Studies in Mycology 101 (March 2022)

ISSN 0166-0616

Regular issue

Robert A. Samson, editor

WESTERDIJK FUNGAL BIODIVERSITY INSTITUTE

An institute of the Royal Netherlands Academy of Arts and Sciences

ISBN/EAN: 978-94-91751-28-8

Cover: Top left: Conidiomata of *Celoporthe foliorum* formed on agar surface with yellow oozing conidial mass; Middle: Asexual structures in *Botryotrichum piluliferum*; Top right: Basidiomata of *Sanguinoderma tricolor*; Bottom left: Conidiogenous cells and conidia of *Colletotrichum bicoloratum*; Bottom middle: Synnemata of *Gibellula puchra* on a spider; Bottom right: Ascomata of *Ophiostoma pilliferum* with sticky ascospores masses at their apices.

AIMS AND SCOPE

The Westerdijk Fungal Biodiversity Institute – an institute of the Royal Netherlands Academy of Arts and Sciences and situated in Utrecht, The Netherlands – maintains a world-renowned collection of living filamentous fungi, yeasts and bacteria. The institute's research programs principally focus on the taxonomy and evolution of fungi as well as on functional aspects of fungal biology and ecology, incorporating molecular and genomics approaches. The Westerdijk Fungal Biodiversity Institute employs circa 60 personnel, among whom circa 32 scientists.

Studies in Mycology is an international journal which publishes systematic monographs of filamentous fungi and yeasts, and special topical issues related to all fields of mycology, biotechnology, ecology, molecular biology, pathology and systematics. The journal is Open-Access and contains monographs or topical issues (5–6 papers per issue). There are no restrictions of length, although it is generally expected that manuscripts should be at least 50 A4 pages in print. The first issue was published in 1972.

Publication
Studies in Mycology is an open access journal that is freely available on the internet. All articles are open access under a Creative Commons BY-NC-ND (Attribution-NonCommercial-NoDerivatives) license. All manuscripts will undergo peer review before acceptance, and will be published as quickly as possible following acceptance. There are no page charges or length restrictions, or fees for colour plates. The official journal language is English. All content submitted to *Studies in Mycology* is checked for plagiarism.

Article submission
Authors who intend to submit monographs or topical issues should contact the Executive Editor in advance. Authors are obliged to meet the requirements as set out in our Instructions for Authors.

Hardcopies
From 2016 onwards hardcopies of new issues are no longer available. Single hardcopies of issues published prior to 2016 can be bought through the Westerdijk Fungal Biodiversity Institute Web shop. A 20% reduction on the list price applies only when 10 or more copies of a specific publication are bought at the same time.

Published by
Westerdijk Fungal Biodiversity Institute, Uppsalalaan 8, 3584 CT Utrecht, The Netherlands.

Hosted by
Ingenta Connect.

CONTENTS

Updating species diversity of *Colletotrichum*, with a phylogenomic overview

F. Liu[1,2#], Z.Y. Ma[1,2#], L.W. Hou[1,2], Y.Z. Diao[3], W.P. Wu[3], U. Damm[4], S. Song[1,2], L. Cai[1,2*]

[1]*State Key Laboratory of Mycology, Institute of Microbiology, Chinese Academy of Sciences, Beijing, 100101, China;* [2]*University of Chinese Academy of Sciences, Beijing, 100049, China;* [3]*Novozymes China, No. 14, Xinxi Rd, Shangdi, Beijing, China;* [4]*Senckenberg Museum of Natural History Görlitz, PF 300 154, 02806 Görlitz, Germany*

[#]These authors contributed equally to this work
**Corresponding author*: Lei Cai, cail@im.ac.cn

Abstract: The genus *Colletotrichum* includes important plant pathogens, endophytes, saprobes and human pathogens. Even though the polyphasic approach has facilitated *Colletotrichum* species identification, knowledge of the overall species diversity and host distribution is largely incomplete. To address this, we examined 952 *Colletotrichum* strains isolated from plants representing 322 species from 248 genera, or air and soil samples, from 87 locations in China, as well as 56 strains from Saudi Arabia, Thailand, Turkey, and the UK. Based on morphological characteristics and multi-locus phylogenetic analyses, the strains were assigned to 107 species, including 30 new species described in this paper and 18 new records for China. The currently most comprehensive backbone tree of *Colletotrichum*, comprising 16 species complexes (including a newly introduced *C. bambusicola* species complex) and 15 singleton species, is provided. Based on these analyses, 280 species with available molecular data are accepted in this genus, of which 139 have been reported in China, accounting for 49.6 % of the species. *Colletotrichum siamense*, *C. karsti*, *C. fructicola*, *C. truncatum*, *C. fioriniae*, and *C. gloeosporioides* were the most commonly detected species in China, as well as the species with the broadest host range. By contrast, 76 species were currently found to be associated with a single plant species or genus in China. To date, 33 *Colletotrichum* species have been exclusively reported as endophytes. Furthermore, we generated and assembled whole-genome sequences of the 30 new and a further 18 known species. The most comprehensive genome tree comprising 94 *Colletotrichum* species based on 1 893 single-copy orthologous genes was hence generated, with all nodes, except four, supported by 100 % bootstrap values. Collectively, this study represents the most comprehensive investigation of *Colletotrichum* diversity and host occurrence to date, and greatly enhances our understanding of the diversity and phylogenetic relationships in this genus.

Key words: Backbone tree, Fungal systematics, Multi-locus phylogeny, New taxa, Phylogenomics, Plant pathogen, Taxonomy
Taxonomic novelties: New species: *Colletotrichum arecacearum* F. Liu, Z.Y. Ma & L. Cai, *Colletotrichum bicoloratum* F. Liu, W.P. Wu & L. Cai, *Colletotrichum bromeliacearum* F. Liu & L. Cai, *Colletotrichum buxi* F. Liu, W.P. Wu & L. Cai, *Colletotrichum chamaedoreae* F. Liu, W.P. Wu & L. Cai, *Colletotrichum crousii* F. Liu, Z.Y. Ma & L. Cai, *Colletotrichum danxiashanense* F. Liu, W.P. Wu & L. Cai, *Colletotrichum diversisporum* F. Liu, W.P. Wu & L. Cai, *Colletotrichum diversum* F. Liu & L. Cai, *Colletotrichum dolichoconidiophori* F. Liu, W.P. Wu & L. Cai, *Colletotrichum iris* F. Liu & L. Cai, *Colletotrichum monsterae* F. Liu, W.P. Wu & L. Cai, *Colletotrichum multiseptatum* F. Liu, W.P. Wu & L. Cai, *Colletotrichum nageiae* F. Liu, W.P. Wu & L. Cai, *Colletotrichum obovoides* F. Liu & L. Cai, *Colletotrichum parabambusicola* F. Liu, W.P. Wu & L. Cai, *Colletotrichum paraendophytum* F. Liu, W.P. Wu & L. Cai, *Colletotrichum reniforme* F. Liu, Z.Y. Ma & L. Cai, *Colletotrichum schimae* F. Liu, W.P. Wu & L. Cai, *Colletotrichum shivasii* F. Liu & L. Cai, *Colletotrichum sinuatum* F. Liu, W.P. Wu & L. Cai, *Colletotrichum subacidae* F. Liu, Z.Y. Ma & L. Cai, *Colletotrichum subsalicis* F. Liu & L. Cai, *Colletotrichum subvariabile* F. Liu, W.P. Wu & L. Cai, *Colletotrichum syngoniicola* F. Liu, Z.Y. Ma & L. Cai, *Colletotrichum telosmae* F. Liu, W.P. Wu & L. Cai, *Colletotrichum tibetense* F. Liu & L. Cai, *Colletotrichum variabile* F. Liu, W.P. Wu & L. Cai, *Colletotrichum zhaoqingense* F. Liu & L. Cai, *Colletotrichum zhejiangense* F. Liu, W.P. Wu & L. Cai.

Citation: Liu F, Ma ZY, Hou LW, Diao YZ, Wu WP, Damm U, Song S, Cai L (2022). Updating species diversity of *Colletotrichum*, with a phylogenomic overview. *Studies in Mycology* **101**: 1–56. doi: 10.3114/sim.2022.101.01
Received: 27 July 2021 ; **Accepted:** 11 October 2021; **Effectively published online:** 11 January 2022
Corresponding editor: Robert A. Samson

INTRODUCTION

Colletotrichum is the only genus of the *Glomerellaceae* (*Glomerellales*, *Sordariomycetes*, *Ascomycota*), and is regarded as one of the 10 most important genera of plant pathogenic fungi in the world (Dean *et al.* 2012). A few species are opportunistic human pathogens, including *C. dematium*, *C. gigasporum*, *C. gloeosporioides* and *C. truncatum* that can cause keratitis and subcutaneous infections (Guarro *et al.* 1998, Damm *et al.* 2009, Shiraishi *et al.* 2011, Shivaprakash *et al.* 2011, Liu *et al.* 2014, Buchta *et al.* 2019). In rare cases, *Colletotrichum* species have been reported to infect animals, *e.g. C. fioriniae* (as *C. acutatum* var. *fioriniae*), infecting a scale insect, and *C. acutatum* (*s. lat.*), infecting a sea turtle (Manire *et al.* 2002, Marcelino *et al.* 2008). *Colletotrichum* also includes plant endophytes, and saprobes from a wide range of substrates, such as the soil, water, and air (Liu *et al.* 2014).

Accurate species identification is important for understanding biodiversity, host-parasite interaction, and evolutionary history, and for monitoring and controlling plant pathogens, and developing quarantine measures. Previous host- and morphology-oriented systematics of *Colletotrichum* is, however, not regarded as natural, does not reflect the phylogenetic relationships, and has largely impeded meaningful investigation of species diversity in this genus. To establish a stable and natural classification system, the use of molecular data in combination with morphological, geographical, and ecological data has increasingly been employed (Cai *et al.* 2009, Cannon *et al.* 2012, Marin-Felix *et al.* 2017, Jayawardena *et al.* 2020).

In the genus *Colletotrichum*, a species complex (also called an 'aggregate') is defined as a group of species that form a monophyletic clade and exhibit shared characteristics (*e.g.* similar conidial morphology) (Cannon *et al.* 2012). The current classification system of *Colletotrichum* comprises 15 species complexes, *i.e.* the *C. acutatum*, *C. agaves*, *C. boninense*, *C. caudatum*, *C. dematium*, *C. destructivum*, *C. dracaenophilum*, *C. gigasporum*, *C. gloeosporioides*, *C. graminicola*, *C. magnum*, *C. orbiculare*, *C.*

orchidearum, *C. spaethianum*, and *C. truncatum* species complexes, as well as a number of singletons (Marin-Felix *et al.* 2017, Damm *et al.* 2019, Jayawardena *et al.* 2020, Bhunjun *et al.* 2021). The *C. caudatum* species complex forms an inner clade of the *C. graminicola* species complex, and was annotated as *C. caudatum* sub-aggregate in the phylogenetic tree, but referred to as a species complex by Crouch (2014). Subsequently, many researchers refer to this group as a *C. caudatum* species complex (*e.g.* Marin-Felix *et al.* 2017, Jayawardena *et al.* 2020). Recently, Bhunjun *et al.* (2021) recommended treating the two species complexes as one, *i.e.* the *C. graminicola-caudatum* species complex.

ITS is a useful DNA barcode for assigning *Colletotrichum* species to species complexes (Cannon *et al.* 2012), but different loci are being employed to resolve the different species complexes. For example, six loci (*act*, *chs-1*, *gapdh*, *his3*, ITS, and *tub2*) have been used for the *C. acutatum*, *C. dematium*, *C. destructivum*, *C. dracaenophilum*, *C. magnum*, *C. orchidearum*, *C. spaethianum* and *C. truncatum* species complexes (Damm *et al.* 2009, 2012a, 2014, 2019), with an additional locus each for the *C. boninense* (*cal*) and *C. orbiculare* (*gs*) species complexes (Damm *et al.* 2012b, 2013), and three additional loci (ApMat, *cal*, and *gs*) for the *C. gloeosporioides* species complex (Weir *et al.* 2012, Liu *et al.* 2015). Meanwhile, *act*, *chs-1*, *gapdh*, ITS, and *tub2* have been used for the *C. gigasporum* species complex (Liu *et al.* 2014), and *apn2*, ITS, Mat1/Apn2, and *sod2* have been used for the *C. caudatum* and *C. graminicola* species complexes (Crouch *et al.* 2009a, Crouch 2014). Furthermore, the combined use of ApMat and *gs* in phylogenetic analysis is very useful for species delimitation in the *C. gloeosporioides* species complex (Liu *et al.* 2015).

Based on phylogenetic analyses of multiple loci, the backbone tree of *Colletotrichum* has been constructed and is frequently updated by the addition of newly described species. The tree includes 119 species in Cannon *et al.* (2012); 189 species in Jayawardena *et al.* (2016) and Marin-Felix *et al.* (2017); 247 species in Jayawardena *et al.* (2020); and 248 species in Bhunjun *et al.* (2021). The continuous discovery of new species indicates very high species diversity in this genus. In China, most *Colletotrichum* taxa are reported in the form of single or few species, or species associated with a certain host (*e.g.* Tao *et al.* 2013, Liu *et al.* 2015, Zhang *et al.* 2020), and there is a lack of systematic and biodiversity investigation of these fungi.

In the current study, we aimed to: 1) resolve the systematic placement of 1 008 *Colletotrichum* strains collected, mostly in China, since 1993; 2) characterise newly discovered species based on all available data; 3) supplement missing sequences of the *act*, *chs-1*, *gapdh*, *his3*, and *tub2* genes of some known species, and build an integrated dataset for *Colletotrichum*; 4) construct a robust and reliable phylogeny of *Colletotrichum* including all species with type-derived sequences; and 5) improve knowledge on the diversity and host occurrence of *Colletotrichum* species in China. In addition, all *Colletotrichum* species with an available genome sequence were used for the construction of a whole-genome species tree to help resolve species boundaries and define species complexes.

MATERIALS AND METHODS

Isolates

In the current study, 1 008 *Colletotrichum* isolates, associated with at least 322 host plant species in 248 genera, from the LC Culture Collection (a personal culture collection of Lei Cai, housed in the Institute of Microbiology, Chinese Academy of Sciences) and the Novozymes Culture Collection were analysed. Of these, 952 were collected at 87 locations in China and 56 at 26 locations in Saudi Arabia, Thailand, Turkey, and the UK. Representative cultures of the new species described herein were deposited in the China General Microbiological Culture Collection (CGMCC). Type specimens were deposited in the Mycological Herbarium, Institute of Microbiology, Chinese Academy of Sciences, Beijing, China (HMAS).

Morphology

The isolates were cultivated on potato dextrose agar (PDA; Difco™, Becton, Dickinson and Company, Sparks, MD, USA) and synthetic nutrient-poor agar (SNA; Nirenberg 1976) supplemented with double-autoclaved pine needles placed on the agar surface. The cultures were incubated at room temperature (25 °C) under a 12 h day/night regime. After 7 d, fungal growth rates were measured and the colony characteristics were noted. Colony colours were rated using the colour charts of Rayner (1970). Morphological observations of reproductive structures were performed using a Nikon AZ100 dissecting microscope (DM) and a Nikon Eclipse 80i compound microscope with differential interference contrast (DIC) illumination, both equipped with a Nikon DS-Ri2 high-definition colour digital camera. Slides were prepared using lactic acid. Measurements and descriptions of microscopic structures were preferentially made from cultures grown on SNA. If sterile on SNA, structures produced on PDA, oatmeal agar (OA), malt extract agar (MEA) (Crous *et al.* 2019), or pine needles were described. Hyphal appressoria were induced using a slide culture technique (Cai *et al.* 2009) or observed directly on the reverse side of colonies grown on SNA. At least 30 measurements were made for each structure, and the mean value, standard deviation, and minimum–maximum values are given, with the extreme measurements in parentheses. Descriptions and illustrations of taxonomic novelties were deposited in MycoBank (www.MycoBank.org; Crous *et al.* 2004).

Molecular analyses using barcoding sequences

Total genomic DNA was extracted from fresh mycelia of each isolate using a modified CTAB protocol (Guo *et al.* 2000). All primers used in the current study are listed in Table 1. PCR amplification was performed as described by Crouch *et al.* (2009a) and Liu *et al.* (2016). PCR amplicons were purified and sequenced by the SinoGenoMax Company (Beijing, China). The forward and reverse reads were paired, and consensus sequences calculated in MEGA v. 7.0.21 (Kumar *et al.* 2016).

Primarily, ApMat, *gapdh*, *gs*, ITS, or *tub2*, which are good discriminative loci in different species complexes in *Colletotrichum* (Damm *et al.* 2012a, b, 2013, 2014, 2019, Liu *et al.* 2015, Jayawardena *et al.* 2016), were selected for PCR amplification and sequencing. All efforts were made to assign isolates to species complexes and to identify them to species level, by BLASTn searches of the NCBI GenBank or by phylogenetic analyses using single locus sequences.

For isolates of species that could not be determined based on the above analyses, an ITS tree was first used for inferring delimitation to the species complex level, and further multi-locus phylogenetic analyses and phenotypic characterisation were then performed for species delimitation. Regarding the multi-locus analyses, a concatenated sequence dataset of *act*, *chs-1*, *gapdh*, *his3*, ITS, and *tub2*, including all *Colletotrichum* species for which molecular data

Table 1. Primers used in this study, with originating loci, sequences and references.

Locus	Product name	Primer name	Direction	Sequence (5'–3')	Reference
act	Actin	ACT-512F	Forward	ATGTGCAAGGCCGGTTTCGC	Carbone & Kohn (1999)
		ACT-783R	Reverse	TACGAGTCCTTCTGGCCCAT	Carbone & Kohn (1999)
apn2	Mat1 and the adjacent DNA lyase gene	Apn1W1F	Forward	ATGGAGCACAAAAACGAACA	Crouch *et al.* (2009b)
		Apn1W1R	Reverse	GCGGAGCAGAGGATGTAGTC	Crouch *et al.* (2009b)
cal	Calmodulin	CL1C	Forward	GAATTCAAGGAGGCCTTCTC	Weir *et al.* (2012)
		CL2C	Reverse	CTTCTGCATCATGAGCTGGAC	Weir *et al.* (2012)
chs-1	Chitin synthase	CHS-79F	Forward	TGGGGCAAGGATGCTTGGAAGAAG	Carbone & Kohn (1999)
		CHS-345R	Reverse	TGGAAGAACCATCTGTGAGAGTTG	Carbone & Kohn (1999)
ApMat	Apn2-Mat1-2 intergenic spacer and partial mating type Mat1-2 gene	AMF1	Forward	CCAGAAATACACCGAACTTGC	Silva *et al.* (2012)
		AMR1	Reverse	TCATTCTACGTATGTGCCCG	Silva *et al.* (2012)
gapdh	Glyceraldehyde-3-phosphate dehydrogenase	GDF1	Forward	GCCGTCAACGACCCCTTCATTGA	Guerber *et al.* (2003)
		GDR1	Reverse	GGGTGGAGTCGTACTTGAGCATGT	Guerber *et al.* (2003)
gs	Glutamine synthetase	GSF1	Forward	ATGGCCGAGTACATCTGG	Guerber *et al.* (2003)
		GSR1	Reverse	GAACCGTCGAAGTTCCAC	Guerber *et al.* (2003)
		GSLF2	Forward	TACACGAGSAAAAGGATACGC	Liu *et al.* (2016)
		GSLR1	Reverse	AGRCGCACATTGTCAGTATCG	Liu *et al.* (2016)
his3	Histone3	CYLH3F	Forward	AGGTCCACTGGTGGCAAG	Crous *et al.* (2004)
		CYLH3R	Reverse	AGCTGGATGTCCTTGGACTG	Crous *et al.* (2004)
ITS	Internal transcribed spacer	ITS1	Forward	TCCGTAGGTGAACCTGCGG	White *et al.* (1990)
		ITS4	Reverse	TCCTCCGCTTATTGATATGC	White *et al.* (1990)
Mat1/Apn2	The 3' end of *apn2* and the 5' end of the mating type gene *Mat1-2*	Mat1M72F	Forward	ACGGCAAACGGCTCAGGGAGTG	Crouch *et al.* (2009b)
		Mat1M72R	Reverse	AATGCCGAGTCCCACGAGGTTCG	Crouch *et al.* (2009b)
sod2	Manganese-superoxide dismutase	SOD625F	Forward	GCCCACAGTACATATTGCCTAAGC	Crouch *et al.* (2006)
		SOD625R	Reverse	TCATCCCGGGAGCCAGAAAACCT	Crouch *et al.* (2006)
tub2	β-tubulin 2	T1	Forward	AACATGCGTGAGATTGTAAGT	O'Donnell & Cigelnik (1997)
		Bt2b	Reverse	ACCCTCAGTGTAGTGACCCTTGGC	Glass & Donaldson (1995)

are available, was used to construct the overview phylogeny for the genus (Cannon *et al.* 2012, Damm *et al.* 2012a, b, 2013, 2014, 2019, Weir *et al.* 2012, Liu *et al.* 2014, Jayawardena *et al.* 2016, Marin-Felix *et al.* 2017). Two additional sequence datasets were used for the *C. caudatum* species complex (*apn2*, ITS, Mat1/Apn2, and *sod2*) and *C. graminicola* species complex (*act*, *chs-1*, ITS, *sod2*, and *tub2*) (Crouch *et al.* 2009a, Cannon *et al.* 2012, Crouch 2014). All novel sequences obtained in the current study were submitted to the NCBI GenBank (www.ncbi.nlm.nih.gov; Tables S1–S3).

Sequence alignments of the individual loci were prepared using MAFFT v. 7 (http://mafft.cbrc.jp/alignment/server/index.html) and manually edited in MEGA v. 7.0.21. Maximum-likelihood (ML) and Bayesian analysis (BA) were used for phylogenetic inferences of the ITS alignment and concatenated alignments. MrModelTest v. 2.2 (Nylander 2004) was used to determine the optimal nucleotide substitution model for each locus. The individual gene trees were assessed for clade conflicts between the individual phylogenies.

Maximum-likelihood and BA were implemented using the CIPRES Science Gateway portal (https://www.phylo.org/; Miller *et al.* 2012) using RAxML-HPC BlackBox v. 8.2.10 (Stamatakis 2014) and MrBayes v. 3.2.6 (Huelsenbeck & Ronquist 2001, Ronquist & Huelsenbeck 2003), respectively. For ML analyses, GTR+GAMMA substitution model with 1 000 bootstrap iterations was set. Bayesian analyses were computed with four simultaneous Markov Chain Monte Carlo chains, 200 M generations, and a sampling frequency of 1 000 generations for the first dataset and 100 generations for the other two datasets, ending the run automatically when standard deviation of split frequencies fell below 0.01. The burn-in fraction was set to 0.25, after which the 50 % majority rule consensus trees and posterior probability (PP) values were calculated. The resulting trees were plotted using FigTree v. 1.4.2 (http://tree.bio.ed.ac.uk/software/figtree).

Whole-genome sequencing

Phylogenomic analysis was performed to better define the species complex boundaries for *Colletotrichum* and help to understand the fungal evolution in this genus. Whole-genome sequences were generated for ex-type strains of new species described in the current study and for 18 known species that were available. Reference genomes were retrieved from NCBI (Table S4). All isolates were purified using a single-spore isolation method (Zhang *et al.* 2013). Hypha of 4-d-old colonies growing on PDA were transferred to 50 mL of potato dextrose broth (PDB) and cultivated

for 3–6 d at 25 °C at 150 rpm. Fresh mycelia were filtered through four layers of sterile gauze and were then stored at -80 °C. DNA libraries were prepared using DNeasy Plant Mini kit (Qiagen). The libraries were sequenced as 150 bp pair-end reads using Illumina NovaSeq 6000 platform. Genome assemblies were deposited in the National Microbiology Data Center (NMDC) under BioProject NMDC10017886.

Genome assembly and gene annotation

Read quality was assessed by using FastQC v. 0.11.8 (Andrews & Babraham 2010). Clean reads were assembled with SPAdes v. 3.12.0 (Bankevich *et al.* 2012), using the 'careful' mode and various kmers (21, 33, 55, 77, 99). Scaffolds shorter than 200 bp were removed from subsequent analyses. Genome assembly quality was assessed using QUAST v. 5.0.2 (Alexey *et al.* 2013). Genome completeness was assessed using genome mode in BUSCOs v. 2.0.1 (Mathieu *et al.* 2019), with Sordaromyceta_odb9 gene set.

Gene prediction for the 48 newly sequenced and 46 previously published genomes of *Colletotrichum* (Table S4) were done using the Funannotate pipeline v. 1.7.0 (Palmer 2016). Repetitive elements were initially soft-masked using default parameters. Next, the prediction step of funannotate pipeline (funannotate predict) was implemented using --busco_db Sordariomycetes, --busco_seed_species Verticillium longporum1 and default parameters. Predicted proteins were firstly annotated using eggNOG-mapper v. 2 (Huerta-Cepas *et al.* 2017) and then compared via BlastP (e-value ≤ 1e-10) against Fungal Cytochrome P450 (Moktali *et al*. 2012) and Transporters Classification Database (Saier *et al.* 2016). Carbohydrate-active enzymes annotation was predicted using dbCAN v. 2.0.6 (Yin *et al.* 2012) with DIAMOND, Hotpep and HMMER as default settings, and the genes found by at least two tools were regarded as candidates. The SignalP v. 5.5 (Armenteros *et al.* 2019), TMHMM v. 2.0 (Krogh *et al.* 2001), TargetP v. 2.0 (Emanuelsson *et al.* 2000), EffectorP v. 1.0 (Sperschneider *et al.* 2016) were incorporated to predict effectors.

Phylogenomic tree construction

The phylogenetic relationships between *Colletotrichum* members were inferred based on orthologs of all (94) assembled genomes (Table S4), using *Verticillium dahliae* as the outgroup. Predicted proteins were clustered into orthologous groups by using Orthofinder v. 2.3.3 (Emms & Kelly 2019). Amino acid sequences of 1 893 single-copy orthologs were aligned using MAFFT v. 7.407 (Katoh & Standley 2013) with default settings. Conserved sites in the alignment were extracted using Gblocks v. 0.91b (Castresana 2000) and then concatenated. A JTT substitution model of the concatenated alignment resulting from analysis in ProtTest v. 3.4.2 (Darriba *et al.* 2011) was used for phylogenomic tree construction using RAxML v. 8.2.12 (Stamatakis 2014) with 1 000 bootstrap iterations.

RESULTS

Single-locus analysis

Based on BLASTn search and single-locus phylogenetic analyses using ApMat, *gapdh*, *gs*, or *tub2*, we attempted to assign the 1 008 strains analysed (Table S5) to species level. For the undetermined strains, a single ITS phylogenetic analysis was performed to allocate them into species complexes. The ITS alignment contained 618 characters, including alignment gaps. The ML search revealed a best tree with an lnL of -8314.217491. The BA was run for 20 025 000 generations, and a 50 % consensus tree and posterior probabilities were calculated from 30 040 trees from two analysis runs. The analysed strains were thus separated into 14 species complexes and six singleton clades. Four taxa (*C. bambusicola*, *C. hsienjenchang*, *C. metake*, and *C. parabambusicola sp. nov.*), characterised by straight conidia, formed a main clade, which was denoted as a new species complex (Fig. S1). The *C. graminicola* species complex was polyphyletic in the ITS tree. *Colletotrichum riograndense*, which had previously been considered as belonging to the *C. spaethianum* species complex, was however phylogenetically basal to the *C. bambusicola* and *C. spaethianum* species complexes. Furthermore, the topologies of the single ITS tree and multi-locus tree were compared to determine whether the grouping of species within species complexes was congruent.

Multi-locus phylogeny

Overview phylogeny of Colletotrichum *based on six loci*

The combined *act*, *chs-1*, *gapdh*, *his3*, ITS, and *tub2* sequence alignment that was used for overview phylogeny construction contained 250 currently accepted *Colletotrichum* species and *Monilochaetes infuscans* (CBS 869.96) as the outgroup. The final alignment contained 2 659 characters (*act*: 322; *chs-1*: 251; *gapdh*: 441; *his3*: 417; ITS: 606; *tub2*: 622) including the alignment gaps, and 1 944 characters were unique site patterns. The ML search revealed a best tree with an lnL of -74738.627777. MrModelTest recommended Dirichlet base frequencies for all data partitions of the BA. The GTR+I+G model was suggested for *act*, *gapdh*, and ITS, and the HKY+I+G model for *chs-1*, *his3*, and *tub2*. The BA was run for 39 980 000 generations, and a 50 % consensus tree and posterior probabilities were calculated from 59 972 trees from two runs.

The topologies of the six-locus phylogenetic trees generated by ML and BA were congruent and consistent with the species complex delimitation reported previously (Cannon *et al.* 2012, Marin-Felix *et al.* 2017, Bhunjun *et al.* 2021), but differed from the ITS tree constructed in the current study in the grouping of *C. guangxiense* and *C. riograndense* on species complex level. In the six-locus tree, *C. guangxiense* and four additional taxa (*C. bambusicola*, *C. hsienjenchang*, *C. metake*, and *C. parabambusicola sp. nov.*) formed a new species complex (Fig. 1). By contrast, *C. guangxiense* was basal to the *C. caudatum*, *C. destructivum* and *C. graminicola* species complexes in the ITS tree (Fig. S1). *Colletotrichum riograndense*, belonging to the *C. spaethianum* species complex in the six-locus phylogeny (Fig. 1), was in the ITS tree basal to a clade formed by the *C. bambusicola*, *C. caudatum*, *C. destructivum*, *C. graminicola*, and *C. spaethianum* species complexes (Fig. S1).

The *C. caudatum* species complex formed a subclade of the *C. graminicola* complex and some taxa in the two species complexes were indistinguishable in the six-locus tree (Fig. 1), *e.g. C. caudatum* and *C. somersetense*, *C. ochraceae* and *C. zoysiae*, *C. axonopodi* and *C. hanaui*.

The phylogenies of the C. caudatum *and* C. graminicola *species complexes*

As two different sets of loci were previously used for the phylogenetic analyses of *C. caudatum* and *C. graminicola* species complexes, separate analyses were performed herein.

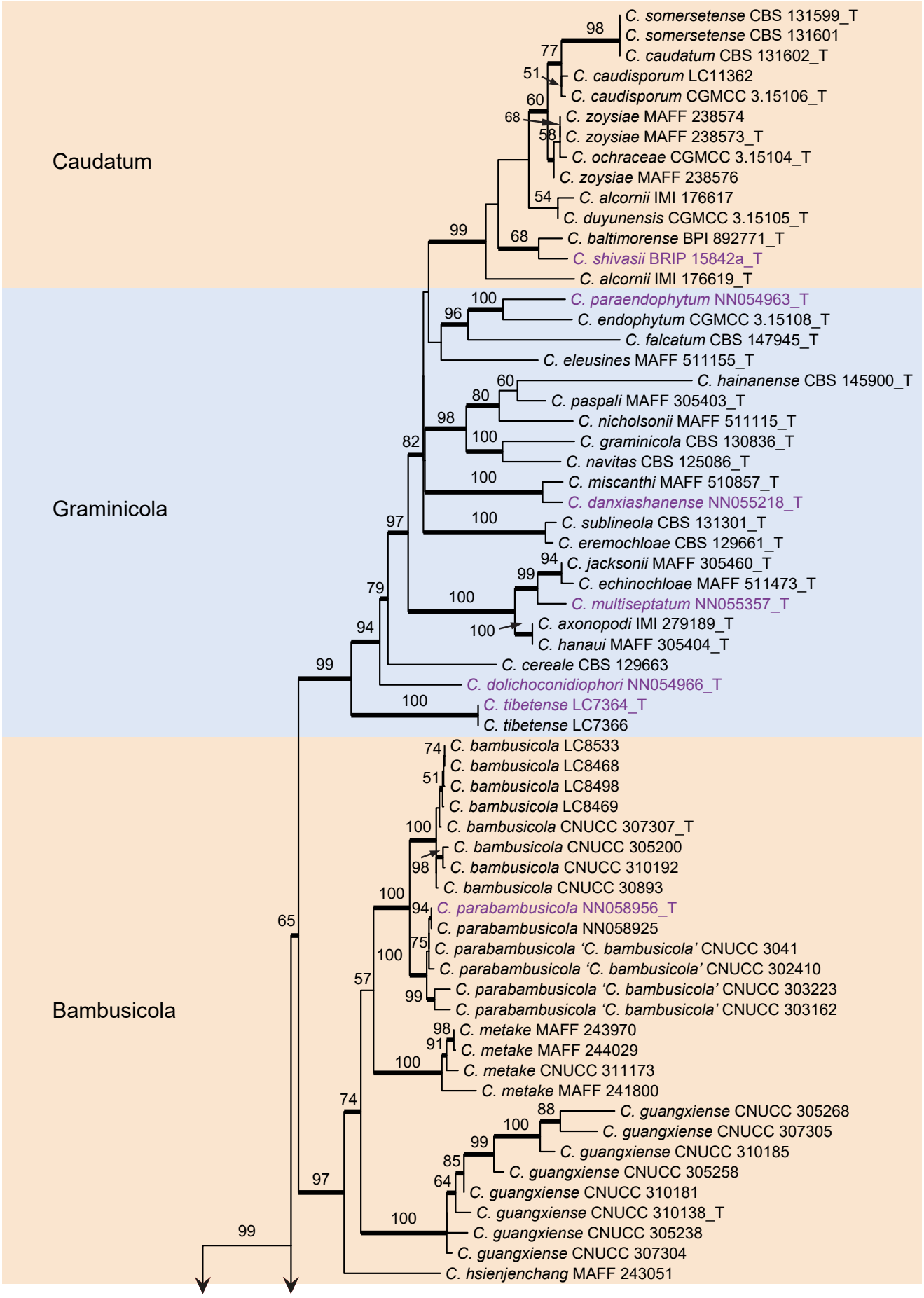

Fig. 1. Phylogenetic tree of *Colletotrichum* calculated with a maximum likelihood analysis of the combined *act*, *chs-1*, *gapdh*, *his3*, ITS, and *tub2* sequence alignment. Bayesian posterior probabilities (PP > 0.90) are emphasised by thickened branches, maximum likelihood bootstrap support values (> 50 %) are shown at the nodes. Species complexes are indicated with coloured boxes, with their names listed at the left. Ex-type strains are indicated with "T" in the end of the taxa labels. Latin names and ex-type strain numbers of the new species described in the current study are shown in purple font.

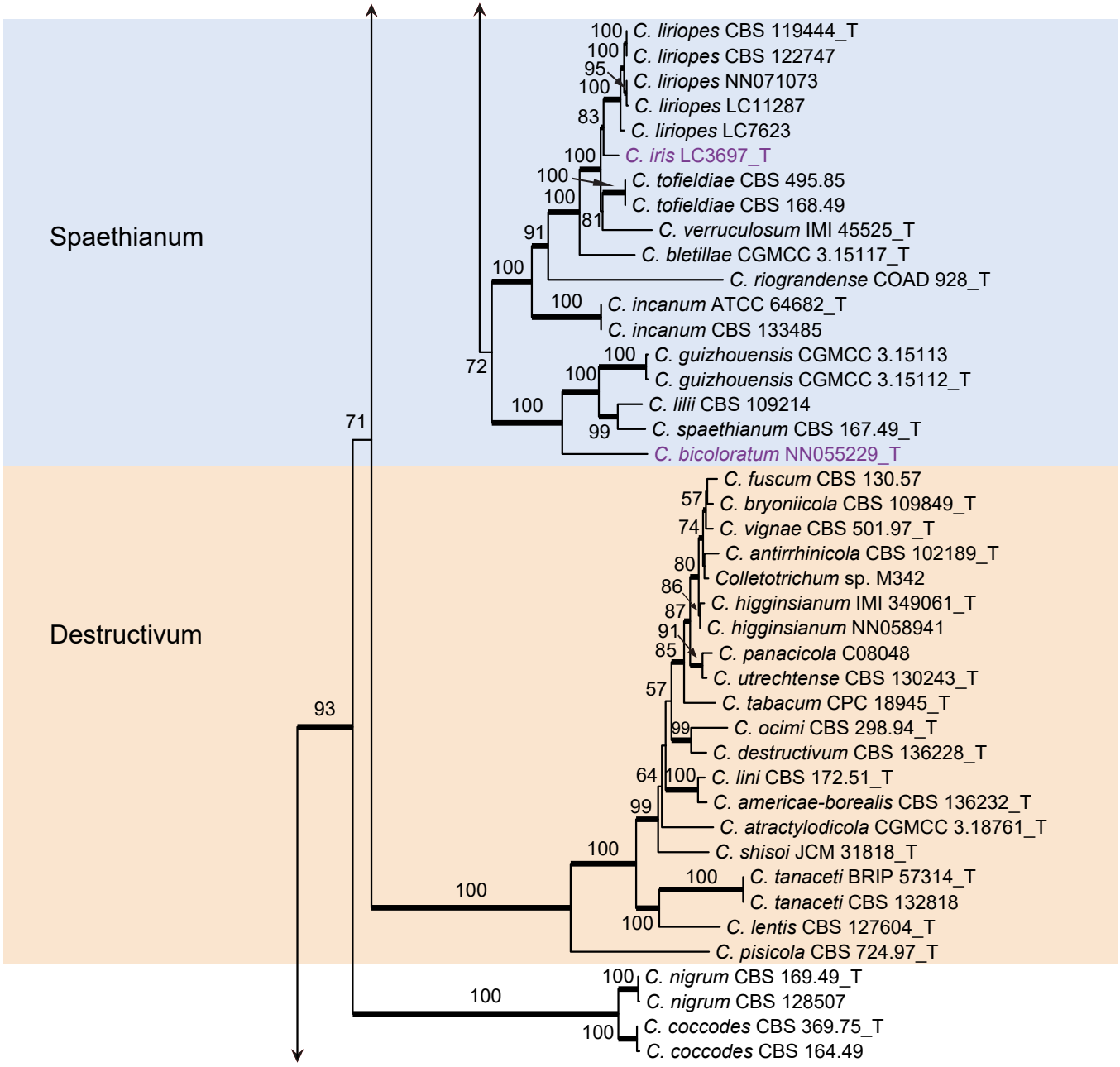

Fig. 1. (Continued).

Colletotrichum caudatum species complex (Fig. 2): The dataset consisted of 14 strains, with *C. gloeosporioides* (IMI 356878) as the outgroup. The final sequence alignment contained 2 949 characters (*apn2*: 805; ITS: 439; Mat1/Apn2: 1253; *sod2*: 452) including alignment gaps, and 301 characters were unique site patterns. The ML search revealed a best tree with an lnL of -6 746.046698. The BA was run for 260 000 generations, and a 50 % consensus tree and posterior probabilities were calculated from 5 202 trees from two runs. The topologies of phylogenetic trees generated by ML and BA were congruent. In the four-locus phylogenetic tree of *C. caudatum* species complex (Fig. 2), strain BRIP 15842a formed a sister clade to the ex-type of *C. baltimorense* on a long branch, distinct from the other clades, representing a novel species. The two strains of *C. alcornii* (IMI 176617 and IMI 176619) were separated into two distant clades, sharing 97 % (419/431) ITS sequence similarity, and may represent different species.

Colletotrichum graminicola species complex (Fig. 3): The dataset consisted of 22 strains, with *C. gloeosporioides* (IMI 356878) as the outgroup. The final alignment contained 2 117 characters (*act*: 255; *chs-1*: 278; ITS: 507; *sod2*: 564; *tub2*: 513) including alignment gaps, and 725 characters were unique site patterns. The ML search revealed a best tree with an lnL of -10629.345037. The BA was run for 1 000 generations, and a 50 % consensus tree and posterior probabilities were calculated from 202 trees from two runs. The topologies of the phylogenetic trees generated by ML and BA were congruent. In the five-locus phylogenetic tree of the *C. graminicola* species complex (Fig. 3), the analysed strains formed five distinct clades on long branches.

Whole-genome data and phylogenomic assessment

The *Colletotrichum* genomes varied from 35.03 Mbp to 109.66 Mbp in size and encoded from 8 424 to 14 841 protein-coding genes (Fig. 4, Table S4), and neither correlated with the phylogenetic position (Fig. 4) nor lifestyle of the species (Table S4), except for the genome sizes of the *C. orbiculare* species complex (> 82 Mbp)

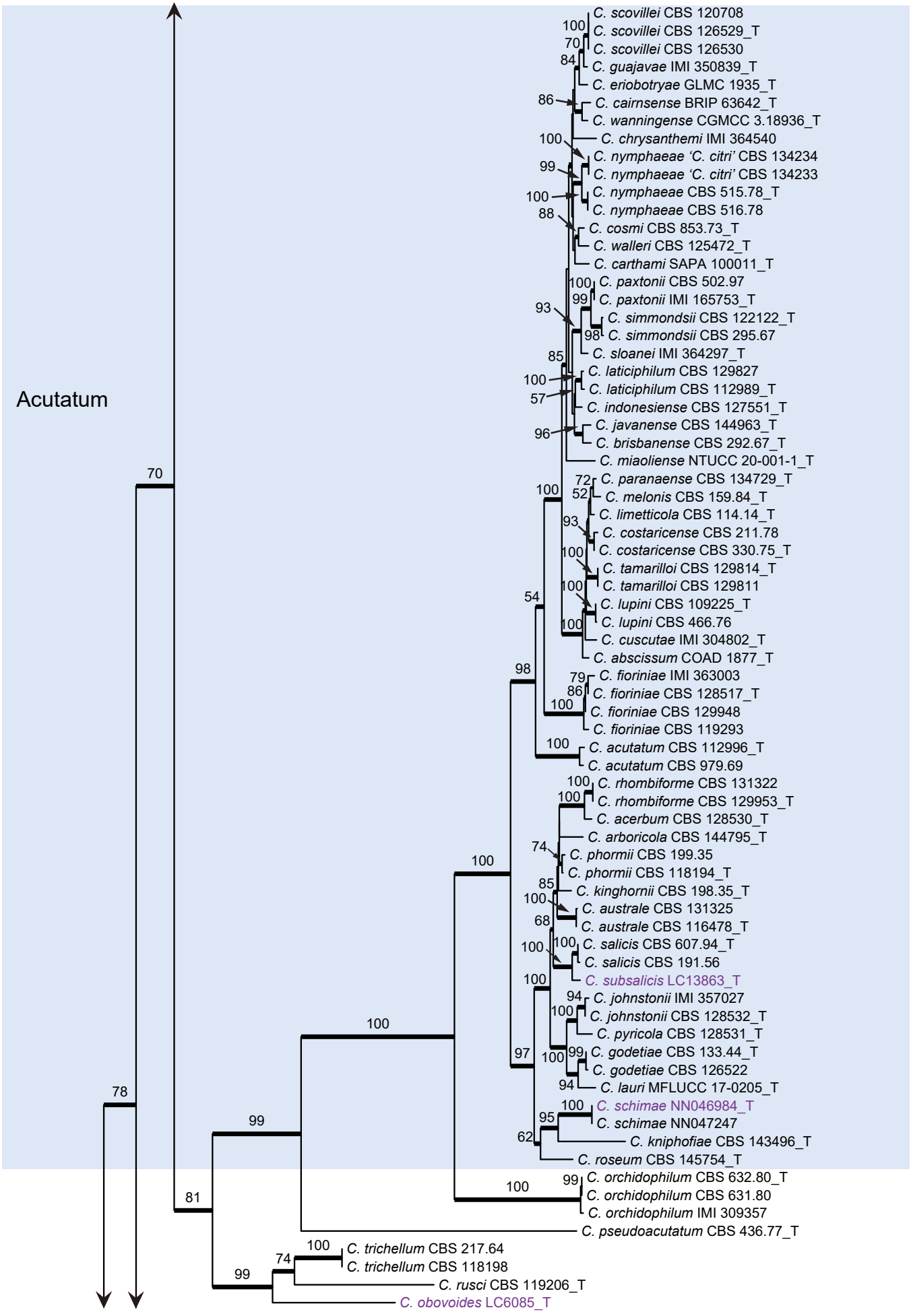

Fig. 1. (Continued).

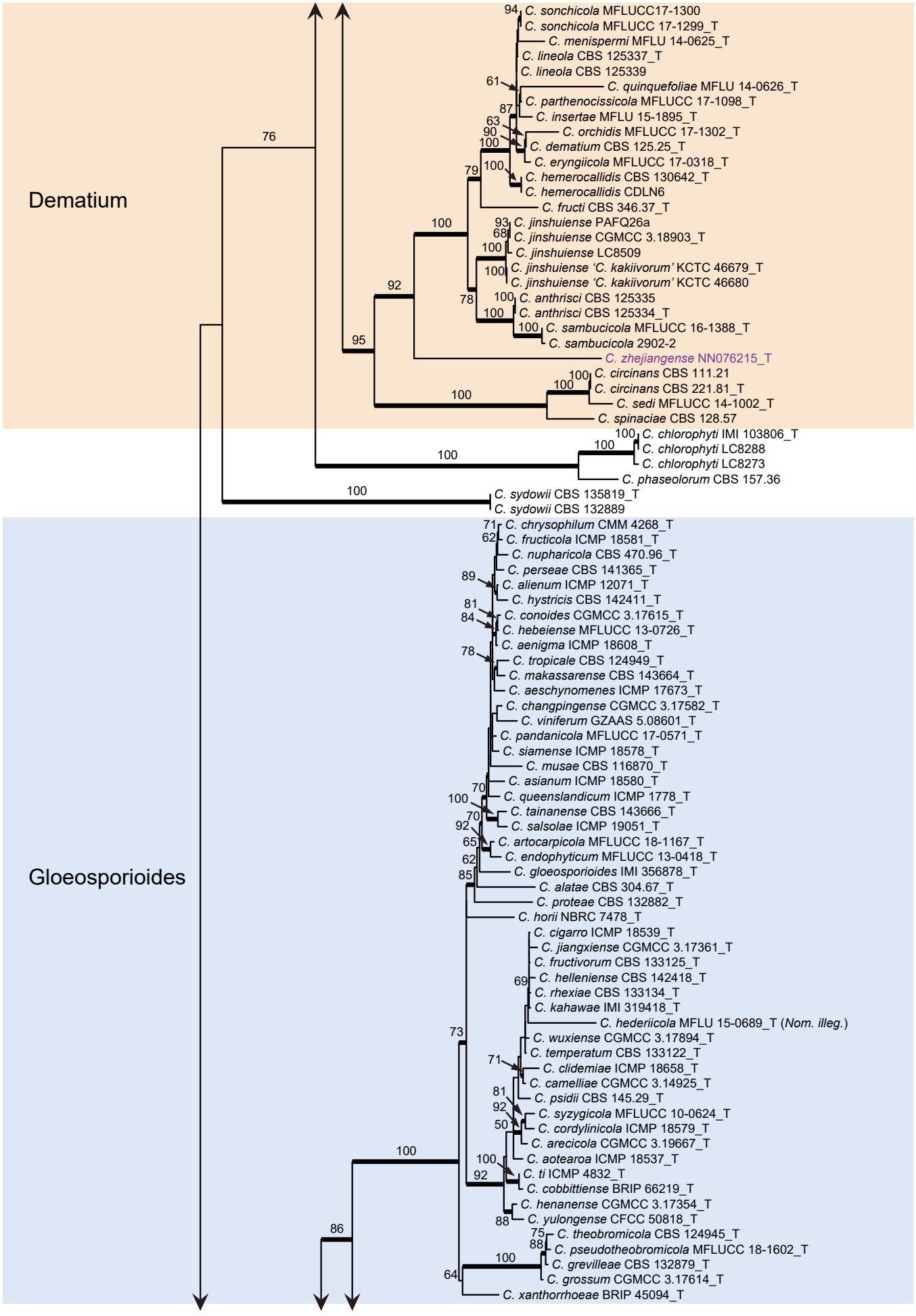

Fig. 1. (Continued).

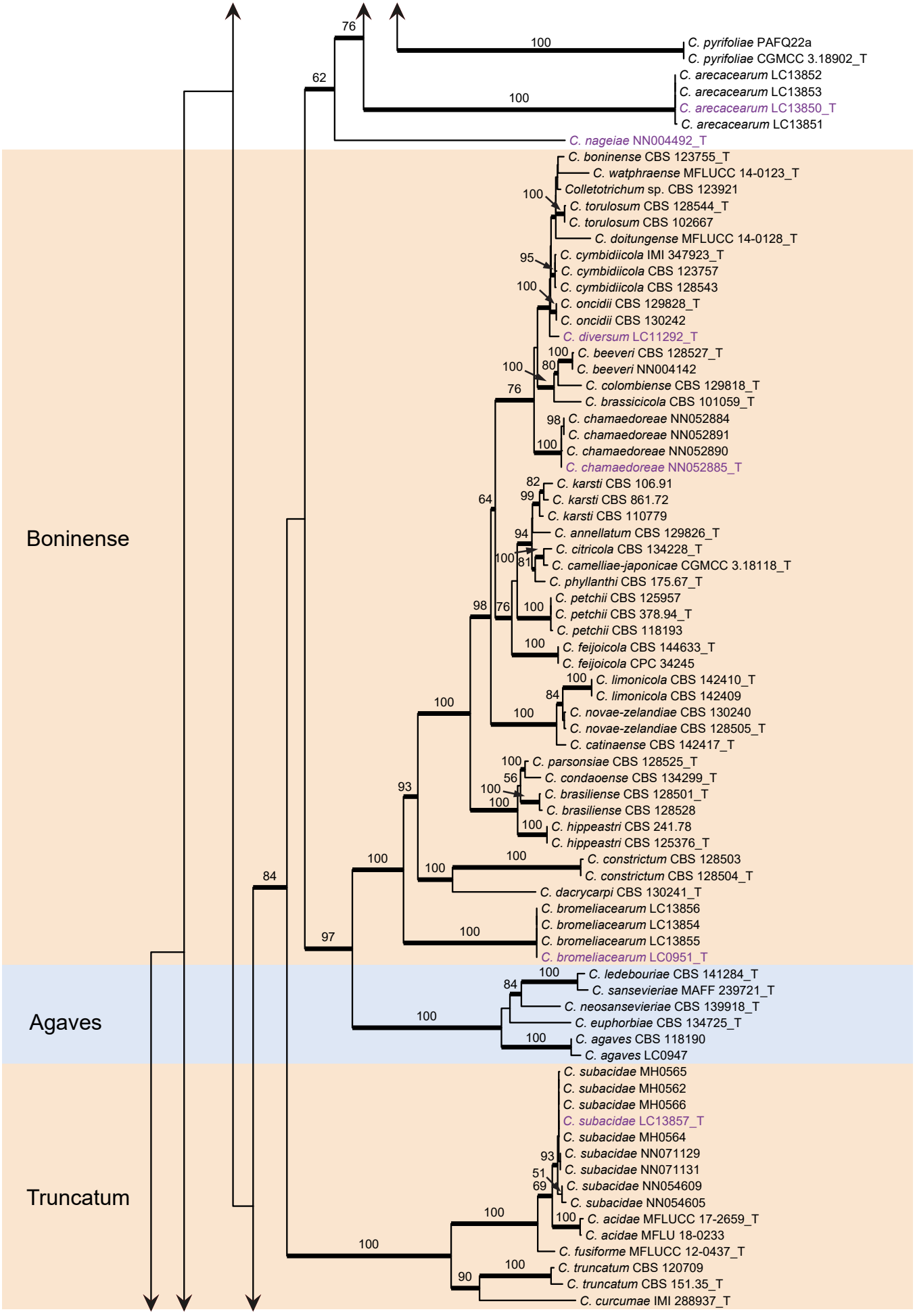

Fig. 1. (Continued).

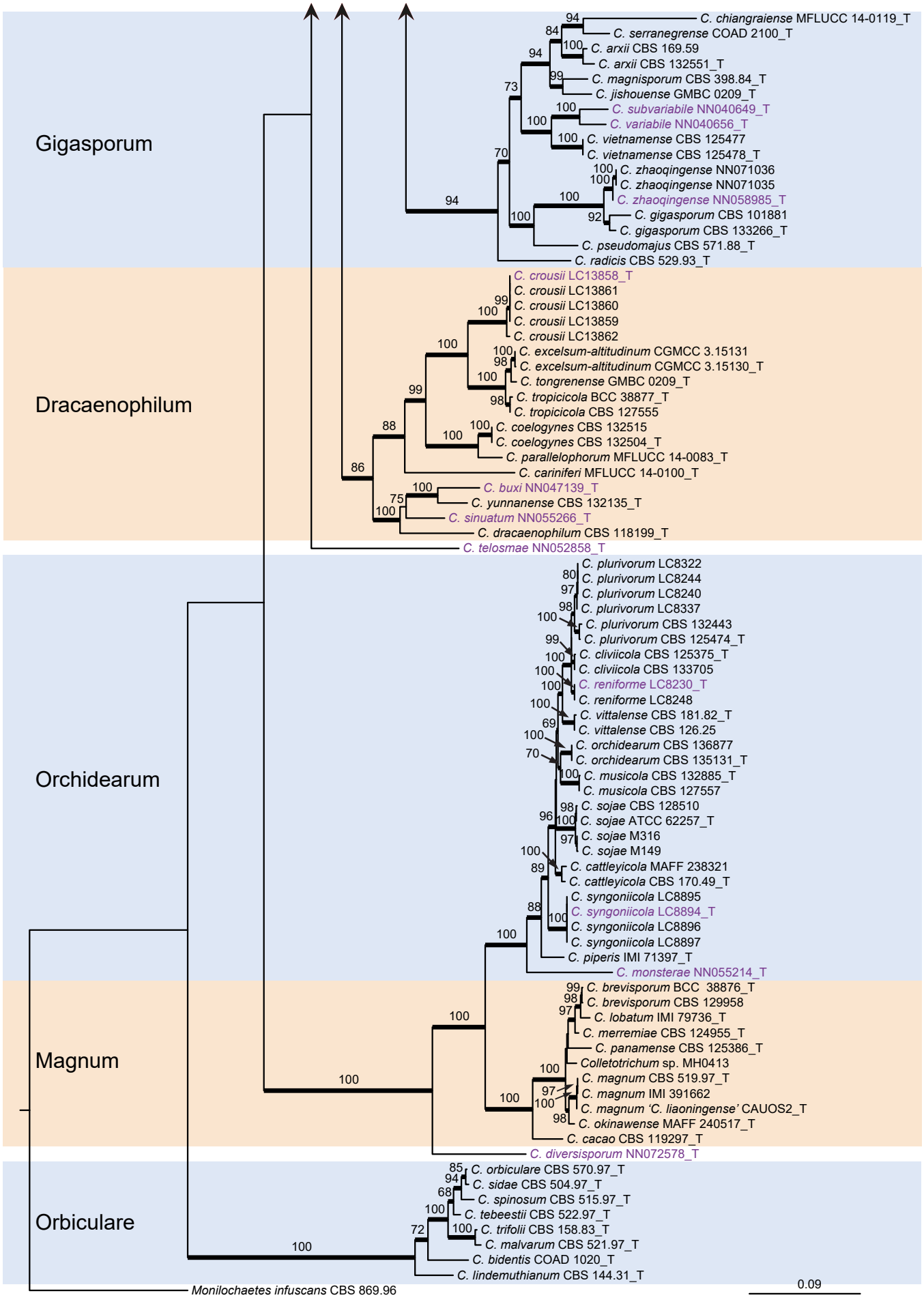

Fig. 1. (Continued).

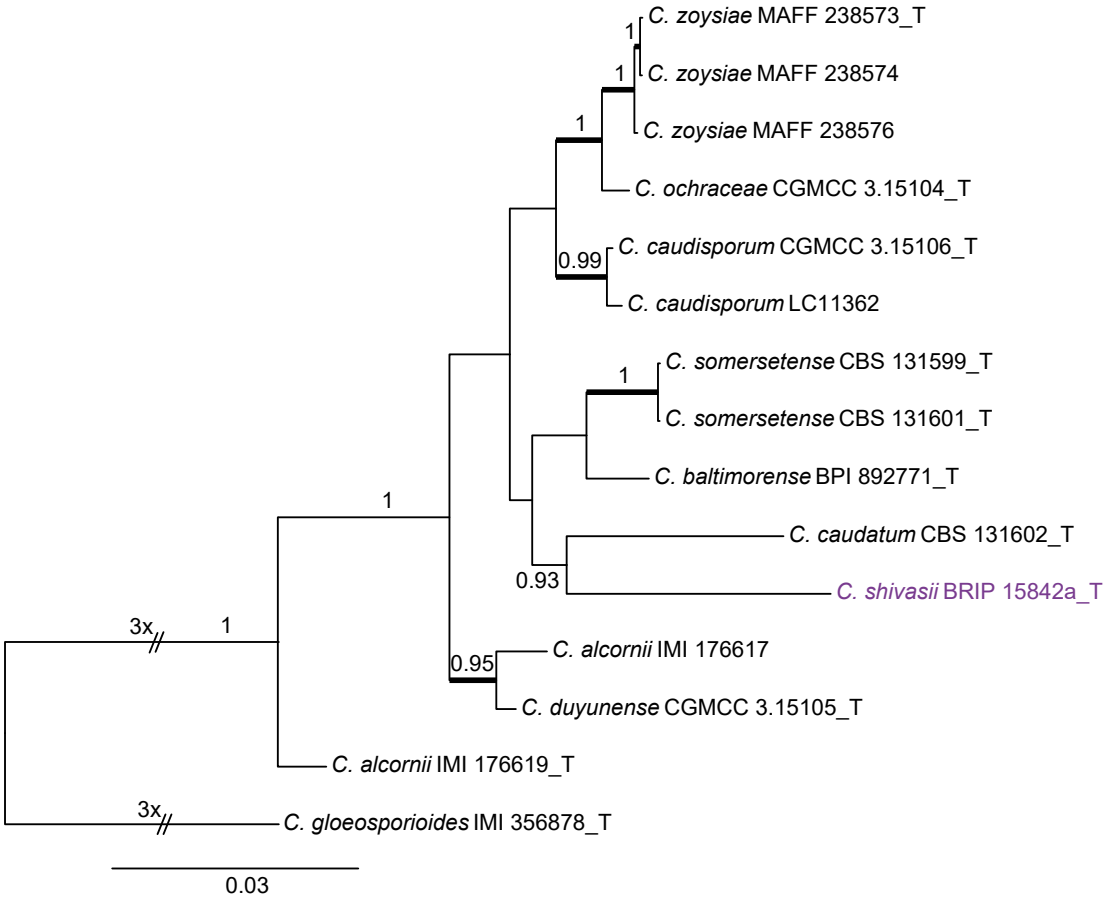

Fig. 2. Phylogenetic tree of the *C. caudatum* species complex resulting from a Bayesian analysis of the combined *apn2*, ITS, Mat1/Apn2, and *sod2* sequence alignment. Maximum likelihood bootstrap support values (> 70 %) are emphasised by thickened branches, bayesian posterior probabilities (PP > 0.90) are shown at the nodes. The scale bar represents the expected number of changes per site. Ex-type strains are indicated with "T" in the end of the taxa labels. Latin names and ex-type strain numbers of the new species described in the current study are shown in purple font.

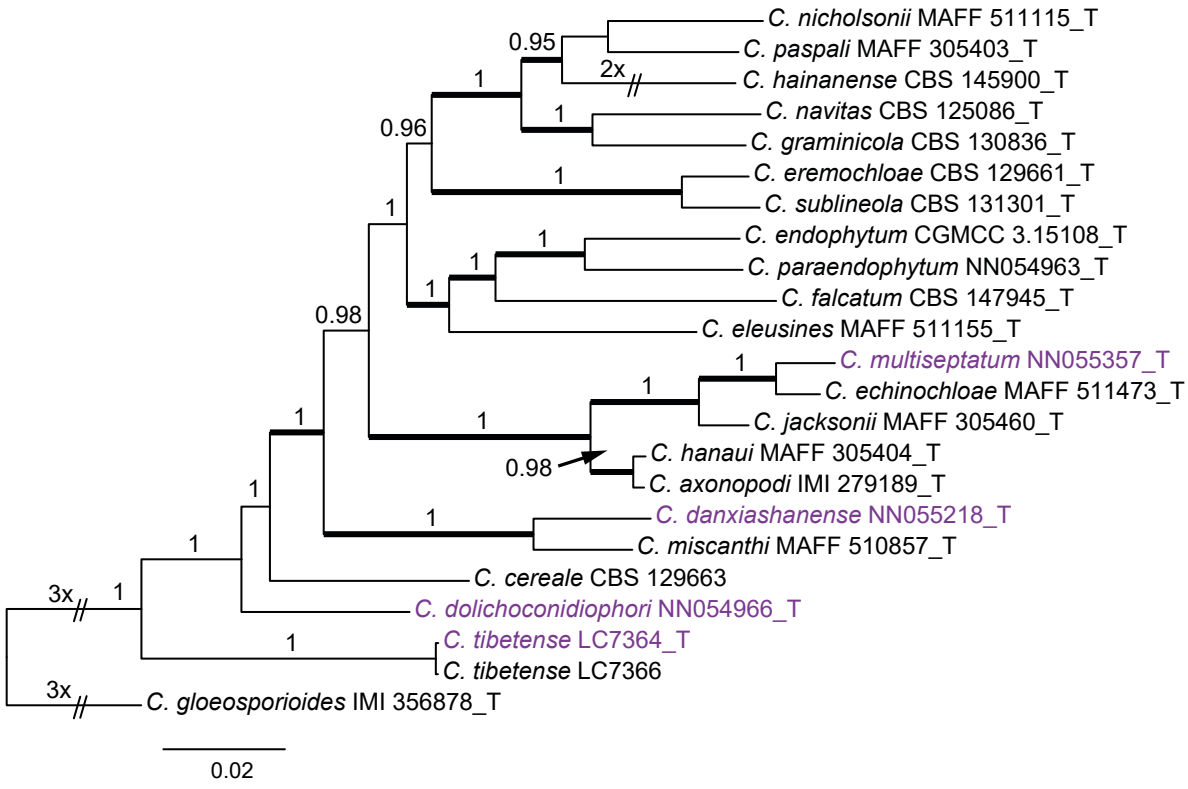

Fig. 3. Phylogenetic tree of the *C. graminicola* species complex resulting from a Bayesian analysis of the combined *act*, *chs-1*, ITS, *sod2*, and *tub2* sequence alignment. Maximum likelihood bootstrap support values (> 70 %) are emphasised by thickened branches, bayesian posterior probabilities (PP > 0.90) are shown at the nodes. The scale bar represents the expected number of changes per site. Ex-type strains are indicated with "T" in the end of the taxa labels. Latin names and ex-type strain numbers of the new species described in the current study are shown in purple font.

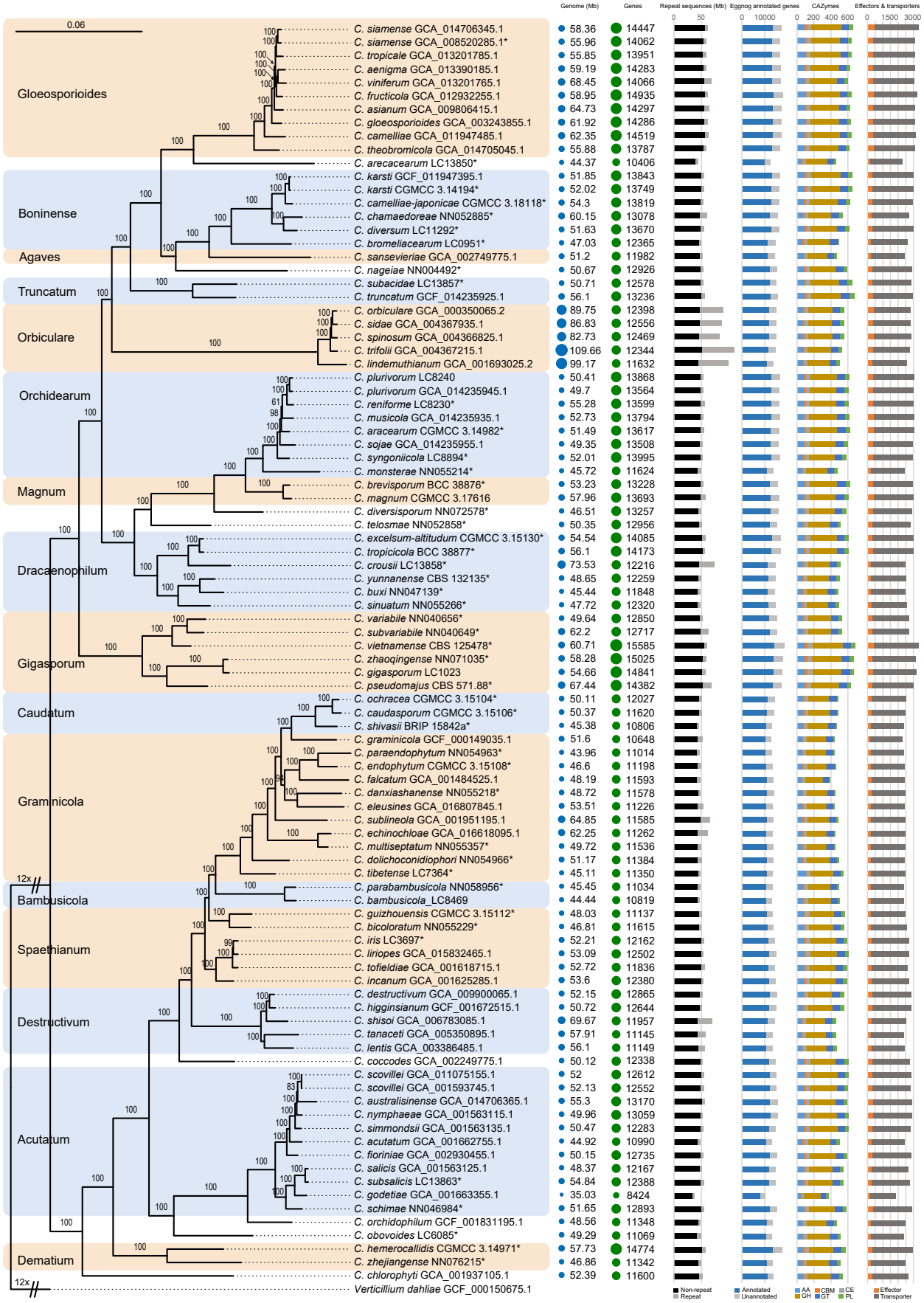

Fig. 4. Maximum likelihood phylogenomic tree generated from a concatenated alignment of sets of orthologous protein sequences. A total of 1 893 single-copy orthologs were retained. The tree was estimated based on the JTT substitution model. Ex-type strains are indicated with "*" in the end of the taxa labels. Genome and assembly features are shown at the right side of the phylogenetic tree. From left to right: Genomes (Mb): genome size in Mb; Genes: number of predicted genes; Repeat sequences (Mb): genome sizes showing proportion of repeat elements in these genomes; Eggnog annotated genes: number of predicted protein coding genes with and without functional annotation based on eggnog database; CAZymes: gene number with the distribution of CAZyme classes, auxiliary activities (AA), carbohydrate binding molecules (CBM), carbohydrate esterases (CE), glycoside hydrolases (GH), glycosyl transferases (GT), polysaccharide lyases (PL); Effectors & transporters: number of predicted effectors and transporters.

that were generally larger than those of other species (Fig. 4). However, disproportionate to the large genome, the *C. orbiculare* species complex encodes relatively smaller number of genes, CAZymes and transporters than a few other species complexes, *e.g. C. gigasporum*, *C. gloeosporioides*, and *C. orchidearum* species complexes. On the contrary, *C. orbiculare* species complex possesses the highest proportion of repeat content than other species in this genus (Fig. 4), which may contribute to its large genome (Haridas *et al.* 2020). Moreover, compared to other members in *Colletotrichum*, species associated with gramineous plants in the *C. bambusicola*, *C. caudatum*, and *C. graminicola* species complexes are characterised by small genome size and small number of genes, CAZymes and transporters.

Using 94 *Colletotrichum* species covering 16 species complexes and one outgroup, a high confidence whole-genome-based phylogenetic tree was generated (Fig. 4). The Gblocks filtered alignment of 1 893 single-copy orthologs consisted of 655 956 characters, including alignment gaps. All nodes, except for four (two in the *C. orchidearum* species complex, and the other two in the *C. graminicola* and *C. spaethianum* species complexes respectively), received 100 % bootstrap support (Fig. 4). The species tree supported the taxonomic status of all species newly described in the current study (Fig. 4). The strain with the assembly accession GCA_001593745.1 was labeled as *C. acutatum* at the time the genome was published; it was however revealed to be *C. scovillei* in the species tree (Fig. 4).

Taxonomy

Five taxa (*C. bambusicola*, *C. guangxiense*, *C. hsienjenchang*, *C. metake*, and *C. parabambusicola sp. nov.*) characterised by straight conidia formed a well-supported clade in the six-locus tree (Fig. 1), representing a new species complex, herein called the *C. bambusicola* species complex. Based on the molecular analyses, morphological examination, and habitat and geographical comparisons, 30 new species are introduced herein.

Colletotrichum arecacearum F. Liu, Z.Y. Ma & L. Cai, ***sp. nov.*** MycoBank MB 841370. Fig. 5.

Etymology: Named after its host plant family, *Arecaceae.*

Description: *Colonies* on PDA 19–22 mm diam in 7 d, flat with entire edge, saffron in the centre, white at the margin, aerial mycelium sparse, reverse creamy white. *Vegetative hyphae* hyaline, smooth-walled, septate, branched. Sporulating on OA, *conidiomata* scattered or confluent, immersed, olivaceous. *Conidiophores* usually reduced to conidiogenous cells. *Conidiogenous cells* hyaline, smooth-walled, ampulliform, rarely subcylindrical, straight or curved, collarette distinct, periclinal thickening sometimes visible, 8.5–15 × 4.5–7.5 µm. *Conidia* hyaline, aseptate, smooth-walled, guttulate, cylindrical, occasionally slightly curved, with one end round and one end subacute, 12.5–18.5 × 4–5.5 µm (av. ± SD = 15.5 ± 1.3 × 4.7 ± 0.3 µm), L/W ratio = 3.3. *Appressoria* and *setae* not observed.

Typus: **China**, Guangxi, Guangxi Botanical Garden of Medicinal Plants, on leaves of an unidentified species in *Arecaceae*, Jun. 2017, Z.Y. Ma & L.W. Hou (**holotype** HMAS 350634, ex-type culture CGMCC 3.20509 = LC13850 = MH0003).

Additional materials examined: **China**, Guangxi, Guangxi Botanical Garden of Medicinal Plants, on leaves of an unidentified species in *Arecaceae*, Jun. 2017, Z.Y. Ma & L.W. Hou, living cultures LC13851 (= MH0003-1), LC13852 (= MH0003-2), LC13853 (= MH0003-3).

Notes: *Colletotrichum arecacearum*, *C. pyrifoliae*, and *C. nageiae sp. nov.* clustered basal to the broadly known *C. gloeosporioides* species complex (Fig. 1). These three species produce cylindrical conidia, similar to those produced by the *C. gloeosporioides* complex (Weir *et al.* 2012), but are temporarily considered as singleton species because the ingroup taxa of the *C. gloeosporioides* complex are much more tightly related to each other than to them. *Colletotrichum arecacearum* is distinct from other species in this genus at each locus sequenced in the current study, and morphologically differs from the most closely related species *C. pyrifoliae* in producing shorter and wider conidiogenous cells (8.5–15 × 4.5–7.5 µm *vs.* 15–32 × 3–5 µm), and slightly shorter and thinner conidia (12.5–18.5 × 4–5.5 µm *vs.* 14–23 × 5.5–7 µm), and differs from *C. nageiae sp. nov.* in producing wider conidiogenous cells (8.5–15 × 4.5–7.5 µm *vs.* 10–20 × 2.5–4.5 µm) and longer conidia (12.5–18.5 × 4–5.5 µm *vs.* 9–13.5 × 4.5–6 µm).

Colletotrichum bambusicola C.L. Hou & Q.T. Wang, Mycologia 113: 452. 2021. Fig. 6.

Description: *Colonies* on PDA 52–56 mm diam in 7 d, flat with undulate edge, white to pale grey, aerial mycelium dense, reverse pale grey with mouse grey to black halo, white at the edge. Sexual morph developed on SNA. *Ascomata* ovoid to obpyriform, medium to dark brown, 180–195 × 95–110 µm, glabrous, ostiolate, neck pale brown, outer layer composed of angular cells, medium brown, 8–18.5 µm diam. *Asci* cylindrical to obclavate, hyaline, 58–72 × 7–10 µm, 8-spored. *Ascospores* uni- to bi-seriate, hyaline, smooth-walled, aseptate, allantoid with rounded ends, rarely straight or very slightly curved, 14–19 × 4–6 µm (av. ± SD = 16 ± 1.1 × 5 ± 0.5 µm), L/W ratio=3.2.

On SNA, *conidiomata* acervular, scattered, semi-immersed, conidiophores and setae formed on a cushion of roundish, hyaline to pale brown cells. *Setae* pale to dark brown, smooth-walled, straight or flexuous, 3–4-septate, 60–74 µm long, basal cell cylindrical, 4–4.5 µm diam, tip more or less acute. *Conidiophores* hyaline to pale brown, smooth-walled, septate, branched. *Conidiogenous cells* hyaline, smooth-walled, cylindrical, occasionally ampulliform, 21–33 × 2.5–3 µm. *Conidia* hyaline, aseptate, smooth-walled, cylindrical, straight, occasionally slightly curved, both ends rounded, or one end rounded and one end ± acute, 12–15.5 × 3.5–6 µm (av. ± SD = 14.0 ± 1.0 × 4.3 ± 0.7 µm), L/W ratio = 3.2. *Appressoria* single or gregarious, olivaceous, irregular outline with crenate or lobed margin, or clavate, 8.5–17.5 × 5–12 µm (av. ± SD = 12.3 ± 2.3 × 8.2 ± 1.7 µm).

Typus: **China**, Guangxi Zhuang Autonomous region, on seeds of *Phyllostachys edulis*, Sep. 2016, C.L. Hou & Q.T. Wang (**holotype** CAF80001, ex-type culture CFCC 54250 = ACCC 39709 = CNUCC 307307).

Additional materials examined: **China**, Fujian, Fuzhou, Wuyi Mountain, on *Petasites hybridus*, Aug. 2016, Z.Y. Ma, WYS14, living culture LC8469 (= M0288); *ibid*. living cultures LC8468 (= M0287); Fujian, Fuzhou, Wuyi Mountain, on *P. hybridus*, Aug. 2016, Z.Y. Ma, WYS40, living culture LC8498 (= M0322); Fujian, Fuzhou, Wuyi Mountain, on *Patrinia villosa*, Aug. 2016, Z.Y. Ma, WYS66, living culture LC8533 (= M0362).

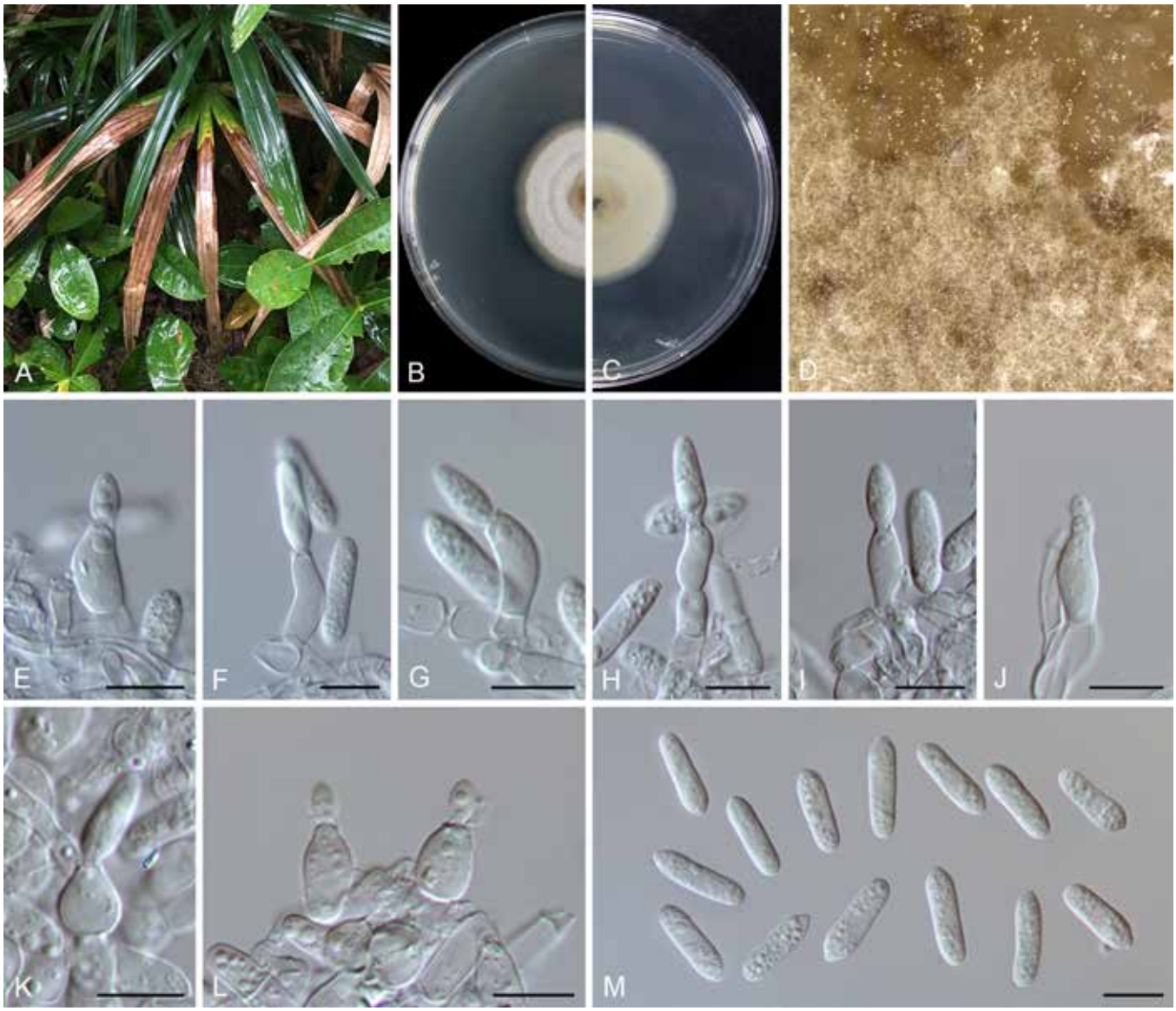

Fig. 5. *Colletotrichum arecacearum* (ex-type culture LC13850). **A.** Disease symptom on the host plant. **B, C.** Front and reverse colony on PDA (7 d). **D.** Colony surface on OA (7 d), with immersed, olivaceous conidiomata. **E–L.** Conidiogenous cells and conidia. **M.** Conidia. Scale bars = 10 µm.

Notes: Here, we describe the sexual morph of *C. bambusicola*, which was lacking in the original description based on collections from bamboo in Wang *et al.* (2021). This fungus was treated in a broader sense although two subclades were recognised. However, after broader sampling for the phylogenetic analysis and detailed morphological comparisons, we concluded that a new species should be proposed to distinguish the two clades (Fig. 1). *Colletotrichum bambusicola* differs in 3 bp in *act*, 2 bp in *gapdh*, 24 in *his3*, 1 bp in ITS, 11 bp in *tub2* from *C. parabambusicola sp. nov*. Morphologically, *C. bambusicola* differs from *C. parabambusicola sp. nov.* in that it produces longer asci (58–72 × 7–10 µm *vs.* 47–55 × 6.5–7.5 µm) and ascospores (14–19 × 4–6 µm *vs.* 10–14.5 × 3–5.5 µm), and a larger conidium L/W ratio (3.2 *vs.* 2.6).

Colletotrichum bicoloratum F. Liu, W.P. Wu & L. Cai, ***sp. nov.*** MycoBank MB 841371. Fig. 7.

Etymology: Named to reflect the bicoloured conidiogenous cells.
Description: *Colonies* on PDA 52 mm diam in 7 d, flat with entire edge, white, aerial mycelium dense, reverse greyish sepia to fuscous black. On MEA, *setae* rarely observed, dark brown, smooth-walled, straight, 3–4-septate, up to 51 µm long, basal cell cylindrical, 3.5 µm diam, tip acute. *Conidiophores* formed directly on hyphae, usually reduced into conidiogenous cells. *Conidiogenous cells* hyaline or dark brown, smooth-walled, ampulliform, 6–10.5 × 4–6 µm (av. ± SD = 8.8 ± 1.4 × 4.8 ± 0.6 µm). *Conidia* hyaline, aseptate, smooth-walled, curved, tapering towards apex and base, base usually obtuse and broader than the apex, 12–16 × 3–4 µm (av. ± SD = 14 ± 0.9 × 3.6 ± 0.3 µm), L/W ratio = 3.9. *Appressoria* single, medium to dark brown, usually ellipsoidal to subcircular, or irregularly shaped, rarely 2-celled, 5–9 × 4–6.5 µm.

Typus: **China**, Guangdong Province, Guangzhou, Yuexiu Park, on dead leaves of *Ophiopogon japonicus*, 29 Dec. 2012, W.P. Wu (**holotype** HMAS 350648, ex-type culture CGMCC 3.20510 = LC13882 = NN055229).

Notes: *Colletotrichum bicoloratum* is phylogenetically closely related to *C. guizhouensis*, *C. lilii* and *C. spaethianum* in the *C. spaethianum* species complex, but differs from *C. guizhouensis* and *C. lilii* in producing shorter and wider conidiogenous cells (6–10.5 × 4–6 µm *vs.* 12–25 × 2–2.5 µm in *C. guizhouensis*, 7–20 × 2–3.5 µm in *C. lilii*) and smaller appressoria (5–9× 4–6.5 µm *vs.* 6–14.5 × 5–11 µm in *C. guizhouensis*, 7.5–28.5 × 4.5–14 µm in *C. lilii*), and differs from *C. spaethianum* in producing wider conidiogenous cells (6–10.5 × 4–6 µm *vs.* 6–16 × 3–4 µm) and shorter conidia

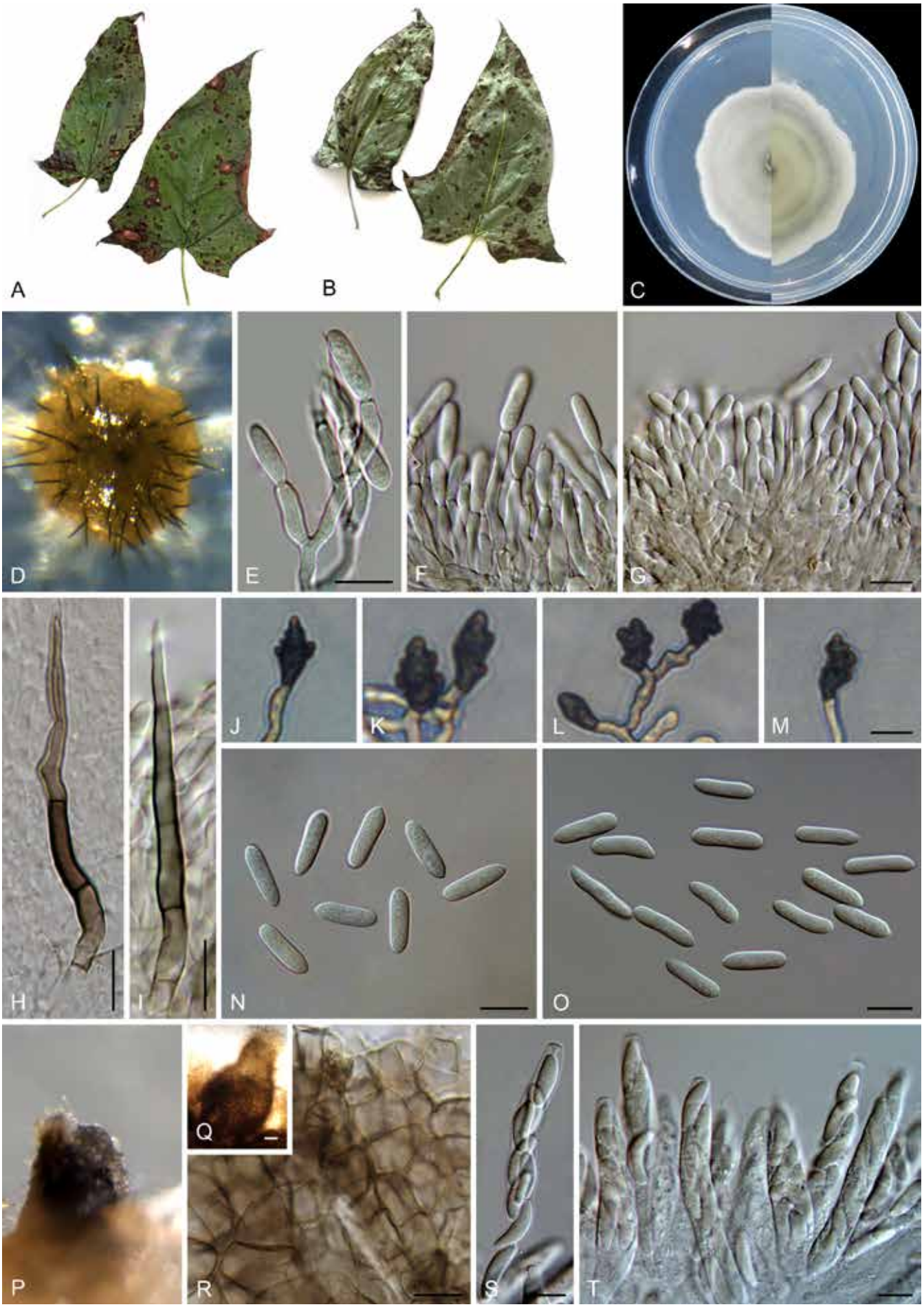

Fig. 6. *Colletotrichum bambusicola* (C–E, H, J–N from LC8469, F–G, I, O from LC8468, P–T from LC8533). **A, B.** Disease symptoms on the host plants. **C.** Front and reverse colony on PDA (7 d). **D.** Acervulus. **E–G**. Conidiophores, conidiogenous cells and conidia. **H, I.** Setae. **J–M.** Appressoria. **N, O.** Conidia. **P, Q.** Ascomata. **R.** Ascomata wall. **S, T.** Asci and ascospores. Scale bars =10 µm. Scale bar of M applies to J–M.

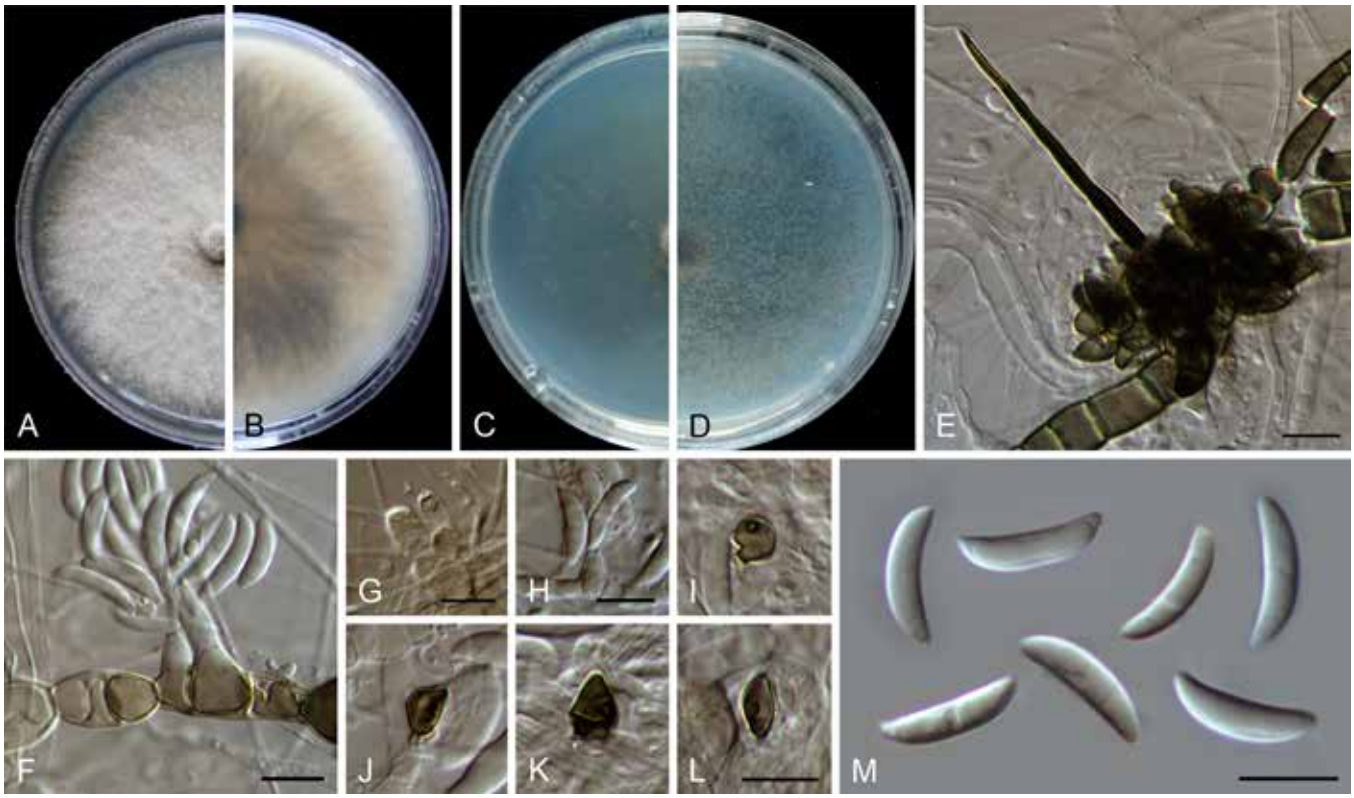

Fig. 7. *Colletotrichum bicoloratum* (ex-type culture NN055229). **A, B.** Front and reverse colony on PDA (7 d). **C, D.** Front and reverse colony on SNA (7 d). **E.** Seta and conidiophores. **F–H.** Conidiogenous cells and conidia. **I–L.** Appressoria. **M.** Conidia. Scale bars = 10 µm.

(12–16 × 3–4 µm *vs.* 13.5–29 × 3–4.5 µm) (Damm *et al.* 2009). *Colletotrichum bicoloratum* can be identified to species level by analysing any of the locus used in the current study.

Like most species in the *C. spaethianum* species complex, the associated host of *C. bicoloratum*, *Ophiopogon japonicus*, is also a petaloid monocotyledon plant. To the best of our knowledge, this is the first report of a *Colletotrichum* species associated with this plant host in China (Farr & Rossman 2021).

Colletotrichum bromeliacearum F. Liu & L. Cai, ***sp. nov.*** MycoBank MB 841372. Fig. 8.

Etymology: Named after the host plant family, *Bromeliaceae*.

Description: *Colonies* on PDA 40–47 mm diam in 7 d, flat with undulate edge, cinnamon in the centre, white towards the margin, aerial mycelia sparse, reverse brown vinaceous, dark brick, white towards margin. On PDA, *conidiomata* acervular, gregarious, pale luteous. *Setae* olivaceous grey to olivaceous black, smooth-walled, 2–3-septate, 21–73 µm long, basal cell cylindrical or cylindric-conical, 3–5 µm diam, tip more or less acute. *Conidiophores* formed from a cushion of roundish and pale brown cells, solitary or branched, septate, hyaline to pale brown. *Conidiogenous cells* hyaline or pale brown, smooth-walled, cylindrical, ovoid, 9–20 × 3.5–7 µm. *Conidia* hyaline, aseptate, smooth-walled, cylindrical with both ends round, 8.5–16 × 5–7.5 µm (av. ± SD = 12 ± 1.8 × 6.2 ± 0.7 µm), L/W ratio =1.9. *Appressoria* single, mostly globose to subglobose, rarely subcylindrical or irregular outline, with undulate edge, 5–8(–15) × 4.5–8 µm (av. ± SD = 6.7 ± 0.9 × 6 ± 0.9 µm).

Typus: **China**, Yunnan, on a bromeliad plant (*Bromeliaceae*), 2010, F. Liu (**holotype** HMAS 350626, ex-type culture CGMCC 3.20527 = LC0951).

Additional materials examined: **China**, Yunnan, on a bromeliad plant (*Bromeliaceae*), 2010, F. Liu, living cultures LC13854, LC13855, LC13856.

Notes: Four strains of *C. bromeliacearum* formed a distinct clade in the *C. boninense* species complex (Fig. 1). This species is distinct from other species in this genus at each locus sequenced in the current study. Hitherto, five *Colletotrichum* species were known from *Bromeliaceae*, *i.e. C. ananas*, *C. brevisporum*, *C. truncatum*, *C. gloeosporioides*, and *C. setosum* (Farr & Rossman 2021). *Colletotrichum bromeliacearum* is easily distinguished from *C. brevisporum*, *C. truncatum*, and *C. gloeosporioides* based on molecular and morphological characters (different species complexes), and from *C. ananas* [*Nom. inval.*, Art. 39.1 (Shenzhen)] and *C. setosum* in producing different shapes of conidia (cylindrical and straight *vs.* curved) (Garud 1968), as well as shorter and wider conidia (8.5–16 × 5–7.5 µm *vs.* 15–17 × 4–5 µm) (Patterson 1900), respectively.

Colletotrichum buxi F. Liu, W.P. Wu & L. Cai, ***sp. nov.*** MycoBank MB 841373. Fig. 9.

Etymology: Named after the host plant genus, *Buxus*.

Description: *Colonies* on PDA growing very slowly, reaching 8–11 mm diam after 7 d, flat with undulate edge, saffron to orange, conidial masses abundant, orange, aerial mycelium sparse, reverse salmon. *Conidiomata* not developed, abundant conidial masses (Fig. 9 E) formed on the surface of PDA, covered by aerial mycelium, orange, confluent. *Conidiophores* formed directly on hyphae, hyaline, septate, branched, 32–74 µm in length. *Conidiogenous cells* hyaline, smooth-walled, cylindrical to subcylindrical, variable in size, 9.5–26 × 2–4.5 µm (av. ± SD =18.6 ± 4.1 × 3.4 ± 0.7 µm). *Conidia* hyaline, mostly aseptate, sometimes

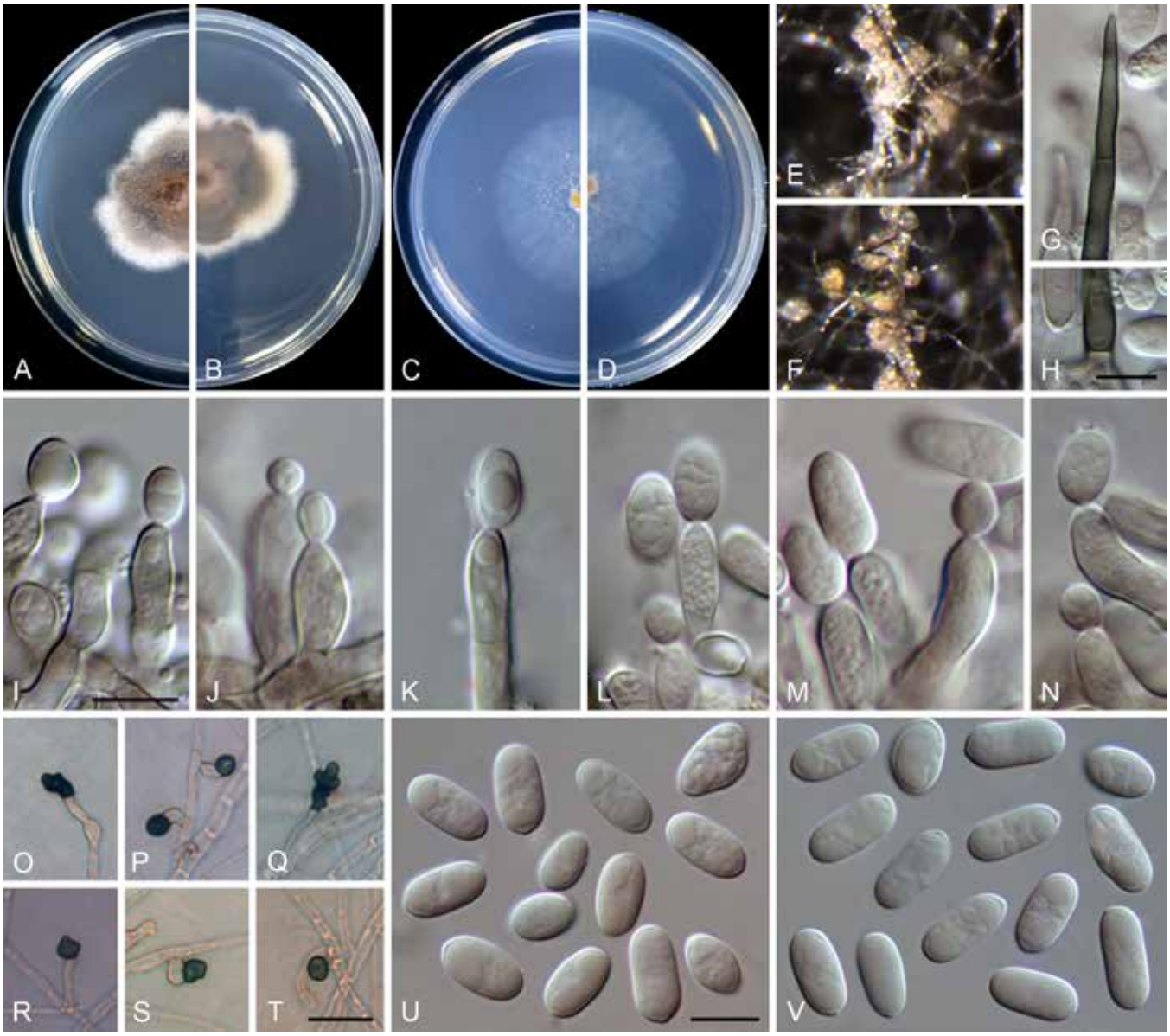

Fig. 8. *Colletotrichum bromeliacearum* (ex-type culture LC0951). **A, B.** Front and reverse colony on PDA (9 d). **C, D.** Front and reverse colony on SNA (9 d). **E, F.** Conidiomata on PDA. **G.** Tip of a seta. **H.** Base of a seta. **I–N.** Conidiogenous cells and conidia. **O–T.** Appressoria. **U, V.** Conidia. Scale bars: H, I, U = 10 µm; T = 20 µm. Scale bar of I applies to I–N; T applies to O–T; U applies to U, V.

1-septate and germinating with thin and flexuous germ tubes developing from the middle or apex of the conidia (Fig. 9 F, J), smooth-walled, cylindrical, both ends round, or one end obtuse and another end round, 9.5–14.5 × 4–6 µm (av. ± SD =12.2 ± 1.2 × 5.1 ± 0.4 µm), L/W ratio =2.4. *Appressoria* mostly clavate, sometimes subcylindrical or with an irregular outline and with a crenate or lobed margin, 5–12 × 3.5–6 µm (av. ± SD = 7.5 ± 1.8 × 4.4 ± 0.7 µm). *Setae* not observed.

Typus: **China**, Yunnan Province, Kunming, Kunming Botanical Garden, on healthy leaves of *Buxus* sp., 10 May 2002, W.P. Wu (**holotype** HMAS 350642, ex-type culture CGMCC 3.20511 = LC13873 = NN047139).

Additional material examined: **China**, Yunnan Province, Kunming, Kunming Botanical Garden, on *Buxus sinica* var. *parvifolia*, 20 Dec. 1993, W.P. Wu, living culture LC14551 (= NN004149).

Notes: *Colletotrichum buxi* resides within the *C. dracaenophilum* species complex in the multi-locus phylogenetic tree (Fig. 1). It shares low sequence similarity with the phylogenetically related species *C. yunnanense* at *act* (93.8 %), *chs-1* (98.8 %), *gapdh* (89.5 %), *his3* (94.9 %), *tub2* (97.3 %), and ITS (97.4 %), and differs in producing longer conidiophores (32–74 µm *vs.* 10–30 µm) and conidiogenous cells (9.5–26 µm *vs.* 6–12 µm), and shorter conidia (9.5–14.5 µm *vs.* 14–21 µm) (Liu *et al.* 2007).

Colletotrichum chamaedoreae F. Liu, W.P. Wu & L. Cai, ***sp. nov.*** MycoBank MB 841374. Fig. 10.

Etymology: Named after the host plant genus, *Chamaedorea*.

Description: *Colonies* on PDA 42–48 mm diam in 7 d, orange in the centre due to the formation of abundant conidial masses, white at the margin, reverse orange in the centre and white towards the margin. *Vegetative hyphae* hyaline, smooth-walled, septate, branched, 2.5–4.5 µm diam. On PDA, *ascomata* globose, subglobose or with an irregular shape, solitary or gregarious, brown to black, sub-immersed or immersed, ostiolate, outer wall composed of pale brown to dark brown angular cells, 6.5–19.5 × 3.5–12 µm diam (av. ± SD = 12.8 ± 3.1 × 7.3 ± 2.2 µm). *Interascal tissue* composed of hyaline, thin-walled, septate paraphyses, 2.5–5.5 µm diam. *Asci* obclavate

or clavate, hyaline, 41–65 × 12–16 µm, 8-spored. *Ascospores* uniseriately or irregularly arranged, hyaline, smooth-walled, aseptate, fusoid or subcylindrical with gently tapering rounded ends, straight or slightly curved, 14.5–21.5 × 4.5–6.5 µm (av. ± SD = 17.7 ± 1.8 × 5.3 ± 0.5 µm), L/W ratio = 3.3.

Conidial masses amber to buff, protruded from the dark brown to black conidiomata. *Setae* medium brown to dark brown, smooth-walled, 1–7-septate, 36–95 µm long, basal cells cylindrical, sometimes inflated in the middle, 4–8 µm diam, the tip acute or rounded. *Conidiophores* 0–1-septate, usually reduced to conidiogenous cells. *Conidiogenous cells* hyaline, cylindrical to subcylindrical, smooth-walled, straight or slight curved, sometimes extending to form new conidiogenous loci, 11–27 × 3.5–9.5 µm. *Conidia* hyaline, aseptate, smooth-walled, guttulate, often with two big and a number of small guttules, cylindrical, the apex round, the base with a prominent truncate scar, straight, 13.5–19 × 4.5–6.5 µm (av. ± SD = 15.7 ± 1.4 × 5.6 ± 0.3 µm), L/W ratio = 2.8. *Appressoria* not observed.

Typus: **China**, Yunnan Province, Jinghong, Xishuangbanna Botanical Garden, on healthy leaves of *Chamaedorea erumpens*, 19 Mar. 2010, W.P. Wu (**holotype** HMAS 350639, ex-type culture CGMCC 3.20512 = LC13868 = NN052885).

Additional materials examined: **China**, Yunnan Province, Jinghong, Xishuangbanna Botanical Garden, on healthy leaves of *Chamaedorea erumpens*, 19 Mar. 2010, W.P. Wu, living cultures LC13867 (= NN052884), LC13869 (= NN052890), LC13870 (= NN052891).

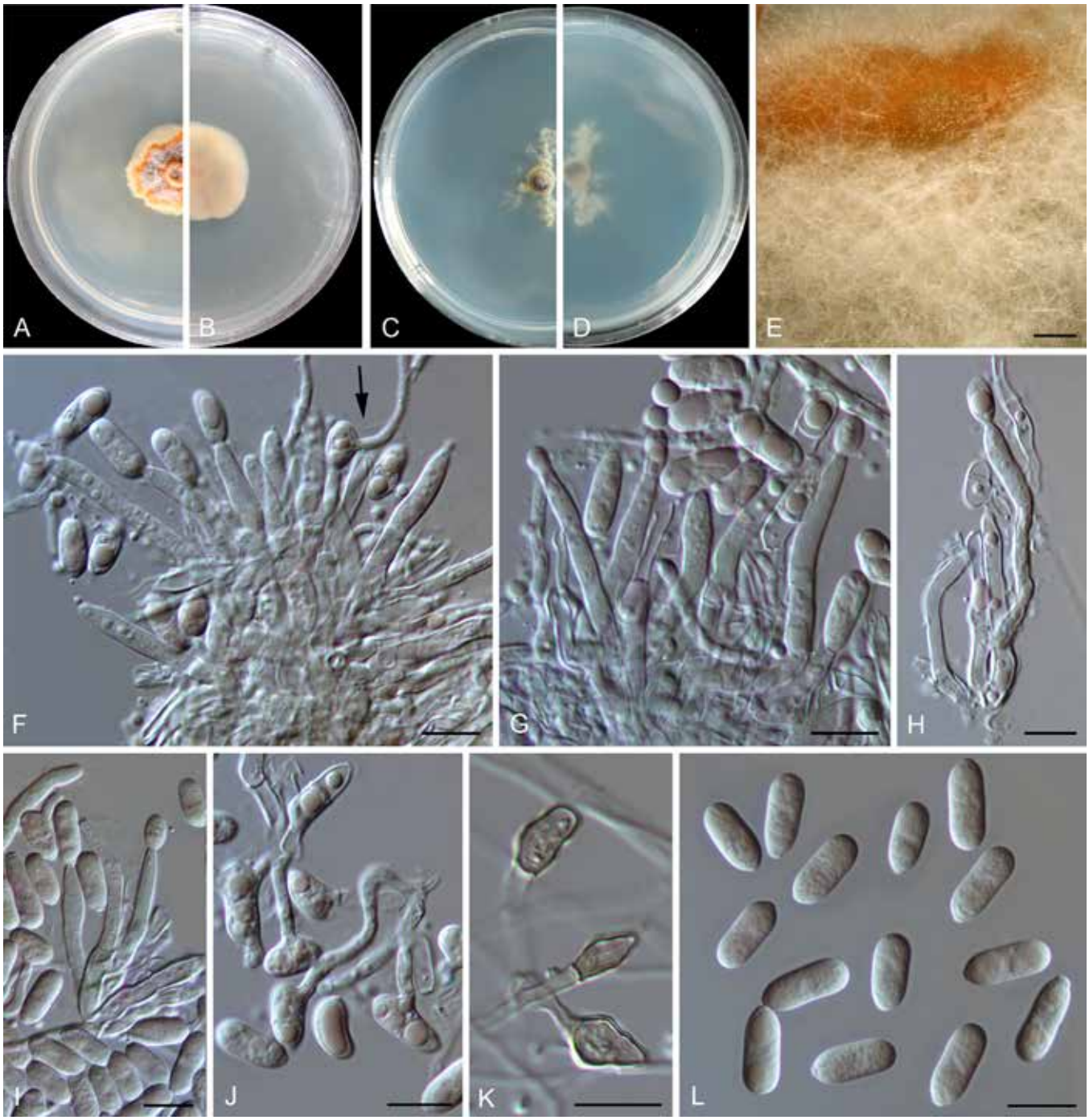

Fig. 9. *Colletotrichum buxi* (ex-type culture NN047139). **A, B.** Front and reverse colony on PDA (7 d). **C, D.** Front and reverse colony on SNA (7 d). **E.** Conidial masses on PDA. **F–I.** Conidiophores, conidiogenous cells and conidia (arrow in F points to a germinating conidium). **J.** Germinating conidia. **K.** Appressoria. **L.** Conidia. Scale bars: E = 300 µm; F–L = 10 µm.

Notes: *Colletotrichum chamaedoreae* belongs to the *C. boninense* species complex (Fig. 1). Conidiogenous cells that extend to form new conidiogenous loci have previously been observed in species of the *C. boninense* species complex, *e.g.* in *C. annellatum*, *C. constrictum*, *C. cymbidiicola*, *C. novae-zelandiae*, and *C. oncidii*. However, their conidia are shorter and the conidium L/W ratio

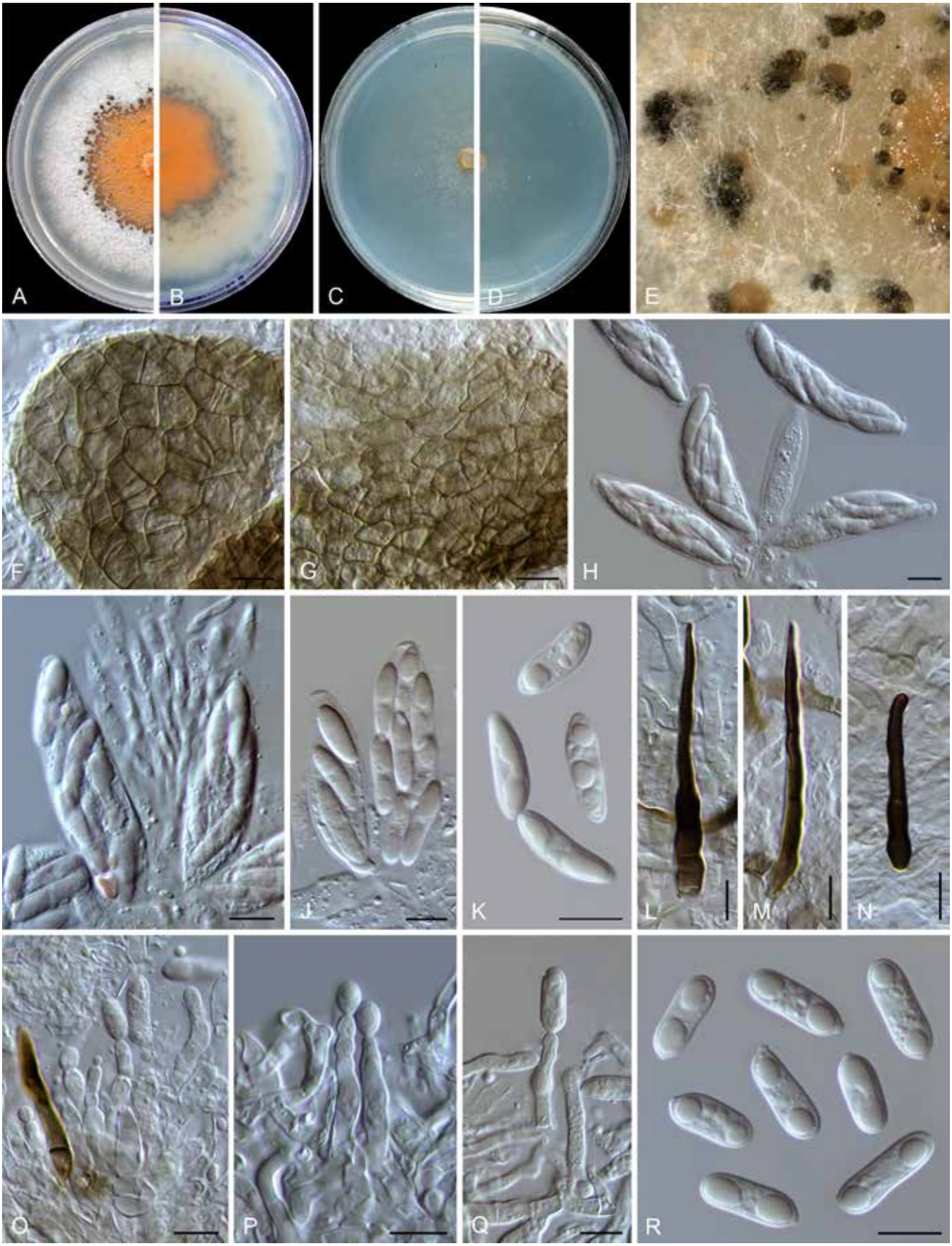

Fig. 10. *Colletotrichum chamaedoreae* (ex-type culture NN052885). **A, B.** Front and reverse colony on PDA (7 d). **C, D.** Front and reverse colony on SNA (7 d). **E.** Conidiomata and ascomata on SNA. **F, G.** Ascomata wall. **H–J.** Asci, ascospores and paraphyses. **K.** Ascospores. **L–N.** Seta. **O–Q.** Conidiophores, conidiogenous cells and conidia. **R.** Conidia. Scale bars = 10 µm.

is lower than those of *C. chamaedoreae* (Damm *et al.* 2012b). In addition, *C. chamaedoreae* is distinct from other species in this genus at each locus sequenced in the current study, and morphologically differs from the most closely related species *C. brassicicola* in that it produces shorter asci (41–65 × 12–16 µm *vs.* 65–105 × 12–13.5 µm), and longer and wider conidiogenous cells (11–27 × 3.5–9.5 µm *vs.* 7–14 × 4–5.5 µm) (Damm *et al.* 2012b).

Colletotrichum chiangraiense X.Y. Ma *et al.*, MycoKeys 43: 34. 2018.

Notes: *Colletotrichum chiangraiense* was shown to be a member of the *C. boninense* species complex in the original description (Ma *et al.* 2018), but resided within the *C. gigasporum* species complex in our multi-locus tree, forming an unusually long branch (Fig. 1). BLASTn search of the NCBI GenBank using ITS and *act* sequences of *C. chiangraiense* (ex-type MFLUCC 14-0119) yielded closest matches with species in the *C. gigasporum* species complex, while using *tub2* yielded closest matches with species in the *C. boninense* species complex. Therefore, it is very likely that the sequences provided in Ma *et al.* (2018) were misplaced or with sequencing errors. The taxonomic status of *C. chiangraiense* requires confirmation by re-examination and re-sequencing of the type.

Colletotrichum crousii F. Liu, Z.Y. Ma & L. Cai, ***sp. nov.*** MycoBank MB 841375. Fig. 11.

Etymology: Named in honour of the mycologist Pedro Crous, one of the major contributors to recent improvements in *Colletotrichum* systematics.

Description: *Colonies* on PDA 44–46 mm diam in 7 d, flat with undulate edge, rosy buff, covered by cottony and white aerial mycelium, reverse dark vinaceous buff, white towards margin. On PDA, *conidiomata* not observed, conidiophores formed directly from hyphae, conidial masses pale vinaceous buff, confluent. *Conidiophores* hyaline, solitary, sometimes branched at the base, up to 35 µm, usually reduced to conidiogenous cells. *Conidiogenous cells* hyaline, aseptate, smooth-walled, cylindrical to ampulliform, 9–22 × 4.5–6 µm. *Conidia* hyaline, aseptate, smooth-walled, cylindrical, both ends obtuse, or apex obtuse and bottom gradually narrowed with an prominent truncate scar, 12.5–18.5 × 6.5–8 µm (av. ± SD =16 ± 1.6 × 7 ± 1.6 µm), L/W ratio =2.2. *Appressoria* and *setae* not observed.

Typus: **China**, Guangxi, Chongzuo, Guangxi Nonggang National Nature Reserve, on leaf of *Rhaphidophora* sp., Jun. 2017, Z.Y. Ma & L.W. Hou, NG56 (**holotype** HMAS 350636, ex-type culture CGMCC 3.20513 = LC13858 = MH0588).

Additional materials examined: **China**, Guangxi, Chongzuo, Guangxi Nonggang National Nature Reserve, on leaf of *Rhaphidophora* sp., Jun. 2017, Z.Y. Ma & L.W. Hou, NG56 (Fig. 11A, B), living cultures LC13859 (= MH0589), LC13860 (= MH0592), LC13861 (= MH0727); on leaf of *Rhaphidophora* sp., Jun. 2017, Z.Y. Ma & L.W. Hou, NG58 (Fig. 11C, D), living culture LC13862 (= MH0759).

Notes: *Colletotrichum crousii* is phylogenetically related to *C. excelsum-altitudinum*, *C. tongrenense*, and *C. tropicicola* in the *C. dracaenophilum* species complex, but differs in that it produces wider conidia (6.5–8 µm *vs.* 5–7 µm in *C. excelsum-altitudinum* and *C. tongrenense*, 4.5–5.5 µm in *C. tropicicola*) with a lower L/W ratio (2.2 *vs.* generally 2.4–3.3) (Tao *et al.* 2013, Damm *et al.* 2019, Zhou *et al.* 2019), and larger conidiogenous cells (9–22 × 4.5–6 µm *vs.* 2–11 × 1–2 µm in *C. tongrenense*) (Zhou *et al.* 2019). Moreover, *C. crousii* is distinct from other species in this genus at each locus sequenced in the current study.

Colletotrichum danxiashanense F. Liu, W.P. Wu & L. Cai, ***sp. nov.*** MycoBank MB 841376. Fig. 12.

Etymology: Named after the location where the fungus was collected, Danxia Mountain.

Description: *Colonies* on PDA 52 mm diam in 7 d, flat with rhizoids edge, surface covered by floccose white, aerial mycelium, reverse pale luteous to brown. *Vegetative hyphae* hyaline or pale brown, smooth-walled, septate, branched. On SNA, *conidiomata* not developed, conidiophores formed directly on hyphae, terminally or laterally. *Setae* not observed. *Conidiophores* reduced to conidiogenous cells. *Conidiogenous cells* hyaline, rarely pale brown, smooth-walled, ampulliform to cylindrical, 6–12 × 2.5–5.5 µm, periclinal thickening not observed. *Conidia* hyaline, aseptate, smooth-walled, guttulate, falcate with ± acute or obtuse ends, 18.5–29.5 × 3–4.5 (av. ± SD ± 24.4 ± 3.1 × 3.8 ± 0.4), L/W ratio = 6.4. *Appressoria* single, medium brown to dark brown, subcircular, subcylindrical, or irregularly shaped, 6–10 × 6–7 µm (av. ± SD = 8.3 ± 1.4 × 6.4 ± 0.4 µm).

Typus: **China**, Guangdong Province, Shaoguan, Danxia Mountain, on dead leaves of probable *Miscanthus* sp., 25 Dec. 2012, W.P. Wu (**holotype** HMAS 350650, ex-type culture CGMCC 3.20514 = LC13885 = NN055218).

Notes: *Colletotrichum danxiashanense* belongs to the *C. graminicola* species complex and forms a sister clade to *C. miscanthi* (Fig. 3). Both species are morphologically similar and associated with the same host genus, *Miscanthus*, but with clearly different *act* (98.3 % identity, with 4 bp differences), *chs-1* (99.6 % identity, with 1 bp difference), ITS (98.9 % identity, with 5 bp differences), *sod2* (90.5 % identity, with 35 bp differences), and *tub2* (97.9 % identity, with 10 bp differences) sequences.

Colletotrichum diversisporum F. Liu, W.P. Wu & L. Cai, ***sp. nov.*** MycoBank MB 841377. Fig. 13.

Etymology: Refers to the diverse shapes of conidia.

Description: *Colonies* on PDA 49 mm diam in 7 d, flat with entire edge, smoke to mouse grey in the centre, white towards the margin, aerial mycelium more or less sparse, reverse smoke grey. *Vegetative hyphae* hyaline, smooth-walled, septate, branched. On PDA, *conidiomata* not developed, conidiophores formed directly on hyphae. *Conidiophores* hyaline or very pale brown, septate, branched. *Conidiogenous cells* hyaline, smooth-walled, cylindrical, 14–33 × 2.5–3.5 µm. *Conidia* hyaline, aseptate, smooth-walled, guttulate, variable in shape and size, cylindrical, ellipsoidal or ovoid, sometimes constricted in the centre or near the base, 9.5–16.5 × 3.5–8 µm (av. ± SD ± 11.5 ± 1.5 × 5.2 ± 1.1 µm), L/W ratio = 2.2. Sometimes conidia becoming 1-septate and germinating after 10 d, germ tubes flexuous and thinner than hyphae (Fig. 13 G). *Appressoria* and *setae* not observed.

Typus: **China**, Guangdong Province, Guangzhou, South China Botanical Garden, on dead leaves of *Dracaena angustifolia*, 28 Feb. 2016, W.P. Wu (**holotype** HMAS 350655, ex-type culture CGMCC 3.20515 = LC13890 = NN072578).

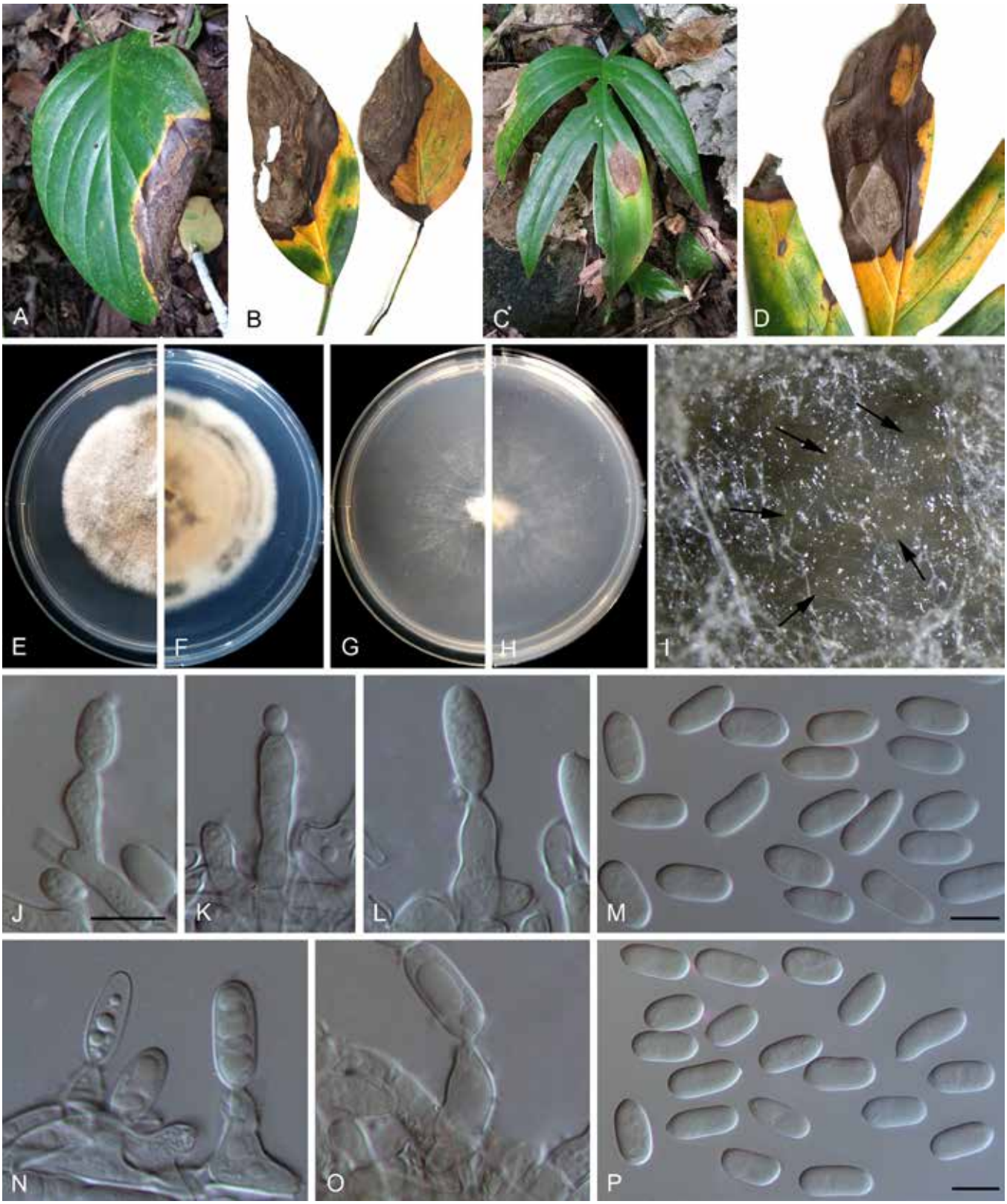

Fig. 11. *Colletotrichum crousii* (ex-type culture LC13858). **A–D.** Disease symptoms on *Rhaphidophora* spp. **E, F.** Front and reverse colony on PDA (7 d). **G, H.** Front and reverse colony on SNA (7 d). **I.** Conidioma on SNA. **J–L, N, O.** Conidiophores, conidiogenous cells and conidia. **M, P.** Conidia. Scale bars = 10 µm. Scale bar of J applies to J–L, N, O.

Notes: *Colletotrichum diversisporum* is basal to the *C. magnum* and *C. orchidearum* species complexes (Fig. 1). It is characterised by a production of conidia of variable shapes and sizes, and can be easily differentiated from other species by analysing any of the loci sequenced in the current study.

Colletotrichum diversum F. Liu & L. Cai, ***sp. nov.*** MycoBank MB 841378. Fig. 14.

Etymology: Named to reflect the formation of two different types of conidiophores.

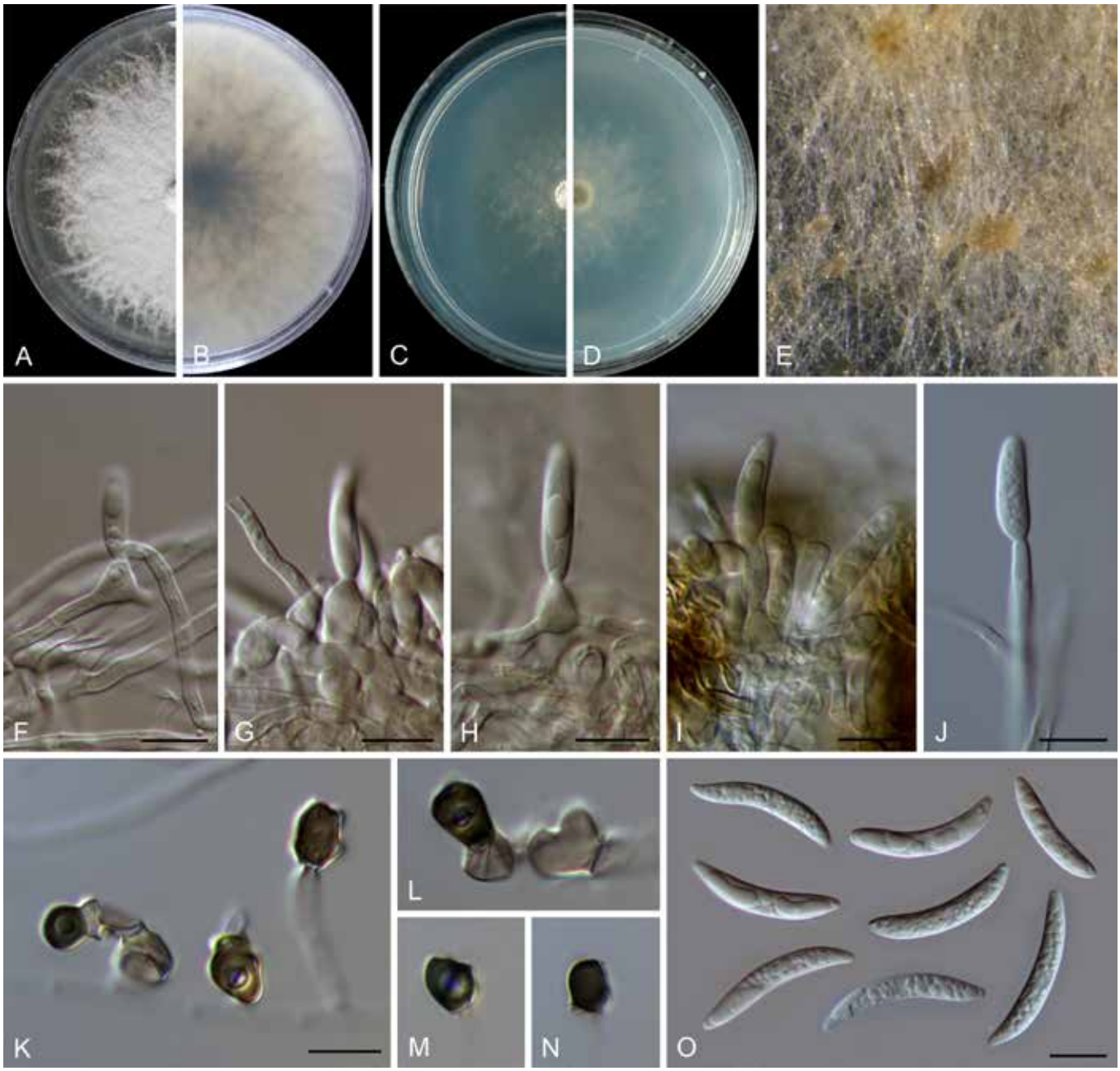

Fig. 12. *Colletotrichum danxiashanense* (ex-type culture NN055218). **A, B.** Front and reverse colony on PDA (7 d). **C, D.** Front and reverse colony on SNA (7 d). **E.** Conidial masses on PDA. **F–J.** Conidiogenous cells and conidia. **K–N.** Appressoria. **O.** Conidia. Scale bars = 10 µm. Scale bar of K applies to K–N.

Description: *Colonies* on PDA 36–39 mm diam in 7 d, flat with undulate edge, pale glaucous grey, aerial mycelium sparse, surface partly covered with orange conidial masses, reverse white. *Vegetative hyphae* hyaline, smooth-walled, septate, branched. On SNA, *conidiomata* acervular, scattered or gregarious, conidiophores formed on a cushion of subglobose pale brown cells (type I, Fig. 14 D–F) or directly from vegetative hyphae (type II, Fig. 14 H–L). The first type of *conidiophores* hyaline, branched, up to 45 µm, sometimes reduced to conidiogenous cells; *conidiogenous cells* hyaline, ampulliform to obclavate, sometimes cylindrical, often extending to form new conidiogenous loci, 11.5–17.5(–22.5) × 3–5.5 µm (av. ± SD = 14.6 ± 2.4 × 4.3 ± 0.6 µm), periclinal thickening distinct. The second type of *conidiophores* hyaline, septate, branched, up to 80 µm; *conidiogenous cells* hyaline, smooth-walled, cylindrical or subcylindrical, sometimes irregularly inflated, variable in length, (7–)12–32 × 3–4.5 µm (av. ± SD = 20.9 ± 6.2 × 3.7 ± 0.6 µm), usually extending to form new conidiogenous loci, periclinal thickening distinct. *Conidia* hyaline, aseptate, smooth-walled, guttulate, straight, cylindrical with one end round and one end slightly acute, 12–15.5 × 4.5–5.5 µm (av. ± SD = 14.1 ± 0.8 × 5.2 ± 0.3), L/W ratio = 2.7. *Appressoria* and *setae* not observed.

Typus: **China**, Yunnan Province, Honghe Hani and Yi Autonomous Prefecture, Mengzi county, Nanhu park, on *Philodendron selloum*, 12 May 2016, Q. Chen (**holotype** HMAS 350633, ex-type culture CGMCC 3.20516 = LC11292 = CQ775).

Notes: *Colletotrichum diversum* is basal to the phylogenetic clade that comprises *C. boninense*, *C. cymbidiicola*, *C. doitungense C. oncidii*, *C. torulosum* and *C. watphraense* in the *C. boninense* species complex (Fig. 1), and shares low sequence similarity with the most closely related species *C. oncidii* at *act* (97.9 %) and *gapdh* (96.9 %) and 99 % similarities at *his3*, ITS and *tub2*. Morphologically, the two species differ with respect to the formation of conidiophores and conidiogenous cells. On SNA, *C. diversum* forms conidiophores either on a cushion of subglobose pale

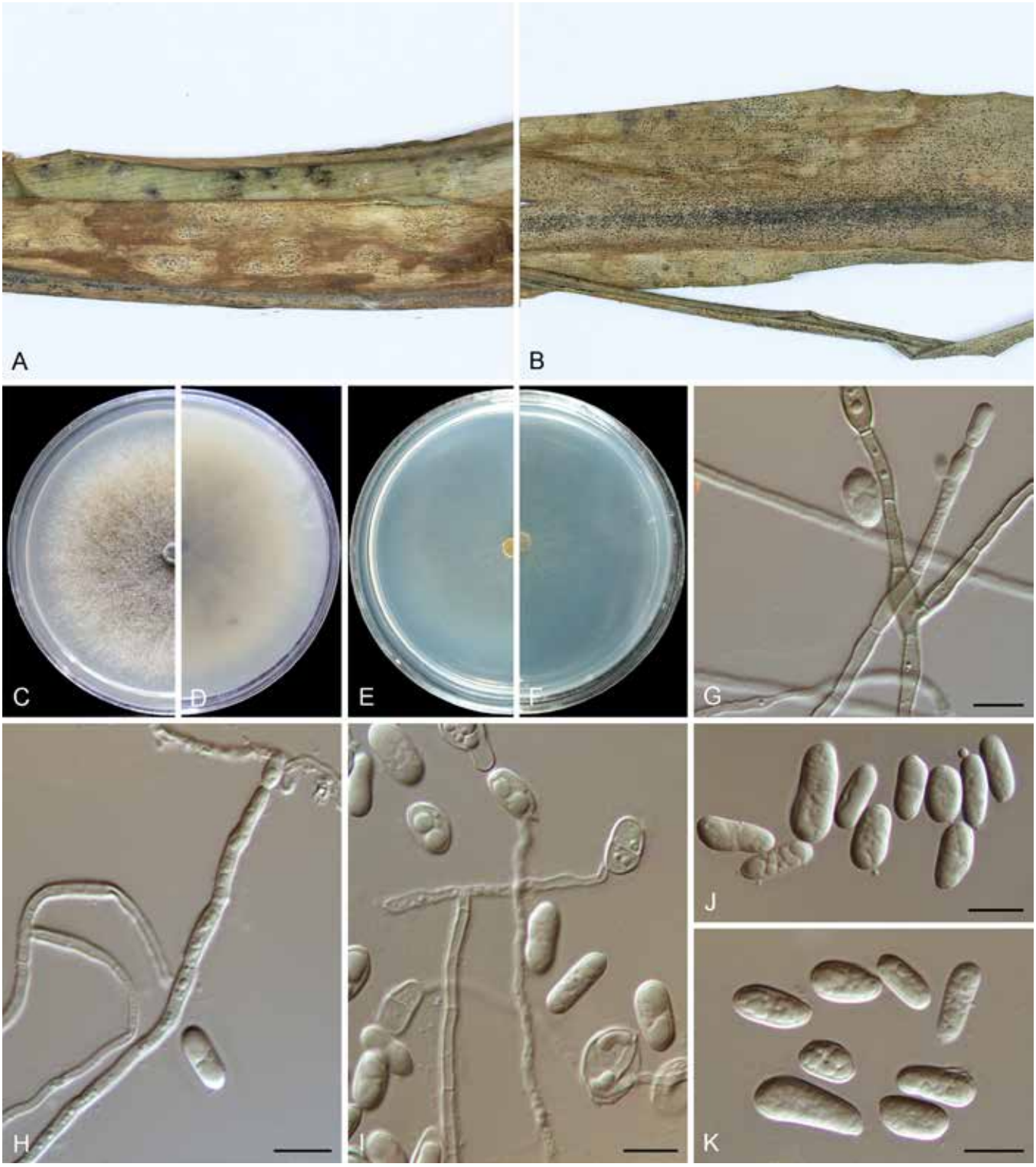

Fig. 13. *Colletotrichum diversisporum* (ex-type culture NN072578). **A, B.** Disease symptoms on host plant. **C, D.** Front and reverse colony on PDA (7 d). **E, F.** Front and reverse colony on SNA (7 d). **G, H.** Conidiophores, conidiogenous cells and conidia. **I.** Germinating conidia. **J, K.** Conidia. Scale bars = 10 µm.

brown cells or directly from vegetative hyphae, while *C. oncidii* only forms conidiophores directly from hyphae. In addition, *C. diversum* produces ampulliform to obclavate or (sub-)cylindrical conidiogenous cells, while only cylindrical cells have been observed for *C. oncidii* (Damm *et al.* 2012b).

To date, *Colletotrichum* species known to be associated with *Philodendron selloum* are *C. orchidearum* (Hou *et al.* 2016, Damm *et al.* 2019), and *C. philodendri* which lacks type-derived sequence data (Alfieri *et al.* 1984). Furthermore, *C. diversum* morphologically differs from *C. philodendri* with respect to the shape (cylindrical with obtuse ends *vs.* round at one end and acute at the other end) and width (4.5–5.5 µm *vs.* 3.5–4 µm) of the conidia. Geographically, *C. philodendri* was reported in the Americas (Brazil and the US) (Hennings 1905, Alfieri *et al.* 1984), while, to date, *C. diversum* is only known in China.

Colletotrichum dolichoconidiophori F. Liu, W.P. Wu & L. Cai, ***sp. nov.*** MycoBank MB 841379. Fig. 15.

Etymology: Named to reflect the formation of long conidiophores.
Description: *Colonies* on PDA 40–41 mm diam in 7 d, flat with fimbriate edge, pale grey in the centre, white toward the margin, aerial mycelium floccose, reverse fuscous black, white at margin.

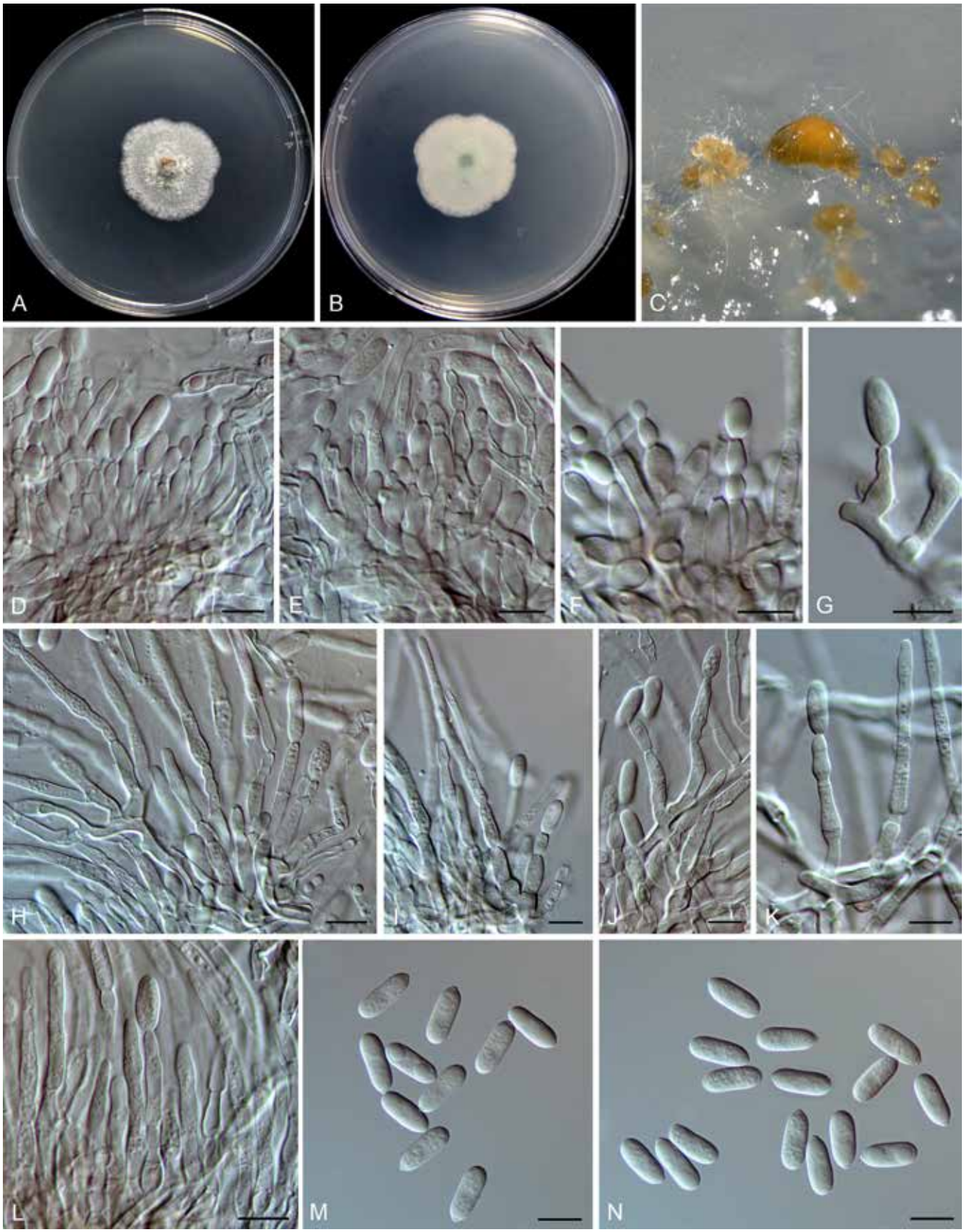

Fig. 14. *Colletotrichum diversum* (ex-type culture LC11292). **A, B.** Front and reverse colony on PDA (6 d). **C.** Conidiomata and conidial masses. **D–G.** Type I of conidiophores and conidia. **H–L.** Type II of conidiophores and conidia. **M, N.** Conidia. Scale bars = 10 µm.

Vegetative hyphae hyaline to pale brown, smooth-walled, septate, branched. *Conidiomata* not developed. On PDA, *conidiophores* formed directly on hyphae, hyaline to very pale brown, smooth-walled, cylindrical, up to 250 µm. *Conidiogenous cells* cylindrical to subcylindrical, rarely ampulliform, hyaline, 6–23 × 2–4 µm. *Setae* abundant, brown, smooth- and thick-walled, 0–3-septate, 41–110 µm long, basal cell cylindrical, inflated, flask shaped or globose, 3.5–8 µm diam, tip ± acute. *Conidia* hyaline, aseptate, smooth-

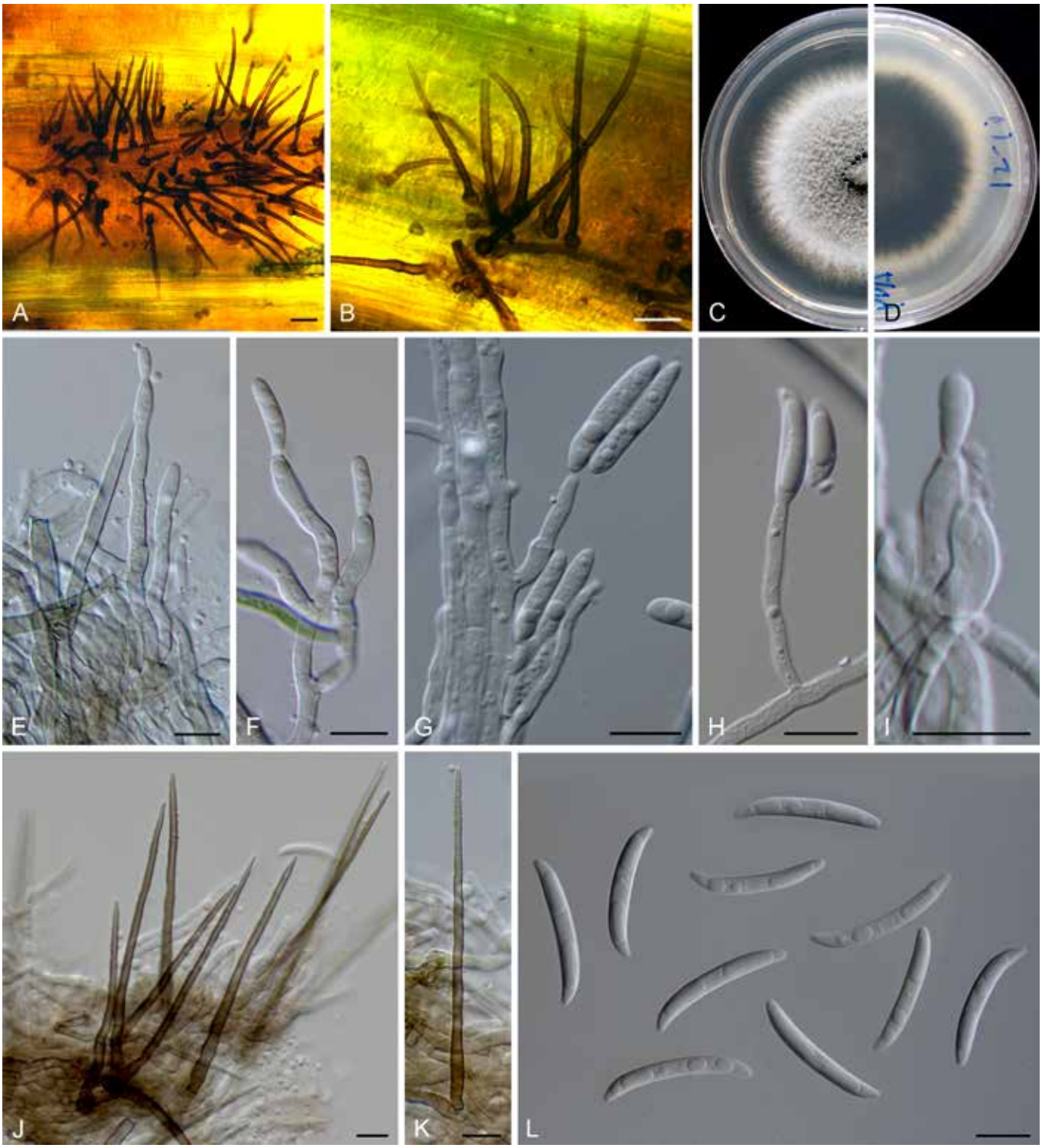

Fig. 15. *Colletotrichum dolichoconidiophori* (ex-type culture NN054966). **A, B.** Conidiomata with setae on the host plant. **C, D.** Front and reverse colony on PDA (7 d). **E–I.** Conidiophores, conidiogenous cells and conidia. **J, K.** Setae. **L.** Conidia. Scale bars: A, B = 20 µm; E–L = 10 µm.

walled, falcate, central part of the conidium almost straight with parallel walls, gradually tapering towards a slightly rounded to ± acute apex and a truncate base, with a similar radian, 19–27.5 × 2.5–3.5 µm (av. ± SD ± 24.9 ± 1.92 × 3.1 ± 0.29 µm), L/W ratio = 8. *Appressoria* not observed.

Typus: **China**, Beijing, Huairou, Beigoucun, on an unidentified grass, 10 Sep. 2012, W.P. Wu (**holotype** HMAS 350654, ex-type culture CGMCC 3.20517 = LC13889 = NN054966).

Notes: *Colletotrichum dolichoconidiophori* belongs to the *C. graminicola* species complex (Fig. 1). It shares very low sequence similarity with all currently accepted species in the genus, even with the most closely related species *C. cereale* CBS 129663 (Figs 1, 3, *act*: 90.7 %; *chs-1*: 96 %; ITS: 96.7 %; *sod2*: 91.8 %; *tub2*: 92.2 %). Morphologically, *C. dolichoconidiophori* differs from *C. cereale* in that it produces longer conidiogenous cells (6–23 × 2–4 µm *vs.* 2–6 × 1–2 µm).

Colletotrichum guangxiense C.L. Hou & Q.T. Wang, Mycologia 113: 454. 2021.

Notes: Intraspecific branches in the *C. guangxiense* clade suggest a high degree of genetic variation in this species, mainly within the *act* and *tub2* sequences examined in the current study.

Colletotrichum iris F. Liu & L. Cai, ***sp. nov.*** MycoBank MB 841383. Fig. 16.

Etymology: Named after the host plant genus, *Iris*.

Description: *Colonies* on PDA 33–34 mm diam in 7 d, flat, aerial mycelium dense, white, reverse pale luteous, centre part fuscous black, and with a fuscous black halo towards margin. On PDA, *conidiomata* scattered or confluent, dark brown to black, immersed. *Setae* not observed. *Conidiophores* hyaline to pale brown, branched, septate, up to 65 µm. *Conidiogenous cells* hyaline or pale brown, smooth-walled, cylindrical, occasionally ampulliform, straight or flexuous, 12.5–22.5 × 3–4.5 µm. *Conidia* hyaline, aseptate, smooth-walled, curved, apex ± acute, base usually broader and truncate, 18–28 × 2–4 µm (av. ± SD = 22 ± 2.6 × 3.4 ± 0.5 µm), L/W ratio = 6.5. *Appressoria* single or in small groups, medium brown, mostly irregular shaped, occasionally ellipsoidal to subcircular, 5–16 × 3–10 µm (av. ± SD = 9.6 ± 2.6 × 6.7 ± 1.8 µm).

Typus: **China**, Jiangxi, Lushan Botanical Garden, on *Iris japonica*, 4 Sep. 2013, N. Zhou (**holotype** HMAS 350628, ex-type culture CGMCC 3.20518 = LC3697).

Notes: *Colletotrichum iris* is closely related to *C. liriopes* in the *C. spaethianum* species complex (Fig. 1), but differs genetically in 2 bp of the *act* nucleotide sequence, 1 bp of *chs-1*, 13 bp of *gapdh*, 12 bp of *his3*, 1 bp of ITS and 3 bp of *tub2*. Morphologically, *C. iris* differs from *C. liriopes* in that it produces thick-walled, pale brown conidiogenous cells and a higher conidium L/W ratio (6.5 *vs*.5.0) (Damm *et al.* 2009). Like most other species in the *C. spaethianum* complex (Damm *et al.* 2009), *C. iris* was isolated from the petaloid monocotyledon plant, *Iris japonica*. Six other *Iris*-associated species in the genus are *C. circinans*, *C.*

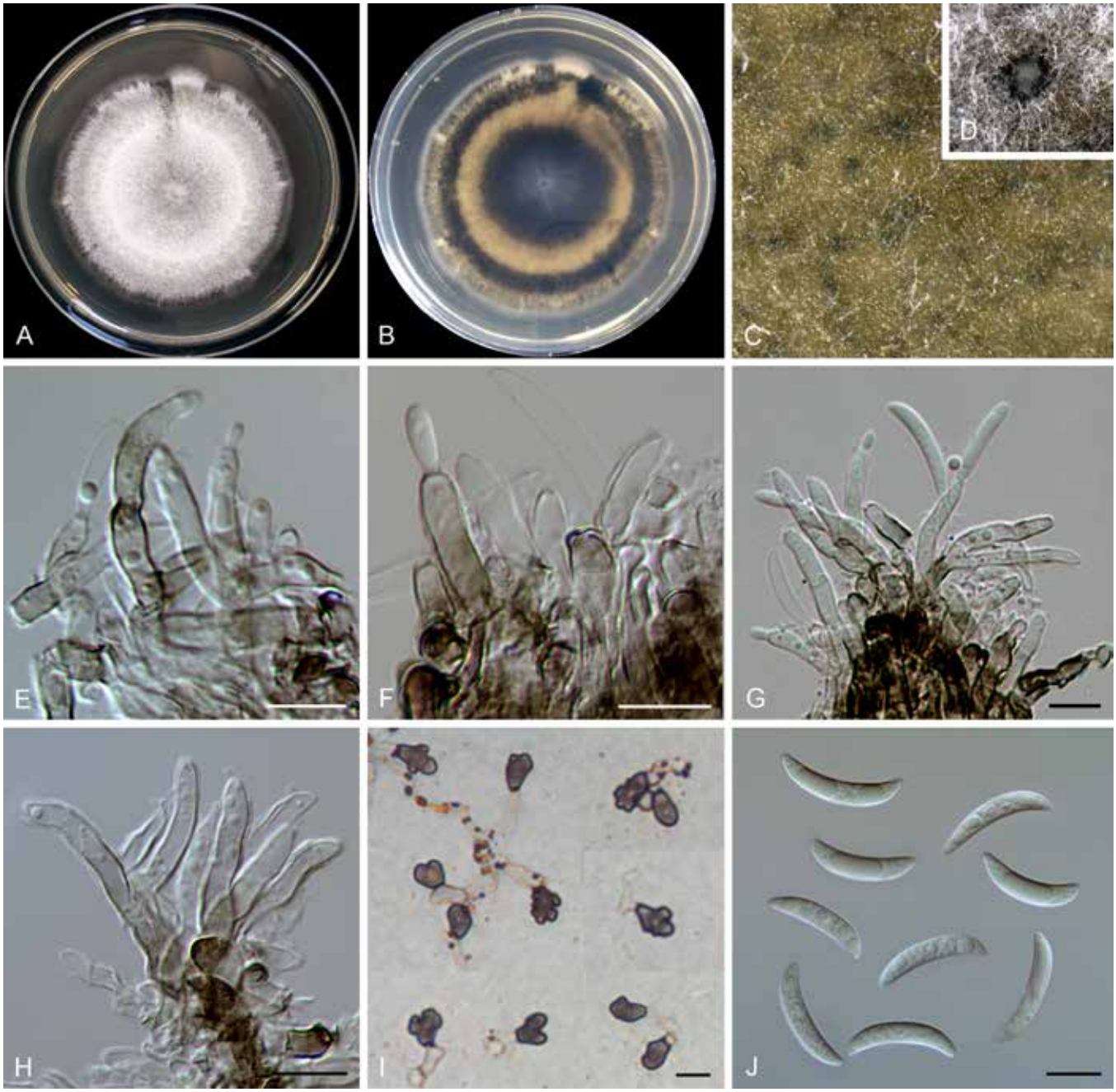

Fig. 16. *Colletotrichum iris* (ex-type culture LC3697). **A, B.** Front and reverse colony on PDA (7 d). **C, D.** Immersed conidiomata. **E–H.** Conidiophores, conidiogenous cells and conidia. **I.** Appressoria. **J.** Conidia. Scale bars = 10 µm.

coccodes, *C. dematium*, *C. gloeosporioides*, *C. siamense*, and *C. tofieldiae* (Farr & Rossman 2021), which are phylogenetically distinct from *C. iris*. Moreover, *C. iris* morphologically differs from another *Iris*-associated species *C. liliacearum* (DNA sequences are unavailable) in producing longer conidia (18–28 × 2–4 µm µm *vs.*12–17 × 2.5–3.5) (Ferraris 1902).

Colletotrichum jasminigenum Wikee *et al.*, Fungal Diversity 46: 174. 2011.

Notes: *Colletotrichum jasminigenum* was shown to be a member of the *C. truncatum* species complex (Hyde *et al.* 2014). However, BLASTn search of the NCBI GenBank using *gapdh* and *act* sequences of *C. jasminigenum* (ex-holotype MFLUCC 10-0273) yielded the closest matches with species of the *C. gloeosporioides* species complex, while using ITS and *tub2* sequences indicated that it belongs to the *C. truncatum* species complex. Therefore, it is likely that the sequences of MFLUCC 10-0273 provided in Wikee *et al.* (2011) were mixed up with those of other species or contained major sequencing errors. To clarify the taxonomic status of *C. jasminigenum*, type specimen and culture inquiries were submitted to the culture collections (CGMCC and MFLUCC) mentioned in the original publication (Wikee *et al.* 2011). Unfortunately, the ex-type could not be located in CGMCC. We suspected that it might not have been preserved in the culture collection, as the strain number was not mentioned in Wikee *et al.* (2011). Furthermore, specimen delivery from MFLUCC was not allowed because of the current quarantine measures for international mail. Therefore, the taxonomic status of *C. jasminigenum* requires further examination and re-sequencing of the type.

Colletotrichum jinshuiense M. Fu & G.P. Wang, Persoonia 42: 21. 2018.
Synonym: *Colletotrichum kakiivorum* H.Y. Jung & S.Y. Lee [as *'kakivorum'*], Mycol. Prog. 17: 1118. 2018.

Typus: **China**, Hubei Province, Wuhan, on leaves of *Pyrus pyrifolia* cv. Jinshui, 1 Aug. 2016, M. Fu (**holotype** HMAS 247824, ex-type culture CGMCC 3.18903).

Additional material examined: **China**, Fujian Province, Fuzhou, Wuyi Mountain, on *Dioscorea zingiberensis*, Aug. 2016, L. Cai & Z.Y. Ma, living culture LC8509 (= M0333).

Notes: The ex-type strains of *C. jinshuiense* (Fu *et al.* 2019, published online 24 Jul. 2018) and *C. kakiivorum* (Lee & Jung 2018, published online: 30 Jul. 2018) cluster together in a well-supported clade within the *C. dematium* species complex (Fig. 1), and their *act*, *chs-1*, *gapdh*, *his3*, ITS, and *tub2* sequences share high similarity (99.8 %), with only two base-pair differences. Morphologically, *C. jinshuiense* and *C. kakiivorum* produce conidiogenous cells, conidia, and appressoria with essentially similar shapes and dimensions. Hence, *C. kakiivorum* is synonymised with the previously published *C. jinshuiense*.

Colletotrichum liriopes Damm *et al.*, Fungal Diversity 39: 71. 2009. Fig. 17.

Typus: **Mexico**, APHIS interception Houston 057263, on *Liriope muscari*, 29 Nov. 2000, M.J. Segall (**holotype** CBS H-20364, ex-type culture CBS 119444).

Additional materials examined: **China**, Shan'xi, Xi An, Huaqing Hot Spring, on dead leaves of *Osmanthus fragrans*, 1 Jul. 2015, W.P. Wu, living culture NN071073; Tibet, Bomi county, Suotong village, on *Poaceae*, 13 Jun. 2015, F. Liu, living culture LC7623; Yunnan Province, Honghe Hani and Yi Autonomous Prefecture, Mengzi county, DaTun Sea, on *Liriope spicata*, 12 May 2016, Q. Chen, living culture LC11287.

Notes: *Colletotrichum liriopes* is phylogenetically related to *C. iris* in the *C. spaethianum* species complex. This species is pathogenic to *Eria coronaria* (Yang *et al.* 2011), *Liriope muscari* (Damm *et al.* 2009), *L. spicata* (this study), and *Rohdea japonica* (Kwon & Kim 2013), endophytic in *Bletilla ochracea* and *Peione bulbocodioides* (Yang *et al.* 2011), and saprophytic on dead stalk of *Hemerocallis fulva* (Yang *et al.* 2011) and dead leaves of *Osmanthus fragrans* (this study).

Colletotrichum magnum (Jenkins & Winstead) Rossman & W.C. Allen, IMA Fungus 7: 4. 2016.
Basionym: *Glomerella magna* Jenkins & Winstead, Phytopathology 54: 453. 1964.
Synonym: *Colletotrichum liaoningense* Y.Z. Diao, *et al.*, Persoonia 38: 34. 2017.

Typus: **USA**, on *Citrullus lanatus*, unknown collection date, R. Rodriguez, ex-epitype culture CBS 519.97.

Additional material examined: **China**, Liaoning Province, Xingcheng city, on chili fruits (*Capsicum annuum* var. *conoides*), Oct. 2012, Y.Z. Diao, ex-type culture of *C. liaoningense* CGMCC 3.17616 (= CAUOS2 = LC6228).

Notes: Since the sequence data and phylogenetic assessment of *C. liaoningense* are questionable (Damm *et al.* 2019), we re-sequenced six loci of its ex-type culture CAUOS2, twice, in the present study. Comparison with sequences deposited in the NCBI GenBank by Diao *et al.* (2017) revealed that the sequences of four loci were consistent except for 1–3 base-pair differences [99 % sequence similarity shared at *cal* (433/435), *chs-1* (294/297), *gapdh* (257/258), and *tub2* (679/680)]; however, the sequences of ITS and *act* differed at many positions [96 % similarity on ITS (478/500) and *act* (252/263)]. Therefore, the original sequences of CAUOS2 are incorrect, and the sequences newly generated in the current study have been deposited in GenBank (Table S1) and used for six-locus phylogenetic analyses (Fig. 1).

Colletotrichum liaoningense is phylogenetically indistinguishable from *C. magnum* (Fig. 1), and their *act*, *chs-1*, *his3*, ITS, and *tub2* sequences are 100 % identical, while the *gapdh* sequences are 96 % (250/260) identical. Consequently, *C. liaoningense* is synonymised with the older name *C. magnum*.

Colletotrichum metake Sacc., Annls Mycol. 6: 557. 1908.

Notes: *Colletotrichum metake* was originally described on a dead culm of bamboo (*Arundinaria japoniea*) in Italy (Costa, Vittorio, Treviso) and characterised by oblong conidia (22 × 5.5–6 µm) (Saccardo 1908), but without type designation. In the current study, four bamboo-associated strains of *C. metake* (Sato *et al.* 2012, Wang *et al.* 2021) clustered in a well-supported clade (Fig. 1). Three of these strains were from *Pleioblastus simonii* in Japan and one from *Chimonobambusa quadrangularis* in China. However, none of these strains is suitable for type designation because of the inconsistency with the original collection site and host of the species (Hyde & Zhang 2008).

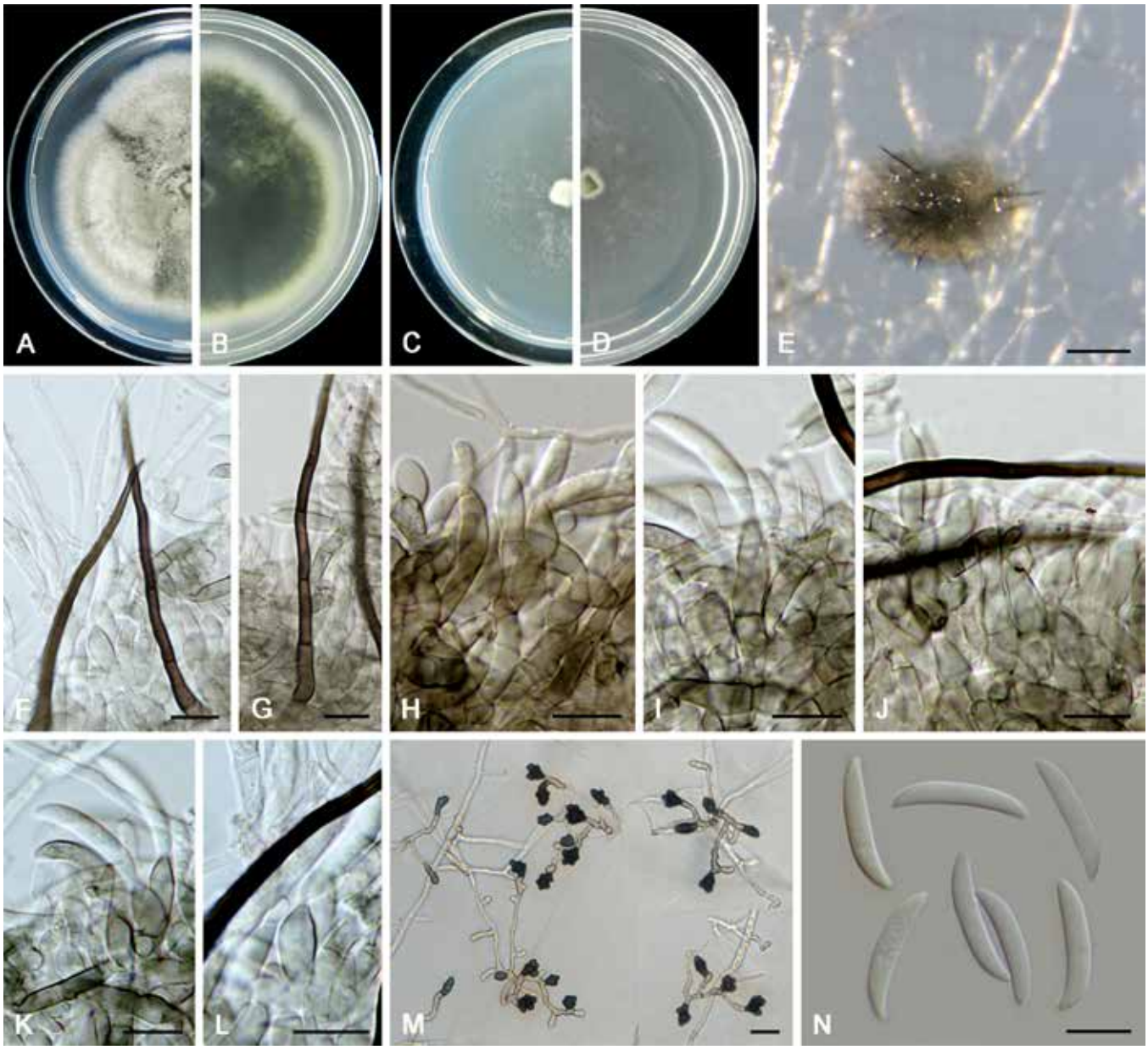

Fig. 17. *Colletotrichum liriopes* (LC11287). **A, B.** Front and reverse colony on PDA (7 d). **C, D.** Front and reverse colony on SNA (7 d). **E.** Conidioma. **F, G.** Setae. **H–L.** Conidiophores, conidiogenous cells and conidia. **M.** Appressoria. **N.** Conidia. Scale bars: E = 80 µm; F–N = 10 µm.

Colletotrichum monsterae F. Liu, W.P. Wu & L. Cai, ***sp. nov.*** MycoBank MB 841384. Fig. 18.

Etymology: Named after the host plant genus, *Monstera.*

Description: *Colonies* on PDA 52 mm diam in 7 d, flat with entire edge, aerial mycelium white and floccose, reverse saffron. *Vegetative hyphae* hyaline to pale brown, smooth-walled, septate, branched. *Conidiomata* black, submerged, conidial masses buff, abundantly formed on the surface of the agar medium or directly on hyphyae. *Setae* not observed. *Conidiophores* brown, base dark brown, mostly gradually becoming paler towards the tip, 1–3-septate, solitary or branched at the bottom, 46–102 µm long. *Conidiogenous cells* pale to medium brown, smooth-walled, cylindrical, 15–51.5 × 3.5–6 µm (av. ± SD ± 33 ± 11.1 × 4.7 ± 0.8). *Conidia* hyaline, aseptate, smooth-walled, guttulate, cylindrical to subcylindrical, rarely obvoid, straight, sometimes slightly curved, with obtuse ends or gradually tapering towards the base, on SNA 13–22.5 × 4.5–6 µm (av. ± SD ± 18.2 ± 2.1 × 5 ± 0.4), L/W ratio = 3.6, on PDA 16.5–24.5 × 3.5–5 (av. ± SD ± 20.6 ± 1.9 × 4.4 ± 0.3), L/W ratio = 4.7. *Appressoria* single, medium to dark brown, mostly irregularly shaped, rarely cylindrical, with undulate to lobate margins, 8.5–19 × 4.5–11.5 µm.

Typus: **China**, Guangdong Province, Guangzhou, Zhaoqing, Seven Star Cave (Qixingyan), on diseased leaf of *Monstera deliciosa*, 24 Dec. 2012, W.P. Wu (**holotype** HMAS 350640, ex-type culture CGMCC 3.20519 = LC13871 = NN055214).

Notes: Although represented by a single strain, *C. monsterae* is phylogenetically distinct from all currently accepted species of *Colletotrichum* at each locus sequenced in the current study and is basal to other species in the *C. orchidearum* species complex (Fig. 1). Morphologically it is different from most species in the genus, including the closest related species, *C. piperis*, and the two other *Monstera deliciosa*-associated species, *C. gloeosporioides* (French 1989) and *C. orchidearum* (Damm *et al.* 2019), by producing long brown conidiophores reminiscent of setae.

Fig. 18. *Colletotrichum monsterae* (ex-type culture NN055214). **A, B.** Front and reverse colony on PDA (7 d). **C, D.** Front and reverse colony on SNA (7 d). **E.** Conidiomata (black, submerged) and conidial masses (buff, superficial). **F–I.** Conidiophores bearing conidia. **J–O.** Appressoria. **P.** Conidia formed on SNA. **Q.** Conidia formed on PDA. Scale bars = 10 µm.

Colletotrichum multiseptatum F. Liu, W.P. Wu & L. Cai, ***sp. nov.*** MycoBank MB 841385. Fig. 19.

Etymology: Named to reflect the multiple septa of its seta.

Description: *Colonies* on PDA 49 mm diam in 7 d, flat with entire edge, saffron to peach, aerial mycelium unconsolidated, reverse peach to umber. *Vegetative hyphae* hyaline to pale brown, smooth-walled, septate, branched. *Conidiomata* not developed, abundant conidial masses formed on the surface of medium, salmon, brown to black, solitary or gregarious. *Setae* medium brown to dark brown, smooth-walled, 50–62 µm long, 2–4-septate, base cylindrical, sometimes slightly inflated, 4.5–6 µm diam, tip ± acute or rounded. *Conidiophores* formed directly from hyphae, hyaline to pale brown, 1–3-septate, usually branched at the bottom and reduced to conidiogenous cells. *Conidiogenous cells* hyaline or pale brown, smooth-walled, ampulliform, bullet-shaped, or subcylindrical, variable in length, 8.5–21.5 × 3–5.5 µm (av. ± SD = 13.1 ± 3 × 4 ± 0.5 µm), collarette observed. *Conidia* hyaline, aseptate, smooth-walled, guttulate, curved, or slightly curved, gradually tapering towards the round apex and truncate base, sometimes less curved towards the base, on PDA 16.5–26 × 3–4.5 µm (av. ± SD = 19.8 ± 2.3 × 3.7 ± 0.3 µm), L/W ratio = 5.4, on SNA 20–25.5 × 3.5–4.5 µm (av. ± SD = 21.8 ± 1.5 × 3.9 ± 0.2 µm), L/W ratio = 5.6. Only one *appressorium* observed, irregular shaped, dark brown, 10 × 5.5 µm.

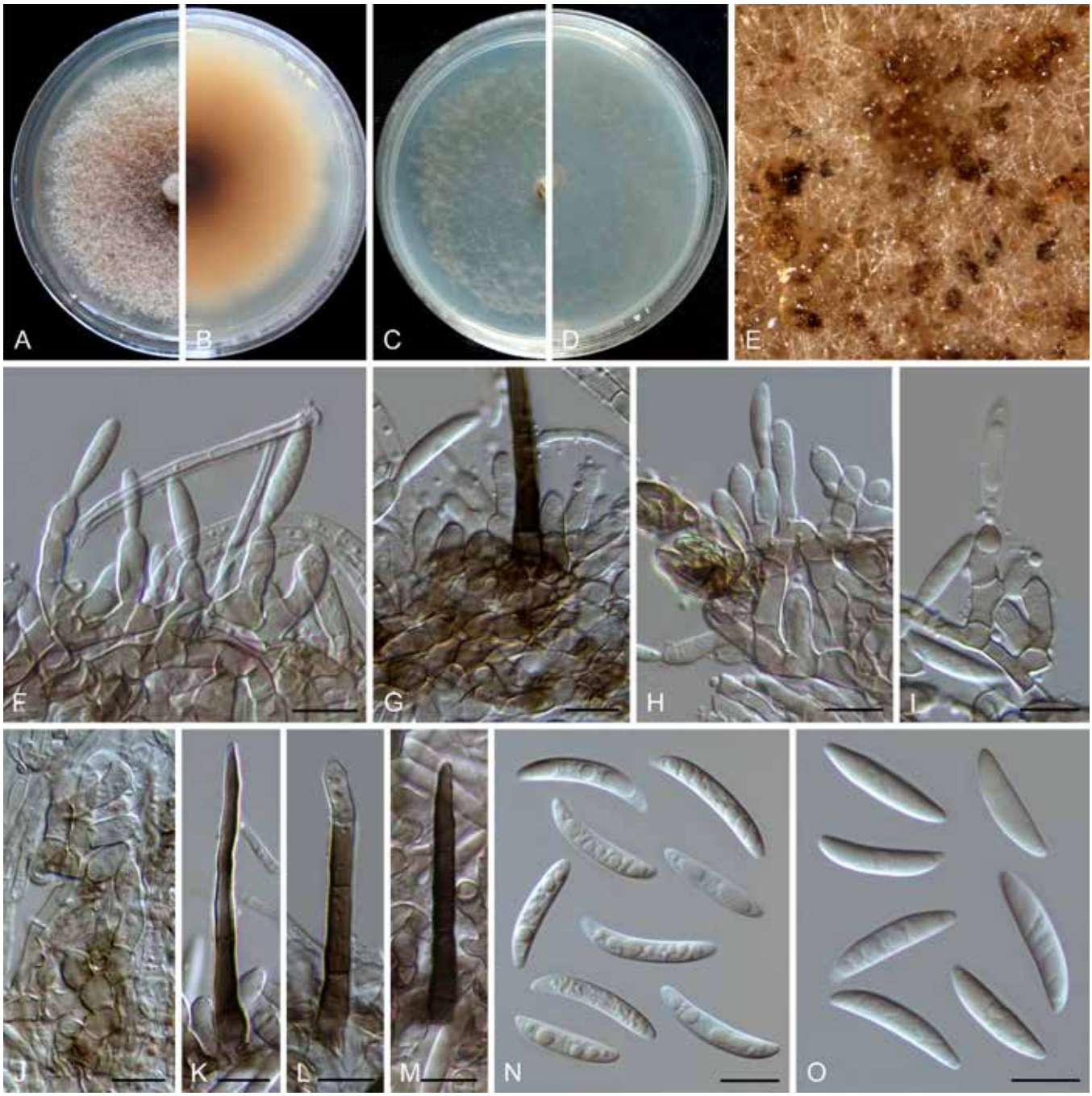

Fig. 19. *Colletotrichum multiseptatum* (ex-type culture NN055357). **A, B.** Front and reverse colony on PDA (7 d). **C, D.** Front and reverse colony on SNA (7 d). **E.** Conidial masses on PDA. **F–I.** Conidiophores, conidiogenous cells and conidia on PDA. **J.** Conidiogenous cells on SNA. **K–M.** Setae on PDA. **N.** Conidia on SNA. **O.** Conidia on PDA. Scale bars = 10 µm.

Typus: **China**, Guangdong Province, Shaoguan, Danxia Mountain, on dead culm of an unidentified grass, 25 Dec. 2012, W.P. Wu (**holotype** HMAS 350651, ex-type culture CGMCC 3.20520 = LC13886 = NN055357).

Notes: *Colletotrichum multiseptatum*, belonging to the *C. graminicola* species complex, is phylogenetically related to *C. echinochloae* (Fig. 3), but shares low sequence similarity at *sod2* (97 %) and even lower whole-genome sequence similarity (95 %) with that species. Morphologically, *C. multiseptatum* differs from *C. echinochloae* in that it produces shorter setae [50–62 µm *vs.*79.8–145.5(–186.3) µm] and exhibits a higher L/W ratio of the conidia (5.4–5.6 *vs.*3.5–5) (Moriwaki & Tsukiboshi 2009). Furthermore, the conidia of *C. echinochloae* are more curved and both ends are more acute than those of *C. multiseptatum.*

Colletotrichum nageiae F. Liu, W.P. Wu & L. Cai, ***sp. nov.*** MycoBank MB 841386. Fig. 20.

Etymology: Named after the host plant genus, *Nageia*.

Description: *Colonies* on PDA growing slowly, reaching 32 mm diam after 7 d, flat with entire edge, white, aerial mycelium sparse, reverse pale buff. On SNA, *vegetative hyphae* hyaline to brown, smooth-walled, septate, branched, 1.5–2 µm diam. *Conidiomata* dark brown to black, beneath the media. *Setae* pale brown to brown, straight to flexuous, smooth-walled, 2–3-septate, 57–62 µm long, basal cells cylindrical, 3.5–4.5 µm diam, the tip rounded. *Conidiophores* septate, branched, *conidiogenous cells* hyaline to pale brown, cylindrical, smooth-walled, straight, 10–20 × 2.5–4.5 µm. *Conidia* hyaline, aseptate, smooth-walled, cylindrical, straight,

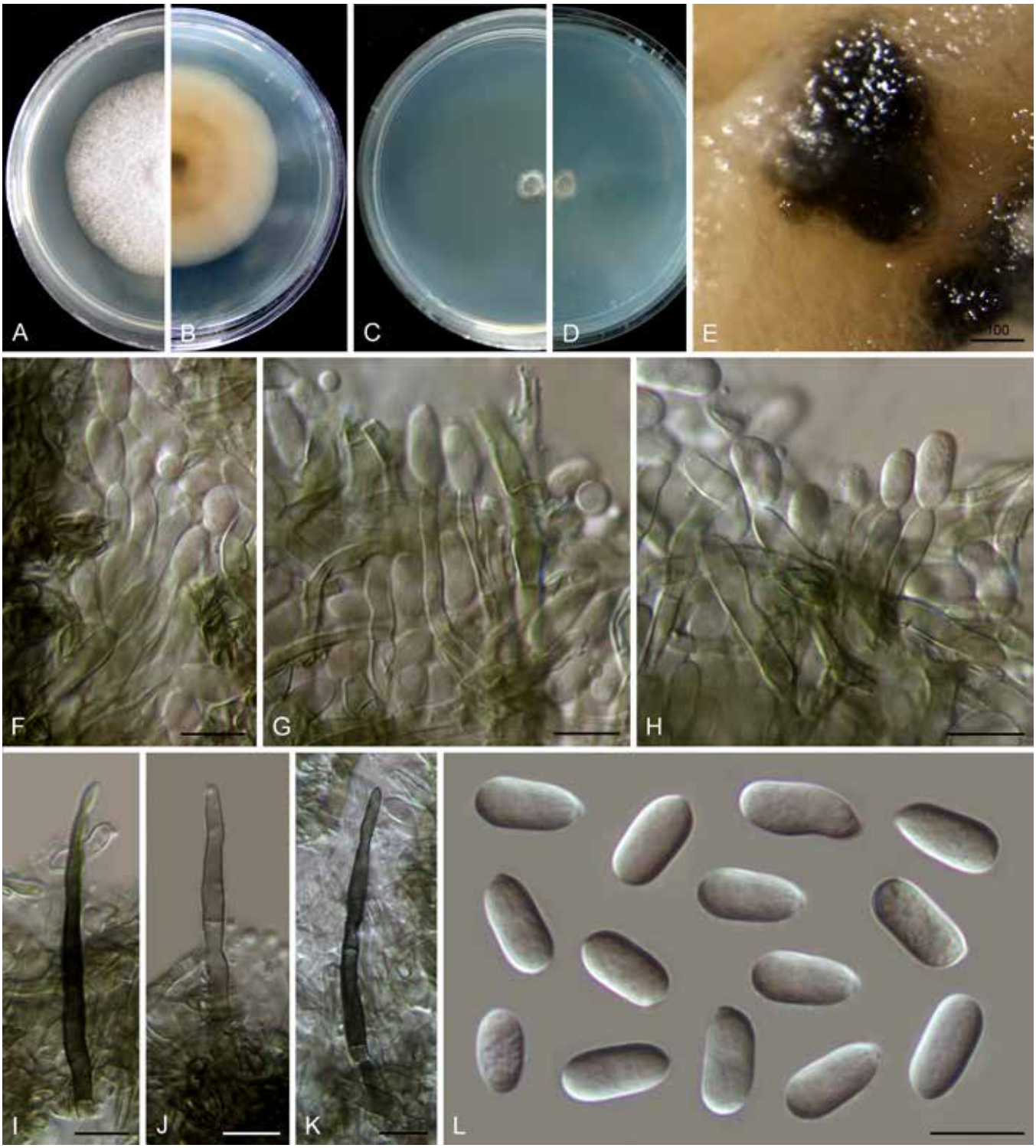

Fig. 20. *Colletotrichum nageiae* (ex-type culture NN004492). **A, B.** Front and reverse colony on PDA (7 d). **C, D.** Front and reverse colony on SNA (7 d). **E.** Conidioma. **F–H.** Conidiogenous cells and conidia. **I–K.** Setae. **L.** Conidia. Scale bars: E = 100 µm; F–L = 10 µm.

9–13.5 × 4.5–6 µm (av. ± SD = 11.5 ± 0.9 × 5.3 ± 0.4 µm), L/W ratio = 2.2, the apex obtuse, the bottom gradually narrowed with a prominent truncate scar. *Appressoria* not observed.

Typus: **China**, Yunnan Province, Kunming, Kunming Botanical Garden, on healthy leaves of *Nageia nagi*, 20 Dec. 1993, W.P. Wu (**holotype** HMAS 350638, ex-type culture CGMCC 3.20521 = LC13866 = NN004492).

Notes: Although the conidial morphology of *C. nageiae* resembles that of species in the *C. boninense* species complex, it is a singleton species that clusters basal to *C. gloeosporioides* species complex and is phylogenetically distinct from all currently accepted *Colletotrichum* species (Fig. 1). Furthermore, BLASTn search revealed very low sequence similarity with the sequences of other species deposited in the NCBI GenBank, based on the comparisons of *act* (up to 86 % identity shared with species in the *C. gloeosporioides* and *C. gigasporum* species complexes), *cal* (up to 80 % identity shared with species in the *C. gloeosporioides* and *C. gigasporum* species complexes), *chs-1* (up to 93 % identity shared with species in the *C. boninense* species complex), *gapdh* (up to 87 % identity shared with species in the *C. boninense* species complex), *gs* (up to 78 % identity shared with species in the *C. boninense* species complex), *his3* (up

to 91 % identity shared with species in the *C. gloeosporioides* and *C. gigasporum* species complexes), and *tub2* (up to 83 % identity shared with species in the *C. boninense* species complex).

Colletotrichum obovoides F. Liu & L. Cai, ***sp. nov.*** MycoBank MB 841387. Fig. 21.

Etymology: Named to reflect the obovoid shape of conidia.

Description: *Colonies* on PDA 28–33 mm diam in 7 d, flat with fimbriate edge, white, abundant pale luteous and confluent conidial masses formed on the surface of medium, reverse white, or buff because of the production of conidial masses. *Vegetative hyphae* hyaline, smooth-walled, septate, branched. On SNA, *conidiomata* acervular, superficial or semi-immersed, black, protruding with white or buff conidial masses. *Setae* not observed. *Conidiophores* hyaline, septate, branched, formed directly from hyphae or on a cushion of pale brown cells, up to 70 µm. *Conidiogenous cells* hyaline, smooth-walled, cylindrical, rarely ampulliform, 5–24 × 2.5–4 µm. *Conidia* hyaline, aseptate, smooth-walled, obovoid, sometimes clavate, 10.5–15.5 × 5.5–7.5 µm (av. ± SD ± 12.7 ± 1.1 × 6.5 ± 0.4), L/W ratio = 1.9. *Appressoria* solitary, brown to dark brown, aseptate, smooth-walled, subglobose, bullet-shaped, clavate, or navicular, 7.5–13 × 4.5–9.5 µm (av. ± SD = 10.2 ± 1.7 × 6.2 ± 1.2 µm).

Typus: **China**, Tibet, Bomi county, Suotong village, on leaf of an unidentified plant, 13 Jun. 2015, Q. Chen, ST10 (**holotype** HMAS 350629, ex-type culture CGMCC 3.20522 = LC6085 = JJR053).

Notes: *Colletotrichum obovoides* is a singleton species, not belonging to any species complex (Fig. 1), and differs genetically from the most closely related species *C. rusci* in 24 bp of the *act* nucleotide sequence, 18 bp of *chs-1*, 41 bp of *his3*, 40 bp of ITS, and 53 bp of *tub2*. Morphologically, *C. obovoides* distinctly differs from the two phylogenetically related species, *C. trichellum* (conidia fusoid, straight or slightly curved, 15–28 × 3–5 µm, Duke 1928) and *C. rusci* (conidia subfusoid or cymbiform, curved, 16–23 × 4–5 µm, Damm *et al.* 2009), in that it produces obovoid or clavate, and smaller conidia (10.5–15.5 × 5.5–7.5 µm).

Colletotrichum orchidis Jayaward. *et al.*, Mycosphere 11: 595. 2020.

Notes: Phylogenetically, *C. orchidis* belongs to the *C. dematium* species complex (Fig. 1). However, BLASTn search of the NCBI GenBank using sequences of different loci of *C. orchidis* yielded controversial results. The closest matches identified by BLASTn search using *gapdh*, *chs-1*, *act*, and *tub2* sequences of the ex-type MFLUCC 17-1302 (Jayawardena *et al.* 2020) are species that belong to the *C. dematium* species complex. However, based on the ITS sequence similarity, the closest matches are *C. panacicola*, *C. destructivum*, and *C. utrechtense*, which belong to the *C. destructivum* species complex, and *C. trifolii*, which belongs to the *C. orbiculare* species complex. This inconsistence might explain the unusually long branch of *C. orchidis* in the six-locus tree (Fig. 1), and requires re-examination of the ex-type.

Colletotrichum parabambusicola F. Liu, W.P. Wu & L. Cai, ***sp. nov.*** MycoBank MB 841388. Fig. 22.

Etymology: Named after its close phylogenetic relationship with *C. bambusicola*.

Description: *Colonies* on PDA 48–52 mm diam in 7 d, flat with crenate edge, pale grey to mouse grey, aerial mycelium dense and floccose, reverse saffron. Sexual morph formed on PDA. *Ascomata* medium to dark brown, outer wall composed of dark brown angular or rarely subglobose cells. *Interascal tissue* composed of paraphyses, thin-walled, hyaline, septate, 1–3 µm diam. *Asci* cylindrical, hyaline, 47–55 × 6.5–7.5 µm, 8-spored. *Ascospores* arranged uniseriately or irregularly, hyaline, smooth-walled, aseptate, allantoid or cylindrical to ellipsoidal, 10–14.5 × 3–5.5 µm, (av. ± SD = 12 ± 1.1 × 4 ± 0.6 µm), L/W ratio=3. *Conidiomata* subimmersed, globose, black, solitary or gregarious, conidial masses buff. *Setae* not observed. *Conidiophores* formed directly on hyphae, hyaline, septate, branched, 21–48 µm long. *Conidiogenous cells* hyaline, smooth-walled, ampulliform, subcylindrical, 8–21.5 × 3–5 µm (av. ± SD = 12.9 ± 3.5 × 3.8 ± 0.5 µm). *Conidia* hyaline, aseptate, smooth-walled, guttulate, variable in shape, ellipsoidal, cylindrical, ovoid, ossiform, obclavate, with obtuse ends, 9.5–20.5 × 4–8 (av. ± SD ± 13.9 ± 2.7 × 5.3 ± 1), L/W ratio = 2.6. *Appressoria* single, brown, subcircular, globose to subglobose, clavate, pyriform, 6.5–15 × 4.5–6.5 µm.

Typus: **China**, Shanghai Botanical Garden, on dead culm of bamboo, 22 May 2015, W.P. Wu (**holotype** HMAS 350649, ex-type culture CGMCC 3.20523 = NN058956 = LC13884).

Additional material examined: **China**, Shanghai Botanical Garden, on dead culm of bamboo, 22 May 2015, W.P. Wu, living culture LC13883 (= NN058925).

Notes: *Colletotrichum parabambusicola* shares low sequence similarity with the phylogenetically related species *C. bambusicola* at *act* (97.7 %), *gapdh* (92.1 %), *his3* (94.2 %), ITS (99.8 %), and *tub2* (97.3 %). Morphologically, it differs from *C. bambusicola* in producing smaller asci (47–55 × 6.5–7.5 µm *vs.*58–72 × 7–10 µm) and ascospores (10–14.5 × 3–5.5 µm *vs.*14–19 × 4–6 µm) and exhibiting a lower conidium L/W ratio (2.6 *vs.*3.2).

Colletotrichum paraendophytum F. Liu, W.P. Wu & L. Cai, ***sp. nov.*** MycoBank MB 841389. Fig. 23.

Etymology: Named to reflect its close phylogenetic relationship with *C. endophytum.*

Description: *Colonies* on PDA 52 mm diam in 7 d, flat with entire edge, mouse grey, aerial mycelium fluffy, reverse fuscous black with a white margin. *Vegetative hyphae* hyaline to pale brown, smooth-walled, septate, branched. On SNA, *conidiomata* scattered, semi-immersed. *Setae* dark brown, smooth-walled, 1–2-septate, 38–160 µm long, basal cell cylindrical, sometimes paler than the other cells, 3–6 µm diam, tip acute or round. *Conidiophores* either septate, branched, formed from a cushion of roundish brown cells, or reduced to conidiogenous cells. *Conidiogenous cells* hyaline to pale brown, smooth-walled, cylindrical to ampulliform, straight, 9.5–15 × 3–5 µm, periclinal thickening distinct, sometimes extending to form a new conidiogenous locus. *Conidia* hyaline, aseptate, guttulate, smooth-walled, slightly curved, gradually tapering towards a rounded apex and a usually truncate base, with a similar radian, 18.5–23 × 3–4.5 (av. ± SD = 21 ± 0.9 × 3.8 ± 0.3 µm), L/W ratio = 5.5. *Appressoria* not observed.

Typus: **China**, Beijing, Huairou, Beigoucun, on an unidentified grass, 10 Sep. 2012, W.P. Wu (**holotype** HMAS 350653, ex-type culture CGMCC 3.20524 = LC13888 = NN054963).

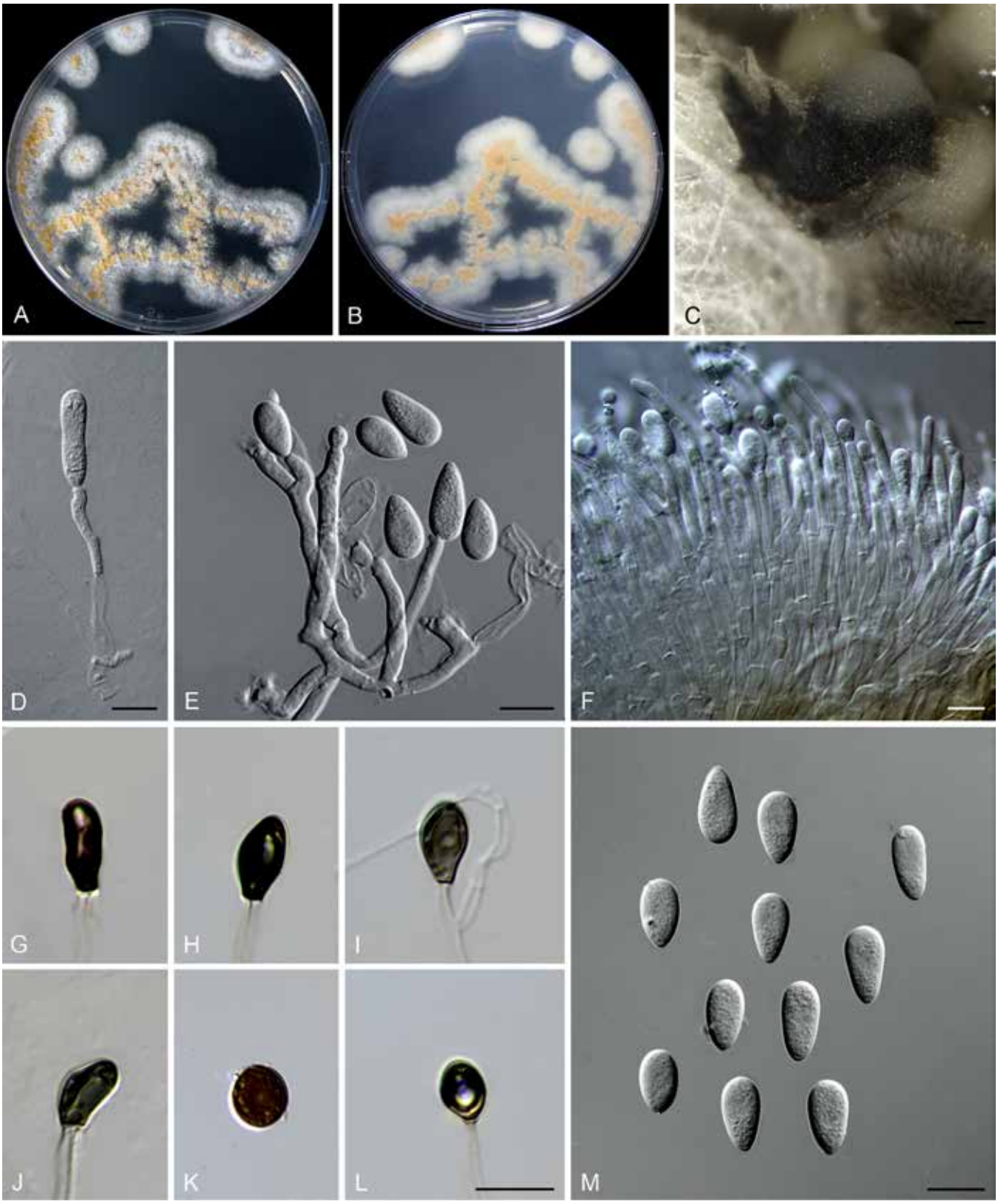

Fig. 21. *Colletotrichum obovoides* (ex-type culture LC6085). **A, B.** Front and reverse colony on PDA (6 d). **C.** Conidioma. **D–F.** Conidiophores, conidiogenous cells and conidia. **G–L.** Appressoria. **M.** Conidia. Scale bars: C = 100 µm; D, E, L, M = 10 µm; F = 20 µm. Scale bar of L applies to G–L.

Notes: *Colletotrichum paraendophytum* is phylogenetically closely related to *C. endophytum* in the *C. graminicola* species complex (Figs 1, 3), but differs in that it produces differently shaped conidia (slightly curved *vs.*pronouncedly curved) and with a different conidium L/W ratio (5.5 *vs.*4.8). In addition, *C. paraendophytum* produces semi-immersed brown conidiomata, which are absent in *C. endophytum* (Tao *et al.* 2013). Furthermore, the two species share low sequence similarity at *act* (95.2 %), *chs-1* (98.2 %), ITS (97.9 %), *sod2* (92.8 %), and *tub2* (92.1 %).

Colletotrichum plurivorum Damm *et al.*, Stud. Mycol. 92: 31. 2018. Fig. 24.

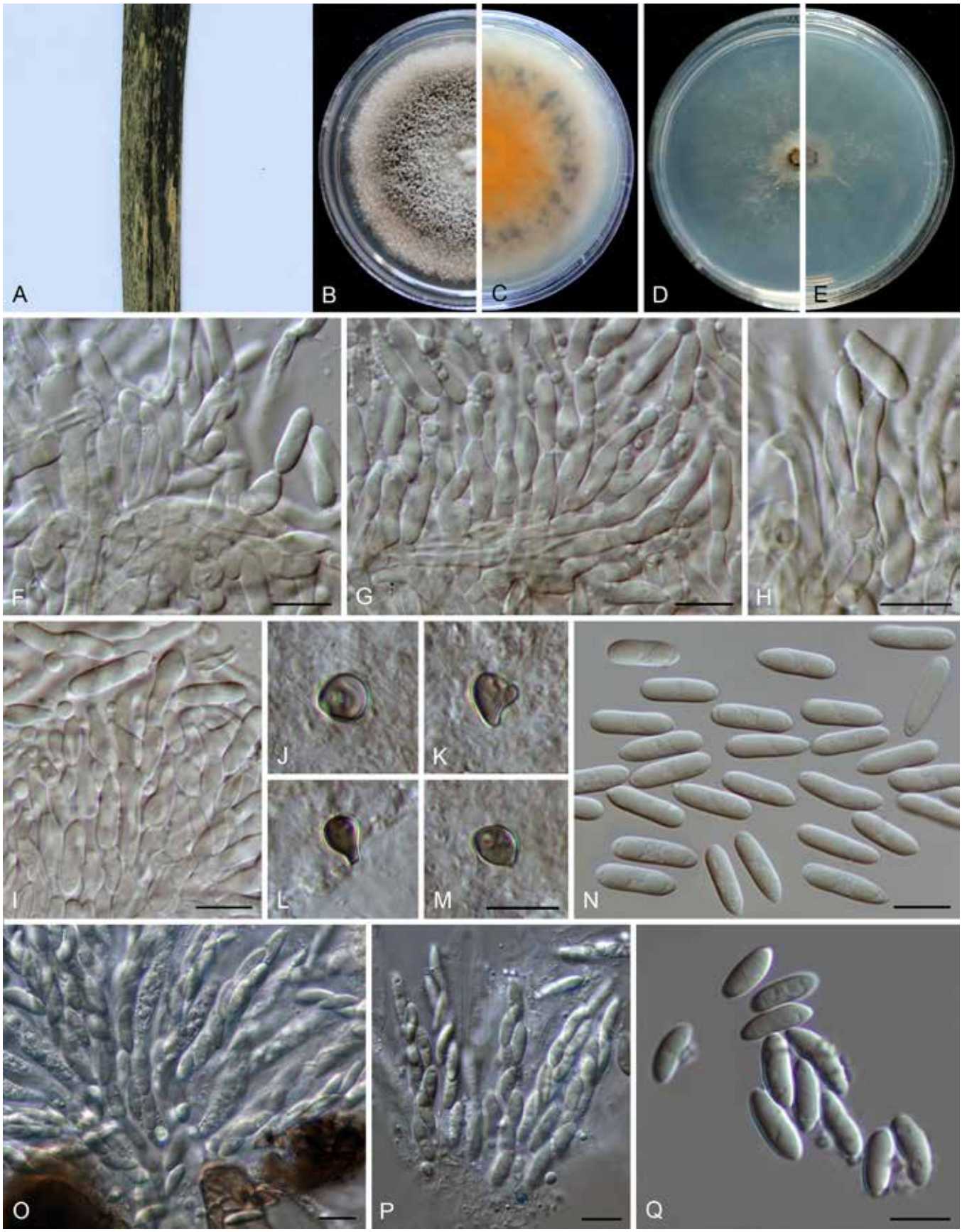

Fig. 22. *Colletotrichum parabambusicola* (ex-type culture NN058956). **A.** Disease symptom on host plant. **B, C.** Front and reverse colony on PDA (7 d). **D, E.** Front and reverse colony on SNA (7 d). **F–I.** Conidiophores, conidiogenous cells and conidia. **J–M.** Appressoria. **N.** Conidia. **O, P.** Asci. **Q.** Ascospores. Scale bars: F–I, M–Q = 10 µm. Scale bar of M applies to J–M.

Description: *Colonies* on PDA 35–51 mm diam in 7 d, flat with undulate edge. *Vegetative hyphae* hyaline to medium brown, smooth-walled, septate, branched. On PDA, *ascomata* globose, subglobose or with an irregular shape, solitary or gregarious, black, 130–300 µm diam, formed on the surface of the medium and usually covered by aerial mycelium, ostiolate, outer wall composed of greenish grey angular cells, 2–6 µm diam. *Interascal tissue* composed of thin-walled, hyaline, septate paraphyses. *Asci* cylindrical, obclavate to clavate,

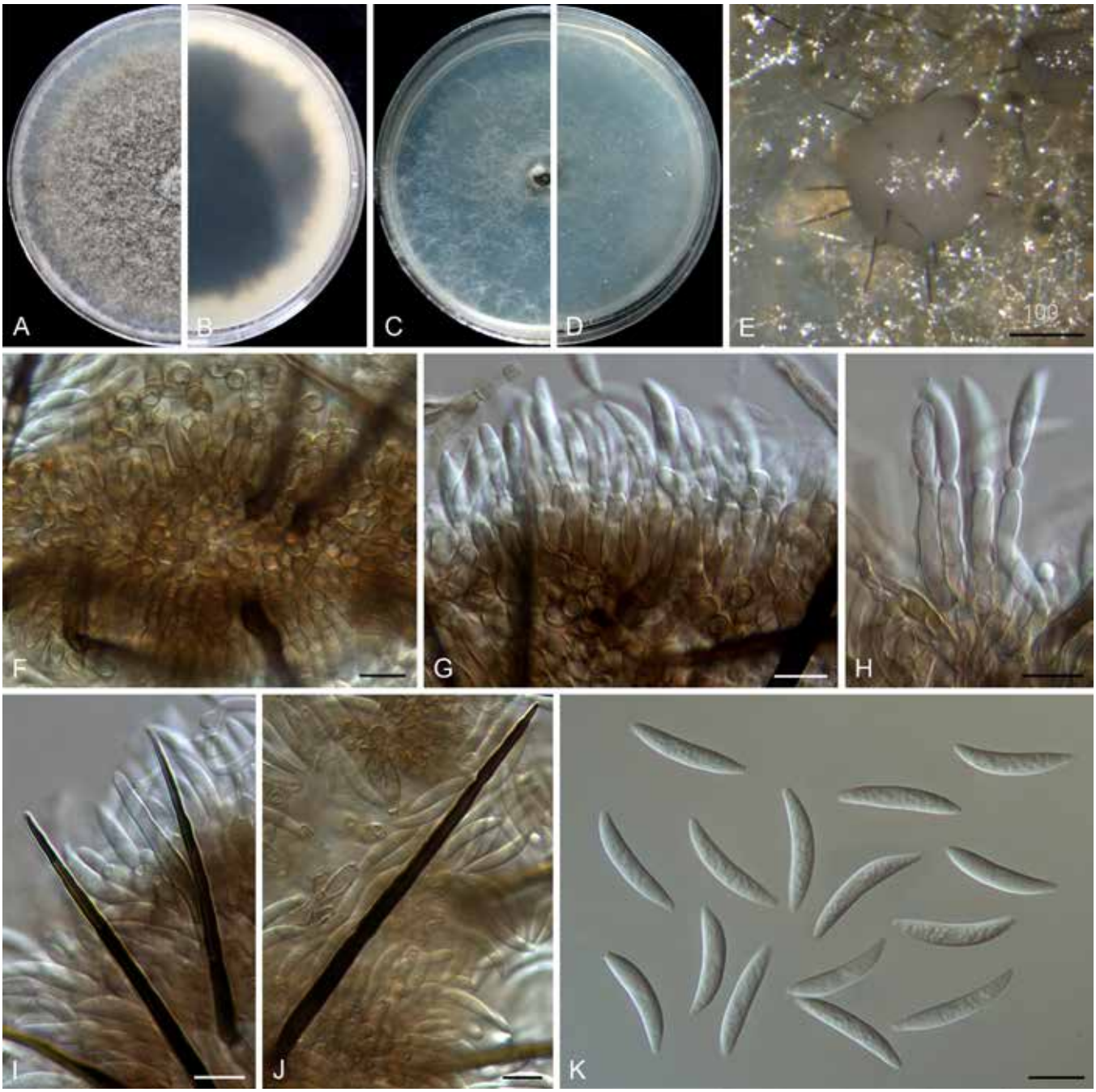

Fig. 23. *Colletotrichum paraendophytum* (ex-type culture NN054963). **A, B.** Front and reverse colony on PDA (7 d). **C, D.** Front and reverse colony on SNA (7 d). **E.** Conidial mass with setae. **F–H.** Conidiophores, conidiogenous cells and conidia. **I, J.** Setae. **K.** Conidia. Scale bars: F–K = 10 µm.

33–54.5 × 7.5–13 µm, 8-spored. *Ascospores* hyaline, smooth-walled, aseptate, fusoid, clavate, with rounded ends, straight or slightly curved, 15–22.5(–25.5) × 4.5–6 µm, (av. ± SD = 18.5 ± 2.7 × 5.3 ± 0.5 µm), L/W ratio = 3.5. *Conidiomata* acervular, solitary or confluent, superficial or semi-immersed, protruding pale luteous conidial masses. *Setae* pale brown to dark brown, usually smooth-walled at the base and verruculose at the top, 1–3-septate, 54–82 µm long, basal cells cylindrical, 3.5–6 µm diam, the tip ± acute. *Conidiophores* solitary or branched, septate, usually reduced to conidiogenous cells. *Conidiogenous cells* hyaline, cylindrical, ovoid to obclavate, smooth-walled, 11–31 × 2.5–5 µm. *Conidia* hyaline, aseptate, smooth-walled, guttulate, cylindrical with obtuse ends, straight, 9–13.5 × 4.5–5.5 µm (av. ± SD = 11.3 ± 1.1 × 5 ± 0.3 µm), L/W ratio = 2.3. *Appressoria* not observed.

Typus: **Vietnam**, Da Lat-Lam Dong, from anthracnose on leaf of *Coffea* sp., collection date unknown, P. Nguyen & E. Liljeroth (**holotype** CBS H-21496, ex-type culture CBS 125474).

Additional materials examined: **China**, Fujian, Fuzhou, Wuyi Mountain, on *Paederia foetida*, Aug. 2016, Z.Y. Ma & L. Cai, WYS8, living cultures LC8240 = (M51), LC8244 (= M55), LC8322 (= M136); on *Vigna unguiculata*, Aug. 2016, Z.Y. Ma & L. Cai, FJWYS01, living culture LC8337 (= M151).

Notes: *Colletotrichum plurivorum* exhibits a large host range and high degree of genetic variation (Damm *et al.* 2019). This is the first report of *C. plurivorum* on *Paederia foetida* and *Vigna unguiculata.*

Colletotrichum quinquefoliae Jayaward. *et al*., Fungal Diversity 78: 83. 2016.

Notes: *Colletotrichum quinquefoliae* was described as a distinct species in the *C. dematium* species complex (Li *et al.* 2016) and

Fig. 24. *Colletotrichum plurivorum* (D–E, H–J. LC8337; F–G, K–S. LC8240). **A, B.** Disease symptoms on *Paederia foetida*. **C.** Disease symptom on *Vigna unguiculata*. **D–G.** Front and reverse colonies on PDA (6 d). **H, I.** Ascomata. **J.** Conidiomata and conidial mass. **K, L.** Setae. **M, N.** Asci. **O.** Ascospores. **P–R.** Conidiophores, conidiogenous cells and conidia. **S.** Conidia. Scale bar = 10 µm.

forms an unusually long branch in the multi-locus phylogenetic tree (Fig. 1). Based on the BLASTn searches, ITS, *gapdh*, and *tub2* sequences of its type MFLU 14-0626 (Li *et al.* 2016) share high similarity with those of species in the *C. dematium* species complex. However, the closest matches using the *act* sequence (KU236389.1) is *C. siamense* (> 99 % identity), belonging to the *C. gloeosporioides* species complex, which very likely reflects a confusion with another specimen and may explain the strangely long branch of *C. quinquefoliae*. The type of *C. quinquefoliae* and its derived sequences are thus in need of reexamination.

Colletotrichum reniforme F. Liu, Z.Y. Ma & L. Cai, ***sp. nov.*** MycoBank MB 841390. Fig. 25.

Etymology: Named to reflect the reniform shape of ascospores.

Description: *Colonies* on PDA 60–64 mm diam in 7 d, flat with entire edge, pale grey with white edge, floccose aerial mycelium, reverse olivaceous grey to iron grey with off-white edge. *Vegetative hyphae* hyaline, smooth-walled, septate, branched. Sexual morph formed on SNA. *Ascomata* solitary or gregarious, superficial to semi-immersed, globose or irregular, black, outer wall composed of angular cells,

Fig. 25. *Colletotrichum reniforme* (ex-type culture LC8230). **A.** Disease symptom on *Smilax cocculoides.* **B.** Front and reverse colony on PDA (6 d). **C, D.** Conidiomata and conidial masses on pine needle and SNA, respectively. **E–H.** Appressoria. **I.** Conidiophores. **J.** Conidia. **K–O.** Setae. **P, Q.** Ascomata on SNA and pine needle, respectively. **R, S.** Asci. **T.** Ascospores. Scale bars: P, Q = 200 µm; R = 20 µm; H–K, M, O, S, T = 10 µm. Scale bar of H applied to E–H.

medium brown. *Interascal tissue* composed of paraphyses, thin-walled, hyaline, septate. *Asci* cymbiform to subcylindrical, hyaline, 33.5–49.5 × 6.5–11.5 µm, 8-spored. *Ascospores* uniseriately arranged, hyaline, smooth-walled, aseptate, allantoid to reniform with rounded ends, 13.5–16 × 4–5 µm (av. ± SD = 14.8 ± 0.7 × 4.5 ± 0.3 µm), L/W ratio = 3.2. On SNA amended with pine needle, *conidiomata* acervular, scattered or gregarious, semi-immersed. *Setae* straight or flexuous, smooth-walled, sometimes verrucous

in the upper half, basal cell medium brown, gradually becoming dark brown towards the tip, 1–2-septate, 65–89 µm long, basal cell cylindrical, 3.5–4.5 µm diam, the tip ± acute. *Conidiophores* hyaline to pale brown, septate, branched, 25–35 µm, usually reduced to conidiogenous cells. *Conidiogenous cells* hyaline, smooth-walled, cylindrical, subcylindrical to ampulliform, 5.5–11.5(–14) × 2.5–5 µm. *Conidia* hyaline, aseptate, smooth-walled, guttulate, straight, cylindrical, both ends obtuse, 11.5–16 × 4–5.5 µm (av. ± SD = 13.6 ± 0.9 × 4.7 ± 0.3), L/W ratio = 2.9. *Appressoria* single, medium to dark brown, various in shape, subcircular, ovoid, navicular, ellipsoidal or irregular in outline, 9–14.5 × 4.5–7.5 µm (av. ± SD = 11.6 ± 1.4 × 5.5 ± 0.7 µm).

Typus: **China**, Fujian, Fuzhou, Wuyi Mountain, on *Smilax cocculoides*, Aug. 2016, Z.Y. Ma & L. Cai, WYS3 (**holotype** HMAS 350631, ex-type culture CGMCC 3.20525 = LC8230 = M41).

Additional material examined: **China**, Fujian, Fuzhou, Wuyi Mountain, on *Paederia foetida*, Aug. 2016, Z.Y. Ma & L. Cai, WYS8, living culture LC8248 (= M59).

Notes: *Colletotrichum reniforme* is closely related to *C. cliviicola* in the *C. orchidearum* species complex (Fig. 1), but these two species are easily differentiated on the basis of morphological characteristics. The conidiophores of *C. reniforme* are inconspicuous on SNA and pine needles, and difficult to distinguish from the pale brown acervulus cells, while those of *C. cliviicola* are easily recognised and usually elongating up to 70 or 80 µm in 3 wk (Damm *et al.* 2019). The conidiogenous cells of *C. reniforme* are shorter and thinner than those of *C. cliviicola* [5.5–11.5(–14) × 2.5–5 µm *vs.*7.5–23 × 4.5–7.5 µm]. Furthermore, microcyclic conidiation is observed in *C. cliviicola*, but not in *C. reniforme*. According to Damm *et al.* (2019) and Yang *et al.* (2009), the appressoria of *C. cliviicola* usually have undulate to lobate margins, while those of *C. reniforme* are flat.

Colletotrichum schimae F. Liu, W.P. Wu & L. Cai, ***sp. nov.*** MycoBank MB 841391. Fig. 26.

Etymology: Named after the host plant genus, *Schima.*

Description: *Colonies* on PDA 33–38 mm diam in 7 d, flat with entire or undulate edge, white, aerial mycelium dense, reverse umber in the centre, pale luteous towards the margin. *Conidiomata* and *setae* not observed. On SNA, *conidiophores* formed directly from aerial mycelium, hyaline, aseptate or septate. *Conidiogenous cells* hyaline, cylindrical, formed terminally or laterally on hyphae, variable in size, up to 45 µm long. *Conidia* hyaline, smooth-walled, guttulate, cylindrical to fusoid, with ± acute ends, 8.5–14 × 2.5–4 µm (av. ± SD = 11.6 ± 1.1 × 3.5 ± 0.3 µm), L/W ratio = 3.3. *Appressoria* pale brown, solitary, ellipsoidal, subglobose, bullet or irregular shape, 5–12.5 × 3.5–7 µm.

Typus: **China**, Hunan Province, Chenzhou, Yizhang County, Mangshan, on healthy leaves of *Schima* sp., 12 Apr. 2002, W.P. Wu (**holotype** HMAS 350647, ex-type culture CGMCC 3.20526 = LC13880 = NN046984).

Additional material examined: **China**, Hunan Province, Chenzhou, Yizhang County, Mangshan, on healthy leaves of *Schima* sp., 12 Apr. 2002, W.P. Wu, living culture LC13881 (= NN047247).

Notes: *Colletotrichum schimae* is phylogenetically related to *C. kniphofiae* in the *C. acutatum* species complex, and shares low sequence similarity at *act* (92 %), *chs-1* (96.2 %), *gapdh* (89.8 %), ITS (98.4 %), and *tub2* (94.9 %). Moreover, *C. schimae* is distinct from all other species in this genus at each locus sequenced in the current study. Morphologically, *C. schimae* differs from *C. kniphofiae* in that it produces smaller-sized conidia (8.5–14 × 2.5–4 µm *vs.*17–37 × 5–7 µm) (Crous *et al.* 2018).

Colletotrichum shivasii F. Liu & L. Cai, ***sp. nov.*** MycoBank MB 841392. Fig. 27.

Etymology: Named in honour of the mycologist Roger Shivas, who provided the ex-type culture of this species for the study.

Description: *Colonies* on PDA 75–80 mm diam in 7 d, flat with fimbriate edge, aerial mycelium white, reverse white at first, becoming orange to black at the centre with time. On PDA, *conidiomata* not observed. *Conidiophores* formed directly from aerial mycelium, hyaline to very pale grey, septate, up to 37 µm. *Setae* not observed. *Conidiogenous cells* cylindrical, smooth-walled, 12–16 µm in length. *Conidia* hyaline, smooth-walled, apex reduced into a filiform appendage (10–)12.5–23 µm, conidia body slightly curved or straight, 27.5–47.5 µm long (including appendages), 2.5–4 µm wide (av ± SD = 39.4 ± 5.2 × 3.6 ± 0.5 µm), L/W ratio = 10.9. *Appressoria* pale to medium brown, pyriform to subcircular, 6–11.5 × 4.5–7.5 µm (av. ± SD = 7.8 ± 1.5 × 6 ± 1.1 µm).

Typus: **Australia**, Queensland, Tablelands, Wongabel Road, Atherton, on leaf of *Themeda triandra*, Feb. 2004, probably J.L. Alcorn (**holotype** HMAS 350627, ex-type culture LC1400 = BRIP 15842a).

Notes: *Colletotrichum shivasii* belongs to the *C. caudatum* species complex. Species in this complex comprise widespread fungal pathogens of warm-season grasses, and are easily differentiated from other species in the genus by producing caudate conidia (Crouch 2014). *Colletotrichum shivasii*, associated with the perennial tussock-forming grass *Themeda triandra* in Australia, is morphologically similar to the closely related species *C. caudatum*, but harbours nucleotide polymorphisms at ITS (96.9 % similarity), *sod2* (92.9 % similarity), and Mat/Apn2 (82.1 % similarity).

Colletotrichum sinuatum F. Liu, W.P. Wu & L. Cai, ***sp. nov.*** MycoBank MB 841393. Fig. 28.

Etymology: Named to reflect the sinuate setae and conidiophores.

Description: *Colonies* on PDA 42 mm diam in 7 d, flat with entire edge, white to pale saffron, aerial mycelium sparse, reverse pale saffron with a black centre. *Conidiomata* not formed, conidial masses and setae abundantly formed on the surface of medium. *Setae* medium to dark brown, smooth-walled or verruculose, mostly sinuate, 2–5-septate, 67–175 µm long, basal cells cylindrical, sometimes inflated, 4–9.5 µm diam, the tip acute or rounded. *Conidiophores* formed directly from hyphae, hyaline to brown, branched, 1–4-septate, 32–122 µm in length. *Conidiogenous cells* hyaline to pale brown, smooth-walled, cylindrical, rarely subulate, variable in length, on SNA 11.5–34 × 2.5–5 µm (av. ± SD = 21.9 ± 5.4 × 3.8 ± 0.6 µm), on PDA 15–37 × 3–5 µm (av. ± SD = 24.8 ± 6.5 × 4 ± 0.5 µm). *Conidia* hyaline, aseptate, smooth-walled, cylindrical, apex obtuse, tapering at base to a truncate hilum, mostly straight, rarely slightly curved, on SNA 14.5–19 × 3.5–5 µm (av. ± SD = 16.9 ± 1.2 × 4.4 ± 0.4 µm), L/W ratio = 3.8, on PDA 14.5–21 × 4.5–5.5 µm (av. ± SD = 17.8 ± 1.5 × 4.8 ± 0.3 µm), L/W ratio = 3.7. *Appressoria* not observed.

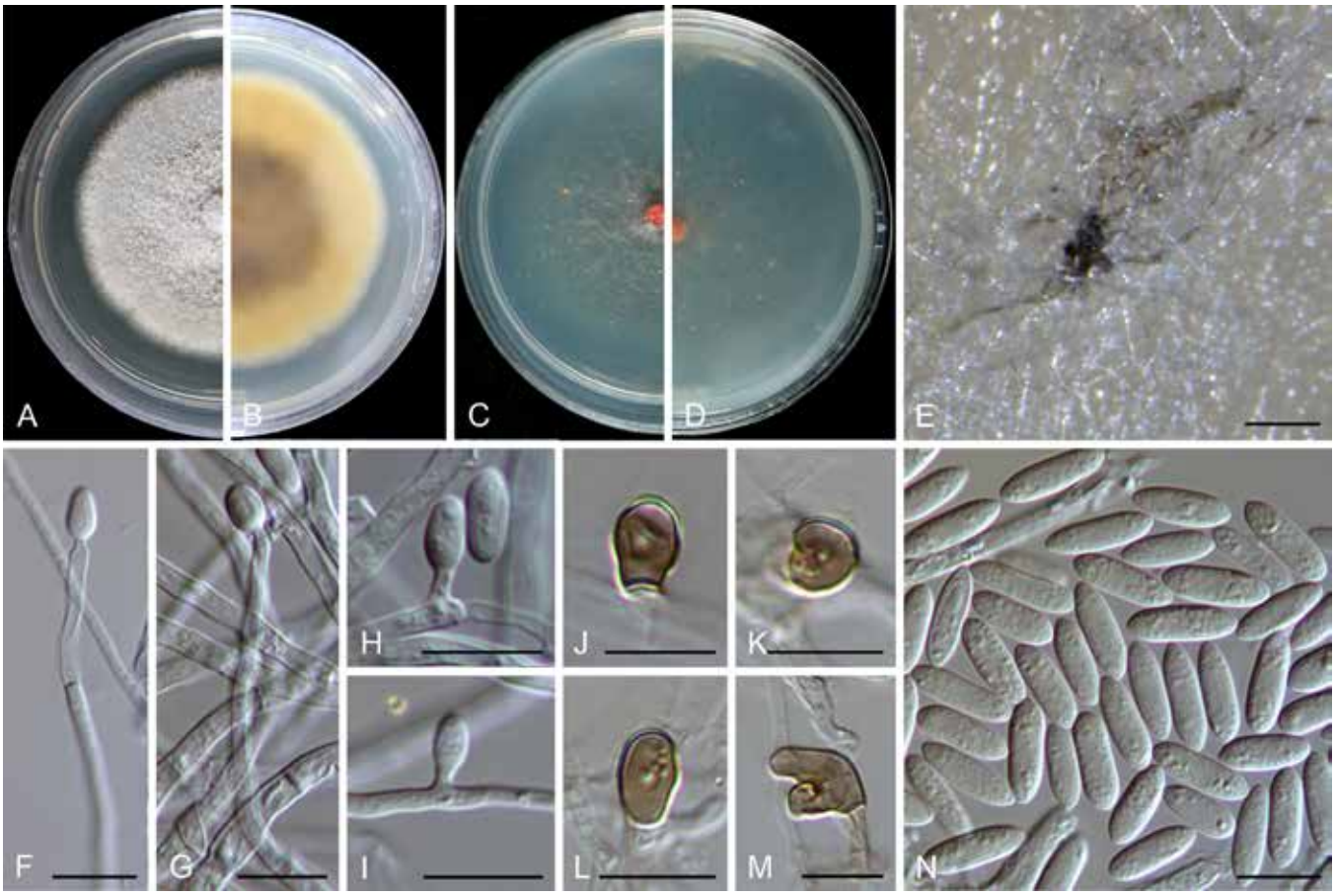

Fig. 26. *Colletotrichum schimae* (ex-type culture NN046984). **A, B.** Front and reverse colony on PDA (7 d). **C, D.** Front and reverse colony on SNA (7 d). **E.** Conidial mass on SNA. **F–I.** Conidiophores, conidiogenous cells and conidia. **J–M.** Appressoria. **N.** Conidia. Scale bars = 10 µm.

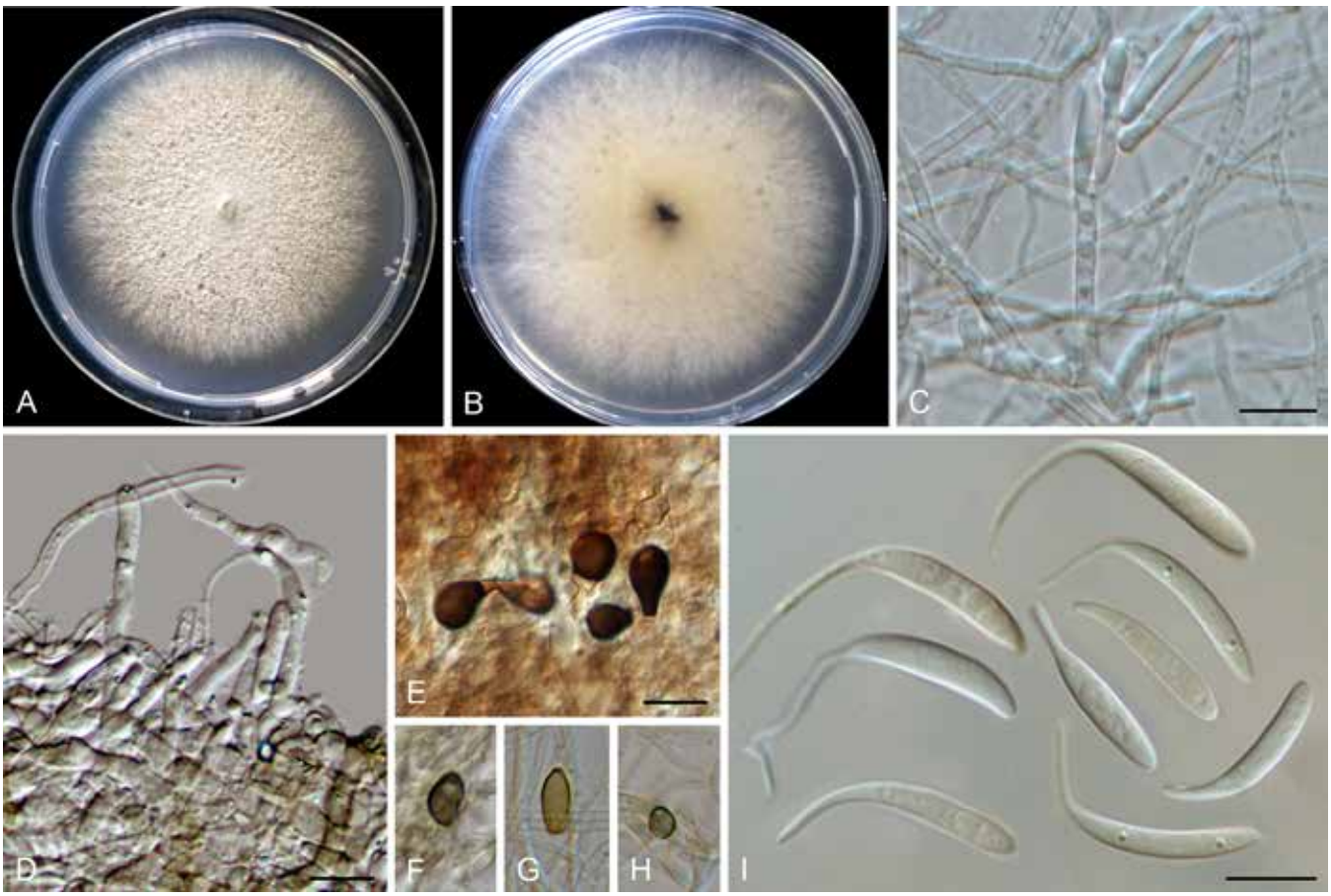

Fig. 27. *Colletotrichum shivasii* (ex-type culture BRIP 15842a). **A, B.** Front and reverse colony on PDA (7 d). **C, D.** Conidiophores and conidiogenous cells. **E–H.** Appressoria. **I.** Conidia. Scale bars = 10 µm.

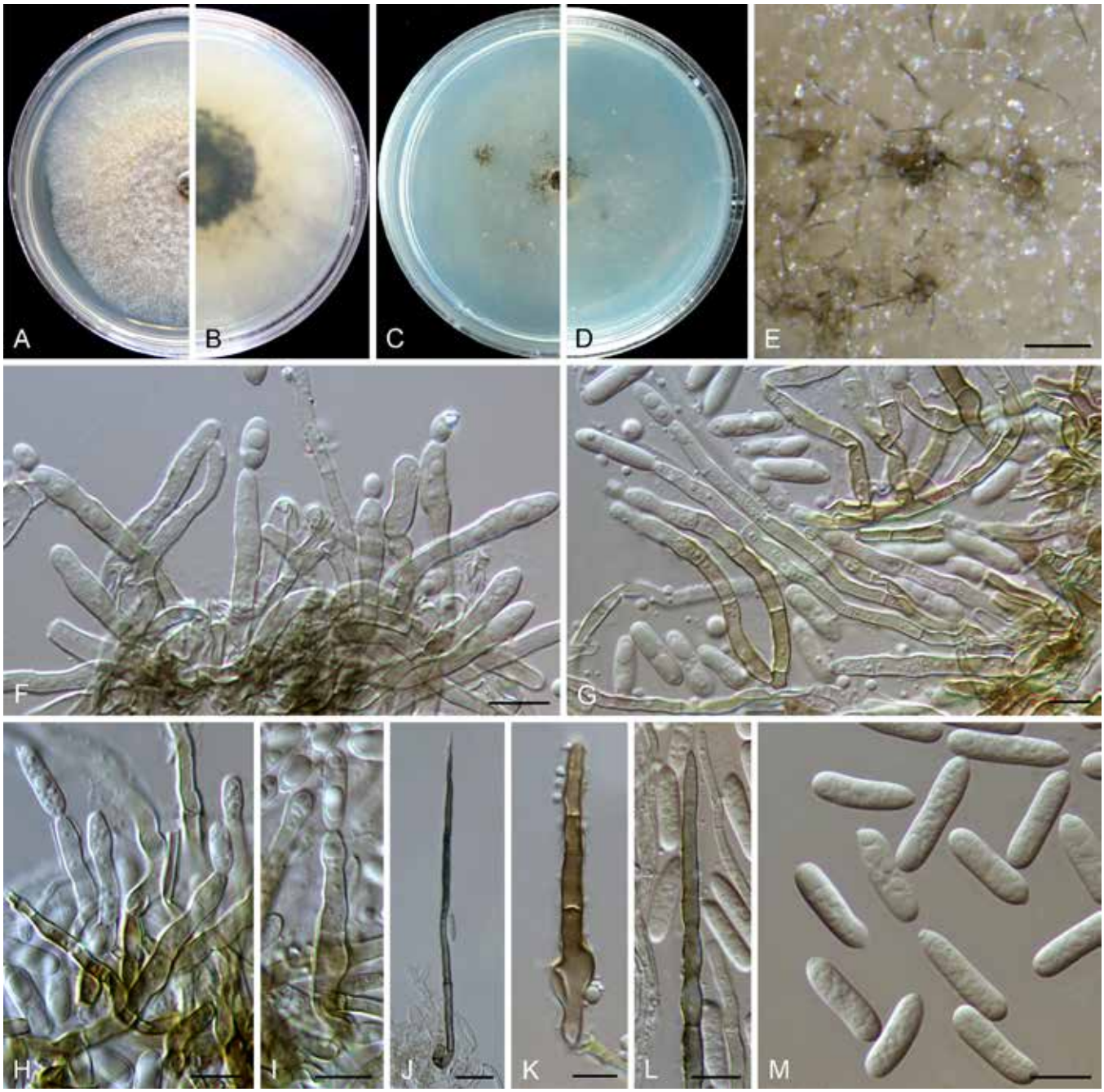

Fig. 28. *Colletotrichum sinuatum* (ex-type culture NN055266). **A, B.** Front and reverse colony on PDA (7 d). **C, D.** Front and reverse colony on SNA (7 d). **E.** Conidial masses and setae on SNA. **F–I.** Conidiophores, conidiogenous cells and conidia. **J–L.** Setae. **M.** Conidia. Scale bars: E = 100 µm; J = 20 µm; F–I, K–M = 10 µm.

Typus: **China**, Guangdong Province, Guangzhou, Yuexiu Park, on dead leaves of *Ophiopogon japonicus*, 29 Dec. 2012, W.P. Wu (**holotype** HMAS 350643, ex-type culture CGMCC 3.20528 = LC13874 = NN055266).

Notes: *Colletotrichum sinuatum* belongs to the *C. dracaenophilum* species complex. It shares low sequence similarity with the most closely related species *C. yunnanense* at *act* (91.6 %), *chs-1* (97.6 %), *gapdh* (87.4 %), *his3* (92.4 %), ITS (96.5 %), and *tub2* (96.3 %). Moreover, *C. schimae* is distinct from all other species in this genus at each locus sequenced in the current study. This species morphologically differs from the phylogenetically related species *C. buxi sp. nov.*, *C. dracaenophilum*, and *C. yunnanense* in that it produces distinctly longer conidiophores and conidiogenous cells. Two other *O. japonicus*-associated species, *C. truncatum* and *C. falcatum* (Raabe *et al.* 1981, Miller 1992), are easily distinguished from *C. sinuatum* in that they produce curved conidia.

Colletotrichum subacidae F. Liu, Z.Y. Ma & L. Cai, ***sp. nov.*** MycoBank MB 841394. Fig. 29.

Etymology: Named to reflect its close phylogenetic relationship with *C. acidae.*

Description: *Colonies* on PDA 43–51 mm diam in 7 d, flat with undulate edge, glaucous grey to smoke grey in the centre, white at the margin, aerial mycelium sparse, reverse greenish grey in the centre, white at the margin. On PDA, *conidiomata* acervular, gregarious, semi-immersed. *Setae* dark brown, 1–3-septate, 80–165 µm long, base cylindrical, smooth-walled, 5–9 µm diam, tip acute to obtuse. *Conidiophores* hyaline to pale brown, smooth-walled, septate, solitary or branched, formed from a cushion of roundish brown cells. *Conidiogenous cells* hyaline, smooth-walled, cylindrical, 9–20 × 2–4.5 µm. *Conidia* hyaline, aseptate, smooth-

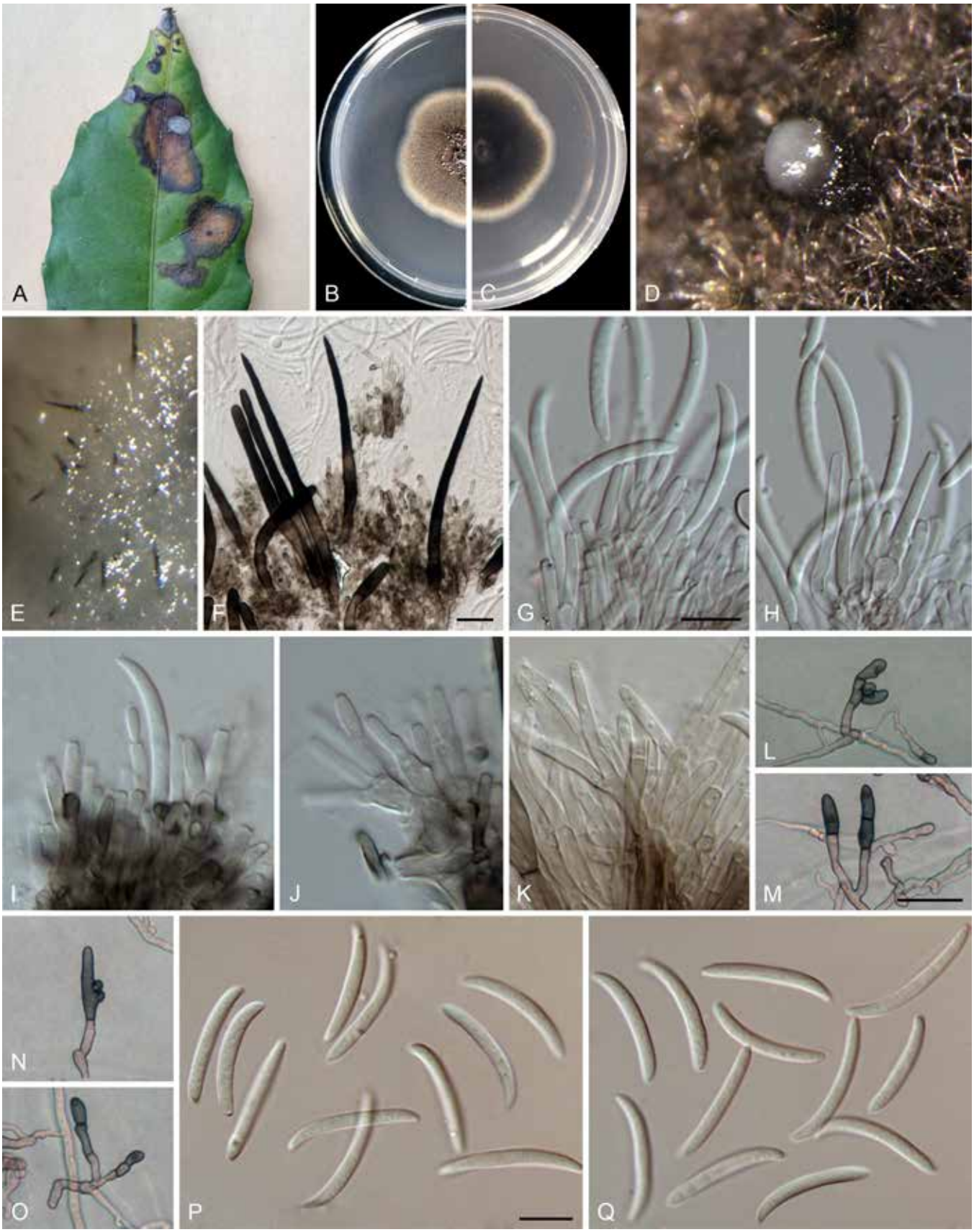

Fig. 29. *Colletotrichum subacidae* (ex-type culture LC13857). **A.** Disease symptom on host plant. **B, C.** Front and reverse colony on PDA (6 d). **D.** Conidioma on PDA. **E, F.** Setae. **G–K.** Conidiophores, conidiogenous cells and conidia. **L–O.** Appressoria. **P, Q.** Conidia. Scale bars: F, M = 20 µm; G, P = 10 µm. Scale bar of G applies to G–K; M applies to L–O; P applies to P–Q.

walled, slightly curved, central part of conidium almost straight with parallel walls, apex more or less acute, base usually truncate, 21–30 × 2.5–4 µm (av. ± SD = 26 ± 2.3 × 3 ± 0.3 µm), L/W ratio = 8.5. *Appressoria* brown, usually in groups, mostly oblong to subcylindrical, rarely irregular in outline, 8–25 × 5–8 µm (av. ± SD = 15.5 ± 4.4 × 6.5 ± 1.0 µm), L/W ratio = 2.3.

Typus: **China**, Guangxi, Chongzuo, Guangxi Nonggang National Nature Reserve, on *Tetrastigma obovatum*, Jun. 2017, Z.Y. Ma & L.W. Hou (**holotype** HMAS 350635, ex-type culture CGMCC 3.20529 = LC13857 = LH01).

Additional materials examined: **China**, Beijing, Xibeiwang, Beijing Medical Botanical Garden, on a diseased stem of *Asparagus officinalis*, 9 Sep. 2012, W.P. Wu, living culture NN054605; on a diseased leaf of *Hosta* sp., 9 Sep. 2012, W.P. Wu, living culture NN054609; Guangxi, Chongzuo, Guangxi Nonggang National Nature Reserve, on *Tetrastigma obovatum*, Jun. 2017, Z.Y. Ma & L.W. Hou, living cultures LC15821, LC15822, LC15823; Hubei Province, Wuhan Botanical Garden, on a dead leaf petiole of *Ailanthus altissima*, 2 Aug. 2015, W.P. Wu, living cultures NN071129, NN071131.

Notes: *Colletotrichum subacidae* is phylogenetically allied with *C. acidae* (Fig. 1), but these two species share low sequence similarity at *gapdh* (93.8 %), *act* (94.3 %), and *tub2* (97.6 %). Morphologically, *C. subacidae* differs from *C. acidae* with respect to the shape and size of appressoria (oblong to subcylindrical, 8–25 × 5–8 µm *vs.*round, oval or irregular, 11–23 × 9–18 µm) and the size of conidiogenous cells (9–20 × 2–4.5 µm *vs.*1–2 × 2–3.5 µm) (Samarakoon *et al.* 2018). Moreover, the conidia of *C. acidae* are more strongly curved than those of *C. subacidae*.

Colletotrichum subsalicis F. Liu & L. Cai, ***sp. nov.*** MycoBank MB 841395. Fig. 30.

Etymology: Named to reflect its close phylogenetic relationship with *C. salicis.*

Description: *Colonies* on PDA 39–40 mm diam in 7 d, flat with entire edge, pale mouse grey in the centre, white at the margin, aerial mycelium sparse, reverse brown vinaceous, mouse grey and white towards the margin. On PDA, *conidiomata* acervular, scattered, semi-immersed, protruding saffron conidial masses. *Setae* not observed. *Conidiophores* formed from a cushion of pale brown angular cells, septate, branched, 17–41 µm. *Conidiogenous cells* hyaline to pale brown, smooth-walled, mostly cylindrical to ampulliform, rarely ovoid, 11–20 × 2–5 µm, periclinal thickening visible. *Conidia* hyaline, aseptate, smooth-walled, fusoid, 13–16 × 3.5–5 µm (av. ± SD = 14 ± 0.9 × 4.5 ± 0.9 µm), L/W ratio = 3.2. *Appressoria* single, olivaceous, smooth-walled, mostly clavate with a truncate base, sometimes irregular, 6–13 × 2–6 µm (av. ± SD = 8.5 ± 1.7 × 4 ± 1.7 µm), L/W ration = 2.1.

Typus: **China**, Beijing, Baihuashan National Nature Reserve Forest Station, *Populus alba*, 19 Sep. 2018, Q. Chen (**holotype** HMAS 350637, ex-type culture CGMCC 3.20530 = LC13863 = CQ1168).

Notes: *Colletotrichum subsalicis* forms a sister clade to *C. salicis* in the *C. acutatum* species complex (Fig. 1), but morphologically differs from the latter in conidium shape (fusoid *vs.*cylindrical to clavate) and appressorium size (6–13 × 2–6 µm, av. ± SD = 8.5 × 4 µm, L/W ratio = 2.1 *vs.* 6–19.5 × 5–9.5 µm, av. ± SD = 11.5 × 7.6 µm, L/W ratio = 1.5) (Damm *et al.* 2012a). Furthermore, the sexual morph of *C. salicis* is more commonly observed in culture than the asexual morph (Damm *et al.* 2012a), but is absent in *C. subsalicis*. *Colletotrichum subsalicis* and *C. salicis* share 98.8 % genomic similarity.

Colletotrichum subvariabile F. Liu, W.P. Wu & L. Cai, ***sp. nov.*** MycoBank MB 841396. Fig. 31.

Etymology: Named to reflect its close phylogenetic relationship with *C. variabile.*

Description: *Colonies* on PDA 48–49 mm diam in 7 d, flat with entire edge, pale salmon, covered by white and pale greenish grey aerial mycelium, reverse pale salmon, variegated with pale greenish grey spots. On PDA, *conidiomata* subimmersed, globose, black, solitary or gregarious, in which conidiophores hardly observed. *Conidiophores*, formed directly on hyphae, usually reduced to conidiogenous cells, terminally or laterally. *Conidiogenous cells* rarely observed, hyaline to pale brown, cylindrical, or ampulliform, 2–12 µm in length. *Conidia* hyaline with salmon guttules, smooth-walled, cylindrical with obtuse apex and truncate base, 18–27 × 5.5–8 µm, av. ± SD = 22.1 ± 2.5 × 6.7 ± 0.8 µm, L/W ratio = 3.3. *Setae* and *appressoria* not observed.

Typus: **China**, Yunnan Province, Kunming, Kunming Botanical Garden, on healthy leaves of an unknown plant (endophyte), 20 Dec. 1993, W.P. Wu (**holotype** HMAS 350645, ex-type culture CGMCC 3.20531 = LC13876 = NN040649).

Notes: *Colletotrichum subvariabile*, belonging to the *C. gigasporum* species complex (Fig. 1), shares low sequence similarity with the phylogenetically related species *C. variabile sp. nov.* at *act* (95.2 %), *chs-1* (97.2 %), *gapdh* (94.2 %), *his3* (95 %), *tub2* (97.9 %), and ITS (97.8 %). Morphologically, *C. subvariabile* differs from *C. variabile* in that it produces shorter conidiogenous cells (2–12 µm *vs.*9–34 µm) and has a lower conidium L/W ratio (3.3 *vs.*3.8).

Colletotrichum syngoniicola F. Liu, Z.Y. Ma & L. Cai, ***sp. nov.*** MycoBank MB 841397. Fig. 32.

Etymology: Named after the host plant genus, *Syngonium.*

Description: Colonies on PDA 56–58 mm diam in 7 d, flat with entire edge, smoke grey to greenish grey with white edge, aerial mycelium sparse and short, reverse greenish grey to olivaceous black, off-white at the margin. On SNA, *vegetative hyphae* hyaline or brown, smooth-walled, septate, branched. *Conidiomata* not developed. *Conidiophores* formed directly from hyphae, conidial masses buff to honey. *Setae* not observed. *Conidiophores* hyaline to brown, septate, branched, up to 130 µm long, basal cells more or less thick-walled. *Conidiogenous cells* hyaline, rarely pale brown, smooth-walled, cylindrical or slightly tapering towards the apex, 8–19(–24) × 3.5–5.5 µm. *Conidia* hyaline, aseptate, smooth-walled, guttulate, cylindrical with obtuse ends, sometimes the base tapering to a truncate hilum, (9–)11–18.5(–23.5) × 3.5–5.5 (av. ± SD = 14.9 ± 1.2 × 4.1 ± 0.4), L/W ratio = 3.6. *Appressoria* single or gregarious, medium to dark brown, terminally at the tip of the hyphae, mostly irregularly shaped, with undulate to lobate margins, sometimes elliptical with an entire margin, 7.5–18 × 3.5–9 µm (av. ± SD = 10.1 ± 2.7 ×5.8 ± 1.7 µm).

Typus: **China**, Guangdong, Shenzhen, from a leaf spot of *Syngonium* sp., Nov. 2016, Y.Z. Diao, SZ36 (**holotype** HMAS 350632, ex-type culture CGMCC 3.20532 = LC8894 = M0745).

Additional materials examined: **China**, Guangdong, Shenzhen, from leaf spots of *Syngonium* sp., Nov. 2016, Y.Z. Diao, SZ36, living cultures LC8895 (= M0746), LC8896 (= M0747), LC8897 (= M0748).

Notes: *Colletotrichum syngoniicola* belongs to the *C. orchidearum* species complex (Fig. 1), and shares low sequence similarity with

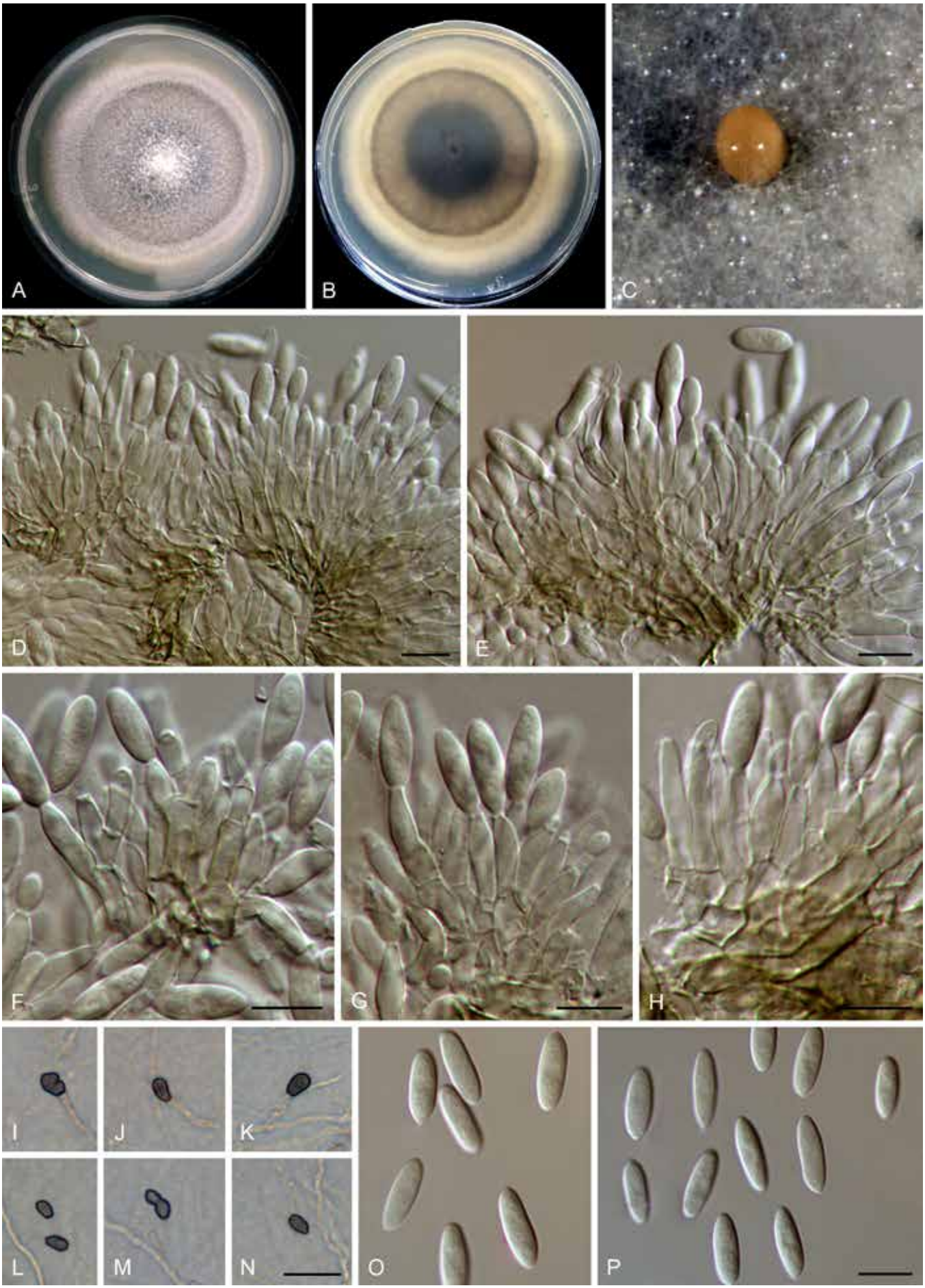

Fig. 30. *Colletotrichum subsalicis* (ex-type culture LC13863). **A, B.** Front and reverse colony on PDA (13 d). **C.** Conidioma on PDA. **D–H.** Conidiophores, conidiogenous cells and conidia. **I–N.** Appressoria. **O, P.** Conidia. Scale bars: D–H, P = 10 µm; N = 20 µm. Scale bar of N applies to I–N; P applies to O, P.

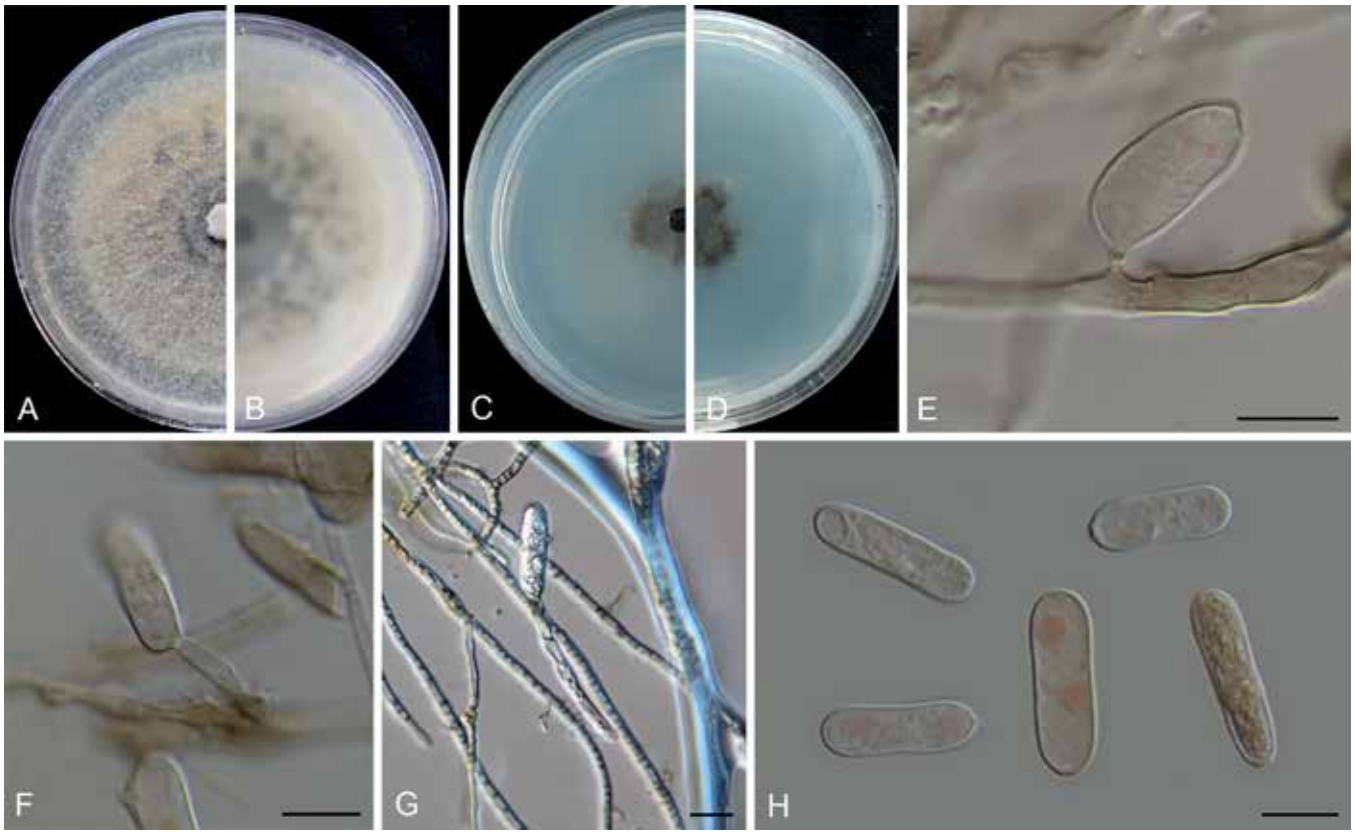

Fig. 31. *Colletotrichum subvariabile* (ex-type culture NN040649). **A, B.** Front and reverse colony on PDA (7 d). **C, D.** Front and reverse colony on SNA (7 d). **E–G.** Conidiophores, conidiogenous cells and conidia. **H.** Conidia. Scale bars = 10 µm.

the phylogenetically related species *C. piperis* at *act* (95.3 %), *chs-1* (98.4 %), *gapdh* (93.2 %), *his3* (96.5 %), *tub2* (97.5 %), and ITS (99 %). Morphologically, *C. syngoniicola* differs from *C. piperis* in that it produces relatively darker conidiophores (Damm *et al.* 2019). Moreover, although *C. syngoniicola* is characterised by the unusual conidiophores that are long-branched and brown, resembling those of *C. monsterae sp. nov.*, the two species share low sequence similarity at *act* (89.3 %), *chs-1* (92.8 %), *gapdh* (87.7 %), *his3* (91.9 %), ITS (97.6 %), and *tub2* (93.5 %).

Colletotrichum telosmae F. Liu, W.P. Wu & L. Cai, ***sp. nov.*** MycoBank MB 841398. Fig. 33.

Etymology: Named after the host plant genus, *Telosma.*

Description: *Colonies* on PDA growing slowly, 28–29 mm diam in 7 d, raised with concave edge, grey, reverse iron grey with pale amber margin, a pale amber ring more towards the centre of the colony corresponds to the production of conidial masses on the surface. *Vegetative hyphae* hyaline to pale brown, smooth-walled, septate, branched. On SNA, *conidiomata* not developed, conidiophores formed directly on hyphae, conidial masses buff to brown. *Setae* not observed. *Conidiophores* hyaline to pale brown, 1–4-septate, branched, up to 80 µm long. *Conidiogenous cells* hyaline, smooth-walled, cylindrical, 8–24 × 2–4 µm (av. ± SD ± 18.3 ± 3.5 × 3 ± 0.3 µm), collarette visible. *Conidia* hyaline, aseptate, smooth-walled, guttulate, cylindrical with obtuse ends, 10.5–11.5 × 3.5–5 µm (av. ± SD ± 11 ± 0.4 × 4 ± 0.2 µm), L/W ratio = 2.8. *Appressoria* ellipsoidal, subcircular, medium brown to dark brown, 5.5–11.5 × 3.5–7 µm (av. ± SD ± 7.2 ± 1.6 × 5 ± 1 µm), with conidia-like cells formed from the appressoria, 6.5–7.5 × 5–5.5 µm.

Typus: **China**, on healthy leaves of *Telosma cordarum*, 24 Mar. 2010, W.P. Wu (**holotype** HMAS 350641, ex-type culture CGMCC 3.20533 = LC13872 = NN052858).

Notes: The endophytic *C. telosmae*, phylogenetically related to the *C. dracaenophilum* species complex (Fig. 1), is a singleton species and can be distinguished from all currently accepted species of *Colletotrichum* at each locus sequenced in the current study. Its cylindrical conidia resemble species in many complexes, especially the *C. gloeosporioides* and *C. dracaenophilum* complexes. However, the conidia-like cells that form on the *C. telosmae* appressoria (Fig. 33L–M) have not been previously observed in this genus. This is the first report of a *Colletotrichum* species on *Telosma cordarum.*

Colletotrichum tibetense F. Liu & L. Cai, ***sp. nov.*** MycoBank MB 841399. Fig. 34.

Etymology: Named after the location where the fungus was collected, Tibet.

Description: *Colonies* on PDA growing slowly, 21–24 mm diam in 7 d, flat with fimbriate edge, straw, aerial mycelium sparse, reverse straw. *Vegetative hyphae* hyaline, smooth-walled, septate, branched. Sporulating on SNA and pine needle, *conidiomata* not developed, *conidiophores* formed directly from hyphae and hardly observed, conidial masses abundant, pale luteous to buff, scattered or confluent. *Setae* not observed. *Conidiophores* hyaline, aseptate, unbranched, reduced to conidiogenous cells. *Conidiogenous cells* hyaline, smooth-walled, cylindrical, straight or flexuous, 19.5–32.5 × 2 µm. *Conidia* hyaline, aseptate, guttulate, smooth-walled, curved, central part of conidium almost straight with parallel walls, gradually

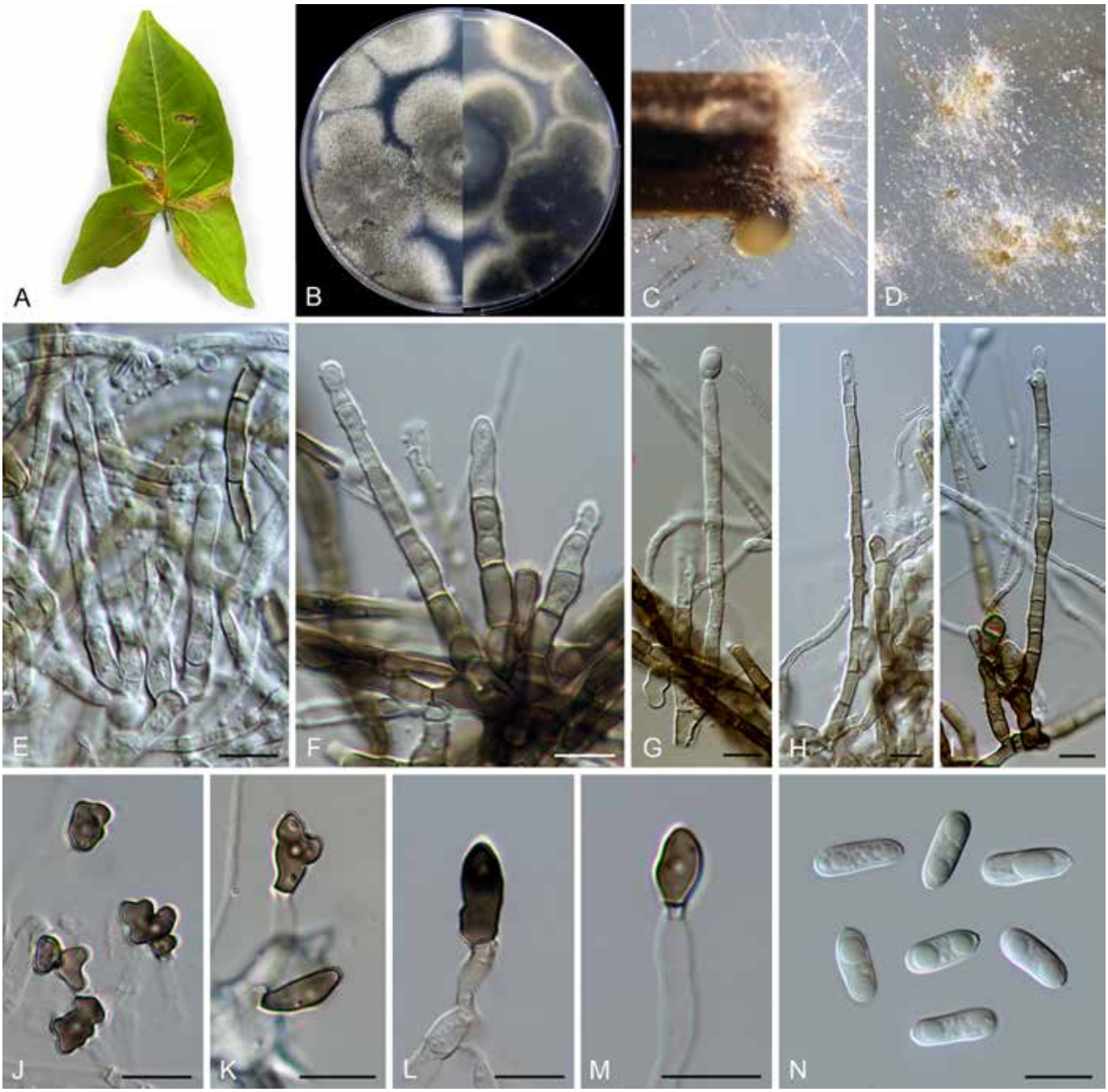

Fig. 32. *Colletotrichum syngoniicola* (ex-type culture LC8894). **A.** Disease symptom on *Syngonium* sp. **B.** Front and reverse colony on PDA (6 d). **C, D.** Conidiomata and conidial masses on pine needle and SNA, respectively. **E–I.** Conidiophores, conidiogenous cells and conidia. **J–M.** Appressoria. **N.** Conidia. Scale bars = 10 µm.

tapering towards a ± acute or slightly rounded apex and a usually truncate base, with a similar radian, 11.5–18.5 × 2.5–4 µm (av. ± SD = 16.4 ± 1.7 × 3.1 ± 0.3 µm), L/W ratio = 5.3. *Appressoria* discrete or gregarious, brown, smooth-walled, subglobose, obovoid, clavate with truncate base, or sometimes irregularly shaped, lobed, 6–9.5 × 3.5–7 µm (av. ± SD = 8.1 ± 0.9 × 5.3 ± 0.8 µm).

Typus: **China**, Tibet, Bomi county, Suotong village, on an unidentified species of *Poaceae*, 13 Jun. 2015, F. Liu, BM12 (**holotype** HMAS 350630, ex-type culture CGMCC 3.20534 = LC7364 = LJM48).

Additional material examined: **China**, Tibet, Bomi county, Suotong village, on *Poaceae*, 13 Jun. 2015, F. Liu, BM12, living culture LC7366.

Notes: *Colletotrichum tibetense* belongs to the *C. graminicola* species complex (Fig. 1) and is characterised by slow growth rate on PDA (21–24 mm diam in 7 d) and abundant sporulation. It morphologically differs from the closely related species *C. dolichoconidiophori* (Figs 1, 3) in producing longer conidiogenous cells (19.5–32.5 × 2 µm *vs.*6–23 × 2–4 µm), shorter conidia (11.5–18.5 × 2.5–4 µm *vs.*19–27.5 × 2.5–3.5 µm), and with a lower conidium L/W ratio (5.3 *vs.*8). The closest matches revealed by BLASTn search using the *act*, *chs-1*, *sod2*, *tub2*, and ITS sequences of the ex-type strain LC7364 were *C. cereale* (92.7 %), *C. hanaui* (95 %), *C. sublineola* (86.3 %), *C. navitas* (89.3 %), and *C. tofieldiae* (99.8 %), respectively.

Colletotrichum variabile F. Liu, W.P. Wu & L. Cai, ***sp. nov.*** MycoBank MB 841400. Fig. 35.

Etymology: Named to reflect the variable length of conidiogenous cells.

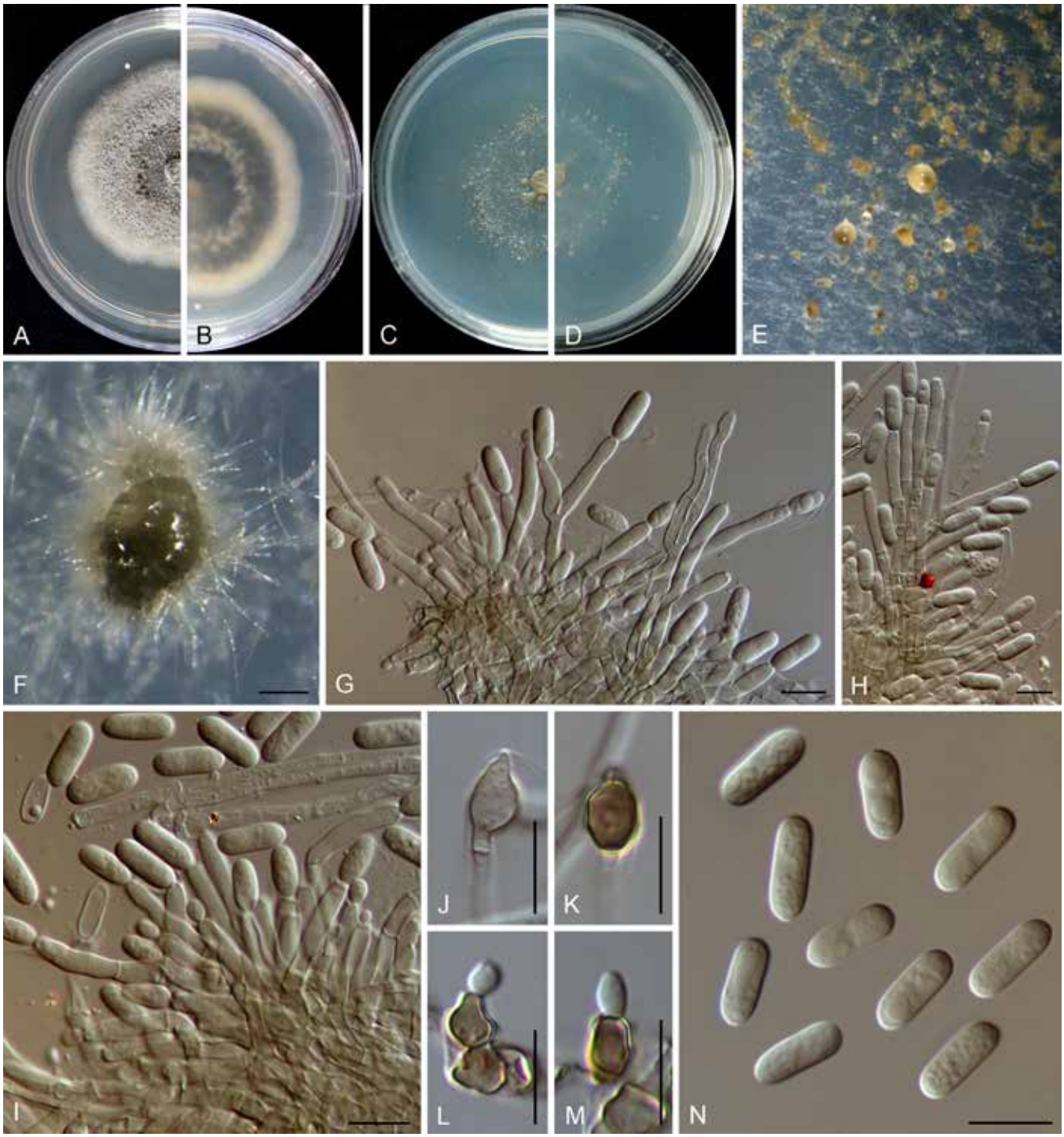

Fig. 33. *Colletotrichum telosmae* (ex-type culture NN052858). **A, B.** Front and reverse colony on PDA (7 d). **C, D.** Front and reverse colony on SNA (7 d). **E, F.** Conidial masses on SNA. **G–I.** Conidiophores, conidiogenous cells and conidia. **J–M.** Appressoria. **N.** Conidia. Scale bars: F = 100 µm; G–N = 10 µm.

Description: *Colonies* on PDA 42 mm diam in 7 d, flat with entire edge, white to pale saffron, aerial mycelium sparse, reverse pale saffron with a black region in the centre. On PDA, *conidiomata* and setae not observed. *Conidial masses* salmon, formed among the aerial mycelium. *Conidiophores* formed directly from the aerial mycelium, hyaline, branched, 1–5-septate. *Conidiogenous cells* cylindrical to subcylindrical, rarely ovoid, hyaline, 9–34 × 4–5.5 µm. *Conidia* hyaline, smooth-walled, guttulate, cylindrical with obtuse ends, sometimes slightly narrowed at the centre, becoming 1–3-septate with age, (16–)19–27.5 × 4.5–7 µm, av. ± SD = 22.5 ± 2.2 × 6.0 ± 0.6 µm, L/W ratio = 3.8. *Appressoria* irregular outline with crenate or lobed margin, clavate, brown, 7.5–9 × 4.5–5.5 µm.

Typus: **China**, Yunnan Province, Kunming, Kunming Botanical Garden, from healthy leaves of an unknown plant, 20 Dec. 1993, W.P. Wu (**holotype** HMAS 350644, ex-type culture CGMCC 3.20535 = LC13875 = NN040656).

Notes: *Colletotrichum variabile* belongs to the *C. gigasporum* species complex. It shares low sequence similarity with the phylogenetically related species *C. subvariabile sp. nov.* at *act* (95.2 %), *chs-1* (97.2 %), *gapdh* (94.2 %), *his3* (95 %), *tub2* (97.9 %), and ITS (97.8 %), and differs from that species in that it produces longer conidiogenous cells (9–34 µm *vs.*2–12 µm). In addition, *C. variabile* differs from other species in the *C. gigasporum* species complex in the mode of conidiophore and conidium formation (directly on the aerial mycelia *vs.*on a cushion of cells).

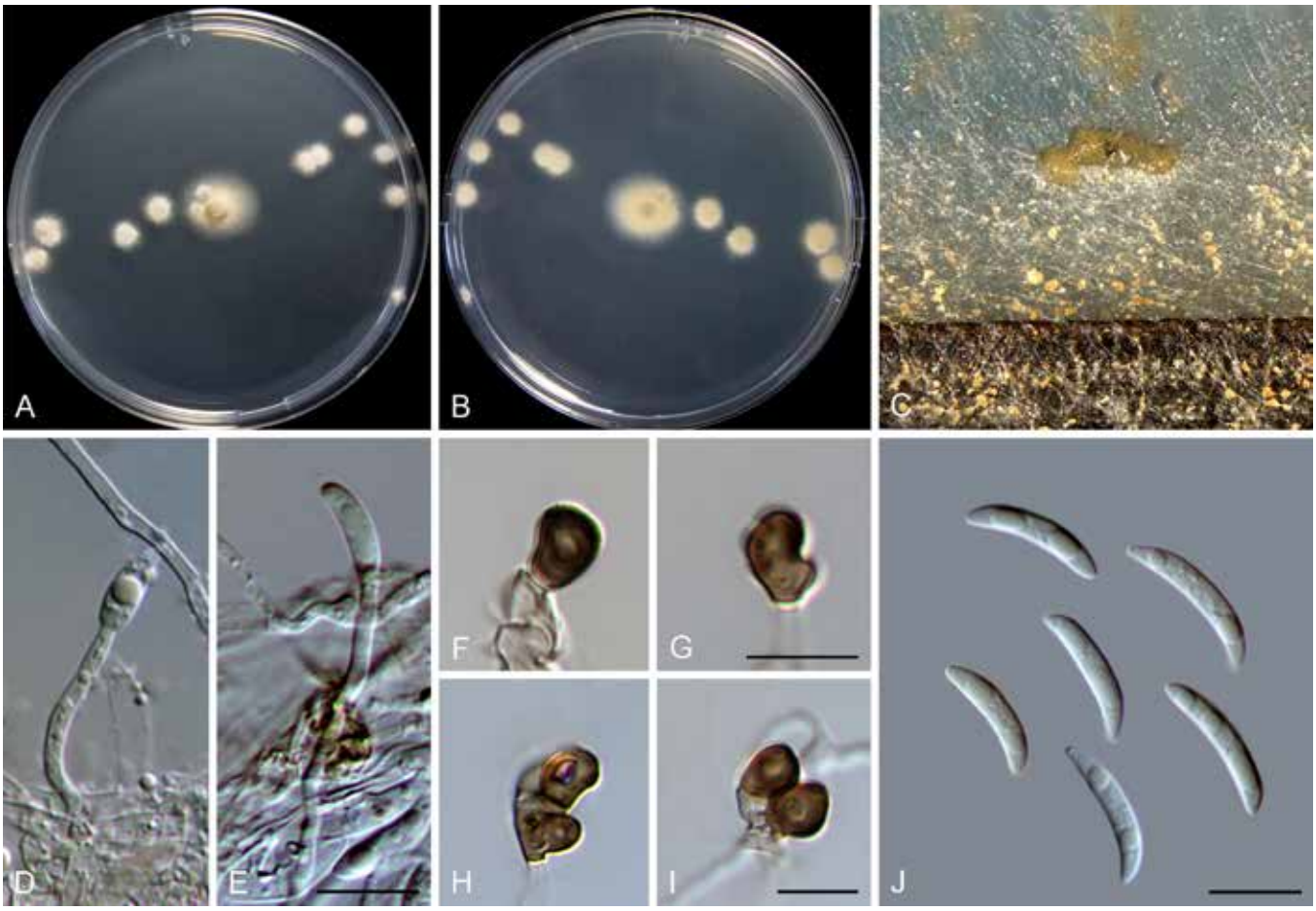

Fig. 34. *Colletotrichum tibetense* (ex-type culture LC7364). **A, B.** Front and reverse colony on PDA (6 d). **C.** Conidial masses on pine needle and SNA. **D, E.** Conidiogenous cells and conidia. **F–I.** Appressoria. **J.** Conidia. Scale bars = 10 µm. Scale bar of E applies to D, E; G applies to F, G; I applies to H, I.

Colletotrichum zhaoqingense F. Liu & L. Cai, ***sp. nov.*** MycoBank MB 841401. Fig. 36.

Etymology: Named after the location at which the fungus was collected, Zhaoqing.

Description: *Colonies* on PDA 52 mm diam in 7 d, flat with entire edge, medium to dark mouse grey, aerial mycelium floccose, reverse dark mouse grey. On SNA, *conidiomata* acervular, scattered, semi-immersed to immersed, protruding hyaline or salmon conidial masses, surrounded by dark brown setae. *Setae* 1–4-septate, 66–112 µm long, basal cells cylindrical, sometimes conical, smooth-walled, 5–6.5 µm diam, tip acute. *Conidiophores* formed from a cushion of roundish to angular pale brown cells, or formed directly on aerial mycelium, solitary or branched, septate, hyaline to pale brown, 0–4-septate. *Conidiogenous cells* cylindrical, rarely ovoid, hyaline to pale brown, 10–22 × 4.5–8 µm. *Conidia* hyaline, smooth-walled, guttulate, cylindrical with obtuse ends, 20–24 × 5.5–7 µm, av. ± SD = 21.3 ± 0.9 × 6.3 ± 0.6 µm, L/W ratio = 3.4. *Appressoria* variable in shape, globose, subglobose, ovoid, or irregular outline with a crenate or lobed margin, pale brown, 5.5–18 × 3.5–6.5 µm.

Typus: **China**, Zhejiang Province, Hangzhou Botanical Garden, on dead petiole of an unidentified palm (*Arecaceae*), 12 Jun. 2015, W.P. Wu (**holotype** HMAS 350646, ex-type culture CGMCC 3.20536 = LC13878 = NN071035).

Additional materials examined: **China**, Guangdong Province, Zhaoqing, Seven Star Cave (Qixingyan), on *Musa* sp., 24 Dec. 2012, W.P. Wu, living culture NN055284; Guangzhou, on *Carica papaya*, 10 Dec. 2013, W.P. Wu, living culture NN057644; Zhejiang Province, Hangzhou Botanical Garden, on dead petiole of palm (*Arecaceae*), 12 Jun. 2015, W.P. Wu, living cultures LC13877 (= NN058985), LC13879 (= NN071036).

Notes: *Colletotrichum zhaoqingense* forms a sister clade to *C. gigasporum* (Fig. 1), but differs morphologically from the latter in producing smaller conidia (20–24 × 5.5–7 µm *vs.*22–32 × 6–9 µm) (Liu *et al.* 2014). Furthermore, on the molecular level, these two species share low sequence similarity at *chs-1* (98 %), *gapdh* (97.3 %), and ITS (93.2 %).

Colletotrichum zhejiangense F. Liu, W.P. Wu & L. Cai, ***sp. nov.*** MycoBank MB 841402. Fig. 37.

Etymology: Named after the location at which the fungus was collected, Zhejiang Province.

Description: *Colonies* on PDA 34–35 mm diam in 7 d, flat with crenate edge, grey to purple slate, aerial mycelium dense, reverse violet slate with grey margin. *Conidiomata* black, columnar, straight, conidial masses hyaline. *Conidiophores* formed from a cushion of elliptical or angular and medium brown cells, branched, septate, hyaline to pale brown. *Setae* brown to olivaceous black, smooth-walled, 1–3-septate, 45–139 µm long, basal cells cylindrical to slightly conical, 4–8 µm diam, tip acute or round. *Conidiogenous cells* smooth-walled, cylindrical, 5.5–11.5 × 2.5–4.5 µm (av. ± SD = 8.8 ± 1.9 × 3.5 ± 0.5 µm). *Conidia* hyaline, aseptate, smooth-walled, curved, central part almost straight with parallel walls, gradually tapering towards the ends with a similar radian, 20.5–

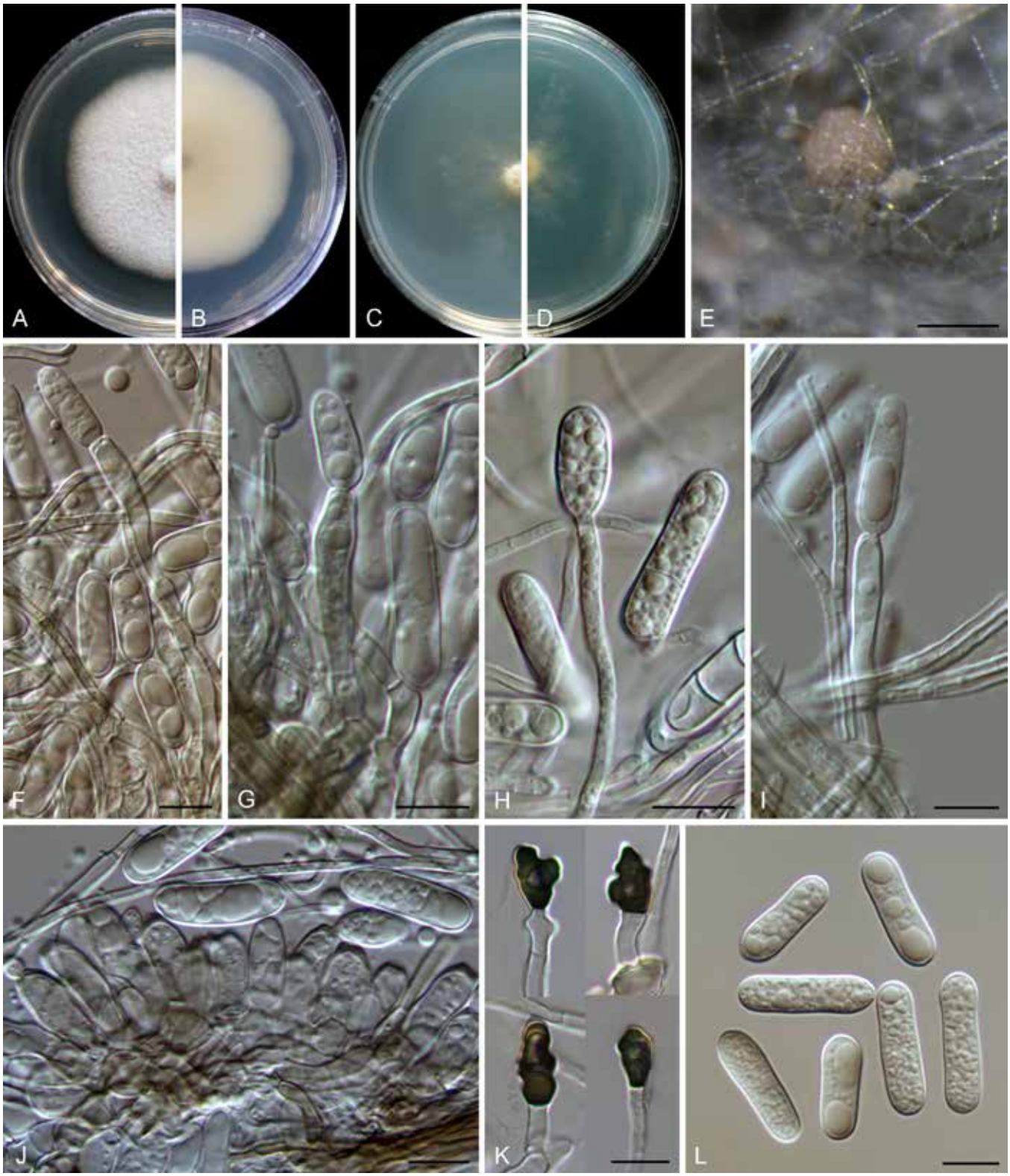

Fig. 35. *Colletotrichum variabile* (ex-type culture NN040656). **A, B.** Front and reverse colony on PDA (7 d). **C, D.** Front and reverse colony on SNA (7 d). **E.** Conidial mass. **F–J.** Conidiophores, conidiogenous cells and conidia. **K.** Appressoria. **L.** Conidia. Scale bars = 10 µm.

24.5 × 3–4 µm (av. ± SD = 22 ± 0.9 × 3.3 ± 0.2 µm), L/W ratio = 6.7. *Appressoria* not observed.

Typus: **China**, Zhejiang Province, Chun'an County, Qiandao Lake, on dead leaves of an unidentified tree, 18 Oct. 2018, W.P. Wu (**holotype** HMAS 350652, ex-type culture CGMCC 3.20537 = LC13887 = NN076215).

Notes: *Colletotrichum zhejiangense* belongs to the *C. dematium* species complex (Figs 1, S1), and is characterised by typical curved conidia with parallel walls in the middle, as is also observed for other species in this group. BLASTn search of *C. zhejiangense* sequences in the NCBI GenBank revealed very low sequence similarity with other species; the closest matches of the *act*, *chs-1*, *gapdh*, ITS and *tub2* sequences were *C. fructi* (89.1 % identity), *C. insertae* (94.4 %), *C. lineola* (68.9 %), *C. fructi* (98.6 %) and *C. dematium* (89.2 %), respectively.

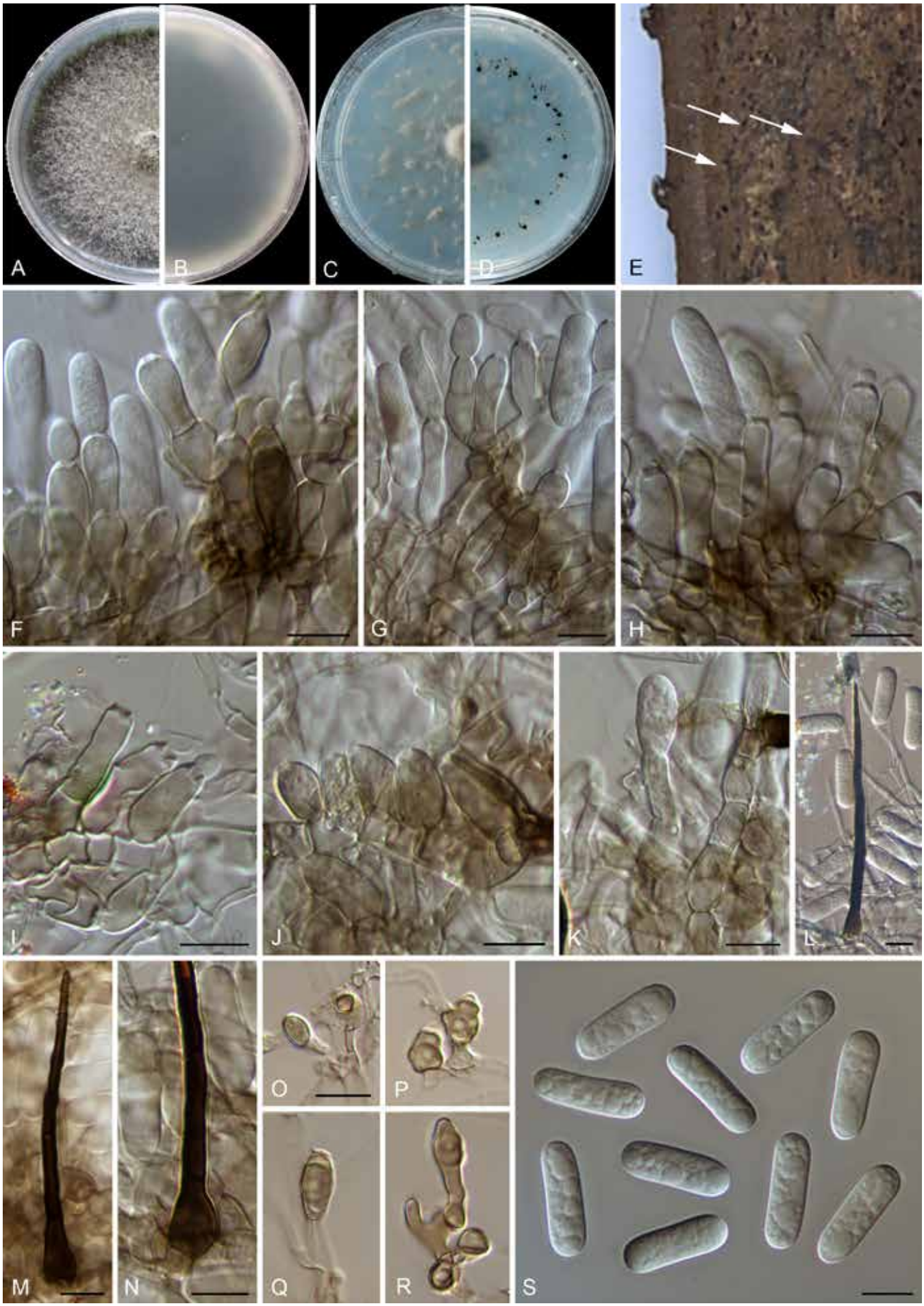

Fig. 36. *Colletotrichum zhaoqingense* (A–D, I–L, N–S: ex-type culture NN058985, E–H, M: NN071035). **A, B.** Front and reverse colony on PDA (7 d). **C, D.** Front and reverse colony on SNA (7 d). **E.** Conidiomata (black) on dead petiole of palm. **F–K.** Conidiophores, conidiogenous cells and conidia. **L–N.** Setae. **O–R.** Appressoria. **S.** Conidia. Scale bars: F–O, S = 10 µm. Scale bar of O applies to O–R.

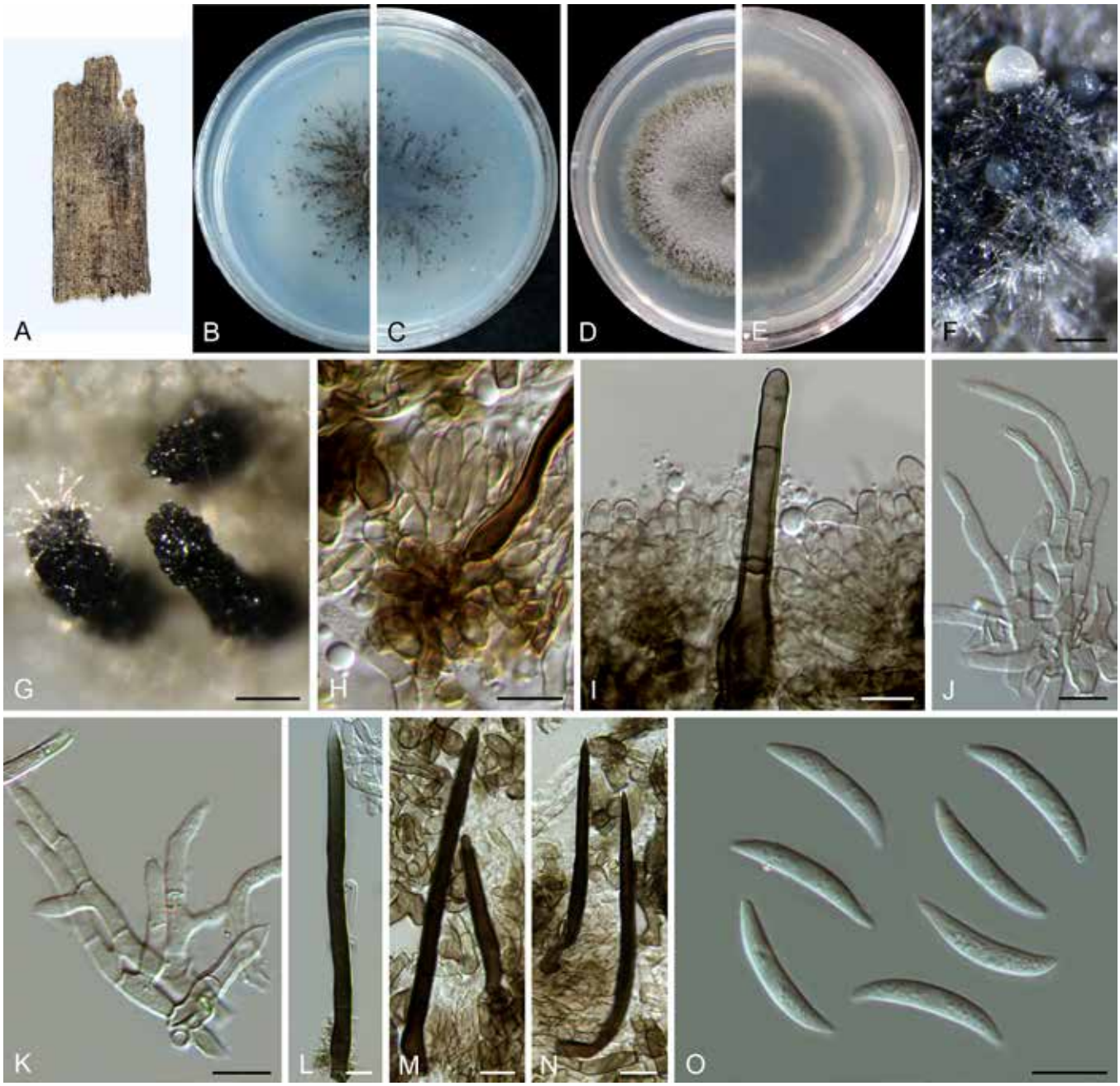

Fig. 37. *Colletotrichum zhejiangense* (ex-type culture NN076215). **A.** Symptom on the dead leaf of an unidentified tree. **B, C.** Front and reverse colony on SNA (7 d). **D, E.** Front and reverse colony on PDA (7 d). **F, G.** Conidiomata. **H, I.** Conidiophores, conidiogenous cells and setae. **J, K.** Conidiophore-like hyphae. **L–N.** Setae. **O.** Conidia. Scale bars: F, G = 100 µm; H–O = 10 µm.

Species diversity of *Colletotrichum* in China

In the current study, based on BLASTn searches and phylogenetic analyses of single-, multi-locus and whole-genome sequences, 1 008 strains were assigned to 107 species, belonging to 16 species complexes and 10 singletons (Fig. 38), of which 97 were isolated in China (Tables S5, S6). The majority of analysed strains belong to the *C. gloeosporioides* species complex (Fig. 38). However, because of the unavailability of ApMat and *gs* sequences for some taxa in the *C. gloeosporioides* species complex, species identification in this group was difficult or unfeasible. Hence, only tentative identification was provided for 183 strains in the current study. Among all the identified species, *C. siamense* was the most common taxon, followed by *C. karsti*, *C. fructicola*, *C. truncatum*, *C. fioriniae*, and *C. gloeosporioides* (Fig. 39).

Furthermore, we summarised the host-association data for *Colletotrichum* species from China, that were retrieved from 224 peer-reviewed papers published in 2009 or later (Table S6), and in which the species had been identified employing a modern classification approach. As of 1 Apr. 2021, 139 species belonging to 15 species complexes and 10 singleton species have been reported in China, including the 30 new species and 18 new records reported in the current study (Table S6, Fig. 38). The top six most common species listed in the preceding paragraph are also the species with the widest host range in China (Fig. 39). On the other hand, 76 species have to date been reported from a single plant species or genus (Table S6).

DISCUSSION

In the current study, we generated 67 type-derived sequences for known *Colletotrichum* species that were omitted or have been erroneously sequenced in various previous publications. This helped

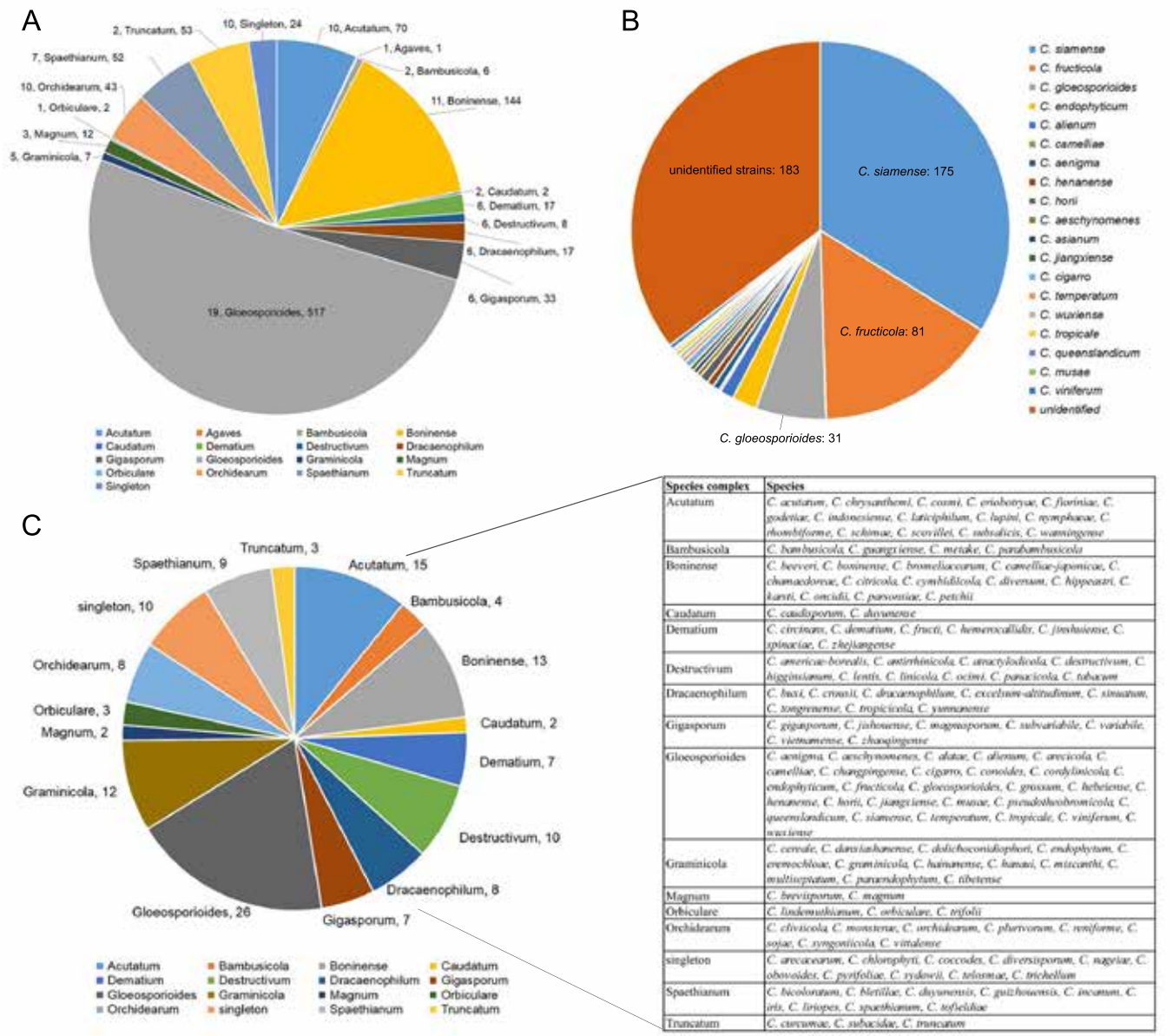

Species complex	Species
Acutatum	*C. acutatum, C. chrysanthemi, C. cosmi, C. eriobotryae, C. floriniae, C. godetiae, C. indonesiense, C. lineolatum, C. lupini, C. nymphaeae, C. rhombiforme, C. schimae, C. scovillei, C. subrufilicis, C. wanningense*
Bambusicola	*C. bambusicola, C. guangxiense, C. menke, C. parabambusicola*
Boninense	*C. beeveri, C. boninense, C. bromeliacearum, C. camelliae-japonicae, C. chamaedoreae, C. citricola, C. cymbidiicola, C. diversum, C. hippeastri, C. karsti, C. orchidi, C. parsonsiae, C. petchii*
Caudatum	*C. caudisporum, C. shivwense*
Dematium	*C. circinans, C. dematium, C. fructi, C. hemerocallidis, C. jinshuiense, C. spinaciae, C. zhejiangense*
Destructivum	*C. americae-borealis, C. antirrhinicola, C. amaryllidicola, C. destructivum, C. higginsianum, C. lentis, C. limicola, C. ocimi, C. panaciicola, C. tabacum*
Dracaenophilum	*C. baci, C. cronartii, C. dracaenophilum, C. excelsum-altitudinum, C. simmondsii, C. songmenense, C. tropicicola, C. yunnanense*
Gigasporum	*C. gigasporum, C. jiahuense, C. magnisporum, C. subvariabile, C. variabile, C. vietnamense, C. zhaoqingense*
Gloeosporioides	*C. aenigma, C. aeschynomenes, C. alatae, C. alienum, C. arecicola, C. camelliae, C. changpingense, C. cigarro, C. conoides, C. cordylinicola, C. endophyticum, C. fructicola, C. gloeosporioides, C. grossum, C. henanense, C. horii, C. jiangxiense, C. musae, C. pseudothwboromicola, C. queenslandicum, C. siamense, C. temperatum, C. tropicale, C. viniferum, C. wuxiense*
Graminicola	*C. cereale, C. darrisiahamense, C. dolichoconidiophori, C. endophytum, C. eremochloae, C. graminicola, C. hainanense, C. hanaui, C. miscanthi, C. multiseptatum, C. paraendophytum, C. tibetense*
Magnum	*C. brevisporum, C. magnum*
Orbiculare	*C. lindemuthianum, C. orbiculare, C. trifolii*
Orchidearum	*C. clidiicola, C. monsterae, C. orchidearum, C. plurivorum, C. reniforme, C. sojae, C. syngoniicola, C. vitalense*
singleton	*C. arecacearum, C. chlorophyti, C. coccodes, C. diversisporum, C. nagriae, C. obovoides, C. pyrifoliae, C. sydowii, C. teleosmae, C. trichellum*
Spaethianum	*C. bicoloratum, C. blastilae, C. dioscoreae, C. guizhouense, C. incanum, C. iris, C. liriopes, C. spaethianum, C. tofieldiae*
Truncatum	*C. curcumae, C. subaciculare, C. truncatum*

Fig. 38. Statistics of *Colletotrichum* strains and species in this study. **A.** Proportion of all 1 008 strains analysed in this study (left: number of species, right: number of strains). **B.** Proportion of the 517 strains (right: number of strains) of species in the *C. gloeosporioides* species complex analysed in this study. **C.** Proportion and summary of species within each species complex distributed in China based on this and previous studies (right: number of species).

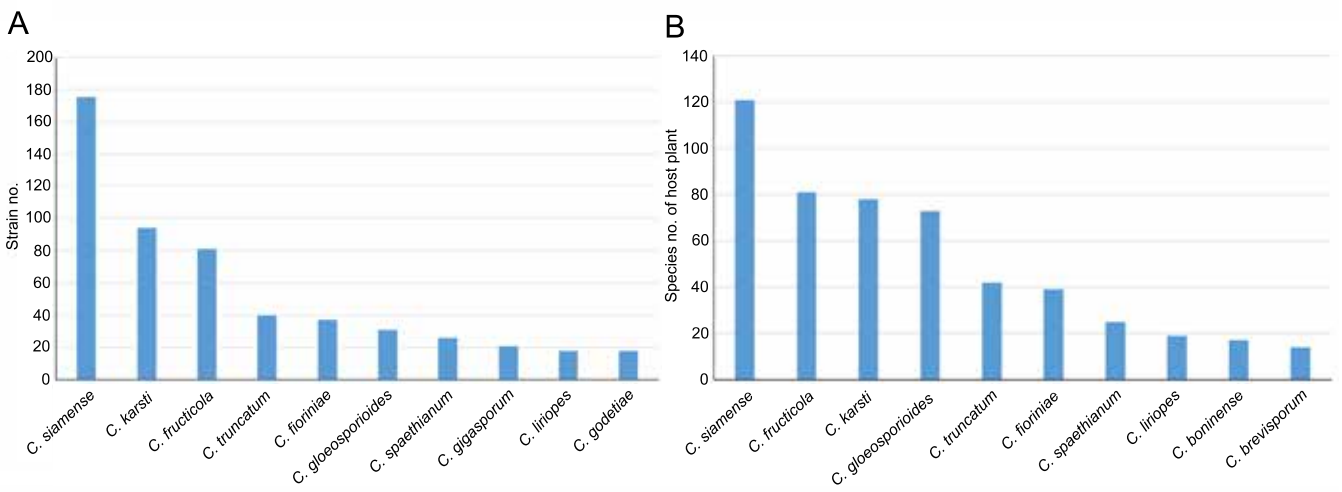

Fig. 39. Statistics of *Colletotrichum* species in this study. **A.** The most common ten species identified in this study. **B.** The ten species with the widest host range in China based on this study.

to clarify the existing taxonomic confusion (*e.g. C. liaoningense* and *C. ochraceae*), and also greatly contributed to the reconstruction of a robust backbone tree for *Colletotrichum*. Nevertheless, the identity of a few ambiguous species is still pending clarification, as we were unable to obtain their type or type-derived DNA, *e.g.* in the case of *C. chiangraiense*, *C. jasminigenum*, and *C. quinquefoliae.* Several strains that had been isolated from different bamboo hosts form a distinct clade in the multi-locus phylogeny (Fig. 1), which we refer to as the *C. bambusicola* species complex. The strains previously identified as *C. metake* and *C. hsienjenchang* (Sato *et al.* 2012) do not include type material, and hence their identity has not yet been clarified. Furthermore, the *C. metake* strains neither originate from the type location (Italy) nor from the host that *C. metake* was originally described on (*Arundinaria japonica*, Saccardo 1908), and might even represent more than one species. The two species will be examined in detail in a subsequent study (U. Damm, unpub. data). Overall, together with the 30 species newly described in the current study, 265 of the 280 *Colletotrichum* species were herein assigned to 16 species complexes, with the remaining 15 species regarded as singletons (Fig. 1, Tables S1–S3).

Among the 16 species complexes, the *C. acutatum*, *C. boninense*, and *C. gloeosporioides* species complexes contain more species than the other species complexes. Coincidentally, most strains analysed in the current study belong to these three species complexes (Fig. 38), with more than half (518/1 008) belonging to the *C. gloeosporioides* species complex. Although the combined use of ApMat and *gs* is very effective in resolving species in the *C. gloeosporioides* species complex (Liu *et al.* 2015), we did not employ the two loci in the multi-locus analyses herein, as they had been only rarely sequenced from species in other species complexes. To date, 51 species for which DNA sequence data are available have been accepted in the *C. gloeosporioides* species complex (Fig. 1); however, the species boundaries are still not well defined for several species. For example, the sequences of the six loci analysed and even whole-genome sequences of *C. kahawae s. str.* and its closest relatives (*C. cigarro*, *C. fructivorum*, *C. hedericola*, *C. helleniense*, *C. kahawae*, *C. rhexiae* and *C. jiangxiense*), *C. conoides* and *C. hebeiense*, *C. wuxiense* and *C. temperatum*, and *C. cobbitiiense* and *C. ti* exhibit very few nucleotide differences (Liu *et al.*, unpub. data). Hence, resolution of the taxonomy of the *C. gloeosporioides* species complex requires a further in-depth study, preferably involving whole-genome data.

Based on the findings of the current study, data retrieved from the USDA fungal database (Farr & Rossman 2021), and data from previous studies (Table S6), we observed that *Colletotrichum* species vary widely with respect to host specificity and host range, although determination of the host range is somewhat biased as pathogenic fungi have received much more attention to date than endophytes and saprobes. Species with both broad and narrow host range are found in most species complexes (Crouch *et al.* 2014, Table S6), especially in the *C. acutatum*, *C. boninense* and *C. gloeosporioides* species complexes. In contrast, species in the *C. caudatum* and *C. graminicola* species complexes are exclusively associated with monocots, and mostly restricted to single species or members of the *Poaceae* (Crouch *et al.* 2009a, 2014). Comparative genomic analyses indicate that host specificity may be related to gene family contractions (Baroncelli *et al.* 2016), loss of functional genes (Gan *et al.* 2016, Stajich 2017), and maintenance of a targeted arsenal of virulence factors (O'Connell *et al.* 2012). In-depth comparative genomic and transcriptomic analyses, as well as verification experiments of functional genes, are required to elucidate the molecular mechanisms of host specialisation and expansion.

Many *Colletotrichum* species have been isolated from healthy plant tissue and are referred to as endophytes, of which some are also known to be plant pathogenic. However, this does not necessarily imply that all endophytes can switch to a necrotrophic lifestyle (Cannon *et al.* 2012), and distinguishing between the two life strategies is difficult. According to Bhunjun *et al.* (2021), 16 out of the 40 endophytic *Colletotrichum* species can cause disease symptoms in host plants. Our large-scale survey revealed only three additional necrotrophs among the previously known endophytic species (*C. caudisporum*, *C. duyunensis*, and *C. metake*) (Table S7). By contrast, six newly described species (*C. buxi*, *C. chamaedoreae*, *C. nageiae*, *C. schimae*, *C. telosmae*, and *C. variabile*) have been isolated exclusively as endophytes to date. This largely implies that some of the 33 *Colletotrichum* species that are currently reported as endophytes only (Table S7) might live as beneficial organisms in the host plant and may not cause plant disease.

Although morphological characters are insufficient to distinguish *Colletotrichum* species, they are considered as important taxonomic characters for the identification of species to species complexes (Cannon *et al.* 2012). For example, conidia of most species in the *C. acutatum* species complex have acute ends or at least one acute end (Damm *et al.* 2012a); conidia of most species in the *C. gigasporum* species complex are notably larger than those formed by other species complexes (Liu *et al.* 2014); and typical conidia of *C. boninense* species complex are cylindrical with a prominent basal scar (Damm *et al.* 2012b). However, many species in various species complexes (*e.g.* the *C. dracaenophilum*, *C. magnum*, and *C. orchidearum* species complexes), as well as singleton species, form cylindrical conidia with round ends, which is regarded as a typical feature of the *C. gloeosporioides* complex (Damm *et al.* 2019). A schematic overview of the typical conidium and ascospore features of each *Colletotrichum* species complex is provided in Fig. 40. In general, species of the *C. acutatum*, *C. bambusicola*, *C. boninense*, *C. dracaenophilum*, *C. gigasporum*, *C. gloeosporioides*, *C. magnum*, *C. orbiculare*, and *C. orchidearum* species complexes produce straight conidia, while species in the *C. caudatum*, *C. dematium*, *C. graminicola*, *C. spaethianum*, and *C. truncatum* species complexes produce curved conidia (Damm *et al.* 2012a, b, 2013, 2014, 2019, 2020, Weir *et al.* 2012, Yang *et al.* 2012, Crouch 2014, Liu *et al.* 2014, 2015, Jayawardena *et al.* 2016, Liu 2016, Fu *et al.* 2019, Zhang *et al.* 2020). Of note, species complexes with curved conidia are scattered throughout the phylogenetic tree, which indicates that curved spores may have evolved more than once within the genus.

The ITS and multi-locus trees constructed in the current study are consistent with previous reports that the species complexes in *Colletotrichum* are monophyletic except for the *C. graminicola* species complex (Cannon *et al.* 2012, Marin-Felix *et al.* 2017, Bhunjun *et al.* 2021). In the multi-locus phylogenetic tree of the current study (Fig. 1), the *C. graminicola* species complex is inclusive of the *C. caudatum* species complex residing at the top of the clade. However, morphologically, the *C. caudatum* species complex is easily differentiated from the *C. graminicola* species complex by the formation of a filiform appendage at the apex of the curved conidia (Crouch 2014, Fig. 40). Initially, we suspected that this incongruence might be a consequence of the largely incomplete sequence dataset for this group. Specifically, the *his3*/*gapdh* sequences of most species in the *C. graminicola* species complex, and those of *gapdh*/*chs-1*/*his3*/*act*/*tub2* of most species in the *C. caudatum* species complex are unavailable, and treated as missing data in the alignments (*e.g.* Marin-Felix *et al.* 2017, Bhunjun *et al.* 2021, and the current study). However, the subsequent species tree based on 1 893 single-copy orthologous

Fig. 40. An illustration of the diversity of conidia and ascospores in different species complexes of *Colletotrichum*. **A, B.** Acutatum (**A.** Conidia of *C. schimae*, NN046984; **B.** Ascospores of *C. salicis*, CBS 607.94). **C.** Agaves (Conidia of *C. agaves*, CBS 118190). **D, E.** Bambusicola (**D.** Conidia of *C. bambusicola*, LC8468; **E.** Ascus and ascospores of *C. bambusicola*, LC8533). **F, G.** Boninense (**F.** Conidia of *C. chamaedoreae*, NN052885; **G.** Ascus and ascospores of *C. chamaedoreae*, NN052885). **H.** Caudatum (Conidia of *C. shivasii*, BRIP 15842a). **I.** Dematium (Conidia of *C. zhejiangense*, NN076215). **J.** Destructivum (Conidia of *Colletotrichum* sp., LC8517). **K.** Dracaenophilum (Conidia of *C. buxi*, NN047139). **L, M.** Gigasporum (**L.** Conidia of *C. magnisporum*, CBS 398.84; **M.** Ascospores of *C. pseudomajus*, CBS 571.88). **N, O.** Gloeosporioides (**N.** Conidia of *C. gloeosporioides*, CGMCC 3.17360; **O.** Ascospores of *C. alienum*, CBS 115183). **P.** Graminicola (Conidia of *C. multiseptatum*, NN055357). **Q.** Magnum (Conidia of *C. magnum*, CGMCC 3.17616). **R.** Orbiculare (Conidia of *C. orbiculare*, CBS 570.97). **S,T.** Orchidearum (**S.** Conidia of *C. orchidearum*, CBS 135131; **T.** Ascospores of *C. reniforme*, LC8230). **U.** Spaethianum (Conidia of *C. iris*, LC3697). **V.** Truncatum (Conidia of *C. subacidae*, LC13857). Scale bars = 10 µm.

genes (Fig. 4) revealed the same topology of this group as that in the multi-locus tree (Fig. 1). It is therefore most likely that species in the *C. caudatum* species complex are descendants of a common ancestor of the *C. graminicola* species complex, from which evolved a filiform appendage at the conidial apex. The two species complexes probably should be regarded as one species complex (the *C. graminicola-caudatum* species complex) as proposed by Bhunjun *et al.* (2021), or as *C. caudatum* sub-aggregate in the *C. graminicola* species complex, as proposed by Crouch (2014).

Although ITS is generally useful for assigning *Colletotrichum* species to species complexes, the allocation of a few individual species within the *C. bambusicola*, *C. caudatum*, *C. destructivum*, *C. graminicola*, and *C. spaethianum* species complexes somewhat contradicts that achieved by using multiple loci. For example, *C. riograndense*, a member of the *C. spaethianum* species complex according to the six-locus phylogeny (Fig. 1), is basal to the *C. bambusicola* and *C. spaethianum* species complexes in the ITS tree (Fig. S1). By contrast, the affiliation of species to species complexes is much more congruent between the six-locus tree and the whole-genome tree (Fig. 4), except for the *C. spaethianum* species complex, which is divided into two subclades in the genome tree. These contradictions among the single- and six-locus gene trees, and the genome tree might result from incomplete lineage sorting, horizontal gene transfer, and hybridisation or recombination through speciation events (Degnan & Rosenberg 2009).

By 3 June 2021, 207 whole genomes of 69 *Colletotrichum* species (Table S4) have been deposited in the NCBI and JGI databases, representing 24.6 % of the currently accepted *Colletotrichum* species. Whole-genome sequences of additional 48 species, including 30 new and 18 known species, were generated and assembled in the current study, increasing the number of genome-sequenced species to 116 (41.4 % of the species, Table S4). To better define the species complex boundaries and reveal the evolutionary relationship of *Colletotrichum*, we generated a whole-genome-based phylogenetic tree in this study. In accordance with the six-locus tree (Fig. 1), most species complexes formed well-supported clades in the species tree, except for the *C. spaethianum* species complex, which did not form a monophyletic clade. As expected, the *C. boninense* and *C. gloeosporioides* species complexes with a large number of species and a wide range of hosts had generally larger number of genes and CAZymes (Fig. 4). This is consistent with the conclusion of Baroncelli *et al.* (2016) that host range is associated with gene family expansion and contraction in *Colletotrichum*. However, the numbers of genes and CAZymes greatly varied among species in the *C. acutatum* species complex, another species rich group with broad host range. For example, *C. godetiae*, associated with at least 18 genera of host plants (Farr & Rossman 2021), possesses the smallest genome size and number of genes, CAZymes and transporters of this genus (Fig. 4). Considering the importance of the genus *Colletotrichum*, we recommend genome sequencing of all species, especially those plant and human pathogens. This effort will not only pave the way toward a fully resolved *Colletotrichum* tree of life, but also provide essential data revealing their evolution and adaptation mechanisms, and improve the understanding of the genetic basis of various biological features and metabolic potential of these fungi.

ACKNOWLEDGEMENTS

We thank Yuanying Su, Wei Sun, Qian Chen, Zhifeng Zhang, Dianming Hu, Parinn Noireung, Dimuthu S. Manamgoda, Dhanushka Udayanga, Junmin Liang and Roger Shivas for providing assistance in sample sharing and culture collection. We also acknowledge Pedro W. Crous for his support on the taxonomy of phytopathogenic fungi and Clement K.M. Tsui for his comments and suggestions on this manuscript. Hui Li, Haoning Qiu and Wanying Kang are thanked for their help on generating partial sequences. This study was financially supported by the National Natural Science Foundation of China (31725001 & 31770009), the Youth Innovation Promotion Association of Chinese Academy of Sciences (2021085), and the National Science and Technology Fundamental Resources Investigation Program of China (2021FY100900). Yongzhao Diao thanks the National Natural Science Foundation of China (31700436) for financial support.

DECLARATION ON CONFLICT OF INTEREST

The authors declare that there is no conflict of interest.

REFERENCES

Alexey G, Vladislav S, Nikolay V, *et al.* (2013). QUAST: quality assessment tool for genome assemblies. *Bioinformatics* **29**: 1072–1075.

Alfieri Jr SA, Langdon KR, Wehlburg C, *et al*. (1984). Index of Plant Diseases in Florida (revised). *Florida Department of Agriculture & Consumer Services, Division of Plant Industry, Bulletin* **11**: 1–389.

Andrews S, Babraham B (2010). FastQC: a quality control tool for high throughput sequence data. <http://www.bioinformatics.babraham.ac.uk/projects/fastqc>.

Armenteros JJA., Tsirigos KD, Sonderby CK, *et al.* (2019). SignalP 5.0 improves signal peptide predictions using deep neural networks. *Nature Biotechnology* **37**: 420–423.

Bankevich A, Nurk S, Antipov D, *et al*. (2012). SPAdes: a new genome assembly algorithm and its applications to single-cell sequencing. *Journal of Computational Biology* **19**: 455–477.

Baroncelli R, Amby DB, Zapparata A, *et al.* (2016). Gene family expansions and contractions are associated with host range in plant pathogens of the genus *Colletotrichum*. *BMC Genomics* **17**: 555.

Bhunjun CS, Phukhamsakda C, Jayawardena R, *et al.* (2021). Investigating species boundaries in *Colletotrichum*. *Fungal Diversity* **107**: 107–127.

Buchta V, Nekolová J, Jirásková N, *et al.* (2019). Fungal keratitis caused by *Colletotrichum dematium*: case study and review. *Mycopathologia* **184**: 441–453.

Cai L, Hyde KD, Taylor PWJ, *et al*. (2009). A polyphasic approach for studying *Colletotrichum*. *Fungal Diversity* **39**: 183–204.

Cannon PF, Damm U, Johnston PR, *et al.* (2012). *Colletotrichum* current status and future directions. *Studies in Mycology* **73**: 181–213.

Carbone I, Kohn LM (1999). A method for designing primer sets for speciation studies in filamentous ascomycetes. *Mycologia* **91**: 553–556.

Castresana J (2000). Selection of conserved blocks from multiple alignments for their use in phylogenetic analysis. *Molecular Biology and Evolution* **17**: 540–552.

Crouch JA, Clarke BB, White JFJ, *et al.* (2009a). Systematic analysis of the falcate-spored graminicolous *Colletotrichum* and a description of six new species from warm-season grasses. *Mycologia* **101**: 717–732.

Crouch JA, Tredway LP, Clarke BB, *et al.* (2009b). Phylogenetic and population genetic divergence correspond with habitat for the pathogen *Colletotrichum* cereale and allied taxa across diverse grass communities. *Molecular Ecology* **18**: 123–135.

Crouch JA (2014). *Colletotrichum caudatum s.l.* is a species complex. *IMA Fungus* **5**: 17–30.

Crouch J, O'Connell R, Gan P, *et al.* (2014). The genomics of *Colletotrichum*. In: *Genomics of plant-associated fungi*: *monocot pathogens* (Dean RA, Lichens-Park A, Kole C, eds). Springer-Verlag Berlin Heidelberg, Germany: 69–102.

Crous PW, Gams W, Stalpers JA, *et al.* (2004). MycoBank: an online initiative to launch mycology into the 21st century. *Studies in Mycology* **50**: 19–22.

Crous PW, Schumacher RK, Wingfield MJ, *et al.* (2018). New and interesting fungi. 1. *Fungal Systematics and Evolution* **1**: 169–215.

Crous PW, Verkley GJM, Groenewald JZ, *et al.* (eds) (2019). *Fungal Biodiversity*, 2nd ed. Westerdijk Fungal Biodiversity Institute, Utrecht, Netherlands [Westerdijk Laboratory Manual Series 1].

Damm U, Cannon PF, Woudenberg JHC, *et al.* (2012a). The *Colletotrichum acutatum* species complex. *Studies in Mycology* **73**: 37–113.

Damm U, Cannon PF, Woudenberg JHC, *et al.* (2012b). The *Colletotrichum boninense* species complex. *Studies in Mycology* **73**: 1–36

Damm U, Cannon PF, Liu F, *et al.* (2013). The *Colletotrichum orbiculare* species complex: Important pathogens of field crops and weeds. *Fungal Diversity* **61**: 29–59.

Damm U, O'Connell RJ, Groenewald JZ, *et al.* (2014). The *Colletotrichum destructivum* species complex – hemibiotrophic pathogens of forage and field crops. *Studies in Mycology* **79**: 49–84.

Damm U, Sato T, Alizadeh A, *et al.* (2019). The *Colletotrichum dracaenophilum*, *C. magnum* and *C. orchidearum* species complexes. *Studies in Mycology* **92**: 1–46.

Damm U, Sun YC, Huang CJ (2020). *Colletotrichum eriobotryae sp. nov.* and *C. nymphaeae*, the anthracnose pathogens of loquat fruit in central Taiwan, and their sensitivity to azoxystrobin. *Mycological Progress* **19**: 367–380.

Damm U, Woudenberg JHC, Cannon PF, *et al.* (2009). *Colletotrichum* species with curved conidia from herbaceous hosts. *Fungal Diversity* **39**: 45–87.

Darriba D, Taboada GL, Doallo R, *et al.* (2011). ProtTest 3: fast selection of best-fit models of protein evolution. *Bioinformatics* **27**: 1164–1165.

Dean R, van Kan JA, Pretorius ZA, *et al.* (2012). The Top 10 fungal pathogens in molecular plant pathology. *Molecular Plant Pathology* **13**: 414–430.

Degnan JH, Rosenberg NA (2009). Gene tree discordance, phylogenetic inference and the multispecies coalescent. *Trends in Ecology & Evolution* **24**: 332–340.

Diao YZ, Zhang C, Liu F, *et al.* (2017). *Colletotrichum* species causing anthracnose disease of chili in China. *Persoonia* **38**: 20–37.

Duke MM (1928). The genera *Vermicularia* Fr. and *Colletotrichum* Cda. *Transactions of the British Mycological Society* **13**: 156–184.

Emanuelsson O, Nielsen H, Brunak S, *et al.* (2000). Predicting subcellular localization of proteins based on their N-terminal amino acid sequence. *Journal of Molecular Biology* **300**: 1005–1016.

Emms DM, Kelly S (2019). OrthoFinder: phylogenetic orthology inference for comparative genomics. *Genome Biology* **20**: 238.

Farr DF, Rossman AY (2021). *Fungal Databases, U.S. National Fungus Collections, ARS, USDA*. <https: //nt.ars-grin.gov/fungaldatabases/>. Accessed on 16 March 2021.

Ferraris T (1902). Materiali per una flora micologica del Piemonte. Miceti raccolti nei dintorni di Crescentino. Seconda contribuzione. *Malpighia* **16**: 1–46.

Fu M, Crous PW, Bai Q, *et al.* (2019). *Colletotrichum* species associated with anthracnose of *Pyrus* spp. in China. *Persoonia* **42**: 1–35.

Gan P, Narusaka M, Kumakura N, *et al.* (2016). Genus-wide comparative genome analyses of *Colletotrichum* species reveal specific gene family losses and gains during adaptation to specific infection lifestyles. *Genome Biology and Evolution* **8**: 1467–1481.

Garud AB (1968). An anthracnose disease of pineapple in India. *Plant Disease Reporter* **52**: 436–437.

Glass NL, Donaldson GC (1995). Development of primer sets designed for use with the PCR to amplify conserved genes from filamentous ascomycetes. *Applied and Environmental Microbiology* **61**: 1323–1330.

Guarro J, Svidzinski TE, Zaror L, *et al.* (1998). Subcutaneous hyalohyphomycosis caused by *Colletotrichum gloeosporioides*. *Journal of Clinical Microbiology* **36**: 3060–3065.

Guo LD, Hyde KD, Liew ECY (2000). Identification of endophytic fungi from *Livistona chinensis* based on morphology and rDNA sequences. *New Phytologist* **147**: 617–630.

Guerber JC, Liu B, Correll JC, *et al.* (2003). Characterization of diversity in *Colletotrichum acutatum sensu lato* by sequence analysis of two gene introns, mtDNA and intron RFLPs, and mating compatibility. *Mycologia* **95**: 872–895.

Haridas S, Albert R, Binder M, *et al.* (2020). 101 *Dothideomycetes* genomes: A test case for predicting lifestyles and emergence of pathogens. *Studies in Mycology* **96**: 141–153.

Hennings P (1905). Fungi Amazonici IV. a cl. Ernesto Ule collecti (Appendix). *Hedwigia* **44**: 57–71.

Hou LW, Liu F, Duan WJ, *et al.* (2016). *Colletotrichum aracearum* and *C. camelliae-japonicae*, two holomorphic new species from China and Japan. *Mycosphere* **7**: 1111–1123.

Huelsenbeck JP, Ronquist F (2001). MrBayes: Bayesian inference of phylogeny. *Bioinformatics* **17**: 754–755.

Huerta-Cepas J, Forslund K, Coelho LP, *et al.* (2017). Fast genome-wide functional annotation through orthology assignment by eggNOG-Mapper. *Molecular Biology and Evolution* **34**: 2115–2122.

Hyde KD, Nilsson RH, Alias SA *et al.* (2014). One stop shop: backbones trees for important pytopathogenic genera: I. *Fungal Diversity* **67**: 21–125.

Hyde KD, Zhang Y (2008). Epitypification: should we epitypify? *Journal of Zhejiang University Science B* **9**: 842–846.

Jayawardena RS, Hyde KD, Damm U, *et al.* (2016). Notes on currently accepted species of *Colletotrichum*. *Mycosphere* **7**: 1192–1260.

Jayawardena RS, Hyde KD, Chen YJ, *et al.* (2020). One stop shop IV: taxonomic update with molecular phylogeny for important phytopathogenic genera: 76–100. *Fungal Diversity* **103**: 87–218.

Katoh K, Standley DM (2013). MAFFT multiple sequence alignment software version 7: improvements in performance and usability. *Molecular Biology and Evolution* **30**: 772–780.

Krogh A, Larsson B, von Heijne G, *et al.* (2001). Predicting transmembrane protein topology with a hidden Markov model: Application to complete genomes. *Journal of Molecular Biology* **305**: 567–580.

Kumar S, Stecher G, Tamura K (2016). MEGA7: molecular evolutionary genetics analysis version 7.0 for bigger datasets. *Molecular Biology and Evolution* **33**: 1870–1874.

Kwon JH, Kim J (2013). First report of anthracnose on *Rohdea japonica* caused by *Colletotrichum liriopes* in Korea. *Plant Disease* **97**: 559.

Lee SY, Jung HY (2018). *Colletotrichum kakivorum sp. nov.*, a new leaf spot pathogen of persimmon in Korea. *Mycological Progress* **17**: 1113–1121.

Li GJ, Hyde KD, Zhao RL *et al.* (2016). Fungal diversity notes 253–366: taxonomic and phylogenetic contributions to fungal taxa. *Fungal Diversity* **78**: 1–237.

Liu F (2016). *Taxonomy and biodiversity of Colletotrichum* Ph.D. dissertation. University Utrecht, The Netherlands.

Liu F, Cai L, Crous PW, *et al.* (2014). The *Colletotrichum gigasporum* species complex. *Persoonia* **33**: 83–97.

Liu F, Wang M, Damm U, *et al.* (2016). Species boundaries in plant pathogenic fungi: a *Colletotrichum* case study. *BMC Evolutionary Biology* **16**: 81.

Liu F, Weir BS, Damm U, *et al.* (2015). Unravelling *Colletotrichum* species associated with *Camellia*: employing ApMat and GS loci to resolve species in the *C. gloeosporioides* complex. *Persoonia* **35**: 63–86.

Liu XJ, Xie X, Duan J (2007). *Colletotrichum yunnanense sp. nov.*, a new endophytic species from *Buxus* sp. *Mycotaxon* **100**: 137–144

Ma X, Nontachaiyapoom S, Jayawardena RS (2018). Endophytic *Colletotrichum* species from *Dendrobium* spp. in China and Northern Thailand. *MycoKeys* **43**: 23–57.

Manire CA, Rhinehart HL, Sutton DA, *et al.* (2002). Disseminated mycotic infection caused by *Colletotrichum acutatum* in a Kemp's ridley sea turtle (*Lepidochelys kempi*). *Journal of Clinical Microbiology* **40**: 4273–4280.

Marcelino J, Giordano R, Gouli S *et al.* (2008). *Colletotrichum acutatum* var. *fioriniae* (teleomorph: *Glomerella acutata* var. *fioriniae var. nov.*) infection of a scale insect. *Mycologia* **100**: 353–374.

Marin-Felix Y, Groenewald JZ, Cai L *et al.* (2017). Genera of phytopathogenic fungi: GOPHY 1. *Studies in Mycology* **86**: 99–216.

Mathieu S, Mosè M, Evgeny MZ (2019). BUSCO: assessing genome assembly and annotation completeness. *Methods in Molecular Biology* **1962**: 227–245.

Miller MA, Pfeiffer W, Schwartz T (2012). The CIPRES science gateway: enabling high-impact science for phylogenetics researchers with

limited resources. In: *Proceedings of the 1st conference of the extreme science and engineering discovery environment*: *Bridging from the extreme to the campus and beyond.* Association for Computing Machinery, USA: 1–8.

Miller JW (1992). Bureau of Plant Pathology. *Tri-ology Technical Report Of Division, Plant Industry, Florida* **31**: 5–8.

Moktali V, Park J, Fedorova-Abrams ND, *et al*. (2012). Systematic and searchable classification of cytochrome P450 proteins encoded by fungal and oomycete genomes. *BMC Genomics* **13**: 525.

Moriwaki J, Tsukiboshi T (2009). *Colletotrichum echinochloae*, a new species on Japanese barnyard millet (*Echinochloa utilis*). *Mycoscience* **50**: 273–280.

Nirenberg HI (1976). Untersuchungen über die morphologische und biologische Differenzierung in der *Fusarium*-Sektion Liseola. *Mitteilungen aus der Biologischen Bundesanstalt für Land- und Forstwirtschaft Berlin-Dahlem* **169**: 1–117.

Nylander JAA (2004). *MrModeltest v2. Program distributed by the author.* Evolutionary Biology Centre, Uppsala University, Sweden.

O'Donnell K, Cigelnik E (1997). Two divergent intragenomic rDNA ITS2 types within a monophyletic lineage of the fungus *Fusarium* are nonorthologous. *Molecular Phylogenetics and Evolution* **7**: 103–116.

O'Connell RJ, Thon MR, Hacquard S *et al.* (2012). Life-style transitions in plant pathogenic *Colletotrichum* fungi deciphered by genome and transcriptome analyses. *Nature Genetics* **44**: 1060–1065.

Palmer JM (2016). Funannotate: pipeline for genome annotation. <https: // funannotate.readthedocs.io/en/latest/index.html>.

Patterson W (1900). New species of fungi. *Bulletin of the Torrey Botanical Club* **27**: 282–286.

Raabe RD, Conners IL, Martinez AP (1981). *Checklist of plant diseases in Hawaii.* College of Tropical Agriculture and Human Resources, University of Hawaii, USA.

Rayner RW (1970). *A Mycological Colour Chart.* Commonwealth Mycological Institute, Kew, UK.

Ronquist F, Huelsenbeck JP (2003). MrBayes 3: Bayesian phylogenetic inference under mixed models. *Bioinformatics* **19**: 1572–1574.

Samarakoon MC, Persoh D, Hyde KD, *et al.* (2018). *Colletotrichum acidae sp. nov.* from northern Thailand and a new record of *C. dematium* on *Iris* sp. *Mycosphere* **9**: 583–597.

Saccardo PA (1908). Notae mycologicae. Series X. *Annales Mycologici* **6**: 553–569.

Saier MH, Reddy VS, Tsu BV, *et al*. (2016). The Transporter Classification Database (TCDB): recent advances. *Nucleic Acids Research* **44**: D372–D379.

Sato T, Moriwaki J, Uzuhashi S, *et al*. (2012). Molecular phylogenetic analyses and morphological re-examination of strains belonging to three rare *Colletotrichum* species in Japan. *Microbiology and Culture Collections* **28**: 121–134.

Shiraishi A, Araki-Sasaki A, Mitani A, *et al.* (2011). Clinical characteristics of keratitis due to *Colletotrichum gloeosporioides*. *Journal of Ocular Pharmacology and Therapeutics* **27**: 487–491.

Shivaprakash MR, Appannanavar SB, Dhaliwal M, *et al.* (2011). *Colletotrichum truncatum*: an unusual pathogen causing mycotic keratitis and endophthalmitis. *Journal of Clinical Microbiology* **49**: 2894–2898.

Silva DN, Talhinhas P, Várzea V, *et al.* (2012). Application of the Apn2/MAT locus to improve the systematics of the *Colletotrichum gloeosporioides* complex: an example from coffee (*Coffea* spp.) hosts. *Mycologia* **104**: 396–409.

Sperschneider J, Gardiner DM, Dodds PN, *et al*. (2016). EffectorP: predicting fungal effector proteins from secretomes using machine learning. *New Phytologist* **210**: 743–761.

Stajich JE (2017). Fungal genomes and insights into the evolution of the kingdom. *Microbiol Spectrum* **5**: FUNK-0055-2016.

Stamatakis A (2014). RAxML version 8: a tool for phylogenetic analysis and post-analysis of large phylogenies. *Bioinformatics* **30**: 1312–1313.

Tao G, Liu ZY, Liu F, *et al.* (2013). Endophytic *Colletotrichum* species from *Bletilla ochracea* (*Orchidaceae*), with descriptions of seven new species. *Fungal Diversity* **61**: 139–164.

Wang Q, Liu F, Hou CL, *et al.* (2021). Species of *Colletotrichum* on bamboos from China. *Mycologia* **113**: 450–458.

Weir BS, Johnston PR, Damm U (2012). The *Colletotrichum gloeosporioides* species complex. *Studies in Mycology* **73**: 115–180.

White TJ, Bruns TD, Lee S, *et al*. (1990). Amplification and direct sequencing of fungal ribosomal RNA genes for phylogenetics. In: *PCR protocols*: *a guide to methods and applications* (White TJ, Sninsky JJ, Gelfand DH, *et al*., eds). Academic Press, San Diego, USA: 315–322.

Wikee S, Cai L, Pairin N, *et al*. (2011). *Colletotrichum* species from Jasmine (*Jasminum sambac*). *Fungal Diversity* **46**: 171–182.

Yang Y, Liu Z, Cai L, *et al.* (2012). New species and notes of *Colletotrichum* on daylilies (*Hemerocallis* spp.). *Tropical Plant Pathology* **37**: 165–174.

Yang YL, Liu ZY, Cai L, *et al.* (2009). *Colletotrichum* anthracnose of *Amaryllidaceae*. *Fungal Diversity* **39**: 123–146.

Yang Y, Cai L, Liu Z, *et al.* (2011). *Colletotrichum* species on *Orchidaceae* in southwest China. *Cryptogamie, Mycologie* **32**: 229–253.

Yin Y, Mao X, Yang J, *et al*. (2012). dbCAN: a web resource for automated carbohydrate-active enzyme annotation. *Nucleic Acids Research* **40**: W445–W451.

Zhang K, Su YY, Cai L (2013). An optimized protocol of single spore isolation for fungi. *Cryptogamie, Mycologie* **34**: 349–356.

Zhang W, Damm U, Crous PW, *et al.* (2020). Anthracnose disease of carpetgrass (*Axonopus compressus*) caused by *Colletotrichum hainanense sp. nov. Plant Disease* **104**: 1744–1750.

Zhou S, Qiao L, Jayawardena RS, *et al.* (2019). Two new endophytic *Colletotrichum* species from *Nothapodytes pittosporoides* in China. *MycoKeys* **49**: 1–14.

Supplementary Material: https://studiesinmycology.org/

Fig. S1. Phylogenetic tree of *Colletotrichum* resulting from the RAxML analysis of the ITS sequence alignment. Bootstrap support values (1 000 replicates, GTR-GAMMA model) > 50 % are shown at the nodes. The scale bar represents the expected number of changes per site. Species complexes are indicated with coloured boxes, their names are listed at the left. Ex-type strains are indicated with "T" in the end of the taxa labels.

Table S1. DNA barcodes of all accepted *Colletotrichum* spp. except for the ones in the *C. graminicola* and *C. caudatum* species complexes.

Table S2. DNA barcodes of the accepted *Colletotrichum* spp. in the *C. caudatum* species complex.

Table S3. DNA barcodes of the accepted *Colletotrichum* spp. in the *C. graminicola* species complex.

Table S4. *Colletotrichum* species for which whole-genome sequences are available, retrieved from NCBI and JGI, or generated in the current study.

Table S5. All strains identified in the current study.

Table S6. The substrate/host information for *Colletotrichum* species analysed in the current study, and host information of species reported in China retrieved from literature.

Table S7. *Colletotrichum* species reported as endophytes in previous publications and in the current study.

Studies in Mycology 101: 57–120 (2022).

Generic boundaries in the *Ophiostomatales* reconsidered and revised

Z.W. de Beer[1#], M. Procter[1#], M.J. Wingfield[1], S. Marincowitz[1], T.A. Duong[1*]

[1]*Department of Biochemistry, Genetics & Microbiology; Forestry and Agricultural Research Institute (FABI), University of Pretoria, Pretoria 0002, South Africa*

[#]These authors contributed equally to this work
[*]*Corresponding author*: tuan.duong@fabi.up.ac.za

Abstract: The *Ophiostomatales* was erected in 1980. Since that time, several of the genera have been redefined and others have been described. There are currently 14 accepted genera in the Order. They include species that are the causal agents of plant and human diseases and common associates of insects such as bark beetles. Well known examples include the Dutch elm disease fungi and the causal agents of sporotrichosis in humans and animals. The taxonomy of the *Ophiostomatales* was confused for many years, mainly due to the convergent evolution of morphological characters used to delimit unrelated fungal taxa. The emergence of DNA-based methods has resolved much of this confusion. However, the delineation of some genera and the placement of various species and smaller lineages remains inconclusive. In this study we reconsidered the generic boundaries within the *Ophiostomatales*. A phylogenomic framework constructed from genome-wide sequence data for 31 species representing the major genera in the Order was used as a guide to delineate genera. This framework also informed our choice of the best markers from the currently most commonly used gene regions for taxonomic studies of these fungi. DNA was amplified and sequenced for more than 200 species, representing all lineages in the Order. We constructed phylogenetic trees based on the different gene regions and assembled a concatenated data set utilising a suite of phylogenetic analyses. The results supported and confirmed the delineation of nine of the 14 currently accepted genera, *i.e. Aureovirgo, Ceratocystiopsis, Esteya, Fragosphaeria, Graphilbum, Hawksworthiomyces, Ophiostoma, Raffaelea* and *Sporothrix*. The two most recently described genera, *Chrysosphaeria* and *Intubia*, were not included in the multi-locus analyses. This was due to their high sequence divergence, which was shown to result in ambiguous taxonomic placement, even though the results of phylogenomic analysis supported their inclusion in the *Ophiostomatales*. In addition to the currently accepted genera in the *Ophiostomatales*, well-supported lineages emerged that were distinct from those genera. These are described as novel genera. Two lineages included the type species of *Grosmannia* and *Dryadomyces* and these genera are thus reinstated and their circumscriptions redefined. The descriptions of all genera in the *Ophiostomatales* were standardised and refined where this was required and 39 new combinations have been provided for species in the newly emerging genera and one new combination has been provided for *Sporothrix*. The placement of *Afroraffaelea* could not be confirmed using the available data and the genus has been treated as *incertae sedis* in the *Ophiostomatales*. *Paleoambrosia* was not included in this study, due to the absence of living material available for this monotypic fossil genus. Overall, this study has provided the most comprehensive and robust phylogenies currently possible for the *Ophiostomatales*. It has also clarified several unresolved One Fungus-One Name nomenclatural issues relevant to the Order.

Key words: Generic boundaries, new taxa, nomenclature, *Ophiostomataceae*, *Ophiostomatales, Sordariomycetidae,* taxonomy.
Taxonomic novelties: New genera: *Harringtonia* Z.W. de Beer & M. Procter, *Heinzbutinia* Z.W. de Beer & M. Procter, *Jamesreidia* Z.W. de Beer & M. Procter, *Masuyamyces* Z.W. de Beer & M. Procter. **New species:** *Masuyamyces massonianae* M. Procter & Z.W. de Beer. **New combinations:** *Dryadomyces montetyi* (M. Morelet) M. Procter & Z.W. de Beer, *Dryadomyces quercivorus* (Kubono & Shin. Ito) M. Procter & Z.W. de Beer, *Dryadomyces quercus-mongolicae* (K.H. Kim *et al.*) M. Procter & Z.W. de Beer, *Dryadomyces sulphureus* (L.R. Batra) M. Procter & Z.W. de Beer, *Graphilbum pusillum* (Masuya) M. Procter & Z.W. de Beer, *Grosmannia abieticolens* (K. Jacobs & M.J. Wingf.) M. Procter & Z.W. de Beer, *Grosmannia altior* (Paciura *et al.*) M. Procter & Z.W. de Beer, *Grosmannia betulae* (Jankowiak *et al.*) M. Procter & Z.W. de Beer, *Grosmannia curviconidia* (Paciura *et al.*) M. Procter & Z.W. de Beer, *Grosmannia euphyes* (K. Jacobs & M.J. Wingf.) M. Procter & Z.W. de Beer, *Grosmannia fenglinhensis* (R. Chang *et al.*) M. Procter & Z.W. de Beer, *Grosmannia gestamen* (de Errasti & Z.W. de Beer) M. Procter & Z.W. de Beer, *Grosmannia innermongolica* (X.W. Liu *et al.*) M. Procter & Z.W. de Beer, *Grosmannia pistaciae* (Paciura *et al.*) M. Procter & Z.W. de Beer, *Grosmannia pruni* (Masuya & M.J. Wingf.) M. Procter & Z.W. de Beer, *Grosmannia taigensis* (Linnak. *et al.*) M. Procter & Z.W. de Beer, *Grosmannia trypodendri* (Jankowiak *et al.*) M. Procter & Z.W. de Beer, *Harringtonia aguacate* (D.R. Simmons *et al.*) M. Procter & Z.W. de Beer, *Harringtonia brunnea* (L.R. Batra) M. Procter & Z.W. de Beer, *Harringtonia lauricola* (T.C. Harr. *et al.*) Z.W. de Beer & M. Procter, *Heinzbutinia grandicarpa* (Kowalski & Butin) Z.W. de Beer & M. Procter, *Heinzbutinia microspora* (Arx) M. Procter & Z.W. de Beer, *Heinzbutinia solheimii* (B. Strzałka & Jankowiak) Z.W. de Beer & M. Procter, *Jamesreidia coronata* (Olchow. & J. Reid) M. Procter & Z.W. de Beer, *Jamesreidia nigricarpa* (R.W. Davidson) M. Procter & Z.W. de Beer, *Jamesreidia rostrocoronata* (R.W. Davidson & Eslyn) M. Procter & Z.W. de Beer, *Jamesreidia tenella* (R.W. Davidson) Z.W. de Beer & M. Procter, *Leptographium cainii* (Olchow. & J. Reid) M. Procter & Z.W. de Beer, *Leptographium europioides* (E.F. Wright & Cain) M. Procter & Z.W. de Beer, *Leptographium galeiforme* (B.K. Bakshi) M. Procter & Z.W. de Beer, *Leptographium pseudoeurophioides* (Olchow. & J. Reid) M. Procter & Z.W. de Beer, *Leptographium radiaticola* (J.J. Kim *et al.*) M. Procter & Z.W. de Beer, *Masuyamyces acarorum* (R. Chang & Z.W. de Beer) M. Procter & Z.W. de Beer, *Masuyamyces ambrosius* (B.K. Bakshi) M. Procter & Z.W. de Beer, *Masuyamyces botuliformis* (Masuya) Z.W. de Beer & M. Procter, *Masuyamyces jilinensis* (R. Chang *et al.*) M. Procter & Z.W. de Beer, *Masuyamyces lotiformis* (Z. Wang & Q. Lu) M. Procter & Z.W. de Beer, *Masuyamyces pallidulus* (Linnak. *et al.*) M. Procter & Z.W. de Beer, *Masuyamyces saponiodorus* (Linnak. *et al.*) M. Procter & Z.W. de Beer, *Sporothrix longicollis* (Massee & E.S. Salmon) M. Procter & Z.W. de Beer.

Citation: de Beer W, Procter M, Wingfield MJ, Marincowitz S, Duong TA (2022). Generic boundaries in the *Ophiostomatales* reconsidered and revised. *Studies in Mycology* **101**: 57–120. doi: 10.3114/sim.2022.101.02
Received: 18 August 2021; **Accepted:** 29 January 2022; **Effectively published online:** 30 March 2022
Corresponding editor: Robert A. Samson

Studies in Mycology

INTRODUCTION

The *Ophiostomatales* (*Sordariomycetidae, Ascomycota*), was described by Benny & Kimbrough (1980) accommodating the single family *Ophiostomataceae*. The Order includes species that are the causal agents of plant and human diseases as well as common associates of wood infesting insects such as bark beetles (Wingfield *et al*. 1993, Seifert *et al.* 2013). Well known examples are the Dutch elm disease fungi and the causal agents of sporotrichosis in humans and animals (Figs 1, 2). As described, this Order originally accommodated four genera, *Ophiostoma*, *Ceratocystiopsis*, *Sphaeronaemella* and *Ceratocystis*. These authors considered *Ceratocystis* distinct from *Ophiostoma* based on cell wall constituents and conidiogenesis (Weijman & De Hoog 1975, Seifert *et al.* 2013). Upadhyay (1981) treated *Ophiostoma* as a synonym of *Ceratocystis* based on morphological similarities such as their long-necked ascocarps that produce sheathed ascospores in sticky droplets to facilitate arthropod dispersal (Upadhyay 1981, Malloch & Blackwell 1993). In the 1990's, DNA sequence data confirmed that *Ophiostoma* and *Ceratocystis* resided in two distinct Orders of the fungi (Hausner *et al.* 1993c, Spatafora & Blackwell 1994). *Ceratocystis* has subsequently been shown to represent several morphologically and ecologically distinct genera in the *Ceratocystidaceae* (*Microascales*) (De Beer *et al.* 2013a, 2014, Nel *et al.* 2018, Mayers *et al.* 2015, 2020).

The *Ophiostomatales* as it is currently defined accommodates a single family, the *Ophiostomataceae* (De Beer *et al.* 2013a), which was initially described in 1932 (Nannfeldt 1932). At the time, it included *Ophiostoma*, with *Endoconidiophora* and *Ceratocystis* as synonyms (Melin & Nannfeldt 1934). The family was treated in various Orders prior to 1980 (De Beer *et al.* 2013a). Apparently unaware of Benny & Kimbrough's (1980) study, Upadhyay (1981) re-defined the *Ophiostomataceae* with *Ceratocystis* as type genus, and *Ophiostoma*, *Sphaeronaemella*, *Grosmannia* and *Europhium* as synonyms, and with *Ceratocystiopsis* as a distinct new genus. However, the DNA-based distinction between *Ceratocystis* and *Ophiostoma* led to their inevitable separation and emended definitions of the *Ceratocystidaceae* and *Ophiostomataceae* (Wingfield *et al.* 1993, Réblová *et al.* 2011, De Beer *et al.* 2013a, 2016a).

The first attempt to resolve generic boundaries within the *Ophiostomatales* subsequent to its separation from the *Ceratocystidaceae* was made by Zipfel *et al.* (2006). Based on phylogenies constructed from ribosomal DNA and β-tubulin sequences and including 55 taxa, they recognised *Ophiostoma, Ceratocystiopsis* and *Grosmannia* as distinct sexual genera. Following the dual nomenclature system at the time, asexual *Sporothrix* and *Leptographium* species retained their names in these genera, although they respectively grouped in *Ophiostoma* and *Grosmannia*.

After 20 years of DNA-based taxonomy and in the wake of the abandonment of a dual nomenclature for the fungi (Hawksworth *et al*. 2011, Hawksworth 2012), De Beer & Wingfield (2013) revised the *Ophiostomatales*, considering all published ribosomal large subunit (LSU) and internal transcribed spacer (ITS) sequences, including 266 species. They redefined *Ophiostoma sensu stricto*, *Raffaelea s.s.*, *Ceratocystiopsis*, *Fragosphaeria* and *Graphilbum*, and recognised 18 species complexes within the various genera of the *Ophiostomatales*. However, they concluded that the rDNA-based phylogenies were not sufficiently robust to resolve the generic status of the *Sporothrix schenckii-Ophiostoma stenoceras* species complex, or that of various lineages within what they defined as *Leptographium sensu lato*. Their phylogenies also suggested that ambrosial species previously treated as *Raffaelea* did not form a monophyletic group.

After the revision of the *Ophiostomatales* by De Beer & Wingfield (2013), the majority of studies focused on new species descriptions (Romón *et al.* 2014a, b, Musvuugwa *et al.* 2015, 2016, De Errasti *et al.* 2016, Simmons *et al.* 2016, Chang *et al.* 2017, Marincowitz *et al.* 2017, 2020, *etc*.) and on resolving issues within species complexes (Ando *et al.* 2016, Linnakoski *et al.* 2016, Jankowiak *et al.* 2017, Yin *et al.* 2019, 2020, *etc*.).

De Beer *et al.* (2016a) reconsidered the status of the *S. schenckii-O. stenoceras* complex, providing sequences for four gene regions of 65 species with sporothrix-like asexual morphs. They concluded that *Sporothrix* represented a distinct genus including 51 species and incorporated the characters of the sexual morphs of many of the species, previously treated as *Ophiostoma*, in the emended definition of *Sporothrix*. A lineage including some of the remaining sporothrix-like species that did not form part of the newly defined genus were provided with the new genus name, *Hawksworthiomyces*, in a subsequent paper (De Beer *et al.* 2016b). In addition, Van der Linde *et al.* (2016) and Bateman *et al.* (2017) described *Aureovirgo* and *Afroraffaelea* respectively as novel, monotypic genera in the Order. In 2018, a fungus was discovered preserved in amber alongside an ambrosia beetle, leading to the description of *Paleoambrosia.* The genus was treated in the *Ophiostomatales* based on morphological characters resembling *Raffaelea* species (Poinar & Vega 2018). Most recently, Nel *et al*. (2021) described two new genera, *Chrysosphaeria* and *Intubia*, from the abandoned combs of fungus-growing termites (*Termitomyces*) in South Africa.

In this study, we reconsidered and redefined the unresolved boundaries of genera including *Leptographium*, *Raffaelea* and some smaller lineages in the *Ophiostomatales*. To achieve this goal, we selected four gene regions based on a phylogenomic framework constructed from genome-wide sequence data for representative ophiostomatalean species. Sequence data for these four gene regions were then generated for as many species in the Order as possible, and phylogenetic analyses were conducted.

MATERIALS AND METHODS

Fungal isolates and DNA extraction

Fungal cultures used in this study were obtained from the Culture Collection (CMW) of the Forestry and Agricultural Biotechnology Institute (FABI), University of Pretoria, South Africa, and the Westerdijk Fungal Biodiversity Institute (CBS), Utrecht, the Netherlands. Isolates were grown on 2 % malt extract agar (MEA: 20 g malt extract, 20 g agar, 1 L dH_2O) at room temperature; initially with streptomycin (0.4 g/L, Sigma-Aldrich, Kempton Park, South Africa) and cycloheximide (0.5 g/L, Sigma-Aldrich, Kempton Park, South Africa) supplemented in the media, then sub-cultured to MEA, and maintained at 4 °C after optimal growth had occurred. DNA was extracted following the protocol described by Duong *et al.* (2012).

Phylogenomic analyses

Available genome sequences for 31 species representing 11 of 14 currently recognised genera (excluding *Afroraffaelea*, *Aureovirgo* and *Paleoambrosia*) in the *Ophiostomatales* (Supplementary

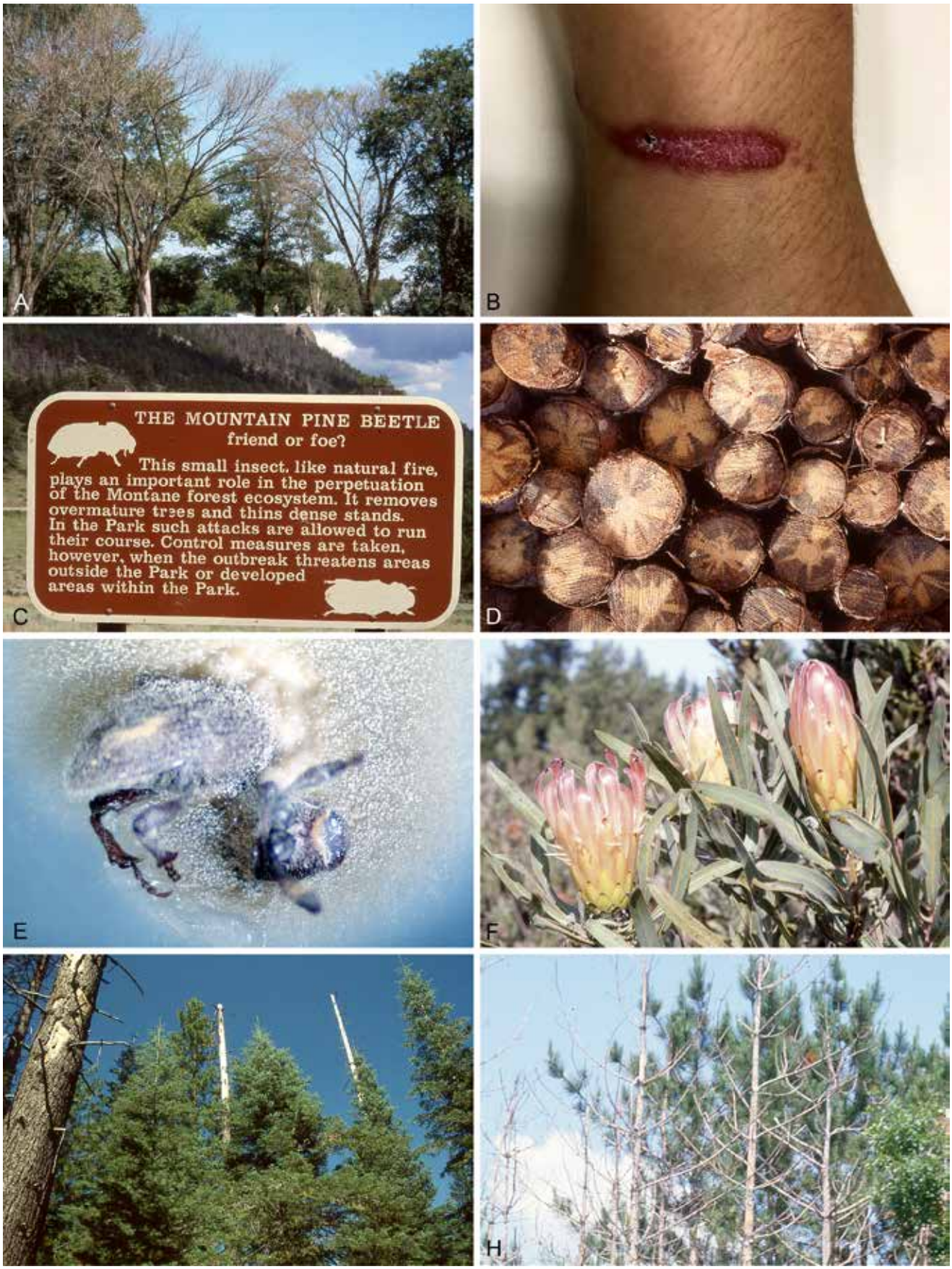

Fig. 1. Ecological niches in which genera and species residing in the *Ophiostomatales* are found. **A.** *Ulmus americana* street trees dying as a result of Dutch Elm Disease (photo: D.W. French). **B.** Symptoms of infection by the human pathogen *Sporothix schenckii* (photo: Prof. Dr Flávio de Queiroz Telles Filho, Federal University of Paraná, Brazil). **C.** Signage in Yellowstone National Park emphasising the important role that bark beetles (and by extension their fungal symbionts) play in the ecology of conifer ecosystems. **D.** Blue stain in conifer timber caused by numerous species of Ophiostomatoid fungi. **E.** *Hylobius rhizophagus* (root collar weevil) squashed onto the surface of agar medium containing cycloheximide selective for many genera and species of *Ophiostomatales* and in this case *Leptographium procerum*. **F.** Infructescences of a *Protea* species in which numerous species of Ophiostomatoid fungi can be found. **G.** Douglas fir (*Pseudotsuga menzesii*) trees dying as a result of black stain root disease caused by *Leptographium wageneri* var. *pseudotsugae* (Photo: F.W. Cobb). **H.** *Pinus resinosa* trees dying as a result of mass infestation by *Ips pini* and associated *Ophiostoma minus*.

Fig. 2. Ecological niches of Ophiostomatoid fungi and micrographs providing examples of structures typical of these fungi. **A.** Transverse stellate gallery systems of *Ips schmutzenhoferi* in the bark of a *Pinus spinulosa* tree, showing blue-stain around nuptial chambers and female galleries. **B.** Section through a *Eucalyptus* stem infested by the ambrosia beetle *Megaplatypus mutatus* showing tunnels in which species of *Ophiostomatales* occur. **C, D.** Ascomata of *Ophiostoma ulmi* (**C**) (photo: D.W. French) and *O. pilliferum* (**D**) (photo: Z.W. de Beer) with sticky ascospores masses at their apices, illustrating the manner by which these fungi easily attach to the insects that carry them. **E.** Conidiophores of *Leptographium procerum*, illustrating asexual structures well suited to being vectored by insects. **F.** Conidiogenous cells of a *Sporothrix* sp. **G.** Typical single-celled conidia found in most species of *Ophiostomatales.* **H.** Many species of *Ophiostomatales* have ascospores with sheaths such as these pillow-shaped spores in *Ophiostoma ips*.

Table S1) were used to construct a phylogenomic tree. Two species of *Diaporthales* (*Cryphonectria parasitica* and *Diaporthe ampelina*), two species of *Magnaporthales* (*Magnaporthe grisea* and *Magnaporthe poae*), and one species of *Togniniales* (*Phaeoacremonium minimum*) were included in the analyses as outgroup taxa. Genome assemblies for all species were subjected to BUSCO v. 4.0.5 (Seppey *et al.* 2019) runs using the Sordariomycetes_odb10 dataset to obtain BUSCO genes. The amino acid sequences were extracted from BUSCO results and datasets were compiled for each of the BUSCO orthologous groups. All BUSCO orthologous groups with duplicated BUSCO genes were excluded from the analysis. PRANK (Löytynoja 2014) was used to align the datasets with default parameters.

Trimal v. 1.4 (Capella-Gutiérrez *et al.* 2009) was used for trimming of the alignments with "-resoverlap 0.8 -seqoverlap 75" parameters. Only datasets with lengths equal or larger than 100 aa after trimming step were retained for further analysis. Permutation Tail Probability (PTP) tests were conducted in

PAUP v. 4.0a (Swofford 2003) to identify and remove datasets having no phylogenetic signal as well as those with less than 50 parsimony-informative characters. Individual gene trees for each BUSCO orthologous group were constructed using IQ-TREE v. 2 with an optimal substitution model automatically determined and 1 000 ultrafast bootstraps (Hoang *et al*. 2018, Minh *et al*. 2020). TreeShrink v. 1.3.7 (Mai & Mirarab 2018) was used to remove outliers (taxa with abnormal branch length) from all trees with default parameters. Newick utilities (Junier & Zdobnov 2010) was used to collapse branches with less than 10 % bootstrap support. A species tree was then constructed from the final set of trees under the multi-species coalescent model using ASTRAL v. 5.7.7 (Mirarab *et al.* 2014). Branch length of the species tree was optimized with RAxML v. 8.2.11 (Stamatakis 2014) using only BUSCO orthogroups that have all 36 taxa present and without any outliner taxon as identified with TreeShrink analysis.

Selection of gene regions for phylogenetic analyses

Sequences for eight gene regions commonly used in phylogenetic studies of the fungi were extracted from 31 draft genome sequences for species in the *Ophiostomatales,* as well as from those used as outgroups in the phylogenomic analysis (Supplementary Table S1). These included β-tubulin (*β-tub*), translation elongation factor 1 alpha (*TEF-1α*), internal transcribed spacer region (ITS), ribosomal large subunit (LSU), mini chromosome maintenance protein complex 7 (*MCM7*), DNA-directed RNA polymerase II second largest subunit (*RPBII*), DNA-directed RNA polymerase II largest subunit (*RPBI*) and ribosomal small subunit (SSU). A phylogenetic tree was constructed for each of these datasets using IQ-TREE v. 2 as indicated above. Based on the level of congruency between individual gene trees and the phylogenomic tree as well as the phylogenetic signal of these gene regions, the LSU, ITS, *TEF-1α* and *RPBII* gene regions were selected as markers to delineate genera in the *Ophiostomatales*. These regions included the primary (ITS) and secondary (*TEF-1α*) barcodes for fungi (Schoch *et al.* 2012, Stielow *et al.* 2015).

Primer selection

Existing primers were used to amplify and sequence the ITS (ITS1F: Gardes & Bruns 1993, ITS4: White *et al.* 1990), *TEF-1α* (EF2F: Marincowitz *et al.* 2015, EF2R: Jacobs *et al.* 2004) and LSU (LR5, LROR: Vilgalys & Hester 1990) gene regions. Since previously available primers for *RPBII* did not consistently amplify the targeted region in most of the isolates investigated, we designed new primers for this gene region based on the available genome sequences: Oph-RPB2F1 (5' - GAYGAYCGIGAYCAYTTYGG - 3'), Oph-RPB2F2 (5' - TICTGGCIAARCTNTTCCG - 3') and Oph-RPB2R1 (5' - CCCATRGCYTGYTTRCCCAT - 3'). A combination of Oph-RPBF1 and Oph-RPBR1 was used in most instances, while Oph-RPBF2 and Oph-RPBR1 were used in cases where the former combination was not successful.

PCR

For the ITS, *TEF-1α* and LSU regions, FastStart *Taq* DNA Polymerase (Roche, Germany) was used. For the *RPBII* gene region the Platinum® Multiplex PCR Master Mix (Applied Biosystems, Foster City, California) was used. The ITS, LSU and *TEF-1α* gene regions were amplified following the protocol described by Duong *et al.* (2012). For the *RPBII* gene region, the protocol provided with the Platinum® Multiplex PCR Master Mix was used but amended as follows: the PCR mixture was made up to a final volume of 12.5 µL, primers were added to a concentration of 1 µM each, and PCR was carried out with 40 cycles of denaturing at 94 °C for 30 s, annealing at 58 °C for 30 s, and elongation at 72 °C for 1 min.

Agarose gel electrophoresis (1 % agarose) was performed on all PCR products to confirm the success of amplification. PCR products were treated with ExoSAP (a mixture of exonuclease I and alkaline phosphatase; one unit of each enzyme was used for approximately 20 µL of PCR product). The mixture was then subjected to two incubation steps at 37 °C for 15 min (for enzymatic action) and 80 °C for 15 min (to deactivate the enzymes). The treated products were stored at 4 °C until PCR sequencing was carried out.

DNA sequencing

Sanger sequencing was performed for all ExoSAP treated PCR products. The PCR sequencing setup reaction (12 µL) consisted of 6.4 µL dH_2O, 2.1 µL 5× sequencing buffer, 0.5 µL BigDye v 3.1, 1 µL of the forward or reverse primer (10 mM), and 2 µL ExoSAP treated PCR product. The reaction was performed under the following conditions: 25 cycles of a denaturing step at 96 °C for 10 s, an annealing step at 55 °C for 5 s, and an elongation step at 60 °C for 4 min. The products were maintained at 4 °C until being used for precipitation.

PCR sequencing products were precipitated using the ethanol/NaOAc precipitation method. For each of the PCR sequencing products (total volume of 12 µL) 8 µL dH_2O, 2 µL NaOAc (3 M, pH 5.2) and 50 µL absolute ethanol (EtOH) was added. The tubes were incubated on ice for 10 min, then centrifuged at 13 400 rpm for 30 min at room temperature. After centrifugation, the supernatant was removed, and the pellet washed twice with 150 µL of 70 % EtOH and centrifuged for 10 min at 13 400 rpm at room temperature. After the final wash, the supernatant was removed, and the pellet was air-dried for approximately 15 min. The samples were kept at -20 °C until they could be analysed. The fragment separations were performed using an ABI PRISM® 3100 Genetic Analyzer (Applied Biosystems). Consensus sequences were derived from sequences obtained with forward and reverse primers. All sequences generated in this study have been submitted to GenBank, and those from ex-type isolates will be included in the RefSeq Targeted Loci (RTL) database in GenBank (Schoch *et al.* 2014).

Phylogenetic analyses

For species with available genome sequences (Supplementary Table S1), gene region data were extracted from assembled genome sequences. Sequences were downloaded from GenBank for newly described species for which cultures were not available during the study period, as well as for species for which our sequence data were incomplete. Datasets were aligned using the online version of MAFFT v. 7 (Katoh & Stanley 2013) with default parameters. Alignments were refined with an online version of Gblocks v. 0.91b (Castresana 2000) using default parameters – *i.e.* no alternative options for more or less stringent selection were selected. Datasets for the various gene regions obtained from Gblocks were concatenated using FASconCAT-G (Kück & Meusemann 2010). Partitionfinder v. 2.1.1 (Lanfear *et al.* 2017) was used to determine best substitution models for the combined dataset.

Maximum Likelihood (ML) analyses using RAxML (Stamatakis 2014) were performed separately for all gene regions and for the concatenated dataset with raxmlGUI v. 1.3 (Silvestro & Michalak

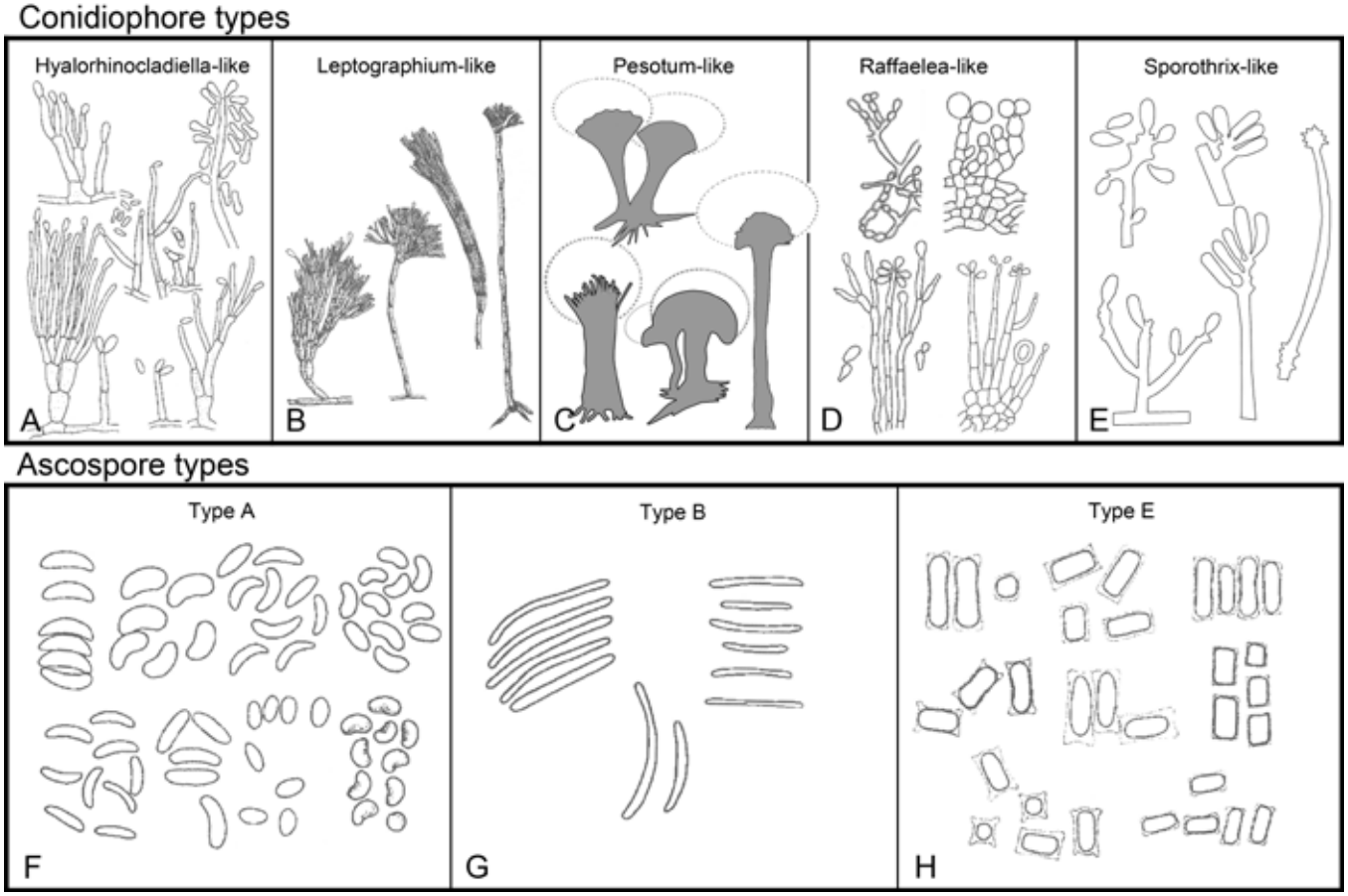

Fig. 3. Conidiophore and ascospore types mentioned in the paper. **A–E.** Conidiophore types. **F–H.** Ascospore types *sensu* De Beer & Wingfield (2013). A, B, D, F–H. Adapted from illustrations in De Beer & Wingfield (2013). Shades of grey depict colours of various structures ranging from hyaline to dematiaceous.

2012) using the GTR+G+I substitution model and 1 000 thorough bootstrap replicates. Bayesian analysis was conducted using PhyloBayes-MPI v. 1.8 (Lartillot *et al.* 2013); two chains were run in parallel under the CAT-GTR model. The program bpcomp was used to assess the convergence in tree space. Runs were terminated when the maxdiff value obtained between two chains reached 0.1 or lower.

Morphology

Of the 11 ascospore morphotypes defined by De Beer & Wingfield (2013) for the *Ophiostomatales*, three (Type A, B, E) were used to describe ascospore types in the present study (Fig. 3). Type A ascospores are those described as allantoid, bean-shaped, crescent to sickle-shaped, clavate to ovate, curved, cylindrical and slightly curved, orange section, lunate or reniform. Type B ascospores are those that are bacilliform, elongate filiform or narrow clavate. Type E ascospores are those with sheaths and are box-shaped, cylindrical, oblong, pillow-shaped, rectangular or rod-shaped. For the asexual morphs, five conidiophore types, hyalorhinocladiella-like, leptographium-like, pesotum-like, raffaelea-like and sporothrix-like, were used as descriptors where applicable (Fig. 3). Three shades of grey were applied in the figures to depict the colours of structures. Thus, hyaline to subhyaline structures were shaded in pale grey. Brown to dark brown structures were a medium-tone grey and fuscous black to black structures were presented in dark grey.

RESULTS

The phylogenomic tree constructed from the genome-wide sequence data for 31 ophiostomatalean species (Fig. 4) showed a similar topology to those obtained in previous studies (Nel *et al.* 2021, Vanderpool *et al.* 2018). The placement of *Graphilbum fragrans* was, however, different from that suggested by Vanderpool *et al*. (2018). This inconsistent placement for *Gra. fragrans* was also observed by Nel *et al.* (2021) where different phylogenomic approaches were applied. Species of *Leptographium s.l.* grouped in two distinct lineages; one of these accommodated the *Grosmannia penicillata* complex and the other the *L. lundbergii*, *L. procerum* and *L. galeiforme* complexes. Species of *Raffaelea s.l.* resolved in three distinct clades, which is consistent with the findings in two previous studies (Nel *et al.* 2021, Vanderpool *et al.* 2018). Otherwise, all remaining species and genera included in the analysis resided in the clades consistent with their current recognition as separate genera in the *Ophiostomatales*.

The maximum likelihood tree (Fig. 5) resulting from analyses of the concatenated dataset (LSU, ITS, *TEF-1α* and *RPBII*) for 264 isolates representing 249 species revealed 24 distinct lineages. Posterior probability values generated from Bayesian Inference analysis are indicated at the genus-level nodes (Fig. 5). Although the topologies of the individual gene trees (Figs S1–S4) were different to one another and to those in the combined tree, (apart from a few exceptions discussed below), the terminal clades were mostly consistent for the gene regions. To facilitate a discussion of the emerging results, the 24 lineages that represent genera or smaller groups were annotated using Roman numerals (I–XXIV). These were applied in the order of appearance in the

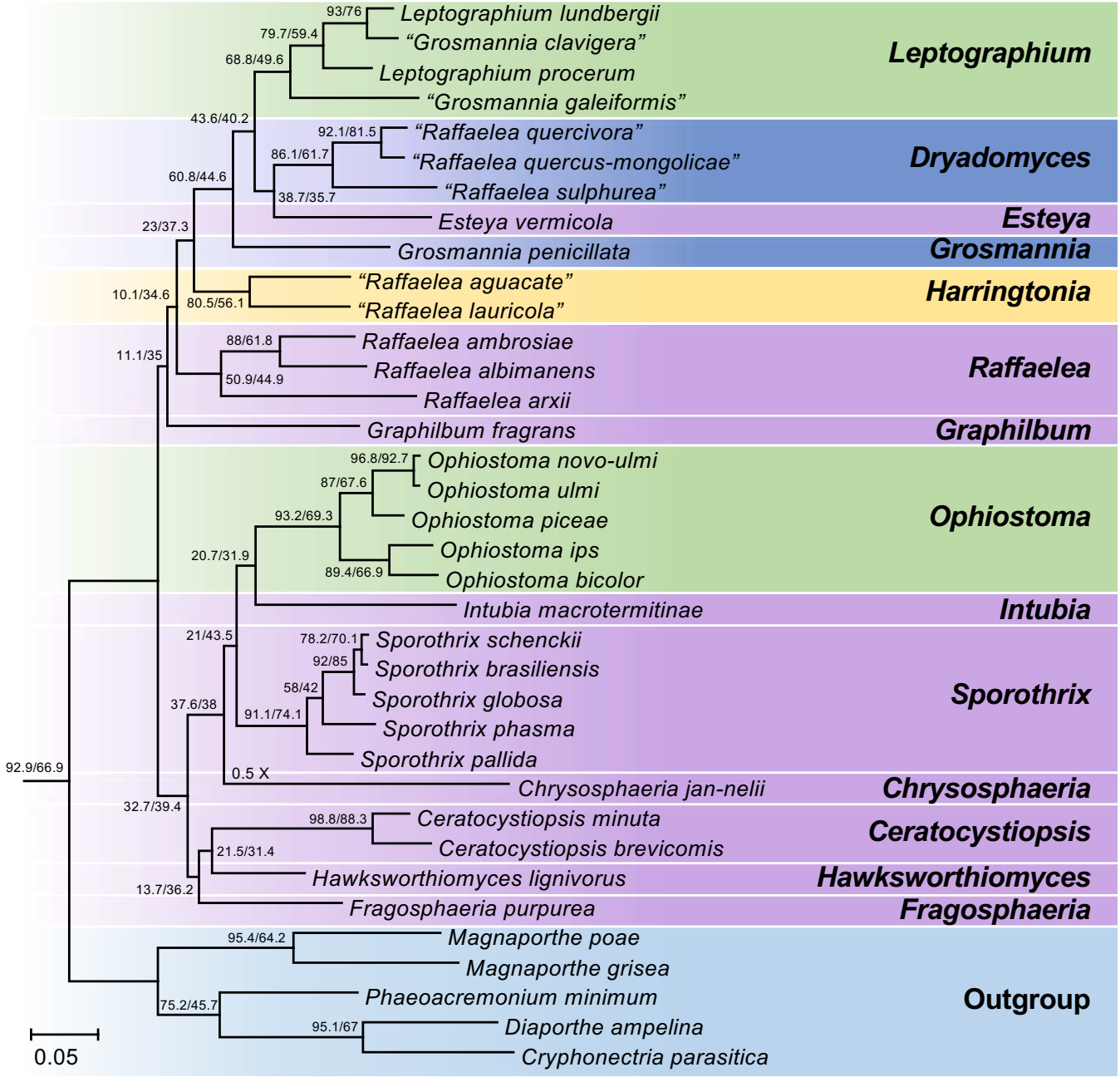

Fig. 4. Phylogenomic tree obtained from supertree analysis with ASTRAL using gene trees constructed from 3 548 BUSCO genes (identified using the sordariomycetes_odb10 dataset; BUSCO v. 4.0.5). All 31 species in the *Ophiostomatales* for which genome sequence currently available were included in the analysis. *Cryphonectria parasitica*, *Diaporthe ampelina*, *Magnaporthe grisea*, *Magnaporthe poae* and *Phaeoacremonium minimum* were included as outgroup taxa. Gene concordance factors (gCF) and site concordance factors (sCF), which indicate the percentage of genes and sites that support a parcular nodes respectively, were determined using IQ-TREE2 are presented at nodes as gCF/sCF. Species names presented in double quotes denote old names which have been changed to their new respective genera subsequent to this study.

concatenated tree (Fig. 5). Single species that grouped within major lineages, but not within defined species complexes, or not consistent within the same lineage in different trees, were labelled alphabetically (A–K).

The overall topology of the LSU tree (Fig. S1) showed some differences from that of the concatenated tree, but 22 of the lineages corresponded between the two trees. The exceptions were Lineages III and XIX. Lineage III consisted of a single species in the concatenated tree, for which no LSU data were available, while Lineage XIX grouped outside the other genera in the concatenated tree, but as part of *Sporothrix* (Lineage XIV) in the LSU tree. Species complexes within *Leptographium*, *Sporothrix* and *Ophiostoma* were generally less well-defined in the LSU tree than in the concatenated tree.

The ITS tree (Fig. S2) showed little resolution below the genus level. Due to the variable nature of the ITS1 and ITS2 regions, the dataset was subjected to a strict Gblocks treatment (using automated parameters). The dataset consisted of 1 132 characters (including gaps) prior to treatment with Gblocks, and only 169 characters thereafter. The remaining dataset on which the tree (Fig. S2) is based, consisted predominantly of the 5.8S region. Nevertheless, we retained this analysis in the study because the ITS region is the officially recognised barcode for the fungi (Schoch *et al.* 2012). The ITS sequences were submitted to the GenBank Refseq database. The ITS tree (Fig. S2) supported separation of most of the genera, but Lineages XI, XII and XXII were not monophyletic in this tree, when compared to the concatenated tree. The relatively small dataset also failed to resolve most of the species complexes for the larger genera.

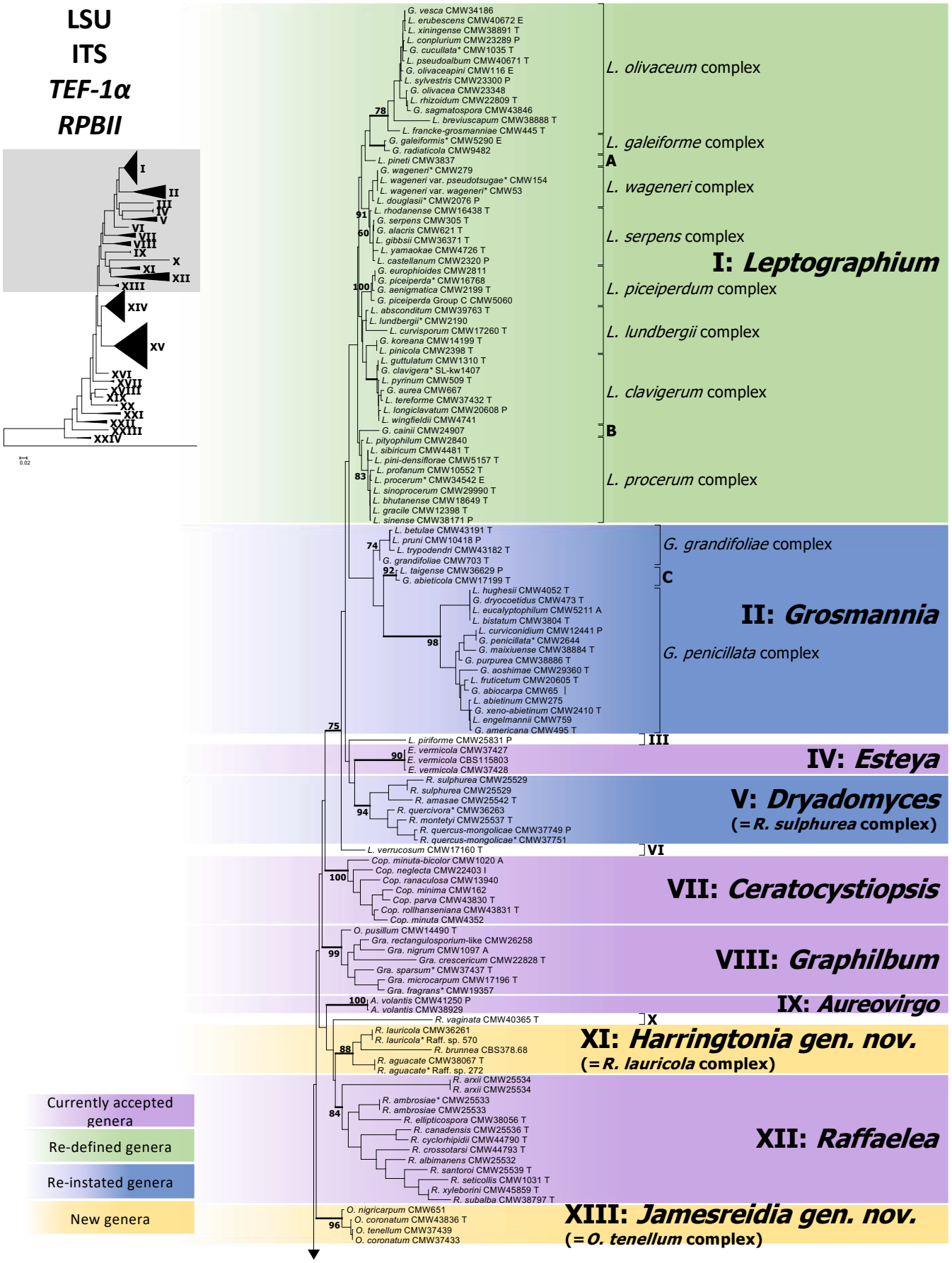

Fig. 5. Phylogenetic tree depicting the boundaries of currently accepted genera in the *Ophiostomatales*. This tree was generated using maximum likelihood analysis of the concatenated dataset of LSU, ITS, *TEF1-α* and *RPBII* gene regions. The dataset consisted of 264 isolates and 2 360 characters (including gaps). Bootstrap values above 60 % are shown. Bold lines indicate Bayesian posterior probabilities values above 0.8. Bootstrap values and Bayesian posterior probabilities values below the species complex level were removed for simplification. Purple blocks indicate existing genera, yellow blocks new genera described in this study, green blocks, genera that we redefine here, and blue blocks indicate genera that that have been reinstated and re-defined. (T = ex-type, E = ex-epitype, P = ex-paratype; L = ex-lectotype; A = authentic isolate, used in the original study; * Genome sequenced).

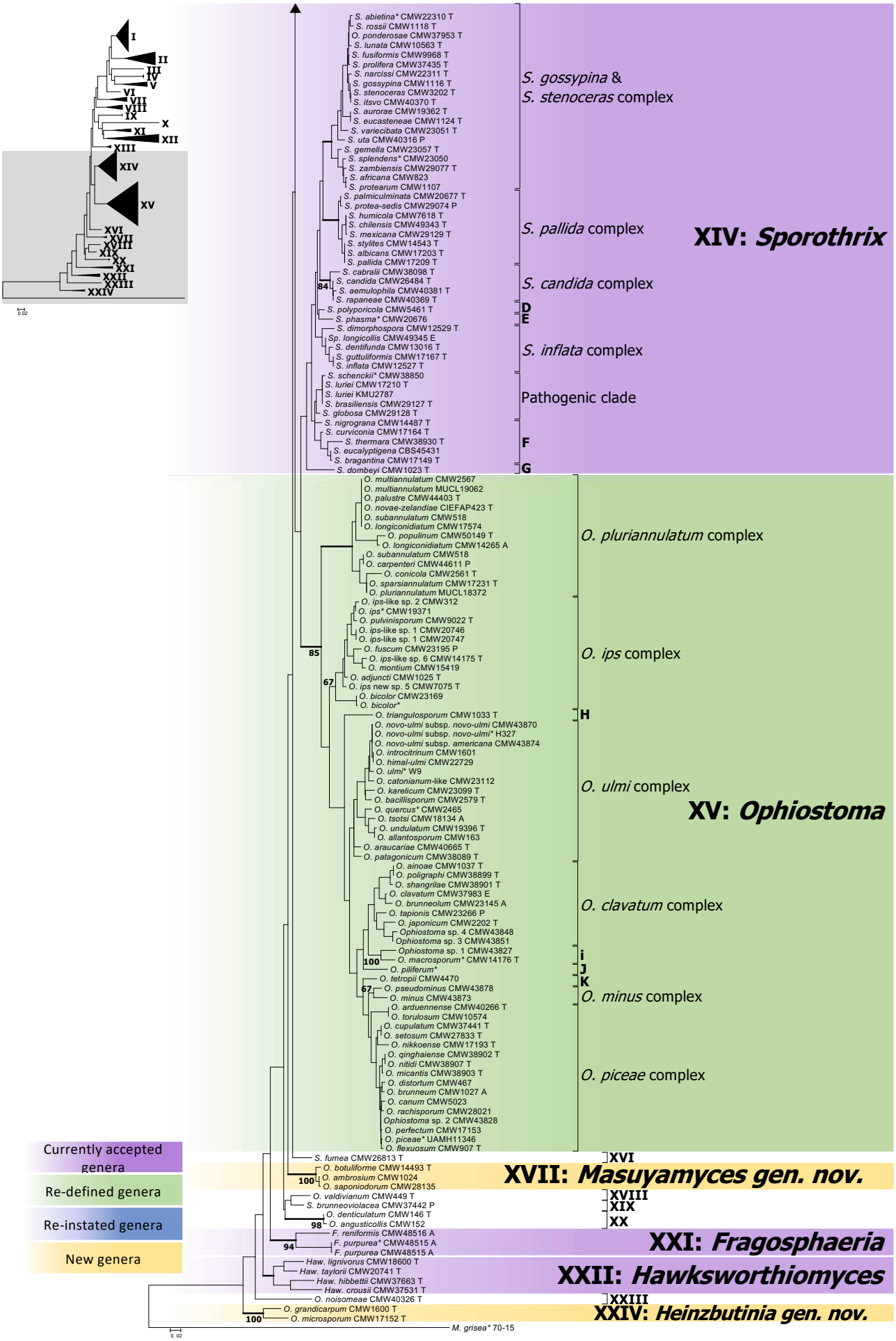

Fig. 5. (Continued).

The *TEF-1α* tree (Fig. S3) resolved almost all the lineages representing species complexes, but failed to support monophyly of Lineages I, II, VIII, XI and XXII.

The *RPBII* tree (Fig. S4) supported the separation of all genera, species complexes and smaller lineages apart from Lineage XII that separated in four clades, and Lineage VIII that grouped within Lineage I.

Based on the concatenated tree (Fig. 5), Lineage I included species complexes previously defined in *Leptographium s.l.* (De Beer & Wingfield 2013), namely the *Leptographium clavigerum, L. galeiforme*, *L. lundbergii*, *L. olivaceum*, *L. piceiperdum*, *L. procerum*, *L. serpens* and *L. wageneri* complexes; as well as two species not forming part of these species complexes (A & B). Lineage II included the *G. grandifoliae* and *G. penicillata* species complexes and a smaller lineage (C). *Leptographium piriforme* was labelled as Lineage III and *L. verrucosum* as Lineage VI, both grouping outside of *Leptographium* (Lineage I). Lineage IV consisted of three isolates of the monotypic genus *Esteya*. The *Raffaelea sulphurea* complex formed Lineage V. *Ceratocystiopsis* spp. formed Lineage VII, *Graphilbum* formed Lineage VIII and *Aureovirgo* formed Lineage IX. *Raffaelea vaginata* grouped outside of *Raffaelea* (Lineage XII) and was labelled Lineage X. Lineage XI consisted of the *R. lauricola* complex, distinct from *Raffaelea* spp., which formed Lineage XII. The *Ophiostoma tenellum* complex formed Lineage XIII. *Sporothrix* and *Ophiostoma*, as defined by De Beer *et al.* (2016a), formed Lineages XIV and XV, respectively. Lineage XIV consisted of the *S. gossypina* and *S. stenoceras* species complexes (which grouped inseparably from each other), the *S. candida*, *S. inflata* and *S. pallida* species complexes, the pathogenic clade (including the type species of *Sporothrix*, *S. schenckii*), as well as groups D to G. Lineage XV included the *O. clavatum*, *O. ips*, *O. minus*, *O. piceae*, *O. pluriannulatum* and *O. ulmi* complexes as well as groups H to K. *Sporothrix fumea* and *S. brunneoviolacea* both grouped separate from *Sporothrix*, and were labelled as Lineages XVI and XIX, respectively. Three *Ophiostoma* species consistently grouped together and distinct from *Ophiostoma* and were labelled Lineage XVII. Lineage XVIII included *O. valdivianum* and Lineage XX consisted of *O. denticulatum* and *O. angusticollis*. Lineage XXI represented *Fragosphaeria*, and Lineage XXII represented *Hawksworthiomyces*. *Ophiostoma noisomeae* was labelled Lineage XXIII, while *O. grandicarpum* and *O. microsporum* together constituted Lineage XXIV.

Afroraffaelea was excluded from the final analyses because the placement of the type for this monotypic species, *Afr. ambrosiae,* was completely incongruent among the separate gene trees (data not shown), most often forming long branches, distinct from all other groups. This impacted negatively on the support for several lineages in the concatenated tree, which prompted the decision to exclude the species from the analyses. Likewise, the two species of *Intubia* and the monotypic *Chrysosphaeria* were excluded from the analyses due to their ambiguous generic placement when using traditionally applied phylogenetic markers (Nel *et al.* 2021).

TAXONOMY

Phylogenetic analyses for four gene regions revealed 16 lineages within the *Ophiostomatales,* which we now recognise as valid genera. Seven of these represent genera currently known and defined in the Order. They include *Esteya* (Lineage IV), *Ceratocystiopsis* (Lineage VII), *Graphilbum* (Lineage VIII), *Aureovirgo* (Lineage IX), *Sporothrix* (Lineage XIV), *Fragosphaeria* (Lineage XXI) and *Hawksworthiomyces* (Lineage XXII). Two Lineages (Lineage II and V), which were clearly distinct from all other genera, included the ex-type cultures of *Grosmannia penicillata* and *Dryadomyces amasae* respectively. These species have previously been treated in the genera *Grosmannia*/*Leptographium* and *Raffaelea* respectively and we have consequently reinstated and redefined the genera *Grosmannia* and *Dryadomyces* with emended descriptions. Four lineages (Lineage XI, XIII, XVII and XXIV) are recognised as representing new genera and are described as such. Characters of these new genera were previously included in the descriptions of *Leptographium*, *Ophiostoma* and *Raffaelea*, and we have consequently emended their descriptions. Although *Afroraffaelea*, *Chrysosphaeria, Intubia,* and the fossil genus *Paleoambrosia* were not included in our analyses, we recognise these genera as valid, retaining them in the *Ophiostomatales*.

The placement of the remaining lineages (III, VI, X, XVI, XVIII, XIX, XX and XXIII) remains uncertain, as most of these lineages were represented by single species that grouped inconsistently in our analyses. We have chosen not to describe new monotypic genera for these lineages, but rather to delay this decision until additional taxa are discovered that support establishing novel genera. In addition to describing and redefining genera, new combinations have been provided for species where necessary.

Circumscription of the *Ophiostomatales* and *Ophiostomataceae*

At present there is no need to revise the description of the *Ophiostomatales*. This is because the emended description by De Beer *et al.* (2013a) broadly encompasses the morphologies of all genera, including the novel genera described in the present study. With more than 300 species and clearly distinct broad morphological groups in the Order, it would make sense to provide a narrower definition for the *Ophiostomataceae,* and to introduce one or more additional families. However, in view of the lack of support for the deeper nodes in our analyses, we have refrained from doing so at present. We suggest that this should be done only when related taxa outside the *Ophiostomatales*, such as those included in the LSU and SSU phylogenies of De Beer *et al.* (2013a), can be incorporated in multigene phylogenies to provide more robust context within the *Sordariomycetidae*.

Currently accepted genera in the *Ophiostomatales*

All currently accepted genera in the *Ophiostomatales* are defined below, and based on our results, descriptions have been emended where necessary. Genera and species complexes are discussed in alphabetical order, with lineage numbers corresponding to their appearance in the concatenated phylogenetic tree (Fig. 5).

New combinations

Where required, new combinations have been provided, and these are listed under the relevant genera. Species that have been treated in a particular genus but were shown based on our data to reside in a different genus, for which a name already exists in the appropriate genus, have been listed under 'current name' in Table 1, and thus not in the following section For example, *Grosmannia serpens* is now treated as *Leptographium serpens* but did not require a new combination and is listed in Table 1.

Afroraffaelea (not included in the phylogenetic analyses)

Afroraffaelea C.C. Bateman *et al.*, Fungal Ecol. 25: 46. 2017. MycoBank MB 816236. Fig. 6A, B.

Etymology: 'Prefix Afro - indicating its likely African origin, and 'raffaelea' to recognise the ecological similarity to the closely related (though probably not monophyletic) ambrosia fungus genus *Raffaelea*' (Bateman *et al.* 2017).

Sexual morph: Unknown.

Asexual morph: No reproductive structures observed. Colonies white becoming brown with age, aerial hyphae present, abundant, subhyaline, extensively branched often perpendicularly, thickened and melanized intercalarily, distal hyphae denticulate, submerged hyphae subhyaline, constricted at septa, frequently branched, with tapering distal ends, monillioid mycelia occurring in peptone-containing medium, fragmented unicellularly or bicellularly.

Type species: *Afroraffaelea ambrosiae* C.C. Bateman *et al.*, Fungal Ecol. 25: 46. 2017. MycoBank MB 816237.

No other species known.

Notes: *Afroraffaelea* was described by Bateman *et al.* (2017) and has a unique morphology relative to the rest of the *Ophiostomatales*. Within a few days of sub-culturing, *Afr. ambrosiae* (the only species in this genus) produces masses of aerial hyphae, unlike any other ophiostomatalean species, and changes colour from white to brown as the culture matures. The fungus is the dominant fungal symbiont of the ambrosia beetle *Premnobius cavipennis,* presumably introduced into North America from Africa (Bateman *et al.* 2017). The phylogenies of Bateman *et al.* (2017) showed *Afr. ambrosiae* grouping close to *Fragosphaeria*, but there was insufficient phylogenetic support for these authors to determine the taxonomic placement of *Afroraffaelea* in the *Ophiostomatales*.

The taxonomic placement of *Afroraffaelea* in our phylogenetic trees is not conclusive. The four known isolates of *Afr. ambrosiae* consistently grouped together as one species. However, the clade grouped inconsistently in the single gene trees. For example, in the LSU and *TEF-1α* trees, *Afr. ambrosiae* isolates grouped in Lineage VIII, but with Lineage V in ITS, and with Lineage XXIII in *RPBII* (data not shown). We consequently excluded these isolates from our datasets. We believe that the taxonomic placement of this fungus will be resolved when additional species are found, or possibly with whole genome data. Until such time, we treat *Afroraffaelea* as *incertae sedis* in the *Ophiostomatales*.

Aureovirgo (Lineage IX)

Aureovirgo J.A. van der Linde *et al.*, Antonie van Leeuwenhoek 109: 593. 2016. MycoBank MB 813870. Fig. 6C, D.

Etymology: 'Refers to the golden appearance of the immature ascomata and the pure white colour of the cultures ("*Aureovirgo*" refers to a golden maiden with an unstated overtone of virginal whiteness)' (Van der Linde *et al.* 2016).

Sexual morph: *Ascomatal bases* subglobose to globose, pale brown when young, becoming darker with age; necks cylindrical, dark brown. *Ostiolar hyphae* hyaline, parallel. *Ascospores* hyaline, 1-celled, enclosed in a sheath, falcate, endospores (the body of ascospores) allantoid.

Asexual morph: Leptographium-like; *conidiophores* macronematous, mononematous, hyaline; *conidiogenous cells* cylindrical, hyaline; *conidia* hyaline, 1-celled, oblong to ellipsoidal.

Type species: *Aureovirgo volantis* J.A. van der Linde *et al.*, Antonie van Leeuwenhoek 109: 593. 2016. MycoBank MB 813872.

No other species known.

Notes: *Aureovirgo* was described from galleries of the ambrosia beetle *Cyrtogenius africus* in dead and dying *Euphorbia ingens* trees in South Africa. It is a monotypic genus accommodating *A. volantis* (Van der Linde *et al.* 2016). The ascomatal bases are honey-coloured when immature, while the rest of the culture is white. This is the only genus in the *Ophiostomatales* associated with *Eurphorbia* trees. In our dataset, *Aureovirgo* formed a well-supported, distinct lineage.

Ceratocystiopsis (Lineage VII)

Ceratocystiopsis H.P. Upadhyay & W.B. Kendr., Mycologia 67: 799. 1975. MycoBank MB 889. Fig. 6E, F.

Etymology: 'Resembling the genus *Ceratocystis*' (Upadhyay & Kendrick 1975, Upadhyay 1981). At the time of the description, Upadhyay & Kendrick (1975) and others treated *Ophiostoma* as a synonym of *Ceratocystis* in the *Ophiostomatales*. *Ceratocystis* was later shown to form part of the *Microascales*, and *Ceratocystiopsis* to be related to *Ophiostoma* in the *Ophiostomatales* (Zipfel *et al.* 2006). Although somewhat of a misnomer, the name *Ceratocystiopsis* remains valid and represents a distinct genus in the *Ophiostomatales*.

Synonym: *Hyalorhinocladiella* H.P. Upadhyay & W.B. Kendr., Mycologia 67: 800. 1975. MycoBank MB 8582. [Type species *Hyalorhinocladiella minuta-bicolor* (R.W. Davidson) H.P. Upadhyay & W.B. Kendr.]

Sexual morph: *Ascomatal bases* subglobose, globose, obpyriform, black or pale brown, upper part surrounded with collar-like structure or corona of globose cells; necks short conical to elongate, cylindrical, black or paler than base. *Ostiolar hyphae* absent or present, convergent, parallel, divergent. *Asci* evanescent, clavate, broadly fusiform, 8-spored. *Ascospores* hyaline, 1-celled, enclosed in a sheath, falcate in side view, fusiform, acicular in face view; endospores elongate orange segment-shaped in side view, cylindrical in face view; cucullate, sometimes forming bulbous swelling toward one end.

Asexual morph: Hyalorhinocladiella-like; *conidiophores* micronematous, semimacronematous, macronematous, mononematous, hyaline; *conidiogenous cells* integrate or discrete, polyblastic, sympodial, with denticle scars; *conidia* hyaline, 1-celled, obovoid, ellipsoidal, oval to globose, clavate, T-shaped, Y-shaped, cylindrical.

Type species: *Ceratocystiopsis minuta* (Siemaszko) H.P. Upadhyay & W.B. Kendr., Mycologia 67: 800. 1975. MycoBank MB 310480.

Other species: Listed in Table 1.

Table 1. Taxa described in the *Ophiostomatales*, based on currently published data.

Previous name	Current name	CMW[1]	CBS or other[1]	Type[2]	Isolated from	Country	Collector	GenBank Accession Numbers[3]			
								ITS	LSU	*TEF1-α*	*RPBII*
Afroraffaelea											
Afr. ambrosiae	*Afr. ambrosiae*	48331	141678	T	*Premnobius cavipennis*	Florida, USA	C. Bateman	OM632703	OM584293	OM631576	OM631577
Aureovirgo											
A. volantis	*A. volantis*	41250	139649	P	*Cyrtogenius africus* on *Euphorbia ingens*	South Africa	J.A. van der Linde	OM501369	OM514700	OM631743	OM631579
A. volantis	*A. volantis*	38929	140081		*Cyrtogenius africus* on *Euphorbia ingens*	South Africa	J.A. van der Linde	OM501368	OM514699	OM631742	OM631578
Ceratocystiopsis											
Cop. brevicomis	*Cop. brevicomis*	40952	333.97	T	*Dendroctonus brevicomis*	California, USA	T. Harrington	EU913722	EU913683	–	–
Cop. collifera	*Cop. collifera*	7074	126.89	T	*Dendroctonus valens* on *Pinus teocote*	Mexico	J. Marmolejo	EU913721	EU913681	–	–
Cop. concentrica	*Cop. concentrica*	–	WIN(M)71-07		*Pinus banksiana*	Canada	J. Reid, A. Olchowecki	–	AF135571	–	–
Cop. conicicollis	*Cop. conicicollis*	–	WIN(M)69-25		*Abies balsemea*	Canada	J. Reid, A. Olchowecki	–	–	–	–
Cop. longispora	*Cop. longispora*	–	UM48		*Pinus* sp.	Canada	A. Olchowecki	EU913723	EU913684	–	–
Cop. lunata[#]	*Cop. lunata*	55897	47171	T	*Xylosandrus crassciusculus*	South Africa	W.J. Nel	MW028169	MW028141	–	–
Cop. manitobensis	*Cop. manitobensis*	13792	UAMH9813	T	Manitoba beetle gallery in *Pinus resinosa*	Canada	J. Reid	EU913714	EU913674	–	–
Cop. minima	*Cop. minima*	162	182.86		*Pinus banksiana*	Wisconsin, USA	M.J. Wingfield	OM501370	OM514701	OM631744	–
Cop. minuta[*]	*Cop. minuta*	4352	138717		*Ips cembrae*	Poland	T. Kirisits	OM501372	OM514703	OM631745	OM631581
Cop. minuta-bicolor[*]	*Cop. minuta-bicolor*	1020	635.66	A	Gallery of *Ips* sp. in *Pinus contorta*	USA	R.W. Davidson	OM501371	OM514702	–	OM631580
Cop. neglecta	*Cop. neglecta*	22403	100596	I	*Hylurgops palliatus*	Germany	R. Kirschner	OM501373	OM514704	OM631746	OM631582
Cop. ochracea	*Cop. ochracea*	–	DAOM100148		*Picea mariana*	Canada	H.D. Griffin	–	–	–	–
Cop. pallidobrunnea	*Cop. pallidobrunnea*	–	UM51		*Populus tremuloides*	Canada	J. Reid	–	EU913682	–	–
Cop. parva	*Cop. parva*	43830	UAMH9650	T	*Abies balsamea*	Canada	A. Olchowecki	OM501374	–	OM631747	OM631583
Cop. ranaculosa	*Cop. ranaculosa*	13940	119683		*Pinus echinata*	North Carolina, USA	F. Hains	OM501375	OM514705	OM631748	OM631584
Cop. rollhanseniana	*Cop. rollhanseniana*	43831	UAMH9774	T	Unknown beetle on *Pinus sylvestris*	Norway	J. Reid	OM501376	OM514706	OM631749	–
Cop. spinulosa	*Cop. spinulosa*		DAOM110151	T	*Tilia americana*	Canada	H.D. Griffin	–	–	–	–
Cop. synnemata[#]	*Cop. synnemata*	–	NRIF 16918DA	T	*Dryocoetes alni* infesting *Populus tremula*	Poland	K. Miśkiewicz	MN900988	MN900988	MN901018	–
Cop. yantaiensis[#]	*Cop. yantaiensis*	–	SNM650	T	*Pinus thunbergii*	China	R. Chang	MW989411	MZ819924	MZ853080	–
Cop. weihaiensis[#]	*Cop. weihaiensis*	–	SNM649	T	*Pinus thunbergii*	China	R. Chang	MW989413	MZ819926	MZ853082	–
Chrysosphaeria											
Chr. jan-nelii[#]	*Chr. jan-nelii*	47058	141570	T	*Termitomyces* fungal comb of *Macrotermes natalensis*	South Africa	W.J. Nel	MT637038	MT637006	–	–
***Dryadomyces* (*R. sulphurea* complex)**											
R. amasae	*D. amasae*	25542	116694	T	*Amasa concitatus* on Angiosperms	Taiwan	H. Gebhardt	–	MT629750	OM631750	OM631585
R. montetyi	*D. montetyi*	25537	463.94	T	*Platypus cylindrus* on *Quercus suber*	France	D. Vouland	–	MT629761	OM631751	–
R. quercivora[*]	*D. quercivorus*	36263	122982		*Quercus mongolica*	Japan	T. Kubono	MT633072	MT629762	OM631752	OM631586
R. quercus-mongolicae	*D. quercus-mongolicae*	37749	KACC44403	P	*Quercus mongolica*	South Korea	K.H. Kim	MT633073	MT629764	OM631754	OM631588
R. quercus-mongolicae[*]	*D. quercus-mongolicae*	37751	KACC44405		*Platypus koryoensis*-infested *Quercus*	South Korea	K.H. Kim	MT633074	MT629763	OM631753	OM631587
R. sulphurea[*]	*D. sulphureus*	25529	380.68		*Xyleborus saxesenii* gallery in *Populus deltoides*	Kansas, USA	L.R. Batra	MT633077	MT629768	OM631755	OM631589

Table 1. (Continued).

Previous name	Current name	CMW[1]	CBS or other[1]	Type[2]	Isolated from	Country	Collector	GenBank Accession Numbers[3]			
								ITS	LSU	*TEF1-α*	*RPBII*
Esteya											
E. vermicola	*E. vermicola*	37427	100821		*Olea europeae*	Italy	S. Frisullo	–	OM514708	OM631757	OM631591
E. vermicola	*E. vermicola*	37428	156.82		*Pinus* sp.	Taiwan	T. Tatsuno	OM501378	OM514709	OM631758	–
E. vermicola[*]	*E. vermicola*	–	115803		*S. intricatus* and its galleries in oak trees	Czech Republic	L. Marvanova	OM501377	OM514707	OM631756	OM631590
Fragosphaeria											
F. purpurea[*]	*F. purpurea*	48515	133.34	A	*Fagus* sp.	England, UK	C.G.C. Chesters	OM501379	OM514710	OM631759	OM631592
F. reniformis	*F. reniformis*	48516	134.34	A	*Fagus* sp.	England, UK	E.W. Mason	OM501381	–	OM631760	OM631593
Graphilbum											
Gra. acuminatum[#]	*Gra. acuminatum*	54769	145828	T	*Ips acuminatus* gallery on *Pinus sylvestris*	Poland	R. Jankowiak	MN548902	–	MN548952	–
Gra. brunneocrinitum	*Gra. brunneocrinitum*	–	TRTC34581	T	*Abies balsamea*	Canada	–	–	–	–	–
Gra. carpaticum[#]	*Gra. carpaticum*	43141	145835	T	*Pissodes piceae* gallery on *Abies alba*	Poland	P. Majka	KY568116	–	MN548956	–
Gra. curvidentis[#]	*Gra. curvidentis*	54779	145832	T	*Pitokteines curvidens* gallery on *Abies alba*	Poland	P. Bilański	KY568111	–	KY56850	–
Gra. crescericum	*Gra. crescericum*	22828	130864	T	*Hylurgops palliatus* on *Pinus radiata*	Spain	P. Romón	OM501403	OM514749	OM631779	OM631604
Gra. curvicolle	*Gra. curvicolle*	–	WIN(M)70-25	T	*Abies balsamea*	Canada	J. Reid, A. Olchowecki	–	–	–	–
Gra. fragrans[*]	*Gra. fragrans*	19357	138720		*Pinus patula*	South Africa	X. D. Zhou	OM501404	OM514750	OM631780	OM631605
Gra. furuicola[#]	*Gra. furuicola*	44770	145813	T	*Tomicus piniperda* in *Pinus sylvestris*	Norway	R.H. Lindseth, T.H. Sundt	MN548907	–	MN548961	–
Gra. gorcense[#]	*Gra. gorcense*	34153	146203	T	*Tetropium* sp. in *Picea abies*	Poland	R. Jankowiak	MN548919	–	MN548972	–
Gra. interstitiale[#]	*Gra. interstitiale*	54780	145816	T	*Hylurgops interstitialis* in *Pinus sylvestris*	Russia	H. Solheim	MN548909	–	MN548963	–
Gra. ipis-grandicollis[#]	*Gra. ipis-grandicollis*	–	VPRI43762		*Ips grandicollis gallery* on *Pinus radiata*	Australia	A.J. Carnegie	MW046071	MW046117	MW066405	–
Gra. kesiyae	*Gra. kesiyae*	41729	139652	T	*Polygraphus szemaoensis* on *Pinus kesiya*	China	S. Taerum	MG205669	–	–	–
Gra. microcarpum	*Gra. microcarpum*	17196	YCC439	T	*Cryphalus montanus*	Japan	Y. Yamaoka	OM501405	OM514751	OM631781	OM631606
Gra. nigrum	*Gra. nigrum*	1097	163.61	A	*Abies lasiocarpa*	Colorado, USA	R.W. Davidson	OM501406	OM514752	–	OM631607
Gra. niveum[#]	*Gra. niveum*	–	SNM145	T	*Pinus thunbergii*	China	R. Chang	MW989418	–	MZ019548	–
Gra. puerense	*Gra. puerense*	41673	139640	T	*Ips acuminatus* on *Pinus kesiya*	China	S. Taerum	MG205671	–	–	–
Gra. rectangulosporium	*Gra. rectangulosporium*	29364	MAFF 238952	T	*Polygraphus proximus* on *Abies mariesii*	Japan	N. Ohtaka	MG205671	–	–	–
Gra. roseum[#]	*Gra. roseum*	40349	141074	T	*Curtisia dentata*	South Africa	T. Musvuugwa	KY050751	–	–	–
Gra. sexdentatum[#]	*Gra. sexdentatum*	54773	145814	T	*Ips sexdentatus* in *Pinus sylvestris*	Norway	H. Solheim, M.E. Waalberg	MN548915	–	MN548968	–
Gra. sparsum[*]	*Gra. sparsum*	37437	405.77	T	Bark beetle gallery on *Picea glauca*	Alaska, USA	R.W. Davidson	OM501409	OM514755	–	OM631608
Gra. translucens[#]	*Gra. translucens*	–	SNM144	T	*Pinus thunbergii*	China	R. Chang	MW989416	–	MZ019546	–
Gra. tsugae	*Gra. tsugae*	–	UAMH11701	T	*Tsuga heterophylla*	Canada	J. Reid, B. Reid	KJ661745	–	–	–
Gra. tubicolle	*Gra. tubicolle*	43837	UAMH9686	T	*Pinus banksiana*	Canada	A. Olchowecki	–	–	–	–
O. pusillum	*Gra. pusilllum*	14490	–	T	*Pinus densiflora*	Japan	H. Masuya	OM501407	OM514753	–	–
***Grosmannia: G. penicillata* complex**											
G. abiocarpa	*G. abiocarpa*	65	594.85	L	*Ips* sp. on *Picea engelmannii*	Colorado, USA	R.W. Davidson	OM501384	OM514715	OM631764	–

Table 1. (Continued).

Previous name	Current name	CMW[1]	CBS or other[1]	Type[2]	Isolated from	Country	Collector	GenBank Accession Numbers[3]			
								ITS	LSU	*TEF1-α*	*RPBII*
G. americana	*G. americana*	495	497.96	T	*Dendroctonus simplex* on *Larix laricina*	Vermont, USA	D. Bergdalh	OM501385	OM514718	OM631765	OM631595
G. aoshimae	*G. aoshimae*	29360	MAFF238948	T	*Polygraphus proximus* on *Abies mariesii*	Japan	N. Ohtaka	OM501386	OM514719	OM631766	OM631596
G. crassifolia[#]	*G. crassifolia*	38885	136505	T	*Polygraphus poligraphus* in *Pinus crassifolia*	China	X.D. Zhou, S. Taerum	–	MN644475	MN647897	–
G. dryocoetis	*G. dryocoetis*	473	376.66	T	*Dryocoetes confusus* on *Abies lasiocarpa*	Canada	A.C. Molnar	OM501392	OM514727	OM631768	OM631597
L. fenglinhense	*G. fenglinhensis*	44579	141896	T	*Ips typographus* on *Pinus* sp.	China	R. Chang, S.F. Chen	MH144128	–	MH124404	–
G. maixiuense	*G. maixiuense*	38884	136502	T	*Polygraphus poligraphus, Ips shangrila* in *Picea crassifolia*	China	M. Yin, S. Taerum, X.D. Zhou	OM501396	MN644474	MN647900	OM631599
G. penicillata[*]	*G. penicillata*	2644	116008		*Picea abies*	Norway	H. Solheim	OM501397	OM514737	OM631774	OM631600
G. purpurea	*G. purpurea*	38886	136975	T	*Ips shangrila* on *Picea purpurea*	China	M. Yin, S. Taerum, X.D. Zhou	OM501399	MN644476	MN647914	–
G. tibetensis	*G. tibetensis*	–	CFCC53415	T	*Orthotomicus* sp. on *Pinus likiangensis* var. *balfouriana*	Tibet	Z. Wang, Q. Lu	MT269759	–	MT268756	–
G. xeno-abietinum	*G. xeno-abietinum*	2410	136514	T	*Pinus ponderosa*	California, USA	T. Harrington	OM501402	MN644471	MN647894	OM631603
G. xianmiense[#]	*G. xianmiense*	38892	136500	T	*Polygraphus poligraphus* in *Pinus crassifolia*	China	X.D. Zhou, S. Taerum	–	MN644479	MN647911	–
G. zekuensis[#]	*G. zekuensis*	41876	141901	T	*Bakerdania* sp. in gallery of *Ips nitidus* on *Picea crassifolia*	China	S.J. Taerum	MH121683	MH121683	MH124546	–
L. abieticolens	*G. abieticolens*	2865	115248	T	*Abies balsamea*	Vermont, USA	D. Bergdalh	AF343701	–	–	–
L. abietinum	*G. abietina*	275	118590		*Picea engelmannii*	Canada	A. Molnar	OM501383	OM514713	OM631763	OM631594
L. altius	*G. altior*	12471	123619	T	*Picea koraiensis*	China	X.D. Zhou, Z.W. de Beer	HQ406851	–	HQ406875	–
L. bistatum	*G. bistata*	3804	120192	T	*Pinus radiata*	Japan	J.J. Kim	OM501388	OM514721	OM631795	–
L. chlamydatum	*G. chlamydata*	36631	128840		*Pityogenes chalcographus* on *Picea abies*	Finland	Z.W. de Beer	JF279965	–	JF280080	–
L. curviconidium	*G. curviconidia*	12441	123617	P	*Ips typographus* on *Picea koraiensis*	China	X.D. Zhou, Z.W. de Beer	OM501390	OM514725	OM631767	–
L. curvisporum	*G. curvispora*	17260	123914	T	*Picea abies*	Norway	M.J. Wingfield, H. Solheim	OM501391	OM514726	EU979347	–
L. engelmannii	= *G. abietina*	759	–		*Picea engemannii*	Canada	R.W. Davidson	–	OM631763	OM631762	–
L. eucalyptophilum	*G. eucalyptophila*	5211	–	A	*Eucalyptus urophylla* × *E. pellita*	Democratic Republic of Congo	J. Roux	OM501393	OM514728	OM631769	–
L. euphyes	*G. euphyes*	259	109701	T	*Pinus strobus*	New Zealand	M. Dick	AF343686	–	–	–
L. fruticetum	*G. fruticetum*	20605	–	T	*Picea engelmannii* × *P. glauca*	Canada	S. Massoumi Alamouti	OM501394	OM514730	OM631770	–
L. hughesii	*G. hughesii*	4052	109709	T	*Aquilaria* sp.	Vietnam	B. Lanchette	OM501395	OM514732	OM631772	OM631598
L. pistaciae	*G. pistaciae*	12499	123626	T	*Pistacia chinensis*	China	X.D. Zhou, Z.W. de Beer	HQ406846	–	HQ406870	–
***Grosmannia: G. grandifoliae* complex**											
G. grandifoliae	*G. grandifoliae*	703	ATCC28746	T	*Fagus grandifolia*	Iowa, USA	R.W. Davidson	–	–	OM631771	–
L. betulae	*G. betulae*	43191	142734	T	*Scolytus ratzeburgi* on *Betula verrucosa*	Poland	R. Jankowiak	KY801840	–	KY801817	–

Table 1. (Continued).

Previous name	Current name	CMW[1]	CBS or other[1]	Type[2]	Isolated from	Country	Collector	GenBank Accession Numbers[3]			
								ITS	LSU	*TEF1-α*	*RPBII*
L. pruni	*G. pruni*	10418	120197	P	*Polygraphus ssiori* on *Prunus jamasakura*	Japan	H. Masuya	OM501398	OM514740	OM631775	–
L. trypodendri	*G. trypodendri*	43182	142724	T	*Trypodendron domesticum* on *Fagus sylvatica*	Norway	R. Jankowiak	KY801828	–	KY801805	–
***Grosmannia*: Group C**											
G. abieticola	*G. abieticola*	17199	–	T	*Dryocoetes hectographus* on *Abies mariesii*	Japan	Y. Yamaoka	OM501382	OM514712	OM631761	–
L. innermongolicum	*G. innermongolica*	–	MUCL55158	T	*Ips subelongatus* on *Larix* sp.	China	Q. Lu	KM236107	–	KM981763	–
L. taigense	*G. taigensis*	36629	–	P	*Ips typographus* on *Picea abies*	Russia	Z.W. de Beer	OM501400	OM514744	OM631777	–
L. gestamen	*G. gestamen*	38096	CIEFAP453	T	*Nothofagus dombeyi*	Argentina	A. de Errasti	KT362234	KT362232	KT381300	–
***Harringtonia gen. nov.* (previously *Raffalea lauricola* complex)**											
R. aguacate	*Har. aguacate*	38067	141672	T	*Persea americana*	Florida, USA	C.L. Harmon	–	KJ909296	–	–
R. aguacate[*]	*Har. aguacate*	–	Raff. sp. 272		*Persea americana*	Florida, USA	C.L. Harmon	MT633065	MT629748	OM631783	OM631613
R. brunnea	*Har. brunnea*	–	378.68		*Monarthrum* sp.	USA	L.R. Batra	–	EU177457	–	–
R. lauricola[*]	*Har. lauricola*	–	Raff. sp. 570		*Xyleborus* sp. on *Persea* sp.	Florida, USA	J. Smith	MT633071	MT629759	OM631784	OM631614
R. lauricola	*Har. lauricola*	36261	PL159		*Xyleborus glabratus*	Georgia, USA	S. Fraedrich	OM501411	MT629760	OM631785	OM631615
Hawksworthiomyces											
Haw. crousii	*Haw. crousii*	37531	MUCL55928	T	Bamboo chips	South Korea	J.J. Kim	KX396551	KX396548	OM652622	OM631609
Haw. hibbettii	*Haw. hibbettii*	37663	MUCL55929	T	*Trachymyrmex* sp.	Texas, USA	U. Mueller	KX396550	KX396547	OM652623	OM631610
Haw. lignivorus[*]	*Haw. lignivorus*	18600	119148	T	*Eucalyptus* pole	South Africa	E.M. de Meyer	OM501410	OM514756	OM631782	OM631611
Haw. taylorii	*Haw. taylorii*	20741	MUCL55927	T	*Eucalyptus* pole	South Africa	E.M. de Meyer	KX396549	KX396546	OM652624	OM631612
'Haw. sequentia ENAS'	*'Haw. sequentia ENAS'*	–	nik62104a_03C_19	T	*Picea* log	Sweden	–	HQ611296	–	–	–
Heinzbutinia gen. nov.											
O. grandicarpum	*He. grandicarpa*	1600	250.88	T	*Quercus robor*	Poland	H. Butin	OM501412	OM514757	OM631786	OM631616
O. longicollum	*He. longicolla*	–	JCM10198	T	*Quercus mongolica* var. *grosseserrata* infested by *Platypus quercivorus*	Japan	H. Masuya	–	–	–	–
O. microsporum	*He. microspora*	17152	440.69	T	*Quercus* sp.	Virginia, USA	R.W. Davidson	–	OM514758	OM631787	OM631617
O. solheimi[#]	*He. solheimii*	52050	144881	T	*Anisandrus dispar* infesting *Quercus robur*	Poland	P.Wieczorek	MH283134	–	MH283488	–
Intubia											
I. macrotermitinarum[#]	*I. macrotermitinarum*	46496	141560	T	*Termitomyces* fungal comb of *Macrotermes natalensis*	South Africa	W.J. Nel	MT637025	–	–	–
I. oerlemansii[#]	*I. oerlemansii*	47048	141564	T	*Termitomyces* fungal comb of *Macrotermes natalensis*	South Africa	W.J. Nel	MT637024	–	–	–
***Jamesreidia gen. nov.* (previously *O. tenellum* complex)**											
O. coronatum	*J. coronata*	43836	UAMH9685	T	*Pinus* sp.	Canada	A. Olchowecki	OM501413	OM514759	OM631788	OM631618
O. nigricarpum	*J. nigricarpa*	651	638.66		*Pseudotsuga menziesii*	Idaho, USA	R.W. Davidson	AY280490	DQ294356	–	–
O. rostrocoronata	*J. rostrocoronata*	456	434.77		Pulpwood chips	Wisconsin, USA	R.W. Davidson	AY194509	KX590871	–	–
O. tenellum	*J. tenella*	37439	189.86		*Pinus* sp.	Colorado, USA	R.W. Davidson	OM501414	OM514760	OM631789	–
***Leptographium*: *L. clavigerum* complex**											
G. aurea	*L. aureum*	667	438.69	A	*Pinus contorta* var. *latifolia*	Canada	R. W. Davidson	OM501387	OM514720	OM631793	OM631621

Table 1. (Continued).

Previous name	Current name	CMW[1]	CBS or other[1]	Type[2]	Isolated from	Country	Collector	GenBank Accession Numbers[3]			
								ITS	LSU	*TEF1-α*	*RPBII*
G. clavigera[*]	*L. clavigerum*	–	SL-Kw1407		Sapwood associated with *Dendroctonus ponderosae*	Canada	S. Lee	OM501421	OM514723	OM631799	OM631624
G. robusta	*L. robustum*	668	–	T	*Pinus ponderosa*	Idaho, USA	R.C.R. Jeffrey, R.W. Davidson	–	AY544619	JF798465	–
L. longiclavatum	*L. longiclavatum*	20608	–	P	*Pinus contorta*	Canada	S. Lee	–	OM514771	–	–
L. pyrinum	*L. pyrinum*	509	120181	T	*Dendroctonus adjunctus*	USA	R.W. Davidson	OM501445	OM514781	OM631819	OM631642
L. terebrantis	*L. terebrantis*	29841	337.70	T	*Dendoctronus terebrantis*	Louisiana, USA	S.J. Baras	JF798477	–	JF798470	–
L. tereforme	*L. tereforme*	37432	125736	T	*Hylurgus ligniperda*	California, USA	S.J. Kim	OM501455	OM514786	OM631828	OM631649
L. wingfieldii	*L. wingfieldii*	4741	–		*Pinus densiflora*	Japan	H. Masuya	OM501461	OM514789	OM631834	OM631654
***Leptographium*: *L. galeiforme* complex**											
G. galeiformis[*]	*L. galeiforme*	5290	115711	E	*Pinus sylvestris*	Scotland	T. Kirisits	OM501428	OM514731	OM631806	OM631631
G. radiaticola	*L. radiaticola*	9482	–		*Hylurgus ligniperda* on *Pinus radiata*	Chile	X.D. Zhou	OM501446	OM514742	OM631820	OM631643
L. doddsii[#]	*L. doddsii*	34479	143470	T	*Dendroctonus valens*	California, USA	M.J. Wingfield	MT637215	MT637212	MT637205	–
L. gordonii[#]	*L. gordonii*	34619	143477	T	*Dendroctonus valens* in *Pinus resinosa*	New Hampshire, USA	M.J. Wingfield	MT637226	MT637213	MT637207	–
L. koraiense	*L. koraiense*	44461	141898	T	*Ips typographus* on *Pinus koraiensis*	China	R. Chang	MH144096	–	MH124372	–
L. owenii[#]	*L. owenii*	34448	143467	T	*Dendroctonus valens*	California, USA	M.J. Wingfield	MT637217	KF515912.1	KF515884.1	–
L. seifertii[#]	*L. seifertii*	34620	143478	T	*Dendroctonus valens* on *Pinus resinosa*	New Hampshire, USA	M.J. Wingfield	MT637224	KF515911.1	KF515885.1	–
***Leptographium*: *L. lundbergii* complex**											
G. koreana	*L. koreanum*	14199	KUC2078	T	*Tomicus piniperda* on *Pinus koraiensis*	South Korea	J.J. Kim	OM501431	OM514733	OM631808	OM631633
G. yunnanensis	*L. yunnanense*	5152	–		*Pinus yunnanensis*	China	X.D. Zhou	AY707207	–	–	–
L. absconditum	*L. absconditum*	39763	136527	T	*Orthotomicus laricis* on *Pinus nigra*	Spain	P. Romón	OM501415	OM514761	OM631790	–
L. celere	*L. celere*	12422	123628	T	*Pinus semaonensis*	China	X.D. Zhou, Z.W. de Beer	HQ406834	–	HQ406858	–
L. conjunctum	*L. conjunctum*	12473	123631	T	*Pinus yunnanensis*	China	X.D. Zhou, Z.W. de Beer	HQ406831	–	HQ406855	–
L. lundbergii[*]	*L. lundbergii*	2190	138716		*Pinus sylvestris*	Norway	H. Roll-Hansen	OM501432	OM514772	OM631809	OM631634
L. manifestum	*L. manifestum*	12436	123622	T	*Larix olgensis*	China	X.D. Zhou, Z.W. de Beer	HQ406839	–	HQ406863	–
L. pinicola	*L. pinicola*	2398	–	T	*Hylastes* sp. on *Pinus* sp.	Canada	J. Juzwik	OM501439	OM514775	–	–
L. shansheni	*L. shansheni*	44462	141895	T	*Ips typographus* on *Picea* sp.	China	R. Chang, S.F. Chen	MH144097	–	MH124373	–
L. sosnaicola[#]	*L. sosnaicola*	52084	147023	T	*Pinus sylvestris*	Poland	D. Jazłowiecka	MT210337	MT210353	MT210397	–
L. truncatum	*L. truncatum*	28	929.85	T	*Pinus taeda*	South Africa	M.J. Wingfield	DQ062052/ AY935626	–	DQ062019	–
L. wushanense	*L. wushanense*	–	YMF1.04936	T	*Pinus* sp.	China	J. Lu	MG878407	–	MG878409	–
***Leptographium*: *L. olivaceum* complex**											
G. cucullata[*]	*L. cucullatum*	1035	218.83	T	*Ips typographus*	Norway	H. Solheim	OM501423	OM514724	OM631801	OM631626
G. davidsonii	*L. davidsonii*	–	YCC611		Logs of *Larix kaempferi* infested with *Ips subelongatus*	Japan	Y. Yamaoka	GU134165	–	–	–

Table 1. (Continued).

Previous name	Current name	CMW[1]	CBS or other[1]	Type[2]	Isolated from	Country	Collector	GenBank Accession Numbers[3]			
								ITS	LSU	*TEF1-α*	*RPBII*
G. olivacea	*L. olivaceum*	23348	–		*Pinus sylvestris*	Finland	Z.W. de Beer, P. Niemelä	OM501434	OM514735	OM631811	–
G. olivaceapini	*L. olivaceapini*	116	504.86	E	*Pinus ponderosa* in *Dendroctonus* sp.	Arizona, USA	T. Hinds	OM501433	OM514736	OM631810	OM631635
G. sagmatospora	*L. sagmatosporum*	43846	UAMH6971		*Pinus strobus*	Canada	B. Grylls, K. Seifert	OM501449	OM514743	OM631823	–
G. vesca	*L. vescum*	34186	800.73		*Ips pilifrons*, *Dendroctonus engelmanni* in *Picea engelmannii*	Colorado, USA	F.F. Lombard, R. W. Davidson	OM501457	OM514745	–	–
L. brevicolle	*L. brevicolle*	–	150.78		Beetle gallery in *Populus tremuloides*	Colorado, USA	R.W. Davidson	MH055549	AF155670	MH055635	–
L. breviuscapum	*L. breviuscapum*	38888	136507	T	*Picea crassifolia* infested with *Polygraphus poligraphus*	China	M.L. Yin, X.D. Zhou	OM501419	OM514763	MN517742	–
L. conplurium	*L. conplurium*	23289	128834	P	*Pinus sylvestris*	Finland	Z.W. de Beer, P. Niemelä	OM501422	OM514765	OM631800	OM631625
L. duchongi	*L. duchongi*	44455	141897	T	*Ips typographus* on *Pinus koraiensis*	China	R. Chang	MH144122	–	MH124398	–
L. erubescens	*L. erubescens*	40672	278.54	E	*Pinus sylvestris*	Sweden	A. Mathiesen-Käärik	OM501425	OM514767	OM631803	OM631628
L. flavum	*L. flavum*	51797	144099	T	*Quercus robur*	Poland	R. Jankowiak	MH055548	–	MH055634	–
L. francke-grosmanniae	*L. francke-grosmanniae*	445	356.77	T	*Hylecoetus dermestoides* on *Quercus* sp.	Germany	H. Francke-Grosmann	OM501427	OM514768	OM631805	OM631630
L. sylvestris	*L. sylvestris*	23300	128833	P	*Picea abies*	Finland	Z.W. de Beer, P. Niemelä	OM501454	OM514777	OM631827	–
L. pseudoalbum	*L. pseudoalbum*	40671	276.54	T	*Blastophagus piniperda* in *Pinus sylvestris*	Sweden	A. Mathiesen-Käärik	MN516723	MN516723	MN517755	OM631641
L. raffai[#]	*L. raffai*	34451	143468	T	*Dendroctonus valens*	California, USA	M.J. Wingfield	MT637219	MT637211	MT637206	–
L. rhizoidum	*L. rhizoidum*	22809	136512	T	*Hylastes ater* on *Pinus radiata*	Spain	P. Romón, X.D. Zhou	MN516724	MN516724	MN517748	OM631644
L. tardum	*L. tardum*	51789	144091	T	*Trypodendron domesticum* on *Fagus sylvatica*	Poland	R. Jankowiak	MH055529	–	MH055615	–
L. vulnerum	*L. vulnerum*	51794	144096	T	*Fagus sylvatica*	Poland	R. Jankowiak	MH055534	–	MH055620	–
L. xiningense[#]	*L. xiningense*	38891	136509	T	*Polygraphus poligraphus* in *Picea crassifolia*	China	M.L. Yin, X.D. Zhou	MN516732	MN516732	MN517752	OM631637
***Leptographium*: *L. piceiperdum* complex**											
G. aenigmatica	*L. aenigmaticum*	2199	–	T	*Ips typographus japonicus* on *Picea jezoensis*	Japan	Y. Yamaoka	OM501416	OM514716	OM631791	OM631619
G. europhioides	*L. europhioides*	2811	115245		*Picea rubens*	New York, USA	T. Harrington	OM501426	OM514729	OM631804	OM631629
G. laricis	*L. laricis*	1913	120188		*Larix* sp.	Japan	Y. Yamaoka	–	DQ294393	–	–
G. piceiperdum[*]	*L. piceiperdum*	16768	138719		*Picea glauca*	Canada	K. Harrison	OM501435	OM514738	OM631812	OM631636
G. pseudoeurophioides	*L. pseudoeurophioides*	–	WIN(M)42		–	Canada	J. Reid	EU879136	–	–	–
L. heilongjiangense	*L. heilongjiangense*	44456	141702	T	*Ips typographus* on *Pinus koraiensis*	China	R. Chang	MH144098	–	MH124374	–
L. zhangii	*L. zhangii*	–	MUCL55162	T	*Ips subelongatus* on *Larix gmelinii*	China	X. Liu	KM236108	–	KM974275	–
***Leptographium*: *L. procerum* complex**											
L. bhutanense	*L. bhutanense*	18649	122076	T	*Pinus wallichiana*	Bhutan	M.J. Wingfield	OM501418	OM514762	OM631794	–
L. gracile	*L. gracile*	12398	123623	T	*Pinus armandii*	China	X.D. Zhou	OM501430	OM514769	–	–

Table 1. (Continued).

Previous name	Current name	CMW[1]	CBS or other[1]	Type[2]	Isolated from	Country	Collector	GenBank Accession Numbers[3]			
								ITS	LSU	*TEF1-α*	*RPBII*
L. latens	*L. latens*	12438	124023	T	*Picea koraiensis*	China	X.D. Zhou, Z.W. de Beer	HQ406845	–	HQ406869	–
L. longiconidiophorum	*L. longiconidiophorum*	2004	135624	T	*Hylastes* sp. on *Pinus densiflora*	Japan	M.J. Wingfield	KM491421	–	KM491471	–
L. peucophilum	*L. peucophilum*	2876	120191		*Picea* sp.	New York, USA	D. Bergdalh	–	–	–	–
L. pini-densiflorae	*L. pini-densiflorae*	5157	115261	T	*Pinus densiflora*	Japan	H. Masuya	OM501438	OM514774	OM631815	
L. procerum[*]	*L. procerum*	34542	138288	E	*Dendroctonus valens* on *Pinus resinosa*	Maine, USA	M.J. Wingfield	OM501442	OM514778	OM631816	OM631639
L. profanum	*L. profanum*	10552	120307	T	*Carya* sp.	Alabama, USA	L. Eckhardt	OM501443	OM514779	OM631817	OM631640
L. sibiricum	*L. sibiricum*	4481	115260	T	*Monochamus urussoni* on *Abies sibitica*	Russia	V.P. Vetrova	OM501451	OM514783	–	–
L. sinense	*L. sinense*	38171	316515	P	*Pinus elliottii*	China	M. Yin, R. Chang, X.D. Zhou	OM501452	OM514784	OM631825	OM631647
L. sinoprocerum	*L. sinoprocerum*	29990	MUCL46532	T	*Pinus tabuliformis*	China	Q. Lu	OM501453	OM514785	OM631826	OM631648
L. yichunense	*L. yichunense*	44464	141705	T	*Ips typographus* on *Picea* sp.	China	R. Chang, S.F. Chen	MH144114	–	MH124390	–
***Leptographium*: *L. serpens* complex**											
G. alacris	*L. alacre*	621	128830	T	*Pinus pinaster*	Portugal	M. de Famtima Moniz	OM501417	OM514717	OM631792	OM631620
G. serpens	*L. serpens*	305	141.36	T	*Pinus sylvestris*	Italy	G. Goidànich	OM501450	–	OM631824	OM631646
L. castellanum	*L. castellanum*	2320	128698	P	*Pinus occidentalis*	Dominican Republic	R. Webb	OM501420	OM514764	OM631798	OM631623
L. gibbsii	*L. gibbsii*	36371	–	T	*Hylastes opacus* on *Pinus sylvestris*	England, UK	J. Gibbs	OM501429	–	OM631807	OM631632
L. rhodanense	*L. rhodanense*	16438	138284	T	*Pinus sylvestris*	Switzerland	U. Heiniger	OM501448	–	OM631822	OM631645
L. yamaokae	*L. yamaokae*	4726	129732	T	*Pinus densiflora*	Japan	H. Masuya	–	–	OM631835	OM631655
***Leptographium*: *L. wageneri* complex**											
G. wageneri[*]	*L. wageneri* var. *ponderosum*	279	–		*Pinus* sp.	USA	T. Harrington	OM501458	OM514746	OM631831	OM631651
L. douglasii[*]	*L. douglasii*	2076	–	P	*Pseudotsuga menziesii*	New Mexico, USA	M. Midke	OM501424	OM514766	OM631802	OM631627
L. neomexicanum	*L. neomexicanum*	2079	168.93	T	*Pinus ponderosa*	New Mexico, USA	T. Harrington, W Livingston	AY553382	–	AY536176	–
L. reconditum	*L. reconditum*	15	116348		*Zea mays*	South Africa	W. Jooste	AF343690	–	AY536177	–
L. wageneri var. *pseudotsugae*[*]	*L. wageneri* var. *pseudotsugae*	154	115246		*Pseudotsuga menziesii*	USA	T. Harrington	OM501459	OM514747	OM631832	OM631652
L. wageneri var. *wageneri*[*]	*L. wageneri* var. *wageneri*	53	139665		*Pinus ponderosa*	California, USA	T. Harrington	OM501460	OM514788	OM631833	OM631653
***Leptographium*: Group A**											
L. pineti	*L. pineti*	3837	115257		*Pinus* sp.	Indonesia	M.J. Wingfield	–	–	OM631814	OM631638
L. ningerense	*L. ningerense*	41786	139663	T	*Coccotrypes cyperi* on *Pinus kesiya*	China	S. Taerum	MG205674	–	MG205765	–
***Leptographium*: Group B**											
G. cainii	*L. cainii*	24907	–		*Picea* sp.	Canada	C. Breuil	OM501389	OM514722	OM631797	OM631622
***Leptographium Incertae sedis* (based on our data)**											
G. huntii	*G. huntii*	2868	118780		*Pinus strobus*	North Carolina, USA	V. Lackner	AY553394	–	DQ354938	–
G. leptographioides	*G. leptographioides*	481	144.59		*Quercus* sp.	New York, USA	R.W. Davidson	–	DQ294382	–	–

Table 1. (Continued).

Previous name	Current name	CMW[1]	CBS or other[1]	Type[2]	Isolated from	Country	Collector	GenBank Accession Numbers[3]			
								ITS	LSU	*TEF1-α*	*RPBII*
G. truncicola	*G. truncicola*	–	–		*Dendroctonus* sp. on *Picea* sp.	USA	–	–	–	–	–
L. albopini	*L. albopini*	^26	–		*Hylastes* sp. on *Pinus* sp.	USA	–	AF343695	–	–	–
L. alethinum	*L. alethinum*	^3763	–		Galleries of *Hylobus abietis* on log of *Pinus nigra* var. *maritima*	England, UK	A. Uzunovic	AY553391	–	AY536185	
L. calophylli	*L. calophylli*	752	277.51		*Cryphalus* sp. on *Calophyllum* sp.	Mauritius	J.A. Stevenson	MH856855	MH868375	–	–
L. microsporum	*L. microsporum*	–	–	T	*Fagus* sp.	Mississippi, USA	R.W. Davidson	–	–	–	–
L. obscurum	*L. obscurum*	37429	125.39		*Pinus* sp.	USA	R.W. Davidson	–	–	–	–
L. pityophilum	*L. pityophilum*	2840	109706		*Pinus nigra*	Italy	S. Frisullo	OM501441	OM514776	–	–
L. rostrocylindricum	*L. rostrocylindricum*	–	–		*Quercus* sp.	Connecticut, USA	R.W. Davidson	–	–	–	–
***Leptographium* & *Grosmannia incertae sedis* (based on our data)**											
L. guttulatum	*L. guttulatum*	1310	120185	T	*Tomicus piniperda* on *Pinus sylvestris*	England, UK	J. Gibbs	–	OM514770	–	–
Lineage III											
G. crassivaginata	*G. crassivaginata*	90	120178		–	–	T. Hinds	AF343673	–	–	–
L. alneum#	*L. alneum*	52076	144901	T	*Dryocoetes alni* infesting *Populus tremula*	Poland	K. Miśkiewicz	MN900997	MN900997	MN901024	–
L. piriforme	*L. piriforme*	25381	UAMH10681	P	Beetle caught in a trap baited with coyote dung	Canada	M.D. Greif	OM501440	–	–	–
Lineage VI											
L. verrucosum	*L. verrucosum*	17160	112420	T	*Xyleborus dryographus*	Germany	H. Gebhardt	OM501456	OM514787	OM631830	OM631650
Masuyamyces gen. nov.											
O. ambrosium	*M. ambrosius*	1024	210.64		Wood of *Pinus sylvestris*	Netherlands	J.A. von Arx	OM501465	OM514793	OM631836	OM631656
O. acarorum	*M. acarorum*	41850	139748	T	*Orthotomicus angulatus* on *Pinus kesiya*	China	S. Taerum	MG205657	–	–	–
O. botuliforme	*M. botuliformis*	14493	–		*Cryphalus jeholensis*	Japan	H. Masuya	OM501471	OM514799	OM631837	–
O. jilinense	*M. jilinensis*	40491	141894	T	*Ips typographus* on *Picea* sp.	China	X. D. Zhou	MH144094	–	MH124370	–
O. lotiforme#	*M. lotiformis*	–	MUCL55165	T	*Ips subelongatus* on *Pinus sylvestris* var. *mongolica*	China	X. Meng	MK748185	–	–	–
O. massoniana	*M. massonianae*	–	MUCL55179	T	*Monochamus* sp. on *Pinus* sp.	China	Q. Lu	KY094067	–	–	–
O. pallidulum	*M. pallidulus*	23278	128118	T	*Pinus sylvestris*	Russia	Z.W. de Beer, P. Niemelä	HM031510	–	–	–
O. saponiodorum	*M. saponiodorus*	28135	128302		*Pinus sylvestris*	Russia	R. Linnakoski	OM501512	OM514838	OM631838	OM631657
***Ophiostoma*: *O. clavatum* complex**											
O. ainoae	*O. ainoae*	1037	205.83	T	*Picea abies*	Norway	H. Solheim	OM501463	OM514791	–	–
O. brevipilosi	*O. brevipilosi*	41873	139660	T	*Tomicus brevipilosus* on *Pinus kesiya*	China	S. Taerum	MG205660	–	MG205732	–
O. brunneociliatum	*O. brunneociliatum*	5212	–		*Larix* sp.	Scotland, UK	T. Kirisits	KU184422	–	KU184379	–
O. brunneolum	*O. brunneolum*	23145	–	A	*Picea abies*	Russia	J. Ahtiainen, P. Niemelä	OM501472	OM514800	OM631843	OM631663
O. clavatum	*O. clavatum*	37983	141080	E	*Ips acuminatus* on *Pinus sylvestris*	Sweden	C. Villari	OM501477	OM514805	OM631848	–
O. hongxingense#	*O. hongxingense*	–	CFCC52695	T	*Ips subelongatus* on *Larix gmelinii*	China	Q. Lu	MK748194	–	MN896068	–
O. japonicum	*O. japonicum*	2202	YCC099	T	*Ips typographus japonicus* on *Picea jezoensis*	Japan	Y. Yamaoka	OM501492	–	OM631855	OM631673
O. jiamusiensis	*O. jiamusiensis*	40512	141893	T	*Ips typographus* on *Picea* sp.	China	X.D. Zhou	MH144064	–	MH124343	–

Table 1. (Continued).

Previous name	Current name	CMW[1]	CBS or other[1]	Type[2]	Isolated from	Country	Collector	GenBank Accession Numbers[3]			
								ITS	LSU	*TEF1-α*	*RPBII*
O. macroclavatum	*O. macroclavatum*	23115	141081	T	*Pinus sylvestris*	Russia	Z.W. de Beer	HM031499	–	KU094765	–
O. peniculi[#]	*O. peniculi*	–	CFCC52687	T	*Ips subelongatus* infesting *Larix gmelinii*	China	Q. Lu	MK748198	–	MN896063	–
O. poligraphi	*O. poligraphi*	38899	136517	T	*Polygraphus poligraphus* on *Picea crassifolia*	China	M. Yin, S. Taerum, X.D. Zhou	OM501507	OM514832	OM631871	OM631688
O. pseudocatenulatum	*O. pseudocatenulatum*	43103	141276	T	*Ips cembrae* on *Larix decidua*	Poland	R. Jankowiak	KU094686	–	KU094774	–
O. shangrilae	*O. shangrilae*	38901	136519	T	*Ips shangrila* on *Picea purpurea*	China	M. Yin, S. Taerum, X.D. Zhou	OM501514	OM514840	OM631879	OM631695
O. songshui	*O. songshui*	44473	141707	T	*Ips typographus* on *Picea* sp.	China	R. Chang, S.F. Chen	MH144065	–	MH124344	–
O. subelongati[#]	*O. subelongati*	–	CFCC52693	T	*Ips subelongatus* infesting *Larix gmelinii*	China	Q. Lu	MK748200	–	MN896064	–
O. tapionis	*O. tapionis*	23266	128122	P	*Picea abies*	Russia	Z.W. de Beer, P. Niemelä	OM501516	OM514842	OM631881	OM631697
Ophiostoma sp. 3 *(Hyalorhinocladiella* sp. 2*)*	*Ophiostoma* sp. 3 *(Hyalorhinocladiella* sp. 2*)*	43851	UAMH10642		*Ips* sp.	Canada	S. Massoumi Alamouti	OM501524	OM514851	OM631888	–
Ophiostoma sp. 4 *(Hyalorhinocladiella* sp. 1*)*	*Ophiostoma* sp. 4 *(Hyalorhinocladiella* sp. 1*)*	43848	UAMH10639		*Ips* sp.	Canada	S. Massoumi Alamouti	OM501525	OM514852	OM631889	OM631704
***Ophiostoma*: *O. ips* complex**											
O. adjuncti	*O. adjuncti*	1025	314.77	T	Stained sapwood in *Pinus ponderosa*	New Mexico, USA	R.W. Davidson	OM501462	OM514790	–	OM631658
'O. arborea'	*'O. arborea'*	–	WIN(M)69-23		*Picea mariana*	Canada	A. Olchowecki, J. Reid	–	–	–	–
O. bicolor	*O. bicolor*	23169	–		*Pinus sylverstris*	Russia	J. Ahtiainen, P. Niemelä	OM501470	OM514798	OM631842	OM631662
O. columnare	*O. columnare*	–	WIN(M)71-27		*Pinus banksiana*	Canada	A. Olchowecki, J. Reid	–	–	–	–
O. fuscum	*O. fuscum*	23195	128124	P	*Pinus sylverstris*	Finland	Z.W. de Beer, P. Niemelä	OM501483	OM514810	–	OM631670
O. gilletteae[#]	*O. gilletteae*	30681	143458	T	*Dendroctonus valens*	Washington, USA	N. Gillette	MT637227	–	–	–
O. guatemalensis	*O. guatemalensis*	44221	–	T	*Pinus patula*	Guatemala	I. Barnes, J. Garnas	–	–	–	–
O. hyalothecium	*O. hyalothecium*	–	ATCC28825		*Pinus contorta*	Wyoming, USA	R.W. Davidson	–	AF137284	–	–
Tubercullariella ips	*O. ips*-like sp. 6	14175	435.34	T	*Ips* sp. on *Pinus* sp.	Minnesota, USA	J.G. Leach	OM501487	OM514813	OM631854	OM631672
O. ips[*]	*O. ips*	19371	138721		*Pinus taeda*	Louisiana, USA	X.D. Zhou	OM501486	OM514812	OM631853	OM631671
O. manchongi[#]	*O. manchongi*	41954	141906		*Uropodoidea* sp. in *Ips shangrila* gallery on *Picea purpurea*	China	S.J. Taerum	MH121662	–	–	–
O. montium	*O. montium*	15419	–		*Pinus contorta*	Idaho, USA	B. Bentz	OM501498	OM514822	OM631861	OM631678
O. pseudobicolor[#]	*O. pseudobicolor*	–	CFCC52683	T	*Ips subelongatus* in *Larix gmelinii*	China	Q. Lu	MK748188	–	–	–
O. pulvinisporum	*O. pulvinisporum*	9022	118673	T	*Pinus pseudostrobus*	Mexico	X.D. Zhou	OM501509	OM514835	OM631874	OM631691
***Ophiostoma*: *O. minus* complex**											
'O. album'	*'O. album'*	–	MUCL55189	T	*Monochamus alternatus* gallery on *Pinus massoniana*	China	Q. Lu, Y.Y. Lun	KY094073	–	–	–
O. exiguum	*O. exiguum*	–	–		*Pinus virginiana*	West Virginia, USA	G.G. Hedgcock	–	–	–	–

Table 1. (Continued).

Previous name	Current name	CMW[1]	CBS or other[1]	Type[2]	Isolated from	Country	Collector	GenBank Accession Numbers[3]			
								ITS	LSU	*TEF1-α*	*RPBII*
O. kryptum	*O. kryptum*	–	116190	T	*Tetropium* on *Picea*	Austria	T. Kirisits	AY305685	–	–	–
O. minus	*O. minus*	43873	UAMH4917		*Dendroctonus ponderosae* on *Pinus flexillis*	Canada	P. Muruyama	OM501497	OM514821	OM631860	OM631677
'O. olgensis'	*'O. olgensis'*	–	CXY1410	T	*Ips subelongatus* on *Larix olgensis*	China	Q. Lu	KU551303	–	KU551297	–
O. minus (in Europe *O. pini*)	*O. minus* (in Europe *O. pini*)	43346	–		*Pinus sylvestris*	Poland	T. Tomasz	–	–	–	–
O. pseudominus	*O. pseudominus*	43878	UAMH9721		*Pseudotsuga menziesii*	Canada	J. Reid, B Reid	OM501508	OM514834	OM631873	OM631690
O. pseudotsugae	*O. pseudotsugae*	–	D48/3		–	Canada	H. Solheim	AY542501	–	–	–
O. wuyingense	*O. wuyingense*	44474	141706	T	*Ips typographus* on *Picea* sp.	China	R. Chang, S.F. Chen	MH144061	–	MH124340	–
***Ophiostoma*: *O. piceae* complex**											
O. arduennense (= *O. distortum*)	*O. distortum*	40266	MUCL44866	T	*Fagus sylvatica*	Belgium	F.X. Carlier, T. Defrance	OM501468	OM514796	KU184376	–
O. brunneum	*O. brunneum*	1027	161.61	A	Standing dead *Abies* sp.	Colorado, USA	R.W. Davidson	OM501473	OM514801	OM631844	OM631664
O. canum (Pachnodium)	*O. canum (Pachnodium)*	5023	118668		*Tomicus minor* on *Pinus sylvestris*	Austria	T. Kirisits	OM501474	OM514802	OM631845	OM631665
O. cupulatum	*O. cupulatum*	37441	102358	T	*Pseudotsuga menziesii*	Washington, USA	T. Harrington	OM501479	OM514806	OM631849	OM631667
O. distortum	*O. distortum*	467	397.77		*Picea engelmannii*	Arizona, USA	R.W. Davidson	OM501481	OM514808	OM631850	OM631668
O. flexuosum	*O. flexuosum*	907	208.83	T	*Picea abies*	Norway	H. Solheim	OM501482	OM514809	OM631851	OM631669
O. floccosum	*O. floccosum*	34182	799.73	T	Wood	Sweden	A. Mathiesen-Käärik	KU184431	–	KU184388	–
O. genhense#	*O. genhense*	–	CFCC52675	T	*Ips subelongatus* infesting *Larix gmelinii*	China	Q. Lu	MK748199	–	MN896074	–
O. kunlunense#	*O. kunlunense*	41927	141903	T	*Uropodoidea* sp. in gallery of *Ips shangrila* on *Picea purpurea*	China	S.J. Taerum	MH121648	–	MH124515	–
O. micantis	*O. micantis*	38903	136523	T	*Dendroctonus micans* on *Picea crassifolia*	China	M. Yin, S. Taerum, X.D. Zhou	OM501496	OM514820	OM631859	OM631676
O. multisynnematum#	*O. multisynnematum*	–	CFCC52677		*Ips subelongatus* infesting *Larix gmelinii*	China	Q. Lu	MK748196	–	MN896071	–
O. nikkoense	*O. nikkoense*	17193	YCC430	T	*Polygraphus proximus*	Japan	Y. Yamaoka	OM501500	OM514824	OM631863	OM631679
O. nitidi	*O. nitidi*	38907	136525	T	*Picea crassifolia*	China	M. Yin, S. Taerum, X.D. Zhou	OM501501	OM514825	OM631864	OM631680
O. perfectum	*O. perfectum*	17153	600.85		Cat hairs	Germany	G.S. de Hoog	OM501506	OM514831	OM631868	OM631685
O. peregrinum	*O. peregrinum*	–	CIEFAP426	T	*Pinus radiata*	Argentina	A. de Errasti	MG345116	–	–	–
*O. piceae**	*O. piceae*	–	UAMH11346		Pine saw timber	Canada	A. Uzunovic	MT633062	MT629745	OM631869	OM631686
O. pityokteinis#	*O. pityokteinis*	52056	144879	T	*Pityokteines curvidens* infesting *Abies alba*	Poland	P. Majka	MH837046	–	MH837055	–
O. qinghaiense	*O. qinghaiense*	38902	136521	T	*Picea crassifolia*	China	M. Yin, S. Taerum, X.D. Zhou	OM501510	OM514836	OM631875	–
O. rachisporum	*O. rachisporum*	28021	–		*Picea abies*	Russia	R. Linnakoski	OM501511	OM514837	OM631877	OM631693
O. rufum#	*O. rufum*	52062	144871	T	*Ips cembrae* galleries on *Larix decidua*	Czech Republic	K. Lukášová	MH837040	–	KY568647	–
O. setosum	*O. setosum*	27833	AU160-38	T	*Tsuga* sp.	Canada	A. Uzunovic	OM501513	OM514839	OM631878	OM631694
O. shanziensis#	*O. shanziensis*	48329	MUCL46456	T	Phloem adjacent to *Dendroctonus valens* gallery in *Pinus tabuliformis*	China	Q. Lu, C. Decock	MT637221	–	–	–
O. sugadairense	*O. sugadairense*	–	YCC589	T	*Polygraphus* sp. on *Larix* sp.	Japan	Y. Yamaoka	LC090227	–	AB934343	–

Table 1. (Continued).

Previous name	Current name	CMW[1]	CBS or other[1]	Type[2]	Isolated from	Country	Collector	GenBank Accession Numbers[3]			
								ITS	LSU	*TEF1-α*	*RPBII*
O. taphrorychi[#]	*O. taphrorychi*	52045	144891	T	*Taphrorychus bicolor* infesting *Fagus sylvatica*	Poland	P. Bilánski	MH837052	–	MH837062	–
O. typographi	*O. typographi*	44483	141709	T	*Picea* sp.	China	R. Chang, S.F. Chen	MH144059	–	MH124337	–
O. torulosum	*O. torulosum*	10574	CTK106		*Fagus sylvatica*	Germany	T. Kirisits	OM501518	OM514844	OM631883	OM631699
O. xinganense[#]	*O. xinganense*	–	CFCC52679		*Ips subelongatus* infesting *Larix gmelinii*	China	Q. Lu	MK748186	–	MN896078	–
***Ophiostoma*: *O. pluriannulatum* complex**											
O. californicum	*O. californicum*	143	796.73		*Prunus domestica*	California, USA	R.W. Davidson	KU756602	AF137280	–	–
O. carpenteri	*O. carpenteri*	44611	UAMH9696	P	*Trypodendron lineatum*	Oregon, USA	S. Carpenter	OM501475	OM514803	OM631846	–
O. conicola	*O. conicola*	2561	127.89	T	*Pinus cembroides*	Mexico	H. Butin	OM501478	–	–	–
O. longiconidiatum	*O. longiconidiatum*	14265	121350	A	*Faurea saligna*	South Africa	G. Kamgan Nkuekam	OM501494	OM514818	OM631857	–
O. longirostellatum	*O. longirostellatum*	–	134.51	T	*Quercus* sp.	Scotland, UK	B.K. Bakshi	–	AF155688	–	–
O. multiannulatum	*O. multiannulatum*	2567	357.77		*Pinus* sp.	North Carolina, USA	R.W. Davidson	OM501499	OM514823	OM631862	–
O. novae-zelandiae	*O. novae-zelandiae*	–	CIEFAP423	T	Dead fallen wood	New Zealand	–	KT362249	KT362226	–	–
O. palustre	*O. palustre*	44403	140596	T	*Barringtonia racemosa*	South Africa	J.A. Osorio	KU865593	–	–	–
O. pluriannulatum	*O. pluriannulatum*	–	MUCL18372		*Quercus* sp.	Oregon, USA	R.W. Davidson	AY934517	DQ294365	–	–
O. populinum	*O. populinum*	50149	212.67	T	*Populus tremuloides*	Colorado, USA	R.W. Davidson	–	OM514833	OM631872	OM631689
O. retusi	*O. retusi*		ATCC22324		*Populus* sp.	Colorado, USA	R.W. Davidson	–	L05783	–	–
O. sparsiannulatum	*O. sparsiannulatum*	17231	122815	T	*Pinus taeda*	Georgia, USA	L. Eckhardt	OM501515	OM514841	OM631880	OM631696
O. subannulatum	*O. subannulatum*	518	188.86		*Pinus* sp.	USA	W.H. Livingston, R.W. Davidson	AY934522	DQ294364	–	–
***Ophiostoma*: *O. ulmi* complex**											
O. allantosporum	*O. allantosporum*	163	185.86		*Pinus resinosa*	Wisconsin, USA	M.J. Wingfield	OM501464	OM514792	OM631839	OM631659
O. araucariae	*O. araucariae*	40665	114.68	T	*Araucaria araucana*	Chile	H. Butin	OM501467	OM514795	–	–
O. australiae	*O. australiae*	6606	121025	T	*Acacia mearnsii*	Australia	M.J. Wingfield	EF408603	–	–	–
O. bacillisporum	*O. bacillisporum*	2579	MUCL45378	T	*Xyloterus domesticus* on *Fagus sylvatica*	Germany	F.X. Carlier	OM501469	OM514797	OM631841	OM631661
O. borealis	*O. borealis*	18966	123222	T	*Betula* logs	Norway	G. Kamgan Nkuekam, H. Solheim	EF408593	–	–	–
O. catonianum	*O. catonianum*	11535	263.35	A	*Pyrus communis*	Italy	G. Goidanich	AF198243	–	–	–
O. denticiliatum	*O. denticiliatum*	29493	124497	T	*Betula pendula*	Norway	R. Linnakoski	FJ804490	–	–	–
O. himal-ulmi	*O. himal-ulmi*	22729	ATCC36204		*Ulmus* sp.	India	H. Rebel	OM501484	OM514811	OM631852	–
O. hylesini	*O. hylesini*	51680	144296	T	*Hylesinus crenatus* on *Fraxinus excelsior*	Poland	P. Wieczorek	MH055636	MH055675	MH062835	–
O. introcitrinum	*O. introcitrinum*	–	UAMH9549	T	*Betula* sp.	Canada	A. Olchowecki	OM501485	–	–	–
O. karelicum	*O. karelicum*	23099	123219	T	*Scolytus* sp. on *Betula* sp.	Russia	Z.W. de Beer, P. Niemelä	OM501493	OM514817	OM631856	OM631674
O. novo-ulmi subsp. *americana*	*O. novo-ulmi* subsp. *americana*	43874	UAMH5030		*Ulmus americana*	–	–	–	OM514828	–	OM631683
O. novo-ulmi subsp. *novo-ulmi*[*]	*O. novo-ulmi* subsp. *novo-ulmi*	–	H327		*Ulmus* sp.	Slovakia	H. Jamnicky	OM501503	OM514827	OM631865	OM631682
O. novo-ulmi subsp. *novo-ulmi*	*O. novo-ulmi* subsp. *novo-ulmi*	43870	UAMH10443		*Ulmus* sp.	Iran	M. Rahju, K. Rahnama	OM501504	OM514829	OM631866	OM631684

Table 1. (Continued).

Previous name	Current name	CMW[1]	CBS or other[1]	Type[2]	Isolated from	Country	Collector	GenBank Accession Numbers[3]			
								ITS	LSU	*TEF1-α*	*RPBII*
O. patagonicum	*O. patagonicum*	38089	CIEFAP431	T	*Nothofagus pumilio*	Argentina	A. de Errasti	OM501505	OM514830	OM631867	–
O. pseudokarelicum	*O. pseudokarelicum*	51704	144281	T	*Trypodendron domesticum* on *Alnus incana*	Norway	T. Aas	MH055659	MH055693	MH062859	–
*O. quercus**	*O. quercus*	2465	117912		*Quercus robur*	France	M. Morelet	MT633064	MT629747	OM631876	OM631692
O. signatum	*O. signatum*	51689	144269	T	*Trypodendron signatum* on *Alnus incana*	Norway	G. Kvammen	MH055645	MH055682	MH062844	–
O. tasmaniense	*O. tasmaniense*	29088	127212	T	*Eucalyptus nitens* stumps	Australia	G. Kamgan Nkuekam	GU797211	–	GU797223	–
O. tsotsi	*O. tsotsi*	18134	123599	A	*Julbenardia globiflora*	Malawi	J. Roux	OM501520	OM514846	–	OM631701
*O. ulmi**	*O. ulmi*	–	W9		*Ulmus* sp.	–	–	OM501521	OM514847	OM631885	OM631702
O. undulatum	*O. undulatum*	19396	127183		*Eucalyptus grandis*	Australia	M.J. Wingfield	–	OM514848	–	–
O. villosum	*O. villosum*	51694	144274	T	*Dryocoetes villosus* on *Quercus robur*	Norway	T. Aas, K.D. Hansen	MH055650	MH055685	MH062849	–
***Ophiostoma*: Group H**											
O. triangulosporum	*O. triangulosporum*	1033	138.77	T	*Araucaria angustifolia*	Brazil	H. Butin	OM501519	OM514845	OM631884	OM631700
***Ophiostoma*: Group I**											
*O. macrosporum**	*O. macrosporum*	14176	367.53	T	*Pinus sylvestris*	Sweden	H. Francke-Grosmann	OM501495	OM514819	OM631858	OM631675
O. tingens	*O. tingens*	25530	366.53		*Xyleborus saxesenii* gallery in *Populus deltoides*	Sweden	H. Francke-Grosmann	–	EU177474	–	–
Ophiostoma sp. 1 (Ambrosiella sp. 1)	*Ophiostoma sp. 1 (Ambrosiella sp. 1)*	43827	UAMH10633		*Ips* sp.	Canada	S. Massoumi Alamouti	OM501522	OM514850	OM631887	OM631703
Ophiostoma sp. 2 (Ambrosiella sp. 2)	*Ophiostoma sp. 2 (Ambrosiella sp. 2)*	43828	UAMH10634		*Ips* sp.	Canada	S. Massoumi Alamouti	OM501523	–	–	–
***Ophiostoma*: Group J**											
*O. piliferum**	*O. piliferum*	–	–		–	–	–	MT633063	MT629746	OM631870	OM631687
O. ponderosae	*O. ponderosae*	37953	ATCC26665	T	Blue stain of *Pinus ponderosa*	Arizona, USA	R.W. Davidson	OM501554	OM514882	–	–
***Ophiostoma*: Group K**											
O. tetropii	*O. tetropii*	4470	428.94		*Picea abies*	Austria	T. Kirisits	OM501517	OM514843	OM631882	OM631698
***Ophiostoma incertae sedis* (based on our data)**											
Lineage XVIII											
O. valdivianum	*O. valdivianum*	449	454.83	T	*Nothofagus alpiva*	Chile	H. Butin	–	OM514849	OM631886	–
Lineage XX											
O. angusticollis	*O. angusticollis*	152	–		*Pinus banksiana*	Wisconsin, USA	M.J. Wingfield	OM501466	OM514794	OM631840	OM631660
O. denticulatum	*O. denticulatum*	146	ATCC38087	T	*Gnathotrichus* sp. on *Pinus* sp.	Colorado, USA	R.W. Davidson	OM501480	OM514807	–	–
O. sejunctum	*O. sejunctum*	–	Ophi 1A	T	*Tomicus* sp. on *Pinus* sp.	Spain	M.R. Bareal	AY934519	–	–	–
Lineage XXIII											
O. noisomeae	*O. noisomeae*	40326	–	T	*Rapanea melanophloeos*	South Africa	T. Musvuugwa	OM501502	OM514826	–	OM631681
Paleoambrosia											
P. entomophila	*P. entomophila*	–	No. B-F-7	T	*Palaeotylus femoralis* in burmese amber	Myanmar	G.O. Poinar, F.E. Vega	–	–	–	–

Table 1. (Continued).

Previous name	Current name	CMW[1]	CBS or other[1]	Type[2]	Isolated from	Country	Collector	GenBank Accession Numbers[3]			
								ITS	LSU	*TEF1-α*	*RPBII*
Raffaelea											
R. albimanens[*]	*R. albimanens*	25532	271.70	T	*Platypus externedentatus* in *Ficus sycomorus*	South Africa	D.B. Scott	MT633066	MT629749	OM631890	OM631705
R. ambrosiae[*]	*R. ambrosiae*	25533	185.64	T	*Platypus cylindrus* tunnel in *Quercus* sp.	England, UK	J.M. Bakeer	MT633067	MT629751	OM631891	OM631706
R. arxii	*R. arxii*	25534	273.70		*Xyleborus torquatus* on *Cussonia* sp.	South Africa	D.B. Scott	–	MT629754	OM631892	OM631708
R. borbonica[#]	*R. borbonica*	51553	PPRI27953	T	*Leucaena leucocephala*	Réunion, France	M.J. Wingfield, P.W. Crous	MT633059	MT629742	–	–
R. campbelliorum	*R. campbelliorum*	44800	139943	T	*Xyleborus glabratus* on *Persea palustris*	Florida, USA	A.S. Campbell	–	KR018414	–	–
R. canadensis	*R. canadensis*	25536	168.66	T	*Platypus wilsonii* in *Pseudotsuga menziessii*	Canada	A. Funk	GQ225699	MT629755	–	–
R. canadensis (=A. sulcati)	*R. canadensis*	25528	805.70	T	*Gmnathotrichus sulcatus* (mycangium) on *Pseudotsuga menziesii*	Canada	A. Funk	–	EU177459	–	–
R. crossotarsi	*R. crossotarsi*	44793	141675	T	Mycangium extract of *Crossotarsus emancipatus* in *Lithocarpus* sp.	Taiwan	J. Hulcr, A. Black, D.R. Simmons	KX267138	MT629756	OM631893	OM631709
R. cyclorhipidii	*R. cyclorhipidii*	44790	141676	T	*Cyclorhipidion* sp. on *Lithocarpus* sp.	Taiwan	J. Hulcr, A. Black, D.R. Simmons	MT633069	MT629757	–	OM631710
R. ellipticospora	*R. ellipticospora*	38056	121569	T	*Xyleborus glabratus* on *Persea* sp.	South Carolina, USA	S. Fraedrich	MT633070	MT629758	OM631894	–
R. fusca	*R. fusca*	38798	121570	T	*Xyleborus glabratus* on *Persea* sp.	South Carolina, USA	S. Fraedrich	–	EU177449	–	–
R. gnathotrichi	*R. gnathotrichi*	25523	379.68	T	*Gnathotrichus retusus* on *Picea engelmannii*	Colorado, USA	L.R. Batra	–	EU177460	–	–
R. promiscua[#]	*R. promiscua*	55899	147173	T	*Xyleborinus saxesenii*	South Afica	W.J. Nel	MW028176	–	–	–
R. rapaneae	*R. rapaneae*	40357	140084	T	*Platypodinae* sp. on *Rapanea melanophloeos*	South Africa	T. Musvuugwa	KT192596	KT182930	–	–
R. santoroi	*R. santoroi*	25539	399.67	T	*Platypus* sp. bore hole	Argentina	J. Wright	MT633075	MT629765	–	–
R. scolytodis	*R. scolytodis*	23001	CCF3566	A	*Scolytodes* sp. on *Cecropia* sp.	Costa Rica	M. Kolarik	AM267264	–	–	–
R. seticollis	*R. seticollis*	1031	634.66	T	*Tsuga canadensis*	New York, USA	R.W. Davidson	MT633076	MT629766	OM631895	OM631711
R. subalba	*R. subalba*	38797	121568	T	*Xyleborus* sp. on *Persea* sp.	South Carolina, USA	S. Fraedrich	–	MT629767	–	OM631712
R. subfusca	*R. subfusca*	38055	121571	T	*Xyleborus glabratus*	South Carolina, USA	S. Fraedrich	–	EU177450	–	–
R. sulcati	*R. sulcati*	25540	806.70	T	*Gnatotrichus sulculcattus* mycangium in *Pseudotsuga menziesii*	Canada	A. Funk	–	EU177462	–	–
R. tritirachium	*R. tritirachium*	25541	726.69	T	*Monarthrum mali* tunnel in *Quercus* sp.	Pennsylvania, USA	D.B. Scott	–	EU177464	–	–
R. xyleborini	*R. xyleborini*	45859	Hulcr6099	T	*Xyleborinus andrewesii*	Florida, USA	C. Bateman	MT633078	MT629769	–	–
Raffaelea sp. A (PL1001)	*Raffaelea* sp. A (PL1001)	38062	–		*Persea* sp.	California, USA	A. Eskalen	–	KJ909293	–	–
***Raffaelea incertae sedis* (based on our data)**											
R. deltoideospora	*R. deltoideospora*	–	WIN(M)41		*Pinus* sp.	Canada	J. Reid	EU879121	KT182932	–	–
Lineage X											
R. vaginata	*R. vaginata*	40365	140086	T	*Lanurgus* sp. on *Olea capensis*	South Africa	T. Musvuugwa	KT192602	–	–	–
***Sporothrix*: *S. candida* complex**											
S. aemulophila	*S. aemulophila*	40381	140087	T	*Rapanea melanophloeos*	South Africa	T. Musvuugwa	OM501527	OM514854	OM631897	–
S. cabralii	*S. cabralii*	38098	CIEFAP456	T	*Nothofagus pumilio*	Argentina	A. de Errasti	OM501533	OM514861	OM631903	OM631716
S. candida	*S. candida*	26484	129713	T	*Eucalyptus cloeziana*	South Africa	G. Kamgan Nkuekam	–	OM514862	OM631904	OM631717
S. itsvo	*S. itsvo*	40370	141063	T	*Rapanea melanophloeos*	South Africa	T. Musvuugwa	KX590840	–	–	–

Table 1. (Continued).

Previous name	Current name	CMW[1]	CBS or other[1]	Type[2]	Isolated from	Country	Collector	GenBank Accession Numbers[3]			
								ITS	LSU	*TEF1-α*	*RPBII*
S. oleae[#]	*S. oleae*	40362	142082	T	*Olea capensis* ssp. *macrocarpa* wound	South Africa	T. Musvuugwa	MN298851	–	–	–
S. rapaneae	*S. rapaneae*	40369	141060	T	*Rapanea melanophloeos*	South Africa	T. Musvuugwa	OM501558	OM514885	OM631926	OM631735
***Sporothrix*: *S. inflata* complex**											
S. dentifunda	*S. dentifunda*	13016	115790	T	*Quercus* wood	Hungary	C. Delatour	OM501535	OM514865	OM631907	OM631718
S. dimorphospora	*S. dimorphospora*	12529	553.74	T	Soil	Canada	R.A.A. Morall	OM501536	OM514866	OM631908	OM631719
S. guttuliformis	*S. guttuliformis*	17167	437.76	T	Soil	Malaysia	T. Furukawa	OM501542	OM514873	OM631915	OM631725
S. inflata	*S. inflata*	12527	239.68	T	Wheat field soil	Canada	W. Gams	OM501544	–	OM631917	OM631727
Spumatoria longicollis	*S. longicollis*	49345	141464	E	Dung	Netherlands	J. vd Lee	–	OM514895	OM631933	–
***Sporothrix*: *S. stenoceras* & *S. gossypina* complexes**											
S. abietina[*]	*S. abietina*	22310	125.89	T	*Pseudohylesinus* gallery on *Abies vejari*	Mexico	J.G. Marmolejo	OM501526	OM514853	OM631896	OM631713
S. africana	*S. africana*	823	116571		*Protea gaguedi*	South Africa	M.J. Wingfield	OM501528	OM514855	OM631898	OM631714
S. aurorae	*S. aurorae*	19362	118837	T	*Hylastes angustatus* on *Pinus elliottii*	South Africa	X.D. Zhou	–	OM514857	OM631900	–
S. cantabriensis	*S. cantabriensis*	39766	136529	T	*Hylastes attenuates* on *Pinus sylvestris*	Spain	P. Romón	KF951554	–	–	–
S. cracoviensis[#]	*S. cracoviensis*	–	147942	T	Adult of *Tryopodendron domesticum* beetle on *Fagus sylvaticum*	Poland	R. Jankowiak	MW768964	–	–	–
S. eucastaneae	*S. eucastaneae*	1124	424.77	T	Canker on *Castanea dentata*	North Carolina, USA	R.W. Davidson	OM501539	OM514868	OM631910	OM631720
S. euskadiensis	*S. euskadiensis*	27318	122138	T	*Hylurgops palliatus* on *Pinus radiata*	Spain	X.D. Zhou	DQ674369	–	–	–
S. fraxini[#]	*S. fraxini*	–	147936	T	Gallery of *Hylesinus varius* on *Fraxinus excelsior*	Poland	R. Jankowiak	MH283150	–	–	–
S. fusiformis	*S. fusiformis*	9968	112912	T	*Populus nigra*	Azerbaijan	D. Aghayeva	–	OM514870	OM631912	OM631722
S. gossypina	*S. gossypina*	1116	ATCC18999	T	*Pinus ponderosa*	New Mexico, USA	R.W. Davidson	–	–	OM631914	OM631724
S. villosa[#]	*S. villosa*	–	SNM188	T	*Pinus thunbergii*	China	R. Chang	MW989428	–	MZ853078	–
S. lunata	*S. lunata*	10563	112927	T	*Carpinus betulus*	Austria	T. Kirisits	OM501545	–	OM631918	OM631728
S. narcissi	*S. narcissi*	22311	138.50	T	*Narcissus* sp.	Netherlands	D.P. Limber	OM501548	OM514876	OM631920	–
S. nsini	*S. nsini*	28602	143281	T	*Protea caffra*	South Africa	F. Roets	EU660458	–	–	–
S. prolifera	*S. prolifera*	37435	251.88	T	*Quercus robur*	Poland	T. Kowalski	OM501555	–	OM631924	OM631732
S. protearum	*S. protearum*	1107	116654		*Protea caffra*	South Africa	M.J. Wingfield	OM501557	OM514884	OM631925	OM631734
S. resoviensis[#]	*S. resoviensis*	–	147927	T	Wound on *Betula pendula*	Poland	R. Jankowiak	MH740962	–	–	–
S. rossii	*S. rossii*	1118	116.78	T	*Dendroctonus adjunctus* gallery on *Pinus ponderosa*	New Mexico, USA	R.W. Davidson	OM501559	OM514886	OM631927	OM631736
S. splendens[*]	*S. splendens*	23050	138722		*Oodinychus* sp. on *Protea repens*	South Africa	F. Roets	OM501561	OM514888	OM631929	OM631738
S. stenoceras	*S. stenoceras*	3202	237.32	T	Pine pulp	Norway	H. Robak	AF484462	DQ294350	–	–
S. uta	*S. uta*	40316	141069	P	*Rapanea melanophloeos*	South Africa	T. Musvuugwa	OM501565	OM514892	OM631930	OM631739
S. variecibata	*S. variecibata*	23051	121961	T	*Trichouropoda* sp. from *Protea repens*	South Africa	F. Roets	OM501566	OM514893	OM631931	OM631740
S. zambiensis	*S. zambiensis*	29077	124914	T	*Protea caffra*	Zambia	F. Roets	OM501567	OM514894	OM631932	OM631741
***Sporothrix*: *S. pallida* complex**											
S. albicans (*syn S. pallida*)	*S. albicans* (*syn S. pallida*)	17203	302.73	T	Soil	England, UK	S.B. Saksena	OM501529	OM514856	OM631899	OM631715

Table 1. (Continued).

Previous name	Current name	CMW[1]	CBS or other[1]	Type[2]	Isolated from	Country	Collector	GenBank Accession Numbers[3]			
								ITS	LSU	*TEF1-α*	*RPBII*
S. chilensis	*S. chilensis*	49343	139890	T	Soil	Chile	R. Cruz Choappa	–	OM514863	OM631905	–
S. gemella	*S. gemella*	23057	121959	T	*Tarsonemus* sp. on *Protea caffra*	South Africa	F. Roets	DQ821560	DQ821531	–	–
S. humicola	*S. humicola*	7618	118129	T	Soil	South Africa	H.F. Vismer	OM501543	–	OM631916	OM631726
S. mexicana	*S. mexicana*	29129	120341	T	Soil	Mexico	A. Espinosa	OM501547	OM514875	OM631919	–
S. pallida	*S. pallida*	17209	131.56	T	*Stemonitis fusca*	Japan	K. Tubaki	OM501550	OM514878	OM631921	OM631729
S. palmiculminata	*S. palmiculminata*	20677	119590	T	*Protea repens*	South Africa	F. Roets	OM501551	OM514879	OM631922	OM631730
S. protea-sedis	*S. protea-sedis*	29074	124911	P	*Protea caffra*	Zambia	F. Roets	OM501556	OM514883	–	OM631733
S. stylites	*S. stylites*	14543	118848	T	Pine utility poles	South Africa	E.M. de Meyer	OM501563	OM514890	–	–
***Sporothrix*: Pathogenic clade**											
S. brasiliensis	*S. brasiliensis*	29127	120339	T	Human skin	Brazil	M.D.S. Lazera	OM501531	OM514859	OM631901	
S. globosa	*S. globosa*	29128	120340	T	Human face	Spain	C. Rubio	OM501541	OM514872	OM631913	OM631723
S. luriei	*S. luriei*	17210	937.72	T	Human skin	South Africa	L. Lurie	OM501546	–	–	–
S. schenckii[*]	*S. schenckii*	38850	138723		Clinical isolate	South Africa	H.F. Vismer	OM501560	OM514887	OM631928	OM631737
***Sporothrix*: Group D**											
S. cavum[#]	*S. cavum*	–	147943	T	Cavity of *Dendrocopos major* on *Salix fragilis*	Poland	R. Jankowiak	MF782813	MF782813	–	–
S. polyporicola	*S. polyporicola*	5461	669.88	T	*Fomitopsis pinicola*	Sweden	S. Ryman	OM501553	OM514881	–	–
***Sporothrix*: Group E**											
S. phasma[*]	*S. phasma*	20676	119722	T	*Protea laurifolia*	South Africa	F. Roets	OM501552	OM514880	OM631923	OM631731
***Sporothrix*: Group F**											
S. bragantina	*S. bragantina*	17149	474.91	T	Soil	Brazil	W. Gams	OM501530	OM514858	–	–
S. curviconia	*S. curviconia*	17164	959.73	T	*Terminalia ivorensis*	Ivory Coast	J. Devois	OM501534	OM514864	OM631906	–
S. epigloea	*S. epigloea*	22308	573.63	T	*Tremella fuciformis*	Argentina	R. T. Guerrero	KX590817	KX590854	–	–
S. eucalyptigena	*S. eucalyptigena*	45431	139899	T	*Eucalyptus* sp.	Australia	P. A. Barber	OM501538	–	OM631909	–
S. nebularis	*S. nebularis*	27319	122135	T	*Hylastes attenuatus* on *Pinus radiata*	Spain	P. Romón	KX590823	KX590862	–	–
S. nigrograna	*S. nigrograna*	14487	MAFF410943	T	*Pinus densiflora*	Japan	H. Masuya	OM501549	OM514877	–	–
S. smangaliso	*S. smangaliso*	50502	143341	T	*Protea gaguedi*	South Africa	N.P. Ngubane	MF103773	–	–	–
S. thermara	*S. thermara*	38930	139747	T	*Cyrtogenius africus* on *Euphorbia ingens*	South Africa	J.A. van der Linde	OM501564	OM514891	–	–
S. zhejiangensis	*S. zhejiangensis*	–	MUCL55183	T	*Monochamus* sp. on *Pinus* sp.	China	Q. Lu, Y.Y. Lun	KY094071	–	–	–
***Sporothrix*: Group G**											
S. dombeyi	*S. dombeyi*	1023	455.83	T	*Nothofagus* sp.	Chile	H. Butin	OM501537	OM514867	–	–
***Sporothrix incertae sedis* (based on our data)**											
Lineage XVI											
S. fumea	*S. fumea*	26813	129712	T	*Phoracantha* sp. galleries on *Eucalyptus*	South Africa	C. Perez	OM501540	OM514869	OM631911	OM631721
Lineage XIX											
S. brunneoviolacea	*S. brunneoviolacea*	37442	124560	P	Soil	Spain	C. Silvera	OM501532	OM514860	OM631902	–
***Sporothrix incertae sedis* (based on published data)**											
S. cryptarchum[#]	*S. cryptarchum*	–	147934	T	Adult of *Cryptarcha undata*	Poland	R. Jankowiak	MW768966	–	–	–
S. hypoxyli[#]	*S. hypoxyli*	47441	141569	T	*Hypoxylon petriniae* on *Fraxinus* wood	Netherlands	E. Osieck & W.J. Nel	MT637058	MW012948	–	–

Table 1. (Continued).

Previous name	Current name	CMW[1]	CBS or other[1]	Type[2]	Isolated from	Country	Collector	GenBank Accession Numbers[3]			
								ITS	LSU	*TEF1-α*	*RPBII*
S. undulata[#]	*S. undulata*	–	147929	T	Adult of *Epuraea guttata*	Poland	R. Jankowiak	MH740976	–	–	–
***Ophiostomatales insertae sedis* (based on published data)**											
L. antibioticum	*L. antibioticum*	2777	DAOM84338	T	*Pinus taeda*	Georgia, USA	S. Alexander	AF343677	–	–	–
L. brachiatum	*L. brachiatum*	2855	C388	T	*Picea rubens*	New York, USA	S. Alexander	AF343676	–	–	–
L. elegans	*L. elegans*	2245	115241		*Chamaecyparis / Hinoke*	Taiwan	M.J. Wingfield	AF343675	–	–	–
O. crenulatum	*O. crenulatum*	–	WIN(M)70-17	T	*Pinus banksiana*	Canada	J. Reid	–	AF135589	–	–
O. fasciatum	*O. fasciatum*	–	UM56		*Pseudotsuga menziesii*	Canada	A. Olchowecki	EU913720	EU913680	–	–
O. breviusculum	*O. breviusculum*	–	YCC522		Single ascospore isolate from YCC-494	Japan	Y. Yamaoka	AB200423	–	–	–
O. ssiori	*O. ssiori*	–	MAFF410973	T	*Polygraphus ssiori* on *Prunus* sp.	Japan	H. Masuya	AB096209	–	–	–
O. subalpinum	*O. subalpinum*	–	YCC408		*Cryphalus* sp. on *Abies* sp.	Japan	Y. Yamaoka	AB200424	–	LC090750	–
O. pseudonigrum	*O. pseudonigrum*	–	WIN(M)71-13		*Picea mariana*	Canada	J. Reid	–	AF135577	–	–
O. pehueninum	*O. pehueninum*	–	142995	T	*Araucaria araucana*	Chile	V. Sepúlveda	MF576438	–	MF576446	–
O. tremulo-aureum	*O. tremulo-aureum*	–	361.65		Black canker on *Populus tremuloides*	Colorado, USA	R.W. Davidson	–	AF135573	–	–

ATCC = American Type Culture Collection, Maryland, USA; CBS = the culture collection of Westerdijk Fungal Biodiversity Institute, Utrecht, the Netherlands; CFCC = China Forestry Culture Collection Center, Research Institute of Forest Ecology, Environment and Protection, Chinese Academy of Forestry, Beijing, China; CIEFAP = the culture collection of the Centro de Investigación y Extensión Forestal Andino Patagónico, Argentina; CMW = the culture collection of the Forestry and Agricultural Biotechnology Institute (FABI), University of Pretoria, South Africa; CTK = the culture collection of the Institute of Forest Entomology, Forest Pathology and Forest Protection, Department of Forest and Soil Sciences, University of Natural Resources and Applied Life Sciences, Vienna, Austria; CXY = the culture collection of the Chinese Academy of Forestry, China; DAOM = Canadian National Mycological Herbarium, Ottawa, Canada; KACC = Korean Agricultural Culture Collection, Suwon, Korea; KUC = Korea University Culture Collection, Seoul, Korea; MAFF = the culture collection of National Institute of Agrobiological Resources, Japan; MUCL = BCCM/MUCL Agro-food & Environmental Fungal Collection, Université catholique de Louvain, Belgium; PPRI = National Collection of Fungi, Pretoria, South Africa; RWD = the private collection of R.W. Davidson; SNM = the microbial culture collection of Shandong Normal University, Jinan, Shandong, China; TRTC = Royal Ontario Museum Fungarium, Toronto, Canada; UAMH = University of Alberta Mold Herbarium and Culture Collection, Edmonton, Canada; VPRI = Victorian Plant Pathology Herbarium, Victoria, Australia; WIN(M) = University of Manitoba, Microbiology and Botany (J. Reid's personal collection); YCC = the private collection of Y. Yamaoka.

[2] T = ex-type, E = ex-epitype, P = ex-paratype; L = ex-lectotype; A = authentic isolate, used in the original study.

* Genome data used in this study.

Species published after 2018, thus not included in the current analyses.

^ CMW culture replaced with a different fungus.

[3] Sequences with accession numbers preceded with "OM" were generated in the current study.

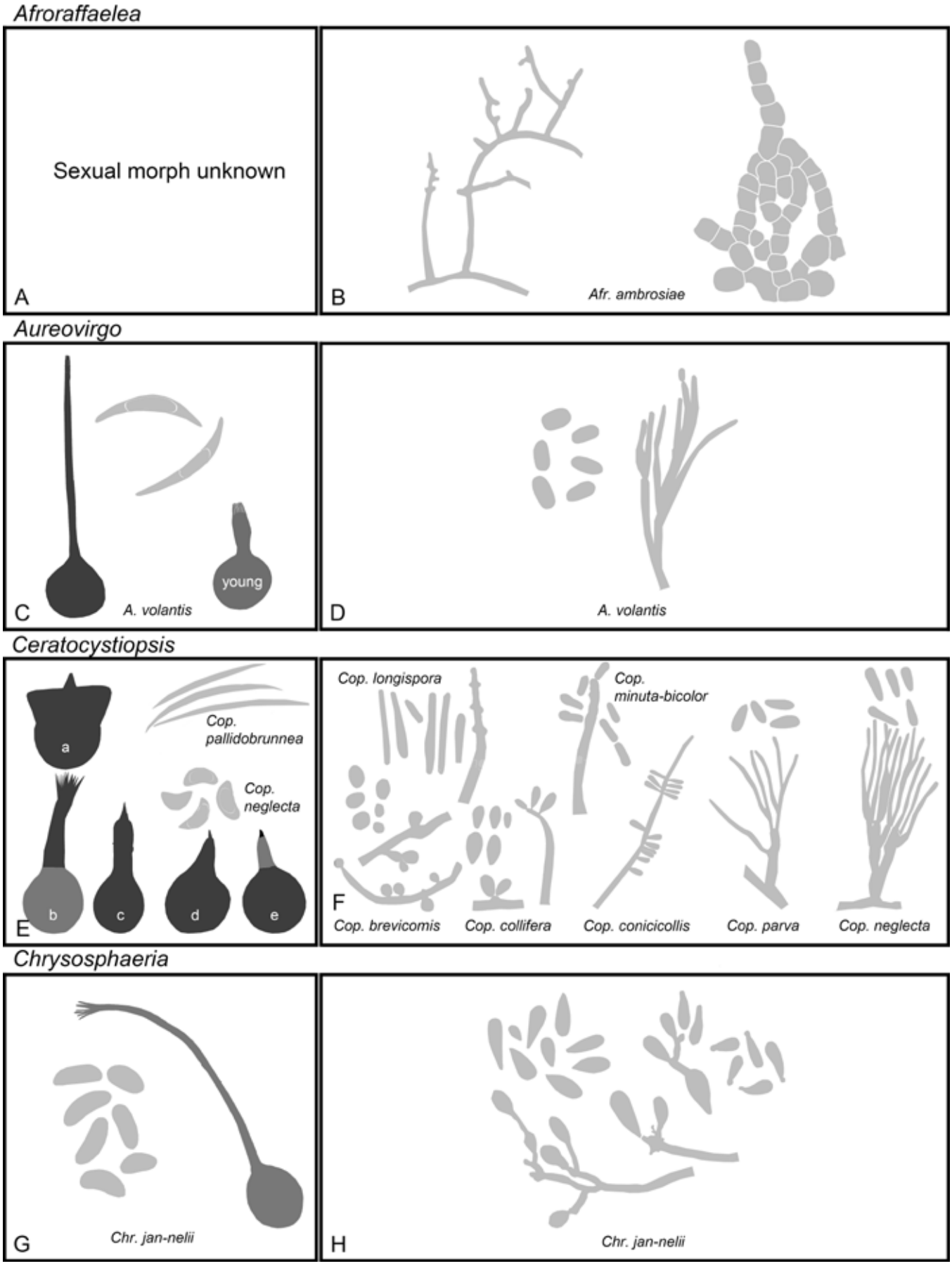

Fig. 6. Genera of the *Ophiostomatales* redrawn from published images with sexual morphs (if known) on the left and asexual morphs on the right. **A, B.** *Afroraffaelea*. **C, D.** *Aureovirgo*. **E, F.** *Ceratocystiopsis* (a. *Cop. collifera*; b. *Cop. ochracea*; c. *Cop. manitobensis*; d. *Cop. concentrica*; e. *Cop. rollhanseniana*). **G, H.** *Chrysosphaeria*. (Pale grey shading reflects hyaline to subhyaline colouration, medium-tone grey brown to dark brown and dark grey reflects fuscous black to dark black colouration).

Notes: In their revision of the genus *Ceratocystis,* Upadhyay & Kendrick (1975) erected *Ceratocystiopsis* for species with falcate ascospores and a *Hyalorhinocladiella* asexual morph. Hausner *et al.* (1993a) reduced *Ceratocystiopsis* to synonymy with *Ophiostoma* based on rDNA sequences, but Zipfel *et al.* (2006) included additional taxa in their study and reinstated the genus that is typified by *Ceratocystiopsis minuta*. Species in this genus have elongated sickle-shaped (falcate) ascospores that are sheathed, produced in very short necked ascomata, characters not seen in any other genus in the *Ophiostomatales* (Upadhyay & Kendrick 1975, Zipfel *et al.* 2006, De Beer & Wingfield 2013). Species of *Ceratocystiopsis* are found in the galleries of conifer-infesting bark beetles (*Dendroctonus* species in North America or *Ips* species in Japan and Europe) in the Northern Hemisphere (Plattner *et al.* 2009).

Ceratocystiopsis spp. formed a well-supported monophyletic clade in all our phylogenies, supporting the decision of Zipfel *et al.* (2006) to reinstate the genus. Our data also supported the placement of *Cop. neglecta* (previously *Ophiostoma neglectum*) in *Ceratocystiopsis*, as shown by De Beer & Wingfield (2013).

Chrysosphaeria

Chrysosphaeria W.J. Nel *et al.*, Mycologia 113: 1206. 2021. MycoBank MB 837564. Fig. 6G, H.

Etymology: 'From Latin chryso-, golden, and -sphaera, sphere or orb, referring to the light colour of the ascoma bases in the type species' (Nel *et al.* 2021).

Sexual morph: *Ascomatal bases* globose, light to golden brown; necks light brown, cylindrical, tapering towards apex, flexible. *Ostiolar hyphae* present, slightly divergent, hyaline. *Ascospores* hyaline, 1-celled, no sheath, short cylindrical to bean-shaped.

Asexual morph: Sporothrix-like; *conidiophores* micronematous, mononematous, hyaline; *conidiogenous cells* hyaline, denticulate; *conidia* hyaline, 1-celled, oblong, occasionally producing secondary spores hyaline, 1-celled, obovoid.

Type species: *Chrysosphaeria jan-nelii* W.J. Nel *et al.*, Mycologia 113: 1206. 2021. MycoBank MB 837566.

Notes: Unlike most species in the *Ophiostomatales,* which occur on wood and have associations with bark or ambrosia beetles, *Chyrysosphaeria* was isolated from abandoned combs of the fungus-growing termite *Macrotermes natalensis*.

Dryadomyces (Lineage V)

Dryadomyces Gebhardt, Mycol. Res. 109: 693. 2005. MycoBank MB 28937, ***emend.*** Z.W. de Beer & M. Procter Fig 7A, B.

Etymology: 'dryads, the tree nymphs in Greek mythology; referring to the habitat of these fungi in woody plants' (Gebhardt *et al.* 2005).

Sexual morph: Unknown.

Asexual morph: *Colony* confluent, mucilaginous. *Conidiophores* single or aggregated in sporodochia, macronematous, mononematous, hyaline, smooth. *Conidiogenous cells* monillioid or oblong, sympodial, with denticles or inconspicuous scars. *Conidia* hyaline to subhyaline, 1-celled, globose to subglobose, obovoid to pyriform with truncate base, smooth, producing secondary spores. *Aleuriospores* absent or present, hyaline, globose to subglobose, terminal.

Type species: *Dryadomyces amasae* Gebhardt, Mycol. Res. 109: 693. 2005. MycoBank MB 369332.

Notes: Based on our analyses, *Dryadomyces* now includes five ambrosia beetle-associated species, previously described in either *Ambrosiella*, *Raffaelea* or *Dryadomyces* (Gebhardt *et al.* 2005, De Beer & Wingfield 2013). *Raffaelea sulphurea* was isolated from hardwood-infesting ambrosia beetles, as was its sister species, *R. montetyi* (Massoumi Alamouti *et al.* 2009). Two Asian species in this complex, *R. quercivora* from Japan and *R. quercus-mongolicae* from Korea, have been implicated in contributing to the death of large numbers of *Quercus* spp. in their native ranges (Dreaden *et al.* 2014).

The fifth species in Clade V of our analyses (Fig. 5), *Drydomyces amasae,* was initially described as the type species of the monotypic genus *Dryadomyces.* It was isolated from the ambrosia beetle *Amasae concitatus* in Taiwan (Gebhardt *et al.* 2005). Although the conidia of *D. amasae* differ from other *Raffaelea* species, Harrington *et al.* (2008) suggested that all ambrosial fungi in the *Ophiostomatales* should be treated in *Raffaelea,* until further studies revealed the taxonomic identities of these fungi. The more robust phylogenies constructed by Massoumi Alamouti *et al.* (2009) revealed a monophyletic lineage including *D. amasae, R. sulphurea* and *R. montetyi*. However, Harrington *et al.* (2010) treated *D. amasae* in *Raffaelea*, not considering the differences between conidia of *D. amasae* and other *Raffaelea* species as sufficient to separate *Dryadomyces* from *Raffaelea*.

De Beer & Wingfield (2013) named the lineage containing *R. amasae*, *R. montetyi*, *R. suphurea*, *R. quercus-mongolicae* and *R. quercivora* as the *R. sulphurea* complex, referring to the oldest of the five described species. This complex grouped within *Leptographium s.l.* in their phylogenies. They did, however, note that the *R. sulphurea* complex is most probably not part of the larger *Leptographium s.l.,* but their data were insufficient to show otherwise. They suggested that when more robust phylogenies support the *R. sulphurea* complex as a monophyletic lineage separate from other genera, *Dryadomyces* would be a suitable name as the complex includes *D. amasae*.

Dreaden *et al.* (2014) investigated the monophyly of *Raffaelea* and showed that the *R. sulphurea* complex grouped close to isolates of *E. vermicola* within *Leptographium s.l.* as defined by De Beer & Wingfield (2013). They concluded that a larger study including additional *Leptographium* and *Raffaelea* species should provide clarity on the placement of these outlying *Raffaelea* lineages.

The *R. sulphurea* complex consistently formed a well-defined lineage distinct from *Leptographium* in our phylogenies. This supported re-instating the name *Dryadomyces* for this lineage. The description of *Dryadomyces* by Gebhardt *et al.* (2005) is emended here to accommodate other species in this lineage.

***New combinations*:**

1) *Dryadomyces montetyi* (M. Morelet) M. Procter & Z.W. de Beer, ***comb. nov.*** MycoBank MB 840313.
Basionym: *Raffaelea montetyi* M. Morelet, Ann. Soc. Sci. Nat. Archéol. Toulon Var 50: 189. 1998. MycoBank MB 445315.

Description: Morelet (1998: 189–191, fig. A).

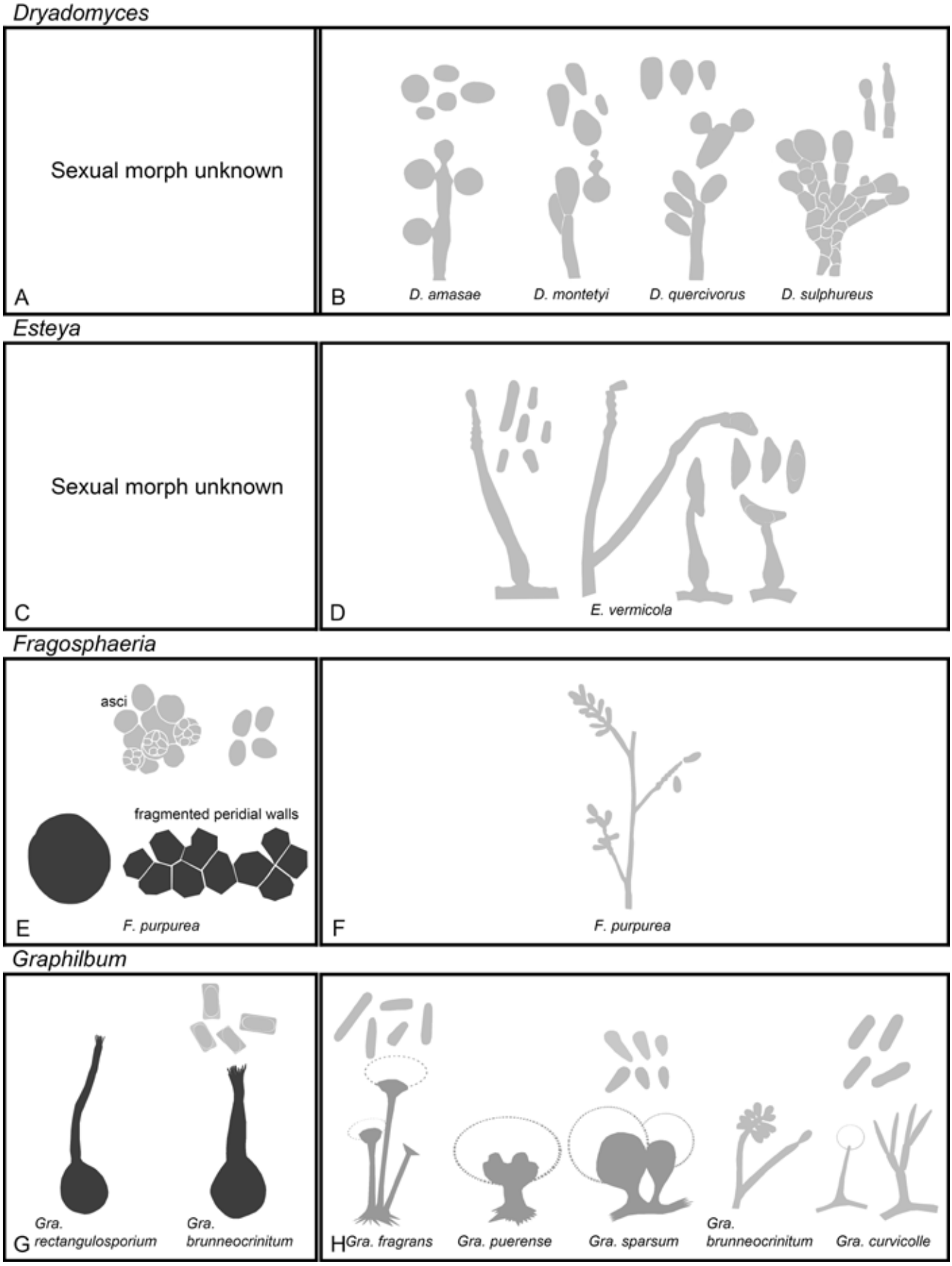

Fig. 7. Genera of the *Ophiostomatales* redrawn from published images with sexual morphs (if known) on the left and asexual morphs on the right. **A, B.** *Dryadomyces.* **C, D.** *Esteya.* **E, F**. *Fragosphaeria.* **G, H.** *Graphilbum*. (Pale grey shading reflects hyaline to subhyaline colouration, medium-tone grey brown to dark brown and dark grey reflects fuscous black to dark black colouration).

Phylogenetic data: Gebhardt *et al.* (2005), Massoumi Alamouti *et al.* (2009), Harrington *et al.* (2010), Matsuda *et al.* (2010), De Beer & Wingfield (2013), Dreaden *et al.* (2014), Musvuugwa *et al.* (2015), De Beer *et al.* (2016a, b), Vanderpool *et al.* (2017), Li *et al.* (2018), Saucedo-Carabez *et al.* (2018).

Notes: It forms part of *Dryadomyces* (Fig. 5), previously designated as the *R. sulphurea* complex (De Beer & Wingfield 2013).

2) *Dryadomyces quercivorus* (Kubono & Shin. Ito) M. Procter & Z.W. de Beer, ***comb. nov.*** MycoBank MB 840316.
Basionym: *Raffaelea quercivora* Kubono & Shin. Ito, Mycoscience 43: 256. 2002. MycoBank MB 483997.

Description: Kubono & Ito (2002: 256–259, figs 1–11).

Phylogenetic data: Kim *et al.* (2009), Seo *et al.* (2010), Matsuda *et. al.* (2010), Endoh *et al.* (2011), Dreaden *et al.* (2014), Musvuugwa *et al.* (2015), Simmons *et al.* (2016), Van der Linde *et al.* (2016), De Beer *et al.* (2016a, b), Vanderpool *et al.* (2017), De Errasti *et al.* (2018), Li *et al.* (2018), Saucedo-Carabez *et al.* (2018).

Notes: *Dryadomyces quercivorus* groups in *Dryadomyces* and was previously accommodated in the *R. sulphurea* complex (Fig. 5; De Beer & Wingfield 2013, De Errasti *et al.* 2018, Li *et al.* 2018, Saucedo-Carabez *et al.* 2018).

3) *Dryadomyces quercus-mongolicae* (K.H. Kim *et al.*) M. Procter & Z.W. de Beer, ***comb. nov.*** MycoBank MB 840318.
Basionym: *Raffaelea quercus-mongolicae* K.H. Kim *et al.*, Mycotaxon 110: 193. 2009. MycoBank MB 515072.

Description: Kim *et al.* (2009: 193–195, fig. 2).

Phylogenetic data: Kim *et al.* (2009), Seo *et al.* (2010), De Beer *et al.* (2016a), Vanderpool *et al.* (2017), De Errasti *et al.* (2018), Li *et al.* (2018), Saucedo-Carabez *et al.* (2018).

Notes: *Dryadomyces quercus-mongolicae* groups in *Dryadomyces*, and was formerly in the *R. sulphurea* complex (Fig. 5; De Beer & Wingfield 2013, Li *et al.* 2018, Saucedo-Carabez *et al.* 2018).

4) *Dryadomyces sulphureus* (L.R. Batra) M. Procter & Z.W. de Beer, ***comb. nov.*** MycoBank MB 840321.
Basionym: *Ambrosiella sulphurea* L.R. Batra, Mycologia 59: 992. 1967. MycoBank MB 326145.
Synonyms: *Raffaelea sulphurea* (L.R. Batra) T.C. Harr., Mycotaxon 111: 353. 2010. MycoBank MB 515298.
Cephalosporium luteum Verrall, J. Agric. Res. 66: 141. 1943. MycoBank MB 284848.

Description: Batra (1967: 992–998, figs 20, 21, 26–29), Verrall (1943: 141, 142. fig 4).

Phylogenetic data: Cassar & Blackwell (1996), Rollins *et al.* (2001), Gebhardt *et al.* (2005), Massoumi Alamouti *et al.* (2009), Harrington *et al.* (2010), Matsuda *et al.* (2010), De Beer & Wingfield (2013), Dreaden *et al.* (2014), Musvuugwa *et al.* (2015), Simmons *et al.* (2016), De Beer *et al.* (2016a, b), Vanderpool *et al.* (2017), Saucedo-Carabez *et al.* (2018).

Notes: This taxon groups in *Dryadomyces* (Fig. 5), previously designated as the *R. sulphurea* species complex (De Beer & Wingfield 2013), and has a heterotypic synonym, *Cephalosporium luteum* (Verrall 1943). Gharabigloozare (2015) proposed *C. luteum* as conspecific with *R. sulphurea*. These two species were isolated from *Xyleborinus saxeseni* (syn. *Xyleborus pecanis*) and their galleries. The culture morphologies and conidial dimensions of Batra (1967) and Verrall (1943) match and we support their conspecificity. In terms of nomenclatural priority, *Cephalosporium luteum* (1943) has precedence over *A. sulphurea* (1967) and the former epithet has a priority over the latter as a basionym. However, since De Beer & Wingfield (2013) introduced *R. sulphurea* complex, the name *R. sulphurea* has been widely used and recognised, and we have chosen not to introduce a new epithet for this species.

Esteya (Lineage IV)

Esteya J.Y. Liou *et al.*, Mycol. Res. 103: 243. 1999. MycoBank MB 28256, ***emend.*** Z.W. de Beer & M. Procter Fig. 7C, D.

Etymology: 'Named in honour of Prof. Ralph H. Estey (Macdonald College, McGill University, Canada), in recognition of his contribution to the study of nematophagous fungi and nematology' (Liou *et al.* 1999).

Sexual morph: Unknown.

Asexual morph: *Conidiophores* macronematous, mononematous, simple, subhyaline to pigmented, smooth to verrucous. *Conidiogenous cells* flask-shaped. *Conidia* hyaline, 1-celled, smooth, asymmetrically ellipsoidal in face view, concave, lunate in side view, ends moderately apiculate, with a layer of adhesive mucus on concave surface, containing ovoid endospore-like structures. Hyalorhinocladiella-like; *conidiophores* macronematous, mononematous, simple or branched, subhyaline to pigmented, smooth to verrucous; *conidiogenous cells* cylindrical to subulate; *conidia* hyaline, 1-celled, cylindrical, smooth.

Type species: *Esteya vermicola* J.Y. Liou *et al.*, Mycol. Res. 103: 243. 1999. MycoBank MB 450702.

No other species known.

Notes: The genus *Esteya* was first described by Liou *et al.* (1999) and includes the single species, *E. vermicola* (Wang *et al.* 2015). *Esteya vermicola* produces two different types of conidia depending on abiotic and biotic factors, with one of the forms lethal to nematodes when consumed (Liou *et al.* 1999). This species was first isolated from the pine wood nematode *Bursaphelencus xylophilus*. It is the only nematode-associated fungus in the *Ophiostomatales*, clearly distinguishing *Esteya* from other genera in the Order. Wang *et al.* (2008) discovered another isolate of *E. vermicola*, and upon performing a BLAST search in GenBank found that members of the *Ophiostomatales* were the closest phylogenetic relatives. They subsequently performed molecular phylogenetic analyses including various *Ophiostomatales* species and found that *Esteya* grouped close to but separately from a clade containing two *Leptographium* and two *Grosmannia* species, and distinct from any other genus in the *Ophiostomatales*. The phylogenies of De Beer & Wingfield (2013) did not resolve the generic placement of *Esteya* in the *Ophiostomatales*, showing that *Esteya* grouped within *Leptographium s.l.* based on both ITS and

LSU sequence data. These authors chose not to reduce *Esteya* to synonymy with *Leptographium* and recommended that *Esteya* should not be treated in *Leptographium* but be retained as a distinct genus until further studies could be conducted on the group. Later studies using LSU data again placed *Esteya* in *Leptographium s.l*. (Musvuugwa *et al.* 2015, De Beer *et al.* 2016a). Dreaden *et al.* (2014) used SSU, LSU and *β-tub* genes, which also placed *Esteya* in *Leptographium s.l.* In the phylogenies of the *TEF-1α* and *β-tub* genes generated by Wang *et al.* (2014), the separate treatment of *Esteya* from *Leptographium s.l.* was well supported.

In our datasets, *Esteya* grouped within what was previously known as *Leptographium s.l*. The separation of *Grosmannia* and *Leptographium* based on our data, allows the recognition of *Esteya* as a distinct genus, forming a well-supported clade including two of the known *E. vermicola* isolates. Our data did not include the type specimen of *E. vermicola*, because cultures of this fungus were not available in the culture collections from which isolates were sought. It is interesting that a nematode-associated fungus groups within a family of fungi not associated with nematodes. The discovery of other *Esteya* isolates may shed light on the evolution of this unique lifestyle within the *Ophiostomatales*.

Fragosphaeria (Lineage XXI)

Fragosphaeria Shear, Mycologia 15: 124. 1923. MycoBank MB 2011, ***emend.*** Z.W. de Beer & M. Procter Fig. 7E, F.

Etymology: Name is derived from the word "fragor" meaning "breaking to pieces" and "sphaera" (Shear 1923), referring to the spherical ascomata of the two species in the genus that easily break into fragments when handled.

Sexual morph: *Ascomatal bases* dark, globose, cleistothecial, walls easily fragmented. *Asci* subglobose. *Ascospores* yellowish-brown, 1-celled, broadly bean-shaped.

Asexual morph: *Conidia* hyaline, 1-celled, oblong to ellipsoidal, subalantoid, inequilateral.

Type species: *Fragosphaeria purpurea* Shear, Mycologia 15: 124. 1923. MycoBank MB 275760.

Other species: Listed in Table 1.

Notes: *Fragosphaeria* was first associated with the *Ophiostomatales* when a study by Suh & Blackwell (1999) showed that *F. purpurea*, the type species of this genus, grouped with some *Ophiostoma* species. The genus currently includes only two species, *F. purpurea* (Shear 1923) and *F. reniformis* (Saccardo 1881). The latter species was originally described in *Cephalotheca*, which Chesters (1935) reduced to synonymy with *Fragosphaeria* based on the similarities between *F. purpurea, Cephalotheca sulfurea* and *C. reniformis*. Malloch & Cain (1970) reinstated *Fragosphaeria*, transferring *Cephalotheca reniformis* to *Fragosphaeria*.

Both *Fragosphaeria* species are associated with stained wood within and surrounding bark beetle galleries in hardwoods and have been isolated in Britain and North America (Chesters 1935, De Beer & Wingfield 2013). Drawings by Chesters (1935) show a sporothrix-like asexual morph and allantoid ascospores produced by the cephalothecoid ascomata, which link this genus with other ophiostomatalean genera. However, the spherical cephalothecoid ascomata distinguish it from other *Ophiostomatales* (De Beer & Wingfield 2013). A study by Yaguchi *et al.* (2006) showed that there was no evident relationship between species of *Cephalotheca* and *Fragosphaeria* and confirmed that the two *Fragosphaeria* isolates group together. Our data confirm the treatment of *Fragosphaeria* as a distinct, monophyletic genus in the *Ophiostomatales*.

Graphilbum (Lineage VIII)

Graphilbum H.P. Upadhyay & W.B. Kendr., Mycologia 67: 800. 1975. MycoBank MB 8393, ***emend.*** Z.W. de Beer *et al*. In *The Ophiostomatoid Fungi*: *Expanding Frontiers*: 268. 2013. Fig. 7G, H.

Etymology: *Graphilbum* was described as the hyaline analogue of the genus *Graphium* (Upadhyay & Kendrick 1975). *Graphium* was later shown to form part of the *Microascales* (Okada *et al.* 1998), while *Graphilbum* resides in the *Ophiostomatales* (Zipfel *et al.* 2006). Although somewhat of a misnomer, the name *Graphilbum* remains valid and represents a distinct genus in the *Ophiostomatales*.

Sexual morph: *Ascomatal bases* globose, subglobose, black; necks dark brown to black, nearly cylindrical, straight or slightly curved. *Ostiolar hyphae* present or absent, parallel or divergent. *Asci* evanescent, broadly clavate to subglobose. *Ascospores* hyaline, 1-celled, cylindrical to oblong in side view, globose in end view, enclosed in rectangular sheath.

Asexual morph: *Conidiophores* micronematous, semimacronematous, macronematous, mononematous, synnematous, branched, unbranched. Hyalorhinocladiella-like; *conidiophores* simple or sparingly branched; *conidiogenous cells* sympodial, subulate; *conidia* hyaline, 1-celled, cylindrical or clavate to broadly clavate, oblong or ellipsoidal, sometimes slightly curved. Pesotum-like; stipes pale to dark pigmented, biverticillate; *conidiogenous cells* sympodial.

Type species: *Graphilbum sparsum* H.P. Upadhyay & W.B. Kendr., Mycologia 67: 800. 1975. MycoBank MB 314730.

Other species: Listed in Table 1.

Notes: *Graphilbum* was originally described to accommodate the asexual morph of some *Ophiostoma* (then *Ceratocystis*) species (Upadhyay & Kendrick 1975). Okada *et al.* (1998) treated *Graphilbum* together with other genera in the *Ophiostomatales*, which have synnematous asexual morphs, as a synonym of *Pesotum.* However, De Beer *et al.* (2013a) showed that the type species of *Pesotum*, *O. ulmi*, grouped within *Ophiostoma s.s.,* while the type species of *Graphilbum*, *O. sparsum*, formed a lineage distinct from *Ophiostoma s.s.* They consequently reduced *Pesotum* to synonymy with *Ophiostoma*, and reinstated *Graphilbum* with *Gra. sparsum* as the type species, including seven additional species in the genus. *Graphilbum* species are characterised by Type E ascospores (Fig. 3H) and either a hyalorhinocladiella- or pesotum-like asexual morph (Fig. 3A, C; *sensu* De Beer & Wingfield 2013). This is with the exception of *Gra. tsugae* that produces a continuum of hyalorhinocladiella-like and pesotum-like asexual morphs. *Graphilbum* species are commonly found in galleries of conifer-infesting bark beetles in the Northern Hemisphere (De Beer *et al.* 2013b, Romón *et al.* 2014a, Reid & Hausner 2015, Jankowiak *et al.* 2020).

In our analyses, *Graphilbum* formed a well-supported monophyletic lineage, distinct from other genera. Interestingly,

Ophiostoma pusillum consistently grouped with *Graphilbum*, supporting previous suggestions that the species might form part of this genus (De Beer & Wingfield 2013).

***New combination*:**

1) *Graphilbum pusillum* (Masuya) M. Procter & Z.W. de Beer, ***comb. nov.*** MycoBank MB 840324.
Basionym: *Ophiostoma pusillum* Masuya, Mycoscience 44: 302. 2003. MycoBank MB 489291.

Description: Masuya *et al.* (2003: 302, figs 1–10).

Phylogenetic data: Fig. 5.

Notes: Masuya *et al.* (2013) treated this species as part of the *O. ips* complex based on morphology. However, due to morphological similarities with the fungus known as *Ophiostoma nigrum* and *Ceratocystis tubicollis* (Masuya *et al.* 2003), De Beer *et al.* (2013b) suggested that it may rather belong in *Graphilbum*. Both *O. nigrum* (now *Gra. nigrum*) and *C. tubicollis* (now *Gra. tubicolle*) were treated in *Graphilbum* by De Beer *et al.* (2013b), and our sequence data also confirm the placement of *O. pusillum* in this genus (Fig. 5). The name should not be confused with *S. pusilla* U. Braun & Crous [= *Quambalaria pusilla* (U. Braun & Crous) J.A. Simpson] (De Beer *et al.* 2006) or *Graphium pusillum* (Wallr.) Sacc. (De Beer *et al.* 2013b).

Grosmannia (Lineage II)

Grosmannia Goid., Boll. Staz. Patol. Veg. Roma 16: 27. 1936. MycoBank MB 2141, ***emend.*** Z.W. de Beer & M. Procter. Fig. 8A–D.

Etymology: Goidànich (1935) named the genus after the German forest pathologist, Helene Grosmann, later Francke-Grosmann (1900–1990), who described both the asexual morph (as *Leptographium penicillatum* Grosmann) and the sexual morph (as *Ceratostomella penicillata* Grosmann) of the type species of this genus.

Synonym: *Verticicladiella* S. Hughes, Canad. J. Bot. 31: 653. 1953. MycoBank MB 10394. [Type species *V. abietina* (Peck) S. Hughes].

Sexual morph: *Ascomatal bases* subglobose to globose, black; necks nearly cylindrical, straight or slightly curved, black. *Ostiolar hyphae* absent or present, divergent or variable. *Asci* evanescent. *Ascospores* hyaline, 1-celled, enclosed in sheath or not, endospores orange segment-shaped in side view, cylindrical in face view, globose to ellipsoidal in end view.

Asexual morph: *Conidiophores* macronematous, micronematous, mononematous, synnematous, singly or in groups. Hyalorhinocladiella-like; *conidia* hyaline, 1-celled, oblong to obovoid. Leptographium-like; *conidiophores* branched; stipes pale brown, branches pale brown, becoming hyaline towards apex, bases simple or rhizoid-like; *conidiogenous cells* hyaline; *conidia* hyaline, 1-celled, oblong, broadly ellipsoidal to slightly obovoid, sometimes allantoid, narrowly obovoid to clavate, straight or distinctly curved. Pesotum-like; *conidiophores* single or in groups; *conidia* hyaline, oblong, 1-celled. Sporothrix-like; *conidiophores* simple; *conidiogenous cells* hyaline, cylindrical, sympodial, denticulate; *conidia* hyaline, 1-celled, oblong, ovoid to ellipsoidal, clavate, sometimes developing into larger ramoconidia, producing secondary spores. *Ramoconidia* hyaline, 1-celled, clavate. Single ascospore cultures yeasty, budding hyaline conidia, ovoid to elongate, colony later darkened. *Aleuriospores* hyaline or pigmented, globose to subglobose, oval to ellipsoid.

Type species: *Grosmannia penicillata* (Grosmann) Goid., Boll. Staz. Patol. Veg. Roma 16: 46. 1936. MycoBank MB 253870.]

Notes: *Grosmannia* was originally erected by Goidànich (1935) to accommodate sexual species of *Ceratostomella* with leptographium-like asexual morphs (Davidson 1942). The genus was later treated as synonym of both *Ophiostoma* (Siemaszko 1939) and *Ceratocystis* (Bakshi 1951). Zipfel *et al.* (2006) showed that *Ophiostoma* and *Grosmannia* were distinct from each other based on ITS and LSU sequences, and separated the two genera based on these and morphological differences. However, the focus of the Zipfel *et al.* (2006) study was primarily on sexually reproducing species.

De Beer & Wingfield (2013) included sequence data for many more asexual *Leptographium* spp. in their study and showed that *Leptographium* and *Grosmannia* spp. grouped together, along with other previously unassociated *Ophiostoma* spp. They applied the older name, *Leptographium* to this group, rather than *Grosmannia*, which following the dual nomenclature system (McNeill *et al.* 2012) had preference because it was considered a sexual genus (De Beer & Wingfield 2013). They referred to the lineage as *Leptographium s.l.*, even though the lineage did not show strong monophyletic support. The type species of *Grosmannia* (*G. penicillata*) grouped in a lineage distinct from the type species of *Leptographium* (*L. lundbergii*). However, they recommended that novel species grouping in what they referred to as the *G. penicillata* complex should be treated as *Grosmannia* species. This was until more robust analyses could confirm whether the *G. penicillata* complex should be treated as a distinct genus.

Based on the data emerging from the present study, we have reinstated *Grosmannia* as a genus distinct from *Leptographium*, for species that produce leptographium-like asexual morphs and have allantoid, hyaline and aseptate ascospores. These species are commonly associated with conifer-infesting bark beetles in the Northern Hemisphere (Jacobs & Wingfield 2001, Linnakoski *et al.* 2012). Based on our phylogenetic analyses, *Grosmannia* includes the fungus previously known as *G. penicillata s.s.* (referred to here as the *G. penicillata* complex), *G. abieticola* and *L. taigense* (Lineage C), and the newly recognised *G. grandifoliae* complex (Jankowiak *et al.* 2017).

***Species complexes*:**

The *G. penicillata* complex
The *G. penicillata* complex as defined by Six *et al.* (2011), Linnakoski *et al.* (2012) and De Beer & Wingfield (2013) included 18 species. Our results and those emerging from other studies add another seven species to the complex within a well-supported lineage. All 25 species are associated in some way with conifer-infesting bark and ambrosia beetles in the Northern Hemisphere. The complex is named based on the first species in the complex to be described, *G. penicillata* [as *Ceratostomella penicillata* (Grosmann 1932)], which is also the type species of *Grosmannia*.

The *G. grandifoliae* complex
The second species complex included in our definition of *Grosmannia*, the *G. grandifoliae* complex, emerged when two new

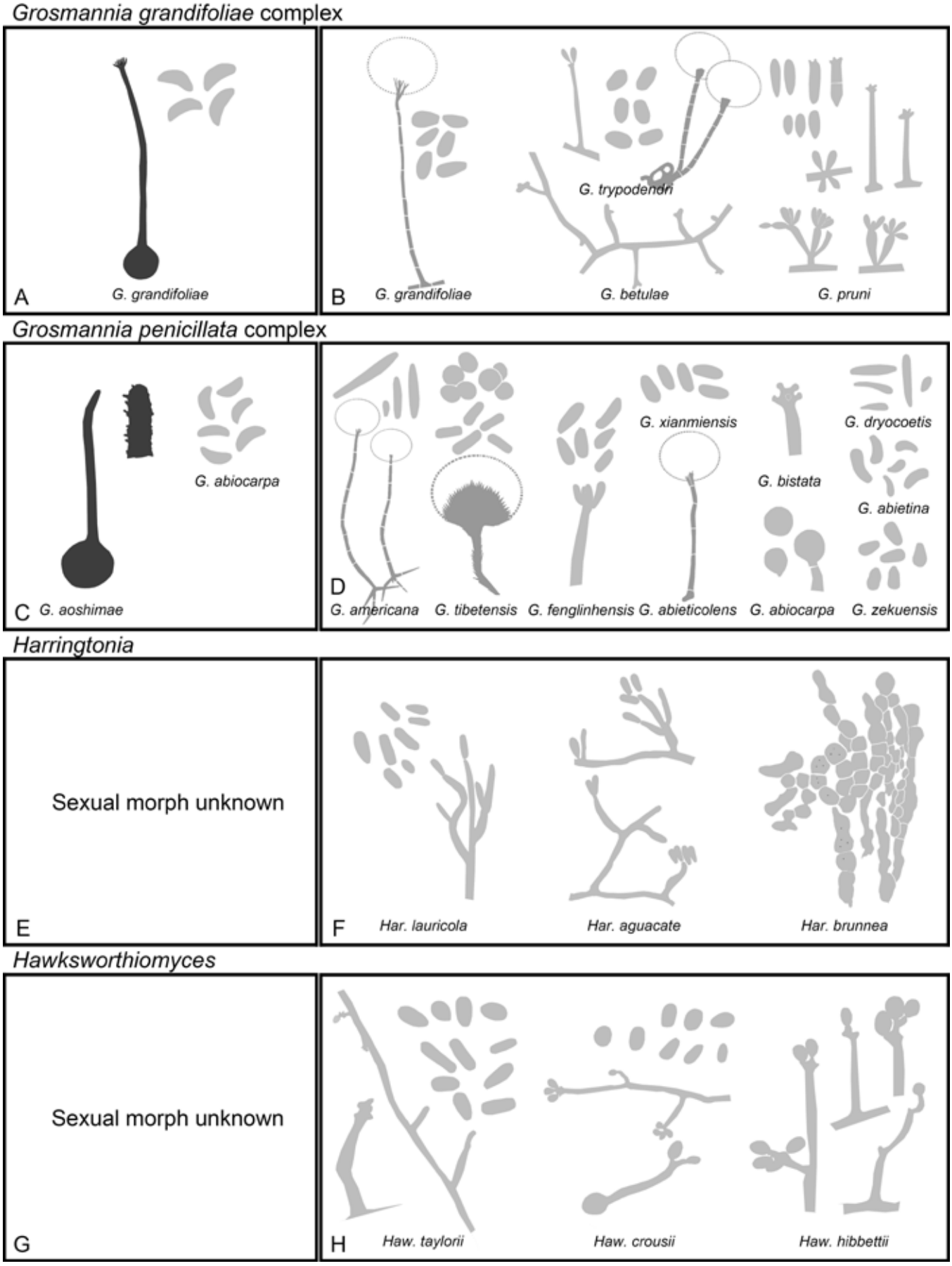

Fig. 8. Genera of the *Ophiostomatales* redrawn from published images with sexual morphs (if known) on the left and asexual morphs on the right. **A, B.** *Grosmannia grandifoliae* complex. **C, D.** *Grosmannia penicillata* complex. **E, F.** *Harringtonia.* **G, H.** *Hawksworthiomyces*. (Pale grey shading reflects hyaline to subhyaline colouration, medium-tone grey brown to dark brown and dark grey reflects fuscous black to dark black colouration).

species of *Leptographium* were described from Poland (Jankowiak *et al.* 2017). Both species formed a well-supported lineage with *G. grandifoliae* and *L. pruni*, sister to the *G. penicillata* complex. Prior to the description of the new species, *L. pruni* and *G. grandifoliae* did not form part of the *G. penicillata* complex or any of the other species complexes recognised by De Beer *et al.* (2013b) in *Leptographium s.l.* Jankowiak *et al.* (2017) suggested that *G. grandifoliae* should be the name-bearing species of this small complex, because it is the oldest known name among the species that it accommodates.

Grosmannia grandifoliae is the only species for which a sexual morph has been observed and that is characterised by ascomata with very long necks (Jacobs & Wingfield 2001). With the addition of the two new species from Poland, *L. trypodendri* and *L. betulae,* it became evident that this complex represents a well-supported hardwood-infesting lineage in *Grosmannia* (Fig. 5) (Jankowiak *et al.* 2017). *Leptographium trypodendri* was isolated mostly from *Trypodendron* (beetle) species and *L. betulae* in association with *Scolytus* species (Jankowiak *et al.* 2017). This is the first species complex in *Leptographium* and *Grosmannia* that accommodates only hardwood-infesting species (Jankowiak *et al.* 2017).

In our datasets, the *G. grandifoliae* complex grouped within Lineage II in all except the *TEF-1α* tree (Fig. S3) where it grouped with Group C (below) among species complexes in *Leptographium*. The clear ecological distinction and the well-supported monophyletic lineage of the *G. grandifoliae* complex, supports its treatment as novel genus. In the future, this will need to be verified using more robust phylogenies including additional gene regions, and if possible, inclusion of a greater number of species in the complex.

Group C

In the phylogenies of Linnakoski *et al.* (2012), *L. taigense* grouped in a distinct lineage between the *G. grandifoliae* and *G. penicillata* complexes. In the LSU tree generated by De Beer & Wingfield (2013), *L. taigense* also grouped outside of the *G. penicillata* complex, close to, but not in a well-supported lineage with *G. abieticola*. With the additional gene regions included in this study, *L. taigense* and *G. abieticola* emerged together in a well-supported lineage distinct from, but between the two complexes defined above. Both these species are associated with conifers, as is true for all species in the *G. penicillata* complex. For the present, we have chosen to treat them in *Grosmannia*, but inclusion of newly discovered species in this lineage in the future could justify the description of a new genus to accommodate these species.

***New combinations*:**

1) *Grosmannia abieticolens* (K. Jacobs & M.J. Wingf.) M. Procter & Z.W. de Beer, ***comb. nov.*** MycoBank MB 840331.
Basionym: *Leptographium abieticolens* K. Jacobs & M.J. Wingf., Mycoscience 41: 599. 2000. MycoBank MB 466545.

Description: Jacobs & Wingfield (2001: 46–48, figs 19–21).

Phylogenetic data: Jacobs *et al.* (2001b), Kim *et al.* (2004, 2005a), Masuya *et al.* (2004), Massoumi Alamouti *et al.* (2006), Paciura *et al.* (2010), Six *et al.* (2011), Duong *et al.* (2012), De Beer & Wingfield (2013), Huang & Chen (2014), Musvuugwa *et al.* (2015), Chang *et al.* (2019).

Notes: Sexual morph unknown. While it was not included in our study, *G. abieticolens* groups in the *G. penicillata* complex based on previously published data (Six *et al.* 2011, De Beer & Wingfield 2013, Chang *et al.* 2019). The name should not be confused with *Grosmannia abieticola* that formed part of Group C in our analyses.

Notes on Grosmannia abietina: Sexual morph unknown. *Grosmannia abietina* groups in the G. *penicillata* species complex (Fig. 4; Six *et al.* 2011, Linnakoski *et al.* 2012, De Beer & Wingfield 2013). The species should not be confused with *Sporothrix abietina,* that resides in *Sporothrix*. Jacobs *et al.* (1998) proposed the synonymy of *G. engelmannii* (as *L. engelmannii*) with *G. abietina* (as *L. abietinum*), which was supported by Jacobs & Wingfield (2001). In our analyses, an isolate of *L. engelmannii* (CMW 759) grouped with *G. abietina* in the *TEF1-α* tree (Fig. S3) and separate from that species in the LSU tree (Fig. S1).

2) *Grosmannia altior* (Paciura, Z.W. de Beer & M.J. Wingf.) M. Procter & Z.W. de Beer, ***comb. nov.*** MycoBank MB 840369.
Basionym: *Leptographium altius* Paciura *et al*., Persoonia 25: 106. 2010. MycoBank MB 516740.

Description: Paciura *et al.* (2010: 106, fig. 7h–m).

Phylogenetic data: Paciura *et al.* (2010), Duong *et al.* (2012), Linnakoski *et al.* (2012), De Beer & Wingfield (2013), Liu *et al.* (2017), Chang *et al.* (2019).

Notes: Sexual morph unknown. This species forms part of the *G. penicillata* complex based on previously published data (Paciura *et al.* 2010, Linnakoski *et al.* 2012, De Beer & Wingfield 2013, Liu *et al.* 2017, Chang *et al.* 2019).

3) *Grosmannia betulae* (Jankowiak *et al*.) M. Procter & Z.W. de Beer, ***comb. nov.*** MycoBank MB 840370.
Basionym: *Leptographium betulae* Jankowiak *et al*., Antonie van Leeuwenhoek 110: 1550. 2017. MycoBank MB 821670.

Description: Jankowiak *et al.* (2017: 1550, fig. 6).

Phylogenetic data: Jankowiak *et al.* (2017, 2018).

Notes: Sexual morph unknown. Groups in the *G. grandifoliae* species complex (Fig. 5; Jankowiak *et al.* 2017).

4) *Grosmannia curviconidia* (Paciura *et al*.) M. Procter & Z.W. de Beer, ***comb. nov.*** MycoBank MB 840373.
Basionym: *Leptographium curviconidium* Paciura *et al*., Persoonia 25: 104. 2010. MycoBank MB 516739.

Description: Paciura *et al.* (2010: 104–105, figs 7a–g).

Phylogenetic data: Paciura *et al.* (2010), Duong *et al.* (2012), Linnakoski *et al.* (2012), De Beer & Wingfield (2013), Huang & Chen (2014), Musvuugwa *et al.* (2015), Jankowiak *et al.* (2017, 2018), Liu *et al.* (2017), Chang *et al.* (2019).

Notes: Sexual morph unknown. *Grosmannia curviconidia* groups in the *G. penicillata* species complex (Fig. 5; Linnakoski *et al.* 2012, De Beer & Wingfield 2013, Huang & Chen 2014, Musvuugwa *et al.* 2015, Jankowiak *et al.* 2017, 2018, Liu *et al.* 2017, Chang *et al.* 2019).

5) *Grosmannia euphyes* (K. Jacobs & M.J. Wingf.) M. Procter & Z.W. de Beer, ***comb. nov*.** MycoBank MB 840376.
Basionym: *Leptographium euphyes* K. Jacobs & M.J. Wingf., Mycol. Res. 105: 497. 2001. MycoBank MB 467761.

Descriptions: Jacobs *et al.* (2001c: 496–498, figs 15–21), Jacobs & Wingfield (2001: 96–99, figs 70–72).

Phylogenetic data: Jacobs *et al.* (2001a), Kim *et al.* (2004, 2005a), Masuya *et al.* (2004), Massoumi Alamouti *et al.* (2006), Paciura *et al.* (2010), Six *et al.* (2011), Duong *et al.* (2012), De Beer & Wingfield (2013), Jankowiak *et al.* (2017, 2018), Liu *et al.* (2017), Chang *et al.* (2019).

Notes: Sexual morph unknown. This species grouped in the *G. penicillata* complex based on previous data (Six *et al.* 2011, De Beer & Wingfield 2013, Jankowiak *et al.* 2017, 2018, Liu *et al.* 2017, Chang *et al.* 2019).

6) *Grosmannia fenglinhensis* (R. Chang *et al*.) M. Procter & Z.W. de Beer, ***comb. nov*.** MycoBank MB 840377.
Basionym: *Leptographium fenglinhense* R. Chang *et al*., Persoonia 42: 67. 2018 (2019). MycoBank MB 825092.

Description: Chang *et al.* (2019: 66–67, fig. 21).

Phylogenetic data: Chang *et al.* (2019)

Notes: Sexual morph unknown. Groups in the *G. penicillata* species complex (Fig. 5; Chang *et al.* 2019).

7) *Grosmannia gestamen* (Errasti & Z.W. de Beer) M. Procter & Z.W. de Beer, ***comb. nov*.** MycoBank MB 840381.
Basionym: *Leptographium gestamen* Errasti & Z.W. de Beer, Mycol. Prog. 15: 11. 2016. MycoBank MB 814177.

Descriptions: De Errasti *et al.* (2016: 11–13, fig. 7).

Phylogenetic data: De Errasti *et al.* (2016), Jankowiak *et al.* (2017, 2018), Chang *et al.* (2019).

Notes: Sexual morph unknown. This species grouped close to *G. taigensis* (as *L. taigense*) in the phylogenies of Jankowiak *et al.* (2017) and Chang *et al.* (2019), and with *G. abieticola* (Jankowiak *et al.* 2018). We have consequently included it in *Grosmannia*, as part of the complex defined by the genus in group C (Fig. 5).

8) *Grosmannia innermongolica* (X.W. Liu *et al*.) M. Procter & Z.W. de Beer, ***comb. nov*.** MycoBank MB 840384.
Basionym: *Leptographium innermongolicum* X.W. Liu *et al*., Mycol. Prog. 16: 8. 2017. MycoBank MB 811204.

Description: Liu *et al.* (2017: 8–10, fig. 6).

Phylogenetic data: Liu *et al.* (2017), Chang *et al.* (2019).

Notes: Sexual morph unknown. This species grouped with *L. taigense* (Group C in Fig. 5) in the phylogenies of Liu *et al.* (2017) and Chang *et al.* (2019). It is consequently included in *Grosmannia* (Fig. 5).

9) *Grosmannia pistaciae* (Paciura *et al*.) M. Procter & Z.W. de Beer, ***comb. nov*.** MycoBank MB 840385.
Basionym: *Leptographium pistaciae* Paciura *et al*., Persoonia 25: 104. 2010. MycoBank MB 516738.

Description: Paciura *et al.* (2010: 104, figs 6g–l).

Phylogenetic data: Paciura *et al.* (2010), Duong *et al.* (2012), Linnakoski *et al.* (2012), De Beer & Wingfield (2013), Jankowiak *et al.* (2017, 2018), Liu *et al.* (2017), Chang *et al.* (2019).

Notes: Sexual morph unknown. *Leptographium pistaciae* has previously been shown to reside in the *G. penicillata* complex (Paciura *et al.* 2010, Linnakoski *et al.* 2012, De Beer & Wingfield 2013, Jankowiak *et al.* 2017, 2018, Liu *et al.* 2017, Chang *et al.* 2019).

10) *Grosmannia pruni* (Masuya & M.J. Wingf.) M. Procter & Z.W. de Beer, ***comb. nov*.** MycoBank MB 840386.
Basionym: *Leptographium pruni* Masuya & M.J. Wingf., Mycologia 96: 553. 2004. MycoBank MB 488574.

Description: Masuya *et al.* (2004: 553–555, figs 1–16).

Phylogenetic data: Masuya *et al.* (2004, 2013), Massoumi Alamouti *et al.* (2006), Matsuda *et al.* (2010), Duong *et al.* (2012), De Beer & Wingfield (2013), De Errasti *et al.* (2016), Jankowiak *et al.* 2017, 2018), Chang *et al.* (2019).

Notes: Sexual morph unknown. This species grouped with *G. grandifoliae* and two other species to form the *G. grandifoliae* species complex (Jankowiak *et al.* 2017).

11) *Grosmannia taigensis* (Linnak. *et al*.) M. Procter & Z.W. de Beer, ***comb. nov*.** MycoBank MB 840387.
Basionym: *Leptographium taigense* Linnak. *et al*., Antonie van Leeuwenhoek 102: 387. 2012. MycoBank MB 564881.

Description: Linnakoski *et al.* (2012: 387–388, fig. 7).

Phylogenetic data: Linnakoski *et al.* (2012), De Beer & Wingfield (2013), Jankowiak *et al.* (2017, 2018), Liu *et al.* (2017), Chang *et al.* (2019).

Notes: Sexual morph unknown. This species grouped with *G. abieticola*, separated from other species complexes in *Grosmannia* (Fig. 5), based on LSU (Fig. S1) and *TEF1-α* (Fig. S3) sequence data.

12) *Grosmannia trypodendri* (Jankowiak *et al*.) M. Procter & Z.W. de Beer, ***comb. nov*.** MycoBank MB 840388.
Basionym: *Leptographium trypodendri* Jankowiak *et al*., Antonie van Leeuwenhoek 110: 1546. 2017. MycoBank MB 821669.

Description: Jankowiak *et al.* (2017: 1546–1550, fig. 5).

Phylogenetic data: Jankowiak *et al.* (2017, 2018).

Notes: Sexual morph unknown. Groups in the *G. grandifoliae* species complex (Fig. 5).

Other species: Listed in Table 1.

Harringtonia (Lineage XI)

Harringtonia Z.W. de Beer & Procter, ***gen. nov.*** MycoBank MB 840400. Fig. 8E, F.

Etymology: Named for the American mycologist Prof. Thomas C. Harrington, who described the type species of this genus as *Raffaelea lauricola* (Harrington *et al.* 2008), and who has contributed substantially to our understanding of the biology and taxonomy of the *Ophiostomatales* (Harrington 1981, 1988, Harrington & Cobb 1987, Harrington *et al.* 2001, 2008, 2010, 2011).

Synonym: *Raffaelea lauricola* complex *sensu* Z.W. de Beer & M.J. Wingf., In *The Ophiostomatoid Fungi*: *Expanding Frontiers*: 34. 2013.

Sexual morph: Unknown.

Asexual morph: *Colonies* initially yeast-like at centre becoming cottony in 2 wk (*Har. lauricola*), cream-coloured, having submerged mycelium at margins, aging to dark green on MEA (*Har. aguacate*). Colonies when repeatedly subcultured forming a filamentous mycelium, with surface becoming finely tomentose (*Har. brunnea*). *Conidiophores* single or aggregated in sporodochia, hyaline, macronematous, semimacronematous, mononematous, simple or branched. *Conidiogenous cells* with inconspicuous annellations at point of conidial dehiscence. *Conidia* hyaline, 1-celled, oblong to ellipsoidal, obovoid, truncated at base, occasionally borne sessile, in some species producing secondary budding cells. Associated with ambrosia beetles.

Type species: ***Harringtonia lauricola*** (T.C. Harr. *et al.*) Z.W. de Beer & M. Procter, ***comb. nov.*** MycoBank MB 840401.
Basionym: *Raffaelea lauricola* T.C. Harr. *et al.*, Mycotaxon 104: 401. 2008. MycoBank MB 511590.

Description: Fraedrich *et al.* (2008: 219–220, fig. 5).

Phylogenetic data: Fraedrich *et al.* (2008), Harrington *et al.* (2008, 2010, 2011), Kim *et al.* (2009), Massoumi Alamouti *et al.* (2009), Matsuda *et al.* (2010), De Beer & Wingfield (2013), Dreaden *et al.* (2014), Musvuugwa *et al.* (2015), Simmons *et al.* (2016), De Beer *et al.* (2016a, b), Bateman *et al.* (2017), Vanderpool *et al.* (2018), Wingfield *et al.* (2017), Li *et al.* (2018), Saucedo-Carabez *et al.* (2018).

Notes: *Harringtonia lauricola* consistently forms a clade together with *Har. brunnea* and *Har. aguacate,* that has previously been referred to as the *R. lauricola* complex (De Beer & Wingfield 2013). This complex has always formed a monophyletic lineage close to, but distinct from *Raffaelea s.s.* in previous studies (Massoumi Alamouti *et al.* 2009, De Beer & Wingfield 2013, Dreaden *et al.* 2014, Simmons *et al.* 2016). When De Beer & Wingfield (2013) first defined this species complex, they chose *R. lauricola* as the name bearing species, because it is the best-known species in this complex. This is despite the fact that it was not the first species in the complex to be described. They suggested that this lineage would likely emerge as a new genus when more robust phylogenetic analyses were performed, as is the case in the present study.

In the analyses of our datasets, the *R. lauricola* complex grouped close to *Raffaelea s.s.* and together they formed a monophyletic clade, although this relationship was not suppoted. Phylogenomic analyses conducted in the current study and previous studies (Nel *et al.* 2021; Vanderpool *et al.* 2018) showed that the *R. lauricola* complex and *Raffaelea s.s.* did not form a monophyletic lineage. Based on these results, we have removed the *R. lauricola* complex from *Raffaelea* and have described the complex as a new genus. While fully cogniscient of the fact that describing a new genus to accommodate an important tree pathogen might result in some early discomfort, this change is based on robust taxonomic data, not only from the present study. Failing to make this change perpetuates a taxonomically confused situation. In our view this decision will also provide opportunities to better understand the biology and evolutionary characteristics of two phylogenetically distinct and important groups of fungi.

All species in the *R. lauricola* complex produce raffaelea-like asexual morphs (De Beer & Wingfield 2013). *Harringtonia lauricola* is the causal agent of laurel wilt, a vascular wilt disease affecting *Lauraceae* species in the south-eastern USA. It is believed to have been introduced into the USA from Asia in the mycangia of *Xyleborus glabratus*, an ambrosia beetle invasive to the USA (Harrington *et al.* 2008). The other species in this complex are *Har. brunnea*, associated with ambrosia beetles infesting hardwoods (De Beer & Wingfield 2013), and *Har. aguacate*, originally isolated from avocado (*Persea americana*) (Simmons *et al.* 2016) and later shown to be vectored by *X. bispinatus* (Saucedo-Carabez *et al.* 2018).

***Other new combinations*:**

1) *Harringtonia aguacate* (D.R. Simmons *et al.*) M. Procter & Z.W. de Beer, ***comb. nov.*** MycoBank MB 840402.
Basionym: *Raffaelea aguacate* D.R. Simmons *et al.*, IMA Fungus 7: 269. 2016. MycoBank MB 817170.

Description: Simmons *et al.* (2016: 269, fig. 2).

Phylogenetic data: Simmons *et al.* (2016), Vanderpool *et al.* (2018), Li *et al.* (2018), Saucedo-Carabez *et al.* (2018).

Notes: This species forms part of *Harringtonia* (Fig. 5), previously the *R. lauricola* complex (De Beer & Wingfield 2013).

2) *Harringtonia brunnea* (L.R. Batra) M. Procter & Z.W. de Beer, ***comb. nov.*** MycoBank MB 840403.
Basionym: *Ambrosiella brunnea* L.R. Batra, Mycologia 59: 980. 1968 (1967). MycoBank MB 326140.
Synonyms: *Monilia brunnea* Verrall, J. Agric. Res. 66: 142. 1943. MycoBank MB 440994. *nom. illegit*., Art. 53. 1.
Raffaelea brunnea (L.R. Batra) T.C. Harr., Mycotaxon 111: 351. 2010. MycoBank MB 515296.

Descriptions: Verrall (1943: 142–143, fig. 5), Batra (1967: 1004–1007, figs 43, 45, 46).

Phylogenetic data: Cassar & Blackwell (1996), Rollins *et al.* (2001), Gebhardt *et al.* (2005), Massoumi Alamouti *et al.* (2009), Harrington *et al.* (2010), Matsuda *et al.* (2010), De Beer & Wingfield (2013), Dreaden *et al.* (2014), Musvuugwa *et al.* (2015), De Beer *et al.* (2016a, b), Vanderpool *et al.* (2018), Wingfield *et al.* (2017), Li *et al.* (2018), Saucedo-Carabez *et al.* (2018).

Notes: This species forms part of *Harringtonia* (Fig. 5), previously the *R. lauricola* species complex (De Beer & Wingfield 2013).

This species should not be confused with *Monilia brunnea*, a soil inhabiting species.

Hawksworthiomyces (Lineage XXII)

Hawksworthiomyces Z.W. de Beer *et al*., Fungal Biol. 120: 1329. 2016. MycoBank MB 815685. Fig. 8G, H.

Etymology: 'Named for Dr David Hawksworth, in recognition of the leading role that he has played in guiding the global mycological community through the controversial and often challenging transition from a dual nomenclature to a One Fungus-One Name-based system' (De Beer *et al.* 2016b).

Sexual morph: Unknown.

Asexual morph: *Conidiophores* hyaline, micronematous to macronematous, mononematous, simple or branched. *Conidiogenous cells* hyaline, polyblastic, denticulate. *Conidia* hyaline, 1-celled, broadly ellipsoidal to cylindrical, producing secondary cells.

Type species: *Hawksworthiomyces lignivorus* (De Mey. *et al*.) Z.W. de Beer *et al*., Fungal Biol. 120: 1329. 2016. MycoBank MB 815686.

Other species: Listed in Table 1.

Notes: *Hawksworthiomyces* was erected to accommodate *Sporothrix lignivora* (now *Haw. lignivora*) and three other species not previously associated with the *Ophiostomatales*. De Beer & Wingfield (2013) listed *S. lignivora* as "*incertae sedis*", as this species formed a lineage on its own, separate from other species in *Ophiostoma* and *Sporothrix*, even though its morphology resembled species of *Sporothrix* (De Meyer *et al.* 2008). BLAST searches on GenBank later revealed sequences from environmental studies and isolates from diversity studies with strong similarity to *S. lignivora*. Consequently, De Beer *et al.* (2016) proceeded to erect the new genus, *Hawksworthiomyces,* to incorporate *S. lignivora* and these "new" species. In the analyses of our data, *Haw. lignivora*, *Haw. taylorii*, *Haw. hibbettii* and *Haw. crousii* formed a well-supported monophyletic lineage, supporting their treatment in a distinct genus. An ENAS (Environmental Nucleic Acid Sequence) species, named *Haw. sequentia* ENAS, was also included in *Hawksworthiomyces* by De Beer *et al.* (2016). *Hawksworthiomyces* species have been isolated from diverse sources (*e.g. Eucalyptus* wood poles, insect fungal gardens, rhizospheres of plants) in South Africa, North and Central America, South Korea and Europe (De Beer *et al.* 2016). In the analyses of our datasets based on protein coding genes (Figs S3, S4) *Hawksworthiomyces* spp. formed two separate lineages. However, in the concatenated (Fig. 5) and LSU (Fig. S1) datasets, a monophyletic lineage emerged.

Heinzbutinia (Lineage XXIV)

Heinzbutinia Z.W. de Beer & M. Procter, ***gen. nov.*** MycoBank MB 840404. Fig. 9A, B.

Etymology: Named for Prof. Heinz Butin (1928–2021), a German forest pathologist who described 10 new species in the *Ophiostomatales* between 1968 and 1990, including the type species of this novel genus.

Sexual morph: *Ascomatal bases* black, subglobose to globose; necks black, cylindrical, curved. *Ostiolar hyphae* absent. *Asci* elongate ovoid or clavate, evanescent. *Ascospores* hyaline, 1-celled, orange segment-like in side view, ellipsoidal in face view.

Asexual morph: Sporothrix-like; *conidiophores* micronematous, macronematous, mononematous, simple or branched, hyaline; *conidiogenous cells* sympodial, denticulate; *conidia* hyaline, 1-celled, ellipsoid, often curved, reniform, secondary conidia originating from swollen ellipsoidal conidia, oblong, straight or curved.

Type species: *Heinzbutinia grandicarpa* (Kowalski & Butin) Z.W. de Beer & M. Procter, ***comb. nov.*** MycoBank MB 840405.
Basionym: *Ceratocystis grandicarpa* Kowalski & Butin, J. Phytopathol. 124: 243. 1989. MycoBank MB 134497.
Synonym: *Ophiostoma grandicarpum* [as '*grandicarpa*'] (Kowalski & Butin) Rulamort, Bull. Soc. Bot. Centre-Ouest 21: 511. 1990. MycoBank MB 130251.

Phylogenetic data: Villarreal *et al.* (2005), De Beer & Wingfield (2013), Reid & Hausner (2015), De Beer *et al.* (2016a, b), De Errasti *et al.* (2018).

Notes: The *O. grandicarpum* complex was described by De Beer *et al.* (2016b) for the monophyletic lineage formed by *O. grandicarpum* and *O. microsporum* among other genera in the *Ophiostomatales* (De Beer & Wingfield 2013, Reid & Hausner 2015, De Beer *et al.* 2016a, De Errasti *et al.* 2018). In our expanded phylogenies, the two species again consistently formed a well-supported lineage distinct from all other genera in the *Ophiostomatales* (Figs 5, S2–S4). Both species are characterised by very long (more than 1 mm) ascomatal necks (Kowalski & Butin 1989, Hunt 1956), sporothrix-like asexual morphs and reniform ascospores (Fig. 3F; Type A as categorised by De Beer & Wingfield 2013). Both species were isolated from hardwoods. Based on the distinct phylogenetic placement and supported by a unique morphology and ecology, we have designated the *O. grandicarpum* complex as the new genus *Heinzbutinia*.

***Other new combinations*:**

1) *Heinzbutinia microspora* (Arx) Z.W. de Beer & M. Procter, ***comb. nov*.** MycoBank MB 840406.
Basionym: *Ophiostoma microsporum* Arx, Antonie van Leeuwenhoek 18: 211. 1952. MycoBank MB 302079.
Synonyms: *Ceratostomella microspora* R.W. Davidson, Mycologia 34: 650. 1942. MycoBank MB 284860. *nom. illegit*., Art. 53.1, later homonym for *Cs. microspora* Ellis & Everh., see De Beer *et al.* 2013, Section C.1.
Ceratocystis perparvispora J. Hunt, Lloydia 19: 46. 1956. MycoBank MB 294227. Art. 52.1, superfluous *nom. nov*.
Ceratocystis microspora (R.W. Davidson) R.W. Davidson & Aoshima, Ph.D. thesis, University of Tokyo: 20. 1965. *nom. inval.,* Arts 29.1, 39.1 or 39.2.
Ceratocystis microspora (Arx) R.W. Davidson, J. Colorado-Wyoming Acad. Sci. 6: 16. 1969. MycoBank MB 453851.

Descriptions: Hunt (1956: 46–47), Griffin (1968: 710), De Hoog (1974: 63–64, fig. 25), Olchowecki & Reid (1974: 1709), Upadhyay (1981: 50, figs 104–108), Maekawa *et al.* (1987: 8, 10, figs 1–6).

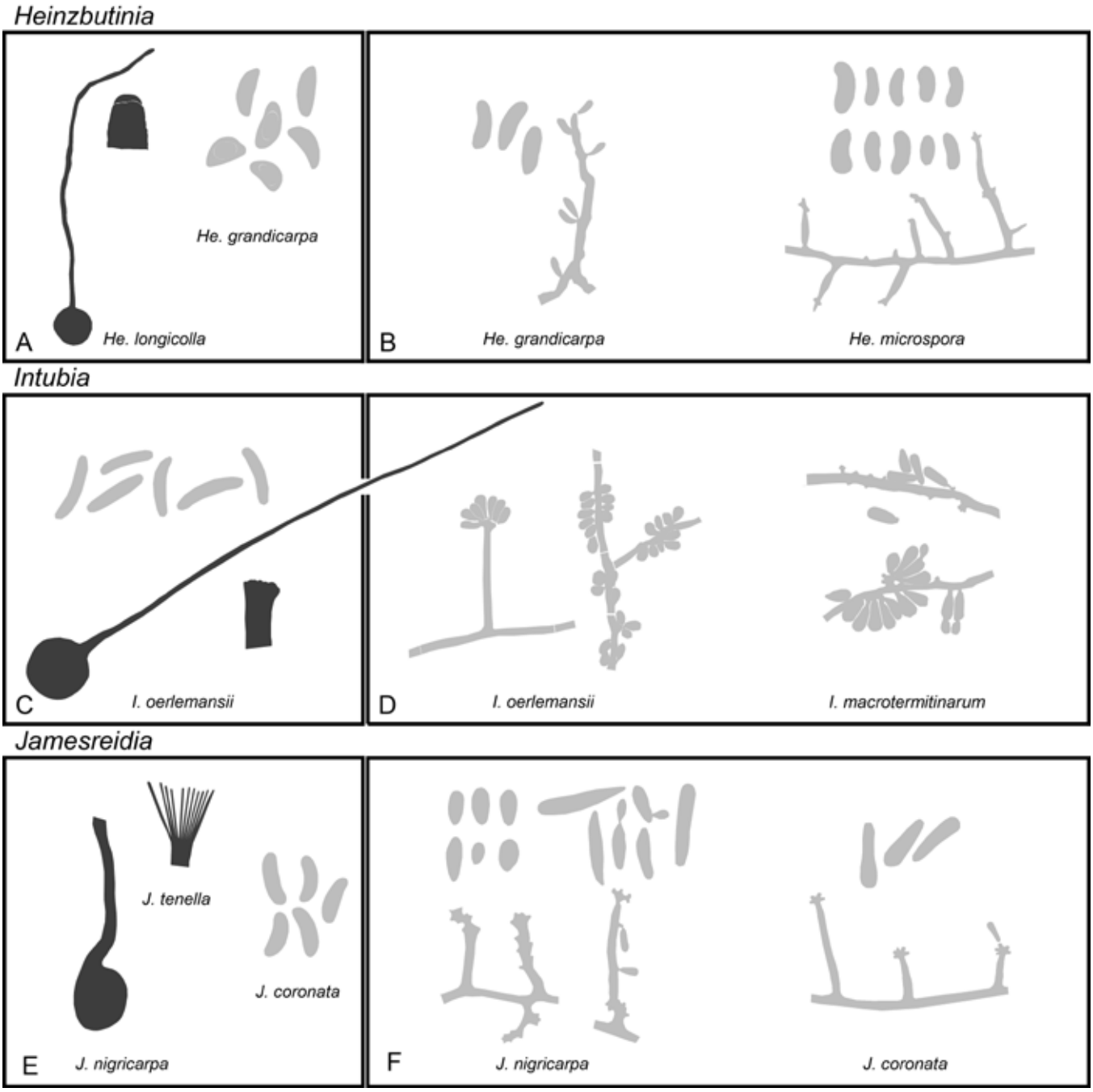

Fig. 9. Genera of the *Ophiostomatales* redrawn from published images with sexual morphs (if known) on the left and asexual morphs on the right. **A, B.** *Heinzbutinia*. **C, D.** *Intubia*. **E, F.** *Jamesreidia*. (Pale grey shading reflects hyaline to subhyaline colouration, medium-tone grey brown to dark brown and dark grey reflects fuscous black to dark black colouration).

Phylogenetic data: Hausner *et al.* (1993b), Mullineux *et al.* (2011), De Beer & Wingfield (2013), Musvuugwa *et al.* (2015), De Beer *et al.* (2016a, b).

Notes: This species grouped with *He. grandicarpa* and distinct from other *Ophiostoma* spp. (De Beer *et al.* 2016a, b), in the *O. grandicarpum* complex as designated by De Beer *et al.* (2016b). See note under *He. grandicarpa*. The name *He. microspora* should not be confused with *Leptographium microsporum* or *Ceratostomella microspora* (see De Beer *et al.* 2013, section C.2).

2) *Heinzbutinia solheimii* (Strzałka & Jankowiak) Z.W. de Beer & M. Procter, ***comb. nov.*** MycoBank MB 840407.
Basionym: *Ophiostoma solheimii* Strzałka & Jankowiak, Antonie van Leeuwenhoek 112: 1517. 2019. MycoBank MB 830198.

Description: Jankowiak *et al.* (2019: 1516–1517, fig. 8).

Phylogenetic data: Jankowiak *et al.* (2019).

Notes: This species is closely related to and formed a well-supported lineage with *He. grandicarpa* and *He. microspora* (Jandowiak *et al.* 2019, figs 1, S4).

Intubia

Intubia W.J. Nel *et al.*, Mycologia 113: 1206. 2021. MycoBank MB 837565. Fig. 9C, D.

Etymology: 'From the Xhosa language, Intubi for termite, recognising the source where the fungus was found' (Nel *et al.* 2021).

Sexual morph: *Ascomatal bases* dark brown, globose; necks uniformly dark, often slightly curved, tapering towards apex, extremely long. *Ostiolar hyphae* absent. *Asci* not seen. *Ascospores* produced in slimy droplet at apex of neck, hyaline, 1-celled, cylindrical, sometimes slightly curved, no sheath.

Asexual morph: *Conidiophores* micronematous, hyaline, arising singly. Hyalorhinocladiella-like; *conidiogenous cells* smooth; *conidia* hyaline, 1-celled, bacilliform tapering toward one end, occasionally producing secondary spores. Sporothrix-like; *conidiogenous cells* denticulate; *conidia* of two types, first type formed on vegetative hyphae, hyaline, 1-celled, round to obovoid, second type formed on conidiophores, hyaline, 1-celled, bacilliform, secondary conidia present.

Type species: *Intubia macrotermitinarum* W.J. Nel *et al*., Mycologia 113: 1208. 2021. MycoBank MB 837567.

Other species: Listed in Table 1.

Notes: Distinguished from other phylogenetically related genera in the *Ophiostomatales* for their unique habitat with dark coloured ascomata embedded in the substrate of abandoned *Termitomyces* combs.

Jamesreidia (Lineage XII)

Jamesreidia Z.W. de Beer & M. Procter, ***gen. nov.*** MycoBank MB 840408. Fig. 9E, F.

Etymology: Named for the Canadian mycologist, Dr James Reid, who described 28 novel ophiostomatoid species, including the type species of this new genus. He was also involved in producing some of the first phylogenetic data based on ribosomal sequences distinguishing between the *Ophiostomatales* and *Microascales* (Olchowecki & Reid 1974, Hausner *et al.* 1992).

Synonym: *Ophiostoma tenellum* complex *sensu* Z.W. de Beer & M.J. Wingf., In *The Ophiostomatoid Fungi*: *Expanding Frontiers*: 34. 2013.

Sexual morph: *Ascomatal bases* black, globose; necks absent or present, black, straight or bent. *Ostiolar hyphae* divergent. *Asci* evanescent, clavate to subglobose. *Ascospores* hyaline, 1-celled, orange segment-like in side view, oblong in face view, broadly ellipsoidal to globose in end view.

Asexual morph: *Conidiophores* macronematous, semimacronematous, mononematous, hyaline, simple or branched. *Conidiogenous cells* polyblastic, denticulate. *Conidia* hyaline, 1-celled, broadly ovoid to nearly cylindrical, slightly curved.

Type species: ***Jamesreidia tenella*** (R.W. Davidson) Z.W. de Beer & M. Procter, ***comb. nov.*** MycoBank MB 840409.
Basionym: *Ceratocystis tenella* R.W. Davidson, Mycologia 50: 666. 1958. MycoBank MB 294240.
Synonyms: *Ophiostoma tenellum* (R.W. Davidson) M. Villarreal, Mycotaxon 92: 263. 2005. MycoBank MB 346181.
Ceratocystis capitata H.D. Griffin, Canad. J. Bot. 46: 699. 1968. MycoBank MB 327623.

Descriptions: Griffin (1968: 713, 715, fig. 93, pl. III), Olchowecki & Reid (1974: 1708, pl. XVI figs 307, 308, 311, 312), Upadhyay (1981: 114, figs 408–412), Maekawa *et al.* (1987: 10–11, figs 19, 20), Hutchison & Reid (1988a: 68).

Phylogenetic data: Villarreal *et al.* (2005), Linnakoski *et al.* (2010, 2016), De Beer & Wingfield (2013), De Errasti *et al.* (2018), De Beer *et al.* (2016a), De Errasti *et al.* (2018), Wang *et al.* (2018), Chang *et al.* (2019).

Notes on the type species: *Jamesreidia tenella* groups with *J. coronata*, *J. nigricarpa* (Fig. 5; Linnakoski *et al.* 2010, De Beer & Wingfield 2013) and *J. rostrocoronata* (in the phylogenies of De Beer *et al.* 2016a) to form *Jamesreidia*, previously designated as the *O. tenellum* species complex (De Beer & Wingfield 2013). This species serves as the type species of the new genus, due to the fact that it is the oldest described species in the genus.

Notes on the genus: The *O. tenellum* complex was defined in *Ophiostoma s.l.* by De Beer & Wingfield (2013), who noted that members of the complex shared a similar morphology with species in the *S. schenckii-O. stenoceras* complex (also treated in *Ophiostoma s.l.* at the time, but now recognised as the genus *Sporothrix*). The asexual morphs of all species can be described as sporothrix-like and sexual morphs form Type A ascospores (Fig. 3F; as categorised by De Beer & Wingfield 2013). All species in this complex colonise conifer wood in North America (Linnakoski *et al.* 2010).

De Beer *et al.* (2016a) noted that the generic status of the *O. tenellum* complex should be further investigated, because it grouped distinctly from both *Sporothrix* and *Ophiostoma s.s.* in their phylogenies. In the present study, this complex grouped separately from what we have designated as *Ophiostoma* and *Sporothrix* in our phylogeny (Fig. 5) as well as in the phylogenies of other authors (Villarreal *et al.* 2005, Linnakoski *et al.* 2010, De Beer & Wingfield 2013, De Beer *et al.* 2016a). We have thus elevated the status of the *O. tenellum* complex to that of a genus, for which we have provided the name *Jamesreidia*.

***Other new combinations*:**

1) *Jamesreidia coronata* (Olchow. & J. Reid) M. Procter & Z.W. de Beer, ***comb. nov.*** MycoBank MB 840410.
Basionym: *Ceratocystis coronata* Olchow. & J. Reid, Canad. J. Bot. 52: 1705. 1974. MycoBank MB 310490.
Synonym: *Ophiostoma coronatum* (Olchow. & J. Reid) M. Villarreal, Mycotaxon 92: 263. 2005. MycoBank MB 346368.

Description: Hutchison & Reid (1988a: 66, 68).

Phylogenetic data: Hausner *et al.* (1993b), Thwaites *et al.* (2005), Villarreal *et al.* (2005), Linnakoski *et al.* (2010), Mullineux *et al.* (2011), De Beer & Wingfield (2013), Linnakoski *et al.* (2016), De Beer *et al.* (2016a), De Errasti *et al.* (2018), Wang *et al.* (2018), Chang *et al.* (2019).

Notes: This species grouped in *Jamesreidia* (Fig. 5), previously designated as the *O. tenellum* species complex (De Beer & Wingfield 2013).

2) *Jamesreidia nigrocarpa* (R.W. Davidson) M. Procter & Z.W. de Beer, ***comb. nov.*** [MycoBank MB 840411]
Basionym: *Ceratocystis nigrocarpa* R.W. Davidson, Mycopathol. Mycol. Appl. 28: 276. 1966. MycoBank MB 327637.

Synonym: *Ophiostoma nigrocarpum* (R.W. Davidson) de Hoog, Stud. Mycol. 7: 62. 1974. MycoBank MB 319024.

Descriptions: De Hoog (1974: 62–63, fig. 24), Olchowecki & Reid (1974: 1709), Upadhyay (1981: 104, figs 378–381), Benade *et al.* (1997: 1110–1111, figs 6–11).

Phylogenetic data: Aghayeva *et al.* (2004), Zhou *et al.* (2004a, 2006), Roets *et al.* (2006, 2008, 2010), Zipfel *et al.* (2006), De Meyer *et al.* (2008), Linnakoski *et al.* (2010), Madrid *et al.* (2010), Romón *et al.* (2014b), De Errasti *et al.* (2016, 2018), Linnakoski *et al.* (2016), De Beer *et al.* (2016a), Giraldo *et al.* (2017), Chang *et al.* (2019).

Notes: This species forms part of *Jamesreidia* (Fig. 5), previously the *O. tenellum* species complex (De Beer & Wingfield 2013).

3) *Jamesreidia rostrocoronata* (R.W. Davidson & Eslyn) M. Procter & Z.W. de Beer, ***comb. nov.*** MycoBank MB 840412.
Basionym: *Ceratocystis rostrocoronata* R.W Davidson & Eslyn, Mem. N.Y. Bot. Gard. 28: 50. 1976. MycoBank MB 310518.
Synonym: *Ophiostoma rostrocoronatum* (R.W. Davidson & Eslyn) de Hoog & R.J. Scheff., Mycologia 76: 297. 1984. MycoBank MB 107077.

Descriptions: Upadhyay (1981: 112), Hutchison & Reid (1988a: 76–78).

Phylogenetic data: Hausner *et al.* (1993b), Jacobs *et al.* (2003), Villarreal *et al.* (2005), Linnakoski *et al.* (2010), De Beer & Wingfield (2013), Reid & Hausner (2015), De Beer *et al.* (2016b), Osorio *et al.* (2016), Jankowiak *et al.* (2017b), Wang *et al.* (2018).

Notes: A LSU sequence generated by Jacobs *et al.* (2003) was shown to group in *Sporothrix* (De Beer & Wingfield 2013, Osorio *et al.* 2016, Jankowiak *et al.* 2017, Wang *et al.* 2018). However, sequence data generated by De Beer *et al.* (2016b) for the same isolate, placed *O. rostrocoronatum* with the *O. tenellum* complex. Based on analyses of sequences from four gene regions and morphological characteristics, De Beer *et al*. (2016b) proceeded to treat *O. rostrocoronatum* in the *O. tenellum* complex. We have consequently treated this species as part of the lineage described here as *Jamesreidia*.

Leptographium (Lineage I)

Leptographium Lagerb. & Melin, Svenska Skogsv.-Fören. Tidskr. 25: 257. 1927. MycoBank MB 8749, ***emend.*** Z.W. de Beer & M. Procter. Figs 10, 11.

Etymology: 'A thin, small brush. From the Greek adjective, λεπτός (thin) and the Greek noun γραφισν (a small brush). The generic name refers to the conidiophores that resemble small brushes' (Jacobs & Wingfield 2001).

Synonyms: *Scopularia* Preuss, Linnaea 24: 133. 1851. MycoBank MB 22345, *nom. illegit*., Art. 53.1. (Type species *Sc. venusta* Preuss).
Phialographium H.P. Upadhyay & W.B. Kendr., Mycologia 66: 183. 1974. MycoBank MB 9340. (Type species *Ph. sagmatosporae* H.P. Upadhyay & W.B. Kendr.).
Graphiocladiella H.P. Upadhyay, A Monograph of *Ceratocystis* and *Ceratocystiopsis*: 138. 1981. MycoBank MB 8394. (Type species *G. clavigera* H.P. Upadhyay).
?= *Europhium* A.K. Parker, Canad. J. Bot. 35: 175. 1957. MycoBank MB 1938. [Type species *E. trinacriforme* A.K. Parker; Placement uncertain, see De Beer *et al.* (2013b)].

Sexual morph: *Ascomata* cleitothecial or perithecial; bases black, subglobose to globose; necks absent or present, very short, elongated, cylindrical, straight or flexuous. *Ostiolar hyphae* absent. *Asci* evanescent, clavate to broadly clavate. *Ascospores* hyaline, 1-celled, enclosed in sheath, reniform or cucullate in side view, oblong or rectangular in face view, ovoid, globose or triangular in end view.

Asexual morph: *Conidiophores* macronematous, micronematous, mononematous, singly or in groups, upright or prone, branches brown, becoming paler towards upper branches, bases simple or rhizoid-like. *Conidiogenous cells* hyaline, cylindrical. *Conidia* hyaline, 1-celled, oblong, pyriform, broadly ellipsoidal to obovoid, with truncate base. Hyalorhinocladiella-like; *conidiophores* simple or branched, upright; *conidia* hyaline, 1-celled, oblong to ellipsoid. Pesotum-like; *conidiophores* pale to dark brown, hyaline to light grey, reddish brown at apex; conidia hyaline, 0–4-celled, oblong, cylindrical to clavate, broadly fusiform, or subglobose to ellipsoid with truncate base. *Ramoconidia* hyaline, clavate to ellipsoid, 1-celled spores. Serprentine hyphae present in *L. lundbergii*, *L. serpens* complexes and *L. douglasii* in *L. wageneri* complex.

Type species: *Leptographium lundbergii* Lagerb. & Melin, Svenska Skogsv.-Fören. Tidskr. 25: 248. 1927. MycoBank MB 269891.
Synonym: *Scopularia lundbergii* (Lagerb. & Melin) Goid., Ann. Mycol. 31: 138. 1933. MycoBank MB 253103.

Notes on the genus: *Leptographium* was originally described as an asexual genus with *L. lundbergii* as type species (Lagerberg *et al.* 1927). Soon afterwards, the sexual genus *Grosmannia* was described to accommodate the sexual morph of another species, *Leptographium penicillatum* (Goidànich 1935). During the course of the next 65 years, an additional 28 asexual species were described in *Leptographium* and 17 species with known sexual morphs that were treated in different genera (Harrington 1988, Wingfield 1993). This prompted a revision of the genus in a comprehensive monograph by Jacobs & Wingfield (2001), who treated the sexual morphs of these species in *Ophiostoma,* of which *Grosmannia* was listed as one of several synonyms (Jacobs & Wingfield 2001). As mentioned in the introduction to this study, Zipfel *et al.* (2006) reinstated *Grosmannia* for all sexual species with *Leptographium* asexual morphs. However, they included only one asexual species, *L. lundbergii,* in their phylogeny.

De Beer & Wingfield (2013) were the first authors to apply the One Fungus-One Name principles to the *Ophiostomatales*, and listed *Grosmannia* as synonym of the older name, *Leptographium*. However, they recognised that the type species for these two genera grouped in different lineages but concluded that their LSU and ITS phylogenies were not sufficiently robust to resolve the generic status of these sub-lineages within what they referred to as '*Leptographium sensu lato*'. They listed 94 valid species in this broad concept but refrained from making new combinations for species that did not have names in *Leptographium*, recommending that phylogenies based on a greater number of gene regions should be used to resolve the genera.

Prior to the study of De Beer & Wingfield (2013), several authors defined phylogenetic species complexes in '*Leptographium sensu*

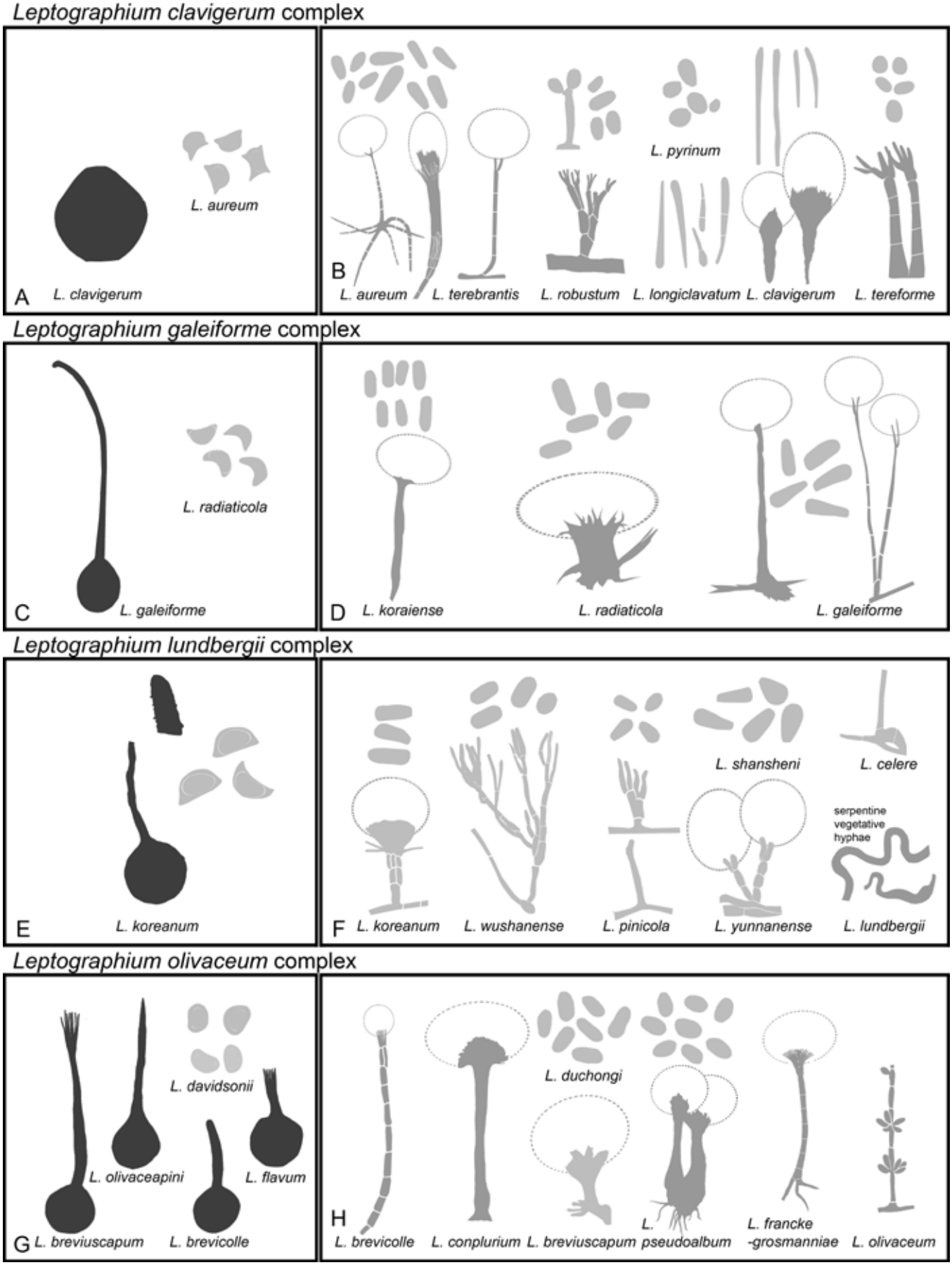

Fig. 10. Genera of the *Ophiostomatales* redrawn from published images with sexual morphs (if known) on the left and asexual morphs on the right. **A, B.** *Leptographium clavigerum* complex. **C, D.** *Leptographium galeiforme* complex. **E, F.** *Leptographium lundbergii* complex. **G, H.** *Leptographium olivaceum* complex. (Pale grey shading reflects hyaline to subhyaline colouration, medium-tone grey brown to dark brown and dark grey reflects fuscous black to dark black colouration).

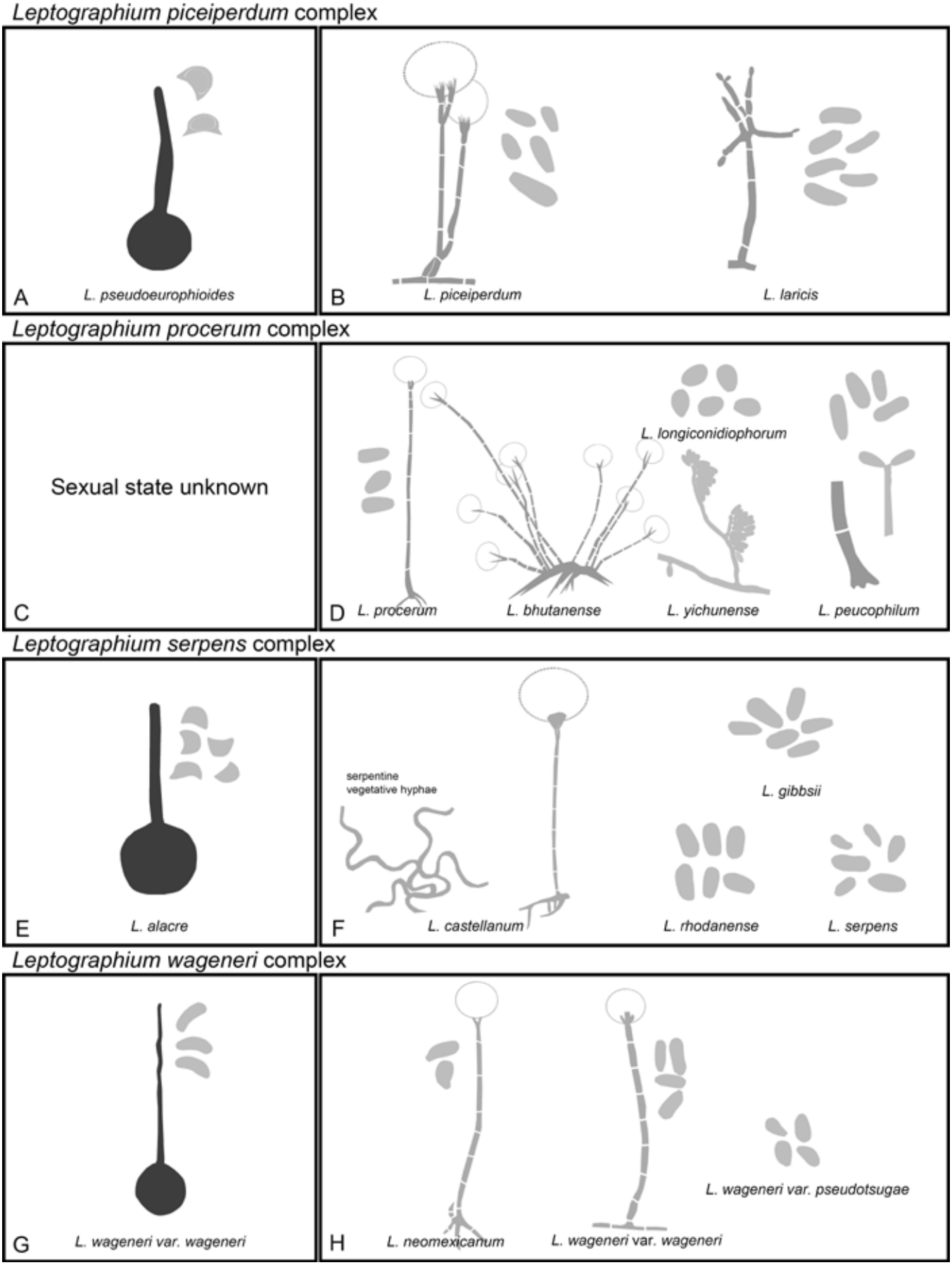

Fig. 11. Genera of the *Ophiostomatales* redrawn from published images with sexual morphs (if known) on the left and asexual morphs on the right. **A, B.** *Leptographium piceiperdum* complex. **C, D.** *Leptographium procerum* complex. **E, F.** *Leptographium serpens* complex. **G, H.** *Leptographium wageneri* complex. (Pale grey shading reflects hyaline to subhyaline colouration, medium-tone grey brown to dark brown and dark grey reflects fuscous black to dark black colouration).

lato' (Massoumi Alamouti *et al.* 2011, Six *et al.* 2011, Duong *et al.* 2012, Linnakoski *et al.* 2012). The results of the present study clearly show that '*Leptographium sensu lato*' represents two distinct genera. These include *Leptographium* (Lineage I) with *L. lundbergii* as type species and including eight species complexes defined below and *Grosmannia* (Lineage II) defined by *G. penicillata* including two species complexes defined above. A third complex could emerge as new species are described in *Grosmannia*.

The last formal morphological description of *Leptographium* was provided by Jacobs & Wingfield (2001) for asexual fungi forming mononematous conidiophores and branched conidiogenous apparatuses. In view of the One Fungus-One Name principles, we have emended the description of *Leptographium* to accommodate the morphology of the sexual morphs, treated previously in *Grosmannia, Ophiostoma, Ceratocystis* or *Europhium* (Upadhyay 1981, Jacobs & Wingfield 2001, De Beer & Wingfield. 2013). Morphology of synnematous asexual morphs previously excluded from *Leptographium* and treated variously as species of *Graphium, Pesotum, Phialographium* or *Graphiocladiella* (Upadhyay & Kendrick 1974, Upadhyay 1981, Seifert & Okada 1993, Okada *et al.* 1998) have also been incorporated in the revised circumscription of the genus.

***Species complexes*:**

The *L. clavigerum* complex

The *L. clavigerum* complex was first described by Massoumi Alamouti *et al.* (2011) as the *G. clavigera* complex. *Grosmannia clavigera* is also the type species of *Graphiocladiella*, a genus originally described for the asexual morphs of '*Ceratocystis*' species forming mononematous and synnematous conidiophores (Upadhyay 1981, Harrington 1988). Harrington (1988) proceeded to reduce *Graphiocladiella* to synonymy with *Graphium* (in which he also included species producing leptographium-like conidiophores). Species in the *G. clavigera* complex produce mostly synnematous aggregates of leptographium-like conidiophores, cleistothecal ascomata and reniform ascospores with hat-shaped sheaths (Linnakoski *et al.* 2012, De Beer & Wingfield 2013).

The first whole genome sequence produced for species in the *Ophiostomatales* was that for *G. clavigera*. This work was justified by the close association of *G. clavigera* with the mountain pine beetle (*Dendroctonus ponderosae*), a native but invasive pest causing devastating losses in the Northwestern USA and Canada (Kim *et al.* 2004, Massoumi Alamouti *et al.* 2011, De Beer & Wingfield 2013). Genome data were then used to show that what was previously thought to be a highly variable population of *G. clavigera*, actually represents a complex including multiple species (Massoumi Alamouti *et al.* 2011). Later studies contributed additional species to this new species complex (Six *et al.* 2011, De Beer & Wingfield 2013). In the present study, the *G. clavigera* complex formed a well-supported monophyletic lineage, and currently includes eight well-defined species, as well as one undescribed species (Massoumi Alamouti *et al.* 2011).

The *L. galeiforme* complex

The *L. galeiforme* complex was first described as the *O. galeiformis* complex when Zhou *et al.* (2004b) designated an epitype for the species (Bakshi 1951). Kim *et al.* (2005b) showed that *G. radiaticola* was part of the complex, and that this species was conspecific with the asexual species, *Hyalopesotum pini*. The latter species name was thus used for the asexual morph of *G. radiaticola* (Kim *et al.* 2005b, De Beer & Wingfield 2013). However, when the One Fungus–One Name principles are applied, the oldest epithet '*pini*' (Hutchison & Reid 1988b) should take precedence over '*radiaticola*' (Kim *et al.* 2005b). We have consequently provided a new combination, *L. pini,* to represent this species. It was previously believed that *G. radiaticola* and *G. galeiformis* were the same species (Thwaites *et al.* 2005). However, data from the studies of Kim *et al.* (2005b) and Linnakoski *et al.* (2012) showed that these are distinct species, and that in addition to these, the complex includes two as yet undescribed cryptic species. Chang *et al.* (2017) reported *L. pini* (as *G. radiaticola*) from China, as well as another possible new species in the complex.

All species in the *L. galeiforme* complex produce synnemata that appear to be loose aggregates of leptographium-like conidiophores (Zhou *et al.* 2004b, Linnakoski *et al.* 2012, De Beer & Wingfield 2013). The distinction between the two species is also supported by the ecology of these fungi, with *L. galeiforme* being associated with conifer-infesting bark beetles in Europe, and *L. pini* (as *G. radiaticola*) associated with pine-infesting bark beetles with a wider distribution (South Africa, Chile, Europe, China, Korea, and New Zealand; Linnakoski *et al.* 2012).

The *L. lundbergii* complex

The *L. lundbergii* complex was first defined by Jacobs *et al.* (2005). In a study emerging from a survey of ophiostomatoid fungi in Finland and Russia, Linnakoski *et al.* (2012) expanded the complex to include additional species that group close to *L. lundbergii*. Although these species always grouped close together, they never formed a well-supported monophyletic lineage, neither in the analyses of Linnakoski *et al.* (2012), various subsequent analyses (De Beer & Wingfield 2013, Jankowiak *et al.* 2017, 2018, Chang *et al.* 2017, Pan *et al.* 2020) nor those in the present study. However, for the sake of convenience, we have chosen to treat these species as a group. All the species produce relatively short conidiophores that have conidia with truncate bases, and the two sexually reproducing species produce cucullate ascospores (Linnakoski *et al.* 2012, De Beer & Wingfield 2013). Most of the species in this complex have been described from conifers in Asia and they have also been found in Europe, Canada, South Africa and New Zealand as the causal agents of sapstain in lumber (Linnakoski *et al.* 2012).

The *L. olivaceum* complex

The *L. olivaceum* complex accommodates species that are characterised by brownish synnematous asexual morphs and cucullate ascospores produced in ascomata with almost cylindrical necks and prominent ostiolar hyphae (Yin *et al.* 2019). The complex was first demarcated in a phylogeny by Six *et al.* (2011), more comprehensively defined by Linnakoski *et al.* (2012), and subsequently recognised by De Beer & Wingfield (2013) and Jankowiak *et al.* (2017, 2018). The complex includes *L. sagmatosporum*, the type species of the genus *Phialographium* (Upadhyay & Kendrick 1974), and its inclusion in the complex renders that name a synonym of *Leptographium* (De Beer & Wingfield 2013).

Most recently, Yin *et al.* (2019) added six new species to the complex. All species in this complex are associated with various bark beetles, mostly infesting spruce and pine trees in North America and Eurasia (Linnakoski *et al.* 2012, Jankowiak *et al.* 2017, 2018, Yin *et al.* 2019). The only exception is *L. francke-grosmanniae* that groups peripheral to the complex, has a morphology quite distinct from other species and was isolated from a bark beetle gallery on oak trees in Europe (Davidson 1971, Mouton *et al.* 1992, Yin *et al.* 2019). It is possible that this species represents a distinct species complex that cannot be distinguished at the present time.

The *L. piceiperdum* complex

Linnakoski *et al.* (2012) first defined this species complex when they showed that isolates described as *G. piceiperda* separated into five distinct species, two of which were unnamed. Ando *et al.* (2016) focused on isolates from different sources in Japan, revealing several additional cryptic species. Both Linnakoski *et al.* (2012) and Ando *et al.* (2016) concluded that epitypification is needed for *L. piceiperdum* and *L. europhioides* in order to confirm the placement of these species, because sequences for them were derived from herbarium type material. All members of this complex form typical leptographium-like asexual morphs, have cucullate ascospores (De Beer & Wingfield 2013, Ando *et al.* 2016), and have been found in association with conifer infesting bark beetles (mostly *Ips* species) in Europe, North America, Russia and Japan (Linnakoski *et al.* 2012, Ando *et al.* 2016).

The *L. procerum* complex

The *L. procerum* complex was first defined by De Beer & Wingfield (2013), and studied by Yin *et al.* (2015). These authors used seven gene regions to evaluate the species boundaries in the complex, and showed that it accommodates nine species. No sexual morph has been observed for any species in this complex, and asexual morphs can be described as leptographium-like (Jacobs *et al.* 2000b, 2006, Jacobs & Wingfield 2001, Lu *et al.* 2008, Paciura *et al.* 2010, De Beer & Wingfield 2013, Yin *et al.* 2015). Species in this complex are associated with conifer-infesting bark beetles in North America and Eurasia, with most described from East Asia. The exception is *L. profanum* that occurs on hardwood trees in the USA (Linnakoski *et al.* 2012, Yin *et al.* 2015). Most species in this complex are not widely distributed, with single species being found only in single countries. However, *L. procerum* has been isolated from *Pinus* spp. in China, Russia and the USA (Yin *et al.* 2015).

The *L. procerum* complex has received considerable attention by researchers. This is due to the fact that *L. procerum*, the type species of the complex has been associated with a root and root-collar disease of *Pinus* spp. in the USA known as white pine root decline (Kendrick 1962, Dochinger 1967, Wingfield 1983, Wingfield *et al*. 1994). Furthermore, *L. procerum* is associated with the red turpentine beetle (*Dendroctonus valens*), which is native to North America and possibly western Europe and was introduced into China resulting in devastating losses of Chinese native pines (Yan *et al.* 2005, Lu *et al.* 2008, Taerum *et al.* 2012, 2013, 2017, Zhou *et al.* 2013, Sun *et al.* 2013, Yin *et al.* 2015).

The *L. serpens* complex

The *L. serpens* species complex was first recognised based on phylogenetic analyses by Six *et al.* (2011). In a focused study to resolve typification issues in the complex, Duong *et al.* (2012) showed that *L. serpens*, previously recognised as a single taxon represented five distinct species. All of these species produce typical leptographium-like conidiophores, with characteristic serpentine hyphae on agar, while ascospores produced by two of the species are sheathed (Wingfield & Marasas 1980, Jacobs & Wingfield 2001, Duong *et al.* 2012). Interestingly, most of the members of the complex have relatively narrow distributions, most being known from only a single country. For example, *L. serpens* occurs in Italy, *L. gibbsii* in the UK, *L. yamaoake* in Japan and *L. castellanum* in Spain and the Dominican Republic. The exception here is *L. alacre* that is more widely distributed and associated with conifer-root infesting bark beetles in South Africa and Italy (Duong *et al.* 2012), although its occurrence in South Africa is certainly due to an accidental introduction likely from Europe. Marincowitz *et al.* (2017) described a morphologically similar species, *L. rhodanense* from Switzerland that groups between the *L. serpens* and the *L. wageneri* complexes.

The *L. wageneri* complex

Six *et al.* (2011) first defined the *L. wageneri* species complex based on phylogenetic analyses. All species in this complex form typical leptographium-like asexual morphs. However, the sexual morph has been observed only for *L. wageneri* var. *ponderosae*, and this was described as *G. wageneri* (Goheen & Cobb 1978, Zipfel *et al.* 2006). This fungus produces allantoid ascospores, but unlike other *Leptographium* ascospores, no sheath was reported (Goheen & Cobb 1978, Jacobs & Wingfield 2001). Most of the species in the complex are associated with conifer-root infesting beetles in the USA (Cobb *et al*. 1974, 1984, Hansen *et al*. 1988, Witcosky & Hansen 1985, Witcosky *et al*. 1986). The only exception is *L. reconditum,* which was isolated from the roots of *Triticum* species in South Africa (Jooste 1978).

The *L. wageneri* complex includes three host-specific varieties that are important pathogens of conifers restricted to the western USA and causing black stain root disease (Cobb 1988, Hessburg & Hansen 2000). These three formally described varieties can be distinguished from each other based on their morphological characteristics and the host tree species that they infect (Harrington & Cobb 1984, 1987, Jacobs & Wingfield 2001). *Leptographium wageneri* var. *pseudotsugae* occurs on Douglas fir (*Pseudotsuga menziesii*), *L. wageneri* var. *ponderosae* on hard pines (*Pinus ponderosa*, *P. jeffreyi* and *P. contorta*), and *L. wageneri* var. *wageneri* on pinyon pines (*P. monophylla* and *P. edulis*). Phylogenetic analyses in this study support the lineage defined as the *G. wageneri* complex by De Beer & Wingfield (2013) and Six *et al.* (2011).

Groups A & B

Leptographium pineti grouped singly in *Leptographium* and this is consistent with phylogenies emerging from other studies (Paciura *et al.* 2010, Six *et al.* 2011, Duong *et al.* 2012, De Beer & Wingfield 2013). Chang *et al.* (2017) described a new species from China, *L. ningerense* (not included in our data), which grouped with *L. pineti* in their datasets.

Grosmannia cainii formed a lineage distinct from others in *Leptographium* in our analyses (Fig. 5) and this was also seen in the phylogenies of De Beer & Wingfield (2013).

***New combinations*:**

1) *Leptographium cainii* (Olchow. & J. Reid) M. Procter & Z.W. de Beer, ***comb. nov.*** MycoBank MB 840389.
Basionym: *Ceratocystis cainii* Olchow. & J. Reid, Canad. J. Bot. 52: 1697. 1974. MycoBank MB 310486.
Synonyms: *Ophiostoma cainii* (Olchow. & J. Reid) T.C. Harr., Mycotaxon 28: 41. 1987. MycoBank MB 128912.
Grosmannia cainii (Olchow. & J. Reid) Zipfel, Z.W de Beer & M.J. Wingf., Stud. Mycol. 55: 89. 2006. MycoBank MB 500812.

Descriptions: Upadhyay (1981: 39, figs 43–47), Seifert & Okada (1993: 32, fig. 3D).

Phylogenetic data: Hausner *et al.* (2000), Masuya *et al.* (2004), Kim *et al.* (2005b), Six *et al.* (2011), Duong *et al.* (2012), De Beer & Wingfield (2013), Jankowiak *et al.* (2017, 2018), Liu *et al.* (2017), De Errasti *et al.* (2018), Chang *et al.* (2019).

Notes: *Leptographium cainii* groups alone and distinct from other species complexes in *Leptographium* in our data (Fig. 5). This is consistent with the data presented by De Beer & Wingfield (2013).

2) *Leptographium europhioides* (E.F. Wright & Cain) M. Procter & Z.W. de Beer, ***comb. nov*.** MycoBank MB 840392.
Basionym: *Ceratocystis europhioides* E.F. Wright & Cain, Canad. J. Bot. 39: 1222. 1961. MycoBank MB 327627.
Synonyms: *Ophiostoma europhioides* (E.F. Wright & Cain) H. Solheim, Nordic J. Bot. 6: 203. 1986. MycoBank MB 102979.
Grosmannia europhioides (E.F. Wright & Cain) Zipfel, Z.W. de Beer & M.J. Wingf., Stud. Mycol. 55: 90. 2006. MycoBank MB 500818.
Ceratocystis shikotsuensis Aoshima, Ph. D. thesis, University of Tokyo: 10. 1965. *nom. inval.,* Arts 29.1, 39.1 or 39.2.

Descriptions: Davidson *et al.* (1967: 929–930), Griffin (1968: 709, 713), Olchowecki & Reid (1974: 1699, pl. XIII, figs 259–261), De Hoog & Scheffer (1984: 295, fig. 2), Yamaoka *et al.* (1997: 1221–1222), Jacobs *et al.* (1998: 290–291), Jacobs *et al.* (2000a: 239).

Phylogenetic data: Hausner *et al.* (1993b, 2000), Okada *et al.* (1998), Schroeder *et al.* (2001), Masuya *et al.* (2004), Greif *et al.* (2006), Mullineux & Hausner (2009), Matsuda *et al.* (2010), Paciura *et al.* (2010), Six *et al.* (2011), Linnakoski *et al.* (2012), De Beer & Wingfield (2013), Musvuugwa *et al.* (2015), Ando *et al.* (2016), Yamaoka (2017), De Errasti *et al.* (2018).

Notes: *Leptographium europhiodes* groups in the *L. piceiperdum* complex (Fig. 5). De Beer & Wingfield (2013) noted that species such as *G. europhioides,* previously treated as synonyms of *G. piceiperda* based on morphology (Jacobs *et al.* 2000a, Jacobs & Wingfield 2001), were possibly distinct species (Linnakoski *et al.* 2012). Ando *et al.* (2016) investigated the phylogenetic relationships of Japanese isolates assigned to the *L. piceiperdum* complex and recognised 13 lineages within the complex. These included lineages representing *G. aenigmatica*, *G. laricis, G. piceiperda* group D and eight representing distinct, but undescribed species (Ando *et al.* 2016, Yamaoka 2017). Ando *et al.* (2016) concluded that although *L. piceiperdum* (as *G. piceiperda*) and *L. europhioides* (as *G. europhioides*) are valid species, epitypification is needed for both species to resolve the identity of the remaining undescribed taxa.

3) *Leptographium galeiforme* (B.K. Bakshi) M. Procter & Z.W. de Beer, ***comb. nov*.** MycoBank MB 840393.
Basionym: *Ceratocystis galeiformis* Bakshi, Mycol. Pap. 35: 13. 1951. MycoBank MB 294208.
Synonyms: *Ophiostoma galeiforme* (B.K. Bakshi) Math.-Käärik, Meddeland. Statens Skogs-Forstningsinst. 43: 47. 1953. MycoBank MB 302075 (as '*galeiformis*').
Grosmannia galeiformis (B.K. Bakshi) Zipfel, Z.W. de Beer & M.J. Wingf., Stud. Mycol. 55: 90. 2006. MycoBank MB 500820.

Descriptions: Mathiesen-Käärik (1953: 47–50), Hunt (1956: 33), Wingfield (1993: 48, fig. 8), Zhou *et al.* (2004b: 1309–1311, fig. 2).

Phylogenetic data: Hausner *et al.* (2000), Zhou *et al.* (2004b), Kim *et al.* (2005b, 2011), Thwaites *et al.* (2005), Greif *et al.* (2006), Zipfel *et al.* (2006), Lu *et al.* (2009), Mullineux & Hausner (2009), Harrington *et al.* (2010), Matsuda *et al.* (2010), Paciura *et al.* (2010), Six *et al.* (2011), Duong *et al.* (2012), Linnakoski *et al.* (2012), De Beer & Wingfield (2013), Taerum *et al.* (2013), Masuya *et al.* (2013), Huang & Chen (2014), Wang *et al.* (2014), Musvuugwa *et al.* (2015), De Beer *et al.* (2016a, b), Chang *et al.* (2017, 2019), Wingfield *et al.* (2017), Jankowiak *et al.* (2017), Liu *et al.* (2017), De Errasti *et al.* (2018).

Notes: This species grouped with *L. radiaticola* and undescribed species (Linnakoski *et al.* 2012, De Beer & Wingfield 2013) to form the *L. galeiforme* species complex (Fig. 5). In the phylogenies of Chang *et al.* (2019), *L. koraiensis* grouped within this species complex. The latter species was not included in our analyses.

4) *Leptographium pseudoeurophioides* (Olchow. & J. Reid) M. Procter & Z.W. de Beer, ***comb. nov*.** MycoBank MB 840413.
Basionym: *Ceratocystis pseudoeurophioides* Olchow. & J. Reid, Canad. J. Bot. 52: 1700. 1974. MycoBank MB 310514.
Synonyms: *Ophiostoma pseudoeurophioides* (Olchow. & J. Reid) Hausner *et al.*, Canad. J. Bot. 71: 1264. 1993. MycoBank MB 362667.
Grosmannia pseudoeurophioides (Olchow. & J. Reid) Zipfel *et al.*, Stud. Mycol. 55: 91. 2006. MycoBank MB 500826.

Descriptions: Olchowecki & Reid (1974: 1700, figs 219–229).

Phylogenetic data: Hausner *et al.* (1993b, 2000), Masuya *et al.* (2004), Mullineux & Hausner (2009), Mullineux *et al.* (2011), De Beer & Wingfield (2013), Musvuugwa *et al.* (2015), De Errasti *et al.* (2018).

Notes: *Leptographium pseudoeurophioides* was assigned to the *G. penicillata* complex (Hausner *et al.* 1993b, 2000). However, based on a short LSU sequence produced by Hausner *et al.* (1993b, 2000) and ascospore morphology, De Beer & Wingfield (2013) suggested that *L. pseudoeurophioides* should form part of the *L. piceiperdum* complex, and that additional collections and fresh material would be required to confirm its placement. For the present, we treat this species in *Leptographium.*

5) *Leptographium radiaticola* (J.J. Kim *et al.*) M. Procter & Z.W. de Beer **comb. nov.** [MycoBank MB 840396]
Basionym: *Ophiostoma radiaticola* J.J. Kim *et al.*, Mycotaxon 91: 486. 2005. MycoBank MB 500832.
Synonyms: *Grosmannia radiaticola* (J.J. Kim *et al.*) Z.W. de Beer & M.J. Wingf., Stud. Mycol. 55: 91. 2006. MycoBank MB 500827.
Hyalopesotum pini L.J. Hutchison & J. Reid, New Zealand J. Bot. 26: 90. 1988. MycoBank MB 135442.
= *Pesotum pini* (L.J. Hutchison & J. Reid) G. Okada & Seifert, Canad. J. Bot. 76: 1504. 1998. MycoBank MB 446360.

Descriptions: Hutchison & Reid (1988b: 90–91, figs 32–35, of *Hy. pini*), Kim *et al.* (2005b: 486–489, figs 1–14).

Phylogenetic data: Masuya *et al.* (2004), Kim *et al.* (2005a, b), Thwaites *et al.* (2005), Zipfel *et al.* (2006), Lu *et al.* (2009), Mullineux & Hausner (2009), Paciura *et al.* (2010), Six *et al.* (2011), Duong *et al.* (2012), Linnakoski *et al.* (2012), De Beer & Wingfield (2013), Taerum *et al.* (2013), Huang & Chen (2014), Wang *et al.* (2014), Romón *et al.* (2014a), Musvuuwga *et al.* (2015), Chang *et al.* (2017, 2019), Liu *et al.* (2017), De Errasti *et al.* (2018).

Notes: This species grouped in the *L. galeiforme* species complex (Fig. 5; Linnakoski *et al.* 2012, De Beer & Wingfield 2013). *Pesotum pini* has been recognised as the asexual morph of *L. radiaticola* (Kim

et al. 2005b). Following the One Fungus-One Name principles, the oldest name, irrespective of morph, should take precedence in the selection of the basionym. In this case, *Hyalopesotum pini* would serve that purpose. However, to avoid confusion with the name *O. pini*, currently treated as a synonym of *O. minus,* but possibly a distinct taxon (De Beer & Wingfield, 2013), we have designated *O. radiaticola* as basionym.

Other species: Listed in Table 1.

Leptographium and *Grosmannia incertae sedis* (Lineages III & VI)

Leptographium piriforme **(Lineage III)**

De Beer & Wingfield (2013) applied a relatively wide taxonomic concept for *Leptographium s.l.* and their phylogenies placed *L. piriforme* in a distinct lineage with *G. crassivaginata.* The data in the present study did not include *G. crassivaginata.* Greif *et al.* (2006) noted some morphological similarities between *L. piriforme* and *G. crassivaginata* when they described *L. piriforme*. Consequently, *G. crassivaginata* may form part of Lineage III if it were included in analyses.

Leptographium piriforme produces curved conidia and pear-shaped cells, distinguishing it from other *Leptographium* species (Greif *et al.* 2006, Jankowiak & Kolařik 2010). In the concatenated dataset utilised in the present study, *L. piriforme* grouped basal to Lineage I and II (Fig. 5). Although the phylogeny presented by Greif *et al.* (2006) was much smaller than that presented here, *L. piriforme* also grouped outside of the lineage containing *Leptographium* and *Grosmannia.* For the present, we have retained *L. piriforme* in *Leptographium* although its taxonomic placement clearly deserves further consideration.

Leptographium verrucosum **(Lineage VI)**

Gebhardt *et al.* (2002) was the first to describe *L. verrucosum* (as *O. verrucosum*) and their description was based solely on morphology. De Beer & Wingfield (2013) transferred *O. verrucosum* to *Leptographium* based on LSU sequences, and their recommendation was that new species grouping with either *Leptographium* or *Grosmannia* should be described in *Leptographium*. In our LSU dataset (Fig. S1), *L. verrucosum* grouped basal to Lineage I (*Leptographium s.s.*), but this grouping was not seen in the other gene trees. For the present and until additional material is available for further analyses, we have chosen to retain it in *Leptographium*.

Masuyamyces (Lineage XVII)

Masuyamyces Z.W. de Beer & M. Procter, ***gen. nov.*** MycoBank MB 840414. Fig. 12A, B.

Etymology: Named for Dr Hayato Masuya, a Japanese mycologist who has described 17 species of ophiostomatoid fungi, including the type species of this novel genus.

Sexual morph: *Ascomatal bases* black, subglobose to globose; necks black, nearly cylindrical, curved or straight. *Ostiolar hyphae* absent or present. *Asci* evanescent, clavate to sub-globose when young. *Ascospores* hyaline, 1-celled, oblong or cylindrical in front view, allantoid in side view, globose in end view, enclosed in uniform hyaline sheath.

Asexual morph: *Conidiophores* macronematous, mononematous to synnematous. Hyalorhinocladiella-like; *conidiophores* simple or branched, hyaline; *conidiogenous cells* annellidic, cylindrical; *conidia* hyaline, obovoid to globose, oblong to ellipsoidal, 1-celled. Pesotum-like; *conidiophores* loosely compacted, stipes hyaline to pale brown; *conidiogenous cells* hyaline annellidic; *conidia* hyaline, oblong to ellipsoidal.

Type species: ***Masuyamyces botuliformis*** (Masuya) Z.W. de Beer & M. Procter, ***comb. nov.*** MycoBank MB 840415.
Basionym: *Ophiostoma botuliforme* Masuya, Mycoscience 44: 304. 2003. MycoBank MB 489292.

Description: Masuya *et al.* (2003: 304, figs 11–21).

Phylogenetic data: Fig. 5.

Notes on the type species: No DNA sequence data were previously available for this species (De Beer & Wingfield 2013). Although *M. botuliformis* resembles *O. allantosporum* morphologically (Masuya *et al.* 2003), it did not group with the latter species, which groups in *Ophiostoma* (Fig. 5). Recently, sequences of *M. botuliformis* (as *O. botuliforme*) have been deposited in GenBank, which are identical to our ITS and LSU sequences. See note under *M. saponiodorus*.

Notes on the genus: In our phylogenies, Lineage XVII consistently formed a monophyletic group, distinct from *Ophiostoma*. This group includes *O. ambrosium*, *O. botuliforme*, *O. pallidulum* (not included in our analyses) and *O. saponiodorum*. All described from conifers and all having reniform ascospores (Fig. 3F; Type A as categorised by De Beer & Wingfield 2013). Although *O. pallidulum* was not included in our analyses, it grouped with *O. saponiodorum* in the phylogenies of Linnakoski *et al.* (2010) and De Beer & Wingfield (2013).

The isolate of *O. ambrosium* included in our analyses is not the ex-type culture but was designated as an "isolate from type collection" by Hausner *et al.* (1993b). Our LSU sequence is almost identical to that of Hausner *et al*. (1993b), although theirs is very short. However, the morphology of this isolate does not match that of the type of *O. ambrosium*, and although this isolate is from the type collection, it may represent a different species.

Our isolate of *O. saponiodorum* was also not the ex-type isolate for the species, but our ITS sequence is identical to the one produced by Linnakoski *et al.* (2010). The latter species grouped with isolate CMW 30883 and was used in the cross to produce the holotype of the species. Therefore, although two species in this clade are not represented by ex-type isolates, we have sufficient confidence in the sequences to justify describing this lineage as a new genus.

Masuyamyces ambrosius was described from *Betula albae* infested by the beetle *Trypodendron domesticum* in Great Britain (Bakshi 1950). *Masuyamyces botuliformis* was isolated from *Pinus densiflora* in Japan (Masuya *et al.* 2003), *M. pallidulus was* from *P. sylvestris* infested by *Hylastes brunneus* in Finland (Linnakoski *et al.* 2010), and *M. saponiodorus* was from *Picea abies* infested with *Ips typographus* and *Pityogenes chalcographus* in Russia as well as Finland (Linnakoski *et al.* 2010). The asexual morph of *M. botuliformis* was described as pesotum-like (Masuya *et al.* 2003), that of *M. ambrosium* as raffaelea-like (De Beer & Wingfield 2013), that of *M. pallidulus* as hyalorhinocladiella-like, and that of *M. saponiodorus* as pesotum-like with a hyalorhinocladiella-like synasexual morph (Linnakoski *et al.* 2010).

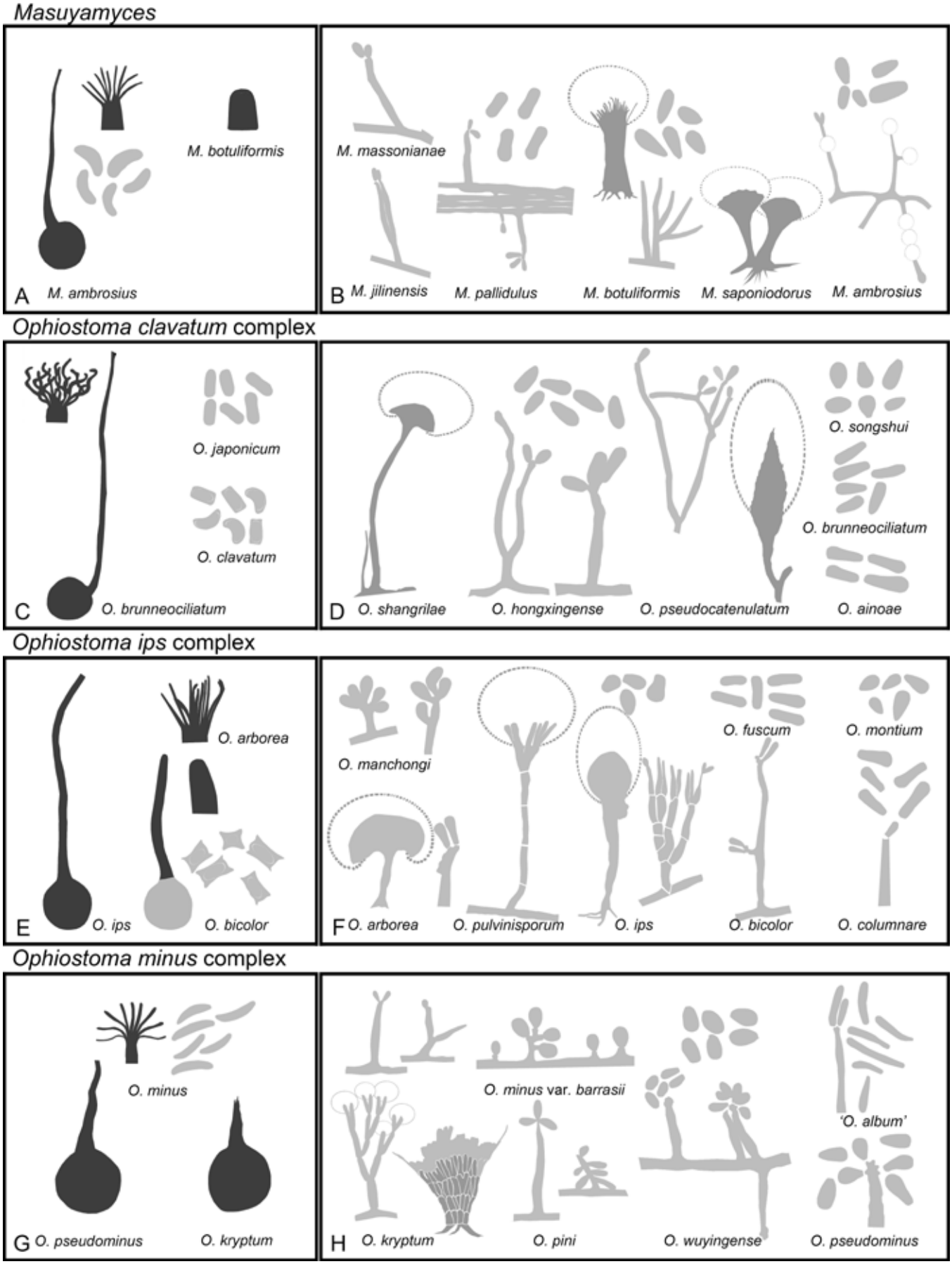

Fig. 12. Genera of the *Ophiostomatales* redrawn from published images with sexual morphs (if known) on the left and asexual morphs on the right. **A, B.** *Masuyamyces*. **C, D.** *Ophiostoma clavatum* complex. **E, F.** *Ophiostoma ips* complex. **G, H.** *Ophiostoma minus* complex. (Pale grey shading reflects hyaline to subhyaline colouration, medium-tone grey brown to dark brown and dark grey reflects fuscous black to dark black colouration).

***Other new combinations*:**

1) *Masuyamyces acarorum* (R. Chang & Z.W. de Beer) M. Procter & Z.W. de Beer, ***comb. nov.*** MycoBank MB 840416.
Basionym: *Ophiostoma acarorum* R. Chang & Z.W. de Beer, MycoKeys 28: 40. 2017. MycoBank MB 823693.

Description: Chang *et al.* (2017: 40–41, fig. 7).

Phylogenetic data: Chang *et al.* (2017, 2019).

Notes: Sexual morph unknown. This species resides in *Masuyamyces* and grouped with *M. saponiodorus* (as *O. saponiodorum*) in the phylogenies of Chang *et al.* (2017, 2019). See note under *M. saponiodorus*.

2) *Masuyamyces ambrosius* (B.K. Bakshi) M. Procter & Z.W. de Beer, ***comb. nov.*** MycoBank MB 840526.
Basionym: *Ceratocystis ambrosia* B.K. Bakshi, Trans. Brit. Myc. Soc. 33: 116. 1950. MycoBank MB 294192.
Synonym: *Ophiostoma ambrosium* (B.K. Bakshi) Georg Hausner, J. Reid & Klassen, Canad. J. Bot. 71: 1264. 1993. MycoBank MB 362662.

Description: Bakshi (1950: 116–118, fig. 2)

Notes: Sexual morph unknown.This species grouped with *M. saponiodorus* and *M. botuliformis* (Fig. 5).

3) *Masuyamyces jilinensis* (R. Chang *et al*.) M. Procter & Z.W. de Beer, ***comb. nov.*** MycoBank MB 840417.
Basionym: *Ophiostoma jilinense* R. Chang *et al*., MycoKeys 28: 63. 2019. MycoBank MB 825086.

Description: Chang *et al.* (2019: 63–65, fig. 16).

Phylogenetic data: Chang *et al.* (2019).

Notes: Sexual morph unknown. This species grouped with *M. saponiodorus* (as *O. saponiodorum*) in the phylogeny of Chang *et al.* (2019), and is consequently included in the the genus. See note under *M. saponiodorus*.

4) *Masuyamyces lotiformis* (Z. Wang & Q. Lu) M. Procter & Z.W. de Beer, ***comb. nov.*** MycoBank MB 840418.
Basionym: *Ophiostoma lotiforme* Z. Wang & Q. Lu, IMA Fungus 11: 17. 2020. MycoBank MB 830612.

Description: Wang *et al.* (2020: 17–18, fig. 14)

Phylogenetic data: Wang *et al.* (2020).

Notes: Sexual morph unknown. This species grouped with *M. saponiodorus* (as *O. saponiodorum*) in the phylogeny of Wang *et al.* (2020), and is consequently included in the genus. See note under *M. saponiodorus*.

5) *Masuyamyces massonianae* M. Procter & Z.W. de Beer, ***sp. nov.*** MycoBank MB 840419.
Synonym: *Ophiostoma massonianae* H.M. Wang & Q. Lu, MycoKeys 39: 15. 2018. *nom. inval.*, Art. 40.7. MycoBank MB 827856.

Description: Wang *et al.* (2018: 15–17, fig. 4).

Holotype: PREM 63310.

Phylogenetic data: Wang *et al.* (2018)

Notes: Sexual morph unknown. This species grouped with *M. saponiodorus* (as *O. saponiodorum*) in the phylogenies of Wang *et al.* (2018), and is thus included in the genus. See note under *M. saponiodorus*.

6) *Masuyamyces pallidulus* (Linnak. *et al*.) M. Procter & Z.W. de Beer, ***comb. nov.*** MycoBank MB 840420.
Basionym: *Ophiostoma pallidulum* Linnak. *et al*., Persoonia 25: 86. 2010. MycoBank MB 518884.

Description: Linnakoski *et al.* (2010: 86, 88, fig. 9).

Phylogenetic data: Linnakoski *et al.* (2010, 2016), De Beer & Wingfield (2013), De Beer *et al.* (2016a, b), Chang *et al.* (2017, 2019), Wang *et al.* (2018).

Notes: Sexual morph unknown. Although not included in our analyses, this species was shown to consistently group with *M. saponiodorus* (as *O. saponiodorum*) and is thus treated in *Masuyamyces* (Linnakoski *et al.* 2010, 2016, De Beer & Wingfield 2013, Chang *et al.* 2017, 2019, Wang *et al.* 2018). See note under *M. saponiodorus*.

7) *Masuyamyces saponiodorus* (Linnak. *et al*.) M. Procter & Z.W. de Beer, ***comb. nov.*** MycoBank MB 840421.
Basionym: *Ophiostoma saponiodorum* Linnak. *et al*., Persoonia 25: 88. 2010. MycoBank MB 518885.

Description: Linnakoski *et al.* (2010: 88, fig. 10).

Phylogenetic data: Linnakoski *et al.* (2010, 2016), Six *et al.* (2011), De Beer & Wingfield (2013), Romón *et al.* (2014b), Chang *et al.* (2017, 2019), Wang *et al.* (2018).

Notes: *Masuyamyces saponiodorus* consistently grouped separately from what we have defined as *Ophiostoma* in our phylogenies (Fig. 5, S1–S4), and with the other species listed above in previously published phylogenies (Linnakoski *et al.* 2010, 2016, De Beer & Wingfield 2013, Chang *et al.* 2017, 2019, Wang *et al.* 2018).

Ophiostoma (Lineage XV)

Ophiostoma Syd. & P. Syd., Ann. Mycol. 17: 43. 1919. MycoBank MB 3614, ***emend.*** Z.W. de Beer & M. Procter. Figs 12C–13F.
Synonyms: *Linostoma* Höhn., Ann. Mycol. 16: 91. 1918. MycoBank MB 2885. *nom. illegit.* Art. 53.1, De Beer *et al.* 2013a. [Type species *Linostoma piliferum* (Fr.) Höhn.].
Pesotum J.L. Crane & Schokn., Amer. J. Bot. 60: 347. 1973. MycoBank MB 9270. [Type species *Pesotum ulmi* (M.B. Schwarz) J.L. Crane & Schokn.].
Hyalopesotum H.P. Upadhyay & W.B. Kendr., Mycologia 67: 801. 1975. MycoBank MB 8579. (Type species *H. introcitrinum* H.P. Upadhyay & W.B. Kendr.).
Pachnodium H.P. Upadhyay & W.B. Kendr., Mycologia 67: 802. 1975. Asexual synonym: MycoBank MB 9189 (Type species *P. canum* H.P. Upadhyay & W.B. Kendr.).

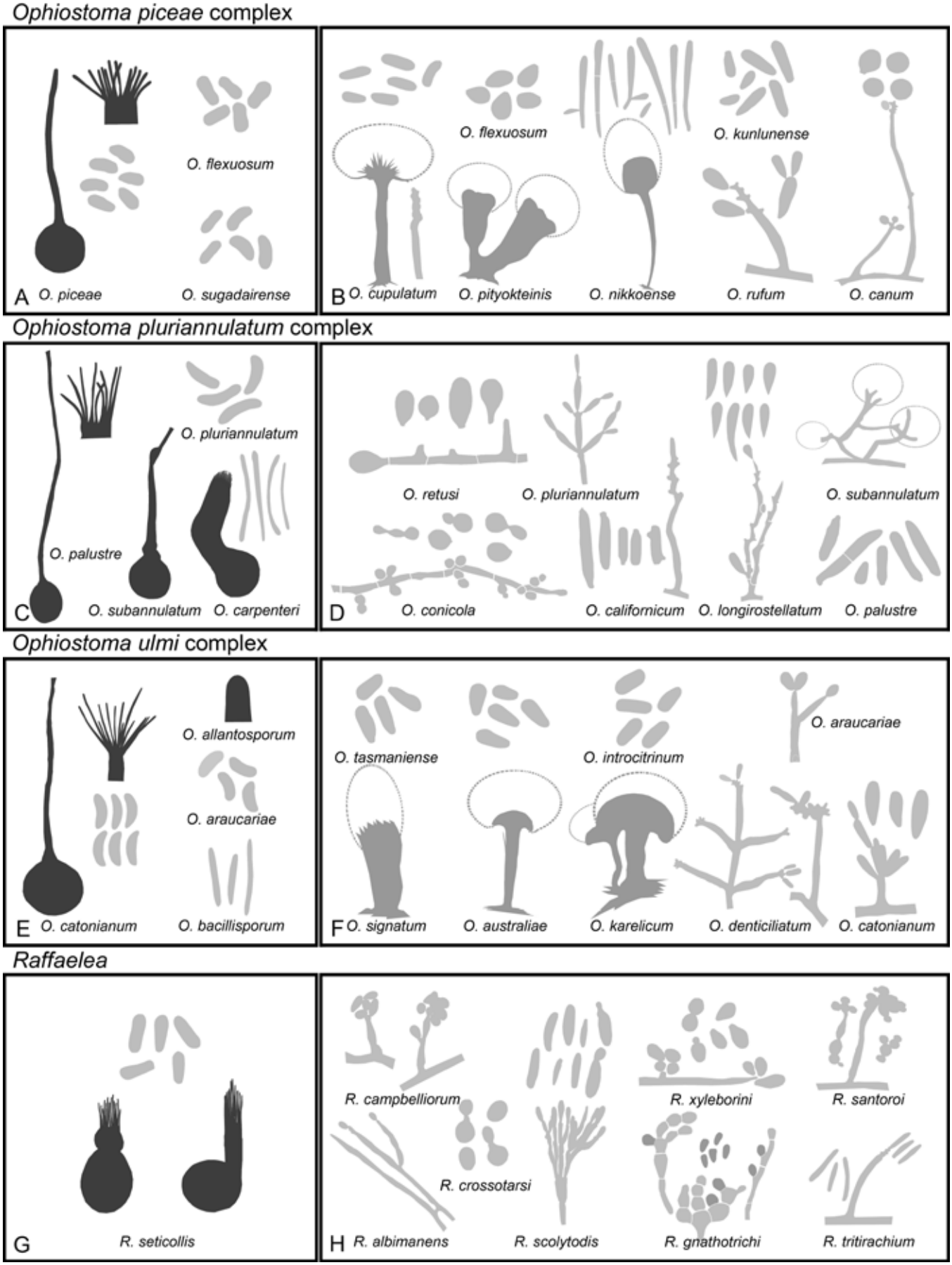

Fig. 13. Genera of the *Ophiostomatales* redrawn from published images with sexual morphs (if known) on the left and asexual morphs on the right. **A, B.** *Ophiostoma piceae* complex. **C, D.** *Ophiostoma pluriannulatum* complex. **E, F.** *Ophiostoma ulmi* complex. **G, H.** *Raffaelea*. (Pale grey shading reflects hyaline to subhyaline colouration, medium-tone grey brown to dark brown and dark grey reflects fuscous black to dark black colouration).

Etymology: *Ophio-* from the Greek for 'snake-like' and '*stoma'* meaning mouth, referring to the long, tubular necks of the ascomata.

Sexual morph: *Ascomatal bases* black, subglobose to globose; necks black, cylindrical, straight or slightly curved. *Ostiolar hyphae* absent or present, divergent. *Asci* evanescent, clavate. *Ascospores* hyaline, 1-celled, enclosed in sheath, allantoid, reniform, cylindrical to ossiform in side view, ellipsoid in face view, globose in end view.

Asexual morph: *Conidiophores* macronematous, micronematous, mononematous, synnematous. Hyalorhinocladiella-like; *conidiophores* simple or branched; *conidia* hyaline, 1-celled, oblong to ellipsoid. Leptographium-like; *conidiophores* upright or prone, bases simple or rhizoid-like; *conidiogenous cells* hyaline, subcylindrical; *conidia* hyaline, 1-celled, oblong to obovoid with truncate base. Pesotum-like; *conidiophores* single or in groups, black becoming paler towards apex; stipes extending beyond conidiogenous cells, becoming seta-like structures (*O. cupulatum*); *conidia* hyaline, mostly 1-celled, oblong to ellipsoid, round apex, tapering towards base, clavate to obovoid; *conidia* elongated cylindrical or clavate with tapering towards base, 1–3-celled (*O. nikkonse*), giving rise to secondary conidia (*O. nikkoense*). Sporothrix-like; *conidiogenous cells* proliferating, sympodial, denticulate; *conidia* hyaline, 1-celled, oblong to ellipsoid, elongate or broadly cylindrical, round apex, tapering towards base, clavate or obovoid, obpyriform, giving rise to secondary spores (*O. cupulatum, O. flexuosum*).

Type species: *Ophiostoma piliferum* (Fr.) Syd. & P. Syd., Ann. Mycol. 17: 43. 1919. MycoBank MB 431882.

Other species: Listed in Table 1.

Notes on the genus: The definition of *Ophiostoma* emerging from this study relates to what was previously treated as *Ophiostoma s.l.* by De Beer & Wingfield (2013). In this case it excludes the *S. schenckii-O. stenoceras* complex (now *Sporothrix*) and the *O. tenellum* complex. Species in the newly defined *Ophiostoma sensu stricto* typically produce Type A or B ascospores (Fig. 3F, G; as categorised by De Beer & Wingfield 2013) and a variety of asexual morphs including those that are sporothrix-like, pesotum-like, hyalorhinocladiella-like; some having more than one morph and commonly a continuum between these morphs (De Beer & Wingfield 2013).

***Species complexes*:**

The *O. clavatum* complex

The *O. clavatum* complex was defined by Linnakoski *et al.* (2016). Species in this complex generally have rectangular to cylindrical shaped ascospores (Fig. 3F; Type A as categorised by De Beer & Wingfield 2013), spirally coiled ostiolar hyphae that are brown in colour and they produce pesotum-like asexual morphs (Mathiesen-Käärik 1960, Linnakoski *et al.* 2016). These fungi are found in Eurasia and are mostly associated with conifer-infesting bark beetles residing in the genus *Ips* and some species cause blue stain in the sapwood of trees (Linnakoski *et al.* 2016).

Ophiostoma ainoae and *O. tapionis* grouped peripherally to other species in the *O. clavatum* complex in the datasets of Linnakoski *et al.* (2016). *Ophiostoma ainoae* has ascospores similar in shape to species in the *O. ips* complex, but groups within the *O. clavatum* complex (Linnakoski *et al.* 2016). *Ophiostoma ainoae* also has a hyphal morphology similar to that of *O. clavatum* but it grouped peripheral to that complex (Linnakoski *et al.* 2016). Due to its morphological similarity with other species in the complex, *O. ainoae* is best treated as part of the *O. clavatum* species complex. This grouping was also supported in our analyses (Fig. 5).

The *O. ips* complex

The *O. ips* complex was first defined by De Beer & Wingfield (2013). Species in the complex all have cylindrical ascospores in a pillow-shaped sheath (Fig. 3H; Type E as categorised by De Beer & Wingfield 2013) and this distinguishes them from other species in *Ophiostoma.* These species form pesotum- to hyalorhinocladiella-like asexual morphs (De Beer & Wingfield 2013). Members of this complex are associated with bark beetles in the genera *Ips* and *Dendroctonus*, infesting conifers mostly in North America and areas where pine trees have been introduced (Upadhyay 1981, Zhou *et al.* 2004a, Linnakoski *et al.* 2010).

The ex-type isolate of the asexual species *Hyalorhinocladiella ips* (CMW 14175) grouped in our analyses within the *O. ips* complex, similar to the results of De Beer & Wingfield (2013). *Hyalorhinocladiella ips* was originally described as *Tuberculariella ips* (Leach *et al.* 1934), later treated in *Ambrosiella* (Batra 1967) and most recently in *Hyalorhinocladiella* (Harrington *et al.* 2010). This fungus has been suggested to represent the asexual morph of *O. montium*, because the two species share morphological similarities and there are minimal differences in their sequence data (Massoumi Alamouti *et al.* 2009, De Beer & Wingfield 2013, De Beer *et al.* 2013b). In our analyses (Fig. 5) *O. montium* and *"H. ips*" grouped very close to each other. De Beer *et al.* (2013b) formally listed *H. ips* as synonym of *O. montium* (Rumbold 1941), even though *H. ips* is the older of the two names (Leach *et al.* 1934) and should thus be designated as basionym for the species. However, the epithet "*ips*" is already in use for *O. ips*, the name bearing species of this complex, that has *Ceratostomella ips* (Rumbold 1931) as basionym. To avoid the creation of a later homonym by using *H. ips* as basionym, we have chosen to select *Ceratostomella montium* (Rumbold 1941) as basionym for the species and for which *O. montium* (Von Arx 1952) is then the appropriate current name. The *O. ips* complex formed a well-supported lineage that might be excluded from *Ophiostoma s.s.* in future to be treated as a distinct genus. However, for the present and in the absence of more robust datasets, we have retained species in this complex in *Ophiostoma s.s.*

The *O. minus* complex

The *O. minus* complex was well supported in our phylogenies even though this was not true in the phylogenies of De Beer & Wingfield (2013). The *O. minus* complex was first defined by Jacobs & Kirisits (2003). Species in this complex produce hyalorhinocladiella-like asexual morphs (Fig. 3A; as categorised by De Beer & Wingfield 2013) and have been isolated from conifers in North America and Europe. *Ophiostoma minus* is a well-known causal agent of blue stain in conifers. It is associated with the southern pine beetle (*Dendroctonus frontalis*), a native but invasive pest in the USA (Jacobs & Kirisits 2003, Gorton *et al.* 2004).

It must be noted that our phylogenies included isolates of only the North American form of *O. minus* and *O. pseudominus*, both available in the CMW collection. This was due to the fact that there were no available cultures of other species included in the complex by previous authors (Jacobs & Kirisits 2003, Gorton *et al.* 2004, Linnakoski *et al.* 2010, De Beer & Wingfield 2013).

The *O. piceae* complex

Harrington *et al.* (2001) first defined the *O. piceae* complex, but the complex was not applied by De Beer & Wingfield (2013). Because the complex did not have any phylogenetic support in their trees, De Beer and Wingfield (2013) treated the species in the complex as part of *Ophiostoma s.s.* Yin *et al.* (2016) redefined the *O. piceae* complex, including the discripiton of three new species described from spruce-infesting bark beetles in China. The two sub-clades seen to be formed by the *O. piceae* complex (Harrington *et al.* 2001) are now known as the *O. ulmi* complex and the *O. piceae* complex. The *O. ulmi* complex includes what was previously referred to as the 'hardwood clade', and the newly redefined *O. piceae* complex includes what was previously referred to as the 'conifer clade' (Harrington *et al.* 2001, Grobbelaar *et al.* 2010, 2011, Kamgan Nkuekam *et al.* 2011, De Beer & Wingfield 2013, Yin *et al.* 2016). Species in this complex form ascomata with long necks of up to 500 µm and can form either sporothrix- or pesotum-like asexual morphs, or both, while some form hyalorhinocladiella-like asexual morphs (Fig. 3A, C, E; as categorised by De Beer & Wingfield 2013). Members of this complex have been isolated from conifers mostly in the Northern Hemisphere, and one species (*O. cupulatum*) was described from New Zealand (Yin *et al.* 2016). In our phylogenies, the *O. piceae* complex grouped distinct from the *O. ulmi* complex.

The *O. pluriannulatum* complex

The *O. pluriannulatum* complex was initially defined as the *O. multiannulatum* complex (Villarreal *et al.* 2005) and later renamed to the *O. pluriannulatum* complex (Kamgan Nkuekam *et al.* 2008, Zanzot *et al.* 2010, De Beer & Wingfield 2013). Ascospores of species in the complex are allantoid (Fig. 3F; Type A in De Beer & Wingfield 2013) (Hunt 1956, Kamgan Nkuekam *et al.* 2008, Zanzot *et al.* 2010, De Beer & Wingfield 2013). This is with the exception of *O. carpenteri* that has Type B (Fig. 3G) narrowly clavate ascospores (Hausner *et al.* 2003, De Beer & Wingfield 2013). Other than *O. carpenteri*, all members of the *O. pluriannulatum* complex have very long ascomatal necks relative to other *Ophiostoma* species (Zanzot *et al.* 2010, De Beer & Wingfield, 2013). *Ophiostoma carpenteri* has very short necks but does produce a sporothrix-like asexual morph as in all other members of the complex (Hausner *et al.* 2003, De Beer & Wingfield 2013). Species in this complex have been found in Eurasia, North America and Africa on conifers and hardwoods, and some associated with bark beetles in the genera *Ips* and *Dendroctonus* (Zhou *et al.* 2004a, Linnakoski *et al.* 2010, Pacuira *et al.* 2010). This complex may represent a discrete genus, but our analyses were not sufficiently robust to support such a distinction.

The *O. ulmi* complex

The *O. ulmi* complex was first known as the 'hardwood clade' in the *O. piceae* complex (Harrington *et al.* 2001, Linnakoski *et al.* 2010). It was later referred to as the *O. quercus* complex (Kamgan Nkuekam *et al.* 2011), until De Beer & Wingfield (2013) defined it as the *O. ulmi* species complex. Most of the members of the complex produce allantoid ascospores (Fig. 3F; Type A) that lack sheaths (Hunt 1956, Brasier 1991, De Beer & Wingfield, 2013). Species in this complex occur in Eurasia, Australia, Africa and North and South America and are associated with a variety of bark beetles (Upadhyay 1981, Brasier 1991, Brasier & Mehrotra 1995, Villarreal *et al.* 2005, Harrington *et al.* 2001, Kamgan Nkuekam *et al.* 2010, 2011, Linnakoski *et al.* 2008, 2009, Grobbelaar *et al.* 2010, Paciura *et al.* 2010). De Beer & Wingfield (2013) chose to have *O. ulmi* as the name bearing species for this complex, justified because it is the best-known species in this complex, as one of the causal agents of Dutch Elm Disease (DED). *Ophiostoma novo-ulmi* and *O. himal-ulmi* are also causal agents of DED (Brasier 1991, Harrington *et al.* 2001). DED is one of the most catastrophic tree disease pandemics in the Northern Hemisphere, leading to the death of large populations of Elm trees (Brasier 1979, 1991, Gibbs 1978). Another species in this complex, *O. quercus,* is associated with substantial economic losses due to sapstain in *Quercus* spp. (Harrington *et al.* 2001).

Ophiostoma bacillisporum, *O. torulosum* and *O. undulatum* have asexual morphs that are different in morphology to other members of the *O. ulmi* complex. Their asexual morphs are mycelial while other members of the complex form sporothrix- and pesotum-like asexual morphs. The ascospores of the species are, however, similar to those in the *O. ulmi* complex (De Beer & Wingfield, 2013). We have supported the decision of De Beer & Wingfield (2013) to include species residing in what was known as the *O. quercus* complex (Kamgan Nkuekam *et al*. 2011) in the *O. ulmi* complex. This decision is justified based on the fact that *O. quercus* groups within the *O. ulmi* complex. However, our analyses grouped *O. torulosum* outside the *O. piceae* complex (Fig. 5) and its position requires further consideration.

Group H

De Beer & Wingfield (2013) included *O. triangulosporium* in the *O. ulmi* complex but noted that its unique ascospore morphology (allantoid ascospores with triangular sheaths) suggested that its placement in the complex required further study, including inspection of the type material and a greater number of isolates. In our analyses (Fig. 5), *O. triangulosporium* grouped peripheral to other species in the *O. ulmi* complex.

Group I

Ophiostoma macrosporum and an undescribed *Ophiostoma* species (previously treated as a *Hyalorhinocladiella* sp.) formed a small lineage outside of any of the species complexes in *Ophiostoma*.

Group J

The type species of *Ophiostoma*, *O. piliferum*, grouped on its own within *Ophiostoma*. Although it is the type of the genus, it does not group in any species complex (De Beer & Wingfield 2013, Yin *et al.* 2016, De Beer *et al.* 2016a, b).

Group K

Ophiostoma tetropii grouped peripheral to the *O. minus* and *O. piceae* complexes (Fig. 5). Linnakoski *et al.* (2010) included *O. tetropii* in the *O. minus* complex. However, the ascospores of *O. tetropii* have a distinct morphology different to species in the *O. minus* complex (De Beer & Wingfield 2013). The phylogenies of De Beer & Wingfield (2013) also showed that *O. tetropii* grouping separately from the *O. minus* complex and it clearly requires further study.

Ophiostoma incertae sedis (Lineages XVIII, XX & XXIII)

***Ophiostoma valdivianum* (Lineage XVIII)**

As mentioned above, *O. valdivianum* formed a lineage with *S. fumea* in the phylogenies of De Beer *et al.* (2016a), grouping basal to most of *Sporothrix*. However, in the phylogenies arising from the present study, these two species did not group together.

***Ophiostoma angusticollis* and *O. denticulatum* (Lineage XX)**

Ophiostoma angusticollis and *O. denticulatum* consistently formed a lineage distinct from *Ophiostoma*. In the phylogenies of De Beer & Wingfield (2013), *O. angusticollis* formed a lineage with *O. sejunctum* (not included in the present study) close to the *O. tenellum* complex (Lineage XIII) but distinct from *Ophiostoma*. We have chosen not to describe this lineage as a new genus because we were not able to include the holotype of *O. angusticollis*.

***Ophiostoma noisomeae* (Lineage XXIII)**

Ophiostoma noisomeae consistently grouped distinct from *Ophiostoma* in our datasets. In the phylogenies of De Beer *et al.* (2016a), *O. noisomeae* also grouped distinct from *Ophiostoma*.

Paleoambrosia (No sequence data available)

Paleoambrosia Poinar & F.E. Vega, Fungal Biol. 122: 1160. 2018. MycoBank MB 840457. *nom. inval.*, Art. F.5.1.

Etymology: 'From the Greek "palaios" = ancient, and the Greek "ambrosia" = immortal, referring to the fossilized ambrosial fungus discovered with a Platypodine beetle in ~100 million-year-old amber in Myanmar' (Poinar & Vega 2018).

Sexual morph: Unknown.

Asexual morph: *Conidiophores* borne in sporodochia, simple, black. *Conidia* black, 1-celled, globose to obovoid, borne in slimy droplet terminally. Yeast-like cells present in mycangium.

Type species: *Paleoambrosia entomophila* Poinar & F.E. Vega, Fungal Biol. 122(12): 1160 (2018). MycoBank MB 840458. *nom. inval.*, Art. F.5.1.

No other species known at present.

Notes: This genus was recently described from a specimen found in amber and was included in the current study for completeness, despite the fact that its placement in the *Ophiostomatales* (Poinar & Vega 2018) is open to debate. The fossil beetle associated with this fungus could have been misidentified and might not be a member of the Platipodinae. Likewise, whether the cavity shown on the beetle reflects a functional mycangium is unclear. The growth form of the fungus growing alongside the beetle is unusual for any beetle-related ophiostomatalean fungus, and mucilage-bound phialidic spores could be those of an asexual morph of an entomopathogenic or another fungus producing phialidica conidiophores.

Raffaelea (Lineage XII)

Raffaelea Arx & Hennebert, Mycopathol. Mycol. Appl. 25: 310. 1965. MycoBank MB 9685, ***emend.*** Z.W. de Beer & M. Procter. Fig 13G, H.

Etymology: Named for the Italian mycologist and plant pathologist, Prof. Raffaele Ciferri (1897–1964).

Sexual morph: *Ascomatal bases* black, subglobose to globose; necks black, straight or curved. *Ostiolar hyphae* present or absent. *Asci* evanescent. *Ascospores* hyaline, 1-celled or rarely 2-celled, cylindrical to oblong, enclosed in hyaline rectangular sheath.

Asexual morph: *Colony* confluent, mucilaginous. *Conidiophores* micronematous, macronematous, mononematous, solitary or aggregated in sporodochia, hyaline, simple or branched, monilioid. *Conidiogenous cells* flask-shaped, proliferating percurrently or sympodially, with denticles, inconspicuous scars or annellations. *Conidia* hyaline, ellipsoidal, obovoid, globose, pyriform, sometimes T- or Y-shaped, 1-celled, producing secondary cells through budding. Associated with ambrosia beetles.

Type species: *R. ambrosiae* Arx & Hennebert, Mycopathol. Mycol. Appl. 25: 310. 1965. MycoBank MB 338171.

Other species: Listed in Table 1.

Notes: *Raffaelea* was originally described to accommodate a number of fungal mutualists of wood-boring ambrosia beetles (Von Arx & Hennebert 1965). In the same paper, Von Arx & Hennebert (1965) validated a similar genus, *Ambrosiella*, with a mode of conidial development different to that in *Raffaelea*. However, confusion persisted regarding the generic placement of species in these two genera until DNA sequence data showed that *Ambrosiella* belonged in the *Ceratocystidaceae* (*Microascales*) and *Raffaelea* in the *Ophiostomatales* (Batra 1967, Cassar & Blackwell 1996, Massoumi Alamouti *et al.* 2009, Harrington *et al.* 2010, De Beer *et al.* 2013a, 2014). Species of *Raffaelea* have reduced conidiophore morphology, distinguishing them from other Ophiostomatalean genera (De Beer & Wingfield 2013). All species in the genus are mutualists of ambrosia beetles in the sub-families *Scolytinae* and *Platypodinae* (*Curculionidae*), respectively, in North America, South Africa, Europe and Asia (Harrington *et al.* 2010, Hulcr & Stelinski 2017).

Prior to the study of Musvuugwa *et al.* (2015), *Raffaelea* was considered as an exclusively asexual genus. Musvuugwa *et al.* (2015) described a *Raffaelea* species forming sexual structures and emended the generic description of *Raffaelea* to accommodate these structures. In our analyses, *R. vaginata* (labelled as Lineage X) did not consistently group within *Raffaelea* (see below). However, our analyses support the inclusion of *R. seticollis* in *Raffaelea,* which was one of the other two sexually reproducing species treated in *Raffaelea* by Musvuugwa *et al.* (2015). This species was originally described from ambrosial galleries in a hemlock (*Tsuga canadensis*) stump in New York State (Davidson 1966) but has not been recorded again. Musvuugwa *et al.* (2015) also transferred *O. deltoideosporum* to *Raffaelea* based on a short LSU sequence of the fungus produced by Hausner *et al.* (1993b), and morphological similarities to *O. seticolle*. We did not have access to material of this species and could therefore not include it in our analyses. For the present, we have followed the suggestion of Musvuugwa *et al.* (2015) and include it in *Raffaelea*.

Raffaelea incertae sedis (Lineage X)

Raffaelea vaginata

Notes: This species was described from a beetle in the genus *Lanurgus* collected from a native tree in the Southern Cape of South Africa (Musvuugwa *et al.* 2015). The fungus formed a sexual morph similar to *O. deltoideosporum* and *O. seticolle* that grouped in *Raffaelea* in the study of De Beer & Wingfield (2013). As stated above, analyses of our data supported the inclusion of *R. seticollis* (*O. seticolle*) in *Raffaelea*. Because *R. vaginata* did not consistently group within *Raffaelea* in our analyses, it is not included in our narrower definition of *Raffaelea*. While it might respresent a novel

genus, there is insufficient information to make this decision and it is thus treated as *incertae sedis*.

Sporothrix (Lineage XIV)

Sporothrix Hektoen & C.F. Perkins, J. Exp. Med. 5: 80. 1900. MycoBank MB 10046, ***emend.*** Z.W. de Beer *et al*., Stud. Mycol. 83: 171. 2016. Figs 14, 15.
Synonyms: *Spumatoria* Massee & E.S. Salmon, Ann. Bot. (Oxford) 15: 350. 1901. MycoBank MB 5175. [Type species *Spumatoria longicollis* Massee & E.S. Salmon, Ann. Bot. (Oxford) 15: 351 (1901)].
Sporotrichopsis Guég., Arch. Parasitol. 15: 104. 1911. MycoBank MB 10048. [Type species *S. beurmannii* (Matr. & Ramond) Guég.; *nom. inval*., Art. 38.1].
Dolichoascus Thibaut & Ansel, Compt. Rend. Hebd. Seances Acad. Sci. 270: 2173. 1970. MycoBank MB 1684. (Type species *D. schenckii* Thibaut & Ansel; *nom. inval*., Art. 40.1).

Etymology: The name is derived from the Latin for 'spore hair' (De Hoog 1974).

Sexual morph: *Ascomatal bases* black, globose; necks black, becoming paler towards apex, straight or slightly curved. *Ostiolar hyphae* parallel to divergent. *Asci* evanescent. *Ascospores* hyaline, 1-celled, allantoid to reniform in side view, almost triangular-shaped, ovoid to oblong.

Asexual morph: *Conidiophores* micronematous, semi-macronematous, mononematous, simple. *Conidiogenous cells* showing sympodial growth, terminal or intercalary, cylindrical, denticulate or not denticulate, hyaline. *Conidia* hyaline to subhyaline, 1-celled, subglobose to oblong, obovoid, clavate to strongly curved, guttuliform to fusiform with round apices and pointed base that sometimes slightly curved, sometimes slightly curved at base; (pathogenic clade and *S. inflata* complex) borne directly on hyphae (sessile) brown to dark brown, subglobose to globose, narrowly obovoid, ellipsoid, 1-celled. *Secondary conidia* borne by yeast-like budding, absent or present.

Type species: *Sporothrix schenckii* Hektoen & C.F. Perkins, J. Exp. Med. 5: 77. 1900.

Other species: Listed in Table 1.

Notes: *Sporothrix* was described as part of a medical case study concerning a child who had contracted a fungal infection after injuring his finger with a hammer (Hektoen & Perkins 1900). The fungus isolated from the infection was described as *Sporothrix schenckii*. The epithet referred to B.R. Schenck who described, but did not name a similar fungus in an earlier study. The genus description of *Sporothrix* by Hektoen & Perkins (1900) was invalid, and the name was validated years later by Nicot & Mariat (1973). In the late 1960's, *S. schenckii* was suggested to represent the asexual morph of *O. stenoceras* (Nicot & Mariat 1973), and subsequently the asexual morphs of many other *Ophiostoma* species were also treated in *Sporothrix* under the dual nomenclature system (De Hoog 1974, De Beer & Wingfield 2013).

The phylogenetic placement of *S. schenckii* in the *Ophiostomatales* based on ribosomal DNA sequences by Berbee & Taylor (1992) became the first example where asexual (anamorph) and sexual (teleomorph) genera were connected based on phylogenetic inference. This represented a first important step towards the abandonment of the the dual nomenclature system for the fungi, which culminated in the Amsterdam Declaration (Hawksworth *et al*. 2011) and subsequent changes to the Code where one fungus could only have one species name.

Following the adoption of the One Fungus-One Name convention, De Beer & Wingfield (2013) listed *Sporothrix* as a synonym of *Ophiostoma*, with the type species of *Sporothrix* (*S. schenckii*) forming part of the *S. schenckii-O. stenoceras* complex in a broad concept for *Ophiostoma*. De Beer & Wingfield (2013) noted that this species complex could represent a genus separate from other species in *Ophiostoma s.l*. However, the available data at the time were insufficient to formally separate the two genera. In a more comprehensive study including sequences of all *Sporothrix* spp. and all *Ophiostoma* spp. with *Sporothrix* asexual morphs, De Beer *et al.* (2016a) showed that the *S. schenckii-O. stenoceras* complex formed a well-supported monophyletic lineage, distinct from other species in *Ophiostoma.* Because this lineage accommodated the type species of *Sporothrix*, they reinstated the genus, transferring all *Ophiostoma* species in this lineage to *Sporothrix*. De Beer *et al*. (2016a) also emended the description of *Sporothrix* to include sexual morphs. Furthermore, they defined several species complexes within *Sporothrix*. The analyses emerging from the present study support the separation of *Sporothrix* and *Ophiostoma* based on strong monophyletic lineages. There are a few exceptions where species formed independent lineages and these are discussed below.

***Species complexes*:**

See De Beer *et al.* (2016a) and below.

The *S. candida* complex
The *S. candida* complex accommodates four species that have been described from hardwoods in South Africa (Kamgan Nkuekam *et al.* 2012, Musvuugwa *et al.* 2016) and one species from hardwoods in Argentina (De Errasti *et al.* 2016). *Sporothrix itsvo* was previously included in this species complex, but it grouped within the *S. gossypina/S. stenoceras* complex in our phylogenetic analyses (Fig. 5).

The *S. inflata* complex
The *S. inflata* complex accommodates species that have been isolated from oak in Europe, soil in Europe, Canada and Malaysia (De Beer *et al.* 2016a). It also includes the epitype isolate of *Spumatoria longicollis*, a coprophilous fungus. In a recent study forming part of The Genera of Fungi project (http://www.mycobank.org), Giraldo *et al.* (2017) showed an isolate of the monotypic genus *Spumatoria* (*Sp. longicollis*) grouping within *Sporothrix,* based on ITS, LSU and *BT* sequence data. These authors considered this as the first report of the fungus after it was initially described. The type of this species has been lost (De Beer *et al.* 2014) and consequently Giraldo *et al.* (2017) designated an epitype, isolated from cow dung in the Netherlands, which was used in the present study. Although this species has a sporothrix-like asexual morph, its septate ascospores distinguished it from all other ophiostomatalean species. Furthermore, its coprophilous nature and pale coloured ascomata distinguish it from other *Sporothrix* species (De Beer *et al.* 2014, Giraldo *et al.* 2017). De Beer *et al.* (2013a) excluded *Spumatoria* from the *Ophiostomatales*, based on these atypical characteristics and characteristics shared with *Kathistes*, which is phylogeneticially distant from the *Ophiostomatales.* Our analyses included LSU and *TEF-1α* sequence data for the epitype isolate,

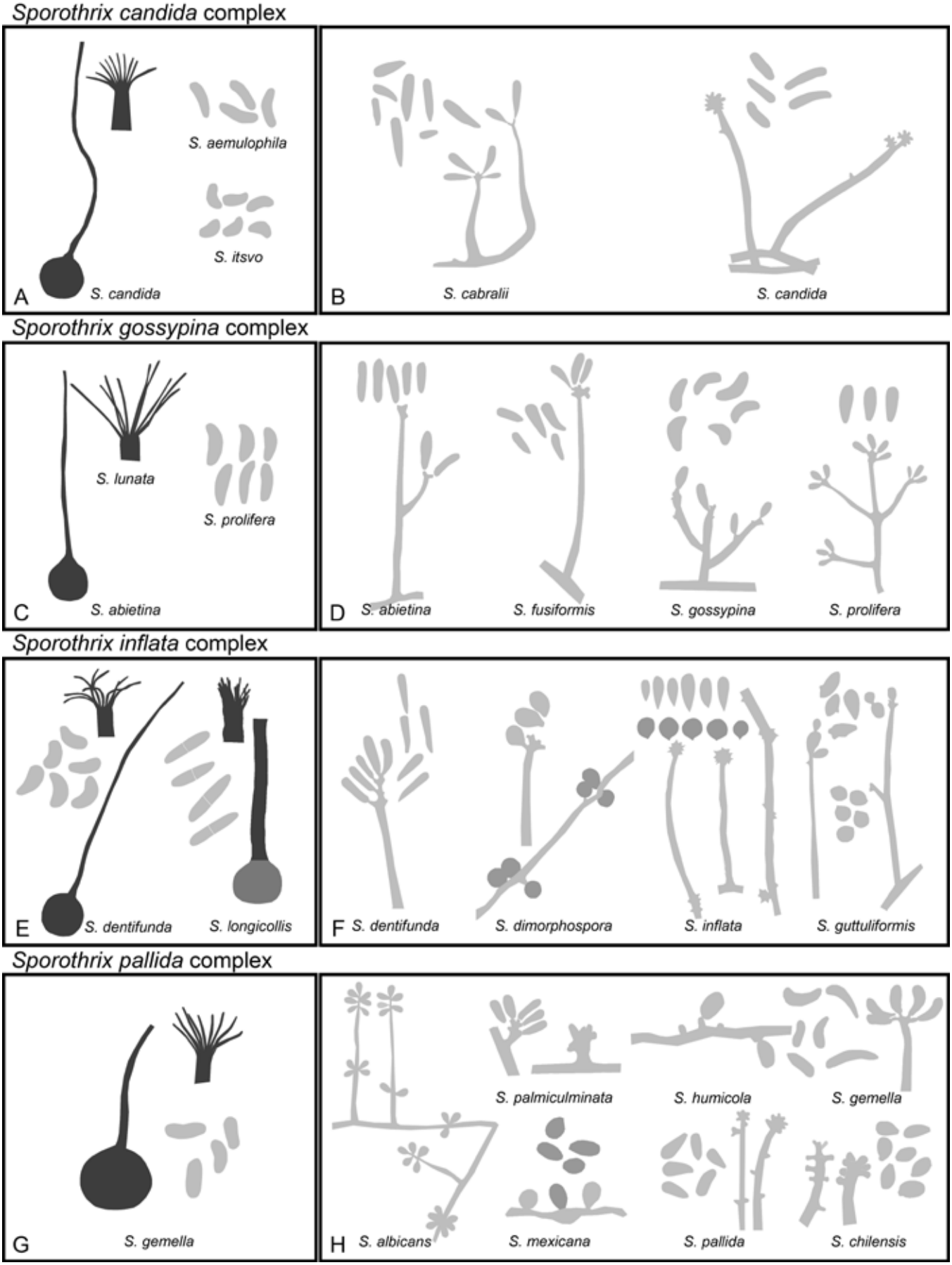

Fig. 14. Genera of the *Ophiostomatales* redrawn from published images with sexual morphs (if known) on the left and asexual morphs on the right. **A, B.** *Sporothrix candida* complex. **C, D.** *Sporothrix gossypina* complex. **E, F.** *Sporothrix inflata* complex. **G, H.** *Sporothrix pallida* complex. (Pale grey shading reflects hyaline to subhyaline colouration, medium-tone grey brown to dark brown and dark grey reflects fuscous black to dark black colouration).

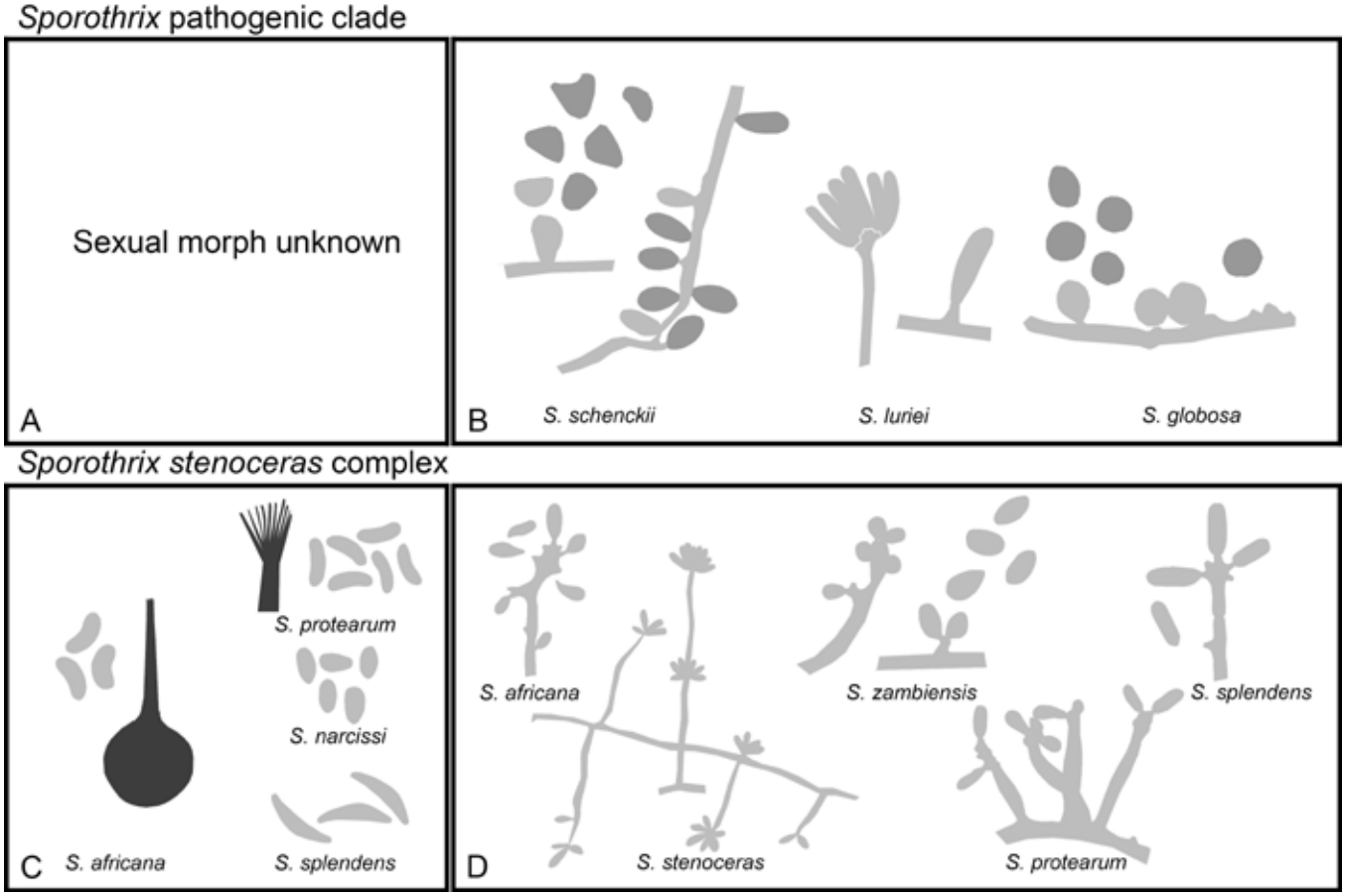

Fig. 15. Genera of the *Ophiostomatales* redrawn published images with sexual morphs (if known) on the left and asexual morphs on the right. **A, B.** *Sporothrix* pathogenic clade. **C, D.** *Sporothrix stenoceras* complex. (Pale grey shading reflects hyaline to subhyaline colouration, medium-tone grey brown to dark brown and dark grey reflects fuscous black to dark black colouration).

which placed it within the *S. inflata* species complex (Figs 5, S1, S3).

The *S. stenoceras* and *S. gossypina* complexes

The *S. stenoceras* and *S. gossypina* species complexes formed an aggregated lineage in the analyses of our datasets (Figs 5, S1, S3). Interestingly, the lineage within the *S. stenoceras* complex including species isolated from *Protea* (De Beer *et al.* 2016a, Ngubane *et al.* 2018), and *S. gemella* (also from *Protea*), formed a lineage distinct from the other species in these complexes, none of which are associated with *Protea*.

The *S. gossypina* complex accommodates species that have diverse ecologies (De Beer *et al.* 2016a). Some species are associated with conifer-infesting bark beetles (Davidson 1971, Marmolejo & Butin 1990, Zhou *et al.* 2004a, 2006, Lu *et al.* 2009, Linnakoski *et al.* 2010, Six *et al.* 2011, Taerum *et al.* 2013), others specifically with pine-infesting bark beetles (Davidson 1971, Zhou *et al.* 2006, Romón *et al.* 2014a, b), and a few species that have been isolated from stained oak wood (Aghayeva *et al.* 2004). Interestingly, there is also a species isolated from cankers on chestnut caused by the aggressive tree pathogen *Cryphonectria parasitica* (Davidson 1978). Species are widely distributed in the USA, Europe, Asia and South Africa (De Beer *et al.* 2016a).

Sporothrix stenoceras has been isolated from soils and hardwoods on many continents. This could explain why it grouped with species in the *S. gossypina* complex.

Sporothrix gemella was previously included in the *S. pallida* complex, but it grouped within the complex in the analyses of our combined dataset (Fig. 5). This species is found on *Protea* species in South Africa and is vectored by mites, a niche similar to that of *S. splendens* (Roets *et al.* 2013, De Beer *et al.* 2016a).

Ophiostoma ponderosae grouped in this species complex in the analyses of our combined dataset (Fig. 5). The LSU sequence generated by De Beer *et al.* (2016a) for the same isolate placed this species in *Ophiostoma s.s.* Our sequence data for *O. ponderosae* differed from the sequence generated by De Beer *et al.* (2016a) in only a small number of bases.

The *S. pallida* complex

Three species forming part of the *S. pallida* complex (*S. pallida*, *S. mexicana* and *S. chilensis*) have been reported as rare and opportunistic pathogens of humans, but mostly occurring in soil along with other species in this complex. Two species are associated with *Protea* species occurring in South Africa. Species in this complex have been found in Japan, Mexico, Chile, England and South Africa (De Beer *et al.* 2016a).

The pathogenic clade

Most *Sporothrix* species are relatively harmless to humans, but there are four species (*S. schenckii*, *S. luriei*, *S. brasiliensis* and *S. globosa*) that are human and animal pathogens. These species are the causal agents of the disease known as sporotrichosis (Teixeira *et al.* 2014). All four species form pigmented blastoconidia, in addition to the more typical sporothrix-like morphology of the asexual morphs. This is possibly an adaptation to both the soil inhabiting and animal-pathogenic lifestyle of these fungi (De

Beer *et al.* 2016a). Collectively, these pathogens have an almost global distribution. *Sporothrix schenckii* has been isolated in the Americas, Australia, Southern Africa and Europe, and S. *globosa* in Central America and parts of Eurasia. However, *S. brasiliensis* is known only from Brazil, where it is responsible for serious epidemic (Rodrigues *et al*. 2013, 2014). *Sporothrix luriei* is known based on only a single isolate from South Africa (Zhang *et al.* 2013, Teixeira *et al.* 2014).

Group D
Sporothrix polyporicola grouped alone in *Sporothrix* in our analyses. (Fig. 5). This is consistent with the phylogenies of Osorio *et al.* (2016) and De Beer *et al.* (2016a).

Group E
In a similar manner, *S. polyporicola* and *S. phasma* grouped alone in *Sporothrix* in our analyses (Fig. 5). Both species were closely related in the LSU dataset of De Beer *et al.* (2016a).

Group F
Group F accommodated *S. nigrograna*, *S. curviconia*, *S. thermara*, *S. eucalyptigena* and *S. bragantina*. *Sporothrix thermara* and *S. bragantina* grouped together as "Lineage H" and *S. curviconia* as "Lineage G" in the phylogenies of De Beer *et al.* (2016a).

Group G
Sporothrix dombeyi formed a single lineage basal to *Sporothrix* in our concatenated dataset (Fig. 5). Previously *S. dombeyi* (as *O. nothofagi*) was transferred to *Sporothrix* and renamed by De Beer *et al.* (2016a). This species also grouped basal to *Sporothrix* in their datasets (along with other species treated here as Lineage XVI, XVIII, XIX).

***New combination*:**

1) *Sporothrix longicollis* (Massee & E.S. Salmon) M. Procter & Z.W. de Beer, ***comb. nov.*** MycoBank MB 841005.
Basionym: *Spumatoria longicollis* Massee & E.S. Salmon, Ann. Bot. 15: 351. 1901. MycoBank MB 171713.

Description: Massee & Salmon (1901: 350–351, fig. 27), Giraldo *et al.* (2017: 344–345, fig. 9).

Phylogenetic data: Giraldo *et al*. (2017).

Notes: *Sporothrix longicollis* is different from other *Sporothrix* spp. by having 1-septate ascospores, pale-coloured ascomata and coprophilous biology. The inclusion of this species in *Sporothrix* was also suggested by Giraldo *et al.* (2017).

Sporothrix incertae sedis (Lineages XVI & XIX)

***Sporothrix fumea* (Lineage XVI)**
Sporothrix fumea grouped basal to all the above-mentioned lineages in the analyses of our combined dataset (Fig. 5). In the phylogenies of De Beer *et al.* (2016a), *S. fumea* formed a lineage with *O. valdivianum* (Lineage XVIII), but in our phylogenies these species grouped separately.

***Sporothrix brunneoviolaceae* (Lineage XIX)**
In the phylogenies of De Beer & Wingfield (2013), *S. brunneoviolaceae* formed a distinct lineage in *Ophiostoma s.l.* with *S. fumea* and *O. fasciatum* but these were not available for the present study. However, this species grouped basal to *Sporothrix* in the phylogenies of De Beer *et al.* (2016a). In the analyses for the present study, *S. brunneoviolaceae* consistently grouped separately from *Sporothrix*.

CONCLUSIONS

The results of this study have provided support for the delineation of most of the genera that have been recognised during the course of the last decade in the *Ophiostomatales*. This study also revealed robust novel lineages described here in four new genera. In addition to phylogenetic support, most of these genera include coherent groups of species that are characterised by similar morphology, ecology and/or geographical origin. The study has also resolved remaining One Fungus-One Name issues that were not dealt with in the revision of De Beer & Wingfield (2013). This is especially by providing new combinations for several species in *Grosmannia* and *Leptographium*.

This study is the most extensive and most comprehensive ever undertaken on the taxonomy of the *Ophiostomatales.* The concatenated dataset included 264 taxa representing all major lineages in the Order. It was not possible to resolve the taxonomic status of some smaller lineages. These lineages may represent new genera or reside in existing genera that will emerge as new species are discovered. We have consequently chosen to retain species in these lineages in their current genera until such data can provide clarity on their taxonomic placement.

The phylogenies generated in this study will serve as a framework for future taxonomic studies on the *Ophiostomatales.* In the short term, they will facilitate the appropriate generic placement of novel species. But they will also provide the required lists of the appropriate species to include in smaller phylogenies of single genera and/or species complexes that will make it possible to confirm whether studied isolates represent novel taxa.

ACKNOWLEDGEMENTS

We thank Dr Hugh Glen for advice on Latinized names and Dr Konstanze Bensch of MycoBank for advice on nomenclatural elements. We acknowledge funding from members of the Tree Protection Cooperative Programme (TPCP), the DST/NRF Centre of Excellence in Plant Health Biotechnology (CPHB), South Africa, and the Fibre Processing & Manufacturing Sector Education and Training Authority (FP&M SETA) bursary programme. We acknowledge the support from the South African Research Chairs Initiative (SARChI), specifically Brenda Wingfield's SARChI Chair in Fugal Genetics for providing early access to some of the fungal genome sequences during this study. Furthermore, thank the many herbaria and culture collections that provided us with material for this study. Reviewers of the originally submitted manuscript, and particularly in one case, provided extensive and important suggestions. These enabled us to re-think particular taxonomic decisions and thus to substantially refine the final product, for which we are most grateful.

DECLARATION ON CONFLICT OF INTEREST

The authors declare that there is no conflict of interest.

REFERENCES

Aghayeva DN, Wingfield MJ, De Beer ZW, *et al.* (2004). Two new *Ophiostoma* species with *Sporothrix* anamorphs from Austria and Azerbaijan. *Mycologia* **96**: 866–878.

Ando Y, Masuya H, Motohashi K, *et al.* (2016). Phylogenetic relationship of Japanese isolates belonging to the *Grosmannia piceiperda* complex (*Ophiostomatales*). *Mycoscience* **57**: 123–135.

Bakshi BK (1950). Fungi associated with ambrosia beetles in Great Britain. *Transactions of the British Mycological Society* **33**: 111–120.

Bakshi BK (1951). Studies on four species of *Ceratocystis*, with a discussion on fungi causing sap-stain in Britain. *Mycological Paper* **35**: 1–16.

Bateman C, Huang Y-T, Simmons DR, *et al.* (2017). Ambrosia beetle *Premnobius cavipennis* (*Scolytinae*: *Ipini*) carries highly divergent ascomycotan ambrosia fungus, *Afroraffaelea ambrosiae gen. nov. et sp. nov.* (*Ophiostomatales*). *Fungal Ecology* **25**: 41–49.

Batra LR (1967). Ambrosia fungi: a taxonomic revision and nutritional studies of some species. *Mycologia* **59**: 976–1017.

Benade E, Wingfield MJ, Van Wyk PS (1997). Conidium development in *Sporothrix* anamorphs of *Ophiostoma*. *Mycological Research* **101**: 1108–1112.

Benny GL, Kimbrough JW (1980). A synopsis of the orders and families of Plectomycetes with keys to genera. *Mycotaxon* **12**: 1–91.

Berbee ML, Taylor JW (1992). 18S Ribosomal RNA gene sequence characters place the human pathogen *Sporothrix schenckii* in the genus *Ophiostoma*. *Experimental Mycology* **16**: 87–91.

Blanco-Ulate B, Rolshausen P, Cantu D (2013). Draft genome sequence of the ascomycete *Phaeoacremonium aleophilum* strain UCR-PA7, a causal agent of the esca disease complex in grapevines. *Genome Announcements* **3**: e00390-13.

Brasier CM (1979). Dual origin of recent Dutch elm disease outbreaks in Europe. *Nature* **281**: 78–80.

Brasier CM (1991). *Ophiostoma novo-ulmi sp nov.* – causative agent of current Dutch elm disease pandemics. *Mycopathologia* **115**: 151–161.

Brasier CM, Mehrotra MD (1995) *Ophiostoma himal-ulmi sp. nov.*, a new species of Dutch elm disease fungus endemic to the Himalayas. *Mycological Research* **99**: 205–215.

Capella-Gutiérrez S, Silla-Martínez JM, Gabaldón T (2009). trimAl: a tool for automated alignment trimming in large-scale phylogenetic analyses. *Bioinformatics* **25**: 1972–1973.

Cassar S, Blackwell M (1996). Convergent origins of ambrosia fungi. *Mycologia* **88**: 596–601.

Castresana J (2000). Selection of conserved blocks from multiple alignments for their use in phylogenetic analysis. *Molecular Biology and Evolution* **17**: 540–552.

Chang R, Duong TA, Taerum SJ, *et al.* (2017). Ophiostomatoid fungi associated with conifer-infesting beetles and their phoretic mites in Yunnan, China. *MycoKeys* **28**: 19–64.

Chang R, Duong TA, Taerum SJ, *et al.* (2019). Ophiostomatoid fungi associated with the spruce bark beetle *Ips typographus,* including 11 new species from China. *Persoonia* **42**: 50–74.

Chesters CGC (1935). Studies on British Pyrenomycetes. I. The life histories of three species of *Cephalotheca* Fuck. *Transactions of the British Mycological Society* **19**: 261–279.

Cobb FW Jr. (1988) *Leptographium wageneri*, cause of black-stain root disease: a review of its discovery, occurrence and biology with emphasis on pinyon and ponderosa pine. *Leptographium root diseases on conifers.* (Harrington TC, Cobb FW, ed.): 41–62. APS press, St. Paul, Minnesota.

Cobb FW Jr., Goheen DJ, Harrington TC (1984). Black-stain root disease caused by *Verticicladiella wageneri*. In: *Proceedings of the Fourth International Congress for Plant Pathology*, Melbourne, Australia. p. 84.

Cobb FW Jr., Parmeter JR Jr., Wood DL, *et al.* (1974). Root pathogens as agents predisposing ponderosa pine and white fir to bark beetles. In: *Proceedings of the fourth international conference on Fomes annosus* (E.G. Kuhlman, ed.): 8–15. USDA Forestry Service, Washington DC, USA.

D'Alessandro E, Giosa D, Huang L, *et al.* (2016). Draft genome sequence of the dimorphic fungus. *Genome Announcements* **4**: e00184-16.

Davidson RW (1942). Some additional species of *Ceratostomella* in the United States. *Mycologia* **34**: 650–662.

Davidson RW (1958). Additional species of *Ophiostomataceae* from Colorado. *Mycologia* **50**: 661–670.

Davidson RW (1966). New species of *Ceratocystis* from conifers. *Mycopathologia et Mycologia Applicata* **28**: 273–286.

Davidson RW (1971). New species of *Ceratocystis*. Mycologia **63**: 5–15.

Davidson RW (1978). A new species of *Ceratocystis* on *Endothia parasitica* canker of American chestnut. *Mycologia* **70**: 856–858.

Davidson RW, Käärik A, Francke-Grosmann H (1967). A restudy of *Ceratocystis penicillata* and report of two American species of this genus from Europe. *Mycologia* **59**: 928–932.

De Beer ZW, Begerow D, Bauer R, *et al.* (2006). Phylogeny of the *Quambalariaceae fam. nov.*, including important *Eucalyptus* pathogens in South Africa and Australia. *Studies in Mycology* **55**: 289–298.

De Beer ZW, Duong TA, Barnes I, *et al.* (2014). Redefining *Ceratocystis* and allied genera. *Studies in Mycology* **79**: 187–219.

De Beer ZW, Duong TA, Wingfield MJ (2016a). The divorce of *Sporothrix* and *Ophiostoma*: solution to a problematic relationship. *Studies in Mycology* **83**: 165–191.

De Beer ZW, Marincowitz S, Duong TA, *et al.* (2016b). *Hawksworthiomyces gen. nov.* (*Ophiostomatales*), illustrates the urgency for a decision on how to name novel taxa known only from environmental nucleic acid sequences (ENAS). *Fungal Biology* **120**: 1323–1340.

De Beer ZW, Seifert K, Wingfield MJ (2013a). The ophiostomatoid fungi: their dual position in the *Sordariomycetes*. In: *The Ophiostomatoid Fungi*: *Expanding Frontiers,* (Seifert KA, De Beer ZW, Wingfield MJ, ed.): 1–19. CBS-KNAW Fungal Biodiversity Centre, Utrecht, The Netherlands.

De Beer ZW, Seifert KA, Wingfield MJ (2013b). A nomenclator for ophiostomatoid genera and species in the *Ophiostomatales* and *Microascales*. In: *The Ophiostomatoid Fungi*: *Expanding Frontiers,* (Seifert KA, De Beer ZW, Wingfield MJ, ed.): 245–322. CBS-KNAW Fungal Biodiversity Centre, Utrecht, The Netherlands.

De Beer ZW, Wingfield MJ (2013). Emerging lineages in the *Ophiostomatales*. In: *The Ophiostomatoid Fungi*: *Expanding Frontiers,* (Seifert KA, De Beer ZW, Wingfield MJ, ed.): 21–46. CBS-KNAW Fungal Biodiversity Centre, Utrecht, The Netherlands.

De Errasti A, De Beer ZW, Coetzee MPA, *et al.* (2016). Three new species of *Ophiostomatales* from *Nothofagus* in Patagonia. *Mycological Progress* **15**: 17.

De Errasti A, Pildain MB, Rajchenberg M (2018). Ophiostomatoid fungi isolated from three different pine species in Argentinian Patagonia. *Forest Pathology* **48**: e12393.

De Hoog GS (1974). The genera *Blastobotrys*, *Sporothrix*, *Calcarisporium* and *Calcarisporiella gen. nov. Studies in Mycology* **7**: 1–84.

De Hoog GS, Scheffer R (1984). *Ceratocystis* versus *Ophiostoma*: a reappraisal. *Mycologia* **76**: 292–299.

De Meyer EM, De Beer ZW, Summerell RC, *et al.* (2008). Taxonomy and phylogeny of new wood- and soil-inhabiting *Sporothrix* species in the *Ophiostoma stenoceras-Sporothrix schenckii* complex. *Mycologia* **100**: 647–661.

Dean RA, Talbot NJ, Ebbole DJ, *et al.* (2005). The genome sequence of the rice blast fungus *Magnaporthe grisea*. *Nature* **434**: 980–986.

DiGuistini S, Wang Y, Liao NY, *et al.* (2011). Genome and transcriptome analyses of the mountain pine beetle-fungal symbiont *Grosmannia clavigera*, a lodgepole pine pathogen. *Proceedings of the National Academy of Sciences* **108**: 2504–2509.

Dochinger LS (1967). *Leptographium* root decline of eastern white pine. *Phytopathology* **57**: 809.

Dreaden TJ, Davis JM, De Beer ZW, *et al.* (2014). Phylogeny of ambrosia beetle symbionts in the genus *Raffaelea*. *Fungal Biology* **118**: 970–978.

Duong TA, De Beer ZW, Wingfield BD, *et al.* (2012). Phylogeny and taxonomy of species in the *Grosmannia serpens* complex. *Mycologia* **104**: 715–732.

Endoh R, Suzuki M, Okada G, *et al.* (2011). Fungus symbionts colonizing

the galleries of the ambrosia beetle *Platypus quercivorus*. *Microbial Ecology* **62**: 106–120.
Fraedrich SW, Harrington TC, Rabaglia RJ, *et al.* (2008). A fungal symbiont of the redbay ambrosia beetle causes a lethal wilt in redbay and other *Lauraceae* in the southeastern United States. *Plant Disease* **92**: 215–224.
Forgetta V, Leveque G, Dias J, *et al.* (2013). Sequencing of the Dutch elm disease fungus genome using the Roche/454 GS-FLX titanium system in a comparison of multiple genomics core facilities. *Journal of Biomolecular Techniques* **24**: 39–49.
Gharabigloozare Y (2015). *Raffaelea* spp. from five ambrosia beetles in the genera *Xyleborinus* and *Cyclorhipidion* (*Coleoptera*: *Curculionidae*: *Scolytinae*: *Xyleborini*): 11–47. Iowa State University, Graduate Theses and Dissertations. 14815. Ames, Iowa, USA.
Gardes M, Bruns TD (1993). ITS primers with enhanced specificity for basidiomycetes - application to the identification of mycorrhizae and rusts. *Molecular Ecology* **2**: 113–118.
Gebhardt H, Kirschner R, Oberwinkler F (2002). A new *Ophiostoma* species isolated from the ambrosia beetle *Xyleborus dryographus* (*Coleoptera*: *Curculionidae*, *Scolytinae*). *Mycological Progress* **1**: 377–382.
Gebhardt H, Weiss M, Oberwinkler F (2005). *Dryadomyces amasae*: a nutritional fungus associated with ambrosia beetles of the genus *Amasa* (*Coleoptera*: *Curculionidae*, *Scolytinae*). *Mycological Research* **109**: 687–696.
Gibbs JN (1978). Development of the Dutch elm disease epidemic in southern England, 1971–6. *Annals of Applied Biology* **88**: 219–228.
Giraldo A, Crous PW, Schumacher RK, *et al.* (2017). The Genera of Fungi—G3: *Aleurocystis, Blastacervulus, Clypeophysalospora, Licrostroma, Neohendersonia* and *Spumatoria*. *Mycological Progress* **16**: 325–348.
Goheen DJ, Cobb F (1978). Occurrence of *Verticicladiella wageneri* and its perfect state, *Ceratocystis wageneri sp. nov.*, in insect galleries. *Phytopathology* **68**: 1192–1195.
Goidànich G (1935). A new species of *Ophiostoma* living on pear and some observations on the exact systematic position of the ascigerous form and the metagenetic forms of the genus. *Bollettino della R Stazione di Patologia Vegetale* **15**: 122–168.
Gorton C, Kim SH, Henricot B, *et al.* (2004). Phylogenetic analysis of the bluestain fungus *Ophiostoma minus* based on partial ITS rDNA and β-tubulin gene sequences. *Mycological Research* **108**: 759–765.
Greif MD, Gibas CFC, Currah RS (2006). *Leptographium piriforme sp. nov.*, from a taxonomically diverse collection of arthropods collected in an aspen-dominated forest in western Canada. *Mycologia* **98**: 771–780.
Griffin HD (1968). The genus *Ceratocystis* in Ontario. *Canadian Journal of Botany* **46**: 689–718.
Grobbelaar JW, Bloomer P, Wingfield MJ, *et al.* (2011). Discovery of *Ophiostoma tsotsi* on *Eucalyptus* wood chips in China. *Mycoscience* **52**: 111–118.
Grobbelaar JW, De Beer ZW, Bloomer P, *et al.* (2010) *Ophiostoma tsotsi sp. nov.*, a wound-infesting fungus of hardwood trees in Africa. *Mycopathologia* **169**: 413–423.
Hansen EM, Goheen DJ, Hessburd PF, *et al.* (1988). Biology and management of black stain root disease in Douglas fir. In: *root disease in conifers* (Harrington TC & Cobb FW, eds): 63–80. American Phytopathological Society, St Paul, Minnesota, USA.
Haridas S, Wang Y, Lim L, *et al.* (2013). The genome and transcriptome of the pine saprophyte *Ophiostoma piceae*, and a comparison with the bark beetle-associated pine pathogen *Grosmannia clavigera*. *BMC Genomics* **14**: 373.
Harrington TC (1981). Cycloheximide sensitivity as a taxonomic character in *Ceratocystis*. *Mycologia* **73**: 1123–1129.
Harrington TC (1988). *Leptographium* species, their distributions, hosts and insect vectors. In: *Leptographium root diseases on conifers,* (Harrington TC & Cobb FW, eds.): 1–40. American Phytopathological Society Press, St. Paul, Minnesota, USA.
Harrington T, Cobb Jr F (1984). Host specialization of three morphological variants of *Verticicladiella wageneri*. *Phytopathology* **74**: 286–290.
Harrington T, Cobb Jr F (1987). *Leptographium wageneri* var. *pseudotsugae*, *var. nov.*, cause of black stain root disease on Douglas fir. *Mycotaxon* **30**: 501–507.
Harrington TC, Aghayeva DN, Fraedrich SW (2010). New combinations in *Raffaelea, Ambrosiella*, and *Hyalorhinocladiella*, and four new species from the redbay ambrosia beetle, *Xyleborus glabratus*. *Mycotaxon* **111**: 337–361.
Harrington T, Fraedrich S, Aghayeva D (2008). *Raffaelea lauricola,* a new ambrosia beetle symbiont and pathogen on the *Lauraceae*. *Mycotaxon* **104**: 399–404.
Harrington TC, McNew D, Steimel J, *et al.* (2001). Phylogeny and taxonomy of the *Ophiostoma piceae* complex and the Dutch Elm Disease fungi. *Mycologia* **93**: 111–136.
Harrington TC, Yun HY, Lu S-S, *et al.* (2011). Isolations from the redbay ambrosia beetle, *Xyleborus glabratus,* confirm that the laurel wilt pathogen, *Raffaelea lauricola*, originated in Asia. *Mycologia* **103**: 1028–1036.
Hausner G, Eyjolfsdottir GG, Reid J (2003). Three new species of *Ophiostoma* and notes on *Cornuvesica falcata*. *Canadian Journal of Botany* **81**: 40.
Hausner G, Reid J, Klassen GR (1992). Do galeate-ascospore members of the *Cephaloascaceae*, *Endomycetaceae* and *Ophiostomataceae* share a common phylogeny? *Mycologia* **84**: 870–881.
Hausner G, Reid J, Klassen GR (1993a). *Ceratocystiopsis*: a reappraisal based on molecular criteria. *Mycological Research* **97**: 625–633.
Hausner G, Reid J, Klassen GR (1993b). On the phylogeny of *Ophiostoma*, *Ceratocystis s.s.*, and *Microascus*, and relationships within *Ophiostoma* based on partial ribosomal DNA sequences. *Canadian Journal of Botany* **71**: 1249–1265.
Hausner G, Reid J, Klassen GR (1993c). On the subdivision of *Ceratocystis s.l.,* based on partial ribosomal DNA sequences. *Canadian Journal of Botany* **71**: 52–63.
Hausner G, Reid J, Klassen GR (2000). On the phylogeny of members of *Ceratocystis s.s.* and *Ophiostoma* that possess different anamorphic states, with emphasis on the anamorph genus *Leptographium*, based on partial ribosomal DNA sequences. *Canadian Journal of Botany* **78**: 903–916.
Hawksworth DL (2012). Managing and coping with names of pleomorphic fungi in a period of transition. *IMA Fungus* **3**: 15–24.
Hawksworth DL, Crous PW, Redhead SA, *et al.* (2011). The Amsterdam Declaration on fungal nomenclature. *IMA Fungus* **2**: 105–112.
Hektoen L, Perkins CF (1900). Refractory subcutaneous abscesses caused by *Sporothrix schenckii*. A new pathogenic fungus. *The Journal of Experimental Medicine* **5(1)**: 77–89.
Hessburg PF, Hansen EM (2000). Infection of Douglas-fir by *Leptographium wageneri*. *Canadian Journal of Botany* **78**: 1254–1261.
Hoang DT, Chernomor O, Von Haeseler A, *et al.* (2018). UFBoot2: Improving the Ultrafast Bootstrap Approximation. *Molecular Biology and Evolution* **35**: 518–522.
Huang Y-T, Chen C-Y (2014). *Leptographium globosum sp. nov.*, a new species with globose conidia. *Mycological Progress* **13**: 841–848.
Huang L, Gao W, Giosa D, *et al.* (2016). Whole-genome sequencing and *in silico* analysis of two strains of *Sporothrix globosa*. *Genome Biology and Evolution* **8**: 3292–3296.
Hulcr J, Stelinski LL (2017). The ambrosia symbiosis: from evolutionary ecology to practical management. *Annual Review of Entomology* **62**: 285–303.
Hunt J (1956). Taxonomy of the genus *Ceratocystis*. *Lloydia* **19**: 1–58.
Hutchison LJ, Reid J (1988a). Taxonomy of some potential wood-staining fungi from New Zealand 1. *Ophiostomataceae*. *New Zealand Journal of Botany* **26**: 63–81.
Hutchison LJ, Reid J (1988b). Taxonomy of some potential wood-staining fungi from New Zealand. 2. Pyrenomycetes, Coelomycetes and Hyphomycetes. *New Zealand Journal of Botany* **26**: 83–98.
Jacobs K, Bergdahl DR, Wingfield MJ, *et al.* (2004). *Leptographium wingfieldii* introduced into North America and found associated with exotic *Tomicus piniperda* and native bark beetles. *Mycological Research* **108**: 411–418.
Jacobs K, Eckhardt LG, Wingfield MJ (2006). *Leptographium profanum sp. nov.*, a new species from hardwood roots in North America. *Canadian Journal of Botany* **84**: 759–766.
Jacobs K, Kirisits T (2003). *Ophiostoma kryptum sp. nov.* from *Larix decidua* and *Picea abies* in Europe, similar to *O. minus*. *Mycological*

Research **107**: 1231–1242.
Jacobs K, Seifert KA, Harrison KJ, *et al.* (2003). Identity and phylogenetic relationships of ophiostomatoid fungi associated with invasive and native *Tetropium* species (*Coleoptera*: *Cerambycidae*) in Atlantic Canada. *Canadian Journal of Botany* **81**: 316–329.
Jacobs K, Solheim H, Wingfield BD, *et al.* (2005). Taxonomic re-evaluation of *Leptographium lundbergii* based on DNA sequence comparisons and morphology. *Mycological Research* **109**: 1149–1161.
Jacobs K, Wingfield MJ (2001). *Leptographium species*: *tree pathogens, insect associates, and agents of blue-stain*. American Phytopathological Society Press, St. Paul, Minnesota, USA.
Jacobs K, Wingfield MJ, Crous PW (2000b). *Ophiostoma europhioides* and *Ceratocystis pseudoeurophioides*, synonyms of *O. piceaperdum*. *Mycological Research* **104**: 238–243.
Jacobs K, Wingfield MJ, Crous PW, *et al.* (1998). *Leptographium engelmannii*, a synonym of *Leptographium abietinum*, and description of *Leptographium hughesii sp. nov. Canadian Journal of Botany* **76**: 1660–1667.
Jacobs K, Wingfield MJ, Jacobs A, *et al.* (2001b). A taxonomic re-evaluation of *Phialocephala phycomyces*. *Canadian Journal of Botany* **79**: 110–117.
Jacobs K, Wingfield MJ, Pashenova NV, *et al.* (2000a). A new *Leptographium* species from Russia. *Mycological Research* **104**: 1524–1529.
Jacobs K, Wingfield MJ, Uzunovic A, *et al.* (2001c) Three new species of *Leptographium* from pine. *Mycological Research* **105**: 490–499.
Jacobs K, Wingfield MJ, Wingfield BD (2001a). Phylogenetic relationships in *Leptographium* based on morphological and molecular characters. *Canadian Journal of Botany* **79**: 719–732.
Jankowiak R, Bilański P, Strzałka B, *et al*. (2019). Four new *Ophiostoma* species associated with conifer- and hardwood-infesting bark and ambrosia beetles from the Czech Repubic and Poland. *Antonie van Leeuwenhoek* **112**: 1501–1521.
Jankowiak R, Ostafińska A, Aas T, *et al.* (2018). Three new *Leptographium* spp. (*Ophiostomatales*) infecting hardwood trees in Norway and Poland. *Antonie van Leeuwenhoek* **111**: 2323–2347.
Jankowiak R, Solheim H, Bilański P, *et al.* (2020) Seven new species of *Graphilbum* from conifers in Norway, Poland, and Russia. *Mycologia* **112**: 1240–1262.
Jankowiak R, Strzałka B, Bilański P, *et al*. (2017). Two new *Leptographium* spp. reveal an emerging complex of hardwood-infecting species in the *Ophiostomatales*. *Antonie van Leeuwenhoek* **110**: 1537–1553.
Jeon J, Kim KT, Song H, *et al.* (2017). Draft Genome Sequence of the Fungus Associated with Oak Wilt Mortality in South Korea, *Raffaelea quercus-mongolicae* KACC44405. *Genome Announ*cements **5**: e00797-17.
Jooste W (1978). *Leptographium reconditum sp. nov.* and observations on conidiogenesis in *Verticicladiella*. *Transactions of the British Mycological Society* **70**: 152–155.
Junier T, Zdobnov EM (2010). The Newick utilities: high-throughput phylogenetic tree processing in the UNIX shell. *Bioinformatics* **26**: 1669–1670.
Kamgan Nkuekam G, De Beer ZW, Wingfield MJ, *et al.* (2011). *Ophiostoma* species (*Ophiostomatales*, *Ascomycota*), including two new taxa on eucalypts in Australia. *Australian Journal of Botany* **59**: 283–297.
Kamgan Nkuekam G, De Beer ZW, Wingfield MJ, *et al.* (2012) A diverse assemblage of *Ophiostoma* species, including two new taxa on eucalypt trees in South Africa. *Mycological Progress* **11(2)**: 515–533.
Kamgan Nkuekam G, Jacobs K, De Beer ZW, *et al.* (2008). *Ceratocystis* and *Ophiostoma* species, including three new taxa, associated with wounds on native South African trees. *Fungal Diversity* **29**: 37–59.
Kamgan Nkuekam G, Solheim H, De Beer ZW, *et al*. (2010) *Ophiostoma* species, including *Ophiostoma borealis sp. nov.*, infecting wounds of native broad-leaved trees in Norway. *Cryptogamie, Mycologie* **31**: 285–303.
Katoh K, Standley DM (2013). MAFFT multiple sequence alignment software version 7: improvements in performance and usability. *Molecular Biology and Evolution* **30**: 772–780.
Kendrick WB (1962). The *Leptographium* complex. *Verticicladiella* Hughes. *Canadian Journal of Botany* **40**: 771–797.
Khoshraftar S, Hung S, Khan S, *et al.* (2013). Sequencing and annotation of the *Ophiostoma ulmi* genome. *BMC Genomics* **14**: 162.
Kim J-J, Lim YW, Breuil C, *et al.* (2005a). A new *Leptographium* species associated with *Tomicus piniperda* infesting pine logs in Korea. *Mycological Research* **109**: 275–284.
Kim J-J, Lim YW, Seifert K, *et al.* (2005b). Taxonomy of *Ophiostoma radiaticola sp. nov.* (*Ophiostomatales*, Ascomycetes), the teleomorph of *Pesotum pini,* isolated from logs of *Pinus radiata*. *Mycotaxon* **91**: 481–496.
Kim J-J, Lim YW, Wingfield MJ, *et al.* (2004). *Leptographium bistatum sp. nov.*, a new species with a *Sporothrix* synanamorph from *Pinus radiata* in Korea. *Mycological Research* **108**: 699–706.
Kim K-H, Choi Y-J, Seo S-T, *et al.* (2009). *Raffaelea quercus-mongolicae sp. nov.* associated with *Platypus koryoensis* on oak in Korea. *Mycotaxon* **110**: 189–197.
Kim S, Harrington TC, Lee JC, *et al.* (2011). *Leptographium tereforme sp. nov.* and other *Ophiostomatales* isolated from the root-feeding bark beetle *Hylurgus ligniperda* in California. *Mycologia* **103**: 152–163.
Kowalski T, Butin H (1989). Taxonomy of known and new species of *Ceratocystis* from oak (*Quercus robur* L.). *Journal of Phytopathology* **124**: 236–248.
Kubono T, Ito S (2002). *Raffaelea quercivora sp. nov.* associated with mass mortality of Japanese oak, and the ambrosia beetle (*Platypus quercivorus*). *Mycoscience* **43**: 255–260.
Kück P, Meusemann K (2010). FASconCAT: convenient handling of data matrices. *Molecular Phylogenetics and Evolution* **56**: 1115–1118.
Lagerberg T, Lundberg G, Melin E (1927). Biological and practical researches into blueing in pine and spruce. *Svenska Skogsvårdsfören Tidskrift* **25**: 145–272.
Lah L, Löber U, Hsiang T, *et al.* (2017). A genomic comparison of putative pathogenicity-related gene families in five members of the *Ophiostomatales* with different lifestyles. *Fungal Biology* **121**: 234–252.
Lanfear R, Fandsen PB, Wright AM, *et al*. (2017). PartitionFinder 2: new methods for selecting partitioned models of evolution for molecular and morphological phylogenetic analyses. *Molecular Biology and Evolution* **34(3)**: 772–773.
Lartillot N, Rodrigue N, Stubbs D, *et al.* (2013). PhyloBayes MPI: Phylogenetic reconstruction with infinite mixtures of profiles in a parallel environment. *Systematic Biology* **62**: 611–615.
Leach JG, Orr LW, Christiansen C (1934). The interrelationship of bark beetles and blue staining fungi in felled Norway pine timber. *Journal of Agricultural Research* **49**: 315–341.
Li Y, Huang Y-T, Kasson MT, *et al.* (2018). Specific and promiscuous ophiostomatalean fungi associated with *Platypodinae* ambrosia beetles in the southeastern United States. *Fungal Ecology* **35**: 42–50.
Linnakoski R, De Beer ZW, Ahtiainen J, *et al.* (2010). *Ophiostoma* spp. associated with pine- and spruce-infesting bark beetles in Finland and Russia. *Persoonia* **25**: 72–93.
Linnakoski R, De Beer ZW, Duong TA, *et al*. (2012). *Grosmannia* and *Leptographium* spp. associated with conifer-infesting bark beetles in Finland and Russia, including *Leptographium taigense sp. nov. Antonie van Leeuwenhoek* **102**: 375–399.
Linnakoski R, De Beer ZW, Rousi M, *et al*. (2008) Fungi including *Ophiostoma karelicum sp. nov.*, associated with *Scolytus ratzeburgi* infesting birch in Finland and Russia. *Mycological Research* **112**: 1475–1488
Linnakoski R, De Beer ZW, Rousi M, *et al.* (2009) *Ophiostoma denticiliatum sp. nov.* and other *Ophiostoma* species associated with the birch bark beetle in southern Norway. *Persoonia* **23**:9–15.
Linnakoski R, Jankowiak R, Villari C, *et al*. (2016). The *Ophiostoma clavatum* species complex: a newly defined group in the *Ophiostomatales* including three novel taxa. *Antonie van Leeuwenhoek* **109**: 987–1018.
Liou JY, Shih JY, Tzean SS (1999). *Esteya*, a new nematophagous genus from Taiwan, attacking the pinewood nematode (*Bursaphelenchus xylophilus*). *Mycological Research* **103**: 242–248.
Liu F, Chen S, Ferreira MA, *et al.* (2019). Draft genome sequences of five *Calonectria* species from *Eucalyptus* plantations in China, *Celoporthe*

dispersa, *Sporothrix phasma* and *Alectoria sarmentosa*. *IMA Fungus* **10**: 22.

Liu X-W, Wang H-M, Lu Q, *et al.* (2017). Taxonomy and pathogenicity of *Leptographium* species associated with *Ips subelongatus* infestations of *Larix* spp. in northern China, including two new species. *Mycological Progress* **16**: 1–13.

Löytynoja A (2014). Phylogeny-aware alignment with PRANK. *Methods in Molecular Biology* **1079**: 155–170.

Lu Q, Decock C, Zhang XY, *et al.* (2008). *Leptographium sinoprocerum sp. nov.*, an undescribed species associated with *Pinus tabuliformis-Dendroctonus valens* in northern China. *Mycologia* **100**: 275–290.

Lu Q, Decock C, Zhang XY, *et al.* (2009). Ophiostomatoid fungi (*Ascomycota*) associated with *Pinus tabuliformis* infested by *Dendroctonus valens* (*Coleoptera*) in northern China and an assessment of their pathogenicity on mature trees. *Antonie van Leeuwenhoek* **96**: 275–293.

Madrid H, Gené J, Cano J, *et al.* (2010). *Sporothrix brunneoviolacea* and *Sporothrix dimorphospora*, two new members of the *Ophiostoma stenoceras-Sporothrix schenckii* complex. *Mycologia* **102**: 1193–1203.

Maekawa N, Tsuneda A, Arita I (1987). *Ceratocystis* species occurring on the *Lentinus edodes* bedlogs. *Reports of the Tottori Mycological Institute* **25**: 6–14.

Mai U, Mirarab S (2018). TreeShrink: fast and accurate detection of outlier long branches in collections of phylogenetic trees. *BMC Genomics* **19**: 272.

Malloch D, Blackwell M (1993). Dispersal biology of the ophiostomatoid fungi. In: *Ceratocystis and ophiostoma*: *taxonomy, ecology, and pathogenicity,* (Wingfield MJ, Seifert KA, Webber JF, ed.): 195–206. American Phytopathological Society Press., St. Paul, Minnesota.

Malloch D, Cain RF (1970). Five new genera in the new family *Pseudeurotiaceae*. *Canadian Journal of Botany* **48**: 1815–1825.

Marincowitz S, Duong TA, De Beer ZW, *et al.* (2015). *Cornuvesica*: A little known mycophilic genus with a unique biology and unexpected new species. *Fungal Biology* **119**: 615–630.

Marincowitz S, Duong TA, Heiniger U, *et al.* (2017). A new *Leptographium* species from the roots of declining *Pinus sylvestris* in Switzerland. *Forest Pathology* **47**: e12346.

Marincowitz S, Duong TA, Stephen SJ, *et al.* (2020) Fungal associates of an invasive pine-infesting bark beetle, *Dendroctonus valens* including seven new Ophiostomatalean fungi. *Persoonia* **45**: 177–195.

Marmolejo JG, Butin H (1990). New conifer-inhabiting species of *Ophiostoma* and *Ceratocystiopsis* (*Ascomycetes*, *Microascales*) from Mexico. *Sydowia* **422**: 193–199.

Massee G, Salmon ES (1901) Researches on coprophilous fungi. *Annals of Botany* **15**: 313–357.

Massoumi Alamouti S, Kim J-J, Breuil C (2006). A new *Leptographium* species associated with the northern spruce engraver, *Ips perturbatus*, in western Canada. *Mycologia* **98**: 149–160.

Massoumi Alamouti S, Tsui CKM, Breuil C (2009). Multigene phylogeny of filamentous ambrosia fungi associated with ambrosia and bark beetles. *Mycological Research* **113**: 822–835.

Massoumi Alamouti S, Wang V, DiGuistini S, *et al.* (2011). Gene genealogies reveal cryptic species and host preferences for the pine fungal pathogen *Grosmannia clavigera*. *Molecular Ecology* **20**: 2581–2602.

Masuya H, Kaneko S, Yamaoka Y (2003). Three new *Ophiostoma* species isolated from Japanese red pine. *Mycoscience* **44**: 301–310.

Masuya H, Manabe RI, Ohkuma M, *et al.* (2016). Draft genome sequence of *Raffaelea quercivora* JCM 11526, a Japanese oak wilt pathogen associated with the platypodid beetle, *Platypus quercivorus*. *Genome Announcements* **4**: e00755-16.

Masuya H, Wingfield M, Kubono T, *et al.* (2004). *Leptographium pruni*, *sp. nov.* from bark beetle-infested *Prunus jamasakura* in Japan. *Mycologia* **96**: 548–557.

Masuya H, Yamaoka Y, Wingfield MJ (2013). Ophiostomatoid fungi and their associations with bark beetles in Japan. In: *Ophiostomatoid Fungi*: *Expanding Frontiers,* (Seifert KA, De Beer ZW, Wingfield MJ, ed.): 77–90. CBS-KNAW Fungal Biodiversity Centre, Utrecht, the Netherlands.

Mathiesen-Käärik A (1953). Eine Übersicht über die gewöhnlichsten mit Borkenkäfern assoziierten Bläuepilze in Schweden und einige für Schweden neue Bläuepilze. *Meddelanden från Statens Skogsforskningsinstitut* **43**: 1–74.

Mathiesen-Käärik A (1960). Studies on the ecology, taxonomy and physiology of Swedish insect-associated blue stain fungi, especially the genus *Ceratocystis*. *Oikos* **11**: 1–25.

Matsuda Y, Kimura K, Ito S-I (2010). Genetic characterization of *Raffaelea quercivora* isolates collected from areas of oak wilt in Japan. *Mycoscience* **51**: 310–316.

Mayers CG, Harrington TC, Masuya H, *et al.* (2020). Patterns of coevolution between ambrosia beetle mycangia and the *Ceratocystidaceae*, with five new fungal genera and seven new species. *Persoonia* **44**: 41–66.

Mayers CG, McNew DL, Harrington TC, *et al.* (2015). Three genera in the *Ceratocystidaceae* are the respective symbionts of three independent lineages of ambrosia beetles with large, complex mycangia. *Fungal Biology* **119**: 1075–1092.

Melin E, Nannfeldt JA (1934). Researches into the blueing of ground wood-pulp. *Svensk Skogsvardsforeningens Tidskrift* **32**: 397–616.

McNeill J, Barrie FR, Buck WR, *et al*. (2012). *International Code of Nomenclature for algae, fungi, and plants (Melbourne Code)*. Regnum Vegetabile 154. ARG Gantner Verlag KG, Germany.

Minh BQ, Schmidt HA, Chernomor O, *et al.* (2020). IQ-TREE 2: New models and efficient methods for phylogenetic inference in the genomic era. *Molecular Biology and Evolution* **37**: 1530–1534.

Mirarab S, Reaz R, Bayzid MS, *et al.* (2014). ASTRAL: genome-scale coalescent-based species tree estimation. *Bioinformatics* **30**: i541–i548.

Morales-Cruz A, Amrine KC, Blanco-Ulate B, *et al.* (2015). Distinctive expansion of gene families associated with plant cell wall degradation, secondary metabolism, and nutrient uptake in the genomes of grapevine trunk pathogens. *BMC Genomics* **16**: 469.

Morelet M (1998). Une espèce nouvelle de *Raffaelea*, isolée de *Platypus cylindrus*, coléoptère xylomycétophage des chênes. *Annales de la Société des Sciences Naturelles et d'Archéologie de Toulon et du Var.* **50**: 185–193.

Mouton M, Wingfield MJ, Van Wyk PS (1992). The anamorph of *Ophiostoma frankae-grosmanniae* is a *Leptographium*. *Mycologia* **84**: 857–862.

Mullineux T, Hausner G (2009). Evolution of rDNA ITS1 and ITS2 sequences and RNA secondary structures within members of the fungal genera *Grosmannia* and *Leptographium*. *Fungal Genetics and Biology* **46**: 855–867.

Mullineux T, Willows K, Hausner G (2011). Evolutionary dynamics of the mS952 Intron: A novel Mitochondrial Group II Intron encoding a LAGLIDADG homing endonuclease gene. *Journal of Molecular Evolution* **72**: 433–449.

Musvuugwa T, De Beer ZW, Duong TA, *et al.* (2015). New species of *Ophiostomatales* from *Scolytinae* and *Platypodinae* beetles in the Cape Floristic Region, including the discovery of the sexual state of *Raffaelea*. *Antonie van Leeuwenhoek* **108**: 933–950.

Musvuugwa T, De Beer ZW, Duong TA, *et al.* (2016). Wounds on *Rapanea melanophloeos* provide habitat for a large diversity of *Ophiostomatales* including four new species. *Antonie van Leeuwenhoek* **109**: 877–894.

Nannfeldt JA (1932). Studien uber die Morphologie und Systematik der nicht-lichenisierten inoperculaten Discomyceten. *Nova Acta Regiae Societatis Scientiarum Upsaliensis* **IV 8**: 1–368.

Nel WJ, De Beer ZW, Wingfield MJ, *et al.* (2021). Phylogenetic and phylogenomic analyses reveal two new genera and three new species of ophiostomatalean fungi from termite-fungus combs. *Mycologia*. **113**: 1199–1217.

Nel WJ, Duong TA, Wingfield BD, *et al.* (2018). A new genus and species for the globally important, multi-host root pathogen *Thielaviopsis basicola*. *Plant Pathology* **67**: 871–882.

Ngubane NP, Dreyer LL, Oberlander KC, *et al.* (2018). Two new *Sporothrix* species from *Protea* flower heads in South African Grassland and Savanna. *Antonie van Leeuwenhoek* **111**: 965–979.

Nicot J, Mariat F (1973). Caractères morphologiques et position systématique de *Sporothrix schenckii,* agent de la sporotrichose humaine. *Mycopathologia et Mycologia Applicata* **49**: 53–65.

Okada G, Seifert KA, Takematsu A, *et al.* (1998). A molecular phylogenetic reappraisal of the *Graphium* complex based on 18S rDNA sequences. *Canadian Journal of Botany* **76**: 1495–1506.

Olchowecki A, Reid J (1974) Taxonomy of the genus *Ceratocystis* in Manitoba. *Canadian Journal of Botany* **52**: 1675–1711.

Osorio JA, De Beer ZW, Wingfield MJ, *et al.* (2016). Ophiostomatoid fungi associated with mangroves in South Africa, including *Ophiostoma palustre sp. nov. Antonie van Leeuwenhoek* **109**: 1555–1571.

Paciura D, De Beer ZW, Jacobs K, *et al.* (2010). Eight new *Leptographium* species associated with tree-infesting bark beetles in China. *Persoonia* **25**: 94–108.

Pan Y, Lu J, Zhou X-D, *et al.* (2020). *Leptographium wushanense sp. nov.*, associated with *Tomicus armandii* on *Pinus armandii* in Southwestern China. *Mycoscience* **61**: 43–48.

Plattner A, Kim J-J, Reid J, *et al.* (2009). Resolving taxonomic and phylogenetic incongruence within species *Ceratocystiopsis minuta*. *Mycologia* **101**: 878–887.

Poinar GO, Vega FE (2018). A mid-Cretaceous ambrosia fungus, *Paleoambrosia entomophila gen. nov. et sp. nov.* (*Ascomycota*: *Ophiostomatales*) in Burmese (Myanmar) amber, and evidence for a femoral mycangium. *Fungal Biology* **122**: 1159–1162.

Réblová M, Gams W, Seifert KA (2011). *Monilochaetes* and allied genera of the *Glomerellales*, and a reconsideration of families in the *Microascales*. *Studies in Mycology* **68**: 163–191.

Reid J, Hausner G (2015). A new *Graphilbum* species from western hemlock (*Tsuga heterophylla*) in Canada. *Mycotaxon* **130**: 399–419.

Rodrigues AM, De Hoog GS, De Camargo ZP (2013). Emergence of pathogenicity in the *Sporothrix schenckii* complex. *Medical Mycology* **51**: 405–412.

Rodrigues AM, De Hoog GS, De Cássia Pires D, *et al.* (2014). Genetic diversity and antifungal susceptibility profiles in causative agents of sporotrichosis. *BMC Infectious Diseases* **14**: 219.

Roets F, De Beer ZW, Dreyer LL, *et al.* (2006). Multi-gene phylogeny for *Ophiostoma* spp. reveals two new species from *Protea* infructescences. *Studies in Mycology* **55**: 199–212.

Roets F, De Beer ZW, Wingfield MJ, *et al.* (2008). *Ophiostoma gemellus* and *Sporothrix variecibatus* from mites infesting *Protea* infructescences in South Africa. *Mycologia* **100**: 496–510.

Roets F, Wingfield MJ, Crous PW, *et al.* (2013). Taxonomy and ecology of ophiostomatoid fungi associated with *Protea* infructescences. In: *The Ophiostomatoid Fungi*: *Expanding Frontiers,* (Seifert KA, De Beer ZW, Wingfield MJ, ed.): 177–187. CBS-KNAW Fungal Biodiversity Centre, Utrecht, The Netherlands.

Roets F, Wingfield BD, De Beer ZW, *et al.* (2010). Two new *Ophiostoma* species from *Protea caffra* in Zambia. *Persoonia*: *Molecular Phylogeny and Evolution of Fungi* **24**: 18–28.

Rollins F, Jones KG, Krokene P, *et al.* (2001). Phylogeny of asexual fungi associated with bark and ambrosia beetles. *Mycologia* **93**: 991–996.

Romón P, De Beer ZW, Fernández M, *et al.* (2014a). Ophiostomatoid fungi including two new fungal species associated with pine root-feeding beetles in northern Spain. *Antonie van Leeuwenhoek* **106**: 1167–1184.

Romón P, De Beer ZW, Zhou X, *et al*. (2014b). Multigene phylogenies of *Ophiostomataceae* associated with Monterey pine bark beetles in Spain reveal three new fungal species. *Mycologia* **106**: 119–132.

Rumbold CT (1931) Two blue-stain fungi associated with bark-beetle infestation of pines. *Journal of Agricultural Research* **43**: 847–873.

Rumbold CT (1941). A blue stain fungus, *Ceratostomella montium n. sp.*, and some yeasts associated with two species of *Dendroctonus*. *Journal of Agricultural Research* **62**: 589–601.

Saccardo PA (1881). Fungi Gallici lecti a cl. viris P. Brunaud, C.C. Gillet, Abb. Letendre, A. Malbranche, J. Therry vel editi in Mycotheca Gallica C. Roumeguèri. Series III. *Michelia* **2**: 302–371.

Saucedo-Carabez JR, Ploetz RC, Konkol JL, *et al.* (2018). Partnerships between ambrosia beetles and fungi: Lineage-specific promiscuity among vectors of the Laurel wilt pathogen, *Raffaelea lauricola*. *Microbial Ecology* **76**: 925–940.

Schoch CL, Robbertse B, Robert V, *et al*. (2014). Finding needles in haystacks: linking scientific names, reference specimens and molecular data. *Database*: 1–21, doi:10.1093/dababase/bau061

Schoch CL, Seifert KA, Huhndorf S, *et al*. (2012). Nuclear ribosomal internal transcribed spacer (ITS) region as a universal DNA barcode marker for *Fungi*. *Proceedings of the National Academy of Sciences* **109**: 6241–6246.

Schroeder S, Kim SH, Cheung WT, *et al.* (2001). Phylogenetic relationship of *Ophiostoma piliferum* to other sapstain fungi based on the nuclear rRNA gene. *FEMS Microbiology Letters* **195**: 163–167.

Seifert KA, De Beer ZW, Wingfield MJ (2013). The ophiostomatoid fungi: expanding frontiers. *CBS Biodiversity Series* **12**. CBS-KNAW Biodiversity Centre, Utrecht, The Netherlands.

Seifert KA, Okada G (1993). *Graphium* anamorphs of *Ophiostoma* species and similar anamorphs of other Ascomycetes. In: *Ceratocystis and Ophiostoma*: *Taxonomy, Ecology and Pathogenicity,* (Wingfield MJ, Seifert KA & Webber J, eds.): 27–41. American Phytopathological Society Press, St. Paul, Minnesota.

Seo ST, Kim KH, Lee SH, *et al.* (2010). Genotypic characterization of Oak Wilt pathogen *Raffaelea quercus-mongolicae* and *R. quercivora* strains. *Research in Plant Disease* **16**: 219–223.

Seppey M, Manni M, Zdobnov EM (2019). BUSCO: assessing genome assembly and annotation completeness. *Methods in Molecular Biology* **1962**: 227–245.

Shear CL (1923). Life Histories and undescribed genera and species of fungi. *Mycologia* **15**: 120–131.

Siemaszko W (1939). Zespoly grzybów towarzyszących kornikom polskim. *Planta Polonica* **7**: 1–54.

Silvestro D, Michalak I (2012). raxmlGUI: a graphical front-end for RAxML. *Organisms Diversity & Evolution* **12**: 335–337.

Simmons DR, De Beer ZW, Huang Y-T, *et al.* (2016). New *Raffaelea* species (*Ophiostomatales*) from the USA and Taiwan associated with ambrosia beetles and plant hosts. *IMA Fungus* **7**: 265–273.

Six D, De Beer ZW, Duong TA, *et al.* (2011). Fungal associates of the lodgepole pine beetle, *Dendroctonus murrayanae*. *Antonie van Leeuwenhoek* **100**: 231–244.

Spatafora JW, Blackwell M (1994). The polyphyletic origins of ophiostomatoid fungi. *Mycological Research* **98**: 1–9.

Stamatakis A (2014). RAxML version 8: a tool for phylogenetic analysis and post-analysis of large phylogenies. *Bioinformatics* **30**: 1312–1313.

Stielow JB, Lévesque CA, Seifert KA, *et al.* (2015). One fungus, which genes? Development and assessment of universal primers for potential secondary fungal DNA barcodes. *Persoonia*: *Molecular Phylogeny and Evolution of Fungi* **35**: 242–263.

Suh S-O, Blackwell M (1999). Molecular phylogeny of the cleistothecial fungi placed in *Cephalothecaceae* and *Pseudeurotiaceae*. *Mycologia* **91**: 836–848.

Sun J, Lu M, Gillette NE, *et al.* (2013). Red Turpentine beetle: innocuous native becomes invasive tree killer in China. *Annual Review of Entomology* **58**: 293–311.

Swofford DL (2003). *PAUP* 4.0*: *phylogenetic analysis using parsimony (*and other methods)*. Sunderland, Massachusetts: Sinauer Associates.

Taerum S, De Beer ZW, Duong TA, *et al.* (2012). Fungal symbionts suggest an alternative origin for the red turpentine beetle (*Dendroctonus valens*) invasion in China. Mycological Society of America 2012 Meeting. Yale University, New Haven, Connecticut.

Taerum SJ, Duong TA, De Beer ZW, *et al.* (2013). Large shift in symbiont assemblage in the invasive red turpentine beetle. *PLoS ONE* **8**: e78126.

Taerum SJ, Hoareau TB, Duong TA, *et al.* (2017). Putative origins of the fungus *Leptographium procerum*. *Fungal Biology* **121**: 82–94.

Teixeira M, De Almeida L, Kubitschek-Barreira P, *et al.* (2014). Comparative genomics of the major fungal agents of human and animal Sporotrichosis: *Sporothrix schenckii* and *Sporothrix brasiliensis*. *BMC Genomics* **15**: 943.

Thwaites JM, Farrell RL, Duncan SM, *et al.* (2005). Survey of potential sapstain fungi on *Pinus radiata* in New Zealand. *New Zealand Journal of Botany* **43**: 653–663.

Upadhyay HP (1981). *A monograph of Ceratocystis and Ceratocystiopsis*. University of Georgia Press.

Upadhyay HP, Kendrick WB (1975). Prodromus for a revision of *Ceratocystis* (*Microascales*, Ascomycetes) and its conidial states. *Mycologia* **67**: 798–805.

Van der Linde J, Six D, De Beer Z, *et al.* (2016). Novel ophiostomatalean

fungi from galleries of *Cyrtogenius africus* (*Scolytinae*) infesting dying *Euphorbia ingens*. *Antonie van Leeuwenhoek* **109**: 589–601.

Van der Nest MA, Bihon W, De Vos L, *et al.* (2014). Draft genome sequences of *Diplodia sapinea*, *Ceratocystis manginecans*, and *Ceratocystis moniliformis*. *IMA Fungus* **5**: 135–140.

Vanderpool D, Bracewell RR, McCutcheon JP (2018). Know your farmer: ancient origins and multiple independent domestications of ambrosia beetle fungal cultivars. *Molecular Ecology* **27**: 2077–2094.

Verrall AF (1943). Fungi associated with certain ambrosia beetles. *Journal of Agricultural Research* **66**: 135–144.

Vilgalys R, Hester M (1990). Rapid genetic identification and mapping of enzymatically amplified ribosomal DNA from several *Cryptococcus* species. *Journal of Bacteriology* **172**: 4238–4246.

Villarreal M, Rubio V, De Troya M, *et al.* (2005). New *Ophiostoma* species isolated from *Pinus pinaster* in the Iberian Peninsula. *Mycotaxon* **92**: 259–268.

Von Arx JA (1952). Ueber die Ascomycetengattungen *Ceratostomella* Sacc., *Ophiostoma* Syd. und *Rostrella* Zimmermann. *Antonie van Leeuwenhoek* **18**: 13–213.

Von Arx JA, Hennebert GL (1965) Deux champignons ambrosia. *Mycopathologia et Mycologia Applicata* **25**: 309–315.

Wang CY, Fang ZM, Sun BS, *et al.* (2008). High infectivity of an endoparasitic fungus strain, *Esteya vermicola,* against nematodes. *Journal of Microbiology* **46**: 380–389.

Wang H, Lun Y, Lu Q, *et al.* (2018). Ophiostomatoid fungi associated with pines infected by *Bursaphelenchusxylophilus* and *Monochamusalternatus* in China, including three new species. *MycoKeys* **39**: 1–27.

Wang X, Wang T, Wang J, *et al.* (2014). Morphological, molecular and biological characterization of *Esteya vermicola*, a nematophagous fungus isolated from intercepted wood packing materials exported from Brazil. *Mycoscience* **55**: 367–377.

Wang Y-B, Pang W-X, Yv X-N, *et al.* (2015). The effects of fluctuating culture temperature on stress tolerance and antioxidase expression in *Esteya vermicola*. *Journal of Microbiology* **53**: 122–126.

Wang Z, Liu Y, Wang H, *et al.* (2020). Ophiostomatoid fungi associated with *Ips subelongatus*, including eight new species from northeastern China. *IMA Fungus* **11**:1–29.

Weijman AC, De Hoog GS (1975). On the subdivision of the genus *Ceratocystis*. *Antonie van Leeuwenhoek* **41**: 353–360.

White TJ, Bruns T, Lee S, *et al.* (1990). Amplification and direct sequencing of fungal ribosomal RNA genes for phylogenetics. *PCR protocols*: *a guide to methods and applications* **18**: 315–322.

Wingfield BD, Ades PK, Al-Naemi FA, *et al.* (2015a). Draft genome sequences of *Chrysoporthe austroafricana*, *Diplodia scrobiculata*, *Fusarium nygamai*, *Leptographium lundbergii*, *Limonomyces culmigenus*, *Stagonosporopsis tanaceti*, and *Thielaviopsis punctulata*. *IMA Fungus* **6**: 233–248.

Wingfield BD, Ambler JM, Coetzee MPA, *et al.* (2016a) Draft genome sequences of *Armillaria fuscipes*, *Ceratocystiopsis minuta*, *Ceratocystis adiposa*, *Endoconidiophora laricicola*, *E. polonica* and *Penicillium freii* DAOMC 242723. *IMA Fungus* **7**: 217–227.

Wingfield BD, Barnes I, De Beer ZW, *et al.* (2015). Draft genome sequences of *Ceratocystis eucalypticola*, *Chrysoporthe cubensis*, *C. deuterocubensis*, *Davidsoniella virescens*, *Fusarium temperatum*, *Graphilbum fragrans*, *Penicillium nordicum*, and *Thielaviopsis musarum*. *IMA Fungus* **6**: 493–506.

Wingfield BD, Berger DK, Steenkamp ET, *et al.* (2017). Draft genome of *Cercospora zeina*, *Fusarium pininemorale*, *Hawksworthiomyces lignivorus*, *Huntiella decipiens* and *Ophiostoma ips*. *IMA Fungus* **8**: 385–396.

Wingfield BD, Duong TA, Hammerbacher A, *et al.* (2016b) Draft genome sequences for *Ceratocystis fagacearum*, *C. harringtonii*, *Grosmannia penicillata*, and *Huntiella bhutanensis*. *IMA Fungus* **7**: 317–323.

Wingfield BD, Liu M, Nguyen HDT, *et al.* (2018). Nine draft genome sequences of *Claviceps purpurea s.lat.*, including *C. arundinis*, *C. humidiphila*, and *C. cf. spartinae*, pseudomolecules for the pitch canker pathogen *Fusarium circinatum*, draft genome of *Davidsoniella eucalypti*, *Grosmannia galeiformis*, *Quambalaria eucalypti*, and *Teratosphaeria destructans*. *IMA Fungus* **9**: 401–418.

Wingfield MJ (1983). Association of *Verticicladiella procera* and *Leptographium terebrantis* with insects in the Lake States. *Canadian Journal of Forest Research* **13**: 1238–1245.

Wingfield MJ (1993). *Leptographium* species as anamorphs of *Ophiostoma*. In: *Ceratocystis and Ophiostoma*: *Taxonomy, Ecology and Pathogenicity,* (Wingfield MJ, Seifert KA & Webber J, eds.): 43–51. American Phytopathological Society Press, St. Paul, Minnesota.

Wingfield MJ, Barnes I, De Beer ZW, *et al.* (2017). Novel associations between ophiostomatoid fungi, insects and tree hosts: current status—future prospects. *Biological Invasions* **19**: 3215–3228.

Wingfield MJ, Harrington TC, Crous PW (1994). Three new *Leptographium* species associated with conifer roots in the United States. *Canadian Journal of Botany* **72**: 227–238.

Wingfield MJ, Marasas WFO (1980). *Verticicladiella alacris sp. nov.*, associated with a root disease of pines in South Africa. *Transactions of the British Mycological Society* **75**: 21–28.

Wingfield MJ, Seifert KA, Webber JF (1993). *Ceratocystis and Ophiostoma*: *taxonomy, ecology, and pathogenicity*. American Phytopathological Society, St. Paul, Minnesota, USA.

Witcosky JJ, Hansen EM (1985). Root-colonizing insects recovered from Douglas-fir in various stages of decline due to black-stain root disease. *Phytopathology* **75**: 399–402.

Witcosky JJ, Schowalter TD, Hansen EM (1986). *Hylastes nigrinus* (*Coleoptera*: *Scolytidae*), *Pissodes fasciatus*, and *Steremnius carinatus* (*Coleoptera*: *Curculionidae*) as Vectors of Black-stain Root Disease of Douglas-fir. *Environmental Entomology* **15**: 1090–1095.

Yaguchi T, Sano A, Yarita K, *et al.* (2006). A new species of *Cephalotheca* isolated from a Korean patient. *Mycotaxon* **96**: 309–322.

Yamaoka Y (2017). Taxonomy and pathogenicity of ophiostomatoid fungi associated with bark beetles infesting conifers in Japan, with special reference to those related to subalpine conifers. *Mycoscience* **58**: 221–235.

Yamaoka Y, Wingfield MJ, Takahashi I, *et al.* (1997). Ophiostomatoid fungi associated with the spruce bark beetle *Ips typographus f. aponicus* in Japan. *Mycological Research* **101**: 1215–1227.

Yan Z, Sun J, Don O, *et al.* (2005). The red turpentine beetle, *Dendroctonus valens* LeConte (Scolytidae): an exotic invasive pest of pine in China. *Biodiversity and Conservation* **14**: 1735–1760.

Yin M, Duong TA, Wingfield MJ, *et al.* (2015). Taxonomy and phylogeny of the *Leptographium procerum* complex, including *Leptographium sinense sp. nov.* and *Leptographium longiconidiophorum sp. nov. Antonie van Leeuwenhoek* **107**: 547–563.

Yin M, Wingfield MJ, Zhou X, *et al.* (2016). Multigene phylogenies and morphological characterization of five new *Ophiostoma* spp. associated with spruce-infesting bark beetles in China. *Fungal Biology* **120**: 454–470.

Yin M, Wingfield MJ, Zhou X, *et al.* (2019). Taxonomy and phylogeny of the *Leptographium olivaceum* complex (*Ophiostomatales*, *Ascomycota*), including descriptions of six new species from China and Europe. *MycoKeys* **60**: 93–123.

Yin ML, Wingfield MJ, Zhou XD, *et al.* (2020). Phylogenetic re-evaluation of the *Grosmania penicillata* complex (*Ascomycota*, *Ophiostomatales*), with the description of five new species from China and USA. *Fungal Biology* **124**: 110–124.

Zanzot JW, De Beer ZW, Eckhardt LG, *et al.* (2010). A new *Ophiostoma* species from loblolly pine roots in the southeastern United States. *Mycological Progress* **9**: 447–457.

Zhang Y, Hagen F, Stielow B, *et al.* (2013). Global evolutionary patterns in pathogenic *Sporothrix* species. 1st International Meeting on *Sporothrix* and Sporotrichosis. Rio de Janeiro, Brazil.

Zhou X, De Beer ZW, Cibrian D, *et al.* (2004a). Characterisation of *Ophiostoma* species associated with pine bark beetles from Mexico, including *O. pulvinisporum sp. nov. Mycological Research* **108**: 690–698.

Zhou X, De Beer ZW, Harrington TC, *et al.* (2004b). Epitypification of *Ophiostoma galeiforme* and phylogeny of species in the *O. galeiforme* complex. *Mycologia* **96**: 1306–1315.

Zhou XD, De Beer ZW, Wingfield MJ (2006). DNA sequence comparisons of *Ophiostoma* spp., including *Ophiostoma aurorae sp. nov*., associated with pine bark beetles in South Africa. *Studies in Mycology* **55**: 269–277.

Zhou X, De Beer ZW, Wingfield M (2013). Ophiostomatoid fungi associated with conifer-infesting bark beetles in China. In: *The Ophiostomatoid Fungi*: *Expanding Frontiers,* (Seifert KA, De Beer ZW, Wingfield MJ, ed.): 91–98. CBS-KNAW Fungal Biodiversity Centre, Utrecht, The Netherlands.

Zipfel RD, De Beer ZW, Jacobs K, *et al.* (2006). Multi-gene phylogenies define *Ceratocystiopsis* and *Grosmannia* distinct from *Ophiostoma*. *Studies in Mycology* **55**: 75–97.

Supplementary Material: https://studiesinmycology.org/

Fig. S1. Phylogenetic tree derived from maximum likelihood analysis of the LSU gene region. The dataset consisted of 233 isolates and 859 characters before and after Gblocks treatment. Bootstrap values above 60 % are shown. Purple blocks indicate existing genera, yellow blocks new genera described in this study, green blocks genera that we redefine here, and blue blocks indicate genera that we here re-instate and re-define.

Fig. S2. Phylogenetic tree derived from maximum likelihood analysis of the ITS gene region. The dataset consisted of 235 isolates and 169 characters after Gblocks treatment (1 171 characters prior to Gblocks, including gaps). ML values above 60 % are shown. Purple blocks indicate existing genera, yellow blocks new genera described in this study, green blocks genera that we redefine here, and blue blocks indicate genera that we here re-instate and re-define.

Fig. S3. Phylogenetic tree derived from maximum likelihood analysis of the *TEF1-α* gene region. The dataset consisted of 207 isolates and 380 characters after Gblocks treatment (655 characters prior to Gblocks, including gaps). ML values above 60 % are shown. Purple blocks indicate existing genera, yellow blocks new genera described in this study, green blocks genera that we redefine here, and blue blocks indicate genera that we here re-instate and re-define.

Fig. S4. Phylogenetic tree derived from maximum likelihood analysis of the *RPBII* gene region. The dataset consisted of 171 isolates and 952 characters after Gblocks treatment (1 108 characters prior to Gblocks, including gaps). ML values above 60 % are shown. Purple blocks indicate existing genera, yellow blocks new genera described in this study, green blocks genera that we redefine here, and blue blocks indicate genera that we here re-instate and re-define.

Table S1. Taxa included in the phylogenomic analyses and their genome sequence statistics

Studies in Mycology 101: 121–243 (2022).

Taxonomy, phylogeny and identification of *Chaetomiaceae* with emphasis on thermophilic species

X.W. Wang[1,2#*], P.J. Han[1#], F.Y. Bai[1], A. Luo[3], K. Bensch[2], M. Meijer[2], B. Kraak[2], D.Y. Han[1], B.D. Sun[1], P.W. Crous[2,4,5], J. Houbraken[2*]

[1]*State Key Laboratory of Mycology, Institute of Microbiology, Chinese Academy of Sciences, No. 3, 1st Beichen West Road, Chaoyang District, Beijing 100101, China;* [2]*Westerdijk Fungal Biodiversity Institute, Uppsalalaan 8, 3584 CT, Utrecht, the Netherlands;* [3]*Key Laboratory of Zoological Systematics and Evolution, Institute of Zoology, Chinese Academy of Sciences, Beijing 100101, China;* [4]*Wageningen University and Research Centre (WUR), Laboratory of Phytopathology, Droevendaalsesteeg 1, 6708 PB Wageningen, The Netherlands;* [5]*Microbiology, Department of Biology, Utrecht University, Padualaan 8, 3584 CH Utrecht, the Netherlands*

[#]These authors contributed equally to the work
**Corresponding authors*: X.W. Wang, wangxw@im.ac.cn; J. Houbraken, j.houbraken@wi.knaw.nl

Abstract: *Chaetomiaceae* comprises phenotypically diverse species, which impact biotechnology, the indoor environment and human health. Recent studies showed that most of the traditionally defined genera in *Chaetomiaceae* are highly polyphyletic. Many of these morphology-based genera, such as *Chaetomium*, *Thielavia* and *Humicola*, have been redefined using multigene phylogenetic analysis combined with morphology; however, a comprehensive taxonomic overview of the family is lacking. In addition, the phylogenetic relationship of thermophilic *Chaetomiaceae* species with non-thermophilic taxa in the family is largely unclear due to limited taxon sampling in previous studies. In this study, we provide an up-to-date overview on the taxonomy and phylogeny of genera and species belonging to *Chaetomiaceae*, including an extensive taxon sampling of thermophiles. A multigene phylogenetic analysis based on the ITS (internal transcribed spacers 1 and 2 including the 5.8S nrDNA), LSU (D1/D2 domains of the 28S nrDNA), *rpb2* (partial RNA polymerase II second largest subunit gene) and *tub2* (β-tubulin gene) sequences was performed on 345 strains representing *Chaetomiaceae* and 58 strains of other families in *Sordariales*. Divergence times based on the multi-gene phylogeny were estimated as aid to determine the genera in the family. Genera were delimited following the criteria that a genus must be a statistically well-supported monophyletic clade in both the multigene phylogeny and molecular dating analysis, fall within a divergence time of over 27 million years ago, and be supported by ecological preference or phenotypic traits. Based on the results of the phylogeny and molecular dating analyses, combined with morphological characters and temperature-growth characteristics, 50 genera and 275 species are accepted in *Chaetomiaceae*. Among them, six new genera, six new species, 45 new combinations and three new names are proposed. The results demonstrate that the thermophilic species fall into seven genera (*Melanocarpus*, *Mycothermus*, *Remersonia*, *Thermocarpiscus gen. nov*., *Thermochaetoides gen. nov*., *Thermothelomyces* and *Thermothielavioides*). These genera cluster in six separate lineages, suggesting that thermophiles independently evolved at least six times within the family. A list of accepted genera and species in *Chaetomiaceae*, together with information on their MycoBank numbers, living ex-type strains and GenBank accession numbers to ITS, LSU, *rpb2* and *tub2* sequences is provided. Furthermore, we provide suggestions how to describe and identify *Chaetomiaceae* species.

Key words: Generic divergence times, Identification, Multi-gene phylogeny, New taxa, Taxonomic novelties, Thermophilic species.
Taxonomic novelties: new genera: *Parvomelanocarpus* X.Wei Wang & Houbraken, *Pseudohumicola* X.Wei Wang, P.J. Han, F.Y. Bai & Houbraken, *Tengochaeta* X.Wei Wang & Houbraken, *Thermocarpiscus* X.Wei Wang & Houbraken, *Thermochaetoides* X.Wei Wang & Houbraken, *Xanthiomyces* X.Wei Wang & Houbraken; **New species:** *Botryotrichum geniculatum* X.Wei Wang, P.J. Han & F.Y. Bai, *Chaetomium subaffine* Sergejeva ex X.Wei Wang & Houbraken, *Humicola hirsuta* X.Wei Wang, P.J. Han & F.Y. Bai, *Subramaniula latifusispora* X.Wei Wang, P.J. Han & F.Y. Bai, *Tengochaeta nigropilosa* X.Wei Wang & Houbraken, *Trichocladium tomentosum* X.Wei Wang, P.J. Han & F.Y. Bai; **New combinations:** *Achaetomiella gracilis* (Udagawa) Houbraken, X.Wei Wang, P.J. Han & F.Y. Bai, *Allocanariomyces americanus* (Cañete-Gibas *et al.*) Cañete-Gibas, Wiederhold, X.Wei Wang & Houbraken, *Amesia dreyfussii* (Arx) X.Wei Wang & Houbraken, *Amesia raii* (G. Malhotra & Mukerji) X.Wei Wang & Houbraken, *Arcopilus macrostiolatus* (Stchigel *et al.*) X.Wei Wang & Houbraken, *Arcopilus megasporus* (Sörgel ex Seth) X.Wei Wang & Houbraken, *Arcopilus purpurascens* (Udagawa & Y. Sugiy.) X.Wei Wang & Houbraken, *Arxotrichum deceptivum* (Malloch & Benny) X.Wei Wang & Houbraken, *Arxotrichum gangligerum* (L.M. Ames) X.Wei Wang & Houbraken, *Arxotrichum officinarum* (M. Raza & L. Cai) X.Wei Wang & Houbraken, *Arxotrichum piluliferoides* (Udagawa & Y. Horie) X.Wei Wang & Houbraken, *Arxotrichum repens* (Guarro & Figueras) X.Wei Wang & Houbraken, *Arxotrichum sinense* (K.T. Chen) X.Wei Wang & Houbraken, *Botryotrichum inquinatum* (Udagawa & S. Ueda) X.Wei Wang & Houbraken, *Botryotrichum retardatum* (A. Carter & R.S. Khan) X.Wei Wang & Houbraken, *Botryotrichum trichorobustum* (Seth) X.Wei Wang & Houbraken, *Botryotrichum vitellinum* (A. Carter) X.Wei Wang & Houbraken, *Collariella anguipilia* (L.M. Ames) X.Wei Wang & Houbraken, *Collariella hexagonospora* (A. Carter & Malloch) X.Wei Wang & Houbraken, *Collariella pachypodioides* (L.M. Ames) X.Wei Wang & Houbraken, *Ovatospora amygdalispora* (Udagawa & T. Muroi) X.Wei Wang & Houbraken, *Ovatospora angularis* (Yu Zhang & L. Cai) X.Wei Wang & Houbraken, *Parachaetomium biporatum* (Cano & Guarro) X.Wei Wang & Houbraken, *Parachaetomium hispanicum* (Guarro & Arx) X.Wei Wang & Houbraken, *Parachaetomium inaequale* (Pidopl. *et al.*) X.Wei Wang & Houbraken, *Parachaetomium longiciliatum* (Yu Zhang & L. Cai) X.Wei Wang & Houbraken, *Parachaetomium mareoticum* (Besada & Yusef) X.Wei Wang & Houbraken, *Parachaetomium muelleri* (Arx) X.Wei Wang & Houbraken, *Parachaetomium multispirale* (A. Carter *et al.*) X.Wei Wang & Houbraken, *Parachaetomium perlucidum* (Sergejeva) X.Wei Wang & Houbraken, *Parachaetomium subspirilliferum* (Sergejeva) X.Wei Wang & Houbraken, *Parathielavia coactilis* (Nicot) X.Wei Wang & Houbraken, *Parvomelanocarpus tardus* (X.Wei Wang & Samson) X.Wei Wang & Houbraken, *Parvomelanocarpus thermophilus* (Abdullah & Al-Bader) X.Wei Wang & Houbraken, *Pseudohumicola atrobrunnea* (X.Wei Wang *et al.*) X.Wei Wang, P.J. Han, F.Y. Bai & Houbraken, *Pseudohumicola pulvericola* (X.Wei Wang *et al.*) X.Wei Wang, P.J. Han, F.Y. Bai & Houbraken, *Pseudohumicola semispiralis* (Udagawa & Cain) X.Wei Wang, P.J. Han, F.Y. Bai & Houbraken, *Pseudohumicola subspiralis* (Chivers) X.Wei Wang, P.J. Han, F.Y. Bai & Houbraken, *Staphylotrichum koreanum* (Hyang B. Lee & T.T.T. Nguyen) X.Wei Wang & Houbraken, *Staphylotrichum limonisporum* (Z.F. Zhang & L. Cai) X.Wei Wang & Houbraken, *Subramaniula lateralis* (Yu Zhang & L. Cai) X.Wei Wang & Houbraken, *Thermocarpiscus australiensis* (Tansey & M.A. Jack) X.Wei Wang & Houbraken, *Thermochaetoides dissita* (Cooney & R. Emers.) X.Wei Wang & Houbraken, *Thermochaetoides thermophila* (La Touche) X.Wei Wang & Houbraken, *Xanthiomyces spinosus* (Chivers) X.Wei Wang & Houbraken; **New names:** *Chaetomium neoglobosporum* X.Wei Wang & Houbraken, *Thermothelomyces fergusii* X.Wei Wang & Houbraken, *Thermothelomyces myriococcoides* X.Wei Wang & Houbraken; **Lecto- and / or epi-typifications (basionyms)**: *Botryoderma rostratum* Papendorf & H.P. Upadhyay, *Botryotrichum piluliferum* Sacc. & Marchal, *Chaetomium carinthiacum* Sörgel, *Thielavia heterothallica* Klopotek.

Studies in Mycology

Citation: Wang XW, Han PJ, Bai FY, Luo A, Bensch K, Meijer M, Kraak B, Han DY, Sun BD, Crous PW, Houbraken J (2022). Taxonomy, phylogeny and identification of *Chaetomiaceae* with emphasis on thermophilic species. *Studies in Mycology* **101**: 121–243. doi: 10.3114/sim.2022.101.03.
Received: 14 September 2021; **Accepted:** 16 February 2022; **Effectively published online:** 1 April 2022
Corresponding editor: Robert A. Samson

INTRODUCTION

Species of the family *Chaetomiaceae* exhibit high phenotypical and ecological diversity and are medically and economically important. Well-known taxa of the family include the indoor contaminant *Chaetomium globosum*, the mycetoma-causing agent *Madurella mycetomatis* and the enzyme producer *Thermothelomyces thermophilus* (= *Myceliophthora thermophila*) (Ahmed *et al.* 2002, van den Brink *et al.* 2012, Samson *et al.* 2019). *Chaetomiaceae* have a worldwide distribution. The majority are saprobes and occur in soil, dung, air, seed, compost, rotting plant materials and indoor environments (Cooney & Emerson 1964, Tiscornia *et al.* 2009, Betancourt *et al.* 2013, Wang *et al.* 2016a).

Species in *Chaetomiaceae* gained attention in biotechnology because they are producers of industrial-relevant enzymes (Berka *et al.* 2011, Harreither *et al.* 2011, Glass *et al.* 2013, Vivi *et al.* 2019), with the thermophilic species being used for the production of plant-biomass degrading thermostable enzymes (Margaritis *et al.* 1986, Haki & Rakshit 2003, Viikari *et al.* 2007, Berka *et al.* 2011, van den Brink *et al.* 2012, Yang *et al.* 2014a, Singh 2016). Other potential applications of *Chaetomiaceae* are their use as biological control organisms of plant diseases, bioorganic fertilisers (Lang *et al.* 2012, Hu *et al.* 2013, Yang *et al.* 2014b, Zhang *et al.* 2014b, Larran *et al.* 2016) or growth promoters of *Agaricus bisporus* mycelium (Straatsma *et al.* 1994). *Chaetomiaceae* are able to produce various bioactive secondary metabolites that display a wide range of cytotoxic, anticancer, antioxidant, antibacterial or antimalarial activities (Kharwar 2011, Gond *et al.* 2012, Gutierrez *et al.* 2012, Zhang *et al.* 2012, Selim *et al.* 2014, Wang *et al.* 2017, Gao *et al.* 2019, Yadav *et al.* 2019)

In contrast to the positive aspects mentioned above, some *Chaetomiaceae* species are negatively associated with human health. For example, *Madurella* species are agents of human subcutaneous mycoses, causing human mycetoma in arid areas of northeastern Africa (Ahmed *et al.* 2002). The presence of medically important species in *Chaetomiaceae* is not restricted to *Madurella*, and infective species are distributed across the family (*e.g., Canariomyces subthermophilus*, *Chaetomium globosum*, *Humicola atrobrunnea* and *Subramaniula anamorphosa*) (Ahmed *et al.* 2016, Wang *et al.* 2019b). Most human infections by *Chaetomiaceae* species are caused by traumatic inoculations into otherwise healthy humans, and rarely occur as deep infections in severely immunocompromised hosts (Abbott *et al.* 1995, Guppy *et al.* 1998, Ahmed *et al.* 2002, Barron *et al.* 2003, Al-Aidaroos *et al.* 2007, Hubka *et al.* 2011). Furthermore, the aflatoxin precursor and mycotoxin sterigmatocystin can be produced by several species within the family (Rank *et al*. 2011). In addition, *Chaetomiaceae* also occur in the indoor environment, causing disfigurement of surfaces and contribute to the development of rhinitis and asthma due to the production of mycotoxins, microbial volatile organic compounds and fungal particles (ascospores, hyphal fragments) (Wang *et al.* 2016b).

In 1817, Gustav Kunze introduced *Chaetomium* with *Ch. globosum* as type (Kunze & Schmidt 1817). The family *Chaetomiaceae* was established in 1885 to accommodate fungi that produce non-stromatic ascomata with a membranaceous ascomatal wall, fasciculate and evanescent asci and single-celled, smooth, pigmented ascospores (Winter 1885, Ames 1963, Hawksworth 1971). In the long taxonomic history of *Chaetomiaceae*, the most important change was made by von Arx *et al.* (1986). Rather than focusing on the variable ascomatal hairs, he laid emphasis on asci and ascospores characters, the presence of germ pores on ascospores and the structure of the ascomatal wall to delimit species. However, there were limited changes to the generic concept. For example, *Chaetomium* remained for species producing ostiolate ascomata covered by relatively well-developed hairs, *Achaetomium* for species having ostiolate ascomata covered by hypha-like ascomatal hairs, *Chaetomidium* for taxa producing non-ostiolate ascomata with pseudoparenchymatous wall covered by well-developed ascomatal hairs, and *Thielavia* for those having non-ostiolate, glabrous or tomentose ascomata with a wall of *textura epidermoidea* (von Arx *et al.* 1986, 1988, Abdel-Azeem 2020). The only change at the generic level was splitting several genera from previously existing genera, such as separating *Corynascus* (for species producing ascospores with two apical germ pores and a chrysosporium-like conidial morph) and *Corynascella* (for species producing ascospores with two apical germ pores but lacking a chrysosporium-like conidial morph) from *Thielavia* (von Arx 1973b, 1975a), and separating *Subramaniula* from *Achaetomium* for species producing urniform and nearly glabrous ascomata with a translucent wall and a wide ostiole surrounded by a hyaline collar (von Arx 1985). The morphologically-defined *Chaetomium* became a large genus with more than 400 proposed species epithets and approximately 270 accepted species (Abdel-Azeem 2020).

Traditional taxonomic studies of *Chaetomiaceae* mainly focused on sexually reproducing species (Zopf 1881, Ames 1963, von Arx *et al.* 1986, 1988). However, phylogenetic studies showed that different asexual morphs are present in the family, and these can be, for example, acremonium-, humicola-, staphylotrichum- or trichocladium-like (Wang *et al.* 2019a). Recent taxonomic studies based on molecular phylogenetic analyses also recognised the polyphyly of many morphologically-defined genera, including *Chaetomium*, *Chaetomidium* and *Thielavia* (Greif *et al.* 2009, van den Brink *et al.* 2015, Wang *et al.* 2016b). A modern classification system of *Chaetomiaceae* that includes monophyletic lineages and that is consistent with the current single name nomenclature system has been established. In total, 26 genera are recently proposed: *Allobotryotrichum* (Raza *et al.* 2019), *Allocanariomyces* (Mehrabi *et al.* 2020), *Amesia* and *Arcopilus* (Wang *et al.* 2016b), *Arxotrichum* (Crous *et al.* 2018), *Batnamyces* (Noumeur *et al.* 2020), *Brachychaeta*, *Carteria*, *Chrysanthotrichum* and *Chrysocorona* (Wang *et al.* 2019b), *Collariella* (Wang *et al.* 2016b), *Condenascus* (Wang *et al.* 2019b), *Crassicarpon* (Marin-Felix *et al.* 2015), *Dichotomopilus* (Wang *et al.* 2016b), *Floropilus*, *Hyalosphaerella* and *Microthielavia* (Wang *et al.* 2019b), *Mycothemus* (Natvig *et al.* 2015, Wang *et al.* 2019a), *Ovatospora* (Wang *et al.* 2016b), *Parachaetomium* (Mehrabi *et al.* 2020), *Parathielavia* (Wang *et al.* 2019b), *Pseudocanariomyces* (Ryan *et al.* 2021), *Pseudothielavia* and *Stolonocarpus* (Wang *et al.* 2019b), *Thermothelomyces* (Marin-Felix *et al.* 2015), *Thermothielavioides* (Wang *et al.* 2019b). Many existing genera have also been re-defined, including *Acrophialophora*, *Botryotrichum*, *Canariomyces*, *Chaetomium*,

Humicola, *Staphylotrichum*, *Subramaniula*, *Thielavia*, and *Trichocladium* (Wang *et al.* 2016b, 2019a, b). Although this series of recent studies have elucidated the phylogenetic relationships of *Chaetomiaceae* (Wang *et al.* 2016a, b, 2019a, b), a comprehensive taxonomic overview is still lacking, which may hamper correct species identification, resulting in incorrect classification at species and generic levels (Raza *et al.* 2019).

Thermophilic fungi were defined as those with a maximum growth temperature above 50 °C and a minimum growth temperature at 20 °C or even higher (Cooney & Emerson 1964), or with a faster growth rate at 45 °C than at 34 °C (Morgenstern *et al.* 2012). They are of great importance as a potential source of thermostable enzymes in industry and as a production platform for biotechnology at elevated temperatures (van den Brink *et al.* 2012). Morgenstern *et al.* (2012) reported the presence of 23 thermophilic species in Kingdom *Fungi* and demonstrated their polyphyly: 13 species (of which three proved to be conspecific, Wang *et al.* 2019a) fell into the *Chaetomiaceae* (*Sordariales*), six belonged to the *Eurotiales* and one to the *Onygenales* in *Ascomycota*, and three in the *Mucoromycota*. This clearly shows that *Chaetomiaceae* harbours the most thermophilic species in Kingdom *Fungi*. Various studies adopted inconsistent names for some of the thermophilic *Chaetomiaceae* species, mainly caused by confusing taxonomy based on morphology. Natvig *et al.* (2015) introduced the name *Mycothermus thermophilus* for a fungus, which historically was named *Scytalidium thermophilum* or *Torula thermophila*. Subsequently, Wang *et al.* (2019b) synonymised *Humicola insolens* and *Humicola grisea* var. *thermoides* with *Mycothermus thermophilus*. During the phylogenetic re-evaluation of the genus *Thielavia*, *Thermothielavioides terrestris* was introduced to accommodate the thermophilic species "*Thielavia terrestris*" which produces thielavia-like ascomata, but is phylogenetically distant from the type species of *Thielavia* (Wang *et al.* 2019b). Marin-Felix *et al.* (2015) segregated *Myceliophthora sensu* van den Brink *et al.* (2012) into four genera: *Myceliophthora*, the resurrected genus *Corynascus*, and two newly-proposed thermophilic genera *Crassicarpon* and *Thermothelomyces*. In their analysis, however, only four other *Chaetomiaceae* species were included as a reference, and their phylogenetic relationships with other genera in the family remain unclear. Despite these studies, the classification and relationships of some other thermophilic species in the family is still poorly addressed. *Chaetomium thermophilum*, for example, is one of the few thermophilic fungal species with the optimum growth temperature at 45–50 °C and maximum up to 60 °C, reaching the upper limit of growth for *Eukarya* (Millner 1977, Morgenstern *et al.* 2012, de Oliveira *et al.* 2015). There has been evidence that *Ch. thermophilum* is distantly related to *Chaetomium sensu stricto* (van den Brink *et al.* 2012, Wang *et al.* 2016a, b, Zhang *et al.* 2017b); however, no taxonomic update has been made for this species.

Molecular-clock dating analysis proved helpful to delimit taxa at different taxonomic levels. The molecular evolutionary clock concept or the molecular clock hypothesis was already proposed in the 1960s, postulating a constant evolutionary rate at the molecular level (Zuckerkandl & Pauling 1965). Molecular-clock dating analysis greatly advanced over the past decades and with the availability of DNA sequence data and suitable fossil calibrations, it has been widely used to estimate timescales for different life forms on earth or in studying the macroevolutionary process (Bourguignon *et al.* 2014, Zanne *et al.* 2014, dos Reis *et al.* 2015, Chen *et al.* 2019, Ho 2020). In mycology, molecular-clock dating has been employed to infer macroevolutionary patterns of speciation and extinction of mushroom-forming fungi (*Agaricomycetes*) (Varga *et al.* 2019), and to infer the origin and diversification of genera and fungi in certain specific environments over time (Wang *et al.* 2018, Zhang *et al.* 2018, Steenwyk *et al.* 2019, Wang *et al.* 2019c, Zhu *et al.* 2019). It has also been used as additional evidence for classification arrangements at different taxonomic levels. Hyde *et al.* (2017) proposed a series of evolutionary periods that could be used as a guide to determine the various higher ranks in Kingdom *Fungi*: phyla >550 million years ago (Mya), subphyla 400–550 Mya; classes 300–400 Mya; subclasses 250–300 Mya, orders 150–250 Mya and families 50–150 Mya. They furthermore proposed that classification schemes and ranking of taxa should, where possible, incorporate a polyphasic approach including phylogeny, phenotype, and estimate of divergence times. Molecular dating analyses have been applied in various taxonomic studies. For example, to standardise taxonomic ranks of *Basidiomycota*, a universal criterion was proposed in which taxa must be monophyletic and statistically well-supported in molecular dating analyses (Zhao *et al.* 2017). In order to stabilise ranks in *Basidiomycota*, He *et al.* (2019) subsequently estimated the divergence times within this phylum (to family level). Examples in *Ascomycota* include those of Píchová *et al.* (2018), who used molecular dating to support their proposal of an infrageneric classification in *Claviceps* and Guterres *et al.* (2018), who used multilocus phylogenetic analyses followed by divergence time estimation to demonstrate a natural placement of *Apiosphaeria guaranitica* (the causal agent of brown crust disease of bignoniaceous plants) within *Diaporthaceae* (*Diaporthales*) rather than in *Phyllachoraceae* (*Phyllachorales*). In the present study, molecular dating analysis was used as an addition to the commonly used phylogenetic analyses for revealing phylogenetic relationships of genera in *Chaetomiaceae*.

Lists of accepted species are compiled to assist users of the taxonomy in basic and applied research fields to obtain the correct species names. These lists have been prepared for various genera, such as *Aspergillus, Cladosporium, Fusarium, Penicillium* and *Trichoderma*, and sometimes also include data on reference sequences, (ex-)type information and MycoBank numbers (Samson *et al.* 2014, Visagie *et al.* 2014, Yilmaz *et al.* 2014, Bissett *et al.* 2015, Marin-Felix *et al.* 2017, Crous *et al.* 2021). Historically, overviews of accepted *Chaetomiaceae* species were provided in monographs dealing with specific genera, but these monographs are outdated (Arx *et al.* 1986, 1988, Abdel-Azeem 2020). Though our recent studies have updated the taxonomy of *Chaetomiaceae* and most of the generic descriptions have been emended (Wang *et al.* 2016a, b, 2019a, b), a comprehensive modern classification of the *Chaetomiaceae* providing a better insight into the evolutionary relationships among the species and genera is lacking. The first aim of this study is to determine the phylogenetic relationships of taxa within the *Chaetomiaceae*, including thermophilic taxa and previously described species and genera that have not yet been treated in phylogenetic studies of the family before. Secondly, we suggest methods for identifying and describing *Chaetomiaceae* species using molecular markers and morphology, and thirdly, we propose a list of accepted species and genera in *Chaetomiaceae* with their MycoBank numbers, type information and GenBank numbers to reference sequences.

SUGGESTED METHODS TO DESCRIBE AND IDENTIFY *CHAETOMIACEAE*

During our studies on the taxonomy of *Chaetomiaceae* (Wang *et al.* 2014, 2016a, b, 2019a, b), we gained experience in describing and

identifying strains belonging to this family. In this section we intend to share our accumulated knowledge.

Markers for identification and phylogenetic analysis

Amplification and sequencing

An overview of primers used for amplification and sequencing of ITS, LSU, *rpb2* and *tub2* is given in Table 1. The primer combination V9G and LS266 is preferred for ITS amplification and sequencing, and the combination ITS5/ITS4 can be used as an alternative. The ITS barcode and a part of LSU region (D1/D2) can also be amplified in one reaction with the primers ITS5 and NL4; however, in that case sequencing should be preferably performed with the additional internal primers, *e.g.,* LR0R and LS266 or ITS4. The primer combination rpb2-5F2/rpb2-7CR is recommended for amplification and sequencing of a part of the *rpb2* gene, and the reverse primer rpb2AM-7R is suggested as alternative. Successful amplification is usually obtained with an annealing temperature of 55 °C in combination with 35 cycles. The PCR enhancer dimethyl sulfoxide (DMSO, 5 %) is added to the PCR master mix for obtaining ITS, LSU and *tub2* amplicons and bovine serum albumin (BSA, 0.05 %) is added to increase the success rate of the *rpb2* PCR reaction.

DNA-based identification

Identification of *Chaetomiaceae* strains using morphological characters is challenging and suffers from phenotypic plasticity and genetic variability (Tekpinar & Kalmer 2019). Strains can lose their typical morphology when preserved over time, or do not or poorly sporulate on the agar media recommended for identification (*e.g.*, *Batnamyces*, *Madurella*) (Wang *et al.* 2019a, Noumeur *et al.* 2020). Comparative sequence-based methods are the current standard for strain identification. The ITS region is the accepted DNA barcode for fungi (Schoch *et al.* 2012). In common with some other ascomycete genera and families, this marker is unreliable for identification because different species can share the same ITS sequence (Wang *et al.* 2016b, 2019a). A good genetic identification marker should have enough variability to allow species identification and an extensive reference sequence dataset should be available for comparison. Of the markers commonly used in *Chaetomiaceae* (LSU, ITS, *rpb2* and *tub2*), the latter two are suitable for strain identification. However, we recommend the use of *tub2* and as secondary identification marker because this gene has a better species resolution (Wang *et al.* 2016b) and is easier to amplify than *rpb2* (pers. obs.).

Some entries in GenBank might not reflect the new taxonomic concepts and/or sequences in GenBank might be deposited under an incorrect name (Nilsson *et al.* 2006); both negatively affecting the identification result. It is recommended to check whether the taxonomy of the identification result is correct, *e.g.*, by using the list of accepted species supplied in this article. In case of doubt, we recommend constructing a phylogram using the *tub2* reference sequences provided in the list of accepted species here and using the phylograms in this article (Fig. 7, Supplementary Fig. S3) as a guide. Alternatively, a local BLAST database can be assembled using verified *tub2* sequences.

Phylogenetic analysis

The *tub2* gene is recommended for routine identification of species, but analysis of a combined dataset of ITS, LSU, *rpb2* and *tub2* sequences is suggested for phylogenetic analysis. β-tubulin is difficult to align, especially when the dataset includes multiple genera, and this also applies, to a lesser extent, to the ITS dataset. The LSU and *rpb2* sequence datasets have the advantage that they are easier to align above species level. For the description of new *Chaetomiaceae* species, we recommend generating at least ITS, LSU, *rpb2* and *tub2* sequences of the ex-type strain. The relationships of the new species will be confidently determined using this 4-gene approach, and it will enable us to recognise new species more easily.

Morphological characters

Nowadays, *Chaetomiaceae* taxonomy often relies more heavily on molecular phylogenetic data than on morphological characters. Morphological observations, however, are essential for describing new taxa in the family, understanding the generic and species concepts and achieving insight into the biology of the species. Before the single name nomenclature era, the production of non-stromatic perithecia covered with hairs was a hallmark for *Chaetomiaceae*. The majority of species in the family reproduces sexually in a homothallic manner and lacks an asexual morph; however, some species produce sexual and asexual morphs in

Table 1. Primers used for amplification and sequencing of *Chaetomiaceae* strains.

Locus	Primer	Direction	Preferred/ alternative	Primer sequence (5'-3')	Reference
Internal Transcribed Spacer (ITS)	V9G	Forward	Preferred	TTA CGT CCC TGC CCT TTG TA	de Hoog & Gerrits van den Ende (1998)
	LS266	Reverse	Preferred	GCA TTC CCA AAC AAC TCG ACT C	Masclaux *et al.* (1995)
	ITS5	Forward	Alternative	GGA AGT AAA AGT CGT AAC AAG G	White *et al.* (1990)
	ITS4	Reverse	Alternative	TCC TCC GCT TAT TGA TAT GC	White *et al.* (1990)
28S large subunit (LSU) nrDNA	LR0R	Forward	Preferred	ACC CGC TGA ACT TAA GC	Vilgalys & Sun (1994)
	LR5	Reverse	Preferred	TCC TGA GGG AAA CTT CG	Vilgalys & Hester (1990)
ITS+LSU, combined	ITS5	Forward	Preferred	GGA AGT AAA AGT CGT AAC AAG G	White *et al.* (1990)
	NL4	Reverse	Preferred	GGT CCG TGT TTC AAG ACG	O'Donnell (1993)
β-tubulin (*tub2*)	T1	Forward	Preferred	AAC ATG CGT GAG ATT GTA AGT	O'Donnell & Cigelnik (1997)
	TUB4Rd	Reverse	Preferred	CCR GAY TGR CCR AAR ACR AAG TTG TC	Woudenberg *et al.* (2009)
RNA polymerase II second largest subunit (*rpb2*)	rpb2-5F2	Forward	Preferred	GGG GWG AYC AGA AGA AGG C	Sung *et al.* (2007)
	rpb2-7CR	Reverse	Preferred	CCC ATR GCT TGY TTR CCC AT	Liu *et al.* (1999)
	rpb2AM-7R	Reverse	Alternative	GAA TRT TGG CCA TGG TRT CCA T	Miller & Huhndorf (2005)

one culture (*e.g.*, many species in *Humicola*, several *Chaetomium* species, *Corynascella humicola*, *Corynascus* species). Other species or genera are only known by their asexual morph (*e.g.*, all species of *Allobotryotrichum*, *Botryoderma*, *Mycothermus* and *Remersonia*, most species in *Acrophialophora* and some species in *Botryotrichum*, *Humicola*, *Staphylotrichum* and *Trichocladium*). Here, we provide recommendations for obtaining morphological data in order to properly identify and describe *Chaetomiaceae* species.

Cultivation of *Chaetomiaceae* strains

Media

Colony characteristics vary on different media. Oatmeal agar (OA; composition and preparation, see Samson *et al*. 2019) is recommended as standard medium for *Chaetomiaceae* and morphological descriptions are mainly based on cultures grown on this medium. Ascomata are key structures for sexually reproducing species. Von Arx *et al*. (1986) recommended cornmeal agar (CMA); however, our experience is that the development of sexual structures is better on OA. Potato carrot agar (PCA; composition and preparation, see Samson *et al*. 2019) is recommended as an alternative medium for species that poorly develop ascomata on OA (*e.g.*, *Arxotrichum repens*), but in contrast to OA, the cultures on PCA often fail to produce coloured exudates. Furthermore, aerial mycelium development is poor on PCA and this hampers preparation of slides for the observation of those asexual morphs which are formed on mycelium. Malt extract agar (MEA, Oxoid) and potato dextrose agar (PDA) are recommended media for extrolite profiling (Wang *et al.* 2016b, Samson *et al*. 2019). However, these media are not suitable for studying the morphology because the formation of a sexual morph is generally poorly induced. Some strains/species easily lose their ability to sporulate sexually. Covering the OA and/or PCA medium with a sterile cellophane membrane before inoculation might help to induce the development of ascomata when adding sterile filter paper fails (Wang *et al.* 2019b).

Inoculation

Inoculations are made from freshly prepared ascospore or conidium suspensions in a solution containing 2.0 g/L agar and 0.5 g/L Tween 80. We recommend using a micropipette for inoculation of the agar media with the spore suspension. The agar plates are inoculated in a three-point pattern with 1–2 µL per spot. For strains that do not or poorly sporulate, we recommend using agar plugs as inoculum. Agar plugs are cut with a cork borer along the edges of fresh colonies. Inoculating media with spore suspensions preserved at -20 °C or -80 °C is not recommended for measuring growth rates because of possible growth delay.

Incubation

Inoculated agar medium plates are incubated reverse side up in the dark at 25 °C. Exceptions are for thermotolerant or thermophilic species where an incubation temperature of 37 °C and/or 45 °C is recommended. Plates should not be wrapped with Parafilm, because this restricts air exchange and often inhibits growth and sporulation. Incubation times for measuring colony diameters are standardised at 7 d with the exception for some thermophilic species that grow fast at 45 °C; for those species the incubation time is shortened to 3 d. Asci are studied in young cultures of generally less than 2 wk old, while ascomata and ascospores are examined from cultures with fully developed ascomata, usually present after 3 wk or more.

Macromorphology

The macromorphology of a *Chaetomiaceae* on an agar medium provides the first impression of a species. Colony characters used for characterising species include colony diameters, degree of sporulation, colour of mycelium and colony reverse, and the presence or absence and texture of aerial mycelium, the presence or absence and distribution of ascomata and asexual morphs, soluble pigments and exudates.

Micromorphology

Microscopy

A dissecting microscope is used to observe the developmental stage of the ascomata in culture. The ostiolate ascomata are studied for the presence of ascomatal hairs, ascospore masses on the ascomata and their colour in reflected light. The top of the ascomata can be observed by placing the agar plate under the dissecting microscope, and the side view by cutting out a block of agar with well-developed ascomata and tipping it onto one side.

Slide preparation

Up to five slides are needed to study the morphology of a holomorphic *Chaetomiaceae* species: 1) ascomata together with ascomatal hairs, 2) asci, 3) ascospores, 4) the ascomatal wall and 5) the asexual morph. Historically, ascomycete taxonomists used water as mounting medium for the observation and measurement of ascospores (von Arx *et al.* 1986). Considering its rapid desiccation and the difficulty of observing germ pore(s) of ascospores properly, we suggest to use lactic acid (80 %) instead of water. We made a tentative study to get insight in the effect of these two mounting fluids on the ascospore size. Ascospore size data of 15 strains derived from previous studies were compared (Supplementary Table S1). Seven strains seemed slightly (0.5–2 µm) smaller in size (both in length and width) in lactic acid than in water, the length of two strains was slightly less in lactic acid than in water (no difference in width), one strain had a similar size in lactic acid and water, two strains were slightly narrower in width or in lateral width (for its bilaterally flattened ascospores) with no difference in length, two strains produces ascospores of similar length, but had a broader width and one strain was slightly shorter in length and broader in width. This tentative comparison shows that the ascospores of *Chaetomiaceae* are slightly smaller in lactic acid than in water, and observing germ pores is more easy in lactic acid. A more detailed study would be needed to confirm these data. Shear's solution (Samson *et al*. 2019) is a good alternative for lactic acid (and water), especially as a mounting medium for asci. In our experience, both lactic acid and Shear's solution are very suitable for photomicrography.

Ascomata and ascomatal hairs (Figs 1, 2)

A fine needle can be used to transfer ascomata into the lactic acid mounting medium. Ascomata are picked up one by one under a dissecting microscope to avoid being damaged. After the preparation is covered with a coverslip, the slide is gently heated on a hotplate or above a low flame on a lab gas burner to remove air bubbles and ascospore masses trapped inside terminal ascomatal hairs. After this procedure, the whole structure

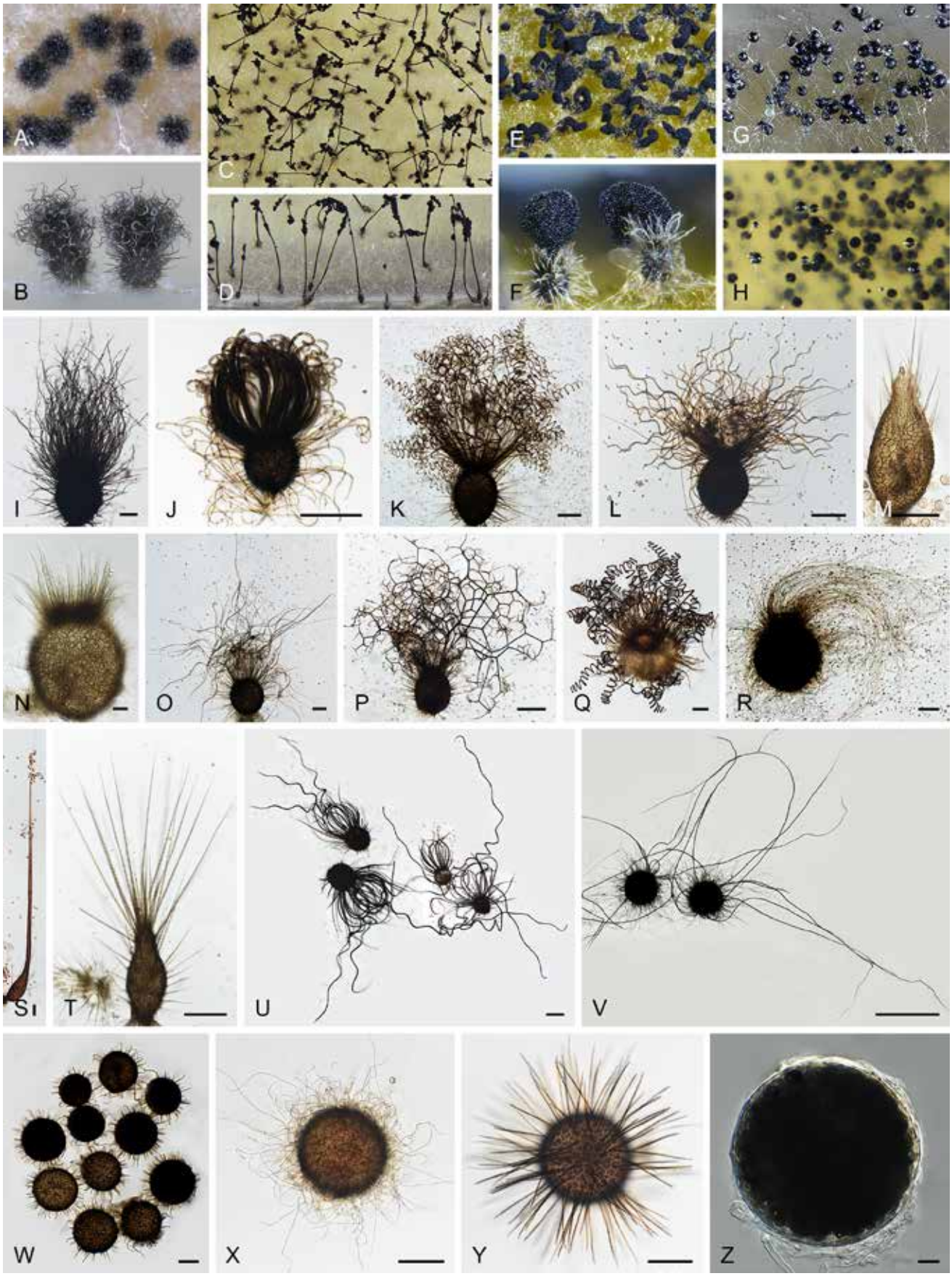

Fig. 1. Ascoma diversity in *Chaetomiaceae* under stereomicroscope (A–H) and light microscope (I–Z). **A, B.** *Amesia nigricolor* CBS 291.83. **C, D.** *Staphylotrichum longicolle* CBS 119.57. **E, F.** *Brachychaeta variospora* CBS 414.73. **G.** *Canariomyces vonarxii* CBS 160.80. **H.** *Hyalosphaerella fragilis* CBS 456.73. **I.** *Chaetomium subaffine* CBS 637.91. **J.** *Arcopilus cupreus* CBS 560.80. **K.** *Collariella bostrychodes* DTO 324-H6. **L.** *Arxotrichum repens* CBS 233.82. **M.** *Humicola seminuda* CBS 368.84. **N.** *Collariella carteri* CBS 128.85. **O.** *Botryotrichum murorum* DTO 324-G9. **P.** *Dichotomopilus pratensis* CBS 860.68. **Q.** *Trichocladium acropullum* CBS 114580. **R.** *Chaetomium umbonatum* CBS 293.83. **S.** *Staphylotrichum longicolle* CBS 119.57. **T.** *Humicola hirsuta* CBS 144492. **U.** *Parachaetomium muelleri* CBS 192.84. **V.** *Chaetomium subfimeti* CBS 370.66. **W.** *Chrysanthotrichum peruvianum* CBS 732.68. **X.** *Botryotrichum geniculatum* CBS 144475. **Y.** *Trichocladium arxii* CBS 104.79. **Z.** *Hyalosphaerella fragilis* CBS 456.73. Scale bars: I–L, O, P, R, U, X, Y, = 100 µm; M, Q, S, T = 50 µm ; N, Z = 20 µm ; V = 500 µm.

of the terminal ascomatal hairs including their lower parts can be observed. Ascomata of *Chaetomiaceae* (Fig. 1) are non-stromatic perithecia (*e.g.*, Fig. 1A–F, I–U) or cleistothecia (*e.g.*, Fig. 1G–H, V–Z) and are usually produced superficially on the agar surface and occasionally immersed in the medium (*e.g.*, Fig. 1H). The ascomata can be glabrous (*e.g.*, Fig. 1G, H, Z) or covered by highly diverse hairs (*e.g.*, Fig. 1A–F, I–Y). The ascomatal hairs can be erect [*e.g.*, Fig. 1M, N, S, T, W (partial), Y], flexuous [*e.g.*, Fig. 1I, W (partial)], undulate [*e.g.*, Fig. 1L, O, U (long)], coiled (*e.g.*, Fig. 1K, Q), arcuate [*e.g.*, Fig. 1J, U (short)], apically circinate or coiled [*e.g.*, Fig. 1J, O, W (partial)], branched (*e.g.*, Fig. 1P), hypha-like [*e.g.*, Fig. 1R, V (short), X], or consisting of two different types (*e.g.*, Fig. 1U, V). The ascomatal walls (peridium) can be membranaceous, composed of *textura epidermoidea* (Fig. 2A), *intricata* (Fig. 2B) or *angularis* (Fig. 2D) in surface view, or cephalothecoid (composed of radially elongated cells and often surrounded by lines of dehiscence in surface view) in a few species (Fig. 2C, E).

Asci (Fig. 3)

Examining asci in *Chaetomiaceae* is a challenge because they are commonly evanescent and disappear before maturation of the ascospores. Because of this, we usually observe hyaline ascospores in an ascus (Fig. 3). In some studies, the ascospores of *Chaetomium globosum* were even wrongly assumed to be conidia (Luo *et al.* 2019). For observing asci, careful attention should be paid to the formation of ascomata. It is very important to prepare slides from young ascomata at the early stage of the culture, normally within 2 wk. When the cultures are incubated longer, the majority of ascomata are mature and it becomes difficult to observe asci, even when you pick up young ascomata at the edge of the colony.

Fig. 2. Structure diversity of ascomatal wall in *Chaetomiaceae*. **A.** *Pseudothielavia arxii* CBS 603.97. **B.** *Chaetomium globosum* MUCL 39526. **C.** *Aporothielavia leptoderma* CBS 538.74. **D.** *Humicola seminuda* CBS 368.84. **E.** *Trichocladium arxii* CBS 104.79. Scale bars = 10 µm.

For species that produce non-ostiolate ascomata, hyaline young ascomata are usually a good choice for ascus observation. Several young ascomata are transferred in a drop of Shear's solution on a microscope slide. After the preparation is covered with a coverslip, the blunt end of a needle can be used to gently squash the ascomata. After tapping several times, fasciculate and dissociated asci can be found beside the cracked ascomata. In some species/strains, persistent asci that retain until ascospores mature can be

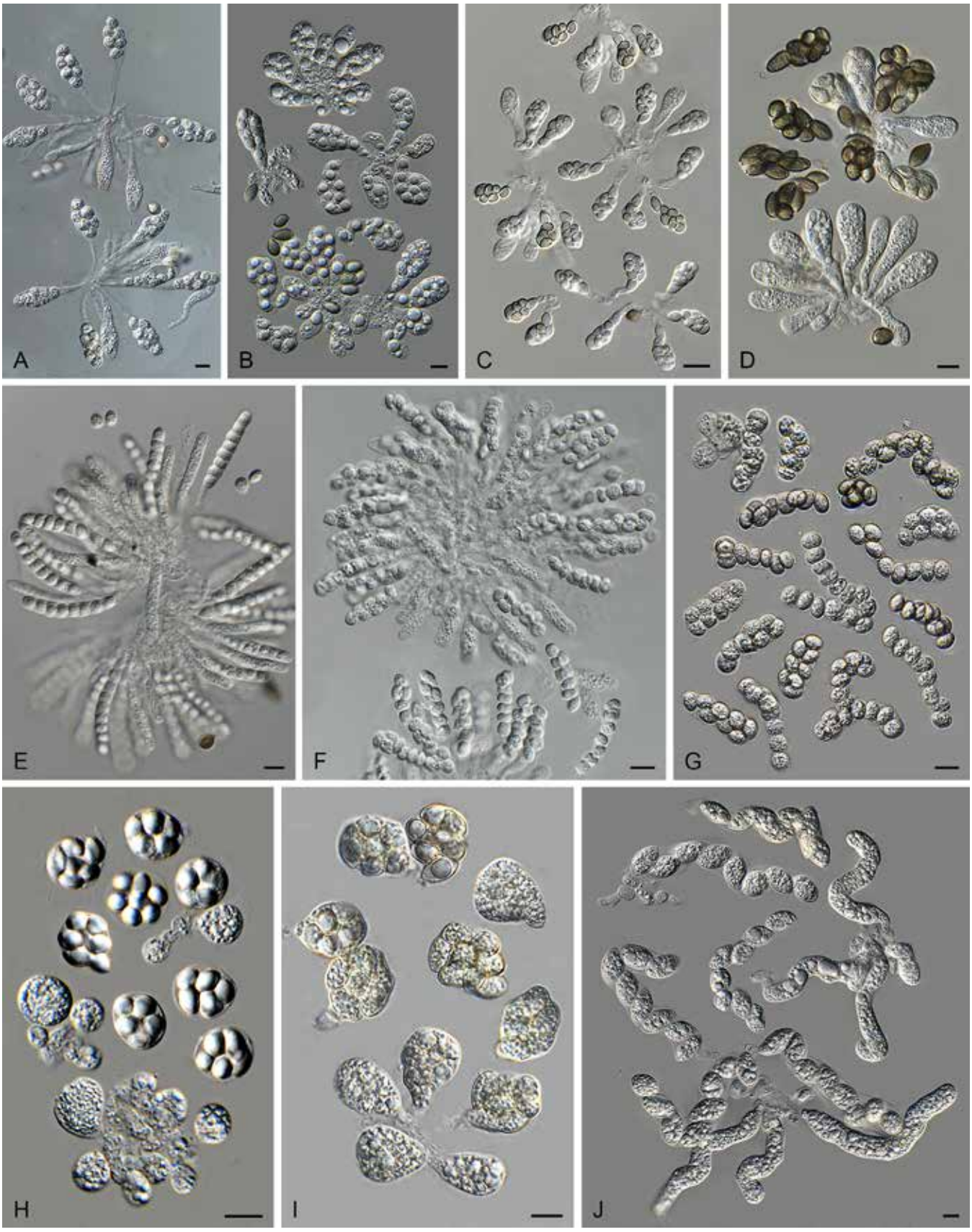

Fig. 3. Ascus diversity in *Chaetomiaceae*. **A.** *Chaetomium globosum* DTO 333-E3. **B.** *Hyalosphaerella fragilis* CBS 456.73. **C.** *Thermothielavioides terrestris* CBS 492.74. **D.** *Parathielavia appendiculata* CBS 723.68. **E.** *Ovatospora pseudomollicella* CBS 251.75. **F.** *Humicola ampulliella* CBS 116735. **G.** *Trichocladium antarcticum* CBS 123565. **H.** *Canariomyces microsporus* CBS 161.80. **I.** *Corynascus fumimontanus* CBS 137294. **J.** *Condenascus tortuosus* CBS 610.97. Scale bars = 10 µm.

observed (Fig. 3D). The shape of the asci can be fusiform (Fig. 3A), clavate (Fig. 3B–D), cylindrical (Fig. 3E–F), ovoid to subglobose (Fig. 3H–I) or twisted (Fig. 3J). The asci contain eight (rarely four) ascospores that are uniseriate [*e.g.*, Fig. 3E, F (partial), G (partial), J (partial)], biseriate [*e.g.*, Fig. 3A, D (partial), F (partial), G (partial)] or irregularly-arranged [*e.g.*, Fig. 3B, D (partial), H, I].

Ascospores (Fig. 4)

The species that produce ostiolate ascomata usually have their mature ascospores extruded in a sticky mass or cirrhus at the top of the ascoma. In many species, these ascospores are wrapped in numerous ascomatal hairs. It is easy to pick up ascospores from the top of these ascomata for slide preparation. To study ascospores produced in non-ostiolate ascomata, the ascomata must be squashed on a slide to release the ascospores. As mentioned above, water, Shear's solution and lactic acid can be used as mounting media. Water has the disadvantage of rapid desiccation and exposure to the air might make ascospores become dehydrated, which may make them shrunken or concave. In our experience, germ pores are not easily observed in such ascospores (*e.g.* in *Aporothielavia leptoderma* (Fig. 11, see notes below) and *Arxotrichum piluliferoides* (= *Chaetomium piluliferoides*; Fig. 14, see notes below)). Heating the ascospore slide gently above a low flame on a lab gas burner or on a hotplate will not only allow ascospores to restore their normal shape, but also helps to visualise the germ pore on the spores. The position and number of germ pores can be observed on rolling ascospores in the (heated) lactic acid. When ascospores are immobile, photos can be taken of ascospores with germ pore(s). The ascospores of *Chaetomiaceae* are aseptate, pigmented, smooth and vary in shape and size, with one (in most species), two (*e.g.*, Fig. 4O, Z, AA, AI, AQ) or rarely more [*e.g.*, Fig. 4U, AQ (partial)] germ pores. The position of the germ pore is apical in most species, or subapical to oblique (*e.g.*, Fig. 4E, AD, AO, AP) or lateral [*e.g.*, Fig. 4N, U, AQ (partial)]. The ascospore measurements should include the extreme values given in parentheses and, in between, the 95 % confidence interval of 30 individual measurements. For the measurements of bilaterally flattened ascospores, the size was reported as "length" × "width in front view" × "width in lateral view".

Asexual morph (Figs 5, 6)

In general, the asexual morph of *Chaetomiaceae* is produced either on the substrate or in the aerial mycelium. The asexual structures of *Corynascella humicola*, *Botryotrichum* spp. (except for *Botry. verrucosum*) and *Remersonia* spp. grow up into the air above the medium (Fig. 5), and it is easy to prepare microscopic slides of these structures in lactic acid (80 %). The asexual morphs developed at mycelium (Fig. 6), especially those produced by species that also produce abundant well-developed ascomata, can easily be missed and cultures should therefore be carefully examined. A slide culture method (Riddell 1950, modified) is recommended. An agar block is cut out of a culture, placed on a sterile glass microscope slide, and a sterile coverslip is subsequently put on the top of the block. After 1–2 wk inoculation in a damp chamber, the coverslip is carefully removed from the block and used for the preparation of a microscope slide. The material that has grown around the block onto the microscope slide is used to make another slide (after removal of the agar block). The inclined coverslip method (Kawato & Shinobu 1959, revised in Nugent *et al*. 2006) can be used as an alternative. A sterile coverslip is inserted into the OA agar medium at a 45° angle, and the target strain is subsequently inoculated at one side of the inserted coverslip to allow the fungus to creep onto it. After 7–10 d, when the mycelium has covered about a third of the coverslip, the coverslip is carefully taken out of the OA medium. After cleaning the other side of the coverslip with tissue paper dipped in alcohol, it is used to make a slide for observation. Lactic acid (80 %) is used as mounting medium. Air bubbles inside the slide can be removed by gently heating the slide above a low flame. Diverse asexual morphs are associated with *Chaetomiaceae* (*e.g.*, acremonium-, humicola-, staphylotrichum- or trichocladium-like, Wang *et al*. 2019a) and we refer to Seifert *et al.* (2011) for more details on these structures.

MATERIALS AND METHODS

Strains

In addition to previously studied strains (Wang *et al*. 2016a, b, 2019a, b), 106 strains were obtained from the CBS culture collection (CBS) housed at the Westerdijk Fungal Biodiversity Institute (WI), Utrecht, the Netherlands. Six isolates were obtained from the personal collection of Xue-Wei Wang (WXW) housed at the State Key Laboratory of Mycology, Institute of Microbiology, Chinese Academy of Sciences, which represent four potential new species. Details on these strains are provided in Table 2.

Morphology

The methods and media used for the morphological analysis are described in the "suggested methods" section above. Mature ascomata (top or side view) or a part of the colony were photographed using a Nikon SMZ25 stereo microscope. Focused images were obtained by z-stacking using the software Nikon NIS-Element D. Microscopic photographs were taken using a Zeiss AxioImager.2A microscope with a Nikon DS-Ri2 camera, or sometimes using Nikon Eclipse 80i microscope with a Nikon Digital Sight DS-Fi1 camera, both equipped with differential interference contrast (DIC) illumination. Ascospores with clear germ pore(s) were selected from the originally taken photos to get composite images using the "Healing Brush Tool" of Adobe Photoshop.

DNA isolation, sequencing and phylogenetic analyses

Genomic DNA was extracted from fungal mycelium grown on oatmeal agar (OA, Samson *et al.* 2019) using the DNeasy® UltraClean® Microbial Kit (Qiagen, Germany) following the manufacturer's instructions. The internal transcribed spacer 1 and 2 including the intervening 5.8S nrDNA (ITS), the D1/D2 domains of the 28S nrDNA (LSU), partial RNA polymerase II second largest subunit gene (*rpb2*) and partial β-tubulin gene (*tub2*) were selected for phylogenetic inference. The PCR conditions, primers used for PCR amplification and sequencing were the same as those described by Wang *et al.* (2019a). Each amplicon was sequenced in both directions using the same set of primers. A consensus sequence for each locus was assembled in MEGA v. 6 (Tamura *et al.* 2013).

Novel sequences generated in this study were deposited in GenBank (http://www.ncbi.nlm.nih.gov, Table 2) and these datasets were merged with reference sequences obtained from previous studies (Wang *et al.* 2016a, b, 2019a, b) or retrieved from GenBank (see list of accepted species below and Supplementary Table S2). Alignments and treefiles are available in Figshare: https://


A
B
C
D
E
F
G
H
I
J
K
L
M
N
O
P
Q
R
S
T
U
V
W
X
Y
Z
AA
AB
AC
AD
AE
AF
AG
AH
AI
AJ
AK
AL
AM
AN
AO
AP
AQ

Fig. 4. (Page 130) Ascospore diversity in *Chaetomiaceae*. **A.** *Collariella bostrychodes* DTO 324-H6. **B.** *Dichotomopilus variostiolatus* CBS 179.84. **C.** *Collariella quandrangulata* CBS 152.59. **D.** *Humicola ampulliella* CBS 116735. **E.** *Parathielavia kuwaitensis* CBS 353.62. **F.** *Ovatospora brasiliensis* CBS 140.50. **G.** *Bommerella trigonospora* CBS 324.69. **H.** *Arcopilus cupreus* CBS 560.80. **I.** *Canariomyces microsporus* CBS 161.80. **J.** *Arxotrichum piluliferoides* CBS 103.77. **K.** *Stellatospora terricola* CBS 811.95. **L.** *Parachaetomium subspirilliferum* CBS 150.60. **M.** *Staphylotrichum longicolle* CBS 119.57. **N.** *Pseudothielavia arxii* CBS 603.97. **O.** *Parachaetomium inaequale* CBS 331.75. **P.** *Dichotomopilus fusus* CBS 114.83. **Q.** *Chaetomium globosum* DTO 319-B2. **R.** *Chaetomium umbonatum* CBS 293.83. **S.** *Chaetomium citrinum* CBS 693.82. **T.** *Chaetomium ascotrichoides* CBS 110.83. **U.** *Chaetomium megalocarpum* CBS 149.59. **V.** *Chaetomium globosporum* CBS 108.83. **W.** *Pseudothielavia hamadae* CBS 499.83. **X.** *Stolonocarpus gigasporus* CBS 112062. **Y.** *Pseudothielavia terricola* CBS 165.88. **Z.** *Corynascus sepedonium* CBS 111.69. **AA.** *Brachychaeta variospora* CBS 414.73. **AB.** *Pseudothielavia subhyaloderma* CBS 473.86. **AC.** *Aporothielavia leptoderma* CBS 538.74. **AD.** *Parachaetomium perlucidum* CBS 141.58. **AE.** *Chrysanthotrichum peruvianum* CBS 732.68. **AF.** *Arxotrichum repens* CBS 233.82. **AG.** *Xanthiomyces spinosus* CBS 789.71. **AH.** *Parachaetomium biporatum* CBS 244.86. **AI.** *Corynascella humicola* CBS 337.72. **AJ.** *Amesia dreyfussii* CBS 376.83. **AK.** *Corynascus sexualis* CBS 827.96. **AL.** *Botryotrichum geniculatum* CBS 144475. **AM.** *Thermochaetoides thermophila* CBS 179.67. **AN.** *Humicola quadrangulata* CBS 111771. **AO.** *Parathielavia hyrcaniae* CBS 353.62**. AP.** *Condenascus tortuosus* CBS 610.97. **AQ.** *Chaetomium nozdrenkoae* CBS 163.62. Scale bars = 10 µm, applies to all.

Figshare.com/s/d251b9512f9d77522ef7. Phylogenetic analyses were based on Bayesian inference (BI) and Maximum Likelihood (ML) as described previously (Wang *et al*. 2019b). For BI, the best evolutionary model for each locus was determined using MrModeltest v. 2.0 (Nylander 2004). Obtained trees were viewed in FigTree v. 1.1.2 (Rambaut 2009) and subsequently visually prepared and edited in Adobe® Illustrator® CS6.

Divergence time estimation within *Chaetomiaceae*

Divergence time analysis was introduced to evaluate the phylogenetically-delimited genera in *Chaetomiaceae*. Five calibration points were selected (Samarakoon *et al.* 2019) (Table 3). Bayesian molecular-clock dating analysis was carried out using BEAST v. 2.6.3 (Bouckaert *et al.* 2019) with the concatenated *rpb2*, *tub2*, ITS and LSU sequence dataset including all genera and representative species of *Chaetomiaceae* as well as reference taxa. The reference sequences were retrieved from GenBank and listed in Supplementary Table S2. The introns in the protein coding genes and ITS1, ITS2 fragments in ITS locus were excluded to avoid an uncertain or dubious estimate.

The GTR substitution model was assigned for each gene with a gamma distribution accounting for rate variation among sites. An uncorrelated lognormal relaxed-clock model was applied to the four genes together with a uniform (10^{-6},1) hyperprior for the mean rate. Following a recent work on divergence time calibrations for ancient lineages of *Ascomycota* based on reliable fossil data (Samarakoon *et al.* 2019), the following five calibrations were used with priors: a uniform (35,55) distribution for *Aspergillus*, a uniform (61.6,72.3) distribution for *Colletotrichum*, a uniform (136,188) distribution for *Diaporthales*, a uniform (98.17,99.41) distribution for *Ophiocordyceps*, and an offset-exponential distribution with a mean 10 million years ago (Mya) and an offset 410 Mya for *Pezizomycotina*. Using the Yule process (Yule 1925) with a gamma (0.001,1000) distribution for the speciation rate, we performed two independent runs of Markov chain Monte Carlo (MCMC) sampling, with samples drawn every 10 000 steps over 100 million steps, discarding the first 25 %. After the convergence was checked based on the combined samples, the maximum-clade-credibility tree was identified among posteriors using TreeAnnotator v. 2.6.0.

RESULTS

Phylogeny

Phylogenetic analyses were performed on the individual LSU, ITS, *rpb2* and *tub2* datasets and a combined dataset of all four loci. The LSU and ITS phylograms were poorly supported. Compared to the phylogram based on the combined dataset (Fig. 7, discussed below), 27 generic clades were supported (ML-BS > 80 %; PP = 1.00) or formed monotypic lineages in the ITS phylogram; the other recognised generic clades did not receive robust support or did not form monophyletic lineages (Supplementary Fig. S1). The LSU failed to resolve most of the recognised species and genera (data not shown). In the *tub2* phylogeny, 45 of the 47 generic clades recognised in the combined phylogram were supported (ML-BS > 78 %; PP > 0.97) or formed monotypic lineages. *Humicola* was not statistical supported and *Melanocarpus albomyces* was distant from the other *Melanocarpus* species (Supplementary Fig. S2). In the *rpb2* phylogeny, the *Remersonia*/*Mycothermus* clade nested on a long branch inside *Staphylotrichum* (Supplementary Fig. S3). The position of the *Remersonia* and *Mycothermus* together is questionable (*rpb2*) or lacks support (LSU, ITS, *tub2*, combined) in the single gene and the combined phylograms (Fig. 7C, Supplementary Figs S1–S3). Furthermore, the *Chaetomium*, *Humicola* and *Melanocarpus* clades did not receive statistical support in the *rpb2* phylogram (Supplementary Fig. S3). No topological conflicts were observed when the 70 % bootstrap reciprocal tree topologies based on the single datasets were compared (Supplementary Figs S1–S3). Therefore, all four loci were combined to reveal the generic relationships in the family following the argument of Cunningham (1997) that combining incongruent partitions could increase phylogenetic accuracy.

The concatenated dataset of LSU, ITS, *rpb2* and *tub2* contains sequences of 404 strains and includes representatives of all genera and most accepted species of *Chaetomiaceae*. Exceptions are species that are only known by their ITS and/or LSU sequence(s), *e.g.*, several *Acrophialophora* species and *Humicola koreana*, as well as *Chaetomium iranicum*, *Collariella capillicompacta*, *Trichocladium amorphum* and *Trichocladium nigrospermum*. Furthermore, representative species belonging to *Lasiosphaeriaceae sensu lato*, *Podosporaceae* and *Sordariaceae* were included, and *Microascus trigonosporus* CBS 218.31 (*Microascales*) was selected as the outgroup. The alignment contained 3 622 characters (including gaps) and was composed of four partitions: 883 characters for *rpb2*, 1 354 characters for *tub2*, 798 characters for ITS and 587 characters for the D1/D2 regions of LSU. Of these, 1 352 characters were constant, 1 980 were parsimony-informative, and 290 were parsimony-uninformative. For the Bayesian inference, GTR+I+G was the most optimal model for all four partitions. The result of the phylogenetic analysis is shown in Fig. 7. Forty-seven monophyletic lineages are recognised in the *Chaetomiaceae*, each corresponding to a previously defined genus or a potential new genus, which were all highly supported (ML-BS ≥ 92 %; PP = 1.00). The only exceptions were the *Melanocarpus* lineage (ML-BS < 70 %; PP = 1.00, Fig. 7D)

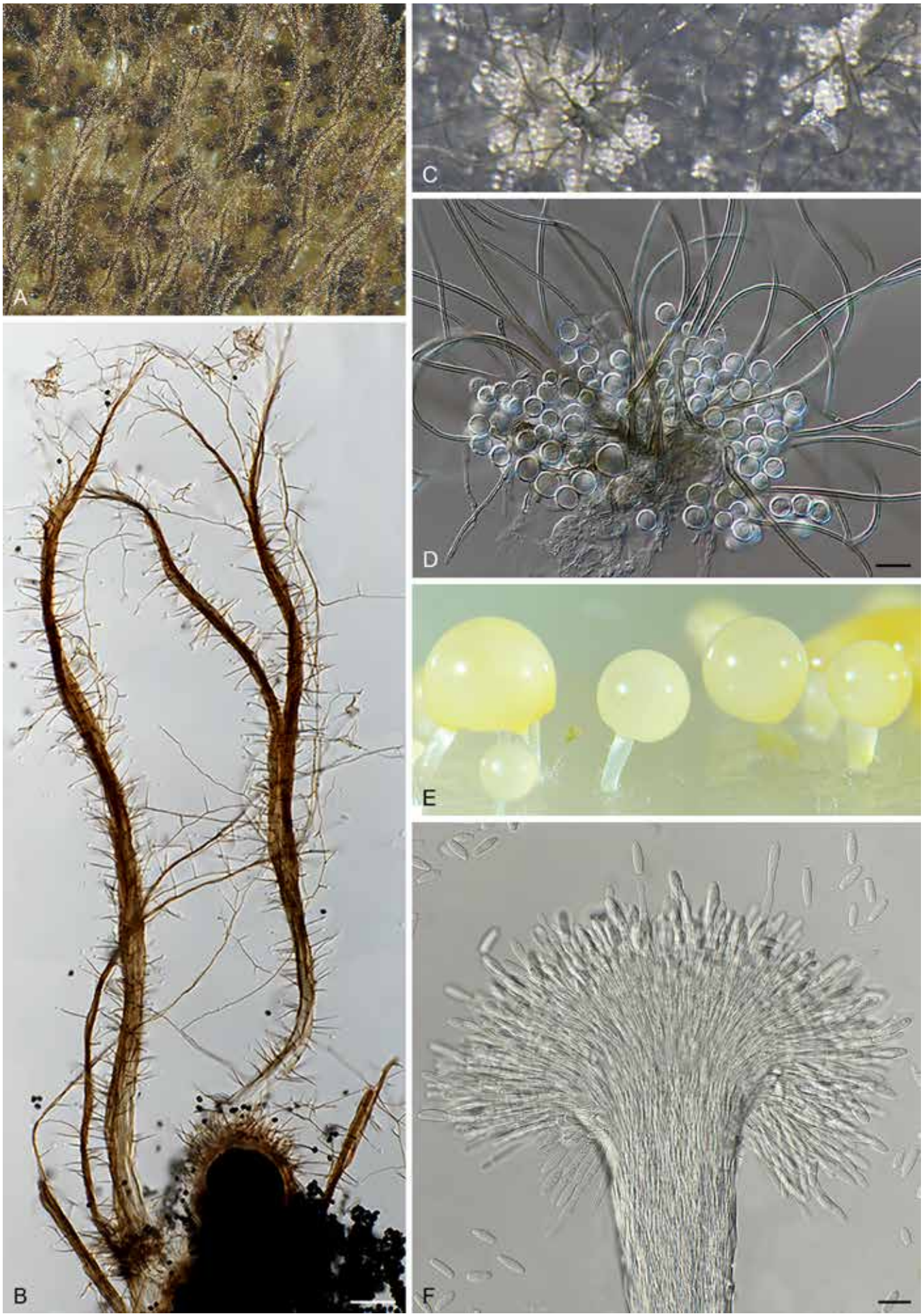

Fig. 5. Diversity of asexual structures growing up into the air above the medium in *Chaetomiaceae*. **A–B.** *Corynascella humicola* CBS 337.72. **C–D.** *Botryotrichum piluliferum* DTO 254-B8. **E–F.** *Remersonia thermophila* CBS 645.91. Scale bars: B = 100 µm; D, F = 20 µm.

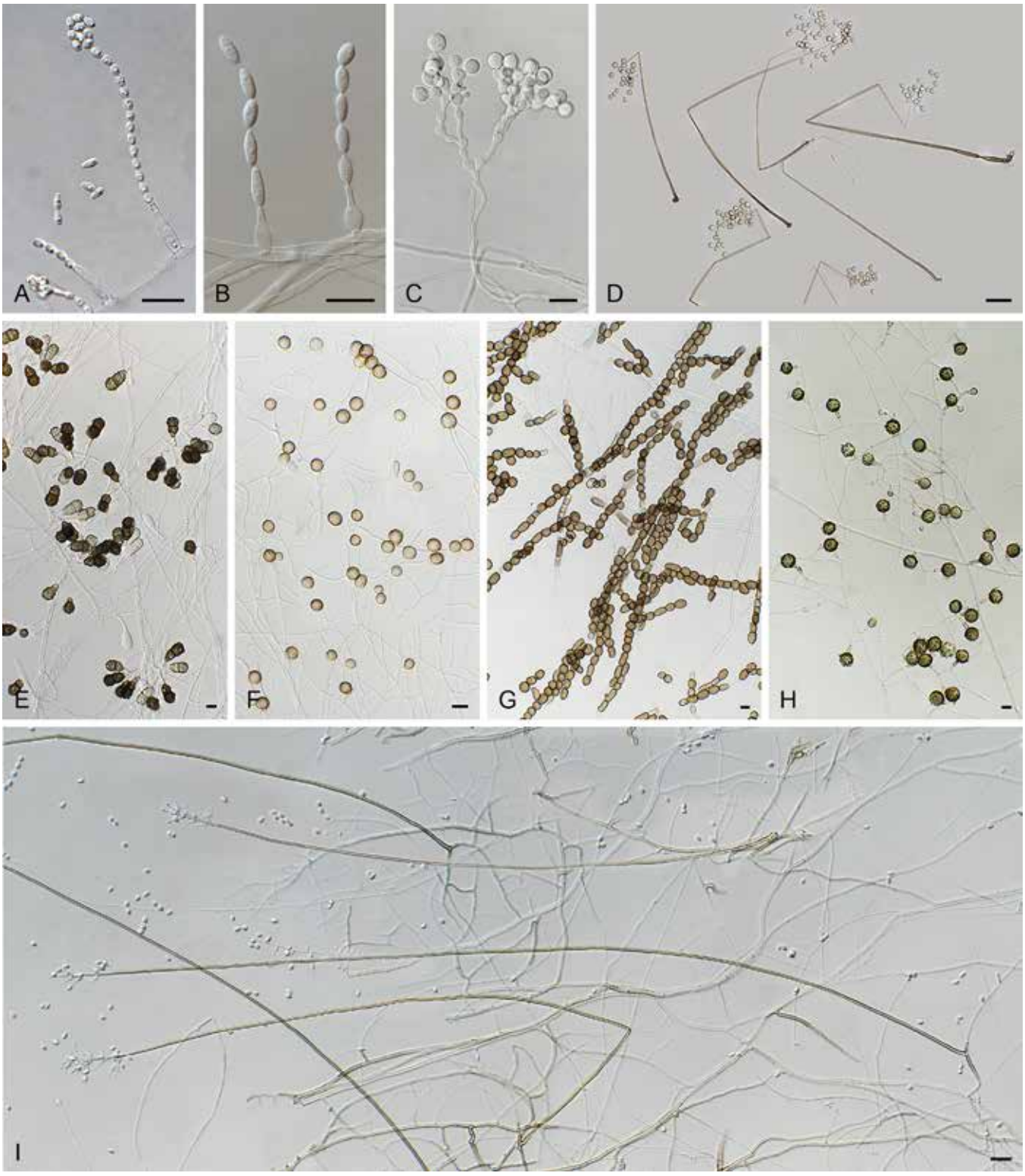

Fig. 6. Asexual diversity in *Chaetomiaceae* observed by means of inclined coverslip method. **A.** *Chaetomium elatum* DTO 319-B3. **B.** *Acrophialophora ellipsoidea* CBS 102.61. **C.** *Trichocladium beniowskiae* CBS 757.74. **D.** *Staphylotrichum coccosporum* CBS 364.58. **E.** *Trichocladium asperum* CBS 903.85. **F.** *Humicola fuscoatra* CBS 118.14. **G.** *Mycothermus thermophilus* CBS 625.91. **H.** *Botryotrichum verrucosum* CBS 116.64. **I.** *Acrophialophora nainiana* CBS 100.60. Scale bars: A, B, E–H = 10 µm; C, D, I = 20 µm.

and *Humicola* lineage (ML-BS = 78 %; PP = 1.00, Fig. 7B). The fifteen thermophilic species grouped into seven genus-level clades (Fig. 7, highlighted in orange blocks). The *Thermothelomyces* clade (ML-BS = 100 %; PP = 1.00) was confirmed as closely related to the four non-thermophilic genera *Arxotrichum*, *Botryoderma*, *Corynascus* and *Myceliophthora* (ML-BS = 100 %; PP = 1.00, Fig. 7A). *Mycothermus* and *Remersonia* were confirmed as sister genera (ML-BS = 100 %; PP = 1.00, Fig. 7C). *Thermothielavioides* was closely related to the non-thermophilic genus *Floropilus* (ML-BS = 97 %; PP = 1.00), and these two genera clustered close to but separate from the non-thermophilic genus *Chrysanthotrichum* (ML-BS = 95 %; PP = 1.00, Fig. 7C). The *Chaetomium thermophilum* clade (ML-BS = 100 %; PP = 1.00, Fig. 7D) consists of two species clades, with no statistically-supported close relatives. The *Thielavia australiensis* clade is sister to the genus *Carteria* (ML-BS = 100 %; PP = 1.00, Fig. 7D).

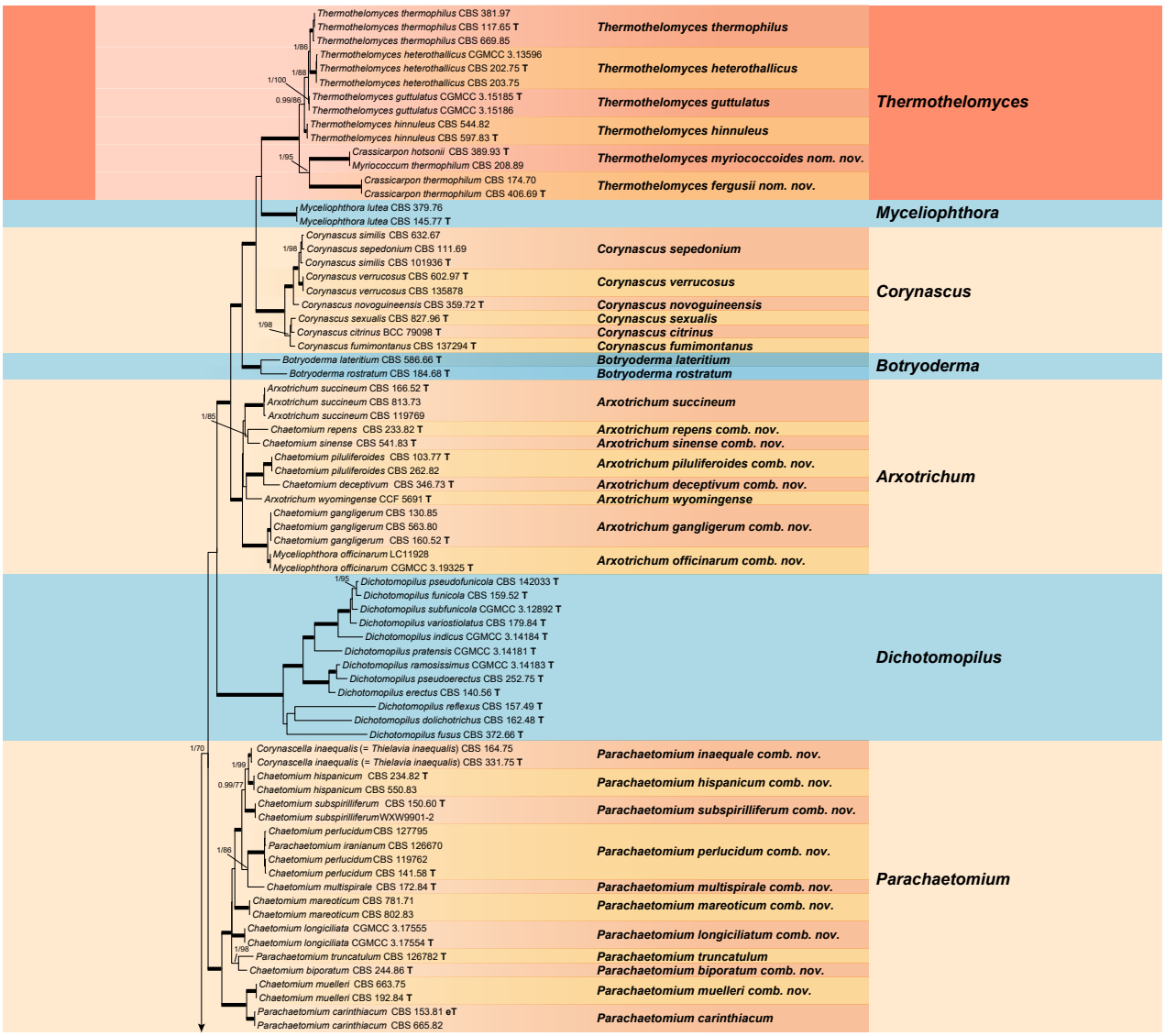

Fig. 7. Phylogenetic tree resulting from ML analysis of the concatenated partial *rpb2*, *tub2*, ITS and LSU gene region alignment, with the confidence values indicated at the notes: the posterior probabilities from the Bayesian analysis before the slash, bootstrap proportions from the ML analysis after the slash. The "-" indicates lacking statistical support (<70 % for bootstrap proportions from ML analysis; <0.95 for posterior probabilities from Bayesian analysis). The branches with full statistical support (PP = 1.0; ML-BS = 100 %) are highlighted by thickened branches. Genus/potential new species or combination clades are discriminated with boxes in different colours and clades containing thermophilic species are highlighted with an orange background. Ex-type strains are marked with "**T**" after the culture number. "**eT**" represents the ex-epitype designated in this study. *Taxa with names of genus/family not necessarily reflecting molecular phylogenetic relationships. The scale bar shows the expected number of changes per site. The tree is rooted with *Microascus trigonosporus* in the *Microascales*.

To delimit species boundaries using the gene concordance phylogenetic species concept (GCPSR), the phylogenies based on ITS (if data available), *tub2* and *rpb2* sequences are compared (see Supplementary Figs S1–S3) and discussed in the notes of the relevant species in the taxonomy section below. The LSU phylogeny failed to resolve most of the recognised species and genera (data not shown) and is therefore not discussed.

Divergence time estimation (Figs 8, 9)

Three hundred and eighteen taxa were selected for dating analysis, containing 204 representative species of *Chaetomiaceae*, 16 *Podosporaceae* species, 38 *Lasiosphaeriaceae sensu lato* species and three *Sordariaceae* species (all in the *Sordariales*), together with 55 *Pezizomycotina* species that included five calibrating points (Table 3, Fig. 8). *Taphrina deformans* and *Candida albicans* were used as outgroups. Divergence time of genera (blue) and species (yellow) in *Chaetomiaceae* are shown in Fig. 9. The Turkey`s test reveals two outliers: 51.15 Mya in the species boxplot and 122.79 Mya in the genus boxplot. After removing these two outliers, the divergence times of the species range from 0.64 Mya to 48.57 Mya and those of the genera range from 27.26 Mya to 93.47 Mya. The molecular dating analysis indicated that all the previously defined genera in the *Chaetomiaceae* diverged from about 27 Mya (*Chrysocorona*) to 123 Mya (*Condenascus*) and that these generic clades are all fully supported (PP = 1.0, highlighted by thickened branches in Fig. 8), with the *Humicola* and *Melanocarpus* clades being the only exception. The previously phylogenetically-defined *Humicola* lineage appeared to be polyphyletic, with two subclades estimated to diverge from each other about 60 Mya, with one of them closer to *Aporothielavia*, having diverged from the latter about 52 Mya. Two subclades within the *Melanocarpus* lineage (PP < 0.9) diverged from each other about 60 Mya. The other thermophilic lineages diverged from their non-thermophilic neighbours at least 30 Mya.

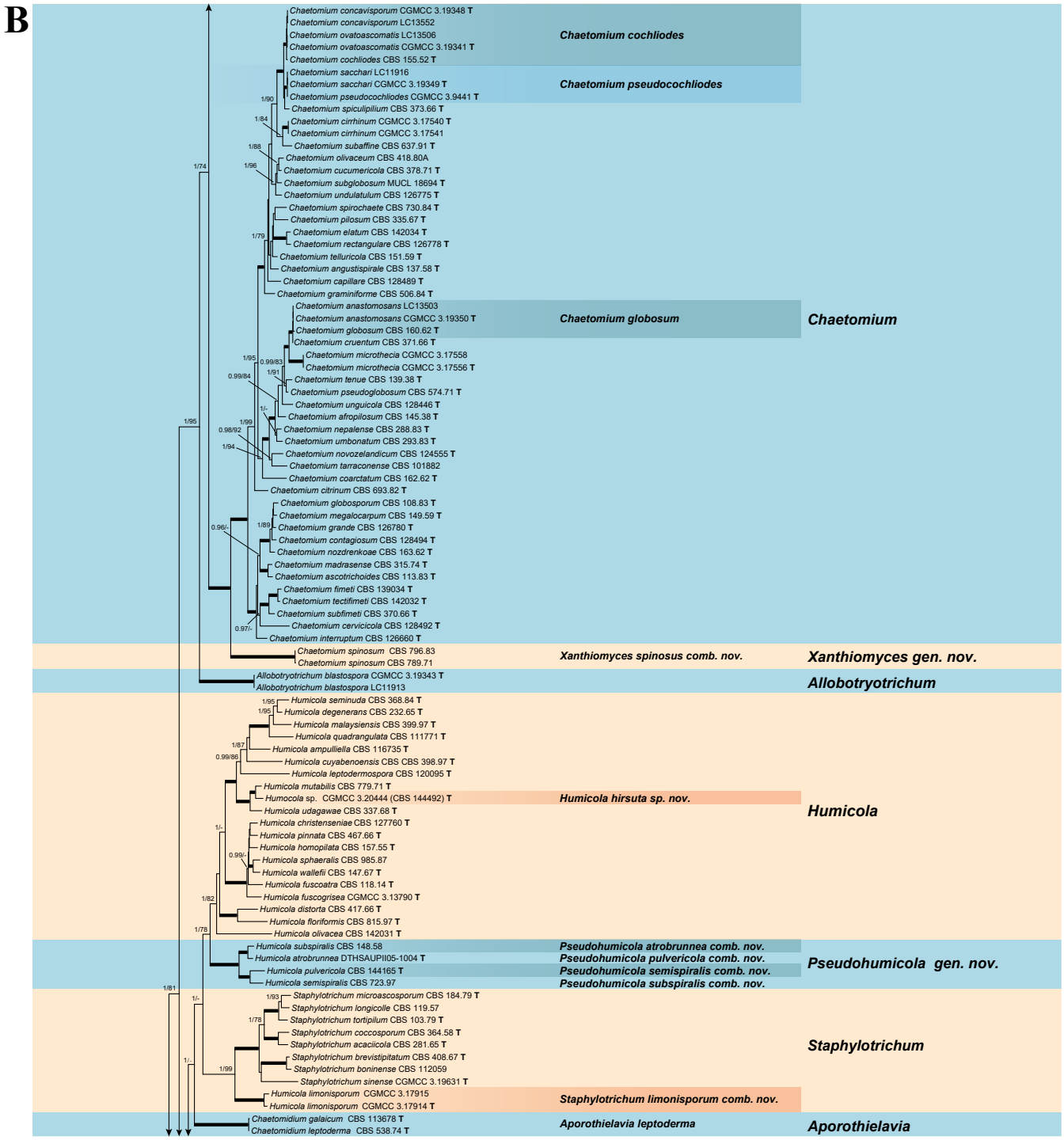

Fig. 7. (Continued).

TAXONOMY

Six genera, *Parvomelanocarpus*, *Pseudohumicola*, *Tengochaeta*, *Thermocarpiscus*, *Thermochaetoides* and *Xanthiomyces*, are newly proposed based on molecular dating and multi-gene phylogenetic analyses (Figs 7, 8) in combination with (shared) morphological characters and/or ecological features. The genus *Botryoderma* is confidentially positioned in the *Chaetomiaceae* and *Achaetomiella*, *Aporothielavia* and *Bommerella* are resurrected and redefined or redescribed. The generic concepts of *Collariella* and *Humicola* are emended because of the introduction of *Achaetomiella* and *Pseudohumicola*. *Allocanariomyces*, *Amesia*, *Arcopilus*, *Arxotrichum, Botryotrichum, Chaetomium, Ovatospora*, *Parachaetomium*, *Parathielavia*, *Staphylotrichum*, *Subramaniula* and *Thermothelomyces* are expanded with new combinations and/or new species. Among them, four genera (*Arxotrichum*, *Botryotrichum*, *Parachaetomium* and *Staphylotrichum*) are redefined. In the current concept, *Corynascella* and *Melanocarpus* are restricted to their type species. Six new species belonging to six different genera (*Botryotrichum geniculatum*, *Chaetomium subaffine*, *Humicola hirsuta*, *Subramaniula latifusispora*, *Tengochaeta nigropilosa* and *Trichocladium tomentosum*) are introduced. The delimitation of *Corynascus* and *Myceliophthora* by Marin-Felix *et al.* (2015) is confirmed. In total, 50 genera and 275 species are accepted in the *Chaetomiaceae*, while "*Chaetomium microascoides*" and "*Chaetomidium triangulare*" proved to be

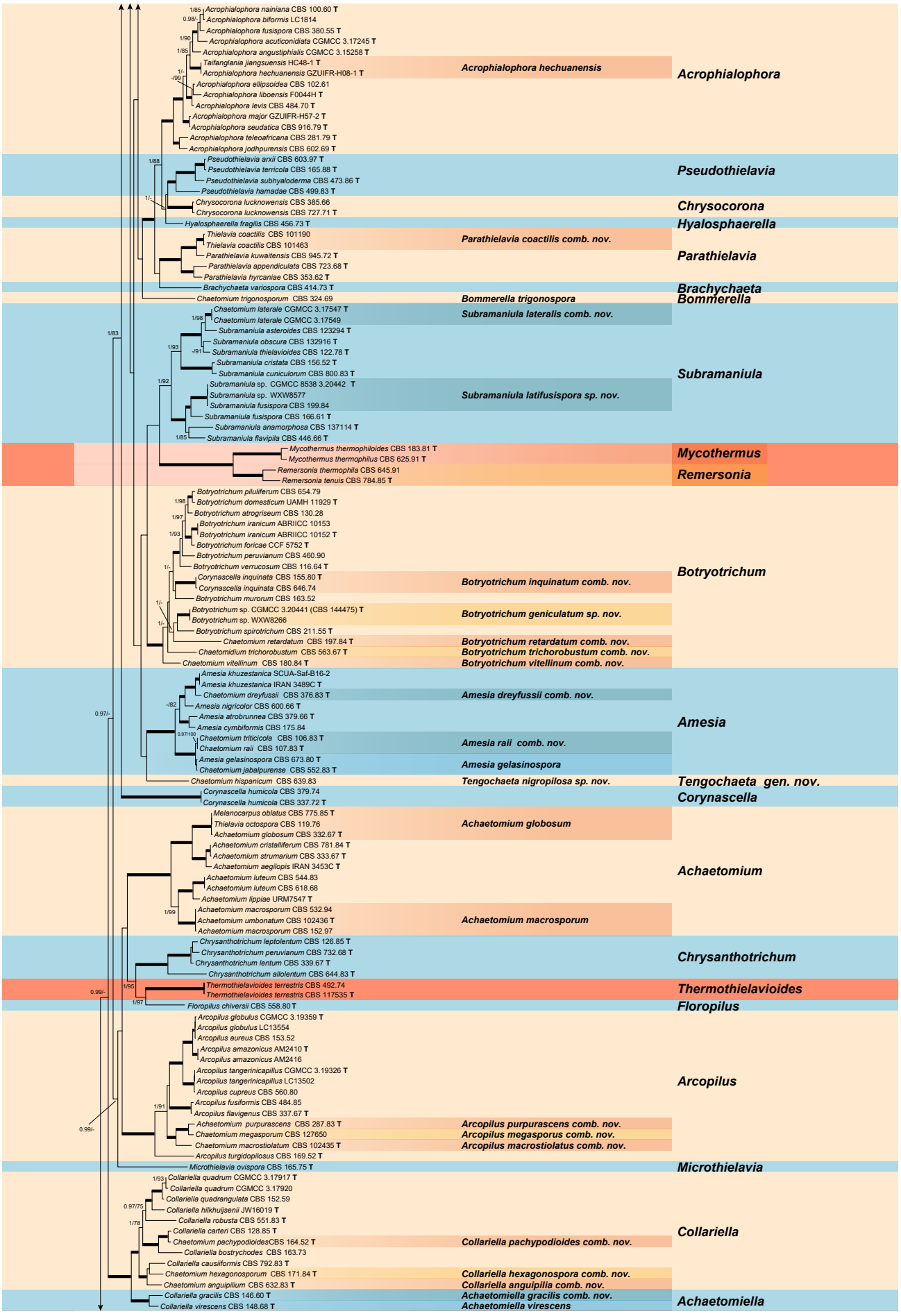

Fig. 7. (Continued).

members of *Lasiosphaeriaceae sensu lato*, distant from the *Chaetomiaceae*.

Arxotrichum, *Botryoderma*, *Corynascus*, *Myceliophthora*, *Parachaetomium* and *Thermothelomyces* are studied here in more detail. These genera include thermophilic species or species phylogenetically related to them. Together with *Dichotomopilus* (Wang *et al.* 2016b), these seven genera share a common ancestor (ML-BS = 70 %; PP = 1.00, Fig. 7A). New combinations are mainly based on the results of the phylogenetic analyses (Fig. 7, Supplementary Figs S1–S3). A number of new species combinations is fully illustrated and described, as examples for a genus.

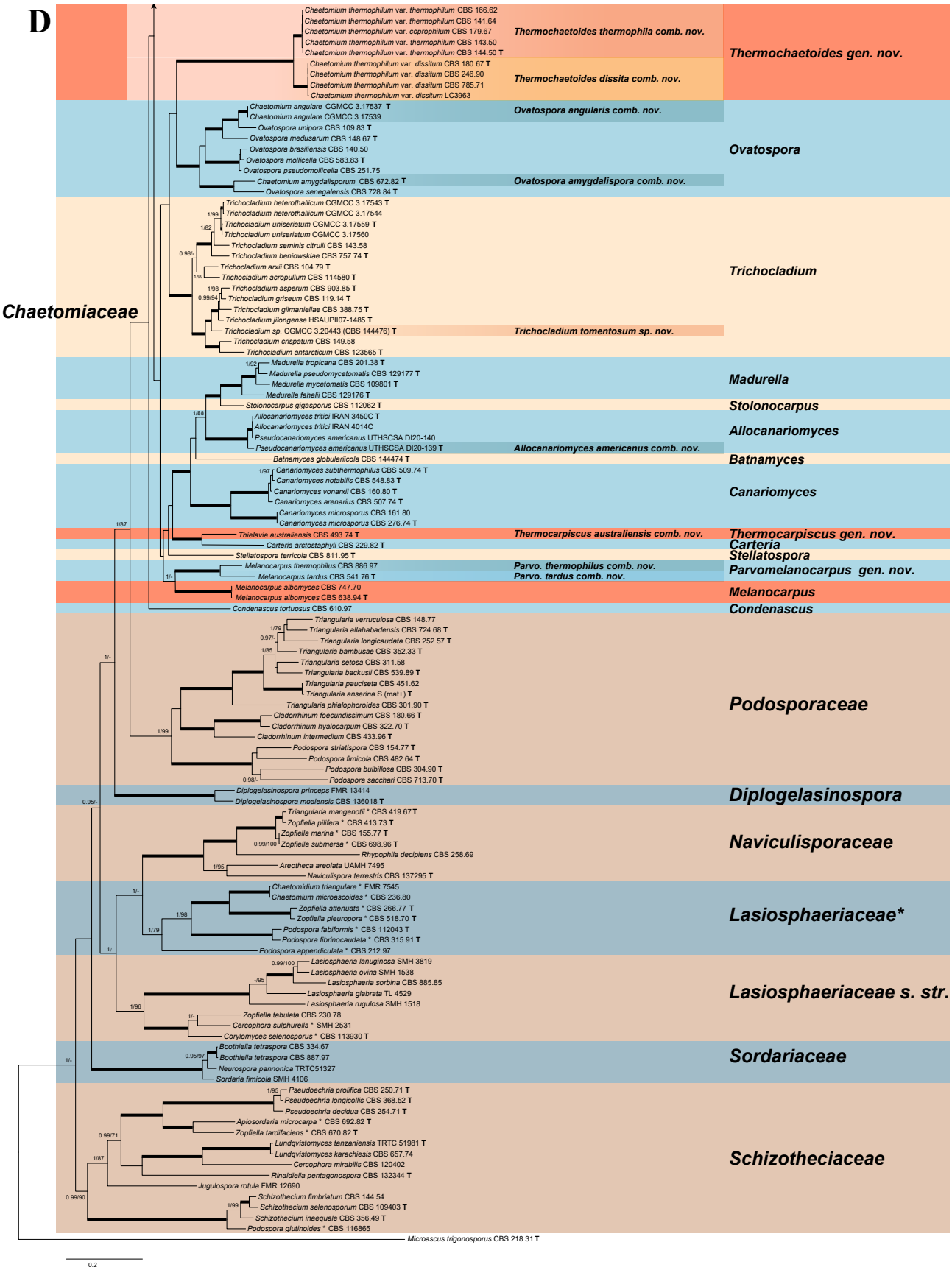

Fig. 7. (Continued).

Table 2. Details of strains sequenced and studied in the present study.

Current name	Culture accession number	Previous identification (if different)	Origin	GenBank accession numbers[1]			
				ITS	LSU	*tub2*	*rpb2*
Achaetomium strumarium	CBS 781.84 = ATCC 58164	*Achaetomium cristalliferum*	Arid saline soil; New Valley Department, near Kharga-Beris, Egypt; type of *Achaetomium cristalliferum*	MH861836	–	**MZ343033**	**MZ342994**
Achaetomium globosum	CBS 775.85	*Melanocarpus oblatus*	Unknown substrate; Niger; type of *Melanocarpus oblatus*	**MZ334727**		**MZ343031**	**MZ342992**
	CBS 119.76 = IMI 291729	*Thielavia octospora*	Dead branch; Pabbi Hills, Pakistan	**MZ334731**	**MZ351416**	**MZ343009**	**MZ342970**
Achaetomium macrosporum	CBS 102436 = FMR 6778 = IMI 381871	*Achaetomium umbonatum*	Garden soil; Kanpur, India; type of *Achaetomium umbonatum*	**MZ334718**	AJ312099	**MZ343007**	**MZ342966**
Amesia dreyfussii	CBS 376.83 = MUCL 40177	*Chaetomium dreyfussii*	Dung of hare; Israel; isotype of *Chaetomium dreyfussii*	MH861613	MH873331	**MZ343023**	**MZ342985**
Amesia gelasinospora	CBS 552.83 = IMI 157256	*Chaetomium jabalpurense*	Unknown substrate and location	–	–	**MZ343026**	**MZ342987**
Amesia raii	CBS 107.83	*Chaetomium raii*	Wood of *Mangifera indica*; India; type of *Chaetomium raii*	–	–	–	**MZ342968**
	CBS 106.83 = IMI 232292	*Chaetomium triticicola*	Stored wheat grain; New Delhi, India; type of *Chaetomium triticicola*	–	–		**MZ342967**
Aporothielavia leptoderma	CBS 538.74 = IMI 054770	*Chaetomidium leptoderma, Thielavia leptoderma*	Soil; Surrey, England; isotype of *Thielavia leptoderma*	NR_164219	NG_067253	**MZ343025**	**MZ342986**
	CBS 113678 = FMR 8192	*Chaetomidium leptoderma*	Black spot on granite rock sample; Serra de Xurés, Galicia, Spain; type of *Chaetomidium galaicum*	–	**MZ351417**	**MZ343008**	**MZ342969**
Arcopilus aureus	CGMCC 3.19359	*Arcopilus globulus*	Root of *Saccharum officinarum*, Guangxi, China	MN215741	MN215579	**MZ343038**	MN255422
Arcopilus cupreus	CGMCC 3.19326	*Arcopilus turgidopilosus*	Root of *Saccharum officinarum*, Guangzhou, China	MN215743	MN215581	MN329904	**MZ342999**
Arcopilus macrostiolatum	CBS 102435 = FMR 6780 = IMI 381870 = MUCL 43147	*Chaetomium macrostiolatum*	Forest soil; Enugu state, Isi-uzo, Nigeria; type of *Chaetomium macrostiolatum*	**MZ334722**	**MZ351418**	**MZ343006**	**MZ342965**
Arcopilus megasporum	CBS 127650	*Chaetomium megasporum*	Agricultural soil; Minnesota, near East Bethel, USA	–	–	**MZ343010**	**MZ342971**
Arcopilus purpurascens	CBS 287.83	*Chaetomium purpurascens*	Soil; Gandaki, Nepal; type of *Achaetomium purpurascens*	–	–	**MZ343021**	**MZ342982**
Arxotrichum deceptivum comb. nov.	CBS 346.73	*Chaetomium deceptivum*	Dung of pack rat; California, USA; isotype of *Chaetomium deceptivum*	**MK919276**	**MK919276**	**MK919390**	**MK919332**
Arxotrichum gangligerum comb. nov.	CBS 160.52 = ATCC 11206	*Chaetomium gangligerum*	Wood sample; Virginia, USA; type of *Chaetomium gangligerum*	**MK919277**	**MK919277**	**MK919391**	**MK919333**
	CBS 130.85	*Chaetomium gangligerum*	Dung of rabbit; Ontario, Canada	**MK919278**	**MK919278**	**MK919392**	**MK919334**
	CBS 563.80	*Chaetomium gangligerum*	Dung of rabbit; Ontario, Canada	**MK919279**	**MK919279**	**MK919393**	**MK919335**
Arxotrichum piluliferoides comb. nov.	CBS 103.77 = IFM 4531 = IMI 210880	*Chaetomium piluliferoides*	Grassland soil; Sugadaira, Naguna Prefecture, Japan; isotype of *Chaetomium piluliferoides*	**MK919280**	**MK919280**	**MK919394**	**MK919336**
	CBS 262.82	*Chaetomium piluliferoides*	Dung; Tarragona, Spain	**MK919281**	**MK919281**	**MK919395**	**MK919337**
Arxotrichum repens comb. nov.	CBS 233.82	*Chaetomium repens*	Soil; Tarragona, Spain; isotype of *Chaetomium repens*	**MK919282**	**MK919282**	**MK919396**	**MK919338**
Arxotrichum sinense comb. nov.	CBS 541.83	*Chaetomium sinense*	Soil; China	**MK919283**	**MK919283**	**MK919397**	**MK919339**

Table 2. (Continued).

Current name	Culture accession number	Previous identification (if different)	Origin	GenBank accession numbers[1]			
				ITS	LSU	*tub2*	*rpb2*
Arxotrichum succineum	CBS 166.52 = ATCC 11216 = MUCL 18704	*Chaetomium succineum*	*Abies magnifica* var. *shastensis*; California, USA; type of *Chaetomium succineum*	**MK919284**	**MK919284**	**MK919398**	**MK919340**
	CBS 813.73 = DAOM 24174 = IMI 044210		*Abies magnifica* var. *shastensis*; California, USA	**MK919285**	**MK919285**	**MK919399**	**MK919341**
	CBS 119769	*Chaetomium succineum*	Soil; Xinjiang, China	**MK919286**	**MK919286**	**MK919400**	**MK919342**
Bommerella trigonospora	CBS 324.69		Soil; Tokyo, Japan		**MZ351419**	**MZ343022**	**MZ342984**
Botryoderma lateritium	CBS 586.66 = ATCC 18926 = IMI 158956 = MUCL 8790		Soil mixed with leaf litter; Transvaal, South Africa	**MK919287**	**MK919287**	**MK919401**	**MK919343**
Botryoderma rostratum	CBS 184.68 = ATCC 18927 = IMI 158957		Sandy soil; Maranhão, Brazil; type of *Botryoderma rostratum*	**MK919288**	**MK919288**	**MK919402**	**MK919344**
Botryotrichum geniculatum sp. nov	CBS 144475 = WXW8287		Soil; Xinjiang, China	**MZ334719**	**MZ351422**	**MZ343011**	**MZ342972**
	WXW8266		Soil; Xinjiang, China	**MZ334720**	**MZ351423**	**MZ343039**	**MZ343000**
Botryotrichum inquinatum comb. nov.	CBS 155.80	*Corynascella inquinata*	Sewage sludge; Nagasaki Pref., Japan; type of *Corynascella inquinata*	**MK919289**	**MK919289**	**MK919403**	**MK919345**
	CBS 646.74	*Thielavia hyalocarpa*	Desert soil; Egypt	**MK919290**	**MK919290**	**MK919404**	**MK919346**
Botryotrichum retardatum	CBS 197.84	*Chaetomium retardatum*	Dung of herbivore; Lake Amboseli, Kenya	–	–	**MZ343019**	**MZ342980**
Botryotrichum trichorobustum	CBS 563.67	*Chaetomidium trichorobustum*	Dung of rabbit; near Hamburg, Germany	–	**MZ351420**	**MZ343027**	**MZ342988**
Botryotrichum vitellinum	CBS 180.84	*Chaetomium vitellinum*	Soil of field; Turkey	**MZ334725**	**MZ351421**	**MZ343018**	**MZ342979**
Chaetomium nepalense	CBS 288.83		Soil; Godawari; Nepal	MH861591	MH873316		**MZ342983**
Chaetomium tarraconense	CBS 101882 = FMR 6638 = IMI 380425 = MUCL 43149		Soil; Tarragona, Spain; type of *Chaetomium tarraconensis*	–	–	**MZ343005**	**MZ342964**
Collariella anguipilia	CBS 632.83	*Chaetomium anguipilium*	Dung of rabbit; New Mexico, USA; type of *Chaetomium anguipilium*	**MZ334721**	**MZ351424**	**MZ343028**	**MZ342989**
Collariella hexagonospora	CBS 171.84 = FMR 7235	*Chaetomium hexagonosporum*	Dung of pack rat; Nevada, USA; type of *Chaetomium hexagonosporum*	MH861717		**MZ343016**	**MZ342977**
Collariella pachypodioides	CBS 164.52 = ATCC 11213 = IMI 012266 = IMI 287299 = MUCL 9586	*Chaetomium pachypodioides*	Vegetable detritus; Tennessee, USA; type of *Chaetomium pachypodioides*	MH856980	MH868500	**MZ343014**	**MZ342975**
Corynascella humicola	CBS 337.72		Soil; North Carolina, Piedmont, USA; type of *Corynascella humicola*	KX976656	KX976751	KX976998	**MK942091**
	CBS 379.74		Soil; North Carolina, Piedmont, USA; type of *Corynascella humicola*	KX976657	KX976752	KX976999	**MK942092**

Table 2. (Continued).

Current name	Culture accession number	Previous identification (if different)	Origin	GenBank accession numbers[1]			
				ITS	LSU	*tub2*	*rpb2*
Corynascus fumimontanus	CBS 137294 = FMR 12372		Forest soil; Tennessee, USA; type of *Corynascus fumimontanus*	LK932694	**MK919291**	**MK919405**	**MK919347**
Corynascus novoguineensis	CBS 359.72	*Myceliophthora novoguineensis*	Soil; New Britain, Rabaul, Papua New Guinea; type of *Thielavia novoguineensis*	HQ871762	**MK919292**	**MK919406**	**MK919348**
Corynascus sepedonium	CBS 111.69 = IMI 136625	*Myceliophthora sepedonium*	Soil; Allahabad, India; type of *Thielavia sepedonium* var. *minor*	HQ871751	KX976777	KX977027	**MK919349**
	CBS 632.67	*Corynascus similis*	Soil; Uzbekistan; type of *Thielavia lutescens*	HQ871759	**MK919293**	**MK919407**	**MK919350**
	CBS 101936 = FMR 5693	*Corynascus similis*	Soil; Ajmed, India	**MK919294**	**MK919294**	**MK919408**	**MK919351**
Corynascus sexualis	CBS 827.96 = FMR 5691		Soil; Jaipur, India	AJ224202	**MK919295**	**MK919409**	**MK919352**
Corynascus verrucosus	CBS 602.97 = IMI 378522 = FMR 5904		Soil; Quilmes, Argentina	AJ224203	**MK919296**	**MK919410**	**MK919353**
	CBS 135878 = FMR 12783		Forest soil; Tennessee, USA	**MK919297**	**MK919297**	**MK919411**	**MK919354**
Humicola hirsuta sp. nov.	CBS 144492 = WXW 9028		Soil; Sanxi, China	**MZ334726**	**MZ351425**	**MZ343013**	**MZ342974**
Melanocarpillus thermophilus	CBS 886.97 = FMR 6190 (representative)	*Thielavia minuta* var. *thermophila*/*Melanocarpus thermophilus*	Soil; Agra, India	KM655350	MH874288	**MZ343037**	xKM655434
	CBS 379.76 = ATCC 14741 = IMI 086454		Usar soil; Lucknow, Uttar Pradesh, India; type of *Sporotrichum carthusioviride*	**MK919302**	**MK919302**	**MK919416**	**MK919359**
Ovatospora amygdalispora	CBS 672.82 = IMI 291735	*Chaetomium amygdalisporum*	Soil; Japan; type of *Chaetomium amygdalisporum*	–	–	**MZ343030**	**MZ342991**
Parachaetomium biporatum comb. nov.	CBS 244.86 = FMR 854 = IMI 330348	*Chaetomium biporatum*	Soil; Valencia, Spain; type of *Chaetomium biporatum*	**MK919303**	**MK919303**	**MK919417**	**MK919360**
Parachaetomium carinthiacum	CBS 153.81	*Chaetomium carinthiacum*	Unknown substrate; Meylan, France	**MK919298**	**MK919298**	**MK919412**	**MK919355**
	CBS 665.82	*Chaetomium carinthiacum*	*Thymus* sp.; Japan	**MK919299**	**MK919299**	**MK919413**	**MK919356**
Parachaetomium hispanicum comb. nov.	CBS 234.82	*Chaetomium hispanicum*	Dung; Tarragona, Spain; type of *Chaetomium hispanicum*	**MK919304**	**MK919304**	**MK919418**	**MK919361**
	CBS 550.83 = FMR 502	*Chaetomium hispanicum*	Soil; Reus, Spain	**MK919305**	**MK919305**	**MK919419**	**MK919362**
Parachaetomium inaequalis comb. nov.	CBS 331.75 = IMI 196527	*Corynascella inaequalis*	Soil of oak forest; Kirovograd, Ukraine; type of *Thielavia inaequalis*	**MK919306**	**MK919306**	**MK919420**	**MK919363**
	CBS 164.75	*Corynascella inaequalis*	Soil; Kirovograd, Ukraine	**MK919307**	**MK919307**	**MK919421**	**MK919364**
Parachaetomium mareoticum comb. nov.	CBS 802.83	*Chaetomium mareoticum*	Dung; Moledet, Israel	**MZ334723**	**MZ351426**	**MZ343036**	**MZ342997**
	CBS 781.71		Dung of gazelle; Israel			**MZ343032**	**MZ342993**
Dimorphopilus muelleri comb. nov.	CBS 192.84	*Chaetomium muelleri*	Decayed twig; Lahore, Pakistan; type of *Chaetomium muelleri*	**MK919300**	**MK919300**	**MK919414**	**MK919357**
	CBS 663.75	*Chaetomium muelleri*	Unknown substrate; Bornova-Izmir, Turkey	**MK919301**	**MK919301**	**MK919415**	**MK919358**

Table 2. (Continued).

Current name	Culture accession number	Previous identification (if different)	Origin	GenBank accession numbers[1]			
				ITS	LSU	*tub2*	*rpb2*
Parachaetomium multispirale comb. nov.	CBS 172.84 = TRTC 66609	*Chaetomium multispirale*	Dung of herbivore; Mt. Kenya, Kenya; type of *Chaetomium multispirale*	**MH861718**	–	**MZ343017**	**MZ342978**
Parachaetomium perlucidum comb. nov.	CBS 141.58 = IMI 074954 = MUCL 18693 = MUCL 39399	*Chaetomium perlucidum*	Dead herbaceous stem; Kiev, Ukraine; type of *Chaetomium perlucidum*	**MK919308**	**MK919308**	**MK919422**	**MK919365**
	CBS 119762 = AS 3.9405	*Chaetomium raii*	Soil; Xinjiang, China	**MK919309**	**MK919309**	**MK919423**	**MK919366**
	CBS 126670	*Chaetomium iranianum*	Leaf of *Hordeum vulgare;* East Azerbaijan Prov., Iran; type of *Chaetomium iranianum*	**MK919310**	**MK919310**	**MK919424**	**MK919367**
	CBS 127795	*Chaetomium perlucidum*	Soil; Wyoming, USA	**MK919311**	**MK919311**	**MK919425**	**MK919368**
Parachaetomium subspirilliferum comb. nov.	CBS 150.60 = ATCC 14534 = IMI 081771 = MUCL 18698	*Chaetomium subspirilliferum*	Soil; Kulundinskaya steppe, Altai, Russia; type of *Chaetomium subspirilliferum*	**MK919312**	**MK919312**	**MK919426**	**MK919369**
	WXW 9901-2	*Chaetomium subspirilliferum*	Soil; Xinjiang, China	**MK919313**	**MK919313**	**MK919427**	**MK919370**
Parathielavia coactilis comb. nov.	CBS 101190 (representative)	*Thielavia coactilis*	Bark of lower branches of *Atraphaxis replicata*; Mangyschlak Peninsula, near Mt. Kunabai, Kazakhstan	–	–	**MZ343003**	**MZ342962**
	CBS 101463		Dead leaves of *Carpinus betulus*; Ile de France, France	–	–	**MZ343004**	**MZ342963**
Subramaniula fusispora	CBS 166.61		Soil, red-brown earth; Adelaide, South Australia, Australia; type of *Chaetomium fusisporum*	MH858011	MH869571	**MZ343015**	**MZ342976**
Subramaniula lateralis comb. nov.	CGMCC 3.17547	*Chaetomium laterale*	*Leymus chinensis*, Inner Mongolia, China	KP336789	KP336838	KP336887	**MZ342998**
Subramaniula latifusispora sp. nov.	CGMCC 20442 = WXW 8538		Sheep dung; Xinjiang, China	**MZ334728**	**MZ351428**	**MZ343040**	**MZ343001**
	WXW 8577		Fallen spruce fruit; Xinjiang, China	**MZ334729**	**MZ351427**	**MZ343041**	**MZ343002**
Tengochaeta nigropilosa gen. et sp. nov.	CBS 639.83		Soil from *Pinus* forest; Tenerife, Spain	**MZ334730**		**MZ343029**	**MZ342990**
Thermocarpusella australiensis gen. et comb. nov.	CBS 493.74 = ATCC 28236 = DAOM 145919	*Thielavia australiensis*	Nesting material of incubator bird; Pulletop Nature Reserve near Griffith, New South Wales, Australia; type of *Thielavia australiensis*	KM655339	KM655378	**MZ343024**	KM655419
Thermochaetoides dissita gen. et comb. nov.	CBS 180.67 = ATCC 16452 = IMI 126332	*Chaetomium thermophilum* var. *dissitum*	Straw of *Typha*; California, USA; type of *Chaetomium thermophilum* var. *dissitum*	**MK919319**	**MK919319**	**MK919433**	**MK919375**
	CBS 246.90	*Chaetomium thermophilum* var. *dissitum*	Dung of pig with sawdust; Netherlands	**MK919320**	**MK919320**	**MK919434**	**MK919376**
	CBS 785.71	*Chaetomium thermophilum* var. *dissitum*	Dung of gazelle; Israel	**MK919321**	**MK919321**	**MK919435**	**MK919377**
Thermochaetoides thermophila comb. nov.	CBS 144.50	*Chaetomium thermophilum* var. *thermophilum*	Decaying wheat straw; Leeds, UK; type of *Chaetomium thermophilum* var. *thermophilum*	**MK919314**	**MK919314**	**MK919428**	KM655436
	CBS 143.50	*Chaetomium thermophilum* var. *thermophilum*	Decaying wheat straw; Leeds, UK	**MK919315**	**MK919315**	**MK919429**	**MK919371**
	CBS 166.62	*Chaetomium thermophilum* var. *thermophilum*	Mushroom compost; Netherlands	**MK919316**	**MK919316**	**MK919430**	**MK919372**

Table 2. (Continued).

Current name	Culture accession number	Previous identification (if different)	Origin	GenBank accession numbers[1]			
				ITS	LSU	*tub2*	*rpb2*
	CBS 141.64	*Chaetomium thermophilum* var. *thermophilum*	Mushroom compost; Zürich, Switzerland	**MK919317**	**MK919317**	**MK919431**	**MK919373**
	CBS 179.67 = ATCC 16451= IMI 126331	*Chaetomium thermophilum* var. *coprophilum*	Horse dung; California, USA; type of *Chaetomium thermophilum* var. *coprophilum*	**MK919318**	**MK919318**	**MK919432**	**MK919374**
Thermothelomyces fergusii nom. nov.	CBS 406.69 = ATCC 22067	*Crassicarpon thermophilum*	Mushroom compost, Pennsylvania, USA; type of *Thielavia thermophila*	HQ871794	KX976776	KX977024	**MK919378**
	CBS 174.70 = IMI 145136	*Myceliophthora fergusii*	Wheat straw compost; Cambridge, England	**MK919322**	**MK919322**	**MK919436**	**MK919379**
Thermothelomyces guttulatus	CGMCC 3.15185		Soil; Hunan, China	KC352943	**MK919323**	**MK919437**	**MK919380**
	CGMCC 3.15186		Soil; Hunan, China	KC352944	**MK919324**	**MK919438**	**MK919381**
Thermothelomyces heterothallicus	CBS 203.75		Soil; Indiana, USA; authentic strain of *Thielavia heterothallica*	HQ871772	**MK919325**	**MK919439**	**MK919382**
	CGMCC 3.13596		Soil; USA	**MK919326**	**MK919326**	**MK919440**	**MK919383**
Thermothelomyces hinnuleus	CBS 597.83		Cultivated soil; Japan; type of *Myceliophthora hinnulea*	HQ871791	**MK919327**	**MK919441**	**MK919384**
	CBS 544.82		Soil; Christchurch, New Zealand	**MK919328**	**MK919328**	**MK919442**	**MK919385**
Thermothelomyces myriococcoides nom. nov.	CBS 389.93 = ATCC 22112 = CBS 736.70	*Myriococcum thermophilum*	Surface of heated compost; Switzerland; type of *Papulaspora thermophila*	**MK919329**	**MK919329**	**MK919443**	**MK919386**
	CBS 208.89	*Myriococcum thermophilum*	Self-heating horse manure; Netherlands	**MK919330**	**MK919330**	**MK919444**	KM655394
Thermothelomyces thermophilus	CBS 117.65		Dry pasture soil; England; isotype of *Sporotrichum thermophilum*	HQ871764	**MK919331**	**MK919445**	**MK919387**
	CBS 669.85		Mutant of CBS 866.85; USA	HQ871767	KX976778	KX977028	**MK919388**
	CBS 381.97		Man; unknown location	HQ871766	KX976779	KX977029	**MK919389**
Trichocladium tomentosum sp. nov.	CBS 144476 = WXW 8615		Soil; Qinghai, China	**MZ334732**	**MZ351431**	**MZ343012**	**MZ342973**
Xanthiomyces spinosum gen. et comb. nov. (representative)	CBS 789.71	*Chaetomium spinosum*	Culture of algae; Zürich, Switzerland	MH860357	**MZ351429**	**MZ343034**	**MZ342995**
	CBS 796.83		Straw; Bloney, Switzerland	**MZ334724**	**MZ351430**	**MZ343035**	**MZ342996**
	CBS 236.80	*Chaetomium microascoides*	Soil; Spain	MH861259	MH873028	**MZ343020**	**MZ342981**

[1] Sequences generated in this study are indicated in **bold**.

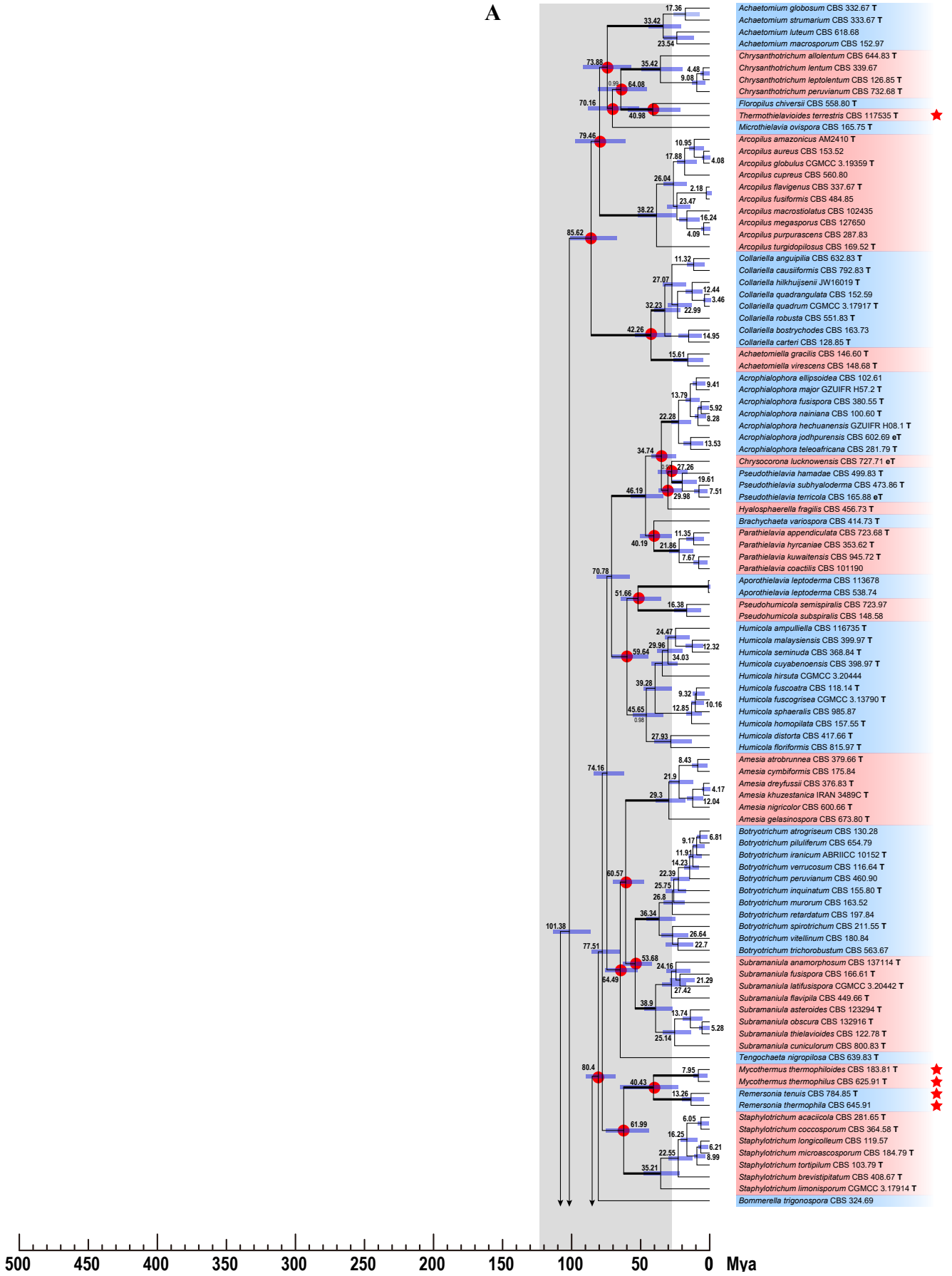

Fig. 8. Maximum clade credibility tree of *Sordariales* based on *rpb2*, *tub2*, ITS and LSU sequences. Blue bars around each internode correspond to 95 % divergence time confidence intervals for each branch. For reference, the time scale is shown right below the phylogenetic tree. Different genera are depicted using different-coloured blocks. Dating estimates were calibrated using five constraints marked by red triangles. Mean divergence times of genera in *Chaetomiaceae* are marked in red dots and those of families in *Sordariales* marked in yellow dots. The robust confidence values (posterior probabilities ≥ 0.95) for genera or higher clades of *Sordariales* indicated at the notes and the branches with full statistical support (PP = 1.0) are highlighted by thickened branches. The red stars at the right of species names highlight the thermophilic species.

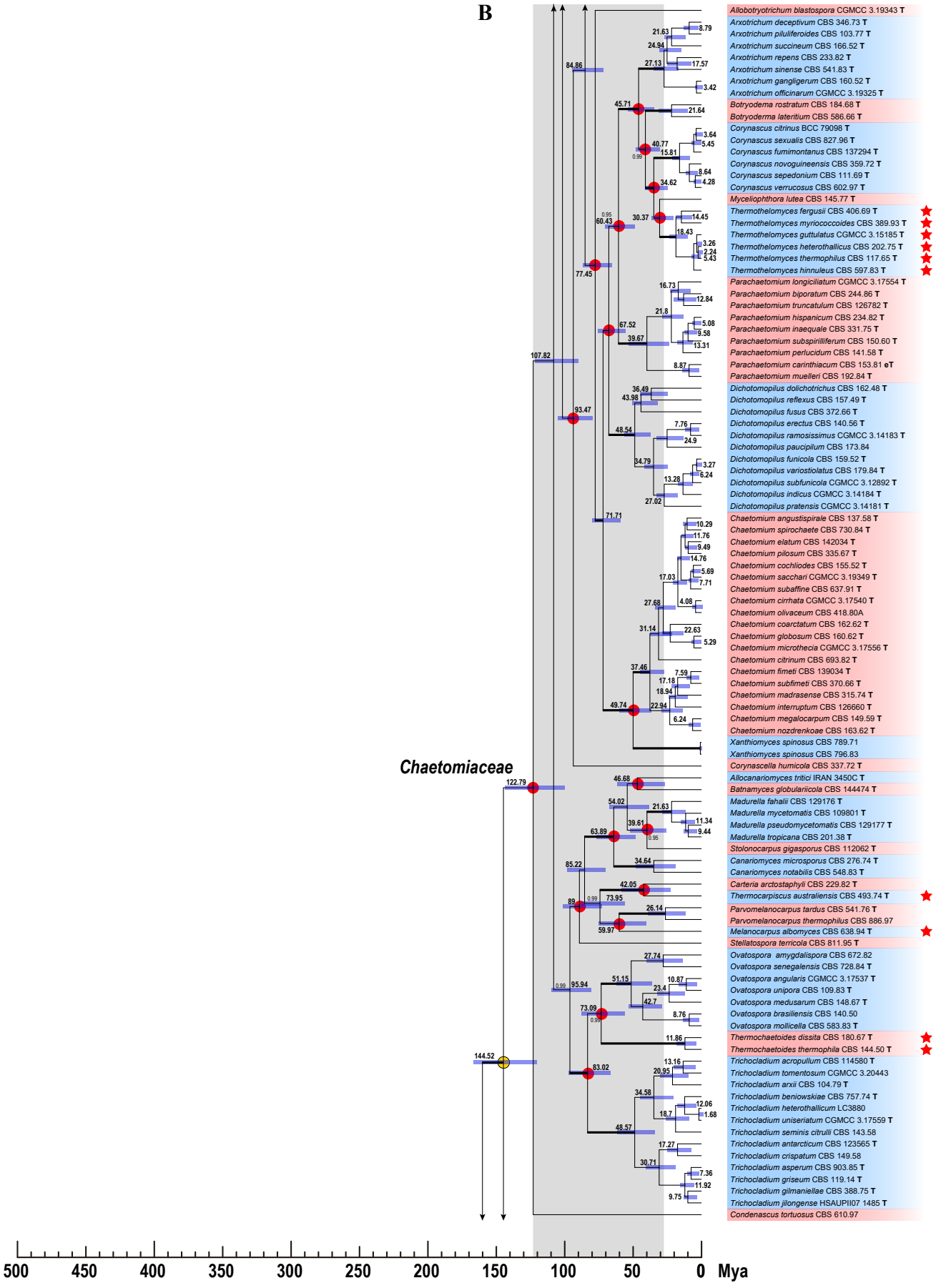

Fig. 8. (Continued).

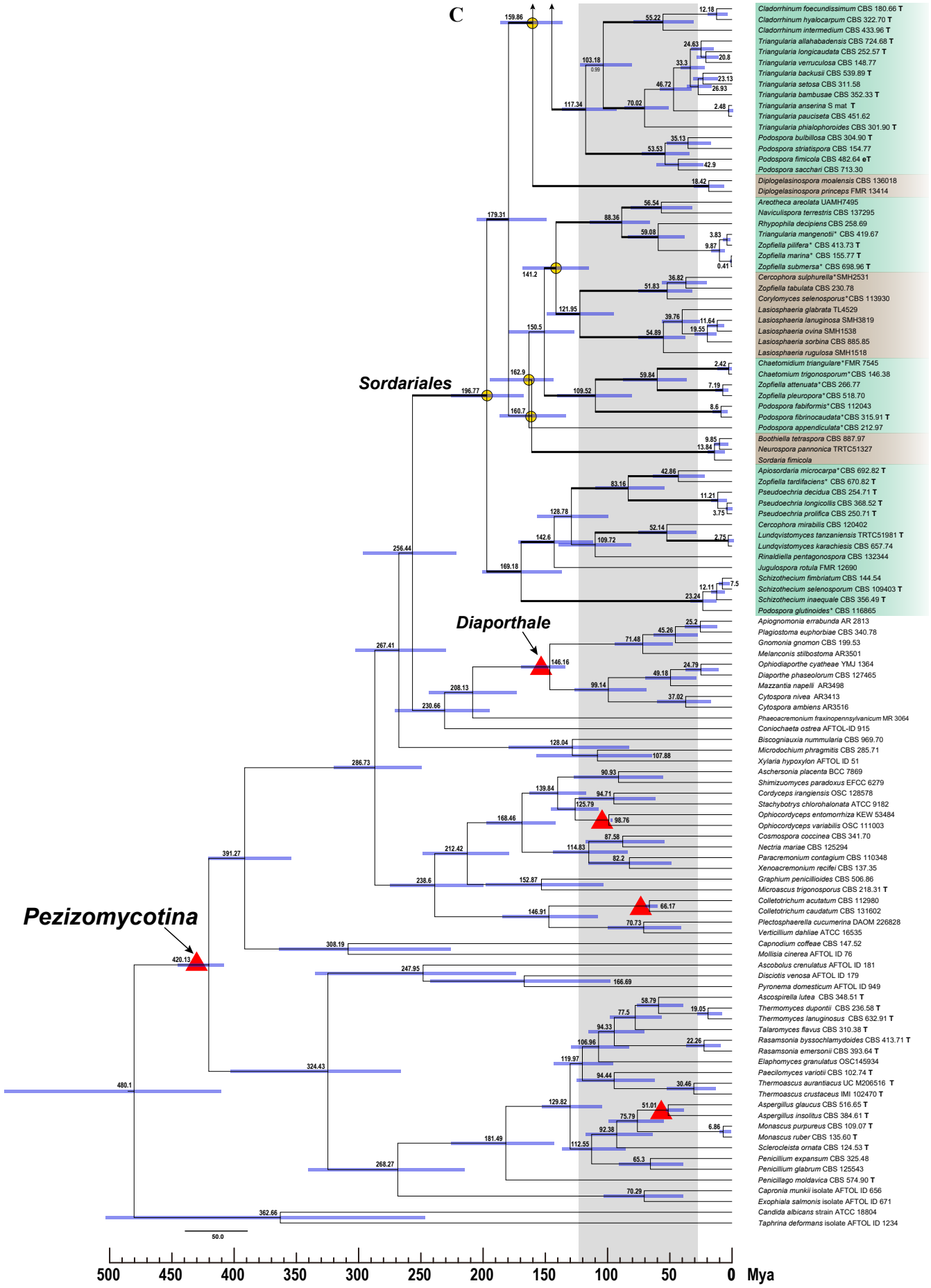

Fig. 8. (Continued).

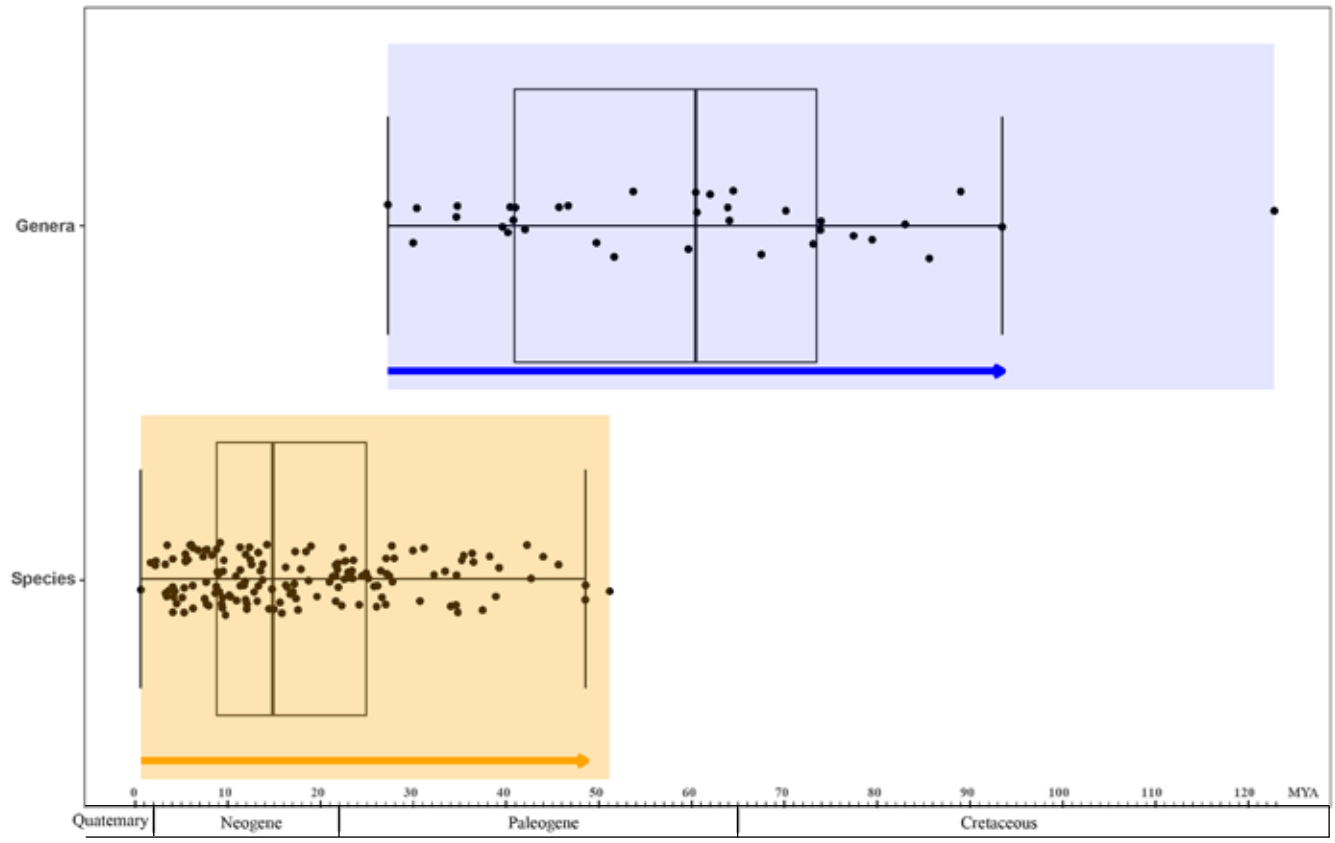

Fig. 9. Comparison of divergence times between species (yellow block) and genera (blue block) in *Chaetomiaceae*.

Table 3. Overview of selected calibration points (Samarakoon *et al.* 2019) in this study.

No.	Crown calibrating point	Fossil taxa	Minimum age (Ma)
1	*Pezizomycotina*	*Paleopyrenomycites devonicus*	410
2	*Diaporthales*	*Spataporthe taylorii*	136
3	*Ophiocordyceps*	*Paleoophiocordyceps coccophagus*	99
4	*Colletotrichum*	*Protocolletotrichum deccanensis*	61
5	*Aspergillus*	*Aspergillus collembolorum*	35

Achaetomiella Arx, The genera of fungi sporulating in pure culture: 247. 1970. Fig. 10.

Micromorphology: *Ascomata* superficial, ostiolate, subglobose or ovate, with brown walls of *textura angularis* in surface view. *Terminal hairs* straight, flexuous, undulate or arcuate. *Lateral hairs* straight, flexuous. *Asci* fasciculate, clavate, fusiform or obovate, with eight irregularly-arranged ascospores, evanescent. *Ascospores* brown when mature, ellipsoidal or fusiform, with an apical or sometimes slightly sub-apical germ pore, usually more than 9 µm in length. *Asexual morph* not observed.

Type species: *Achaetomiella virescens* Arx

Notes: *Achaetomiella*, typified by *Ach. virescens*, was introduced by von Arx (1970) as an intermediate between *Achaetomium* and *Chaetomium*. This genus was characterised by the production of simple ascomatal hairs that are evenly distributed over the ascoma. Udagawa (1980) transferred *Ach. virescens* to *Chaetomium* and this was accepted by Cannon (1986) and von Arx *et al.* (1986). Based on a multigene phylogenetic analysis (Wang *et al.* 2016b), *Ach. virescens* was transferred to *Collariella*. At that time, two morphologically distinct groups were observed within the genus. Molecular dating analysis indicated that these two groups diverged from each other as early as about 42 Mya (Fig. 8A). Group I includes the type species of *Collariella* and is redefined here as *Collariella sensu stricto* (Fig. 10), and *Achaetomiella* is resurrected to accommodate taxa belonging to group II (Fig. 22). *Collariella* and *Achaetomiella* are sister genera (Fig. 7C, Supplementary Figs S2, S3) and the generic concept of *Collariella* is redefined below. *Collariella* is characterised by 1) ascomata that usually have a darkened collar around the ostiolar pore, 2) broadly limoniform to quadrangular, bilaterally flattened ascospores with an apical germ pore, 3) ascospores length usually less than 7.5 µm, with *Col. hexagonospora* (9–10.5 µm long) being the only exception (see also notes of *Collariella sensu stricto* below). In contrast, *Achaetomiella* species lack a darkened collar around the ostiolar pore of ascomata, and their ascospores can be ellipsoidal or fusiform, but never limoniform or quadrangular, and never bilaterally flattened. Two species are accepted in this genus, *Achaetomiella gracilis* and *Achaetomiella virescens.* Ascomatal hairs cannot be used as a diagnostic characteristic for *Achaetomiella*.

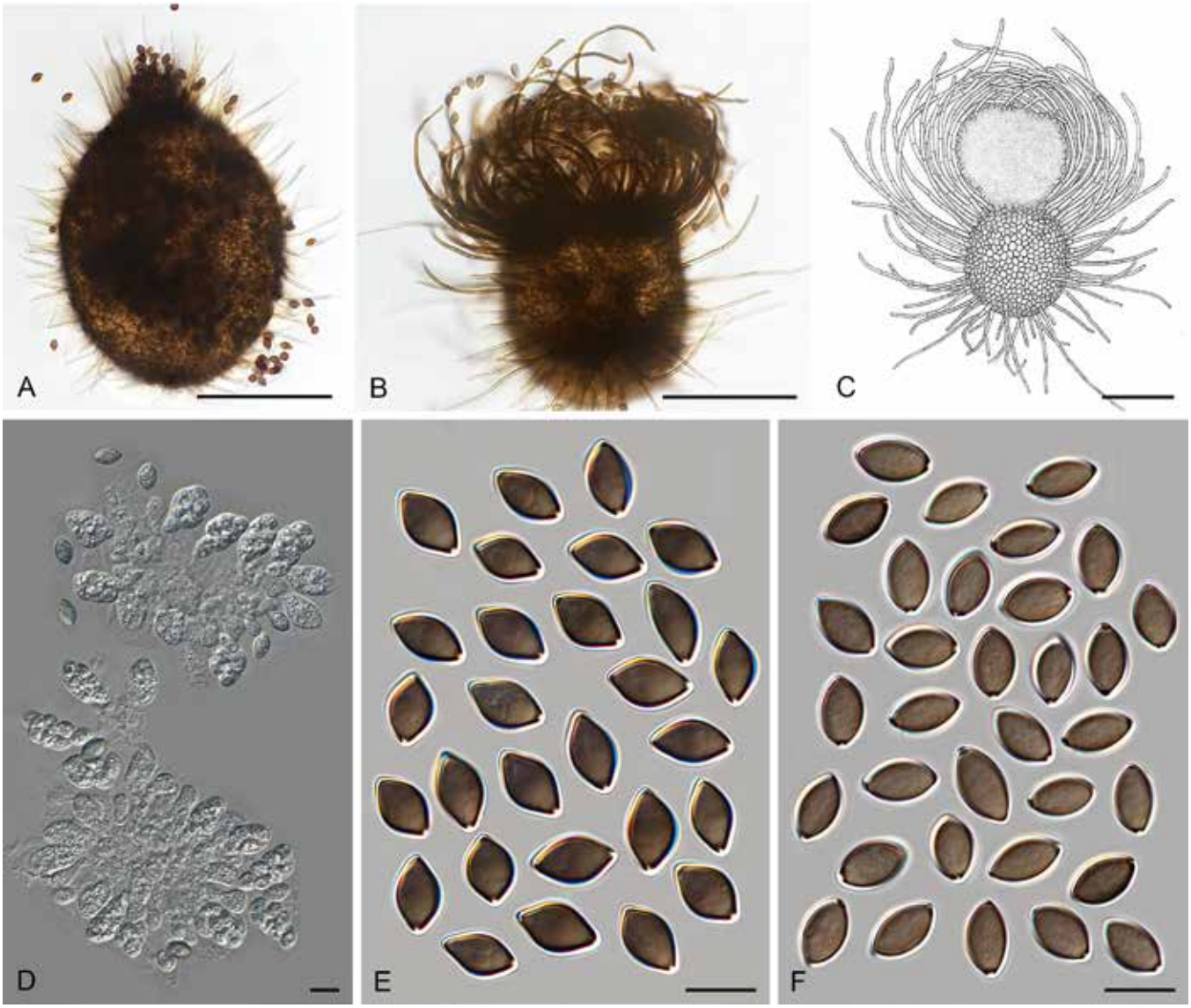

Fig. 10. Morphology of *Achaetomiella*. Ascomata (A–C): **A.** *Ach. virescens* (CBS 148.68[T]). **B.** *Ach. gracilis* (CBS 249.75). **C.** Line drawing of *Ach. gracilis* (CGMCC 3.3782). **D.** Asci of *Ach. gracilis* (CBS 249.75). Ascospores (E, F): **E.** *Ach. virescens* (CBS 148.68 [T]). **F.** *Ach. gracilis* (CBS 249.75). Scale bars: A–C = 100 µm; D–F =10 µm.

Achaetomiella gracilis (Udagawa) Houbraken, X.Wei Wang, P.J. Han & F.Y. Bai, ***comb. nov.*** MycoBank MB 840195. Fig. 10B–D, F.
Basionym: *Chaetomium gracile* Udagawa, J. Gen. Appl. Microbiol. 6: 235. 1960.
Synonym: *Collariella gracilis* (Udagawa) X.Wei Wang & Samson, Stud. Mycol. 84: 185. 2016.

Notes: This species can be distinguished from *Ach. virescens* by numerous arcuate ascomatal hairs surrounding the truncated apical ostiole (Fig. 10B, C), while the ascomata of *Ach. virescens* are tapered at the apex and covered by sparse, straight and short hairs (Fig. 10A).

Achaetomiella virescens Arx, The genera of fungi sporulating in pure culture: 247. 1970. Fig. 10A, E.
Synonyms: *Chaetomium virescens* (Arx) Udagawa, Trans. Mycol. Soc. Japan 21: 34. 1980.
Collariella virescens (Arx) X.Wei Wang & Samson, Stud. Mycol. 84: 217. 2016.

Notes: According to the description of von Arx *et al.* (1986), this species produces ascospores with two apical germ pores, but the figure in their monograph (Plate 91D) shows ascospores with only one apical germ pore. Our observations confirmed that ascospores have one apical germ pore (Fig. 10E).

Allocanariomyces Mehrabi *et al.*, Mycol. Prog. 19: 1417. 2020.
Synonym: *Pseudocanariomyces* Cañete-Gibas *et al.*, Mycopathologia 186: 443. 2021.

Micromorphology and illustrations: See Mehrabi *et al.* (2020). Species producing both a sexual and asexual morph.

Type species: *Allocanariomyces tritici* Mehrabi, Asgari & Zare

Notes: *Allocanariomyces* was first proposed for a seed endophyte of *Triticum boeoticum*. This genus is morphologically similar to *Canariomyces* in its asexual (solitary and appressonium-like conidia laterally produced from hyphae) and sexual morph (producing non-ostiolate ascomata and ellipsoidal-fusiform ascospores with a subapical or apical germ pore), but is phylogenetically distinct (Mehrabi *et al.* 2020). Later, Ryan *et al.* (2021) proposed *Pseudocanariomyces* to accommodate strains isolated from a prosthetic hip infection of a 65-yr-old white woman and a

human ear respectively. Our phylogenetic analysis showed that *Pseudocanariomyces* is a synonym of *Allocanariomyces* (Fig. 7D).

Allocanariomyces americanus (Cañete-Gibas *et al*.) Cañete-Gibas, Wiederhold, X.Wei Wang & Houbraken, ***comb. nov.*** MycoBank MB 840154.
Basionym: *Pseudocanariomyces americanus* Cañete-Gibas *et al*., Mycopathologia 186: 443. 2021.

Notes: Two strains identified as *Pseudocanariomyces americanus* were reported in Ryan *et al*. (2021). The ex-type strain UTHSCSA DI20-139 (= CBS 147185), isolated from a prosthetic hip infection of a patient, represents a species belonging to *Allocanariomyces* and this combination is proposed here. The other strain (UTHSCSA DI20-140 = CBS 147186), isolated from a human ear, is phylogenetically different and is re-identified here as *Allocanariomyces tritici* (Fig. 7D). *Allocanariomyces americanus* produces smaller ascomata than *Allocan. tritici* (15–90 × 20–92.5 µm *vs* 100–130 µm diam), but has ascospores (12.5–25 × 8.75–15 µm *vs* 13–22.8 × 9–16 µm) and conidia (5–7.75 × 2.5–5 µm *vs* 3–9 × 3–4.5 µm) similar to those of *Allocan. tritici* in shapes and sizes (Mehrabi *et al.* 2020, Ryan *et al*. 2021).

Amesia X.Wei Wang *et al*., Stud. Mycol. 84: 156. 2016.

Micromorphology and illustrations: See Wang *et al.* (2016b; p. 156–163). Species producing only a sexual morph.

Type species: *Amesia atrobrunnea* (L.M. Ames) X.Wei Wang & Samson

Notes: The genus *Amesia* was proposed for four species that originally were described in *Chaetomium* (Wang *et al.* 2016b). These four species produce ostiolate ascomata, but the morphological diversity in ascomatal hairs and ascospores among species in the genus proved to be large. The ascomatal hairs of *Amesia* species can be straight, flexuous, undulate or spirally coiled, and ascopores can be fusiform, elongated fusiform, ovate, elongated ovate or pyriform, with an apical or sub-apical germ pore. Two more chaetomium-like species proved to be members of this genus based on our phylogenetic analysis (Fig. 7C). Both morphologically fit in the definition of *Amesia* (von Arx *et al.* 1986, Wang *et al.* 2016b).

Amesia dreyfussii (Arx) X.Wei Wang & Houbraken, ***comb. nov.*** MycoBank MB 840132.
Basionym: *Chaetomium dreyfussii* Arx, Beih. Nova Hedwigia 84: 6. 1986.

Notes: This species can be distinguished from other *Amesia* species by the production of seta-like terminal hairs surrounding the apical ostioles and elongated fusiform or pyriform ascospores with an apical germ pore at the relatively broad end (Fig. 4-AJ). Von Arx *et al.* (1986) incorrectly described the ascospores of this species with an apical germ pore at the most attenuated end; however, this does not match with what is shown in their supplied illustration (Plate 22D).

Amesia raii (G. Malhotra & Mukerji) X.Wei Wang & Houbraken, ***comb. nov.*** MycoBank MB 840137.
Basionym: *Chaetomium raii* G. Malhotra & Mukerji, Rev. Mycol. (Paris) 40: 182. 1976.

Notes: *Amesia raii* produces ascomata covered by undulate to spirally coiled terminal hairs and fusiform or elongated ovate ascospores with a subapical germ pore. As indicated by von Arx *et al.* (1986), this species is morphologically quite like *Para. perlucidum* (Fig. 37, see below), but phylogenetically distant (Fig. 7A, C). *Amesia gelasinospora* is phylogenetically related to *Am. raii* (Fig. 7C, Supplementary Fig. S3; ITS and *tub2* sequences of *Am. raii* are not available) and produces ascospores with a subapical germ pore. The former species can be distinguished by the production of numerous and more regularly coiled ascomatal hairs, and by the shape of its ascospores that are ovate or broadly fusiform (Wang *et al.* 2016b).

Aporothielavia Malloch & Cain, Mycologia 65: 1074. 1973.

Micromorphology: *Ascomata* superficial, non-ostiolate, spherical, pilose. *Ascomatal wall* brown, consisting of cephalothecoid plates in surface view. *Ascomatal hairs* brown, slightly undulate, tapering towards the tips, smooth, sometimes absent. *Asci* pyriform to fusiform with eight irregularly-arranged ascospores. *Ascospores* olivaceous when mature, fusiform, with an apical or slightly subapical germ pore. *Asexual morph* produced as intercalary or terminal chlamydospores, solitary or catenulate, ellipsoidal to globose, brown, 1-celled, smooth-walled, lacking germ pores. Containing only one species with both asexual and sexual morphs.

Type species: *Aporothielavia leptoderma* (C. Booth) Malloch & Cain

Notes: Booth (1961) originally described the type species of *Aporothielavia* in *Thielavia*. In the original description it was mentioned that this species produces fusiform ascospores with an indistinct germ pore. However, Malloch & Cain (1973) re-examined the ex-type culture and noted that their strain produced ascospores without germ pores. Based on these observations, they introduced *Aporothielavia* to accommodate this species. Later, Greif & Currah (2007) transferred *Apor. leptoderma* to *Chaetomidium* because they observed an apical germ pore and noticed the species' morphological similarity to *Chaetomidium arxii* (= *Trichocladium arxii*) (both have non-ostiolate ascomata with long hairs). Our examination confirmed the presence of a germ pore in the ascospores (Fig. 11J), but phylogenetic analysis showed that this species forms a unique clade in the family (Fig. 7B). The monotypic genus *Aporothielavia* is therefore resurrected and redefined.

Aporothielavia leptoderma (C. Booth) Malloch & Cain, Mycologia 65: 1074. 1973. Fig. 11.
Basionym: *Thielavia leptoderma* C. Booth [as '*leptodermus*'], Mycol. Pap. 83: 3. 1961.
Synonyms: *Chaetomidium leptoderma* (C. Booth) Greif & Currah, Mycol. Res. 111: 74. 2007.
Chaetomidium gallecicum Stchigel & Guarro [as '*galaicum*'], Stud. Mycol. 50: 217. 2004.

Micromorphology: *Ascomata* superficial or covered by aerial mycelium, solitary to loosely aggregated, non-ostiolate, leaden black when mature in reflected light due to the dark ascomatal wall, spherical, pilose, (100–)155–475 µm diam. *Ascomatal wall* brown, consisting of cephalothecoid plates which are composed of radially elongated cells in surface view. *Ascomatal hairs* brown, slightly undulate, tapering towards the tips, smooth, (2.5–)3–5 µm diam near the base, sometimes absent. *Asci* pyriform to fusiform, spore-bearing part 20–43 × 12–18 µm, with stalks 7–15

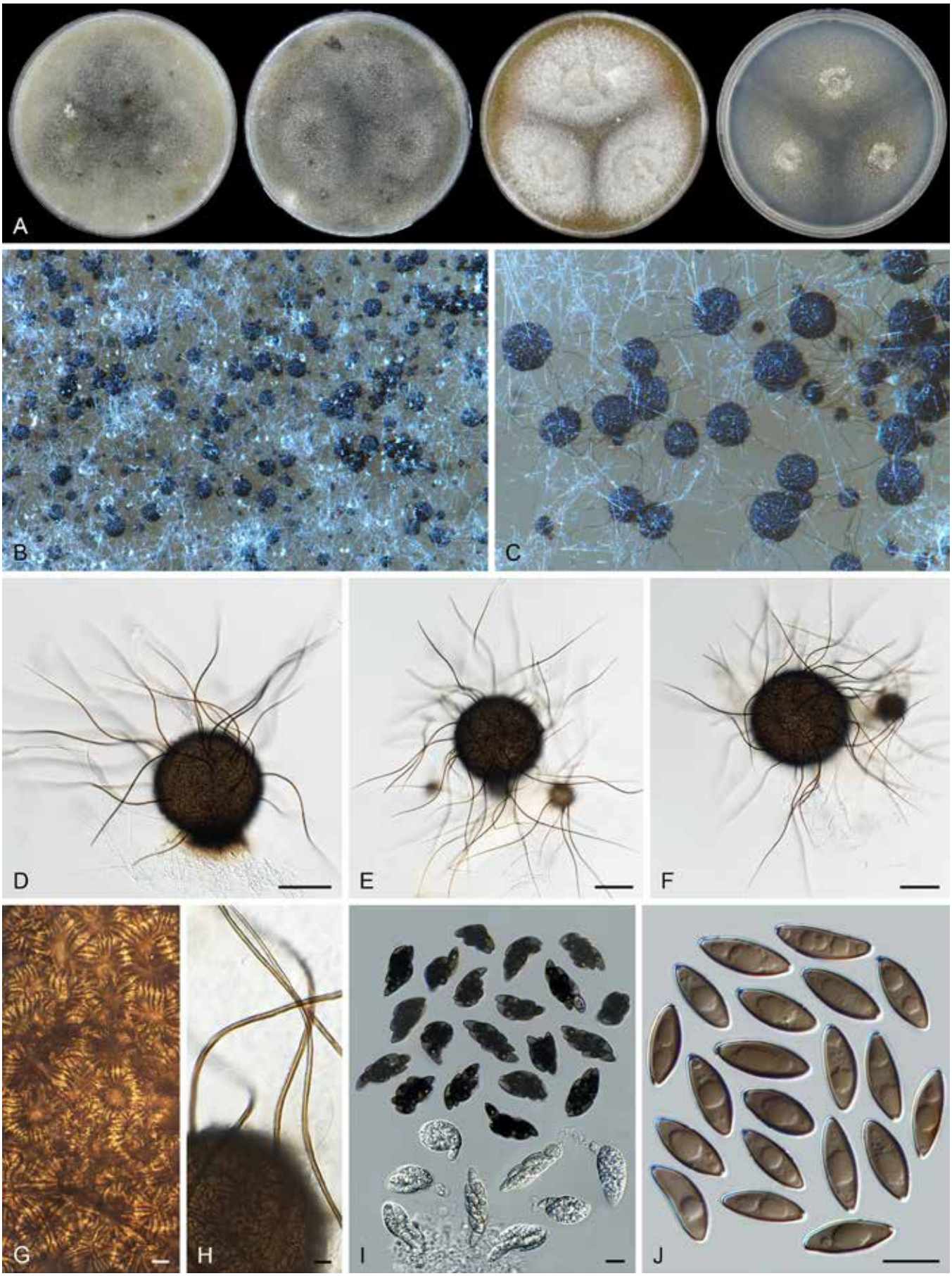

Fig. 11. Sexual morph of *Aporothielavia leptoderma* (CBS 538.74, ex-type culture). **A.** Colonies from left to right on OA, CMA, MEA and PCA after 3 wk incubation. **B.** Part of the colony on OA. **C.** Mature ascomata on OA, top view. **D–F.** Ascomata mounted in lactic acid. **G.** Structure of ascomatal wall in surface view. **H.** Ascomatal hairs. **I.** Asci. **J.** Ascospores. Scale bars: D–F = 100 µm; G–J = 10 µm.

µm long, with eight irregularly-arranged ascospores, sometimes persistent till ascospores mature. *Ascospores* olivaceous when mature, fusiform, often inequilateral, (14–)14.5–16.5(–18) × (5–)5.5–6.5(–7.5) µm, with an apical or slightly subapical germ pore. *Asexual morph* (*fide* Malloch & Cain 1973), formed as intercalary or terminal chlamydospores, solitary or catenulate, ellipsoidal to globose, brown, 1-celled, smooth-walled, 4–14 µm diam, lacking germ pores.

Culture characteristics: Colonies on OA with an entire edge, 51–57 mm diam in 7 d at 25 °C, with white aerial mycelium, without coloured exudates; reverse pale mouse grey. Colonies on CMA similar to those on OA, 45–51 mm diam in 7 d at 25 °C. Colonies on MEA with an entire edge, 52–58 mm diam in 7 d at 25 °C, with white aerial mycelium, texture floccose, obverse white; reverse ochreous to fulvous. Colonies on PCA with an entire edge, 45–51 mm diam in 7 d at 25 °C, with sparse aerial mycelium, obverse uncoloured, without coloured exudates, reverse uncoloured.

Material examined: **UK**, England, Surrey, Chobham, isolated from soil, 1953, G.W.F. Sewell (ex-type culture of *Thielavia leptoderma*, CBS 538.74 = IMI 054770). **Spain**, Galicia, Orense, Serra de Xurés, isolated from black spot on granite rock sample, 10 Nov. 2001, V. Jato & A.M. Stchigel (CBS 113678 = FMR 8192, ex-type of *Chaetomidium gallecicum*).

Notes: Based on the phylogenetic analyses, *Chaetomidium gallecicum* is a synonym of *Apor. leptoderma* (Fig. 7B, Supplementary Figs S2, S3; ITS sequences of the two strains are not available). *Aporothielavia leptoderma* can be easily recognised by the cephalothecoid ascomatal wall of non-ostiolate ascomata with long hairs (sometimes missing), pyriform to fusiform asci and elongated fusiform ascospores with an apical or slightly subapical germ pore.

Arcopilus X.Wei Wang *et al.*, Stud. Mycol. 84: 159. 2016.

Micromorphology and illustrations: See Wang *et al.* (2016b; p.159, 165). Containing species with only sexual morph.

Type species: *Arcopilus aureus* (Chivers) X.Wei Wang & Samson

Notes: The genus *Arcopilus* was proposed based on phylogenetic analysis (Wang *et al.* 2016b) and species belonging to this genus produce arcuate ascomatal hairs, colourful colonies (due to its ascomata and exudates) and diverse ascospores that are more or less inequilateral with one or two apical germ pores. Three more chaetomium-like species proved to be members of this genus based on our phylogenetic analysis (Fig. 7C). Each of them morphologically fits in the definition of *Arcopilus* (Wang *et al.* 2016b).

Arcopilus macrostiolatus (Stchigel *et al.*) X.Wei Wang & Houbraken, ***comb. nov.*** MycoBank MB 840138.
Basionym: *Chaetomium macrostiolatum* Stchigel *et al.*, Mycologia 94: 121. 2002.

Notes: *Arcopilus macrostiolatus* produces terminal hairs arcuate and recurved at the apex, fitting the general morphology of the genus. This species is phylogenetically most closely related to *Ar. megasporus* and *Ar. purpurascens* (Fig. 7C). *Arcopilus macrostiolatus* can be distinguished from these and other species in the genus by its limoniform, umbonate, bilaterally flattened ascospores that have an apical germ pore (Rodríguez *et al.* 2002). *Arcopilus turgidopilosus* also produces limoniform and bilaterally flattened ascospores, but can be distinguished by production of biapiculate or less umbonate ascospores with two apical germ pores (von Arx *et al.* 1986, Wang *et al.* 2016b).

Arcopilus megasporus (Sörgel ex Seth) X.Wei Wang & Houbraken, ***comb. nov.*** MycoBank MB 840139.
Basionym: *Chaetomium megasporum* Sörgel ex Seth, Beih. Nova Hedwigia 37: 82. 1972.

Notes: *Arcopilus megasporus* produces fusiform or navicular ascospores with two germ pores at the ends and red exudates on OA and/or CMA, fitting the overall morphology of the genus (von Arx *et al.* 1986). It can be distinguished from the other species in the genus by its ascomata covered by sparse, hypha-like flexuous hairs.

Arcopilus purpurascens (Udagawa & Y. Sugiy.) X.Wei Wang & Houbraken, ***comb. nov.*** MycoBank MB 840140.
Basionym: *Achaetomium purpurascens* Udagawa & Y. Sugiy., Rep. Cryptogam. Stud. Nepal: 13. 1982.
Synonym: *Chaetomium purpurascens* (Udagawa & Y. Sugiy.) Arx, Proc. Indian Acad. Sci., Pl. Sci. 94: 344. 1985.

Notes: *Arcopilus purpurascens* is morphologically similar to *Ar. megasporus* and was treated as a synonym of the latter by von Arx *et al.* (1986). The four-locus phylogeny as well as the *tub2* and *rpb2* phylograms show *Ar. purpurascens* is a distinct species, most closely related to *Ar. megasporus* (Fig. 7C, Supplementary Figs S2, S3).

Arxotrichum A. Nováková & M. Kolařík, Persoonia 40: 259. 2018.

Micromorphology: Containing asexual species, sexual species and species with both asexual and sexual morphs. *Ascomata* superficial, occasionally sub-immersed in the medium, ostiolate, ovoid, in some species possessing a short tapering beak fading towards the tip with a pale brown to subhyaline apex. *Ascomatal wall* brown, composed of irregular or angular cells. *Ascomatal hairs* pale to pale brown, finely verrucose, verrucose or punctulate, septate, in some species without differentiation between terminal and lateral ones, hypha-like, straight or flexuous, tapering and fading towards the tips; in other species terminal hairs spirally coiled, loosely coiled, undulate or flexuous, usually erect or flexuous at lower part, lateral hairs flexuous, shorter than terminal ones. *Asci* fasciculate, fusiform or clavate, stalked, containing eight irregularly-arranged ascospores, evanescent. *Ascospores* olivaceous brown when mature, ellipsoidal with attenuated or rounded ends, or fusiform, sometimes reniform or navicular, not bilaterally flattened, with an apical, subapical, oblique or lateral germ pore, or with two apical or slightly subapical germ pores, each at one end. *Asexual morph* present in four species. *Conidiophores* ramified, unbranched or reduced to conidiogenous cells. *Conidiogenous cells* developing at the ends of branches of conidiophores, or lateral or intercalary directly from the hyphae, monoblastic. *Conidia* 1-celled, smooth, verruculose or rugose, hyaline or pinkish coloured.

Type species: *Arxotrichum wyomingense* A. Nováková & M. Kolařík

Notes: *Arxotrichum* was recently proposed to accommodate an asexual species, *Arx. wyomingense* (the type species), and the sexual species *Chaetomium succineum* which was renamed *Arx. succineum* (Crous *et al.* 2018). The type species produces poorly differentiated conidiophores that resemble the micronematous ones of a *Staphylotrichum* species. Based on our four-gene

phylogenetic analysis (Fig. 7A), six additional chaetomium-like species are transferred into the genus *Arxotrichum*. Several species in the genus, *e.g.*, *Arx. gangligerum*, *Arx. officinarum* and *Arx. piluliferoides*, produce both sexual and asexual morphs. They link the asexual species *Arx. wyomingense* to the strictly sexually reproducing species in the genus.

Arxotrichum deceptivum (Malloch & Benny) X.Wei Wang & Houbraken, ***comb. nov.*** MycoBank MB 830917. Fig. 12.
Basionym: *Chaetomium deceptivum* Malloch & Benny, Mycologia 65: 648. 1973.

Micromorphology: *Ascomata* superficial, sometimes sub-immersed in the medium, leaden black to amber due to ascomata and masses of ascospores in reflected light, ostiolate, ovoid, with a short papillate beak fading towards the tip, usually with a hyaline apex, 190–335 µm high, 150–300 µm diam. *Ascomatal wall* brown, composed of irregular or angular cells. *Ascomatal hairs* pale brown, short, straight or flexuous, tapering and fading towards the tips, finely verrucose, septate, 2.5–3.5 µm diam near the base, usually less than 70 µm long. *Asci* fusiform, sometimes clavate, spore-bearing part 37–55 × 15–20.5 µm, with stalks being 7–16.5 µm long, containing eight irregularly-arranged ascospores, evanescent. *Ascospores* olivaceous brown when mature, fusiform or ellipsoidal with both ends attenuated, often inequilateral, occasionally navicular, (14.5–)16.5–19.5(–21.5) × (8–)8.5–9.5(–10) µm, with an apical or subapical germ pore. *Asexual morph* unknown.

Culture characteristics: On OA with an entire edge, 39–45 mm diam in 7 d at 25 °C, with sparse aerial mycelium, obverse olivaceous buff due to ascomata; reverse hazel. On CMA similar to those on OA. On MEA with an entire edge, 44–50 mm diam in 7 d at 25 °C, texture floccose, obverse white to smoke grey due to aerial mycelium mixed with ascomata, reverse ochreous, or mouse grey in the central part. On PCA with an entire edge, 42–48 mm diam in 7 d at 25 °C, without sparse aerial mycelium, obverse pale olivaceous grey, without coloured exudates; reverse uncoloured.

Material examined: **USA**, California, Riverside County, Lake Hemet, isolated from dung of pack rat, 10 Nov. 1968, coll. R.K. Benjamin, isol. C.L. Benny (culture ex-type CBS 346.73 = RSA 1993).

Notes: *Arxotrichum deceptivum* can easily be distinguished from the other known species in the genus by its short, hypha-like ascomatal hairs. The ascomata produced by *Arx. deceptivum* are reminiscent of those of *Achaetomiella virescens* and an *Achaetomium* species. Von Arx *et al.* (1986) suggested that *Arx. deceptivum* was related to *Chaetomium murorum* (= *Botryotrichum murorum*, Wang *et al.* 2016b) based on the similarities of their ascospores. These two species are phylogenetically distant from each other (Fig. 7A, C, Supplementary Figs S1–S3). Morphologically, *Arx. deceptivum* can be distinguished from *Botryot. murorum* by its larger (16.5–19.5 × 8.5–9.5 µm *vs* 12.5–15 × 7.5–8.5 µm) and often inequilateral ascospores, and the production of undeveloped ascomatal hairs.

Arxotrichum gangligerum (L.M. Ames) X.Wei Wang & Houbraken, ***comb. nov.*** MycoBank MB 830918. Fig. 13.
Basionym: *Chaetomium gangligerum* L.M. Ames, Mycologia 41: 640. 1950.

Micromorphology: *Ascomata* superficial, vinaceous buff due to ascomatal hairs in reflected light, ostiolate, ovoid or ellipsoidal, 140–230 µm high, 130–200 µm diam. *Ascomatal wall* brown, composed of *textura epidermoidea* in surface view. *Ascomatal hairs* numerous, brown, spirally coiled, finely verrucose, septate, erect or flexuous at lower part, 2–3.5 µm diam near the base. *Lateral hairs* flexuous. *Asci* fusiform or clavate, spore-bearing part 31.5–45.5 × 12–17.5 µm, with stalks being 14–36.5 µm long, containing eight irregularly-arranged ascospores, evanescent. *Ascospores* olivaceous brown when mature, ellipsoidal with both ends attenuated, (9.5–)10.5–12.5(–13.5) × (6.5–)7–8.5 µm, with a subapical or oblique germ pore. *Asexual morph* (*fide* von Arx *et al.* 1986): *Conidia* spherical or ellipsoidal, mostly formed intercalary, singly or catenate, occasionally clustered, smooth or verrucose, hyaline or pale brown, 5–8 µm diam.

Culture characteristics: On OA with an entire edge, 46–52 mm diam in 7 d at 25 °C, obverse primrose or pale mouse grey to grey olivaceous due to ascomata mixed with aerial mycelium; reverse mouse grey. On CMA with an entire edge, 49–55 mm diam in 7 d at 25 °C, with a thicker layer of aerial mycelium, obverse olivaceous buff to greenish olivaceous, reverse greenish olivaceous. On MEA with an entire edge, 45–51 mm diam in 7 d at 25 °C, texture floccose, obverse smoke grey to olivaceous buff, reverse fuscous black. On PCA with an entire edge, 49–55 mm diam in 7 d at 25 °C, with sparse aerial mycelium, obverse smoke grey, or grey olivaceous in the central part, without coloured exudates; reverse uncoloured, or olivaceous grey in the central part.

Material examined: **Canada**, Ontario, Haliburton Co., Dorset, isolated from dung of rabbit, Oct. 1979, A. Carter (CBS 563.80 = CBS 130.85 = TRTC 48537). **USA**, Virginia, Fort Belvoir, isolated from wood sample under test conditions in Tropical Testing Chamber, date unknown, L.M. Ames (culture ex-type CBS 160.52 = ATCC 11206).

Notes: *Arxotrichum gangligerum* is characterised by ascospores with a subapical or oblique germ pore, and by the production of numerous spirally coiled ascomatal hairs that are relatively long and often intertwined with aerial mycelium. *Arxotrichum sinense* produces similar ascospores (with an oblique to lateral germ pore), but can be distinguished from *Arx. gangligerum* by its pyriform or ovoid asci, larger ascospores (13.5–15 × 8.5–9.5 µm *vs* 10.5–13 × 7–8.5 µm), and flexuous or undulate rather than spirally coiled ascomatal hairs. The asexual morph was not observed in our study and more work is required to compare the conidia of this species with those of *Arx. piluliferoides* and *Arx. wyomingense*.

Arxotrichum officinarum (M. Raza & L. Cai) X.Wei Wang & Houbraken, ***comb. nov.*** MycoBank MB 840142.
Basionym: *Myceliophthora officinarum* M. Raza & L. Cai, Fungal Diversity 99: 89. 2019.

Micromorphology: See Raza *et al.* (2019; p. 87, 89).

Notes: Raza *et al.* (2019) classified this species in *Myceliophthora* based on their phylogenetic analysis. However, no representatives of *Arxotrichum* were included in their phylogenetic analysis. In our phylogenetic analyses (Fig. 7A, Supplementary Figs S1–S3), *Arx. officinarum* forms a sister lineage to *Arx. gangligerum*. This species is morphologically similar to *Arx. gangligerum* with both sexual and asexual morphs, but can be distinguished by thicker ascomatal hairs (2.5–4 µm *vs* 2–3.5 µm diam near the base) and larger conidia (7.0–10.5 × 6–10.5 µm *vs* 5–8 µm diam). The original description reported that the ascospores of *Arx. officinarum* have an "apical germ slit", and the ex-type strain needs to be re-examined to confirm this observation.

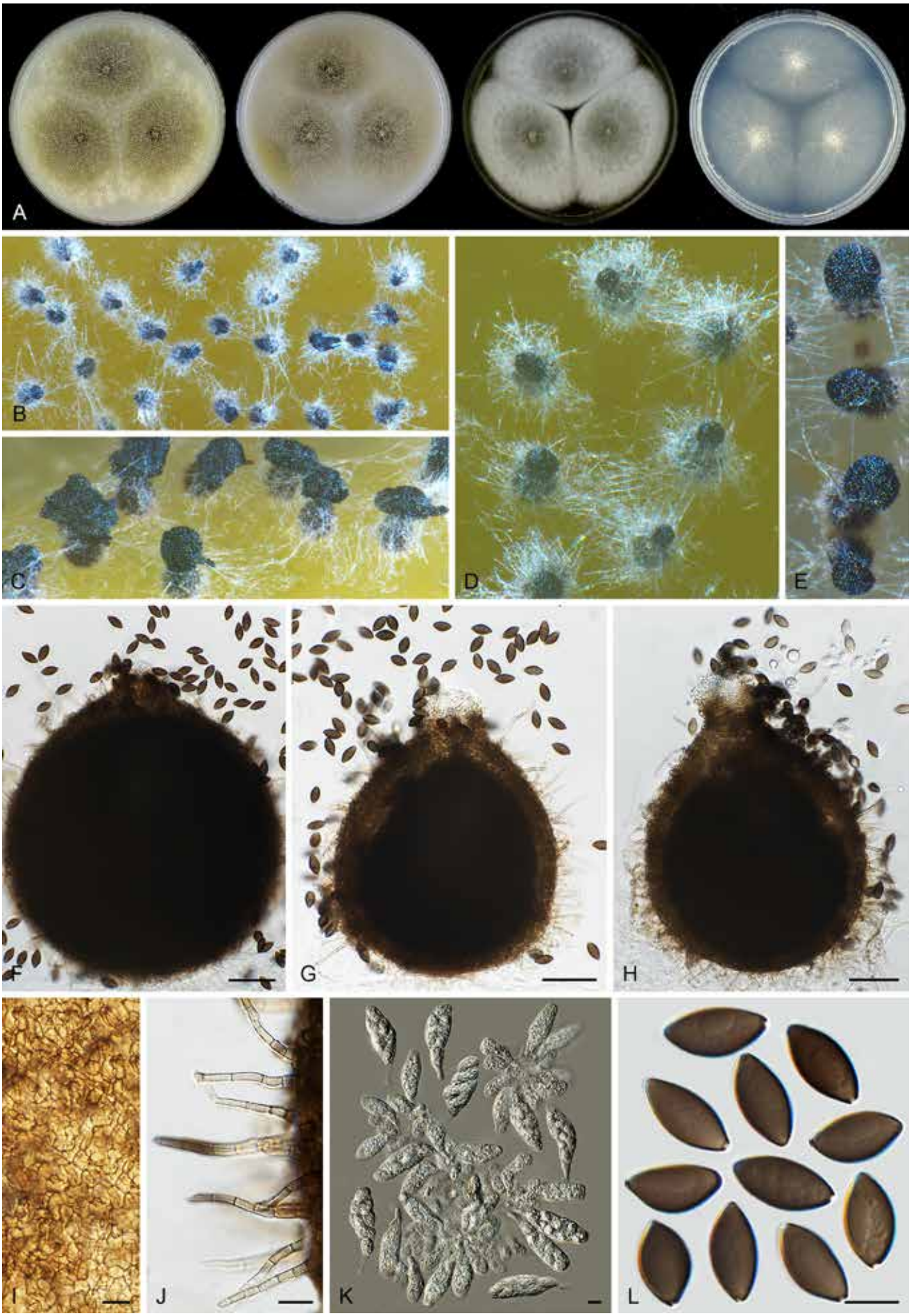

Fig. 12. *Arxotrichum deceptivum* (CBS 346.73, ex-type culture). **A.** Colonies from left to right on OA, CMA, MEA and PCA after 2 wk incubation. **B.** Part of the colony on OA. **C.** Mature ascomata on OA, side view. **D, E.** Mature ascomata on OA, top view. **F–H.** Ascomata mounted in lactic acid. **I.** Structure of ascomatal wall in surface view. **J.** Terminal ascomatal hairs. **K.** Asci. **L.** Ascospores. Scale bars: F–H = 50 µm; I–L = 10 µm.

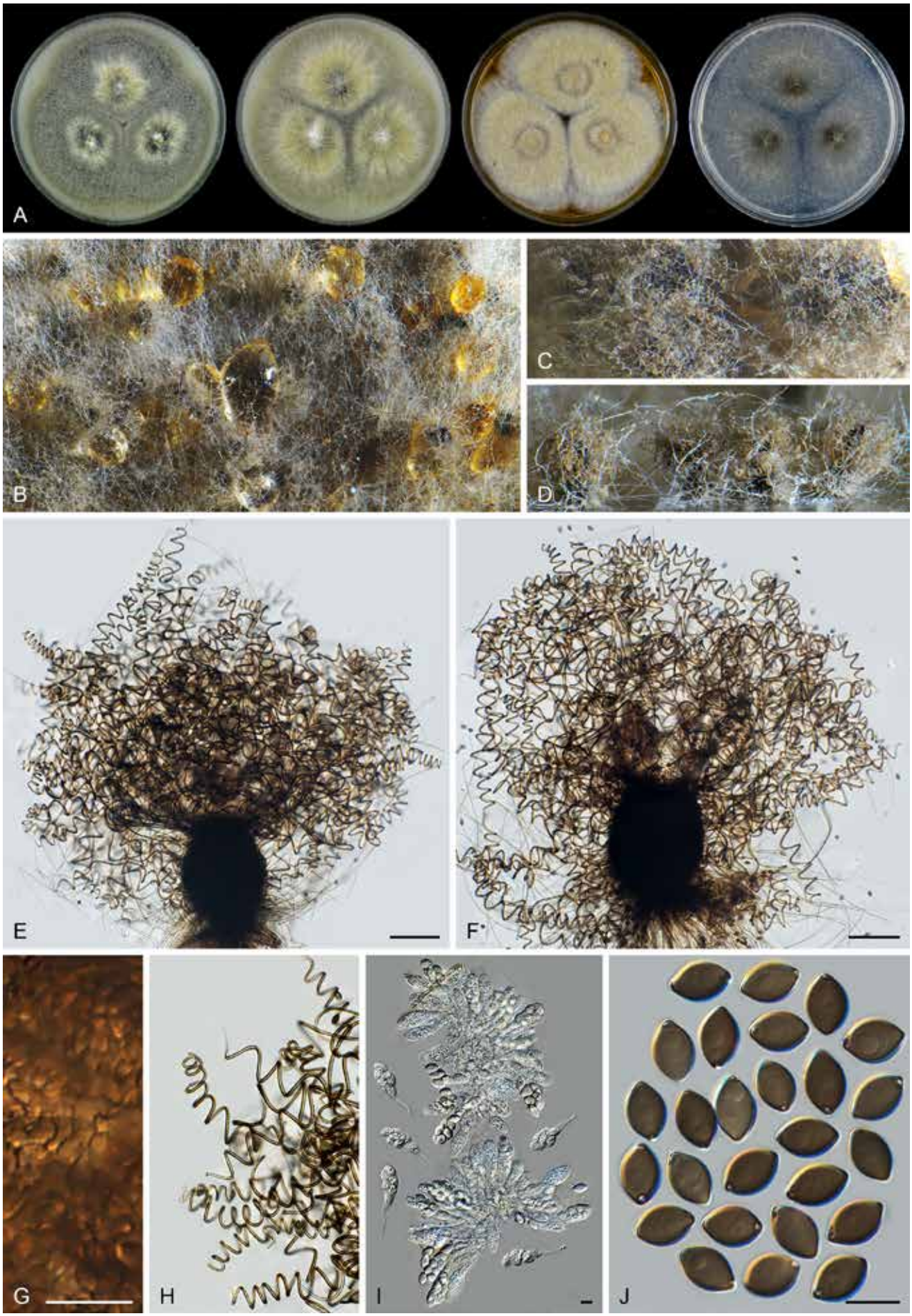

Fig. 13. Sexual morph of *Arxotrichum gangligerum* (CBS 160.52, ex-type culture). **A.** Colonies from left to right on OA, CMA, MEA and PCA after 2 wk incubation. **B.** Part of the colony on OA. **C.** Mature ascomata on OA, top view. **D.** Mature ascomata on OA, side view. **E, F.** Ascomata mounted in lactic acid. **G.** Structure of ascomatal wall in surface view. **H.** Terminal ascomatal hairs. **I.** Asci. **J.** Ascospores. Scale bars: E, F = 100 µm; G–J = 10 µm.

Arxotrichum piluliferoides (Udagawa & Y. Horie) X.Wei Wang & Houbraken, ***comb. nov.*** MycoBank MB 830920. Fig. 14.
Basionym: *Chaetomium piluliferoides* Udagawa & Y. Horie, Trans. Mycol. Soc. Japan 16: 337. 1975.

Micromorphology: *Ascomata* superficial, olivaceous grey in reflected light due to ascomatal hairs, ovoid to obpyriform or subglobose, often with a short beak, 140–245 µm high, 115–195 µm diam. *Ascomatal wall* brown, composed of irregular or angular cells. *Ascomatal hairs* flexuous, punctulate or verrucose, brown, septate, 1.5–3 µm diam near the base. *Asci* pyriform to clavate, spore-bearing part 31–58 × 18–24 µm, with stalks being 9–10 µm long, containing eight irregularly-arranged or biseriate ascospores, evanescent, sometimes persistent until ascospores mature. *Ascospores* olivaceous brown when mature, fusiform, often inequilateral, (19–)21–24(–26) × 7.5–9 (–9.5) µm, with one or two apical or slightly subapical germ pores. *Conidiophores* absent. *Conidiogenous cells* reduced to a hyphal cell, monoblastic, laterally or terminally producing conidia. *Conidia* arising laterally from aerial hyphae, or from short branches of hyphae, sometimes intercalary, hyaline, globose to subglobose, sometimes ovate to fusiform, hyaline, verrucose, 4.5–9 µm diam.

Culture characteristics: On OA with an entire edge, 51–57 mm diam in 7 d at 25 °C, texture floccose, obverse olivaceous buff to pale luteous due to conidia on mycelium mixed with ascomata; reverse olivaceous grey. On CMA similar to those on OA, 49–55 mm diam in 7 d at 25 °C. On MEA with an entire edge, 47–53 mm diam in 7 d at 25 °C, texture thick floccose, obverse buff to pale luteous; reverse ochreous to umber. On PCA with an entire edge, 46–52 mm diam in 7 d at 25 °C, without aerial mycelium, obverse smoke grey due to ascomata, without coloured exudates, reverse smoke grey or dark brick.

Material examined: **Japan**, Sugadaira, Naguna Prefecture, isolated from grassland soil, 17 Oct. 1972, J.Y. Horie (culture ex-type CBS 103.77 = IFM 4531 = IMI 210880 = NHL 2738). **Spain**, Tarragona, isolated from dung, date unknown, J. Guarro (CBS 262.82).

Notes: *Arxotrichum piluliferoides* is closely related to *Arx. deceptivum* (Fig. 7A, Supplementary Figs S1–S3). Both species produce hypha-like ascomatal hairs with no differentiation between the terminal and lateral ones. *Arxotrichum piluliferoides* can be distinguished from *Arx. deceptivum* by olivaceous grey ascomatal hairs and elongated fusiform ascospores. Conidia of this species can easily be observed in the aerial mycelium (Fig. 14B–F). Von Arx *et al.* (1986) described the ascospores of this species "with paler ends, but without sharply delimited germ pores". In our study we used lactic acid as mounting fluid and two apical germ pores (Fig. 14L) could be observed in the ascospores.

Arxotrichum repens (Guarro & Figueras) X.Wei Wang & Houbraken, ***comb. nov.*** MycoBank MB 830921. Fig. 15.
Basionym: *Chaetomium repens* Guarro & Figueras, Beih. Nova Hedwigia 84: 6. 1986.

Micromorphology: *Ascomata* superficial, buff to greyish sepia due to ascomatal hairs in reflected light, ovoid or subglobose, ostiolate, 160–230 µm high, 130–220 µm diam. *Ascomatal wall* brown, composed of irregular or angular cells. *Terminal hairs* brown, regularly undulate to slightly coiled, verrucose, septate, erect or flexuous in the lower parts, 2.5–4.5 µm diam near the base. *Lateral hairs* flexuous. *Asci* fusiform, sometimes clavate or pyriform, spore-bearing part 16.5–28.5 × 11–16 µm, with stalks being 4–20.5 µm long, containing eight irregularly-arranged ascospores, evanescent. *Ascospores* olivaceous brown when mature, ellipsoidal or reniform, rounded or slightly attenuated at both ends, often inequilateral, (7.5–)8–10(–10.5) × (4.5–)5–6 µm, with an inconspicuous apical germ pore. *Asexual morph* unknown.

Culture characteristics: On OA with an entire edge, 47–53 mm diam in 7 d at 25 °C, texture floccose, obverse white to smoke grey due to aerial mycelium, non-sporulating; reverse bay due to coloured exudates diffusing into the medium. On CMA similar to those on OA. On MEA with an entire edge, 47–53 mm diam in 7 d at 25 °C, texture floccose, obverse white with margins rosy or rosy vinaceous, reverse rust. On PCA with an entire edge, 50–56 mm diam in 7 d at 25 °C, without aerial mycelium, obverse buff due to ascomata, without coloured exudates; reverse uncoloured or buff.

Material examined: **Spain**, Tarragona, isolated from soil in Montblanc, date unknown, J. Guarro (culture ex-type CBS 233.82 = FFBA 310).

Notes: *Arxotrichum repens* is phylogenetically most closely related to *Arx. sinense* (Fig. 7A). These two species could be differentiated based in their *tub2* and *rpb2* sequences. In contrast, the ITS phylogeny fails to separate these two species (Supplementary Figs S1–S3). *Arxotrichum repens* can be distinguished from *Arx. sinense* by its regularly undulate to slightly coiled ascomatal hairs, often fusiform and smaller asci (16.5–28.5 × 11–16 µm *vs* 22–35 × 17.5–23 µm in spore-bearing part), and ellipsoidal or reniform and smaller ascospores (8–10 × 5–6 µm *vs* 13.5–15 × 8.5–9.5 µm) with an inconspicuous apical germ pore. This species is only known from the ex-type strain. Our cultures on OA and CMA remained sterile after prolonged incubation, but ascomata were obtained on PCA. *Arxotrichum repens* is mainly characterised by its ellipsoidal or reniform ascospores with rounded ends. In contrast, the majority of *Chaetomiaceae* species produce ascospores with at least one attenuated end. The only exceptions are those that produce spherical and bilaterally flattened ascospores, such as *Chaetomium globosporum*, *Ch. grande* and *Ch. megalocarpum* (von Arx *et al.* 1986, 1988, Wang *et al.* 2016a, b, 2019a, b).

Arxotrichum sinense (K.T. Chen) X.Wei Wang & Houbraken, ***comb. nov.*** MycoBank MB 830922. Fig. 16.
Basionym: *Chaetomium sinense* K.T. Chen, Acta Microbiol. Sin. 13: 125. 1973.

Micromorphology: *Ascomata* superficial, sulphur-yellow to pure yellow due to ascomatal hairs in reflected light, ovoid or subglobose, ostiolate, often with a short papillate beak, 100–145 µm high, 82–120 µm diam. *Ascomatal wall* brown, with apical beak paler, composed of irregular or angular cells. *Terminal hairs* brown, flexuous or undulate, sometimes recurved or slightly circinate at the apex, tapering towards the tips, finely verrucose, septate, erect or flexuous in the lower parts, 2–3.5 µm diam near the base. *Lateral hairs* flexuous. *Asci* pyriform or ovoid, spore-bearing part 22–35 × 17.5–23 µm, with short stalks being 3.5–7 µm long, containing eight irregularly-arranged ascospores, evanescent. *Ascospores* olivaceous brown when mature, ellipsoidal with both ends attenuated, (13–)13.5–15(–15.5) × (7.5–)8.5–9.5(–10) µm, with an oblique to lateral germ pore. *Asexual morph* unknown.

Culture characteristics: On OA with an entire edge, 47–53 mm diam in 7 d at 25 °C, without aerial mycelium, obverse olivaceous buff

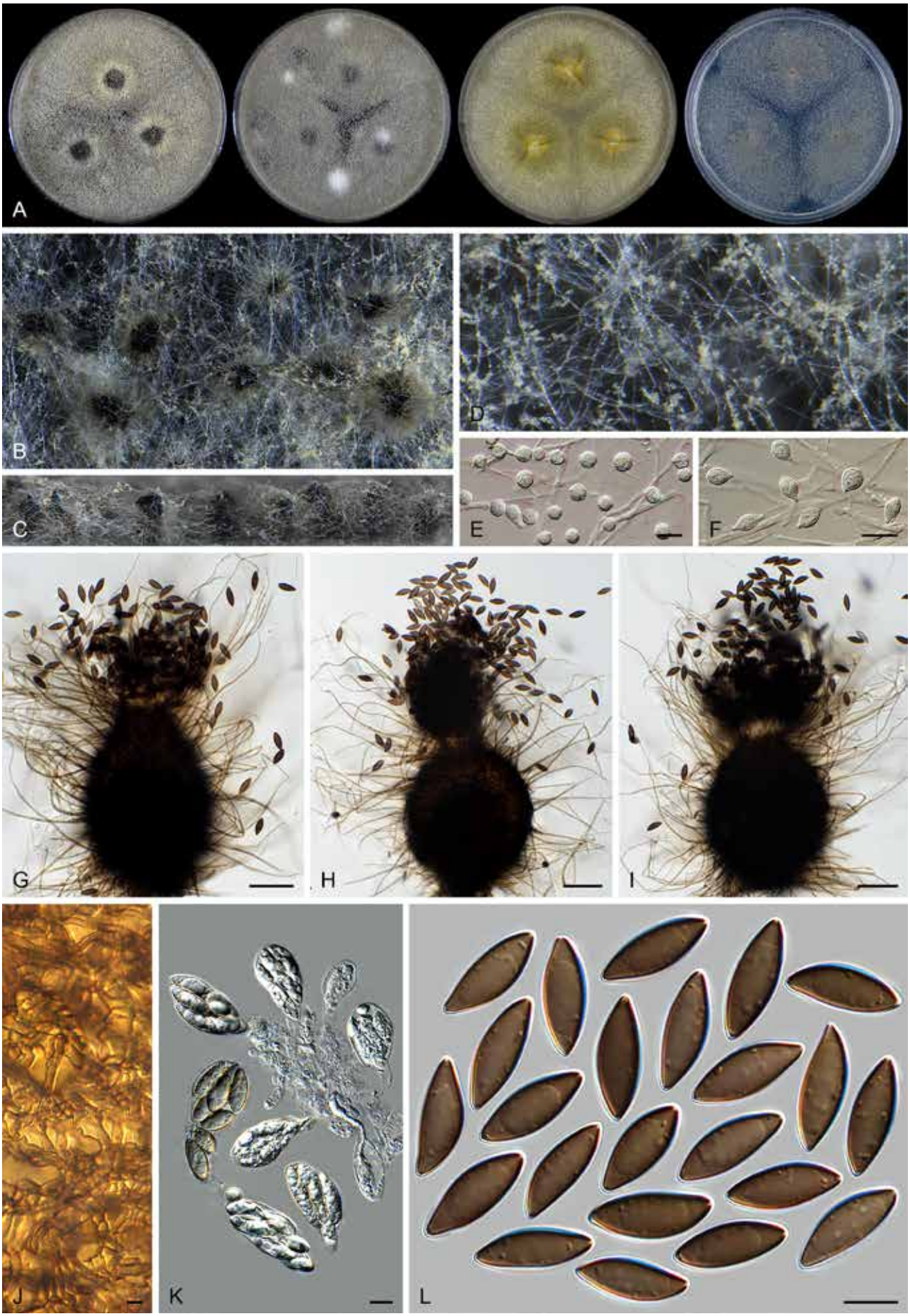

Fig. 14. *Arxotrichum piluliferoides* (CBS 103.77, ex-type culture). **A.** Colonies from left to right on OA, CMA, MEA and PCA after 4 wk incubation. **B.** Part of the colony showing mature ascomata on OA, top view. **C.** Mature ascomata on OA, side view. **D.** Conidia on aerial hyphae. **E, F.** Conidia and hyphae. **G–I.** Ascomata mounted in lactic acid. **J.** Structure of ascomatal wall in surface view. **K.** Asci. **L.** Ascospores. Scale bars: E, F, J–L = 10 µm; G–I = 50 µm.

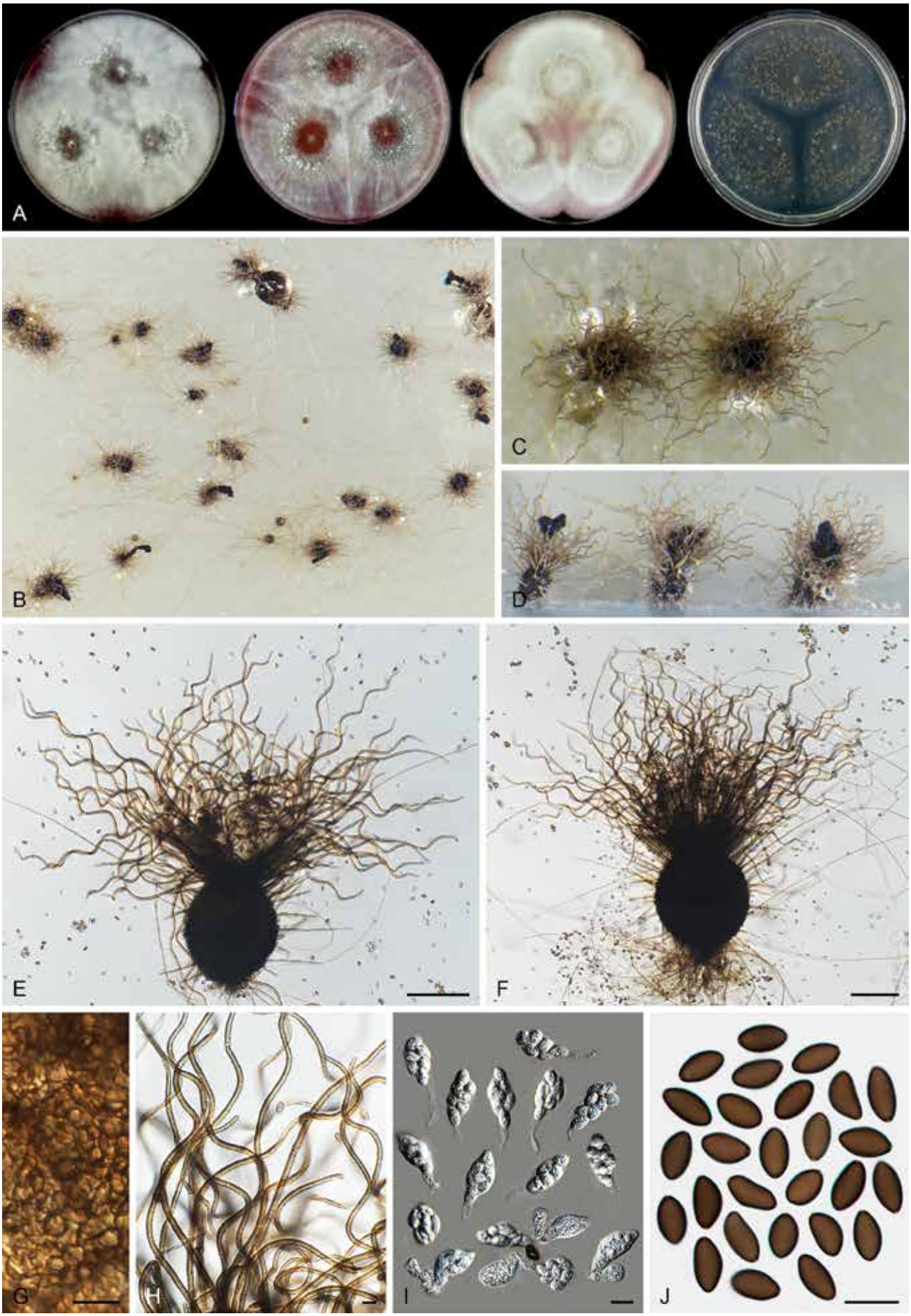

Fig. 15. *Arxotrichum repens* (CBS 233.82, ex-type culture). **A.** Colonies from left to right on OA, CMA, MEA and PCA after 3 wk incubation. **B.** Part of the colony on PCA. **C.** Mature ascomata on PCA, top view. **D.** Mature ascomata on PCA, side view. **E, F.** Ascomata mounted in lactic acid. **G.** Structure of ascomatal wall in surface view. **H.** Terminal ascomatal hairs. **I.** Asci. **J.** Ascospores. Scale bars: E, F = 100 µm; G–J = 10 µm.

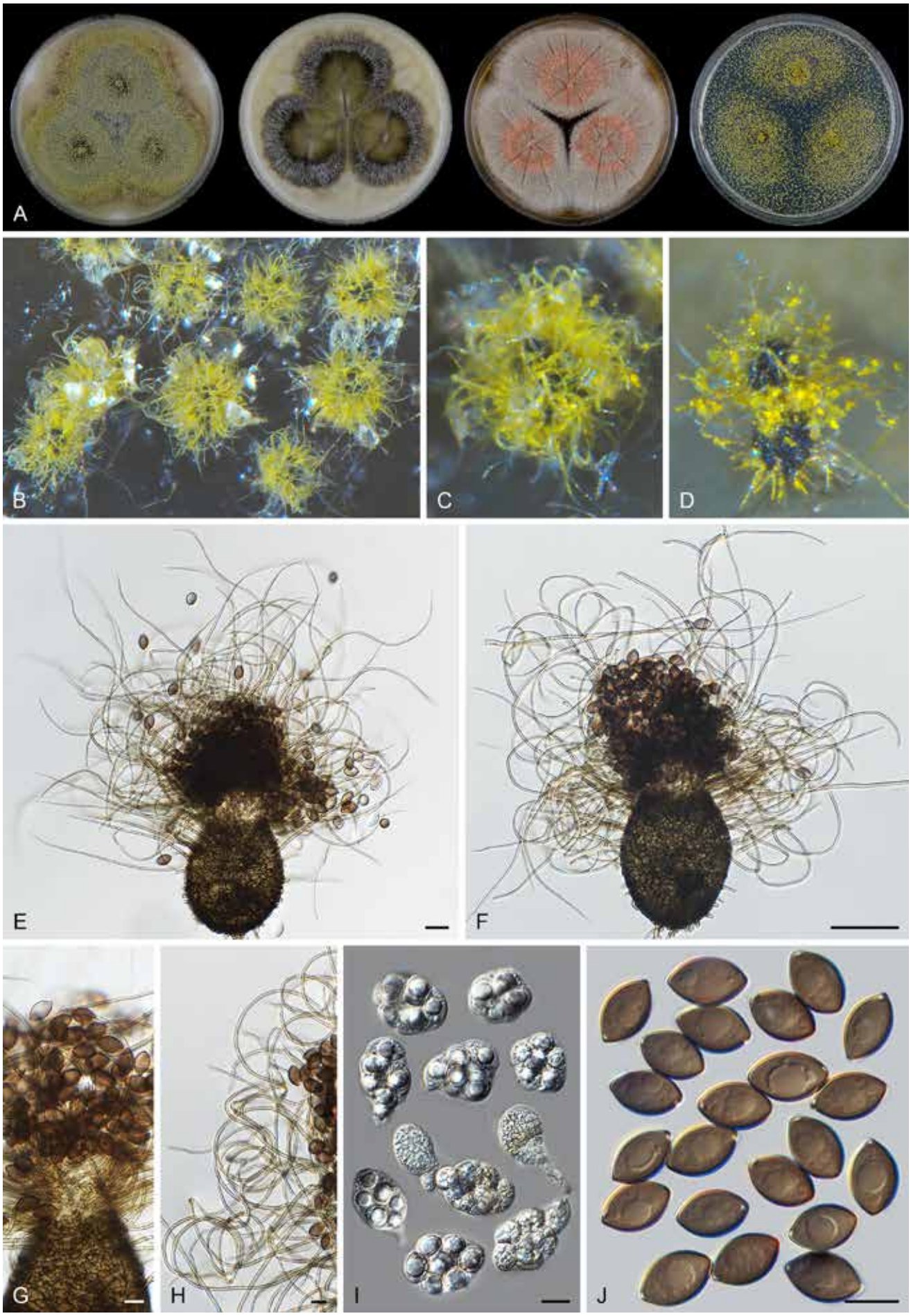

Fig. 16. *Arxotrichum sinense* (CBS 541.83, ex-type culture). **A.** Colonies from left to right on OA, CMA, MEA and PCA after 3 wk incubation. **B.** Part of the colony on OA. **C.** Mature ascomata on OA, top view. **D.** Mature ascomata on OA, side view. **E, F.** Ascomata mounted in lactic acid. **G.** Structure of ascomatal wall in surface view. **H.** Terminal ascomatal hairs. **I.** Asci. **J.** Ascospores. Scale bars: E = 20 µm; F = 50 µm; G–J = 10 µm.

to greenish olivaceous due to ascomata, with margins hazel due to coloured exudates diffusing into the medium; reverse buff, or fuscous black in the central part. On CMA with an entire edge, 47–53 mm diam in 7 d at 25 °C, poorly sporulating, obverse olivaceous due to coloured exudates diffusing into the medium, with a ring of aerial mycelium around the centre; reverse mouse grey. On MEA with an entire edge, 47–53 mm diam in 7 d at 25 °C, obverse smoke grey or slightly peach due to aerial mycelium, reverse sienna or umber. On PCA with an entire edge, 45–51 mm diam in 7 d at 25 °C, without aerial mycelium, obverse sulphur-yellow to amber due to ascomata, without coloured exudates; reverse smoke grey.

Material examined: **China**, isolated from soil, date unknown, J.D. Chen (culture ex-type CBS 541.83 = FFBA 388).

Notes: *Chaetomium sinense* was synonymised with *Ch. gangligerum* by von Arx *et al.* (1986). These two species are phylogenetically not closely related (Fig. 7A, Supplementary Figs S1–S3). Our morphological examination showed that *Arx. sinense* (= *Ch. sinense*) produces similar shaped ascospores; however, they are larger than those of *Arx. gangligerum* (= *Ch. gangligerum*) (13.5–15 × 8.5–9.5 µm *vs* 10.5–13 ×7–8.5 µm). Furthermore, the terminal hairs of *Arx. sinense* are never spirally coiled, different from those of *Arx. gangligerum*. For more details, see notes of *Arx. gangligerum*.

Arxotrichum succineum (L.M. Ames) A. Nováková & M. Kolařík, Persoonia 40: 259. 2018. Fig. 17.
Basionym: *Chaetomium succineum* L.M. Ames, Mycologia 41: 645. 1949.

Micromorphology: *Ascomata* superficial, buff to greenish olivaceous due to ascomatal hairs in reflected light, subglobose to ovoid, ostiolate, 110–280 µm high, 90–255 µm diam. *Ascomatal wall* brown, composed of irregular or angular cells. *Terminal hairs* brown, flexuous, undulate or irregularly loosely coiled in the upper part, finely verrucose, septate, erect or flexuous at lower part, 2–4 µm diam near the base. *Lateral hairs* flexuous. *Asci* clavate or fusiform, spore-bearing part 30.5–38.5 × 13–17 µm, with stalks being 11–20 µm long, containing eight irregularly-arranged ascospores, evanescent. *Ascospores* olivaceous when mature, ellipsoidal or fusiform with both ends attenuated, sometimes inequilateral, (11.5–)12.5–14(–15) × (6–)6.5–7.5(–8.5) µm, with an apical germ pore. *Asexual morph* unknown.

Culture characteristics: On OA with an entire edge, 39–45 mm diam in 7 d at 25 °C, obverse greenish olivaceous to hazel due to ascomata mixed with aerial mycelium and conidia; reverse cinnamon. On CMA similar to those on OA, obverse grey olivaceous; reverse honey or hazel. On MEA with an entire edge, 40–46 mm diam in 7 d at 25 °C, texture floccose, obverse smoke grey or slightly buff to pale luteous due to conidia on aerial mycelium, reverse rust. On PCA with an entire edge, 43–49 mm diam in 7 d at 25 °C, without aerial mycelium, obverse olivaceous buff due to ascomata, without coloured exudates; reverse uncoloured.

Material examined: **China**, Xinjiang, Altai, isolated from soil, 2003, X.W. Wang (CBS 119769 = CGMCC 3.9426). **USA**, California, Mount Shasta, isolated from *Abies magnifica* var. *shastensis*, date unknown, G.W. Martin (culture ex-type CBS 166.52 = ATCC 11216 = MUCL 18704); (CBS 813.73 = DAOM 24174 = IMI 044210 = QM 1044).

Notes: *Arxotrichum succineum* can be distinguished from the other known species in the genus by its thin, flexuous, undulate or irregularly coiled ascomatal hairs and fusiform ascospores having an apical germ pore. When *Arxotrichum* was introduced, this was the only known sexually reproducing species in the genus (Crous *et al.* 2018). The description of the sexual morph of *Arxotrichum* was therefore based on the description of *Ch. succineum* as reported by von Arx *et al.* (1986). In the present study, we re-describe six additional species in *Arxotrichum* and then redefine the genus.

Arxotrichum wyomingense A. Nováková & M. Kolařík, Persoonia 40: 259. 2018.

Micromorphology: *See* Nováková and Kolařík (Crous *et al.* 2018): On MEA. *Conidiophores* septate, 250–400 µm long, stipe with basal part yellowish brown, smooth to finely rough-walled, 3 µm wide, upper part colourless, smooth, 2.5 µm wide, ramified, branches racemose. *Conidiogenous cells* borne at the ends of branches, hyaline. *Conidia* solitary, aseptate, 5(–7) µm diam, hyaline to pinkish coloured, subglobose, rough-walled to rugose, flattened from side view with distinct spiral (bands) and visible scars. *Sexual morph* not observed.

Notes: Although *Arx. wyomingense* was designated as the type species of *Arxotrichum*, this is the only species in the genus that only produces an asexual morph (Crous *et al.* 2018). The conidiophores of this species are ramified with racemose branches and the aseptate conidia are produced solitary, are flattened from side view and have rough to rugose walls with distinct spiral (bands) and visible scars. Three other species in the genus (*Arx. gangligerum*, *Arx. officinarum* and *Arx. piluliferoides*) also produce solitary and aseptate conidia. However, these species do not produce conidiophores and the conidia develop lateral or intercalary directly from the hyphae. We did not study the ex-type of this species. It needs to be noted that the description of *Arx. wyomingense* was based on MEA, and this medium is often unsuitable for *Chaetomiaceae* species to develop ascomata. It is therefore necessary to check whether this species is able to produce a sexual morph on more suitable media such as OA or PCA.

Bommerella Marchal, Bull. Soc. Roy. Bot. Belgique 24: 164. 1885.

Micromorphology (from von Arx *et al.* 1986): *Ascomata* ostiolate, with a short conical beak. *Ascomatal wall* composed of elongate cells arranged in petaloid patterns (cephalothecoid). *Ascomatal hairs* seta-like, straight, septate, smooth or verrucose, tapering towards the tips. *Asci* fasciculate, clavate or fusiform, stalked, containing eight ascospores, evanescent. *Ascospores* triangular in front view, ellipsoidal in side view, brown when mature, with an apical germ pore. *Conidia* formed in basipetal chains on percurrently elongating conidiogenous cells, pyriform, truncate at base, punctulate, hyaline. Containing species with both asexual and sexual morphs.

Type species: *Bommerella trigonospora* Marchal

Notes: This is a monotypic genus. *Bommerella trigonospora* is characterised by its ascospores which are triangular in front view and elliosoidal in side view (Fig. 4G), and by the presence of conidia which are pyriform, hyaline, and formed in basipetal chains (von Arx *et al.* 1986). Chivers (1915) combined this species in *Chaetomium* (*Ch. trigonosporum*) and this was followed by others (Ames 1963, von Arx *et al.* 1986). Our phylogenetic analyses showed that this species forms a single lineage with no known close

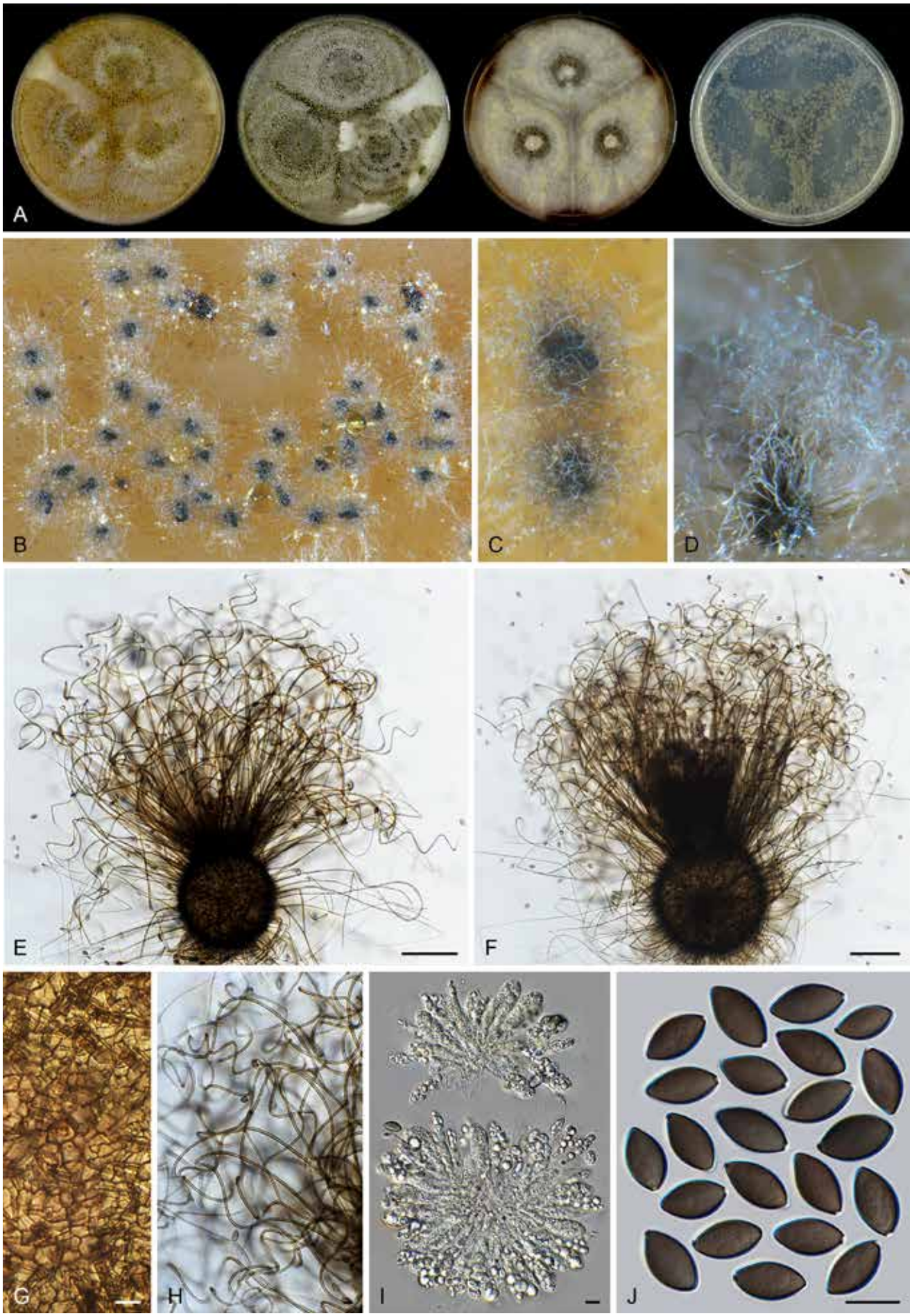

Fig. 17. *Arxotrichum succineum* (CBS 166.52, ex-type culture). **A.** Colonies from left to right on OA, CMA, MEA and PCA after 3 wk incubation. **B.** Part of the colony on OA. **C.** Mature ascomata on OA, top view. **D.** Mature ascomata on OA, side view. **E, F.** Ascomata mounted in lactic acid. **G.** Structure of ascomatal wall in surface view. **H.** Terminal ascomatal hairs. **I.** Asci. **J.** Ascospores. Scale bars: E, F = 100 µm; G–J = 10 µm.

relatives (Fig. 7C), thus the generic name is resurrected. Another chaetomium-like species that produces trianglar ascospores is "*Chaetomium microascoides*" which can be distinguished by the absence of conidia and terminal ascomatal hairs around ostiolates. Phylogenetic analysis indicated that "*Chaetomium microascoides*" belongs to *Lasiosphaeriaceae sensu lato*, distant from *Chaetomiaceae* (Fig. 7D).

Botryoderma Papendorf & H.P. Upadhyay, Trans. Brit. Mycol. Soc. 52: 257. 1969.

Micromorphology: *Fertile hyphae* hyaline, 1–4 µm wide. *Conidiophores* reduced. *Conidiogenous cells* arising laterally or terminally from fertile hyphae, densely clustered with some sterile hyphal branches, hyaline, subglobose, ellipsoidal or ovoid, monoblastic or polyblastic. *Conidia* produced singly, rhexolytic when seceding, single-celled, hyaline, smooth, ellipsoidal or obovoid, with a rounded apex or an apical spine-like beak and a narrow basal or oblique secession scar where a membranous frill is often attached. *Sterile hyphal branches* arising laterally or terminally from fertile hyphae and forming dense clusters together with conidiogenous cells, erect, seta-like, flexuous or recurved. *Sexual morph* not observed.

Type species: *Botryoderma lateritium* Papendorf & H.P. Upadhyay

Notes: Since the genus *Botryoderma* was established (Papendorf & Upadhyay 1969), it remained as "*incertae sedis*" in the *Pezizomycotina*, *Ascomycota* (Kirk *et al.* 2008, www.mycobank.org, www.indexfungorum.org). In the present study, phylogenetic analysis clearly located *Botryoderma* in the *Chaetomiaceae*, *Sordariales*. This genus forms a lineage closely related to the genera *Arxotrichum*, *Corynascus*, *Myceliophthora* and *Thermothelomyces* (Fig. 7A). *Botryoderma lateritium* and *Botryod. rostratum* can easily be recognised by their conidiogenous cells and sterile hyphal branches arising laterally or terminally from fertile hyphae in dense clusters. The other two species described in this genus, *Botryod. gigasporum* (Kapoor & Lal 1982) and *Botryod. nigrum* (Lopez *et al.* 1995) also produce single-celled conidia attached with remains of ruptured conidiogenous cell due to rhexolytic secession, but differ in lacking sterile hyphal branches within the clusters of conidiogenous cells. Furthermore, *Botryod. gigasporum* produces conspicuous conidiophores (Kapoor & Lal 1982) and *Botryod. nigrum* pigmented to black conidia (Lopez *et al.* 1995). It remains necessary to confirm the classification of the latter two species in *Botryoderma*.

Botryoderma lateritium Papendorf & H.P. Upadhyay, Trans. Brit. Mycol. Soc. 52: 258. 1969. Fig. 18.

Micromorphology: *Conidiophores* usually reduced. *Conidiogenous cells* arising laterally or terminally from fertile hyphae, densely clustered with some sterile hyphal branches, hyaline, subglobose, ellipsoidal or ovoid, polyblastic or monoblastic, 2.5–4 × 2–3 µm. *Conidia* single-celled, hyaline, smooth, ellipsoidal or obovoid, (4.5–)5.5–8(–9) × 3–5 µm, rhexolytic when seceding, usually with a rounded apex and a truncate base or a narrow secession scar often attached with ruptured remain of conidiogenous cell when detached. *Sterile filaments* arising laterally or terminally from fertile hyphae and forming dense clusters together with conidiogenous cells, erect, flexuous or recurved, 1.5–2.5 µm diam near the bases, up to 40 µm long. *Sexual morph* not observed.

Culture characteristics: On OA with an entire edge, 12–18 mm diam after 7 d at 25 °C, without aerial mycelium, obverse peach to brick due to the clusters of conidiogenous cells and conidia; reverse cinnamon. On CMA with a crenate edge, 12–18 mm diam after 7 d at 25 °C, without aerial mycelium, obverse olivaceous to brown vinaceous due to coloured exudates diffusing into the medium, with several peach to brick and crenate concentric rings due to the formation of clusters of conidiogenous cells and conidia; reverse dark mouse grey. On MEA with a crenate edge, 13–19 mm diam after 7 d at 25 °C, obverse saffron in the central part, with several salmon, buff or rosy buff concentric rings; reverse fawn to hazel. On PCA translucent, with an entire or lobate edge, 5–11 mm diam after 7 d at 25 °C, without aerial mycelium, obverse peach to brick, reverse saffron.

Material examined: **South Africa**, Transvaal, Potchefstroom, isolated from soil mixed with leaf litter of *Acacia karroo*, Jan.–Feb. 1964, M.C. Papendorf (culture ex-type CBS 586.66 = ATCC 18926 = IMI 158956 = MUCL 8790 = PRE 44223).

Notes: *Botryoderma lateritium*, the type species of the genus, produces conidia that usually have a rounded apex and a truncate base or a narrow secession scar. Two subsequently described species, *Botryod. gigasporum* and *Botryod. nigrum* have similar conidia. In comparison with *Botryod. lateritium*, *Botryod. gigasporum* (Kapoor & Lal 1982) produces larger conidia (11.5–30 × 10–22 µm *vs* 5.5–8 × 3–5 µm), while *Botryod. nigrum* (Lopez *et al.* 1995) produces smaller and brown to black conidia (3–6 × 2.5–3.5 µm *vs* 5.5–8 × 3–5 µm). Furthermore, *Botryod. gigasporum* and *Botryod. nigrum* lack sterile hyphal branches in the clusters of the conidiogenous cells.

Botryoderma rostratum Papendorf & H.P. Upadhyay, Trans. Brit. Mycol. Soc. 52: 260. 1969. Fig. 19.

Micromorphology: *Conidiophores* reduced. *Conidiogenous cells* arising laterally from fertile hyphae, densely clustered with seta, hyaline, subglobose, ellipsoidal or ovoid, monoblastic or polyblastic, 2.5–4 × 2–3 µm. *Conidia* single-celled, hyaline, smooth, ellipsoidal or obovoid, usually with an apical spine-like beak which is 1–3.5 µm long, rhexolytic when seceding, usually with a truncate base or a secession scar often attached with ruptured remain of conidiogenous cell when detached, (7.5–)8–10(–11.5) × 4–6 µm (excluding beak). *Sterile seta* arising laterally or terminally from fertile hyphae and forming dense clusters together with conidiogenous cells, sometimes branched, erect or recurved, 1–2 µm diam near the bases, up to 80 µm long. *Sexual morph* not observed.

Culture characteristics: On OA with an entire edge, 23–29 mm diam after 7 d at 25 °C, with sparse aerial mycelium, obverse vinaceous buff due to clusters of conidiogenous cells and conidia; reverse iron grey. On CMA like those on OA, with clusters of conidiogenous cells and conidia mainly in the central part and forming several concentric rings. On MEA with a lobate edge, 6–12 mm diam after 7 d at 25 °C, obverse white to buff or saffron, with a sienna margin, olivaceous around the colonies due to coloured exudates diffusing into the medium; reverse sienna. On PCA with an entire or slightly crenate edge, 16–22 mm diam after 7 d at 25 °C, without aerial mycelium, obverse white to rosy buff, reverse buff.

Material examined: **Lectotype** designated here: CBS H-24915, MBT 10004828. **Brazil**, Prov. Maranhâo, isolated from sandy soil, 1964, M.C. Papendorf (culture ex-lectotype CBS 184.68 = ATCC 18927 = IMI 158957).

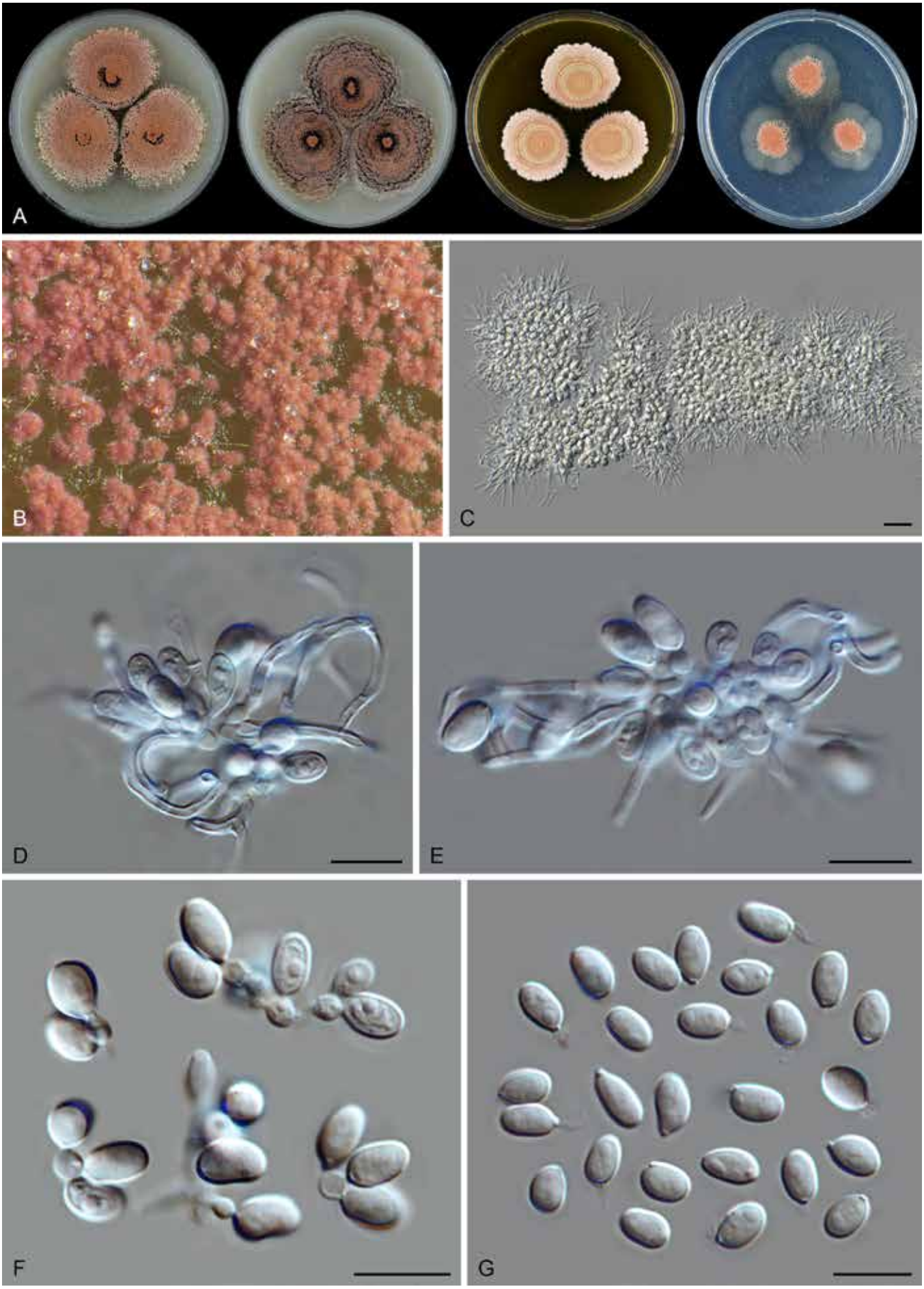

Fig. 18. *Botryoderma lateritium* (CBS 586.66, ex-type culture). **A.** Colonies from left to right on OA, CMA, MEA and PCA after 3 wk incubation. **B.** Part of the colony on OA. **C.** Clusters of conidiogenous cells with conidia and sterile hyphal branches. **D, E.** Part of the clusters of conidiogenous cells with conidia and sterile hyphal branches. **F.** Conidiogenous cells and conidia. **G.** Conidia. Scale bars: C = 20 µm; D–G = 10 µm.

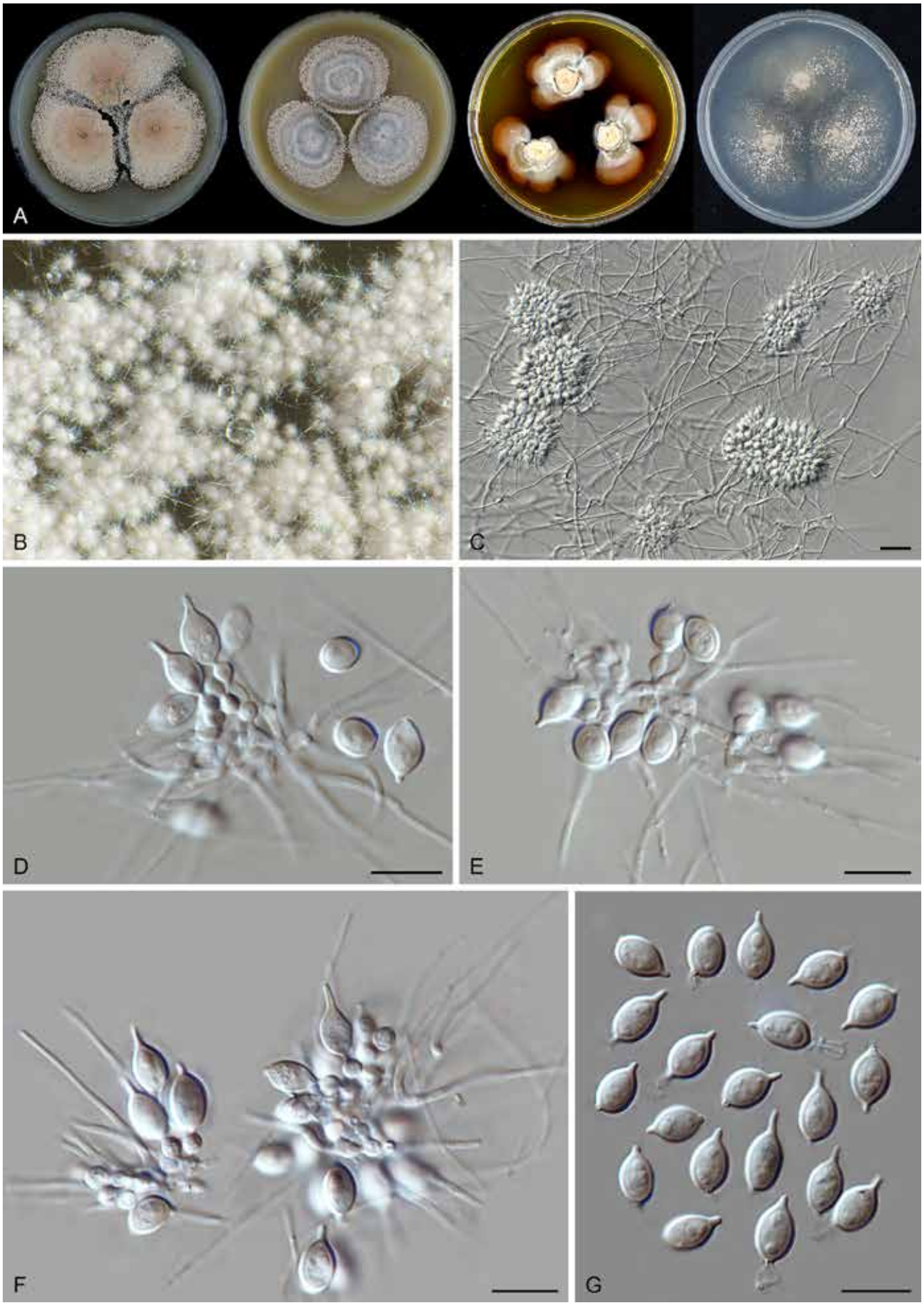

Fig. 19. *Botryoderma rostratum* (CBS 184.68, ex-type culture). **A.** Colonies from left to right on OA, CMA, MEA and PCA after 3 wk incubation. **B.** Part of the colony on OA. **C.** Hyphae, clusters of conidiogenous cells with conidia and sterile hyphal branches arising from hyphae. **D–F.** Part of the clusters of conidiogenous cells with conidia and sterile hyphal branches arising from hyphae. **G.** Conidia. Scale bars: C = 20 µm; D–G = 10 µm.

Notes: Papendorf & Upadhyay (1969) described *Botryoderma rostratum* and *Botryod. lateritium* in the same article, but only designated a holotype of *Botryod. lateritium*. For *Botryod. rostratum*, the protologue simply mentioned that "Cultures of the type have been deposited in the Mycotheca, University of Recife, Brazil; the Centraalbureau voor Schimmelcultures, Baarn, Netherlands, and the Cryptogamic Herbarium, University of Potchefstroom." Consequently, we prepared a herbarium specimen from the type culture CBS 184.68 as lectotype of this species. Both species described by Papendorf & Upadhyay (1969) produce conidiogenous cells and sterile hyphal branches in dense clusters. *Botryoderma rostratum* can easily be distinguished from *Botryod. lateritium*, *Botryod. gigasporum* and *Botryod. nigrum*, by its conidia having an apical spine-like beak. For more morphological comparisons, see notes of *Botryod. lateritium*.

Botryotrichum Sacc. & Marchal, Bull. Soc. Roy. Bot. Belgique 24: 66. 1885.

Micromorphology: Containing asexual species, sexual species and species with both asexual and sexual morphs. *Ascomata* superficial, or sub-immersed to immersed in the medium, ostiolate or non-ostiolate, subglobose to ovoid, covered by well-developed ascomatal hairs, or in some species glabrous or with sparse and hypha-like hairs. *Ascomatal wall* brown, non-translucent to semi-translucent, or in some species subhyaline to olivaceous grey and translucent, composed of *textura epidermoidea*, *intricata* or *angularis* in surface view. *Ascomatal hairs*, if present, flexuous or undulate and often circinate at the apex, or spirally coiled, or sparse and hyphal-like. *Asci* fasciculate, clavate, fusiform, ovoid or irregular, stalked, containing eight ascospores, evanescent. *Ascospores* olivaceous brown when mature, smooth, ellipsoidal with attenuated ends, or ellipsoidal-fusiform, not bilaterally flattened, with one or two apical germ pores. *Conidiophores* solitary or clustered with a tuft of sterile setae, hyaline to slightly pigmented, sympodially branched to produce several conidiogenous cells, or unbranched, sometimes reduced to conidiogenous cells. *Conidiogenous cells* hyaline, subhyaline to pale brown, cylindrical or slightly swollen, monoblastic or sympodially polyblastic. *Conidia* 1-celled, hyaline or pigmented, globose to subglobose, smooth to warted, solitary or rarely formed in chains of a few spores.

Type species: *Botryotrichum piluliferum* Sacc. & Marchal

Notes: As described above, *Botryotrichum* encompasses a high morphological diversity (Wang *et al.* 2016b, 2019a). Based on previous phylogenetic analyses, ten species have been included in this genus. Among the seven asexually reproducing species, *Botryot. atrogriseum*, *Botryot. peruvianum* and the type species *Botryot. piluliferum* produce monoblastic or sympodially polyblastic conidiogenous cells on sympodially or simply branched conidiophores that often cluster with sterile setae (Wang *et al.* 2016b). *Botryotrichum domesticum* (Schultes *et al.* 2019), *Botryot. foricae* (Crous *et al.* 2019) and *Botryot. iranicum* (Alidadi *et al.* 2020) produce similar conidiogenous cells, but usually lack sterile setae clustering with conidiophores or conidiogenous cells. *Botryotrichum verrucosum* produces solitary and often unbranched conidiophores (Wang *et al.* 2019a). Although the type species *Botryot. piluliferum* was originally described as an asexual species (Marchal 1885, Saccardo 1886), its sexual morph was later discovered (Daniels 1961). The sexual morph of *Botryot. piluliferum* is morphologically similar to that of *Botryot. murorum* and both produce ostiolate ascomata covered by unbranched ascomatal hairs with circinate tips and ellipsoidal ascospores (Daniels 1961, von Arx *et al.* 1986). *Botryotrichum murorum* has no asexual morph. *Botryotrichum spirotrichum* can be distinguished from the other species in the genus by its non-ostiolate ascomata which are usually ellipsoidal to doliiform and have two (or three) tufts of spirally coiled hairs at the two opposite ends. Based on phylogenetic data (Fig. 7), four new combinations in *Botryotrichum* are proposed below and one new species is described. The morphological diversity of *Botryotrichum* expands with the addition of this new species and four chaetomium- or corynascella-like species. Two of those species are (re)described and illustrated here: *Botryot. geniculatum* with a chaetomidium-like sexual morph and *Botryot. inquinatum* with a corynascella-like sexual morph. More details are given below.

Botryotrichum geniculatum X.Wei Wang, P.J. Han & F.Y. Bai, ***sp. nov.*** MycoBank MB 840127. Fig. 20.

Etymology: The name refers to its ascomatal hairs, which are geniculate in the lower parts.

Micromorphology: *Ascomata* superficial, occasionally immersed, solitary to several clustered, non-ostiolate, pale olivaceous grey in reflected light due to ascomatal hairs, spherical, 150–310 µm diam. *Ascomatal wall* dark brown, composed of *textura epidermoidea* or *intricata* when young, and then *textura angularis* when mature in surface view. *Ascomatal hairs* covering the whole ascomata, hypha-like, smooth or finely verrucose, flexuous or slightly undulate in the upper part, tapering and fading to hyaline towards the tips, geniculate in the lower part, brown at the base, 2–3.5 µm near the base, varying in length, some up to 400 µm long, occasionally up to 1 300 µm long. *Asci* clavate, spore-bearing part 48–72 × 20–26 µm, with stalks 12–35(–59) µm long, containing eight irregularly-arranged or biseriate ascospores, evanescent. *Ascospores* 1-celled, smooth, dark brown when mature, elongated limoniform to broadly fusiform, sometimes inequilateral, (16.5–)17–20(–30) × (11–)11.5–13(–14) µm, with an apical germ pore. *Asexual morph* unknown.

Culture characteristics: On OA with an entire edge, 18–24 mm diam in 7 d at 25 °C, aerial mycelium absent; obverse pale olivaceous grey due to the masses of ascomata, with soluble pigment greenish glaucous to greenish olivaceous; reverse smoke grey to greenish olivaceous due to exudates diffusing into the medium. On CMA similar to those on OA, 17–23 mm diam in 7 d at 25 °C, with soluble pigment pale vinaceous grey to vinaceous grey. On MEA with an fimbriate edge, 11–17 mm diam in 7 d at 25 °C, obverse pale mouse grey due to thick aerial mycelium, texture floccose, reverse cinnamon. On PCA with an entire edge, 10–16 mm diam in 7 d at 25 °C, obverse white, aerial mycelium absent, without coloured exudates, reverse uncoloured.

Material examined: **China**, Burjin County, Altay Prefecture, Xinjiang, isolated from soil under herb, Aug. 2004 , X.W. Wang (**holotype** HMAS 350293, isotype CBS H-23629, culture ex-type CGMCC 3.20441 = CBS 144475 = WXW 8287); Yili Prefecture, Xinjiang, near Sayram Lake, isolated from soil under *Trollius chinensis*, Aug. 2004, X.W. Wang (culture WXW 8266).

Notes: This species is characterised by its non-ostiolate ascomata covered by hypha-like ascomatal hairs, which are geniculate in their lower part and by its large limoniform to broadly fusiform ascospores (17–20 × 11.5–13 µm) with an apical germ pore. Three

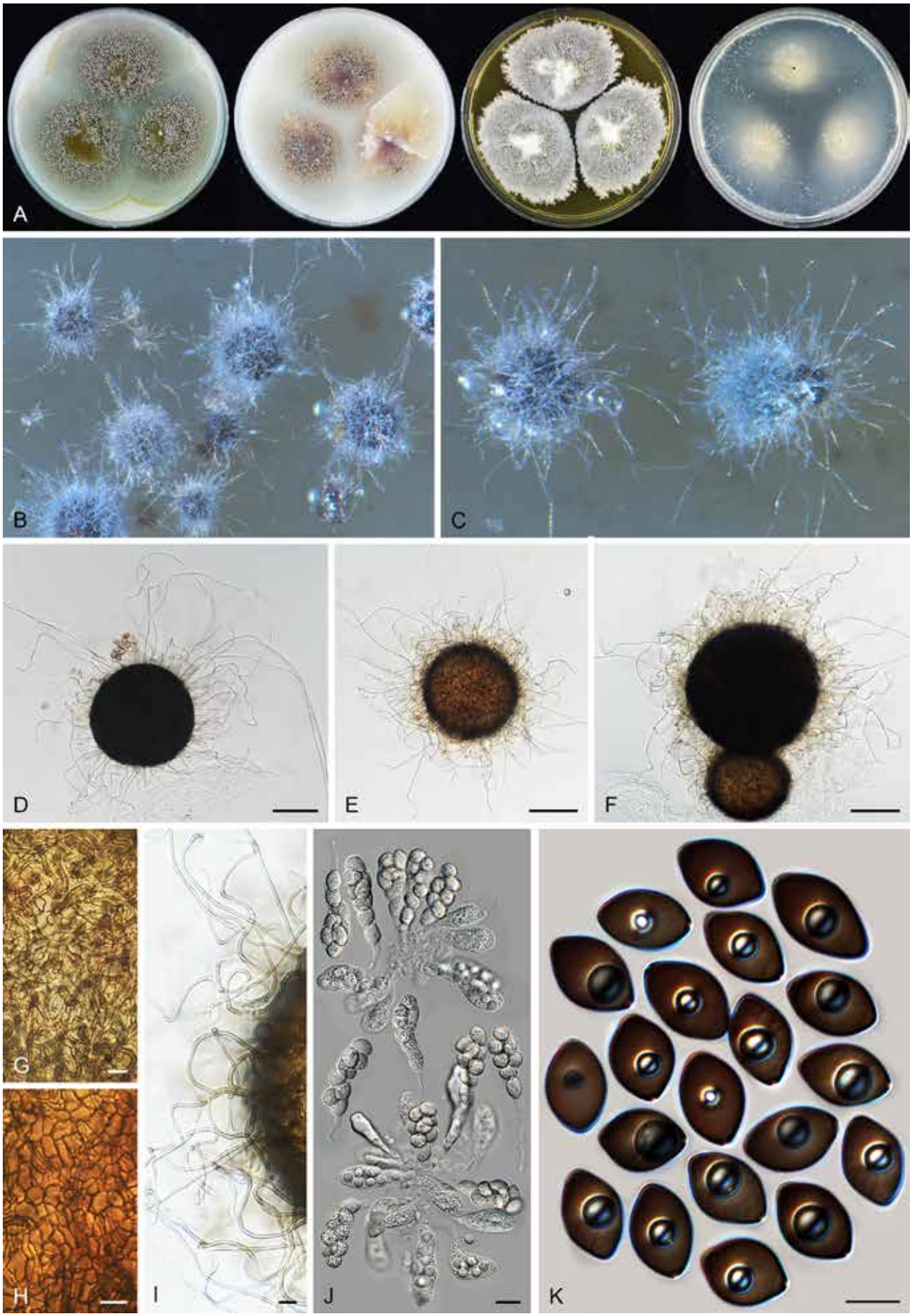

Fig. 20. *Botryotrichum geniculatum* (CGMCC 3.20441, ex-type culture). **A.** Colonies from left to right on OA, CMA, MEA and PCA after 3 wk incubation. **B, C.** Mature ascomata on OA, top view. **D–F.** Ascomata mounted in lactic acid. **G, H.** Structure of ascomatal wall in surface view. **I.** Ascomatal hairs. **J.** Asci. **K.** Ascospores. Scale bars: D–F = 100 µm; G–I, K = 10 µm; J = 20 µm.

other *Botryotrichum* species produce non-ostiolate ascomata: *Botry. inquinatum* also has large ascospores (17–19 × 12.5–14.5 µm), but can be distinguished by two apical or subapical germ pores on each ascospore and by glabrous ascomata (see below); *Botry. spirotrichum* can be distinguished by smaller ascospores (5.5–8.0 × 4.5–6.5 µm) and by ascomata covered by coiled hairs (von Arx *et al.* 1988); *Botry. trichorobustum* is different in ascomata covered by flexuous or slightly undulate hairs, partly recurved or circinate at the apex, and in slightly smaller ascospores (10.5–18.5 × 10.5–13.5 µm) (Seth 1968, see below).

Botryotrichum inquinatum (Udagawa & S. Ueda) X.Wei Wang & Houbraken, ***comb. nov.*** MycoBank MB 830923. Fig. 21.
Basionym: *Corynascella inquinata* Udagawa & S. Ueda, Mycotaxon 8: 292. 1979.

Micromorphology: *Ascomata* superficial, subimmersed to immersed in the medium, solitary or aggregated, non-ostiolate, mouse grey to dark mouse grey when mature in reflected light, subglobose, glabrous, or with sparse, hypha-like hairs, (120–)175–330 µm diam. *Ascomatal wall* subhyaline to olivaceous grey, translucent, composed of *textura epidermoidea* in surface view. *Asci* pyriform, clavate, ovoid or irregular, spore-bearing part 42–86 × 21–31 µm, with stalks being 17–36.5 µm long, containing eight irregularly-arranged ascospores, evanescent. *Ascospores* olivaceous brown when mature, ellipsoidal, often biapiculate, (16–)17–19(–20.5) × (11.5–)12.5–14.5 µm, with two apical or subapical germ pores. *Asexual morph* unknown.

Culture characteristics: On OA with an entire or crenate edge, 10–16 mm diam in 7 d at 25 °C, without aerial mycelium, obverse olivaceous buff due to coloured exudates diffusing into the medium, producing mouse grey ascomata; reverse buff to olivaceous buff. On CMA a crenate edge, 7–13 mm diam in 7 d at 25 °C, without aerial mycelium, obverse buff to olivaceous buff; reverse olivaceous buff. On MEA with a lobate edge, 5–11 mm diam in 7 d at 25 °C, without aerial mycelium, obverse buff to rosy buff, wrinkled; reverse cinnamon. On PCA with a crenate edge, 3–9 mm diam in 7 d at 25 °C, without aerial mycelium, obverse grey white, with thin and translucent margins, without coloured exudates, reverse uncoloured.

Material examined: **Egypt**, isolated from desert soil, date unknown, J. Mouchacca (CBS 646.74). **Japan**, Nagasaki Pref., Isahaya-shi, isolated from sewage sludge, 22 Mar. 1978, S. Ueda (culture ex-type CBS 155.80 = ATCC 18927 = NHL 2841).

Notes: *Botryotrichum inquinatum* was originally placed in *Corynascella* based on its production of non-ostiolate ascomata and ascospores with two germ pores (Udagawa & Ueda 1979). Our phylogenetic analysis indicates that this species belongs to *Botryotrichum*, distantly related to the type species of *Corynascella*, *C. humicola* (Fig. 7C). This species is distinguished from the other species in the genus by its translucent, nearly glabrous non-ostiolate ascomata and its ascospores with two apical or subapical germ pores.

Botryotrichum retardatum (A. Carter & R.S. Khan) X.Wei Wang & Houbraken, ***comb. nov.*** MycoBank MB 840141.
Basionym: *Chaetomium retardatum* A. Carter & R.S. Khan, Canad. J. Bot. 60: 1255. 1982.

Notes: The position of this species in *Botryotrichum* (Fig. 7C) is supported in the combined and the *tub2* and *rpb2* phylogenies (Fig. 7C, Supplementary Figs S2, S3, ITS sequence not available). *Botryotrichum retardatum* can be distinguished from other species by the production of ostiolate ascomata covered by sparse hairs and ellipsoidal to fusiform ascospores with two subapical germ pores (von Arx *et al.* 1986).

Botryotrichum trichorobustum (Seth) X.Wei Wang & Houbraken, ***comb. nov.*** MycoBank MB 840143.
Basionym: *Chaetomidium trichorobustum* Seth, Nova Hedwigia 16: 430. 1968.

Notes: The phylogenetic relationship of *Botryo. trichorobustum* with other species in the genus is unresolved and it seems to take a basal position in the genus, though bootstrap support is lacking. *Botryotrichum trichorobustum* can be distinguished from other species in the genus by the production of non-ostiolate ascomata covered by smooth and thick (9–14 µm near the base) ascomatal hairs, partly with recurved or circinate apex. The species produces limoniform to broadly fusiform ascospores. No germ pores were observed and reported in the original description of the species (Seth 1968).

Botryotrichum vitellinum (A. Carter) X.Wei Wang & Houbraken, ***comb. nov.*** MycoBank MB 840144.
Basionym: *Chaetomium vitellinum* A. Carter, Mycologia 75: 531. 1983.

Notes: Phylogenetically, *Botryo. vitellinum* is sister to all other species in the genus (Fig. 7C). It can be distinguished from other species in the genus by the production of ostiolate ascomata covered by sparse, delicate hairs and ovate to fusiform ascospores with an apical germ pore (von Arx *et al.* 1986).

Chaetomium Kunze, Mykol. Hefte 1: 15. 1817.

Micromorphology and illustrations: See Wang *et al.* (2016a; p.167). Containing sexual species and species with both asexual and sexual morphs.

Type species: *Chaetomium globosum* Kunze

Notes: *Chaetomium sensu stricto* is characterised by the production of globose, ellipsoid to ovate or obovate ascomata, most often ostiolate and non-ostiolate in a few species. The ascomatal wall is usually composed of *textura intricata* or *epidermoidea* in surface view, or of *textura angularis* in a few species; the ascomatal hairs are hypha-like, flexuous, undulate, coiled to simply branched or dichotomously branched, mostly with verrucose surface and smooth in a few species. The asci of *Chaetomium* species are clavate or fusiform with eight biseriate or irregularly arranged ascospores. The ascospores are limoniform to globose (irregular in a few species), bilaterally flattened and usually more than 7 µm in length. An asexual morph is produced in some species and is, if present, acremonium-like (Wang *et al.* 2016a, b). We accept 43 species in *Chaetomium*. It is the largest genus in the family (Fig. 7B).

Chaetomium neoglobosporum X.Wei Wang & Houbraken, ***nom. nov.*** MycoBank MB 841112.
Replaced synonym: *Chaetomium globosporum* Rikhy & Mukerji, Kavaka 1: 38. 1974, non *Chaetomium globisporum* Lodha. 1964.

Fig. 21. *Botryotrichum inquinatum* (CBS 155.80, ex-type culture). **A.** Colonies from left to right on OA, CMA, MEA and PCA after 4 wk incubation. **B, C.** Mature ascomata on OA, top view. **D–F.** Ascomata mounted in lactic acid. **G.** Structure of ascomatal wall in surface view. **H.** Asci. **I.** Ascospores. Scale bars: D–F = 50 µm; G–I = 10 µm.

Etymology: The species name refers to *"globosporum"*, the epithet of the replaced synonym.

Micromorphology and illustrations: See Wang *et al.* (2016a; p. 101–102).

Notes: The epithets of *Ch. globosporum* and *Ch. globisporum* are similar, have the same meaning and can be easily confused. Because of this, *Ch. globosporum* is regarded as an illegitimate later homonym of *Ch. globisporum* (Art. 53.1), and we therefore propose the replacement name "*neoglobosporum*" for the former one. No (ex-)type material of the latter one "*Ch. globisporum*" was included in our study, so the taxonomic position of the latter species remains unknown.

Chaetomium subaffine Sergejeva ex X.Wei Wang & Houbraken, ***sp. nov.*** MycoBank MB 842311.
Synonym: *Chaetomium subaffine* Sergejeva, Bot. Mater. Otd. Sporov. Rast. Bot. Inst. Komarova Akad. Nauk S.S.S.R. 14: 148. 1961. (*nom. inval.*, Art. 39.1).

Etymology: The epithet "subaffine" was used in the description of Sergejeva (1961), referring to *Chaetomium affine* Corda *sensu* Bainier.

Diagnosis: Phylogenetic inference (Fig. 7B) indicates that *Ch. subaffine* is most closely related to *Ch. cirrhatum*, *Ch. cochliodes*, *Ch. pseudocochliodes* and *Ch. spiculipilium*. *Chaetomium subaffine* can be distinguished from them by the abundant white mycelia covering the ascomata, mostly straight to flexuous ascomatal hairs, and the production of an acremonium-like asexual morph. The ascospores of *Ch. subaffine* are also larger (11.5–13.5 × 8.5–10 × 6.5–7.5 µm) than those of *Ch. cochliodes* (9–10 × 7.5–8.5 × 5–6 µm), *Ch. pseudocochliodes* (9.5–11 × 7.5–8.5 × 5.5–6.5 µm) and *Ch. spiculipilium* (10–13 × 7.5–9 × 5.5–6.5 µm) (Wang *et al*. 2016a, Zhang *et al*. 2017).

Description and illustration: See Wang *et al*. (2016a; p.121–122).

Material examined: **Russia**, isolated from seed and dead stem of cereal, date unknown, K.S. Sergejeva (**holotype** CBS H-24916, culture ex-type CBS 637.91 = ATCC 14531 = IMI 090489 = MUCL 18695 = VKM F-1945).

Notes: Bainier's concept (1910) of *Ch. affine* differs from the original description of Corda (1840) and therefore Sergejeva (1961) introduced *Ch. subaffine* for Bainier's species. *Chaetomium subaffine* Sergejeva lacks a Latin diagnosis and is therefore invalidly described. Sergejeva (1961) refers to Bainier (1910), but this publication also lacks a Latin description (only in French). In addition, the reference to Bainier's illustration is insufficient. To validate this species, an English diagnosis is given above, with the name of the original author maintained.

Collariella X.Wei Wang, Samson & Crous, Stud. Mycol. 84: 177. 2016. Fig. 22.

Micromorphology (*emended description*): *Ascomata* superficial, ostiolate, ovate, obovate, ampulliform or cylindrical with brown walls of *textura angularis* in surface view. *Apices of ascomata* truncated, usually with a darkened collar around the ostiolar pore. *Terminal hairs* highly diverse, straight, flexuous, undulate or spirally coiled or presenting two different types. *Lateral hairs* straight, flexuous. *Asci* fasciculate, fusiform or clavate, stalked, with eight biseriate or irregularly-arranged ascospores, evanescent. *Ascospores* olivaceous brown at maturity, broadly limoniform to quadrangular, bilaterally flattened, with an apical germ pore, usually less than 7.5 µm in length, occasionally up to 10.5 µm long. *Asexual morph* not observed.

Type species: *Collariella bostrychodes* (Zopf) X.Wei Wang & Samson

Notes: *Collariella* was originally delimited based on phylogenetic data and included two subclades (Wang *et al.* 2016b). Species in each subclade share certain morphological characters, yet the two subclades are distinctively different in the morphology of their ascomata and ascospores (Figs 10, 22). The molecular dating analysis performed here (Fig. 8A) indicated that these two subclades diverged from each other about 42 Mya, before the later time limit (about 27 Mya, Figs 8A, 9) of the other accepted genera in the family. This result supports segregating them as two genera. Thus, *Collariella sensu stricto* is restricted to subclade 1 (Wang *et al.* 2016b) and *Achaetomiella* is revived above to accommodate species belonging to the other subclade.

Phylogenetic analyses showed that three additional chaetomium-like species belong to *Collariella* (Fig. 7C, Supplementary Figs S1, S2). The morphology of these species fits in the modified definition of *Collariella* as given above.

Collariella anguipilia (L.M. Ames) X.Wei Wang & Houbraken, ***comb. nov.*** MycoBank MB 840145.
Basionym: *Chaetomium anguipilium* L.M. Ames, A monograph of the *Chaetomiaceae*: 12. 1963.

Notes: *Collariella anguipilia* is phylogenetically closely related to *Col. causiiformis* and *Col. hexagonospora* (Fig. 7C, Supplementary Figs S1–S3). Morphologically, *Col. anguipilia* is similar to *Col. causiiformis*. Both have two types of ascomatal hairs, partly shorter and partly longer, and possess ascospores of similar shape and size. *Collariella anguipilia* can be distinguished from *Col. causiiformis* by its shorter type of ascomatal hairs, which are undulate and unbranched (Ames 1963, von Arx *et al.* 1986). *Collariella hexagonospora* can be distinguished by coiled ascomatal hairs and larger ascospores.

Collariella hexagonospora (A. Carter & Malloch) X.Wei Wang & Houbraken, ***comb. nov.*** MycoBank MB 840146.
Basionym: *Chaetomium hexagonosporum* A. Carter & Malloch, Canad. J. Bot. 60: 1249. 1982.

Notes: *Collariella hexagonospora* has the largest ascospores (9–10.5 µm long) in the genus (von Arx *et al.* 1986). Ascospores of the other known *Collariella* species are usually less than 7.5 µm long. The presence of a darkened collar around the ostiolar pore was not reported in the original description, though von Arx *et al.* (1986) mentioned that its ascomata were darker than those of other species (von Arx *et al.* 1986). More work is required to verify whether this species also produces a darkened collar around the ostiolar pore, as do the other species in the genus.

Collariella pachypodioides (L.M. Ames) X.Wei Wang & Houbraken, ***comb. nov.*** MycoBank MB 840147.
Basionym: *Chaetomium pachypodioides* L.M. Ames, Mycologia 37: 145. 1945.

Notes: This species was once treated as a synonym of *Col. bostrychodes* (von Arx *et al.* 1986). Our phylogenetic analysis indicated that it is distinct (Supplementary Figs S1–S3), and closer to *Col. carteri* than to *Col. bostrychodes* (Fig. 7C). *Collariella carteri* can be distinguished from *Col. pachypodioides* by short and seta-like terminal ascomatal hairs (Wang *et al.* 2016b), while the latter only produces spirally coiled terminal hairs. *Collariella pachypodioides* can be distinguished from *Col. bostrychodes* by

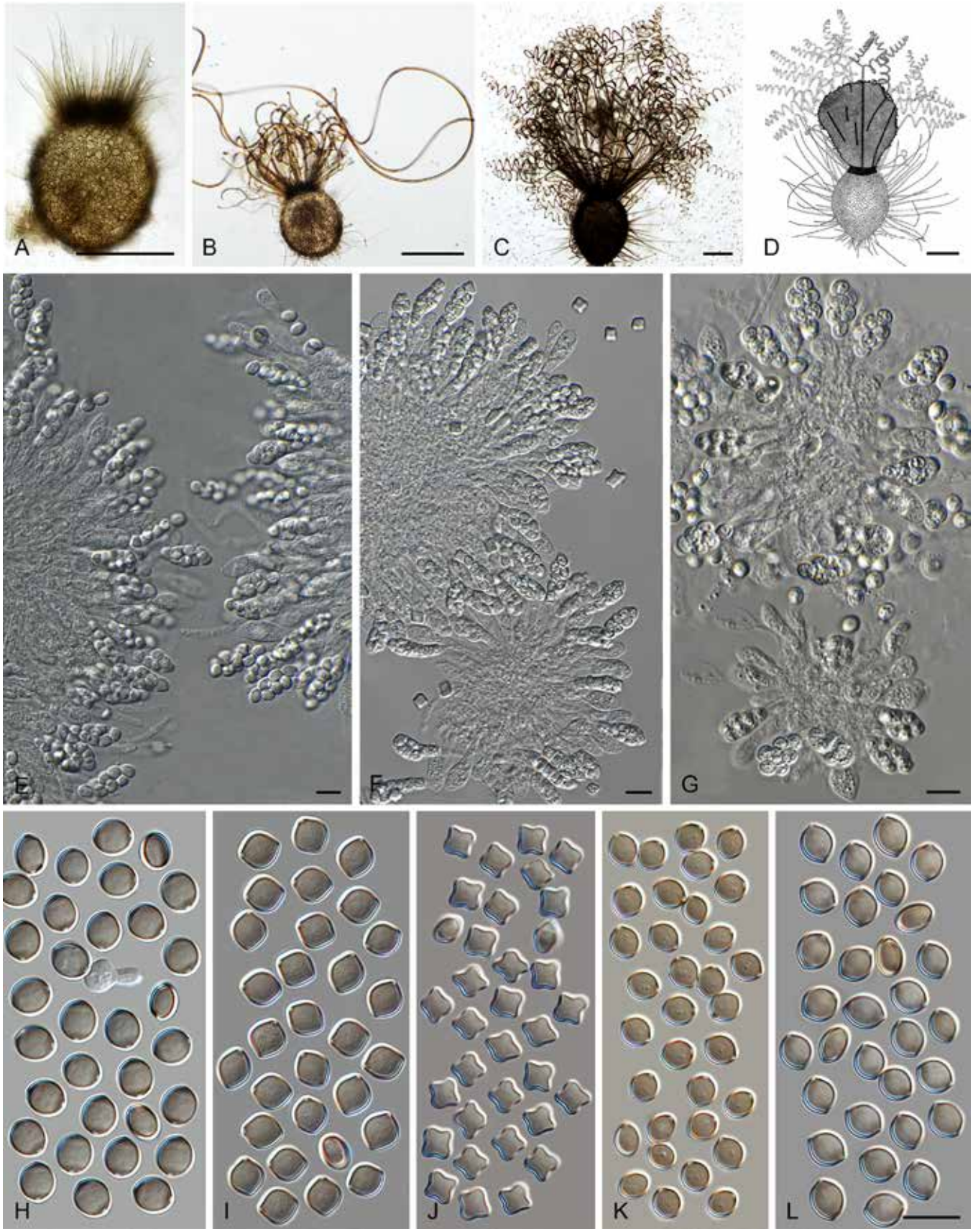

Fig. 22. Morphology of *Collariella*. Ascomata (A–D): **A.** *Collariella intricata* (CBS 128.85^{T}). **B.** *Col. causiiformis* (CBS 792.83^{T}). **C.** *Col. bostrychodes* (DTO 326-H6). **D.** Line drawing of *Col. bostrychodes* (CGMCC 3.1054). Asci (E–G): **E.** *Col. bostrychodes* (DTO 326-H6). **F.** *Col. quandrangulata* (CBS 152.59). **G.** *Col. causiiformis* (CBS 792.83^{T}). Ascospores (H–L): **H.** *Col. bostrychodes* (DTO 326-H6). **I.** *Col. robusta* (CBS 551.83^{T}). **J.** *Col. quandrangulata* (CBS 152.59). **K.** *Col. causiiformis* (CBS 792.83^{T}). **L.** *Col. intricata* (CBS 128.85^{T}). Scale bars: A–D = 100 µm; E–G = 10 µm; L = 10 µm, also applied to H–K.

its ascomatal shape (elongated ovate *vs* globose or subglobose) (Greathouse & Ames 1945, Wang *et al.* 2016b). *Collariella capillicompacta* is recently described as being closely related to *Col. carteri* and is phenotypically similar as *Col. pachypodioides* (Aghyl *et al.* 2021).

Corynascella Arx & Hodges, Stud. Mycol. 8: 23. 1975.

Micromorphology: *Ascomata* superficial, immersed or sub-immersed into the medium, solitary or aggregated, non-ostiolate at the beginning, later ostiolate especially on CMA, with masses of released ascospores on the top, subglobose or ovoid, usually covered by sparse aerial hyphae on which conidia are produced. *Ascomatal wall* brown, composed of *textura epidermoidea* in surface view. *Ascomatal hairs* straight or flexuous, brown, fading towards the tips, septate, smooth. *Asci* fasciculate, clavate, stalked, containing eight biseriate or irregularly-arranged ascospores, evanescent. *Ascospores* brown when mature, ellipsoidal, oblate, ovoid or doliiform, usually irregular and inequilateral, with two apical germ pores. *Synnemata* composed of compact groups of parallel or sometimes intricate hyphae, brown, often split in two or more branches in the upper part and tapering and fading towards the tips. *Conidiophores* arising laterally from synnemata or from aerial hyphae, erect or flexuous, brown, septate, unbranched or simply branched near the base. *Conidiogenous cells* hyaline to buff, cylindrical or clavate, apically surrounded by masses of conidia, polyblastic, with conidiogenous scars after conidial secession. *Conidia* formed in slimy heads, single-celled, hyaline, smooth, ellipsoidal, obovate or clavate with a truncate base. Containing species with both asexual and sexual morphs.

Type species: *Corynascella humicola* Arx & Hodges

Notes: In his morphological treatment of *Thielavia*, von Arx (1973a, 1975b) classified species producing ascospores with two germ pores in *Corynascus* (see below in detail) and *Corynascella*, and species with a single germ pore in *Thielavia*. *Corynascella* was distinguished from *Corynascus* by lacking a myceliophthora-like asexual morph (von Arx 1973b, 1975a). In the protologue of the type species *Corynascella humicola*, von Arx (1975a) simply mentioned that occasionally some blastoconidia were formed in the aerial mycelium or on tips of hyphal branches. Up to now, four species have been described in this genus, but except for the type species, none of the other species produce an asexual morph (von Arx 1975b, Udagawa & Ueda 1979, von Arx *et al.* 1988, Guarro *et al.* 1997). In the present study, three of the four species were examined. Our phylogenetic analysis demonstrated that these three *Corynascella* species belong to three different genera (Fig. 7A, C). *Corynascella* is restricted only to its type species. *Corynascella inaequalis* is transferred below to *Parachaetomium* as *Parach. inaequale* and *Corynascella inquinata* is transferred to *Botryotrichum* as *Botryot. inquinatum*. The unique structure of the asexual morph in the type species was re-described and illustrated (Fig. 24). No asexual morph is reported in *Corynascella arabica* (Guarro *et al.* 1997) and the phylogenetic position of this species remains to be resolved.

Corynascella humicola Arx & Hodges, Stud. Mycol. 8: 23. 1975. Figs 23, 24.

Micromorphology: *Ascomata* on OA and CMA usually superficial, sometimes immersed or sub-immersed into the medium, solitary or aggregated, non-ostiolate at the beginning, later ostiolate especially on CMA, with masses of released ascospores on the top, cinnamon due to ascomatal hairs, or fuscous black when mature due to exposed ascospores in reflected light, subglobose or ovoid, 110–170 µm high, 95–140 µm diam, usually covered by sparse aerial hyphae on which conidia are produced. *Ascomatal wall* brown, composed of *textura epidermoidea* in surface view. *Ascomatal hairs* straight or flexuous, brown, fading towards the tips, septate, smooth, 1–3 µm diam near the base, up to 105 µm long. *Asci* clavate, spore-bearing part 38–52 × 16–20 µm, with stalks being 7–20.5 µm long, containing eight biseriate or irregularly-arranged ascospores, evanescent. *Ascospores* dark brown when mature, irregularly ellipsoidal, oblate, ovoid or doliiform, usually irregular and inequilateral, (11–)12.5–14.5(–16.5) × (9–)9.5–11(–12.5) µm, with two apical germ pores. *Synnemata* usually produced in the central part of colonies on OA or forming a circle ring around the centre on CMA, composed of compact groups of parallel or sometimes intricate hyphae, brown, 10–100 µm diam near the bases, often split in two or more branches in the upper part and tapering and fading towards the tips, up to 2.5 mm long. *Conidiophores* arising laterally from synnemata or from aerial hyphae, erect or flexuous, brown, septate, unbranched or simply branched near the base, 2–4 µm diam near the base, 20–80 µm long. *Conidiogenous cells* hyaline to buff, cylindrical or clavate, surrounded by masses of conidia, 9–16 × 2–2.5 µm, polyblastic, with conidiogenous scars after conidial secession (Fig. 24H). *Conidia* formed compactly in slimy heads on top of the conidiogenous cells, single-celled, hyaline, smooth, ellipsoidal, obovate or clavate with a truncate base, 2.5–8 × 2–4.5 µm, schizolytic when seceding.

Culture characteristics: On OA with an entire edge, 30–36 mm diam in 7 d at 25 °C, with sparse olivaceous aerial hyphae on which simple conidiophores and conidia are produced; reverse uncoloured. On CMA with an entire edge, 30–36 mm diam in 7 d at 25 °C, olivaceous black due to masses of ascospores on top of ascomata, with a greyish sepia and floccose circle ring composed of synnemata around the central part; reverse buff. On MEA with an entire edge, about 29–35 mm diam in 7 d at 25 °C, with thick olivaceous floccose aerial hyphae covering the aggregated ascomata, obverse fuscous black; reverse buff to olivaceous black. On PCA with a lobate or crenate edge, about 27–33 mm diam in 7 d at 25 °C, translucent, obverse pale mouse grey to dark mouse grey due to simple conidiophores and ascomata; reverse olivaceous to olivaceous black due to the immersed hyphae, immersed ascomata and coloured exudates diffusing into the medium.

Material examined: **USA**, North Carolina, Piedmont, isolated from soil, 1971, C.S. Hodges (culture ex-type CBS 337.72); North Carolina, Piedmont, isolated from soil, 1971, C.S. Hodges (CBS 379.74).

Notes: The asexual morph of *Corynascella humicola* was carefully examined for the first time in the present study (Fig. 24). The same asexual morph was observed in the cultures CBS 337.72^{T} and CBS 379.74. The synnemata seem to be better developed on CMA than on OA, MEA and PCA. Von Arx (1975a) observed solitary conidiophores in the aerial mycelium and conidia measuring 4–8 × 1.5–3 µm, similar to those arising directly from the aerial hyphae in our observations. The conidia are usually aggregated compactly in slimy heads, and it is not easy to find discrete conidia free from the aggregations. The ascomata of *Corynascella humicola* were always described as being non-ostiolate; however, we observed ostioles on the mature ascomata where masses of released ascospores are clearly present (Fig. 23C).

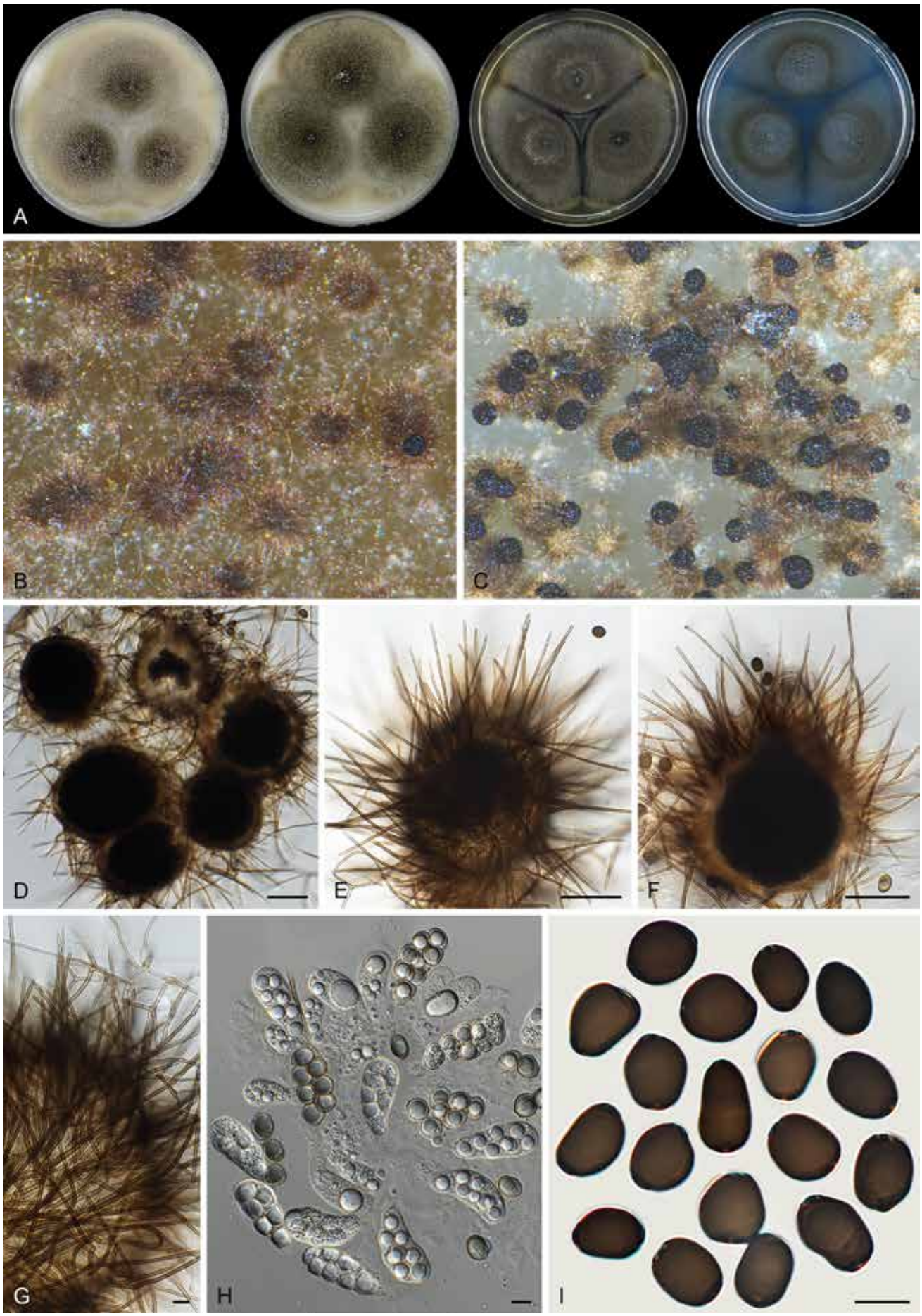

Fig. 23. Sexual morph of *Corynascella humicola* (CBS 337.72, ex-type culture). **A.** Colonies from left to right on OA, CMA, MEA and PCA after 3 wk incubation. **B.** Part of the colony, showing ascomata on OA, top view; most non-ostiolate. **C.** Part of the colony, showing mature and ostiolate ascomata with masses of ascospores on the top, top view on OA. **D–F.** Ascomata mounted in lactic acid. **G.** Ascomatal hairs. **H.** Asci. **I.** Ascospores. Scale bars: D–F = 50 µm; G–I = 10 µm.

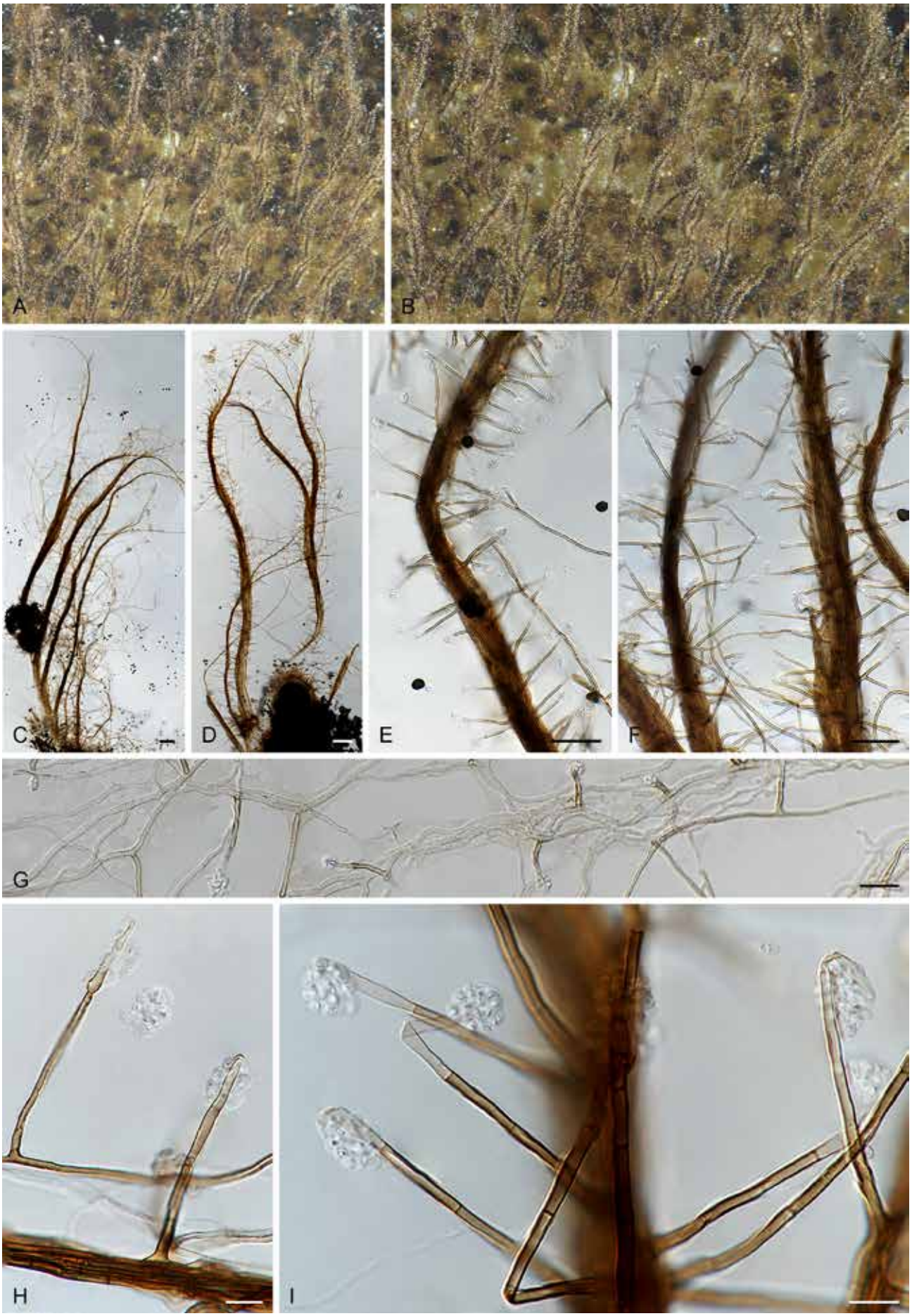

Fig. 24. Asexual morph of *Corynascella humicola* (CBS 337.72, ex-type culture). **A, B.** Aerial part of the colony, showing synnemata bearing conidiophores on sides and apex, on CMA. **C–D.** Synnemata bearing conidiophores on sides and apex, mounted in lactic acid. **E, F.** Part of synnemata and solitary fertile hyphae, from which conidiophores arise. **G.** Hyphae from which solitary conidiophores arise. **H, I.** Conidiophores, hyaline conidiogenous cells and masses of conidia. Scale bars: C, D = 100 µm; E, F = 50 µm; G = 20 µm; H, I = 10 µm.

Corynascus Arx, Proc. Kon. Ned. Akad. Wetensch., C 76: 295. 1973.

Micromorphology: *Ascomata* superficial to immersed, often covered by aerial hyphae together with conidial structures, non-ostiolate, small (usually less than 115 µm diam), glabrous, globose or subglobose. *Ascomatal wall* brown, composed of *textura epidermoidea* in surface view. *Asci* obovoid, pyriform or clavate, usually with short or indistinct stalks, containing eight irregularly-arranged ascospores, evanescent. *Ascospores* olivaceous brown when mature, single-celled, smooth, fusiform to limoniform, with two apical, subapical or oblique germ pores. *Conidiophores* usually reduced to conidiogenous cells that arise laterally or terminally from hyphae. *Conidiogenous cells* hyaline, denticle-like or inflated and ampulliform, fusiform, clavate or obovoid, sometimes reduced to a hyphal cell, monoblastic or polyblastic synchronous. *Conidia* schizolytic when seceding, hyaline, single-celled, verrucose, or smooth in a few species, globose, subglobose, ellipsoidal or obovoid, sometimes with a narrow and truncate base. Containing species with both asexual and sexual morphs.

Type species: *Corynascus sepedonium* (C.W. Emmons) Arx

Notes: *Corynascus* was defined to produce homothallic ascomata together with a myceliophthora-like (historically called chrysosporium-like, see "*Myceliophthora*" below) asexual morph and this genus was therefore considered a sexual morph of *Myceliophthora* (von Arx 1973b, van Oorschot 1980, von Arx *et al.* 1988, Stchigel *et al.* 2000). Several recent studies dealt with the generic delimitation of *Myceliophthora sensu lato*. Van den Brink *et al.* (2012) studied the phylogeny of 48 strains representing five *Myceliophthora* and three *Corynascus* species, but only a limited number of other *Chaetomiaceae* species was included in their analysis. Even though their study indicated segregation of homothallic *Corynascus* from the other species, they nevertheless suggested a broad generic concept for *Myceliophthora*, in which all *Corynascus* species were included. Zhang *et al.* (2014a) followed the taxonomy of van den Brink *et al.* (2012), but Marin-Felix *et al.* (2015) segregated *Myceliophthora sensu* van den Brink *et al.* (2012) into four genera: the two non-thermophilic genera *Corynascus* and *Myceliophthora* and the two thermophilic genera *Crassicarpon* and *Thermothelomyces*. Phylogenetically, *Corynascus* is sister to *Myceliophthora* and *Thermothelomyces* (Fig. 7A). Our molecular dating analysis (Fig. 8B) indicated that *Myceliophthora sensu* van den Brink *et al.* (2012) has a mean stem age of about 41 Mya. The *Corynascus* clade within this *Myceliophthora sensu* van den Brink *et al.* clade diverged from the others about 35 Mya. Based on literature (von Arx 1975a, Stchigel *et al.* 2000, van den Brink *et al.* 2015, Marin-Felix *et al.* 2015), *Corynascus* species are mesophilic or thermotolerant, and no species are thermophilic. All described *Corynascus* species are homothallic, produce ascomata and a myceliophothora-like morph in culture. The combination of these characters sets this genus apart from the other genera in *Chaetomiaceae*.

Corynascus fumimontanus Y. Marín *et al.*, Mycologia 107: 628. 2015. Fig. 25.

Micromorphology: See Marín-Felix *et al.* (2015).

Notes: Based on our measurements, *Corynascus fumimontanus* produces larger ascomata (up to 165 µm diam) than other *Corynascus* species, which are usually less than 120 µm diam. Its conidia arise laterally or terminally from hyphae rather than from well-differentiated conidiogenous cells. Marín-Felix *et al.* (2015) emphasised the morphological characters of this species such as verrucose ascomatal wall cells, mostly irregularly shaped ascospores and sessile conidia. Our examination showed that similar ascomatal wall cells are also found in *Corynascus novoguineensis*, *Coryn. sexualis* and *Coryn. verrucosus*, and ascospores of the accepted species of that genus are more or less inequilateral as well. *Corynascus sepedonium* produces a similar asexual morph, but has smaller ascomata (25–45 µm *vs* 65–165 µm), broader and shorter ascospores (12–14.5 × 7.5–9 µm *vs* 13–15.5 × 7.5–8.5 µm) and smooth-walled conidia (see below).

Corynascus novoguineensis (Udagawa & Y. Horie) Arx, Proc. Kon. Ned. Akad. Wetensch., C 76: 295. 1973. Fig. 26.
Basionym: *Thielavia novoguineensis* Udagawa & Y. Horie, Bull. Natl. Sci. Mus. Tokyo 15: 191. 1972.
Synonym: *Myceliophthora novoguineensis* (Udagawa & Y. Horie) van den Brink & Samson, Fungal Diversity 52: 206. 2011 [2012], *nom. inval*., Art. 41.5.

Micromorphology: *Ascomata* superficial, often covered by aerial mycelium together with conidial structures, solitary or aggregated, non-ostiolate, honey to leaden black, glabrous, globose or subglobose, 50–115 µm diam. *Ascomatal wall* brown, composed of *textura epidermoidea* in surface view. *Asci* obovoid or pyriform, 24–43 × 20–28 µm, with short stalks being 2–9 µm long, containing eight irregularly-arranged ascospores, evanescent. *Ascospores* dark brown when mature, fusiform or ellipsoidal with attenuated ends, often inequilateral, (16.5–)18.5–21(–22) × (7.5–)8–9(–9.5) µm, with two apical germ pores. *Conidiophores* hypha-like, usually reduced to conidiogenous cells. *Conidiogenous cells* produced terminally on the short branches of hyphae or arising laterally from hyphae, hyaline, ampulliform, fusiform or obovoid due to swollen conidiogenous part, usually synchronously polyblastic, 4–10.5 × 1.5–4 µm. *Conidia* produced on the pedicels arising from the conidiogenous cells, hyaline, smooth, subglobose, ellipsoidal, obovoid, with a narrow and truncate base, (5–)5.5–7.5(–9) × (4.5–)5.5 –7.5(–8.5) µm.

Culture characteristics: On OA with an entire edge, 41–47 mm diam in 7 d at 25 °C, obverse pale luteous or honey due to the formation of conidia on aerial mycelium together with liquid drops of coloured exudates on the surface of the mycelium; reverse luteous. On CMA similar to those on OA, 39–45 mm diam in 7 d at 25 °C. On MEA with a crenate or lobate edge, 32–38 mm diam in 7 d at 25 °C, texture floccose, obverse olivaceous buff due to aerial mycelium, with orange liquid drops of coloured exudates near the central part; reverse sienna. On PCA with an entire or slightly crenate edge, 36–42 mm diam in 7 d at 25 °C, with sparse aerial mycelium, obverse olivaceous buff; reverse uncoloured.

Material examined: **Papua New Guinea**, New Britain, Rabaul, isolated from soil, 27 Dec. 1969, S. Udagawa (culture ex-type CBS 359.72 = NHL 22501).

Notes: *Corynascus novoguineensis* can easily be distinguished from the other species in the genus by the production of smooth-walled conidia that often synchronously arise from swollen and polyblastic conidiogenous cells. This species also produces large ascospores (18.5–21 × 8–9 µm), while the ascospores of other *Corynascus* species are usually less than 16 µm in length.

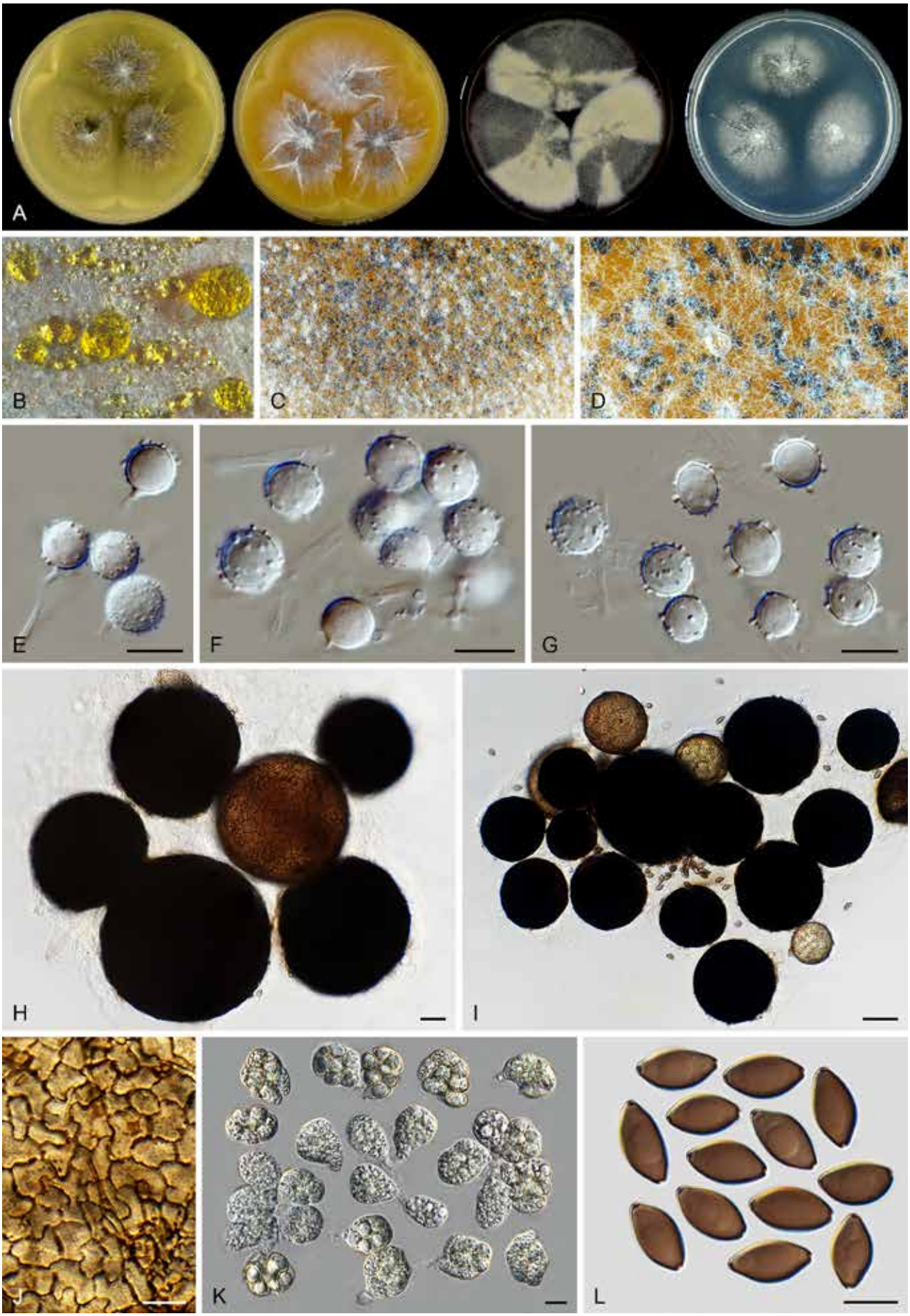

Fig. 25. *Corynascus fumimontanus* (CBS 137294, ex-type culture). **A.** Colonies from left to right on OA, CMA, MEA and PCA after 4 wk incubation. **B–D.** Part of the colony on OA, showing ascomata mixed with hyphae and conidia on OA, top view. **E–G.** Hyphae, conidiogenous cells and conidia. **H, I.** Ascomata mounted in lactic acid. **J.** Structure of ascomatal wall in surface view. **K.** Asci. **L.** Ascospores. Scale bars: E–G, J–L = 10 µm; H = 20 µm; I = 50 µm.

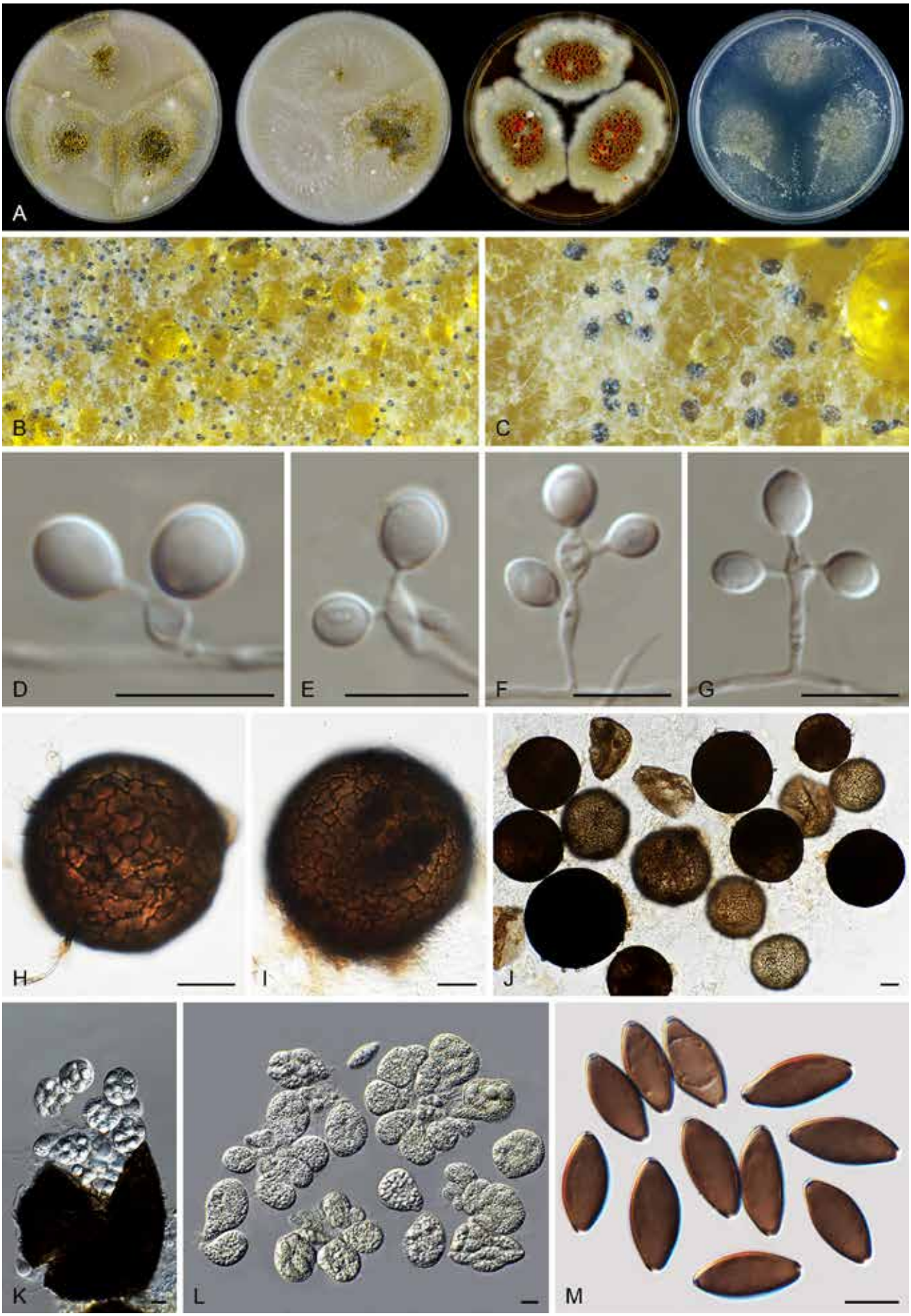

Fig. 26. *Corynascus novoguineensis* (CBS 359.72, ex-type culture). **A.** Colonies from left to right on OA, CMA, MEA and PCA after 4 wk incubation. **B, C.** Part of the colony on OA, showing ascomata mixed with hyphae and conidia on OA, top view. **D–G.** Hyphae, conidiogenous cells and conidia. **H–J.** Ascomata mounted in lactic acid. **K.** Asci coming from a broken ascoma. **L.** Asci. **M.** Ascospores. Scale bars: D–G, K–M = 10 µm; H–J = 20 µm.

Corynascus sepedonium (C.W. Emmons) Arx, Proc. Kon. Ned. Akad. Wetensch., C 76: 292. 1973. Fig. 27.
Basionym: *Thielavia sepedonium* C.W. Emmons, Bull. Torrey Bot. Club 59: 417. 1932.
Synonyms: *Myceliophthora sepedonium* (C.W. Emmons) van den Brink & Samson, Fungal Diversity 52: 206. 2011 [2012], *nom. inval.*, Art. 41.5.
Thielavia lutescens Kamyschko, Novosti Sist. Nizsh. Rast. 2: 116. 1965.
Corynascus similis Stchigel *et al.*, Mycol. Res. 104: 881. 2000.
Myceliophthora similis (Stchigel *et al.*) van den Brink & Samson, Fungal Diversity 52: 206. 2011 [2012], *nom. inval.*, Art. 41.5.

Micromorphology: *Ascomata* superficial, often covered by aerial mycelium together with conidial structures, solitary or aggregated, non-ostiolate, leaden black in reflected light, glabrous, globose or subglobose, 25–45 µm diam. *Ascomatal wall* brown, composed of angular or irregular cells in surface view. *Asci* clavate or pyriform, 24–28 × 13–18 µm, with indistinct stalks, containing eight irregularly-arranged ascospores, quickly evanescent. *Ascospores* olivaceous brown when mature, ellipsoidal with attenuated ends to fusiform, sometimes slightly inequilateral, (11.5–)12–14.5(–16) × (7–)7.5–9(–10.5) µm, with two apical germ pores. *Conidiophores* reduced. *Conidiogenous cells* arising laterally from hyphae, hyaline, ampulliform or denticle-like, monoblastic, 1.5–6 × 1–3 µm. *Conidia* hyaline, verrucose, globose or subglobose, (6–)7–9(10.5) µm diam, occasionally ovoid, 9.5–13 × 8–8.5 µm.

Culture characteristics: On OA with an entire edge, 31–37 mm diam in 7 d at 25 °C, obverse buff or olivaceous buff due to aerial mycelium and conidia; reverse cinnamon. On CMA with an entire edge, 28–34 mm diam in 7 d at 25 °C, obverse grey white with cinnamon margins; reverse buff to honey. On MEA with an entire or slightly crenate edge, 28–34 mm diam in 7 d at 25 °C, texture floccose, obverse buff with white margins; reverse apricot. On PCA with an entire edge, 27–33 mm diam in 7 d at 25 °C, with sparse aerial mycelium, obverse pale smoke grey; reverse uncoloured.

Material examined: **India**, Allahabad, isolated from soil, 1968, B.S. Mehrotra (CBS 111.69 = IMI 136625, ex-type of *Coryn. sepedonium* var. *minor*); Ajmed, isolated from soil, 2 Nov. 1995, J. Guarro (CBS 101936 = FMR 5693, ex-type of *Coryn. similis*). **Uzbekistan**, isolated from soil, date unknown, O.P. Kamyschko (CBS 632.67 = VKM F-1142, ex-type of *Thielavia lutescens*).

Notes: CBS 340.33 was isolated by the original author C.W. Emmons and was considered as ex-type of *Coryn. sepedonium* (originally *Thielavia sepedonium*) by von Arx (1975a). Von Arx (1975a) treated *Coryn. sepedonium* var. *minor* and *Thielavia lutescens* as synonyms of *Coryn. sepedonium*. In his study, von Arx also reported that *Coryn. sepedonium* had a large variation in the size and shape of ascospores and conidia. His treatment was supported by multigene phylogenetic analysis (van den Brink *et al.* 2012). CBS 111.69, the ex-type of *Coryn. sepedonium* var. *minor*, was often incorrectly assumed to be the ex-type of *Coryn. sepedonium* (van den Brink *et al.* 2012, Marin-Felix *et al.* 2015). According to von Arx (1975a), the type strain of *Coryn. sepedonium* (CBS 340.33) produced similar sized conidia (8–12 µm), but larger ascospores than those of CBS 111.69 [15–19 × 8–10 µm *vs* (11.5–)12–14.5(–16) × (7–)7.5–9(–10.5) µm]. Our measurements of ascomata of CBS 111.69 (25–45 µm diam) were also much smaller than those in the previous description given by von Arx (50–120 µm diam, 1975a) or by Malloch & Cain (20–150 µm diam, 1973). Its asci are evanescent and difficult to observe and measure. Our phylogenetic analysis (Fig. 7A) confirmed that the ex-type culture of *Coryn. similis* clustered with the strains of *Coryn. sepedonium*, and we therefore follow Marín-Felix *et al.* (2015) and treat *Coryn. similis* as a synonym of *Coryn. sepedonium*. In the original description, however, *Coryn. similis* was described to produce ascospores with two subapical or oblique germ pores. We did not see such ascospores and cannot confirm this observation.

Corynascus sexualis Stchigel *et al.*, Mycol. Res. 104: 880. 2000. Fig. 28.
Synonym: *Myceliophthora sexualis* (Stchigel *et al.*) van den Brink & Samson, Fungal Diversity 52: 206. 2011 [2012], *nom. inval.*, Art. 41.5.

Micromorphology: *Ascomata* superficial to immersed in the medium, often covered by aerial mycelium, solitary or aggregated, non-ostiolate, fawn to olivaceous in reflected light, glabrous, globose or subglobose, 60–115 µm diam. *Ascomatal wall* brown, composed of *textura epidermoidea* in surface view. *Asci* obovoid or pyriform, 18–25 × 14–18 µm, with short stalks being 3–7 µm long, containing eight irregularly-arranged ascospores, evanescent. *Ascospores* olivaceous brown when mature, limoniform or broad fusiform, umbonate at both ends, sometimes slightly inequilateral, 11.5–13.5(–14.5) × 8–9 µm, with two apical germ pores. *Conidiophores* reduced. *Conidiogenous cells* reduced to a hyphal cell, inconspicuous, monoblastic. *Conidia* inconspicuous, arising laterally or terminally from hyphae, subhyaline, thin-walled, smooth, subglobose, ellipsoidal, obovoid, 6–11 × 5–10.5 µm.

Culture characteristics: On OA with an entire or slightly lobate edge, 24–30 mm diam in 7 d at 25 °C, obverse olivaceous buff or smoke grey due to ascomata mixed with aerial mycelium, pale luteous to luteous around the colonies due to coloured exudates diffusing into the mycelium; reverse pale luteous to sienna. On CMA with an entire edge, 26–32 mm diam in 7 d at 25 °C, less producing ascomata, obverse buff to rosy buff, without coloured exudates; reverse pale luteous to luteous. On MEA with a slightly lobate edge, 16–22 mm diam in 7 d at 25 °C, texture floccose, obverse white due to aerial mycelium; reverse luteous to orange. On PCA translucent, with an entire or slightly crenate edge, 22–28 mm diam in 7 d at 25 °C, without or with sparse aerial mycelium; reverse uncoloured.

Material examined: **India**, Jaipur, isolated from soil, Oct. 1995, J. Guarro (culture ex-type CBS 827.96 = FMR 5691 = IMI 378520).

Notes: The conidiophores and conidiogenous cells of *Coryn. sexualis* are extremely reduced, and its conidia are sparsely produced. This might explain why the original description of this species lacks the description of an asexual morph. Phylogenetic analysis showed that *Coryn. sexualis* is closely related to *Coryn. citrinus* and *Coryn. fumimontanus* (Fig. 7A). These species can be identified using *tub2* and *rpb2* sequencing; the ITS sequence fails to distinguish the three species (Supplementary Figs S1–S3). *Corynascus sexualis* is distinct in sparsely producing conidia, and can also be distinguished from *Coryn. citrinus* by its larger ascospores (11.5–13.5 × 8–9 µm *vs* 9–12 × 6–8 µm) and from *Coryn. fumimontanus* by shorter and broader ascospores (11.5–13.5 × 8–9 µm *vs* 13–15.5 × 7.5–8.5 µm).

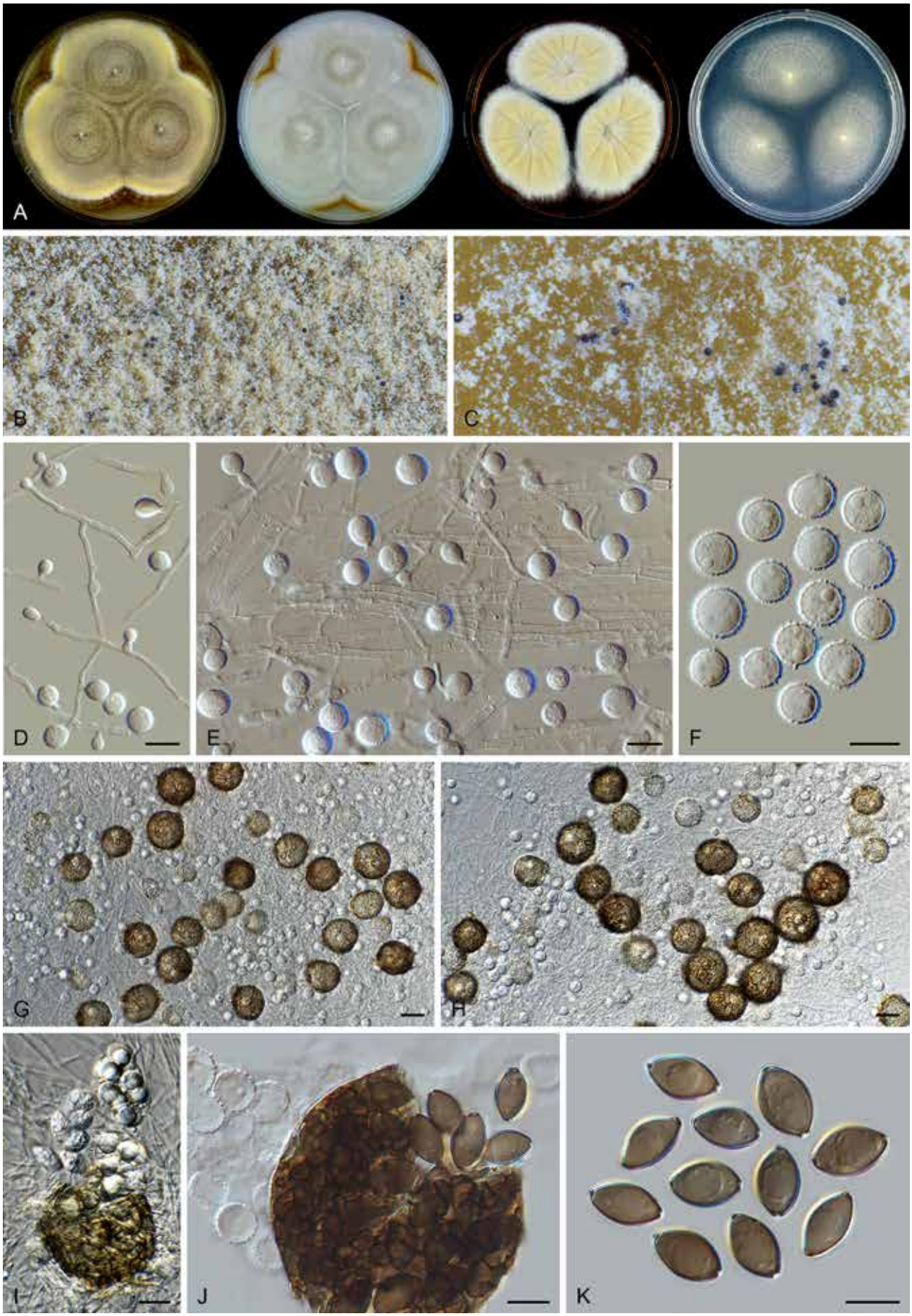

Fig. 27. *Corynascus sepedonium* (CBS 111.69, ex-type culture). **A.** Colonies from left to right on OA, CMA, MEA and PCA after 2 wk incubation. **B, C.** Part of the colony on OA, showing ascomata mixed with hyphae and conidia on OA, top view. **D, E.** Hyphae, conidiogenous cells and conidia. **F.** Conidia. **G, H.** Mature ascomata mixed with hyphae and conidia. **I.** Asci coming from a broken ascoma. **J.** Mature ascospores and a broken ascoma. **K.** Ascospores. Scale bars: D–F, I–K = 10 µm; G, H = 20 µm.

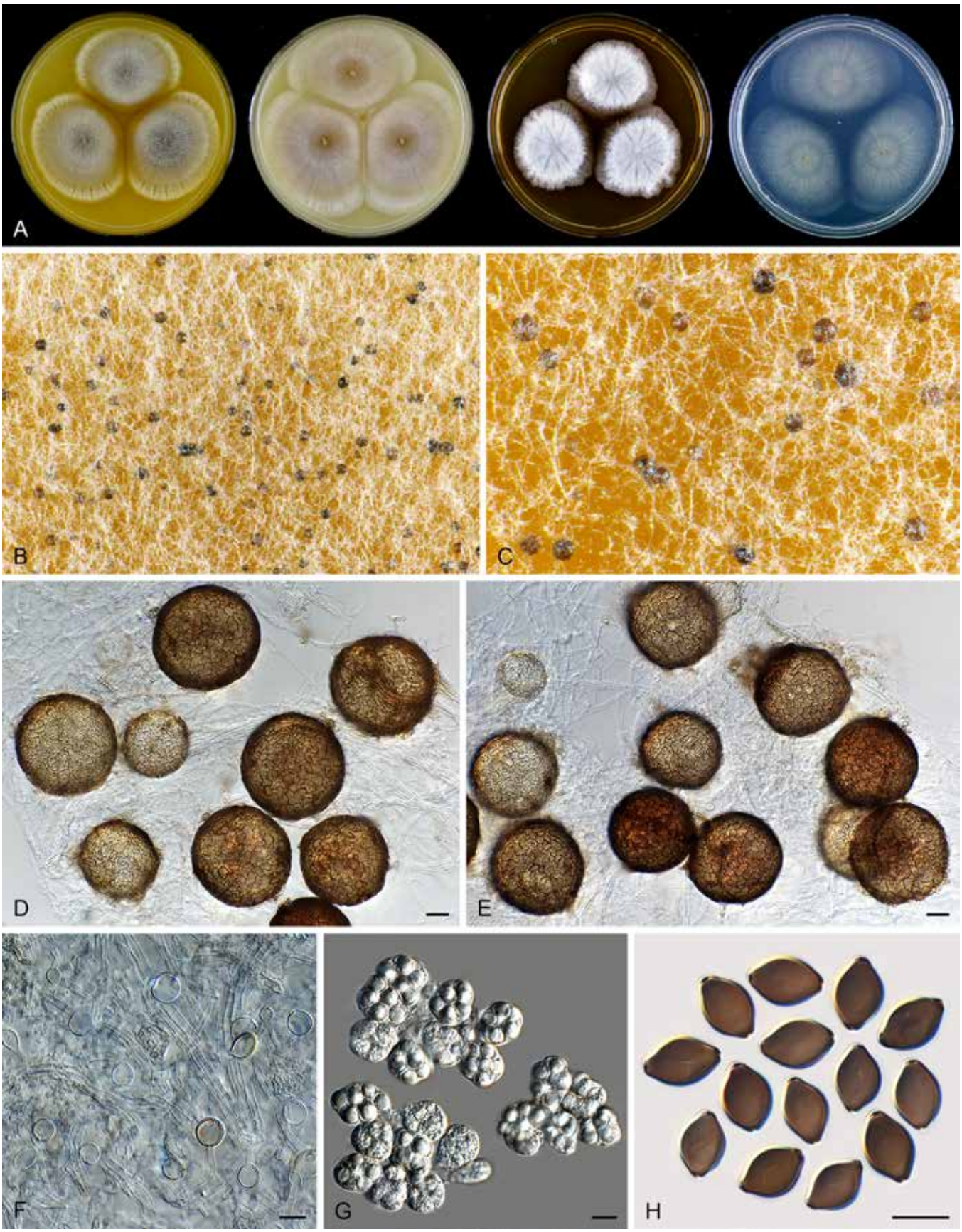

Fig. 28. *Corynascus sexualis* (CBS 827.96, ex-type culture). **A.** Colonies from left to right on OA, CMA, MEA and PCA after 3 wk incubation. **B, C.** Part of the colony on OA, showing ascomata mixed with hyphae and conidia on OA, top view. **D, E.** Ascomata, hyphae and conidia mounted in lactic acid. **F.** Hyphae and conidia. **G.** Asci. **H.** Ascospores. Scale bars: D, E = 20 µm; F–H = 10 µm.

Corynascus verrucosus Stchigel *et al.*, Mycol. Res. 104: 884. 2000. Fig. 29.
Synonym: *Myceliophthora verrucosa* (Stchigel *et al.*) van den Brink & Samson, Fungal Diversity 52: 206. 2011 [2012], nom. inval., Art. 41.5.

Micromorphology: *Ascomata* superficial, often covered by aerial mycelium together with conidial structures, solitary or aggregated, non-ostiolate, leaden black in reflected light, glabrous, globose or subglobose, 50–85 µm diam. *Ascomatal wall* brown, composed of *textura epidermoidea* in surface view. *Asci* obovoid or pyriform, 20–28 × 14–22 µm, with short or indistinct stalks being 0–5 µm long, containing eight irregularly-arranged ascospores, evanescent. *Ascospores* olivaceous brown when mature, ellipsoidal with attenuated ends or fusiform, often inequilateral, (9–)11–13(–13.5) × (6–)7–8 µm, with two apical or slightly subapical germ pores. *Conidiophores* hypha-like or reduced to conidiogenous cells. *Conidiogenous cells* arising laterally from hyphae, hyaline, often sympodially polyblastic or proliferating, swollen to ampulliform, doliiform or clavate, 5–15 × 1.5–4 µm. *Conidia* produced on pedicels arising from the conidiogenous cells, hyaline, verrucose, globose or subglobose, (6–)7.5–9.5(–11) µm diam.

Culture characteristics: On OA with an entire edge, 37–43 mm diam in 7 d at 25 °C, obverse olivaceous buff due to the formation of conidia on aerial mycelium, often partly with white floccose aerial mycelium; reverse ochreous. On CMA similar to those on OA, 37–43 mm diam in 7 d at 25 °C, obverse buff. On MEA with an entire or slightly crenate edge, 27–33 mm diam in 7 d at 25 °C, texture floccose, obverse white to buff; reverse apricot to chestnut. On PCA translucent, with an entire edge, 23–29 mm diam in 7 d at 25 °C, without aerial mycelium, obverse buff; reverse buff.

Material examined: **Argentina**, Quilmes, Buenos Aires Province, isolated from soil, Aug. 1996, A.M. Stchigel (culture ex-type CBS 602.97 = FMR 5904 = IMI 378522). **USA**, Tennessee, Great Smokey Mountain National Park, isolated from forest soil, 10 Aug. 2008, A. Miller, M. Calduch & A. Stchigel (CBS 135878 = FMR 12783).

Notes: Phylogenetic analysis shows that *Coryn. verrucosus* is sister to *Coryn. sepedonium* (Fig. 7A). Partial *tub2* and *rpb2* sequencing can be used for identification but ITS fails to distinguish the two species (Supplementary Figs S1–S3). This species can be distinguished from *Coryn. sepedonium* by larger, better developed conidiogenous cells (2–15 × 1.5–4 µm *vs* 1.5–6 × 1–3 µm) which are polyblastic or proliferating and often swollen. This species was originally described to produce ascospores with a larger length range (11–18 µm, Stchigel *et al.* 2000) than what we measured (11–13 µm).

Humicola Traaen, Nytt Mag. Naturvidensk. 52: 31. 1914.

Micromorphology (*emended description*): *Asexual morphs* producing aleurioconidia-like conidia, humicola-like, an acremonium-like morph co-occurring in several species. *Humicola-like morph*: *conidiogenous cells* reduced to a hyphal cell, intercalary or lateral, monoblastic; conidiophores absent. *Aleurioconidia-like conidia* arising laterally, intercalary or terminally, 1-celled, solitary or rarely in chains of a few spores, globose, subglobose, oblate, occasionally obovoid, pyriform or irregular-shaped, light olivaceous, olivaceous, brown or dark brown, smooth, in persisted state on hyphae or rhexolytic when seceding, germ pores rare. *Acremonium-like morph*: *Phialides* lateral or occasionally terminal, hyaline. *Conidia* in basipetal chains, hyaline, aseptate, smooth, obovoid, usually with a truncated base and a rounded apex. *Ascomata* absent or present, when present superficial, or covered by aerial hyphae, ostiolate. *Ascomatal wall* brown, composed of *textura angularis* in surface view. *Terminal hairs* seta-like, flexuous, undulate, or arcuate with apices incurved. *Asci* clavate, with eight biseriate or irregularly-arranged ascospores, evanescent before ascospores become mature. *Ascospores* limoniform to quadrangular, bilaterally flattened, with an apical germ pore. Containing asexual species and species with both asexual and sexual morphs.

Type species: *Humicola fuscoatra* Traaen

Notes: In our phylogenetic analyses, we noticed that our previously defined *Humicola* (MP-BS < 50 %, ML-BS = 78 %; PP = 1.0, Wang *et al.* 2019a) seemed unstable. With the addition of *rpb2* sequences of CBS 113678 and CBS 538.74 to our analysis, representing *Aporothielavia*, *Humicola* splits into two clades, with one of them clustering with *Aporothielavia* (ML-BS < 70 %; PP = 1.0, Supplementary Fig. S3). This result suggested that not all the species in the *Humicola* clade share a common recent ancestor. Molecular dating analysis reinforced our suspicion that a small clade splits from the other *Humicola* species and is here named *Aporothielavia* (Fig. 8A). Molecular dating analysis was based on a dataset in which ITS1, ITS2 and introns in protein coding genes were excluded. The topology of the resulting tree is expected to be more stable than the normal phylogenetic tree. Therefore, we segregate *Humicola sensu* Wang *et al.* (2019a) into two genera. Our molecular dating estimation showed that the two "*Humicola*" clades diverged from each other as early as about 60 Mya, supporting their segregation. *Humicola sensu stricto* is modified as shown above, and a new genus (*Pseudohumicola*) is proposed for the other clade (see below for more details). Morphologically, both genera produce similar asexual morphs, but the ascomata in *Pseudohumicola* (if produced) usually have coiled terminal hairs, while such hairs are rare in sexual *Humicola s. str*. species.

Humicola hirsuta X.Wei Wang, P.J. Han & F.Y. Bai, ***sp. nov.*** MycoBank MB 840128. Fig. 30.

Etymology: The name refers to its terminal ascomatal hairs, which are relatively long and erect.

Micromorphology: *Ascomata* superficial, ostiolate, leaden black with honey hairs in reflected light, elongated obpyriform, obclavate or ampulliform below, apically attenuated to an elongated conical or short cylindrical neck, 190–290 µm high, 70–130 µm diam at the widest part. *Ascomatal wall* brown, composed of angular and irregular cells, or elongate to cylindrical cells in the neck part in surface view. *Terminal hairs* around ostiole relatively short, seta-like and delicate, smooth, tapering and fading to hyaline towards the tips, 1.5–4 µm diam near the base, usually surrounded by numerous long, thick and seta-like hairs which are 3.5–5.5 µm diam near the base, closely septate. *Lateral hairs* similar to thick terminal ones, tapering and fading towards the tips. *Asci* clavate, spore-bearing part 23–31 × 9–12 µm, with stalks about 12–25 µm long, containing eight biseriate or irregularly-arranged ascospores, evanescent. *Ascospores* olivaceous or olivaceous brown when mature, limoniform, biapiculate or slightly umbonate at both ends, bilaterally flattened, (7–)7.5–9(–10.5) × (5.5–)6–7.5(–8) × 4.5–5.5 µm, with an apical germ pore. *Conidia* usually subglobose, arising laterally or terminally from the hyaline aerial hyphae, solitary,

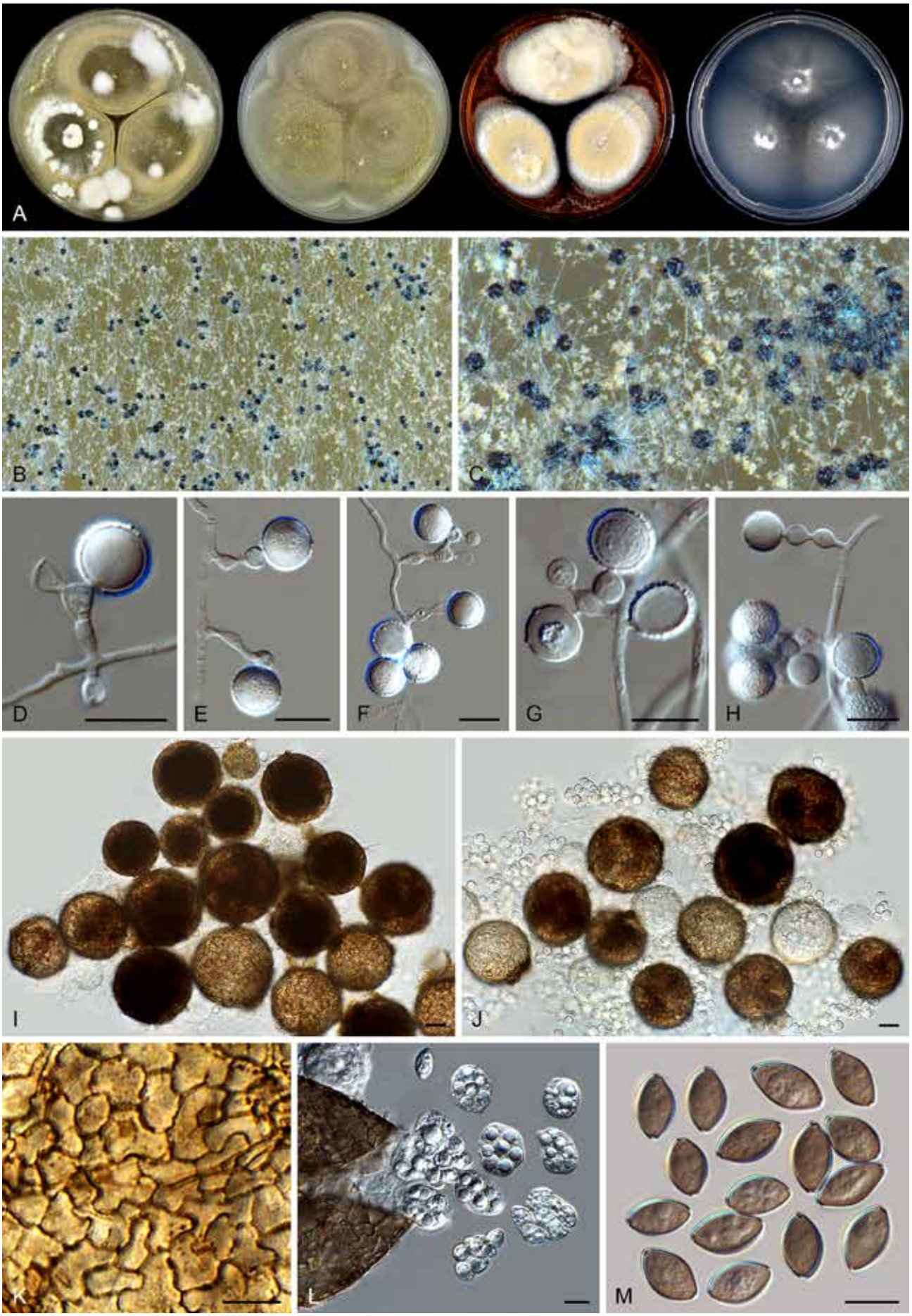

Fig. 29. *Corynascus verrucosus* (CBS 602.97, ex-type culture). **A.** Colonies from left to right on OA, CMA, MEA and PCA after 4 wk incubation. **B, C.** Part of the colony on OA, showing ascomata mixed with hyphae and conidia on OA, top view. **D–H.** Hyphae, conidiogenous cells and conidia. **I, J.** Ascomata and conidia mounted in lactic acid. **K.** Structure of ascomatal wall in surface view. **L.** Asci coming from a broken ascoma. **M.** Ascospores. Scale bars: D–H, K–M = 10 µm; I, J = 20 µm.

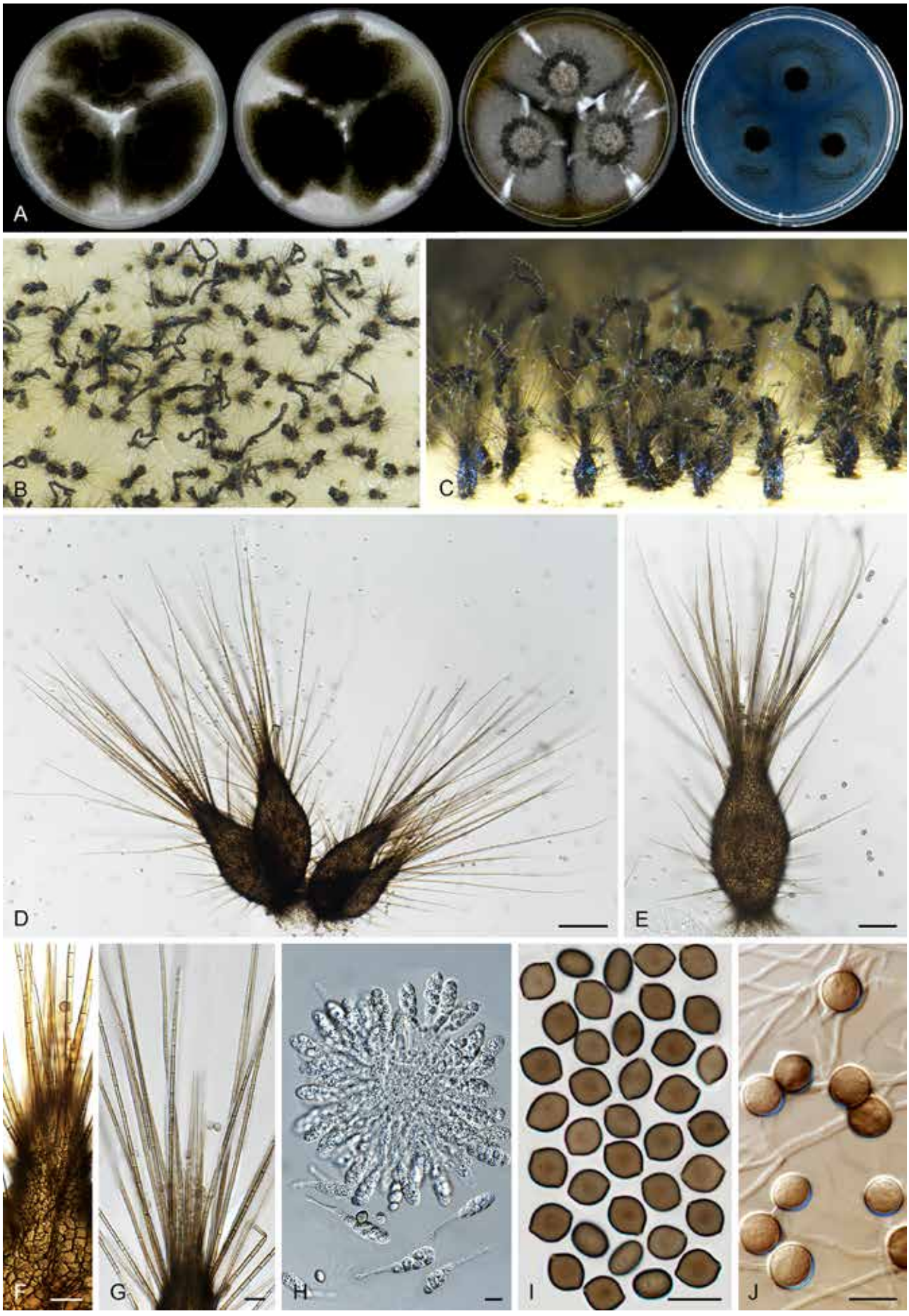

Fig. 30. *Humicola hirsuta* (CGMCC 3.20444, ex-type culture). **A.** Colonies from left to right on OA, CMA, MEA and PCA after 3 wk incubation. **B.** Part of the colony showing mature ascomata on OA, top view. **C.** Mature ascomata on OA, side view. **D, E.** Ascomata mounted in lactic acid. **F.** Structure of ascomatal wall in surface view. **G.** Terminal ascomatal hair. **H.** Asci. **I.** Ascospores. **J.** Hyphae and conidia. Scale bars: D = 100 µm; E = 50 µm; F, G = 20 µm; H–J = 10 µm.

sometimes two cells in chains or several in clusters, cinnamon to fawn, 6–10.5 µm diam.

Culture characteristics: Colonies on OA 33–39 mm diam after 7 d at 25 °C; edge entire or slightly crenate; obverse showing leaden black mature ascomata mixed with young ascomata covered by pale luteous to amber ascomata hairs, and sparse white aerial hypha; soluble pigment absent; reverse uncoloured. Colonies on CMA similar to those on OA, 31–37 mm diam after 7 d at 25 °C. Colonies on MEA 29–35 mm diam after 7 d at 25 °C; edge entire, obverse showing a thin layer of white aerial mycelium mixed with sparse ascomata; reverse saffron to ochreous. Colonies on PCA 27–33 mm diam after 7 d at 25 °C, edge entire; translucent; aerial hyphae absent; soluble pigment absent; reverse uncoloured.

Material examined: **China**, Qinling Mountains in Shaanxi Province, isolated from soil, Jun. 2004, X.W. Wang (**holotype** HMAS 350292, **isotype** CBS H-23638, culture ex-type CGMCC 3.20444 = CBS 144492 = WXW 9028).

Notes: *Humicola hirsuta* is phylogenetically most closely related to *H. mutabilis* (Fig. 7B) and this relationship is also concordant among the single gene phylograms (Supplementary Figs S1–S3). *Humicola hirsuta* produces uniformly-shaped ascomata and long, honey (in reflected light) terminal hairs around the beak, while *H. mutabilis* produces ascomata that are variable in shape, with buff to amber hairs in reflected light. *Humicola hirsuta* is morphologically similar to *H. ampulliella*, but differs in ascus and ascospore shape. *Humicola ampulliella* produces narrowly clavate to cylindrical asci and prominently umbonate ascospores, while clavate asci and biapiculate or slightly umbonate ascospores are present in *H. hirsuta*.

Melanocarpus Arx, Stud. Mycol. 8: 17. 1975.

Micromorphology (*fide* von Arx *et al.* 1988, Guarro *et al.* 1996): *Colonies* expanding rapidly. *Ascomata* superficial, non-ostiolate, spherical, smooth, black. *Ascomatal wall* dark brown, composed of *textura angularis* in surface view. *Asci* fasciculate, obovate or clavate, stalked, containing eight ascospores, evanescent. *Ascospores* bilaterally flattened, globose to broadly ovate in face view and elliptical in side view, dark brown, with an apical germ pore. *Conidia* usually catenate, cylindrical, fusiform or clavate with a truncate base, hyaline. Thermophilic. Containing species with both asexual and sexual morphs.

Type species: *Melanocarpus albomyces* (Cooney & R. Emers.) Arx

Notes: *Melanocarpus* was first introduced for *Myriococcum albomyces* Cooney & R. Emers., a thermophilic species producing non-ostiolate ascomata with a pseudoparenchymatous wall, ovoid-oblate ascospores with an apical germ pore, and hyaline, cylindrical, fusiform or clavate, usually catenate conidia (von Arx 1975a). Later, four more species (*Mel. coprophilus*, *Mel. oblatus*, *Mel. tardus* and *Mel. thermophilus*) were described or transferred to the genus, all with similar ascomata and ascospores (Guarro *et al.* 1996, Wang *et al.* 2016b).

Our present analysis indicates that the morphologically defined *Melanocarpus* is polyphyletic. *Melanocarpus oblatus* is a synonym of *Achaetomium globosum* (Fig. 7C, Supplementary Figs S1–S3). In the phylogram based on the combined dataset, *Mel. tardus* and *Mel. thermophilus* cluster together as a sister clade to *Mel. albomyces* (Fig. 7D). A similar clustering is observed in the *rpb2* phylogram (Supplementary Fig. S3), but the *tub2* and ITS phylogenies place *Mel. albomyces* distantly from the two other species (Supplementary Figs S1, S2). These three species have different growth rates and temperature growth profiles (Fig. 39): *Mel. albomyces* grows fast and has a higher growth rate at 45 °C than at 37 °C (thermophilic), while *Mel. tardus* and *Mel. thermophilus* grow very slowly and show optimal growth at 37 °C (thermotolerant). Molecular dating analysis shows that *Mel. albomyces* diverged from the two other species quite early (about 59.97 Mya, Fig. 8B). Therefore, we restrict *Melanocarpus* to its thermophilic type species and at the same time, the new genus *Parvomelanocarpus* is proposed for *Mel. tardus* and *Mel. thermophilus* (see below for more details).

No material of *Mel. coprophilus* was included in our study. According to the original description (Guarro *et al.* 1996), this species is mesophilic and does not produce an asexual morph. It is therefore unlikely that this species belongs to *Melanocarpus*.

Myceliophthora Costantin, Compt. Rend. Hebd. Séances Acad. Sci. D 114: 849. 1892.

Micromorphology: *Conidiophores* absent. *Conidiogenous cells* reduced to a hyphal cell, or originating laterally or terminally from hyphae, swollen, subglobose, fusiform, clavate or ampulliform, monoblastic or synchronously polyblastic with one or more conidia developing from one conidiogenous cell. *Conidia* solitary or in short acropetal chains, single-celled, smooth, hyaline, ovoid or subglobose, apically rounded, often with a narrow and truncate base, rhexolytic when seceding. *Sexual morph* not observed. Thermotolerant.

Type species: *Myceliophthora lutea* Costantin

Notes: For many years, thermophilic species that produce single-celled blastoconidia with narrow bases attached directly to hyphae or conidiogenous cells were placed in *Myceliophthora* (van Oorschot 1977, Berka *et al.* 2011, van den Brink *et al.* 2012, Zhang *et al.* 2014a). The taxonomy of this genus has long been tumultuous.The type species, *Myceliophthora lutea* was first described as a pathogen in mushroom cultivation (Costantin 1892). Apinis (1962) described *Sporotrichum thermophilum*, a thermophilic species that produces a conidial morph similar to that of *My. lutea*. In the same year, Carmichael (1962) transferred *My. lutea* into his broad genus *Chrysosporium* as *Chry. luteum*. Von Arx (1973a) re-described *Sporotrichum* as a basidiomycete genus because clamp connections were observed on the septa of the hyphae of the type species, *Sporotrichum aureum*, and suggested moving *Chry. luteum* from *Chrysosporium* back to *Myceliophthora*. Other "sporotrichum-like" fungi were classified in *Chrysosporium*, which produce conidia with a broad base (being separated from the conidiogenous cell by a cross wall) and lack clamp connections, such as *Sp. thermophilum* (von Arx 1973a). Later, another thermophilic species, *Chrysosporium fergusii* was described (von Klopotek 1974). Van Oorschot (1977) formally reintroduced *Myceliophthora* for species producing blastoconidia with a narrow base and lacking intercalary arthroconidia. Three species mentioned above were accepted in *Myceliophthora*: the type species *My. lutea*, *My. thermophila* (= *Sporotrichum thermophilum*) and *My. fergusii* (= *Chrysosporium fergusii*). Marín-Felix *et al.* (2015) suggested to restrict *Myceliophthora* only to its type species *My. lutea* on the basis of their multigene phylogenetic analysis. Our phylogenetic analyses (Fig. 7A) confirmed the treatment of

Marín-Felix *et al.* (2015). *Myceliophthora lutea* grows faster at 37 °C than at 45 °C, indicating that it is thermotolerant rather than thermophilic. Our molecular dating analysis indicated that *Myceliophthora* diverged from its thermophilic relatives about 30 Mya, before the later time limit (about 27 Mya, Figs 8, 9) of the other accepted genera in the family.

Myceliophthora lutea Costantin, Compt. Rend. Hebd. Séances Acad. Sci., Sér. D 114: 850.1892. Fig. 31.
Synonyms: *Scopulariopsis lutea* (Costantin) Tubaki, Nagaoa 5: 29. 1955.
Chrysosporium luteum (Costantin) J.W. Carmich., Canad. J. Bot. 40: 1158. 1962.
Sporotrichum carthusioviride J.N. Rai & Mukerji, Mycopathol. Mycol. Appl. 18: 122. 1962.

Micromorphology: *Conidiophores* absent. *Conidiogenous cells* often reduced to a hyphal cell, or originating laterally or terminally from hyphae, swollen, subglobose, fusiform, clavate or ampulliform, synchronously polyblastic or monoblastic, 1–4 conidia developing from one conidiogenous cell, 3–5 × 2.5–3.5 µm. *Conidia* solitary or in short chains, single-celled, smooth, hyaline, ovoid or subglobose, rhexolytic when seceding, with a truncate base, (3.5–)4.5–5.5(–6) × (3–)3.5–4.5(–5) µm diam. *Sexual morph* unknown.

Culture characteristics: On OA with a crenate edge, 11–17 mm diam in 7 d at 25 °C, texture cottony, obverse olivaceous buff or hazel due to conidia mixed with aerial mycelium, isabelline around the colonies due to coloured exudates diffusing in to the medium; reverse olivaceous. On CMA similar to those on OA, obverse olivaceous buff or greenish olivaceous. On MEA with a crenate edge, 11–17 mm diam in 7d at 25 °C, texture cottony, obverse olivaceous buff; reverse umber. On PCA with an entire edge, 12–18 mm diam in 7 d at 25 °C, obverse olivaceous buff due to the formation of conidia on aerial mycelium, without coloured exudates; reverse olivaceous buff.

Material examined: **India**, Uttar Pradesh, Lucknow, isolated from usar soil, date unknown, Rai & Mukerji (CBS 379.76, ex-type culture of *Sporotrichum carthusioviride*). **UK**, Newmarket, isolated from hay, 1974, M.T. Archer (culture ex-neotype CBS 145.77 = IMI 182034).

Notes: *Myceliophthora lutea* has been isolated from mushroom beds, soil, hay, *Hordeum vulgare*, air in pig sty, and dust in a stable (van Oorschot 1977). This species produces a similar asexual morph as *Thermothelomyces* species, but can be distinguished by its restricted growth on the agar media (Fig. 31A) and by its thermotolerant rather than thermophilic nature. Because a type specimen was not designated by the original author with no illustration in the original publication, van Oorschot (1977) designated CBS 145.77 as neotype for this species.

Ovatospora X.Wei Wang *et al.*, Stud. Mycol. 84: 207. 2016.

Micromorphology and illustrations: See Wang *et al.* (2016b; p. 207, 214–216). Containing species with only the sexual morph.

Type species: *Ovatospora brasiliensis* (Batista & Pontual) X.Wei Wang *et al.*

Notes: The genus *Ovatospora* is mainly characterised by its ascospore shape and the arrangement of these ascospores in the asci (Wang *et al.* 2016b). The ascospores of *Ovatospora* are broadly ovate, bilaterally flattened, rounded at one end, with an apical or subapical germ pore at another attenuate or apiculate end. The eight ascospores are usually uniseriate in cylindrical asci, in a few species biseriate or irregularly-arranged in clavate asci. Species in the genus produce ostiolate ascomata with walls of *textura angularis* in surface view, and usually covered by coiled terminal hairs, sometimes with coiled branches, which were originally placed in *Chaetomium*. Two more chaetomium-like species proved to be members of this genus based on our phylogenetic analysis (Fig. 7D). Morphologically, each taxon fits the definition of *Ovatospora* (Udagawa & Muroi 1981, Wang *et al.* 2016b, Zhang *et al.* 2017).

Ovatospora amygdalispora (Udagawa & T. Muroi) X.Wei Wang & Houbraken, ***comb. nov.*** MycoBank MB 840155.
Basionym: *Chaetomium amygdalisporum* Udagawa & T. Muroi, Trans. Mycol. Soc. Japan 22: 13. 1981.

Notes: This species is combined in *Ovatospora* based on our phylogenetic analysis of the ex-type culture (Fig. 7D). It is closely related to *O. senegalensis* (Fig. 7D), but the latter produces smaller ascospores with a subapical or oblique germ pore (9–11 × 7–8 × 6–7 µm *vs* 13–18 × 10–14 × 9–12 µm). Apparently, *O. amygdalispora* is the species with the largest ascospores in the genus. Von Arx *et al.* (1986) treated this species as a synonym of *Ch. uniapiculatum*, but there is no type material of the latter species available to confirm this treatment using DNA sequence data.

Ovatospora angularis (Yu Zhang & L. Cai) X.Wei Wang & Houbraken, ***comb. nov.*** MycoBank MB 840156.
Basionym: *Chaetomium angulare* Yu Zhang & L. Cai, Fungal Biol. 121: 28. 2016.

Notes: *Ovatospora angularis* produces broadly ovate and bilaterally flattened ascospores with an apical germ pore, uniseriate in cylindrical asci (Zhang *et al.* 2017), morphologically fitting the definition of *Ovatospora*. Species previously recognised in *Ovatospora* produce coiled terminal hairs covering their ostiolate ascomata. *Ovatospora angularis* is the only known *Ovatospora* species producing flexuous or slightly undulate ascomatal hairs with no differentiation between terminal and lateral hairs. It is phylogenetically closely related to *O. unipora* (Fig. 7D), but the latter produces clavate asci and larger ascospores (9–11 × 8–10 × 5–7 µm *vs* 6.5–8.5 × 5.5–7.5 × 5–6 µm) in addition to their difference in ascomatal hairs.

Parachaetomium Mehrabi *et al.*, Mycol. Prog. 19: 1422. 2020.

Micromorphology (*emended description*): *Ascomata* superficial, sometimes immersed in the medium, ostiolate, non-ostiolate in one species (*Parach. inaequale*), globose, subglobose to ovate. *Ascomatal wall* brown, composed of irregular or angular cells. *Ascomatal hairs* highly diverse, some verrucose, undulate to loosely coiled, or irregularly coiled, erect or flexuous in the lower part, with lateral hairs flexuous; or finger-like (short) to hypha-like, unbranched, straight or flexuous, finely verrucose, covering the whole ascoma or without differentiation between terminal and lateral ones; sometimes with two distinct types of hairs (called type I and type II): type I numerous, shorter and thinner, often arcuate, apically circinate, undulate or irregularly coiled, verrucose, brown, tapering and fading towards the tips; type II only a few, longer and thicker, undulate or loosely coiled, verrucose, brown, tapering towards the tips, sometimes recurved or circinate at the apex. *Asci* fasciculate, fusiform, clavate or pyriform, stalked, containing eight irregularly-

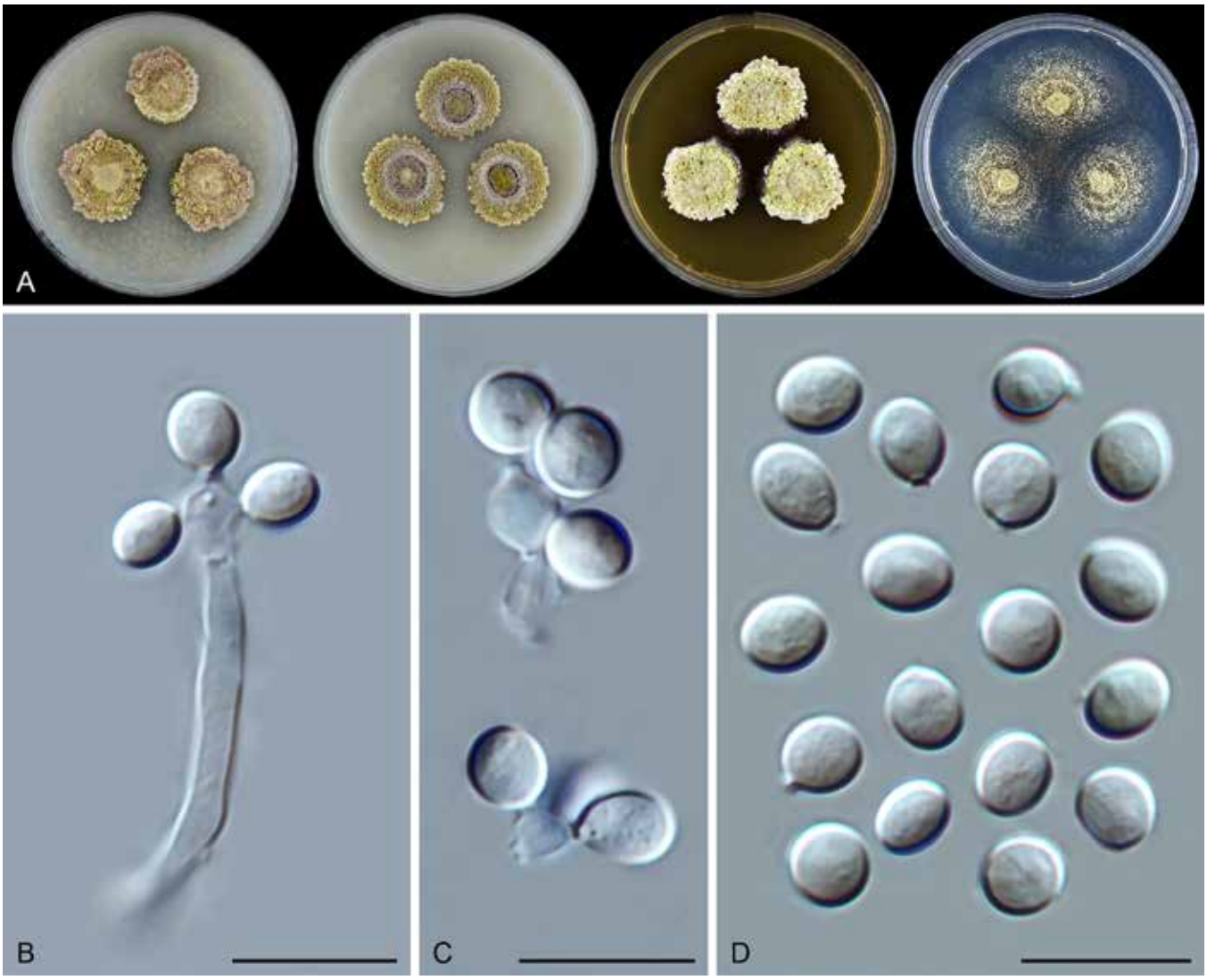

Fig. 31. *Myceliophthora lutea* (CBS 145.77, ex-neotype culture). **A.** Colonies from left to right on OA, CMA, MEA and PCA after 3 wk incubation. **B, C.** Conidiogenous cells and conidia. **D.** Conidia. Scale bars = 10 µm.

arranged ascospores, evanescent. *Ascospores* olivaceous or olivaceous brown when mature, elongated ellipsoidal or fusiform, with an apical, subapical or oblique germ pore, or with two apical germ pores, each at one end. *Asexual morph* not observed.

Type species: *Parachaetomium perlucidum* (Sergejeva) X.Wei Wang & Houbraken

Notes: *Parachaetomium* was introduced to accommodate three chaetomium-like species with *Parach. iranianum* as the type species (Mehrabi *et al.* 2020). Our phylogenetic analysis revealed that *Parach. iranianum* resides in a clade along with the older species *Ch. perlucidum*, here combined in *Parachaetomium* as *Parach. perlucidum* (Fig. 7A, Supplementary Figs S1–S3). The species resemble each other morphologically (von Arx *et al.* 1986, Mehrabi *et al.* 2020) and we therefore consider *Parach. iranianum* a synonym of *Parach. perlucidum*. Nine more species are transferred to this genus, resulting in a total of eleven accepted species (Fig. 7A). All species only produce a sexual morph. A high morphological diversity is present (for more details, see below). Ten species produce ostiolate ascomata and were previously classified in *Chaetomium*. *Parachaetomium inaequale* produces non-ostiolate ascomata and was previously classified in *Corynascella*.

Parachaetomium biporatum (Cano & Guarro) X.Wei Wang & Houbraken, ***comb. nov.*** MycoBank MB 830926. Fig. 32.
Basionym: *Chaetomium biporatum* Cano & Guarro, Nova Hedwigia 44: 543. 1987.

Micromorphology: *Ascomata* superficial, solitary, usually covered by white aerial mycelium, leaden black due to masses of ascospores, with smoke grey ascomatal hairs in reflected light, subglobose, ostiolate, 95–165 µm high, 95–155 µm diam. *Ascomatal wall* brown, composed of *textura epidermoidea* in surface view. *Terminal hairs* brown, septate, verrucose, irregularly undulate to irregularly coiled, often with undulate to irregularly coiled branches, erect or flexuous at lower part, 1.5–3 µm diam near the base. *Lateral hairs* flexuous. *Asci* fusiform, spore-bearing part 34–51 × 16–24 µm, with stalks being 10–36.5 µm long, containing eight irregularly-arranged ascospores, evanescent. *Ascospores* olivaceous brown when mature, elongated ovoid or fusiform, often inequilateral, (13.5–)15.5–18(–19.5) × (7.5–)8–9(–10) µm, with two apical germ pores. *Asexual morph* unknown.

Culture characteristics: On OA with an entire edge, 34–40 mm diam in 7 d at 25 °C, texture floccose, obverse white due to aerial mycelium; reverse buff. On CMA similar to those on OA, 31–37 mm diam in 7

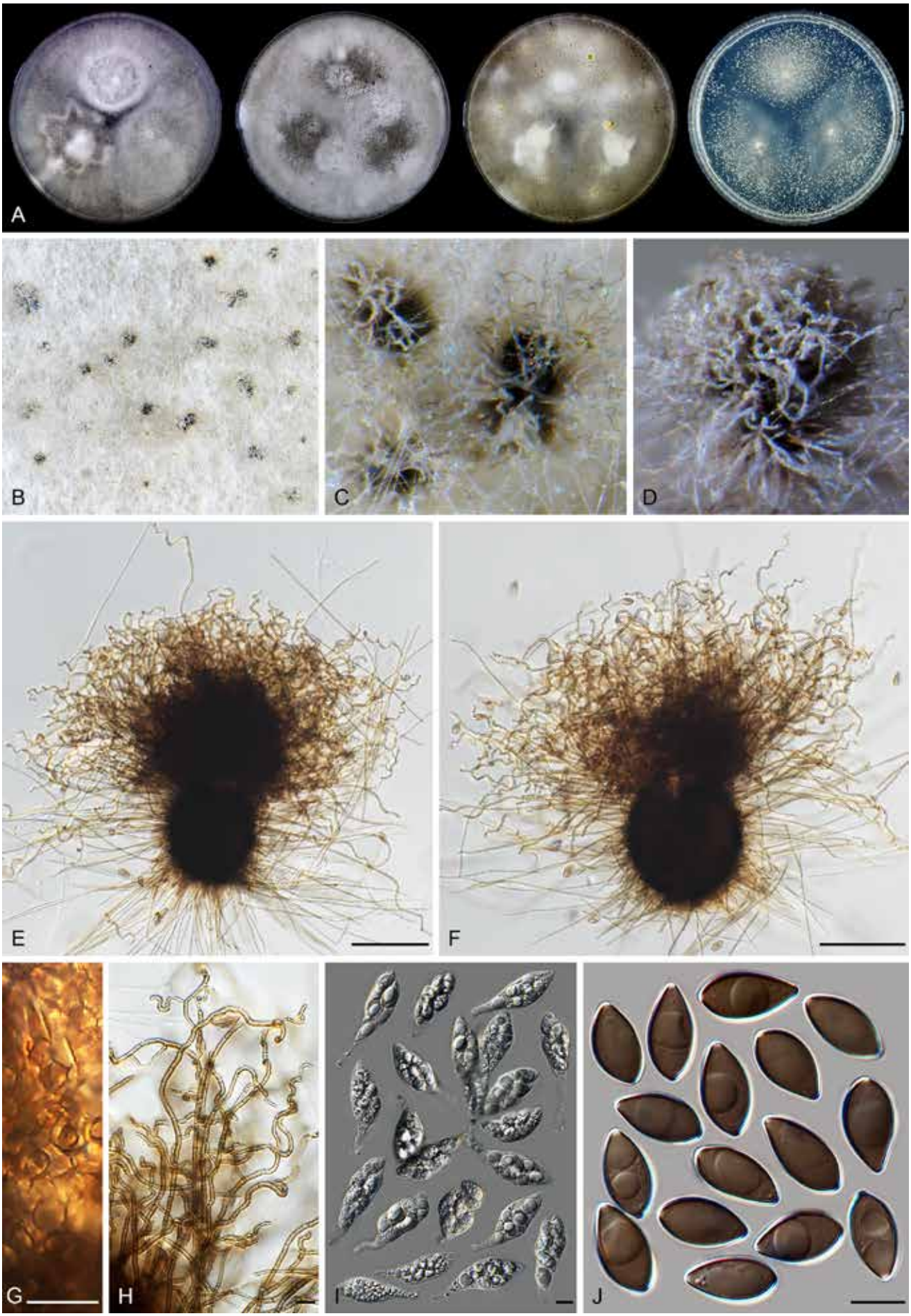

Fig. 32. *Parachaetomium biporatum* (CBS 244.86, ex-type culture). **A.** Colonies from left to right on OA, CMA, MEA and PCA after 5 wk incubation. **B.** Part of the colony on OA. **C.** Mature ascomata on OA, top view. **D.** Mature ascomata on OA, side view. **E, F.** Ascomata mounted in lactic acid. **G.** Structure of ascomatal wall in surface view. **H.** Terminal ascomatal hairs. **I.** Asci. **J.** Ascospores. Scale bars: E, F = 100 µm; G–J = 10 µm.

d at 25 °C; reverse buff to ochreous. On MEA with an entire edge, 30–36 mm diam in 7 d at 25 °C, obverse white or grey olivaceous due to ascomata mixed with aerial mycelium, reverse ochreous to olivaceous grey. On PCA with an entire edge, 30–36 mm diam in 7 d at 25 °C, without aerial mycelium, producing pale olivaceous grey ascomata, without coloured exudates; reverse uncoloured.

Material examined: **Spain**, Valencia, Betera, isolated from soil, Aug. 1985, J. Guarro (culture ex-type CBS 244.86 = FMR 854 = IMI 330348).

Notes: *Parachaetomium biporatum* can be distinguished from the other known species in the genus by the production of elongated ovoid or fusiform ascospores with two apical germ pores (Fig. 32J) and by the occurrence of numerous irregularly undulate to coiled terminal hairs with undulate to irregularly coiled branches (Fig. 32H).

Parachaetomium carinthiacum (Sörgel) Mehrabi *et al.*, Mycol. Prog. 19: 1422. 2020. Fig. 33.
Basionym: *Chaetomium carinthiacum* Sörgel, Arch. Mikrobiol. 40: 393. 1961.

Micromorphology: *Ascomata* superficial, mouse grey in reflected light due to ascomatal hairs, globose or ovoid, ostiolate, 140–190 µm high, 125–165 µm diam. *Ascomatal wall* brown, composed of angular or irregular cells in surface view. *Terminal hairs* of two types: type I numerous, shorter, often erect or arcuate in the lower part, irregularly undulate to loosely and irregularly coiled in the upper part, verrucose, brown, septate, tapering and fading towards the tips, 2–4 µm diam near the base; type II only a few, longer, undulate, verrucose, brown, septate, tapering towards the tips, sometimes recurved or circinate at the apex, 4–6 µm diam near the base. *Lateral hairs* straight or flexuous. *Asci* fusiform or clavate, spore-bearing part 20–31.5 × 10.5–13 µm, with stalks being 6–16.5 µm long, containing eight irregularly-arranged ascospores, evanescent. *Ascospores* olivaceous when mature, ellipsoidal-fusiform, attenuated at both ends, sometimes often slightly inequilateral, (7.5–)8–9(–10) × 5–6 µm, with an apical or subapical to oblique germ pore. *Asexual morph* unknown.

Culture characteristics: On OA with an entire edge, 39–45 mm diam in 7 d at 25 °C, without aerial mycelium, grey olivaceous due to ascomata; reverse olivaceous grey. On CMA similar to those on OA, obverse greenish olivaceous; reverse olivaceous buff to honey. On MEA with an entire edge, 42–48 mm diam in 7 d at 25 °C, obverse greenish olivaceous with white margins due to aerial mycelium; reverse cinnamon to umber. On PCA with an entire edge, 37–43 mm diam in 7 d at 25 °C, without aerial mycelium and coloured exudates; reverse uncoloured.

Material examined: **Lectotype** designated here: Abb. 7 a, b. in Sörgel, Arch. Mikrobiol. 40: 392, 1961 (based on the ex-type culture from a dead leaf collected in Germany), MBT 10002835. **France**, Meylan, date and substrate unknown, Laboratoire de Biologie Végétale Cryptogamie Meylan (CBS H-10007, **epitype** of *Chaetomium carinthiacum* designated here, MBT 10002836, culture ex-epitype CBS 153.81). **Japan**, isolated from *Thymus* sp., date unknown, S. Udagawa (CBS 665.82 = NHL 2884).

Notes: *Parachaetomium carinthiacum* is characterised by the production of two types of terminal ascomatal hairs. Another species in the genus, *Parach. muelleri*, also has two types of terminal ascomatal hairs. The two species are sister taxa (Fig. 7A). They are indistinguishable in ITS phylogeny (Supplementary Fig. S1), but can be identified using *tub2* and *rpb2* sequencing. *Parachaetomium carinthiacum* differs from *Parach. muelleri* by numerous short type I hairs, which are often erect or arcuate in the lower part, and irregularly undulate to loosely and irregularly coiled in the upper part, while type I hairs of *Parach. muelleri* are arcuate, but relatively sparse, some may be apically recurved, but not undulate or coiled. Type II terminal hairs of *Parach. carinthiacum* are flexuous or undulate, but never coiled like those of *Parach. muelleri*.

Parachaetomium hispanicum (Guarro & Arx) X.Wei Wang & Houbraken, ***comb. nov.*** MycoBank MB 830927. Fig. 34.
Basionym: *Chaetomium hispanicum* Guarro & Arx, Beih. Nova Hedwigia 84: 6. 1986.

Micromorphology: *Ascomata* superficial, solitary, grey olivaceous due to ascomatal hairs and masses of ascospores in reflected light, ovoid, ostiolate, 110–220 µm high, 100–190 µm diam. *Ascomatal wall* brown, composed of angular or irregular cells. *Terminal hairs* hypha-like, pale brown, septate, finely verrucose, straight or flexuous, sometimes apically recurved, unbranched, 1.5–3 µm diam near the base. *Lateral hairs* similar to terminal ones. *Asci* clavate, spore-bearing part 30–35 × 13.5–16 µm, with stalks being 9–20 µm long, containing eight irregularly-arranged ascospores, evanescent. *Ascospores* olivaceous brown when mature, ellipsoidal, attenuated at both ends, often slightly inequilateral, 12–14(–15) × 7–8 µm, with an apical germ pore. *Asexual morph* unknown.

Culture characteristics: On OA with an entire edge, 32–38 mm diam in 7 d at 25 °C, without aerial mycelium, obverse grey olivaceous to isabelline due to ascomata; reverse isabelline. On CMA with an entire edge, 30–36 mm diam in 7 d at 25 °C, without aerial mycelium, poorly sporulating, obverse olivaceous buff due to coloured exudates diffusing into the medium; reverse olivaceous buff. On MEA with an entire edge, 28–34 mm diam in 7 d at 25 °C, texture floccose, obverse pale smoke grey due to ascomata mixed with aerial mycelium, reverse ochreous or dark brick. On PCA with an entire edge, 25–34 mm diam in 7 d at 25 °C, without aerial mycelium, without coloured exudates; reverse uncoloured.

Material examined: **Spain**, Tarragona, isolated from dung, date unknown, J. Guarro (culture ex-type CBS 234.82 = FFBA 313); Reus, isolated from soil, date unknown, J. Guarro (CBS 550.83 = FMR 502).

Notes: The ex-type culture of this species is degenerated as sterile and the description above is based on the culture CBS 550.83. *Parachaetomium hispanicum* is characterised by the production of hypha-like and unbranched ascomatal hairs, with no differentiation between the terminal and lateral ones.

Parachaetomium inaequale (Pidopl. *et al.*) X.Wei Wang & Houbraken, ***comb. nov.*** MycoBank MB 830928. Fig. 35.
Basionym: *Thielavia inaequalis* Pidopl. *et al.*, Mikrobiol. Zhurn. 35: 723. 1973.
Synonym: *Corynascella inaequalis* (Pidopl. *et al.*) Arx, Kavaka 3: 34. 1976.

Micromorphology: *Ascomata* superficial or immersed in the medium, solitary or aggregated, non-ostiolate, fuscous black when mature in reflected light, spherical to oblate, pilose, 65–110 µm diam. *Ascomatal wall* brown, composed of *textura epidermoidea* in surface view. *Ascomatal hairs* short, finger-like, straight or

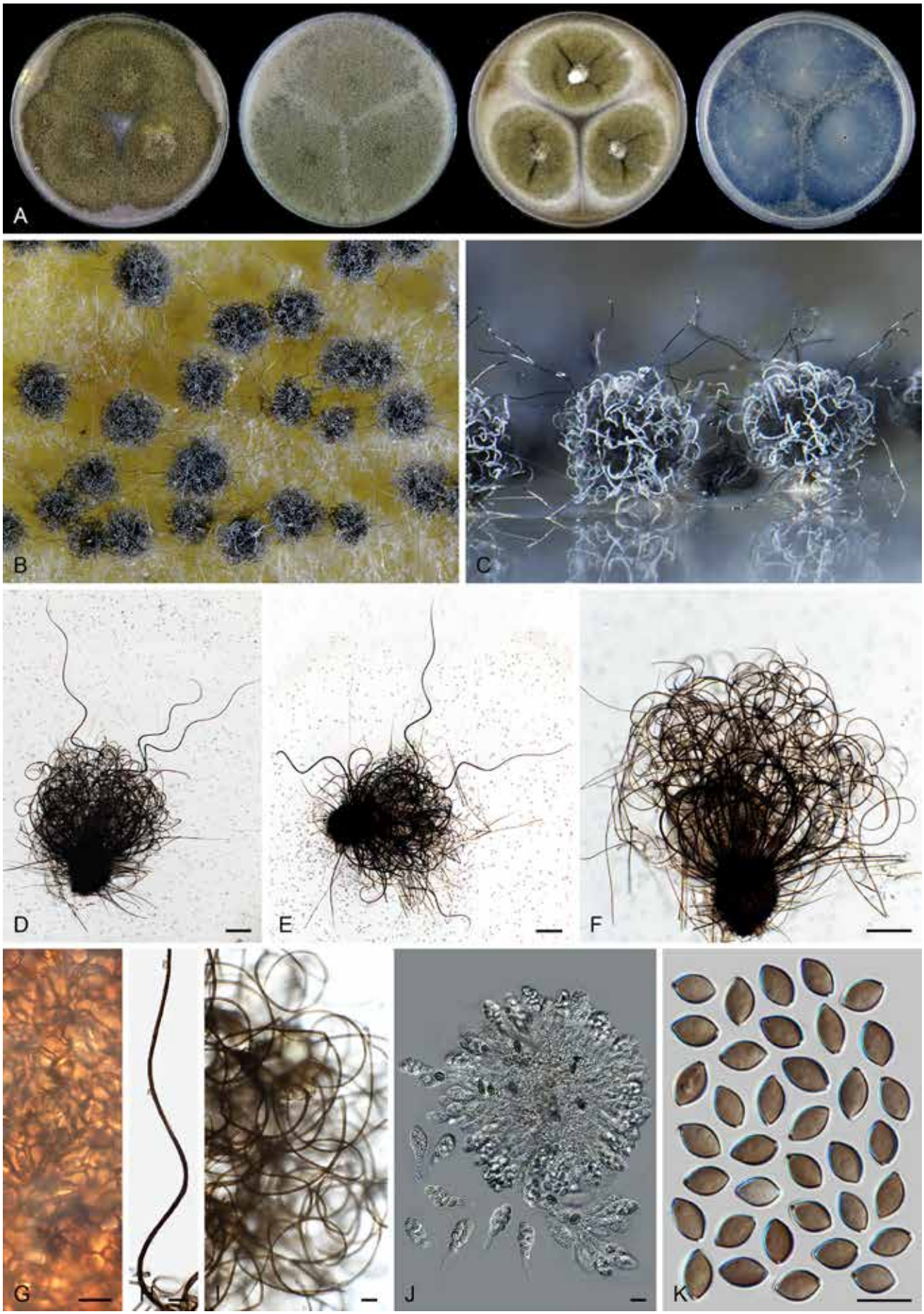

Fig. 33. *Parachaetomium carinthiacum* (CBS 153.81, ex-epitype culture). **A.** Colonies from left to right on OA, CMA, MEA and PCA after 18 d incubation. **B.** Part of the colony showing mature ascomata on OA, top view. **C.** Mature ascomata on OA, side view. **D–F.** Ascomata mounted in lactic acid. **G.** Structure of ascomatal wall in surface view. **H.** Part of a long terminal ascomatal hair. **I.** Short terminal ascomatal hairs. **J.** Asci. **K.** Ascospores. Scale bars: D–F = 100 µm; H, I = 20 µm; G, J–K = 10 µm.

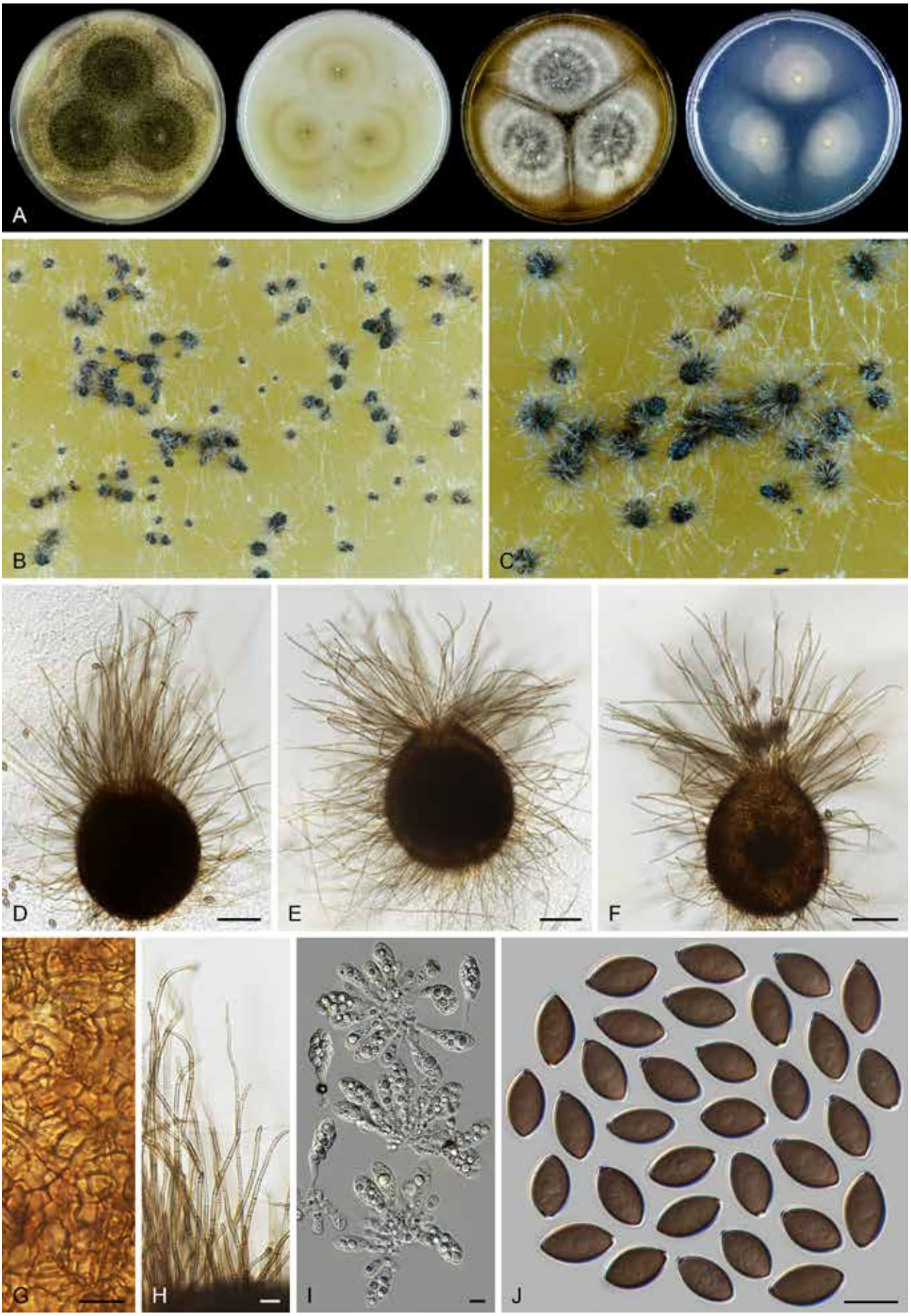

Fig. 34. *Parachaetomium hispanicum* (CBS 550.83). **A.** Colonies from left to right on OA, CMA, MEA and PCA after 3 wk incubation. **B, C.** Part of the colony, showing ascomata on OA, top view. **D–F.** Ascomata mounted in lactic acid. **G.** Structure of ascomatal wall in surface view. **H.** Terminal ascomatal hairs. **I.** Asci. **J.** Ascospores. Scale bars: D–F = 50 µm; G–J = 10 µm.

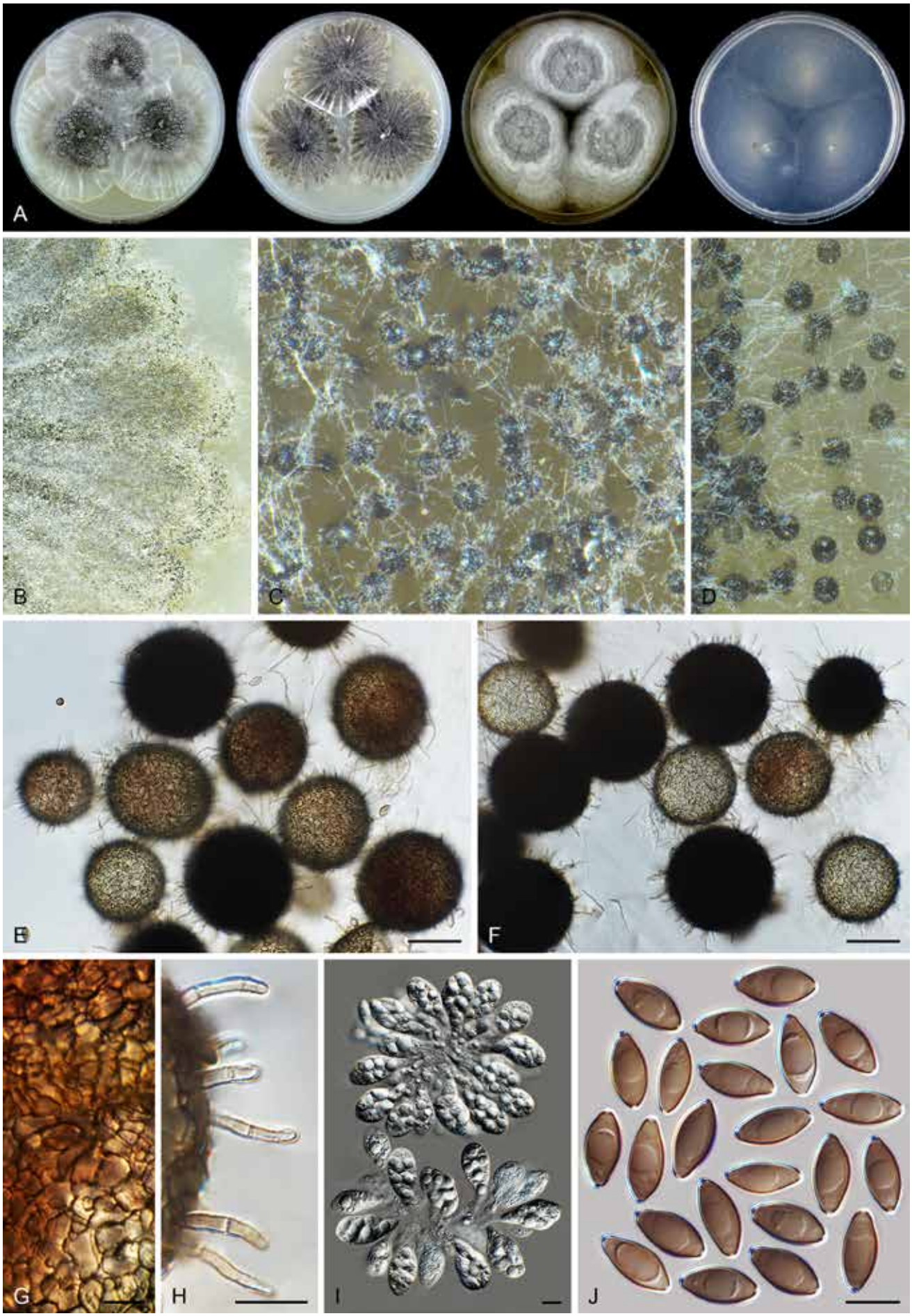

Fig. 35. *Parachaetomium inaequale* (CBS 331.75, ex-type culture). **A.** Colonies from left to right on OA, CMA, MEA and PCA after 18 d incubation. **B.** Part of the colony on CMA. **C.** Mature ascomata on OA, top view. **D.** Mature ascomata on CMA, top view. **E, F.** Ascomata mounted in lactic acid. **G.** Structure of ascomatal wall in surface view. **H.** Terminal ascomatal hairs. **I.** Asci. **J.** Ascospores. Scale bars: E, F = 50 µm; G–J = 10 µm.

flexuous, finely verrucose, septate, 1.5–2 µm diam near the base, less than 30 µm long. *Asci* clavate or pyriform, spore-bearing part 25.5–33.5 × 15–17 µm, with stalks being 5–13 µm long, containing eight irregularly-arranged ascospores, evanescent. *Ascospores* olivaceous brown when mature, elongated ellipsoidal or fusiform, often inequilateral, (12–)13.5–15.5(–16.5) × (5.5–)6.5–7.5(–8.5) µm, with two apical germ pores. *Asexual morph* unknown.

Culture characteristics: On OA with a crenate edge, 27–33 mm diam in 7 d at 25 °C, with a thin layer of white aerial mycelium, obverse mouse grey due to ascomata; reverse buff. On CMA similar to those on OA, 28–34 mm diam in 7 d at 25 °C, forming masses of ascomata radially straited with lobate margins. On MEA with an entire or slightly crenate edge, 26–32 mm diam in 7 d at 25 °C, with white aerial mycelium, obverse pale mouse grey in the central part, wrinkled, with several white concentric and crenated rings; reverse ochreous. On PCA with an entire edge, 29–35 mm diam in 7 d at 25 °C, without aerial mycelium, without coloured exudates, reverse uncoloured.

Material examined: **Ukraine**, Kirovograd, isolated from soil in oak forest, May 1968, collector unknown (culture ex-type CBS 331.75 = IMI 196527 = VKM F-1922); Kirovograd District, Ashen plantation, isolated from soil, 1 Jun. 1968, T.S. Kirilenko (CBS 164.75 = VKM F-1565).

Notes: *Parachaetomium inaequale* is the only species in the genus with non-ostiolate ascomata. This species was originally described in *Thielavia*, and later combined in *Corynascella* because of the production of ascospores with two apical germ pores (von Arx 1975b). Phylogenetic analysis indicates that *Parach. inaequale* is a sister species of *Parach. hispanicum*, distantly related to the type species of *Corynascella* (Fig. 7A). *Parachaetomium inaequale* differs morphologically from the type species of *Corynascella* (Figs 23, 24) by lacking an asexual morph and having elongated, ellipsoidal or fusiform ascospores, rather than irregularly ellipsoidal, oblate, ovoid or doliiform and usually irregular and inequilateral ascospores produced by the latter.

Parachaetomium muelleri (Arx) X.Wei Wang & Houbraken, ***comb. nov.*** MycoBank MB 830925. Fig. 36.
Basionym: *Chaetomium muelleri* Arx, Beih. Nova Hedwigia 84: 6. 1986.

Micromorphology: *Ascomata* superficial, olivaceous grey in reflected light due to ascomatal hairs and masses of ascospores, subglobose, ostiolate, 100–200 µm high, 90–195 µm diam. *Ascomatal wall* brown, composed of angular or elongate cells in surface view. *Terminal hairs* in two types: type I shorter, arcuate, some apically recurved, verrucose, brown, septate, tapering and fading towards the tips, 3.5–6 µm diam near the base; type II longer, undulate or loosely coiled, verrucose, dark brown, tapering towards the tips, sometimes recurved or circinate at the apex, 5.5–7 µm diam near the base. *Lateral hairs* short, straight or flexuous. *Asci* fusiform, occasionally clavate, spore-bearing part 23–36.5 × 11.5–15 µm, with stalks being 6–15 µm long, containing eight irregularly-arranged ascospores, evanescent. *Ascospores* olivaceous when mature, ellipsoidal-fusiform, attenuated at both ends, sometimes slightly inequilateral, (9–)9.5–10.5(–11) × 5.5–6.5 µm, with an apical or slightly subapical germ pore. *Asexual morph* unknown.

Culture characteristics: On OA with an entire edge, 49–55 mm diam in 7 d at 25 °C, without aerial mycelium, obverse lavender to violet due to coloured exudates diffusing into the medium; reverse olivaceous grey. On CMA with an entire edge, 50–56 mm diam in 7 d at 25 °C, with white aerial mycelium, obverse citrine due to ascomata; reverse violet slate. On MEA with an entire edge, 52–58 mm diam in 7 d at 25 °C, with aerial mycelium, obverse buff to isabelline; reverse cinnamon. On PCA with an entire edge, 52–58 mm diam in 7 d at 25 °C, without aerial mycelium, without coloured exudates, obverse and reverse olivaceous buff.

Material examined: **Pakistan**, Lahore, isolated from decayed twig, 1976, S. Ahmed (culture ex-type CBS 192.84). **Turkey**, Bornova-Izmir, date and substrate unknown, M. Esentepe (CBS 663.75).

Notes: *Parachaetomium muelleri* can be easily recognised by the production of lavender to violet exudates on OA. It differs from its sister species, *Parach. carinthiacum*, by sparser, thicker (3.5–6 µm *vs* 2–4 µm diam near the base) and shorter type I terminal hairs, which are arcuate, some apically recurved, and by thicker terminal hairs of type II (5.5–7 µm diam *vs* 4–6 µm near the base), which are undulate to loosely coiled. *Parachaetomium muelleri* also produces larger ascospores than *Parach. carinthiacum* (9.5–10.5 × 5.5–6.5 µm *vs* 8–9 × 5–6 µm).

Parachaetomium perlucidum (Sergejeva) X.Wei Wang & Houbraken, ***comb. nov.*** MycoBank MB 830930. Fig. 37.
Basionym: *Chaetomium perlucidum* Sergejeva, Bot. Mater. Otd. Sporov. Rast. Bot. Inst. Komarova Akad. Nauk S.S.S.R. 11: 108. 1956.
Synonyms: *Chaetomium iranianum* Asgari & Zare, Mycologia 103: 877. 2011.
Parachaetomium iranianum (Asgari & Zare) Mehrabi *et al*., Mycol. Prog. 19: 1422. 2020.

Micromorphology: *Ascomata* superficial, smoke grey due to ascomatal hairs in reflected light, subglobose to ovate, ostiolate, 95–230 µm high, 85–200 µm diam. *Ascomatal wall* brown, composed of irregular or angular cells. *Terminal hairs* in reflected light orange or luteous near the base, fading to pale smoke grey towards the tips, brown when mounting, septate, verrucose, loosely coiled, erect or flexuous in the lower part, 2–3.5 µm diam near the base. *Lateral hairs* flexuous. *Asci* fusiform, spore-bearing part 28–38 × 12–14 µm, with stalks being 8–18 µm long, containing eight irregularly-arranged ascospores, evanescent. *Ascospores* olivaceous when mature, fusiform or elongated ovoid, (11–)12–13.5(–14.5) × (5.5–)6–6.5(–7.5) µm, with a subapical or oblique germ pore. *Asexual morph* unknown.

Culture characteristics: On OA with an entire edge, 38–44 mm diam in 7 d at 25 °C, obverse smoke grey due to ascomatal hairs, without aerial mycelium; reverse honey. On CMA similar to those on OA, 35–41 mm diam in 7 d at 25 °C, with a thin layer of white aerial mycelium; reverse buff or ochreous. On MEA with an entire or slightly crenate edge, 37–43 mm diam in 7 d at 25 °C, obverse white and floccose due to aerial mycelium, reverse ochreous or fulvous. On PCA with an entire edge, 37–43 mm diam in 7 d at 25 °C, with sparse aerial mycelium, without coloured exudates; reverse uncoloured.

Material examined: **China**, Xinjiang, Changji, isolated from soil, 2013, X.W. Wang (culture CBS 119762). **Iran**, East Azerbaijan Prov., Sarab, isolated from leaf of *Hordeum vulgare*, 22 May 2005, B. Asgari (CBS 126670 = IRAN 861C, ex-type of *Chaetomium iranianum*). **Ukraine**, Kiev, isolated from dead herbaceous stem, date unknown, K.S. Sergejeva (culture ex-type CBS 141.58 = IMI 074954 = MUCL 18693 = MUCL 39399 = VKM F-1950). **USA**, Wyoming, isolated from soil, 1976, M. Christensen (CBS 127795 = RMF H 140).

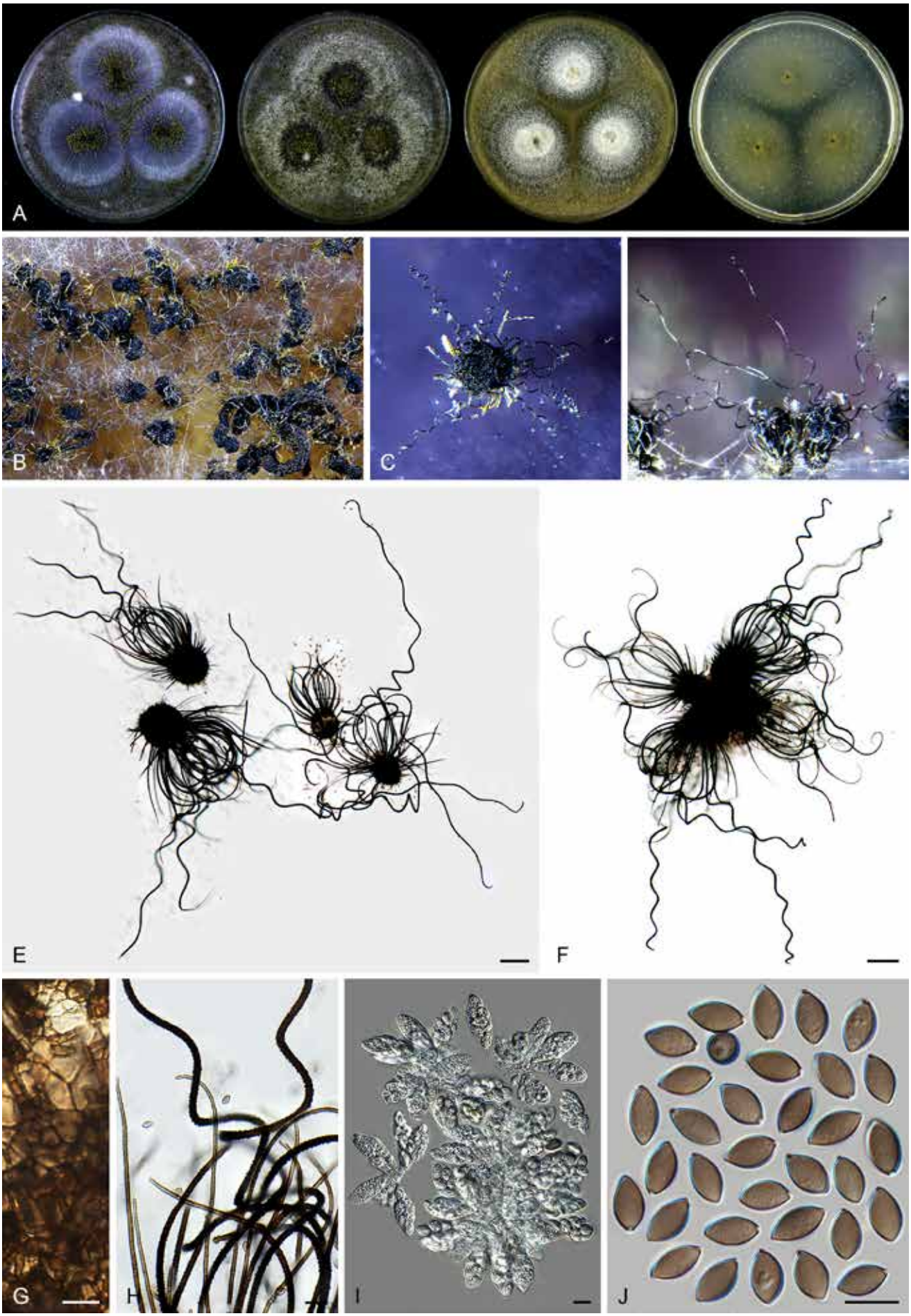

Fig. 36. *Parachaetomium muelleri* (CBS 192.84, ex-type culture). **A.** Colonies from left to right on OA, CMA, MEA and PCA after 3 wk incubation. **B.** Part of the colony on OA. **C.** Mature ascomata on OA, top view. **D.** Mature ascomata on OA, side view. **E, F.** Ascomata mounted in lactic acid. **G.** Structure of ascomatal wall in surface view. **H.** Terminal ascomatal hairs. **I.** Asci. **J.** Ascospores. Scale bars: E, F = 100 µm; G–J = 10 µm.

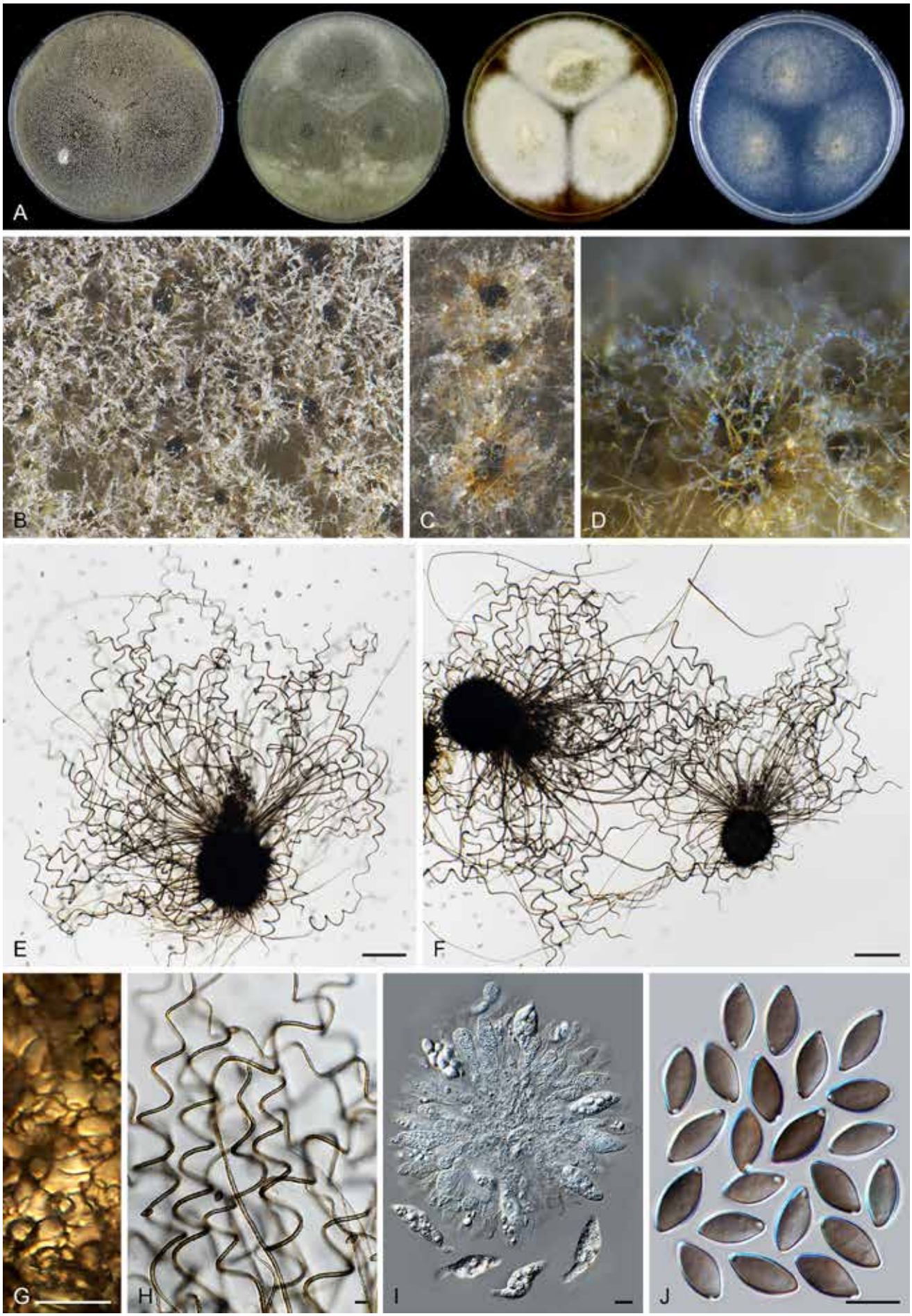

Fig. 37. *Parachaetomium perlucidum* (CBS 141.58, ex-type culture). **A.** Colonies from left to right on OA, CMA, MEA and PCA after 18 d incubation. **B.** Part of the colony on OA. **C.** Mature ascomata on OA, top view. **D.** Mature ascomata on OA, side view. **E, F.** Ascomata mounted in lactic acid. **G.** Structure of ascomatal wall in surface view. **H.** Terminal ascomatal hairs. **I.** Asci. **J.** Ascospores. Scale bars: E, F = 100 µm; G–J = 10 µm.

Notes: *Parachaetomium perlucidum* is characterised by having ascospores with a subapical or oblique germ pore, fusiform asci and loosely coiled terminal hairs. As noted above, *Parach. iranianum* is treated as a synonym of this species based on morphological similarities and phylogenetic analysis.

Parachaetomium subspirilliferum (Sergejeva) X.Wei Wang & Houbraken, ***comb. nov.*** MycoBank MB 830931. Fig. 38.
Basionym: *Chaetomium subspirilliferum* Sergejeva, Bot. Mater. Otd. Sporov. Rast. Bot. Inst. Komarova Akad. Nauk S.S.S.R. 13: 174. 1960.

Micromorphology: *Ascomata* superficial, greenish olivaceous due to ascomatal hairs in reflected light, spherical to ovate, ostiolate, 95–150 µm high, 80–130 µm diam. *Ascomatal wall* brown, composed of angular or elongate cells. *Terminal hairs* brown, septate, finely verrucose, undulate to loosely coiled, erect or flexuous at lower part, 1.5–3 µm diam near the base. *Lateral hairs* flexuous. *Asci* clavate, spore-bearing part 25.5–36 × 12–14.5 µm, with stalks being 11–21 µm long, containing eight irregularly-arranged ascospores, evanescent quickly in one week. *Ascospores* olivaceous brown when mature, elongated ellipsoidal, elongated ovoid, attenuated at both ends, or fusiform, often slightly inequilateral, (10.5–)12–13.5(–14) × (6–)6.5–7.5 µm, with an apical or occasionally slightly subapical germ pore. *Asexual morph* unknown.

Culture characteristics: On OA with an entire edge, 34–40 mm diam in 7 d at 25 °C, obverse grey olivaceous to isabelline due to ascomatal hairs, with sparse white aerial mycelium; reverse hazel. On CMA similar to those on OA. On MEA with an entire edge, 28–34 mm diam in 7 d at 25 °C, obverse white or greenish olivaceous due to ascomata mixed with aerial mycelium, reverse ochreous or fulvous. On PCA with an entire edge, 34–40 mm diam in 7 d at 25 °C, without aerial mycelium, sparsely producing ascomata, without coloured exudates; reverse uncoloured.

Material examined: **China**, Xingjiang, Altai, isolated from soil, 2003, X.W. Wang (WXW 9901-2). **Russia**, Altai, Kulundinskaya steppe, isolated from soil, date unknown, D.T. Degtyareva & M.V. Nosdrenko (culture ex-type CBS 150.60 = ATCC 14534 = IMI 081771 = MUCL 18698 = VKM F-1943).

Notes: *Parachaetomium subspirilliferum* produces undulate to loosely coiled terminal hairs, similar to *Parach. perlucidum*. This species can be differentiated from the latter species by its ascospores, which have an apical (occasionally slightly subapical, but never oblique) germ pore, clavate rather than fusiform asci and slightly thinner terminal hairs (1.5–3 µm diam *vs* 2–3.5 µm diam near the base).

Three more chaetomium-like species are combined in *Parachaetomium* based on phylogenetic data (Fig. 7A, Supplementary Figs S2, S3). These species produce fusiform ascospores and coiled terminal hairs covering ostiolate ascomata, similar to *Parach. perlucidum* and *Parach. subspirilliferum*:

Parachaetomium longiciliatum (Yu Zhang & L. Cai) X.Wei Wang & Houbraken, ***comb. nov.*** MycoBank MB 840157.
Basionym: *Chaetomium longiciliatum* [as '*longiciliata*'] Yu Zhang & L. Cai, Fungal Biol. 121: 31. 2016.

Note: *Parachaetomium longiciliatum* is characterised by producing shorter ascospores (9–12.5 × 5.5–8 µm) than *Parach. perlucidum* (12–13.5 × 6–6.5 µm) and *Parach. subspirilliferum* (12–13.5 × 6.5–7.5 µm), and having an apical or slightly subapical germ pore (Zhang *et al.* 2017).

Parachaetomium mareoticum (Besada & Yusef) X.Wei Wang & Houbraken, ***comb. nov.*** MycoBank MB 840158.
Basionym: *Chaetomium mareoticum* Besada & Yusef, Trans. Brit. Mycol. Soc. 52: 502. 1969.

Notes: *Parachaetomium mareoticum* produces rather thin terminal hairs (2–3 µm diam near the base), similar to *Parach. perlucidum* and *Parach. subspirilliferum*. This species can be distinguished by its large ascospores (15–18 × 7–8.5 µm) with two apical germ pores (von Arx *et al.* 1986). Apparently, *Parach. mareoticum* produces the largest ascospores in the genus.

Parachaetomium multispirale (A. Carter *et al.*) X.Wei Wang & Houbraken, ***comb. nov.*** MycoBank MB 840159.
Basionym: *Chaetomium multispirale* A. Carter *et al.*, Canad. J. Bot. 60: 1256. 1982.

Notes: *Parachaetomium multispirale* produces relatively thick terminal hairs (2.5–4 µm diam near the base), similar to *Parach. perlucidum*, but can be distinguished by its smaller ascospores (7–10 × 5–6 µm *vs* 11.5–13.5 × 6–7 µm) with an apical germ pore (Carter & Khan 1982, von Arx *et al.* 1986), rather than a subapical or oblique germ pore like the latter. *Parachaetomium multispirale* produces more regularly coiled terminal hairs (Carter & Khan 1982), in contrast to the loosely coiled hairs of *Parach. perlucidum*.

Parathielavia X.Wei Wang & Houbraken, Stud. Mycol. 93: 208. 2019.

Micromorphology and illustrations: See Wang *et al.* (2019b; p. 208, 210–212).

Type species: *Parathielavia hyrcaniae* (Nicot) X.Wei Wang & Houbraken

Notes: *Parathielavia* is characterised by producing non-ostiolate, pilose or glabrous ascomata, with a brown and semi-translucent wall and having ascospores with a subapical germ pore (Wang *et al.* 2019b). *Thielavia coactilis*, previously not studied when introducing *Parathielavia* (Wang *et al*. 2019b), proved to belong to this genus based on our phylogenetic analysis (Fig. 7C). The morphology of this species fits in the current circumscription of the genus. The combination is introduced below.

Parathielavia coactilis (Nicot) X.Wei Wang & Houbraken, ***comb. nov.*** MycoBank MB 840160.
Basionym: *Thielavia coactilis* Nicot, Compt. Rend. Hebd. Séances Acad. Sci., Sér. D 253: 304. 1961.

Notes: *Parathielavia coactilis* was published together with *Parath. hyrcaniae* (= *Thielavia hyrcaniae*), and can be distinguished by glabrous ascomata and smaller ascospores (6–11 × 5–7 µm *vs* 11–13 × 6–7 µm) (von Arx 1975a, Wang *et al.* 2019b). No type material of this species is available. Our sequence data are from two recent isolates deposited in the CBS culture collection and these are phylogenetically most closely related to the type of *Parath. kuwaitensis*.

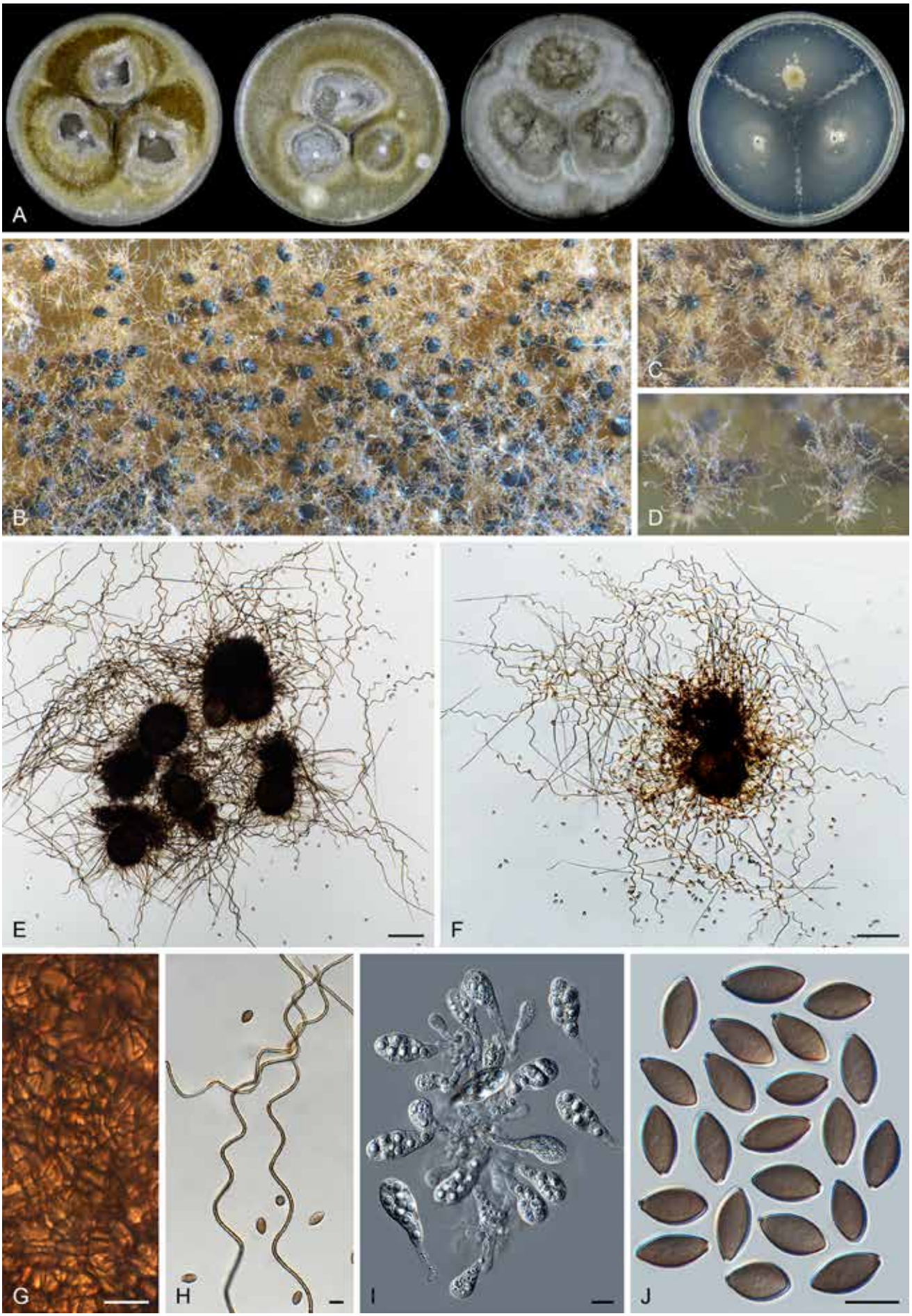

Fig. 38. *Parachaetomium subspirilliferum* (CBS 150.60, ex-type culture). **A.** Colonies from left to right on OA, CMA, MEA and PCA after 3 wk incubation. **B.** Part of the colony on OA. **C.** Mature ascomata on OA, top view. **D.** Mature ascomata on OA, side view. **E, F.** Ascomata mounted in lactic acid. **G.** Structure of ascomatal wall in surface view. **H.** Terminal ascomatal hairs. **I.** Asci. **J.** Ascospores. Scale bars: E, F = 100 µm; G–J = 10 µm.

Parvomelanocarpus X.Wei Wang & Houbraken, ***gen. nov.*** MycoBank MB 840124.

Etymology: The name refers to its smaller ascospores and slower growth than those of the genus *Melanocarpus*.

Micromorphology: *Ascomata* superficial, or embedded in aerial mycelium, discrete to aggregated, non-ostiolate, spherical, glabrous or covered by finger-like ascomatal hairs, black when mature in reflected light due to the dark ascomatal wall. *Ascomatal wall* brown, composed of *textura angularis*, *epidermoidea* or *intricata* in surface view. *Asci* ovate to broadly ovate, containing eight irregularly-arranged ascospores, evanescent. *Ascospores* 1-celled, smooth, olivaceous brown or brown when mature, ovate to broadly ovate, bilaterally flattened, with an apical germ pore, usually shorter than 10 µm. *Asexual morph* unknown.

Culture characteristics: *Colonies* on agar media growing slowly, less than 20 mm diam in 5 d at optimal temperature (about 37 °C). Thermotolerant.

Type species: *Parvomelanocarpus tardus* (X.Wei Wang & Samson) X.Wei Wang & Houbraken

Notes: The proposal of this new genus is supported by its differences from *Melanocarpus albomyces* in morphology, reproduction, temperature adaptation (Fig. 39) and by their divergence time (Fig. 8B). *Parvomelanocarpus* species are thermotolerant, while *Melanocarpus* species are thermophilic. Furthermore, no asexual morph is observed in *Parvomelanocarpus* species, they grow very slow on agar media and produce smaller ascospores. The genus diverged from *Melanocarpus* about 60 Mya (Fig. 8B). For more details, see notes of *Melanocarpus*.

Parvomelanocarpus tardus (X.Wei Wang & Samson) X.Wei Wang & Houbraken, ***comb. nov.*** MycoBank MB 840152.

Basionym: *Melanocarpus tardus* X.Wei Wang & Samson, Stud. Mycol. 84: 205. 2016.

Micromorphology and illustrations: See Wang *et al.* (2016b; p. 205, 213).

Note: *Parvomelanocarpus tardus* is characterised by the production of non-ostiolate, glabrous ascomata; the ascospores of this species are ovate to broadly ovate, bilaterally flattened, 7–8(–8.5) × (6–) 6.5–7.5 × 5–6 µm, having an apical germ pore at the attenuated end.

Parvomelanocarpus thermophilus (Abdullah & Al-Bader) X.Wei Wang & Houbraken, ***comb. nov.*** MycoBank MB 840167. Fig. 40.
Basionym: *Thielavia minuta* var. *thermophila* Abdullah & Al-Bader, Basrah J. Agric. Sci. 5: 116. 1992.
Synonym: *Melanocarpus thermophilus* (Abdullah & Al-Bader) Guarro *et al.*, Mycol. Res. 100: 75. 1996.

Micromorphology: *Ascomata* superficial, discrete or aggregated to form a ring around the central point, non-ostiolate, dark slate blue in reflected light, covered by hairs, globose or subglobe, 60–160 µm diam. *Ascomatal wall* brown, ochreous or fulvous when young, dark brown when mature, *textura epidermoidea* or *intricata* in surface view. *Ascomatal hairs* brown, finger-like, often geniculate, finely verrucose, septate, 2–4 µm diam near the base, usually less than 20 µm long. *Asci* fasciculate, ovate to broadly ovate, spore-bearing portion 13.5–20 × 10.5–14.5 µm, with short or indistinct stalks being 0–5 µm long, containing eight irregularly-arranged ascospores, quickly evanescent. *Ascospores* dark brown when mature, broadly ovate, slightly bilaterally flattened, (6–)7–9(–9.5) × (6–)6.5–8(–8.5) × 6–7 µm, with an apical germ pore at the attenuated end. *Asexual morph* unknown.

Culture characteristics: On OA with a crenated edge, 8–14 mm diam in 5 d at 37 °C, obverse mouse grey due to the formation

Fig. 39. Comparison of growth temperature between *Melanocarpus* and *Parvomelanocarpus*. Left to right: 5-d-old colonies on OA 25 °C, OA 37 °C, OA 45 °C, PDA 25 °C, PDA 37 °C, PDA 45 °C; top to bottom: *Melanocarpus albomyc*es CBS 638.94, *Parvomelanocarpus tardus* CBS 541.76, *Parvomelanocarpus thermophilus* CBS 886.97.

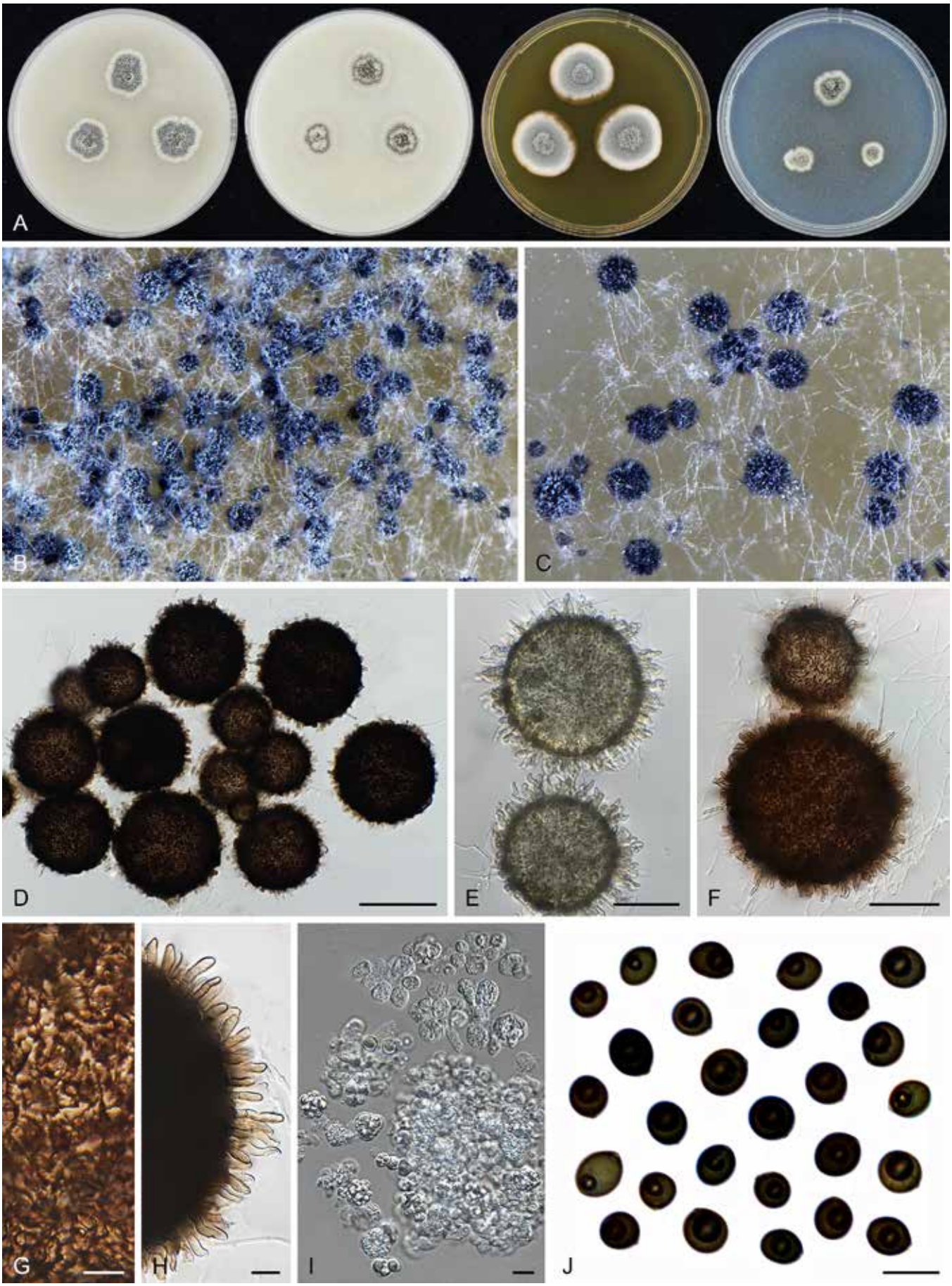

Fig. 40. *Parvomelanocarpus thermophilus* (CBS 886.97). **A.** Colonies from left to right on OA, CMA, MEA and PCA after 3 wk incubation. **B.** Part of the colony. **C.** Mature ascomata on OA, top view. **D, F.** Mature ascomata mounted in lactic acid. **E.** Young ascomata mounted in lactic acid. **G.** Structure of ascomatal wall in surface view. **H.** Ascomatal hairs. **I.** Asci. **J.** Ascospores. Scale bars: D = 100 µm; E, F = 50 µm; G–J = 10 µm.

of ascomata, with sparse white aerial mycelium, without coloured exudates; reverse uncoloured. On CMA similar to those on OA. On MEA with an entire or slightly lobate edge, 14–20 mm diam in 5 d at 37 °C, obverse pale mouse grey due to ascomata mixed with aerial mycelium, reverse saffron. On PCA with a crenated edge, 6–12 mm diam in 5 d at 37 °C, with sparse aerial mycelium, without coloured exudates; reverse uncoloured.

Material examined: **India**, Agra, isolated from soil, 3 Nov. 1995, A.M. Stchigel (CBS 886.97 = FMR 6190).

Notes: *Parvomelanocarpus thermophilus* can be distinguished from *Par. tardus* by its ascomata, which are covered by finger-like ascomatal hairs, while those of *Par. tardus* are usually glabrous (Wang *et al*. 2016b). The ascospores of *Par. thermophilus* are slightly larger than those of *Par. tardus* (7–9 × 6.5–8 × 6–7 µm *vs* 7–8 × 6.5–7.5 × 5–6 µm).

Pseudohumicola X.Wei Wang, P.J. Han, F.Y. Bai & Houbraken, ***gen. nov.*** MycoBank MB 840123.

Etymology: The name refers to the morphologically related genus *Humicola*.

Micromorphology: Containing asexual species and species with both asexual and sexual morphs. *Asexual morphs* humicola-like and producing aleurioconidia-like conidia and/or acremonium-like. *Conidiogenous cells of humicola-like morph* reduced to a hyphal cell, intercalary or lateral, monoblastic. *Aleurioconidia-like conidia* arising laterally, intercalary or terminally, 1-celled, solitary or rarely in chains or in clusters of a few spores, globose, subglobose, oblate, occasionally obovoid, pyriform or clavate, light olivaceous, olivaceous, brown or dark brown, smooth or not, in persisted state on hyphae or rhexolytic when seceding, germ pores or thinning area of wall present. *Acremonium-like phialides* lateral or occasionally terminal, hyaline. *Acremonium-like conidia* in basipetal chains, hyaline, aseptate, smooth, obovoid, usually with a truncated base and a rounded apex. *Ascomata* absent or present, when present superficial, or covered by aerial hyphae, ostiolate. *Terminal hairs* straight, flexuous, undulate or coiled in the upper part. *Asci* clavate, containing eight biseriate or irregularly-arranged ascospores, evanescent. *Ascospores* limoniform, bilaterally flattened, with an apical germ pore.

Type species: *Pseudohumicola subspiralis* (Chivers) X.Wei Wang, P.J. Han, F.Y. Bai & Houbraken

Notes: *Humicola sensu* Wang *et al.* (2019a) receives moderate statistic support in our phylogenetic analysis (ML-BS = 78 %; PP = 1.0, Fig. 7B). In contrast, our molecular dating analysis shows that a group of species (*Humicola atrobrunnea*, *H. pulvericola*, *H. semispiralis*, *H. subspiralis*) closely clusters to *Aporothielavia*, separating them from the other *Humicola* species. The new genus *Pseudohumicola* is therefore proposed here for these species. The ascomata (if produced) in *Pseudohumicola* usually have coiled terminal hairs, while such ascomatal hairs are rare in the sexual species of *Humicola s. str*. In addition, germ pores or a thin area on the aleurioconidia-like conidia is more often observed in *Pseudohumicola* than in *Humicola* species. For more details, see notes on *Humicola* above.

Pseudohumicola atrobrunnea (X.Wei Wang *et al.*) X.Wei Wang, P.J. Han, F.Y. Bai & Houbraken, ***comb. nov.*** MycoBank MB 840148.
Basionym: *Humicola atrobrunnea* X.Wei Wang *et al.*, Stud. Mycol. 93: 76. 2018.

Micromorphology and illustrations: See Wang *et al.* (2019a; p. 76, 78).

Notes: This species only produces an asexual morph with aleurioconidia-like conidia. The smooth, dark brown and thick-walled conidia are produced solitary, sometimes in a chain of 2–3 conidia or in a cluster. A germ pore can be observed on some conidia.

Pseudohumicola pulvericola (X.Wei Wang *et al.*) X.Wei Wang, P.J. Han, F.Y. Bai & Houbraken, ***comb. nov.*** MycoBank MB 840149.
Basionym: *Humicola pulvericola* X.Wei Wang *et al.*, Stud. Mycol. 93: 96. 2018.

Micromorphology and illustrations: See Wang *et al.* (2019a; p. 96, 98).

Notes: *Pseudohumicola pulvericola* only produces an asexual morph with both aleurioconidia-like conidia and an acremonium-like morph. The slightly verrucose, dark brown and thick-walled aleurioconidia-like conidia are mostly produced solitary and occasionally in chains of two. A germ pore or thinning area of wall can sometimes be observed on the conidia. Acremonium-like conidiophores can be present in the aerial mycelium.

Pseudohumicola semispiralis (Udagawa & Cain) X.Wei Wang, P.J. Han, F.Y. Bai & Houbraken, ***comb. nov.*** MycoBank MB 840150.
Basionym: *Chaetomium semispirale* Udagawa & Cain, Canad. J. Bot. 47: 1947. 1969.
Synonym: *Humicola semispiralis* (Udagawa & Cain) X.Wei Wang & Houbraken, Stud. Mycol. 93: 100. 2018.

Micromorphology and illustrations: See Wang *et al.* (2019a; p. 100, 102).

Notes: *Pseudohumicola semispiralis* produces a sexual morph and an asexual morph with aleurioconidia-like conidia. The terminal ascomatal hairs are partly straight to flexuous, partly spirally coiled in the upper part. The conidia are smooth, subhyaline or olivaceous. A germ pore or thinning area of wall can be observed on some conidia.

Pseudohumicola subspiralis (Chivers) X.Wei Wang, P.J. Han, F.Y. Bai & Houbraken, ***comb. nov.*** MycoBank MB 840151.
Basionym: *Chaetomium subspirale* Chivers, Proc. Amer. Acad. Arts 48: 84. 1912.
Synonym: *Humicola subspiralis* (Chivers) X.Wei Wang & Houbraken, Stud. Mycol. 93: 104. 2018.

Micromorphology and illustrations: See Wang *et al.* (2019a; p. 104, 105).

Notes: *Pseudohumicola subspiralis* produces both a sexual and asexual morph. Von Arx *et al.* (1986) observed aleurioconidia-like conidia and noted that such thick-walled conidia could occasionally be absent. In our study, only acremonium-like phialides were observed in the ex-type culture. Apparently, this species can

potentially produce both aleurioconidia-like conidia and an acremonium-like morph. The ascomatal hairs of this species are undulate to spirally coiled in the upper parts, without differentiation between the terminal and lateral ones.

Staphylotrichum J.A. Mey. & Nicot, Bull. Trimestriel Soc. Mycol. France 72: 322. 1957.

Micromorphology (*emended description*): Species producing only an asexual morph or both an asexual and sexual morph. *Asexual morphs* usually of two types. Type one macronematous. *Conidiophores* arising from an intercalary, thick-walled, pigmented foot cell, usually pigmented and thick-walled in the lower part, tapering and fading towards the tips, apically branched. *Conidiogenous cells* terminally on the top branches of conidiophores, cylindrical or denticle-like, monoblastic or sympodial polyblastic. Type two micronematous. *Conidiophores* absent. *Conidiogenous cells* arising directly from hyphae, cylindrical or denticle-like, monoblastic, rarely sympodial polyblastic. *Conidia* solitary, single-celled, smooth or slightly verrucose, hyaline to pale brown, usually globose, subglobose or obovoid, rhexolytic when seceding. *Sexual morph* absent or present. If present, of two types: *Ascomata* of type I with a conspicuous neck, superficial or covered by aerial hyphae, ostiolate, elongated obpyriform, obclavate or ampulliform below, usually apically attenuated to a cylindrical, thread-like neck which is composed of fused basal part of the terminal hairs, with terminal hairs seta-like or whip-like, smooth, fused in the lower part to form a channel through which a column of ascospores emerges from the ascomata. *Ascomata* of type II without a conspicuous neck, superficial, ostiolate, ovate to subglobose, with terminal hairs spirally or loosely coiled in the upper parts. *Asci* clavate to fusiform, with eight irregularly-arranged ascospores, evanescent. *Ascospores* broad limoniform to nearly globose, often somewhat biapiculate, bilaterally flattened, with an apical germ pore.

Type species: *Staphylotrichum coccosporum* J.A. Mey. & Nicot.

Notes: Asexual species usually produce both macro- and micronematous asexual morphs, while sexual species only produce a micronematous asexual morph. With the addition of *Staph. limonisporum*, the concept of *Staphylotrichum* needs to be emended (see above) to include species producing ascomata lacking a long neck. All known species produce similar conidia, asci and ascospores. The ascospores of *Staphylotrichum* are limoniform to broad limoniform, bilaterally flattened, with an apical germ pore. The conidia of *Staphylotrichum* species are easily confused with those of *Humicola* species. *Staphylotrichum* species produce cylindrical or denticle-like conidiogenous cells, while *Humicola* species produce conidia that arise laterally, intercalary or terminally from hyphae without differentiated conidiophores or conidiogenous cells (Fig. 6F). Two more species are transferred to this genus.

Staphylotrichum koreanum (Hyang B. Lee & T.T.T. Nguyen) X.Wei Wang & Houbraken, ***comb. nov.*** MycoBank MB 840161.
Basionym: *Humicola koreana* Hyang B. Lee & T.T.T. Nguyen, Fungal Diversity 78: 97. 2016.

Notes: Based on the illustration in the original description, *H. koreana* produces typical micronematous conidia on denticle-like to cylindrical conidiogenous cells (Li *et al.* 2016), similar to other *Staphylotrichum* species. ITS and LSU sequences indicate that *H. koreana* belongs to *Staphylotrichum* (Supplementary Fig. S4). No *rpb2* and *tub2* sequences are available for this species and it is therefore not included in our multigene phylogenetic tree.

Staphylotrichum limonisporum (Z.F. Zhang & L. Cai) X.Wei Wang & Houbraken, ***comb. nov.*** MycoBank MB 840162.
Basionym: *Humicola limonispora* [as '*limonisporum*'] Z.F. Zhang & L. Cai, Persoonia 39: 15. 2017.

Notes: *Staphylotrichum limonisporum* was originally described as a *Humicola* species (Zhang *et al.* 2017a). This was mainly due to the limited taxon sampling in their phylogenetic analysis. The phylogenetic position in *Staphylotrichum* is supported by multigene phylogeny (Fig. 7B), as well as the *tub2* and *rpb2* phylogenies (Supplementary Figs S2, S3). *Staphylotrichum limonisporum* is the only known *Staphylotrichum* species that produces ascomata without a conspicuous neck. Molecular dating indicated that this species diverged from the other *Staphylotrichum* species about 35 Mya. Considering that *Staph. limonisporum* produces similar ascospores and conidia as those of typical *Staphylotrichum* species, it is transferred to *Staphylotrichum* above.

Subramaniula Arx, Proc. Indian Acad. Sci., Pl. Sci. 94: 344. 1985.

Micromorphology: Containing sexual species and asexual species. Sexual species: *Ascomata* superficial to immersed in the medium, ostiolate, urniform, subglobose or ovoid. *Ascomatal wall* brown, usually composed of *textura angularis* in surface view. *Ascomatal hairs* absent or present and highly diverse, if present, hypha-like, flexuous or undulate, sometimes coiled in the upper part, or apically irregularly-curved and branched repeatedly to form a network in some species. *Asci* fasciculate, clavate, fusiform or obovate, stalked, containing eight ascospores, evanescent. *Ascospores* olivaceous brown or dark brown when mature, smooth, fusiform or ellipsoidal-fusiform, sometimes inaequilateral or irregular, not bilaterally flattened, with an apical, subapical or lateral germ pore. *Asexual morph* unknown. Asexual species: *Somatic hyphae* hyaline, sometimes becoming pigmented with age, or forming chlamydospore- or microsclerotium-like structures. *Chlamydospores* formed in chains, pigmented, thick-walled. *Microsclerotium-like structures* composed of brown or dark brown, thick-walled, subglobose or irregular cells. *Conidiophores* phialidic, terminally or intercalary from hyphae, hyaline, cylindrical, obclavate or reduced to conidiogenous cells. *Conidia* smooth-walled, hyaline, unicellular, obovoidal or ellipsoidal in slimy heads or in basipetal chains. *Sexual morph* unknown.

Type species: *Subramaniula thielavioides* (Arx *et al.*) Arx

Notes: *Subramaniula* species exhibit a highly diverse morphology. Three asexually-reproducing species (*Sub. anamorphosa*, *Sub. asteroides* and *Sub. obscura*) are opportunistic human pathogens that were once misclassified as *Papulaspora* spp. (Ahmed *et al.* 2016). These asexual species intermingle among the sexual species in the phylogenetic tree (Fig. 7C), although their sexual morphs are unknown. One new species is described here and an additional chaetomium-like species is transferred to this genus. In total, seven sexual species are now included in the genus with no asexual morph observed. *Subramaniula thielavioides*, the type species, produces glabrous ascomata, while the other species have ascomata covered by different ascomatal hairs.

Subramaniula latifusispora X.Wei Wang, P.J. Han & F.Y. Bai, ***sp. nov.*** MycoBank MB 840129. Fig. 41.

Etymology: The name refers to the ascospores, which are broader than those of its closest relative *Subramaniula fusispora*.

Micromorphology: *Ascomata* superficial, ostiolate, olivaceous buff due to ascomatal hairs in reflected light, then becoming greenish black due to ascospores aggregating on the top, ovate or subglobose, 140–220 µm high, 125–190 µm diam. *Ascomatal wall* brown, of *textura angularis* in surface view. *Terminal hairs* brown, septate, fading towards the tips, flexuous in the lower part, 2–3 µm diam near the base, coiled or undulate in the upper part. *Lateral hairs* flexuous, undulate or slightly coiled. *Asci* fasciculate, fusiform or clavate, spore-bearing part 32–45 × 16–21 µm, with stalks 10–20.5 µm long, containing eight biseriate or irregularly-arranged ascospores, evanescent. *Ascospores* olivaceous brown when mature, fusiform, (11–)13–15.5(–17.5) × 7.5–9(–11) µm, with a subapical or lateral germ pore. *Asexual morph* unknown.

Culture characteristics: On OA with an entire edge, 28–38 mm diam in 7 d at 25 °C, without aerial hyphae, obverse luteous or ochreous to orange due to exudates diffusing into the medium, often forming ascomata sparsely; reverse luteous to ochreous or orange. On CMA similar to those on OA, 23–33 mm diam after 7 d at 25 °C. On MEA with an entire edge, 25–35 mm diam in 7 d at 25 °C, without aerial hyphae, obverse orange with a luteous edge due to exudates diffusing into the medium, forming ascomata; reverse orange with a luteous edge. On PCA with an entire edge, 26–33 mm diam in 7 d at 25 °C, without aerial hyphae, sparsely forming ascomata, obverse amber in the centre due to exudates diffusing into the medium; reverse amber in the centre due to exudates diffusing into the medium.

Material examined: **Canada**, Banff, isolated from dung of marmot, 10 Sep. 1977, D.W. Malloch (culture CBS 199.84). **China**, Gongliu Forest Farm in Yili, Xinjiang, isolated from dung of sheep, Aug. 2004, X.W. Wang (**holotype** HMAS 350267, culture ex-type CGMCC 3.20442 = WXW 8538); near Sayram Lake in Yili, Xinjiang, isolated from fallen spruce fruit, Aug. 2004, X.W. Wang (WXW 8577).

Notes: *Subramaniula latifusispora* is phylogenetically related, but separate, to *Sub. fusispora* (Fig. 7C). Morphologically, *Sub. latifusispora* can be distinguished from *Sub. fusispora* by broader ascospores (13–15.5 × 7.5–9 µm *vs* 12.5–14.5 × 6.5–7 µm) and luteous or ochreous to orange exudates on OA.

Subramaniula lateralis (Yu Zhang & L. Cai) X.Wei Wang & Houbraken, ***comb. nov.*** MycoBank MB 840164.
Basionym: *Chaetomium laterale* Yu Zhang & L. Cai, Fungal Biol. 121: 30. 2017.

Notes: *Subramaniula lateralis* is characterised by hypha-like ascomatal hairs that are flexuous or slightly undulate, and by fusiform ascospores with a subapical germ pore (Zhang *et al.* 2017a). It is closely related to the asexual species *Sub. asteroides* (Fig. 7C). *Subramaniula flavipila* (= *Chaetomium irregulare*) also produces hypha-like ascomatal hairs, but can be distinguished by ascospores with an apical germ pore.

Tengochaeta X.Wei Wang & Houbraken, ***gen. nov.*** MycoBank MB 830915.

Etymology: Named after S.C. Teng (1902–1975), honouring his pioneering study on Chinese *Chaetomiaceae*.

Micromorphology: *Ascomata* superficial, often covered by aerial mycelium, ostiolate, ellipsoidal or subglobose, sometimes forming two ostioles from one ascoma. *Ascomatal wall* brown, composed of angular or irregular cells. *Terminal hairs* brown, septate, verrucose, flexuous to undulate, unbranched. *Lateral hairs* similar to terminal ones. *Asci* pyriform or broadly clavate, evanescent. *Ascospores* olivaceous brown when mature, ellipsoidal to fusiform, attenuated at both ends, often slightly inequilateral, with an apical germ pore. *Asexual morph* unknown.

Type species: *Tengochaeta nigropilosa* X.Wei Wang & Houbraken

Tengochaeta nigropilosa X.Wei Wang & Houbraken, ***sp. nov.*** MycoBank MB 840130. Fig. 42.

Etymology: The name refers to the ascomatal hairs of the species that look like dark hairs fully covering the ascoma.

Micromorphology: *Ascomata* superficial, often covered by white aerial mycelium, solitary or clustered, grey olivaceous due to ascomatal hairs in reflected light, ellipsoidal or subglobose, ostiolate, sometimes forming two ostioles from one ascoma, 105–195 µm high, 85–140 µm diam, or 130–280 µm diam when with two ostioles. *Ascomatal wall* brown, composed of angular or irregular cells. *Terminal hairs* brown, septate, verrucose, flexuous to undulate, unbranched, 2–3 µm diam near the base. *Lateral hairs* similar to terminal ones, but shorter. *Asci* pyriform or broadly clavate, spore-bearing part 25–30 × 13–16.5 µm, with stalks being 8–13 µm long, containing eight irregularly-arranged ascospores, evanescent. *Ascospores* olivaceous brown when mature, ellipsoidal to fusiform, attenuated at both ends, often slightly inequilateral, (9.5–)10.5–12(–12.5) × (5.5–)6–7 µm, with an apical germ pore. *Asexual morph* unknown.

Culture characteristics: On OA with an entire edge, 27–33 mm diam in 7 d at 25 °C, obverse ochreous to umber due to coloured exudates diffusing into the medium, or forming thick aerial mycelium, texture floccose; reverse apricot. On CMA with an entire edge, 25–31 mm diam in 7 d at 25 °C, obverse white due to thick aerial mycelium, texture floccose, often pale luteous at the edge due to coloured exudates diffusing into the medium; reverse pale luteous to orange. On MEA with an entire edge, 32–38 mm diam in 7 d at 25 °C, texture floccose, obverse white due to thick aerial mycelium, reverse apricot to scarlet. On PCA with an entire edge, 25–31 mm diam in 7 d at 25 °C, obverse white due to aerial mycelium, without coloured exudates; reverse uncoloured or pale luteous in the centre.

Material examined: **Spain**, Tenerife, Aguamansa, isolated from soil in *Pinus* forests, date unknown, M. Dreyfuss (**holotype** CBS H-24774, culture ex-type CBS 639.83).

Notes: Based on morphology, von Arx *et al.* (1986) identified CBS 639.83 as *Ch. hispanicum* (= *Par. hispanicum*). Our phylogenetic analysis shows that CBS 639.83 is distinct from *Parachaetomium* (Fig. 7A) and forms a separate lineage, with no statistically supported close relatives (Fig. 7C). *Tengochaeta nigropilosa* and *Par. hispanicum* have different morphologies. *Tengochaeta nigropilosa* can be distinguished from *Par. hispanicum* (Fig. 34) by

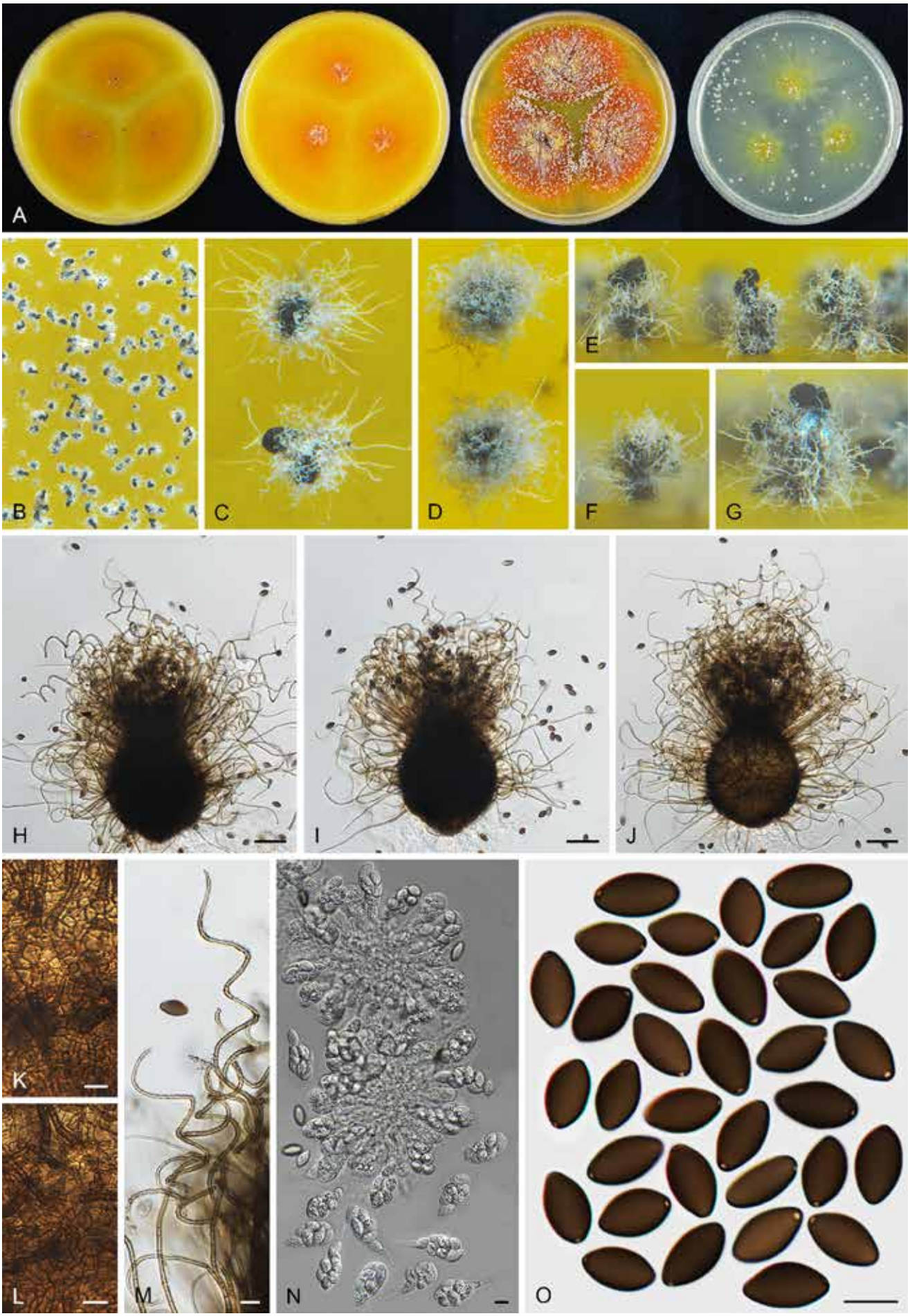

Fig. 41. *Subramaniula latifusispora* (CGMCC 3.20442, ex-type culture). **A.** Colonies from left to right on OA, CMA, MEA and PCA after 3 wk incubation. **B.** Part of the colony. **C, D.** Mature ascomata on OA, top view. **E–G.** Mature ascomata on OA, side view. **H–J.** Ascomata mounted in lactic acid. **K, L.** Structure of ascomatal wall in surface view. **M.** Terminal ascomatal hairs. **N.** Asci. **O.** Ascospores. Scale bars: H–J = 50 µm; K–O = 10 µm.

producing darker ascomatal hairs which are flexuous to undulate and often covered by aerial mycelium, pyriform or broadly clavate asci, while *Par. hispanicum* produces straight or flexuous, hyphae-like ascomatal hairs and clavate asci. *Tengochaeta nigropilosa* also produces smaller ascospores than those of *Par. hispanicum* (10.5–12 × 6–7 µm *vs* 12–14 × 7–8 µm).

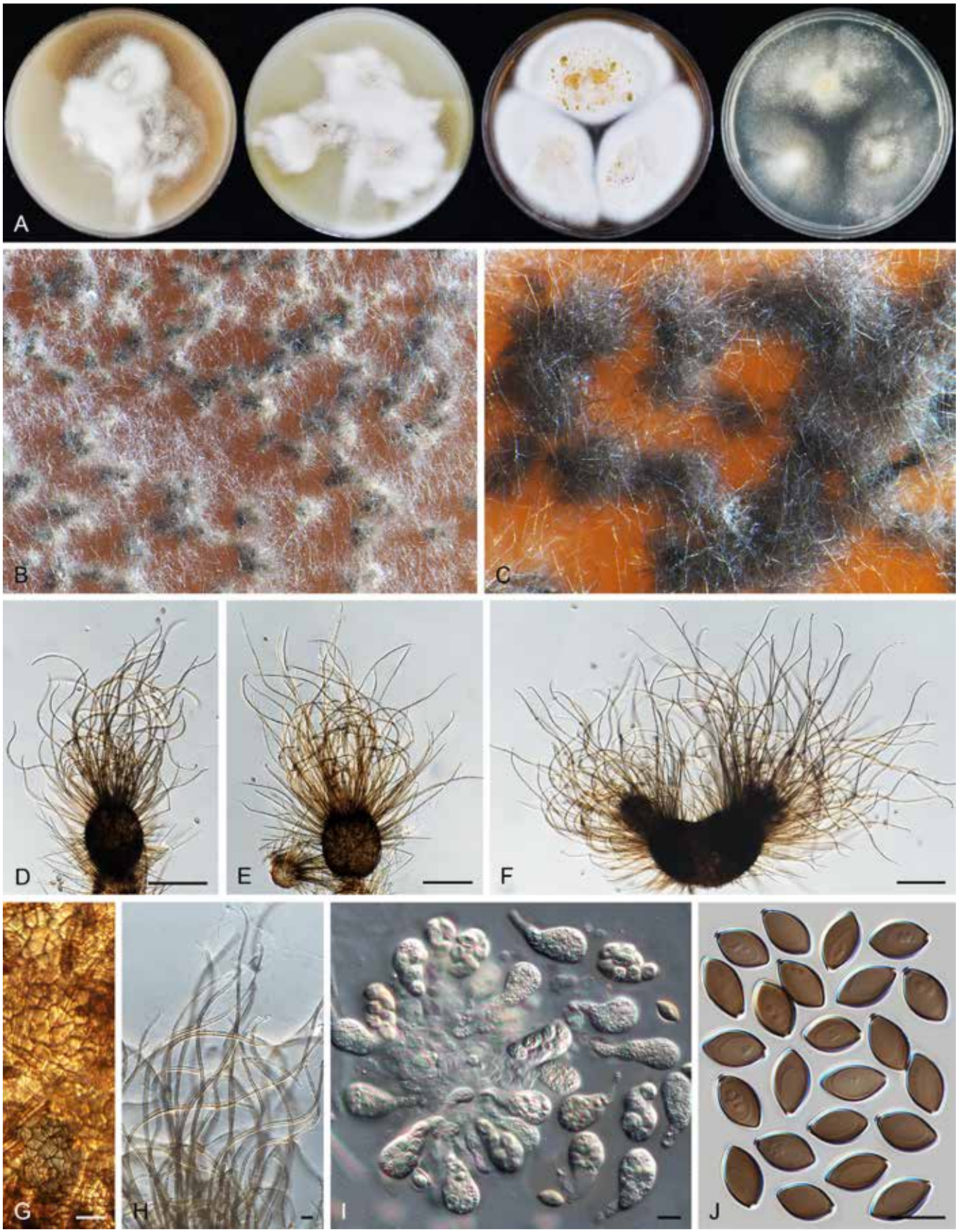

Fig. 42. *Tengochaeta nigropilosa* (CBS 639.83, ex-type culture). **A.** Colonies from left to right on OA, CMA, MEA and PCA after 3 wk incubation. **B.** Part of the colony. **C.** Mature ascomata on OA, top view. **D–F.** Ascomata mounted in lactic acid. **G.** Structure of ascomatal wall in surface view. **H.** Terminal ascomatal hairs. **I.** Asci. **J.** Ascospores. Scale bars: D–F = 100 µm; G–J = 10 µm.

Thermocarpiscus X.Wei Wang & Houbraken, ***gen. nov.*** MycoBank MB 840163.

Etymology: The name refers to the thermophilic nature of the genus and the production of small cleistothecia.

Micromorphology (*fide* Tansey & Jack 1975): *Ascomata* superficial, spherical, glabrous, usually less than 100 µm diam, black when mature in reflected light due to the dark ascomatal wall. *Ascomatal wall* brown, composed of *textura epidermoidea* in surface view. *Asci* broadly ovate to subglobose, containing eight irregularly-arranged ascospores. *Ascospores* 1-celled, smooth, olivaceous brown when mature, ovate, with an apical germ pore. *Conidiophores* absent. *Conidiogenous cells* arising laterally or terminally from hyphae, or reduced to a hyphal cell, monoblastic. *Conidia* 1-celled, solitary, hyaline, smooth, usually ovoid. Containing one species with both sexual and asexual morph.Thermophilic.

Type species: *Thermocarpiscus australiensis* (Tansey & M.A. Jack) X.Wei Wang & Houbraken

Notes: This is a monotypic genus. The ex-type culture of the type species CBS 493.74 is in poor condition and is no longer producing ascomata, and we failed to study the phenotypic characteristics of this species. According to the original description, the species had a growth minimum temperature of 20 °C and they observed that the fungus grew at above 50 °C.

Thermocarpiscus australiensis (Tansey & M.A. Jack) X.Wei Wang & Houbraken, ***comb. nov.*** MycoBank MB 840165.
Basionym: *Thielavia australiensis* Tansey & M.A. Jack, Canad. J. Bot. 53: 81. 1975.

Micromorphology and illustrations: See Tansey & Jack (1975).

Thermochaetoides X.Wei Wang & Houbraken, ***gen. nov.*** MycoBank MB 830916.

Etymology: The name refers to the thermophilic habit and its morphological similarity to *Chaetomium*.

Micromorphology: *Ascomata* superficial, subglobose or ovoid, ostiolate. *Ascomatal wall* brown, composed of irregular or angular cells. *Ascomatal hairs* brown, flexuous, usually tortuous or geniculate, unequally thickened and being frequently and irregularly constricted along their length, dichotomously or irregularly branched, verrucose, septate. *Asci* fasciculate, cylindrical, occasionally elongated clavate, stalked, containing eight uniseriate (occasionally biseriate) ascospores, evanescent. *Ascospores* olivaceous when mature, single-celled, smooth, globose, subglobose or broad ovoid, bilaterally flattened, with a distinctly protuberant apical germ pore. *Asexual morph* unknown.

Type species: *Thermochaetoides thermophila* (La Touche) X.Wei Wang & Houbraken

Notes: Our phylogenetic analysis (Fig. 7D) shows that this genus forms an isolated lineage with no known close relatives in the *Chaetomiaceae*. After the description of *Chaetomium thermophilum* (La Touche 1950), Cooney & Emerson (1964) proposed two new varieties based on cultural characteristics. In our phylogenetic analyses, these varieties clearly group into two lineages (Fig. 7D, Supplementary Figs S1–S3). We here propose two new combinations, *Thermoc. dissita* and *Thermoc. thermophila* (see below).

Thermochaetoides dissita (Cooney & R. Emers.) X.Wei Wang & Houbraken, ***comb. nov.*** MycoBank MB 830932. Fig. 43.
Basionym: *Chaetomium thermophilum* var. *dissitum* Cooney & R. Emers., Thermophilic Fungi: 68. 1964.

Micromorphology: *Ascomata* superficial, pale olivaceous grey due to ascomatal hairs in reflected light, subglobose or ovoid, ostiolate, 100–200 µm high, 90–155 µm diam. *Ascomatal wall* brown, composed of irregular or angular cells. *Terminal hairs* brown, geniculate and flexuous, dichotomously or irregularly branched, verrucose, septate, 2–4 µm diam near the base. *Lateral hairs* similar but sparse and shorter. *Asci* cylindrical, sometimes elongated clavate or elongated obclavate, spore-bearing part 32–52 × 7.5–11 µm, with stalks being 4–8 µm long, containing eight uniseriate, occasionally biseriate ascospores, evanescent. *Ascospores* olivaceous when mature, globose, subglobose or ovoid, bilaterally flattened, (6.5–)7–8(–9) × (6–)6.5–7.5(–9) × (4.5–)5–5.5(–6) µm, with a distinctly protuberant apical germ pore. *Asexual morph* unknown.

Culture characteristics: Optimum growth temperature 45–55 °C. On OA with an entire or slightly crenate edge, over 70 mm diam in 3 d at 45 °C, obverse pale smoke grey to grey olivaceous; reverse smoke grey. On CMA similar to those on OA. On MEA with an entire edge, over 70 mm diam in 3 d at 45 °C, obverse olivaceous buff or smoke grey, radially or irregularly striated due to wrinkling; reverse dark mouse grey. On PCA with an entire or slightly crenate edge, over 70 mm diam in 3 d at 45 °C, obverse mouse grey to dark mouse grey; reverse mouse grey.

Material examined: **Israel**, isolated from dung of gazelle, date unknown, E. Müller (CBS 785.71). **Netherlands**, isolated from dung of pig with sawdust, date unknown, G. Straatsma & Proefstation voor de Champignoncultuur (CBS 246.90). **USA**, California, Alameda Co., isolated from straw of *Typha* used as nesting material by the common coot or mud hen, 1949, D.G. Cooney & R. Emerson (culture ex-type CBS 180.67 = ATCC 16452 = DSM 1494 = IMI 126332).

Notes: *Thermochaetoides dissita* can be distinguished from *Thermoc. thermophila* by smaller ascospores (7–8 × 6.5–7.5 × 5–5.5 µm *vs* 8–9.5 × 8–9 × 5.5–6.5 µm) and the absence of crenate concentric rings in colonies grown on OA and CMA. Colonies of this species grow faster at 45 °C (over 70 mm diam *vs* < 60 mm diam on MEA after 3 d) and ascomata often develop discretely over the colony. Furthermore, *Thermoc. thermophila* has numerous ascomatal hairs covering the whole ascoma without differentiation of terminal and lateral hairs, while distinct forms of terminal and lateral hairs can be found in *Thermoc. dissita*.

Thermochaetoides thermophila (La Touche) X.Wei Wang & Houbraken, ***comb. nov.*** MycoBank MB 830933. Figs 44, 45.
Basionym: *Chaetomium thermophilum* La Touche (as '*thermophile*'), Trans. Brit. Mycol. Soc. 33: 95. 1950.
Synonyms: *Chaetomium thermophilum* var. *thermophilum* La Touche, Trans. Brit. Mycol. Soc. 33: 95. 1950.
Chaetomium thermophilum var. *coprophilum* Cooney & R. Emers., Thermophilic Fungi: 68. 1964.

Micromorphology: *Ascomata* superficial, olivaceous grey or greyish sepia due to ascomatal hairs in reflected light, subglobose, ostiolate,

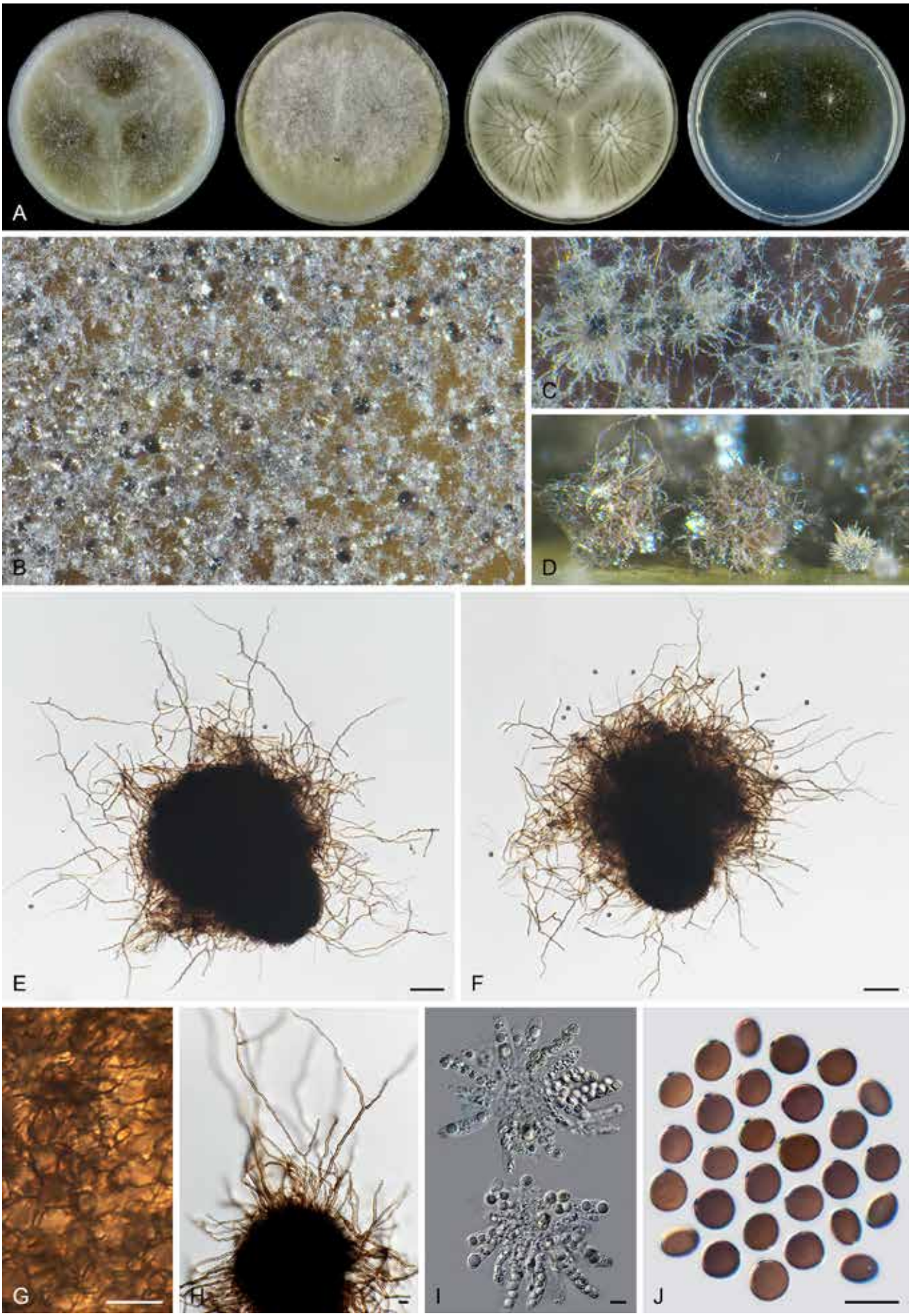

Fig. 43. *Thermochaetoides dissita* (CBS 180.67, ex-type culture). **A.** Colonies from left to right on OA, CMA, MEA and PCA after 3 d incubation at 45 °C. **B.** Part of the colony. **C.** Mature ascomata on OA, top view. **D.** Mature ascomata on OA, side view. **E, F.** Ascomata mounted in lactic acid. **G.** Structure of ascomatal wall in surface view. **H.** Terminal ascomatal hairs. **I.** Asci. **J.** Ascospores. Scale bars: E, F = 50 µm; G–J = 10 µm.

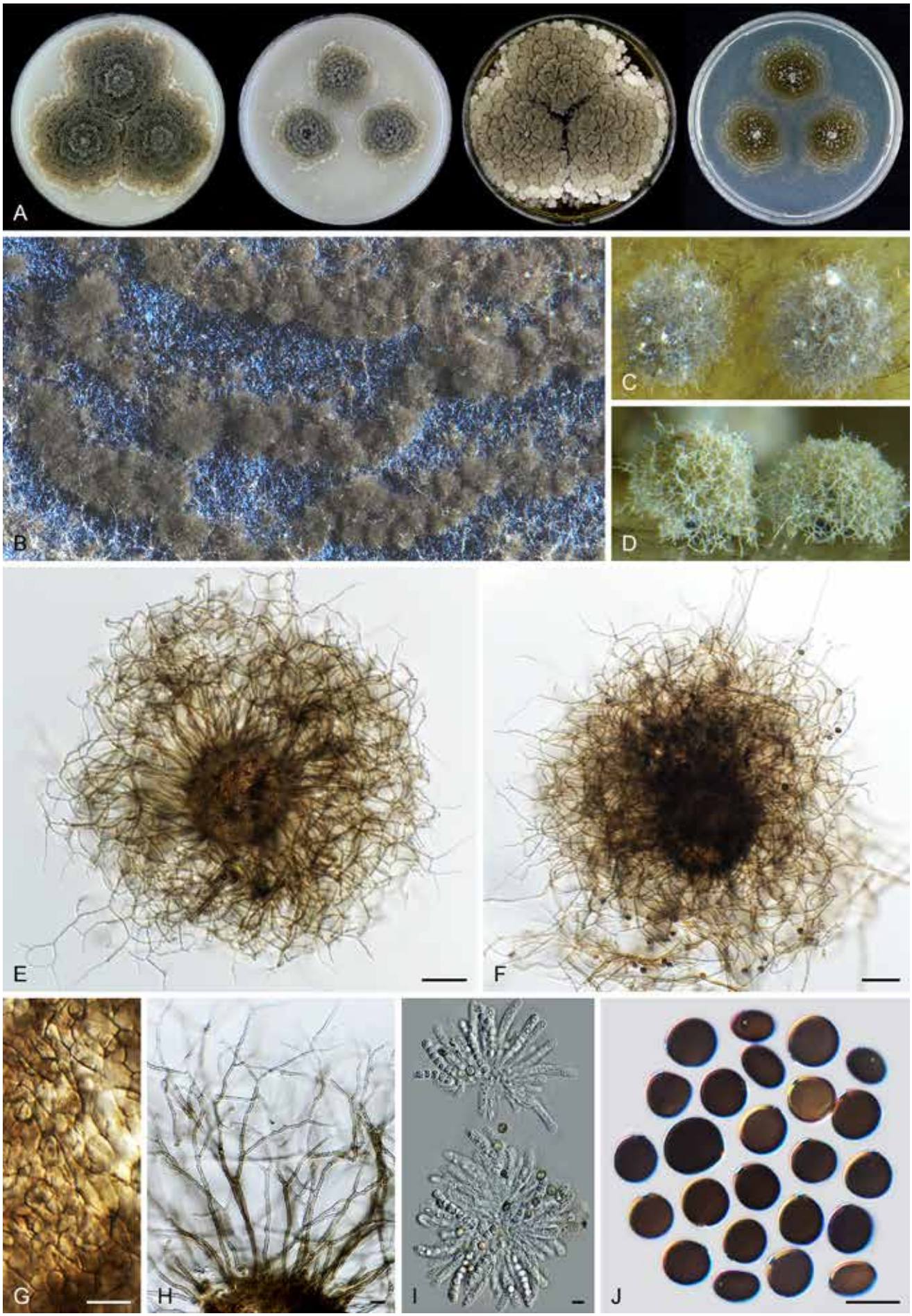

Fig. 44. *Thermochaetoides thermophila* (CBS 144.50, ex-type culture). **A.** Colonies from left to right on OA, CMA, MEA and PCA after 3 d incubation at 45 °C. **B.** Part of the colony. **C.** Mature ascomata on OA, top view. **D.** Mature ascomata on OA, side view. **E, F.** Ascomata mounted in lactic acid. **G.** Structure of ascomatal wall in surface view. **H.** Terminal ascomatal hairs. **I.** Asci. **J.** Ascospores. Scale bars: E, F = 50 µm; G–J = 10 µm.

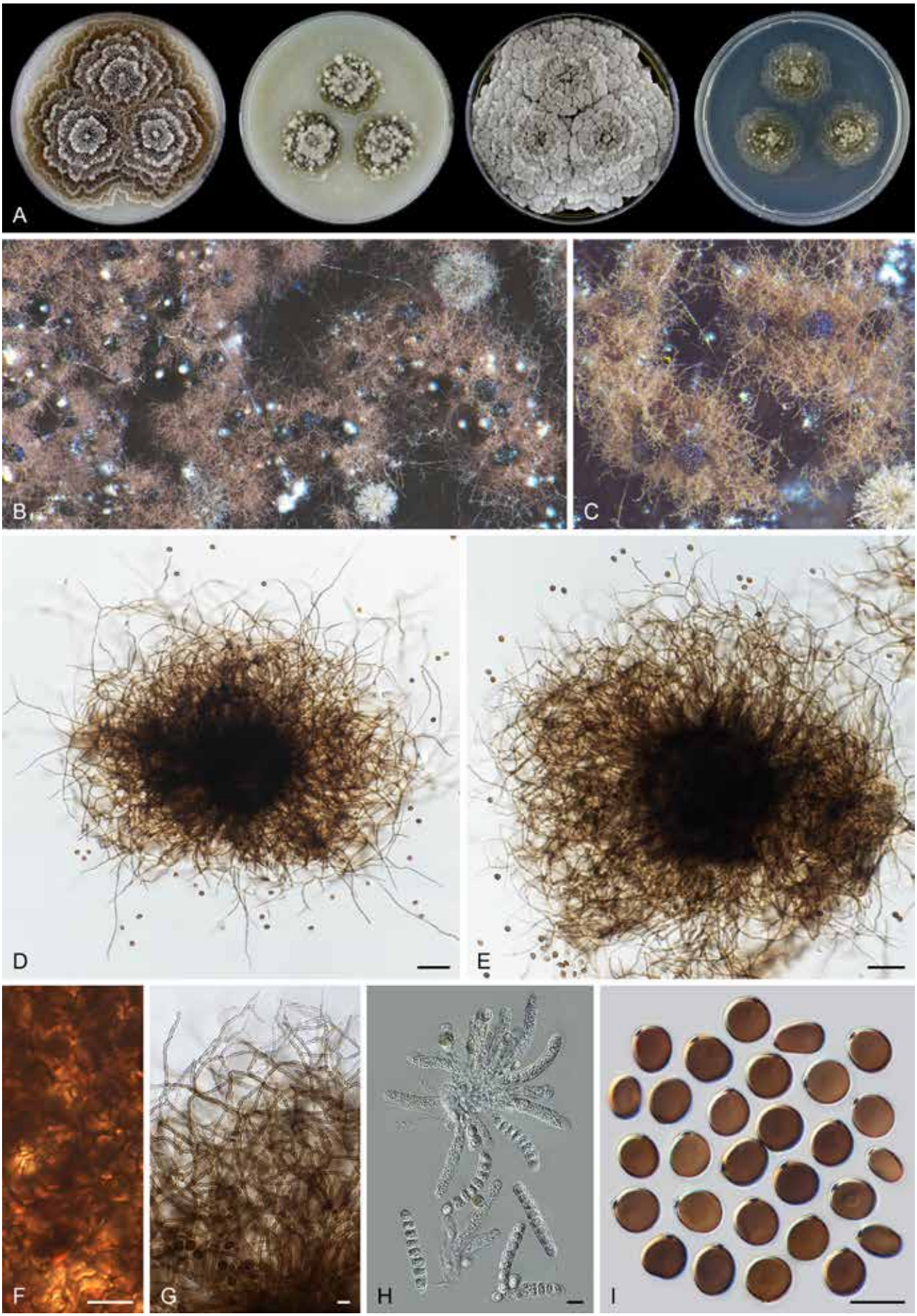

Fig. 45. *Thermochaetoides thermophila* (CBS 179.67). **A.** Colonies from left to right on OA, CMA, MEA and PCA after 3 d incubation at 45 °C. **B, C.** Part of the colony, showing ascomata on OA, top view. **D, E.** Ascomata mounted in lactic acid. **F.** Structure of ascomatal wall in surface view. **G.** Terminal ascomatal hairs. **H.** Asci. **I.** Ascospores. Scale bars: D, E = 50 µm; F–I = 10 µm.

(80–)105–160 µm diam. *Ascomatal wall* brown, composed of irregular or angular cells. *Ascomatal hairs* numerous, covering the whole ascoma with no differentiation between terminal hairs and lateral hairs, brown, geniculate and flexuous, dichotomously or irregularly branched, verrucose, septate, 2–4 µm diam near the base. *Asci* cylindrical, spore-bearing part 46–58 × 8–11.5 µm, with stalks being 6–17 µm long, containing eight uniseriate ascospores, evanescent. *Ascospores* olivaceous when mature, globose, subglobose or ovoid, bilaterally flattened, 8–9.5(–10.5) × (7.5–)8–9(–9.5) × 5.5–6.5 µm, with a distinctly protuberant germ pore. *Asexual morph* unknown.

Culture characteristics: Optimum growth temperature 45–55 °C. On OA with a crenate-lobate edge, 44–73 mm diam in 3 d at 45 °C, obverse smoke grey to mouse grey or greyish sepia, with several crenate concentric rings due to the formation of ascomata; reverse olivaceous or fawn. On CMA with a crenate-lobate edge, 25–55 mm diam in 3 d at 45 °C, obverse smoke grey or olivaceous buff to greenish olivaceous, sometimes with crenate concentric rings; reverse pale mouse grey. On MEA with a crenate-lobate edge, 53–over 70 mm diam in 3 d at 45 °C, obverse pale mouse grey or olivaceous grey, radially or irregularly striated to form several concentric rings; reverse iron grey. On PCA with a lobate edge, 26–62 mm diam in 7 d at 45 °C, obverse smoke grey to grey olivaceous or mouse grey to olivaceous grey, with several lobate concentric rings; reverse pale olivaceous grey to olivaceous grey or hazel.

Material examined: **Netherlands**, isolated from mushroom compost, date unknown, H.C. Bels-Koning (CBS 166.62). **Switzerland**, isolated from mushroom compost, date unknown, E. Müller (CBS 141.64). **UK**, Leeds, isolated from decaying wheat straw, 1949, C.J. La Touche (culture ex-type CBS 144.50 = DAOM 24625 = DSM 1495 = IMI 039719; CBS 143.50). **USA**, California, Alameda Co., isolated from horse dung, 1950, D.G. Cooney & R. Emerson (CBS 179.67, ex-type culture of *Chaetomium thermophilum* var. *coprophilum*).

Notes: The variety *Ch. thermophilum* var. *coprophilum* (Fig. 45) is morphologically undistinguishable from the ex-type culture of *Ch. thermophilum* (Fig. 44). Our phylogenetic analysis confirmed that these two taxa are conspecific (Fig. 7D, Supplementary Figs S1–S3). *Thermochaetoides thermophila* can easily be distinguished from *Thermoc. dissita*, as noted above.

Thermothelomyces Y. Marín *et al.*, Mycologia 107: 630. 2015.

Micromorphology: *Asexual morph*: *Conidiophores* hypha-like, sometimes simply branched, or reduced to conidiogenous cells. *Conidiogenous cells* reduced to a hyphal cell, or terminally or occasionally laterally from conidiophores, solitary, sometimes verticillate, or in short unbranched or branched chain, sometimes swollen, subglobose, fusiform, clavate or ampulliform, monoblastic or synchronously polyblastic with two or more conidia developing from one conidiogenous cell. *Conidia* solitary or in short chains, single-celled, mostly hyaline and smooth, in a few species pigmented and verrucose, ovoid, ellipsoidal, pyriform or subglobose, often apically rounded, in a few species apically attenuated, with a narrow and truncate base, rhexolytic when seceding. In one species (*Thermoth. myriococcoides*), only sterile microsclerotia-like structures were formed, mainly in aerial mycelium, subglobose, ellipsoidal to irregular, composed of angular or irregular cells, surrounded by several layers of outer cells; conidial morph not observed. *Sexual morph* (*fide* Fergus & Sinden 1969, von Klopotek 1976) not observed in the culture of an individual strain, but in two heterothallic species (*Thermoth. fergusii* and *Thermoth. heterothallicus*), different and compatible strains growing together induce the formation of ascomata. *Ascomata*, if present, superficial, sub-immersed to immersed, non-ostiolate, globose, glabrous, black when mature. *Asci* globose, ovoid, clavate or ellipsoidal, containing four or eight ascospores, evanescent. *Ascospores* brown when mature, unicellular, ellipsoidal or ovoid, with one or two apical germ pores. The genus contains asexual species and heterothallic species with asexual and sexual morphs when both mating types present. Thermophilic.

Type species: *Thermothelomyces thermophilus* (Apinis) Y. Marín *et al.*

Notes: Marín-Felix *et al.* (2015) segregated the thermophilic species of *Myceliophthora sensu* van den Brink *et al.* (2012) into two genera: *Crassicarpon* (with hyaline, smooth-walled conidia) and *Thermothelomyces* (with brown, ornamented conidia). The present study does not accept the invalidly described genus *Crassicarpon* (Art. F.5.1). Three of the four species in *Thermothelomyces sensu* Marín-Felix *et al.* (2015) are observed to produce hyaline and smooth conidia (Figs 46–48), which means that "*Crassicarpon*" and *Thermothelomyces* species have, besides their thermophilicity, also overlapping morphological characters. In addition, molecular dating analysis shows that divergence between "*Crassicarpon*" and *Thermothelomyces sensu* Marín-Felix *et al.* (2015) happened more recently (at about 18 Mya) than the later time limit (at about 27 Mya, Figs 8B, 9) of the other accepted genera in the family. We therefore merge "*Crassicarpon*" in *Thermothelomyces sensu* Marín-Felix *et al.* (2015) and redefine this genus. *Thermothelomyces* diverged from the closest relative *Myceliophthora* about 30 Mya (Fig. 8B).

Thermothelomyces fergusii X.Wei Wang & Houbraken, ***nom. nov.*** MycoBank MB 830934. Fig. 46.
Replaced synonym: *Thielavia thermophila* Fergus & Sinden, Canad. J. Bot. 47: 1635. 1969, non *Thermothelomyces thermophilus* (Apinis) Y. Marín *et al.*, Mycologia 107: 630. 2015.
Synonyms: *Chrysosporium fergusii* Klopotek, Arch. Mikrobiol. 98: 366. 1974. (conidial morph).
Corynascus thermophilus (Fergus & Sinden) Klopotek, Arch. Mikrobiol. 98: 366. 1974.
Myceliophthora fergusii (Klopotek) Oorschot, Persoonia 9: 406. 1977.
Crassicarpon thermophilum (Fergus & Sinden) Y. Marín *et al.*, Mycologia 107: 630. 2015, *nom. inval.*, Art. 35.1.

Micromorphology: *Conidiophores* absent. *Conidiogenous cells* reduced to an intercalary or terminal hyphal cell or as a denticle laterally arising from a hyphal cell, monoblastic, or occasionally polyblastic. *Conidia* single-celled, solitary, occasionally in chains of two, smooth, hyaline, subglobose, ovoid, ellipsoidal, pyriform or clavate, usually apically rounded, with a narrow and truncate base, (4–)5–7(–9) × 4–6(–7.5) µm. *Sexual morph* heterothallic formed by crossing between compatible strains (*fide* Fergus & Sinden 1969): *Ascomata* superficial to immersed, non-ostiolate, globose, glabrous, black when mature, 190–260 µm diam. *Asci* globose or ovoid, 30–37 × 40–52 µm, without distinct stalks, containing four irregularly-arranged ascospores, quickly evanescent. *Ascospores* brown when mature, unicellular, ellipsoidal, 23–32 × 17–23 µm, with two apical germ pores.

Culture characteristics: On OA with an entire edge, over 70 mm diam in 3 d at 45 °C, texture floccose, obverse white due to aerial mycelium, without coloured exudates; reverse uncoloured. On

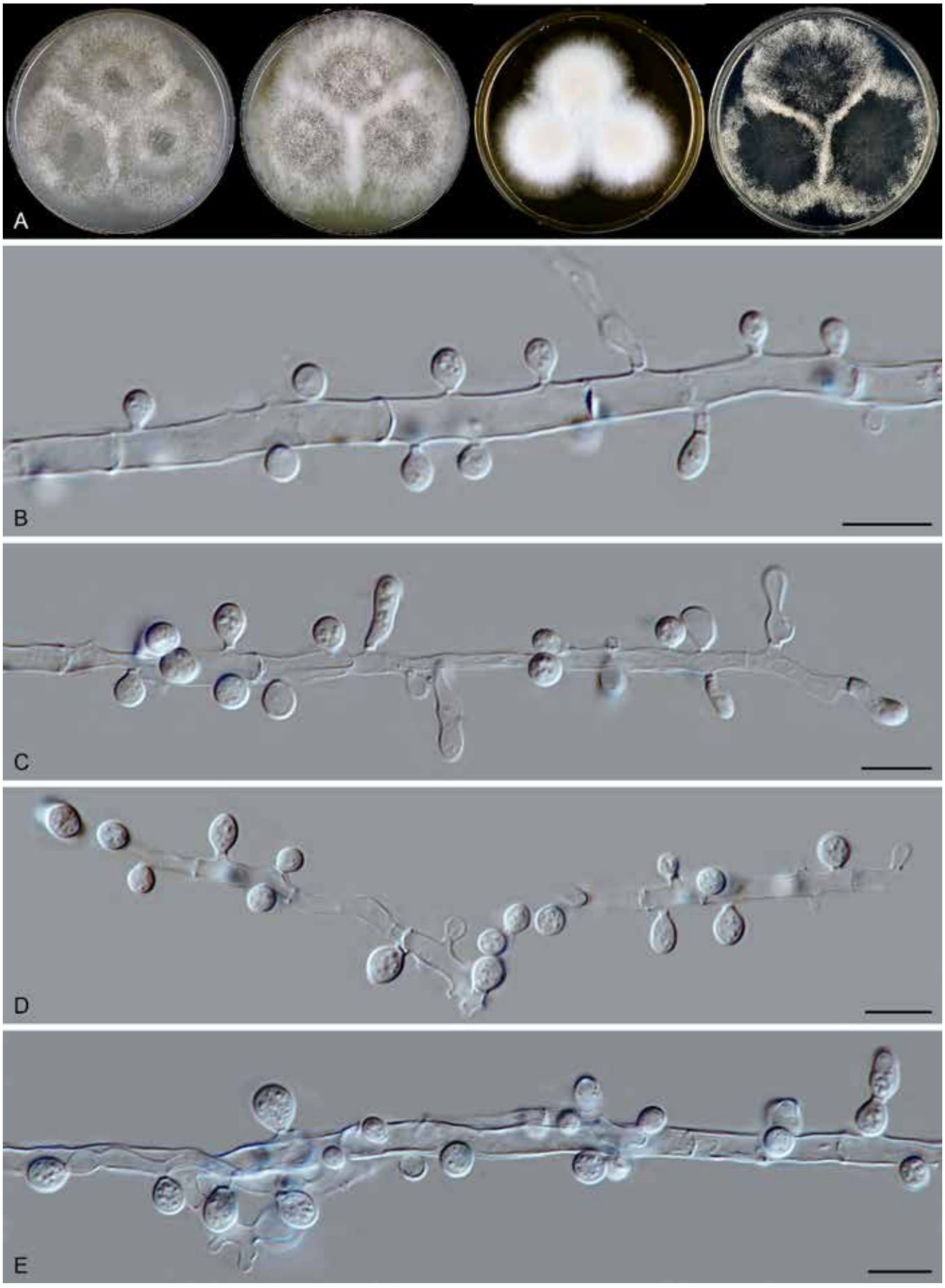

Fig. 46. *Thermothelomyces fergusii* (CBS 406.69, ex-type culture). **A.** Colonies from left to right on OA, CMA, MEA and PCA after 7 d incubation at 37 °C. **B–E.** Hyphae, conidiogenous cells and conidia. Scale bars = 10 µm.

CMA similar to those on OA. On MEA with an entire edge, over 70 mm diam in 3 d at 45 °C, with a thick layer of aerial mycelium, obverse white; reverse uncoloured. On PCA translucent, with an entire edge, over 70 mm diam in 3 d at 45 °C, with sparse aerial mycelium mainly at the margins, without coloured exudates; reverse uncoloured.

Material examined: **UK**, Cambridge, isolated from wheat straw compost, date unknown, H.J. Hudson (CBS 174.70 = IMI 145136). **USA**, Pennsylvania, isolated from mushroom compost, date unknown, C.L. Fergus (culture ex-type CBS 406.69 = ATCC 22067 = R46w2).

Notes: Fergus & Sinden (1969) induced ascomata after growing compatible strains (CBS 406.69 and CBS 405.69) together, and they described this holomorph as *Thielavia thermophila*. Subsequently, von Klopotek (1974) transferred *Thielavia thermophila* to *Corynascus* and redescribed its conidial morph as *Chrysosporium fergusii* (based on "strain S22", isolated from Germany designated as ex-type). He also determined the mating types of the following strains: CBS 405.69 and S22 (+); CBS 406.69 and CBS 174.70 (-). The asexual species was later transferred into *Myceliophthora* as *My. fergusii* by van Oorschot (1977). Based on a three-locus phylogenetic analysis, Marín-Felix *et al.* (2015) combined this species in the invalidly-proposed *Crassicarpon* (published without identifier, Art. F.5.1), a genus related to *Thermothelomyces*. *Crassicarpon* is not accepted here (see notes of *Thermothelomyces* above). In the present study, we only examined the individual strains and did not attempt mating experiments to induce ascomata.

Thermothelomyces guttulatus (Yu Zhang & L. Cai) Y. Marín *et al.*, Mycologia 107: 630. 2015. Fig. 47.
Basionym: *Myceliophthora guttulata* Yu Zhang & L. Cai, Mycol. Prog. 13: 168. 2013.

Micromorphology: *Conidiophores* hypha-like, or simply branched, hyaline, sometimes reduced. *Conidiogenous cells* often several formed in unbranched or branched chains, swollen, subglobose, ellipsoidal, doliiform, ampulliform or fusiform, monoblastic, or polyblastic with two or more conidia formed from one cell, 3.5–6.5(–8) × 2–5.5 µm. *Conidia* solitary or in short chains, single-celled, smooth, hyaline, subglobose, ellipsoidal or ovoid, apically rounded or slightly attenuated, with a narrow and truncate base, (4–)4.5–7.5(–10) × (3–)3.5–5(–5.5) µm diam. *Sexual morph* not observed.

Culture characteristics: On OA with an entire edge, over 70 mm diam in 3 d at 45 °C, texture cottony, obverse white due to the formation of conidia on aerial mycelium, greyish yellow-green around the colonies due to coloured exudates diffusing into the medium; reverse buff. On CMA similar to those on OA, over 70 mm diam in 3 d at 45 °C, reverse cinnamon due to coloured exudates diffusing into the medium. On MEA with an entire edge, over 70 mm diam in 3 d at 45 °C, texture thick cottony, obverse white to pale smoke grey; reverse umber. On PCA translucent, with an entire edge, over 70 mm diam in 3 d at 45 °C, with sparse aerial mycelium, without coloured exudates; reverse uncoloured.

Material examined: **China**, Hunan Province, Yizhang county, Mangshan National Forest Park, isolated from soil, 10 Sep. 2000, W.-P. Wu (culture ex-type CGMCC 3.15185; culture CGMCC 3.15186).

Notes: No sexual morph was observed and we speculate that this species is heterothallic. Mating type analysis in combination with growth experiments might induce ascomata formation. *Thermothelomyces guttulatus* can be distinguished from other species by its swollen conidiogenous cells.

Thermothelomyces heterothallicus (Klopotek) Y. Marín *et al.*, Mycologia 107: 630. 2015. Fig. 48.
Basionym: *Thielavia heterothallica* Klopotek, Arch. Mikrobiol. 107: 223. 1976.
Synonyms: *Corynascus heterothallicus* (Klopotek) Arx, Persoonia 12: 174. 1984.
Myceliophthora heterothallica (Klopotek) van den Brink & Samson, Fungal Diversity 52: 206. 2012, *nom. inval.*, Art. 41.5.

Micromorphology: *Conidiophores* absent. *Conidiogenous cells* reduced to intercalary hyphal cells, or differentiated laterally from hyphae, sometimes two or more in short simple or branched chains, slightly swollen, fusiform, clavate or ampulliform, monoblastic, or polyblastic with two or more conidia developed from one cell, 2–7 × 1–4 µm. *Conidia* solitary or in short chains, single-celled, smooth, hyaline, ovoid, ellipsoidal, pyriform, usually apically rounded, with a narrow and truncate base, (3–)3.5–5(–6.5) × (2–)2.5–3 µm. *Sexual morph* heterothallic formed by crossing between compatible strains (*fide* von Klopotek 1976): *Ascomata* sub-immersed to immersed, non-ostiolate, globose, brown or black when mature, 70–180 µm diam. *Ascomatal wall* composed of *textura epidermoidea*. *Asci* clavate or ellipsoidal, 25–35 × 10–15 µm, with stalks, containing eight ascospores, evanescent. *Ascospores* brown when mature, unicellular, ellipsoidal or ovoid, 7.5–11 × 4.5–7 µm, with one apical germ pore.

Culture characteristics: On OA with an entire edge, 42–55 mm diam in 3 d at 45 °C, with a thick layer of aerial mycelium, texture cottony, obverse white to buff due to the formation of conidia on aerial mycelium; reverse pale luteous. On CMA similar to those on OA, 46–54 mm diam in 3 d at 45 °C, obverse white. On MEA similar to those on OA, 51–58 mm diam in 3 d at 45 °C, obverse white to rosy buff; reverse ochreous. On PCA translucent, with an entire edge, 36–50 mm diam in 3 d at 45 °C, with sparse aerial mycelium, without coloured exudates; reverse uncoloured.

Material examined: **Germany**, Giessen, isolated from garden soil, date unknown, A. von Klopotek (CBS 202.75), (**holotype** CBS H-18810, dried culture of crossing of CBS 202.75 and CBS 203.75, designated by von Klopotek (1976), **epitype** CBS H-24878, designated here, MBT 10004825; culture ex-epitype CBS 202.75) **USA**, Indiana, Bloomington, isolated from soil, 8 Aug. 1974, M.R. Tansey (CBS 203.75); isolated from soil, date and collector unknown (CGMCC 3.13596 = ACCC 30346 = IFFI 2441).

Notes: A holotype specimen was prepared by von Klopotek (1976) consisting of a dried culture of a crossing with CBS 202.75 and CBS 203.75. This specimen, which was later labeled as CBS H-18810 contains many ascomata. Although this specimen demonstrates the sexual component of the life cycle, it is necessary to designate an epitype from one of the strains in order to present the phylogenetic relationship of this species with other ones. Here, we designate CBS H-24878, derived from CBS 202.75, as the epitype. *Thermothelomyces heterothallicus* is phylogenetically closely related to *Thermoth. thermophilus*, but can be distinguished by its simpler conidiogenous structures and the production of conidia with a rounded apex. Within the genus, *Thermot. heterothallicus* is phylogenetically more distant from *Thermoth. fergusii* (Fig. 7A). Nevertheless, the conidial morphs of the two species are quite similar. However, *Thermot.*

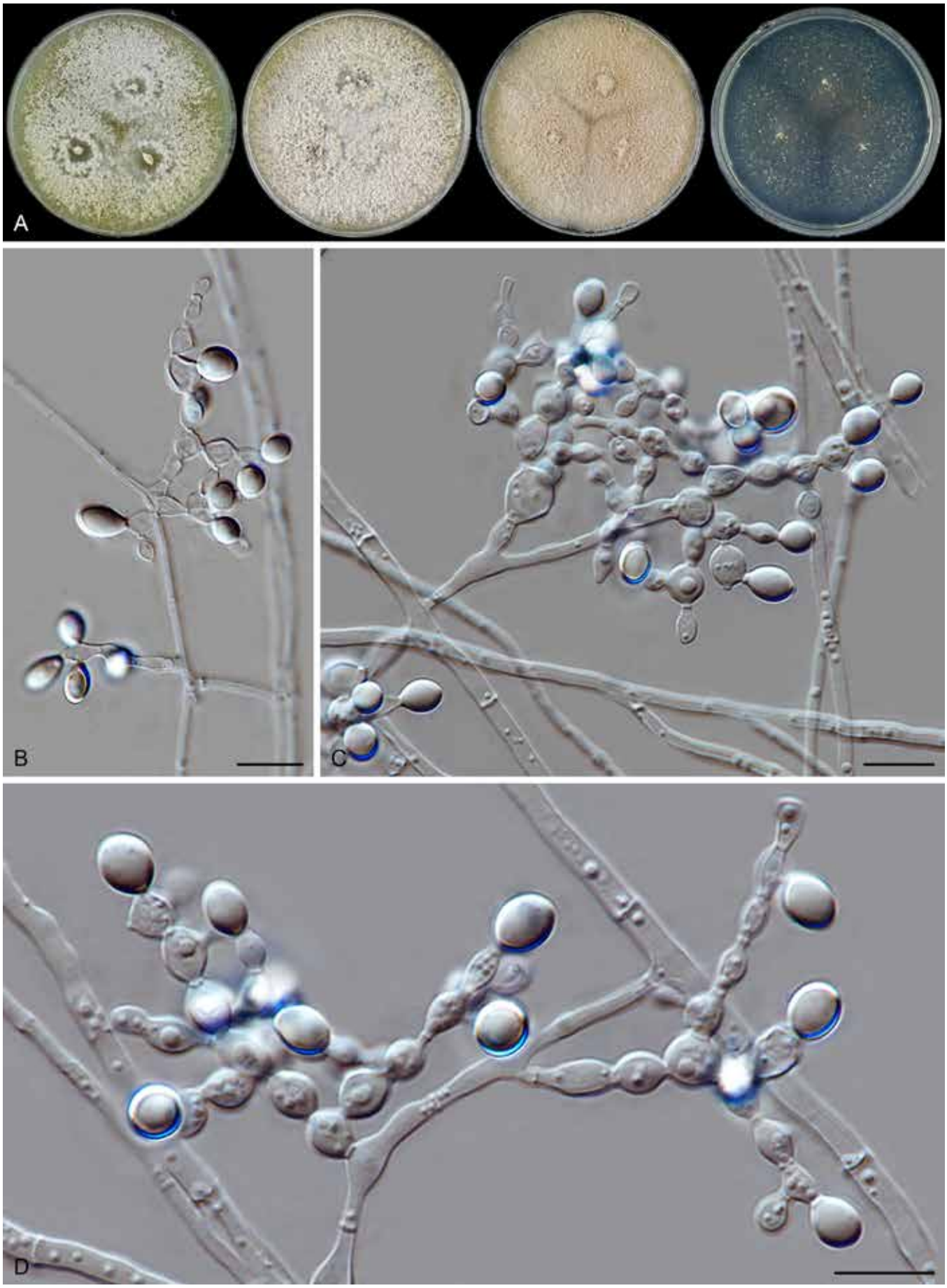

Fig. 47. *Thermothelomyces guttulatus* (CGMCC 3.15185, ex-type culture). **A.** Colonies from left to right on OA, CMA, MEA and PCA after 3 d incubation at 45 °C. **B–D.** Hyphae, conidiogenous cells and conidia. Scale bars = 10 µm.

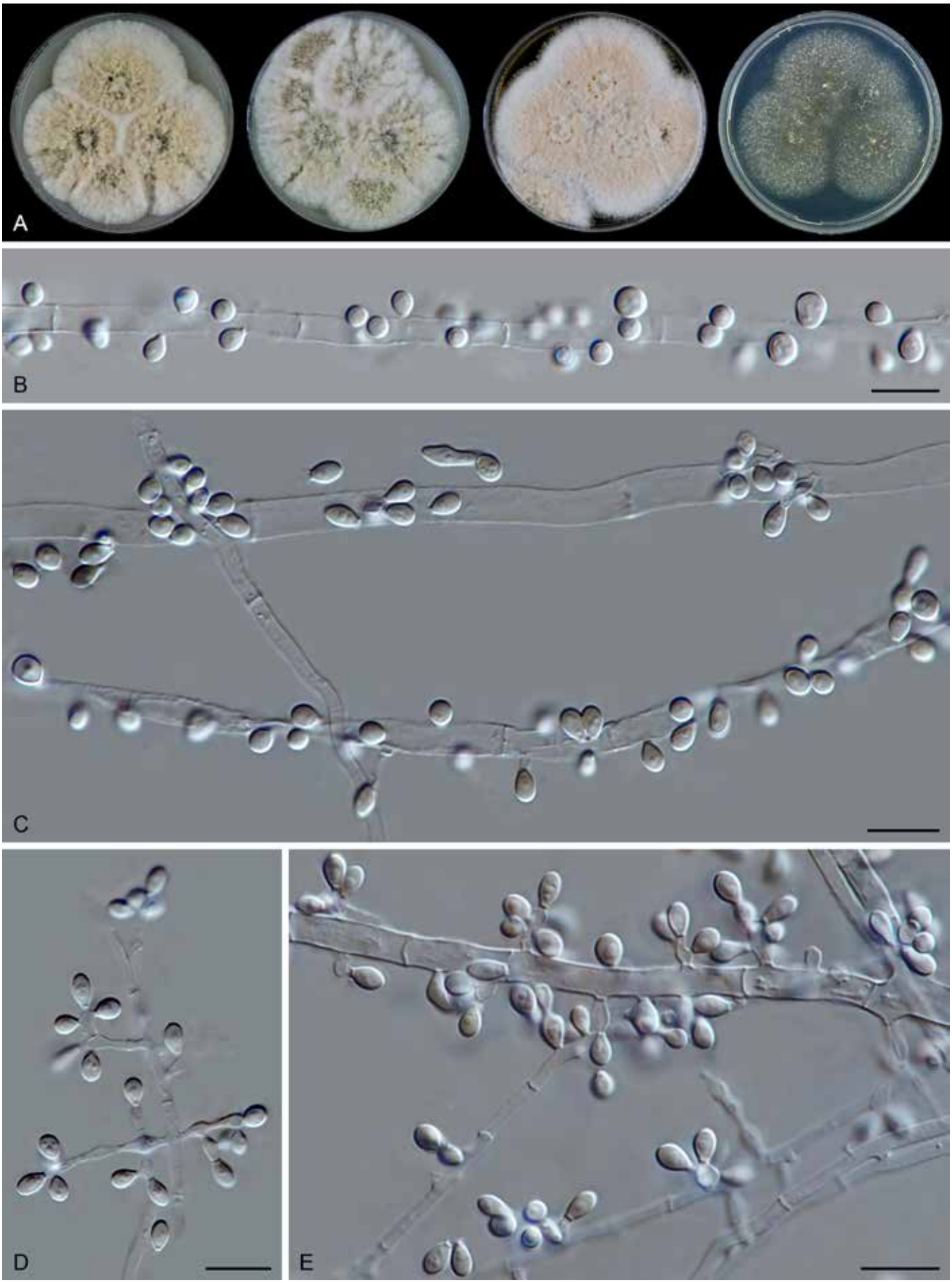

Fig. 48. *Thermothelomyces heterothallicus* (CBS 202.75, ex-epitype culture). **A.** Colonies from left to right on OA, CMA, MEA and PCA after 3 d incubation at 45 °C. **B–E.** Hyphae, conidiogenous cells and conidia. Scale bars = 10 µm.

heterothallicus produces smaller and narrower conidia (3.5–5 × 2.5–3 µm *vs* 5–7 × 4–6 µm). Both species are hetherothallic. The sexual morph of *Thermoth. heterothallicus* distinctively differs from that of *Thermoth. fergusii*. The former species produces clavate or ellipsoidal asci containing eight smaller ascospores (7.5–11 × 4.5–7 µm) with an apical germ pore, while the latter species has globose or ovoid asci containing four larger ascospores (23–32 × 17–23 µm) with two apical germ pores (Fergus & Sinden 1969, von Klopotek 1976). In the present study, we only examined the individual strains and did not undertake mating experiments to induce ascomata for study.

Thermothelomyces hinnuleus (Awao & Udagawa) Y. Marín *et al.*, Mycologia 107: 630. 2015. Fig. 49.
Basionym: *Myceliophthora hinnulea* Awao & Udagawa, Mycotaxon 16: 436. 1983.

Micromorphology: *Conidiophores* hypha-like or reduced. *Conidiogenous cells* lateral or terminal, solitary or several in simple or branched chains, swollen, pyriform, clavate or ampulliform, usually monoblastic, 4–7 × 2.5–3.5 µm. *Conidia* solitary or in short chains, single-celled, verrucose, orange, umber or fulvous, subglobose, (7–)7.5–9 (–10.5) × (6–)6.5–8(–8.5) µm diam. *Sexual morph* not observed.

Culture characteristics: On OA with an entire edge, 50–56 mm diam in 3 d at 45 °C, with sparse aerial mycelium, obverse pale luteous; reverse pale luteous. On CMA similar to those on OA. On MEA with an entire edge, 48–54 mm diam in 3 d at 45 °C, obverse white due to aerial mycelium, forming radiating furrows; reverse ochreous to orange. On PCA translucent, with an entire edge, 48–54 mm diam in 3 d at 45 °C, without coloured exudates; reverse uncoloured.

Material examined: **Japan**, Shizuoka Pref., Tagatagun, Niriayama-machi, isolated from cultivated soil, 24 Feb. 1973, T. Awao (culture ex-type CBS 597.83 = AJ 6773 = ATCC 52474 = NHL 2909). **New Zealand**, Christchurch, isolated from soil, date unknown, A.L.J. Cole (CBS 544.82).

Notes: *Thermothelomyces hinnuleus* is the only species of the genus that produces verrucose, pigmented conidia. Phylogenetic analysis shows that it is closely related to *Thermoth. guttulatus*, *Thermoth. heterothallicus* and *Thermoth. thermophilus* (Fig. 7A). No sexual morph has been observed or described for this species.

Thermothelomyces myriococcoides X.Wei Wang & Houbraken, ***nom. nov.*** MycoBank MB 830935. Fig. 50.
Replaced synonym: *Papulaspora thermophila* Fergus, Mycologia 632: 426. 1971, non *Thermothelomyces thermophilus* (Apinis) Y. Marín *et al.*, Mycologia 107: 630. 2015.
Synonyms: *Myriococcum thermophilum* (Fergus) Aa, Verh. Kon. Ned. Akad. Wetensch., Afd. Natuurk. 61(4): 60. 1973.
Crassicarpon hotsonii (Fergus) Koukol, Pl. Syst. Evol. 302: 967. 2016, *nom. inval.*, Art. 35.1.

Etymology: The epithet refers to the genus *Myriococcum*, to which the species is morphologically similar.

Micromorphology: *Microsclerotium-like structures* originating mainly from aerial mycelium, subglobose, ellipsoidal to irregular, pale luteous to apricot in reflected light, pale luteous to luteous when mounted in lactic acid, 85–230 × 75–180 µm, composed of angular or irregular cells, surrounded by the outer 2–5 layers consisting of pale or hyaline, elongate cells. *Other reproductive structures* not observed. Thermophilic.

Culture characteristics: On OA with a crenate edge, 59–65 mm diam in 3 d at 45 °C, texture cottony, with white aerial mycelium, obverse grey white to buff due to microsclerotium-like structures mixed with aerial mycelium, without coloured exudates; reverse uncoloured. On CMA similar to those on OA. On MEA with a crenate edge, over 70 mm diam in 3d at 45 °C, obverse vinaceous buff, wrinkled to form radiating furrows, reverse ochreous. On PCA with a crenate or lobate edge, 36–48 mm diam in 3 d at 25 °C, with sparse aerial mycelium, without coloured exudates; reverse uncoloured.

Material examined: **Netherlands**, Limburg, isolated from self-heating horse manure, 30 Mar. 1987, G. Straatsma (CBS 208.89). **Switzerland**, Gossau-Zürich, isolated from surface of heated compost, 1969, C.L. Fergus (culture ex-type CBS 389.93 = CBS 736.70 = ATCC 22112).

Notes: Neither a conidial nor a sexual (ascomata) morph has been observed in *Thermoth. myriococcoides*. This species is thermophilic and produces numerous microsclerotium-like structures in the aerial mycelium. *Thermothelomyces myriococcoides* was originally described in *Papulaspora* (Fergus 1971), and later transferred to *Myriococcum* by van der Aa (1973). *Myriococcum*, typified by *Myriococcum praecox*, was described by Fries (1823) as a sterile fungus producing sclerotia. As a consequence, several unrelated species were classified in this genus, including the thermophilic species *Myriococcum thermophilum*. Koukol (2016) showed that the genus is highly polyphyletic and the generic type belongs to the family *Stephanosporaceae* (*Agaricomycetes*). Furthermore, *Myriococcum thermophilum* was transferred to the invalidly proposed genus *Crassicarpon* as *Crass. hotsonii*. Based on our phylogenetic analysis, this species belongs to *Thermothelomyces*.

Thermothelomyces thermophilus (Apinis) Y. Marín *et al.*, Mycologia 107: 630. 2015. Fig. 51.
Basionym: *Sporotrichum thermophilum* [‘*thermophile*’] Apinis, Nova Hedwigia 5: 74. 1962.
Synonyms: *Chrysosporium thermophilum* (Apinis) Klopotek, Arch. Mikrobiol. 98: 366. 1974.
Myceliophthora thermophila (Apinis) Oorschot, Persoonia 9: 403. 1977.

Micromorphology: *Conidiophores* hyaline, hypha-like. *Conidiogenous cells* verticillate, lateral or terminal, occasionally intercalary, slightly swollen, fusiform, clavate or ampulliform, usually polyblastic with two or more conidia developed from one cell, 4–7 × 1.5–3 µm. *Conidia* solitary or in short chains, single-celled, smooth, hyaline to buff, ovoid, ellipsoidal, pyriform, often apically attenuated, with a narrow and truncate base, (3.5–)4–5.5(–6) × (2.5–)3–3.5(–4) µm diam. *Sexual morph* not observed.

Culture characteristics: On OA with an entire edge, 38–44 mm diam in 3 d at 45 °C, texture cottony, obverse grey white to rosy buff due to the formation of conidia on aerial mycelium, without coloured exudates; reverse uncoloured. On CMA similar to those on OA, 44–50 mm diam in 3 d at 45 °C, obverse grey white. On MEA with an entire edge, 59–65 mm diam in 3 d at 45 °C, texture thick cottony, obverse grey white to rosy buff due to the formation of conidia on aerial mycelium; reverse ochreous. On PCA translucent, with an entire edge, 40–46 mm diam in 3 d at 45 °C, with sparse aerial mycelium, without coloured exudates; reverse uncoloured.

Fig. 49. *Thermothelomyces hinnuleus* (CBS 597.83, ex-type culture). **A.** Colonies from left to right on OA, CMA, MEA and PCA after 7 d incubation at 37 °C. **B–E.** Hyphae, conidiogenous cells and conidia. Scale bars = 10 µm.

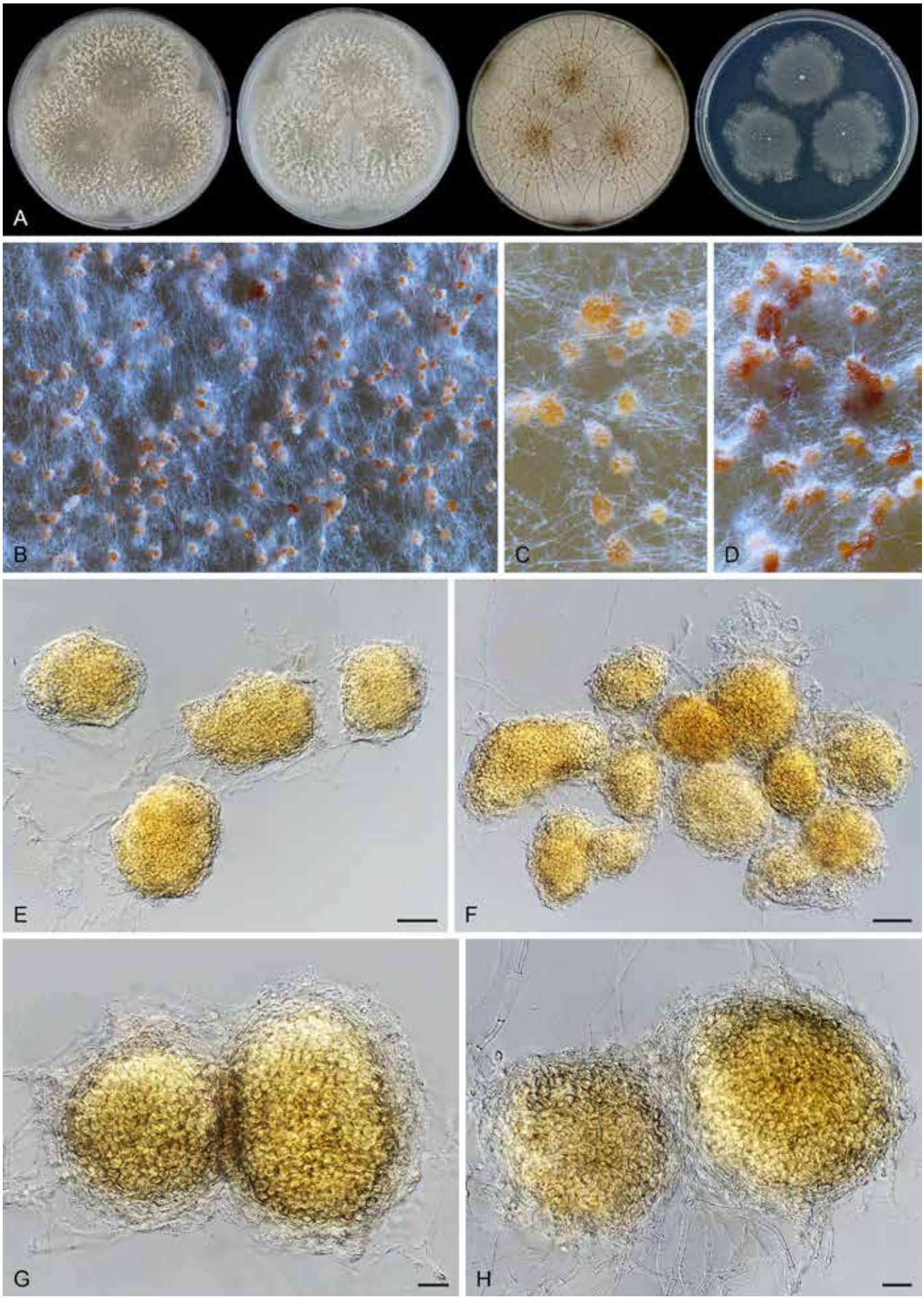

Fig. 50. *Thermothelomyces myriococcoides* (CBS 389.93, ex-type culture). **A.** Colonies from left to right on OA, CMA, MEA and PCA after 3d incubation at 45 °C. **B–D.** Part of the colony, showing microsclerotium-like structures on aerial mycelium. **E–H.** Hyphae and microsclerotium-like structures. Scale bars: E, F = 50 µm; G, H = 20 µm.

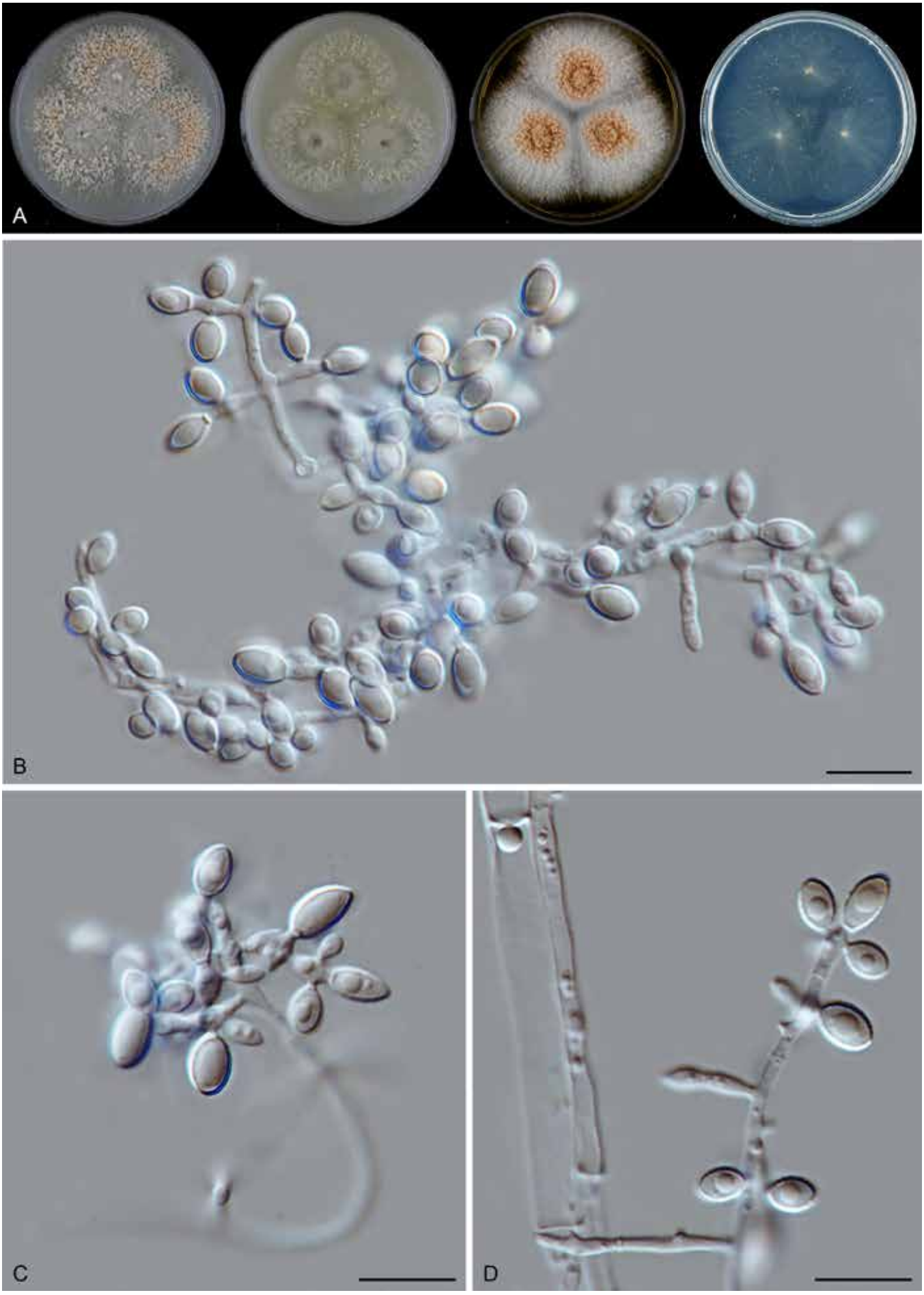

Fig. 51. *Thermothelomyces thermophilus* (CBS 117.65, ex-type culture). **A.** Colonies from left to right on OA, CMA, MEA and PCA after 3 d incubation at 37 °C. **B–D.** Hyphae, conidiogenous cells and conidia. Scale bars = 10 µm.

Material examined: **UK**, Attenborough, isolated from dry pasture soil, Jul. 1951, A.E. Apinis (culture ex-type CBS 117.65 = BDUN 274). **Unknown**, isolated from man, biopsy of nasal cavity, HIV pos. patient affected by sinusitis with infiltration of the orbit & exophthalmos, date unknown, L. Polonelli (CBS 381.97). **USA**, Ajinomoto Co., substrate and date unknown (CBS 669.85, mutant of CBS 866.85 producing cellulase).

Notes: Von Klopotek (1976) treated *Thielavia heterothallica* (= *Myceliophthora heterothallica* = *Thermothelomyces heterothallicus*) as the sexual morph of this species, followed by van Oorschot (1977). Previous studies showed that these two species are closely related, but distinct (van den Brink *et al.* 2015, Marín-Felix *et al.* 2015). Our phylogenetic analysis confirmed their separation (Fig. 7A, Supplementary Figs S1–S3). Morphologically, *Thermoth. thermophilus* and *Thermoth. heterothallicus* can be differentiated by their conidiophore structure. The former species produces conidiophores with verticillate, lateral or terminal conidiogenous cells and its conidia are often apically attenuated, while the conidiogenous cells of *Thermoth. heterothallicus* are often reduced or arise laterally from hyphae, developing apically rounded conidia.

Trichocladium Harz, Bull. Soc. Imp. Naturalistes Moscou 44: 125. 1871.

Micromorphology: Containing asexual species, sexual species and species with both asexual and sexual morphs. *Conidiophores* originating laterally or terminally from hyphae, simple or branched, sometimes reduced. *Conidiogenous cells* monoblastic or polyblastic, occasionally reduced to a hyphal cell, in one species (*Tri. beniowskiae*) swollen and in simple or branched chains. *Conidia* solitary or in chains of a few spores, 1-celled, didymo-, phragmo- or muriform, globose, subglobose, oblate, ellipsoid, obovoid, pyriform or quadrangular, olivaceous, brown or dark brown, or hyaline in *Tri. beniowskiae*, smooth to verrucose, rhexolytic when seceding, often with germ pore(s). *Acremonium-like phialides* present in a few species, lateral or occasionally terminal, hyaline. *Acremonium-like conidia* in basipetal chains or in a false slimy head, hyaline, aseptate, smooth, obovoid, usually with a truncated base and a rounded apex. In one species (*Tri. amorphum*) only intercalary arthroconidia, chlamydospores or microsclerotia produced. *Ascomata*, if present, superficial or immersed in the thick mycelium, ostiolate or non-ostiolate. *Asci* cylindrical with eight (four) uniseriate ascospores, or clavate to fusiform with eight biseriate ascospores, evanescent. *Ascospores* typically broadly ovate, bilaterally flattened, sometimes ellipsoidal and non-flattened, with an apical germ pore.

Type species: *Trichocladium asperum* Harz

Notes: *Trichocladium* is morphologically highly diverse in both its asexual and sexual morphs (Wang *et al.* 2019a). Among the sexual species, ascomata are ostiolate in five species, and non-ostiolate in two species (*Tri. antarcticum* and *Tri. arxii*). Here we describe a third species producing non-ostiolate ascomata.

Trichocladium tomentosum X.Wei Wang, P.J. Han & F.Y. Bai, ***sp. nov.*** MycoBank MB 840131. Fig. 52.

Etymology: The name refers to its downy ascomatal hairs.

Micromorphology: *Ascomata* superficial, solitary to aggregated, non-ostiolate, leaden black when mature in reflected light due to the dark ascomatal wall covered with short ascomatal hairs, spherical, 50–150 µm diam. *Ascomatal wall* brown, semi-translucent, composed of *textura epidermoidea* in surface view. *Ascomatal hairs* covering the whole ascomata, hypha-like, smooth or finely verrucose, brown at the base, septate, tapering and fading to hyaline in the upper part, with basal cells swelling, 2.5–4.5 µm wide. *Asci* clavate, spore-bearing part 28.5–35 × 12–15 µm, with stalks 7–15 µm long, containing eight irregularly-arranged ascospores, evanescent. *Ascospores* 1-celled, smooth, olivaceous when mature, smooth, broadly ovoid, bilaterally flattened, (6.5–)8–9.5(–10) × (7–)7.5–8.5(–9.5) × (5–)5.5–6.5(–7) µm, with an apical germ pore at the attenuated end. Asexual morph unknown.

Culture characteristics: On OA with an entire edge, 15–21 mm diam in 7 d at 25 °C, with sparse white aerial mycelium, obverse white or pale olivaceous grey due to masses of ascomata, without coloured exudates, or greyish sepia in the centre of the old culture due to exudates diffusing into the medium; reverse buff to fawn. On CMA similar to those on OA, 17–23 mm diam in 7 d at 25 °C, usually without coloured exudates. On MEA with an entire or slightly undulate edge, 18–24 mm diam in 7 d at 25 °C, with thick white aerial mycelium, texture floccose, obverse white, reverse ochraceous to umber. On PCA with an entire edge, 17–23 mm diam in 7 d at 25 °C, without aerial mycelium, obverse uncoloured, without coloured exudates, reverse uncoloured.

Material examined: **China**, Qinghai, isolated from soil near Qinghai Lake, Jul. 2003, X.W. Wang (**holotype** HMAS 350294, **isotype** CBS H-23643, culture ex-type CGMCC 3.20443 = CBS 144476 = WXW 8615).

Notes: *Trichocladium tomentosum* is phylogenetically closely related to several asexually reproducing species, such as *Tri. asperum*, *Tri. gilmaniellae*, *Tri. griseum* and *Tri. jilongense* (Fig. 7D). No asexual morph was found in our single *Tri. tomentosum* strain. The closest sexually reproducing species are *Tri. crispatum* with ostiolate ascomata and *Tri. antarcticum* with non-ostiolate ascomata (Wang *et al.* 2019a). The new species produces non-ostiolate ascomata and broadly ovoid, bilaterally flattened ascospores with an apical germ pore, similar to those of *Tri. antarcticum*, but can be differentiated by the production of hypha-like ascomatal hairs and clavate asci (rather than glabrous ascomata and cylindrical to elongated clavate asci as in *Tri. antarcticum*) and by the lack of an acremonium-like asexual morph.

Xanthiomyces X.Wei Wang & Houbraken, ***gen. nov.*** MycoBank MB 840125.

Etymology: The name refers to its ascomata, which look like the fruit of the plant genus *Xanthium*.

Micromorphology: *Ascomata* superficial, ellipsoidal, subglobose or ovoid, ostiolate. *Ascomatal wall* dark brown, composed of angular or irregular cells in surface view. *Ascomatal hairs* erect, seta-like, verrucose. *Asci* fasciculate, elongated fusiform or clavate, stalked, containing eight irregularly-arranged ascospores, evanescent. *Ascospores* olivaceous grey when mature, ovate to elongated ovate, with an apical germ pore. *Asexual morph* unknown.

Type species: *Xanthiomyces spinosus* (Chivers) X.Wei Wang & Houbraken

Notes: "*Chaetomium spinosum*" forms a sister clade to *Chaetomium sensu stricto* (Fig. 7B). This species produces ovate ascospores

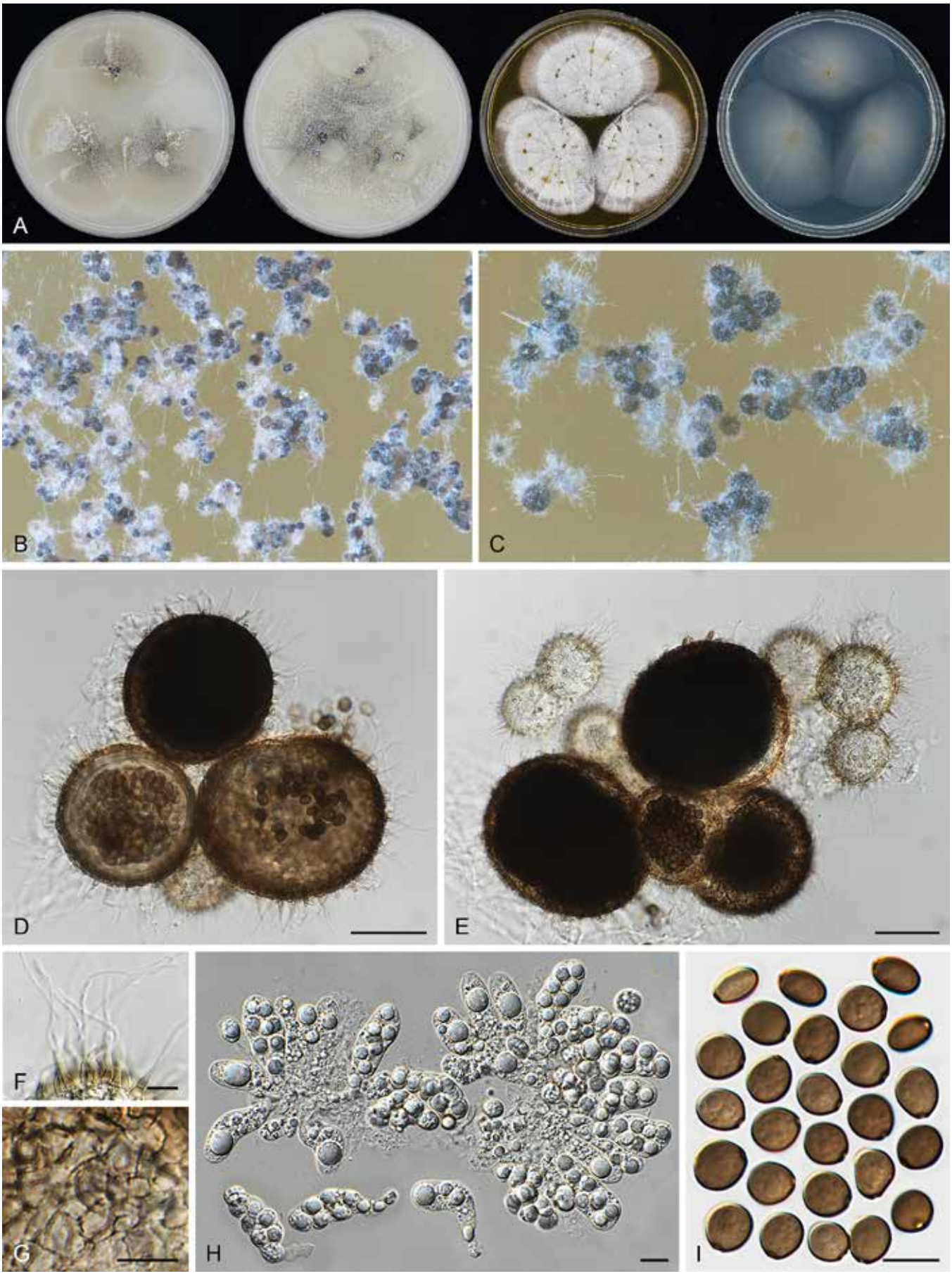

Fig. 52. *Trichocladium tomentosum* (CGMCC 3.20443, ex-type culture). **A.** Colonies from left to right on OA, CMA, MEA and PCA after 3 wk incubation. **B.** Part of the colony on OA. **C.** Mature ascomata on OA, top view. **D, E.** Ascomata mounted in lactic acid. **F.** Ascomatal hairs. **G.** Structure of ascomatal wall in surface view. **H.** Asci. **I.** Ascospores. Scale bars: D, E = 50 µm; F–I = 10 µm.

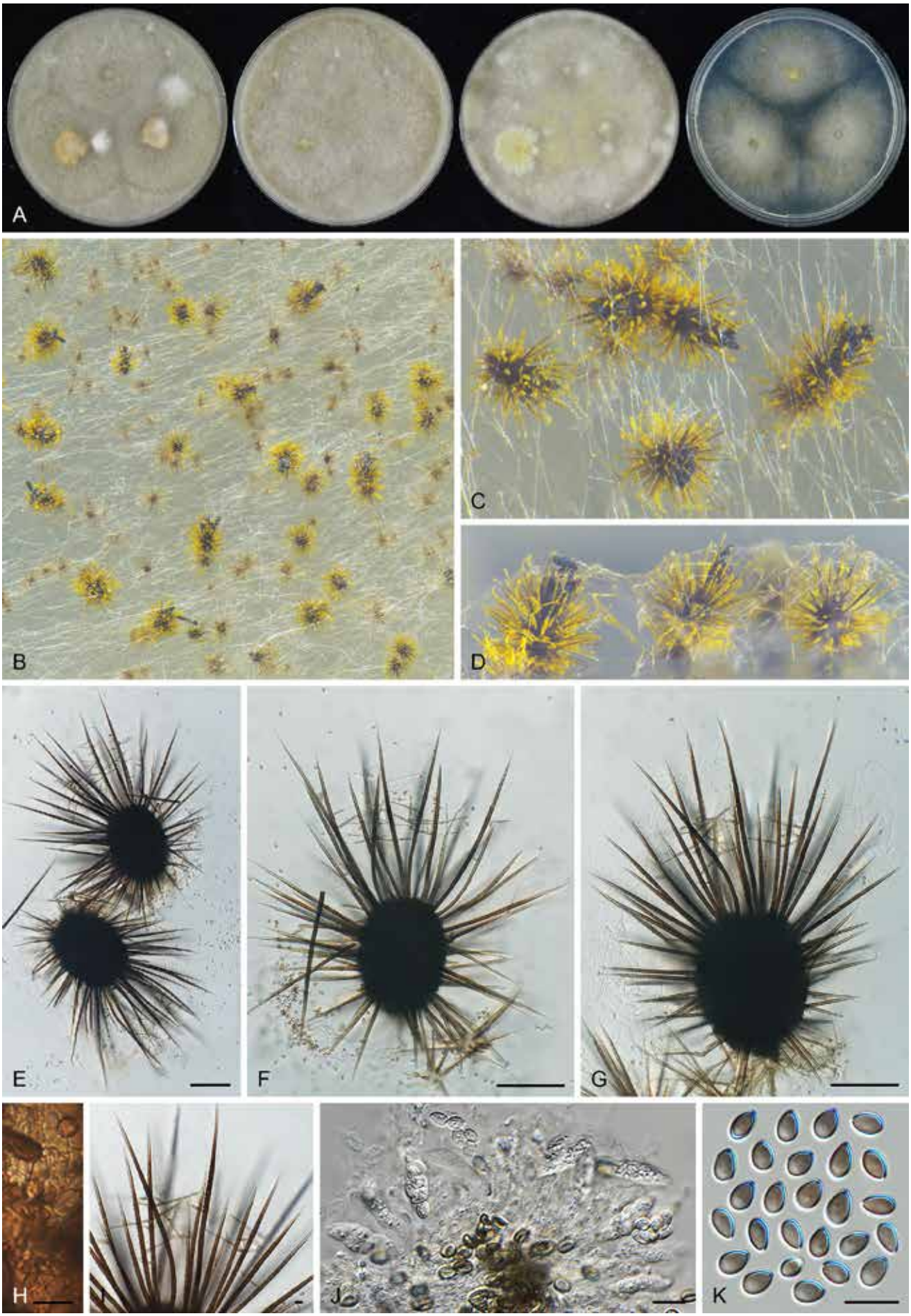

Fig. 53. *Xanthiomyces spinosus* (CBS 789.71). **A.** Colonies from left to right on OA, CMA, MEA and PCA after 3 wk incubation. **B.** Part of the colony on OA. **C, D.** Mature ascomata on OA. **E–G.** Ascomata mounted in lactic acid. **H.** Structure of ascomatal wall in surface view. **I.** Terminal ascomatal hairs. **J.** Asci. **K.** Ascospores. Scale bars: E–G = 100 µm; H–K = 10 µm.

that are usually less than 7 µm in length (Fig. 53K), in contrast to the limoniform to globose ascospores of *Chaetomium*, which are longer than 7 µm (Fig. 4Q–V). The molecular dating analysis indicates that this species diverged from *Chaetomium* about 50 Mya, significantly earlier than the later time limit of the other accepted genera in the family (about 27 Mya, Figs 8B, 9). Based on the morphological difference and the divergence date, the new genus *Xanthiomyces* is proposed here to accommodate *Chaetomium spinosum*.

Xanthiomyces spinosus (Chivers) X.Wei Wang & Houbraken, ***comb. nov.*** MycoBank MB 840166. Fig. 53.
Basionym: *Chaetomium spinosum* Chivers, Proc. Amer. Acad. Arts 48: 86. 1912.

Micromorphology: *Ascomata* superficial, ostiolate, yellow in reflected light due to ascomatal hairs, ellipsoidal, suglobose or ovoid, 150–230 µm high, 120–180 µm diam. *Ascomatal wall* dark brown, composed of angular or irregular cells in surface view. *Terminal hairs* dark brown, often covered by yellow crystals, seta-like, verrucose, tapering, 4–7 µm near the base. *Lateral hairs* similar to, but shorter than terminal ones. *Asci* elongated fusiform or clavate, with spore-bearing part 15–27 × 7–9 µm, with stalks 6–11 µm long, containing eight irregularly-arranged or biseriate ascospores, evanescent. *Ascospores* 1-celled, olivaceous grey when mature, smooth, ovate to elongated ovate, slightly bilaterally flattened, with an apical germ pore, (5–)5.5–6.5(–7) × (3–)3.5–4(–4.5) × 3–4 µm, with an apical germ pore at the attenuated end. *Asexual morph* unknown.

Culture characteristics: On OA with an entire edge, 53–59 mm diam in 7 d at 25 °C, obverse olivaceous buff or white, sometimes pale luteous due to aerial mycelium, or primrose due to the formation of ascomata; reverse buff to pale luteous, or saffron due to exudates diffusing into the medium. On CMA similar to those on OA, 54–60 mm diam in 7 d at 25 °C; reverse honey. On MEA with an entire edge, over 70 mm diam in 7 d at 25 °C, obverse olivaceous buff, primrose or straw due to aerial mycelium, reverse umber. On PCA with an entire edge, 34–42 mm diam in 7 d at 25 °C, obverse white, aerial mycelium sparse, without coloured exudates; reverse uncoloured.

Material examined: **Switzerland**, Zürich, isolated from culture of algae, date unknown, E. Müller (representative strain CBS 789.71 = ETH 7700); Bloney, isolated from straw, date unknown, M. Dreyfuss (culture CBS 796.83).

Notes: *Xanthiomyces spinosus* is morphologically reminiscent of *Dichotomopilus* species which are characterised by their seta-like to dichotomously or irregularly branched ascomatal hairs, and small (usually less than 7.5 µm long) and narrowly ovate, ovate or broad ovate ascospores with an apical or slightly sub-apical germ pore (Fig. 4B, Wang *et al.* 2016b). Phylogenetically, this species is distantly related to *Dichotomopilus* (Fig. 7A, B).

List of genera and species in *Chaetomiaceae*

Since its introduction, over 400 species were described in genera of *Chaetomiaceae*. In the list provided below, we accept only the species that we could classify in the family using DNA sequence data (species shown in bold font). Species originally described in genera of *Chaetomiaceae*, but excluded or reclassified by other authors, or which have not been re-examined recently, are not included in our list. A few excluded species that we have examined, or were sequenced by other authors, are included in a brief overview at the end of this list. Synonyms of the accepted species are provided (in italics, non-bold font) only when these are known and confirmed by sequence data. Most of these data originate from previous studies (Wang *et al.* 2016a, b, 2019 a, b). The list includes 275 accepted species, distributed across 50 genera. For each species, we provide the full reference including MycoBank number, provide information (if known) of the holotype and ex-type strain/specimen and GenBank numbers of reference sequences. In addition, we indicate if the species is able to produce a sexual and/or an asexual morph.

List of accepted genera in *Chaetomiaceae*

Achaetomiella Arx, The genera of fungi sporulating in pure culture: 247. 1970. [MB 37]. — Type: *Achaetomiella virescens*. Reproduction: sexual.

Achaetomium J.N. Rai *et al.*, Canad. J. Bot. 42: 693. 1964. [MB 38]. — Type: *Achaetomium globosum*. Reproduction: sexual.

Acrophialophora Edward, Mycologia 51: 784. 1961. [MB 7037]. — Type: *Acrophialophora nainiana*. Reproduction: asexual or sexual.

Allobotryotrichum M. Raza & L. Cai, Fungal Diversity 99: 74. 2019. [MB 556672]. — Type: *Allobotryotrichum blastosporum*. Reproduction: asexual.

Allocanariomyces Mehrabi *et al.*, Mycol. Prog. 19: 1417. 2020. [MB 835853]. — Type: *Allocanariomyces tritici*. Reproduction: sexual & asexual.

Amesia X.Wei Wang *et al.*, Stud. Mycol. 84: 156. 2016. [MB 818829]. — Type: *Amesia atrobrunnea*. Reproduction: sexual.

Aporothielavia Malloch & Cain, Mycologia 65: 1074. 1973. [MB 283]. — Type: *Aporothielavia leptoderma*. Reproduction: sexual.

Arcopilus X.Wei Wang *et al.*, Stud. Mycol. 84: 159. 2016. [MB 818835]. — Type: *Arcopilus aureus*. Reproduction: sexual.

Arxotrichum A. Nováková & M. Kolařík, Persoonia 40: 259. 2018. [MB 824080]. — Type: *Arxotrichum wyomingense*. Reproduction: sexual & asexual.

Batnamyces Noumeur, Mycol. Prog. 19: 593. 2020. [MB 832844]. — Type: *Batnamyces globulariicola*. Reproduction: asexual.

Bommerella Marchal, Bull. Soc. Roy. Bot. Belgique 24: 164. 1885. [MB 622]. — Type: *Bommerella trigonospora*. Reproduction: sexual.

Botryoderma Papendorf & H.P. Upadhyay, Trans. Brit. Mycol. Soc. 52: 257. 1969. [MB 7419]. — Type: *Botryoderma lateritium*. Reproduction: asexual.

Botryotrichum Sacc. & Marchal, Bull. Soc. Roy. Bot. Belgique 24: 66. 1885. [MB 7431]. — Type: *Botryotrichum piluliferum*. Reproduction: asexual & sexual.

Brachychaeta X.Wei Wang & Houbraken, Stud. Mycol. 93: 186. 2019. [MB 829842]. — Type: *Brachychaeta variospora*. Reproduction: sexual.

Canariomyces Arx, Persoonia 12: 185. 1984. [MB 25789]. — Type: *Canariomyces notabilis*. Reproduction: sexual & asexual.

Carteria X.Wei Wang & Houbraken, Stud. Mycol. 93: 194. 2019. [MB 829850]. — Type: *Carteria arctostaphyli*. Reproduction: sexual.

Chaetomium Kunze, Mykol. Hefte 1: 15. 1817. [MB 953]. — Type: *Chaetomium globosum*. Reproduction: sexual & asexual.

Chrysanthotrichum X.Wei Wang & Houbraken, Stud. Mycol. 93: 194. 2019. [MB 829852]. — Type: *Chrysanthotrichum lentum*. Reproduction: sexual.

Chrysocorona X.Wei Wang & Houbraken, Stud. Mycol. 93: 201. 2019. [MB 829858]. — Type: *Chrysocorona lucknowensis*. Reproduction: sexual.

Collariella X.Wei Wang *et al.*, Stud. Mycol. 84: 177. 2016. [MB 818839]. — Type: *Collariella bostrychodes*. Reproduction: sexual.

Condenascus X.Wei Wang & Houbraken, Stud. Mycol. 93: 203. 2019. [MB 829860]. — Type: *Condenascus tortuosus*. Reproduction: sexual.

Corynascella Arx & Hodges, Stud. Mycol. 8: 23. 1975. [MB 1256]. — Type: *Corynascella humicola*. Reproduction: sexual & asexual.

Corynascus Arx, Proc. Kon. Ned. Akad. Wetensch., Sect. C 76: 295. 1973. [MB 1257]. — Type: *Corynascus sepedonium*. Reproduction: sexual & asexual.

Dichotomopilus X.Wei Wang *et al.*, Stud. Mycol. 84: 185. 2016. [MB 818840]. — Type: *Dichotomopilus indicus*. Reproduction: sexual.

Floropilus X.Wei Wang & Houbraken, Stud. Mycol. 93: 203. 2019. [MB 829862]. — Type: *Floropilus chiversii*. Reproduction: sexual.

Humicola Traaen, Nytt Mag. Naturvidensk. 52: 31. 1914. [MB 8566]. — Type: *Humicola fuscoatra*. Reproduction: sexual & asexual.

Hyalosphaerella X.Wei Wang & Houbraken, Stud. Mycol. 93: 205. 2019. [MB 829864]. — Type: *Hyalosphaerella fragilis*. Reproduction: sexual.

Madurella Brumpt, Compt.-Rend. Séances Mém. Soc. Biol. 58: 999. 1905. [MB 8824]. — Type: *Madurella mycetomatis*. Reproduction: asexual/sterile.

Melanocarpus Arx, Stud. Mycol. 8: 17. 1975. [MB 3063]. — Type: *Melanocarpus albomyces*. Reproduction: sexual & asexual.

Microthielavia X.Wei Wang & Houbraken, Stud. Mycol. 93: 208. 2019. [MB 829866]. — Type: *Microthielavia ovispora*. Reproduction: sexual.

Myceliophthora Costantin, Compt. Rend. Hebd. Séances Acad. Sci. 114: 849. 1892. [MB 9013]. — Type: *Myceliophthora lutea*. Reproduction: asexual.

Mycothermus D.O. Natvig *et al.*, Mycologia 107: 321. 2015. [824453]. — Type: *Mycothermus thermophilus*. Reproduction: asexual.

Ovatospora X.Wei Wang *et al.*, Stud. Mycol. 84: 207. 2016. [MB 818850]. — Type: *Ovatospora brasiliensis*. Reproduction: sexual.

Parachaetomium Mehrabi *et al.*, Mycol. Prog. 19: 1422. 2020. [MB 835855]. — Type: *Parachaetomium perlucidum*. Reproduction: sexual.

Parathielavia X.Wei Wang & Houbraken, Stud. Mycol. 93: 208. 2019. [MB 829868]. — Type: *Parathielavia hyrcaniae*. Reproduction: sexual & asexual.

Parvomelanocarpus X.Wei Wang *et al.*, this study. [MB 840124]. — Type: *Parvomelanocarpus tardus*. Reproduction: sexual.

Pseudohumicola X.Wei Wang *et al.*, this study. [MB 840123]. — Type: *Pseudohumicola subspiralis*. Reproduction: sexual & asexual.

Pseudothielavia X.Wei Wang & Houbraken, Stud. Mycol. 93: 213. 2019. [MB 829872]. — Type: *Pseudothielavia terricola*. Reproduction: sexual.

Remersonia Samson & Seifert, Canad. J. Bot. 75: 1160. 1997. [MB 27809]. — Type: *Remersonia thermophila*. Reproduction: asexual.

Staphylotrichum J. Mey. & Nicot, Bull. Trimestriel Soc. Bot. France 72: 322. 1957. [MB 10065]. — Type: *Staphylotrichum coccosporum*. Reproduction: sexual & asexual.

Stellatospora Tad. Ito & Nakagiri, Mycoscience 35: 413. 1994. [MB 27456]. — Type: *Stellatospora terricola*. Reproduction: sexual.

Stolonocarpus X.Wei Wang & Houbraken, Stud. Mycol. 93: 221. 2019. [MB 829877]. — Type: *Stolonocarpus gigasporus*. Reproduction: sexual.

Subramaniula Arx, Proc. Indian Acad. Sci., Pl. Sci. 94: 344. 1985. [MB 25699]. — Type: *Subramaniula thielavioides*. Reproduction: sexual & asexual.

Tengochaeta X.Wei Wang & Houbraken, this study. [MB 830915]. — Type: *Tengochaeta nigropilosa*. Reproduction: sexual.

Thermocarpiscus X.Wei Wang & Houbraken, this study. [MB 840163]. — Type: *Thermocarpiscus australiensis*. Reproduction: sexual & asexual.

Thermochaetoides X.Wei Wang & Houbraken, this study. [MB 830916]. — Type: *Thermochaetoides thermophila*. Reproduction: sexual.

Thermothelomyces Y. Marín *et al.*, Mycologia 107: 630. 2015. [MB 809489]. — Type: *Thermothelomyces thermophilus*. Reproduction: asexual & sexual (heterothallic).

Thermothielavioides X.Wei Wang & Houbraken, Stud. Mycol. 93: 223. 2019. [MB 829879]. — Type: *Thermothielavioides terrestris*. Reproduction: sexual & asexual.

Trichocladium Harz, Bull. Soc. Imp. Naturalistes Moscou 44: 125. 1871. [MB 10278]. — Type: *Trichocladium asperum*. Reproduction: sexual & asexual.

Xanthiomyces X.Wei Wang & Houbraken, this study. [MB 840125]. — Type: *Xanthiomyces spinosus*. Reproduction: sexual.

List of accepted species and their synonyms

Achaetomiella

Achaetomiella gracilis (Udagawa) Houbraken *et al.*, this study. [MB 840195]. Basionym: *Chaetomium gracile*. — Type: NHL 2251. Ex-type: CBS 146.60 = ATCC 16153 = IFO 6568 = IMI 084227 = NHL 2251. Reproduction: sexual. ITS barcode: KX976648 (alternative markers: LSU = KX976743; *tub2* = KX976990; *rpb2* = KX976842).

Achaetomiella virescens Arx, The genera of fungi sporulating in pure culture: 247. 1970. [MB 308086]. — Type: CBS 148.68. Ex-type: CBS 148.68 = IMI 136212 = IMI 159035. Reproduction: sexual. ITS barcode: KX976654 (alternative markers: LSU = KX976749; *tub2* = KX976996; *rpb2* = KX976848).

Achaetomium

Achaetomium aegilopis Mehrabi *et al.*, Mycol. Prog. 19: 1422. 2020. [MB 835859]. — Type: IRAN 17712F. Ex-type: IRAN 3453C. Reproduction: sexual. ITS barcode: MT568841 (alternative markers: LSU = MT568844; *tub2* = MT568852; *rpb2* = n/a).

Achaetomium cristalliferum Faurel & Locq.-Lin., Cryptog. Mycol. 1: 235. 1980. [MB 113114]. — Type: PC 3252. Ex-type: CBS 781.84. Reproduction: sexual. ITS barcode: MH861836 (alternative markers: LSU = n/a; *tub2* = MZ343033; *rpb2* = MZ342994). *Note*: Based on the phylogenetic analysis (Fig. 7), we consider *Achaetomium cristalliferum* a synonym of *Achaetomium strumarium*.

Achaetomium globosum J.N. Rai & J.P. Tewari, Canad. J. Bot. 42: 693. 1964. [MB 325764]. — Type: IMI 82626. Ex-type: CBS 332.67 = IMI 082626 = IMI 082626ii = IMI 136483 = NRRL A-10899. Reproduction: sexual. ITS barcode: KX976570

(alternative markers: LSU = KX976695; *tub2* = KX976911; *rpb2* = KX976793).

Achaetomium hamadae Udagawa, Trans. Mycol. Soc. Japan 23: 287. 1982. [MB 124435]; basionym of *Pseudothielavia hamadae*.

Achaetomium irregulare (Sörgel ex W. Gams) K. Rodr. *et al.*, Stud. Mycol. 50: 81. 2004. [MB 500020]. *Note*: The basionym of *Achaetomium irregulare*, *Chaetomium irregulare*, was replaced by a new name in *Subramaniula* (as *flavipila*).

Achaetomium lippiae M.G. Viana *et al.*, Persoonia 39: 283. 2017. [MB 820711]. — Type: URM 90067. Ex-type: URM 7547. Reproduction: sexual. ITS barcode: KY855413 (alternative markers: LSU = KY855414; *tub2* = KY855412; *rpb2* = n/a).

Achaetomium luteum J.N. Rai & J.P. Tewari, Canad. J. Bot. 42: 694. 1964. [MB 325765]. — Type: IMI 96678. Ex-type: IMI 96678; Representative strain: CBS 618.68 = ATCC 18524 = IMI 141563. Reproduction: sexual. ITS barcode: KX976571 (alternative markers: LSU = KX976696; *tub2* = KX976912; *rpb2* = KX976794).

Achaetomium macrosporum J.N. Rai *et al.*, Indian Phytopathol. 23: 54. 1970. [MB 308089]. — Type: IMI 132137. Representative strain: CBS 152.97. Reproduction: sexual. ITS barcode: KX976573 (alternative markers: LSU = KX976698; *tub2* = KX976914; *rpb2* = KX976796).

Achaetomium nepalense Udagawa & Y. Sugiy., Rep. Cryptog. Stud. Nepal: 11. 1982 [MB 115709]; basionym of *Chaetomium nepalense*.

Achaetomium purpurascens Udagawa & Y. Sugiy., Rep. Cryptog. Stud. Nepal: 13. 1982. [MB 115710]; basionym of *Arcopilus purpurascens*.

Achaetomium strumarium J.N. Rai *et al.*, Canad. J. Bot. 42: 694. 1964. [MB 325766]. — Type: IMI 82624. Ex-type: CBS 333.67 = ATCC 58165 = IMI 082624 = IMI 082624ii = MI 136213 = NRRL A-10898. Reproduction: sexual. ITS barcode: AY681204 (alternative markers: LSU = AY681170; *tub2* = AY681238; *rpb2* = KC503254).

Achaetomium thielavioides Arx *et al.*, Persoonia 10: 144. 1978. [MB 308092]; basionym of *Subramaniula thielavioides*.

Achaetomium umbonatum K. Rodr. *et al.*, Stud. Mycol. 50: 78. 2004. [MB 500019]. — Type: IMI 38289. Ex-type: CBS 102436 = FMR 6778 = IMI 381871. Reproduction: sexual. ITS barcode: MZ334718 (alternative markers: LSU = AJ312099; *tub2* = MZ343007; *rpb2* = MZ342966). *Note*: Based on the phylogenetic analysis (Fig. 7), we consider *Ach. umbonatum* a synonym of *Achaetomium macrosporum*.

Acremonium (*Hypocreales, Sordariomycetes*)

Acremonium nigrospermum Schwein., Trans. Amer. Philos. Soc., n.s. 4: 283. 1832. [MB 248467]; basionym of *Trichocladium nigrospermum*.

Acrophialophora

Acrophialophora acuticonidiata Yu Zhang & L. Cai, Mycologia 107: 771. 2015. [MB 807461]. — Type: HMAS 245076. Ex-type: CGMCC 3.17245. Reproduction: asexual. ITS barcode: KJ026975 (alternative markers: LSU = n/a; *tub2* = KJ147441; *rpb2* = n/a).

Acrophialophora angustiphialis Yu Zhang & L. Cai, Mycologia 107: 772. 2015. [MB 807078]. — Type: HMAS 244840. Ex-type: CGMCC 3.15258. Reproduction: asexual. ITS barcode: KJ026972 (alternative markers: LSU = n/a; *tub2* = KJ147438; *rpb2* = n/a).

Acrophialophora biformis (Z.Q. Liang *et al.*) Yu Zhang & L. Cai, Mycologia 107: 772. 2015. [MB 810301]. Basionym: *Paecilomyces biformis*. — Type: GZDXIFR-H28. Ex-type: GZDXIFR-H28-1. Reproduction: asexual. ITS barcode: DQ191963 (alternative markers: LSU = n/a; *tub2* = n/a; *rpb2* = n/a).

Acrophialophora cinerea (Z.Q. Liang *et al.*) Yu Zhang & L. Cai, Mycologia 107: 772. 2015. [MB 810302]. Basionym: *Paecilomyces cinereus*. — Type: GZDXIFR-H57-1. Ex-type: GZDXIFR-H57-1. Reproduction: asexual. ITS barcode: DQ243694 (alternative markers: LSU = n/a; *tub2* = n/a; *rpb2* = n/a).

Acrophialophora curticatenata (Z.Q. Liang & Y.F. Han) Yu Zhang & L. Cai, Mycologia 107: 772. 2015. [MB 810303]. Basionym: *Paecilomyces curticatenatus*. — Type: GZDXIFR-H-125-2. Ex-type: GZUIFR-H125-2. Reproduction: asexual. ITS barcode: EU004811 (alternative markers: LSU = n/a; *tub2* = n/a; *rpb2* = n/a).

Acrophialophora ellipsoidea Yu Zhang & L. Cai, Mycologia 107: 772. 2015. [MB 807077]. — Type: HMAS 244841. Ex-type: CGMCC 3.15256. Reproduction: asexual. ITS barcode: MK926786 (alternative markers: LSU = MK926786; *tub2* = MK926886; *rpb2* = MK876748).

Acrophialophora furcata (Z.Q. Liang *et al.*) Yu Zhang & L. Cai, Mycologia 107: 775. 2015. [MB 810304]. Basionym: *Paecilomyces furcatus*. — Type: GZDXIFR-H104-1. Ex-type: GZDXIFR-H104-1. Reproduction: asexual. ITS barcode: DQ243695 (alternative markers: LSU = n/a; *tub2* = n/a; *rpb2* = n/a).

Acrophialophora fusispora (S.B. Saksena) Samson, Acta Bot. Neerl. 19: 805. 1970. [MB 308237]. Basionym: *Paecilomyces fusisporus*. — Type: n/a. Ex-type: CBS 380.55 = ATCC 22556 = IMI 057442 = UAMH 10771. Reproduction: asexual. ITS barcode: MK926788 (alternative markers: LSU = MK926788; *tub2* = MK926888; *rpb2* = MK876750).

Acrophialophora hechuanensis (Z.Q. Liang *et al.*) Yu Zhang & L. Cai, Mycologia 107: 775. 2015. [MB 810305]. Basionym: *Taifanglania hechuanensis*. — Type: GZUIFR H08-1. Ex-type: GZUIFR-H08-1. Reproduction: asexual. ITS barcode: MK926789 (alternative markers: LSU = MK926789; *tub2* = MK926889; *rpb2* = MK876751).

Acrophialophora jiangsuensis (Y.F. Han & Z.Q. Liang) Yu Zhang & L. Cai, Mycologia 107: 775. 2015. [MB 810306]. Basionym: *Taifanglania jiangsuensis*. — Type: GZUIFR HC48.1. Ex-type: GZUIFR HC48.1. Reproduction: asexual. ITS barcode: KF719171 (alternative markers: LSU = n/a; *tub2* = KP143112; *rpb2* = n/a). *Note*: Based on the comparison of the available ITS and *tub2* sequences (Fig. 7), we consider this species a synonym of *Acrophialophora hechuanensis*.

Acrophialophora jodhpurensis (Lodha) X.Wei Wang & Houbraken, Stud. Mycol. 93: 179. 2019. [MB 829844]. Basionym: *Chaetomium jodhpurense*. — Type: fig. 8 in Lodha, J. Indian Bot. Soc. 43: 132, 1964 (lectotype). CBS H-10019 (epitype). Ex-epitype: CBS 602.69. Reproduction: sexual. ITS barcode: MK926790 (alternative markers: LSU = MK926790; *tub2* = MK926890; *rpb2* = MK876752).

Acrophialophora levis Samson & T. Mahmood, Acta Bot. Neerl. 19: 807. 1970. [MB 308238]. — Type: CBS 484.70. Ex-type: CBS 484.70 = ATCC 22557 = UAMH 10773. Reproduction: asexual. ITS barcode: KP233038 (alternative markers: LSU = KM995840; *tub2* = KP233044; *rpb2* = n/a).

Acrophialophora liboensis Y.W. Zhang *et al.*, Phytotaxa 302: 270. 2016. [MB 818669]. — Type: GZUIFR-F0044. Ex-type:

CGMCC 3.18309. Reproduction: asexual. ITS barcode: KP192127 (alternative markers: LSU = n/a; *tub2* = KP999978; *rpb2* = n/a).

Acrophialophora major (Z.Q. Liang *et al.*) Yu Zhang & L. Cai, Mycologia 107: 775. 2015. [MB 810307]. Basionym: *Paecilomyces inflatus* var. *major*. — Type: GZDX-IFR H-57-2. Ex-type: GZUIFR-H57-2. Reproduction: asexual. ITS barcode: MK926792 (alternative markers: LSU = MK926792; *tub2* = MK926892; *rpb2* = MK876754).

Acrophialophora nainiana Edward, Mycologia 51: 784. 1961. [MB 325807]. — Type: IMI, anon. s.n.; MPPD, anon. s.n.; WVA, anon. s.n.; Department of Biology, Allahabad Agricultural Institute, anon. s.n. Ex-type: CBS 100.60. Reproduction: asexual. ITS barcode: MK926793 (alternative markers: LSU = MK926793; *tub2* = MK926893; *rpb2* = MK876755).

Acrophialophora seudatica (Subrahm.) Sand.-Den. *et al.*, J. Clin. Microbiol. 53: 1552. 2015. [MB 811225]. Basionym: *Ampullifera seudatica*. — Type: CBS 916.79. Ex-type: CBS 916.79 = ATCC 36866. Reproduction: asexual. ITS barcode: LN736030 (alternative markers: LSU = LN736031; *tub2* = LN736032; *rpb2* = n/a). *Note*: Based on ITS, LSU and *tub2* sequence data (Fig. 7), we consider this species a synonym of *Acrophialophora major*.

Acrophialophora teleoafricana X.Wei Wang & Houbraken, Stud. Mycol. 93: 185. 2019. [MB 829843]. — Type: CBS H-23631. Ex-type: CBS 281.79. Reproduction: sexual. ITS barcode: MK926795 (alternative markers: LSU = MK926795; *tub2* = MK926895; *rpb2* = MK876757).

Allobotryotrichum

Allobotryotrichum blastosporum [as '*blastospora*'] M. Raza & L. Cai, Fungal Diversity 99: 74. 2019. [MB 636270]. — Type: HMAS 248065. Ex-type: CGMCC 3.19343 = LC11912. Reproduction: asexual. ITS barcode: MN215716 (alternative markers: LSU = MN215554; *tub2* = MN329887; *rpb2* = MN255397).

Allocanariomyces

Allocanariomyces americanus (Cañete-Gibas *et al.*) Cañete-Gibas *et al.*, this study. [MB 840154]. Basionym: *Pseudocanariomyces americanus*. — Type: CBS H-24761. Ex-type: CBS 147185 = UTHSCSA DI20-139. Reproduction: sexual & asexual. ITS barcode: MT902181 (alternative markers: LSU = MT902391; *tub2* = MT904876; *rpb2* = MT904877).

Allocanariomyces tritici Mehrabi *et al.*, Mycol. Prog. 19: 1420. 2020. [MB 835854]. — Type: IRAN 17711F. Ex-type: IRAN 3450C. Reproduction: sexual & asexual. ITS barcode: MT568839 (alternative markers: LSU = MT568842; *tub2* = MT568850; *rpb2* = MT568845).

Amesia

Amesia atrobrunnea (L.M. Ames) X.Wei Wang & Samson, Stud. Mycol. 84: 158. 2016. [MB 818832]. Basionym: *Chaetomium atrobrunneum*. — Type: BPI 1100755. Ex-type: CBS 379.66. Reproduction: sexual. ITS barcode: JX280771 (alternative markers: LSU = JX280666; *tub2* = KX976916; *rpb2* = KX976798).

Amesia cymbiformis (Lodha) X.Wei Wang & Samson, Stud. Mycol. 84: 158. 2016. [MB 818833]. Basionym: *Chaetomium cymbiforme*. — Type: n/a. Representative strain: CBS 175.84. Reproduction: sexual. ITS barcode: KX976576 (alternative markers: LSU = KX976701; *tub2* = KX976918; *rpb2* = KX976800).

Amesia dreyfussii (Arx) X.Wei Wang & Houbraken, this study. [MB 840132]. Basionym: *Chaetomium dreyfussii*. — Type: CBS H-6864. Ex-type: CBS 376.83 = MUCL 40177. Reproduction: sexual. ITS barcode: MH861613 (alternative markers: LSU = MH873331; *tub2* = MZ343023; *rpb2* = MZ342985).

Amesia gelasinospora (Aue & E. Müll.) X.Wei Wang & Samson, Stud. Mycol. 84: 217. 2016. [MB 818854]. Basionym: *Chaetomium gelasinosporum*. — Type: ETH. Ex-type: CBS 673.80. Reproduction: sexual. ITS barcode: KX976580 (alternative markers: LSU = KX976705; *tub2* = KX976922; *rpb2* = KX976804).

Amesia khuzestanica Mehrabi-Koushki *et al.*, Mycol. Prog. 19: 939. 2020. [MB 832229]. — Type: IRAN 17597F. Ex-type: IRAN 3489C = SCUA-Saf-B16. Reproduction: sexual. ITS barcode: MT551117 (alternative markers: LSU = n/a; *tub2* = MN275701; *rpb2* = MN275706).

Amesia nigricolor (L.M. Ames) X.Wei Wang & Samson, Stud. Mycol. 84: 159. 2016. [MB 818834]. Basionym: *Chaetomium nigricolor*. — Type: BPI. Ex-type: CBS 600.66 = ATCC 11211 = DSM 3703 = IMI 250971. Reproduction: sexual. ITS barcode: KX976578 (alternative markers: LSU = KX976703; *tub2* = KX976920; *rpb2* = KX976802). *Notes*: Several specimens in BPI are labeled as type according to Mycoportal: BPI 1101431, BPI 1101434, BPI 580553, BPI 580554, BPI 580555, BPI 580556, BPI 580557, BPI 580558, BPI 580559. A database search and/or examination of these specimens is needed to determine which of them is the holotype and which are isotypes, or if a lectotypification is necessary.

Amesia raii (G. Malhotra & Mukerji) X.Wei Wang & Houbraken, this study. [MB 840137]. Basionym: *Chaetomium raii*. — Type: DUH KG 326. Ex-type: CBS 107.83 = ITCC 1944. Reproduction: sexual. ITS barcode: n/a (alternative markers: LSU = n/a; *tub2* = n/a; *rpb2* = MZ342968).

Aporothielavia

Aporothielavia leptoderma (C. Booth) Malloch & Cain, Mycologia 65: 1074. 1973. [MB 308869]. Basionym: *Thielavia leptoderma* [as '*leptodermus*']. — Type: IMI 54770. Ex-type: CBS 538.74. Reproduction: sexual. ITS barcode: NR_164219 (alternative markers: LSU = NG_067253; *tub2* = MZ343025; *rpb2* = MZ342986).

Arcopilus

Arcopilus amazonicus T.F. Sousa & G.F. Silva, Phytotaxa 456: 150. 2020. [MB 835577]. — Type: INPA2410. Ex-type: INPA2410. Reproduction: sexual. ITS barcode: MH777083 (alternative markers: LSU = MH780043; *tub2* = MH784466; *rpb2* = MH784457).

Arcopilus aureus (Chivers) X.Wei Wang & Samson, Stud. Mycol. 84: 217. 2016. [MB 818855]. Basionym: *Chaetomium aureum*. — Type: BPI 1100494. Representative strain: CBS 153.52. Reproduction: sexual. ITS barcode: KX976582 (alternative markers: LSU = KX976707; *tub2* = KX976924; *rpb2* = KX976806). *Notes*: BPI 1100494 is tentatively indicated as holotype. Thaxter is indicated as the collector of this specimen, which is in agreement with the protologue. However, specimen BPI 1100497 rather than BPI 1100494 is labeled as type. No collector information is given for BPI 1100497.

Arcopilus cupreus (L.M. Ames) X.Wei Wang & Samson, Stud. Mycol. 84: 217. 2016. [MB 818856]. Basionym: *Chaetomium cupreum*. — Type: BPI 580275. Representative strain: CBS

560.80. Reproduction: sexual. ITS barcode: KX976584 (alternative markers: LSU = KX976709; *tub2* = KX976926; *rpb2* = KX976808).

***Arcopilus eremanthi* [as *'eremanthusum'*]** D.G. Tavares *et al.*, Arch. Microbiol. 204: 156, 5. 2022. [MB 843294]. — Type: VIC 47,499. Ex-type: CML 3766 = A2C54. Reproduction: sexual. ITS barcode: MN539886 (alternative markers: LSU = MN539910, *tub2* = n/a, *rpb2* = MN551186).

Arcopilus flavigenus (Van Warmelo) X.Wei Wang & Samson, Stud. Mycol. 84: 217. 2016. [MB 818858]. Basionym: *Chaetomium flavigenum*. — Type: PRE 43080. Ex-type: CBS 337.67. Reproduction: sexual. ITS barcode: KX976587 (alternative markers: LSU = KX976712; *tub2* = KX976929; *rpb2* = KX976811).

Arcopilus fusiformis (Chivers) X.Wei Wang & Samson, Stud. Mycol. 84: 217. 2016. [MB 818857]. Basionym: *Chaetomium fusiforme*. — Type: n/a. Representative strain: CBS 484.85. Reproduction: sexual. ITS barcode: KX976585 (alternative markers: LSU = KX976710; *tub2* = KX976927; *rpb2* = KX976809).

Arcopilus globulus M. Raza & L. Cai, Fungal Diversity 99: 75. 2019. [MB 556674]. — Type: HMAS 248066. Ex-type: CGMCC 3.19359 = LC11930. Reproduction: sexual. ITS barcode: MN215741 (alternative markers: LSU = MN215579; *tub2* = MZ343038; *rpb2* = MN255422). *Note*: Based on sequence data, we consider this species a synonym of *Arcopilus aureus*.

Arcopilus macrostiolatus (Stchigel *et al.*) X.Wei Wang & Houbraken, this study. [MB 840138]. Basionym: *Chaetomium macrostiolatum* [as '*macrostiolum*']. — Type: IMI 382896. Ex-type: CBS 102435. Reproduction: sexual. ITS barcode: MZ334722 (alternative markers: LSU = MZ351418; *tub2* = MZ343006; *rpb2* = MZ342965).

Arcopilus megasporus (Sörgel ex Seth) X.Wei Wang & Houbraken, this study. [MB 840139]. Basionym: *Chaetomium megasporum*. — Type: IMA 73514. Representative strain: CBS 127650. Reproduction: sexual. ITS barcode: n/a (alternative markers: LSU = n/a; *tub2* = MZ343010; *rpb2* = MZ342971).

Arcopilus navicularis Kubátová *et al.*, Persoonia 46: 417. 2021. [MB 839209]. — Type: PRM 954081. Ex-type: CCF 3252 = CBS 147158. Reproduction: sexual. ITS barcode: MW798185 (alternative markers: LSU = MW798181; *tub2* = MW816125; *rpb2* = MW816124).

Arcopilus purpurascens (Udagawa & Y. Sugiy.) X.Wei Wang & Houbraken, this study. [MB 840140]. Basionym: *Achaetomium purpurascens*. — Type: NHL 2896. Ex-type: CBS 287.83. Reproduction: sexual. ITS barcode: n/a (alternative markers: LSU = n/a; *tub2* = MZ343021; *rpb2* = MZ342982).

Arcopilus tangerinicapillus M. Raza & L. Cai, Fungal Diversity 99: 78. 2019. [MB 556675]. — Type: HMAS 248067. Ex-type: CGMCC 3.19326 = LC11936. Reproduction: sexual. ITS barcode: MN215743 (alternative markers: LSU = MN215581; *tub2* = MN329904; *rpb2* = MZ342999). *Note*: Based on sequence data, we consider *Ar. tangerinicapillus* a synonym of *Arcopilus cupreus*.

Arcopilus turgidopilosus (L.M. Ames) X.Wei Wang & Samson, Stud. Mycol. 84: 159. 2016. [MB 818836]. Basionym: *Chaetomium turgidopilosum*. — Type: ISC-F-0123588. Ex-type: CBS 169.52. Reproduction: sexual. ITS barcode: KX976588 (alternative markers: LSU = KX976713; *tub2* = KX976930; *rpb2* = KX976812).

Arxotrichum

Arxotrichum deceptivum (Malloch & Benny) X.Wei Wang & Houbraken, this study. [MB 830917]. Basionym: *Chaetomium deceptivum*. — Type: TRTC 46369. Ex-type: CBS 346.73. Reproduction: sexual. ITS barcode: MK919276 (alternative markers: LSU = MK919276; *tub2* = MK919390; *rpb2* = MK919332).

Arxotrichum gangligerum (L.M. Ames) X.Wei Wang & Houbraken, this study. [MB 830918]. Basionym: *Chaetomium gangligerum*. — Type: BPI. Ex-type: CBS 160.52 = ATCC 11206. Reproduction: sexual. ITS barcode: MK919277 (alternative markers: LSU = MK919277; *tub2* = MK919391; *rpb2* = MK919333). *Notes*: Two specimens in BPI are labeled as type according to Mycoportal: BPI 1100713 and BPI 580418. A database search and/or examination of these specimens is needed to determine which is the holotype and which the isotype, or if a lectotypification is necessary.

Arxotrichum officinarum (M. Raza & L. Cai) X.Wei Wang & Houbraken, this study. [MB 840142]. Basionym: *Myceliophthora officinarum*. — Type: HMAS 248073. Ex-type: CGMCC 3.19325. Reproduction: sexual & asexual. ITS barcode: MN215767 (alternative markers: LSU = MN215605; *tub2* = MN337032; *rpb2* = MN255448).

Arxotrichum piluliferoides (Udagawa & Y. Horie) X.Wei Wang & Houbraken, this study. [MB 830920]. Basionym: *Chaetomium piluliferoides*. — Type: NHL 2738. Ex-type: CBS 103.77 = IFM 4531 = IMI 210880 = NHL 2738. Reproduction: sexual & asexual. ITS barcode: MK919280 (alternative markers: LSU = MK919280; *tub2* = MK919394; *rpb2* = MK919336).

Arxotrichum repens (Guarro & Figueras) X.Wei Wang & Houbraken, this study. [MB 830921]. Basionym: *Chaetomium repens*. — Type: CBS H-6890. Ex-type: CBS 233.82 = FFBA 310. Reproduction: sexual. ITS barcode: MK919282 (alternative markers: LSU = MK919282; *tub2* = MK919396; *rpb2* = MK919338).

Arxotrichum sinense (K.T. Chen) X.Wei Wang & Houbraken, this study. [MB 830922]. Basionym: *Chaetomium sinense*. — Type: CBS H-10001 (isotype). Ex-type: CBS 541.83 = FFBA 388. Reproduction: sexual. ITS barcode: MK919283 (alternative markers: LSU = MK919283; *tub2* = MK919397; *rpb2* = MK919339).

Arxotrichum succineum (L.M. Ames) A. Nováková & M. Kolařík, Persoonia 40: 259. 2018. [MB 824082]. Basionym: *Chaetomium succineum*. — Type: ISC-F-0123587?. Ex-type: CBS 166.52 = ATCC 11216 = MUCL 18704. Reproduction: sexual. ITS barcode: MK919284 (alternative markers: LSU = MK919284; *tub2* = MK919398; *rpb2* = MK919340).

Arxotrichum wyomingense A. Nováková & M. Kolařík, Persoonia 40: 259. 2018. [MB 824081]. — Type: PRM 945788. Ex-type: CCF 5691. Reproduction: asexual. ITS barcode: LT968153 (alternative markers: LSU = LT968143; *tub2* = LT971393; *rpb2* = n/a).

Batnamyces

Batnamyces globulariicola Noumeur, Mycol. Prog. 19: 593. 2020. [MB 832845]. — Type: CBS H-23624. Ex-type: CBS 144474. Reproduction: asexual. ITS barcode: MT075917 (alternative markers: LSU = MT075917; *tub2* = MT075919; *rpb2* = MT075918).

Beniowskia

Beniowskia macrospora M.D. Mehrotra, Sydowia 17: 149. 1964 [MB 326968]; replaced synonym of *Trichocladium beniowskiae*.

Bommerella

Bommerella trigonospora Marchal, Bull. Soc. Roy. Bot. Belgique. 24: 164. 1885. [MB 221255]. — Type: BR5020093738364. Representative strain: CBS 324.69. Reproduction: sexual. ITS barcode: n/a (alternative markers: LSU = MZ351419; *tub2* = MZ343022; *rpb2* = MZ342984).

Botryoderma

Botryoderma lateritium Papendorf & H.P. Upadhyay, Trans. Brit. Mycol. Soc. 52: 258. 1969. [MB 327102]. — Type: PRE 44223. Ex-type: CBS 586.66 = ATCC 18926 = IMI 158956 = MUCL 8790. Reproduction: asexual. ITS barcode: MK919287 (alternative markers: LSU = MK919287; *tub2* = MK919401; *rpb2* = MK919343).

Botryoderma rostratum Papendorf & H.P. Upadhyay, Trans. Brit. Mycol. Soc. 52: 260. 1969. [MB 327103]. — Type: CBS H-24915 (lectotype). Ex-lectotype: CBS 184.68 = ATCC 18927 = IMI 158957. Reproduction: asexual. ITS barcode: MK919288 (alternative markers: LSU = MK919288; *tub2* = MK919402; *rpb2* = MK919344).

Botryotrichum

Botryotrichum atrogriseum J.F.H. Beyma, Verh. Kon. Ned. Akad. Wetensch., Afd. Natuurk. 26: 14. 1928. [MB 257744]. — Type: CBS 130.28. Ex-type: CBS 130.28 = IMI 092902 = MUCL 1110. Reproduction: asexual. ITS barcode: KX976589 (alternative markers: LSU = KX976714; *tub2* = KX976931; *rpb2* = KX976813).

Botryotrichum domesticum D.W. Li & N.P. Schultes, Botany 97: 314. 2019. [MB 828185]. — Type: NHES L1707. Ex-type: UAMH 11929. Reproduction: asexual. ITS barcode: MH899168 (alternative markers: LSU = MH899169; *tub2* = MH899172; *rpb2* = MH899171).

Botryotrichum foricae Jurjević & Hubka, Persoonia 42: 389. 2019. [MB 830668]. — Type: BPI 910933. Ex-type: CCF 5752 = EMSL 2683. Reproduction: asexual. ITS barcode: LR584032 (alternative markers: LSU = LR584033; *tub2* = LR584034; *rpb2* = n/a).

Botryotrichum geniculatum X.Wei Wang *et al*., this study. [MB 840127]. — Type: HMAS 350293 (holotype); CBS H-23629 (isotype). Ex-type: CGMCC 3.20441 = CBS 144475 = WXW 8287. Reproduction: sexual. ITS barcode: MZ334719 (alternative markers: LSU = MZ351422; *tub2* = MZ343011; *rpb2* = MZ342972).

Botryotrichum inquinatum (Udagawa & S. Ueda) X.Wei Wang & Houbraken, this study. [MB 830923]. Basionym: *Corynascella inquinata*. — Type: NHL 2841. Ex-type: CBS 155.80 = NHL 2841. Reproduction: sexual. ITS barcode: MK919289 (alternative markers: LSU = MK919289; *tub2* = MK919403; *rpb2* = MK919345).

Botryotrichum iranicum A. Alidadi, Mycol. Prog. 19: 1578. 2020. [MB 831975]. — Type: ABRIICC 106H. Ex-type: ABRIICC 10152. Reproduction: asexual. ITS barcode: MN134583 (alternative markers: LSU = n/a; *tub2* = MN128435; *rpb2* = MN128437).

Botryotrichum murorum (Corda) X.Wei Wang & Samson, Stud. Mycol. 84: 164. 2016. [MB 818837]. Basionym: *Chaetomium murorum*. — Type: PRM. Representative strain: CBS 163.52 = ATCC 11210 = MUCL 40179. Reproduction: sexual. ITS barcode: KX976591 (alternative markers: LSU = KX976716; *tub2* = KX976933; *rpb2* = KX976815). *Note*: No ex-type strains are available and epitypification of the species based on a suitable specimen needs to be performed.

Botryotrichum peruvianum Matsush., Icones Microfungorum a Matsushima lectorum: 17. 1975. [MB 309895]. — Type: MFC 2649. Representative strain: CBS 460.90 = FMR 3674. Reproduction: asexual. ITS barcode: KX976595 (alternative markers: LSU = KX976720; *tub2* = KX976937; *rpb2* = KX976819).

Botryotrichum piluliferum Sacc. & Marchal, Bull. Soc. Roy. Bot. Belgique 24: 66. 1885. [MB 221757]. — Type: Pl. II, figs 5–8, in Marchal, Bull. Soc. Roy. Bot. Belgique 24: 68, 1885 (lectotype designated here, MBT 10005041; CBS H-24868 [dried culture] – epitype designated here, MBT 10005042). Ex-epitype: CBS 654.79. Reproduction: asexual and sexual. ITS barcode: KX976597 (alternative markers: LSU = KX976722; *tub2* = KX976939; *rpb2* = KX976821). *Note*: No holotype specimen could be located (*e.g.*, in BR) and therefore the illustration in the protologue is designated here as lectotype.

Botryotrichum retardatum (A. Carter & R.S. Khan) X.Wei Wang & Houbraken, this study. [MB 840141]. Basionym: *Chaetomium retardatum*. — Type: TRTC 66.1778b. Ex-type: CBS 197.84. Reproduction: sexual. ITS barcode: n/a (alternative markers: LSU = n/a; *tub2* = MZ343019; *rpb2* = MZ342980).

Botryotrichum spirotrichum (R.K. Benj.) X.Wei Wang & Samson, Stud. Mycol. 84: 217. 2016. [MB 818860]. Basionym: *Magnusia spirotricha*. — Type: RSABG 116. Ex-type: CBS 211.55 = ATCC 12128 = IMI 060034. Reproduction: sexual. ITS barcode: KX976601 (alternative markers: LSU = KX976726; *tub2* = KX976943; *rpb2* = KX976825).

Botryotrichum trichorobustum (Seth) X.Wei Wang & Houbraken, this study. [MB 840143]. Basionym: *Chaetomidium trichorobustum*. — Type: CBS H-6840. Ex-type: CBS 563.67 = ATCC 18247 = IMI 130230. Reproduction: sexual. ITS barcode: n/a (alternative markers: LSU = MZ351420; *tub2* = MZ343027; *rpb2* = MZ342988).

Botryotrichum verrucosum (Pugh *et al*.) X.Wei Wang & Houbraken, Stud. Mycol. 93: 72. 2018. [MB 824410]. Basionym: *Thermomyces verrucosus*. — Type: IMI 96466. Ex-type: CBS 116.64 = ATCC 22222 = IMI 096466 = IMI 096466ii = MUCL 30565. Reproduction: asexual. ITS barcode: LT993567 (alternative markers: LSU = LT993567; *tub2* = LT993648; *rpb2* = LT993486).

Botryotrichum vitellinum (A. Carter) X.Wei Wang & Houbraken, this study. [MB 840144]. Basionym: *Chaetomium vitellinum*. — Type: TRTC 48873. Ex-type: CBS 180.84 = IMI 283627 = TRTC 48873. Reproduction: sexual. ITS barcode: MZ334725 (alternative markers: LSU = MZ351421; *tub2* = MZ343018; *rpb2* = MZ342979).

Brachychaeta

Brachychaeta variospora (Udagawa & Y. Horie) X.Wei Wang & Houbraken, Stud. Mycol. 93: 186. 2019. [MB 829845]. Basionym: *Chaetomium variosporum*. — Type: NHL 22698. Ex-type: CBS 414.73 = IMI 172986 = NHL 2698. Reproduction: sexual. ITS barcode: MK926797 (alternative markers: LSU = MK926797; *tub2* = MK926897; *rpb2* = MK876759).

Canariomyces

Canariomyces arenarius (Mouch.) X.Wei Wang & Houbraken, Stud. Mycol. 93: 189. 2019. [MB 829846]. Basionym: *Thielavia arenaria*. — Types: PC (holotype); CBS H-7846 (isotype); CBS H-7847 (isotype). Ex-type: CBS 507.74. Reproduction: sexual & asexual. ITS barcode: MK926798 (alternative markers: LSU

= MK926798; *tub2* = MK926898; *rpb2* = KM655438).

Canariomyces microsporus (Mouch.) X.Wei Wang & Houbraken, Stud. Mycol. 93: 190. 2019. [MB 829847]. Basionym: *Thielavia microspora*. — Type: PC. Ex-type: CBS 276.74. Reproduction: sexual & asexual. ITS barcode: MK926799 (alternative markers: LSU = MK926799; *tub2* = MK926899; *rpb2* = MK876760).

Canariomyces notabilis Arx, Persoonia 12: 185. 1984. [MB 107785]. — Type: CBS 548.83. Ex-type: CBS 548.83. Reproduction: sexual & asexual. ITS barcode: MK926802 (alternative markers: LSU = MK926802; *tub2* = MK926902; *rpb2* = MK876763).

Canariomyces subthermophilus (Mouch.) X.Wei Wang & Houbraken, Stud. Mycol. 93: 190. 2019. [MB 829848]. Basionym: *Thielavia subthermophila*. — Type: PC. Ex-type: CBS 509.74. Reproduction: sexual & asexual. ITS barcode: MK926804 (alternative markers: LSU = MK926804; *tub2* = MK926904; *rpb2* = MK876764).

Canariomyces vonarxii X.Wei Wang & Houbraken, Stud. Mycol. 93: 190. 2019. [MB 829849]. — Type: CBS H-18817. Ex-type: CBS 160.80 = NHL 2831. Reproduction: sexual & asexual. ITS barcode: MK926805 (alternative markers: LSU = MK926805; *tub2* = MK926905; *rpb2* = MK876765).

Carteria

Carteria arctostaphyli X.Wei Wang & Houbraken, Stud. Mycol. 93: 194. 2019. [MB 829851]. — Type: CBS H-23640. Ex-type: CBS 229.82. Reproduction: sexual. ITS barcode: MK926807 (alternative markers: LSU = MK926807; *tub2* = MK926907; *rpb2* = MK876767).

Chaetomidium (synonym of *Chaetomium*)

Chaetomidium arxii Benny, Mycologia 80: 832. 1980. [MB 112727]; basionym of *Trichocladium arxii*.

Chaetomidium fimeti (Fuckel) Sacc., Syll. Fung. 1: 39. 1882. [MB 174464]; synonym of *Chaetomium fimeti*.

Chaetomidium fragile Natarajan, Proc. Indian Acad. Sci., B 37: 124. 1972 [1971]. [MB 310876]; basionym of *Hyalosphaerella fragilis*.

Chaetomidium gallecicum [as '*galaicum*'] Stchigel & Guarro, Stud. Mycol. 50: 217. 2004. [MB 368919]; synonym of *Aporothielavia leptoderma*.

Chaetomidium leptoderma (C. Booth) Greif & Currah, Mycol. Res. 111: 74. 2007. [MB 510052]; synonym of *Aporothielavia leptoderma*.

Chaetomidium peruvianum Goch., Mycologia 60: 1118. 1968. [MB 328015]; basionym of *Chrysanthotrichum peruvianum*.

Chaetomidium pilosum (C. Booth & Shipton) Arx, Stud. Mycol. 8: 16. 1975. [MB 310879]; synonym of *Chaetomium pilosum*.

Chaetomidium spirotrichum (R.K. Benj.) Malloch & Cain, Mycologia 65: 1069. 1973. [MB 310882]; synonym of *Botryotrichum spirotrichum*.

Chaetomidium subfimeti Seth, Trans. Brit. Mycol. Soc. 50: 46. 1967. [MB 328016]; basionym of *Chaetomium subfimeti*.

Chaetomidium thermophilum (Fergus & Sinden) Lodha, Taxonomy of fungi (Proc. Int. Symp. Madras, 1973) 1: 248. 1978. [MB 310883]; synonym of *Thermothelomyces fergusii*.

Chaetomidium trichorobustum Seth, Nova Hedwigia 16: 430. 1968. [MB 328017]; basionym of *Botryotrichum trichorobustum*.

Chaetomium

Chaetomium acropullum X.Wei Wang, Nova Hedwigia 80: 414. 2005. [MB 336138]; basionym of *Trichocladium acropullum*.

Chaetomium afropilosum X.Wei Wang *et al.*, Persoonia 36: 91. 2015 [2016]. [MB 812942]. — Type: CBS H-22192. Ex-type: CBS 145.38 = DAOM 19448. Reproduction: sexual. ITS barcode: KT214574 (alternative markers: LSU = KT214605; *tub2* = KT214751; *rpb2* = KT214675).

Chaetomium amberpetense P. Rama Rao & Ram Reddy, Mycopathol. Mycol. Appl. 24: 114. 1964. [MB 328021]; synonym of *Amesia nigricolor*.

Chaetomium amesii Sergejeva, Novosti Sist. Nizsh. Rast. 2: 112. 1965. [MB 328022]; synonym of *Humicola homopilata*.

Chaetomium ampulliellum X.Wei Wang, Nova Hedwigia 81: 248. 2005. [MB 356099]; basionym of *Humicola ampulliella*.

Chaetomium amygdalisporum Udagawa & T. Muroi, Trans. Mycol. Soc. Japan 22: 13. 1981. [MB 111238]; basionym of *Ovatospora amygdalispora*.

Chaetomium anamorphosum S.A. Ahmed *et al.*, Fungal Diversity 76: 18. 2015. [MB 810426]; basionym of *Subramaniula anamorphosa*.

Chaetomium anastomosans M. Raza & L. Cai, Fungal Diversity 99: 78. 2019. [MB 556676]. — Type: HMAS 248069. Ex-type: CGMCC 3.19350 = LC11926. Reproduction: sexual. ITS barcode: MN215745 (alternative markers: LSU = MN215583; *tub2* = MN337028; *rpb2* = MN255426). *Note*: This species is a synonym of *Chaetomium globosum*.

Chaetomium anguipilium L.M. Ames, A monograph of the *Chaetomiaceae*: 12. 1963. [MB 328023]; basionym of *Collariella anguipilia*.

Chaetomium angulare Yu Zhang & L. Cai, Fungal Biol. 121: 28. 2016 [2017]. [MB 811149]; basionym of *Ovatospora angularis*.

Chaetomium angustispirale Sergejeva, Not. Syst. Sect. Crypt. Inst. Bot. Acad. Sci. USSR 11: 115. 1956. [MB 294684]. — Type: –. Ex-type: CBS 137.58 = IMI 074952 = VKM F-1942. Reproduction: sexual & asexual. ITS barcode: JN209862 (alternative markers: LSU = JN209862; *tub2* = JN256141; *rpb2* = KF001824).

Chaetomium ascotrichoides Calviello, Revista Mus. Argent. Ci. Nat., Bernardino Rivadavia Inst. Nac. Invest. Ci. Nat., Bot. 3: 372. 1972. [MB 310890]. — Type: n/a. Ex-type: CBS 113.83 = IMI 182725. Reproduction: sexual. ITS barcode: KC109752 (alternative markers: LSU = KC109752; *tub2* = KC109770; *rpb2* = KF001832).

Chaetomium atrobrunneum L.M. Ames, Mycologia 41: 641. 1949. [MB 294685]; basionym of *Amesia atrobrunnea*.

Chaetomium aureum Chivers, Proc. Amer. Acad. Arts Sci. 48: 86. 1912. [MB 161470]; basionym of *Arcopilus aureus*.

Chaetomium biporatum Cano & Guarro, Nova Hedwigia 44: 543. 1987. [MB 130544]; basionym of *Parachaetomium biporatum*.

Chaetomium bostrychodes Zopf, Verh. Bot. Vereins Provinz Brandenburg 19: 173. 1877. [MB 161575]; basionym of *Collariella bostrychodes*.

Chaetomium brasiliense Bat. & Pontual, Bol. Agric. Pernambuco 15: 70. 1948. [MB 294688]; basionym of *Ovatospora brasiliensis*.

Chaetomium camelliae Jayaward. *et al.*, Mycosphere 12: 471. 2021. [MB 558001]. — Type: JZBH3340001. Ex-type: JZB3340001. Reproduction: sexual. ITS barcode: MT535751 (alternative markers: LSU = MT535749, *tub2* = MT535533, *rpb2* = MT535537).

Chaetomium cancroideum Tschudy, Amer. J. Bot. 24: 472. 1938. [MB 120075]; synonym of *Dichotomopilus funicola*.

Chaetomium capillare X.Wei Wang *et al.*, Persoonia 36: 92. 2015. [2016]. [MB 812975]. — Type: CBS H-22187. Ex-type: CBS 128489 = UTHSC 03-1339. Reproduction: sterile. ITS barcode:

KT214583 (alternative markers: LSU = KT214614; *tub2* = KT214760; *rpb2* = KT214686).

Chaetomium carinthiacum Sörgel, Arch. Mikrobiol. 40: 393. 1961. [MB 328032]; basionym of *Parachaetomium carinthiacum*.

Chaetomium causiiforme L.M. Ames, Mycologia 41: 637. 1949. [MB 118825]; basionym of *Collariella causiiformis*.

Chaetomium cervicicola X.Wei Wang *et al.*, Persoonia 36: 93. 2015 [2016]. [MB 812976]. — Type: CBS H-22188. Ex-type: CBS 128492 = UTHSC 07-3593. Reproduction: sterile. ITS barcode: KT214558 (alternative markers: LSU = KT214592; *tub2* = KT214735; *rpb2* = KT214662).

Chaetomium chiversii (J.C. Cooke) A. Carter, Nova Hedwigia 84: 19. 1986. [MB 104874]; synonym of *Floropilus chiversii*.

Chaetomium cirrhatum [as '*cirrhata*'] Yu Zhang & L. Cai, Fungal Biol. 121: 28. 2016 [2017]. [MB 840133]. — Type: HMAS 245784. Ex-type: CGMCC 3.17540. Reproduction: sexual. ITS barcode: KP336792 (alternative markers: LSU = KP336841; *tub2* = KP336890; *rpb2* = KT149508).

Chaetomium citrinum Udagawa & T. Muroi, Trans. Mycol. Soc. Japan 22: 15. 1981. [MB 111239]. — Type: NHL 2873. Ex-type: CBS 693.82 = NHL 2873. Reproduction: sexual. ITS barcode: KT214587 (alternative markers: LSU = KT214617; *tub2* = KT214764; *rpb2* = KT214691).

Chaetomium coarctatum Sergejeva, Bot. Mater. Otd. Sporov. Rast. Bot. Inst. Komarova Akad. Nauk S.S.S.R. 14: 146. 1961. [MB 328033]. — Type: –. Ex-type: CBS 162.62 = ATCC 14530 = IMI 090491 = MUCL 18697 = VKM F-1946. Reproduction: sexual. ITS barcode: JN209863 (alternative markers: LSU = JN209863; *tub2* = JN256142; *rpb2* = KF001802).

Chaetomium cochliodes Palliser, North American Flora 3: 61. 1910. [MB 257241]. — Type: NY01050409; HMAS 244354 (epitype). Ex-epitype: CBS 155.52. Reproduction: sexual. ITS barcode: KC109754 (alternative markers: LSU = KC109754; *tub2* = KC109772; *rpb2* = KF001811).

Chaetomium concavisporum M. Raza & L. Cai, Fungal Diversity 99: 80. 2019. [MB 556677]. — Type: HMAS 248070. Ex-type: CGMCC 3.19348 = LC11924. Reproduction: sexual. ITS barcode: MN215747 (alternative markers: LSU = MN215585; *tub2* = MN329916; *rpb2* = MN255428); synonym of *Chaetomium cochliodes.*

Chaetomium contagiosum X.Wei Wang *et al.*, Persoonia 36: 98. 2015 [2016]. [MB 812977]. — Type: CBS H-22189. Ex-type: CBS 128494 = UTHSC 10-726. Reproduction: sterile. ITS barcode: KT214555 (alternative markers: LSU = KT214589; *tub2* = KT214732; *rpb2* = KT214659).

Chaetomium crispatum (Fuckel) Fuckel, Jahrb. Nassauischen Vereins Naturk. 23-24: 90. 1870. [MB 156792]; synonym of *Trichocladium crispatum*.

Chaetomium cristatum L.M. Ames, Mycologia 41: 639. 1950. [MB 294690]; basionym of *Subramaniula cristata*.

Chaetomium cruentum L.M. Ames, A monograph of the *Chaetomiaceae*: 20. 1963. [MB 120272]. — Type: n/a, see Notes, CBS H-6860 (isotype). Ex-type: CBS 371.66. Reproduction: sexual. ITS barcode: JN209871 (alternative markers: LSU = JN209871; *tub2* = JN256148; *rpb2* = KF001795). *Notes*: This species is phylogenetically identical to *Chaetomium globosum*, but is morphologically distinct (Wang *et al*. 2016a). We tentatively accept this species in *Chaetomium*. Several specimens are labeled as type according to Mycoportal: BPI 1101395, NY01050414 and NY01050415. A database search and/or examination of these specimens is needed to determine which of them is the holotype and which are isotypes, or if a lectotypification is necessary.

Chaetomium cucumericola X.Wei Wang *et al.*, Persoonia 36: 98. 2015 [2016]. [MB 812978]. — Type: CBS H-22190. Ex-type: CBS 378.71. Reproduction: sterile. ITS barcode: KT214579 (alternative markers: LSU = KT214610; *tub2* = KT214756; *rpb2* = KT214680).

Chaetomium cuniculorum Fuckel, Fungi Rhen. Exs. Suppl. Fasc. 5: no. 1961. 1867. [MB 171246]; basionym of *Subramaniula cuniculorum*.

Chaetomium cupreum L.M. Ames, Mycologia 41: 642. 1949. [MB 294691]; basionym of *Arcopilus cupreus*.

Chaetomium cuyabenoense [as '*cuyabenoensis*'] Decock & Hennebert, Mycol. Res. 101: 309. 1997. [MB 628862]; basionym of *Humicola cuyabenoensis*.

Chaetomium cymbiforme Lodha, J. Indian Bot. Soc. 43: 129. 1964. [MB 328037]; basionym of *Amesia cymbiformis*.

Chaetomium deceptivum Malloch & Benny, Mycologia 65: 648. 1973. [MB 310899]; basionym of *Arxotrichum deceptivum*.

Chaetomium distortum L.M. Ames, A monograph of the *Chaetomiaceae*: 21. 1963. [MB 328039]; basionym of *Humicola distorta*.

Chaetomium dolichotrichum L.M. Ames, Mycologia 37: 145. 1945. [MB 285133]; basionym of *Dichotomopilus dolichotrichus*.

Chaetomium dreyfussii Arx, Beih. Nova Hedwigia 84: 6. 1986. [MB 104875]; basionym of *Amesia dreyfussii*.

Chaetomium elatum Kunze, Deutschl. Schwämme, Achte Lieferung: 3, no. 184. 1818. [MB 172050]. — Type: CBS H-22851 (neotype). Ex-neotype: CBS 142034. Reproduction: sexual & asexual. ITS barcode: KX976612 (alternative markers: LSU = KX976733; *tub2* = KX976954; *rpb2* = KX976832).

Chaetomium erectum Skolko & J.W. Groves, Canad. J. Res. 26: 277. 1948. [MB 285134]; basionym of *Dichotomopilus erectus*.

Chaetomium fimeti Fuckel, Jahrb. Nassauischen Vereins Naturk. 15: 64. 1860. [MB 160431]. — Type: G00127165 (holotype), CBS H-22198 (epitype). Ex-epitype: DSM 62108 = CBS 139034. Reproduction: sexual. ITS barcode: KT214559 (alternative markers: LSU = KT214593; *tub2* = KT214736; *rpb2* = KT214663).

Chaetomium flavigenum Van Warmelo, Mycologia 58: 847. 1966. [MB 328042]; basionym of *Arcopilus flavigenus*.

Chaetomium floriforme Gené & Guarro, Mycol. Res. 100: 1005. 1996. [MB 415630]; basionym of *Humicola floriformis*.

Chaetomium funicola Cooke, Grevillea 1: 176. 1873. [MB 172830]; basionym of *Dichotomopilus funicola*.

Chaetomium fusiforme Chivers, Proc. Amer. Acad. Arts 48: 87. 1912. [MB 172131]; basionym of *Arcopilus fusiformis*.

Chaetomium fusisporum G. Sm., Trans. Brit. Mycol. Soc. 44: 46. 1961. [MB 328044]; basionym of *Subramaniula fusispora*.

Chaetomium fusum L.M. Ames, A monograph of the *Chaetomiaceae* Ser. 2: 25. 1963. [MB 328045]; basionym of *Dichotomopilus fusus*.

Chaetomium gangligerum L.M. Ames, Mycologia 41: 640. 1950. [MB 294695]; basionym of *Arxotrichum gangligerum*.

Chaetomium gelasinosporum Aue & E. Müll., Ber. Deutsch. Bot. Ges. 77: 193. 1967. [MB 328046]; basionym of *Amesia gelasinospora*.

Chaetomium globosporum Rikhy & Mukerji, Kavaka: 38. 1974. [MB 310902]; replaced synonym of *Chaetomium neoglobosporum*.

Chaetomium globosum Kunze, Mykol. Hefte 1: 16. 1817. [MB 172545]. — Type: CBS H-22185 (neotype). Ex-neotype: CBS 160.62. Reproduction: sexual. ITS barcode: KT214565

(alternative markers: LSU = KT214596; *tub2* = KT214742; *rpb2* = KT214666).

Chaetomium globosum var. *flavoviride* E.K. Novák, Ann. Univ. Sci. Budapest. Rolando Eötvös, Sect. Biol. 8: 207. 1966. [MB 349175]; synonym of *Chaetomium globosum*.

Chaetomium globosum var. *griseum* E.K. Novák, Ann. Univ. Sci. Budapest. Rolando Eötvös, Sect. Biol. 8: 207. 1966. [MB 353346]; synonym of *Chaetomium globosum*.

Chaetomium gracile Udagawa, J. Gen. Appl. Microbiol. Tokyo 6: 235. 1960. [MB 328048]; basionym of *Achaetomiella gracilis*.

Chaetomium graminiforme X.Wei Wang *et al.*, Persoonia 36: 106. 2015 [2016]. [MB 812979]. — Type: CBS H-22193. Ex-type: CBS 506.84 = TRTC 47862. Reproduction: sexual. ITS barcode: KT214584 (alternative markers: LSU = KT214615; *tub2* = KT214761; *rpb2* = KT214687).

Chaetomium grande Asgari & Zare, Mycologia 103: 874. 2011. [MB 519105]. — Type: IRAN 14608F. Ex-type: IRAN 1064C = CBS 126780. Reproduction: sexual. ITS barcode: HM365253 (alternative markers: LSU = HM365253; *tub2* = HM365273; *rpb2* = KT214657).

Chaetomium hamadae (Udagawa) Arx, Proc. Indian Acad. Sci., Pl. Sci. 94: 343. 1985. [MB 105136]; synonym of *Pseudothielavia hamadae*.

Chaetomium heterothallicum Yu Zhang & L. Cai, Fungal Biol. 121: 29. 2016 [2017]. [MB 811151]; basionym of *Trichocladium heterothallicum*.

Chaetomium hexagonosporum A. Carter & Malloch, Canad. J. Bot. 60: 1249. 1982. [MB 109668]; basionym of *Collariella hexagonospora*.

Chaetomium hispanicum Guarro & Arx, Beih. Nova Hedwigia 84: 6. 1986. [MB 104876]; basionym of *Parachaetomium hispanicum*.

Chaetomium homopilatum Omvik, Mycologia 47: 749. 1955. [MB 294697]; basionym of *Humicola homopilata*.

Chaetomium indicum Corda, Icon. Fung. 4: 38, tab. 8, fig. 104. 1840. [MB 150904]; basionym of *Dichotomopilus indicus*.

Chaetomium interruptum Asgari & Zare, Mycologia 103: 874. 2011. [MB 519104]. — Type: IRAN 14607F. Ex-type: IRAN 1278C = CBS 126660. Reproduction: sexual. ITS barcode: HM365246 (alternative markers: LSU = HM365246; *tub2* = KT214741; *rpb2* = KT214665).

Chaetomium iranianum Asgari & Zare, Mycologia 103: 877. 2011. [MB 519106]. — Type: IRAN 14609F. Ex-type: IRAN 861C = CBS 126670. Reproduction: sexual. ITS barcode: HM365257 (alternative markers: LSU = HM365257; *tub2* = HM365297; *rpb2* = MT568848). *Note*: This species was transferred to the genus *Parachaetomium* (as *P. iranianum*); however, the current name is *Parachaetomium perlucidum* (this study).

Chaetomium iranicum M. Mehrabi-Koushki *et al.*, Sydowia 73: 24. 2020. [MB 835248]. — Type: IRAN 17599F. Ex-type: IRAN 3379C = SCUA-Agh-26. Reproduction: sexual. ITS barcode: n/a (alternative markers: LSU = n/a; *tub2* = MN520421; *rpb2* = MT273944).

Chaetomium irregulare Sörgel ex W. Gams, Nova Hedwigia 12: 386. 1966. [MB 328055]; replaced synonym of *Subramaniula flavipila*.

Chaetomium jabalpurense D.P. Tiwari *et al.*, Curr. Sci. 46: 578. 1977. [MB 310905]. — Type: IMI 157256. Ex-type: CBS 552.83 = IMI 157256. Reproduction: sexual. ITS barcode: n/a (alternative markers: LSU = n/a; *tub2* = MZ343026; *rpb2* = MZ342987). *Note*: Based on the phylogenetic analysis (Fig. 7), we consider *Chaetomium jabalpurense* a synonym of *Amesia gelasinospora*.

Chaetomium jatrophae Rohit Sharma, Mycotaxon 124: 120. 2013. [MB 563940]. — Type: AMH 9558. Ex-type: CBS 13426 = MCC 1025. Reproduction: sexual. ITS barcode: JQ246354 (alternative markers: LSU = HE981193; *tub2* = HE981190; *rpb2* = n/a). *Notes*: The *tub2* sequence deposited on GenBank is 99.3 % similar to that of CBS 673.80, the ex-type of *Amesia gelasinospora*. We therefore consider this species a synonym of *Amesia gelasinospora*.

Chaetomium jodhpurense Lodha, J. Indian Bot. Soc. 43: 132. 1964. [MB 328056]; basionym of *Acrophialophora jodhpurensis*.

Chaetomium laterale Yu Zhang & L. Cai, Fungal Biol. 121: 30. 2016. [MB 811152]; basionym of *Subramaniula lateralis*.

Chaetomium lentum Van Warmelo, Mycologia 58: 850. 1967. [MB 328057]; basionym of *Chrysanthotrichum lentum*.

Chaetomium longiciliatum [as '*longiciliata*'] Yu Zhang & L. Cai, Fungal Biol. 121: 31. 2016 [2017]. [MB 840134]; basionym of *Parachaetomium longiciliatum*.

Chaetomium longicolle [as '*longicolleum*'] Krzemien. & Badura, Acta Soc. Bot. Poloniae 23: 748. 1954. [MB 491886]; basionym of *Staphylotrichum longicolle* [as '*longicolleum*'].

Chaetomium longirostre (Farrow) L.M. Ames, A monograph of the *Chaetomiaceae*: 29. 1963. [MB 282966]; synonym of *Staphylotrichum longicolle*.

Chaetomium lucknowense J.N. Rai & J.P. Tewari, Canad. J. Bot. 40: 1379. 1963. [MB 328059]; basionym of *Chrysocorona lucknowensis*.

Chaetomium luteum (J.N. Rai & J.P. Tewari) P.F. Cannon, Trans. Brit. Mycol. Soc. 87: 60. 1986. [MB 103140]; synonym of *Achaetomium luteum*.

Chaetomium macrostiolatum [as '*macrostiolum*'] Stchigel *et al.*, Mycologia 94: 121. 2002. [MB 484629]; basionym of *Arcopilus macrostiolatus*.

Chaetomium madrasense Natarajan, Proc. Indian Acad. Sci., Sect. B 74: 255. 1971. [MB 310909]. — Type: CBS H-6877. Ex-type: CBS 315.74. Reproduction: sexual. ITS barcode: KC109751 (alternative markers: LSU = KC109751; *tub2* = KC109769; *rpb2* = KF001831).

Chaetomium malaysiense (D. Hawksw.) Arx, Beih. Nova Hedwigia 84: 38. 1986. [MB 104877]; synonym of *Humicola malaysiensis*.

Chaetomium mareoticum Besada & Yusef, Trans. Brit. Mycol. Soc. 52: 502. 1969. [MB 310911]; basionym of *Parachaetomium mareoticum*.

Chaetomium medusarum J.A. Mey. & Lanneau, Bull. Trimestriel Soc. Bot. France 83: 318. 1967. [MB 328061]; basionym of *Ovatospora medusarum*.

Chaetomium megalocarpum Bainier, Bull. Trimestriel Soc. Bot. France 25: 202. 1910. [MB 165525]. — Type: Pl. XVI, figs 1–4 in Bainier, Bull. Trimestriel Soc. Bot. France 25: 202, 1910 (lectotype); CBS H-22186 (epitype). Ex-epitype: MUCL 9589 = CBS 149.59. Reproduction: sexual. ITS barcode: KC109744 (alternative markers: LSU = KC109744; *tub2* = KC109762; *rpb2* = KF001828).

Chaetomium megasporum Sörgel ex Seth, Beih. Nova Hedwigia 37: 82. 1972. [MB 310912]; basionym of *Arcopilus megasporus*.

Chaetomium microthecium [as '*microthecia*'] Yu Zhang & L. Cai, Fungal Biol. 121: 32. 2016 [2017]. [MB 840135]. — Type: HMAS 245781. Ex-type: CGMCC 3.17556. Reproduction: sexual. ITS barcode: KP336785 (alternative markers: LSU = KP336834; *tub2* = KP336883; *rpb2* = KT149505).

Chaetomium mollicellum L.M. Ames, A monograph of the *Chaetomiaceae*: 30. 1963. [MB 328063]; basionym of *Ovatospora mollicella*.

Chaetomium mollipilium L.M. Ames, Mycologia 42: 644. 1950. [MB 294702]; synonym of *Chaetomium globosum*.

Chaetomium muelleri Arx, Beih. Nova Hedwigia 84: 6. 1986. [MB 104878]; basionym of *Parachaetomium muelleri*.

Chaetomium multispirale A. Carter *et al.*, Canad. J. Bot. 60: 1256. 1982. [MB 109669]; basionym of *Parachaetomium multispirale*.

Chaetomium murorum Corda, Icon. Fung. 1: 24, tab. 7, fig. 293B. 1837. [MB 165260]; basionym of *Botryotrichum murorum*.

Chaetomium neoglobosporum X.Wei Wang & Houbraken, [MB 841112]. Replaced synonym: *Chaetomium globosporum*. — Type: IMI 166876. Ex-type: CBS 108.83 = ITCC 1835. Reproduction: sexual. ITS barcode: KC109750 (alternative markers: LSU = KC109750; *tub2* = KC109768; *rpb2* = KF001825).

Chaetomium nepalense (Udagawa & Y. Sugiy.) Arx, Proc. Indian Acad. Sci., Sect. B 94: 344. 1985. [MB 105137]. Basionym: *Achaetomium nepalense*. — Type: NHL 2895. Ex-type: CBS 288.83 = IMI 288623 = NHL 2895. Reproduction: sexual. ITS barcode: MH861591 (alternative markers: LSU = MH873316; *tub2* = n/a; *rpb2* = MZ342983).

Chaetomium nigricolor L.M. Ames, Mycologia 42: 645. 1950. [MB 294703]; basionym of *Amesia nigricolor*.

Chaetomium novozelandicum X.Wei Wang *et al.*, Persoonia 36: 110. (2015) [2016]. [MB 812980]. — Type: AEB 1071 (holotype); CBS H-22191 (isotype). Ex-type: CBS 124555. Reproduction: sterile. ITS barcode: KT214576 (alternative markers: LSU = KT214607; *tub2* = KT214753; *rpb2* = KT214677).

Chaetomium nozdrenkoae Sergejeva, Bot. Mater. Otd. Sporov. Rast. Bot. Inst. Komarova Akad. Nauk S.S.S.R. 14: 140. 1961. [MB 328064]. — Type: –. Ex-type: CBS 163.62 = ATCC 14528 = IMI 090490 = IMI 090490 = MUCL 18703 = VKM F-1953. Reproduction: sexual. ITS barcode: KT214556 (alternative markers: LSU = KT214590; *tub2* = KT214733; *rpb2* = KT214660).

Chaetomium olivaceum Cooke & Ellis, Grevillea 6: 96. 1878. [MB 164649]. — Type: n/a. Representative strain: CBS 418.80A. Reproduction: sexual. ITS barcode: JN209914 (alternative markers: LSU = JN209914; *tub2* = JN256184; *rpb2* = KF001806). *Notes*: Two collections of Ellis are cited in the protologue and an illustration is available. *Chaetomium olivaceum* remains to be lecto- and epitypified based on suitable specimens.

Chaetomium ovatoascomatis M. Raza & L. Cai, Fungal Diversity 99: 82. 2019. [MB 556679]. — Type: HMAS 248072. Ex-type: CGMCC 3.19341 = LC13510. Reproduction: sexual. ITS barcode: MN215753 (alternative markers: LSU = MN215591; *tub2* = MN329920; *rpb2* = MN255434); synonym of *Chaetomium cochliodes*.

Chaetomium pachypodioides L.M. Ames, Mycologia 37: 145. 1945. [MB 285136]; basionym of *Collariella pachypodioides*.

Chaetomium perlucidum Sergejeva, Not. Syst. Sect. Crypt. Inst. Bot. Acad. Sci. USSR 11: 108. 1956. [MB 294704]; basionym of *Parachaetomium perlucidum*.

Chaetomium pilosum (C. Booth & Shipton) X.Wei Wang & Crous, Persoonia 36: 112. 2015 [2016]. [MB 812981]. Basionym: *Thielavia pilosa*. — Type: IMI 113231. Ex-type: CBS 335.67 = IMI 113231 = VKM F-1851. Reproduction: sexual. ITS barcode: KT214586 (alternative markers: LSU = FJ666356; *tub2* = KT214763; *rpb2* = FJ666387).

Chaetomium piluliferoides Udagawa & Y. Horie, Trans. Mycol. Soc. Japan: 337. 1975. [MB 310914]; basionym of *Arxotrichum piluliferoides*.

Chaetomium piluliferum J. Daniels, Trans. Brit. Mycol. Soc. 44: 84. 1961. [MB 328069]; synonym of *Botryotrichum piluliferum*.

Chaetomium pinnatum L.M. Ames, A monograph of the *Chaetomiaceae*: 33. 1963. [MB 328070]; basionym of *Humicola pinnata*.

Chaetomium pratense X.Wei Wang, Mycol. Prog. 13: 723. 2014. [MB 563348]; basionym of *Dichotomopilus pratensis*.

Chaetomium pseudocochliodes X.Wei Wang *et al.*, Persoonia 36: 113. 2015 [2016]. [MB 812982]. — Type: CBS H-22197. Ex-type: CGMCC 3.9441. Reproduction: sexual. ITS barcode: JN209925 (alternative markers: LSU = JN209925; *tub2* = JN256195; *rpb2* = KF001816).

Chaetomium pseudoglobosum X.Wei Wang *et al.*, Persoonia 36: 115. 2015 [2016]. [MB 812983]. — Type: CBS H-10083. Ex-type: CBS 574.71. Reproduction: sexual. ITS barcode: KT214573 (alternative markers: LSU = KT214604; *tub2* = KT214750; *rpb2* = KT214674).

Chaetomium quadrangulatum Chivers, Proc. Amer. Acad. Arts Sci. 48: 85. 1912. [MB 173351]; basionym of *Collariella quadrangulata*.

Chaetomium raii G. Malhotra & Mukerji, Rev. Mycol., (Paris) 40(2): 182. 1976. [MB 283388]; basionym of *Amesia raii*.

Chaetomium ramipilosum Schaumann, Arch. Mikrobiol. 91: 98. 1973. [MB 310916]; synonym of *Chaetomium elatum*.

Chaetomium ramosissimum X.Wei Wang & L. Cai, Mycol. Prog. 13: 725. 2014. [MB 801734]; basionym of *Dichotomopilus ramosissimus*.

Chaetomium rectangulare Asgari & Zare, Mycologia 103: 872. 2011. [MB 519103]. — Type: IRAN 14606F. Ex-type: IRAN 1641C = CBS 126778. Reproduction: sexual & asexual. ITS barcode: HM365239 (alternative markers: LSU = HM365239; *tub2* = HM365285; *rpb2* = KT214688).

Chaetomium reflexum Skolko & J.W. Groves, Canad. J. Res. 26: 279. 1948. [MB 285137]; basionym of *Dichotomopilus reflexus*.

Chaetomium repens Guarro & Figueras, Beih. Nova Hedwigia 84: 6. 1986. [MB 104870]; basionym of *Arxotrichum repens*.

Chaetomium retardatum A. Carter & R.S. Khan, Canad. J. Bot. 60: 1255. 1982. [MB 109670]; basionym of *Botryotrichum retardatum*.

Chaetomium robustum L.M. Ames, A monograph of the *Chaetomiaceae*: 35. 1963. [MB 328075]; basionym of *Collariella robusta*.

Chaetomium sacchari M. Raza & L. Cai, Fungal Diversity 99: 88. 2019. [MB 556680]. — Type: HMAS 248071. Ex-type: CGMCC 3.19349 = LC11918. Reproduction: sexual. ITS barcode: MN215759 (alternative markers: LSU = MN215597; *tub2* = MN329926; *rpb2* = MN255440); synonym of *Chaetomium cryptocochliodes*.

Chaetomium seminis-citrulli [as '*semen-citrulli*'] Sergejeva, Not. Syst. Sect. Crypt. Inst. Bot. Acad. Sci. USSR 11: 113. 1956. [MB 537941]; basionym of *Trichocladium seminis-citrulli*.

Chaetomium seminudum L.M. Ames, Mycologia 41: 642. 1949. [MB 294709]; basionym of *Humicola seminuda*.

Chaetomium semispirale Udagawa & Cain, Canad. J. Bot. 47: 1947. 1969. [MB 310918]; basionym of *Pseudohumicola semispiralis*.

Chaetomium senegalense L.M. Ames, A monograph of the *Chaetomiaceae*: 36. 1963. [MB 328077]; basionym of *Ovatospora senegalensis*.

Chaetomium serpentinum L.M. Ames ex A. Carter, Canad. J. Bot. 61: 2605. 1983. [MB 106675]; synonym of *Amesia cymbiformis*.

Chaetomium sinense K.T. Chen, Acta Microbiol. Sin. 13(2): 125. 1973. [MB 310920]; basionym of *Arxotrichum sinense*.

Chaetomium sphaerale Chivers, Proc. Amer. Acad. Arts Sci. 48: 84. 1912. [MB 158635]; basionym of *Humicola sphaeralis*.

Chaetomium spiculipilium L.M. Ames, A monograph of the *Chaetomiaceae*: 37. 1963. [MB 328078]. — Type: BPI 1100708 (holotype); CBS H-6893 (isotype). Ex-type: CBS 373.66. Reproduction: sexual. ITS barcode: KC109756 (alternative markers: LSU = KC109756; *tub2* = KC109774; *rpb2* = KF001809).

Chaetomium spinosum Chivers, Proc. Amer. Acad. Arts 48: 86. 1912. [MB 152061]; basionym of *Xanthiomyces spinosus*.

Chaetomium spirochaete Palliser, North American Flora 3: 61. 1910. [MB 167661]. — Type: NY01050443 (holotype); HMAS 244438 (epitype). Ex-epitype: CBS 730.84 = IMI 287303 = QM 6702. Reproduction: sexual. ITS barcode: JN209921 (alternative markers: LSU = JN209921; *tub2* = JN256191; *rpb2* = KF001819).

Chaetomium strumarium (J.N. Rai *et al.*) P.F. Cannon, Trans. Brit. Mycol. Soc. 87: 64. 1986. [MB 103141]; synonym of *Achaetomium strumarium*.

Chaetomium subaffine Sergejeva ex X.Wei Wang & Houbraken, this study. [MB 842311]. — Type: CBS H-24916. Ex-type: CBS 637.91 = ATCC 14531 = IMI 90489 = VKM F-1945. Reproduction: sexual & asexual. ITS barcode: JN209929 (alternative markers: LSU = JN209929; *tub2* = JN256199; *rpb2* = KF001817).

Chaetomium subfimeti (Seth) X.Wei Wang & Crous, Persoonia 36: 121. 2015 [2016]. [MB 812984]. Basionym: *Chaetomidium subfimeti.* — Type: IMI 116692 (holotype); CBS H-6839 (isotype). Ex-type: CBS 370.66 = ATCC 18209 = IMI 116692 = LCP 82.3317. Reproduction: sexual. ITS barcode: KT214562 (alternative markers: LSU = FJ666354; *tub2* = KT214739; *rpb2* = FJ666385).

Chaetomium subfunicola X.Wei Wang & L. Cai, Mycol. Prog. 13: 723. 2014. [MB 801733]; basionym of *Dichotomopilus subfunicola*.

Chaetomium subglobosum Sergejeva, Bot. Mater. Otd. Sporov. Rast. Bot. Inst. Komarova Akad. Nauk S.S.S.R. 13: 172. 1960. [MB 328081]. — Type: –. Ex-type: CBS 149.60 = ATCC 14533 = IMI 081770 = MUCL 18694 = VKM F-1951. Reproduction: sexual. ITS barcode: JN209930 (alternative markers: LSU = JN209930; *tub2* = JN256200; *rpb2* = KF001808).

Chaetomium subspirale Chivers, Proc. Amer. Acad. Arts Sci. 48: 84. 1912. [MB 167796]; basionym of *Pseudohumicola subspiralis*.

Chaetomium subspirilliferum Sergejeva, Bot. Mater. Otd. Sporov. Rast. Bot. Inst. Komarova Akad. Nauk S.S.S.R. 13: 174. 1960. [MB 328082]; basionym of *Parachaetomium subspirilliferum*.

Chaetomium subterraneum Swift & Povah, Mycologia 21: 210. 1929. [MB 168290]; synonym of *Chaetomium globosum*.

Chaetomium succineum L.M. Ames, Mycologia 41: 645. 1949. [MB 294710]; basionym of *Arxotrichum succineum*.

Chaetomium tarraconense [as '*tarraconensis*'] Stchigel *et al.*, Mycologia 94: 125. 2002. [MB 541276]. — Type: IMI 382893. Ex-type: CBS 101882 = FMR 6638 = IMI 380425 = MUCL 43149. Reproduction: sexual. ITS barcode: n/a (alternative markers: LSU = n/a; *tub2* = MZ343005; *rpb2* = MZ342964).

Chaetomium tectifimeti X.Wei Wang & Samson, Stud. Mycol. 84: 177. 2016. [MB 818838]. — Type: CBS H-22844. Ex-type: CBS 142032. Reproduction: sexual. ITS barcode: KX976640 (alternative markers: LSU = KX976737; *tub2* = KX976982; *rpb2* = KX976836).

Chaetomium telluricola X.Wei Wang *et al.*, Persoonia 36: 124. 2015 [2016]. [MB 812985]. — Type: CBS H-676. Ex-type: CBS 151.59 = IMI 032543. Reproduction: sexual. ITS barcode: KT214582 (alternative markers: LSU = KT214613; *tub2* = KT214759; *rpb2* = KT214685).

Chaetomium tenue X.Wei Wang *et al.*, Persoonia 36: 125. 2015 [2016]. [MB 812986]. — Type: CBS H-22195. Ex-type: CBS 139.38. Reproduction: sexual. ITS barcode: KT214568 (alternative markers: LSU = KT214599; *tub2* = KT214745; *rpb2* = KT214669).

Chaetomium thermophilum La Touche, Trans. Brit. Mycol. Soc. 33: 95. 1950. [MB 344053]; basionym of *Thermochaetoides thermophila*.

Chaetomium thermophilum var. *dissitum* Cooney & R. Emers., Thermophilic Fungi: 68. 1964. [MB 353347]; basionym of *Thermochaetoides dissita*.

Chaetomium trigonosporum (Marchal & É.J. Marchal) Chivers, Mem. J. Torrey Bot. Soc. 14: 166. 1915. [MB 162780]; synonym of *Bommerella trigonospora*.

Chaetomium trilaterale var. *chiversii* J.C. Cooke, Mycologia 65: 1218. 1973. [MB 347891]; basionym of *Floropilus chiversii*.

Chaetomium triticicola Lal & J.N. Kapoor, Indian Phytopathol. 30: 136. 1978. [MB 310928]. — Type: n/a. Ex-type: CBS 106.83 = IMI 232292 = ITCC 2038. Reproduction: sexual. ITS barcode: n/a (alternative markers: LSU = n/a; *tub2* = n/a; *rpb2* = MZ342967). *Note*: This species shares identical *rpb2* sequences with *Amesia raii* and is tentatively considered a synonym of this species.

Chaetomium truncatulum Asgari & Zare, Mycologia 103: 877. 2011. [MB 519107]; basionym of *Parachaetomium truncatulum*.

Chaetomium turgidopilosum L.M. Ames, Mycologia 41: 639. 1949. [MB 294711]; basionym of *Arcopilus turgidopilosus*.

Chaetomium udagawae Sergejeva ex Udagawa, Trans. Mycol. Soc. Japan 20: 476. 1979. [MB 118491]; basionym of *Humicola udagawae*.

Chaetomium umbonatum D. Brewer, Proc. & Trans. Nova Scotian Inst. Sci. 27(2): 59. 1974. [MB 310929]. — Type: IMI 138895 (holotype); CBS H-6904 (isotype). Ex-type: CBS 293.83 = ATCC 28768 = IMI 138895. Reproduction: sexual. ITS barcode: KT214575 (alternative markers: LSU = KT214606; *tub2* = KT214752; *rpb2* = KT214676).

Chaetomium undulatulum Asgari & Zare, Mycologia 103: 870. 2011. [MB 519102]. — Type: IRAN 14605F. Ex-type: CBS 126775 = IRAN 857C. Reproduction: sexual. ITS barcode: HM365251 (alternative markers: LSU = HM365251; *tub2* = HM365279; *rpb2* = KT214682).

Chaetomium unguicola X.Wei Wang *et al.*, Persoonia 36: 128. 2015 [2016]. [MB 812987]. — Type: CBS H-22196. Ex-type: CBS 128446 = UTHSC 07-2213. Reproduction: sexual. ITS barcode: KT214567 (alternative markers: LSU = KT214598; *tub2* = KT214744; *rpb2* = KT214668).

Chaetomium uniporum Aue & E. Müll., Ber. Schweiz. Bot. Ges. 77: 189. 1967. [MB 328088]; basionym of *Ovatospora unipora*.

Chaetomium uniseriatum Yu Zhang & L. Cai, Fungal Biol. 121: 33. 2016. [MB 811156]; basionym of *Trichocladium uniseriatum*.

Chaetomium variosporum Udagawa & Y. Horie, Rep. Tottori Mycol. Inst. 10: 430. 1973. [MB 310931]; basionym of *Brachychaeta variospora*.

Chaetomium variostiolatum A. Carter, Canad. J. Bot. 61: 2603. 1983. [MB 106676]; basionym of *Dichotomopilus variostiolatus*.

Chaetomium venezuelense L.M. Ames, A monograph of the *Chaetomiaceae*: 42. 1963. [MB 328089]; synonym of *Chrysocorona lucknowensis*.

Chaetomium virescens (Arx) Udagawa, Trans. Mycol. Soc. Japan 21: 34. 1980. [MB 121660]; synonym of *Collariella virescens*.

Chaetomium virgicephalum [as '*virgecephalum*'] L.M. Ames, A

monograph of the *Chaetomiaceae*: 42. 1963. [MB 121663]; synonym of *Chaetomium elatum*.

Chaetomium vitellinum A. Carter, Mycologia 75: 531. 1983. [MB 108760]; basionym of *Botryotrichum vitellinum*.

Chaetomium wallefii J.A. Mey. & Lanneau, Bull. Trimestriel Soc. Bot. France 83: 320. 1967. [MB 328093]; basionym of *Humicola wallefii*.

Chrysanthotrichum

Chrysanthotrichum allolentum X.Wei Wang & Houbraken, Stud. Mycol. 93: 196. 2019. [MB 829853]. — Type: CBS H-23634. Ex-type: CBS 644.83. Reproduction: sexual. ITS barcode: MK926808 (alternative markers: LSU = MK926808; *tub2* = MK926908; *rpb2* = MK876768).

Chrysanthotrichum lentum (Van Warmelo) X.Wei Wang & Houbraken, Stud. Mycol. 93: 196. 2019. [MB 829855]. Basionym: *Chaetomium lentum*. — Type: PRE 43084. Ex-type: CBS 339.67 = IMI 128308. Reproduction: sexual. ITS barcode: MK926809 (alternative markers: LSU = MK926809; *tub2* = MK926909; *rpb2* = MK876769).

Chrysanthotrichum leptolentum X.Wei Wang & Houbraken, Stud. Mycol. 93: 196. 2019. [MB 829856]. — Type: CBS H-23633. Ex-type: CBS 126.85. Reproduction: sexual. ITS barcode: MK926810 (alternative markers: LSU = MK926810; *tub2* = MK926910; *rpb2* = MK876770).

Chrysanthotrichum peruvianum (Goch.) X.Wei Wang & Houbraken, Stud. Mycol. 93: 201. 2019. [MB 829857]. Basionym: *Chaetomidium peruvianum*. — Type: NY, Gochenaur 68-11. Ex-type: CBS 732.68 = ATCC 18511 = IMI 135024. Reproduction: sexual. ITS barcode: MK926812 (alternative markers: LSU = MK926812; *tub2* = MK926912; *rpb2* = MK876772).

Chrysocorona

Chrysocorona lucknowensis (J.N. Rai & J.P. Tewari) X.Wei Wang & Houbraken, Stud. Mycol. 93: 201. 2019. [MB 829859]. Basionym: *Chaetomium lucknowense*. — Type: figs 16–28 in Rai & Tewari, Canad. J. Bot. 40: 1380, 1962 (lectotype); CBS H-10081 (epitype). Ex-epitype: CBS 727.71 = LUP-22. Reproduction: sexual. ITS barcode: MK926813 (alternative markers: LSU = MK926813; *tub2* = MK926913; *rpb2* = MK876773).

Chrysosporium (*Onygenales, Eurotiomycetes*)

Chrysosporium fergusii Klopotek, Arch. Mikrobiol. 98: 366. 1974. [MB 311104]; synonym of *Thermothelomyces fergusii*.

Coccospora

Coccospora agricola Goddard, Bot. Gaz. 56: 264. 1913. [MB 206263]; synonym of *Botryotrichum piluliferum*.

Collariella

Collariella anguipilia (L.M. Ames) X.Wei Wang & Houbraken, this study. [MB 840145]. Basionym: *Chaetomium anguipilium*. — Type: BPI 1101397. Ex-type: CBS 632.83. Reproduction: sexual. ITS barcode: MZ334721 (alternative markers: LSU = MZ351424; *tub2* = MZ343028; *rpb2* = MZ342989).

Collariella bostrychodes (Zopf) X.Wei Wang & Samson, Stud. Mycol. 84: 179. 2016. [MB 818862]. Basionym: *Chaetomium bostrychodes*. — Type: n/a. Representative strain: CBS 163.73 = ATCC 24468 = IMI 171508 = TRTC 661727b. Reproduction: sexual. ITS barcode: KX976641 (alternative markers: LSU = KX976738; *tub2* = KX976983; *rpb2* = KX976837).

Collariella capillicompacta M. Mehrabi-Koushki *et al.*, Sydowia 73: 27. 2020. [MB 832919]. — Type: IRAN 17599F. Ex-type: IRAN 3496C = SCUA-Agh-20H. Reproduction: sexual. ITS barcode: n/a (alternative markers: LSU = n/a; *tub2* = MN520423; *rpb2* = MN520427).

Collariella carteri X.Wei Wang *et al.*, Stud. Mycol. 84: 179. 2016. [MB 818863]. — Type: CBS H-22845. Ex-type: CBS 128.85 = TRTC 50691. Reproduction: sexual. ITS barcode: KX976647 (alternative markers: LSU = KX976742; *tub2* = KX976989; *rpb2* = KX976841).

Collariella causiiformis (L.M. Ames) X.Wei Wang & Samson, Stud. Mycol. 84: 179. 2016. [MB 818864]. Basionym: *Chaetomium causiiforme*. — Type: BPI. Ex-type: CBS 792.83 = ATCC 11198 = CBS 139.56 = IFO 9139. Reproduction: sexual. ITS barcode: KX976646 (alternative markers: LSU = KX976741; *tub2* = KX976988; *rpb2* = KX976840). *Notes*: Several specimens are labeled as type according to Mycoportal: BPI 845270, BPI 1100724 and BPI 1101427. A database search and/or examination of these specimens is needed to determine which of them is the holotype and which are isotypes, or if a lectotypification is necessary.

Collariella gracilis (Udagawa) X.Wei Wang & Samson, Stud. Mycol. 84: 185. 2016. [MB 818865]; synonym of *Achaetomiella gracilis*.

Collariella hexagonospora (A. Carter & Malloch) X.Wei Wang & Houbraken, this study. [MB 840146]. Basionym: *Chaetomium hexagonosporum*. — Type: TRTC 48872. Ex-type: CBS 171.84 = TRTC 48872 = FMR 7235. Reproduction: sexual. ITS barcode: MH861717 (alternative markers: LSU = n/a; *tub2* = MZ343016; *rpb2* = MZ342977).

Collariella hilkhuijsenii X.Wei Wang, Persoonia 39: 463. 2017. [MB 823460]. — Type: CBS H-23232. Ex-type: CBS 143305. Reproduction: sexual. ITS barcode: MG432011 (alternative markers: LSU = MG432012; *tub2* = MF716586; *rpb2* = MF716587).

Collariella pachypodioides (L.M. Ames) X.Wei Wang & Houbraken, this study. [MB 840147]. Basionym: *Chaetomium pachypodioides*. — Type: FH, Ames 1044.3 (holotype); CBS H-6883 (isotype). Ex-type: CBS 164.52 = ATCC 11213 = IFO 9109 = IMI 012266 = IMI 287299 = MUCL 9586. Reproduction: sexual. ITS barcode: MH856980 (alternative markers: LSU = MH868500; *tub2* = MZ343014; *rpb2* = MZ342975).

Collariella quadrangulata (Chivers) X.Wei Wang & Samson, Stud. Mycol. 84: 217. 2016. [MB 818861]. Basionym: *Chaetomium quadrangulatum*. — Type: Chivers No. 29, CUP. Representative strain: CBS 152.59. Reproduction: sexual. ITS barcode: KX976651 (alternative markers: LSU = KX976746; *tub2* = KX976993; *rpb2* = KX976845).

Collariella quadrum Z.F. Zhang *et al.*, Persoonia 39: 14. 2017. [MB 818249]. — Type: HMAS 246923. Ex-type: CGMCC 3.17917. Reproduction: sexual. ITS barcode: KU746675 (alternative markers: LSU = KU746721; *tub2* = KU746767; *rpb2* = KY575870).

Collariella robusta (L.M. Ames) X.Wei Wang & Samson, Stud. Mycol. 84: 217. 2016. [MB 818872]. Basionym: *Chaetomium robustum*. — Type: BPI 1101399. Ex-type: CBS 551.83. Reproduction: sexual. ITS barcode: KX976652 (alternative markers: LSU = KX976747; *tub2* = KX976994; *rpb2* = KX976846).

Collariella virescens (Arx) X.Wei Wang & Samson, Stud. Mycol. 84: 217. 2016. [MB 819488]; synonym of *Achaetomiella virescens*.

Condenascus

Condenascus tortuosus (Udagawa & Y. Sugiy.) X.Wei Wang & Houbraken, Stud. Mycol. 93: 203. 2019. [MB 829861]. Basionym: *Thielavia tortuosa*. — Type: NHL 2890. Ex-type: CBS 691.82 (contaminated); CBS 610.97 (representative strain) = FMR 5780. Reproduction: sexual. ITS barcode: MK926817 (alternative markers: LSU = MK926817; *tub2* = MK926917; *rpb2* = MK876777).

Coniothyrium (*Pleosporales, Dothideomycetes*)

Coniothyrium terricola J.C. Gilman & E.V. Abbott, Iowa St. Coll. J. Sci. 1: 267. 1927. [MB 255077]; basionym of *Pseudothielavia terricola*.

Corynascella

Corynascella humicola Arx & Hodges, Stud. Mycol. 8: 23. 1975. [MB 312209]. — Type: CBS H-6963. Ex-type: CBS 337.72. Reproduction: sexual & asexual. ITS barcode: KX976656 (alternative markers: LSU = KX976751; *tub2* = KX976998; *rpb2* = MK942091).

Corynascella inaequalis (Pidopl. *et al.*) Arx, Kavaka 3: 34. 1975. [MB 312210]; synonym of *Parachaetomium inaequale*.

Corynascella inquinata Udagawa & S. Ueda, Mycotaxon 8: 292. 1979. [MB 312211]; basionym of *Botryotrichum inquinatum*.

Corynascus

Corynascus citrinus A. Giraldo & Crous, Persoonia 36: 449. 2016. [MB 816971]. — Type: BCC 79098 (metabolically inactive). Ex-type: BCC 79098. Reproduction: sexual & asexual. ITS barcode: KX262667 (alternative markers: LSU = KX228351; *tub2* = n/a; *rpb2* = KX262668).

Corynascus fumimontanus Y. Marín *et al.*, Mycologia 107: 628. 2015. [MB 809486]. — Type: CBS H-21594. Ex-type: CBS 137294 = FMR 12372. Reproduction: sexual & asexual. ITS barcode: MK919291 (alternative markers: LSU = MK919291; *tub2* = MK919405; *rpb2* = MK919347).

Corynascus heterothallicus (Klopotek) Arx, Persoonia 12: 174. 1984, nom. inval., Art. 41.4. [MB 107879]; synonym of *Thermothelomyces heterothallicus* [as '*heterothallica*'].

Corynascus novoguineensis (Udagawa & Y. Horie) Arx, Proc. Kon. Ned. Akad. Wetensch., Sect. C 76: 292. 1973. [MB 312212]. Basionym: *Thielavia novoguineensis*. — Type: NHL 22501. Ex-type: CBS 359.72 = NHL 22501. Reproduction: sexual & asexual. ITS barcode: MK919292 (alternative markers: LSU = MK919292; *tub2* = MK919406; *rpb2* = MK919348).

Corynascus sepedonium (C.W. Emmons) Arx, Proc. Kon. Ned. Akad. Wetensch., Sect. C 76: 292. 1973. [MB 312213]. Basionym: *Thielavia sepedonium*. — Type: n/a. Ex-type: CBS 340.33; representative strain: CBS 111.69 = IMI 136625. Reproduction: sexual & asexual. ITS barcode: HQ871751 (alternative markers: LSU = KX976777; *tub2* = KX977027; *rpb2* = MK919349).

Corynascus sexualis Stchigel *et al.*, Mycol. Res. 104: 880. 2000. [MB 467480]. — Type: IMI 378520 (holotype); FMR 5691 (isotype). Ex-type: CBS 827.96 = FMR 5691. Reproduction: sexual & asexual. ITS barcode: MK919295 (alternative markers: LSU = MK919295; *tub2* = MK919409; *rpb2* = MK919352).

Corynascus similis Stchigel *et al.*, Mycol. Res. 104: 881. 2000. [MB 467481]; synonym of *Corynascus sepedonium*.

Corynascus thermophilus (Fergus & Sinden) Klopotek, Arch. Mikrobiol. 98: 366. 1974. [MB 312215]; synonym of *Thermothelomyces fergusii*.

Corynascus verrucosus Stchigel *et al.*, Mycol. Res. 104: 884. 2000. [MB 467482]. — Type: IMI 378522 (holotype); FMR 5904 (isotype). Ex-type: CBS 602.97 = FMR 5904. Reproduction: sexual & asexual. ITS barcode: MK919296 (alternative markers: LSU = MK919296; *tub2* = MK919410; *rpb2* = MK919353).

Crassicarpon nom. inval., Art. F.5.1; synonym of *Thermothelomyces*.

Crassicarpon hotsonii Koukol, Pl. Syst. Evol. 302: 967. 2016. *nom. inval.*, Art. 35.1. (Shenzhen). [MB 816112]; synonym of *Thermothelomyces myriococcoides*.

Crassicarpon thermophilum (Fergus & Sinden) Y. Marín *et al.*, Mycologia 107: 629. 2015. *nom. inval.*, Art. 35.1. (Shenzhen). [MB 809488]; synonym of *Thermothelomyces fergusii*.

Dichotomopilus

Dichotomopilus dolichotrichus (L.M. Ames) X.Wei Wang & Samson, Stud. Mycol. 84: 217. 2016. [MB 818866]. Basionym: *Chaetomium dolichotrichum*. — Type: FH, Ames 1044.7. Ex-type: CBS 162.48 = ATCC 11203 = IMI 012264 = MUCL 9598. Reproduction: sexual. ITS barcode: HM449049 (alternative markers: LSU = HM449063; *tub2* = JF772462; *rpb2* = KX976852).

Dichotomopilus erectus (Skolko & J.W. Groves) X.Wei Wang & Samson, Stud. Mycol. 84: 217. 2016. [MB 818867]. Basionym: *Chaetomium erectum*. — Type: DAOM 14205. Ex-type: CBS 140.56 = DAOM 14205 = IMI 032249. Reproduction: sexual. ITS barcode: HM449044 (alternative markers: LSU = HM449058; *tub2* = JF772458; *rpb2* = KX976854).

Dichotomopilus finlandicus O. Kedves *et al.*, Pathogens 10, 1133: 9. 2021. [MB 840621]. — Type: SZMC 26529. Ex-type: SZMC 26529 (metabolically inactive). Reproduction: sexual. ITS barcode: MW541926 (alternative markers: LSU = n/a, *tub2* =MZ665529, *rpb2* = MZ665531).

Dichotomopilus funicola (Cooke) X.Wei Wang & Samson, Stud. Mycol. 84: 189. 2016. [MB 818841]. Basionym: *Chaetomium funicola*. — Type: K(M) 189267 (holotype), HMAS 244231 (epitype). Ex-epitype: CBS 159.52. Reproduction: sexual. ITS barcode: GU563369 (alternative markers: LSU = GU563354; *tub2* = JF772461; *rpb2* = KX976856).

Dichotomopilus fusus (L.M. Ames) X.Wei Wang & Samson, Stud. Mycol. 84: 217. 2016. [MB 818868]. Basionym: *Chaetomium fusum*. — Type: BPI 579938. Ex-type: CBS 372.66. Reproduction: sexual. ITS barcode: KX976660 (alternative markers: LSU = KX976754; *tub2* = KX977002; *rpb2* = KX976859).

Dichotomopilus indicus (Corda) X.Wei Wang & Samson, Stud. Mycol. 84: 189. 2016. [MB 818842]. Basionym: *Chaetomium indicum*. — Type: PRM 155406 (holotype), HMAS 244232 (epitype). Ex-epitype: CGMCC 3.14184. Reproduction: sexual. ITS barcode: GU563367 (alternative markers: LSU = GU563360; *tub2* = JF772453; *rpb2* = KX976861).

Dichotomopilus pratensis (X.Wei Wang & L. Cai) X.Wei Wang & Samson, Stud. Mycol. 84: 191. 2016. [MB 818843]. Basionym: *Chaetomium pratense*. — Type: HMAS 242921. Ex-type: CBS 133396 = CGMCC 3.14181. Reproduction: sexual. ITS barcode: GU563372 (alternative markers: LSU = GU563357; *tub2* = JF772450; *rpb2* = KX976866).

Dichotomopilus pseudoerectus X.Wei Wang & Samson, Stud. Mycol. 84: 191. 2016. [MB 818844]. — Type: CBS H-22846. Ex-type: CBS 252.75. Reproduction: sexual. ITS barcode: KX976667 (alternative markers: LSU = KX976761; *tub2* =

KX977009; *rpb2* = KX976869).

Dichotomopilus pseudofunicola X.Wei Wang & Samson, Stud. Mycol. 84: 195. 2016. [MB 818845]. — Type: CBS H-22847. Ex-type: CBS 142033. Reproduction: sexual. ITS barcode: KX976668 (alternative markers: LSU = KX976762; *tub2* = KX977010; *rpb2* = KX976870).

Dichotomopilus ramosissimus (X.Wei Wang & L. Cai) X.Wei Wang & Samson, Stud. Mycol. 84: 217. 2016. [MB 818869]. Basionym: *Chaetomium ramosissimum*. — Type: HMAS 244195. Ex-type: CGMCC 3.14183. Reproduction: sexual. ITS barcode: GU563371 (alternative markers: LSU = GU563361; *tub2* = JF772452; *rpb2* = KX976871).

Dichotomopilus reflexus (Skolko & J.W. Groves) X.Wei Wang & Samson, Stud. Mycol. 84: 217. 2016. [MB 818870]. Basionym: *Chaetomium reflexum*. — Type: DAOM 14201. Ex-type: CBS 157.49 = DAOM 14201 = IMI 032252 = MUCL 18700. Reproduction: sexual. ITS barcode: HM449051 (alternative markers: LSU = HM449055; *tub2* = JF772460; *rpb2* = KX976873).

Dichotomopilus subfunicola (X.Wei Wang & L. Cai) X.Wei Wang & Samson, Stud. Mycol. 84: 195. 2016. [MB 818846]. Basionym: *Chaetomium subfunicola*. — Type: HMAS 244194. Ex-type: CGMCC 3.12892. Reproduction: sexual. ITS barcode: JX867125 (alternative markers: LSU = JX867125; *tub2* = JX867122; *rpb2* = KX976875).

Dichotomopilus variostiolatus (A. Carter) X.Wei Wang & Samson, Stud. Mycol. 84: 203. 2016. [MB 818847]. Basionym: *Chaetomium variostiolatum*. — Type: TRTC QM 36d. Ex-type: CBS 179.84. Reproduction: sexual. ITS barcode: KX976672 (alternative markers: LSU = KX976766; *tub2* = KX977014; *rpb2* = KX976879).

Farrowia synonym of *Staphylotrichum*.

Farrowia cuyabenoensis (Decock & Hennebert) D. Hawksw., Systema Ascomycetum 16 (1-2): 52. 1998. [MB 442618]; synonym of *Humicola cuyabenoensis*.

Farrowia longicollis [as '*longicollea*'] (Krzemien. & Badura) D. Hawksw., Persoonia 8: 174. 1975. [MB 314068]; synonym of *Staphylotrichum longicolle*.

Farrowia malaysiensis D. Hawksw., Persoonia 8: 178. 1975. [MB 314069]; basionym of *Humicola malaysiensis*.

Farrowia seminuda (L.M. Ames) D. Hawksw., Persoonia 8: 181. 1975. [MB 314070]; synonym of *Humicola seminuda*.

Floropilus

Floropilus chiversii (J.C. Cooke) X.Wei Wang & Houbraken, Stud. Mycol. 93: 205. 2019. [MB 829863]. Basionym: *Chaetomium trilaterale* var. *chiversii*. — Type: CBS H-10077 (neotype). Ex-neotype: CBS 558.80 = IMI 250966 = MUCL 40052 = TRTC 48533. Reproduction: sexual. ITS barcode: MK926818 (alternative markers: LSU = MK926818; *tub2* = MK926918; *rpb2* = MK876778).

Gilmaniella

Gilmaniella macrospora Moustafa, Persoonia 8: 332. 1975. [MB 314495]. Replaced synonym of *Trichocladium gilmaniellae*.

Humicola

Humicola ampulliella (X.Wei Wang) X.Wei Wang & Houbraken, Stud. Mycol. 93: 76. 2018. [MB 824419]. Basionym: *Chaetomium ampulliellum*. — Type: HMAS 86813. Ex-type: CBS 116735 = CGMCC 3.6696. Reproduction: sexual & asexual. ITS barcode: LT993568 (alternative markers: LSU = LT993568; *tub2* = LT993649; *rpb2* = LT993487).

Humicola atrobrunnea X.Wei Wang *et al*., Stud. Mycol. 93: 76. 2018. [MB 824420]; basionym of *Pseudohumicola atrobrunnea*.

Humicola christenseniae [as '*christensenii*'] X.Wei Wang & Houbraken, Stud. Mycol. 93: 76. 2018. [MB 827854]. — Type: CBS H-23482. Ex-type: CBS 127760 = RMF 9051. Reproduction: sexual & asexual. ITS barcode: LT993571 (alternative markers: LSU = LT993571; *tub2* = LT993652; *rpb2* = LT993490).

Humicola cuyabenoensis (Decock & Hennebert) X.Wei Wang & Houbraken, Stud. Mycol. 93: 80. 2018. [MB 824423]. Basionym: *Chaetomium cuyabenoense*. — Type: MUCL 38838. Ex-type: CBS 398.97 = MUCL 38838. Reproduction: sexual & asexual. ITS barcode: LT993573 (alternative markers: LSU = LT993573; *tub2* = LT993654; *rpb2* = LT993492).

Humicola degenerans X.Wei Wang & Houbraken, Stud. Mycol. 93: 80. 2018. [MB 824424]. — Type: CBS H-23483. Ex-type: CBS 232.65 = IMI 109880. Reproduction: sexual & asexual. ITS barcode: LT993574 (alternative markers: LSU = LT993574; *tub2* = LT993655; *rpb2* = LT993493).

Humicola distorta (L.M. Ames) X.Wei Wang & Houbraken, Stud. Mycol. 93: 80. 2018. [MB 824427]. Basionym: *Chaetomium distortum*. — Type: BPI 579118 (holotype); NY01050417 (isotype). Ex-type: CBS 417.66. Reproduction: sexual & asexual. ITS barcode: LT993577 (alternative markers: LSU = LT993577; *tub2* = LT993658; *rpb2* = LT993496).

Humicola floriformis (Gené & Guarro) X.Wei Wang & Houbraken, Stud. Mycol. 93: 85. 2018. [MB 824429]. Basionym: *Chaetomium floriforme*. — Type: IMI 368520. Ex-type: CBS 815.97 = MUCL 40181. Reproduction: sexual (easy to lose) and asexual. ITS barcode: LT993578 (alternative markers: LSU = LT993578; *tub2* = LT993659; *rpb2* = LT993497).

Humicola fuscoatra Traaen, Nytt Mag. Naturvidensk. 52: 33. 1914. [MB 188714]. — Type: n/a. Ex-type: CBS 118.14 = ATCC 22721 = MUCL 8010. Reproduction: asexual. ITS barcode: LT993579 (alternative markers: LSU = LT993579; *tub2* = LT993660; *rpb2* = LT993498).

Humicola fuscogrisea Y.L. Jiang & T.Y. Zhang, Mycosystema 28: 649. 2009. [MB 513355]. — Type: HSAUP II 04 6083. Ex-type: CGMCC 3.13790. Reproduction: asexual. ITS barcode: LT993581 (alternative markers: LSU = LT993581; *tub2* = LT993662; *rpb2* = LT993500).

Humicola grisea Traaen, Nytt Mag. Naturvidensk. 52: 34. 1914. [MB 148670]; basionym of *Trichocladium griseum*.

Humicola grisea var. *thermoidea* Cooney & R. Emers., Thermophilic Fungi: 74. 1964. [MB 349549]; synonym of *Mycothermus thermophilus*.

Humicola hirsuta X.Wei Wang *et al.*, this study. [MB 840128]. — Type: HMAS 350292 (holotype); CBS H-23638 (isotype). Ex-type: CBS 144492 = CGMCC 3.20444 = WXW 9028. Reproduction: sexual & asexual. ITS barcode: MZ334726 (alternative markers: LSU = MZ351425; *tub2* = MZ343013; *rpb2* = MZ342974).

Humicola homopilata (Omvik) X.Wei Wang & Houbraken, Stud. Mycol. 93: 89. 2018. [MB 824432]. Basionym: *Chaetomium homopilatum*. — Type: CBS 157.55. Ex-type: CBS 157.55 = IMI 182125 = MUCL 40178. Reproduction: sexual & asexual. ITS barcode: LT993582 (alternative markers: LSU = LT993582; *tub2* = LT993663; *rpb2* = LT993501).

Humicola insolens Cooney & R. Emers., Thermophilic Fungi: 79. 1964. [MB 332024]; synonym of *Mycothermus thermophilus*.

Humicola jilongensis Y.M. Wu & T.Y. Zhang, Mycotaxon 121: 148. 2012. [MB 563887]; basionym of *Trichocladium jilongense*.

Humicola koreana Hyang B. Lee & T.T.T. Nguyen, Fungal Diversity 78: 97. 2016. [MB 814402]; basionym of *Staphylotrichum koreanum*.

Humicola leptodermospora X.Wei Wang & Houbraken, Stud. Mycol. 93: 89. 2018. [MB 824435]. — Type: CBS H-23484. Ex-type: CBS 120095 = FMR 9050. Reproduction: sexual (easy to lose) and asexual. ITS barcode: LT993584 (alternative markers: LSU = LT993584; *tub2* = LT993665; *rpb2* = LT993503).

Humicola limonispora [as '*limonisporum*'] Z.F. Zhang & L. Cai, Persoonia 39: 15. 2017. [MB 840136]; basionym of *Staphylotrichum limonisporum*.

Humicola malaysiensis (D. Hawksw.) X.Wei Wang & Houbraken, Stud. Mycol. 93: 89. 2018. [MB 824437]. Basionym: *Farrowia malaysiensis*. — Type: IMI 183184. Ex-type: CBS 399.97 = IMI 183184 = MUCL 39402. Reproduction: sexual & asexual. ITS barcode: LT993586 (alternative markers: LSU = LT993586; *tub2* = LT993667; *rpb2* = LT993505).

Humicola mutabilis X.Wei Wang & Houbraken, Stud. Mycol. 93: 93. 2018. [MB 824438]. — Type: CBS H-23485. Ex-type: CBS 779.71. Reproduction: sexual & asexual. ITS barcode: LT993588 (alternative markers: LSU = LT993588; *tub2* = LT993669; *rpb2* = LT993507).

Humicola olivacea X.Wei Wang & Samson, Stud. Mycol. 84: 203. 2016. [MB 818848]. — Type: CBS H-22848. Ex-type: CBS 142031. Reproduction: asexual. ITS barcode: LT993589 (alternative markers: LSU = LT993589; *tub2* = LT993670; *rpb2* = LT993508).

Humicola pinnata (L.M. Ames) X.Wei Wang & Houbraken, Stud. Mycol. 93: 96. 2018. [MB 824440]. Basionym: *Chaetomium pinnatum*. — Type: BPI 580625. Ex-type: CBS 467.66. Reproduction: sexual & asexual. ITS barcode: LT993590 (alternative markers: LSU = LT993590; *tub2* = LT993671; *rpb2* = LT993509).

Humicola pulvericola X.Wei Wang *et al.*, Stud. Mycol. 93: 96. 2018. [MB 824444]; basionym of *Pseudohumicola pulvericola*.

Humicola quadrangulata X.Wei Wang & Houbraken, Stud. Mycol. 93: 96. 2018. [MB 825446]. — Type: CBS H-23487. Ex-type: CBS 111771. Reproduction: sexual & asexual. ITS barcode: LT993593 (alternative markers: LSU = LT993593; *tub2* = LT993674; *rpb2* = LT993512).

Humicola seminuda (L.M. Ames) X.Wei Wang & Houbraken, Stud. Mycol. 93: 100. 2018. [MB 824447]. Basionym: *Chaetomium seminudum*. — Type: figs 23–29 in Ames, Mycologia 41: 643, 1949 (lectotype); CBS H-23488 (epitype). Ex-epitype: CBS 368.84. Reproduction: sexual & asexual. ITS barcode: LT993594 (alternative markers: LSU = LT993594; *tub2* = LT993675; *rpb2* = LT993513).

Humicola semispiralis (Udagawa & Cain) X.Wei Wang & Houbraken, Stud. Mycol. 93: 100. 2018. [MB 824448]; synonym of *Pseudohumicola semispiralis* (based on *Chaetomium semispirale*).

Humicola sphaeralis (Chivers) X.Wei Wang & Houbraken, Stud. Mycol. 93: 100. 2018. [MB 824449]. Basionym: *Chaetomium sphaerale*. — Type: NY01050440. Ex-type: CBS 985.87. Reproduction: sexual & asexual. ITS barcode: LT993598 (alternative markers: LSU = LT993598; *tub2* = LT993679; *rpb2* = LT993517).

Humicola subspiralis (Chivers) X.Wei Wang & Houbraken, Stud. Mycol. 93: 104. 2018. [MB 824450]; synonym of *Pseudohumicola subspiralis*.

Humicola udagawae (Sergejeva ex Udagawa) X.Wei Wang & Houbraken, Stud. Mycol. 93: 104. 2018. [MB 824451]. Basionym: *Chaetomium udagawae*. — Type: NHL 2259. Ex-type: CBS 337.68 = NHL 2259. Reproduction: sexual & asexual. ITS barcode: LT993601 (alternative markers: LSU = LT993601; *tub2* = LT993682; *rpb2* = LT993520).

Humicola wallefii (J.A. Mey. & Lanneau) X.Wei Wang & Houbraken, Stud. Mycol. 93: 107. 2018. [MB 824452]. Basionym: *Chaetomium wallefii*. — Type: n/a. Ex-type: CBS 147.67 = IMI 126039. Reproduction: sexual (easy to lose) and asexual. ITS barcode: LT993602 (alternative markers: LSU = LT993602; *tub2* = LT993683; *rpb2* = LT993521).

Hyalosphaerella

Hyalosphaerella fragilis (Natarajan) X.Wei Wang & Houbraken, Stud. Mycol. 93: 205. 2019. [MB 829865]. Basionym: *Chaetomidium fragile*. — Type: n/a. Ex-type: CBS 456.73 = IMI 169641. Reproduction: sexual. ITS barcode: KX976693 (alternative markers: LSU = KX976791; *tub2* = KX977042; *rpb2* = MK876779).

Madurella

Madurella fahalii de Hoog *et al.*, J. Clin. Microbiol. 50: 991. 2012. [MB 560128]. — Type: CBS H-20690. Ex-type: CBS 129176. Reproduction: asexual/sterile. ITS barcode: MK926819 (alternative markers: LSU = MK926819; *tub2* = MK926919; *rpb2* = MK876780).

Madurella mycetomatis (Laveran) Brumpt, Compt.-Rend. Séances Mém. Soc. Biol. 58: 997. 1905. [MB 535193]. Basionym: *Streptothrix mycetomatis*. — Type: CBS 109801 (neotype, de Hoog *et al.* 2004). Ex-neotype: CBS 109801. Reproduction: asexual/sterile. ITS barcode: MK926820 (alternative markers: LSU = MK926820; *tub2* = MK926920; *rpb2* = MK876781).

Madurella pseudomycetomatis Yan *et al.* ex de Hoog *et al.*, J. Clin. Microbiol. 50: 991. 2012. [MB 509682]. — Type: CBS H-20691. Ex-type: CBS 129177. Reproduction: asexual/sterile. ITS barcode: MK926821 (alternative markers: LSU = MK926821; *tub2* = MK926921; *rpb2* = MK876782).

Madurella tropicana de Hoog *et al.*, J. Clin. Microbiol. 50: 993. 2012. [MB 800571]. — Type: CBS H-20692. Ex-type: CBS 201.38. Reproduction: asexual/sterile. ITS barcode: MK926824 (alternative markers: LSU = MK926824; *tub2* = MK926924; *rpb2* = MK876785).

Magnusia (*Microascales, Sordariomycetes*)

Magnusia spirotricha R.K. Benj., Aliso 3: 199. 1955. [MB 300049]; basionym of *Botryotrichum spirotrichum*.

Melanocarpus

Melanocarpus albomyces (Cooney & R. Emers.) Arx, Stud. Mycol. 8: 17. 1975. [MB 317449]. Basionym: *Myriococcum albomyces*. — Type: UPS F-646091. Ex-type: CBS 638.94 = ATCC 16460 = CBS 177.67 = IMI 126326. Reproduction: sexual & asexual. ITS barcode: KX976679 (alternative markers: LSU = KX976773; *tub2* = KX977021; *rpb2* = KX976886). *Note*: A specimen of Cooney and Emersons material is deposited in Uppsala University, Museum of Evolution (UPS:BOT) under UPS F-646091.

Melanocarpus oblatus Guarro & Aa, Persoonia 13: 270. 1987. [MB 132107]. — Type: CBS 775.85. Ex-type: CBS 775.85. Reproduction: sexual. ITS barcode: MZ334727 (alternative markers: LSU = n/a; *tub2* = MZ343031; *rpb2* = MZ342992).

Note: This species is a synonym of *Achaetomium globosum*.

Melanocarpus tardus X.Wei Wang & Samson, Stud. Mycol. 84: 205. 2016. [MB 818849]; basionym of *Parvomelanocarpus tardus*.

Melanocarpus thermophilus (Abdullah & Al-Bader) Guarro *et al.*, Mycol. Res. 100: 75. 1996. [MB 413444]; synonym of *Parvomelanocarpus thermophilus*.

Microthielavia

Microthielavia ovispora (Pidopl. *et al.*) X.Wei Wang & Houbraken, Stud. Mycol. 93: 208. 2019. [MB 829867]. Basionym: *Thielavia ovispora*. — Type: Instituto Microbiol. et Virusol. Acad. Sci., Ucrainae (Kiovia) sub N 52128. Ex-type: CBS 165.75 = IMI 196525 = VKM F-1596. Reproduction: sexual. ITS barcode: MK926826 (alternative markers: LSU = MK926826; *tub2* = MK926926; *rpb2* = MK876787).

Myceliophthora

Myceliophthora fergusii (Klopotek) Oorschot, Persoonia 9: 406. 1977. [MB 317954]; synonym of *Thermothelomyces fergusii*.

Myceliophthora guttulata Yu Zhang & L. Cai, Mycol. Prog. 13: 168. 2013. [MB 80233]; basionym of *Thermothelomyces guttulatus* [as '*guttulata*'].

Myceliophthora heterothallica (Klopotek) van den Brink & Samson, Fungal Diversity 52: 206. 2011 [2012], nom. inval., Art. 41.5. [MB 519538]; synonym of *Th. heterothallicus*.

Myceliophthora hinnulea Awao & Udagawa, Mycotaxon 16: 436. 1983. [MB 109090]; basionym of *Thermothelomyces hinnuleus* [as '*hinnulea*'].

Myceliophthora lutea Costantin, Compt. Rend. Hebd. Séances Acad. Sci. 114: 850. 1892. [MB 232833]. — Type: CBS 145.77 (neotype). Ex-neotype: CBS 145.77 = IMI 182034. Reproduction: asexual. ITS barcode: HQ871775(alternative markers: LSU = KM655351; *tub2* = KX977026; *rpb2* = KM655395).

Myceliophthora novoguineensis (Udagawa & Y. Horie) van den Brink & Samson, Fungal Diversity 52: 206. 2011 [2012], nom. inval., Art. 41.5. [MB 561526]; synonym of *Corynascus novoguineensis*.

Myceliophthora officinarum M. Raza & L. Cai, Fungal Diversity 99: 89. 2019. [MB 556681]; basionym of *Arxotrichum officinarum*.

Myceliophthora sepedonium (C.W. Emmons) van den Brink & Samson, Fungal Diversity 52: 206. 2011 [2012], nom. inval., Art. 41.5. [MB 561525]; synonym of *Corynascus sepedonium*.

Myceliophthora sexualis (Stchigel *et al.*) van den Brink & Samson, Fungal Diversity 52: 206. 2011 [2012], nom. inval., Art. 41.5. [MB 561527]; synonym of *Corynascus sexualis*.

Myceliophthora similis (Stchigel *et al.*) van den Brink & Samson, Fungal Diversity 52: 206. 2011 [2012], nom. inval., Art. 41.5. [MB 561528]; synonym of *Corynascus similis*.

Myceliophthora verrucosa (Stchigel *et al.*) van den Brink & Samson, Fungal Diversity 52: 206. 2011 [2012], nom. inval., Art. 41.5. [MB 561529]; synonym of *Corynascus verrucosus*.

Mycothermus

Mycothermus thermophiloides X.Wei Wang & Houbraken, Stud. Mycol. 93: 107. 2018. [MB 824455]. — Type: CBS H-23489. Ex-type: CBS 183.81. Reproduction: asexual. ITS barcode: LT993603 (alternative markers: LSU = LT993603; *tub2* = LT993684; *rpb2* = LT993522).

Mycothermus thermophilus (Cooney & R. Emers.) X.Wei Wang *et al.*, Stud. Mycol. 93: 107. 2018. [MB 824454]. Basionym: *Torula thermophila*. — Type: UC 1206525. Ex-type: CBS 625.91 = ATCC 16463. Reproduction: asexual. ITS barcode: LT993604 (alternative markers: LSU = LT993604; *tub2* = LT993685; *rpb2* = LT993523).

Myriococcum (*Atheliales, Agaricomycetes*)

Myriococcum albomyces Cooney & R. Emers., Thermophilic Fungi: 60. 1964. [MB 335011]; basionym of *Melanocarpus albomyces*.

Myriococcum thermophilum (Fergus) Aa, Verh. Kon. Ned. Akad. Wetensch., Afd. Natuurk., Sect. 2 61(4): 60. 1973. [MB 318413]; synonym of *Thermothelomyces myriococcoides*.

Ovatospora

Ovatospora amygdalispora (Udagawa & T. Muroi) X.Wei Wang & Houbraken, this study. [MB 840155]. Basionym: *Chaetomium amygdalisporum*. — Type: NHL 2874. Ex-type: CBS 672.82 = IMI 291735 = NHL 2874. Reproduction: sexual. ITS barcode: n/a (alternative markers: LSU = n/a; *tub2* = MZ343030; *rpb2* = MZ342991).

Ovatospora angularis (Yu Zhang & L. Cai) X.Wei Wang & Houbraken, this study. [MB 840156]. Basionym: *Chaetomium angulare*. — Type: HMAS 245780. Ex-type: CGMCC 3.17537. Reproduction: sexual. ITS barcode: KP336763 (alternative markers: LSU = KP336812; *tub2* = KP336861; *rpb2* = KT149486).

Ovatospora brasiliensis (Bat. & Pontual) X.Wei Wang & Samson, Stud. Mycol. 84: 207. 2016. [MB 818851]. Basionym: *Chaetomium brasiliense*. — Type: n/a. Representative strain: CBS 140.50 = IMI 031638 = MUCL 9590. Reproduction: sexual. ITS barcode: KX976683 (alternative markers: LSU = KX976781; *tub2* = KX977031; *rpb2* = KX976896).

Ovatospora medusarum (J.A. Mey. & Lanneau) X.Wei Wang & Samson, Stud. Mycol. 84: 217. 2016. [MB 818871]. Basionym: *Chaetomium medusarum*. — Type: n/a. Ex-type: CBS 148.67 = IMI 126040 = IMI 126040ii = MUCL 10171. Reproduction: sexual. ITS barcode: KX976684 (alternative markers: LSU = KX976782; *tub2* = KX977032; *rpb2* = KX976897).

Ovatospora mollicella (L.M. Ames) X.Wei Wang & Samson, Stud. Mycol. 84: 217. 2016. [MB 818873]. Basionym: *Chaetomium mollicellum*. — Type: BPI. Ex-type: CBS 583.83. Reproduction: sexual. ITS barcode: KX976685 (alternative markers: LSU = KX976783; *tub2* = KX977033; *rpb2* = KX976898). *Notes*: Ames' type of *Ch. mollicellum* is probably maintained in BPI. Specimen BPI 580521 is not labeled as type, but could well be used for the species description. More work is needed to eludicate the status of this specimen.

Ovatospora pseudomollicella X.Wei Wang & Samson, Stud. Mycol. 84: 207. 2016. [MB 818852]. — Type: CBS H-22850. Ex-type: CBS 251.75. Reproduction: sexual. ITS barcode: KX976686 (alternative markers: LSU = KX976784; *tub2* = KX977034; *rpb2* = KX976899).

Ovatospora senegalensis (L.M. Ames) X.Wei Wang & Samson, Stud. Mycol. 84: 217. 2016. [MB 818874]. Basionym: *Chaetomium senegalense*. — Type: BPI. Ex-type: CBS 728.84. Reproduction: sexual. ITS barcode: KX976687 (alternative markers: LSU = KX976785; *tub2* = KX977035; *rpb2* = KX976900). *Notes*: Three specimens are labeled as type: BPI 1100707, BPI 1101433 (collected in 1974, so should not be the type material) and BPI 580647. More work is needed to eludicate the status of these specimens.

Ovatospora unipora (Aue & E. Müll.) X.Wei Wang & Samson, Stud. Mycol. 84: 217. 2016. [MB 818875]. Basionym: *Chaetomium uniporum*. — Type: ETH 7503. Ex-type: CBS

109.83. Reproduction: sexual. ITS barcode: KX976689 (alternative markers: LSU = KX976787; *tub2* = KX977037; *rpb2* = KX976902).

Paecilomyces (*Eurotiales, Eurotiomycetes*)

Paecilomyces biformis Z.Q. Liang *et al.*, Fungal Diversity 27: 97. 2007. [MB 510977]; basionym of *Acrophialophora biformis*.

Paecilomyces cinereus Z.Q. Liang *et al.*, Mycotaxon 97: 16. 2006. [MB 501355]; basionym of *Acrophialophora cinerea*.

Paecilomyces curticatenatus Z.Q. Liang & Y.F. Han, Mycosystema 26: 14. 2007. [MB 510908]; basionym of *Acrophialophora curticatenata*.

Paecilomyces furcatus Z.Q. Liang *et al.*, Mycotaxon 97: 16. 2006. [MB 501356]; basionym of *Acrophialophora furcata*.

Paecilomyces fusisporus S.B. Saksena, J. Indian Bot. Soc. 32: 186. 1953. [MB 302189]; basionym of *Acrophialophora fusispora*.

Paecilomyces inflatus var. *major* Z.Q. Liang *et al.*, J. Fungal Res. 2: 43. 2004. [MB 509628]; basionym of *Acrophialophora major*.

Papulaspora (*Melanosporales, Sordariomycetes*)

Papulaspora thermophila Fergus, Mycologia 63: 426. 1971. [MB 319160]; synonym of *Thermothelomyces myriococcoides*.

Parachaetomium

Parachaetomium biporatum (Cano & Guarro) X.Wei Wang & Houbraken, this study. [MB 830926]. Basionym: *Chaetomium biporatum*. — Type: FMR 854. Ex-type: CBS 244.86 = FMR 854 = IMI 330348. Reproduction: sexual. ITS barcode: MK919303 (alternative markers: LSU = MK919303; *tub2* = MK919417; *rpb2* = MK919360).

Parachaetomium carinthiacum (Sörgel) Mehrabi *et al.*, Mycol. Prog. 19: 1422. 2020. [MB 835858]. Basionym: *Chaetomium carinthiacum*. — Type: Abb. 7a and b in Sörgel, Arch. Mikrobiol. 40: 392, 1961 (lectotype), CBS H-10007 (epitype). Ex-epitype: CBS 153.81. Reproduction: sexual. ITS barcode: HM365265 (alternative markers: LSU = HM365265; *tub2* = HM365299; *rpb2* = MT568847).

Parachaetomium hispanicum (Guarro & Arx) X.Wei Wang & Houbraken, this study. [MB 830927]. Basionym: *Chaetomium hispanicum*. — Type: CBS 234.82. Ex-type: CBS 234.82. Reproduction: sexual. ITS barcode: MK919304 (alternative markers: LSU = MK919304; *tub2* = MK919418; *rpb2* = MK919361).

Parachaetomium inaequale (Pidopl. *et al.*, X.Wei Wang & Houbraken, this study. [MB 830928]. Basionym: *Thielavia inaequalis*. — Type: Instituto Microbiol. et Virusol. Acad. Sci., Ucrainae (Kiovia) sub N 55042. Ex-type: CBS 331.75 = IMI 196527 = VKM F-1922. Reproduction: sexual. ITS barcode: MK919306 (alternative markers: LSU = MK919306; *tub2* = MK919420; *rpb2* = MK919363).

Parachaetomium iranianum (Asgari & Zare) Mehrabi *et al.*, Mycol. Prog. 19: 1422. 2020. [MB 835856]. Basionym: *Chaetomium iranianum*. — Type: IRAN 14609F. Ex-type: IRAN 861C = CBS 126670. Reproduction: sexual. ITS barcode: HM365257 (alternative markers: LSU = HM365257; *tub2* = HM365297; *rpb2* = MT568848); synonym of *Parachaetomium perlucidum.*

Parachaetomium longiciliatum (Yu Zhang & L. Cai) X.Wei Wang & Houbraken, this study. [MB 840157]. Basionym: *Chaetomium longiciliatum* [as '*longiciliata*']. — Type: HMAS 245782. Ex-type: CGMCC 3.17554. Reproduction: sexual. ITS barcode: KP336774 (alternative markers: LSU = KP336823; *tub2* = KP336872; *rpb2* = KT149497).

Parachaetomium mareoticum (Besada & Yusef) X.Wei Wang & Houbraken, this study. [MB 840158]. Basionym: *Chaetomium mareoticum*. — Type: IMI 78435. Representative strain: CBS 802.83. Reproduction: sexual. ITS barcode: MZ334723 (alternative markers: LSU = MZ351426; *tub2* = MZ343036; *rpb2* = MZ342997).

Parachaetomium muelleri (Arx) X.Wei Wang & Houbraken, this study. [MB 830925]. Basionym: *Chaetomium muelleri*. — Type: CBS H-6879. Ex-type: CBS 192.84. Reproduction: sexual. ITS barcode: MK919300 (alternative markers: LSU = MK919300; *tub2* = MK919414; *rpb2* = MK919357).

Parachaetomium multispirale (A. Carter *et al.*) X.Wei Wang & Houbraken, this study. [MB 840159]. Basionym: *Chaetomium multispirale*. — Type: TRTC 66.609f. Ex-type: CBS 172.84 = TRTC 66609. Reproduction: sexual. ITS barcode: MH861718 (alternative markers: LSU = n/a; *tub2* = MZ343017; *rpb2* = MZ342978).

Parachaetomium perlucidum (Sergejeva) X.Wei Wang & Houbraken, this study. [MB 830930]. Basionym: *Chaetomium perlucidum*. — Type: –; CBS H-6885 (isotype). Ex-type: CBS 141.58 = IMI 074954 = MUCL 18693 = MUCL 39399 = VKM F-1950. Reproduction: sexual. ITS barcode: MK919308 (alternative markers: LSU = MK919308; *tub2* = MK919422; *rpb2* = MK919365).

Parachaetomium subspirilliferum (Sergejeva) X.Wei Wang & Houbraken, this study. [MB 830931]. Basionym: *Chaetomium subspirilliferum*. — Type: CBS H-6894; CBS H-6895 (isotype). Ex-type: CBS 150.60 = ATCC 14534 = IMI 081771 = MUCL 18698 = VKM F-1943. Reproduction: sexual. ITS barcode: MK919312 (alternative markers: LSU = MK919312; *tub2* = MK919426; *rpb2* = MK919369).

Parachaetomium truncatulum (Asgari & Zare) Mehrabi *et al.*, Mycol. Prog. 19: 1422. 2020. [MB 835857]. Basionym: *Chaetomium truncatulum*. — Type: IRAN 14610F. Ex-type: CBS 126782 = IRAN 918C. Reproduction: sexual. ITS barcode: HM365263 (alternative markers: LSU = HM365263; *tub2* = HM365298; *rpb2* = MT568849).

Parathielavia

Parathielavia appendiculata (M.P. Srivast. *et al.*) X.Wei Wang & Houbraken, Stud. Mycol. 93: 210. 2019. [MB 829869]. Basionym: *Thielavia appendiculata*. — Type: IMI 104944. Ex-type: CBS 723.68 = IMI 104944. Reproduction: sexual. ITS barcode: MK926827 (alternative markers: LSU = MK926827; *tub2* = MK926927; *rpb2* = MK876788).

Parathielavia coactilis (Nicot) X.Wei Wang & Houbraken, this study. [MB 840160]. Basionym: *Thielavia coactilis*. — Type: PC 1644. Representative strain: CBS 101190 = TRTC 52103. Reproduction: sexual. ITS barcode: n/a (alternative markers: LSU = n/a; *tub2* = MZ343003; *rpb2* = MZ342962).

Parathielavia hyrcaniae (Nicot) X.Wei Wang & Houbraken, Stud. Mycol. 93: 210. 2019. [MB 829870]. Basionym: *Thielavia hyrcaniae*. — Type: PC 1645. Ex-type: CBS 353.62 = IFO 8807 = LCP 1645. Reproduction: sexual. ITS barcode: KM655329(alternative markers: LSU = KM655368; *tub2* = KX977043; *rpb2* = KM655401).

Parathielavia kuwaitensis (Moustafa) X.Wei Wang & Houbraken, Stud. Mycol. 93: 210. 2019. [MB 829871]. Basionym: *Thielavia kuwaitensis*. — Type: CBS H-7848. Ex-type: CBS 945.72. Reproduction: sexual & asexual. ITS barcode: KM655332 (alternative markers: LSU = KM655371; *tub2* = KX977044; *rpb2* = KM655404).

Parvomelanocarpus

Parvomelanocarpus tardus (X.Wei Wang & Samson) X.Wei Wang & Houbraken, this study. [MB 840152]. Basionym: *Melanocarpus tardus*. — Type: CBS H-22849. Ex-type: CBS 541.76. Reproduction: sexual. ITS barcode: KX976681 (alternative markers: LSU = KX976775; *tub2* = KX977023; *rpb2* = KX976888).

Parvomelanocarpus thermophilus (Abdullah & Al-Bader) X.Wei Wang & Houbraken, this study. [MB 840167]. Basionym: *Thielavia minuta* var. *thermophila*. — Type: BSR 1006. Representative strain: CBS 886.97 = FMR 6190. Reproduction: sexual. ITS barcode: KM655350 (alternative markers: LSU = MH874288; *tub2* = MZ343037; *rpb2* = KM655434).

Pseudocanariomyces (synonym of *Allocanariomyces*; this study).

Pseudocanariomyces americanus Cañete-Gibas *et al.*, Mycopathologia 186: 443. 2021. [MB 839083]; basionym of *Allocanariomyces americanus*.

Pseudohumicola

Pseudohumicola atrobrunnea (X.Wei Wang *et al.*) X.Wei Wang *et al.*, this study. [MB 840148]. Basionym: *Humicola atrobrunnea*. — Type: CBS H-23481. Ex-type: HSAUP II 05-1004 = CBS 114167. Reproduction: asexual. ITS barcode: LT993570 (alternative markers: LSU = LT993570; *tub2* = LT993651; *rpb2* = LT993489).

Pseudohumicola pulvericola (X.Wei Wang *et al.*) X.Wei Wang *et al.*, this study. [MB 840149]. Basionym: *Humicola pulvericola*. — Type: CBS H-23486. Ex-type: CBS 144165. Reproduction: asexual. ITS barcode: LT993591 (alternative markers: LSU = LT993591; *tub2* = LT993672; *rpb2* = LT993510).

Pseudohumicola semispiralis (Udagawa & Cain) X.Wei Wang *et al.*, this study. [MB 840150]. Basionym: *Chaetomium semispirale*. — Type: TRTC 30103. Ex-type: CBS 723.97 = IMI 250972 = MUCL 40089. Reproduction: sexual & asexual. ITS barcode: LT993597 (alternative markers: LSU = LT993597; *tub2* = LT993678; *rpb2* = LT993516).

Pseudohumicola subspiralis (Chivers) X.Wei Wang *et al.*, this study. [MB 840151]. Basionym: *Chaetomium subspirale*. — Type: NY01050446. Representative strain: CBS 148.58 = IMI 075855. Reproduction: sexual & asexual. ITS barcode: LT993599 (alternative markers: LSU = LT993599; *tub2* = LT993680; *rpb2* = LT993518).

Pseudothielavia

Pseudothielavia arxii (Stchigel & Guarro) X.Wei Wang & Houbraken, Stud. Mycol. 93: 213. 2019. [MB 829873]. Basionym: *Thielavia arxii*. — Type: IMI 374725. Ex-type: CBS 603.97 = FMR 5875. Reproduction: sexual. ITS barcode: MK926830 (alternative markers: LSU = MK926830; *tub2* = MK926930; *rpb2* = MK876791). *Note*: This species is phylogenetically close to *Pseudothielavia terricola*, though phenotypically distinct.

Pseudothielavia hamadae (Udagawa) X.Wei Wang & Houbraken, Stud. Mycol. 93: 213. 2019. [MB 829874]. Basionym: *Achaetomium hamadae*. — Type: NHL 2910. Ex-type: CBS 499.83 = IMI 288714ii = NHL 2910. Reproduction: sexual. ITS barcode: MK926832 (alternative markers: LSU = MK926832; *tub2* = MK926932; *rpb2* = MK876793).

Pseudothielavia subhyaloderma X.Wei Wang & Houbraken, Stud. Mycol. 93: 217. 2019. [MB 829875]. — Type: CBS H-6866. Ex-type: CBS 473.86 = TRTC 36863. Reproduction: sexual. ITS barcode: MK926833 (alternative markers: LSU = MK926833; *tub2* = MK926933; *rpb2* = MK876794).

Pseudothielavia terricola (J.C. Gilman & E.V. Abbott) X.Wei Wang & Houbraken, Stud. Mycol. 93: 217. 2019. [MB 829876]. Basionym: *Coniothyrium terricola*. — Type: fig. 17 in Gilman & Abbott, Iowa St. Coll. J. Sci. 1(3): 267, 1927 (lectotype); CBS H-24049 (epitype). Ex-epitype: CBS 165.88 = TRTC 50997. Reproduction: sexual. ITS barcode: KX976694 (alternative markers: LSU = KX976792; *tub2* = KX977045; *rpb2* = MK876795).

Remersonia

Remersonia tenuis X.Wei Wang *et al.*, Stud. Mycol. 93: 111. 2018. [MB 824456]. — Type: CBS H-18610. Ex-type: CBS 784.85 = IMI 295313. Reproduction: asexual. ITS barcode: LT993609 (alternative markers: LSU = LT993609; *tub2* = LT993690; *rpb2* = LT993528).

Remersonia thermophila (Fergus) Seifert & Samson, Canad. J. Bot. 75: 1160. 1997. [MB 437277]. Basionym: *Stilbella thermophila*. — Type: PAC. Ex-type: ATCC 22073; Representative strain: CBS 645.91. Reproduction: asexual. ITS barcode: JF412016 (alternative markers: LSU = n/a; *tub2* = LT993692; *rpb2* = KF958020).

Scytalidium (*Helotiales, Leotiomycetes*)

Scytalidium thermophilum (Cooney & R. Emers.) Austwick, New Zealand J. Agric. Res. 19: 29. 1976. [MB 123497]; synonym of *Mycothermus thermophilus*.

Sphaeria

Sphaeria crispata Fuckel, Fungi Rhen. Exs., Suppl. Fasc. 6: no 2022. 1867. [MB 165726]; basionym of *Trichocladium crispatum*.

Sporotrichum (*Agaricomycotina, Basidiomycota*)

Sporotrichum thermophilum Apinis, Nova Hedwigia 5: 74. 1963. [MB 344529]; basionym of *Thermothelomyces thermophilus* [as '*thermophila*'].

Staphylotrichum

Staphylotrichum acaciicola X.Wei Wang & Houbraken, Stud. Mycol. 93: 113. 2018. [MB 824457]. — Type: CBS H-23490. Ex-type: CBS 281.65. Reproduction: asexual. ITS barcode: LT993613 (alternative markers: LSU = LT993613; *tub2* = LT993694; *rpb2* = LT993532).

Staphylotrichum boninense Nonaka *et al.*, Mycoscience 53: 315. 2012. [MB 561191]. — Type: TNS-F-41734. Ex-type: JCM 17908; Representative strain: CBS 112059. Reproduction: asexual. ITS barcode: LT993616 (alternative markers: LSU = LT993616; *tub2* = LT993697; *rpb2* = LT993535).

Staphylotrichum brevistipitatum X.Wei Wang & Houbraken, Stud. Mycol. 93: 118. 2018. [MB 824458]. — Type: CBS H-18521. Ex-type: CBS 408.67. Reproduction: asexual. ITS barcode: LT993619 (alternative markers: LSU = LT993619; *tub2* = LT993700; *rpb2* = LT993538).

Staphylotrichum coccosporum J.A. Mey. & Nicot, Bull. Trimestriel Soc. Bot. France 72: 323. 1957. [MB 306413]. — Type: n/a. Ex-type: CBS 364.58 = CBS 293.55 = IMI 57899. Reproduction: asexual. ITS barcode: LT993620 (alternative markers: LSU = LT993620; *tub2* = LT993701; *rpb2* = LT993539).

Staphylotrichum koreanum (Hyang B. Lee & T.T.T. Nguyen) X.Wei Wang & Houbraken, this study. [MB 840161]. Basionym: *Humicola koreana*. — Type: EML-UD33-1. Ex-

type: JMRC:SF:012183. Reproduction: asexual. ITS barcode: KU058192 (alternative markers: LSU = KU058190; *tub2* = n/a; *rpb2* = n/a).

Staphylotrichum limonisporum (Z.F. Zhang & L. Cai) X.Wei Wang & Houbraken, this study. [MB 840162]. Basionym: *Humicola limonispora*. — Type: HMAS 246922. Ex-type: CGMCC 3.17914. Reproduction: sexual & asexual. ITS barcode: KU746672 (alternative markers: LSU = KU746718; *tub2* = KU746764; *rpb2* = KY575867).

Staphylotrichum longicolle [as '*longicolleum*'] (Krzemien. & Badura) X.Wei Wang & Houbraken, Stud. Mycol. 93: 122. 2018. [MB 827915]. Basionym: *Chaetomium longicolle* [as '*longicolleum*']. — Type: n/a. Representative strain: CBS 119.57. Reproduction: sexual. ITS barcode: LT993621 (alternative markers: LSU = LT993621; *tub2* = LT993702; *rpb2* = LT993540).

Staphylotrichum microascosporum X.Wei Wang & Houbraken, Stud. Mycol. 93: 122. 2018. [MB 824460]. — Type: CBS H-12643. Ex-type: CBS 184.79. Reproduction: sexual. ITS barcode: LT993624 (alternative markers: LSU = LT993624; *tub2* = LT993705; *rpb2* = LT993543).

Staphylotrichum sinense M. Qiao *et al.*, Int. J. Syst. Evol. Microbiol. 71 (3, no. 004747): 2. 2021. [MB 832671]. — Type: YMFT 1.05760. Ex-type: YMF 1.05760 = CGMCC3.19631. Reproduction: asexual. ITS barcode: MN271027 (alternative markers: LSU = MN271026; *tub2* = MN340040; *rpb2* = MN233643).

Staphylotrichum tortipilum X.Wei Wang & Houbraken, Stud. Mycol. 93: 126. 2018. [MB 824461]. — Type: CBS H-12642. Ex-type: CBS 103.79. Reproduction: sexual. ITS barcode: LT993625 (alternative markers: LSU = LT993625; *tub2* = LT993706; *rpb2* = LT993544).

Stellatospora

Stellatospora terricola Tad. Ito & Nakagiri, Mycoscience 35: 413. 1994. [MB 414193]. — Type: IFO H-12166. Ex-type: CBS 811.95 = IFO 32597. Reproduction: sexual. ITS barcode: MK926835 (alternative markers: LSU = MK926835; *tub2* = MK926935; *rpb2* = MK876797).

Stilbella (*Hypocreales, Sordariomycetes*)

Stilbella thermophila Fergus, Mycologia 56: 277. 1964. [MB 339742]; basionym of *Remersonia thermophila*.

Stolonocarpus

Stolonocarpus gigasporus (Mustafa & Abdel-Azeem) X.Wei Wang & Houbraken, Stud. Mycol. 93: 221. 2019. [MB 829878]. Basionym: *Thielavia gigaspora*. — Type: IMI 39131. Ex-type: CBS 112062 = IMI 39131. Reproduction: sexual. ITS barcode: MK926836 (alternative markers: LSU = MK926836; *tub2* = MK926936; *rpb2* = MK876798).

Streptothrix

Streptothrix mycetomatis Laveran, Bull. Acad. Méd. Paris, ser. 3, 47: 776. 1902. [MB 492359]; basionym of *Madurella mycetomatis*.

Subramaniula

Subramaniula anamorphosa (S.A. Ahmed *et al.*) X.Wei Wang & Samson, Stud. Mycol. 84: 220. 2016. [MB 818876]. Basionym: *Chaetomium anamorphosum*. — Type: CBS H-21973. Ex-type: CBS 137114. Reproduction: asexual. ITS barcode: KP862598 (alternative markers: LSU = KP970641; *tub2* = KP900704; *rpb2* = KP900667).

Subramaniula asteroides S.A. Ahmed *et al.*, Fungal Diversity 76: 20. 2015. [MB 810427]. — Type: CBS H-21971. Ex-type: CBS 123294. Reproduction: asexual. ITS barcode: HQ906667 (alternative markers: LSU = JX280731; *tub2* = KP900703; *rpb2* = KP900666).

Subramaniula cristata (L.M. Ames) X.Wei Wang & Samson, Stud. Mycol. 84: 212. 2016. [MB 818853]. Basionym: *Chaetomium cristatum*. — Type: ISC-F-0123561. Ex-type: CBS 156.52 = ATCC 11201 = DSM 3702. Reproduction: sexual. ITS barcode: KX976690 (alternative markers: LSU = KX976788; *tub2* = KX977038; *rpb2* = KX976903).

Subramaniula cuniculorum (Fuckel) X.Wei Wang & Samson, Stud. Mycol. 84: 220. 2016. [MB 818877]. Basionym: *Chaetomium cuniculorum*. — Type: Fuckel, Fungi Rhen. 1961, *e.g.*, HAL, S-F267436. Representative strain: CBS 800.83. Reproduction: sexual. ITS barcode: KX976692 (alternative markers: LSU = KX976790; *tub2* = KX977040; *rpb2* = KX976905).

Subramaniula flavipila X.Wei Wang & Samson, Stud. Mycol. 84: 220. 2016. [MB 818878]. Replaced synonym: *Chaetomium irregulare*. — Type: B 505 (holotype); CBS H-6876 (isotype). Ex-type: CBS 446.66 = IMI 153340. Reproduction: sexual. ITS barcode: KP862600 (alternative markers: LSU = KP970647; *tub2* = KP900706; *rpb2* = KP900669).

Subramaniula fusispora (G. Sm.) X.Wei Wang & Samson, Stud. Mycol. 84: 220. 2016. [MB 818879]. Basionym: *Chaetomium fusisporum*. — Type: LSHTM BB382. Ex-type: CBS 166.61 = IMI 086560. Reproduction: sexual. ITS barcode: MH858011 (alternative markers: LSU = MH869571; *tub2* = MZ343015; *rpb2* = MZ342976).

Subramaniula lateralis (Yu Zhang & L. Cai) X.Wei Wang & Houbraken, this study. [MB 840164]. Basionym: *Chaetomium laterale*. — Type: HMAS 245785. Ex-type: CGMCC 3.17547. Reproduction: sexual. ITS barcode: KP336789 (alternative markers: LSU = KP336838; *tub2* = KP336887; *rpb2* = MZ342998).

Subramaniula latifusispora X.Wei Wang *et al.*, this study. [MB 840129]. — Type: HMAS 350267. Ex-type: CGMCC 3.20442 = WXW 8538. Reproduction: sexual. ITS barcode: MZ334728 (alternative markers: LSU = MZ351428; *tub2* = MZ343040; *rpb2* = MZ343001).

Subramaniula obscura S.A. Ahmed *et al.*, Fungal Diversity 76: 21. 2015. [MB 810428]. — Type: CBS H-21972. Ex-type: CBS 132916. Reproduction: asexual. ITS barcode: KP862595 (alternative markers: LSU = KP970653; *tub2* = KP900700; *rpb2* = KP900662).

Subramaniula thielavioides (Arx *et al.*) Arx, Proc. Indian Acad. Sci. Sect. B 94: 344. 1985. [MB 105812]. Basionym: *Achaetomium thielavioides*. — Type: CBS H-6628. Ex-type: CBS 122.78 = IMI 288625. Reproduction: sexual. ITS barcode: KP862597 (alternative markers: LSU = KP970654; *tub2* = KP900708; *rpb2* = KP900670).

Taifanglania (synonym of *Acrophialophora*)

Taifanglania biformis (Z.Q. Liang *et al.*) Z.Q. Liang *et al.*, Fungal Diversity 34: 74. 2009. [MB 512815]; synonym of *Acrophialophora biformis*.

Taifanglania hechuanensis Z.Q. Liang *et al.*, Fungal Diversity 34: 72. 2009. [MB 512804]; basionym of *Acrophialophora hechuanensis*.

Taifanglania jiangsuensis Y.F. Han & Z.Q. Liang, Mycotaxon 112: 328. 2010. [MB 516504]; basionym of *Acrophialophora jiangsuensis*.

Tengochaeta

Tengochaeta nigropilosa X.Wei Wang & Houbraken, this study. [MB 840130]. — Type: CBS H-24774. Ex-type: CBS 639.83. Reproduction: sexual. ITS barcode: MZ334730 (alternative markers: LSU = n/a; *tub2* = MZ343029; *rpb2* = MZ342990).

Thermocarpiscus

Thermocarpiscus australiensis (Tansey & M.A. Jack) X.Wei Wang & Houbraken, this study. [MB 840165]. Basionym: *Thielavia australiensis*. — Type: DAOM, microscope slide no. 3/19/74-8. Ex-type: CBS 493.74 = ATCC 28236 = DAOM 145919. Reproduction: sexual & asexual. ITS barcode: KM655339 (alternative markers: LSU = KM655378; *tub2* = MZ343024; *rpb2* = KM655419).

Thermochaetoides

Thermochaetoides dissita (Cooney & R. Emers.) X.Wei Wang & Houbraken, this study. [MB 830932]. Basionym: *Chaetomium thermophilum* var. *dissitum*. — Type: UC 1206513. Ex-type: CBS 180.67 = ATCC 16452 = DSM 1494 = IMI 126332. Reproduction: sexual. ITS barcode: MK919319 (alternative markers: LSU = MK919319; *tub2* = MK919433; *rpb2* = MK919375).

Thermochaetoides thermophila (La Touche) X.Wei Wang & Houbraken, this study. [MB 830933]. Basionym: *Chaetomium thermophilum*. — Type: IMI, anon. MRA112. Ex-type: CBS 144.50 = DAOM 24625 = DSM 1495 = IMI 039719. Reproduction: sexual. ITS barcode: MK919314 (alternative markers: LSU = MK919314; *tub2* = MK919428; *rpb2* = KM655436).

Thermomyces (*Eurotiales, Eurotiomycetes*)

Thermomyces verrucosus Pugh *et al.*, Trans. Brit. Mycol. Soc. 47: 116. 1964. [MB 340048]; basionym of *Botryotrichum verrucosum*.

Thermothelomyces

Thermothelomyces fergusii X.Wei Wang & Houbraken, this study. [MB 830934]. Replaced synonym: *Thielavia thermophila*. — Type: PAC, Fergus & Sinden R46w1×R46w2. Ex-type: CBS 406.69 = ATCC 22067. Reproduction: asexual & sexual (heterothallic). ITS barcode: HQ871794 (alternative markers: LSU =KX976776; *tub2* = KX977024; *rpb2* = MK919378).

Thermothelomyces guttulatus [as '*guttulata*'] (Y. Zhang & L. Cai) Y. Marín *et al.*, Mycologia 107: 630. 2015. [MB 823051]. Basionym: *Myceliophthora guttulata*. — Type: HMAS 244238. Ex-type: CGMCC 3.15185. Reproduction: asexual. ITS barcode: MK919323 (alternative markers: LSU = MK919323; *tub2* = MK919437; *rpb2* = MK919380).

Thermothelomyces heterothallicus [as '*heterothallica*'] (Klopotek) Y. Marín *et al.*, Mycologia 107: 630. 2015. [MB 823052]. Basionym: *Thielavia heterothallica*. — Type: CBS H-18810 (holotype), CBS H-24878 (epitype). Ex-epitype: CBS 202.75. Reproduction: asexual & sexual (heterothallic). ITS barcode: HQ871771 (alternative markers: LSU = KM655354; *tub2* = KX977025; *rpb2* = KM655391).

Thermothelomyces hinnuleus [as '*hinnulea*'] (Awao & Udagawa) Y. Marín *et al.*, Mycologia 107: 630. 2015. [MB 823053]. Basionym: *Myceliophthora hinnulea*. — Type: NHL AJ-6773. Ex-type: CBS 597.83 = ATCC 52474 = NHL 2909. Reproduction: asexual. ITS barcode: MK919327 (alternative markers: LSU = MK919327; *tub2* = MK919441; *rpb2* = MK919384).

Thermothelomyces myriococcoides (Fergus) X.Wei Wang & Houbraken, this study. [MB 830935]. Replaced synonym: *Papulaspora thermophila*. — Type: BPI 844852. Ex-type: CBS 389.93 = ATCC 22112. Reproduction: asexual. ITS barcode: MK919329 (alternative markers: LSU = MK919329; *tub2* = MK919443; *rpb2* = MK919386).

Thermothelomyces thermophilus [as '*thermophila*'] (Apinis) Y. Marín *et al.*, Mycologia 107: 630. 2015. [MB 823054]. Basionym: *Sporotrichum thermophilum*. — Type: BDUN 274 (holotype); CBS H-7380, CBS H-7381 (isotypes). Ex-type: CBS 117.65 = BDUN 274. Reproduction: asexual. ITS barcode: MK919331 (alternative markers: LSU = MK919331; *tub2* = MK919445; *rpb2* = MK919387).

Thermothielavioides

Thermothielavioides terrestris (Apinis) X.Wei Wang & Houbraken, Stud. Mycol. 93: 223. 2019. [MB 829880]. Basionym: *Allescheria terrestris*. — Type: BDUN 278. Ex-type: CBS 117535 = CBS 355.66 = BDUN 278 = UAMH 3988. Reproduction: sexual & asexual. ITS barcode: MK926837 (alternative markers: LSU = MK926837; *tub2* = MK926937; *rpb2* = MK876799).

Thielavia (*Melanosporales, Sordariomycetes*)

Thielavia antarctica Stchigel & Guarro, Mycologia 95: 1225. 2004. [MB 489459]; basionym of *Trichocladium antarcticum*.

Thielavia appendiculata M.P. Srivast. *et al.*, Mycopathol. Mycol. Appl. 30: 205. 1966. [MB 340050]; basionym of *Parathielavia appendiculata*.

Thielavia arenaria Mouch., Bull. Trimestriel Soc. Mycol. France 89: 308. 1973. [MB 324545]; basionym of *Canariomyces arenarius*.

Thielavia arxii Stchigel & Guarro, Mycol. Res. 106: 979. 2002. [MB 483974]; basionym of *Pseudothielavia arxii*.

Thielavia australiensis Tansey & M.A. Jack, Canad. J. Bot. 53: 81. 1975. [MB 324546]; basionym of *Thermocarpiscus australiensis*.

Thielavia coactilis Nicot, Compt. Rend. Hebd. Séances Acad. Sci. Paris 253: 304. 1961. [MB 340051]; basionym of *Parathielavia coactilis*.

Thielavia fimeti (Fuckel) Malloch & Cain, Mycologia 65: 1064. 1973. [MB 324554]; synonym of *Chaetomium fimeti*.

Thielavia fragilis (Natarajan) Arx, Stud. Mycol. 8: 8. 1975. [MB 324555]; synonym of *Hyalosphaerella fragilis*.

Thielavia gigaspora Moustafa & Abdel-Azeem, Microbiol. Res. 163: 442. 2008. [MB 487453]; basionym of *Stolonocarpus gigasporus*.

Thielavia heterothallica Klopotek, Arch. Microbiol. 107: 223. 1976. [MB 324556]; basionym of *Thermothelomyces heterothallicus* [as '*heterothallica*'].

Thielavia hyrcaniae Nicot, Compt. Rend. Hebd. Séances Acad. Sci., Sér. D 253: 304. 1961. [MB 340053]; basionym of *Parathielavia hyrcaniae*.

Thielavia inaequalis Pidopl. *et al.*, Mikrobiol. Zhurn. 35(6): 723. 1973. [MB 324558]; basionym of *Parachaetomium inaequale*.

Thielavia kirilenkoae Beliakova, Mikol. Fitopatol. 8(2): 73. 1974. [MB 324559]; synonym of *Microthielavia ovispora*.

Thielavia kuwaitensis Moustafa, Trans. Brit. Mycol. Soc. 66: 336. 1976. [MB 324560]; basionym of *Parathielavia kuwaitensis*.

Thielavia leptoderma C. Booth [as '*leptodermus*'], Mycol. Pap. 83: 3. 1961. [MB 340054]; basionym of *Aporothielavia leptoderma*.

Thielavia microspora Mouch., Bull. Trimestriel Soc. Mycol. France 89: 300. 1973. [MB 324563]; basionym of *Canariomyces microsporus*.

Thielavia novoguineensis Udagawa & Y. Horie, Bull. Nat. Sci. Mus. Tokyo 15: 191. 1972. [MB 324566]; basionym of *Corynascus novoguineensis*.

Thielavia octospora (Natarajan) Arx, Stud. Mycol. 8: 6. 1975. [MB 283722]. Basionym: *Thielaviella octospora*. — Type: MUBL 2250. Representative strain: CBS 119.76. ITS barcode: MZ334731 (alternative markers: LSU = MZ351416; *tub2* = MZ343009; *rpb2* = MZ342970). *Note*: Based on the phylogenetic analysis (Fig. 7), we consider *Thielavia octospora* a synonym of *Achaetomium globosum.*

Thielavia ovispora Pidopl. *et al.*, Mikrobiol. Zhurn. 35(6): 724. 1973. [MB 324568]; basionym of *Microthielavia ovispora*.

Thielavia peruviana (Goch.) Malloch & Cain, Mycologia 65: 1067. 1973. [MB 324571]; synonym of *Chrysanthotrichum peruvianum*.

Thielavia pilosa C. Booth & Shipton, Trans. Brit. Mycol. Soc. 49: 665. 1966. [MB 340058]; basionym of *Chaetomium pilosum*.

Thielavia sepedonium C.W. Emmons, Bull. Torrey Bot. Club 59: 417. 1932. [MB 277883]; basionym of *Corynascus sepedonium*.

Thielavia spirotricha (R.K. Benj.) Malloch & Cain, Mycologia 65: 1069. 1973. [MB 324575]; synonym of *Botryotrichum spirotrichum*.

Thielavia subfimeti (Seth) Malloch & Cain, Mycologia 65: 1070. 1973. [MB 324576]; synonym of *Chaetomium subfimeti*.

Thielavia subthermophila Mouch., Bull. Trimestriel Soc. Mycol. France 89: 297. 1973. [MB 324577]; basionym of *Canariomyces subthermophilus*.

Thielavia terrestris (Apinis) Malloch & Cain, Canad. J. Bot. 50: 66. 1972. [MB 324578]; synonym of *Thermothielavioides terrestris*.

Thielavia terricola (J.C. Gilman & E.V. Abbott) C.W. Emmons, Bull. Torrey Bot. Club 57: 124. 1930. [MB 255078]; synonym of *Pseudothielavia terricola*.

Thielavia tetraspora (Lodhi & Mirza) Arx, The genera of fungi sporulating in pure culture: 115. 1974. [MB 283723]; synonym of *Boothiella tetraspora*.

Thielavia thermophila Fergus & Sinden, Canad. J. Bot. 47: 1635. 1969. [MB 340061]. Replaced synonym of *Thermothelomyces fergusii*.

Thielavia tortuosa Udagawa & Y. Sugiy., Trans. Mycol. Soc. Japan 22: 197. 1981. [MB 111966]; basionym of *Condenascus tortuosus*.

Thielavia minuta var. *thermophila* Abdullah & Al-Bader, Basrah J. Agric. Sci. 5: 116. 1992. [MB 444607]; basionym of *Parvomelanocarpus thermophilus*.

Torula (*Pleosporales, Dothideomycetes*)

Torula thermophila Cooney & R. Emers., Thermophilic Fungi: 92. 1964. [MB 340149]; basionym of *Mycothermus thermophilus*.

Trichocladium

Trichocladium acropullum (X.Wei Wang) X.Wei Wang & Houbraken, Stud. Mycol. 93: 126. 2018. [MB 824462]. Basionym: *Chaetomium acropullum*. — Type: HMAS 86808. Ex-type: CBS 114580. Reproduction: sexual & asexual. ITS barcode: LT993626 (alternative markers: LSU = LT993626; *tub2* = LT993707; *rpb2* = LT993545).

Trichocladium amorphum X.Wei Wang & Houbraken, Stud. Mycol. 93: 130. 2018. [MB 824463]. — Type: CBS H-23491. Ex-type: CBS 127763. Reproduction: asexual. ITS barcode: LT993628 (alternative markers: LSU = LT993628; *tub2* = LT993709; *rpb2* = LT993547).

Trichocladium antarcticum (Stchigel & Guarro) X.Wei Wang & Houbraken, Stud. Mycol. 93: 130. 2018. [MB 824464]. Basionym: *Thielavia antarctica*. — Type: IMI 389346. Ex-type: CBS 123565 = FMR 7920. Reproduction: sexual & asexual. ITS barcode: LT993629 (alternative markers: LSU = LT993629; *tub2* = LT993710; *rpb2* = LT993548).

Trichocladium arxii (Benny) X.Wei Wang & Houbraken, Stud. Mycol. 93: 130. 2018. [MB 824465]. Basionym: *Chaetomidium arxii*. — Type: FLAS-F52103. Ex-type: CBS 104.79. Reproduction: sexual. ITS barcode: LT993631 (alternative markers: LSU = LT993631; *tub2* = LT993712; *rpb2* = LT993550).

Trichocladium asperum Harz, Bull. Soc. Imp. Naturalistes Moscou 44: 125. 1871. [MB 171452]. — Type: Tab. II fig. 1 in Harz, Bull. Soc. Imp. Naturalistes Moscow 44, 1871 (lectotype), CBS H-23060 (epitype, designated here; MBT 10002832). Ex-epitype: CBS 903.85. Reproduction: asexual. ITS barcode: LT993632 (alternative markers: LSU = LT993632; *tub2* = LT993713; *rpb2* = LT993551).

Trichocladium beniowskiae X.Wei Wang & Houbraken, Stud. Mycol. 93: 134. 2018. [MB 824466]. Replaced synonym: *Beniowskia macrospora*. — Type: IMI 99625. Ex-type: CBS 757.74 = IMI 099625. Reproduction: asexual. ITS barcode: LT993635 (alternative markers: LSU = LT993635; *tub2* = LT993716; *rpb2* = LT993554).

Trichocladium crispatum (Fuckel) X.Wei Wang & Houbraken, Stud. Mycol. 93: 137. 2018. [MB 824467]. Basionym: *Sphaeria crispata*. — Type: G00127921 (holotype), CBS H-23492 (epitype). Ex-epitype: CBS 149.58. Reproduction: sexual. ITS barcode: LT993636 (alternative markers: LSU = LT993636; *tub2* = LT993717; *rpb2* = LT993555).

Trichocladium gilmaniellae X.Wei Wang & Houbraken, Stud. Mycol. 93: 137. 2018. [MB 824468]. Replaced synonym: *Gilmaniella macrospora*. — Type: CBS 388.75. Ex-type: CBS 388.75. Reproduction: asexual. ITS barcode: LT993638 (alternative markers: LSU = LT993638; *tub2* = LT993719; *rpb2* = LT993557).

Trichocladium griseum (Traaen) X.Wei Wang & Houbraken, Stud. Mycol. 93: 141. 2018. [MB 824469]. Basionym: *Humicola grisea*. — Type: CBS H-23493 (neotype). Ex-neotype: CBS 119.14 = ATCC 22724 = IMI 075664 = MUCL 8008. Reproduction: asexual. ITS barcode: LT993639 (alternative markers: LSU = LT993639; *tub2* = LT993720; *rpb2* = LT993558).

Trichocladium heterothallicum (Yu Zhang & L. Cai) X.Wei Wang & Houbraken, Stud. Mycol. 93: 141. 2018. [MB 824470]. Basionym: *Chaetomium heterothallicum*. — Type: HMAS 245783. Ex-type: CGMCC 3.17543 = LC3796. Reproduction: sexual & asexual. ITS barcode: KP336755 (alternative markers: LSU = KP336804; *tub2* = KP336853; *rpb2* = n/a).

Trichocladium jilongense (Y.M. Wu & T.Y. Zhang) X.Wei Wang & Houbraken, Stud. Mycol. 93: 141. 2018. [MB 824471]. Basionym: *Humicola jilongensis*. — Type: HSAUP II 07 1485. Ex-type: HSAUP II 07 1485. Reproduction: asexual. ITS barcode: LT993642 (alternative markers: LSU = LT993642; *tub2* = LT993723; *rpb2* = LT993561).

Trichocladium nigrospermum (Schwein.) X.Wei Wang & Houbraken, Stud. Mycol. 93: 141. 2018. [MB 824472]. Basionym: *Acremonium nigrospermum*. — Type: PH. Representative strain: CBS 103.36. Reproduction: asexual. ITS barcode: LT993644 (alternative markers: LSU = LT993644; *tub2* = LT993725; *rpb2* = LT993563).

Trichocladium seminis-citrulli (Sergejeva) X.Wei Wang & Houbraken, Stud. Mycol. 93: 145. 2018. [MB 824473].

Basionym: *Chaetomium seminis-citrulli*. — Type: –; CBS H-6892 (isotype). Ex-type: CBS 143.58 = IMI 074953 = VKM F-1952. Reproduction: sexual & asexual. ITS barcode: LT993645 (alternative markers: LSU = LT993645; *tub2* = LT993726; *rpb2* = LT993564).

Trichocladium tomentosum X.Wei Wang *et al.*, this study. [MB 840131]. — Type: HMAS 350294 (holotype); CBS H-23643 (isotype). Ex-type: CGMCC 3.20443 = CBS 144476 = WXW 8615. Reproduction: sexual. ITS barcode: MZ334732 (alternative markers: LSU = MZ351431; *tub2* = MZ343012; *rpb2* = MZ342973).

Trichocladium uniseriatum (Yu Zhang & L. Cai) X.Wei Wang & Houbraken, Stud. Mycol. 93: 145. 2018. [MB 824475]. Basionym: *Chaetomium uniseriatum*. — Type: HMAS 245787. Ex-type: CGMCC 3.17559 = LC3756. Reproduction: sexual & asexual. ITS barcode: KP336751 (alternative markers: LSU = KP336800; *tub2* = KP336849; *rpb2* = KT149475).

Xanthiomyces

Xanthiomyces spinosus (Chivers) X.Wei Wang & Houbraken, this study. [MB 840166]. Basionym: *Chaetomium spinosum*. — Type: CUP, Chivers No. 7. Representative strain: CBS 789.71. Reproduction: sexual. ITS barcode: MH860357 (alternative markers: LSU = MZ351429; *tub2* = MZ343034; *rpb2* = MZ342995).

Doubtful and excluded species

Achaetomium thermophilum M. Basu, Curr. Sci. 51: 524. 1982. [MB 109578]. — Type: n/a. Ex-type: CBS 250.85 = CBS 152.97. Reproduction: sexual. ITS barcode: JX280859 (alternative markers: LSU = JX280740; *tub2* = n/a; *rpb2* = n/a). *Notes*: The two representative cultures of *Achaetomium thermophilum* in the CBS collection differ: one resembles *Chaetomium vitellinum* and the other one *Achaetomium macrosporum*. The taxonomic position of this species is doubtful and needs further study.

Chaetomidium triangulare Stchigel & Guarro, Stud. Mycol. 50: 218. 2004. [MB 500062]. — Type: IMI 392313. Ex-type: CBS 113677 = FMR 7545. Reproduction: sexual. ITS barcode: (alternative markers: LSU = FJ666362; *tub2* = n/a; *rpb2* = FJ666393). *Note*: *Chaetomidium triangulare* and *Chaetomium microascoides* cluster together in "clade 6, *Lasiosphaeriaceae*" outside the *Chaetomiaceae* (Fig. 7).

Chaetomium microascoides Guarro, Nova Hedwigia 41: 445. 1985. [MB 103923]. — Type: n/a. Ex-type: CBS 236.80 = CBS 540.83. Reproduction: sexual. ITS barcode: MH861259 (alternative markers: LSU = MH873028; *tub2* = MZ343020; *rpb2* = MZ342981). *Note*: *Chaetomium microascoides* and *Chaetomidium triangulare* cluster together in "clade 6, *Lasiosphaeriaceae*" outside the *Chaetomiaceae* (Fig. 7).

Chaetomium olivicolor K. Rodr. *et al.*, Mycologia 94: 123. 2002. [MB 484630]. — Type: IMI 382895. Ex-type: CBS 102434 = FMR 6779 = IMI 381869 = MUCL 43148. Reproduction: sexual. ITS barcode: KM655318 (alternative markers: LSU = KM655357; *tub2* = n/a; *rpb2* = KM655428). *Note*: *Chaetomium olivicolor* is phylogenetically related to *Achaetomiella* and more research is needed to determine the position of this species.

Chaetomium siamense Pornsuriya & Soytong, Mycotaxon 115: 21. 2011. [MB 514033]. — Type: TMACC001. Ex-type: CP-2009. Reproduction: sexual. ITS barcode: AB506801 (alternative markers: LSU = n/a; *tub2* = n/a; *rpb2* = n/a). *Notes*: A BLAST search with the ITS sequence deposited on GenBank showed a 97.2 % homology with CBS 337.67, the ex-type of *Ar. flavigenus*. More research is needed to confidentially combine this species in *Arcopilus*.

Chaetomium tetrasporum S. Hughes, Trans. Brit. Mycol. Soc. 29: 72. 1946. [MB 285138]. — *Notes*: No ex-type or authentic representative culture was available to determine the position of this species. A strain maintained in the CBS culture collection (CBS 351.77) as *Chaetomium tetrasporum* is sterile.

Humicola siamensis Chatmala & E.B.G. Jones, Nova Hedwigia 83: 226. 2006. [MB 522318]. — Type: BCC 9511. Ex-type: BCC 9511. Reproduction: sexual & asexual. ITS barcode: n/a (alternative markers: LSU = DQ237875; *tub2* = n/a; *rpb2* = n/a). *Note*: A BLAST search with the LSU sequence present in GenBank shows that this species doesn't belong to the *Chaetomiaceae*, and probably belongs to *Halosphaeriaceae* (*Microascales*).

Taifanglania parvispora Y. Wang *et al.*, Mycosystema 34: 347. 2015. [MB 805936]. — Type: GZUIFR-E21402H. Ex-type: GZUIFR-E21402H. Reproduction: asexual. ITS barcode: KF719170 (alternative markers: LSU = n/a; *tub2* = n/a; *rpb2* = n/a). *Notes*: The morphology of *Tai. parvispora* is that of a typical *Acrophialophora* species; however, comparison of the ITS sequence indicated a relationship with species in *Subramaniula*. More data are needed to confidentially determine its generic position.

DISCUSSION

Fifty genera are recognised in *Chaetomiaceae*, of which six are newly proposed in this study. Multi-gene phylogenetic analysis resolved most of the genera as monophyletic lineages with robust support. However, in some cases we are faced with the choice to define genera in a broader or narrower sense. In combination with ecological, morphological and phylogenetic data, we used divergence times as an additional criterion for evaluating genera that are difficult to delimit. The results indicate that all the well-defined genera in the *Chaetomiaceae* diverged earlier than 27 Mya (Figs 8, 9). *Chrysocorona*, *Pseudothielavia* and *Hyalosphaerella* seem to have diverged most recently from each other at about 27 and 30 Mya, respectively. Even though they cluster together, no statistical evidence supports the close relationships of these three genera in our combined phylogenetic analysis (Fig. 7C). Furthermore, they do have striking morphological differences and we therefore accept them as separate genera. The criteria used here to delimit genera led to the introduction of the new genera *Parvomelanocarpus*, *Pseudohumicola* and *Xanthiomyces*, the reintroduction of *Achaetomiella*, the synonymy of "*Crassicarpon*" with *Thermothelomyces*, and the acceptance of *Parachaetomium* delimited by Mehrabi *et al.* (2020). Divergence times also helped us to confirm several genera which were delimitated in our previous studies. For example, the two sexually-reproducing chaetomium-like species *Acro. jodhpurensis* and *Acro. teleoafricana* were classified in the traditionally asexual genus *Acrophialophora* based on their close phylogenetic relationship. The molecular dating analysis showed that the two sexual species diverged about 22 Mya, more recent than the later time limit of the other accepted genera in the family (about 27 Mya, Figs 8, 9), supporting them within the genus. The phylogenetically-defined *Trichocladium* is also supported by molecular dating analysis. The species in this genus possess a highly diverse morphology in their asexual and sexual morphs. In total, the mean stem ages of the genera in the family range from 27 to 122 Mya (Figs 8, 9).

Most of the morphologically-defined traditional genera in *Chaetomiaceae* have proven to be poly- or paraphyletic with a few exceptions like *Achaetomium*, *Corynascus* and *Stellatospora* (von Arx 1973, von Arx *et al.* 1988, Ito & Nakagiri 1994, Wang *et al.* 2016a, b, 2019a, b). Species with a chaetomium-like morph (the traditionally morphology-based concept of *Chaetomium*) are distributed in 23 genera, namely *Achaetomiella*, *Acrophialophora*, *Amesia*, *Arcopilus*, *Arxotrichum*, *Botryotrichum*, *Brachychaeta*, *Chaetomium sensu stricto*, *Chrysanthotrichum*, *Chrysocorona*, *Collariella*, *Dichotomopilus*, *Floropilus*, *Humicola*, *Ovatospora*, *Parachaetomium*, *Pseudohumicola*, *Staphylotrichum*, *Subramaniula*, *Tengochaeta*, *Thermochaetoides*, *Trichocladium*, *Xanthiomyces* (Wang *et al.* 2016a, Crous *et al.* 2018, Wang *et al.* 2019a, b, Mehrabi *et al.* 2020, this study). The thielavia-like species in *Chaetomiaceae* (species once placed in *Thielavia*) are distributed in 11 genera: *Carteria*, *Chrysanthotrichum*, *Condenascus*, *Hyalosphaerella*, *Microthielavia*, *Parathielavia*, *Pseudothielavia*, *Stolonocarpus*, *Thermocarpiscus*, *Trichocladium* and *Thermothielavioides* (Wang *et al.* 2019a, b, this study). Three species, which produce non-ostiolate ascomata containing ascospores with two apical germ pores, were previously classified in *Corynascella* and current insight shows that these belong to three different genera: *Corynascella sensu stricto* (*Coryl. humicola*; Figs 23, 24), *Botryotrichum* (*Bot. inquinatum*; Fig. 21) and *Parachaemium* (*Parach. inaequale* = *Coryl. inaequalis* = *Thielavia inaequalis*; Fig. 35). Species with a chaetomidium-like morph are distributed over four lineages: *Aporothielavia* (*Ap. leptoderma* = *Chd. leptoderma*; Fig. 11), *Botryotrichum* (*Bot. trichorobustum* = *Chd. trichorobustum*), *Chaetomium* (*Ch. fimeti* = *Chd. fimeti*, *Ch. pilosum* = *Chd. pilosum*, *Ch. subfimeti* = *Chd. subfimeti*, *Ch. tectifimeti*, Wang *et al.* 2016a, b) and *Lasiosphaeriaceae sensu lato* outside *Chaetomiaceae* ("*Chaetomidium triangulare*").

After this phylogenetic revision, most of the genera in the family consist of species which share morphological features. Examples are *Collariella* and *Dichotomopilus. Collariella* can be easily recognised by the production of 1) broadly limoniform to quadrangular and bilaterally flattened ascospores with an apical germ pore which are usually less than 7.5 µm long, and 2) a darkened collar around the ostiolar pore of ascomata. *Dichotomopilus* is characterised by seta-like to dichotomously or irregularly branched ascomatal hairs and by narrowly ovate to broad ovate and slightly bilaterally-flattened small ascospores, which are usually less than 7.5 µm long, and have an apical or slightly sub-apical germ pore. On the other hand, some genera, such as *Botryotrichum* and *Trichocladium* are morphologically highly diverse. Species in these genera can reproduce asexually with different asexual structures or sexually with ostiolate or non-ostiolate ascomata.

At species level, 275 species are accepted in *Chaetomiaceae* based on the results of the phylogenetic analyses (Fig. 7, Supplementary Figs S1, S2). Few species were not included in the multigene analysis because these were very recently described (*Arcopilus eremanthi*, *Chaetomium camelliae*, *Dichotomopilus finlandicus*) or only ITS and/or LSU sequences were available (*e.g.*, several *Acrophialophora* species, *Staphylotrichum koreanum* = *Humicola koreana*) and these failed to be combined in the analysis. Most of the species have been recently (re)described and photo plates of these species are available (Asgar & Zare 2011, Marin-Felix *et al.* 2015, Wang *et al.* 2016a, b, 2019a, b, Crous *et al.* 2016, 2017, 2018, 2019, Zhang *et al.* 2017a, b, Raza *et al.* 2019, Schultes *et al.* 2019, Alidadi *et al.* 2020, Mehrabi *et al.* 2020, Safi *et al.* 2020, Sousa *et al.* 2020, Qiao *et al.* 2021, Ryan *et al.* 2021, this study), making identification easier. In addition, "*Chaetomium microascoides*" (ex-type culture CBS 236.80) and "*Chaetomidium triangulare*" (ex-type culture CBS 113677) proved to be members of *Lasiosphaeriaceae sensu lato*, outside the *Chaetomiaceae*. Further study is needed to determine their exact position at both genus and family level. A few species in *Chaetomiaceae* were found to have a distinct morphology, while no differences in their molecular barcodes (ITS, LSU, *rpb2* and *tub2*) were present (*e.g.*, *Ch. globosum* and *Ch. cruentum*; figs 14, 16 in Wang *et al.* 2016a). These species are morphologically distinct, but phylogenetically undistinguishable (Fig. 7B, Supplementary Figs S1–S3). We decided to tentatively accept these species and genome studies may give more insight into the evolution of these taxa.

Morgenstern *et al.* (2012) demonstrated that thermophilic species are polyphyletic in kingdom *Fungi*, and that they are present in *Sordariales*, *Eurotiales* and *Onygenales* in *Ascomycota* and in *Mucoromycota*. The study of van den Brink *et al.* (2015) showed that thermophilic species in *Chaetomiaceae* are also polyphyletic. The present study resolved 15 thermophilic *Chaetomiaceae* species in seven genera: *Melanocarpus*, *Mycothermus*, *Remersonia*, *Thermocarpusella*, *Thermochaetoides*, *Thermothelomyces* and *Thermothielavioides*. It is clear that thermophiles independently evolved at least six times within *Chaetomiaceae*. *Mycothermus* and *Remersonia* are sister genera with a mean stem age of about 40 Mya. The other five thermophilic genera do not have thermophilic sister genera and clearly diverged from mesophilic genera, probably by adaptation to elevated temperatures. Each of them is estimated to diverge from their close non-thermophilic relatives over 30 Mya.

Some genera have optimum and maximum growth temperatures over a relatively large temperature range. One example is the genus *Trichocladium*. *Trichocladium antarcticum* was reported to have optimal growth temperature at about 15 °C (Stchigel *et al.* 2003), and the optimal growth temperature of *Tri. acropullum* is between 25–28 °C (maximum growth temperature at 32 °C) (Wang & Zheng 2005). In contrast, *Tri. seminis-citrulli* has an optimal growth temperature of about 30 °C and a maximum growth temperature at 40 °C (Millner 1977). Another example is *Collariella*, in which *Col. quadrangulata* has an optimal growth temperature at about 25 °C and maximum growth temperature at 37–38 °C, while *Col. causiiformis* and *Col. gracilis* have an optimal growth temperature around 35–40 °C and maximum growth temperature between 45 and 50 °C (Millner 1977). This suggests that species with psychrophilic, mesophilic and even thermotolerant habits in a certain genus have diverged rather recently.

A few species which can grow at 37 °C have been reported as causal agents of systemic and deep infections in humans, such as *Achaetomium strumarium* (= *Chaetomium atrobrunneum*, Abbott *et al.* 1995), *Amesia atrobrunnea* (= *Chaetomium atrobrunneum*, Abbott *et al.* 1995) and *Parachaetomium perlucidum* (= *Chaetomium perlucidum*, Barron *et al.* 2003). To our knowledge, no thermophilic species in *Chaetomiaceae* have been reported to infect humans although some of them can also grow well at 37 °C. More work is required to determine the cardinal growth temperature of each *Chaetomiaceae* species, and to clarify the correlations between cardinal growth temperatures, infection potential in humans and the ability to produce useful enzymes for industry.

ACKNOWLEDGEMENTS

This study was financially supported by the National Natural Science Foundation of China (NSFC, Project No. 32070014). The authors are grateful to the CBS culture collection at the Westerdijk Fungal Biodiversity Institute, the curator Gerard Verkleij and the technical staff Yda Vlug, Trix Merkx, Diana Vos and Arien van Iperen for their kind help in providing strains from the culture collection, preparing cultures and in the deposit of fungarium material. The authors acknowledge prof. dr Keith Seifert for his kind help in the study of asexual morphs of *Chaetomiaceae*. The first author would like to thank Dr Ewald Groenewald for his valuable comments on this study.

DECLARATION ON CONFLICT OF INTEREST

The authors declare that there is no conflict of interest.

REFERENCES

Abbott SP, Sigler L, McAleer R, *et al.* (1995). Fatal cerebral mycoses caused by the ascomycete *Chaetomium strumarium*. *Journal of Clinical Microbiology* **33**: 2692–2698.

Abdel-Azeem AM (2020). *Recent developments on genus Chaetomium*. Springer International Publishing, Cham.

Aghyl H, Mehdi Mehrabi-Koushki M, Esfandiari M (2021). *Chaetomium iranicum* and *Collariella capillicompacta spp. nov.* and notes to new hosts of *Amesia* species in Iran. *Sydowia* **73**: 21–30.

Ahmed A, Adelmann D, Fahal A, *et al.* (2002). Environmental occurrence of *Madurella mycetomatis*, the major agent of human eumycetoma in Sudan. *Journal of Clinical Microbiology* **40**: 1031–1036.

Ahmed SA, Khan Z, Wang XW, *et al.* (2016). Chaetomium-like fungi causing opportunistic infections in humans: a possible role for extremotolerance. *Fungal Diversity* **76**: 11–26.

Al-Aidaroos A, Bin-Hussain I, Solh HE*, et al.* (2007). Invasive *Chaetomium* infection in two immunocompromised pediatric patients. *The Pediatric Infectious Disease Journal* **26**: 456–458.

Alidadi A, Vala SA, Jouzani GS (2020). *Botryotrichum iranicum sp. nov.* and *Trematosphaeria magenta sp. nov.* as two new species from Iran. *Mycological Progress* **19**: 1575–1586.

Ames LM (1963). A Monograph of the *Chaetomiaceae*. *Research and Development Service of U. S. Army.*

Apinis AE (1962). Occurrence of thermophilous microfungi in certain alluvial soils near Nottingham. *Nova Hedwigia*. **5**: 57–78.

Asgari B, Zare R (2011). The genus *Chaetomium* in Iran, a phylogenetic study including six new species. *Mycologia* **103**: 863–882.

Bainier G. 1910. Monographie des *Chaetomidium* et des *Chaetomium*. *Bulletin de la Société Mycologique de France* **25**: 191–237.

Barron MA, Sutton DA, Veve R, *et al.* (2003). Invasive mycotic infections caused by *Chaetomium perlucidum*, a new agent of cerebral phaeohyphomycosis. *Journal of Clinical Microbiology* **41**: 5302–5307.

Berka RM, Grigoriev IV, Otillar R, *et al.* (2011). Comparative genomic analysis of the thermophilic biomass-degrading fungi *Myceliophthora thermophila* and *Thielavia terrestris*. *Nature Biotechnology* **29**: 922–927.

Betancourt O, Zaror L, Senn C (2013). Isolation of filamentous fungi from haircoat cats without skin lesions in temuco, Chile. *Revista Cientifica de la Facultad de Ciencias Veterinarias de la Universidad del Zulia* **23**: 380–387.

Bissett J, Gams W, Jaklitsch W*, et al.* (2015). Accepted *Trichoderma* names in the year 2015. *IMA Fungus* **6**: 263–295.

Booth C (1961). Studies of *Pyrenomycetes*. VI *Thielavia*. With notes on some allied genera. *Mycological Papers* **83**: 1–15.

Bouckaert R, Vaughan TG, Barido-Sottani J, *et al.* (2019). BEAST 2.5: an advanced software platform for Bayesian evolutionary analysis. *PLOS Computational Biology* **15**: e1006650.

Bourguignon T, Lo N, Cameron SL, *et al.* (2014). The Evolutionary History of Termites as Inferred from 66 Mitochondrial Genomes. *Molecular Biology and Evolution* **32**: 406–421.

Cannon PF (1986). A revision of *Achaetomium*, *Achaetomiella*, and *Subramaniula*, and some silimar species of *Chaetomium*. *Transactions of the British Mycological Society* **87**: 45–76.

Carmichael JW (1962). *Chrysosporium* and some other aleuriosporic hyphomycetes. *Canadian Journal of Botany* **40**: 1137–1173.

Carter A, Khan RS (1982). New and interesting *Chaetomium* species from East Africa. *Canadian Journal of Botany* **60**: 1253–1262.

Chen L, Qiu Q, Jiang Y, *et al.* (2019). Large-scale ruminant genome sequencing provides insights into their evolution and distinct traits. *Science* **364**: eaav6202.

Chivers AH (1915). A monograph of the genera *Chaetomium* and *Ascotricha*. *Memoirs of the Torrey Botanical Club* **14**: 155–240.

Cooney DG, Emerson R (1964). *Thermophilic Fungi*: *an account of their biology, activities and classification*. W.H. Freeman and Co., San Francisco, London

Corda ACJ (1840). Icones fungorum hucusque cognitorum. **4**: 1–53.

Costantin J (1892). Sur quelques maladies du blanc de Champignon. *Comptes Rendues des Séances Hebdomadaires de l'Académie des Sciences Paris* **114**: 849–851.

Crous PW, Carnegie AJ, Wingfield MJ, *et al.* (2019). Fungal Planet description sheets: 868–950. *Persoonia* **42**: 291–473.

Crous PW, Lombard L, Sandoval-Denis M, *et al.* (2021). *Fusarium*: more than a node or a foot-shaped basal cell. *Studies in Mycology* **98**: 100116: 1–184.

Crous PW, Wingfield MJ, Burgess TI, *et al.* (2017). Fungal Planet description sheets: 625–715. *Persoonia* **39**: 270–467.

Crous PW, Wingfield MJ, Burgess TI, *et al.* (2018). Fungal Planet description sheets: 716–784. *Persoonia* **40**: 240–393.

Crous PW, Wingfield MJ, Richardson DM, *et al.* (2016). Fungal Planet description sheets: 400–468. *Persoonia* **36**: 316–458.

Cunningham CW (1997). Can three incongruency tests predict when data should be combined? *Molecular Biology and Evolution* **14**: 733–740.

Daniels J (1961). *Chaetomium piluliferum sp. nov.*, the perfect state of *Botryotrichum piluliferum*. *Transactions of the British Mycological Society* **44**: 79–86.

de Hoog GS, Adelmann D, Ahmed AOA, *et al.* (2004). Phylogeny and typification of *Madurella mycetomatis*, with a comparison of other agents of eumycetoma. *Mycoses*. **47**: 121–130.

de Hoog GS, Gerrits van den Ende AHG (1998). Molecular diagnostics of clinical strains of filamentous Basidiomycetes. *Mycosis* **41**: 183–189.

de Oliveira TB, Gomes E, Rodrigues A (2015). Thermophilic fungi in the new age of fungal taxonomy. *Extremophiles* **19**: 31–37.

dos Reis M, Donoghue PCJ, Yang ZH (2015). Bayesian molecular clock dating of species divergences in the genomics era. *Nature Reviews Genetics* **17**: 71-80.

Fergus CL, Sinden JW (1969). A new thermophilic fungus from mushroom compost: *Thielavia thermophila spec. nov. Canadian Journal of Botany*. **47**: 1635–1637.

Fergus CL (1971). The temperature relationships and thermal resistance of a new thermophilic *Papulaspora* from mushroom compost. *Mycologia* **63**: 426–431.

Fries EM (1823). *Systema mycologicum*, vol 2. Officina Berlingiana, Lundae.

Gao WX, He Y, Li FL, *et al.* (2019). Antibacterial activity against drug-resistant microbial pathogens of cytochalasan alkaloids from the arthropod-associated fungus *Chaetomium globosum* TW1-1. *Bioorganic Chemistry* **83**: 98–104.

Glass NL, Schmoll M, Cate JHD, *et al.* (2013). Plant cell wall deconstruction by ascomycete fungi. *Annual Review of Microbiology* **67**: 477–98.

Gond SK, Mishra A, Sharma VK, *et al.* (2012). Diversity and antimicrobial activity of endophytic fungi isolated from *Nyctanthes arbor-tristis*, a well-known medicinal plant of India. *Mycoscience* **53**: 113–121.

Greathouse GA, Ames LM (1945). Fabric deterioration by thirteen described and three new species of *Chaetomium*. *Mycologia* **37**: 138–155.

Greif MD, Currah RS (2007). Development and dehiscence of the

cephalothecoid peridium in *Aporothielavia leptoderma* shows it belongs in *Chaetomidium*. *Mycological Research* **111**: 70–77.
Greif MD, Stchigel AM, Huhndorf SM (2009). A re-evaluation of genus *Chaetomidium* based on molecular and morphological characters. *Mycologia* **101**: 554–564.
Guarro J, Abdullah SK, Al-Bader SM, *et al.* (1996). The genus *Melanocarpus*. *Mycological Research* **100**: 75–78.
Guarro J, Al-Saadoon AH, Gene J, *et al.* (1997). Two new cleistothecial *Ascomycetes* from Iraq. *Mycologia* **89**: 955–961.
Guppy KH, Thomas C, Thomas K, *et al.* (1998). Cerebral fungal infections in the immunocompromised host: a literature review and a new pathogen – *Chaetomium atrobrunneum*: case report. *Neurosurgery* **43**: 1463–1469.
Guterres DC, Galvão-Elias S, de Souza BCP, *et al.* (2018). Taxonomy, phylogeny, and divergence time estimation for *Apiosphaeria guaranitica*, a Neotropical parasite on bignoniaceous hosts. *Mycologia* **110**: 526–545.
Gutierrez RMP, Gonzalez AMN, Ramirez AM (2012). Compounds derived from endophytes: a review of phytochemistry and pharmacology. *Current Medicinal Chemistry* **19**: 2992–3030.
Haki GD, Rakshit SK (2003). Developments in industrially important thermostable enzymes: a review. *Bioresource Technology* **89**: 17–34.
Harreither W, Sygmund C, Augustin M, *et al.* (2011). Catalytic properties and classification of cellobiose dehydrogenases from ascomycetes. *Applied and Environmental Microbiology* **77**: 1804–1815.
Hawksworth DL (1971). A revision of the genus *Ascotricha* Berk. *Mycological Papers* **126**: 1–28.
He MQ, Zhao RL, Hyde KD, *et al.* (2019). Notes, outline and divergence times of *Basidiomycota*. *Fungal Diversity* **99**: 105–367.
Ho SYW (2020). The Molecular Evolutionary Clock: Theory and Practice. Springer, Cham, Switzerland.
Hubka V, Mencl K, Skorepova M, *et al.* (2011). Phaeohyphomycosis and onychomycosis due to *Chaetomium* spp., including the first report of *Chaetomium brasiliense* infection. *Medical Mycology* **49**: 724–733.
Hu Y, Zhang WP, Zhang P, *et al.* (2013). Nematicidal activity of chaetoglobosin A produced by *Chaetomium globosum* NK102 against *Meloidogyne incognita*. *Journal of Agricultural and Food Chemistry* **61**: 41–46.
Hyde KD, Maharachchikumbura SSN, Hongsanan S, *et al.* (2017). The ranking of fungi: a tribute to David L. Hawksworth on his 70th birthday. *Fungal Diversity* **84**: 1–23.
Ito T, Nakagiri A (1994). *Stellatospora*, a new genus of the *Sordariaceae*. *Mycoscience* **35**: 413–415.
Kapoor JN, Lal SP (1982). A new species of *Botryoderma* from India. *Indian Phytopathology* **35**: 732–733.
Kawato M, Shinobu R (1959). On *Streptomyces herbaricolor*, *nov. sp.*, supplement: a simple technique for the microscopic observation. Memoirs of Osaka University of the Liberal Arts and Education. Series B. *Natural Sciences* **8**: 114–119.
Kharwar RN, Mishra A, Gond SK, *et al.* (2011). Anticancer compounds derived from fungal endophytes: their importance and future challenges. *Natural Product Reports* **28**: 1208–1228.
Kirk PM, Cannon PF, Minter DW, *et al.* (2008). *Ainsworth & Bisby's Dictionary of the Fungi*, 10th ed. CABI, UK.
Koukol O (2016). *Myriococcum* revisited: a revision of an overlooked fungal genus. *Plant Systematics and Evolution* **302**: 957–969.
Kunze G, Schmidt JK (1817). *Mykologische Hefte* **1**: 1–109. Leipzig, Germany.
Lang J, Hu J, Ran W, *et al.* (2012). Control of cotton *Verticillium* wilt and fungal diversity of rhizosphere soils by bio-organic fertilizer. *Biology and Fertility of Soils* **48**: 191–203.
Larran S, Simón MR, Moreno MV, *et al.* (2016). Endophytes from wheat as biocontrol agents against tan spot disease. *Biological Control* **92**: 17–23.
La Touche CJ (1950). On a thermophile species of *Chaetomium*. *Transactions of the British Mycological Society* **33**: 95–104.
Li GJ, Hyde HD, Zhao RL, *et al.* (2016). Fungal diversity notes 253–366: taxonomic and phylogenetic contributions to fungal taxa. *Fungal diversity* **78**: 1–237.
Liu YJJ, Whelen S, Benjamin DH (1999). Phylogenetic relationships among ascomycetes: evidence from an RNA polymerase II subunit. *Molecular Biology and Evolution* **16**: 1799–1808
Lopez SE, Nelson EE, Thies WG (1995). A new species of *Botryoderma* and other hyphomycetes isolated from roots of fumigated and nonfumigated Douglas-fir stumps in Oregon. *Mycotaxon* **55**: 269–274.
Luo ZL, Hyde KD, Liu JK, *et al.* (2019). Freshwater *Sordariomycetes*. *Fungal Diversity* **99**: 451–660.
Malloch D, Cain RF (1973). The genus *Thielavia*. *Mycologia* **65**: 1055–1077.
Marchal E (1885). Champignons coprophiles de Belgique. *Bulletin de la Société Royale de Botanique de Belgique* **24**: 57–77.
Margaritis A, Merchant RFJ, Yaguchi M (1986). Thermostable cellulases from thermophilic microorganisms. *Critical Reviews in Biotechnology* **4**: 327–367.
Marín-Felix Y, Groenewald JZ, Cai L, *et al.* (2017). Genera of phytopathogenic fungi: GOPHY1. *Studies in Mycology* **86**: 99–216.
Marín-Felix Y, Stchigel AM, Miller AN, *et al.* (2015). A re-evaluation of the genus *Myceliophthora* (*Sordariales*, *Ascomycota*): its segregation into four genera and description of *Corynascus fumimontanus sp. nov.* *Mycologia* **107**: 619–632.
Masclaux F, Guého E, de Hoog GS, *et al.* (1995). Phylogenetic relationships of human-pathogenic *Cladosporium* (*Xylohypha*) species inferred from partial LS rRNA sequences. *Journal of Medical and Veterinary Mycology* **33**: 327–338.
Mehrabi M, Asgari B, Zare R (2020). Description of *Allocanariomyces* and *Parachaetomium*, two new genera, and *Achaetomium aegilopis sp. nov.* in the *Chaetomiaceae*. *Mycological Progress* **19**: 1415–1427.
Miller AN, Huhndorf SM (2005). Multi-gene phylogenies indicate ascomal wall morphology is a better predictor of phylogenetic relationships than ascospore morphology in the *Sordariales* (*Ascomycota*, Fungi). *Molecular Phylogenetics and Evolution* **35**: 60–75.
Millner PD (1977). Radial growth responses to temperature by 58 *Chaetomium* species, and some taxonomic relationships. *Mycologia* **69**: 492–502.
Morgenstern I, Powlowski J, Ishmael N, *et al.* (2012). A molecular phylogeny of thermophilic fungi. *Fungal Biology* **116**: 489–502.
Natvig DO, Taylor JW, Tsang A, *et al.* (2015). *Mycothermus thermophilus gen. et comb. nov.*, a new home for the itinerant thermophile *Scytalidium thermophilum* (*Torula thermophila*). *Mycologia* **107**: 319–327.
Nilsson RH, Ryberg M, Kristiansson E, *et al.* (2006). Taxonomic reliability of DNA sequences in public sequence databases: a fungal perspective. *PLoS ONE* **1**: e59.
Noumeur SR, Teponno RB, Helaly SE (2020). Diketopiperazines from *Batnamyces globulariicola*, *gen. & sp. nov.* (*Chaetomiaceae*), a fungus associated with roots of the medicinal plant *Globularia alypum* in Algeria. *Mycological Progress* **19**: 589–603.
Nugent LK, Sangvichen E, Sihanonth P, *et al.* (2006). A revised method for the observation of conidiogenous structures in fungi. *Mycologist* **20**: 111–114.
Nylander JAA (2004). *MrModeltest v. 2.* Programme distributed by the author. Evolutionary Biology Centre, Uppsala University.
O'Donnell K (1993). *Fusarium* and its near relatives. In: *The Fungal Holomorph*: *mitotic, meiotic and pleomorphic speciation in fungal systematics* (Reynolds D & Taylor JW, eds). CAB International, Wallingford: 225–233.
O'Donnell K, Cigelnik E (1997). Two divergent intragenomic rDNA ITS2 types within a monophyletic lineage of the fungus *Fusarium* are nonorthologous. *Molecular Phylogenetics and Evolution* **7**: 103–116.
Papendorf MC, Upadhyay HP (1969). *Botryoderma lateritium* and *B. rostratum gen. et spp. nov.* from soil in South Africa and Brazil. *Transactions of the British Mycological Society* **52**: 257–265.
Píchová K, Pažoutová S, Martin Kostovčík M, *et al.* (2018). Evolutionary history of ergot with a new infrageneric classification (*Hypocreales*: *Clavicipitaceae*: *Claviceps*). *Molecular Phylogenetics and Evolution* **123**: 73–87.
Qiao M, Zhang Z, Yang LY, *et al.* (2021). *Staphylotrichum sinense sp. nov.*, a new hyphomycete (*Chaetomiaceae*) from China. *International Journal of Systematic and Evolutionary Microbiology* **71**: 1–8.

Rambaut A (2009). *FigTree v. 1.3.1.* Computer program and documentation distributed by the author at http://tree.bio.ed.ac.uk/software/.

Rank C, Nielsen KF, Larsen TO, *et al.* (2011). Distribution of sterigmatocystin in filamentous fungi. *Fungal Biology* **115**: 406–420.

Raza M, Zhang ZF, Hyde KD, *et al.* (2019). Culturable plant pathogenic fungi associated with sugarcane in southern China. *Fungal Diversity* **99**: 1–104.

Riddell RW (1950). Permanent stained mycological preparations obtained by slide culture. *Mycologia* **42**: 265–270.

Rodríguez K, Stchigel A, Guarro J (2002). Three new species of *Chaetomium* from soil. *Mycologia* **94**: 116–126.

Ryan K, Cañete-Gibas C, Sanders C, *et al.* (2021). *Pseudocanariomyces americanus*, *gen. nov., sp. nov.*, a new thielavia-like species in the *Chaetomiaceae*: identification and management of a prosthetic hip infection. *Mycopathologia* **186**: 441–447.

Saccardo PA (1886). *Sylloge Fungorum* **4**: 1–807.

Safi A, Mehrabi-Koushki M, Farokhinejad R (2020). *Amesia khuzestanica* and *Curvularia iranica spp. nov.* from Iran. *Mycological Progress* **19**: 935–945.

Samarakoon MC, Hyde KD, Hongsanan S, *et al.* (2019). Divergence time calibrations for ancient lineages of *Ascomycota* classification based on a modern review of estimations. *Fungal Diversity* **96**: 285–346.

Samson RA, Houbraken J, Thrane U, *et al.* (2019). *Food and Indoor Fungi.* 2nd Ed. Westerdijk Laboratory Manual series 2. Westerdijk Fungal Biodiversity Institute, Utrecht, The Netherlands.

Samson RA, Visagie CM, Houbraken J, *et al.* (2014). Phylogeny, identification and nomenclature of the genus *Aspergillus*. *Studies in Mycology* **78**: 141–173.

Schoch CL, Seifert KA, Huhndorf S, *et al.* (2012). Nuclear ribosomal internal transcribed spacer (ITS) region as a universal DNA barcode marker for fungi. *Proceedings of the National Academy of Sciences of the United States of America* **109**: 6241–6246.

Schultes NP, Strzalkowski N, Li DW, *et al.* (2019). *Botryotrichum domesticum sp. nov.*, a new hyphomycete from an indoor environment. *Botany* **97**: 311–319.

Seifert K, Morgan-Jones G, Gams W, *et al.* (2011). *The genera of Hyphomycetes*. CBS Biodiversity series 9. Westerdijk Fungal Biodiversity Institute, Utrecht, The Netherlands.

Selim KA, El-Beih AA, Abdel-Rahman TM, *et al.* (2014). Biological evaluation of endophytic fungus, *Chaetomium globosum* J N711454, as potential candidate for improving drug discovery. *Cell Biochemistry and Biophysics* **68**: 67–82.

Sergejeva KS (1961). Species novae generis *Chaetomium* III. *Notulae Systematicae e Sectione Cryptogamica Instituti Botanici Komarovii Academiae Scientiarum U.R.S.S.* **14**: 139–150.

Seth HK (1968). *Chaetomidium trichorobustum sp. nov.* from Germany. *Nova Hedwigia* **16**: 429–432.

Singh B. (2016). *Myceliophthora thermophila* syn. *Sporotrichum thermophile*: a thermophilic mould of biotechnological potential. *Critical Reviews in Biotechnology* **36**: 59–69.

Sousa TF, Santos AO, Silva FMA, *et al.* (2020). *Arcopilus amazonicus* (*Chaetomiaceae*), a new fungal species from the Amazon rainforest native plant *Paullinia cupana*. *Phytotaxa* **456**: 145–156.

Stchigel AM, Guarro J, Cormack WM (2003). *Apiosordaria antarctica* and *Thielavia antarctica*, two new ascomycetes from Antarctica. *Mycologia* **95**: 1218–1226.

Stchigel AM, Sagués M, Cano J, *et al.* (2000). Three new thermotolerant species of *Corynascus* from soil, with a key to the known species. *Mycological Research* **104**: 879–887.

Steenwyk JL, Shen XX, Lind AL, *et al.* (2019). A robust phylogenomic time tree for biotechnologically and medically important fungi in the genera *Aspergillus* and *Penicillium*. *mBio* **10**: e00925-19.

Straatsma G, Samson RA, Olijnsma TW, *et al.* (1994). Ecology of thermophilic fungi in mushroom compost, with emphasis on *Scytalidium thermophilum* and growth stimulation of *Agaricus bisporus* mycelium. *Applied and Environmental Microbiology* **60**: 454–458.

Sung GH, Sung JM, Hywel-Jones NL, *et al.* (2007). A multi-gene phylogeny of *Clavicipitaceae* (*Ascomycota*, Fungi): identification of localized incongruence using a combinational bootstrap approach. *Molecular Phylogenetics and Evolution* **44**: 1204–1223.

Tamura K, Stecher G, Peterson D, *et al.* (2013). MEGA6: molecular evolutionary genetics analysis version 6.0. *Molecular Biology and Evolution* **30**: 2725–2729.

Tansey MR, Jack MA (1975). *Thielavia australiensis sp. nov.*, a new thermophilic fungus from incubator-bird (mallee fowl) nesting material. *Canadian Journal of Botany* **53**: 81–83.

Tekpinar AD, Kalmer A (2019). Utility of various molecular markers in fungal identification and phylogeny. *Nova Hedwigia* **109**: 87–224.

Tiscornia S, Seguí C, Bettucci L (2009). Composition and characterization of fungal communities from different composted materials. *Cryptogamie, Mycologie* **30**: 363–376.

Udagawa SI, Ueda S (1979). *Corynascella inquinata*, a new cleistothecial ascomycete from sewage sludge. *Mycotaxon* **8**: 292–296.

Udagawa S (1980). New or noteworthy ascomycetes from Southeast Asian soil. I. *Transactions of the Mycological Society of Japan* **21**: 17–34.

Udagawa S, Muroi T (1981). Notes on some Japanese Ascomycetes XVI. *Transactions of the Mycological Society of Japan* **22**: 11–26.

van den Brink J, Facun K, de Vries M, *et al.* (2015). Thermophilic growth and enzymatic thermostability are polyphyletic traits within *Chaetomiaceae*. *Fungal Biology* **119**: 1255–1266.

van den Brink J, Samson RA, Hagen F, *et al.* (2012). Phylogeny of the industrial relevant, thermophilic genera *Myceliophthora* and *Corynascus*. *Fungal Diversity* **52**: 197–207.

van der Aa HA (1973). Progress report. *Verhandelingen der Koninklijke Nederlandsche Akademie van Wetenschappen Afdeeling Natuurkunde, Sectie 2* **61**: 60–61.

van Oorschot CAN (1977). The genus *Myceliophthora*. *Persoonia* **9**: 401–408.

van Oorschot CAN (1980). A revision of *Chrysosporium* and allied genera. *Studies in Mycology* **20**: 1–89.

Varga T, Krizsán K, Földi C, *et al.* (2019). Megaphylogeny resolves global patterns of mushroom evolution. *Nature Ecology & evolution* **3**: 668–678.

Viikari L, Alapuranen M, Puranen T, *et al.* (2007). Thermostable enzymes in lignocellulose hydrolysis. *Advances in Biochemical Engineering Biotechnology* **108**: 121–145.

Vilgalys R, Hester M (1990). Rapid genetic identification and mapping of enzymatically amplified ribosomal DNA from several *Cryptococcus* species. *Journal of Bacteriology* **172**: 4238–4246.

Vilgalys R, Sun BL (1994). Ancient and recent patterns of geographic speciation in the oyster mushroom *Pleurotus* revealed by phylogenetic analysis of ribosomal DNA sequences. *Proceedings of the National Academy of Sciences of the United States of America* **91**: 4599–4603.

Visagie CM, Houbraken J, Frisvad JC, *et al.* (2014). Identification and nomenclature of the genus *Penicillium*. *Studies in Mycology* **78**: 343–371.

Vivi VK, Martins-Franchetti SM, Attili-Angelis D (2019). Biodegradation of PCL and PVC: *Chaetomium globosum* (ATCC 16021) activity. *Folia Microbiologica* **64**:1–7.

von Arx JA (1970). *The Genera of Fungi Sporulating in Pure Culture.* Lehre: J. Cramer.

von Arx JA (1973a). Further observations on *Sporotrichum* and some similar fungi. *Persoonia* **7**: 127–130.

von Arx JA (1973b). Ostiolate and nonostiolate pyrenomycetes. *Proceedings Proceedings, Koninklijke Nederlandse Akademie van Wetenschappen, Series C, Biological and Medical Sciences* **76**: 289–296.

von Arx JA (1975a). On *Thielavia* and some similar genera of ascomycetes. *Studies in Mycology* **8**: 1–32.

von Arx JA (1975b). On *Thielavia angulata* and some recently described *Thielavia* species. *Kavaka* **3**: 33–36.

von Arx JA (1985). On *Achaetomium* and a new genus *Subramaniula*. *Proceedings of the Indian Academy of Science (Plant Science)* **94**: 341–345.

von Arx JA, Figueras MJ, Guarro J (1988). Sordariaceous ascomycetes without ascospore ejaculation. *Beihefte zur Nova Hedwigia* **94**: 1–104.

von Arx JA, Guarro J, Figueras MJ (1986). The Ascomycete genus *Chaetomium*. *Beihefte zur Nova Hedwigia* **84**: 1–162.

von Klopotek A (1974). Revision der thermophilen *Sporotrichum*-Arten: *Chrysosporium thermophilum* (Apinis) *comb. nov.* Und *Chrysosporium fergusii spec. nov.* = status conidialis von *Corynascus thermophilus* (Fergus und Sinden) *comb. nov. Archiv für Mikrobiologie* **98**: 365–369.

von Klopotek A (1976). *Thielavia heterothallica spec. nov.,* die perfekte Form von *Chrysosporium thermophilum*. *Archives of Microbiology* **107**: 223–224.

Wang FQ, Jiang J, Hu S, *et al.* (2017). Secondary metabolites from endophytic fungus *Chaetomium* sp. induce colon cancer cell apoptotic death. *Fitoterapia* **121**: 86–93.

Wang XH, Halling RE, Hofstetter V, *et al.* (2018). Phylogeny, biogeography and taxonomic reassessment of *Multifurca* (*Russulaceae*, *Russulales*) using three-locus data. *PLoS ONE* **13**: e0205840.

Wang XW, Bai FY, Bensch K, *et al.* (2019b). Phylogenetic re-evaluation of *Thielavia* with the introduction of a new family *Podosporaceae*. *Studies in Mycology* **93**: 155–252.

Wang XW, Houbraken J, Groenewald JZ, *et al.* (2016b). Diversity and taxonomy of *Chaetomium* and chaetomium-like fungi from indoor environments. *Studies in Mycology* **84**: 145–224.

Wang XW, Lombard L, Groenewald JZ, *et al.* (2016a). Phylogenetic reassessment of the *Chaetomium globosum* species complex. *Persoonia* **36**: 83–133.

Wang XW, Wang XL, Fu-Jiang Liu FJ, *et al.* (2014). Phylogenetic assessment of *Chaetomium indicum* and allied species, with the introduction of three new species and epitypification of *C. funicola* and *C. indicum*. *Mycological Progress* **13**: 719–732.

Wang XW, Yang FY, Meijer M, *et al.* (2019a). Redefining *Humicola sensu stricto* and related genera in the *Chaetomiaceae*. *Studies in Mycology* **93**: 65–153.

Wang XW, Zheng RY (2005). *Chaetomium acropullum sp. nov.* (*Chaetomiaceae*, *Ascomycota*), a new psychrotolerant mesophilic species from China. *Nova Hedwigia* **80**: 413–418.

Wang Y, Youssef NH, Couger MB, *et al.* (2019c). Molecular dating of the emergence of anaerobic rumen fungi and the impact of laterally acquired genes. *mSystems* **4**: e00247-19.

White TJ, Bruns TD, Lee S, *et al*. (1990). Amplification and direct sequencing of fungal ribosomal RNA genes for phylogenetics. In: *PCR Protocols*: *A Guide to Methods and Applications* (Innis MA & Gelfand DH, eds). Academic Press, London: 315–322.

Winter G (1885). Ascomyceten: Gymnoasceen und Pyrenomyceten. *Dr. L. Rabenhorst's Kryptogamen Flora von Deutschland, Oesterreich und der Schweiz. Zweite Auflage* **1(2)**: i–viii: 1–928.

Woudenberg JH, Aveskamp MM, de Gruyter J, *et al*. (2009). Multiple *Didymella* teleomorphs are linked to the *Phoma clematidina* morphotype. *Persoonia* **22**: 56–62.

Yadav M, Singh A, Balan V, *et al.* (2019). Biological treatment of lignocellulosic biomass by *Chaetomium globosporum*: process derivation and improved biogas production. *International Journal of Biological Macromolecules* **128**: 176–183.

Yang CH, Lin MJ, Su HJ, *et al.* (2014a). Multiple resistance-activating substances produced by *Humicola phialophoroides* isolated from soil for control of *Phytophthora* blight of pepper. *Botanical Studies* **55**: 40.

Yang X, Shi P, Huang H, *et al.* (2014b). Two xylose-tolerant GH43 bifunctional β-xylosidase/α-arabinosidases and one GH11 xylanase from *Humicola insolens* and their synergy in the degradation of xylan. *Food Chemistry* **148**: 381–387.

Yilmaz N, Visagie CM, Houbraken J, *et al.* (2014). Polyphasic taxonomy of the genus *Talaromyces*. *Studies in Mycology* **78**: 175–341.

Yule GU (1925). A Mathematical theory of evolution, based on the conclusions of Dr. J. C. Willis, F.R.S. *Philosophical Transactions of the Royal Society B* **213**: 21–87.

Zanne AE, Tank DC, Cornwell WK, *et al.* (2014). Three keys to the radiation of angiosperms into freezing environments. *Nature* **506**: 89–92.

Zhang Q, Li HQ, Zong SC, *et al.* (2012). Chemical and bioactive diversities of the genus *Chaetomium* secondary metabolites. *Mini-Reviews in Medicinal Chemistry* **12**: 127–148.

Zhang Y, Wu W, Cai L (2017b). Polyphasic characterisation of *Chaetomium* species from soil and compost revealed high number of undescribed species. *Fungal Biology* **121**: 21–43.

Zhang Y, Wu WP, Dian MH, *et al.* (2014a). A new thermophilic species of *Myceliophthora* from China. *Mycological Progress* **13**: 165–170.

Zhang QH, Zhang J, Yang L, *et al.* (2014b). Diversity and biocontrol potential of endophytic fungi in *Brassica napus*. *Biological Control* **72**: 98–108.

Zhang ZF, Liu F, Zhou X, *et al*. (2017a). Culturable mycobiota from Karst caves in China, with descriptions of 20 new species. *Persoonia* **39**: 1–31.

Zhang ZF, Zhao P, Cai L (2018). Origin of cave fungi. *Frontiers in Microbiology* **9**: 1407.

Zhao RL, Li GJ, Sánchez-Ramírez S, *et al.* (2017). A six-gene phylogenetic overview of *Basidiomycota* and allied phyla with estimated divergence times of higher taxa and a phyloproteomics perspective. *Fungal Diversity* **84**: 43–74.

Zhu L, Song J, Zhou JL, *et al.* (2019) Species diversity, phylogeny, divergence time, and biogeography of the genus *Sanghuangporus* (*Basidiomycota*). *Frontiers in Microbiology* **10**: 812.

Zopf W (1881). Zur Entwicklungsgeschichte der Ascomyceten: *Chaetomium*. *Nova Acta Academiae Caesareae Leopoldino-Carolinae Germanicae Naturae Curiosorum* **42**: 199–292.

Zuckerkandl E, Pauling L (1965). Evolutionary divergence and convergence in proteins. In: *Evolving genes and proteins* (Bryson V, Vogel HJ, eds). Academic Press INC, USA: 97–166.

Supplementary Material: https://studiesinmycology.org/

Fig. S1. Phylogenetic tree resulting from ML analysis of the ITS gene region alignment. The confidence values are indicated at the nodes in the same way as in Fig. 7. Genus clades are discriminated with boxes in different colours and clades containing thermophilic species are highlighted with an orange background. The scale bar shows the expected number of changes per site. The tree is rooted with *Pseudoechria longicollis* and *Schizotheciaceae*, in the *Schizotheciaceae.*

Fig. S2. Phylogenetic tree resulting from ML analysis of the partial *tub2* gene region alignment. The confidence values are indicated at the nodes in the same way as in Fig. 7. Genus clades are discriminated with boxes in different colours and clades containing thermophilic species are highlighted with an orange background. The scale bar shows the expected number of changes per site. The tree is rooted with *Pseudoechria longicollis* and *Schizotheciaceae*, in the *Schizotheciaceae*, *Sordariales*.

Fig. S3. Phylogenetic tree resulting from ML analysis of the partial *rpb2* gene region alignment. The confidence values are indicated at the nodes in the same way as in Fig. 7. Genus clades are discriminated with boxes in different colours and clades containing thermophilic species are highlighted with an orange background. The scale bar shows the expected number of changes per site. The tree is rooted with *Pseudoechria longicollis* and *Pseudoechria prolifica*, in the *Schizotheciaceae*.

Fig. S4. Phylogenetic location of "*Humicola koreana*" based on the separate analyses of partial gene sequences of ITS (A) and LSU (B). The confidence values are indicated at the nodes in the same way as in Fig. 7. The scale bar shows the expected number of changes per site. The tree is rooted with *Achaetomium strumarium*.

Table S1. Comparison ascospore sizes measured in lactic acid (present study) and water (literature) as mounting medium.

Table S2. Overview species and strains used in phylogenetic analysis.

Studies in Mycology 101: 245–286 (2022).

Multi-locus phylogeny unmasks hidden species within the specialised spider-parasitic fungus, *Gibellula* (*Hypocreales, Cordycipitaceae*) in Thailand

W. Kuephadungphan[1], B. Petcharad[2], K. Tasanathai[1], D. Thanakitpipattana[1], N. Kobmoo[1], A. Khonsanit[1], R.A. Samson[3], J.J. Luangsa-ard[1*]

[1]*National Center for Genetic Engineering and Biotechnology (BIOTEC), 113 Thailand Science Park, Phahonyothin Road, Khlong Nueng, Khlong Luang, Pathum Thani 12120 Thailand;* [2]*Department of Biotechnology, Faculty of Science and Technology, Thammasat University, Pathum Thani 12120 Thailand;* [3]*Westerdijk Fungal Biodiversity Institute, Uppsalalaan 8, Utrecht, NL-3584 CT, The Netherlands*

**Corresponding author*: J.J. Luangsa-ard, jajen@biotec.or.th

Abstract: Over 80 species of hypocrealean fungi are reported as pathogens of spiders and harvestmen. Among these fungi, the genus *Gibellula* is highly regarded as a specialised spider-killer that has never been reported to infect other arthropods. While more than 20 species of *Gibellula* are known, few attempts to identify the infected spiders have been made despite the fact that the host specificity can help identify the fungal species. Here, we morphologically describe and illustrate eight new species of *Gibellula* and three new records from Thailand of known species along with the multi-gene phylogeny that clearly showed the segregation among the proposed species. Examination of the *Gibellula*-infected spider hosts identified *Oxyopidae*, *Uloboridae* and, for the first time, the ant-mimicking genus *Myrmarachne*.

Key words: araneogenous fungus, *Gibellula,* new taxa, spider predator.
Taxonomic novelties: New species: *Gibellula brevistipitata* Kuephadungphan, Tasanathai & Luangsa-ard, *G. longicaudata* Tasanathai, Kuephadungphan & Luangsa-ard, *G. longispora* Kuephadungphan & Luangsa-ard, *G. nigelii* Kuephadungphan, Tasanathai & Luangsa-ard, *G. parvula* Kuephadungphan, Tasanathai & Luangsa-ard, *G. pilosa* Kuephadungphan, Tasanathai & Luangsa-ard, *G. solita* Kuephadungphan, Tasanathai & Luangsa-ard, *G. trimorpha* Tasanathai, Khonsanit, Kuephadungphan & Luangsa-ard.

Citation: Kuephadungphan W, Petcharad B, Tasanathai K, Thanakitpipattana D, Kobmoo N, Khonsanit A, Samson RA, Luangsa-ard JJ (2022). Multi-locus phylogeny unmasks hidden species within the specialised spider-parasitic fungus, *Gibellula* (*Hypocreales*, *Cordycipitaceae*) in Thailand. *Studies in Mycology* **101**: 245–286. doi: 10.3114/sim.2022.101.04.
Received: 4 January 2022; **Accepted:** 5 April 2022; **Effectively published online:** 29 April 2022
Corresponding editor: Pedro W. Crous

INTRODUCTION

Spiders are cosmopolitan carnivorous arthropods that play a pivotal role in maintaining the balance of ecological systems (Lee & Kim 2001) by killing 400–800 million tons of insects every year (Nyffeler & Birkhofer 2017). Nevertheless, they are predated by other animals including spiders themselves (Foelix 2011). Fungi are important, but neglected natural enemies of spiders (Evans 2013) as pathogenic fungi can be confused with saprophytic fungi on spider cadavers. Pathogenic fungi can establish dense hyphal networks that hinder species identification of the spider host. Nonetheless, *Araneomorphae* and *Mygalomorphae* spiders frequently appear to be parasitised by hypocrealean fungi (*Ascomycota*), in which over 80 species from 13 genera are reported (Shrestha *et al.* 2019).

Among the hypocrealean fungi, *Gibellula* is well-known as a pathogenic genus of spiders, but has never been found infecting any other arthropod. This genus has a very long taxonomic history. The synonymising of *G. pulchra* (the type species) with *G. leiopus*, limited access to certain holotypes, a lack of holotype sequences as well as living cultures, have created nomenclatural and taxonomic complications which unavoidably created confusion and difficulty in species identification. According to Shrestha *et al.* (2019) and our previous reports on the five new species of *Gibellula* (Kuephadungphan *et al.* 2019, 2020), there are currently 21 species accepted in this genus. *Gibellula* can be identified by producing aspergillus-like conidiophores on synnemata with the appearance of lupines growing on the spider host. For the species that produce penicillium-like conidiophores such as *G. leiopus*, *G. clavulifera* and *G. scorpioides*, they can be distinguished from others by forming tufted synnemata fully covered with very short conidiophores. Some species possess unique distinguishing morphology, including *G. mainsii* forming mononematous conidiophores (Samson & Evans 1992), *G. brunnea* producing synnemata that widen into globose to pyriform fertile areas with pale brown, long, slender sterile tips (Samson & Evans 1992) and *G. alata* having wing-like synnemata (Petch 1932). However, other species are indistinguishable based solely on the macroscopic features. For instance, *G. cebrennini* can be discriminated from *G. fusiformispora* only by having much longer conidiophores (Kuephadungphan *et al.* 2020). As *Gibellula* is known to be linked with a *Torrubiella* sexual morph, it may occur on a spider host either with or without the presence of *Gibellula*. *Gibellula cebrennini* is an example of a species that can be found producing only *Torrubiella* perithecia on spider hosts (Kuephadungphan *et al.* 2020). *Torrubiella* was proven by phylogenetic analyses to be a polyphyletic group distributed across several genera, not only within the *Cordycipitaceae* but also the *Clavicipitaceae* (Sung *et al.* 2007, Johnson *et al.* 2009, Kepler *et al.* 2017). Considering only the hypocrealean fungi that infect spiders, *Akanthomyces* and *Hevansia* are also known to be connected with a *Torrubiella* sexual morph besides *Gibellula* (Kepler *et al.* 2017, Mongkolsamrit *et al.* 2018). To identify such fungi bearing only sexual morphs to the genus or species ranks, molecular phylogenetic analysis is highly recommended.

Thus far, 12 spider families consisting of *Agelenidae, Anyphaenidae*, *Araneidae*, *Corinnidae*, *Deinopidae*, *Linyphiidae*, *Pholcidae*, *Salticidae*, *Sparassidae*, *Theridiidae*, *Thomisidae* and *Zodariidae* have been reported as hosts of *Gibellula* (Bishop 1990, Hughes *et al.* 2016, Savić *et al.* 2016, Kuephadungphan *et al.* 2020). Our previous report suggested host-specificity in certain species of *Gibellula* (Kuephadungphan *et al.* 2020). Therein, *G. cebrennini* was found only on *Cebrenninus cf. magnus* whereas *G. pigmentosinum* and *G. scorpioides* appeared to be highly specific to *Storenomorpha* sp. (*Zodariidae*) and *Portia* sp. (*Salticidae*), respectively.

In the exploration of the diversity of the spider-parasitic fungi in Thailand, fungi tentatively identified as *Gibellula* spp. deposited in the BIOTEC Bangkok Herbarium (BBH) and the BIOTEC Culture Collection (BCC), Thailand, were selected and taxonomically studied using an integrative approach, which revealed the existence of eight new and three known taxa within the genus. The new species described herein are illustrated morphologically and phylogenetically along with the identification of their spider hosts to better understand the spider-fungus relationship.

MATERIALS AND METHODS

Fungal materials and isolation

Spiders parasitised by *Gibellula* spp. were collected from various locations throughout Thailand. The living leaves with spider cadavers attached on the underside were picked carefully, kept individually in plastic boxes and transported to the laboratory for isolation. The isolation was performed immediately after returning specimens to the laboratory. An agar plug of potato dextrose agar (PDA; fresh diced potato 200 g, dextrose 20 g, agar 15 g, in 1 L distilled water) was cut into small pieces (approximately 0.1 mm^3) using a sterile fine needle and was gently swiped over the spores located on the conidiophores along the synnemata and then placed on a PDA plate. Plates were incubated at 25 °C, roughly 12:12 light-dark cycle, and examined daily for conidial germination and also for fungal contaminants. Pure cultures were isolated onto fresh PDA plates by hyphal tip isolation. These were then allowed to grow for 6–8 wk before preparation for storage. Daily observation of conidial germination as well as fungal contamination is important. The fresh fungal specimens are stored at 4 °C until the cultures could be obtained. Notably, the longer the specimen is kept, the lesser is the chance a culture can be made. After the pure cultures of each fungus could be established onto PDA, the fungal specimens were dried at 55 °C for 24 h. All living cultures and dried specimens were then deposited in the BCC and BBH, respectively.

Morphological characterisation

Morphological characterisation of invertebrate-pathogenic fungi depends primarily on the presence of structures associated with asexual and sexual reproductive morphs on the host and the observation should be conducted at various levels from the naked eye via a dissecting microscope and compound microscope. Macroscopic features of asexual morph involve noting the number, colour, shape and length of synnemata as well as the colour of mycelia covering the host while microscopic characters involve the shape and size of vesicles, metulae, phialides, conidial heads, conidia and conidiophores including the arrangement of conidiophores on the surface of synnemata. For the sexual morph the shapes and sizes of perithecia, asci and ascopores are noted. The fungus materials, such as phialides and conidia from the asexual morph and perithecia, asci and ascospores of the sexual morph were mounted in lactophenol cotton blue solution and measured using a compound microscope (Olympus SZ31, Olympus Corporation, Japan). Up to 10 perithecia, and 20–40 asci, part-spores, phialides and conidia were measured, and the amount of variability was calculated using standard deviation (with absolute minima and maxima in brackets) and average +/– standard deviation values. These were photographed by using an Olympus BX51 (Olympus Corporation, Japan). PDA cultures were studied for important morphological characters such as conidia and phialides.

Identification of spider hosts

To identify the spider hosts, the World Spider Catalog (2021) (https://wsc.nmbe.ch/) as well as an expert on spider taxonomy were employed. As a spider host is covered with fungi allowing only certain parts, such as the legs and cephalic region to be seen, variation in characteristics of legs and accessories such as setae, spines, and tarsal claws on legs and variation in characteristics of eyes among taxa are useful for identification. Accordingly, we used not only the necessary identification guides, *e.g.* Deeleman-Reinhold (2001), Jocqué & Dippenaar-Schoeman (2007), but also literature relating to morphological characteristics of legs, for example Deeleman-Reinhold (2009), Wolff & Gorb (2012), Wolff *et al*. (2013), Labarque *et al*. (2017), and Ramírez & Michalik (2019), and literature relating to characteristics of eyes, for example Morehouse *et al*. (2017), and Long (2021). The aforementioned literature substantially support identification of spiders.

Molecular phylogenetic analyses

Fungal mycelia were scraped out from the surface of fungal colonies actively growing on PDA and DNA subsequently extracted following the protocol previously described by Thanakitpipattana *et al.* (2020). Five nuclear DNA regions were PCR-amplified including the internal transcribed spacer regions (ITS), the nuclear large subunit (LSU) of the ribosomal DNA, translation elongation factor 1-alpha (*TEF1*), and the largest and second-largest subunits of RNA polymerase II (*RPB1* and *RPB2*). PCR reactions were done in 25 µL volumes consisting of 1× Dream *Taq* Buffer (containing 2.5 mM $MgCl_2$), 0.4 M betaine, 200 µM dNTP mix, 0.5 µM of each primer, 1 U Dream *Taq* DNA polymerase (Thermo Scientific, US) and 50 ng of DNA template.

DNA sequences were assembled using BioEdit v. 7.2.5 (Hall 1999). The alignment was conducted using MUSCLE v. 3.6 software (Edgar 2004) and manually corrected to minimise gaps. The final sequence alignment of 4 219 bps of the combined dataset was used for analyses using maximum likelihood and Bayesian inference. Maximum likelihood-based phylogeny was performed with RAxML-HPC2 on XSEDE in CIPRES Science Gateway v. 3.3 (https://www.phylo.org/) using a GTRCAT model of evolution with 1 000 bootstrap replicates (Stamatakis 2014). Bayesian analysis was performed with MrBayes on XSEDE v. 3.2.7a using the best fit models of evolution (SYM+G) selected by AIC in MrModeltest v. 2.2 (Nylander 2004). Four Markov chains were run for 5 M generations and trees were sampled every 100 generations. A burn-in value of 25 % was set that discarded the first 2 500 generations.

Estimation of divergence between closely related species

P-distances were calculated between sequences using MEGA X (Kumar *et al.* 2018). P-distances were averaged between putative species. Other closely related known taxa were included in the analysis to evaluate whether the divergence among putatively new clades would support their status as distinct species. The p-distance between *G. cebrennini* and *G. fusiformispora*, two sister species proposed in a previous taxonomic work on *Gibellula* (Kuephadungphan *et al.* 2020), was used as a threshold to discriminate between closely related species.

RESULTS

Molecular phylogeny

According to the phylogenetic tree inferred from multiple loci of 47 taxa (Fig. 1 and Table 1), seven genera including *Akanthomyces*, *Beauveria*, *Blackwellomyces*, *Cordyceps*, *Gibellula*, *Hevansia*, and *Engyodontium* (as outgroup) formed monophyletic clades that corresponded to the phylogeny-based classification of the *Cordycipitaceae* contributed by Kepler *et al.* (2017), Kuephadungphan *et al.* (2019, 2020) and Wang *et al.* (2020). All taxa pertaining to this study were distributed in the strongly supported *Gibellula* clade (100 %), which is regarded as a sister lineage to *Hevansia* – another well-known specialised spider-parasitic genus along with *Gibellula*. This multilocus-based phylogeny clearly supports the segregation of three new records of known species, eight new taxa, and seven known species within the genus. New records in Thailand are reported for *G. dimorpha*, *G. pulchra* and *G. unica*. *Gibellula dimorpha* formed a strongly supported clade with *Gibellula trimorpha*, a new species. *Gibellula brevistipitata*, *G. longicaudata*, *G. longispora*, *G. nigelii*, *G. parvula* and *G. pilosa* were recognised as new taxa with strong bootstrap supports for their phylogenetic placements.

Analyses of divergence

We calculated the p-distances between sequences constituting putative new species (*G. brevistipitata*, *G. parvula*, *G. pilosa*, *G. solita* and *G. trimorpha*), new records for Thailand (*G. dimorpha*, *G. pulchra* and *G. unica*) and between closely related known taxa in their respective clades (Fig. 1). The p-distance between *G. cebrennini* and *G. fusiformispora* (0.014 ± 0.003; ~ 1.4 % divergence) was used as a threshold of divergence between two closely related cryptic species of *Gibellula*.

Figure 2 shows the distribution of p-distances between putative new and closely related *Gibellula* species. The p-distance analysis supports *G. dimorpha*, *G. trimorpha*, *G. parvula*, *G. pigmentosinum*, *G. longispora*, *G. brevistipitata*, *G. pilosa*, *G. solita*, *G. unica*, *G. pulchra*, and *G. nigelii* as distinct species. These findings illustrate the cryptic trends in cordycipitoid morphological evolution as demonstrated in other works (Khonsanit *et al.* 2020, Kobmoo *et al.* 2019, 2021, Mongkolsamrit *et al.* 2018, 2020, Wang *et al.* 2020).

Taxonomy

Gibellula brevistipitata Kuephadungphan, Tasanathai & Luangsa-ard, ***sp. nov.*** MycoBank MB 841093. Fig. 3.

Etymology: Refers to the short stipes of synnemata.

Typus: **Thailand**, Buri Ram Province, Dong Yai Wildlife Sanctuary, Pong Kao Nature Trail, on *Thomisidae* attached to the underside of a dicot leaf, 11 Dec. 2010, *K. Tasanathai, P. Srikitikulchai, A. Khonsanit, K. Sansatchanon, W. Noisripoom, A. Saksrikrom, B. Saracam* & *S. Mongkolsamrit* (**holotype** BBH 38549, culture ex-type BCC 45580). GenBank: ITS = OK040729, LSU = OK040706, *TEF1* = OK040697, *RPB1* = OK040715.

Spider covered by a yellowish-white mycelial mat (Fig. 3A). *Synnemata* cylindrical, multiple, brownish white, becoming brown towards the tip, approximately 2 mm long, 200 µm wide, terminal part ovoid tapering towards the end, 175 µm wide (Fig. 3B). *Conidiophores* arising along the entire length of the synnemata, absent on the swollen tip, occasionally from a network of hyphae loosely attached to the host, crowded, septa conspicuous, distinctly roughened, (47.5–)58–100(–115) × 6–8(–8.5) µm, narrowing to a slender apex, and terminating in a swollen vesicle (Fig. 3C–D). *Vesicles* spherical to broadly obovoid, (7.5–)8–9(–10) µm diam (Fig. 3E). *Metulae* borne on vesicle, broadly obovoid or broadly ellipsoid, (7–)7.5–9.5(–10.5) × 5–7 µm, bearing multiple phialides (Fig. 3E). *Phialides* cylindrical to narrowly clavate, often apically thickened, (7–)7.5–9(–10) × 2–2.5(–3) µm (Fig. 3E). A vesicle together with metulae and phialides forming a spherical conidial head, (33–)34.5–37.5(–40) µm diam (Fig. 3E). *Conidia* ellipsoid or narrowly almond-shaped, (3–)3.5–4(–4.5) × 1.5–2 µm (Fig. 3F). Sexual morph and *Granulomanus* synasexual morph not observed.

Culture characteristics: Colonies on PDA attaining a diam of 2 cm in 28 d at 25 °C, white, floccose; reverse cream, becoming light brown with age at the centre (Fig. 3G). Sporulation not observed in culture.

Gibellula dimorpha Tzean, L.S. Hsieh & W.J. Wu, Mycol. Res. 102: 1350. 1998. Fig. 4.

Spider host covered by yellowish white to cream mycelial mat. *Synnema* solitary, brownish white (Fig. 4A–B). *Conidiophores* 100–175 × 5–7.5 µm. *Conidial heads* spherical, (32–)33–45(–50) µm diam (Fig. 4D). *Vesicles* globose to subglobose, 5–6(–7) µm bearing multiple metulae (Fig. 4D). *Metulae* broadly obovoid, 5–7 × 4–5 µm (Fig. 4D). *Phialides* borne on metulae, cylindrical to narrow clavate with a short neck, hyaline, 6.5–8.5 × 1.5–3 µm (Fig. 4D). *Conidia* hyaline, broadly fusiform, smooth, single or in chains, 3–5 × 1.5–2 µm (Fig. 4E). *Granulomanous* synasexual morph present, well differentiated, forming aspergillus-like conidiophores (Fig. 4C). *Conidiophores* cylindrical, septate, verrucose, (70–)94–144.5(–157.5) × 7.5–10(–11) µm (Fig. 4C, 4F). *Vesicles* well developed, often absent, globose to subglobose, smooth-walled, (4.5–)5–7 µm (Fig. 4G). Multiple metulae borne on a vesicle, occasionally hardly developed, broadly obovoid, smooth-walled, 6–7 × 4–5.5(–6) µm (Fig. 4G). *Phialides* narrowly clavate to irregularly shaped, apically thickened often with a short neck, or cylindrical bearing 1–3 denticles at the apices, smooth-walled (Fig. 4G), or irregularly shaped, polyblastic, distinctly verrucose, (6–)7.5–10(–11) × 2.5–3.5(–4) µm (Fig. 4H). *Conidia* filiform, smooth, hyaline, 10–15 × 1–1.5 µm (Fig. 4I). *Conidial head* spherical, formed by a vesicle,

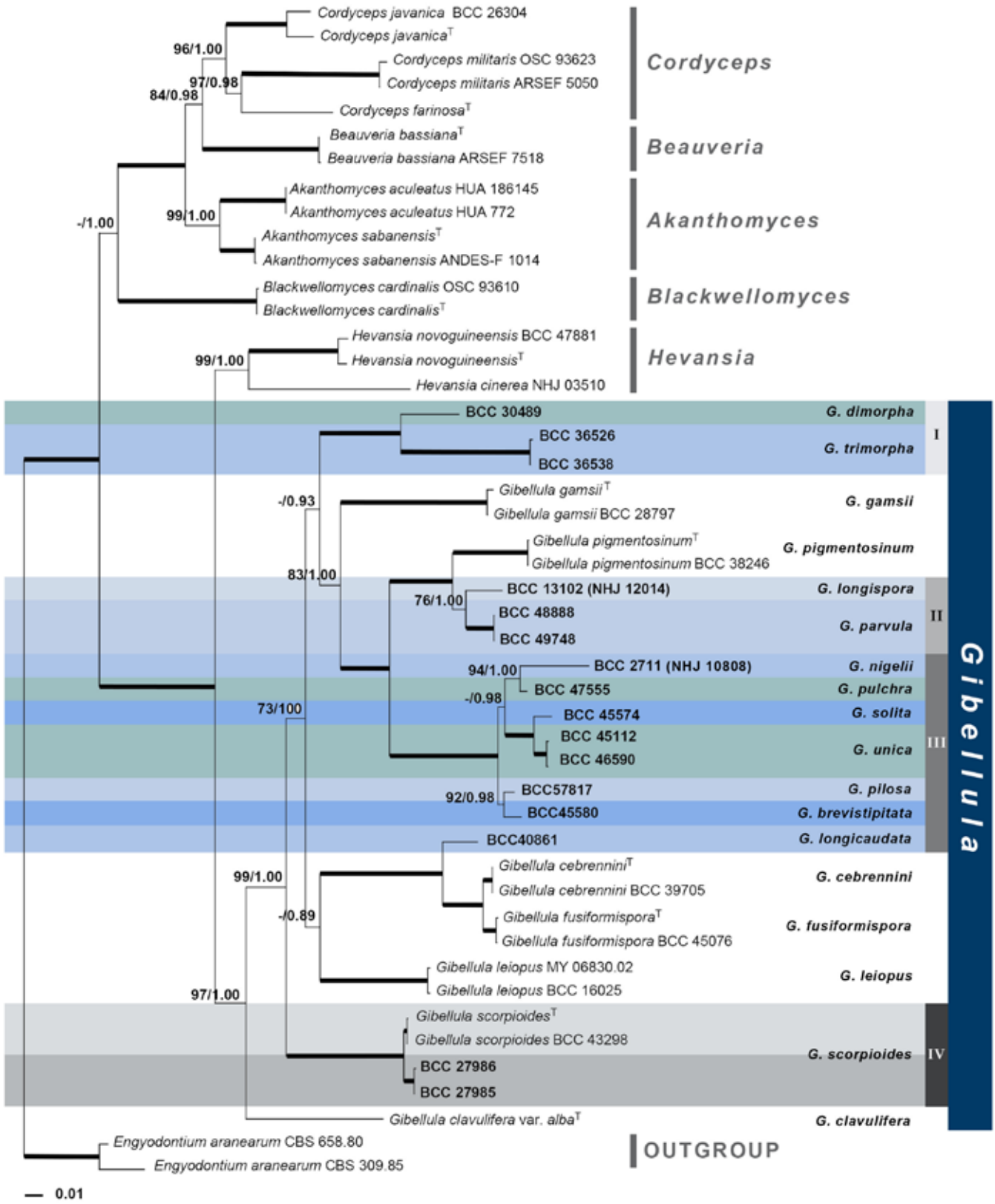

Fig. 1. RAxML tree based on the concatenated five gene datasets (ITS, LSU, *TEF1, RPB1* and *RPB2*) showing the relationship among *Gibellula* and related genera. Bootstrap proportions/ Bayesian posterior probabilities ≥ 50 % are provided above corresponding nodes; nodes with 100 % support are shown as thick lines. The ex-type strains are marked with a superscript T (^{T}) and the isolates reported in this study are bold. All proposed species are highlighted in grey.

several metulae and phialides, (37–)39–56(–59) µm (Fig. 4G–H). *Perithecia* produced on the mycelial mat covering the body of the spider, absent on its legs, superficial with mycelia covering the bottom two-thirds of the perithecium, ovoid narrowing towards the ostiole, reddish-brown, (640–)645–691.5(–700) × (280–)285–310 µm (Fig. 4J–K). *Asci* cylindrical, up to 688 µm long, (5–)6–7(–8) µm wide. *Asci caps*, (4–)4.5–6(–7) × (6.5–)7–8(–8.5) µm (Fig. 4L). *Ascospores* filiform, multiseptate, arranged in parallel rows, breaking into bacilliform part-spores, (5–)6–10(–12) × 1.5–2 µm (Fig. 4M).

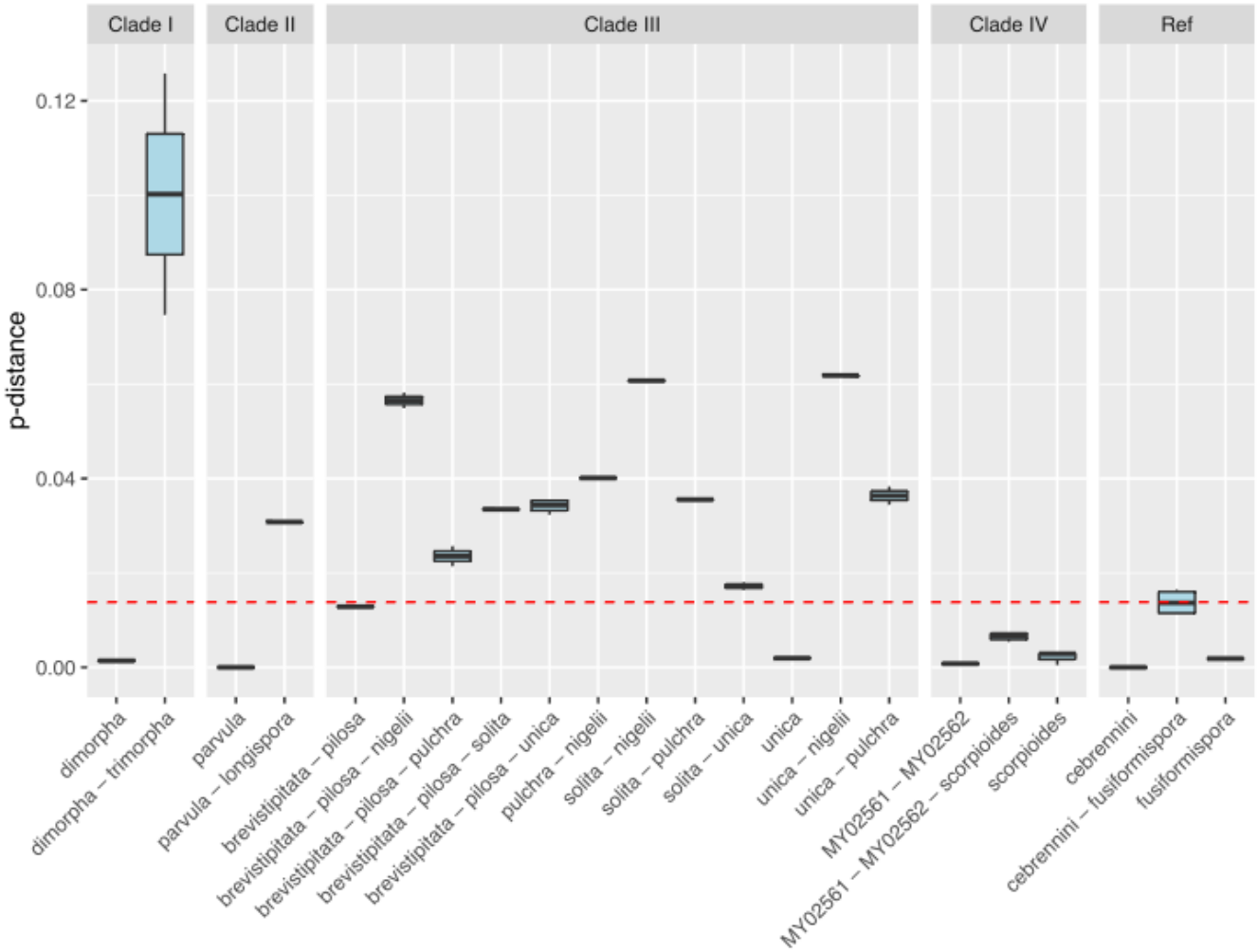

Fig. 2. Distribution of p-distances between putative new species and closely related known taxa. Within Clade III (*G. brevistipitata–G. pilosa–G. solita–G. unica–G. pulchra–G. nigelii)*, all pairwise p-distances between putative species exceeded the threshold supporting their species status (*G. brevistipitata–G. pilosa–G. solita*: 0.033 ± 0.000, *G. brevistipitata–G. pilosa–G. unica*: 0.034 ± 0.001, *G. brevistipitata–G. pilosa–G. pulchra*: 0.024 ± 0.003, *G. brevistipitata–G. pilosa–G. nigelii*: 0.056 ± 0.002, *G. solita–G. unica*: 0.017 ± 0.001, *G. solita–G. pulchra*: 0.038, *G. solita–G. nigelii*: 0.069, *G. unica–G. pulchra*: 0.036 ± 0.003, *G. unica–G. nigelii*: 0.062 ± 0.000, *G. pulchra–G. nigelii*: 0.044). The p-distance between *G. brevistipitata* (BCC 45580) and *G. pilosa* (BCC 57817) is just below the threshold (0.013). However, there are sufficient distinguishing morphological characters to establish them as separate species. Pairwise p-distances also exceeded the threshold in Clade II (*G. parvula–G. longispora*: 0.031 ± 0.000), and Clade I, in which the average p-distance of *G. trimorpha–G. dimorpha* was notably greater (0.061) than for any other pair In clade IV, the average p-distances of the isolates BCC 27985 and BCC 27986 to *G. scorpioides* were well below the threshold indicating that these isolates belong to *G. scorpioides.*

Culture characteristics: Colonies on PDA attaining a diam of 2 cm in 20 d at 25 °C, white, floccose; reverse cream, becoming light brown with age at the centre (Fig. 4N). Sporulation not observed in culture.

Material examined: **Thailand**, Ranong Province, Khuan Mae Yai Mon Wildlife Sanctuary, Heo Lom Waterfall, on *Miagrammopes* sp. attached to the underside of a dicot leaf, 9 Mar. 2011, *K. Tasanathai, P. Srikitikulchai, A. Khonsanit, K. Sansatchanon* & *D. Thanakitpipattana* (BBH30489, living culture BCC 47518). GenBank: ITS = MH532884, LSU = MH394679, *TEF1* = MH521892, *RPB1* = MH521819, *RPB2* = MH521863.

Notes: *Gibellula dimorpha* was first described by Tzean *et al.* in the late 1990s and there has been no report on this species since then. In this study, we described for the first time *G. dimorpha* from Thailand; moreover, we obtained a culture of this species. Typically, *G. dimorpha* is recognised by having a *Granulomanus* conidial morph that develops aspergillus-like conidiophores and by producing broadly fusoid conidia in the *Gibellula* conidial morph. A *Granulomanus* conidiophore often bears both types of phialides: narrowly clavate, smooth-walled phialides, which is typically found in the *Gibellula* conidial morph and irregular-shaped, rough-walled phialides with 1–3 denticles. Remarkably, the narrowly clavate phialides of the *Granulomanus* conidial morph are significantly longer, (6–)7.5–10(–11) µm, than those found in the *Gibellula* conidial morph (6.5–8.5 µm). The size of the conidial heads varies over a wide range, in which the largest is up to 59 µm diam. In comparison to the type, the Thai specimen shared similarity in shape but shows difference in size (Table 2). For instance, the Thai specimen has *Gibellula* conidiophores, *Granulomanus* phialides and conidia that are much shorter than the type whereas the part-spores of the *Torrubiella* sexual morph are slightly longer.

Gibellula longicaudata Tasanathai, Kuephadungphan & Luangsa-ard, ***sp. nov.*** MycoBank MB 841095. Fig. 5.

Etymology: Long tail, referring to the long synnema.

Typus: **Thailand**, Ranong Province, Khuan Mae Yai Mon Wildlife Sanctuary, Heo Lom Waterfall, on *Indoxysticus* sp. (*Thomisidae*) attached

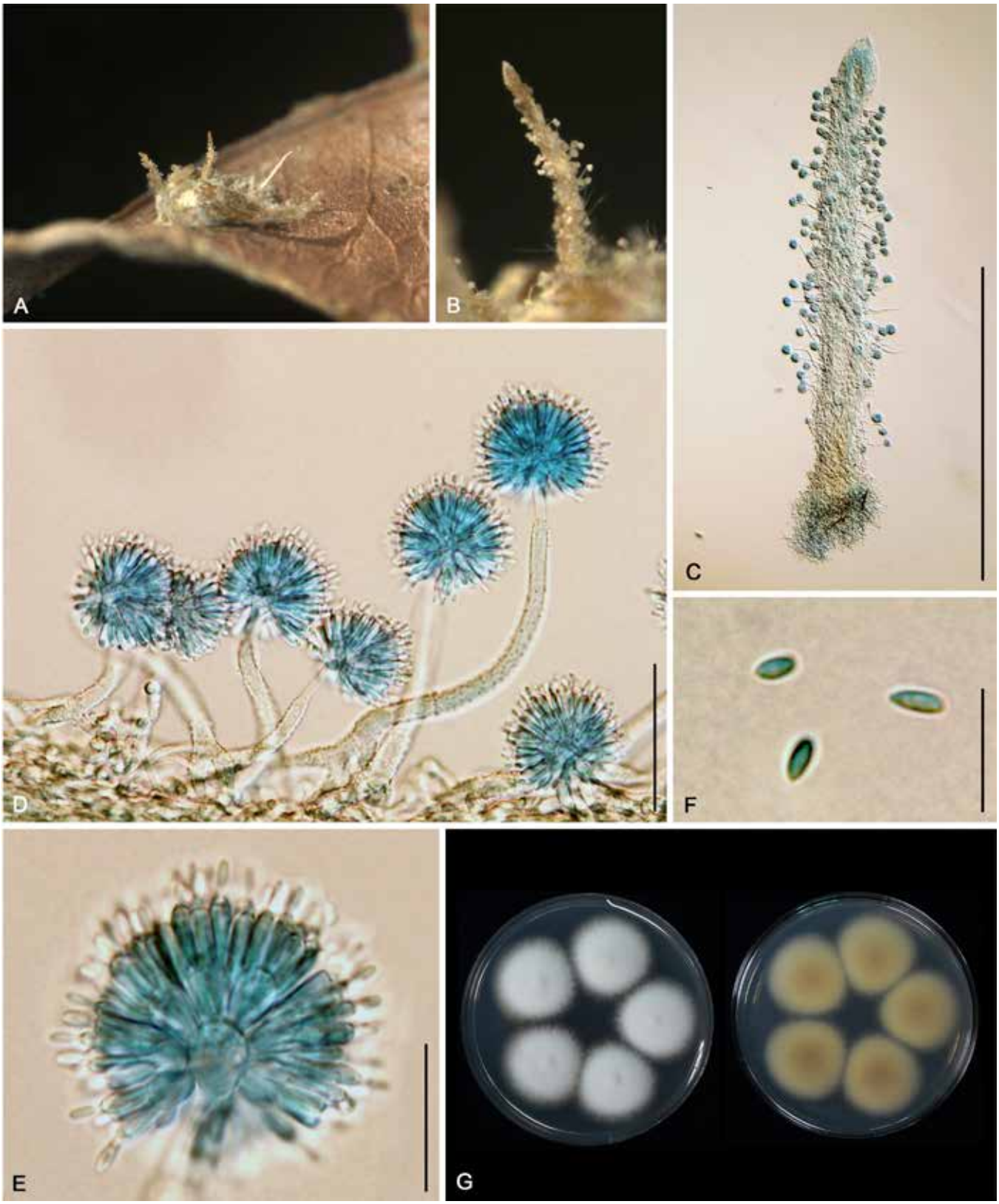

Fig. 3. *Gibellula brevistipitata*. **A.** Fungus on spider. **B–C.** Synnemata. **D.** Conidiophores showing spherical conidial heads. **E.** A conidial head bearing conidia. **F.** Conidia. **G.** Colonies obverse and reverse on PDA at 25 °C after 28 d. Scale bars: C = 1 mm; D = 50 µm; E = 20 µm; F = 10 µm.

Fig. 4. *Gibellula dimorpha*. **A.** Fungus on a spider. **B.** Part of synnema showing conidiophores. **C.** Conidiophores arising from the mycelia covering a spider's leg. **D.** Conidial head of *Gibellula* conidial stage. **E.** Conidia of *Gibellula* conidial stage. **F.** Aspergillus-like conidiophore of *Granulomanus* conidial stage. **G.** *Granulomanus* conidial stage forming typical *Gibellula* phialides. **H.** Conidial head of *Granulomanus* conidial stage showing irregular-shaped phialides. **I.** Filiform conidia of *Granulomanus* conidial stage. **J.** Perithecium occurring on the mycelial network covering the spider's body. **K.** Perithecium. **L.** Asci. **M.** Part-spores **N**. Colonies obverse and reverse on PDA at 25 °C after 20 d. Scale bars: C, K = 250 µm; F, L = 50 µm; J = 50 µm; D, G, H = 20 µm; E, I, M = 10 µm.

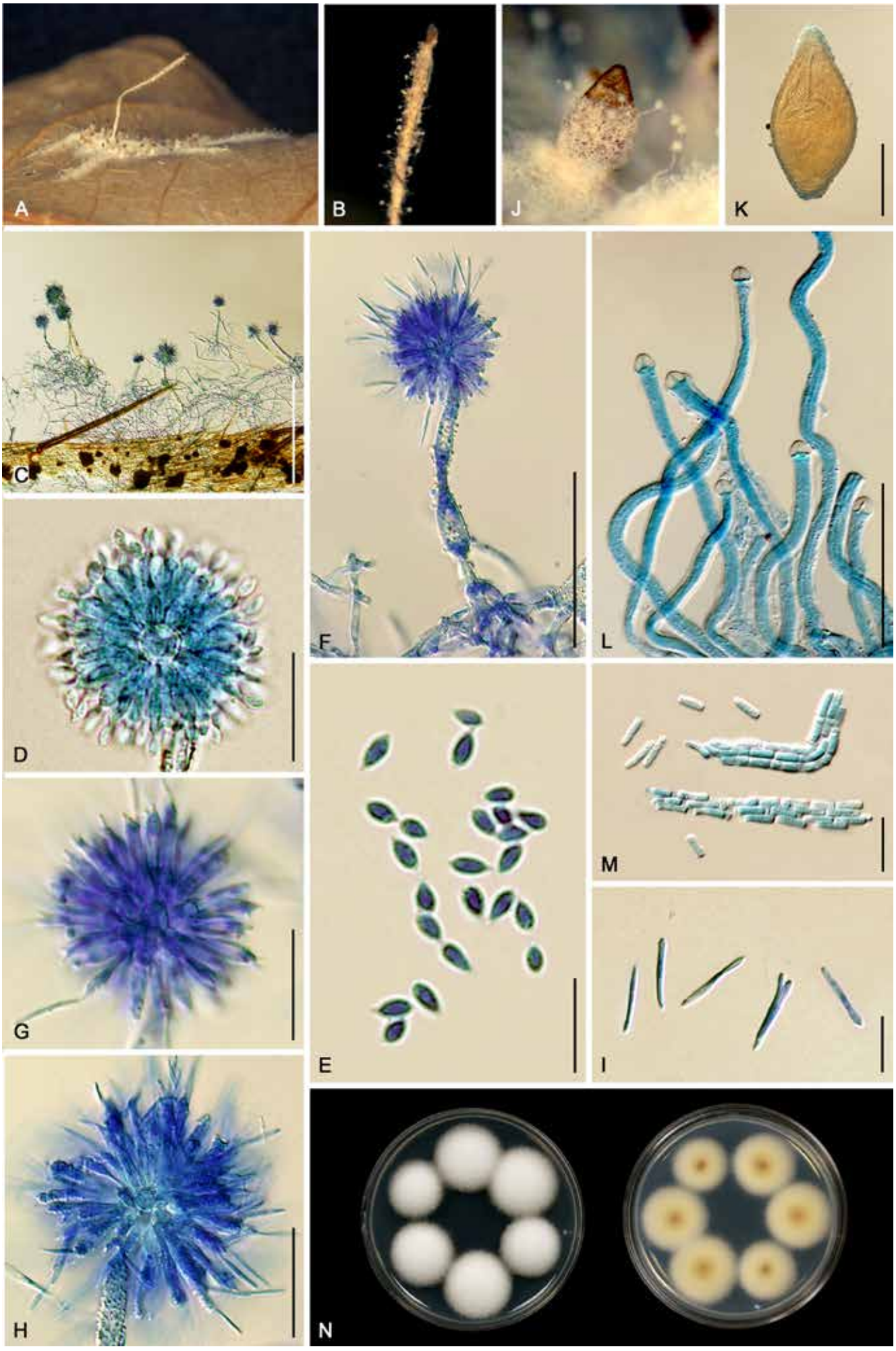
A
B
J
K
C
F
L
D
E
M
G
I
H
N

Table 1. List of taxa included in the multi-locus based phylogenetic analyses and their GenBank accession numbers. The isolates representing the new taxa are marked in bold.

		GenBank accession numbers					
Species	**Code**	**ITS**	**LSU**	***TEF1***	***RPB1***	***RPB2***	**References**
Akanthomyces aculeatus	HUA 772	KC519371	KC519370	KC519366	–	–	Sanjuan *et al.* (2014)
	HUA 186145	–	MF416520	MF416465	–	–	Kepler *et al.* (2017)
Akanthomyces sabanensis	ANDES-F 1014	KC633245	KC633248	KC875221	–	–	Chirivi-Salomon *et al.* (2015)
	ANDES-F 1024	KC633232	KC875225	KC633266	–	KC633249	Chirivi-Salomon *et al.* (2015)
Beauveria bassiana	ARSEF 1564^{T}	NR111594	–	HQ880974	HQ880833	HQ880905	Rehner *et al.* (2011)
	ARSEF 7518	HQ880762	–	HQ880975	HQ880834	HQ880906	Rehner *et al.* (2011)
Blackwellomyces cardinalis	OSC 93609^{T}	–	AY184962	DQ522325	DQ522370	DQ522422	Sung & Spatafora (2004), Spatafora *et al.* (2007)
	OSC 93610	JN049843	AY184963	EF469059	EF469088	EF469106	Kepler *et al.* (2012), Sung & Spatafora (2004), Sung *et al.* (2007)
Cordyceps farinosa	CBS 111113^{T}	AY624181	MF416554	MF416499	MF416656	MF416450	Luangsa-ard *et al.* (2005), Kepler *et al.* (2017)
Cordyceps javanica	CBS 134.22^{T}	NR111172	NG059048	MF416504	MF416661	MF416455	Luangsa-ard *et al.* (2005), Kepler *et al.* (2017)
	BCC26304	MH532851	MH394660	MH521903	MH521825	MH521868	Helaly *et al*. (2019), Kuephadungphan *et al*. (2020)
Cordyceps militaris	ARSEF 5050	HQ880829	–	HQ881020	HQ880901	HQ880973	Rehner *et al.* (2011)
	OSC 93623	JN049825	AY184966	DQ522332	DQ522377	AY545732	Kepler *et al.* (2012), Spatafora *et al.* (2007), Sung & Spatafora (2004)
Engyodontium aranearum	CBS 309.85	JN036556	AF339526	DQ522341	DQ522387	DQ522439	Spatafora *et al.* (2007), Sung *et al.* (2001)
	CBS 658.80	LC092897	LC092916	–	–	–	Tsang *et al.* (2016)
Gibellula brevistipitata	**BCC45580**	**OK040729**	**OK040706**	**OK040697**	**OK040715**	**–**	**This study**
Gibellula cebrennini	BCC39705	MH532874	MH394673	MH521895	MH521822	MH521859	Kuephadungphan *et al*. (2020)
	BCC53605^{T}	MT477069	MT477062	MT503328	MT503321	MT503336	Kuephadungphan *et al*. (2020)
Gibellula clavulifera var. *alba*	ARSEF 1915^{T}	–	DQ518777	DQ522360	DQ522408	DQ522467	Spatafora *et al.* (2007)
Gibellula dimorpha	**BCC47518**	**MH532884**	**MH394679**	**MH521892**	**MH521819**	**MH521863**	**This study**
Gibellula fusiformispora	BCC 45076	MH532882	–	–	MH521823	MH521860	Kuephadungphan *et al*. (2020)
	BCC56802^{T}	MT477070	MT477063	MT503329	MT503322	MT503337	Kuephadungphan *et al*. (2020)
Gibellula gamsii	BCC27968^{T}	MH152529	MH152539	MH152560	MH152547	–	Kuephadungphan *et al*. (2019)
	BCC28797	MH152531	MH152541	MH152562	MH152549	MH152557	Kuephadungphan *et al*. (2019)
Gibellula leiopus	BCC16025	–	MF416548	MF416492	MF416649	–	Kepler *et al.* (2017)
	BCC49250	**OK070780**	**OK070781**	**OK070782**	**OK070783**	**OK070784**	**This study**
Gibellula longicaudata	**BCC40861**	**OK040730**	**OK040707**	**OK040698**	**OK040716**	**OK040724**	**This study**
Gibellula longispora	**NHJ 12014**	–	–	EU369017	EU369055	EU369075	Johnson *et al.* (2009)
Gibellula nigelii	**NHJ 10808**	–	EU369035	EU369018	EU369056	EU369076	Johnson *et al.* (2009)
Gibellula parvula	**BCC48888**	**OK040731**	**OK040708**	**OK040699**	**OK040717**	**OK040725**	**This study**
	BCC49748	**OK040732**	**OK040709**	**OK040700**	**OK040718**	**OK040726**	**This study**
Gibellula pigmentosinum	BCC38246	MH532872	MH394672	MH521893	MH521800	MH521855	Helaly *et al*. (2019), Kuephadungphan *et al*. (2020)
	BCC41203^{T}	MT477071	–	MT503330	MT503323	–	Kuephadungphan *et al*. (2020)
Gibellula pilosa	**BCC57817**	**OK040733**	**OK040710**	**OK040701**	**OK040719**	**–**	**This study**
Gibellula pulchra	**BCC47555**	**MH532885**	**–**	**MH521897**	**MH521804**	**–**	**This study**
Gibellula scorpioides	**BCC27985**	**OK040734**	**MH394662**	**MH521899**	**MH521815**	**MH521857**	**This study**

Table 1. (Continued).

Species	Code	GenBank accession numbers					References
		ITS	LSU	*TEF1*	*RPB1*	*RPB2*	
	BCC27986	**OK040735**	**OK040711**	**OK040702**	**OK040720**	**OK040727**	**This study**
	BCC43298	MT477074	MH394677	MH521900	MH521816	MH521858	Kuephadungphan *et al*. (2020)
	BCC47976[T]	MT477078	MT477066	MT503335	MT503325	MT503339	Kuephadungphan *et al*. (2020)
Gibellula solita	**BCC45574**	**OK040736**	**OK040712**	**OK040703**	**OK040721**	**–**	**This study**
Gibellula trimorpha	**BCC36526**	**OK040737**	**–**	**OK040704**	**OK040722**	**OK040728**	**This study**
	BCC36538	**MH532867**	**MH394668**	**MH521890**	**MH521817**	**MH521861**	**This study**
Gibellula unica	**BCC45112**	**OK040738**	**OK040713**	**OK040705**	**OK040723**	**–**	**This study**
	BCC46590	**MH532883**	**MH394678**	**–**	**MH521803**	**MH521866**	**This study**

Table 2. Morphological comparison between *G. trimorpha*, Thai *G. dimorpha* and the type.

Characters	*Gibellula trimorpha*	*Gibellula dimorpha* (New record from Thailand)	*Gibellula dimorpha* (Tzean *et al*. 1998)
***Gibellula* asexual morph**	Present	Present	Present
Mycelia	Brown	Brownish-white	White, yellowish-white to orange white
Synnemata (mm)	Brownish-white, solitary cylindrical, attenuated	Brownish-white, solitary cylindrical, attenuated	Greenish white to pale green solitary, cylindrical, attenuated curved, 5 × 200
Conidiophores (µm)	Arising from the aerial mycelium and from synnema, septate, rough-walled, 65–230 × 7–9	Arising from the aerial mycelium and from synnema, 100–175 × 5–7.5	Arising from the aerial mycelium or from synnemata, septate, thickened, conspicuous, often darkly pigmented, rough-walled, in particular at base, 140–422 × 7.1–10.3
Conidial heads (µm)	Spherical, 37–44	Spherical, 32–50	Spherical, 36–54
Vesicle (µm)	Globose to subglobose, 9–12 × 7–10	Globose to subglobose, 5–7	Globose to subglobose, 7.9 × 11.1
Metulae (µm)	Hyaline, broadly ellipsoid, 7–10 × 6–7	Broadly obovoid to cylindrical, 5–7 × 4–5	Hyaline, broadly obovoid, narrowing towards base, 7.1–11.9 × 6.4–8.7
Phialides (µm)	n/a	Hyaline, cylindrical to narrow clavate, with a short neck, 6.5–8.5 × 1.5–3	Hyaline, cylindrical to narrowly clavate, with a short neck, smooth-walled, 5.6–8.7 × 2.5–4
Conidia (µm)	Fusoid In short chains, 4–5 × 2	Hyaline, fusoid, smooth-walled, single or in chains, 3–5 × 1.5–2	Hyaline, fusoid, ellipsoidal or lemon-shaped, smooth-walled, single or catenate, 3.2–4.1 × 2–2.4
***Granulomanus* asexual morph**	Present	Present	Present
Conidiophores (µm)	Rough-walled to distinctly verrucose	Rough-walled to distinctly verrucose, 77.5–157.5 × 7.5–11	Rough-walled to distinctly verrucose, 68–140 × 5.2–7.1
Conidial heads (µm)	n/a	Spherical, 37–59	Spherical, n/a
Vesicle (µm)	n/a	Globose to subglobose, often absent, 4.5–7	Hardly developed
Metulae (µm)	n/a	Broadly obovoid, occasionally hardly developed, smooth-walled, 6–7 × 4–6	Broadly obovoid, smooth-walled, occasionally minutely warted, 5.6–8.7 × 4.4–6.4
Phialides (µm)	Holoblastic, cylindrical, clavate, flask-shaped, or irregularly shaped, rough-walled, rarely smooth, bearing 1–3 conspicuous denticles, 8–13 × 3	Holoblastic, cylindrical, clavate, or irregularly shaped, rough- or smooth-walled, bearing 1–3 conspicuous denticles, 6–11 × 2.5–4	Cylindrical, ellipsoidal, narrowly clavate, conoid, or irregularly shaped, smooth-walled, occasionally roughened, bearing 1–3 conspicuous denticles, 7.9–20.6 × 3.2–4
Conidia (µm)	Hyaline, filiform, smooth-walled, 10–19 × 1–1.5	Hyaline, filiform, smooth-walled, 10–15 × 1–1.5	Hyaline, filiform, smooth-walled, 9.1–23.8 × 0.8–2.4
Sexual morph	Present	Present	Present

Table 2. (Continued).

Characters	***Gibellula trimorpha***	***Gibellula dimorpha* (New record from Thailand)**	***Gibellula dimorpha* (Tzean *et al.* 1998)**
Perithecia (µm)	Reddish-brown, superficial, scattered, ovoid, 340–690 × 200–310	Reddish-brown, superficial, scattered, ovoid, 640–700 × 280–310	Yellowish-white, superficial or partly embedded, scattered, ovoid, 490–600 × 250–320
Asci (µm)	Cylindrical, >455 × 7–10 with ascus cap	Cylindrical, >688 × 5–8 with ascus cap	Cylindrical, eight-spored, 220–310 × 6.4–8.2 with a thickened perforated apex
Apex (µm)	4–5.5 × 5–8	4–7 × 6.5–8.5	4.8–6.4 × 6.8–8.7
Ascospores (µm)	Filiform, multi-septate	Filiform, multi-septate	Filiform, multi-septate, no data × 1.6–2.4
Part-spores (µm)	Bacilliform, 3–9 × 1.5–2.5	Bacilliform, 5–12 × 1.5–2	Hyaline, cylindrical, smooth-walled, 3–8.7 × 2–2.3

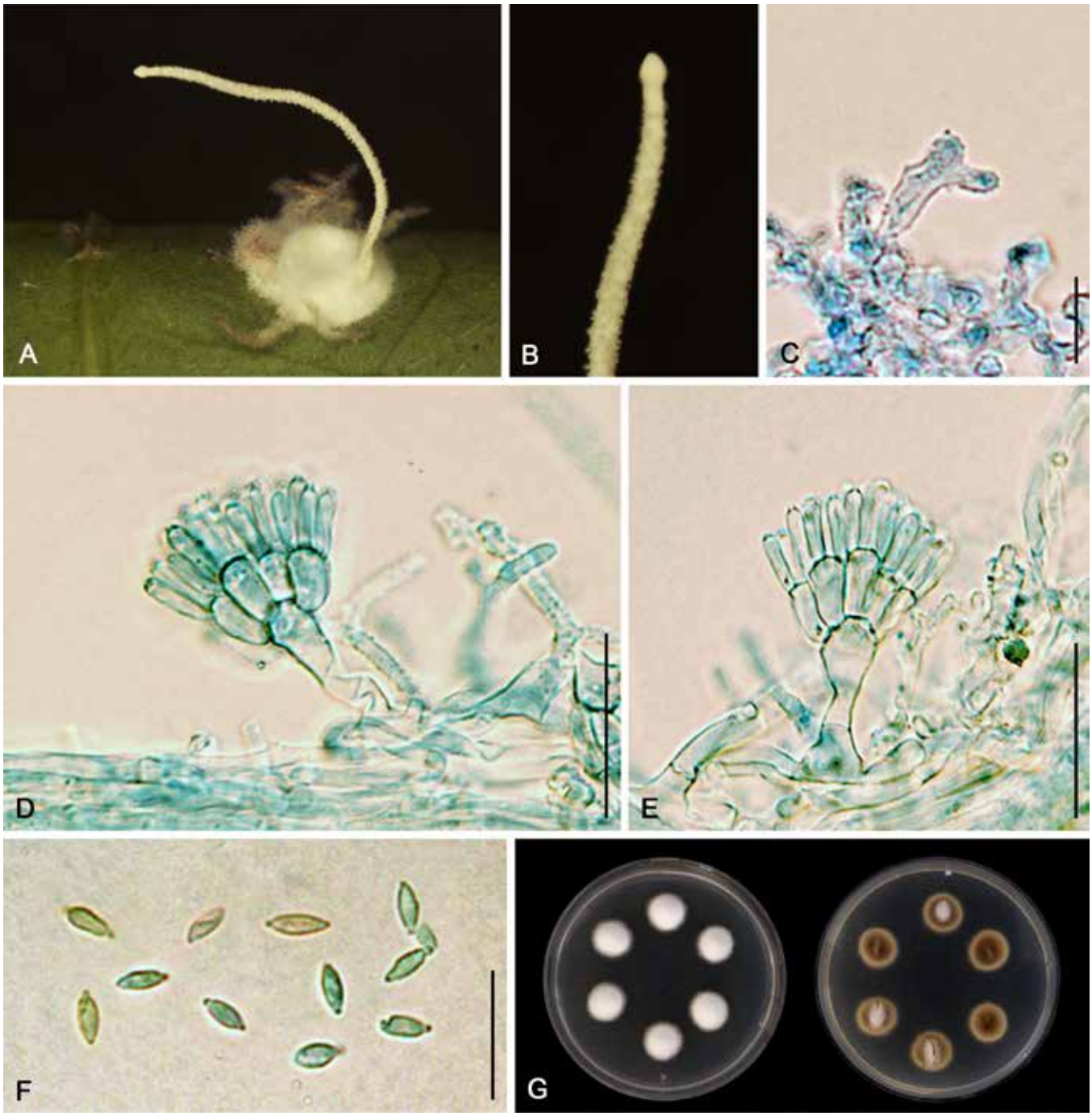

Fig. 5. *Gibellula longicaudata*. **A.** Fungus on spider. **B.** Upper part of a synnema showing a slight enlarged tip. **C.** Conidiophore showing a penicillium-like conidial head. **D–E.** *Granulomanus* phialides. **F.** Conidia. **G.** Colonies obverse and reverse on PDA at 25 °C after 20 d. Scale bars: D–E = 20 µm; C, F = 10 µm.

to the underside of dicot leaf, 9 Mar. 2011, *K. Tasanathai, P. Srikitikulchai, A. Khonsanit, K. Sansatchanon* & *D. Thanakitpipattana* (**holotype** BBH29604, culture ex-type BCC 40861). GenBank: ITS = OK040730, LSU = OK040707, *TEF1* = OK040698, *RPB1* = OK040716, *RPB2* = OK040724.

A long *synnema* arising from white mycelial mat covering the host, posterior part of a spider, greyish white, cylindrical, tufted surface, slightly tapering into sterile ovoid tip (Fig. 5A–B). *Conidiophores* crowded, smooth, enlarging upward into obovoid apices, (10–)15–28(–35) × 3–4(–5) µm, bearing multiple metulae (Fig. 5D–E). *Metulae* broadly obovoid to ellipsoid, 7–8(–10) × 3–3.5(–4) µm (Fig. 5D–E). *Phialides* borne on metulae, narrowly clavate to cylindrical, thickened at the tip, (7–)7.5–9(–10) × 2(–3) µm (Fig. 5D–E). Metulae and phialides together forming wedge-shaped conidial head. *Conidia* fusoid or occasionally ovoid with acute ends, (3–)3.5–5(–6) × 1–2 µm (Fig. 5F). *Granulomanus* synasexual morph observed, occurring on the synnema, arising from the septate hyphae loosely attached to the surface of synnema (Fig. 5C). *Conidiophores* distinctly roughened, very short, bearing polyblastic and irregularly shaped phialides with inconspicuous denticles (Fig. 5C). Sexual morph not observed.

Culture characteristics: Colonies on PDA attaining a diam of 1.1 cm in 20 d at 25 °C, floccose, white; reverse light brown, darkening with age, starting from the centre (Fig. 5G). Sporulation not observed in culture.

Gibellula longispora Kuephadungphan & Luangsa-ard, ***sp. nov.*** MycoBank MB 841091. Fig. 6.

Etymology: Refers to the long conidia.

Typus: **Thailand**, Nakhon Ratchasima Province, Khao Yai National Park, on *Myrmarachne* sp. (*Salticidae*) attached to the underside of monocot leaf, 1 Sep. 2002, *N.L. Hywel-Jones* (**holotype** BBH8638, culture ex-type BCC 13102). GenBank: *TEF1* = EU369017, *RPB1* = EU369055, *RPB2* = EU369075.

White mycelia covering the body of a spider host, occasionally its legs (Fig. 6A). Multiple synnemata produced, cylindrical, attenuated, brown when dried, 5–5.5 mm long, 175–200 µm wide, narrowing upward to a slender tip, 62.5–75 µm wide, consisting of parallel multiseptated longitudinal hyphae (Fig. 6A–C). *Conidiophores* arising from the outer layer of hyphal network loosely attached to the synnemata, crowded along the entire length of the synnemata, multiseptate, minutely roughened, (105–)159.5–290.5(–415) × (6–)8.5–11(–15) µm, abruptly narrowing to a distinct long slender stipe, bearing an aspergillus-like conidial head (Fig. 6D). *Conidial head* spherical, (37–)39–41.5(–42) µm diam (Fig. 6E). *Vesicles* terminated from apices of conidiophores, globose to subglobose, 7–8.5(–9) µm diam, bearing multiple metulae (Fig. 6E). *Metulae* broadly obovoid, (6.5–)7.5–9.5(–10) × (5.5–)6–6.5(–7) µm (Fig. 6E). *Phialides* narrowly clavate to cylindrical, (8.5–)9.5–11(–11.5) × (2.5–)3–3.5(–4) µm (Fig. 6E). *Conidia* borne on phialides, single, often in chains of up to four, bacilliform to cylindrical, (3.5–)5.5–8(–9) × 1–1.5 µm (Fig. 6F). *Granulomanus* synasexual morph and sexual morph not observed.

Culture characteristics: *Gibellula longispora* was once established in culture on PDA. DNA was extracted and sequenced but unfortunately the culture lost its viability after storage.

Notes: *Gibellula longispora* has often been used as a representative of the genus *Gibellula* in phylogenetic analyses (Johnson *et al.* 2009, Kepler *et al.* 2011, Chiriví-Salomón *et al.* 2015, Thanakitpipattana *et al.* 2020). *Gibellula longispora* is in fact an invalid name which is not yet listed in the global fungal nomenclatural databases including Index Fungorum (www.indexfungorum.org) and MycoBank (www.mycobank.org). In order to validate this name, the species is therefore morphologically described and illustrated herein. The specimen BBH8638 (formerly known as NHJ12014) is reminiscent of *G. pulchra* in having numerous synnemata and producing aspergillus-like conidiophores. Nonetheless, *G. longispora* distinctly differs from the type of *G. pulchra* (Cavara 1894) not only in the length of conidia which are twice as long as those of the type (Table 3), but also from the phylogenetic evidence that *G. longispora* is more closely related to *G. parvula* than to *G. pulchra* (Fig. 1).

Gibellula nigelii Kuephadungphan, Tasanathai & Luangsa-ard ***sp. nov.*** MycoBank MB 841096. Fig. 7.

Etymology: In honour of Dr Nigel Hywel-Jones, for his outstanding contribution to our knowledge of spider-parasitic fungi.

Typus: **Thailand**, Nakhon Ratchasima Province, Khao Yai National Park, Mo Sing To Nature trail, on *Linyphiidae* attached to the underside of a dicot leaf, 16 Jun. 2000, *R. Nasit* (**holotype** BCC 2711, culture ex-type BCC 2711). GenBank: LSU = EU369035, *TEF1* = EU369018, *RPB1* = EU369056, *RPB2* = EU369076.

White mycelia growing over the spider, densely on the abdomen, occasionally on the cephalothorax and legs (Fig. 7A). *Synnema* arising from the posterior part of the host, cylindric, attenuated, approximately 3 mm long, 70 µm wide, white at the base, becoming brown to greenish brown upward, enlarging into inconspicuous swollen tip with acute apex (Fig. 7A–D). *Conidiophores* arising from outer layer of hyphal network of the synnema, absent in the lower part, scattered, occasionally septate at base, minutely roughened, (42.5–)55–85(–90) × 7.5–9.5(–10) µm, tapering abruptly in a slender apex and terminating into a swollen vesicle (Fig. 7E–F). *Vesicles* globose to subglobose, (7.5–)8.5–10.5(–11) µm diam bearing multiple metulae (Fig. 7G). *Metulae* broadly obovoid, (7–)7.5–9(–10) × (5–)5.5–6.5(–7) µm (Fig. 7G). *Phialides* borne on metulae, narrowly clavate to cylindrical, apically thickened, occasionally with very short neck, (6–)7–8(–9) × 2–2.5(–3) µm, each bearing a conidium (Fig. 7G). A vesicle, metulae and phialides forming a spherical conidial head, 38–41(–42) µm diam (Fig. 7E–G). *Conidia* ellipsoid, narrowly ovoid, sometimes with an acute end, (2.5–)3–3.5(–4) × 1–1.5 µm (Fig. 7H). *Granulomanus* synasexual morph and sexual morph not observed.

Culture characteristics: Colonies on PDA attaining a diam of 1.5 cm in 24 d at 25 °C, cottony, brownish white; reverse light brown, darkening with age, starting from the centre (Fig. 7I). Sporulation not observed in culture.

Notes: Besides *G. longispora*, *G. nigelii* (formerly known as *G. pulchra* NHJ 10808) has also frequently been included in phylogenetic analyses to represent *G. pulchra* (Johnson *et al.* 2009, Kepler *et al.* 2011, Chiriví-Salomón *et al.* 2015, Thanakitpipattana *et al.* 2020). However, morphological data indicate that NHJ10808 represents a different species. Even though *G. nigelii* and *G. pulchra* show morphological resemblance in having nearly the same microscopic characters, they can be distinguished from each other by the outer appearances. *Gibellula pulchra* typically produces numerous synnemata; however, *G. nigelii* formed only a single synnema and could thus not be assigned to the same species. In addition, the arrangement of conidiophores on

Table 3. Morphological comparison of *G. longispora*, *G. nigelii*, *G. parvula*, *G. pulchra* and *G. solita* with the type strain of *G. pulchra* and other records of the species.

Characters	***G. longispora***	***G. nigelii***	***G. parvula***	***G. pulchra***	***G. solita***	**The type of *G. pulchra* (Cavara 1894)**	***G. pulchra* (Mains 1950)**	***G. pulchra* (Kobayasi *et al.* 1977)**	***G. pulchra* (Tzean *et al.* 1997)**	***G. pulchra* (Selcuk *et al.* 2004)**
Locality	Thailand	Thailand	Thailand	Thailand	Thailand	Italy	America	Japan	Taiwan	Turkey
***Gibellula* asexual morph**	Present	Present	Present	Present	Present	Present	Present	Present	Present	Present
Mycelia	White	White	Yellowish-white	Yellow	Yellow	—	Yellow or yellowish-white	White	White or yellowish-white	Whitish brown, pinkish when dried
Synnemata	At least 20 synnemata cylindrical attenuated	Solitary, white at the base, becoming brown to greenish-brown upward, cylindrical, with indistinct swollen tip, 3 mm × 70 µm	A pair of two yellowish-white, cylindrical, with ovoid tips	Numerous, yellowish-white, cylindrical attenuated, 5 mm × 150 µm	A group of three, brownish-white, cylindrical, attenuated, with ovoid tips, 7 mm × 175 µm	—	Numerous, yellowish-brown, cylindrical, sometimes slightly enlarged above	Numerous, cylindrical, attenuated, 4–5 mm × 400–800 µm	Solitary to numerous, cylindrical	Whitish brown, pinkish when dried cylindrical, 1.5–3 mm × 100–200 µm
Conidiophores (µm)	Crowded, minutely rough-walled, multi-septate, 105–415 × 6–15	Scattered, minutely rough-walled, septate at base, 42.5–90 × 7.5–10	Crowded, rough-walled, multi-septate	Hyaline, rough-walled, 87.5–250 × 6–10	Rough-walled, multi-septate, 62.5–180 × 7.5–10	Multi-septate, 100–120 × 7–8	Hyaline, smooth-walled, 150–600 × 7–12	Septate, 5–8 µm wide	Darkly pigmented, rough-walled, 110–640 × 7.9–10.3	Pale brown, smooth-walled, 155–170 × 6–10
Conidial heads (µm)	Spherical, 37–42	Spherical, 38–42	Spherical, 30–40	Spherical, 34–41	Spherical, 30–33	Spherical, 30–40	Spherical, 30–42	Spherical, 40–50	Spherical, 40–48	Spherical, 40–43
Vesicle (µm)	Globose to subglobose, 7–9	Globose to subglobose, 7.5–11	Globose to subglobose, 6.5–9	Ellipsoidal to globose, 9–11	Globose to subglobose, 6.5–8.5	—	Ellipsoidal, obovoid, 6.4–10	Globose, 6–8	Ellipsoidal to globose, 8.7–10.3 × 7.9–8.7	Globose, obovoid or broadly-clavate, 7.5–10
Metulae (µm)	Broadly obovoid, 6.5–10 × 5.5-7	Broadly obovoid, 7–10 × 5–7	Broadly obovoid, 6–10 × 4.5–8	Broadly obovoid, 8–10 × 6–8	Broadly obovoid, 6.5–8 × 5–7	—	Broadly obovoid, 6–12 × 4–6	Obpyriform, 8–12 × 3–4	Broadly obovoid, 7.9–9.9 × 5.2–6.4	Narrowly clavate, 7.5–8 × 1.5–2.5
Phialides (µm)	Narrowly clavate to cylindric, 8.5–11.5 × 2.5–4	Narrowly clavate to cylindric, 6–9 × 2–3	Narrowly clavate to cylindric, 6–10 × 2–4	Clavate to cylindric, 6–9 × 2–3	Narrowly clavate to cylindric, 6–7.5 × 2–2.5	—	Clavate, 6–10 × 2–3	Sub-cylindric or clavate, 7–10 × 2–2.5	Narrowly clavate with a short neck, 6.4–10.3 × 2–2.4	Cylindrical with a short neck, 6.2–7.5 × 5

Table 3. (Continued).

Characters	*G. longispora*	*G. nigelii*	*G. parvula*	*G. pulchra*	*G. solita*	The type of *G. pulchra* (Cavara 1894)	*G. pulchra* (Mains 1950)	*G. pulchra* (Kobayasi *et al.* 1977)	*G. pulchra* (Tzean *et al.* 1997)	*G. pulchra* (Selcuk *et al.* 2004)
Conidia (µm)	Bacilliform to cylindric, often in chains of up to 4 conidia, 3.5–9 × 1–1.5	Ellipsoid, narrowly ovoid, sometimes with an acute end, 2.5–4 × 1–1.5	Narrowly ovoid or narrowly ellipsoid or bacilliform, 4–6 × 2–4	Ellipsoid, 2–4 × 1–1.5	Ellipsoid to ovoid, 1.5–3 × 1–2	Cylindric to ovate-oblong, 3–4 × 1	Fusoid to fusoid-ellipsoid, 2.5–6.4 × 1.5–2.5	Single or in chains, fusiform-ellipsoidal, 4–6 × 1.5–2	Ellipsoid to fusiform, smooth-walled, 4–6 × 2–2.4	Fusiform to fusiform-ellipsoid, smooth-walled, 3–5 × 1.5–2.5
***Granulomanus* asexual morph**	Absent	Absent	Absent	Absent	Absent	Absent	Absent	Absent	Absent	Absent
Sexual morph	Absent	Absent	Absent	Absent	Absent	Absent	Present	Present	Absent	Absent
Perithecia (µm)	—	—	—	—	—	—	Superficial, light yellowish brown to reddish brown above, narrowly ovoid to conoid, 550–1 200 × 230–350	Almost covered with white hypha, dark ashy grey, narrowly ovoid to conoid, 1 000–1 200 × 250–300	—	—
Asci (µm)	—	—	—	—	—	—	Narrowly cylindrical, with thickened cap, 450–660 × 4–6	Narrowly cylindrical, with thickened cap, 1.5–2.5 µm wide	—	—
Ascospores (µm)	—	—	—	—	—	—	Hyaline, filiform, multi-septate, 450–660 × 1.5	n/a	—	—
Part-spores (µm)	—	—	—	—	—	—	No data, 4–10 × 1.5	Bacilliform to cylindric, 5–7 × 1.2–1.5	—	—

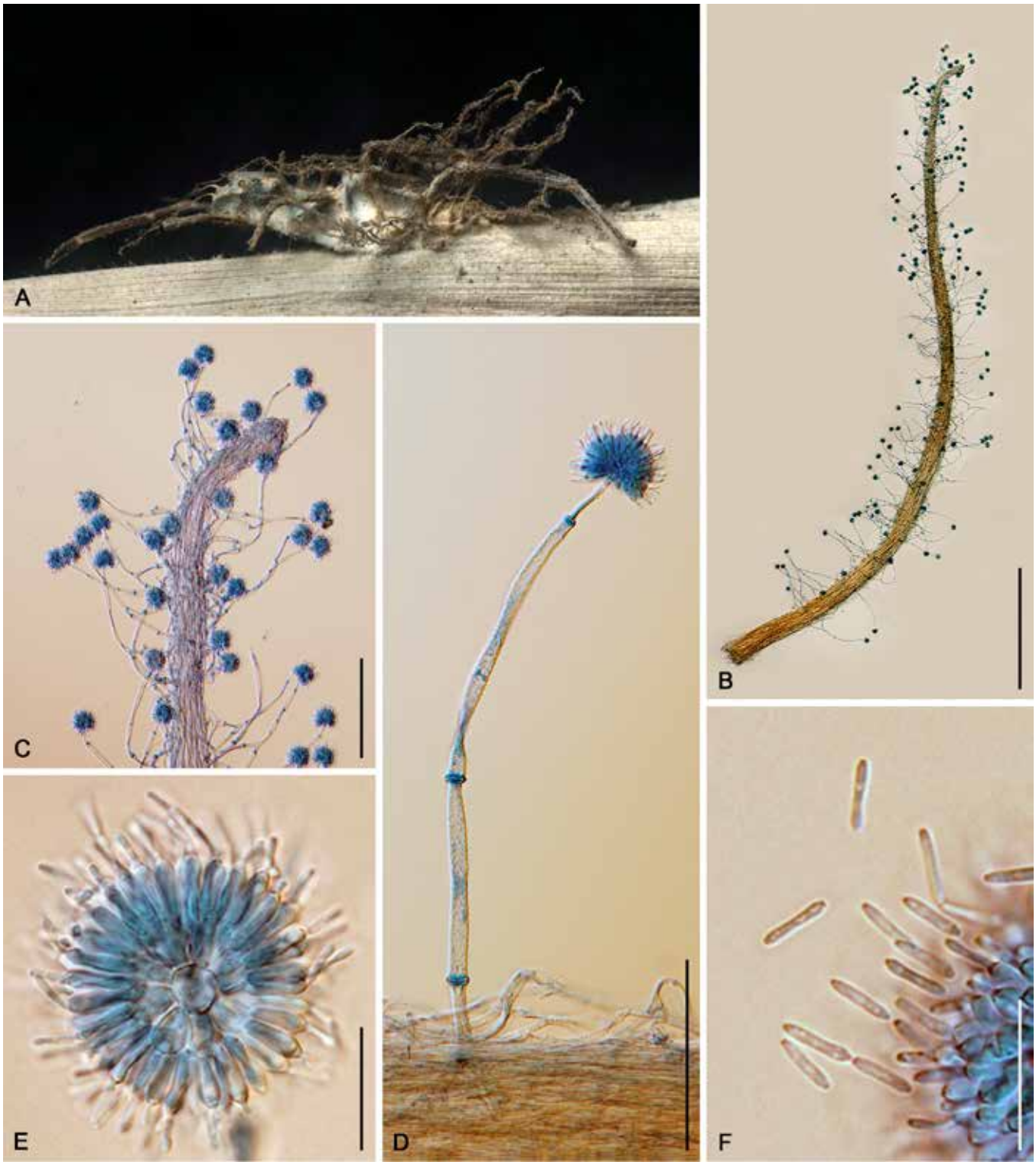

Fig. 6. *Gibellula longispora*. **A.** Fungus on spider. **B.** Synnema. **C.** Upper part of synnema. **D.** Conidiophore bearing aspergillus-like conidial head. **E.** Conidial head bearing conidia. **F.** Conidia. Scale bars: B = 1 mm; C= 200 µm; D = 100 µm; E = 20 µm; F = 10 µm.

synnemata appeared to be an informative character for species discrimination – the conidiophores are scattered in *G. nigelii* but crowded in *G. pulchra*. These differences together with the phylogenetic placements suggested proposing the strain NHJ 10808 as a new species.

Herein, the conidiophore lengths of *G. nigelii* might be inaccurate as the actual length might be longer. In general, the conidiophore is shorter the further up the synnema. To preserve the fungal specimens, only the upper part of a synnema (approximately 830 µm) was taken for the morphological study.

Gibellula parvula Kuephadungphan, Tasanathai & Luangsa-ard, ***sp. nov.*** MycoBank MB 841090. Fig. 8.

Etymology: Refers to the tiny spider host.

Typus: **Thailand**, Nakhon Ratchasima Province, Khao Yai National Park, Mo Sing To Nature Trail, on *Theridiidae* attached to the underside of a dicot leaf, 30 Aug. 2011, *K. Tasanathai, P. Srikitikulchai* & *S. Mongkolsamrit* (**holotype** BBH31330, culture ex-type BCC 49748). GenBank: ITS = OK040732, LSU = OK040709, *TEF1* = OK040700, *RPB1* = OK040718, *RPB2* = OK040726.

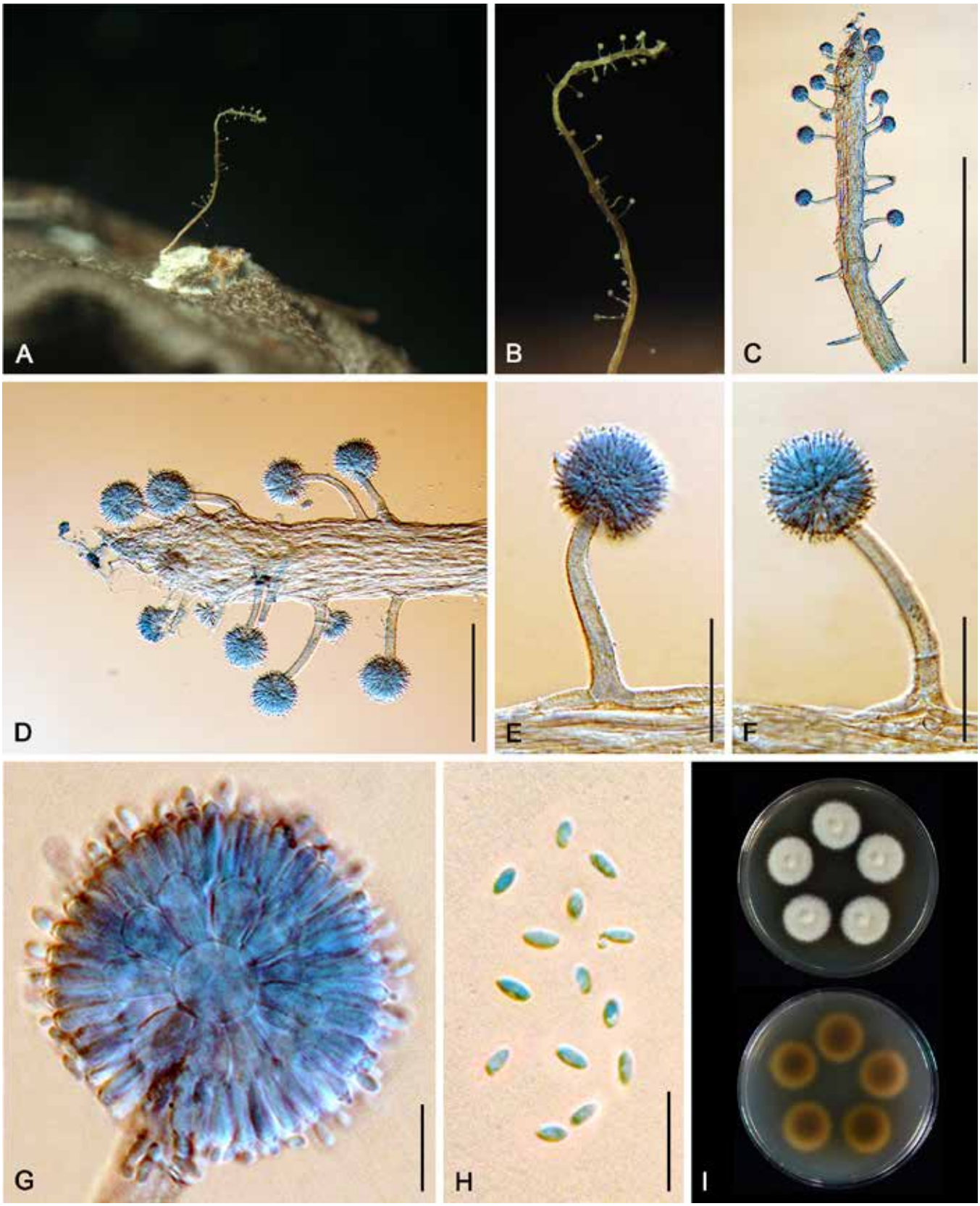

Fig. 7. *Gibellula nigelii*. **A.** Fungus on spider. **B–C.** Synnema. **D.** Upper part of a synnema showing a slight enlarged tip. **E–F.** Conidiophore showing a spherical conidial head. **G.** Conidial head bearing conidia. **H.** Conidia. **I.** Colonies obverse and reverse on PDA at 25 °C after 28 d. Scale bars: C = 500 µm; D = 100 µm; E–F = 50 µm; G–H = 10 µm.

Spider completely covered by a yellowish white mycelial mat (Fig. 8A). *Synnemata* yellowish white, a pair of two, cylindrical, swollen into an ovoid tip, 125 µm wide (Fig. 8B–C). *Conidiophores* arising from the mycelium covering the host and from a network of hyphae loosely attached to the surface of the synnemata, along its entire length, crowded, septa conspicuous, verrucose, (47.5–)85–145(–185) × (6–)8–10(–11) µm, narrowing abruptly to a slender apex, and terminating in a swollen vesicle (Fig. 8D–F). *Vesicles* globose to subglobose, (6.5–)7–8(–9) µm diam, bearing multiple broadly obovoid metulae, (6–)7–8.5(–10) × (4.5–)5–6.5(–8) µm (Fig. 8G). *Phialides* borne on metulae, narrowly clavate to cylindric with both round ends, (6–)7–9(–10) × (2–)2.5–3(–4) µm, each bearing a

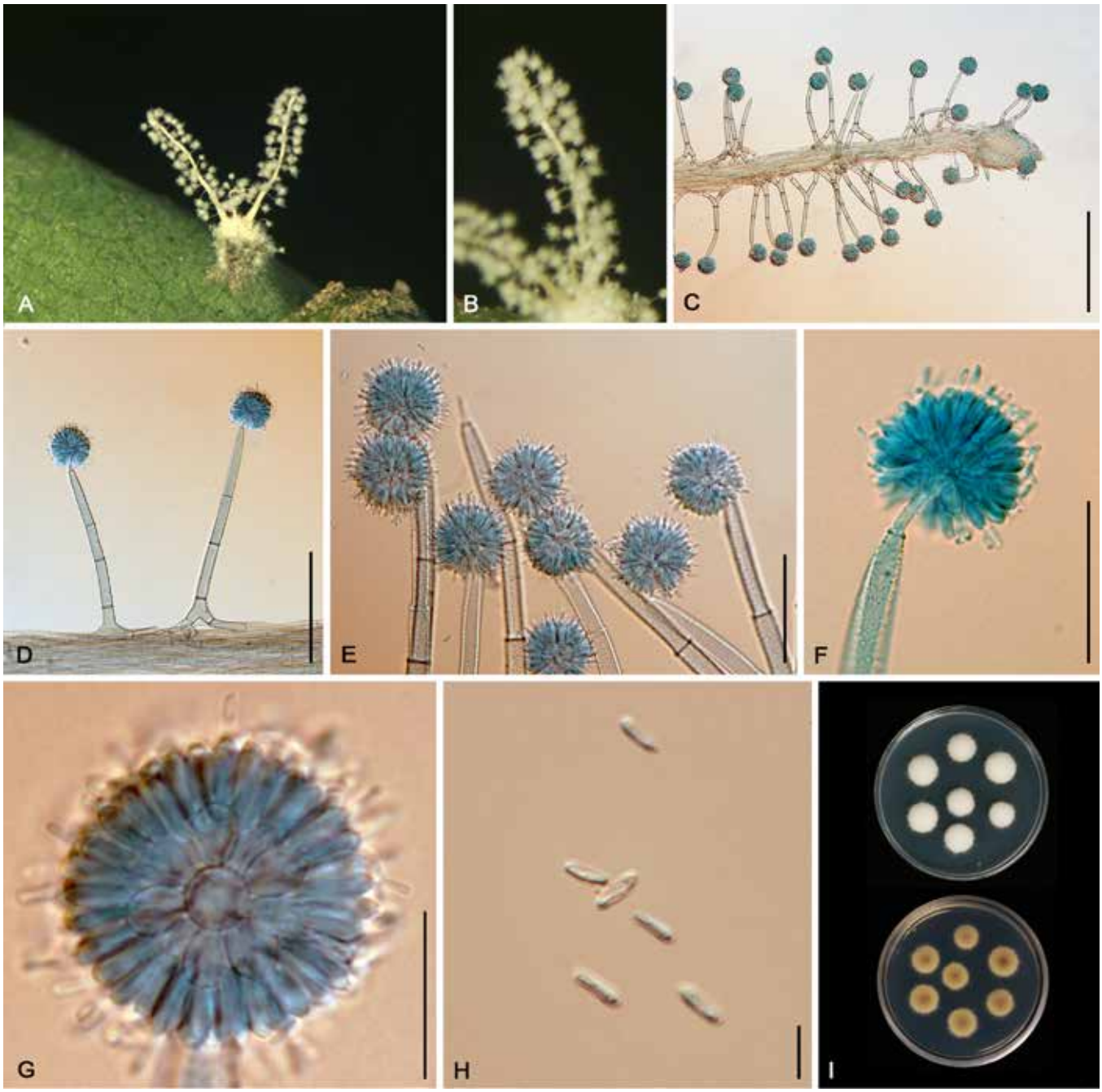

Fig. 8. *Gibellula parvula*. **A.** Fungus on spider (BBH 31330). **B.** Synnemata (BBH 31330). **C.** Upper part of a synnema showing enlarged tip (BBH 31330). **D–F.** Conidiophores showing spherical conidial heads (BBH 31330 and BBH 31446). **G.** Conidial head bearing conidia (BBH 31330). **H.** Conidia (BBH 31446). **I.** Colonies obverse and reverse on PDA at 25 °C after 20 d. Scale bars: C = 250 µm; D = 100 µm; E–F = 50 µm; G = 20 µm; H = 5 µm.

conidium or occasionally a chain of conidia. *Conidia* narrowly ovoid or narrowly ellipsoid or bacilliform, 4–5.5(–6) × (2–)2.5–3(–4) µm (Fig. 8H). Vesicle, metulae and phialides forming spherical conidial heads, (30–)33.5–37(–40) µm diam (Fig. 8D–G).

Culture characteristics: Colonies on PDA attaining a diam of 1 cm in 20 d at 25 °C, white, cottony; reverse light brown, darkening with age toward center (Fig. 8I). Sporulation not observed in culture.

Material examined: **Thailand**, Nakhon Ratchasima Province, Khao Yai National Park, Mo Sing To Nature Trail, on *Theridiidae* attached to the underside of a dicot leaf, 5 Jul. 2011, *K. Tasanathai, P. Srikitikulchai* & *S. Mongkolsamrit* (BBH31446, living culture BCC 48888).

Gibellula pilosa Kuephadungphan, Tasanathai & Luangsa-ard, ***sp. nov.*** MycoBank MB 841092. Fig. 9.

Etymology: Refers to the outer appearance of the species that is very hairy.

Typus: **Thailand**, Nakhon Ratchasima Province, KhaoYai National Park, Fern Nature Trail, on non-web builder *Araneomorphae* attached to the underside of a dicot leaf, 8 Nov. 2012, *S. Mongkolsamrit, A. Khonsanit, W. Noisripoom, P. Srikitikulchai* & *R. Somnuk* (**holotype** BBH35197, culture ex-type BCC 57817). GenBank: ITS = OK040733, LSU = OK040710, *TEF1* = OK040701, *RPB1* = OK040719.

Spider completely covered by yellowish-light brown mycelial mat (Fig. 9A). *Synnemata* pale brown, cylindrical, in pairs, 6 mm long,

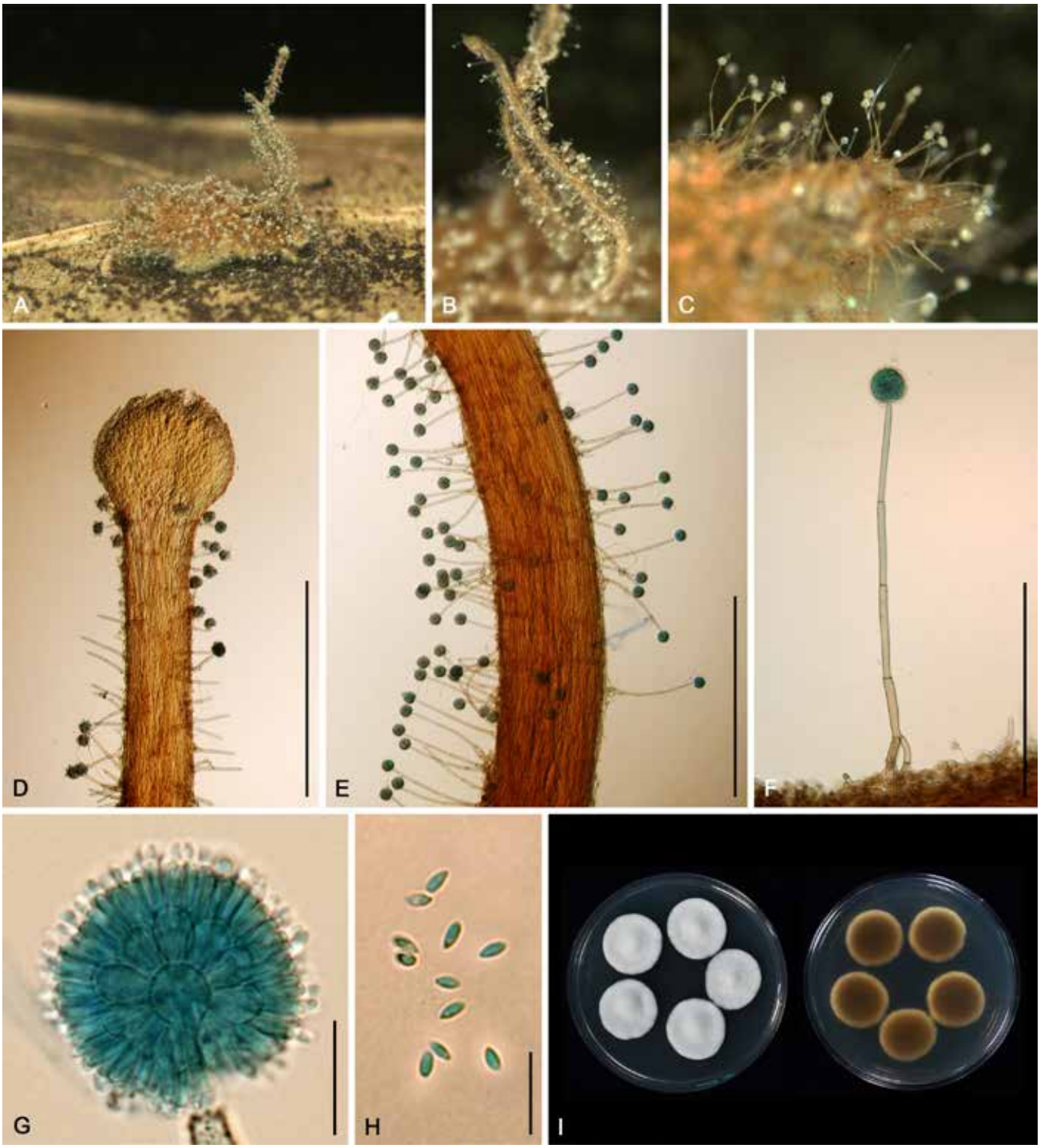

Fig. 9. *Gibellula pilosa*. **A.** Fungus on spider. **B.** Synnemata. **C.** Conidiophores arising from the mycelial mat covering the host. **D.** Upper part of a synnema showing globose tip. **E.** Part of synnema showing conidiophores. **F.** Conidiophore bearing a spherical conidial head. **G.** Conidial head bearing conidia. **H.** Conidia. **I.** Colonies obverse and reverse on PDA at 25 °C after 28 d. Scale bars: D = 1 mm; E = 500 µm; F = 250 µm; G = 20 µm; H = 10 µm.

475 µm wide, terminating in a swollen sterile globose tip, 600 µm wide (Fig. 9A–D). *Conidiophores* arising laterally from the outer layer of synnemata and from the mycelia covering all over the host, distinctly crowded, septa conspicuous, minutely roughened, (140–)151–265(–420) × (8.5–)9–11(–13.5) µm, narrowing to a slender apex, and terminating in a swollen vesicle (Fig. 9C–G). *Vesicles* spherical, (9–)10–11(–12) µm diam, bearing multiple metulae (Fig. 9G). *Metulae* broadly obovoid, (9–)9.5–11(–12) × (6–)7–8(–9) µm (Fig. 9G). *Phialides* borne on metulae, narrowly clavate to cylindrical, 7–9(–10) × 2.5–3 µm, bearing conidia (Fig. 9G). *Conidia* narrowly almond-shaped, 3–4 × 1.5–2 µm (Fig. 9H). Vesicle, metulae, phialides forming a spherical conidial head, (41–)41.5–43(–45) µm diam (Fig. 9G). Sexual morph and *Granulomanus* synasexual morph not observed.

Culture characteristics: Colonies on PDA attaining a diam of 1.7 cm in 28 d at 25 °C, white, cottony; reverse pale brown, darkening with age toward centre (Fig. 9I). Sporulation not observed in culture.

Gibellula pulchra (Sacc.) Cavara, Atti Ist. Bot. Univ. Pavia Ser II, 3: 347. 1894. Figs 10, 11.

Spider host fully covered by yellow mycelial mat (Fig. 10A). *Synnemata* consisting of multiseptate longitudinal hyphae, numerous, arising from all over the host body, yellowish white, cylindrical, slightly narrowing towards the indistinct enlarged tip, 5 mm long, 150 µm wide (Fig. 10B–D). *Conidiophores* arising from a network of hyphae loosely attached to the surface of the synnemata along the entire length of synnemata, except for the base, roughened conspicuous, (87.5–)120–215(–250) × (6–)7.5–9(–10) µm, becoming short towards the tip of synnemata, abruptly tapering into a slender apex and terminating in a swollen vesicle, bearing a group of metulae, phialides and forming a spherical conidial head, (34–)35.5–38.5(–41) µm diam (Fig. 10C–E). *Vesicles* subglobose to globose, (9–)9.5–10.5(–11) µm diam (Fig. 10F). *Metulae* borne on vesicle, broadly obovoid, 8–9.5(–10) × 6–7(–8) µm, bearing phialides (Fig. 10F). *Phialides* narrowly clavate to cylindrical, 6–8(–9) × 2–2.5(–3) µm, each bearing a single conidium (Fig. 10F). *Conidia* ellipsoid, occasionally with an indistinct acute apex, (2–)2.5–3(–4) × 1–1.5 µm (Fig. 10G). Sexual morph and *Granulomanus* synasexual morph not observed.

Culture characteristics: Colonies on PDA attaining a diam of 1.3 cm in 20 d at 25 °C, white, cottony; reverse pale brown, becoming dark brown with age at the centre (Fig. 10H). Sporulation not observed in culture.

Material examined: **Thailand**, Nakhon Ratchasima Province, Khao Yai National Park, Mo Sing To Nature Trail, on *Salticidae* attached to the underside of a dicot leaf, 27 Apr. 2011, *K. Tasanathai, P. Srikitikulchai, S. Mongkolsamrit, A. Khonsanit, K. Sansatchanon* & *W. Noisripoom* (BBH30518, living culture BCC 47555).

Notes: Among *Gibellula* spp. producing aspergillus-like conidiophores, *G. longispora* bears the greatest morphological resemblance to *G. pulchra* in having almost identical macroscopic and microscopic features. They can be distinguished from each other only by the shape of conidia – *G. pulchra* typically produces cylindrical, ellipsoid to ovoid conidia (Fig. 11) whereas *G. longispora* produces only bacilliform conidia which are significantly longer than those reported for *G. pulchra*. Even though their outer appearances can easily mislead species identification, the multilocus-based phylogenetic analysis showed very clear segregation between them by placing *G. longispora* far from *G. pulchra* (Fig. 1). Considering the sister clades of *G. pulchra* and *G. nigelii*, *G. nigelii* has markedly smaller conidia (Table 3). Since the number of synnemata and the arrangement of conidiophores on synnemata are important features used effectively in species discrimination within the genus *Gibellula*, *G. pulchra* can be simply distinguished from *G. nigelii* by forming numerous synnemata with crowded conidiophores (Fig. 10A–D) whereas *G. nigelii* produces a single synnema with scattered conidiophores.

Gibellula solita Kuephadungphan, Tasanathai & Luangsa-ard, ***sp. nov.*** MycoBank MB 841094. Fig. 12.

Etymology: From the Latin '*solitus*', meaning usual, referring to the original feature of *Gibellula* of producing aspergillus-like conidiophores.

Typus: **Thailand**, Buri Ram Province, Dong Yai Wildlife Sanctuary, Pa Takong Nature Trail, on *Theridiidae* attached to the underside of a dicot leaf, 10 Dec. 2010, *K. Tasanathai, P. Srikitikulchai, A. Khonsanit, K. Sansatchanon, W. Noisripoom, A. Saksrikrom, B. Saracam* & *S. Mongkolsamrit* (**holotype** BBH38545, culture ex-type BCC 45574). GenBank: ITS = OK040736, LSU = OK040712, *TEF1* = OK040703, *RPB1* = OK040721.

Yellow mycelia fully covering the spider body, occasionally on its legs (Fig. 12A). *Synnemata* brownish white in a group of three, cylindrical, attenuated, 7 mm long, 175 µm wide, narrowing to a slender apex, terminating into a swollen tip (Fig. 12B–D). *Conidiophores* scattered, arising from the outer layer of synnemata and the mycelia somewhat loosely attached to the host body and legs, multiseptate, verrucose, (62.5–)82–146(–180) × 7.5–9.5(–10) µm, becoming shorter towards the tip of synnemata, tapering abruptly to a distinct neck, enlarging into a vesicle (Fig. 12G). *Vesicle* globose to subglobose, (6.5–)7–8(–8.5) µm diam, bearing a group of metulae (Fig. 12G). *Metulae* broadly obovoid, (6.5–)7–7.5(–8) × 5–6(–7) µm. *Phialides* borne on metulae, narrowly clavate to cylindrical, 6–7(–7.5) × 2–2.5 µm, each bearing a conidium (Fig. 12G). A vesicle, metulae and phialides forming a spherical conidial head, (30–)30.5–32.5(–33) µm diam (Fig. 12G). *Conidia* ellipsoid to ovoid, occasionally globose, (1.5–)2–2.5(–3) × 1–1.5(–2) µm (Fig. 12H).

Culture characteristics: Colonies on PDA attaining a diam of 1.1 cm in 20 d at 25 °C, white, cottony; reverse pale brown, darkening with age towards the centre (Fig. 12I). Sporulation not observed in culture.

Notes: In comparison with *G. unica* which was phylogenetically placed close to *G. solita* as a sister clade (Fig. 1), *G. solita* can be easily distinguished from *G. unica* in mostly having ovoid conidia with the length almost twice shorter as well as distinctly producing shorter conidiophores. However, it might be difficult to tell them apart based solely on the outer appearances as they both produce a single to a few long synnemata.

Gibellula trimorpha Tasanathai, Khonsanit, Kuephadungphan & Luangsa-ard, ***sp. nov.*** MycoBank MB 841089. Fig. 13.

Etymology: Refers to the three different reproductive morphs occurring simultaneously on a single specimen.

Typus: **Thailand**, Phetchabun Province, Nam Nao National Park, Headquarter Nature Trail, on *Salticidae* attached to the underside of a dicot leaf, 6 May 2009, *K. Tasanathai, P. Srikitikulchai, S. Mongkolsamrit* & *T. Chohme* (**holotype** BBH27981, culture ex-type BCC 36526). GenBank: ITS = OK040737, *TEF1* = OK040704, *RPB1* = OK040722, *RPB2* = OK040728.

Spider host covered by brown mycelial mat. *Synnema* arising directly from the host abdomen, erect, cylindrical, short stipe, white, 3 mm long, composed of parallel, densely compacted hyphae (Fig. 13A). *Conidiophores* hyaline, septate, 65–230 × 7–9 µm (Fig. 13B–C). *Conidial heads*, 37–44 µm diam (Fig. 13C). *Vesicle* ellipsoidal, subglobose to globose, smooth, hyaline, 9–12 × 7–10 µm. *Metulae* broadly ellipsoidal, hyaline, smooth occasionally, 7–10 × 6–7 µm. *Conidia* fusiform, in short chains, 4–5 × 2 µm. *Conidiophores* of *Granulomanus* synasexual morph present, well-differentiated, roughened to distinctly verrucose, particularly around the base. *Phialides* holoblastic, cylindrical, clavate, flask-shaped, to irregularly shaped, mostly verrucose, rarely smooth, with one to three conspicuous denticles, 8–13 × 3 µm, bearing solitary, long, filiform conidia. *Conidia* smooth, hyaline, 10–19 × 1–1.5 µm (Fig.

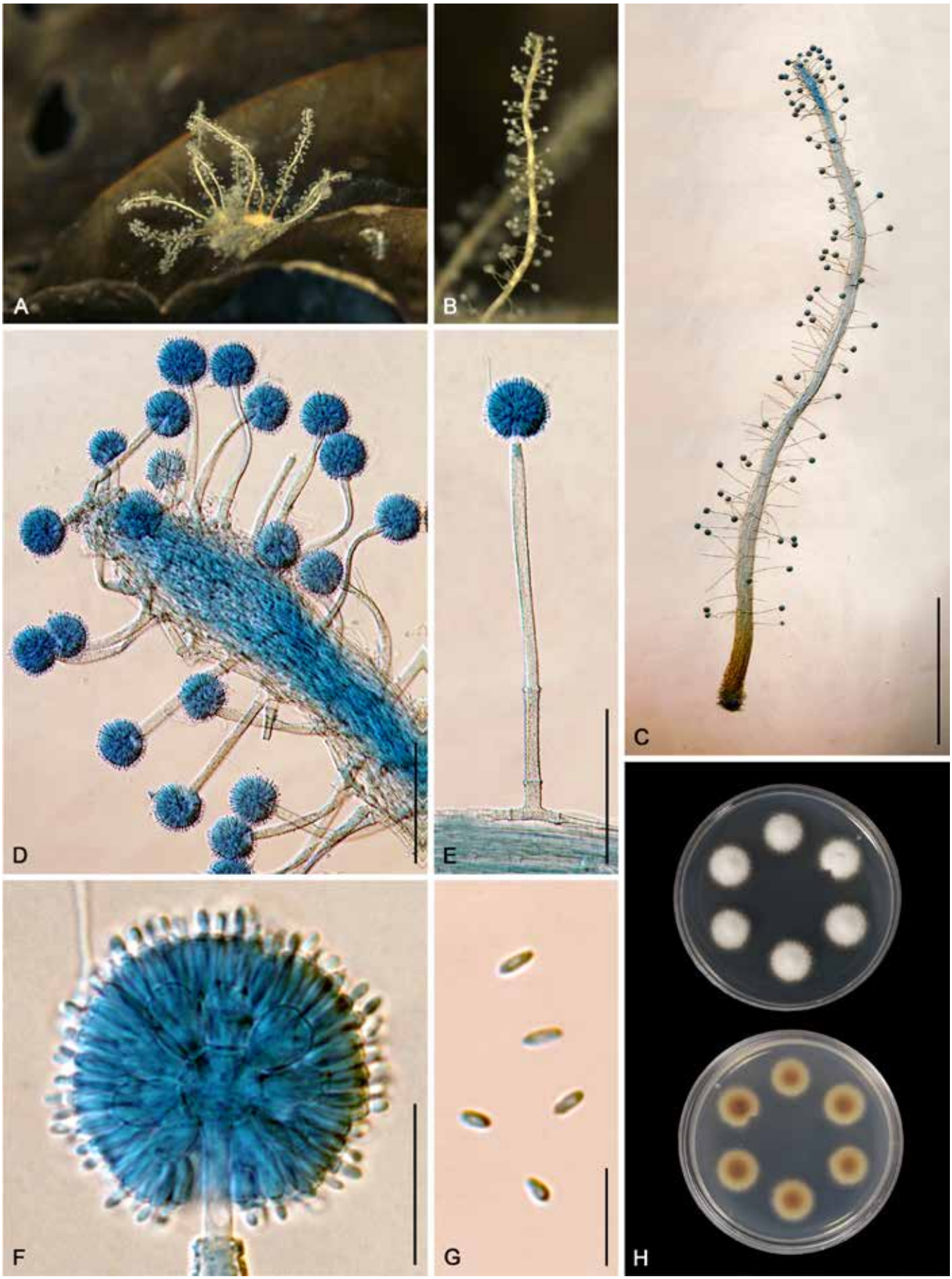

Fig. 10. *Gibellula pulchra*. **A.** Fungus on spider. **B–C.** Synnemata. **D.** Upper part of synnema showing a slight enlarged tip. **E.** Conidiophore showing a spherical conidial head. **F.** Conidial head bearing conidia. **G.** Conidia. **H.** Colonies obverse and reverse on PDA at 25 °C after 20 d. Scale bars: C = 1 mm; D–E = 100 µm; F = 20 µm; G = 10 µm.

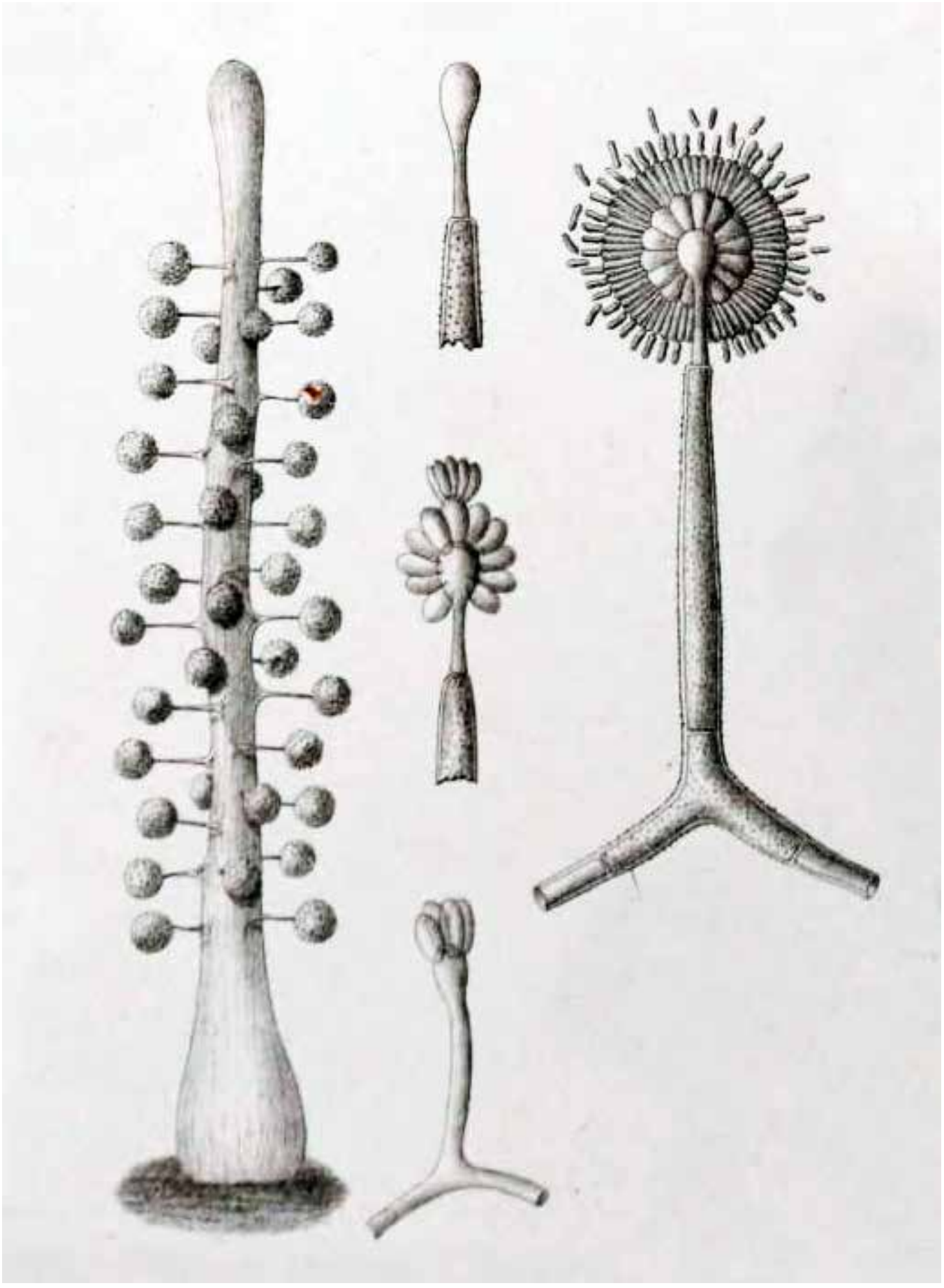

Fig. 11. *Gibellula pulchra* (Sacc.) Cavara, Atti Ist. Bot. Univ. Pavia Ser II, 3: 347. 1894.

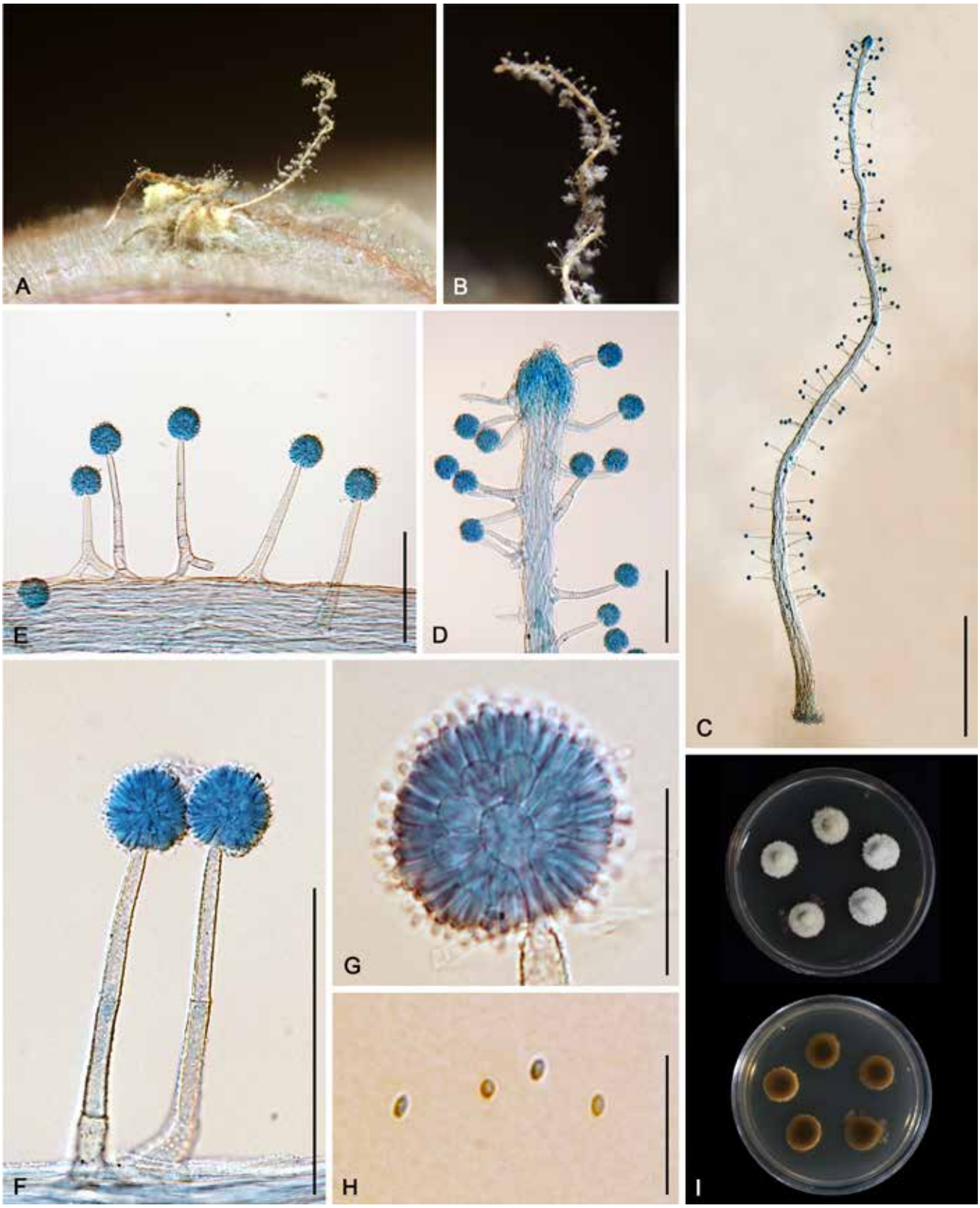

Fig. 12. *Gibellula solita*. **A.** Fungus on spider. **B–C.** Synnema. **D.** Upper part of synnema showing a swollen tip. **E–F.** Conidiophores showing spherical conidial heads. **G.** Conidial head bearing conidia. **H.** Conidia. **I.** Colonies obverse and reverse on PDA at 25 °C after 20 d. Scale bars: C = 1 mm; D–F = 100 µm; G = 25 µm; H = 10 µm.

13D). Sexual morph present. *Perithecia* occurring on the mycelial mat covering the host body, superficial, ovoid, reddish-brown, two-third covered with the loose network of mycelia, (340–)470–690 × (200–)214–282(–310) µm (Fig. 13E). *Asci* cylindrical, 340–530 × (7–)7.5–9(–10) µm. *Asci caps*, 4–5(–5.5) × (5–)6–7.5(–8) µm (Fig. 13F–G). *Ascospores* filiform, multiseptate, breaking into bacilliform part-spores, (3–)4–6(–9) × 1.5–2(–2.5) µm (Fig. 13H).

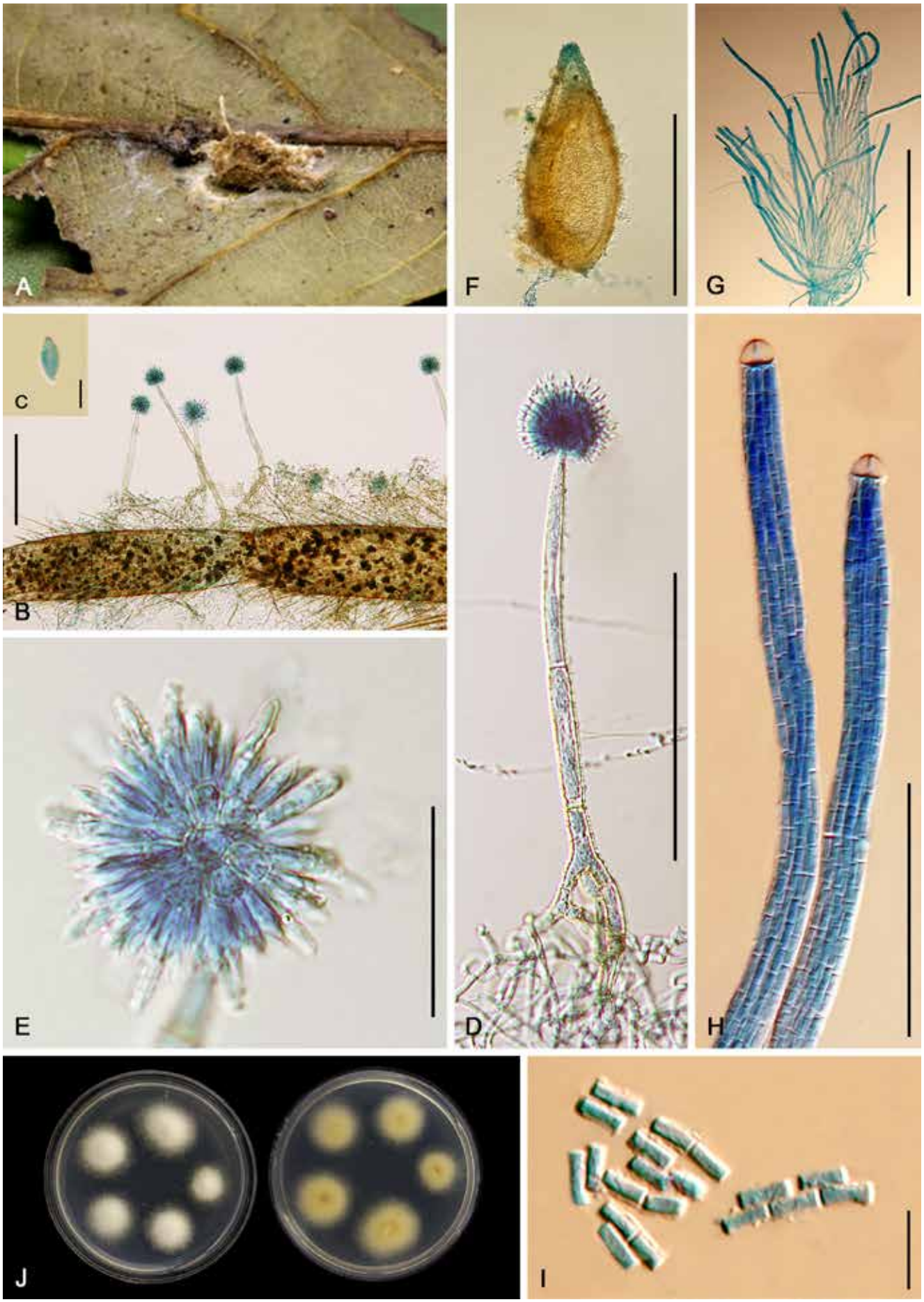

Fig. 13. *Gibellula trimorpha*. **A.** Fungus on a spider. **B.** Conidiophores arising from the mycelia covering the spider's leg. **C.** Conidium. **D.** Conidiophore of *Gibellula* conidial stage. **E.** *Granulomanus* conidial stage forming aspergillus-like conidial head. **F.** Perithecium. **G.** Asci. **H.** Asci with ascus caps. **I.** Part-spores. **J.** Colonies obverse and reverse on PDA at 25 °C after 20 d. Scale bars: F = 500 µm; B, G = 250 µm; D = 100 µm; H = 50 µm; E = 20 µm; I = 10 µm; C = 2 µm.

Culture characteristics: Colonies on PDA attaining a diam of 1.5 cm in 20 d at 25°C, white, velvety; reverse cream, becoming pale brown with age towards the centre (Fig. 13I).

Material examined: **Thailand**, Phetchabun Province, Nam Nao National Park, Headquarter Nature Trail, on *Oxyopidae* attached to the underside of a dicot leaf, 6 May 2009, *K. Tasanathai, P. Srikitikulchai, S. Mongkolsamrit & T. Chohme* (BBH29456, living culture BCC 36538).

Notes: *Gibellula trimorpha* shows morphological resemblance to *G. dimorpha* (Tzean *et al.* 1998) in bearing three different reproductive morphs consisting of a *Gibellula* conidial morph, *Granulomanus* conidial morph and *Torrubiella* sexual morph. It displays a distinct feature of aspergillus-like conidiophores bearing both *Gibellula* and *Granulomanus* phialides. Morphological comparison between *G. trimorpha* and *G. dimorpha* did not show any significant difference as all characters share similarity in shape and size falling within nearly the same ranges (Table 2), making it difficult to discriminate these two species based solely on morphology. Even so, the phylogenetic evidence highly supported *G. trimorpha* as a new species.

Gibellula unica L.S. Hsieh, Tzean & W.J. Wu, Mycologia 89: 312. 1997. Fig. 14.

Spider host covered by white mycelial mat. *Synnemata* cylindrical, attenuated, in groups of 2–3, white to brownish white (Fig. 14A–B). *Conidiophores* arising laterally from the outer layer of synnemata and directly from the mycelial mat covering the host, scattered, septate, roughed, (225–)235–273(–280) × (7.5–)8–11(–12) µm, terminating in a swollen vesicle (Fig. 14C–D). *Conidial heads* spherical, (28–)32–39(–40) µm diam (Fig. 14D). *Vesicles* subglobose to globose, 4–6 µm diam. *Metulae* broadly obovoid, 5–7(–9) × (3–)3.5–5(–6) µm. *Phialides* borne on metulae, broadly cylindrical to clavate, (5–)7–9(–10) × 2–3 µm, bearing a conidium. *Conidia* narrowly ellipsoid, (3–)4–5 × 2 µm (Fig. 14E). *Granulomanus* synasexual morph present, occurring on the synnemata or the mycelial mat covering the host, forming conidiophores or branched hyphae bearing polyblastic, irregularly shaped phialides (Fig. 14F–G). *Conidiophores* septate, roughened, 39.5–44.5 × 5–6 µm, abruptly narrowing toward the apex, forming a vesicle. *Vesicles* obovoid, 7.5 µm diam. *Metulae* broadly obovoid or irregularly shaped, 7.5 × 6 µm. *Phialides* broad cylindrical to clavate, 6–10(–11.5) × 3.5–4 µm (Fig. 14F), developing multiple denticles, each bearing a filiform conidium, (6–)17–22(–23) × 1 µm (Fig. 14H). Sexual morph not observed.

Table 4. Morphological comparison of Thai *G. unica* and the ex-type specimen.

Characters	***G. unica* from Thailand**	***G. unica* (Tzean *et al.* 1997)**
Locality	Thailand	Taiwan
Host	*Pholcidae*	*Arachnida*
***Gibellula* anamorph**	Present	Present
Mycelia	White	White
Synnemata	White to brownish-white, cylindrical, attenuated, in groups of 2–3	Yellowish grey, cylindrical, attenuated, in groups of 5–6, 4–5 mm × 96–184
Conidiophores (µm)	Arising from the synnemata and the mycelial mat covering the host, scattered, septate, rough-walled, 225–280 × 7.5–12	Arising from the synnemata and the mycelial mat covering the host, scattered or densely compacted, septate, rough-walled, 122–244 × 6.4–13.5
Conidial heads (diameter, µm)	Spherical, 28–40	Spherical, 40–52
Vesicle (diameter, µm)	Globose to subglobose, 4–6	Ellipsoidal, subglobose to globose, 7.1–9.9 × 5.6–7.9
Metulae (µm)	Broadly obovoid, 5–9 × 3–6	Broadly ellipsoidal, obovoid, 5.6–9.1 × 4.8–7
Phialides (µm)	Broadly cylindrical to clavate, 5–10 × 2–3	Broadly cylindrical to ellipsoidal with a short neck, apically thickened, 6.4–9.5 × 2.8–4.2
Conidia (µm)	Narrowly ellipsoid, 3–5 × 2	Fusiform, occasionally apiculate, in short chains, 4.0–6.8 × 1.6–2.2
***Granulomanus* anamorph**	Present, formed both aspergillus- and granulomanus-like conidiophores	Present, formed both aspergillus- and granulomanus-like conidiophores
Conidiophores (µm)	Occurring on the synnemata and the mycelial mat covering the host, septate, rough-walled, 39.5–44.5 × 5–6	Occurring particularly around the base of the synnemata, septate[1], rough-walled[1], (No data)
Vesicle (diameter, µm)	Obovoid, 7.5	Subglobose[1], (No data)
Metulae (µm)	Broadly obovoid, 7.5 × 6	Broadly ellipsoidal[1], (No data)
Phialides (µm)	Broadly cylindrical to clavate, 6–11.5 × 3.5–4	Holoblastic, cylindrical, clavate, flask-shaped to irregularly shaped, with 1–3 denticles, 6.8–11.9 × 3.2–4
Conidia (µm)	Filiform, 6–23 × 1	Filiform, 11.1–17.5 × 1.0–1.6
Teleomorph	Absent	Absent

[1]Based on the species description contributed by Tzean *et al*. (1997).

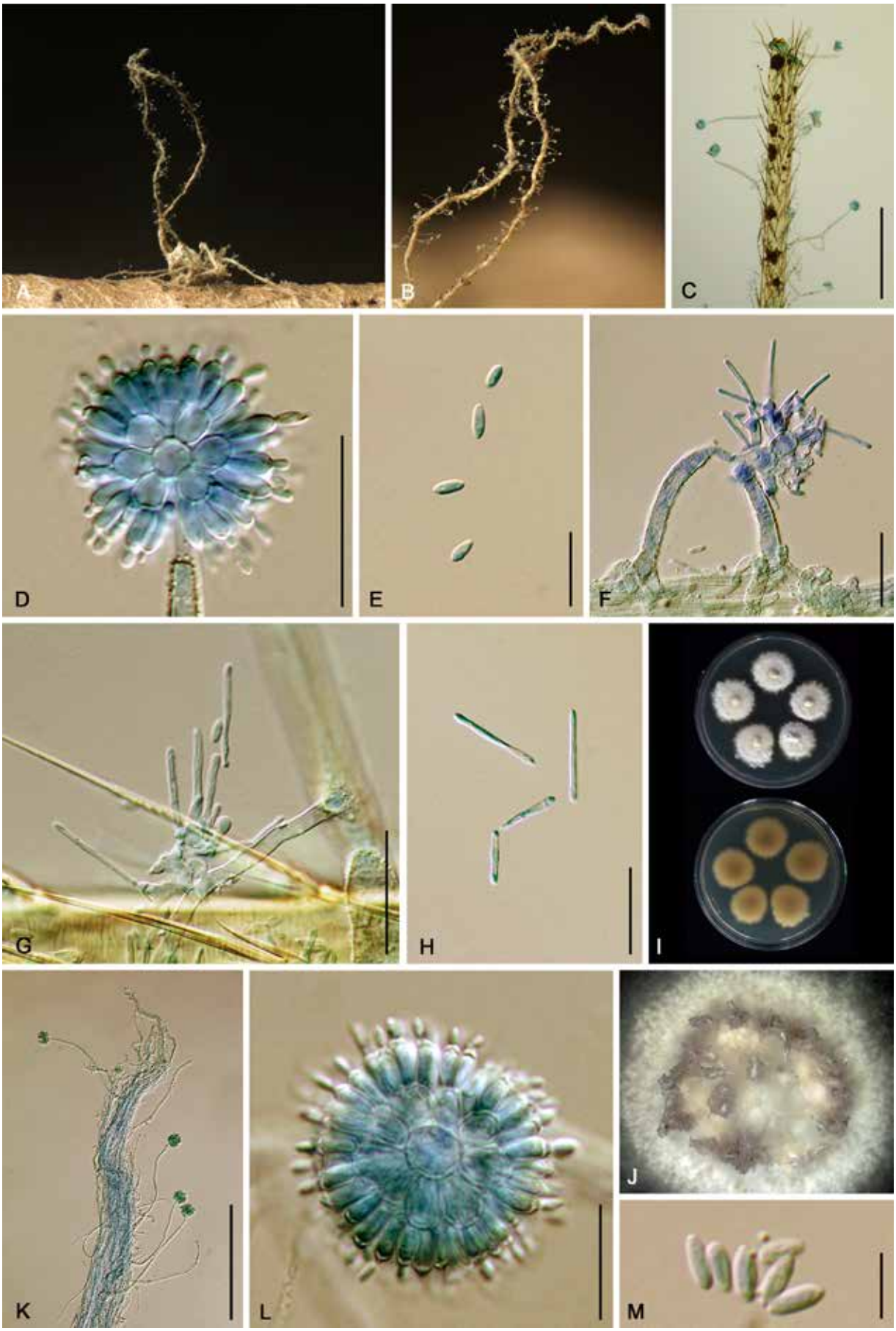

Fig. 14. *Gibellula unica*. **A.** Fungus on spider (BBH30027). **B.** Part of synnema showing conidiophores (BBH30034). **C.** Conidiophores arising from the mycelia covering a spider's leg (BBH30034). **D.** Conidial head of *Gibellula* conidial stage (BBH30034). **E.** Conidia of *Gibellula* conidial stage (BBH30034). **F.** *Granulomanus* conidial stage forming aspergillus-like conidiophores (BBH30034). **G.** Typical *Granulomanus* conidial stage occurring on the mycelial network covering a spider's leg. **H.** Filiform conidia of *Granulomanus* conidial stage. **I.** Colonies obverse and reverse on PDA at 25 °C at 28 d. **J.** Grayish-brown synnema formed on PDA after a month. **K.** Part of a synnema formed on PDA showing aspergillus-like conidiophores. **L.** Conidial head produced on PDA. **M.** Conidia produced on PDA. Scale bars: C = 500 µm; J = 200 µm; D, F, G, K, L = 20 µm; E, H = 10 µm; M = 5 µm.

Culture characteristics: Colonies on PDA attaining a diam of 1.7 cm in 28 d at 25 ºC, floccose, forming irregular margin, white to yellowish-white, reverse light brown, darkening towards the centre with age (Fig. 14I). Sporulation occurring after a month, forming synnemata in a circle, powdery, brownish grey. *Synnemata* composed of loose hyphae, white, becoming yellowish white toward base, cylindrical, tapered toward the apex, curved (Fig. 14J). *Conidiophores* crowded, septate, roughened, 192–227(–239) × (5–)6–8.5(–9) µm. *Conidial heads* spherical, (27–)29–33(–35) µm diam (Fig. 14K). *Vesicles* spherical, 7–9(–10) µm diam. *Metulae* borne on vesicle, obovoid, (5–)5.5–7.5(–10) × 4–6 µm, bearing multiple phialides. *Phialides* broad cylindrical to clavate, 5–6.5(–8) × 2–3 µm. *Conidia* narrow ellipsoid, (3–)4–5 × 1–2 µm (Fig. 14M).

Materials examined: **Thailand**, Kalasin Province, Phu Si Than Wildlife Sanctuary, Khok Pa Si Community Forest, on *Pholcidae* attached to the underside of dicot leaf, 24 Oct. 2010, *A. Khonsanit* (BBH30027, living culture BCC 45112 and BBH30034, living culture BCC 46590).

Notes: Besides *G. trimorpha* and *G. dimorpha*, *G. unica* is also known to have a *Granulomanus* conidial morph producing aspergillus-like conidiophores along with a *Gibellula* conidial morph. Nonetheless, *G. unica* can be distinguished from *G. trimorpha* and *G. dimorpha* by producing narrowly ellipsoidal *Gibellula* conidia instead of fusoid conidia. Moreover, its asexual-sexual link has not yet been found. Herein, we report *G. unica* from Thailand for the first time since the species was described *(*Tzean *et al.* 1997*)*. We also provide the description of colony morphology and the evidence of sporulation on an artificial medium. The Thai specimens were found to be very similar to the type of *G. unica* by having all morphological features in common. The Thai specimens only show slight differences in the size of *Gibellula (*shorter than type*)* and *Granulomanus (*longer than type*)* conidia *(*Table 4*)*. As the *Granulomanus* conidial morph could not be observed in specimen BBH30027, *G. unica* does not always produce a *Granulomanus* conidial morph along with a *Gibellula* morph.

DISCUSSION

Among *Gibellula* spp., *G. pulchra* has the longest and the most complicated nomenclatural history (Figs 10, 11). Several species were synonymised with *G. pulchra* (see Shrestha *et al.* 2019) causing confusion in the taxonomy of the genus. As *G. pulchra* is a cosmopolitan species, it has been recorded from many countries including Hawaii (USA), Puerto Rico, Venezuela, Guyana, Trinidad, Chile, Papua New Guinea (Mains 1950), Ghana (Samson & Evans 1973), Japan (Kobayasi 1977), Solomon Islands (Humber & Rombach 1987), Canada (Strongman 1991), Ecuador (Samson & Evans 1992), South Africa (Rong & Botha 1993), Taiwan (Tzean *et al.* 1997), Turkey (Selçuk *et al.* 2004), Thailand (Luangsa-ard *et al.* 2007) and Brazil (Costa 2014). According to the species description contributed by Mains (1950), Humber & Rombach (1987) and Tzean *et al.* (1997), *G. pulchra* can occur either in the absence or presence of a *Torrubiella* sexual morph or *Granulomanus* synasexual morph. Synnemata are numerous or solitary, clavate to cylindrical, yellow or yellowish white to brown or white or greyish or violet, violaceous brown to brown with age or when dried, sometimes slightly enlarged upwards of the tip, and consist of multiseptated longitudinal hyphae. Conidiophores arise from a network of hyphae loosely attached to the surface of the synnemata or occasionally from the mycelia covering the host body or legs. They are usually rough-walled and arranged in a hymenium along the length of synnemata, each abruptly tapering into a slender apex which subsequently enlarges into a globose, subglobose or obovoid vesicle which bears multiple broadly obovoid metulae. Phialides borne on metulae are narrowly clavate, thickened apically and sometimes extended into a short neck. A vesicle, together with multiple metulae and phialides, form a spherical head that bear either ovoid, fusoid, fusoid-ellipsoid or ellipsoid conidia. Conidia can be found singly or in chains. Based on these descriptions, the species proposed herein as *G. longispora*, *G. nigelii*, *G. parvula* as well as *G. solita* seemed to fit well with previous identifications as *G. pulchra*.

Based on our continuous survey and study of *Gibellula*, over 2 000 specimens exhibiting *Gibellula* traits have been collected, of which around 5 % were preliminarily identified as *G. pulchra*. However, multilocus phylogenetic analyses showed many of them to represent new species, including *G. pigmentosinum.* From our observations, *G. pulchra* can be recognised only by producing numerous whitish, greyish, yellowish to violaceous, cylindrical, attenuated, long synnemata with a tapered tip or slightly enlarged tip, long aspergillus-like conidiophores densely crowded on the surface and along the entire length of synnemata and forming fusoid to ellipsoid conidia either singly or in chains. These descriptions exclude *G. nigelii*, *G. parvula* and *G. solita* from *G. pulchra sensu lato* as they produce a single, a pair of two and a group of three synnemata, respectively, as well as *G. longispora* which produces long bacilliform conidia. Considering the specimen BBH30518, its morphology is strongly reminiscent of *G. pulchra* by having all characters similar to *G. pulchra* in both shape and size (Table 3). Owing to a lack of DNA sources of the type as well as the loss of original material, comparison between our specimen and the holotype is infeasible. To solve the problem of the lost holotype and a lack of its DNA sequences, epitypification and neotypification have been suggested (Ariyawansa *et al.* 2014). Nevertheless, our specimen with affinity to *G. pulchra* could not be designated as either epitype or neotype according to the epitypification and neotypification principle that the epitype or neotype should be obtained from the same location as the type, in this case Italy.

Considering the phylogenetic placements of *G. longispora*, *G. nigelii*, *G. parvula*, *G. pulchra* and *G. solita*, they were distinctly placed in different relatively well-supported clades representing separate species, consistent with morphology-based classification. Since these species have most of the morphological characters in common, only a few can be used to tell them apart. In our study the number of synnemata appears to be an informative feature that can discriminate *G. parvula*, *G. nigelii* and *G. solita* from *G. longispora*, and *G. pulchra* and *G. nigelii* from *G. parvula* and *G. solita*, whereas the shape of conidia can be used to distinguish *G. longispora* from *G. pulchra* and *G. parvula* from *G. solita*. However, due to the limited number of specimens studied for each taxon these observations may change.

Microscopic features including vesicles, metulae and phialides are considered to be inappropriate features for discriminating species that produce aspergillus-like conidiophores, because the sizes of these characters often fall into the same ranges with nearly identical shapes. Vesicles are commonly globose to subglobose, metulae are broadly obovoid to obovoid whereas phialides are often narrowly clavate to cylindrical. In addition to these characters, conidiophore length can sometimes appear to be a misleading feature. As conidiophores become shorter upwards the synnema, the length of conidiophores thus varies depending on where they are observed. Owing to the fact that fungal herbaria are

supposed to preserve specimens under the best condition which forbids studying a whole synnema, particularly when only a single synnema is produced, the actual range of conidiophore lengths is rarely recorded.

The conidiophores of *G. brevistipitata* and *G. pilosa* can be measured along the entire length of synnemata, which is particularly useful for distinguishing these species. These two species produced aspergillus-like conidiophores that are at least twice as short in *G. brevistipitata* (47.5–)58–100(–115) µm than *G. pilosa* (140–)151–265(–420) µm (Table 5). Besides the length of conidiophores, the shape of synnematal tips and the length of synnemata are considered to be reliable characters for differentiating closely related species within *Gibellula*, including *G. brevistipitata* and *G. pilosa,* that are phylogenetically regarded as sister taxa (Fig. 1). *Gibellula brevistipitata* forms distinctly short synnemata with slightly enlarged ovoid tips, whereas *G. pilosa* produces longer synnemata with globose to subglobose apices (Fig. 6). *Gibellula pilosa* can be easily recognised at first glance by the numerous long conidiophores on the mycelia covering the host body and legs.

Among the proposed new species, *G. longicaudata* is the only one that produces penicillium-like conidiophores (Fig. 5). Thus far, only *G. clavulifera*, *G. leiopus* and *G. scorpioides* are known to produce such conidiophores. Based on morphology, *G. longicaudata* was found to be rather close to *G. scorpioides* by having a long cylindrical synnema arising from the posterior part of the spider host, and producing very short penicillium-like conidiophores bearing fusoid conidia. Table 6 shows the comparison of important morphological characters between these species. Interestingly, *G. longicaudata* was phylogenetically placed far from the ex-type strain of *G. scorpioides*, but rather close to *G. cebrennini* and *G. fusiformispora* that have penicillium-like conidiophores (Fig. 15B) instead of aspergillus-like conidiophores (Fig. 15A).

In this study, we also newly reported *G. dimorpha* and *G. unica* from Thailand. These two species are well-known to form a *Granulomanus* conidial morph that can develop aspergillus-like conidiophores. The Thai specimen BBH30034 was found to be morphologically similar to *G. unica* from Taiwan in having white mycelia, a few synnemata on the spider hosts, aspergillus-like conidiophores bearing narrowly ellipsoid conidia and a *Granulomanus* synasexual morph forming gibellula-like conidiophores. The morphological characters of the specimens from different countries showed the same shapes and sizes falling into the same ranges with some minor differences (Table 4, see notes for the species). In contrast, specimen BBH30489 was morphologically reminiscent of *G. dimorpha* (Tzean *et al.* 1998). Based on the comparison of morphological characters between BBH30489 and the type, they share similarities in shape but not size of characters (Table 2, also see notes for the species). The morphological differences between these specimens and a lack of DNA sequence data corresponding to the type have thus left us to question whether our specimen truly represents a new species or falls within the species boundary of *G. dimorpha*. To avoid introducing taxonomic confusion by proposing a new species from the fungus that might later turn out to be the described species, we decided to assign *Gibellula* strain BBH30489 to *G. dimorpha*. With regard to its sister clade, *G. trimorpha* appeared to be very much closer to *G. dimorpha* in having all morphological characters in common which could easily mislead species identification. Nevertheless, the molecular traits segregated them into two taxa (Fig. 1). Although morphological data of some certain characters of *G. trimorpha* remains incomplete, the molecular evidence was sufficient to propose it as a new species.

Recently, Lücking *et al.* (2020) raised awareness of how not only phenotypes can mislead the identification of cryptic species, but also how a single morphologically well-defined species can possess a complex genetic structure. The approach of integrative (polyphasic) taxonomy is highly suggested for accurate species delimitation to overcome these obstacles. For closely related species with typically few distinguishing characters, phylogeny-based classification and identification is important. Nevertheless, it is sometimes questionable whether the observed genetic divergence between putative species could be considered as sufficient for proposing a new species. One approach is to use the genetic distance between known sister species in a given taxonomic group as a threshold for assignment of species status (Baker & Bradley 2006). Although this approach is not widespread in fungal taxonomy, it has been used successfully in some studies (*Ophiocordyceps unilateralis*: Kobmoo *et al.* 2012, *O. myrmecophila*: Khonsanit *et al.* 2019) and is useful for proposing new species. Using the divergence between *G. cebrennini* and *G. fusiformispora* as the threshold, *G. longicaudata*, *G. longispora*, *G. nigelii*, *G. parvula*, *G. pilosa*, *G. solita* and *G. trimorpha* could be proposed as new species. Particular attention should be paid to the taxa BCC45580 and BCC57817 in which the divergence between them was just below the threshold. However, the morphological evidence strongly supported the segregation between them. From the integrative phylogeny considering the morphological and genetic data together, *G. brevistipitata* and *G. pilosa* were thus proposed to accommodate these taxa, respectively.

To identify species of invertebrate-parasitic fungi those that have a narrow host range or are restricted to a single host, host specificity was suggested to be a very informative character (Johnson 1968, Evans *et al*. 2011, Vialle *et al.* 2013, Araújo *et al*. 2018).

The identification of the spider hosts of *Gibellula* spp. at the family ranks was first made by Van der Bijl (1922), who reported *Lycosidae* as a host of *G. haygarthii*, which is now synonymised with *G. pulchra* (Shrestha *et al.* 2019). Later, many attempts were made to identify the hosts of several species of *Gibellula* at the genus and species ranks (Petch 1948, Samson & Evans 1973, 1977, Strongman 1991, Costa 2014, Savić *et al.* 2016). Nevertheless, host specificity has not yet been clearly determined for most *Gibellula* species. For instance, the host morphologies of *G. leiopus* and *G. pulchra* reported by Savić *et al.* (2016) and Strongman (1991), respectively, seemed not to fit well the concepts of the individual species. In our previous study, we also attempted to identify the spider hosts parasitised by four new species of *Gibellula* (Kuephadungphan *et al.* 2020). Therein, *Cebrenninus cf. magnus*, *Storenomorpha* sp. and *Portia* sp. appeared to be exclusively associated to *G. cebrennini*, *G. pigmentosinum* and *G. scorpioides*, respectively, whereas the family *Deinopidae* was described for the first time as a host for *G. fusiformispora*. In total, *Gibellula* hosts have been reported among 16 spider families thus far (Table 7).

Salticidae is the largest family of spiders, and several *Gibellula* species have been reported to parasitise salticid spiders, including *G. pulchra* in this study, confirming a previous study by Samson & Evans (1973). Besides *G. pulchra*, other species of *Gibellula* parasitising salticid spiders include *G. clavulifera* (Samson & Evans 1977), *G. clavulifera* var. *alba* (Humber & Rombach 1987) and three new species reported in this study (*G. longispora*, *G. pilosa* and *G. trimorpha*). *Gibellula trimorpha* also appeared on *Oxyopidae* indicating that is not restricted to a single spider species and can infect a broad host range across multiple spider families.

Table 5. Morphological comparison of accepted species within *Gibellula* and all species proposed herein.

Species	Distribution	Synnemata	*Gibellula* anamorph					Granulomanus-like asexual morph		
			Conidiophores	Vesicles	Metulae	Phialides	Conidia	Conidiophores	Phialides	Conidia
G. alata	Sri Lanka (Peteh 1932) Ghana (Samson & Evans 1973)	Up to 12, white, up to 0.8 mm long, 0.1 mm wide	Aspergillus-like	—	—	—	Oblong-oval or clavate, 4–9 × 2–4 µm	—	—	—
G. brevistipitata	Thailand	In a group of 5, cylindrical, brownish-white, becoming brown towards the tip, 2 mm long, 200 µm, swollen ovoid tip	Aspergillus-like, 47.5–115 × 6–8.5 µm, distinctly roughened	Spherical to broadly obovoid, 7.5–10 µm diam	Broadly obovoid or ellipsoidal, 7–10.5 × 5–7 µm	Cylindrical to narrowly clavate, 7–10 × 2–3 µm	Ellipsoidal, 3–4.5 × 1.5–2 µm	n/d	n/d	n/d
G. brunnea	Brazil (Samson & Evans 1992)	Multiple, with a stout yellow-tan stipe, 0.2–0.8 × 0.2–0.4 cm, broadening into globose to pyriform fertile area, 0.5–0.8 × 0.8–1.4 cm, and narrowed into a pale brown compact acuminate sterile tip	Aspergillus-like, 350 µm long, distinctly verrucose at the base	Ellipsoidal to globose, verrucose, pigmented, 10–15 µm diam	Ellipsoidal to obovoidal, smooth to roughened walled, hyaline, 10–12 × 6–9 µm	Mostly cylindrical also ellipsoidal, smooth to verrucose, pigmented, 10–15 × 3–4 µm	Fusiform, 8–10 × 2–2.5 µm	Mostly arising from the base of synnemata, verrucose, darkly pigmented, bearing 2–5 conidiogenous cells	Cylindrical, ellipsoidal, with 1–3 distinct denticles, smooth-walled	Filiform, 10–21 × 1–1.5 µm
G. cebrennini	Thailand (Kuephadungphan *et al*. 2020)	Single, white to cream, slightly enlarged toward the sterile tip	Aspergillus-like, 45–150 µm long, scattered verrucose	Broadly ellipsoidal to globose, 23–33.5 µm diam	Obovoidal, 5–9 × 3–6.5 µm	Narrowly obovoid, 4–9 × 1.5–3.5 µm	Fusiform, 4–9 × 1.5–3.5 µm	Mostly arising from the mycelial mat covering the host body	Polyblastic and irregularly shaped with multiple denticles	Filiform, 6–12 × 1–1.5 µm
G. clavata	Ecuador (Samson & Evans 1992)	Single, rarely paired, broadly clavate, 4–6 mm long, with a compact stipe, 1.5–2 x 0.1–0.2 mm, broadening into an ellipsoidal, pink to lilac fertile area	Aspergillus-like, 30–50 µm long, slightly verrucose at the base	Ellipsoidal to globose, verrucose, 5–8 µm diam	Ellipsoidal to obovoidal, smooth, hyaline, 6–7.5 × 4–5 µm	Cylindrical, smooth, hyaline, 5.5–7.5 × 2-3 µm	Fusiform, 6–7 × 2–2.7 µm	Arising from irregularly branched hyphae, bearing solitary conidiogenous cells	Flask-or irregularly shaped with 1–2 distinct denticles, 5–15 × 3–5.5 µm, smooth-walled	Filiform, 12–15 × 1–1.5 µm
G. clavispora	China (Chen *et al*. 2014)	Solitary, cylindrical, slender, scattered, attenuated, acuminate sterile tip	Aspergillus-like, 96–113 µm long, scattered	Obovate, hyaline, smooth-walled	Obovate,smooth-walled, 7.6–8.6 × 3.2 µm	Clavate, smooth-walled, with a short neck, 8.6–10.8 × 2.2 µm	Clavate to ellipsoidal, 5.4–6.5 × 1.1–2.2 µm	Absent	—	—
G. dabieshanensis	China (Huang *et al*. 1998)	—	Aspergillus-like, smooth-walled	—	—	Cylindrical, 7.9–10.8 × 1.8–2.9 µm	Fusiform, 3.2–4 × 1.1–1.8	Present	—	—

Table 5. (Continued).

Species	Distribution	Synnemata	*Gibellula* anamorph					Granulomanus-like asexual morph		
			Conidiophores	Vesicles	Metulae	Phialides	Conidia	Conidiophores	Phialides	Conidia
G. dimorpha	Taiwan (Tzean *et al.*1998) Thailand (Luangsa-ard *et al*. 2010) Japan (Okuzawa 2012) Brazil (Costa 2014)	Solitary, attenuated, brownish-white, cylindrical, 5 mm x 200 µm	Aspergillus-like, 140–422 × 7.1–10.3 µm, roughened	Globose to subglobose, 7.9 × 11.1 µm	Broadly obovoid, 7.1–11.9 × 6.4–8.7 µm	Cylindrical to narrowly clavate, 5.6–8.7 × 2.5–4 µm	Fusoid, ellipsoidal to lemon shaped, 3.2–4.1 × 2–2.4 µm	Rough-walled to distinctly verrucose, 68–140 × 5.2–7.1 µm	Cylindrical, ellipsoidal, narrowly clavate, with 1–3 conspicuous denticles, 7.9–20.6 × 3.2–4 µm, smooth walled	Filiform, 9.1–23.8 × 0.8–2.4 µm
G. fusiformispora	Thailand (Kuephadungphan *et al*. 2020)	Single or in pairs, cream to light brown swollen sterlie tip with acute apex	Aspergillus-like, 23–83 µm long, crowded verrucose	Subglobose to globose, 6–8 µm diam	Obovoid to broadly obovoid, 7–10 × 4.5-6 µm	Narrowly obovoid, 7-10 × 2-3 µm	Fusiform, 3.5-6 × 1.5-2.5 µm	Absent	Absent	Absent
G.gamsii	Thailand (Kuephadungphan *et al*. 2019)	Single or in groups of three, yellowish white to pale yellow, 5–15 mm long, short stipe and clavate brush-like fertile area terminating in a wing-like, yellow to gloden brown sterile tip	10–91 µm long, scattered verrucose	Ellipsoidal to globose, 6–10 x 5–10 µm diam	Ellipsoidal to obovoidal, 6–8.5 × 4–6 µm	Mostly oblong-elliptical, 6.5–8.5 × 1.5–3 µm	Fusiform, 3.5–5 × 1.5–2.5 µm	n/d	n/d	n/d
G.leiopus	Austria (Tkaczuk *et al*. 2011) Brazil (Costa 2014) Canada (Mains 1950) Czech Republic (Kubátová 2004) Ghana (Samson & Evans 1973) Japan (Kobayasi & Shimizu 1977) Mexico (Sánchez-Peña 1990) Sweden (Lundquist 1998, referred in Kubátová 2004) Taiwan (Tzean *et al*. 1997) Trinidad (Evans & Samson 1987) US (Mains 1950)	Yellow to whitish, cylindrical , 1.5–8 mm long, 80–300 µm wide	Penicillium-like, very short, crowded, smooth	Broadly obovoid or obpyriform, 10–18 × 4.5–8 µm	Broadly obovoid to ellipsoid, 7.5–12 × 3–5 µm	Narrowly clavate to subcylindric, 7.5–12 × 2.5–3.5 µm	Fusoid to fusoid-ellipsoid, 3–8 × 1–2 µm, singly or in short chains	n/d	n/d	n/d

Table 5. (Continued).

Species	Distribution	Synnemata	*Gibellula* anamorph					Granulomanus-like asexual morph		
			Conidiophores	Vesicles	Metulae	Phialides	Conidia	Conidiophores	Phialides	Conidia
G. longicaudata	Thailand	Single, greyish-white, cylindrical, tufted surface, sterile broadly ovoid tip	Penicillium-like, 10–35 × 3–5 µm, crowded, smooth	n/d	Broadly obovoid to ellipsoidal, 7–10 × 3-4 µm	Narrowly clavate to cylindrical, 7–10 × 2–3 µm	Fusoid, 3–6 × 1-2 µm	Arising from the septate hyphae	Distinctly roughened, very short, bearing polyblastic and irregularly shaped	n/d
G. longispora	Thailand	At least 20, cylindrical, attenuated, 5–5.5 mm × 175–200 µm	Aspergillus-like, 105–415 × 6–15 µm, crowded, minutely roughened	Globose to subglobose, 7–9 µm diam	Broadly obovoid, 6.5–11 × 5.5–7 µm	Narrowly clavate to cylindrical, 8.5–11.5 × 2.5–4 µm	Bacilliform to cylindrical, 3.5–9 × 1–1.5 µm	n/d	n/d	n/d
G. mainsii	Brazil (Samson & Evans 1992)	Vegetative mycelium hyaline, smooth-walled or irregularly verrucose, mostly 2–2.5 µm wide but occasionally thinner, 1.5–2 µm	Aspergillus-like, up to 350 µm in length, hyaline, smooth-walled	Ellipsoidal to globose, 10–15 µm diam	Ellipsoidal to obvoidal, 10–12 × 6–9 µm	Cylindrical with a short neck, 10–13 × 3–4 µm	Fusiform, smooth-walled, 8–10 × 2–2.5 µm	n/d	n/d	n/d
G. mirabilis	Ecuador (Samson & Evans 1992)	Paired, pale to golden yellow, 1.5–2 × 0.6–1 mm, consisting of a short stipe and clavate brush-like fertile area, terminating in a short, golden brown sterile tip	Aspergillus-like, 80 µm long, slightly verrucose at the base	Ellipsoidal to globose, smooth to verrucose, 8–10 µm diam	Ellipsoidal to obovoidal, smooth, hyaline, 6–9 × 5–8 µm	Broadly cylindrical to ellipsoidal, smooth, hyaline, 5.5–7.5 × 3–4 µm	Fusiform, 5–7 × 2–3.5 µm	Arising from irregularly branched hyphae, bearing solitary or densely whorled conidiogenous cells	Flask or irregularly shaped with 1–2 distinct denticles, 5–12 × 3–4 µm, smooth-walled	Filiform, 14–25 × 1–1.5 µm
G. nigelii	Thailand	Single, white at the base becoming brown to greenish-brown upward, cylindrical, attenuated, 3 mm long, 70 µm wide, swollen tip with acute apex	Aspergillus-like, 42.5–90 × 7.5–10 µm, scattered, minutely roughened	Globose to subglobose, 7.5–11 µm diam	Broadly obovoid, 7–10 × 5–7 µm	Narrowly clavate to cylindrical, 6–9 × 2–3 µm	Ellipsoidal, 2.5–4 × 1–1.5 µm	n/d	n/d	n/d

Table 5. (Continued).

Species	Distribution	Synnemata	*Gibellula* anamorph					Granulomanus-like asexual morph		
			Conidiophores	Vesicles	Metulae	Phialides	Conidia	Conidiophores	Phialides	Conidia
G. pulchra	Austria (Tkaczuk *et al*. 2011) Belgium (Bosselaers 1984) Brazil (Costa 2014) British Guiana (Mains 1950) Canada (Strongman 1991) Chile (Mains 1950) Ecuador and Brazil (Samson & Evans 1992) Ghana (Samson & Evans 1973) Mexico (Sánchez-Peña 1990) Papua New Guinea (Mains 1950) Poland (Bałazy 2004) Solomon Islands (Humber & Rombach 1987) Spain (Santamaria & Girbal 1996) Taiwan (Tzean *et al*. 1997) Trinidad (Mains 1950) Turkey (Selçuk *et al*. 2004) USA (Mains 1950) Venezuela (Mains 1950)	Numerous, yellowish-brown, cylindrical	Aspergillus-like, 150–600 × 7–12 µm, smooth-walled	Ellipsoidal to obvoidal, 6.4–10 µm diam	Broadly obovoid, 6–12 × 4–6 µm	Clavate, 6–10 × 2–3 µm	Fusoid to ellipsoid, 2.5–6.4 × 1.5–2.3 µm	Absent	Absent	Absent
G. parvula	Thailand	A pair of two, yellowish-white, cylindrical with ovoid tips	Aspergillus-like, 47.5–185 × 6–11 µm, crowded, rough-walled	Globose to subglobose, 6.5–9 µm diam	Broadly obovoid, 6–10 × 4.5–8 µm	Narrowly clavate to cylindrical, 6–10 × 2–4 µm	Narrowly ovoid or ellipsoid or bacilliform, 4–6 × 2–4 µm	n/d	n/d	n/d
G. pigmentosinum	Thailand (Kuephadungphan *et al*. 2020)	Single or in pairs, white becoming yellowish white at the base	Aspergillus-like, 55–226 µm long, crowded verrucose	Mostly globose, 5–10 µm diam	Broadly obovoid, 5.5–10 × 3–7.5 µm	Obovoid to clavate, 5–9 × 2–4.5 µm	Obovoid, 2.5–5.5 × 1–3 µm	Arising from irregularly branched hyphae	Irregularly shaped with one or more conspicuous denticles, mostly smooth	Filiform, 16–22.5 × 1–1.5 µm
G. pilosa	Thailand	A pair of two, light brown, cylindrical with globose tips, 6 mm × 475 µm	Aspergillus-like, 140–420 × 8.5–13.5 µm, crowded, minutely roughened	Spherical, 9–12 µm diam	Broadly obovoid, 9–12 × 6–9 µm	Narrowly clavate to cylindrical, 7–10 × 2.5–3 µm	Almond shaped, 3–4 × 1.5–2 µm	n/d	n/d	n/d

Table 5. (Continued).

Species	Distribution	Synnemata	*Gibellula* anamorph					Granulomanus-like asexual morph		
			Conidiophores	Vesicles	Metulae	Phialides	Conidia	Conidiophores	Phialides	Conidia
G. scorpioides	Thailand (Kuephadungphan *et al.* 2020)	Single, arising all over the host, 15–20 mm long with blunt tip	Penicillium-like, 20–30 µm long, stout, smooth, mostly biverticillate	Absent or hardly developed, bearing multiple metulae	Obovoid, 7–15 × 2–7 µm	Broadly cylindrical, 9–14 × 2–4 µm	Fusiform, 5–9 × 1.5–3 µm	Absent	Absent	Absent
G. shennongjiaensis	China (Zou *et al.* 2016)	Solitary, arising from mycelial mat, cylindrical, attenuated	Aspergillus-like, 77–107 µm long, distinctly roughened	—	Ellipsoidal, 5.4–7.6 × 2.1–4.3 µm	Clavate with a short neck, smooth, hyaline, 5.4–10.8 × 1.1–2.2 µm	Cylindrical or fusiform, 3.2–6.5 × 1.1–1.6	Present on culture	—	—
G. solita	Thailand	In a group of three, cylindrical, attenuated, 7 mm long, 175 µm wide, brownish white, swollen tip	Aspergillus-like, 62.5–180 × 7.5–10 µm, verrucose	Globose to subglobose, 6.5–8.5 µm diam	Broadly obovoid, 6.5–8 × 5–7 µm	Narrowly clavate to cylindrical, 6–7.5 × 2–2.5 µm	Ellipsoidal to ovoid, 1.5–3 × 1–2 µm	n/d	n/d	n/d
G. trimorpha	Thailand	Single, cylindrical, short stipe, white, 3 mm long	Aspergillus-like, 65–230 × 7–9 µm	Subglobose to globose, 9–12 x 7–10 µm	Broadly ellipsoidal, 7–10 × 6–7 µm	Not observed	Fusiform, in short chains, 4–5 × 2 µm	Well-differentiated, roughened to distinctly verrucose,	Cylindrical, clavate, flask- or irregularly shaped, mostly verrucose with 1–3 conspicuous denticles, 8–13 × 3 µm	Filiform, 10–19 × 1–1.5 µm
G. unica	Taiwan (Tzean *et al.* 1997) Thailand (Luangsa-ard *et al.* 2010, this study) Japan (Okuzawa 2012)	In a group of 5–6, arising all over the host, cylindrical, slender acuminate towards the apex, yellowish grey, 4–5 mm × 96–184 µm, fertile along the length	Aspergillus-like, 112–244 × 6.4–13.5 µm, distinctly verrucose along the length	Ellipsoidal, subglobose to globose, smooth, hyaline, 7.1–9.9 × 5.6–7.9 µm	Broadly ellipsoidal to obovoidal, smooth, hyaline, 5.6–9.1 × 4.8–7.0 µm	Broadly cylindrical to ellipsoidal, smooth, hyaline, 6.4–9.5 × 2.8–4.2 µm	Fusiform, occasionally apiculate, 4.0–6.8 × 1.6–2.2 µm	Mostly arising from the base of synnemata, verrucose	Cylindrical, clavate, flask- or irregularly shaped, verrucose, with 1–3 conspicuous denticles, 6.8–11.9 × 3.2–4.0 µm	Filiform, 11.1–17.5 × 1.0–1.6 µm

Table 6. Morphological comparison of Thai *G. longicaudata* and three varieties of *G. clavulifera* (Data partly after Tzean *et al*. 1997).

Characters	***G. leiopus* (Mains 1950)**	***G. longicaudata***	***G. scorpioides* (Kuephadungphan *et al.* 2020)**	***G. clavulifera* var. *clavulifera***	***G. clavulifera* var. *alba* (Humber & Rombach 1987)**	***G. clavulifera* var. *major* (Tzean *et al*. 1997)**
Locality	USA	Thailand	Thailand	n/a	Solomon Islands	Taiwan
Host	Spider	*Arachnida*	*Portia* sp.	n/a	*Euophrys cf. trivittata*	*Arachnida*
***Gibellula* anamorph**	Present	Present	Present	Present	Present	Present
Mycelia	Yellow to whitish	White	Greyish- or brownish-white	Lilac	White	White to yellowish-white
Synnemata (length × width)	Yellow to whitish, cylindrical, 1.5–8 mm long, 80–300 µm wide	Solitary, greyish-white, whip-like, slightly tapering into sterile broadly ovoid tip, arising from the posterior of the host abdomen	Solitary, greyish- or brownish-white, whip-like with blunt end, arising from the posterior of the host abdomen	Solitary, greyish to purple, stout, short, cylindrical	Mononematous	Solitary, white to yellowish-white, whip-like
Conidiophores (µm)	Hyaline, smooth-walled, enlarged upward, broadly obovoid or obpyriform, 10–18 × 4.5–8	Hyaline, smooth-walled, enlarged upward into obovoid apices, 10–35 × 3–5	Hyaline, smooth-walled, 20–30 × 4	Brown, smooth-walled, 97.3 × 5.4	Hyaline, long and stout, smooth to asperulate, 100 × no data	Hyaline, smooth- to slightly roughed-walled, up to 140 × 4.8–7.1
Metulae (µm)	—	Broadly obovoid to ellipsoid, 7–10 × 3–4	Narrowly obovoid to cylindrical, 7–15 × 2–7	Cylindrical, 11.6–15.4 × 3.8–5	Cylindrical or clavate, 9–15 × 3–4	Clavate to cylindrical, in groups of 3–10, 12.7–19.8 × 4–5.6
Phialides (µm)	Narrowly clavate to sub-cylindrical, 7.5–12 × 2.5–3.5	Narrowly clavate to cylindrical, apically thickened, 7–10 × 2–3	Broadly cylindrical, apically thickened, often with distinct short neck, 9–14 × 2–4	Cylindrical, in groups of 2–4, 13–17 × 3–3.5	Cylindrical, in groups of 2–6, 10–12.4 × 1.5–2.5	Ampulliform to cylindrical, in groups of 2–8, 12.7–19.8 × 3.6–6
Conidia (µm)	Fusoid to fusoid-ellipsoid, 3–8 × 1–2	Fusoid or occasionally ovoid with an acute end, 3–6 × 1–2	Fusiform, 5–9 × 1.5–3	Purplish in mass, fusiform to cylindrical, 6–9 × 1.7–2	Pure white in mass, fusiform, 5–7.5 × 1.5–2	Pure white in mass, fusiform to broadly fusiform, often distinctly apiculate at both ends, 7.1–13.9 × 2.4–5.6
***Granulomanus* anamorph**	Absent	Present	Absent	Present	Present	Present
Phialides (µm)	—	Polyblastic, irregular, rough-walled, arising from a synnema	—	Holoblastic, cylindrical or irregular, pigmented, arising from hyphae, 10–18 × 3–4	Holoblastic, irregular, smooth-walled, arising from hyphae, 9–15 × 3–5	Verticillate, holoblastic, cylindrical to flask-shaped, arising from stipe, 9.5–14.6 × 2.7–4.4
Conidia (µm)	—	n/d	—	Hyaline, filiform, smooth-walled, 11–17 × 1.2–1.5	Hyaline, bacilliform, often swollen at one end, smooth-walled, 20–30 × 0.5–1.5	Hyaline, smooth- to slightly roughed-walled, up to 140 × 4.8–7.1, bacilliform to filiform, apiculate or round end, smooth-walled, 15.9–34.1 × 1.3–2.4

Table 6. (Continued).

Characters	*G. leiopus* (Mains 1950)	*G. longicaudata*	*G. scorpioides* (Kuephadungphan *et al.* 2020)	*G. clavulifera* var. *clavulifera*	*G. clavulifera* var. *alba* (Humber & Rombach 1987)	*G. clavulifera* var. *major* (Tzean *et al.* 1997)
Teleomorph	Present	Absent	Present	Absent	Present	Absent
Perithecia (µm)	Ovoid, 550–900 × 230–350	—	Superficial, one-third immersed in the loose network of mycelia, mostly arranged in groups, reddish-yellow to light honey-brown, ovoid, 750–870 × 310–380	—	Superficial, one-third immersed in the loose network of mycelia, bright to reddish-yellow or light honey-brown, ovoid, up to 600 × 150–250	—
Asci (µm)	Cylindrical, 400–600 × 5–6	—	Cylindrical, over 550 × 3–7, with ascus tips, 4–5 × 3–4	—	Cylindrical, up to 125 × 5–7, with ascus tips, 5–6 × 5–6	—
Ascospores (µm)	Filiform, multi-septate	—	Cylindrical, multi-septate, often break into part-spores	—	Vermiform, septate, 8 per ascus, each breaks into 8 part-spores	—
Part-spores (µm)	Cylindrical	—	Bacilliform, 9–22× 1.5–2	—	Bacilliform, 7–10 × 1.5–2	—

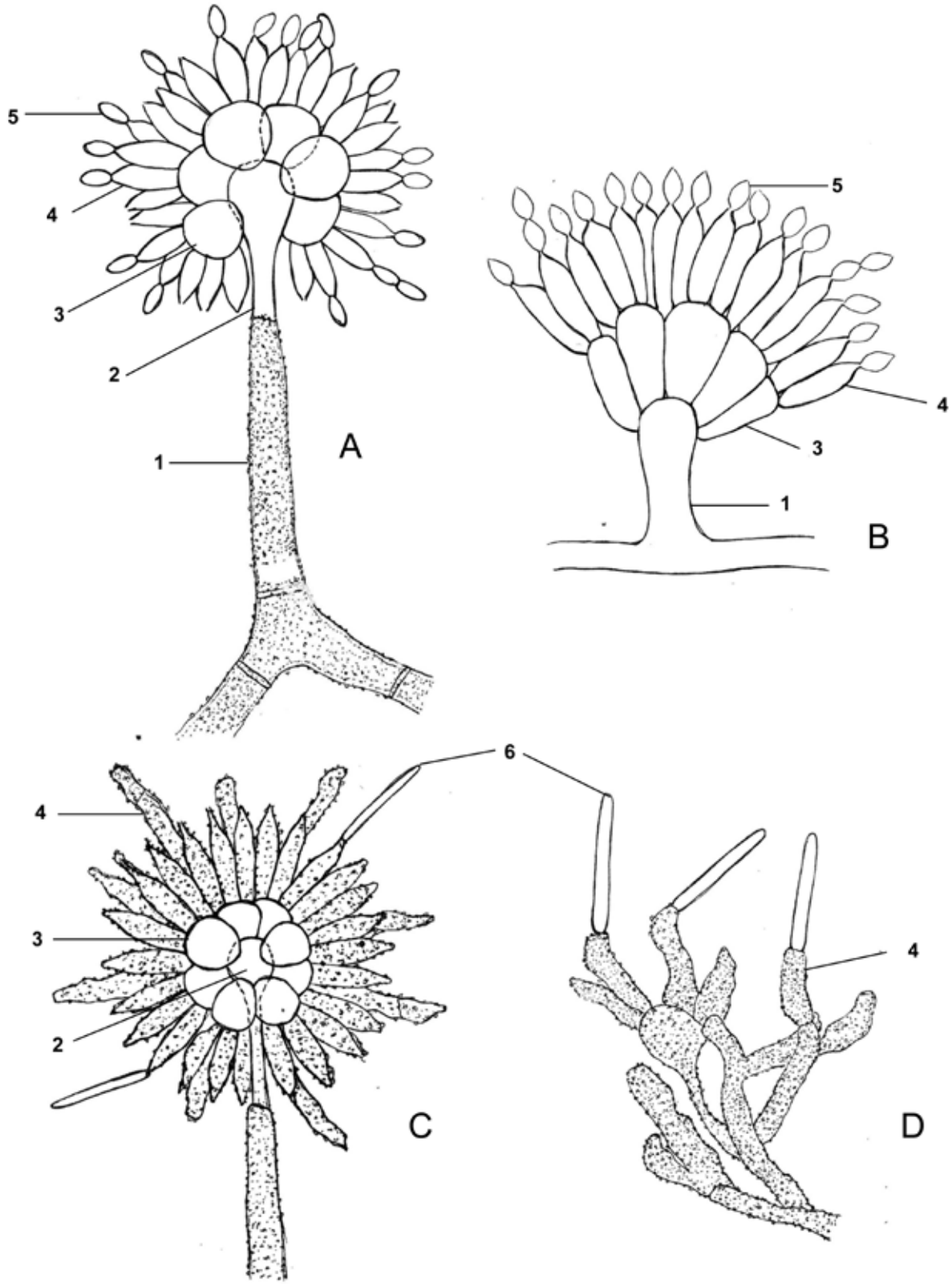

Fig. 15. Illustration of *Gibellula* and *Granulomanus* anamorphs. **A.** Aspergillus-like conidiophore of *Gibellula*. **B.** Penicillium-like conidiophore of *Gibellula*. **C.** Aspergillus-like conidiophore of *Granulomanus*. **D.** *Granulomanus* anamorph. **1.** Conidiophore. **2.** Vesicle. **3.** Metulae. **4.** Phialide. **5.** Conidium of *Gibellula*. **6.** Conidium of *Granulomanus*.

According to Shrestha *et al.* (2019), *Linyphiidae*, the second largest family of spiders after the *Salticidae* (World Spider Catalog 2021) has so far been reported as the hosts of only a few species of hypocrealean fungi including *Cordyceps* sp. from Panama (Nentwig 1985), *G. pulchra* and *Torrubiella albolanata* from the British Isles (Petch 1944, 1948) and *Gibellula* sp. from Brazil (Costa 2014). In this study, this spider family was found to be infected by *G. nigelii*. Interestingly, although at least 46 species of *Linyphiidae* spiders have been reported in Thailand, none of them have previously been reported to be mummified by any hypocrealean fungi. Therefore, to our knowledge, this study includes the first report of *Linyphiidae* as the host of hypocrealean fungi from Asia.

Theridiidae, also known as tangle-web spiders, cobweb spiders, and comb-footed spiders is one of the largest spider families in

Table 7. Classification of spiders parasitised by *Gibellula*. Those encountered in the current study are in bold. The data compiled in part from Shrestha *et al.* (2019).

Spider	*Gibellula*	Reference
Agelenidae		
Urocoras longispinus	*Gibellula* sp.	Savić *et al.* (2016)
Anyphaenidae		
Iguarima censorial	*Gibellula* sp.	Costa *et al.* (2014)
Anyphaenid spider	*G. leiopus*	Costa *et al.* (2014)
Araneidae		
Eustala sp.	*Gibellula* sp.	Costa *et al.* (2014)
Corinnidae		
Trachelas aff. *robustus*	*G. leiopus*	Costa *et al.* (2014)
Deinopidae		
Deinopid spider	*G. fusiformispora*	Kuephadungphan *et al.* (2020)
Linyphiidae		
Gongylidium rufipes	*G. pulchra*	Petch (1948)
Linyphiid spiders	***G. nigelii***	**This study**
	Gibellula sp.	Costa *et al.* (2014)
Lycosidae		
Lycosid spider	*G. pulchra*	Van der Bijl (1922)
Oxyopidae		
Oxyopid spider	***G. trimorpha***	**This study**
Pholcidae		
Metagonia aff. *beni*	*Gibellula* sp.	Costa *et al.* (2014)
Pholcid spiders	***G. unica***	**This study**
Salticidae		
Corythalia sp.	*Gibellula* sp.	Costa *et al.* (2014)
Euophrys nr. trivittata	*G. clavulifera* var. *alba*	Humber & Rombach (1987)
***Myrmarachne* sp.**	***G. longispora***	**This study**
Portia sp.	*G. scorpioides*	Kuephadungphan *et al.* (2020)
Salticid spiders	*G. clavulifera*	Samson & Evans (1977)
	G. pilosa	**This study**
	G. pulchra	Samson & Evans (1973), **this study**
	G. trimorpha	**This study**
	Gibellula sp.	Strongman (1991)
Sparassidae		
Caayguara cupepema	*Gibellula* sp.	Costa *et al.* (2014)
Tetragnathidae		
Metellina (= *Meta*) *merianae*	*Gibellula cf. leiopus*	McNeil (2012)
Theridiidae		
Episinus cognatus	*Gibellula* sp.	Costa *et al.* (2014)
Helvibis longicauda	*Gibellula cf. pulchra*	Gonzaga *et al.* (2006)
Hetschia gracilis	*Gibellula* sp.	Costa *et al.* (2014)
Janula biocorniger	*Gibellula* sp.	Costa *et al.* (2014)
Theridion evexum	*Gibellula* sp.	Costa *et al.* (2014)
Theridiid spiders	***G. parvula***	**This study**
	G. solita	**This study**

Table 7. (Continued).

Spider	*Gibellula*	Reference
Thomisidae		
Cebrenninus cf. magnus	*G. cebrennini*	Kuephadungphan *et al.* (2020)
Tmarus spp.	*Gibellula* spp.	Costa *et al.* (2014)
***Indoxysticus* sp.**	***G. longicaudata***	**This study**
Thomisid spider	***G. brevistipitata***	**This study**
Uloboridae		
***Miagrammopes* sp.**	***G. dimorpha***	**This study**
Zodariidae		
Epicratinus aff. *takutu*	*Gibellula* sp.	Costa *et al.* (2014)
Storenomorpha sp.	*G. pigmentosinum*	Kuephadungphan *et al.* (2020)

the world, ranking among the top five most diverse families with over 120 described genera (World Spider Catalog 2021). Certain genera including *Achaearanea*, *Argyrodes*, *Carniella*, *Chrysso*, *Coleosoma*, *Coscinida*, *Dipoena*, *Episinus*, *Janula*, *Latrodectus*, *Meotipa*, *Parasteatoda*, and *Theridion* (Knoflach 1996, Chotwong & Tanikawa 2013, Wongprom & Košulič 2016, Chaiphongpachara *et al.* 2019, World Spider Catalog 2021, Petcharad & Tanikawa, unpublished data) have been recorded from Thailand but none has previously been reported to be hosts of hypocrealean fungi. Nonetheless, other members of this family are known to be exclusively associated with *Gibellula*, including *Helvibis longicauda* that was found to be parasitised by *Gibellula cf. pulchra* (Gonzaga *et al.* 2006), and *Neopisinus cf. cognatus*, and *Janula bicornigera* that were the hosts of two unidentified *Gibellula* (Marques *et al.* 2011, Costa 2014, World Spider Catalog 2021). In the current study, *G. parvula* and *G. solita* were also found growing on members of *Theridiidae*. However, the host could not be identified at the species nor genus rank. Host identification is important for further study of the fungus/host interaction as the fungus may require specific nutrients from certain hosts, or the physiology or behaviour of the spider could facilitate the fungal infection. Gonzaga *et al.* (2006) noted different susceptibility of two *Theridiidae* species (*Chrysso intervales* and *H. longicauda*) to *Gibellula* fungal attack. These spiders are known to share similarities in body size, web placement as well as habitat selection; however, the latter appeared to encounter *Gibellula* more frequently in nature.

Myrmarachne is a family of ant-mimetic spiders that was found to include a host of *G. longispora* in this study. It is worth pursuing whether *G. longispora* can be found on other spiders beyond *Myrmarachne* or not. As the exoskeleton structure is different between insects and spiders (Evans 2013, Machałowski 2020), a focus on pathogenic fungi parasitising *Myrmarachne* spiders and the ant species mimicked by the spider would provide insight on whether the exoskeleton is the main factor driving the evolution of *Gibellula*. Interestingly, as *Myrmarachne* spiders tend to be herbivores or nectarivores rather than carnivores in comparison with other spiders (Jackson *et al.* 2001, Jackson *et al.* 2008, Nyffeler *et al.* 2017, Hashimoto *et al.* 2020), nutrients could be a key factor driving the speciation of *G. longispora*.

In the spider family *Pholcidae*, *Metagonia* aff. *beni* was reported as a host of an unidentified *Gibellula* (Costa 2014). In this study, two isolates were assigned to *G. unica* that parasitised unidentified species of *Pholcidae*. The morphology of the aforementioned specimen illustrated by Costa (2014) is reminiscent of *G. unica* by the outer appearance and the presence of both *Gibellula* and *Granulomanus* anamorphic states on the same specimen. *Metagonia* is distributed only in the Americas (World Spider Catalog 2021); hence, the *Pholcidae* host of *G. unica* identified in this study is unlikely to belong to *Metagonia*.

Miagramopes sp. is a member of the spider family *Uloboridae*, which is mainly distributed in tropical and subtropical regions (World Spider Catalog 2021) and was found herein to be parasitised by *G. dimorpha*. This fungus is a cosmopolitan species reported in Taiwan (Tzean *et al.* 1998), Thailand (Luangsa-ard *et al.* 2010), probably Brazil (Costa 2014), and Japan (Shrestha *et al.* 2019).

Thomisidae are widely known as crab spiders with more than 2 100 species currently described. Only a few among them have ever been reported as prey for the invertebrate-parasitic fungi. This includes *Cebrenninus cf. magnus* as the host for *G. cebrennini* (Kuephadungphan *et al.* 2020), *Tmarus* for *Gibellula* spp. (Costa 2014) and unidentified thomisid spiders for *Torrubiella albolanata* (Petch 1944) and *Torrubiella fusiformis* (Kobayasi & Shimizu 1982). Based on Ramírez (2014), Wongprom & Košulič (2016), World Spider Catalog (2021), in addition to *Cebrenninus*, there are 16 *Thomisidae* genera reported in Thailand including *Amyciaea*, *Angaeus*, *Boliscus*, *Borboropactus*, *Camaricus*, *Epidius*, *Misumenops*, *Oxytate*, *Pagida*, *Pharta*, *Platythomisus*, *Runcinia*, *Smodicinodes*, *Thomisus*, *Tmarus*, *Zygometis*. However, in the present study, *G. longicaudata* was found on an *Indoxysticus* host that we report as *Thomisidae cf. Indoxysticus*. To our knowledge, this is the first report of *Indoxysticus* in Thailand. Furthermore, *G. brevistipitata* was also found in this study to parasitise a *Thomisidae* host; however, the host could not be identified unequivocally to even the genus rank.

Identifying a spider to the species rank is challenging, which is made more difficult when dealing with a spider fully covered with fungal mycelia that obscure the spider's morphological features. The tarsal claws and scopulate are the most informative characters when the legs appear to be the only part slightly covered by fungal mycelia (Kuephadungphan *et al.* 2020). However, the identification of such a spider to the species rank without severely damaging the fungus highly requires experienced araneologists, and preferably, fresh specimens from fieldwork (Savić *et al.* 2016, Kuephadungphan *et al.* 2020). To promote the investigation of araneophagous fungi, we herein provide a simple protocol of how to handle the specimens in the Methods section. To enable the isolation of spider-parasitic fungi, the parasitised spiders are preferably delivered to mycologists within the same day they are

collected. The molecular data generated from pure cultures often gives much more accurate identification to the species level when it is not feasible to obtain DNA from the fungal stroma. In the case that the specimens cannot be transferred to mycologists or within a day, they can be stored at 4 °C or air-dried. However, the longer they are stored, the lower chance they can be established in cultures.

During our field work for this study, several observations were made that raise the possibility of manipulation of spider behaviour by *Gibellula* during infection. *Gibellula* were noticeably found only on *Araneomorphae* spiders, whereas these fungi have never been reported on *Mygalomorphae* (Shrestha *et al.* 2019, Kuephadungphan *et al*. 2020), suggesting that *Gibellula* is only able to infect the very thin body surface of the former. The exoskeletal parts of the abdomen and leg joints are much thinner than that of other body parts (Jocqué & Dippenaar-Schoeman 2007, Pérez-Miles 2020, Göttler *et al*. 2021a, b) and are much softer after molting (Baerg 1926, Stefoff 2009, Foelix 2011), making them the most vulnerable entry parts for infection, as well as the joints which are composed by thin membranes. *Gibellula* infection thus probably initiates from spores that contact the abdomen or leg joints during molting, which then invade the haemocoel and proliferate via a budding yeast-like phase (Evans 2013), eventually reaching the cephalothorax in which a brain is located and spreading to the appendages via hemolymph. Once the fungus has invaded the brain, the spider's behaviour could be manipulated to enhance fungal growth and dispersal creating "zombie" spiders. The indirect evidence supporting zombie spiders includes 1) the frequency of *Gibellula*-infected cadavers that were found to be firmly attached to the underside of leaves (97.67 %, n = 43) (Kuephadungphan & Petcharad unpubl. data), seems to be not a coincidence as in nature, spiders could randomly stay on the upper surface and underside of leaves (Petcharad pers. obs., Jackson 1986, Li *et al*. 1999, Pekár 2005, Huber & Schütte 2009, Suter *et al.* 2011, Roff & Haddad 2015, Uetz & Dillery 2017, Guarisco 2018), and 2) the cadavers of web-building spiders, such as *Theridiidae* that were found dead off their webs where they spend much of their life time on (Gonzaga *et al*. 2006, Kuephadungphan & Petcharad, unpubl. data) seems to be abnormal. In addition, signs of behaviour manipulation by *G. scorpioides* on the spider assassin *Portia* were reported previously (Kuephadungphan *et al.* 2020). With their thin exoskeleton, desiccation is a significant stress to *Araneomorphae* spiders (Oxbrough *et al.* 2005, Ziesche & Roth 2008, Canal *et al.* 2015, Kwok & Eldridge 2016) and moisture is a limiting factor for araneophagous fungi to grow (Hajek & Leger 1994). The propensity of *Gibellula*-infected spiders to be found on the underside of leaves could be a consequence of behavior for maintaining moisture via avoidance of sunlight exposure.

CONCLUSIONS

A survey of the spider-parasitic genus *Gibellula* led to the discovery of eight new taxa along with three new records from Thailand of previously described species. Among the new species, *G. nigelii* was herein proven to represent a new taxon that had previously been used to represent the type species *G. pulchra* in the phylogeny of *Cordycipitaceae*. New data validate *G. longispora* as a species. Divergence within the genus was estimated from DNA sequence data and shown to be useful in species delimitation of closely related taxa. In addition to the morphological descriptions and DNA sequence data of the fungi, the spider hosts were carefully examined to determine whether the host specificity can aid in species identification of *Gibellula* and to extend our understanding of the spider-fungus association. Most of the spiders being examined could be identified to the family rank. Although this did not give much information on the species delimitation of *Gibellula*, several observations of the hosts indicated aspects of the interaction between spiders and *Gibellula* that are worth further pursuing such as behavioural modification.

Accepted names for *Gibellula*

The following taxa are accepted species of *Gibellula* based on their species descriptions and/or phylogenetic placements. These has been compiled in part from Shrestha *et al*. (2019).

Gibellula alata Petch, Annls. mycol. 30: 391. 1932. MycoBank MB 256143.
Gibellula brunnea Samson & H.C. Evans, Mycologia 84: 301. 1992. MycoBank MB 358123.
Gibellula cebrennini Tasan. *et al.*, MycoKeys 72: 21. 2020. MycoBank MB 835113.
Gibellula clavata Samson & H.C. Evans, Mycologia 84: 306. 1992. MycoBank MB 358125.
Synonym: *Torrubiella clavata* Samson & H.C. Evans, Mycologia 84: 306. 1992.
Gibellula clavispora Z.Q. Liang *et al.*, Mycotaxon 131: 111. 2016. MycoBank MB 810567.
Gibellula clavulifera (Petch) Samson & H.C. Evans, Proc. K. Ned. Akad. Wet., Ser. C, Biol. Med. Sci. 80: 131. 1977. MycoBank MB 314478.
Basionym: *Spicaria clavulifera* Petch, Trans. Br. mycol. Soc. 16: 238. 1932.
Synonym: *Gibellula clavulifera* var. *clavulifera* (Petch) Samson & H.C. Evans, Proc. K. Ned. Akad. Wet., Ser. C, Biol. Med. Sci. 80: 131. 1977.
Gibellula clavulifera* var. *alba Humber & Rombach, Mycologia 79: 376. 1987. MycoBank MB 132411.
Synonym: *Torrubiella ratticaudata* Humber & Rombach, Mycologia 79: 376. 1987.
Gibellula clavulifera* var. *major Tzean *et al.*, Mycologia 89: 311. 1997. MycoBank MB 437910.
Gibellula dabieshanensis B. Huang *et al.*, Mycosystema 17: 110. 1998. MycoBank MB 446535.
Gibellula dimorpha Tzean *et al.*, Mycol. Res. 102: 1350. 1998. MycoBank MB 446667.
Synonym: *Torrubiella dimorpha* Tzean *et al.,* Mycol. Res. 102: 1350. MycoBank MB 446666.
Gibellula fusiformispora Tasan. *et al.*, MycoKeys 72: 26. 2020. MycoBank MB 835114.
Gibellula gamsii Kuephadungphan, *et al.*, Mycol. Prog. 18: 138. 2018. MycoBank MB 825141.
Gibellula leiopus (Vuill. ex Maubl.) Mains, Mycologia 42: 313. 1950. MycoBank MB 485289.
Basionym: *Gibellula arachnophila f. leiopus* Vuill. ex Maubl., Bull. Soc. mycol. France 36: 42. 1920. MycoBank MB 137604.
Synonym: *Gibellula araneae* Sawada, Rep. Dept Agric., Govern. Res. Inst. Formosa, Spec. Bull. Agric. Exp. Station Formosa 35: 114. 1928. MycoBank MB 257173.
Gibellula perexigua (Kobayasi) Koval, Klavitsipital'nye Griby SSSR (Kiev): 57. 1984. MycoBank MB 132451.
Gibellula mainsii Samson & H.C. Evans, Mycologia 84: 300. 1992. MycoBank MB 358122.
Gibellula mirabilis Samson & H.C. Evans, Mycologia 84: 310. 1992. MycoBank MB 358126.

Gibellula pigmentosinum Tasan. *et al*., MycoKeys 72: 27. 2020. MycoBank MB 835112.
Gibellula pulchra (Sacc.) Cavara, Atti Ist. bot. R. Univ. Pavia 3: 347. 1894. MycoBank MB 215909.
Basionym: *Corethropsis pulchra* Sacc., Michelia 1: 84. 1877. MycoBank MB 206516.
Synonyms: *Gibellula aranearum* P. Syd., Bot. Jb. 57: 321. 1922. MycoBank MB 257177.
Gibellula arachnophila f. macropus Vuill., Bull. Soc. mycol. Fr. 36: 41. 1920. MycoBank MB 137624.
Gibellula haygarthii Van der Byl, Trans. Roy. Soc. South Africa 10: 149. 1922. MycoBank MB 266863.
Gibellula globosa Kobayasi & Shimizu, Bull. natn. Sci. Mus., Tokyo, B 8: 45. 1982. MycoBank MB 114288.
Gibellula globosostipitata Kobayasi & Shimizu, Bull. natn. Sci. Mus., Tokyo, B 8: 49. 1982. MycoBank MB 114291.
Gibellula suffulta Speare, Phytopathology 2: 137. 1912. MycoBank MB 216044.
Gibellula tropicalis Sawada, Special Publ. Coll. Agric. Natl. Taiwan Univ. 8: 231. 1959. MycoBank MB 331320.
Gibellula scorpioides Tasan., *et al*., MycoKeys 72: 30. 2020. MycoBank MB 835115.
Gibellula shennongjiaensis X. Zou *et al*., Mycosystema 35: 1163. 2016. MycoBank MB 814470.
Gibellula unica L.S. Hsieh *et al*., Mycologia 89: 312. 1997. MycoBank MB 437911.

Residual species of *Gibellula*
The following species of *Gibellula* could not be confidently assigned to the genus as their morphologies did not fit the concept of the genus or the molecular phylogeny presented is inconclusive or unavailable.

Gibellula arachnophila (Ditmar) Vuill., Bull. Séanc. Soc. Sci. Nancy, Sér. 3 11: 156. 1910. MycoBank MB 227937.
Basionym: Isaria arachnophila Ditmar, Deutschlands Flora, Abt. III. Die Pilze Deutschlands 1–4: 111, t. 55. 1817. MycoBank MB 203061.
Note: Mains (1950) and Evans & Samson (1987) stated that this Ditmar's fungus actually was *Akanthomyces aranearum* (Petch) Mains.
Gibellula araneicola Sawada, Special Publ. Coll. Agric. Natl. Taiwan Univ. 8: 231. 1959. MycoBank MB 331319.
Note: Tzean *et al*. (1997) doubted the identity of *G. araneicola* Sawada that produces an isarioid morph instead of *Gibellula*.
Gibellula aspergilliformis (Rostr.) Vuill., Bull. Séanc. Soc. Sci. Nancy, Sér. 3 11: 158. 1910. MycoBank MB 521547.
Basionym: *Isaria aspergilliformis* Rostr., Botan. Zbl. 57: 185. 1894.
Note: Petch (1932) expressed doubt towards the identity of *G. aspergilliformis* because of the narrow metulae and spherical conidia in chains present in this species were uncommon features of *Gibellula*.
Gibellula capillaris Morgan, J. Mycol. 11: 50. 1905. MycoBank MB 215873.
Note: According to Mains (1950), the description of *G. capillaris* did not fit the concept of *Gibellula* and re-examination of the type specimen is infeasible as it is no longer in a good condition.
Gibellula curvispora Y.F. Han *et al*., Mycosystema 32: 778. 2013. MycoBank MB 516621.
Note: Judging by the species illustration, *Gibellula curvispora* does not fit the concept of *Gibellula*. Importantly, its ITS sequence appeared close to *Bionectriaceae*.
Gibellula formosana Sawada, Rep. Dept. Agric. Gov. Res. Inst. Formosa. 19: 1. 1919. MycoBank MB 646527.
Note: Mains (1950) expressed doubt on the assignment of *Gibellula formosana* Sawada to the genus since it was found infecting a moth while Kobayasi suggested that it resembled *Isaria japonica*.
Gibellula eximia Höhn., Denkschr. Kaiserl. Akad. Wiss., Math.-Naturwiss. Kl. 83: 37. 1907. MycoBank MB 216040.
Note: The species description of *Gibellula eximia* does not fit *Gibellula* (Petch 1932).
Gibellula elegans Henn., Hedwigia 41: 148. 1902. MycoBank MB 216113.
Note: Since *Gibellula* is well-known as an obligate parasite of spiders, Mains (1950) reported that the assignment of *G. elegans* to this genus might be erroneous, as this species is found parasitising locusts.
Gibellula petchii Humber & Rombach, Mycologia 79: 380. 1987. MycoBank MB 132409.
Basionym: *Cylindrophora aranearum* Petch, Trans. Br. mycol. Soc. 27: 85. 1944. MycoBank MB 285924.
Synonym: *Granulomanus aranearum* (Petch) de Hoog & Samson, Persoonia 10: 70. 1978. MycoBank MB 314729.
Notes: It is still unclear whether the species name should be retained or abandoned. *Gibellula petchii* was proposed to accommodate *Cylindrophora aranearum*, which was originally described as the conidial morph of *Torrubiella albolanata* and later elevated to generic rank as a new genus, *Granulomanus* (Petch 1944, de Hoog 1978, Humber & Rombach 1987). From the point of view of Humber & Rombach (1987), *Granulomanus* should be synonymised with *Gibellula* as it almost never occurs in the absence of *Gibellula* and/or its torrubiella-ike teleomorph. *Cylindrophora aranearum* (≡*Granulomanus aranearum*) was henceforth synonymised with *G. petchii*. On the other hand, Samson & Evans (1992) argued that *Granulomanus* naturally occurs independently on spider hosts either with or without *Gibellula*. Thus, the genus should be retained as an independent asexually typified genus resulting in rejection of *G. petchii*. According to a recent taxonomic revision of the *Cordycipitaceae*, which was largely based on molecular data, several generic names including *Granulomanus* were suppressed (Kepler *et al*. 2017). Nevertheless, the taxonomic dilemma of *G. petchii* cannot yet be resolved owing to the lack of sequence data.
Gibellula phialobasia Penz. & Sacc., Malpighia 15: 252. 1902. MycoBank MB 216177.
Note: Petch (1932) expressed doubt towards the identity of *G. phialobosia* because of its flask-shaped phialides regarded as an uncommon feature of *Gibellula*.

KEY TO *GIBELLULA* SPECIES

Aspergillus-like conidiophores 1
Penicillium-like conidiophores 12

1a. Mononematous ..... ***G. mainsii***
1b Synnematous 2

2a. Synnematal shape wing-like structure ..... ***G. alata***
2b. Synnematal shape globose to pyriform fertile area with a short sterile stipe ..... ***G. brunnea***
2c. Synnematal shape clavate 3
2d. Synnematal shape cylindrical 5

3a. Conidiophores 30–50 µm in length ..... ***G. clavata***
3b. Conidiophores longer than 50 µm 4

4a. Conidial heads (31–)37–42.5(−48) µm diam bearing fusoid to fusoid-ellipsoid conidia, smooth-walled, hyaline, (3–)3.5–5(−5.5) × (1–)1.5–2.5(−3) µm ..... ***G. gamsii***
4b. Conidial heads 25–40 µm diam bearing fusoid conidia, 5–7 x 2–3.5 µm ..... ***G. mirabilis***

5a. 1 synnema 6
5b. 2–5 synnemata. 9
5c. More than 5 synnemata 11

6a. *Granulomanus* synasexual morph present 7
6b. *Granulomanus* synasexual morph absent 8

7a. Conidiophores aspergillus-like ..... ***G. dimorpha/G. trimorpha***[1]
7b. Conidiophores irregular-shaped ..... ***G. cebrennini***

8a. Conidia ellipsoid, narrowly ovoid, sometimes with an acute end, (2.5–)3–3.5(–4) × 1–1.5 µm ..... ***G. nigelii***
8b. Conidia ellipsoid to ovoid, occasionally globose, (1.5–)2–2.5(–3) × 1–1.5(–2) µm ..... ***G. solita***
8c. Conidia cylindrical or fusoid, 3.2–6.5 × 1.1–1.6 µm ..... ***G. shennongjiaensis***

9a. Synnematal tips regular, not swollen ..... ***G. unica***
9b. Synnematal tips globose ..... ***G. pilosa***
9c. Synnematal tips ovoid 10

10a. Conidia ellipsoid or narrowly almond-shaped, (3–)3.5–4(–4.5) × 1.5–2 µm ..... ***G. brevistipitata***
10b. Conidia fusiform to broadly fusoid conidia, (3.5–)4–5(–6) × 1.5–2(–2.5) µm ..... ***G. fusiformispora***
10c. Conidia narrowly ovoid or narrowly ellipsoid or bacilliform, 4–5.5(–6) × (2–)2.5–3(–4) µm ..... ***G. parvula***
10d. Conidia broadly almond-shaped, (2.5–)3.5–5(–5.5) × 1–2(–3) µm ..... ***G. pigmentosinum***

11a. Conidia fusoid to ellipsoid ..... ***G. pulchra***
11b. Conidia bacilliform ..... ***G. longispora***
11c. Conidia clavate ..... ***G. clavispora***

12a. Mononematous ..... ***G. clavulifera* var. *alba***
12b. Synnematous 13

13a. Numerous synnemata 14
13b. A single synnema 15

14a. Conidia fusoid or fusoid-ellipsoid, 3–8 × 1–2 µm ..... ***G. leiopus***
14b. Conidia fusoid, 3.2–4 × 1.1–1.8 µm ..... ***G. dabieshanensis***

15a. Synnematal tip swollen ..... ***G. longicaudata***
15b. Synnematal tip regular, not swollen 16

16a. Conidia filiform ..... ***G. clavulifera***
16b. Conidia fusoid ..... ***G. scorpioides***
16c. Conidia bacilliform ..... ***G. clavulifera* var. *major***

[1] *Gibellula dimorpha* and *G. trimorpha* showed identical morphology. Only molecular data could distinguish one from the other.

ACKNOWLEDGEMENTS

This work was supported by the National Center for Genetic Engineering and Biotechnology (BIOTEC) Platform Technology Management (Grant no. P19-50231), National Science and Technology Development Agency (NSTDA). The National Park, Wildlife and Plant Conservation Department in Thailand is gratefully acknowledged for permission to conduct a study in the protected area. We are grateful to Dr Akio Tanikawa from the University of Tokyo, Japan for guidance and advice on the spider taxonomy, to Sasiporn Tongman from Thammasat University, Thailand for her effort in searching and gathering the data of spider's records from our country, and to Dr Philip James Shaw for the careful English editing of the manuscript.

DECLARATION ON CONFLICT OF INTEREST

The authors declare that there is no conflict of interest.

REFERENCES

Araújo JPM, Evans HC, Kepler RM, *et al*. (2018). Zombieant fungi across continents: 15 new species and new combinations within *Ophiocordyceps*. I. Myrmecophilous hirsutelloid-species. *Studies in Mycology* **90**: 1–42.

Ariyawansa HA, Hawksworth DL, Hyde KD, *et al*. (2014). Epitypification and neotypification: guidelines with appropriate and inappropriate examples. *Fungal Diversity* **69**: 57–91.

Baerg WJ (1926). Regeneration of appendages in the tarantula *Eurypelma califonica* Ausserer. *Annals of Entomological Society of America* **19**: 512–513.

Baker RJ, Bradley RD (2006). Speciation in mammals and the genetic species concept. *Journal of Mammalogy* **87**: 643–662.

Bałazy S (2004). Znaczenie obszarów chronionych dla zachowania zasobów grzybów entomopatogenicznych. *KOSMOS* **53**: 5–16.

Bishop L (1990). Entomophagous fungi as mortality agents of ballooning spiderlings. *Journal of Arachnology* **18**: 237–238.

Bosselaers JP (1984). *Gibellula pulchra* (Sacc.) Cavara in het gebied van de Slangebeekbron te Zonhoven (België). *Natuurhistorisch Maandblad* **73**: 166–168.

Cavara F (1894). Ulteriore contribuzione alla micologia lombarda. *Atti del'Istituto Botanico e del Laboratorio Crittogamico dell'Università di Pavia* **3**: 313–350.

Chaiphongpachara T, Lotulit A, Sumruayphol S (2019). Microhabitat use, morphology, and life cycle of brown widow spider *Latrodectus geometricus* (*Araneae: Theridiidae*) in Thailand: A case study of community housing in Samut Songkhram province. *Journal of Animal and Plant Science* **29**: 1793–1799.

Chen WH, Han YF, Liang ZQ, *et al.* (2016). Morphological traits, DELTA system, and molecular analysis for *Gibellula clavispora sp. nov*. from China. *Mycotaxon* **131**: 111–121.

Chiriví-Salomón JS, Danies G, Restrepo S, *et al.* (2015). *Lecanicillium sabanense sp. nov.* (*Cordycipitaceae*) a new fungal entomopathogen of coccids. *Phytotaxa* **234**: 63–74.

Chotwong W, Tanikawa A (2013). Four spider species of the families *Theridiidae*, *Araneidae*, and *Salticidae* (*Arachnida*: *Araneae*) new to Thailand. *Acta Arachnologica* **62**: 1–5.

Costa PP (2014). Gibellula *spp. associadas a aranhas da Mata do Paraíso, Viçosa-MG*. M.Sc. dissertation Minas Gerais, Universidade Federal de Viçosaans, Brazil.

Deeleman-Reinhold CL (2001). Forest spiders of South-East Asia: with a revision of the sac and ground spiders (*Araneae*: *Clubionidae*, *Corinnidae*, *Liocranidae*, *Gnaphosidae*, *Prodidomidae* and *Trochanterriidae* [*sic*]). Brill, Leiden.

Deeleman-Reinhold CL (2009). Spiny theridiids in the Asian tropics. Systematics, notes on behaviour and species richness (*Araneae*: *Theridiidae*: *Chrysso*, *Meotipa*). *Contributions to Natural History* **12**: 403–436.

Edgar RC (2004). MUSCLE: multiple sequence alignment with high accuracy and high through-put. *Nucleic Acids Research* **32**: 1792–1797.

Evans HC (2013). *Fungal pathogens of spiders*. In: Spider ecophysiology (Nentwig W, ed). Springer, Germany: 107–121.

Evans HC, Elliot SL, Hughes DP (2011). Hidden diversity behind the zombie-ant fungus *Ophiocordyceps unilateralis*: four new species described from carpenter ants in Minas Gerais, Brazil. *PLoS ONE* **6**: e17024.

Evans HC, Samson RA (1987). Fungal pathogens of spiders. *The Mycologist* **1**: 152–159.

Foelix RF (2011). *Biology of Spiders*. 3rd edn. Oxford University Press, Oxford, UK.

Gonzaga MO, Leiner NO, Santos AJ (2006). On the sticky cob-webs of two theridiid spiders (*Araneae*: *Theridiidae*). *Journal of Natural History* **40**: 293–306.

Hajek AE, St Leger RJ (1994). Interactions between fungal pathogens and insect hosts. *Annual Review of Entomology* **39**: 293–322.

Hall T (1999). BioEdit: a user-friendly biological sequence alignment editor and analysis program for Windows 95/98/NT. *Nucleic Acids Symposium Series* **41**: 95–98.

Hashimoto Y, Endo T, Yamasaki T, *et al*. (2020). Constraints on the jumping and prey-capture abilities of ant-mimicking spiders (*Salticidae*, *Salticinae*, *Myrmarachne*). *Scientific Reports* **10**: 18279.

Helaly SE, Kuephadungphan W, Phainuphong P, *et al.* (2019). Pigmentosins from *Gibellula* sp. as antibiofilm agents and a new glycosylated asperfuran from *Cordyceps javanica*. *Beilstein Journal of Organic Chemistry* **15**: 2968–2981.

Huang B, Ding DG, Fan MZ, *et al.* (1998). A new entomopathogenic fungus on spiders. *Mycosystema* **17**: 109–113.

Hughes DP, Araújo J, Loreto R, *et al.* (2016). From So Simple a Beginning: The Evolution of Behavioral Manipulation by Fungi. In: *Genetics and molecular biology of entomopathogenic fungi* (Advances in genetics) (Lovett B, St. Leger RJ, eds). Academic Press, Cambridge: 1–33.

Humber RA, Rombach MC (1987). *Torrubiella ratticaudata sp. nov*. (*Pyrenomycetes*: *Clavicipitales*) and other fungi from spiders on the Solomon Islands. *Mycologia* **79**: 375–382.

Jackson RR, Nelson AJ, Salm K (2008). The natural history of *Myrmarachne melanotarsa*, a social ant-mimicking jumping spider. *New Zealand Journal of Zoology* **35**: 225–235.

Jackson RR, Pollard SD, Nelson AJ, *et al.* (2001). Jumping spider (*Araneae*: *Salticidae*) that feed on nectar. *Journal of Zoology* **255**: 25–29.

Jocqué R, Dippenaar-Schoeman AS (2007). *Spider families of the world*. 2nd edn. Peeters nv, Belgium.

Johnson D, Sung GH, Hywel-Jones NL, *et al.* (2009). Systematics and evolution of the genus *Torrubiella* (*Hypocreales*, *Ascomycota*). *Mycological Research* **113**: 279–289.

Johnson T (1968). Host specialization as a taxonomic criterion. In: *The fungi advanced treatise vol. 3 the fungal population* (Ainsworth GC, Sussman AS, eds). Academic Press, New York: 543–554.

Kepler RM, Kaitsu Y, Tanaka E, *et al.* (2011). *Ophiocordyceps pulvinata sp. nov*., a pathogen with a reduced stroma. *Mycoscience* **52**: 39–47.

Kepler RM, Luangsa-ard JJ, Hywel-Jones NL, *et al.* (2017). A phylogenetically-based nomenclature for *Cordycipitaceae* (*Hypocreales*). *IMA Fungus* **8**: 335–353.

Kepler RM, Sung GH, Ban S, *et al.* (2012). New teleomorph combinations in the entomopathogenic genus *Metacordyceps*. *Mycologia* **104**: 182–197.

Khonsanit A, Luangsa-ard JJ, Thanakitpipattana D, *et al*. (2019). Cryptic species within *Ophiocordyceps myrmecophila* complex on formicine ants from Thailand. *Mycological Progress* **18**: 147–161.

Khonsanit A, Luangsa-ard JJ, Thanakitpipattana D, *et al.* (2020). Cryptic diversity of the genus *Beauveria* with a new species from Thailand. *Mycological Progress* **19**: 291–315.

Knoflach B (1996). Three new species of *Carniella* from Thailand (*Araneae, Theridiidae*). *Revue Suisse de Zoologie* **103**: 567–579.

Kobayasi Y, Shimizu D (1977). Some species of *Cordyceps* and its allies on spiders. *Kew Bulletin* **31**: 557–566.

Kobayasi Y, Shimizu D (1982). Monograph of the genus *Torrubiella*. *Bulletin of the National Science Museum, Tokyo, Series B* **8**: 43–78.

Kobmoo N, Arnamnart N, Pootakham W, *et al*. (2021). The integrative taxonomy of *Beauveria asiatica* and *B. bassiana* species complexes with whole-genome sequencing, morphometric and chemical analyses. *Persoonia* **47**: 136–150.

Kobmoo N, Mongkolsamrit S, Tasanathai K, *et al.* (2012). Molecular phylogenies reveal host-specific divergence of *Ophiocordyceps unilateralis sensu lato* following its host ants. *Molecular Ecology* **21**: 3022–3031.

Kobmoo N, Mongkolsamrit, S, Arnamnart N, *et al.* (2019). Population genomics revealed cryptic species within host-specific zombie-ant fungi (*Ophiocordyceps unilateralis*). *Molecular Phylogenetics and Evolution* **140**: 106580.

Kubátová A (2004). The arachnogenous fungus *Gibellula leiopus* – second find from the Czech Republic. *Czech Mycology* **56**: 185–191.

Kuephadungphan W, Macabeo APG, Luangsa-ard JJ, *et al.* (2019). Studies on the biologically active secondary metabolites of the new spider parasitic fungus *Gibellula gamsii*. *Mycological Progress* **18**: 135–146.

Kuephadungphan W, Tasanathai K, Petcharad B, *et al.* (2020). Phylogeny- and morphology-based recognition of new species in the spider-parasitic genus *Gibellula* (*Hypocreales*, *Cordycipitaceae*) from Thailand. *MycoKeys* **72**: 17–42.

Kumar S, Stecher G, Li M, *et al.* (2018). MEGA X: molecular evolutionary genetics analysis across computing platforms. *Molecular Biology and Evolution* **35**: 1547–1549.

Kwok ABC, Eldridge DJ (2016). The influence of shrub species and fine-scale plant density on arthropods in a semiarid shrubland. *Rangeland Journal* **38**: 381–389.

Labarque FM, Wolff JO, Michalik P, *et al.* (2017). The evolution and function of spider feet (*Araneae*: *Arachnida*): multiple acquisitions of distal articulations. *Zoological Journal of the Linnean Society*, 1–34.

Lee JH, Kim ST (2001). *Use of spiders as natural enemies to control rice pests in Korea*. Food and Fertilizer Technology Center, Korea.

Long SM (2021). Variations on a theme: Morphological variation in the secondary eye visual pathway across the order of *Araneae*. *Journal of Comparative Neurology* **529**: 259–280.

Luangsa-ard JJ, Hywel-Jones NL, Manoch L, *et al.* (2005). On the relationships of *Paecilomyces* sect. *Isarioidea* species. *Mycological Research* **109**: 581–589.

Luangsa-ard JJ, Tasanathai K, Mongkolsamrit S, *et al.* (2007). *Atlas of Invertebrate-Pathogenic Fungi of Thailand Volume 1*. National Center of Genetic Engineering and Biotechnology, National Science and Technology Development: Thailand.

Luangsa-ard JJ, Tasanathai K, Mongkolsamrit S, *et al.* (2010). *Atlas of invertebrate-pathogenic fungi of Thailand volume 3*. National Center of Genetic Engineering and Biotechnology, National Science and Technology Development: Thailand.

Lücking R, Aime MC, Robbertse B, *et al.* (2020). Unambiguous identification of fungi: where do we stand and how accurate and precise is fungal DNA barcoding? *IMA Fungus* **11**: 1–32.

Machałowski T, Amemiya C, Jesionowski T (2020). Chitin of *Araneae* origin: structural features and biomimetic applications: a review. *Applied Physics A* **126**: 678.

Mains EB (1950). The genus *Gibellula* on spiders in North America. *Mycologia* **42**: 306–321.

Marques MAL, Buckup EH, Rodrigues ENL (2011). Novo gênero neotropical de *Spintharinae* (*Araneae, Theridiidae*). *Iheringia, Série Zoologia* **101**: 372–381.

McNeil D (2012). Entomogenous fungi. *Shropshire Entomology* **5**: 5–6.

Mongkolsamrit S, Noisripoom W, Tasanathai K, *et al.* (2020). Molecular phylogeny and morphology reveal cryptic species in *Blackwellomyces* and *Cordyceps* (*Cordycipitaceae*) from Thailand. *Mycological Progress* **19**: 957–983.

Mongkolsamrit S, Noisripoom W, Thanakitpipattana D, *et al.* (2018). Disentangling cryptic species with isaria-like morphs in *Cordycipitaceae*. *Mycologia* **110**: 230–257.

Morehouse NI, Buschbeck EK, Zurek DB, *et al.* (2017). Molecular evolution of spider vision: new opportunities, familiar players. *Biology Bulletin* **233**: 21–38.

Nentwig W (1985). Parasitic fungi as a mortality factor of spiders. *Journal of Arachnology* **13**: 272–274.

Nyffeler M, Birkhofer K (2017). An estimated 400–800 million tons of prey are annually killed by the global spider community. *The Science of Nature* **104**: 30.

Nylander JAA (2004). MrModeltest 2.2. Program distributed by the author. Evolutionary Biology Centre, Uppsala University.

Okuzawa Y (2012). Cultural history of vegetable wasps and plant worms. Ishida Taiseisha.

Oxbrough AG, Gittings T, O'Halloran J, *et al.* (2005). Structural indicators of spider communities across the forest plantation cycle. *Forest Ecology and Management* **212**: 171–183.

Pérez-Miles F (2020). Introduction to the *Theraphosidae*. In: *New World Tarantulas*. Zoological Monographs (Pérez-Miles F, ed.) **6**: 1–23.

Petch T (1932). *Gibellula*. *Annales Mycologici* **30**: 386–393.

Petch T (1944). Notes on entomogenous fungi. *Transactions of the British Mycological Society* **27**: 81–93.

Petch T (1948). A revised list of British entomogenous fungi. *Transactions of the British Mycological Society* **31**: 286–304.

Ramírez MJ (2014). The morphology and phylogeny of dionychan spiders (*Araneae*: *Araneomorphae*). *Bulletin of the American Museum of Natural History* **390**: 1–374.

Ramírez MJ, Michalik P (2019). Web-building behavior of the odd-clawed spider *Progradungula otwayensis* (*Araneae*: *Gradungulidae*) and implications for the evolution of combing behavior in spiders. *The Journal of Arachnology* **47**: 299–309.

Rehner SA, Minnis AM, Sung GH, *et al.* (2011). Phylogeny and systematic of the anamorphic, entomopathogenic genus *Beauveria*. *Mycologia* **103**: 1055–1073.

Rong IH, Botha A (1993). New and interesting records of South African fungi XII. Synnematous Hyphomycetes. *South African Journal of Botany* **59**: 514–518.

Samson RA, Evans HC (1973). Notes on entomogenous fungi from Ghana. 1 The genera *Gibellula* and *Pseudogibellula*. *Acta Botanica Neerlandica* **22**: 522–528.

Samson RA, Evans HC (1977). Notes on entomogenous fungi from Ghana. IV. The genera *Paecilomyces* and *Nomuraea*. *Proceedings of the Koninklijke Nederlandse Akademie van Wetenschappen* Ser C **80**: 128–134.

Samson RA, Evans HC (1992). New species of *Gibellula* on spiders (*Araneida*) from South America. *Mycologia* **84**: 300–314.

Sánchez-Peña SR (1990). Some insect and spider pathogenic fungi from Mexico with data on their host ranges. *Florida Entomologist* **73**: 517–522.

Sanjuan T, Tabima J, Restrepo S, *et al.* (2014). Entomopathogens of Amazonian stick insects and locusts are members of the *Beauveria* species complex (*Cordyceps sensu stricto*). *Mycologia* **106**: 260–275.

Santamaria S, Girbal J (1996) *Gibellula pulchra* (Saccardo) Cavara, un fong patogen d'aranyes, a Catalunya. *Orsis* **11**: 179–181.

Savić D, Grbić G, Bošković E, *et al.* (2016). First records of fungi pathogenic on spiders for the Republic of Serbia. *Arachnologiche Mitteilungen/ Arachnology Letters* **52**: 31–34.

Selçuk F, Huseyin E, Gaffaroglu M (2004). Occurrence of the araneogenous fungus *Gibellula pulchra* in Turkey. *Mycologia Balcanica* **1**: 61–62.

Shrestha B, Kubátová A, Tanaka E, *et al.* (2019). Spider-pathogenic fungi within *Hypocreales* (*Ascomycota*): their current nomenclature, diversity, and distribution. *Mycological Progress* **18**: 983–1003.

Spatafora JW, Sung, GH, Sung JM, *et al.* (2007). Phylogenetic evidence for an animal pathogen origin of ergot and the grass endophytes. *Molecular Ecology* **16**: 1701–1711.

Stamatakis A (2014). RAxML version 8: a tool for phylogenetic analysis and post-analysis of large phylogenies. *Bioinformatics* **30**: 1312–1313.

Stefoff R (2009). *The Arachnid Class*. Marshall Cavendish.

Strongman DB (1991). *Gibellula pulchra* from a spider (*Salticidae*) in Nova Scotia, Canada. *Mycologia* **83**: 816–817.

Sung GH, Hywel-Jones NL, Sung JM, *et al.* (2007). Phylogenetic classification of *Cordyceps* and the clavicipitaceous fungi. *Studies in Mycology* **57**: 5–59.

Sung GH, Spatafora JW (2004). *Cordyceps cardinalis* sp. nov., a new species of *Cordyceps* with an east Asian-eastern North American distribution. *Mycologia* **96**: 658–666.

Sung GH, Spatafora JW, Zare R, *et al*. (2001). A revision of *Verticillium* sect. *Prostrata*. II. Phylogenetic analyses of SSU and LSU nuclear rDNA sequences from anamorphs and teleomorphs of the *Clavicipitaceae*. *Nova Hedwigia* **72**: 311–328.

Thanakitpipattana D, Tasanathai K, Mongkolsamrit S, *et al.* (2020). Fungal pathogens occurring on *Orthopterida* in Thailand. *Persoonia* **44**: 140–160.

Tkaczuk C, Balazy S, Krzyczkowski T *et al.* (2011). Extended studies on the diversity of arthropod-pathogenic fungi in Austria and Poland. *Acta Mycologica* **46**: 211–222.

Tsang CC, Chan JF, Pong WM, *et al.* (2016). Cutaneous hyalohyphomycosis due to *Parengyodontium album gen. et. comb. nov*. *Medical Mycology* **54**: 699–713.

Tzean SS, Hsieh LS, Wu WJ (1997). The genus *Gibellula* on spiders from Taiwan. *Mycologia* **89**: 309–318.

Tzean SS, Hsieh LS, Wu WJ (1998). *Torrubiella dimorpha*, a new species of spider parasite from Taiwan. *Mycological Research* **102**: 1350–1354.

Van der Bijl PA (1922). A fungus – *Gibellula haygarthii*, *sp. n*. - on a spider of the family *Lycosidae*. *Transactions of the Royal Society of South Africa* **10**: 149–150.

Vialle A, Feau N, Frey P (2013). Phylogenetic species recognition reveals host-specific lineages among poplar rust fungi. *Molecular Phylogenetics and Evolution* **66**: 628–644.

Wang YB, Wang Y, Fan Q, *et al.* (2020). Multigene phylogeny of the family *Cordycipitaceae* (*Hypocreales*): new taxa and the new systematic position of the Chinese cordycipitoid fungus *Paecilomyces hepiali*. *Fungal Diversity* **103**: 1–46.

Wolff JO, Gorb SN (2012). Comparative morphology of pretarsal scopulae in eleven spider families. *Arthropod Structure & Development* **41**: 419–433.

Wolff JO, Nentwig W, Gorb SN (2013). The great silk alternative: multiple co-evolution of web loss and sticky hairs in spiders. *PLoS ONE* **8**: e62682.

Wongprom P, Košulič O (2016). First data on spiders (*Arachnida: Araneae*) from dry dipterocarp forests of Thailand. *Check List Journal of Biodiversity Data* **12**: 1–13.

World Spider Catalog (2021). World Spider Catalog. Version 22.5. Natural History Museum Bern. <http://wsc.nmbe.ch> Accessed on 9 October 2021.

Ziesche TM, Roth M (2008). Influence of environmental parameters on small-scale distribution of soil-dwelling spiders in forest: What makes the difference, tree species or microhabitat? *Forest Ecology and Management* **255**: 738–752.

Zou X, Chen WH, Han YF, *et al*. (2016). A new species of the genus *Gibellula*. *Mycosystema* **35**: 1161–1168.

Studies in Mycology 101: 287–415 (2022).

Species diversity, systematic revision and molecular phylogeny of *Ganodermataceae* (*Polyporales*, *Basidiomycota*) with an emphasis on Chinese collections

Y.-F. Sun[1#], J.-H. Xing[1#], X.-L. He[2], D.-M. Wu[3], C.-G. Song[1], S. Liu[1], J. Vlasák[4], G. Gates[5], T.B. Gibertoni[6], B.-K. Cui[1*]

[1]*Institute of Microbiology, School of Ecology and Nature Conservation, Beijing Forestry University, Beijing 100083, China;* [2]*Sichuan Institute of Edible Fungi, Sichuan Academy of Agricultural Sciences, Chengdu, Sichuan 610066, China;* [3]*Biotechnology Research Institute, Xinjiang Academy of Agricultural and Reclamation Sciences / Xinjiang Production and Construction Group Key Laboratory of Crop Germplasm Enhancement and Gene Resources Utilization, Shihezi, Xinjiang 832000, China;* [4]*Biology Centre, Czech Academy of Sciences, Institute of Plant "Molecular Biology, Branišovská 31, CZ-370 05 České Budějovice, Czech Republic;* [5]*Tasmanian Institute of Agriculture, Private Bag 98, Hobart, Tasmania 7001, Australia;* [6]*Universidade Federal de Pernambuco, Centro de Biociências, Departamento de Micologia, Av. Avenida da Engenharia, s/n, CEP 50740-600, Recife, Pernambuco, Brasil*

[#]These authors contributed equally to the work
[*]*Corresponding author*: Bao-Kai Cui, cuibaokai@bjfu.edu.cn, baokaicui2013@gmail.com

Abstract: *Ganodermataceae* is one of the main families of macrofungi since species in the family are both ecologically and economically important. The double-walled basidiospores with ornamented endospore walls are the characteristic features of *Ganodermataceae*. It is a large and complex family; although many studies have focused on *Ganodermataceae*, the global diversity, geographic distribution, taxonomy and molecular phylogeny of *Ganodermataceae* still remained incompletely understood. In this work, taxonomic and phylogenetic studies on worldwide species of *Ganodermataceae* were carried out by morphological examination and molecular phylogenetic analyses inferred from six gene loci including the internal transcribed spacer regions (ITS), the large subunit of nuclear ribosomal RNA gene (nLSU), the second largest subunit of RNA polymerase II gene (*rpb2*), the translation elongation factor 1-α gene (*tef1*), the small subunit mitochondrial rRNA gene (mtSSU) and the small subunit nuclear ribosomal RNA gene (nSSU). A total of 1 382 sequences were used in the phylogenetic analyses, of which 817 were newly generated, including 132 sequences of ITS, 139 sequences of nLSU, 83 sequences of *rpb2*, 124 sequences of *tef1*, 150 sequences of mtSSU and 189 sequences of nSSU. The combined six-gene dataset included sequences from 391 specimens representing 146 taxa from *Ganodermataceae*. Based on morphological and phylogenetic analyses, 14 genera were confirmed in *Ganodermataceae*: *Amauroderma*, *Amaurodermellus*, *Cristataspora*, *Foraminispora*, *Furtadoella*, *Ganoderma*, *Haddowia*, *Humphreya*, *Magoderna*, *Neoganoderma*, *Sanguinoderma*, *Sinoganoderma*, *Tomophagus* and *Trachydermella*. Among these genera, *Neoganoderma gen. nov.* is proposed for *Ganoderma neurosporum*; *Sinoganoderma gen. nov.* is proposed for *Ganoderma shandongense*; *Furtadoella gen. nov.* is proposed to include taxa previously belonging to *Furtadoa* since *Furtadoa* is a homonym of a plant genus in the *Araceae*; *Trachydermella gen. nov.* is proposed to include *Trachyderma tsunodae* since *Trachyderma* is a homonym of a lichen genus in the *Pannariaceae*. Twenty-three new species, *viz*., *Ganoderma acaciicola*, *G. acontextum*, *G. alpinum*, *G. bubalinomarginatum*, *G. castaneum*, *G. chuxiongense*, *G. cocoicola*, *G. fallax*, *G. guangxiense*, *G. puerense*, *G. subangustisporum*, *G. subellipsoideum*, *G. subflexipes*, *G. sublobatum*, *G. tongshanense*, *G. yunlingense*, *Haddowia macropora*, *Sanguinoderma guangdongense*, *Sa. infundibulare*, *Sa. longistipitum*, *Sa. melanocarpum*, *Sa. microsporum* and *Sa. tricolor* are described. In addition, another 33 known species are also described in detail for comparison. Scanning electron micrographs of basidiospores of 10 genera in *Ganodermataceae* are provided. A key to the accepted genera of *Ganodermataceae* and keys to the accepted species of *Ganoderma*, *Haddowia*, *Humphreya*, *Magoderna*, *Sanguinoderma* and *Tomophagus* are also provided. In total, 278 species are accepted as members of *Ganodermataceae* including 59 species distributed in China.

Key words: *Ganoderma*, macro fungi, medicinal mushrooms, new taxa, phylogeny, ultrastructure, white-rot fungi.
Taxonomic novelties: New genera: *Furtadoella* B.K. Cui & Y.F. Sun, *Neoganoderma* B.K. Cui & Y.F. Sun, *Sinoganoderma* B.K. Cui, J.H. Xing & Y.F. Sun and *Trachydermella* B.K. Cui & Y.F. Sun; **New species:** *Ganoderma acaciicola* B.K. Cui, J.H. Xing & Y.F. Sun, *G. acontextum* B.K. Cui, J.H. Xing & Vlasák, *G. alpinum* B.K. Cui, J.H. Xing & Y.F. Sun, *G. bubalinomarginatum* B.K. Cui, J.H. Xing & Y.F. Sun, *G. castaneum* B.K. Cui, J.H. Xing & Y.F. Sun, *G. chuxiongense* B.K. Cui, J.H. Xing & Y.F. Sun, *G. cocoicola* B.K. Cui, J.H. Xing & Y.F. Sun, *G. fallax* B.K. Cui, J.H. Xing & Vlasák, *G. guangxiense* B.K. Cui, J.H. Xing & Y.F. Sun, *G. puerense* B.K. Cui, J.H. Xing & Y.F. Sun, *G. subangustisporum* B.K. Cui, J.H. Xing & Y.F. Sun, *G. subellipsoideum* B.K. Cui, J.H. Xing & Y.F. Sun, *G. subflexipes* B.K. Cui, J.H. Xing & Y.F. Sun, *G. sublobatum* B.K. Cui, J.H. Xing & Y.F. Sun, *G. tongshanense* B.K. Cui, J.H. Xing & Y.F. Sun, *G. yunlingense* B.K. Cui, J.H. Xing & Y.F. Sun, *Haddowia macropora* B.K. Cui, Vlasák & Y.F. Sun, *Sanguinoderma guangdongense* B.K. Cui & Y.F. Sun, *Sa. infundibulare* B.K. Cui & Y.F. Sun, *Sa. longistipitum* B.K. Cui & Y.F. Sun, *Sa. melanocarpum* B.K. Cui & Y.F. Sun, *Sa. microsporum* B.K. Cui & Y.F. Sun and *Sa. tricolor* B.K. Cui & Y.F. Sun; **New combinations**: *Furtadoella biseptata* (Costa-Rezende *et al.*) B.K. Cui & Y.F. Sun, *Fu. brasiliensis* (Singer) B.K. Cui & Y.F. Sun, *Fu. corneri* (Gulaid & Ryvarden) B.K. Cui & Y.F. Sun, *Neoganoderma neurosporum* (J.S. Furtado) B.K. Cui & Y.F. Sun, *Sinoganoderma shandongense* (J.D. Zhao & L.W. Xu) B.K. Cui, J.H. Xing & Y.F. Sun and *Trachydermella tsunodae* (Yasuda ex Lloyd) B.K. Cui & Y.F. Sun.

Citation: Sun Y-F, Xing J-H, He X-L, Wu D-M, Song C-G, Liu S, Vlasák J, Gates G, Gibertoni TB, Cui B-K (2022). Species diversity, systematic revision and molecular phylogeny of *Ganodermataceae* (*Polyporales*, *Basidiomycota*) with an emphasis on Chinese collections. *Studies in Mycology* **101**: 287–415. doi: 10.3114/sim.2022.101.05.
Received: 13 December 2021; **Accepted:** 6 April 2022; **Effectively published online:** 20 May 2022
Corresponding editor: Robert A. Samson

INTRODUCTION

Ganodermataceae as an important family in the *Polyporales* has been researched for many decades due to its high medicinal and ecological values. As traditional medicine, *Ganoderma lingzhi*, *G. sinense* and *Amauroderma rugosum* have been used for anti-cancer treatment, for lowering blood pressure and for improving immunity (Dai *et al.* 2009, Cao *et al.* 2012, Chan *et al.* 2013, Zhou *et al.* 2015, Zhang *et al.* 2019). Tree pathogens such as *G. boninense* can cause a basal stem rot on oil palm trees (Pilotti 2005), and *G. philippii* can cause a red root rot on *Acacia mangium* (Glen *et al.* 2009). Besides, *Ganoderma lucidum* and *A. rugosum*

have been used biotechnologically in the production of biofuel and degradation of environmental pollutants (Jong *et al.* 2017, Wang *et al.* 2021).

The systematics of the *Ganodermataceae* have been carried out for about 100 years. Donk (1948) introduced *Ganodermataceae* as a family based on its unique double-walled basidiospores with obvious ornamentation on the endospore walls, which only included *Ganoderma* with a laccate pileal surface and truncated basidiospores and *Amauroderma* with globose to ellipsoid basidiospores without a truncated apex. Murrill (1905) introduced a genus *Tomophagus* that included pale-coloured basidiomata with pale and soft context and truncated basidiospores. In the past decades, specimens of *Ganodermataceae* have been collected from all over the world (Steyaert 1972, Moncalvo & Ryvarden 1997, Ryvarden 2004b, Hapuarachchi *et al.* 2019b) except for the polar region. More genera have been established by evidence of morphological characters and/or molecular data. Imazeki (1952) presented *Trachyderma* as a genus with a fleshy succulent context and truncated basidiospores with spinules. Steyaert (1972) examined several known species in *Ganoderma*, then established *Haddowia* based on non-truncated basidiospores with longitudinal ridges partly connected with short transverse walls on the endospore walls; *Humphreya* with reticular or erratic irregularly ridged double walls on truncated basidiospores; and *Magoderna* based on anticlinal hyphae in pileipellis and ellipsoid to ovoid basidiospores without truncated apex. Costa-Rezende *et al.* (2017) established *Foraminispora* according to the hollow columnar endospore ornamentation, which persist to the exospore wall sometimes forming holes on the basidiospores, and *Furtadoa* based on a monomitic hyphal system in context with clamped and simple-septate generative hyphae. Sun *et al.* (2020) studied one group of *Amauroderma* with a unique pore surface that changes to blood red when bruised, and established *Sanguinoderma*. Costa-Rezende *et al.* (2020b) established *Amaurodermellus* with a dull pileal surface and ovoid basidiospores, and *Cristataspora* with double-walled basidiospores which have endosporic ornamentation as vertical or transverse ridges.

However, the uncertainty about the family level of *Ganodermataceae* should not be ignored. Binder *et al.* (2013) carried out the phylogenetic and phylogenomic analyses of *Polyporales* based on 356 single-copy genes from 10 genomes of this order, which showed that *Ganoderma* was involved in the 'core polyporoid clade'. Justo *et al.* (2017) suggested *Ganodermataceae* as a synonym of *Polyporaceae* based on ITS, nLSU and *rpb1* sequences. The conclusions based on phylogenetic evidence have certain credibility, while in this study, *Ganodermataceae* is still regarded as an independent family based on its remarkable morphological features to clarify the intergeneric and interspecific relationships. For the time being, we prefer to treat *Ganodermataceae* as an independent family different from *Polyporaceae* according to previous specialised studies on the *Ganoderma* group (Moncalvo & Ryvarden 1997, Robledo *et al.* 2015, Zhou *et al.* 2015, Hapuarachchi *et al.* 2018a, b, 2019a, b, Xing *et al.* 2018, Costa-Rezende *et al.* 2020a, b, Sun *et al.* 2020, Luangharn et al. 2021). The scientific status of *Ganodermataceae* within the *Polyporales* should be considered in morphology, phylogeny, and even whole genome sequences.

Ongoing taxonomic studies of *Ganodermataceae* from Asia, Africa, Europe, Neotropics and North America have been conducted for a long time with many new species and combinations continually being reported (Otieno 1968, Steyaert 1972, Moncalvo & Ryvarden 1997, Ryvarden 2004a, b, Gibertoni *et al.* 2008, Cao *et al.* 2012, Le *et al.* 2012, Coetzee *et al.* 2015, Gomes-Silva *et al.* 2015, Hapuarachchi *et al.* 2019b, Sun *et al.* 2020, Costa-Rezende *et al.* 2020b). China has a complex and diverse natural environment resulting in high species richness, and a total of 130 species of *Ganodermataceae* have been reported (Zhao & Zhang 2000, Dai 2012, Cao & Yuan 2012, Wang & Wu 2014, Li *et al.* 2015, Zhou *et al.* 2015, Hapuarachchi *et al.* 2018b, Xing *et al.* 2018, Ye *et al.* 2019, Sun *et al.* 2020). The great variability in the macroscopic characters of the basidiomata and the relatively uniform macro- and micro-morphology of most species in *Ganodermataceae* have resulted in many confusions in taxonomy. As of 10 March 2022, there were 642 records of *Ganodermataceae* recorded in Index Fungorum (http://www.indexfungorum.org/), and 698 records in MycoBank (http://www.mycobank.org/). Nearly half of these records have been identified as synonyms, especially in *Ganoderma* and *Amauroderma* and it is necessary to assess the validity of these records.

With the rapid development of molecular techniques in recent years, DNA sequence data have been widely used in the taxonomic studies of *Ganodermataceae*. Moncalvo (1995) used ITS sequences and the D2 region of nLSU sequences to construct the relationships among species in *Ganoderma*, and concluded that the combined data is useful for intrageneric segregation while the D2 region is suitable for intergeneric or higher ranks segregation. Subsequently, ITS and nLSU sequences were often used to identify species (Cao *et al.* 2012, Le *et al.* 2012, de Lima Júnior *et al.* 2014, Gomes-Silva *et al.* 2015, Li *et al.* 2015). It is worth mentioning that Fryssouli *et al.* (2020) carried out a phylogenetic study of *Ganoderma* based only on 3 970 ITS sequences obtained from the GenBank/ENA/DDBJ database which evaluated the accuracy of sequences and showed that *Ganoderma* can be divided into five main lineages. However, for the complex groups in *Ganoderma* or for the higher rank classification of *Ganodermataceae*, most researchers use multi-gene datasets to construct phylogenetic trees (Zhou *et al.* 2015, Costa-Rezende *et al.* 2017, 2020b, Justo *et al.* 2017, Cabarroi-Hernández *et al.* 2019, Hapuarachchi *et al.* 2019b, Luangharn *et al.* 2020, Sun *et al.* 2020). At present, eight genes have been applied to the phylogenetic analyses in *Ganodermataceae*, *viz*., the internal transcribed spacer regions (ITS), the large subunit of nuclear ribosomal RNA gene (nLSU), the largest subunit of RNA polymerase II gene (*rpb1*), the second largest subunit of RNA polymerase II gene (*rpb2*), the translation elongation factor 1-α gene (*tef1*), the β-tubulin gene (*tub*), the small subunit mitochondrial rRNA gene (mtSSU) and the small subunit nuclear ribosomal RNA gene (nSSU). According to the records in GenBank (https://www.ncbi.nlm.nih.gov/) as of 21 April 2021, 150 801 items were found by searching '*Ganodermataceae*' directly, but only about 65 000 items among them were identified as species of *Ganodermataceae*. The number of sequences is considerable, but repetitive sequences of the same species or specimens, inaccurate identification and low quality of sequences make it necessary to select only the reliable molecular data for phylogenetic analyses.

In this study, the specimens collected from all over the world were studied by macromorphological and microscopic examinations together with ultrastructural observations and phylogenetic analyses based on six gene loci (ITS, nLSU, *rpb2*, *tef1*, mtSSU and nSSU). A total of 146 species in *Ganodermataceae* with available DNA sequences were involved in the phylogenetic analyses. Based on morphological characters and phylogenetic evidence, 14 genera were confirmed within *Ganodermataceae*, *Furtadoella gen. nov.*, *Neoganoderma gen. nov.*, *Sinoganoderma gen. nov.* and *Trachydermella gen. nov.* were proposed as new genera;

278 species were confirmed in *Ganodermataceae* including 23 new species which are listed in Table 2. The ultrastructural features observed under SEM of basidiospores of 10 genera in *Ganodermataceae* were described and photographed. In total, 56 species and nine genera are described and illustrated here. A key to accepted genera of *Ganodermataceae* and keys to accepted species of *Ganoderma*, *Haddowia*, *Humphreya*, *Magoderna*, *Sanguinoderma*, *Tomophagus* are also provided.

MATERIALS AND METHODS

Morphological studies

The studied specimens are deposited at the fungaria of the Institute of Microbiology, Beijing Forestry University (BJFC, Beijing, China), the Institute of Applied Ecology, Chinese Academy of Sciences (IFP, Shenyang, China), the private fungarium of J. Vlasák of Czech Republic (JV) and the Universidade Federal de Pernambuco, Brazil (URM). Macro-morphological descriptions of the new taxa (or selected taxa) were based on field notes and fungarium specimens. Special colour terms followed Petersen (1996). Micro-morphological data were obtained from dried specimens and observed under a compound microscope following Cui *et al.* (2019) and Sun *et al.* (2020). Sections were studied at a magnification up to 1 000× using Nikon E80i microscope and phase contrast illumination (Nikon, Tokyo, Japan). Line drawings were made with the aid of a drawing tube. Ultrastructure of basidiospores was observed with Scanning Electron Microscopy (SEM) using a Field Emission Scanning Electron Microscope (FESEM) Hitachi SU-8010 (Hitachi, Ltd, Tokyo, Japan) at Beijing Forestry University, China (BJFU). Microscopic features, measurements and drawings were made from slide preparations stained with Cotton Blue and Melzer's reagent. Spores were measured from sections cut from the tubes. To represent the variation in the size of the basidiospores, 5 % of measurements were excluded from each end of the range, and are given in parentheses. The following abbreviations are used: IKI = Melzer's reagent, IKI – = neither amyloid nor dextrinoid, KOH = 5 % potassium hydroxide, CB = Cotton Blue, CB + = cyanophilous, L = mean spore length (arithmetic average of all spores), W = mean spore width (arithmetic average of all spores), Q = variation in the L/W ratios between the specimens studied, n (a/b) = number of spores: (a) measured from given number, (b) of specimens.

DNA extraction, amplification and sequencing

A cetyl trimethylammonium bromide (CTAB) rapid plant genome extraction kit-DN14 (Aidlab Biotechnologies Co., Ltd, Beijing, China) and a FH plant DNA kit II (Demeter Biotech Co., Ltd., Beijing, China) were used to extract total genomic DNA from dried specimens and to perform the polymerase chain reaction (PCR) according to the manufacturer's instructions with some modifications (Xing *et al.* 2018, Sun *et al.* 2020). The ITS regions were amplified with primer pairs ITS5 and ITS4 (White *et al.* 1990). The nLSU regions were amplified with primer pairs LR0R and LR7, and the primer LR5 was used sometimes as an alternative to LR7 (Vilgalys & Hester 1990). The *rpb2* regions were amplified with primer pairs fRPB2-5F and fRPB2-7CR (Liu *et al.* 1999). The *tef1* regions were amplified with primer pairs EF1-983F and EF1-1567R (Rehner & Buckley 2005). The mtSSU regions were amplified with primer pairs MS1 and MS2 (White *et al.* 1990). The nSSU regions were amplified with primer pairs PNS1 and NS41 (White *et al.* 1990).

The PCR cycling schedule for ITS, *tef1* and mtSSU included an initial denaturation at 95 °C for 3 min, followed by 35 cycles at 94 °C for 40 s, 54 °C for ITS and mtSSU, 55 °C for *tef1* for 45 s, 72 °C for 1 min, and a final extension at 72 °C for 10 min. The PCR cycling schedule for nLSU and nSSU included an initial denaturation at 94 °C for 1 min, followed by 35 cycles at 94 °C for 30 s, 50 °C for nLSU and 53 °C for nSSU for 1 min, 72 °C for 1.5 min, and a final extension at 72 °C for 10 min. The PCR cycling schedule for *rpb2* included an initial denaturation at 94 °C for 2 min, followed by 10 cycles at 94 °C for 40 s, 60 °C for 40 s and 72 °C for 2 min, then followed by 37 cycles at 94 °C for 45 s, 55 °C for 1.5 min and 72 °C for 2 min, and a final extension of 72 °C for 10 min. The PCR products were purified and sequenced at the Beijing Genomics Institute (BGI), China, with the same primers. All sequences analysed in this study were deposited at GenBank and are listed in Table 1.

Phylogenetic analyses

The sequences generated in this study and retrieved from GenBank were combined with ITS, nLSU, *rpb2*, *tef1*, mtSSU and nSSU. *Perenniporia subtephropora* was selected as the outgroup (Xing 2019). Phylogenetic analyses used in this study followed the approach of Song & Cui (2017) and Shen *et al.* (2019). All sequences of ITS, nLSU, *rpb2*, *tef1*, mtSSU and nSSU were respectively aligned in MAFFT v. 7 (Katoh & Standley 2013, https://mafft.cbrc.jp/alignment/server/) and manually adjusted in BioEdit v. 7.0.9. (Hall 1999). Alignments were spliced in Mesquite v. 3.2. (Maddison & Maddison 2017). The partition homogeneity test (PHT) (Farris *et al.* 1994) of the six-gene dataset was tested by PAUP v. 4.0b10 (Swofford 2002) under 1 000 homogeneity replicates. The best-fit evolutionary model was selected by hierarchical likelihood ratio tests (hLRT) and Akaike information criterion (AIC) in MrModeltest v. 2.3 (Nylander 2004) after scoring 24 models of evolution by PAUP v. 4.0b10.

The Maximum Likelihood (ML) and Bayesian Inference (BI) analyses were performed based on the combined dataset. Each gene of ITS, nLSU, *rpb2*, *tef1*, mtSSU and nSSU was used to perform ML analyses respectively. The ML analyses were performed in RAxML-HPC v. 8.2.3 (Stamatakis 2014) and involved 1 000 ML searches under the GTRGAMMA model, and only the Maximum Likelihood best tree from all searches was provided. In addition, 1 000 rapid bootstrap replicates were run with the GTRCAT model to assess ML bootstrap values of the nodes. Bayesian Inference was calculated using MrBayes v. 3.1.2 (Ronquist & Huelsenbeck 2003) with four Markov chains, starting trees for 80 M generations until the split deviation frequency < 0.01, and trees were sampled every 100 generations. The first 25 % of the sampled trees were discarded as burn-in and the remaining ones were used to reconstruct a majority rule consensus and calculate Bayesian Posterior Probabilities (BPP) of the clades.

All trees were viewed in FigTree v. 1.4.2 (http://tree.bio.ed.ac.uk/software/figtree/). The ML bootstrap support values ≥ 50 % and Bayesian Posterior Probabilities ≥ 0.95 were presented on topologies from ML analyses respectively. The final alignments and the retrieved topologies were deposited in TreeBASE (http:// www.treebase.org), under accession ID: 27788 (http://purl.org/phylo/treebase/phylows/study/TB2:S27788).

Table 1. Taxa information and GenBank accession numbers of the sequences used in this study. Species in bold are new species or new combinations.

		GenBank accession No.						
Species	**Voucher**	**ITS**	**nLSU**	***rpb2***	***tef1***	**mtSSU**	**nSSU**	**References**
Amauroderma aurantiacum	FLOR 52205	KR816510	KU315205	–	–	–	–	Costa-Rezende *et al.* (2016)
	DHCR540	MF409961	MF409953	–	–	–	–	Costa-Rezende *et al.* (2017)
A. calcigenum	FLOR 52315	KR816514	–	–	–	–	–	Costa-Rezende *et al.* (2016)
	URM 89213	MK119792	MK119870	MK121484	MK121541	MZ352778[a]	MZ355137[a]	Sun *et al.* (2020), this study
	JV 1808/51	MZ354865[a]	MZ354997[a]	MZ245374[a]	MZ221624[a]	MZ352779[a]	MZ355138[a]	This study
	URM83864	JX982565	–	–	–	–	–	Gomes-Silva *et al.* (2015)
	URM86847	KT006601	–	–	–	–	–	Gomes-Silva *et al.* (2015)
	URM 89566	MZ354866[a]	MZ355111[a]	MZ245375[a]	MZ221625[a]	MZ352780[a]	MZ355146[a]	This study
A. calcitum	FLOR 50931/DHCR538	KR816528	KU315207	–	–	–	–	Costa-Rezende *et al.* (2016)
	FLOR 52230 (TYPE)	KR816529	–	–	–	–	–	Costa-Rezende *et al.* (2016)
A. camerarium	FLOR 52169	KR816523	–	–	–	–	–	Costa-Rezende *et al.* (2016)
	FLOR 52216	KR816509	–	–	–	–	–	Costa-Rezende *et al.* (2016)
A. cf. schomburgkii	URM 89271	MK119802	MK119880	MK121495	MK121552	–	MZ355289[a]	Sun *et al.* (2020), this study
	URM 89272	MK119803	MK119881	MK121496	MK121553	–	MZ355280[a]	Sun *et al.* (2020), this study
	JV 1908/39	MZ354989[a]	MZ354999[a]	MZ245376[a]	MZ221626[a]	–	MZ355147[a]	This study
A. elegantissimum	Dai 17431	MK119794	MK119872	MK121493	MK121543	–	MZ355288[a]	Sun *et al.* (2020), this study
	URM 83822	MK119795	MK119873	MK121494	MK121544	MZ352784[a]	MZ355308[a]	Sun *et al.* (2020), this study
A. exile	URM82794	JX310845	–	–	–	–	–	Gomes-Silva *et al.* (2015)
	URM 89226	MK119796	MK119874	–	MK121545	–	MZ355249[a]	Sun *et al.* (2020), this study
A. floriformum	URM83250 (TYPE)	JX310846	–	–	–	–	–	Gomes-Silva *et al.* (2015)
A. intermedium	GAS910	MF409959	–	–	–	–	–	Costa-Rezende *et al.* (2017)
	FLOR 52248	KR816527	KU315209	–	–	–	–	Costa-Rezende *et al.* (2016)
	JV 1312/E14-J	MZ354868[a]	MZ355096[a]	–	MZ221627[a]	–	MZ355151[a]	This study
A. laccatostipitatum	HFSL ACGS7	KT006602	–	–	–	–	–	Gomes-Silva *et al.* (2015)
	URM 89240	MK119797	MK119875	MK121489	MK121546	MZ352781[a]	MZ355262[a]	Sun *et al.* (2020), this study
A. omphalodes	DHCR499/501	MF409956	MF409951	–	MF421238	–	–	Costa-Rezende *et al.* (2017)
	DHCR500	MF409957	MF409952	–	MF421239	–	–	Costa-Rezende *et al.* (2017)
	JV 1909/23-J	MZ354991[a]	MZ355000[a]	MZ245377[a]	MZ221628[a]	MZ352785[a]	MZ355250[a]	This study
A. partitum	URM82882	JX310852	–	–	–	–	–	Gomes-Silva *et al.* (2015)
	URM83039	JX310853	–	–	–	–	–	Gomes-Silva *et al.* (2015)
A. praetervisum	URM 89233	MK119801	MK119879	MK121486	MK121551	MZ352926[a]	MZ355315[a]	Sun *et al.* (2020), this study

Table 1. (Continued).

Species	Voucher	GenBank accession No.						References
		ITS	nLSU	*rpb2*	*tef1*	mtSSU	nSSU	
	JV 1467/40	MZ354867[a]	–	–	–	–	–	This study
A. pseudoboletum	FLOR 52318	KR816516	–	–	–	–	–	Costa-Rezende *et al.* (2016)
A. robledoi	FLOR 52249	KR816511	–	–	–	–	–	Costa-Rezende *et al.* (2016)
	URM84230	KC348461	–	–	–	–	–	Unpublished
	URM 87687	MK119800	MK119878	MK121487	MK121550	MZ352786[a]	MZ355290[a]	Sun *et al.* (2020), this study
A. schomburgkii	JV 1908/9	MZ354990[a]	–	–	MZ221629[a]	–	MZ355152[a]	This study
	URM 89225	MK119805	MK119883	MK121498	MK121555	–	MZ355324[a]	Sun *et al.* (2020), this study
	URM83228	JX310848	KT006621	–	–	–	–	Gomes-Silva *et al.* (2015)
Amauroderma sp.	URM 89239	MZ354869[a]	MZ355112[a]	MZ245378[a]	MZ221630[a]	MZ352927[a]	MZ355253[a]	This study
A. subsessile	URM 89293	MK119806	MK119885	MK121490	MK121556	MZ352782[a]	MZ355319[a]	Sun *et al.* (2020), this study
	URM 89294	MK119807	MK119886	MK121491	MK121557	MZ352783[a]	MZ355317[a]	Sun *et al.* (2020), this study
Amaurodermellus ovisporum	DHCR127 (FLOR)	MN077530	–	–	–	–	–	Costa-Rezende *et al.* (2020b)
	DHCR546 (HUEFS)	MN077528	–	–	–	–	–	Costa-Rezende *et al.* (2020b)
	DHCR547 (HUEFS)	MN077527	MN077553	–	–	–	–	Costa-Rezende *et al.* (2020b)
	DHCR539 (HUEFS)	MN077529	–	–	–	–	–	Costa-Rezende *et al.* (2020b)
Cristataspora coffeata	FLOR 50933	KU315204	–	–	–	–	–	Costa-Rezende *et al.* (2020b)
	1504/50	MZ354891[a]	–	–	MZ221631[a]	–	–	This study
	Robledo 3183 (FCOS)	MN077526	MN077560	–	MN061695	–	–	Costa-Rezende *et al.* (2020b)
	Robledo 3182 (FCOS)	MN077525	MN077559	–	–	–	–	Costa-Rezende *et al.* (2020b)
C. flavipora	G299	MN077521	MN077555	–	MN061694	–	–	Costa-Rezende *et al.* (2020b)
Foraminispora austrosinensis	Cui 16425	MK119809	MK119888	–	MK121559	MZ352835[a]	MZ355257[a]	Sun *et al.* (2020), this study
	Cui 14318	MK119810	MK119889	–	MK121560	MZ352848[a]	MZ355309[a]	Sun *et al.* (2020), this study
Fo. concentrica	Cui 12644 (TYPE)	MK119812	MK119891	MK121499	MK121561	MZ352839[a]	MZ355310[a]	Sun *et al.* (2020), this study
	Cui 16238	MK119816	MK119895	–	MK121565	MZ352840[a]	MZ355279[a]	Sun *et al.* (2020), this study
	Cui 17141	MZ354892[a]	MZ355001[a]	MZ245379[a]	–	MZ352837[a]	MZ355311[a]	This study
	Cui 12648	MK119815	MK119894	MK121501	MK121564	MZ352849[a]	MZ355314[a]	Sun *et al.* (2020), this study
Fo. rugosa	DHCR512	MF409960	–	–	MF421240	–	–	Costa-Rezende *et al.* (2017)
	DHCR560	MF409963	MF409955	–	MF421241	–	–	Costa-Rezende *et al.* (2017)
	URM 86888	MZ354945[a]	MZ355131[a]	MZ245380[a]	–	MZ352921[a]	MZ355277[a]	This study
	JV 1608/889-ND	MZ354946[a]	–	–	–	MZ352919[a]	–	This study
Fo. yinggelingensis	Cui 13618 (TYPE)	MK119821	MK119900	MK121536	MK121570	MZ352838[a]	MZ355275[a]	Sun *et al.* (2020), this study

Table 1. (Continued).

Species	Voucher	GenBank accession No.						References
		ITS	nLSU	*rpb2*	*tef1*	mtSSU	nSSU	
	Cui 13630	MK119822	MK119901	–	–	MZ352836[a]	MZ355276[a]	Sun *et al.* (2020), this study
Fo. yunnanensis	Cui 7974	KJ531653	KU220013	–	–	MZ352841[a]	–	Li & Yuan (2015), this study
	Yuan 2253	KJ531655	–	–	–	–	–	Li & Yuan (2015)
Furtadoella biseptata	FLOR 50932 (TYPE)	KU315196	KU315206	–	–	–	–	Costa-Rezende *et al.* (2016)
Fu. brasiliensis	URM83578	JX310841	–	–	–	–	–	Gomes-Silva *et al.* (2015)
	TBG58	JX982569	–	–	–	–	–	Gomes-Silva *et al.* (2015)
	JV 1909/75	MZ354994[a]	MZ355100[a]	MZ245381[a]	MZ221632[a]	MZ352922[a]	MZ355214[a]	This study
Ganoderma acaciicola	Cui 16813	MZ354893[a]	MZ355003[a]	MZ245382[a]	–	–	MZ355221[a]	This study
	Cui 16814	MZ354894[a]	MZ355004[a]	MZ245383[a]	–	–	MZ355219[a]	This study
	Cui 16815 (TYPE)	MZ354895[a]	MZ355005[a]	MZ245384[a]	–	–	MZ355282[a]	This study
G. acontextum	JV 0611/21G (TYPE)	KF605667	–	MG367489	MG367538	–	–	This study
	JV 1208/11J	KF605668	–	MG367490	MG367540	–	–	This study
	JV 1407/64	MG279151	–	MG367491	MG367539	–	–	This study
G. adspersum	Dai 13191	MG279153	–	MG367492	MG367541	–	MZ355157[a]	Xing *et al.* (2018), this study
	HSBU-200894	MG279154	–	–	MG367542	–	MZ355158[a]	Xing *et al.* (2018), this study
G. alpinum	Cui 18402	MZ354910[a]	–	–	–	–	–	This study
	Cui 17325	MZ354911[a]	–	–	–	–	–	This study
	Cui 17467 (TYPE)	MZ354912[a]	–	–	–	–	–	This study
G. angustisporum	Cui 13817 (TYPE)	MG279170	MZ355090[a]	MG367507	MG367563	MZ352850[a]	MZ355166[a]	Xing *et al.* (2018), this study
	Dai 19603	MZ354978[a]	MZ355047[a]	MZ245385[a]	MZ221633[a]	MZ352856[a]	MZ355207[a]	This study
	Cui 18240	MZ354979[a]	MZ355074[a]	MZ245386[a]	MZ221634[a]	MZ352851[a]	MZ355246[a]	This study
G. applanatum	Cui 14062	MZ354913[a]	MZ355076[a]	MZ358846[a]	MZ221635[a]	MZ352857[a]	MZ355202[a]	This study
	Cui 14070	MZ354914[a]	MZ355079[a]	MZ245387[a]	MZ221636[a]	–	MZ355203[a]	This study
G. aridicola	Dai 12588 (TYPE)	KU572491	–	–	KU572502	MZ352842[a]	MZ355195[a]	Xing *et al.* (2016), this study
	GanoTK01	JN105707	–	–	–	JN105734	–	Unpublished
	GanoTK25	JN105708	–	–	–	JN105719	–	Unpublished
G. australe	DHCR411	MF436675	MF436672	–	MF436677	–	–	Costa-Rezende *et al.* (2017)
	DHCR417	MF436676	MF436673	–	MF436678	–	–	Costa-Rezende *et al.* (2017)
G. austroafricanum	CBS 138724	KM507324	KM507325	MK611970	–	–	–	Coetzee *et al.* (2015)
G. boninense	WD 2085	KJ143906	–	KJ143965	KJ143925	–	–	Zhou *et al.* (2015)
	WD 2028	KJ143905	KU220015	KJ143964	KJ143924	–	–	Zhou *et al.* (2015)

Table 1. (Continued).

Species	Voucher	GenBank accession No.						References
		ITS	nLSU	*rpb2*	*tef1*	mtSSU	nSSU	
G. brownii	JV 1105/9J	MG279159	–	MG367494	MG367547	–	–	Xing *et al.* (2018)
	JV 0709/109	KF605662	–	MG367495	MG367548	–	–	Unpublished
G. bubalinomarginatum	Dai 20074	MZ354926[a]	MZ355010[a]	MZ245388[a]	MZ221637[a]	MZ352881[a]	MZ355312[a]	This study
	Dai 20075 (TYPE)	MZ354927[a]	MZ355040[a]	MZ245389[a]	MZ221638[a]	MZ352882[a]	MZ355224[a]	This study
G. calidophilum	MFLU 19-2174	MN398337	–	–	–	–	–	Luangharn *et al.* (2021)
	MFLU 19-2219	MN398338	–	–	–	–	–	Luangharn *et al.* (2021)
G. carnosum	MUCL 49464	MG706220	MG706168	–	–	–	–	Unpublished
	LGAM 1642	MG706217	MG706165	–	–	–	–	Unpublished
G. carocalcareum	DMC 322 (TYPE)	EU089969	–	–	–	–	–	Douanla-Meli & Langer (2009)
	DMC 513	EU089970	–	–	–	EU089971	–	Douanla-Meli & Langer (2009)
G. castaneum	Dai 16500	MZ354918[a]	–	MZ245390[a]	MZ221639[a]	MZ352914[a]	MZ355173[a]	This study
	Cui 13893	MZ354919[a]	MZ355013[a]	MZ245391[a]	MZ221640[a]	MZ352915[a]	MZ355185[a]	This study
	Dai 13710	KU572489	MZ355045[a]	–	KU572499	MZ352917[a]	MZ355229[a]	Xing *et al.* (2016), this study
	Cui 17283 (TYPE)	MZ354920[a]	–	–	–	MZ352916[a]	MZ355230[a]	This study
G. casuarinicola	Dai 16336 (TYPE)	MG279173	MZ355103[a]	MG367508	MG367565	MZ352843[a]	MZ355297[a]	Xing *et al.* (2018), this study
	Dai 16337	MG279174	MZ355104[a]	MG367509	MG367566	MZ352844[a]	MZ355196[a]	Xing *et al.* (2018), this study
	Dai 19678	MZ354995[a]	MZ355105[a]	–	MZ221641[a]	MZ352845[a]	MZ355204[a]	This study
	Dai 19470	MZ354996[a]	–	MZ245392[a]	MZ221642[a]	–	MZ355142[a]	This study
G. chalceum	URM80457	JX310812	JX310826	–	–	–	–	De Lima Júnior *et al.* (2014)
G. chocoense	QCAM 3123 (TYPE)	MH890527	–	–	–	–	–	Crous *et al.* (2018)
G. chuxiongense	Cui 17262 (TYPE)	MZ354907[a]	–	–	–	MZ352925[a]	MZ355316[a]	This study
G. cocoicola	Cui 16791 (TYPE)	MZ354984[a]	MZ355091[a]	MZ245393[a]	MZ221643[a]	–	MZ355321[a]	This study
	Cui 16792	MZ354985[a]	MZ355092[a]	MZ245394[a]	MZ221644[a]	–	MZ355278[a]	This study
G. concinnum	Robledo 3192	MN077522	MN077556	–	–	–	–	Costa-Rezende *et al.* (2020b)
	Robledo 3235	MN077523	MN077557	–	–	–	–	Costa-Rezende *et al.* (2020b)
G. cupreum	GanoTK4	JN105701	–	–	–	JN105732	–	Unpublished
	GanoTK7	JN105702	–	–	–	JN105730	–	Unpublished
G. curtisii	CBS 100131	JQ781848	–	KJ143966	KJ143926	–	–	Cao *et al.* (2012), Zhou *et al.* (2015)
	CBS 100132	JQ781849	–	KJ143967	KJ143927	–	–	Cao *et al.* (2012), Zhou *et al.* (2015)
G. destructans	CMW43670 (TYPE)	KR183856	–	–	–	–	–	Coetzee *et al.* (2015)
	Dai 16431	MG279177	–	–	–	–	–	Xing *et al.* (2018)

Table 1. (Continued).

Species	Voucher	GenBank accession No.						References
		ITS	nLSU	*rpb2*	*tef1*	mtSSU	nSSU	
G. dunense	CMW42149	MG020248	–	–	MG020226	–	–	Tchotet Tchoumi *et al.* (2018)
	CMW42157 (TYPE)	MG020255	–	–	MG020227	–	–	Tchotet Tchoumi *et al.* (2018)
G. ecuadorense	Dai 17397	MZ354950[a]	MZ355019[a]	MZ245398[a]	MZ221648[a]	–	MZ355180[a]	This study
	Dai 17418	MZ354951[a]	MZ355020[a]	MZ245399[a]	MZ221649[a]	–	MZ355181[a]	This study
	JV 1808/85	MZ354952[a]	MZ355075[a]	–	MZ221650[a]	–	MZ355247[a]	This study
G. eickeri	CMW50325	MH571689	–	–	MH567290	–	–	Tchotet Tchoumi *et al.* (2019)
	CMW49692 (TYPE)	MH571690	–	–	MH567287	–	–	Tchotet Tchoumi *et al.* (2019)
	Dai 12595	MZ354964[a]	MZ355035[a]	–	MZ221651[a]	–	MZ355159[a]	This study
	Dai 12598	MZ354965[a]	MZ355036[a]	–	MZ221652[a]	–	MZ355160[a]	This study
G. ellipsoideum	MFLU 19-2221	MN398339	–	–	–	–	–	Luangharn *et al.* (2021)
	CMW 14080966 (TYPE)	MH106867	–	–	–	–	–	Hapuarachchi *et al.* (2018b)
	Dai 19683	MZ354970[a]	MZ355018[a]	–	MZ221653[a]	MZ352893[a]	MZ355217[a]	This study
	Dai 20544	MZ354971[a]	MZ355033[a]	MZ245400[a]	MZ221654[a]	MZ352895[a]	MZ355205[a]	This study
G. enigmaticum	CMW43669 (TYPE)	KR183855	KR183859	–	–	–	–	Coetzee *et al.* (2015)
	Dai 15970	KU572486	MZ355106[a]	MG367513	KU572496	MZ352846[a]	MZ355197[a]	Xing *et al.* (2016, 2018), this study
	Dai 15971	KU572487	MZ355107[a]	MG367514	KU572497	MZ352847[a]	MZ355198[a]	Xing *et al.* (2016, 2018), this study
G. fallax	JV 1009/27 (TYPE)	KF605655	–	–	–	–	–	This study
	JV 0709/39	KF605658	–	–	–	–	–	This study
	JV 0509/93K	KF605653	–	–	–	–	–	This study
G. flexipes	Cui 13841	MZ354923[a]	MZ355063[a]	MZ245401[a]	MZ221655[a]	MZ352905[a]	MZ355177[a]	This study
	Cui 13863	MZ354924[a]	MZ355064[a]	MZ245402[a]	MZ221656[a]	–	MZ355178[a]	This study
	Dai 20461	MZ354925[a]	MZ355065[a]	MZ245403[a]	MZ221657[a]	–	MZ355153[a]	This study
G. fornicatum	BCRC35374	JX840349	–	–	–	–	–	Wang *et al.* (2014)
	TNM-F0010592	JX840347	–	–	–	–	–	Wang *et al.* (2014)
G. gibbosum	KUMCC17-0003	MH035681	MH553157	–	–	–	–	Luangharn *et al.* (2020)
	KUMCC17-0005	MH035682	MH553158	–	–	–	–	Luangharn *et al.* (2020)
	Cui 13940	MZ354972[a]	MZ355021[a]	MZ245404[a]	MZ221658[a]	MZ352894[a]	MZ355161[a]	This study
	Cui 14338	MZ354969[a]	MZ355014[a]	MZ245405[a]	MZ221659[a]	MZ352876[a]	MZ355162[a]	This study
	Cui 17769	MZ354967[a]	–	–	–	–	–	This study
	Cui 17780	MZ354968[a]	–	–	–	–	–	This study
	Cui 17254	MZ354966[a]	MZ355115[a]	MZ245406[a]	MZ221660[a]	MZ352877[a]	MZ355286[a]	This study

Table 1. (Continued).

Species	Voucher	GenBank accession No.						References
		ITS	nLSU	*rpb2*	*tef1*	mtSSU	nSSU	
G. guangxiense	Cui 14453 (TYPE)	MZ354939[a]	MZ355037[a]	MZ245407[a]	MZ221661[a]	MZ352896[a]	MZ355163[a]	This study
	Cui 14454	MZ354941[a]	MZ355039[a]	MZ245408[a]	MZ221662[a]	MZ352897[a]	MZ355164[a]	This study
	Cui 14508	MZ354940[a]	MZ355038[a]	–	MZ221663[a]	MZ352865[a]	MZ355240[a]	This study
G. hochiminhense	MFLU 19-2224 (TYPE)	MN398324	MN396390	–	MN423176	–	–	Luangharn *et al.* (2021)
	MFLU 19-2225	MN396662	MN396391	–	MN423177	–	–	Luangharn *et al.* (2021)
	Cui 18229	MZ354986[a]	MZ355094[a]	MZ245409[a]	MZ221664[a]	–	MZ355283[a]	This study
	Dai 18488	MZ354987[a]	MZ355093[a]	MZ245410[a]	MZ221665[a]	–	MZ355218[a]	This study
G. hoehnelianum	Cui 13904	MZ354935[a]	MZ355135[a]	MZ245411[a]	MZ221666[a]	MZ352888[a]	MZ355169[a]	This study
	Cui 13982	MG279178	MZ355071[a]	MG367515	MG367570	–	MZ355170[a]	Xing *et al.* (2018), this study
	Dai 20783	–	MZ355002[a]	MZ245412[a]	MZ221667[a]	MZ352892[a]	MZ355255[a]	This study
G. japonicum	AS569	AY593864	–	–	–	–	–	Wang & Yao (2005)
	Gja-1	GU213475	–	–	–	–	–	Unpublished
G. knysnamense	CMW47755 (TYPE)	MH571681	–	–	MH56726	–	–	Tchotet Tchoumi *et al.* (2019)
	CMW49688	MH571683	–	–	MH567266	–	–	Tchotet Tchoumi *et al.* (2019)
G. leucocontextum	Dai 15601	KU572485	MZ355049[a]	MG367516	KU572495	MZ352899[a]	MZ355318[a]	Xing *et al.* (2018), this study
	GDGM 40200 (TYPE)	KF011548	–	–	–	–	–	Li *et al.* (2015)
G. lingzhi	Wu 1006-38 (TYPE)	JQ781858	–	JX029980	JX029976	–	–	Cao *et al.* (2012)
	Cui 9166	KJ143907	–	JX029978	JX029974	JX029987	–	Zhou *et al.* (2015)
	Dai 20895	MZ354904[a]	MZ355006[a]	MZ245413[a]	MZ221668[a]	–	–	This study
	Cui 18161	MZ354905[a]	–	–	–	–	–	This study
	Cui 18167	MZ354906[a]	–	–	–	–	–	This study
G. lobatum	JV 1008/31	KF605671	–	MG367499	MG367553	–	–	Xing *et al.* (2018)
	JV 1008/32	KF605670	–	MG367500	MG367554	–	–	Xing *et al.* (2018)
G. lucidum	Cui 14404	MG279181	MZ355051[a]	MG367519	MG367573	MZ352858[a]	MZ355191[a]	Xing *et al.* (2018), this study
	Cui 14405	MG279182	MZ355089[a]	MG367520	MG367574	–	MZ355194[a]	Xing *et al.* (2018), this study
	K 175217	KJ143911	–	KJ143971	KJ143929	–	–	Zhou *et al.* (2015)
	MT 26/10	KJ143912	–	–	KJ143930	–	–	Zhou *et al.* (2015)
	Dai 20017	MZ354937[a]	MZ355050[a]	–	MZ221669[a]	–	MZ355256[a]	This study
G. magniporum	Zhou 439	MZ354936[a]	MZ355097[a]	–	–	MZ352863[a]	–	This study
	Dai 19966	–	MZ355098[a]	MZ345728[a]	MZ221670[a]	–	MZ355223[a]	This study
G. martinicense	LIP SW-Mart08-55 (TYPE)	KF963256	–	–	–	–	–	Unpublished

Table 1. (Continued).

Species	Voucher	GenBank accession No.						References
		ITS	nLSU	*rpb2*	*tef1*	mtSSU	nSSU	
	He 2240	MG279163	–	MG367503	MG367557	–	–	Xing *et al.* (2018)
G. mastoporum	K15-86	MF680427	–	–	–	–	–	Unpublished
	TNM-F0018835	JX840351	–	–	–	–	–	Wang *et al.* (2014)
G. mbrekobenum	UMN7-3 GHA (TYPE)	KX000896	KX000897	–	–	–	–	Crous *et al.* (2016)
	UMN7-4 GHA	KX000898	KX000899	–	–	–	–	Crous *et al.* (2016)
G. meredithiae	UMNFL50	MG654103	–	–	–	–	–	Loyd *et al.* (2018)
	UMNFL64	MG654106	–	MG754863	–	–	–	Loyd *et al.* (2018)
G. mexicanum	MUCL 49453	MK531811	–	MK531836	MK531825	–	–	Cabarroi-Hernández *et al.* (2019)
	MUCL 55832	MK531815	–	MK531839	MK531829	–	–	Cabarroi-Hernández *et al.* (2019)
G. mirabile	Cui 16408	–	MZ355066[a]	–	MZ221671[a]	–	MZ355227[a]	This study
	Cui 18271	MZ354958[a]	MZ355067[a]	MZ345729[a]	MZ221672[a]	MZ352860[a]	MZ355231[a]	This study
	Cui 18283	MZ354959[a]	MZ355069[a]	MZ345730[a]	MZ221673[a]	MZ352861[a]	MZ355248[a]	This study
	Cui 18237	MZ354960[a]	MZ355068[a]	MZ345731[a]	MZ221674[a]	MZ352862[a]	MZ355243[a]	This study
G. mizoramense	UMN-MZ4 (TYPE)	KY643750	–	–	–	–	–	Crous *et al.* (2017a)
	UMN-MZ5	KY643751	KY747490	–	–	–	–	Crous *et al.* (2017a)
	JZ8	MG437336	–	–	–	–	–	Unpublished
G. multipileum	Cui 13597	MZ354899[a]	MZ355043[a]	MZ345732[a]	MZ221675[a]	MZ352866[a]	MZ355174[a]	This study
	Dai 17569	MZ354896[a]	MZ355007[a]	MZ345733[a]	MZ221676[a]	MZ352867[a]	MZ355175[a]	This study
	Dai 19690	MZ354897[a]	MZ355008[a]	–	MZ221677[a]	MZ352868[a]	MZ355215[a]	This study
	Dai 19691	MZ354898[a]	MZ355041[a]	–	–	MZ352869[a]	–	This study
G. multiplicatum	SPC9	KU569553	KU570951	–	–	–	–	Bolaños *et al.* (2016)
	CC8	KU569515	KU570915	–	–	–	–	Bolaños *et al.* (2016)
	URM83346	JX310823	JX310837	–	–	–	–	De Lima Júnior *et al.* (2014)
	Dai 17395	MZ354903[a]	–	MZ345734[a]	MZ221678[a]	MZ352870[a]	MZ355209[a]	This study
G. mutabile	Yuan 2289 (TYPE)	JN383977	–	–	–	–	–	Cao & Yuan (2012)
	Cui 17189	MZ354976[a]	–	–	MZ221679[a]	–	–	This study
	Dai 20414	MZ354977[a]	MZ355110[a]	MZ345735[a]	MZ221680[a]	MZ352864[a]	MZ355292[a]	This study
G. myanmarense	MFLU 19-2167 (TYPE)	MN396330	MN428672	–	–	–	–	Luangharn *et al.* (2021)
	MFLU 19-2211/2169	MN396329	MN398325	–	–	–	–	Luangharn *et al.* (2021)
G. nasalanense	CACP17060211 (TYPE)	MK345441	MK346831	–	–	–	MK346842	Hapuarachchi *et al.* (2019b)
	CACP17060212	MK345442	MK346832	–	–	–	MK346843	Hapuarachchi *et al.* (2019b)

Table 1. (Continued).

Species	Voucher	GenBank accession No.						References
		ITS	nLSU	*rpb2*	*tef1*	mtSSU	nSSU	
G. neojaponicum	AS5.541 (TYPE)	AY593866	–	–	–	–	–	Wang & Yao (2005)
	36073	AY335163	–	–	–	–	–	Unpublished
G. nitidum	JV 1504/73	MZ354933[a]	–	–	MZ221681[a]	MZ352883[a]	–	This study
G. orbiforme	Cui 13880	MG279187	MZ355016[a]	MG367523	MG367577	MZ352908[a]	MZ355188[a]	Xing *et al.* (2018), this study
	Cui 13891	MZ354953[a]	MZ355017[a]	MZ345736[a]	MZ221682[a]	MZ352910[a]	MZ355167[a]	This study
	Cui 18301	MZ354954[a]	MZ355070[a]	–	MZ221683[a]	MZ352911[a]	MZ355232[a]	This study
	Cui 18302	MZ354955[a]	MZ355072[a]	–	MZ221684[a]	MZ352912[a]	MZ355233[a]	This study
	Cui 18317	MZ354956[a]	MZ355059[a]	–	MZ221685[a]	MZ352909[a]	MZ355285[a]	This study
	Cui 18326	MZ354957[a]	MZ355062[a]	–	MZ221686[a]	MZ352913[a]	MZ355244[a]	This study
G. oregonense	CBS 266.88	JQ781876	–	KJ143975	–	–	–	Cao *et al.* (2012), Zhou *et al.* (2015)
	CBS 265.88	JQ781875	–	KJ143974	KJ143933	–	–	Cao *et al.* (2012), Zhou *et al.* (2015)
G. parvulum	URM83345	JX310820	JX310834	–	–	–	–	De Lima Júnior *et al.* (2014)
	URM83344	JX310819	JX310833	–	–	–	–	De Lima Júnior *et al.* (2014)
G. pfeifferi	Dai 12153	MG279164	MZ355109[a]	–	MG367559	–	MZ355168[a]	Xing *et al.* (2018), this study
	Dai 12683	MG279165	MZ355108[a]	–	MG367560	–	–	Xing *et al.* (2018), this study
	CBS 221.48	–	MH867868	–	–	–	–	Unpublished
G. philippii	Cui 14443	MG279188	MZ355023[a]	MG367524	MG367578	MZ352871[a]	MZ355186[a]	Xing *et al.* (2018), this study
	Cui 14444	MG279189	MZ355022[a]	MG367525	MG367579	–	MZ355187[a]	Xing *et al.* (2018), this study
G. platense	BAFC384	AH008109	–	–	–	–	–	Gottlieb *et al.* (2000)
	BAFC2374	AH008110	–	–	–	–	–	Gottlieb *et al.* (2000)
G. podocarpense	QCAM 6422 (TYPE)	MF796661	MF796660	–	–	–	–	Crous *et al.* (2017b)
	JV 1504/126	MZ354942[a]	–	MZ345737[a]	MZ221687[a]	–	–	This study
G. polychromum	UMNOR3	MG654204	–	–	MG754744	–	–	Loyd *et al.* (2018)
	MS343OR	MG654197	–	–	MG754743	–	–	Loyd *et al.* (2018)
G. puerense	Dai 20427 (TYPE)	–	MZ355012[a]	MZ345738[a]	MZ221688[a]	MZ352884[a]	MZ355241[a]	This study
G. ravenelii	MS187FL	MG654211	–	MG754865	MG754745	–	–	Loyd *et al.* (2018)
	151FL	MG654208	–	–	–	–	–	Loyd *et al.* (2018)
G. resinaceum	MS1211	MT397406	–	–	MT415669	–	–	Náplavová *et al.* (2020)
	MS1212	MT397407	–	–	MT415670	–	–	Náplavová *et al.* (2020)
	LGAM 462	MG706250	MG706196	MG837821	MG837858	–	–	Unpublished
	LGAM 448	MG706249	MG706195	MG837820	MG837857	–	–	Unpublished

Table 1. (Continued).

Species	Voucher	GenBank accession No.						References
		ITS	nLSU	*rpb2*	*tef1*	mtSSU	nSSU	
G. ryvardenii	HKAS 58053 (TYPE)	HM138671	–	–	–	–	–	Kinge & Mih (2011)
	HKAS 58054	HM138672	–	–	–	–	–	Kinge & Mih (2011)
	HKAS 58055	HM138670	–	–	–	–	–	Kinge & Mih (2011)
G. sanduense	SA18012501 (TYPE)	MK345450	–	–	–	–	–	Hapuarachchi *et al.* (2019b)
	SA18012502	MK345451	–	–	–	–	–	Hapuarachchi *et al.* (2019b)
G. sessile	Dai 16403	MZ354934[a]	MZ355015[a]	MZ345739[a]	MZ221689[a]	MZ352907[a]	MZ355184[a]	This study
	JV 1209/27	KF605630	–	KJ143976	KJ143937	–	–	Zhou *et al.* (2015)
G. shanxiense	HSA 539	MK764269	–	MK789681	–	–	–	Liu *et al.* (2019)
	BJTC FM423 (TYPE)	MK764268	–	MK783940	MK783937	–	–	Liu *et al.* (2019)
	Cui 14565	MZ354908[a]	–	–	MZ221690[a]	–	MZ355245[a]	This study
	Dai 18921	MZ354909[a]	MZ355044[a]	MZ345740[a]	MZ221691[a]	–	MZ355320[a]	This study
G. sichuanense	HMAS42798 (TYPE)	JQ781877	–	–	–	–	–	Cao *et al.* (2012)
	Cui 16343	MZ354928[a]	MZ355011[a]	MZ345741[a]	MZ221692[a]	MZ352885[a]	MZ355171[a]	This study
	Dai 19651	MZ354929[a]	MZ355031[a]	MZ345742[a]	MZ221693[a]	MZ352889[a]	MZ355208[a]	This study
G. sinense	Cui 14526	MZ354961[a]	MZ355056[a]	MZ345743[a]	MZ221694[a]	–	MZ355189[a]	This study
	Cui 14461	MZ354963[a]	MZ355057[a]	MZ345744[a]	MZ221695[a]	–	MZ355190[a]	This study
	Dai 20079	MZ354962[a]	MZ355058[a]	MZ345745[a]	MZ221696[a]	–	MZ355284[a]	This study
Ganoderma sp.	N.1	MH806359	–	–	–	–	–	Le *et al.* (2018)
	N.3	MH806363	–	–	–	–	–	Le *et al.* (2018)
G. steyaertianum	6-WN-15(M)-A	KJ654459	–	–	–	–	–	Unpublished
	6-WN-16(M)-A	KJ654461	–	–	–	–	–	Unpublished
G. stipitatum	THC 16	KC884264	–	–	–	–	–	Unpublished
G. subangustisporum	Cui 18592 (TYPE)	MZ354981[a]	MZ355027[a]	–	MZ221697[a]	MZ352854[a]	–	This study
	Cui 18593	MZ354982[a]	MZ355028[a]	–	MZ221698[a]	MZ352852[a]	–	This study
	Cui 18596	MZ354983[a]	MZ355029[a]	–	MZ221699[a]	MZ352853[a]	–	This study
	Cui 18597	MZ354980[a]	MZ355025[a]	MZ345746[a]	MZ221700[a]	MZ352855[a]	MZ355216[a]	This study
G. subellipsoideum	Cui 18241	–	MZ355132[a]	–	MZ221701[a]	MZ352878[a]	–	This study
	Cui 18325 (TYPE)	–	MZ355134[a]	–	MZ221702[a]	–	MZ355295[a]	This study
	Cui 18327	–	MZ355133[a]	–	MZ221703[a]	MZ352859[a]	MZ355296[a]	This study
G. subflexipes	Cui 17247	MZ354921[a]	MZ355128[a]	MZ245395[a]	MZ221645[a]	–	MZ355140[a]	This study
	Cui 17257 (TYPE)	MZ354922[a]	MZ355129[a]	MZ245396[a]	MZ221646[a]	–	MZ355220[a]	This study

Table 1. (Continued).

Species	Voucher	GenBank accession No.						References
		ITS	nLSU	*rpb2*	*tef1*	mtSSU	nSSU	
	Cui 17258	–	MZ355130[a]	MZ245397[a]	MZ221647[a]	–	MZ355143[a]	This study
G. sublobatum	Cui 16804 (TYPE)	MZ354973[a]	–	MZ345747[a]	MZ221704[a]	MZ352879[a]	MZ355293[a]	This study
	Cui 16806	MZ354974[a]	MZ355034[a]	–	MZ221705[a]	MZ352918[a]	MZ355165[a]	This study
G. thailandicum	HKAS 104640 (TYPE)	MK848681	MK849879	MK875831	MK875829	–	–	Luangharn *et al.* (2019)
	HKAS 104641	MK848682	MK849880	MK875832	MK875830	–	–	Luangharn *et al.* (2019)
G. tongshanense	Cui 17168 (TYPE)	MZ354975[a]	MZ355024[a]	–	MZ221706[a]	–	MZ355206[a]	This study
G. tornatum	URM82776	JQ514110	JX310800	–	–	–	–	Unpublished
	TBG01AM2009	JQ514108	JX310808	–	–	–	–	Unpublished
G. tropicum	Dai 16434	MG279194	MZ355026[a]	MG367532	MG367585	MZ352872[a]	MZ355176[a]	Xing *et al.* (2018), this study
	Dai 19679	MZ354900[a]	MZ355009[a]	MZ358825[a]	MZ221707[a]	MZ352873[a]	MZ355222[a]	This study
	Dai 20029	MZ354902[a]	–	MZ358826[a]	MZ221708[a]	MZ352880[a]	MZ355225[a]	This study
	Dai 19491	MZ354901[a]	–	MZ358827[a]	MZ221709[a]	MZ352874[a]	MZ355141[a]	This study
G. tsugae	Cui 14110	MG279195	–	MG367533	MG367586	MZ352903[a]	MZ355192[a]	Xing *et al.* (2018), this study
	Cui 14112	MG279196	–	MG367534	MG367587	MZ352904[a]	MZ355193[a]	Xing *et al.* (2018), this study
G. tuberculosum	Dai 17412	MZ354943[a]	–	–	–	MZ352906[a]	MZ355199[a]	This study
	JV 1607/62	MZ354944[a]	MZ355087[a]	–	MZ221710[a]	MZ352875[a]	MZ355294[a]	This study
G. weberianum	Cui 16359	–	MZ355116[a]	MZ358828[a]	MZ221711[a]	MZ352886[a]	MZ355172[a]	This study
	CBS 219.36	MK603804	MH867289	MK611972	MK611974	–	–	Cabarroi-Hernández *et al.* (2019)
	CBS 128581	MK603805	MH876427	MK611971	MK636693	–	–	Cabarroi-Hernández *et al.* (2019)
	Dai 19673	MZ354930[a]	MZ355032[a]	MZ358829[a]	MZ221712[a]	MZ352890[a]	MZ355210[a]	This study
	Dai 19682	MZ354932[a]	MZ355042[a]	MZ358830[a]	MZ221713[a]	MZ352887[a]	MZ355213[a]	This study
	Dai 19689	MZ354931[a]	MZ355046[a]	–	MZ221714[a]	MZ352891[a]	MZ355226[a]	This study
G. weixiense	HKAS 100649 (TYPE)	MK302444	MK302446	–	MK302442	–	–	Ye *et al.* (2019)
	HKAS 100650	MK302445	MK302447	–	MK302443	–	–	Ye *et al.* (2019)
G. wiiroense	UMN-20-GHA	KT952361	KT952362	–	–	–	–	Crous *et al.* (2015)
	MIN 938704 (TYPE)	KT952363	KT952364	–	–	–	–	Crous *et al.* (2015)
G. williamsianum	Dai 17790	MZ354947[a]	MZ355060[a]	–	MZ221715[a]	–	MZ355182[a]	This study
	Dai 16809	MG279183	MZ355030[a]	MG367535	MG367588	–	MZ355183[a]	Xing *et al.* (2018), this study
	Dai 20553	MZ354948[a]	MZ355061[a]	MZ358831[a]	MZ221716[a]	–	MZ355242[a]	This study
	Dai 19611	MZ354949[a]	MZ355048[a]	MZ358832[a]	MZ221717[a]	–	–	This study
G. yunlingense	Cui 16288 (TYPE)	MZ354915[a]	MZ355077[a]	–	MZ221718[a]	–	MZ355179[a]	This study

Table 1. (Continued).

Species	Voucher	GenBank accession No.						References
		ITS	nLSU	*rpb2*	*tef1*	mtSSU	nSSU	
	Cui 17043	MZ354916[a]	MZ355078[a]	–	MZ221719[a]	–	MZ355228[a]	This study
	Cui 17958	MZ354917[a]	–	–	–	–	–	This study
G. zonatum	FL-03	KJ143922	–	KJ143980	KJ143942	–	–	Zhou *et al.* (2015)
	FL-02	KJ143921	–	KJ143979	KJ143941	–	–	Zhou *et al.* (2015)
Haddowia longipes	LPDR17072708	MK345423	MK346828	–	–	–	MK346836	Hapuarachchi *et al.* (2019b)
	LPDR17072709	MK345424	MK346829	–	–	–	MK346837	Hapuarachchi *et al.* (2019b)
Ha. macropora	JV 1908/46 (TYPE)	MZ354870[a]	MZ354998[a]	MZ358847[a]	MZ221720[a]	MZ352923[a]	MZ355251[a]	This study
Magoderna subresinosum	Dai 18626	MK119823	MK119902	MK121507	MK121571	MZ352831[a]	MZ355211[a]	Sun *et al.* (2020), this study
	Cui 18262	MZ354871[a]	MZ355088[a]	–	–	MZ352832[a]	MZ355258[a]	This study
	Cui 18280	MZ354872[a]	MZ355095[a]	–	MZ221721[a]	MZ352833[a]	MZ355304[a]	This study
Neoganoderma neurospora	DHCR559	MN077531	–	–	–	–	–	Costa-Rezende *et al.* (2020b)
	GAS1013	MN077532	–	–	–	–	–	Costa-Rezende *et al.* (2020b)
Sanguinoderma bataanense	Cui 6285	MK119831	MK119910	MK121537	MK121580	MZ352793[a]	MZ355238[a]	Sun *et al.* (2020), this study
	Dai 10746	MK119832	MK119911	MK121511	MK121581	MZ352801[a]	MZ355267[a]	Sun *et al.* (2020), this study
	Zhou 153	KJ531657	–	–	–	–	–	Li & Yuan (2015)
	Dai 7862	KJ531658	–	–	–	–	–	Li & Yuan (2015)
Sa. elmerianum	Cui 8940	MK119833	MK119912	–	–	MZ352812[a]	MZ355305[a]	Sun *et al.* (2020), this study
	HMAS 133187	MK119834	MK119913	–	–	MZ352824[a]	MZ355234[a]	Sun *et al.* (2020), this study
	Cui 18234	MZ354873[a]	MZ355080[a]	–	MZ221722[a]	MZ352814[a]	MZ355236[a]	This study
	Dai 20503	MZ354874[a]	MZ355081[a]	–	MZ221723[a]	MZ352813[a]	MZ355154[a]	This study
	Dai 20634	MZ354875[a]	MZ355082[a]	–	MZ221724[a]	MZ352821[a]	MZ355148[a]	This study
Sa. flavovirens	Cui 16935 (TYPE)	–	MK119914	MK121532	MK121582	MZ352811[a]	MZ355254[a]	Sun *et al.* (2020), this study
Sa. guangdongense	Dai 16724	MZ354876[a]	MZ355117[a]	MZ358833[a]	MZ221725[a]	MZ352815[a]	MZ355271[a]	This study
	Cui 17259 (TYPE)	MZ354877[a]	MZ355123[a]	MZ358834[a]	MZ221726[a]	MZ352816[a]	MZ355139[a]	This study
	Dai 20419	MZ354890[a]	MZ355083[a]	MZ358835[a]	MZ221727[a]	MZ352818[a]	MZ355155[a]	This study
	Cui 17240	–	MZ355124[a]	MZ358836[a]	MZ221728[a]	MZ352817[a]	MZ355287[a]	This study
Sa. infundibulare	Dai 18148	MK119846	MK119925	MK121528	MK121596	MZ352789[a]	MZ355259[a]	Sun *et al.* (2020), this study
	Dai 18149	MK119847	MK119926	MK121529	MK121597	MZ352790[a]	MZ355239[a]	Sun *et al.* (2020), this study
	Cui 17238	OM780277	–	MZ358837[a]	MZ221729[a]	MZ352800[a]	MZ355149[a]	This study
	Cui 17248 (TYPE)	MZ354880[a]	MZ355125[a]	–	MZ221730[a]	MZ352787[a]	MZ355150[a]	This study
	Dai 18151	MK119848	–	MK121530	MK121598	MZ352788[a]	MZ355274[a]	Sun *et al.* (2020), this study

Table 1. (Continued).

Species	Voucher	GenBank accession No.						References
		ITS	nLSU	*rpb2*	*tef1*	mtSSU	nSSU	
	Cui 17256	MZ354885[a]	–	MZ358838[a]	MZ221731[a]	MZ352791[a]	MZ355144[a]	This study
	URM 450213	MK119849	MK119927	–	–	MZ352792[a]	MZ355252[a]	Sun *et al.* (2020), this study
Sa. laceratum	Cui 8155 (TYPE)	MK119851	MK119928	–	–	MZ352810[a]	–	Sun *et al.* (2020), this study
	A5	MG383652	–	–	–	–	–	Unpublished
Sa. longistipitum	Dai 20696 (TYPE)	MZ354881[a]	MZ355084[a]	–	MZ221732[a]	MZ352822[a]	MZ355145[a]	This study
	Cui 13903	MZ354882[a]	MZ355114[a]	MZ358839[a]	MZ221733[a]	MZ352809[a]	MZ355301[a]	This study
	Dai 13891	MZ354886[a]	MZ355126[a]	–	–	MZ352834[a]	MZ355325[a]	This study
	Dai 16635	MZ354883[a]	MZ355120[a]	MZ358840[a]	MZ221734[a]	MZ352802[a]	MZ355260[a]	This study
Sa. melanocarpum	Dai 18512	MZ354888[a]	MZ355118[a]	–	MZ221735[a]	MZ352794[a]	MZ355313[a]	This study
	Dai 18603 (TYPE)	MZ354889[a]	MZ355113[a]	MZ358841[a]	MZ221736[a]	MZ352796[a]	MZ355281[a]	This study
Sa. microporum	Cui 13851 (TYPE)	MK119854	MK119933	MK121512	MK121602	MZ352797[a]	MZ355270[a]	Sun *et al.* (2020), this study
	Cui 18270	–	MZ355086[a]	–	–	MZ352808[a]	MZ355235[a]	This study
	Cui 14022	MK119856	MK119935	MK121515	MK121604	MZ352798[a]	MZ355298[a]	Sun *et al.* (2020), this study
Sa. microsporum	Dai 16726 (TYPE)	–	MZ355119[a]	–	MZ221737[a]	MZ352795[a]	MZ355272[a]	This study
	Cui 13901	MZ354879[a]	MZ355121[a]	–	MZ221738[a]	MZ352803[a]	MZ355299[a]	This study
	Cui 13897	MZ354878[a]	MZ355127[a]	–	MZ221739[a]	MZ352804[a]	MZ355300[a]	This study
Sa. perplexum	Cui 6496	KJ531650	KU220001	MK121538	MK121583	MZ352825[a]	MZ355263[a]	Li & Yuan (2015), this study
	Cui 6554	MK119835	MK119915	MK121540	MK121585	MZ352826[a]	MZ355264[a]	Sun *et al.* (2020), this study
	Wei 5562	KJ531652	–	–	–	–	–	Li & Yuan (2015)
	Dai 10811	KJ531651	KU220002	MK121539	MK121584	MZ352827[a]	MZ355302[a]	Li & Yuan (2015), this study
Sa. reniforme	Cui 16511 (TYPE)	MK119850	MK119929	MK121531	MK121599	–	MZ355322[a]	Sun *et al.* (2020), this study
Sa. rude	Cui 16592	MK119836	MK119916	MK121521	MK121586	MZ352924[a]	MZ355307[a]	Sun *et al.* (2020), this study
	DHCR457	MN077517	MN077551	–	MN061693	–	–	Costa-Rezende *et al.* (2020b)
	MEL 2317411	MK119842	–	MK121524	MK121592	MZ352819[a]	MZ355306[a]	Sun *et al.* (2020), this study
Sa. rugosum	Cui 8795	MK119843	MK119922	MK121516	MK121593	MZ352799[a]	MZ355266[a]	Sun *et al.* (2020), this study
	Cui 9011	KJ531664	KU220010	MK121517	KU572504	MZ352805[a]	MZ355237[a]	Li & Yuan (2015), this study
	Cui 9066	MZ354884[a]	MZ355122[a]	–	MZ221740[a]	MZ352806[a]	MZ355268[a]	This study
	Dai 20582	MZ354887[a]	MZ355085[a]	MZ358842[a]	MZ221741[a]	MZ352823[a]	MZ355156[a]	This study
	Cui 9012	KJ531665	KU220011	MK121518	KU572503	MZ352807[a]	MZ355269[a]	Li & Yuan (2015), this study
Sa. sinuosum	MEL 2366586	MK119852	MK119930	MK121527	MK121600	MZ352920[a]	MZ355261[a]	Sun *et al.* (2020), this study
	MEL 2341763 (TYPE)	MK119853	MK119931	MK121525	MK121601	MZ352820[a]	MZ355291[a]	Sun *et al.* (2020), this study

Table 1. (Continued).

Species	Voucher	GenBank accession No.						References
		ITS	nLSU	*rpb2*	*tef1*	mtSSU	nSSU	
Sa. tricolor	Cui 18292 (TYPE)	–	MZ355101[a]	–	MZ221742[a]	MZ352828[a]	MZ355273[a]	This study
	Cui 18242	MZ354992[a]	MZ355099[a]	MZ358843[a]	MZ221743[a]	MZ352829[a]	MZ355303[a]	This study
	Dai 18574	MZ354993[a]	MZ355102[a]	MZ358844[a]	MZ221744[a]	MZ352830[a]	MZ355265[a]	This study
Sinoganoderma shandongense	Dai 15785	MG279190	MZ355052[a]	MG367526	MG367580	MZ352900[a]	MZ355200[a]	Xing *et al.* (2018), this study
	Dai 15787	MG279191	MZ355053[a]	MG367527	MG367581	MZ352901[a]	MZ355201[a]	Xing *et al.* (2018), this study
	Dai 15791	MG279192	MZ355054[a]	MG367528	MG367582	MZ352902[a]	MZ355323[a]	Xing *et al.* (2018), this study
	Dai 20243	–	MZ355055[a]	–	MZ221745[a]	–	–	This study
	Dai 20244	MZ354938[a]	MZ355073[a]	–	MZ221746[a]	–	–	This study
	xsd08032	EU918700	–	–	–	–	–	Unpublished
	xsd08085	FJ478127	–	–	–	–	–	Unpublished
Tomophagus cattienensis	CT119	JN184398	–	–	–	–	–	Le *et al.* (2012)
	CT99 (TYPE)	JN184397	–	–	–	–	–	Le *et al.* (2012)
	Dai 18487	MZ354988[a]	–	MZ358845[a]	MZ221747[a]	MZ352898[a]	MZ355212[a]	This study
To. colossus	URM80450	JX310825	JX310839	–	–	–	–	De Lima Júnior *et al.* (2014)
	URM83330	JQ618247	JX310811	–	–	–	–	De Lima Júnior *et al.* (2014)
Trachydermella tsunodae	GR363	FJ154773	–	–	–	–	–	Unpublished
	WD2034	AB588989	AB368069	AB368127	–	–	–	Sotome *et al.* (2011)
Perenniporia subtephropora	Dai 10962 (TYPE)	JQ861752	JQ861768	KX880850	KF286329	KF218323	–	Zhao & Cui (2013)
	Dai 10964	JQ861753	JQ861769	KX880851	KF286330	KF218324	–	Zhao & Cui (2013)

[a] Newly generated sequences for this study.

RESULTS

Molecular phylogeny

In this study, 1 382 sequences derived from six gene loci (ITS, nLSU, *rpb2*, *tef1*, mtSSU and nSSU) were used to reconstruct phylogenetic trees of *Ganodermataceae*, including 374 sequences of ITS, 242 sequences of nLSU, 173 sequences of *rpb2*, 242 sequences of *tef1*, 158 sequences of mtSSU and 193 sequences of nSSU. The combined six-gene dataset (ITS + nLSU + *rpb2* + *tef1* + mtSSU + nSSU) included sequences from 391 specimens representing 146 taxa from *Ganodermataceae* and *Perenniporia subtephropora* as the outgroup. The partition homogeneity test indicated all the six different genes displayed a congruent phylogenetic signal (P value = 1.00). The best-fit evolutionary models selected by MrModeltest v. 2.3 for each region of the six genes were GTR + I + G (ITS1), K80 (5.8S), HKY + I + G (ITS2), GTR + I + G (nLSU), K80 + I + G (*rpb2* introns), K80 + G (*rpb2* 1st codon), GTR + I + G (*rpb2* 2nd codon), GTR + I + G (*tef1* introns), HKY + I + G (*tef1* 1st codon), SYM + I + G (*tef1* 2nd codon), SYM + I + G (*tef1* 3rd codon), GTR + I + G (mtSSU) and GTR + I + G (nSSU). These models were applied in Bayesian analyses for the combined dataset.

The combined six-gene dataset has an aligned length of 5 172 total characters including gaps, of which 3 780 are constant, 197 are variable and parsimony-uninformative, and 1 195 are parsimony-informative. The average standard deviation of split frequencies in the Bayesian analyses reached 0.008329. The calculated values based on the combined six-gene dataset are shown in Fig. 1. Thirteen clades were obtained in the phylogenetic analyses of *Ganodermataceae*: *Amauroderma* clade (100 % ML, 1.00 BPP), *Amaurodermellus* clade (100 % ML, 1.00 BPP), *Cristataspora* clade (100 % ML, 1.00 BPP), *Foraminispora* clade (99 % ML, 1.00 BPP), *Furtadoella gen. nov.* clade (100 % ML, 1.00 BPP), *Ganoderma* clade (58 % ML), *Haddowia* clade (85 % ML, 0.99 BPP), *Magoderna* clade (100 % ML, 1.00 BPP), *Neoganoderma gen. nov.* clade (100 % ML, 1.00 BPP), *Sanguinoderma* clade (88 % ML, 0.98 BPP), *Sinoganoderma gen. nov.* clade (100 % ML, 1.00 BPP), *Tomophagus* clade (100 % ML, 1.00 BPP) and *Trachydermella gen. nov.* clade (100 % ML, 1.00 BPP)

The *Ganoderma* clade is composed of 95 taxa including 16 new species. All taxa in this clade were divided into two groups according to laccate or dull pileal surface, and 10 subclades are separated by this feature: subclade I-laccate/dull (84 % ML, 1.00 BPP), subclade II-laccate (100 % ML, 1.00 BPP), subclade III-laccate (100 % ML, 1.00 BPP), subclade IV-dull (100 % ML, 1.00 BPP), subclade V-laccate/dull (93 % ML, 1.00 BPP), subclade VI-dull (98 % ML, 1.00 BPP), subclade VII-laccate/dull (75 % ML, 0.99 BPP), subclade VIII, subclade IX (100 % ML, 1.00 BPP) and subclade X (99 % ML, 1.00 BPP), these subclades were shown in Fig. 1.

The phylogenetic topologies of *Ganodermataceae* based on ITS, nLSU, *rpb2*, *tef1*, mtSSU and nSSU sequences respectively with ML bootstrap support values ≥ 50 % are shown in Figs 2–7. Besides, including *Perenniporia subtephropora* as outgroup, there were 146 taxa included in the ITS dataset, 107 taxa included in the nLSU dataset, 87 taxa included in the *rpb2* dataset, 102 taxa included in the *tef1* dataset, 70 taxa included in the mtSSU dataset, and 81 taxa included in the nSSU dataset.

Taxonomy

Ganodermataceae Donk, Bull. Bot. Gdns Buitenz. 17: 474. 1948. Fig. 8. MycoBank MB 80782.

Type genus: *Ganoderma* P. Karst.

Description: *Basidiomata* annual to perennial, sessile to stipitate, pileate, fleshy to woody hard. *Pilei* variable in shape and colour, with or without laccate surface. *Hyphal system* dimitic to trimitic, rarely monomitic in context; generative hyphae mostly bearing clamp connections, rarely simple-septate. *Basidiospores* subglobose to ovoid or reniform, truncated or not, double-walled and slightly to distinctly thick-walled with varied ornamentation.

Notes: In this study, 12 genera of *Ganodermataceae*: *Amauroderma*, *Amaurodermellus*, *Cristataspora*, *Foraminispora*, *Furtadoella*, *Ganoderma*, *Haddowia*, *Humphreya*, *Magoderna*, *Sanguinoderma*, *Tomophagus*, *Trachydermella* and two new genera: *Neoganoderma* and *Sinoganoderma* were confirmed based on morphological and molecular studies. *Humphreya* was not included in the phylogenetic analyses since there are no available specimens to obtain sequences, but it is treated as an independent genus within *Ganodermataceae* based on its unique basidiospore ornamentation.

Key to accepted genera of *Ganodermataceae*

1a. Colour of fresh pore surface becoming blood red when bruised ..... *Sanguinoderma*
1b. Colour of fresh pore surface darkening or unchanged when bruised 2

2a. Basidiospores non-truncated 3
2b. Basidiospores truncated 8

3a. Hyphal system monomitic in context, generative hyphae clamped to simple-septate ..... *Furtadoella*
3b. Hyphal system di-trimitic in context, generative hyphae clamped 4

4a. Exospore wall incomplete and smooth, endospore wall with two longitudinal crests and transverse membranes ..... *Haddowia*
4b. Exospore wall complete and uneven to foveolate or verrucose, endospore wall with obvious spinules 5

5a. Endospore wall with hollow spinules which persist until exospore wall forming holes ..... *Foraminispora*
5b. Endospore wall with solid spinules, exospore wall verrucose 6

6a. Basidiospores globose to oblong ..... *Amauroderma*
6b. Basidiospores ellipsoid to ovoid 7

7a. Basidiomata woody hard, with short stipe or sessile ..... *Magoderna*
7b. Basidiomata corky, with long stipe ..... *Amaurodermellus*

8a. Basidiomata soft to fleshy when fresh 9
8b. Basidiomata soft corky to woody hard when fresh 10

9a. Hyphal system dimitic, generative hyphae branched ..... *Tomophagus*
9b. Hyphal system trimitic, generative hyphae unbranched ..... *Trachydermella*

10a. Endospore wall with spiny ornamentation 11
10b. Endospore wall with ridged ornamentation 12

11a. Pore dissepiments thin, context cream; exospore wall uneven to foveolate ..... *Sinoganoderma*
11b. Pore dissepiments thick, context pale white to dark brown; exospore wall verrucose to vermicular ..... *Ganoderma*

12a. Basidiomata sessile to subsessile; basidiospores inconspicuously truncated ..... *Neoganoderma*
12b. Basidiomata stipitate; basidiospores conspicuously truncated 13

13a. Context white; endospore wall with vertical or transverse ridges ..... *Cristataspora*
13b. Context honey; endospore wall with reticular ridges ..... *Humphreya*

Amauroderma Murrill, Bull. Torrey Bot. Club 32: 366. 1905. MycoBank MB 17052.

Type species: *Amauroderma schomburgkii* (Mont. & Berk.) Torrend.

For a detailed description of *Amauroderma*, see Costa-Rezende *et al.* (2016) and Sun *et al.* (2020).

Notes: The *Amauroderma* clade is composed of species from the Neotropics. According to Costa-Rezende *et al.* (2020a), 24 species of *Amauroderma* have been recorded from the Neotropics, 16 species with available DNA sequences were included in the current phylogenetic analyses. Besides these species, this genus contains 40 taxa which have been recorded from Africa, Southeast Asia and Central America, and the sequences of these taxa are not available. Until now, 58 species (Table 2) can be recognised in *Amauroderma* based on previous literature (Furtado 1967b, Steyaert 1972, Corner 1983, Henao-M 1997, Moncalvo & Ryvarden 1997, Gulaid & Ryvarden 1998, Aime *et al.* 2003, Ryvarden 2004b, Gomes-Silva *et al.* 2015, Ryvarden 2020).

Amaurodermellus Costa-Rezende *et al.*, Mycol. Prog. 19: 727. 2020. MycoBank MB 833561.

Type species: *Amaurodermellus ovisporum* (Gomes-Silva *et al.*) Costa-Rezende *et al.*

For a detailed description of *Amaurodermellus*, see Costa-Rezende *et al.* (2020b).

Notes: *Amaurodermellus* was established by Costa-Rezende *et al.* (2020b) with type species, *Amaurodermellus ovisporum*. It can be distinguished from the other genera in *Ganodermataceae* by ovoid basidiospores with inconspicuous spinules on the endospore wall. Several species in *Ganoderma* also have ovoid basidiospores such as *G. sichuanense*, but *Amaurodermellus ovisporum* has a dark dull pileal surface and non-truncated basidiospores which is similar to *Amauroderma*. In this study, the taxonomic status of *Amaurodermellus* was further confirmed by multi-gene based phylogenetic analyses (Fig. 1).

Cristataspora Robledo & Costa-Rezende, Mycol. Prog. 19: 733. 2020. MycoBank MB 833558.

Type species: *Cristataspora coffeata* (Berk.) Robledo *et al.*

For a detailed description of *Cristataspora*, see Costa-Rezende *et al.* (2020b).

Notes: *Cristataspora coffeata* as the only species in *Cristataspora* was previously placed in *Humphreya* due to the reticulate or disjointed crests on the endospore wall (Steyaert 1972). Costa-Rezende *et al.* (2020b) examined the specimens of *C. coffeata* collected from neotropical areas, and the vertical or transverse ridges on the endospore wall observed under SEM rendered it distinct from *Humphreya*. Therefore, *Cristataspora* was established as a new genus based on its different basidiospores and independent clade in the phylogenetic analysis (Fig. 1).

Foraminispora Robledo *et al.*, Persoonia 39: 258. 2017. MycoBank MB 819015.

Type species: *Foraminispora rugosa* (Berk.) Costa-Rezende *et al*.

For a detailed description of *Foraminispora*, see Costa-Rezende *et al.* (2017) and Sun *et al.* (2020).

Notes: *Foraminispora* is characterised by the unique ultrastructure of its basidiospores, which shows an uneven exospore wall with holes caused by hollow and columnar spinules on the endospore wall. In this study, *Foraminispora* is recognised as an independent clade including five species with high support (Fig. 1). Species of this genus were reported from East Asia and Neotropics, and the descriptions of these species can be found in Costa-Rezende *et al.* (2017) and Sun *et al.* (2020).

Furtadoella B.K. Cui & Y.F. Sun, ***gen. nov.*** MycoBank MB 840977.

Diagnosis: Differs from other genera by its soft basidiomata, white context, monomitic hyphal system in context, with both clamped and simple-septate generative hyphae.

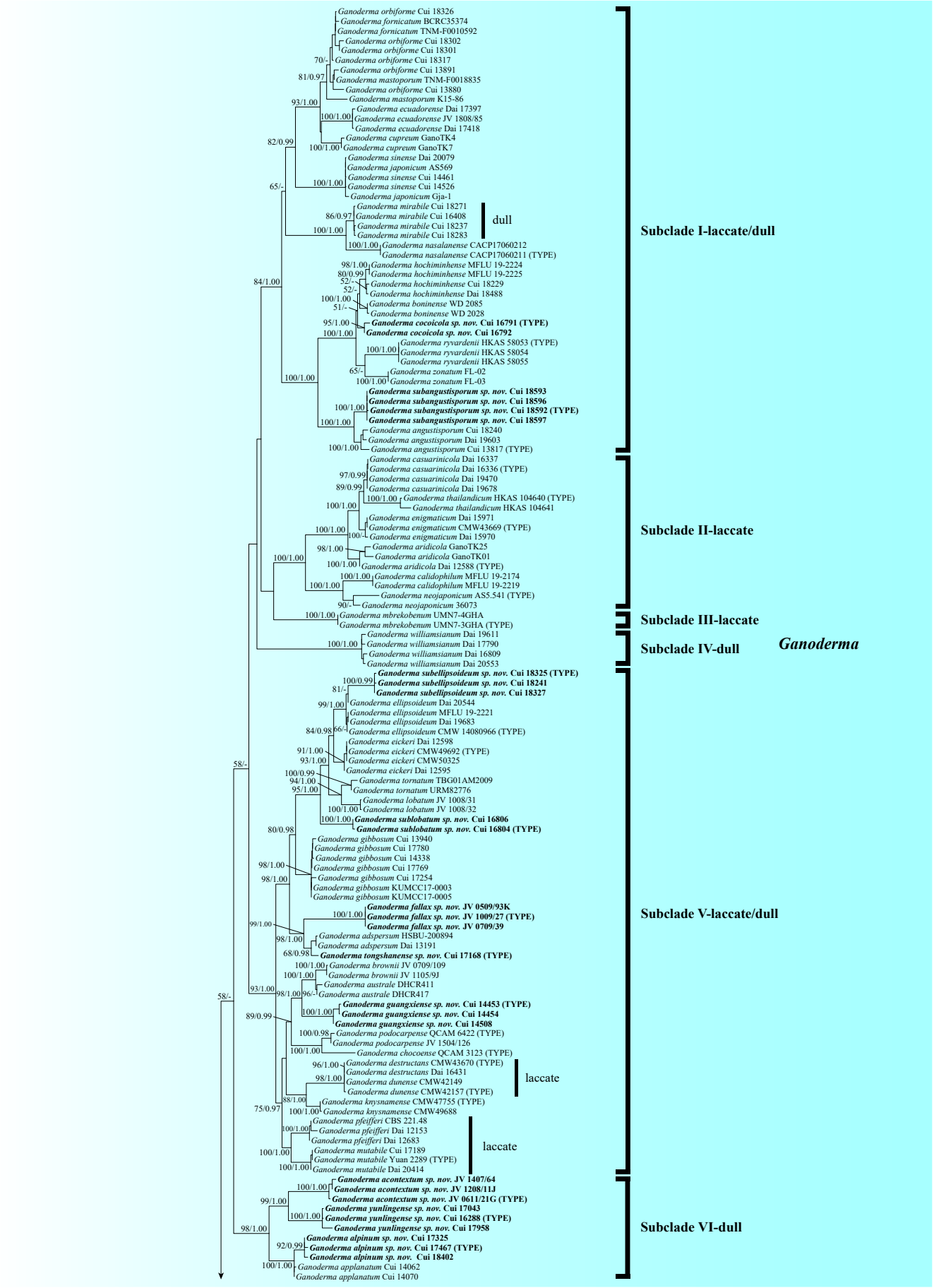

Fig. 1. Maximum Likelihood analyses of *Ganodermataceae* based on dataset of ITS + nLSU + *rpb2* + *tef1* + mtSSU + nSSU. Maximum Likelihood bootstrap values higher than 50 % and Bayesian posterior probabilities values more than 0.95 are shown. New species are in bold. *Ganoderma* clade is divided by laccate or dull pileal surface.

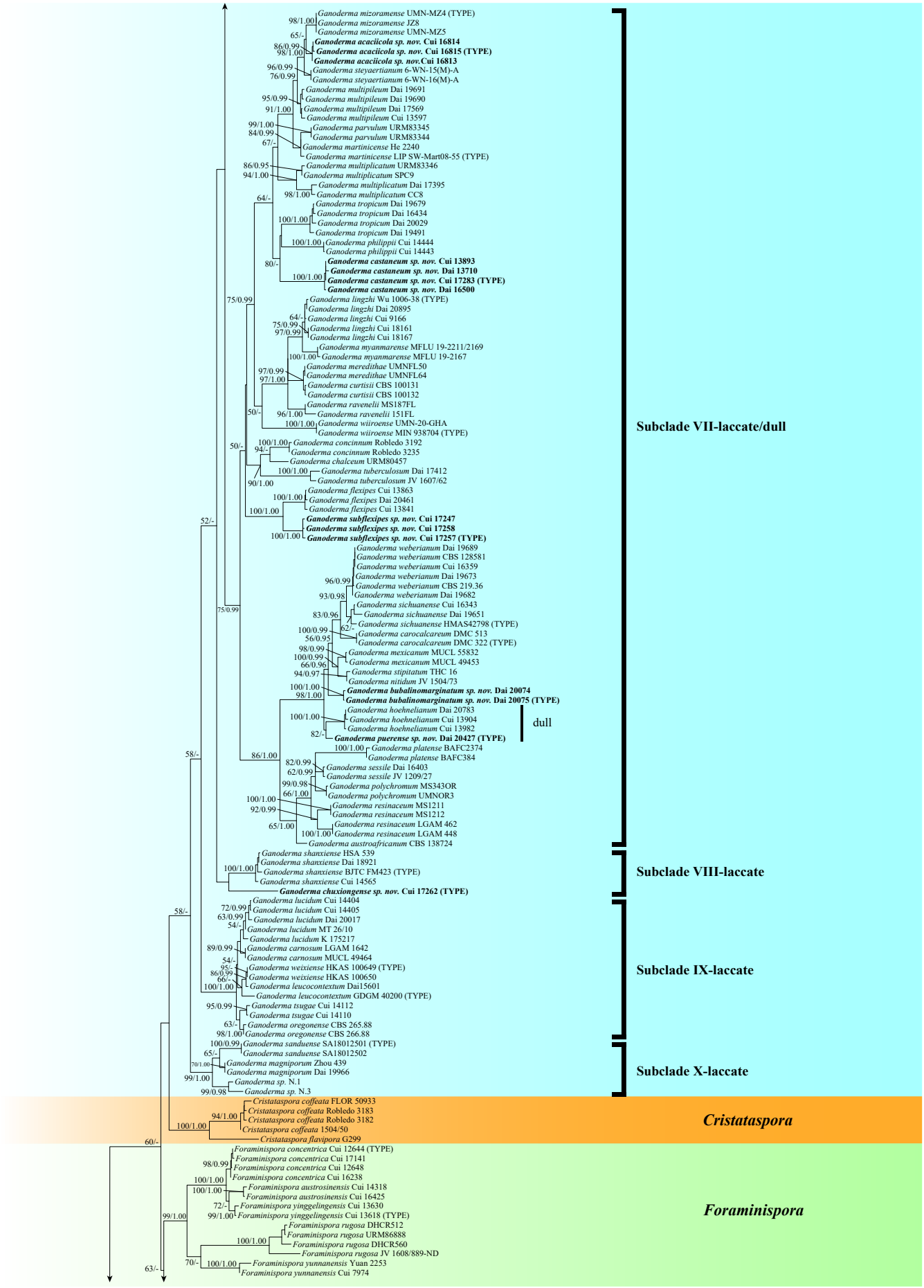

Fig. 1. (Continued).

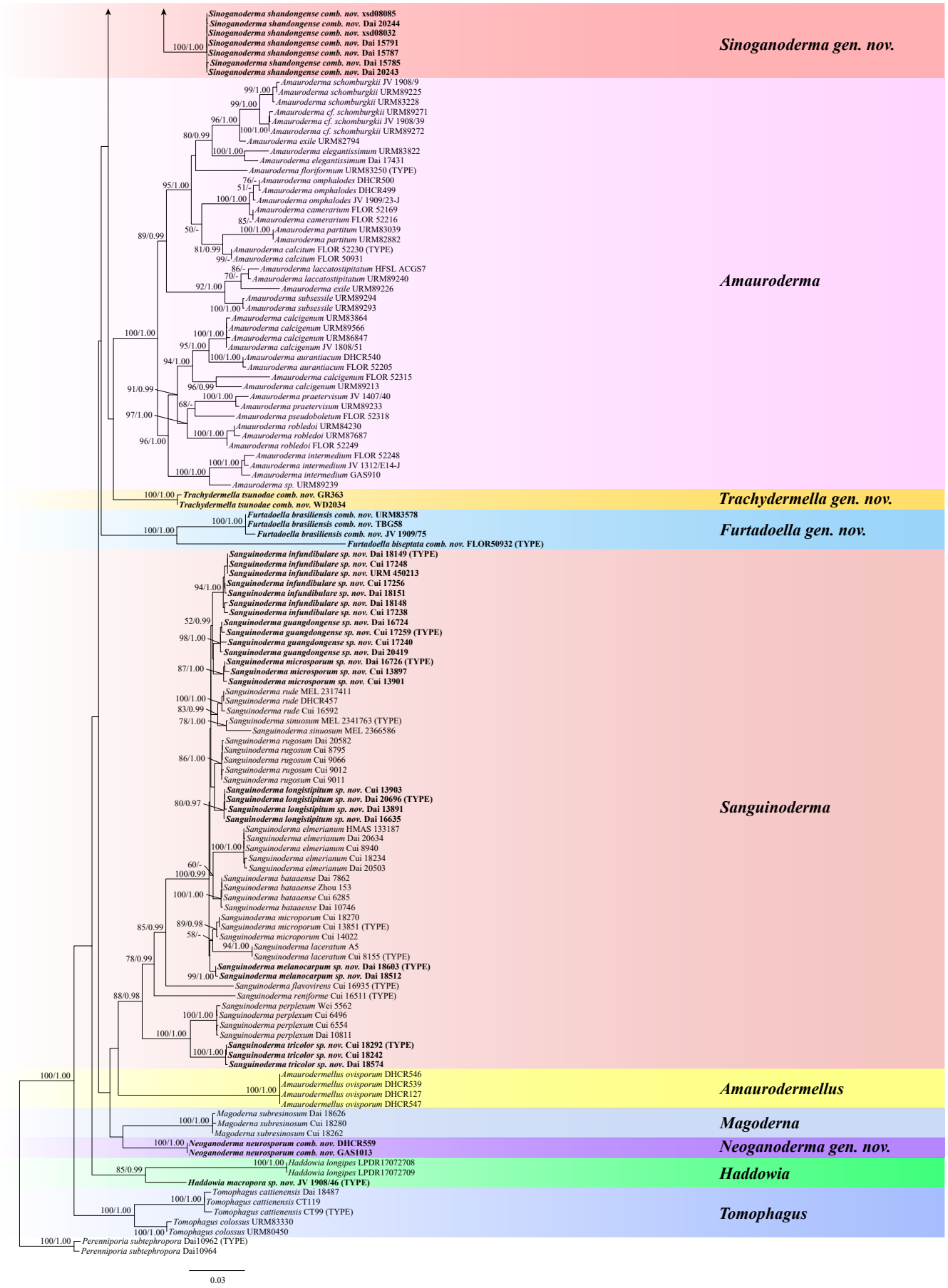

Fig. 1. (Continued).

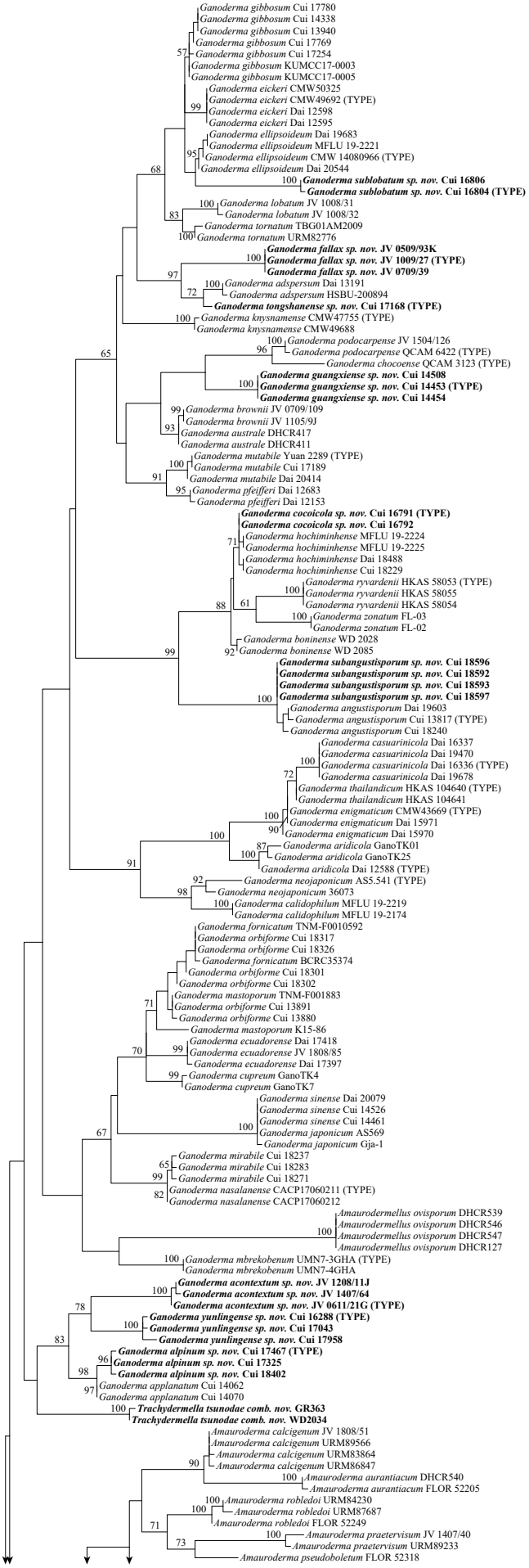

Fig. 2. Maximum Likelihood analyses of *Ganodermataceae* based on dataset of ITS. Maximum Likelihood bootstrap values higher than 50 % are shown. New species are in bold.

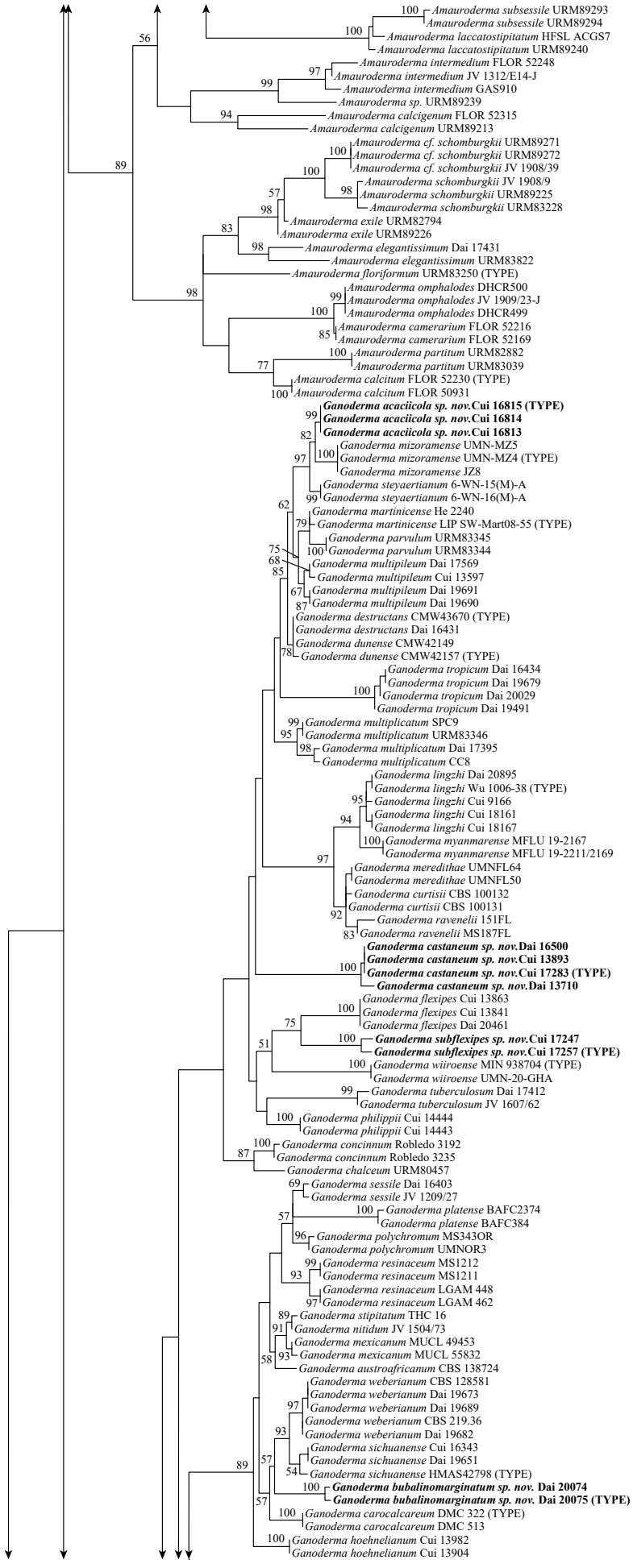

Fig. 2. (Continued).

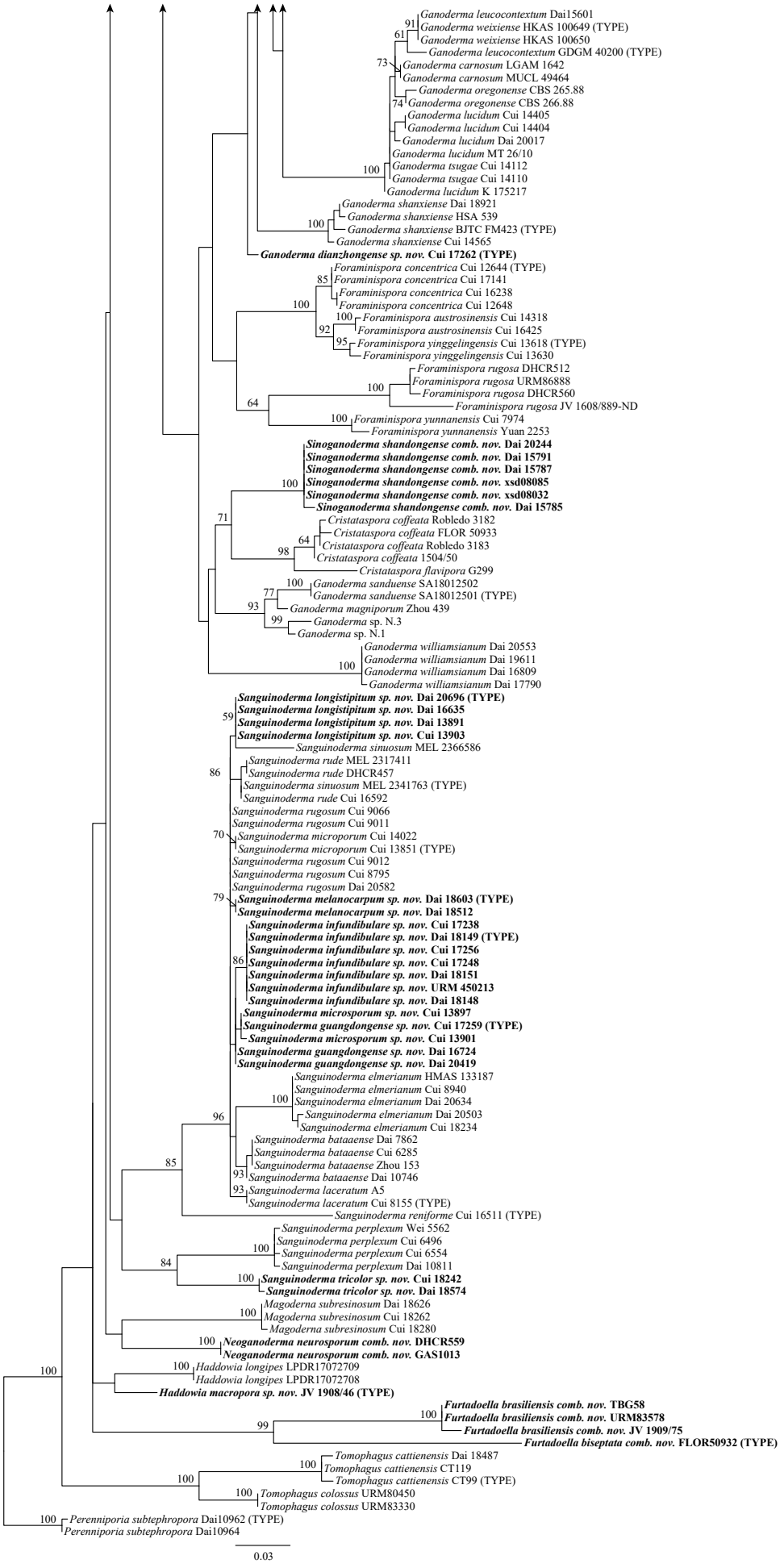

Fig. 2. (Continued).

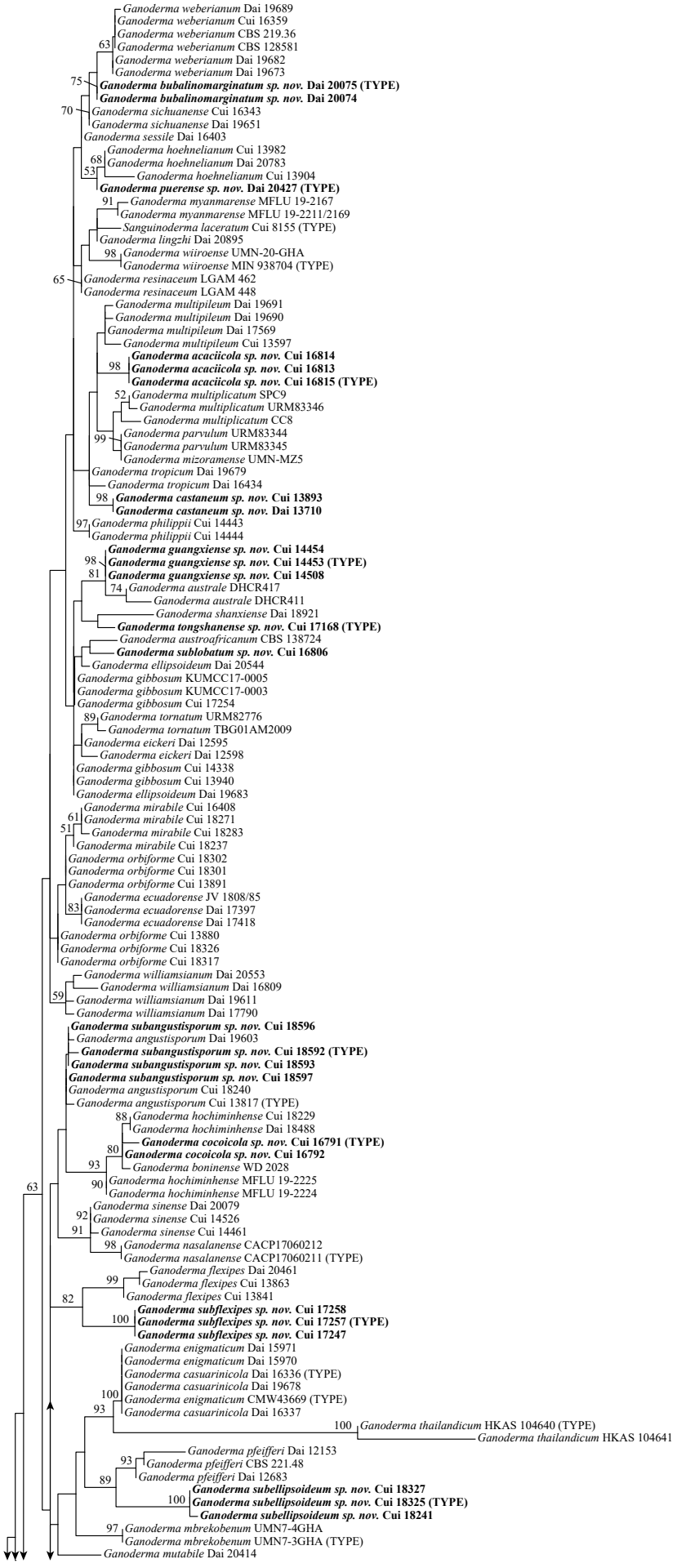

Fig. 3. Maximum Likelihood analyses of *Ganodermataceae* based on dataset of nLSU. Maximum Likelihood bootstrap values higher than 50 % are shown. New species are in bold.

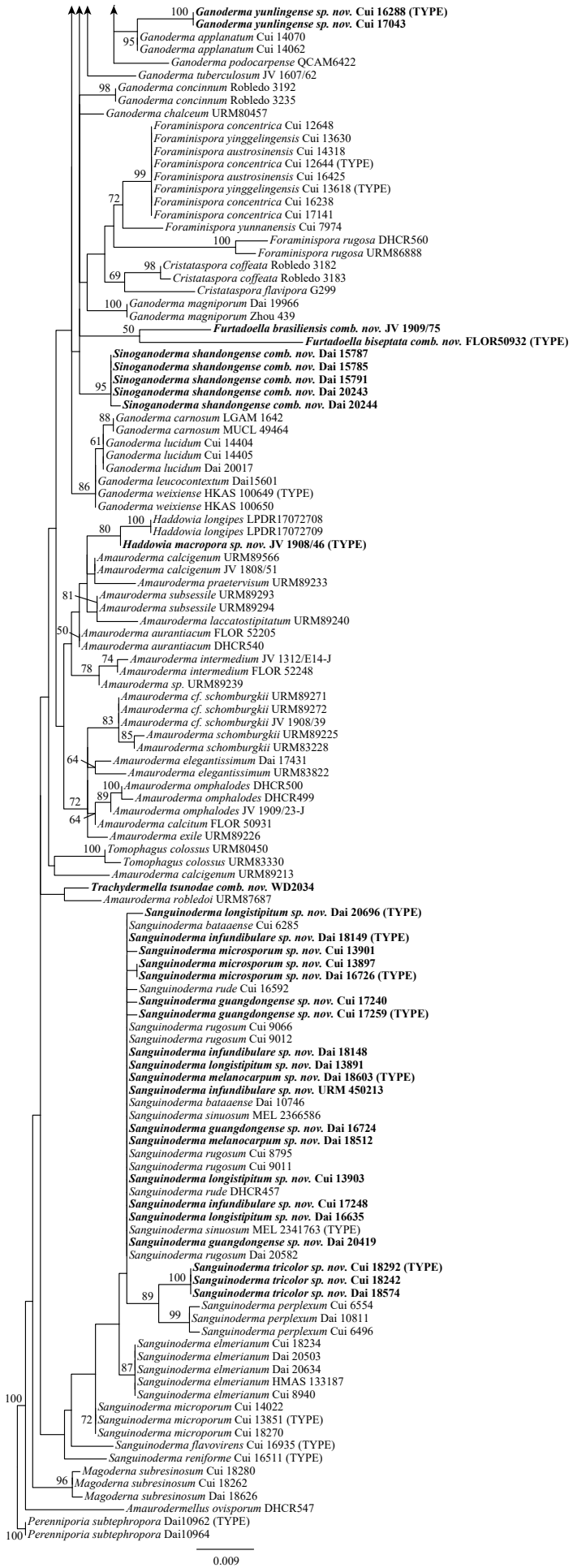

Fig. 3. (Continued).

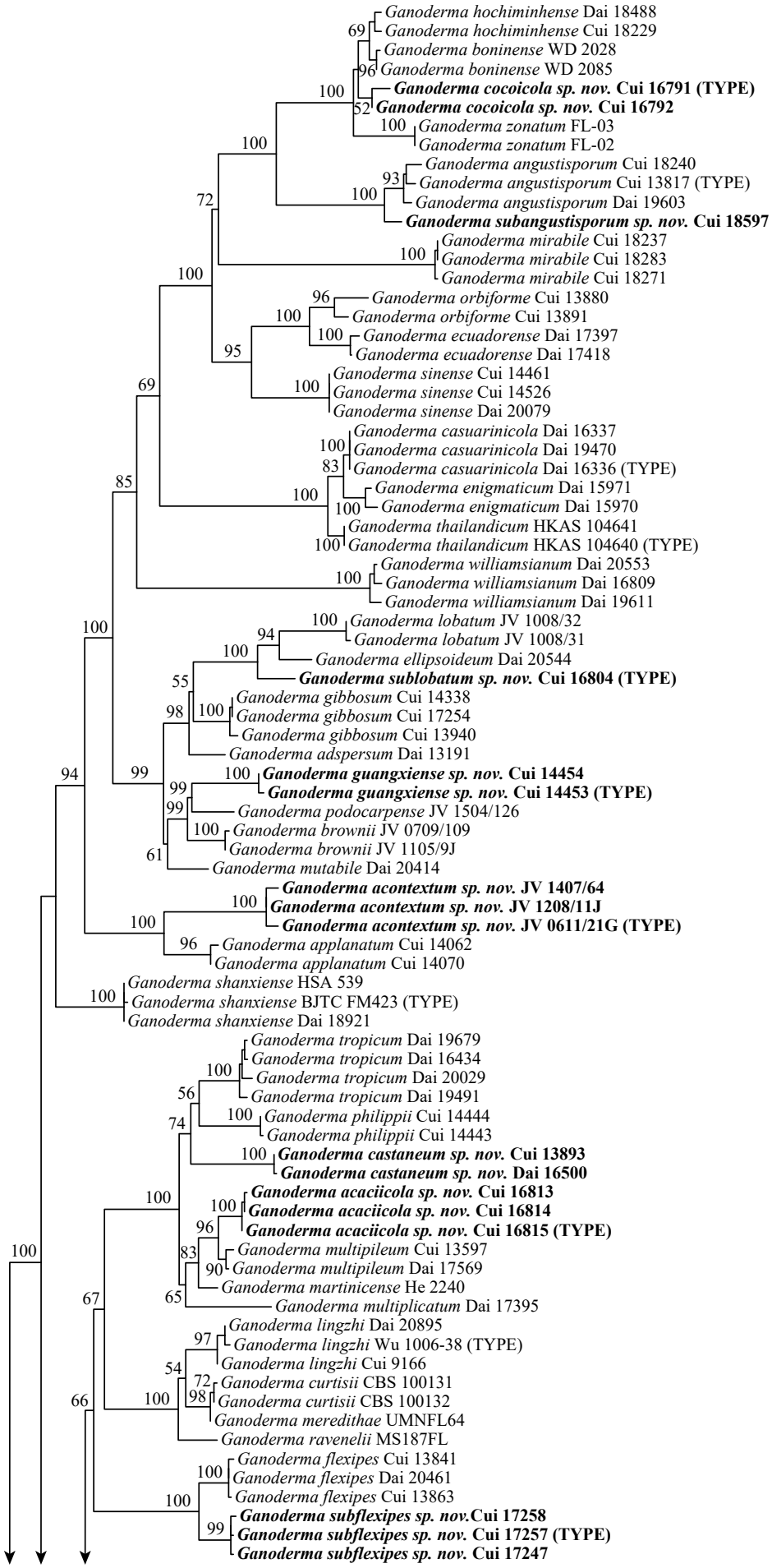

Fig. 4. Maximum Likelihood analyses of *Ganodermataceae* based on dataset of *rpb2*. Maximum Likelihood bootstrap values higher than 50 % are shown. New species are in bold.

Fig. 4. (Continued).

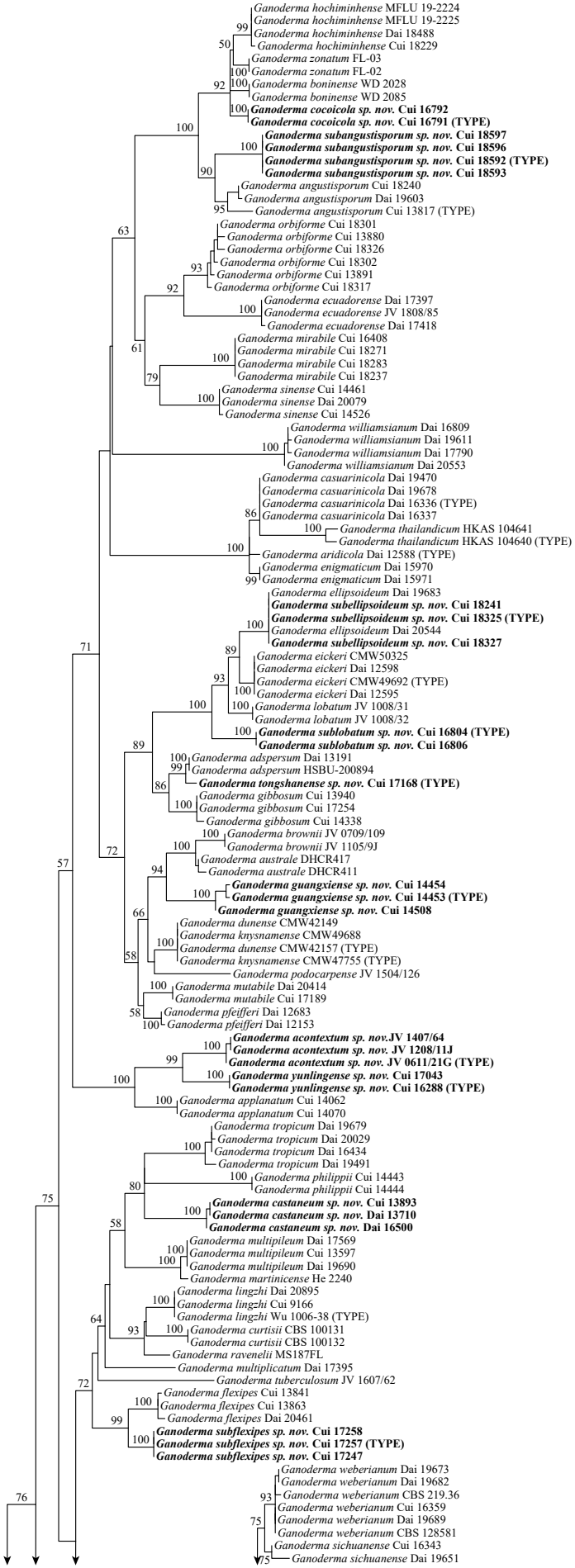

Fig. 5. Maximum Likelihood analyses of *Ganodermataceae* based on dataset of *tef1*. Maximum Likelihood bootstrap values higher than 50 % are shown. New species are in bold.

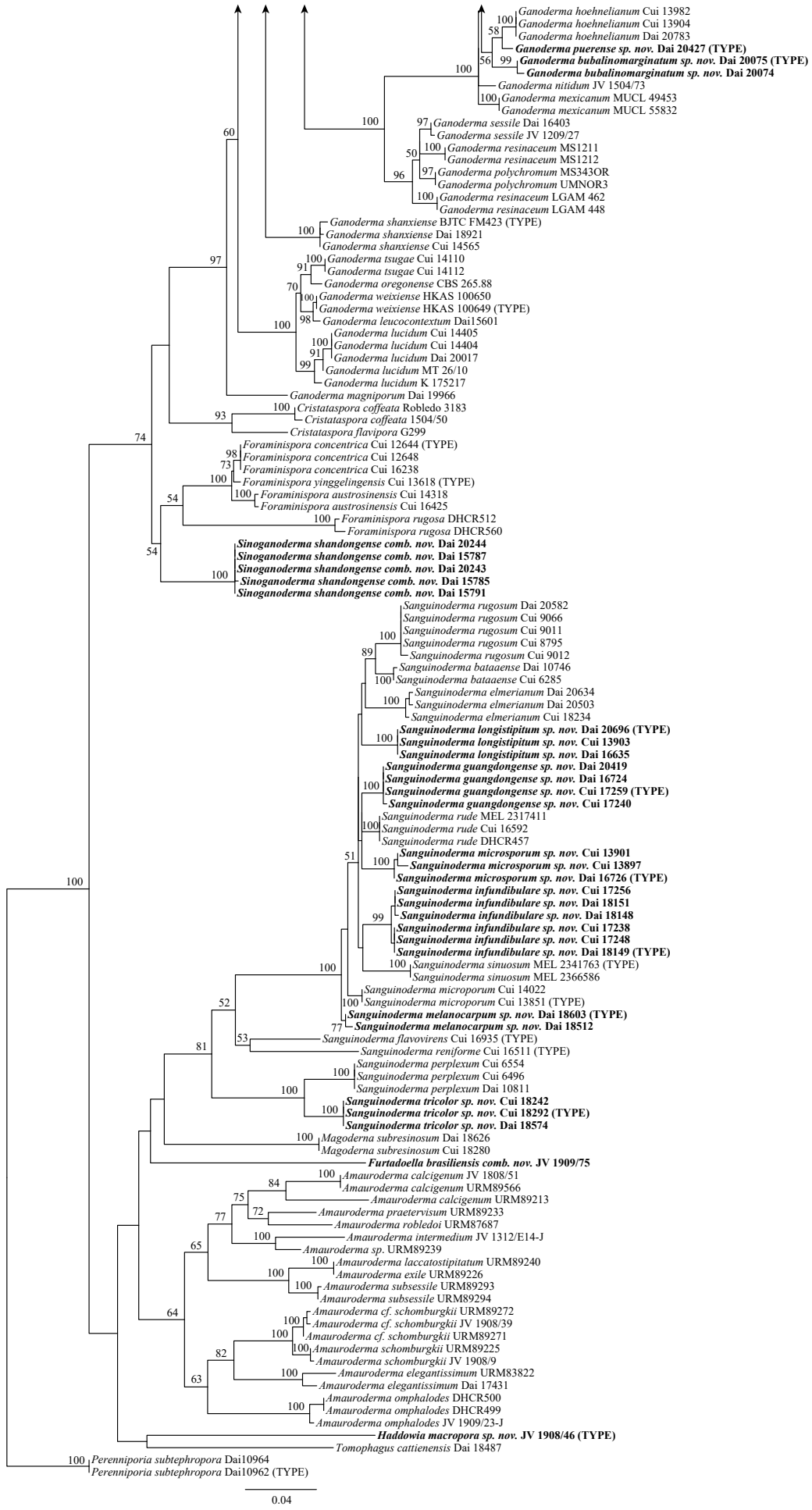

Fig. 5. (Continued).

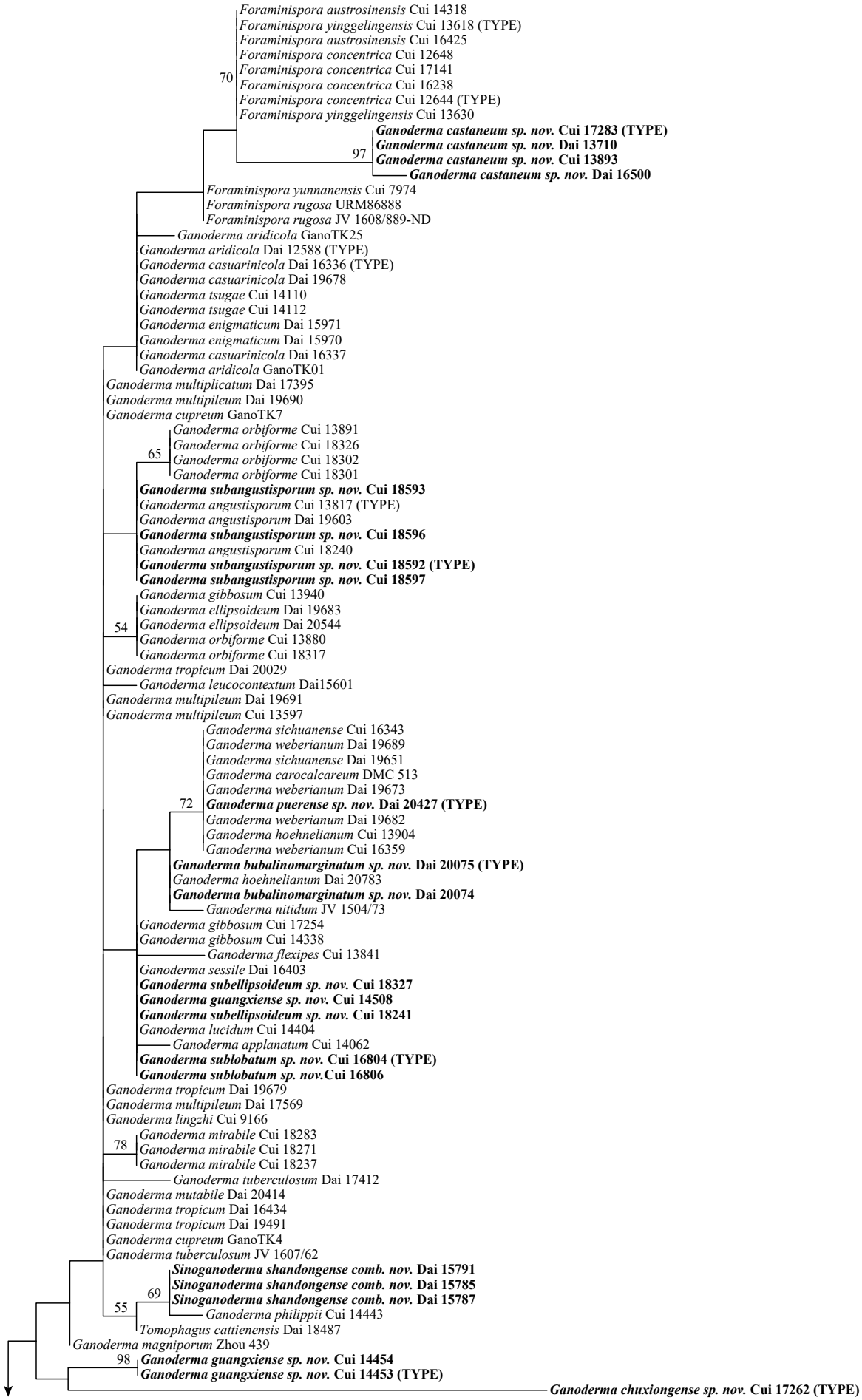

Fig. 6. Maximum Likelihood analyses of *Ganodermataceae* based on dataset of mtSSU. Maximum Likelihood bootstrap values higher than 50 % are shown. New species are in bold.

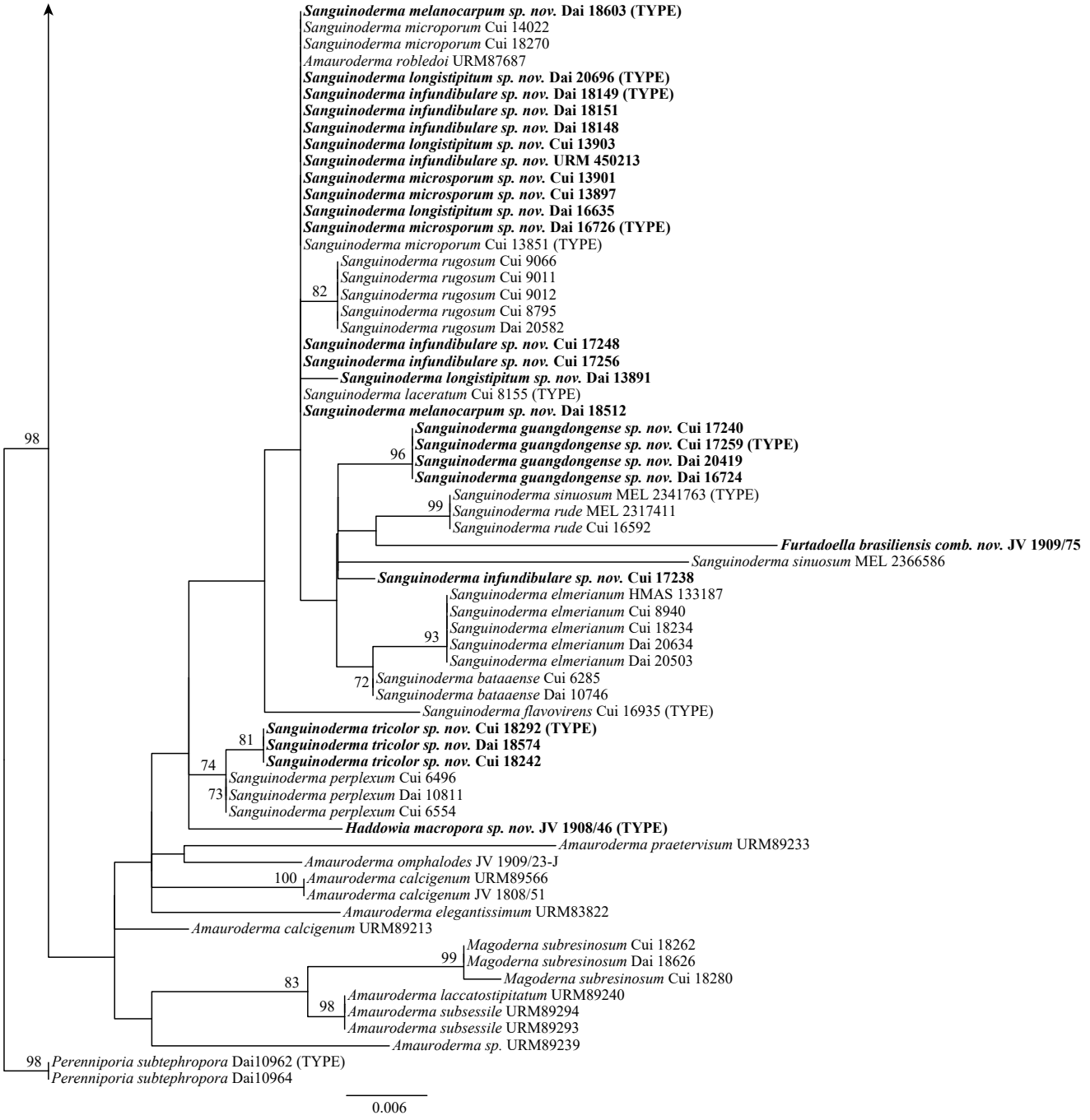

Fig. 6. (Continued).

Etymology: *furtadoella* (*Lat.*), refers to the Dr João Salvador Furtado who contributed significantly to the taxonomy of *Ganodermataceae*.

Type species: *Furtadoella biseptata* (Costa-Rezende *et al.*) B.K. Cui & Y.F. Sun.

Description: *Basidiomata* annual, stipitate, soft to corky. *Pilei* solitary, orbicular to flabelliform or infundibuliform. *Pileal surface* yellowish brown to greyish brown, dull, glabrous to tomentose, obviously concentrically zonate. *Pore surface* white to straw colour; pores circular to angular; dissepiments thin to thick, entire to lacerate. *Context* white to pale brown, with dark resinous lines, soft corky. *Hyphal system* dimitic in trama and monomitic in context; context composed of clamped to simple-septate generative hyphae, thin- to slightly thick-walled; tubes composed of clamped generative hyphae and arboriform skeletal hyphae. *Basidiospores* subglobose to ellipsoid, colourless, double-walled with verrucose to reticulate exospore wall, IKI–.

Notes: *Furtadoa* is an illegitimate name as it is a homonym of one genus in *Araceae* and was renamed as *Furtadoella* in this study. *Furtadoella* was described from the Neotropics comprising three species in Costa-Rezende *et al.* (2017). In this study one specimen collected in French Guiana supported the views of Costa-Rezende *et al.* (2017) and Sun *et al.* (2020) in the morphological and phylogenetic analyses. Under SEM, the ornamentation of basidiospores in *Furtadoella* (Fig. 8C) was obviously shown to have a verrucose to reticulate exospore wall which is similar with the ultrastructural features of *Amauroderma* and *Trachydermella*. However, *Furtadoella* can be distinguished from other genera in *Ganodermataceae* by its soft basidiomata, a monomitic hyphal structure in context and non-truncated basidiospores.

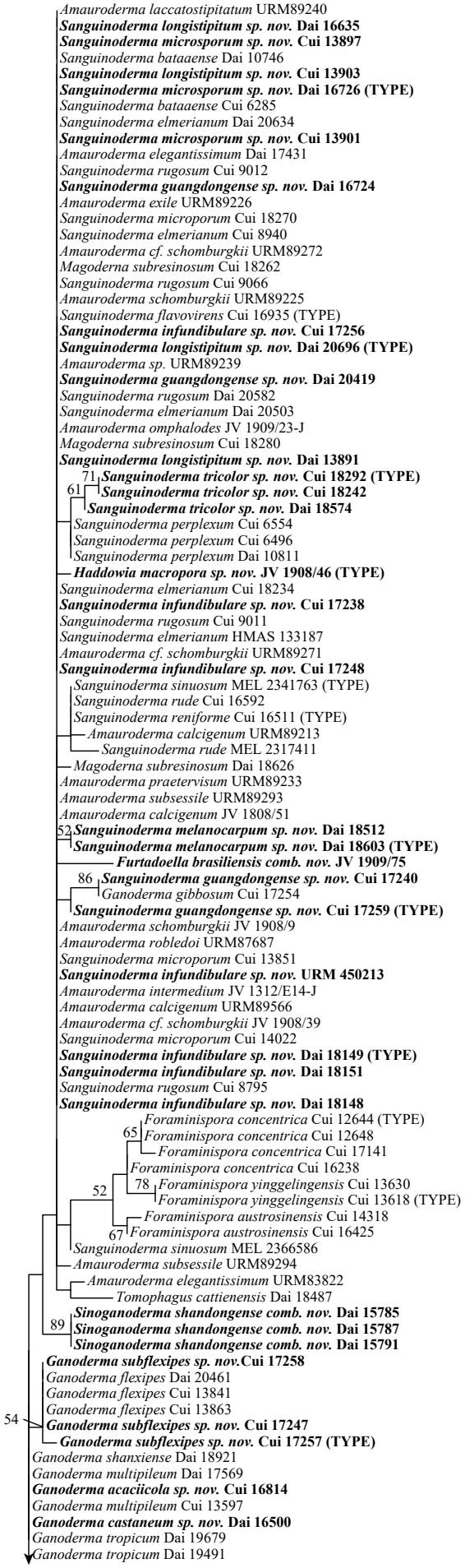

Fig. 7. Maximum Likelihood ML analyses of *Ganodermataceae* based on dataset of nSSU. Maximum Likelihood bootstrap values higher than 50 % are shown. New species are in bold.

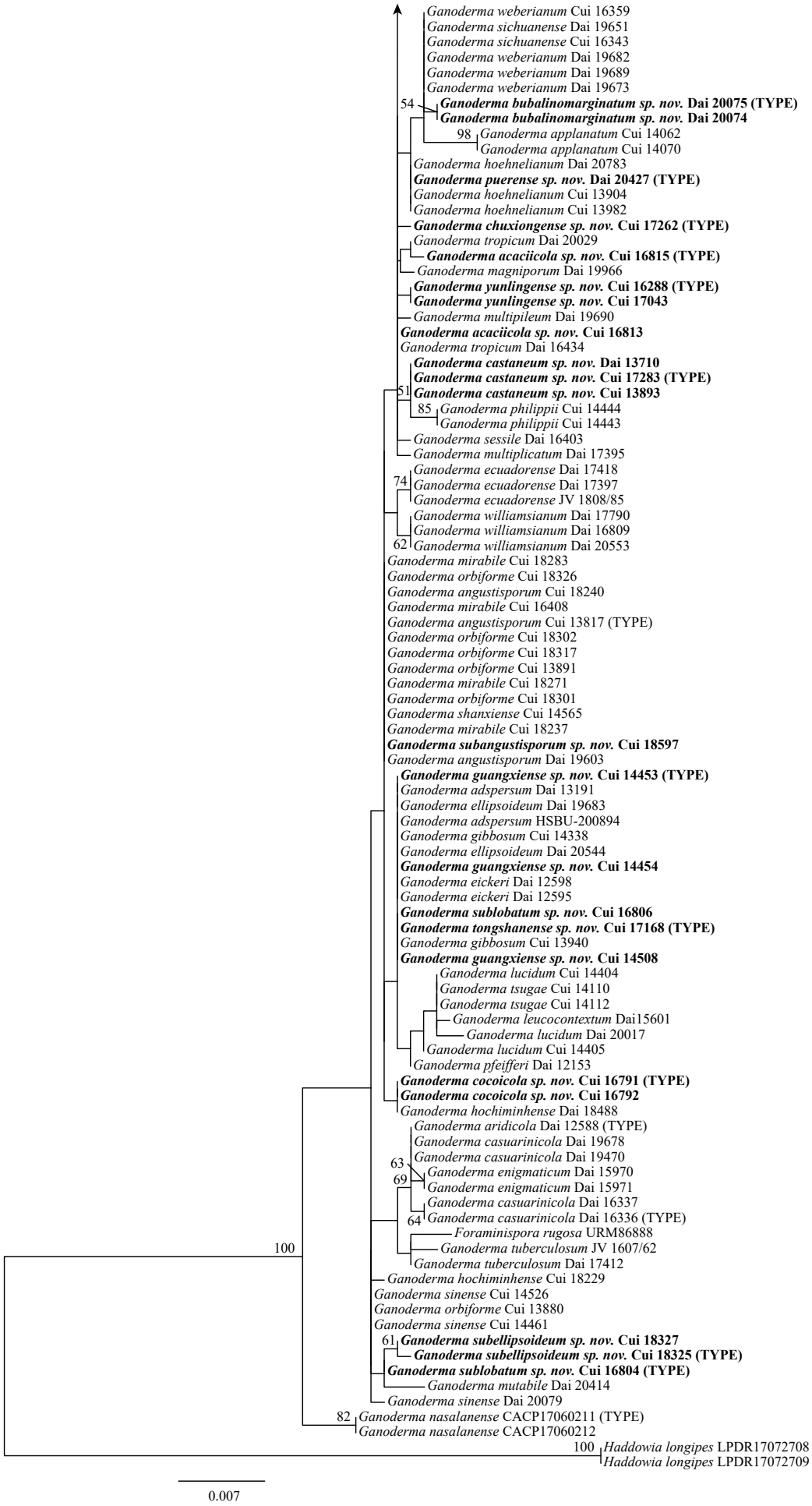

Fig. 7. (Continued).

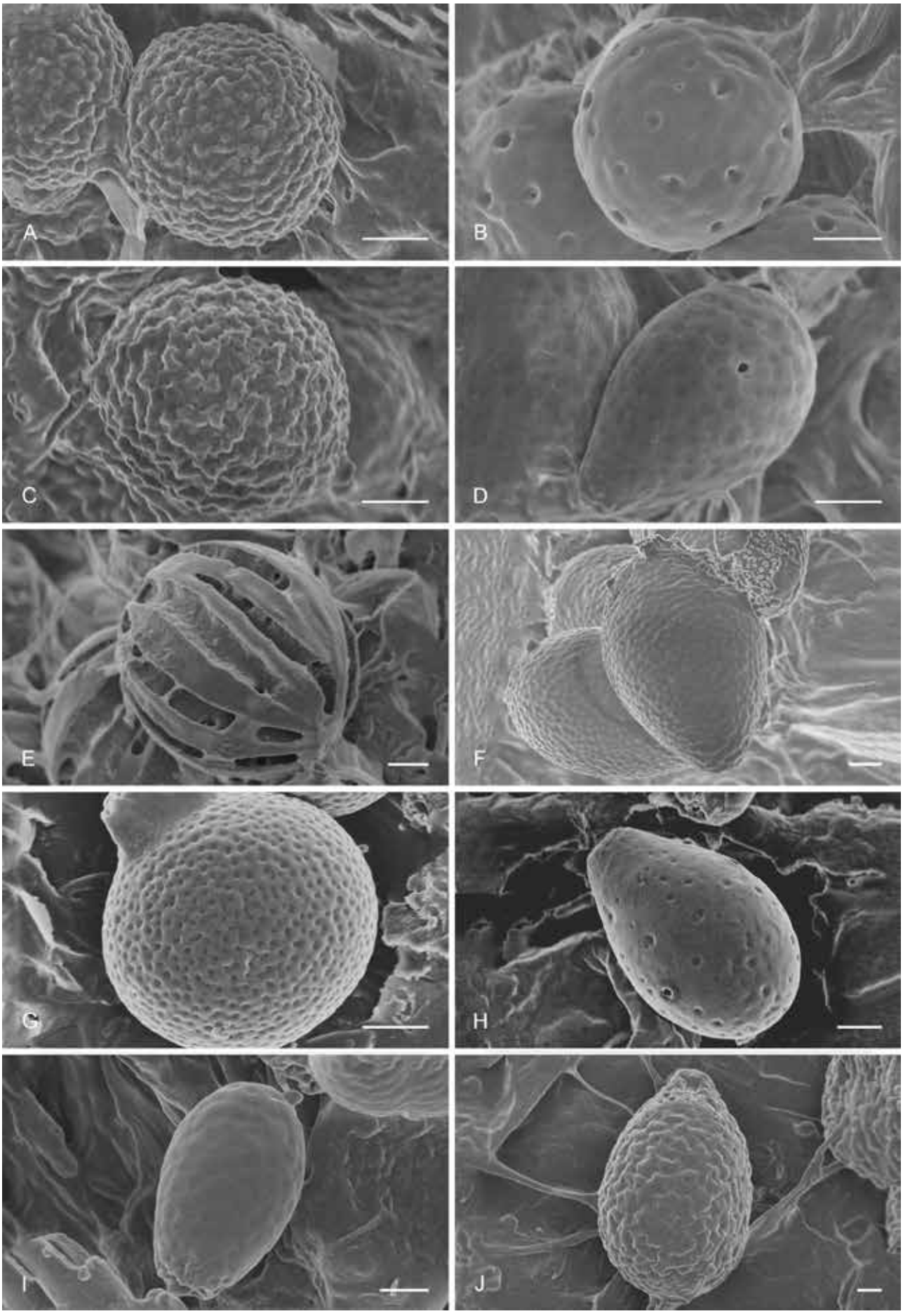

Fig. 8. Scanning Electron Micrograph (SEM) of basidiospores of 10 genera in *Ganodermataceae*. **A.** *Amauroderma schomburgkii* (JV 1908/9). **B.** *Foraminispora rugosa* (JV 1608/889-ND). **C.** *Furtadoella brasiliensis* (JV 1909/75). **D.** *Ganoderma lucidum* (Cui 14405). **E.** *Haddowia macropora* (JV 1908/46). **F.** *Magoderna subresinosum* (Cui 18280). **G.** *Sanguinoderma rude* (MEL 2150776). **H.** *Sinoganoderma shandongense* (Dai 20244). **I.** *Tomophagus cattienensis* (Dai 18487). **J.** *Trachydermella tsunodae* (Dai 3221c). Scale bars = 2 µm.

Table 2. The list of confirmed species in *Ganodermataceae*. Species in bold occur in China.

Genus	Species	Type locality	Sequences	References
Amauroderma (58)	*A. africanum*	Liberia	–	Ryvarden (2004b)
	A. albocontextum	Cameroon	–	Ryvarden (2020)
	A. albostipitatum	Brazil	–	Gomes-Silva *et al.* (2015)
	A. andinum	Venezuela	–	Ryvarden (2004b)
	A. argenteofulvum	Zimbabwe	–	Moncalvo & Ryvarden (1997)
	A. aurantiacum	Brazil	√	Gibertoni *et al.* (2008)
	A. boleticeum	Venezuela	–	Ryvarden (2004a)
	A. buloloi	Papua New Guinea	–	Moncalvo & Ryvarden (1997)
	A. calcigenum	Brazil	√	Ryvarden (2004a)
	A. calcitum	Brazil	√T	Costa-Rezende *et al.* (2016)
	A. camerarium	Brazil	√	Ryvarden (2004a)
	A. coltricioides	Guyana	–	Aime *et al.* (2003)
	A. congregatum	Malaysia	–	Corner (1983)
	A. conicum	Madagascar	–	Moncalvo & Ryvarden (1997)
	A. conjunctum	Africa	–	Moncalvo & Ryvarden (1997)
	A. deviatum	Ecuador	–	Ryvarden (2004a)
	A. ealaense	Zaire	–	Moncalvo & Ryvarden (1997)
	A. elegantissimum	Venezuela	√	Ryvarden (2004a)
	A. exile	Brazil	√	Ryvarden (2004a)
	A. faculum	Colombia	–	Henao-M (1997)
	A. flabellatum	Guyana	–	Aime *et al.* (2007)
	A. floriformum	Brazil	√T	Gomes-Silva *et al.* (2015)
	A. fuscatum	Uganda	–	Moncalvo & Ryvarden (1997)
	A. fuscoporia	Zimbabwe	–	Moncalvo & Ryvarden (1997)
	A. grandisporum	Burundi	–	Gulaid & Ryvarden (1998)
	A. insulare	Pacific: New Caledonia	–	Moncalvo & Ryvarden (1997)
	A. intermedium	Brazil	√	Ryvarden (2004a)
	A. kwiluense	Zaire	–	Ryvarden (1974)
	A. laccatostipitatum	Brazil	√	Gomes-Silva *et al.* (2015)
	A. leptopus	New Guinea	–	Furtado (1967b)
	A. leucosporum	Singapore	–	Corner (1983)
	A. malesianum	Malaysia	–	Corner (1983)
	A. minuta	Zimbabwe	–	Ryvarden (2018)
	A. nigrum	Cameroon	–	Moncalvo & Ryvarden (1997)
	A. oblongisporum	Angola	–	Campacci & Gugliotta (2009)
	A. omphalodes	Brazil	√	Ryvarden (2004a)
	A. parasiticum	Singapore	–	Corner (1983)
	A. partitum	Brazil	√	Gomes-Silva *et al.* (2010)
	A. picipes	Brazil	–	Gomes-Silva & Gibertoni (2012)
	A. praetervisum	Brazil	√	Ryvarden (2004a)
	A. preussii	Cameroon	–	Steyaert (1972)
	A. pseudoboletus	Paraguay	√	Ryvarden (2004a)
	A. pudens	India	–	Moncalvo & Ryvarden (1997)
	A. renidens	Brazil	–	Furtado (1967b), Ryvarden (2004a)
	A. robledoi	Brazil	√	Costa-Rezende *et al.* (2020a)
	A. ryvardenii	Zambia	–	Ryvarden (2020)
	A. salisburiense	Zimbabwe	–	Moncalvo & Ryvarden (1997)

Table 2. (Continued).

Genus	Species	Type locality	Sequences	References
	A. schomburgkii	Guyana	√	Ryvarden (2004a)
	A. secedens	Malaysia: Pahang	–	Corner (1983)
	A. sericatum	Nigeria	–	Moncalvo & Ryvarden (1997)
	A. sessile	Brazil	–	Gomes-Silva *et al.* (2015)
	A. solomonense	Solomon Islands	–	Corner (1983)
	A. subrugosum	Samoa Islands	–	Moncalvo & Ryvarden (1997)
	A. subsessile	Brazil	√	Gomes-Silva *et al.* (2015)
	A. tapetellum	Colombia	–	Henao-M (1997)
	A. trichodermatum	Brazil	–	Robledo *et al.* (2015)
	A. unilaterum	Brazil	–	Ryvarden (2004a)
	A. velutina	Cameroon	–	Ryvarden (2020)
Amaurodermellus (1)	*Amaurodermellus ovisporum*	Brazil	√	Gomes-Silva *et al.* (2015), Costa-Rezende *et al.* (2020b)
Cristataspora (2)	*C. coffeata*	St. Vincent	√	Costa-Rezende *et al.* (2020b)
	C. flavipora	Jamaica	√	Costa-Rezende *et al.* (2020b)
Foraminispora (5)	***Fo. austrosinensis***	China: Hainan	√	Zhao *et al.* (1984), Sun *et al.* (2020)
	Fo. concentrica	China: Sichuan	√T	Song *et al.* (2016), Sun *et al.* (2020)
	Fo. rugosa	Brazil	√	Costa-Rezende *et al.* (2017)
	Fo. yinggelingensis	China: Hainan	√T	Sun *et al.* (2020)
	Fo. yunnanensis	China: Yunnan	√	Zhao & Zhang (1986b), Sun *et al.* (2020)
Furtadoella (3)	*Fu. biseptata comb. nov.*	Brazil	√T	Costa-Rezende *et al.* (2017)
	Fu. brasiliensis comb. nov.	Brazil	√	Costa-Rezende *et al.* (2017)
	Fu. corneri comb. nov.	Brazil	–	Costa-Rezende *et al.* (2017)
Ganoderma (181)	*G. acaciicola sp. nov.*	Australia	√T	This study
	G. acontextum sp. nov.	Guatemala	√T	This study
	G. adspersum	Slovenia: Vinkovce	√	Steyaert (1972), this study
	G. aetii	Indonesia: Kalimantan	–	Zmitrovich (2018)
	G. ahmadii	Pakistan: Sialkot	–	Steyaert (1972)
	G. alluaudii	Kenya: Nairobi	–	Ryvarden (1983)
	G. alpinum sp. nov.	China: Yunnan	√T	This study
	G. amazonense	Brazil: Para State	–	Furtado (1967a)
	G. angustisporum	China: Fujian	√T	Xing *et al.* (2018)
	G. applanatum	Europe	√	Patouillard (1887)
	G. aridicola	South Africa: Durban	√T	Xing *et al.* (2016)
	G. aureolum	Angola: Tchivinguiro	–	Moncalvo & Ryvarden (1997)
	G. australe	Pacific island	√	Ryvarden (2004a)
	G. austroafricanum	South Africa: Gauteng	√	Crous *et al.* (2014)
	G. barretoi	Brazil: Madeira	–	Moncalvo & Ryvarden (1997)
	G. baudonii	Central African Republic	–	Moncalvo & Ryvarden (1997)
	G. bilobum	–	–	–
	G. boninense	Japan: Bonin Islands	√	Ryvarden (1983)
	G. brownii	USA: California	√	Steyaert (1972)
	G. bruggemanii	Indonesia: Java	–	Steyaert (1972)
	G. bubalinomarginatum sp. nov.	China: Guangxi	√T	This study
	G. calidophilum	China: Hainan	√	Cao (2013), this study
	G. capense	South Africa	–	Teng (1963)
	G. carnosum	France: Pyrenees	√	Moncalvo & Ryvarden (1997)

Table 2. (Continued).

Genus	Species	Type locality	Sequences	References
	G. carocalcareum	Cameroon	√T	Douanla-Meli & Langer (2009)
	G. castaneum sp. nov.	China: Hainan	√T	This study
	G. casuarinicola	China: Guangdong	√T	Xing *et al.* (2018)
	G. cervinum	Papua New Guinea	–	Moncalvo & Ryvarden (1997)
	G. chalceum	Sierra Leone: Kenema	√	Steyaert (1967)
	G. chocoense	Ecuador: Esmeraldas	√T	Crous *et al.* (2018)
	G. chonoides	Zaire: Shaba	–	Moncalvo & Ryvarden (1997)
	G. chuxiongense sp. nov.	China: Yunnan	√T	This study
	G. cinnamomea	Cameroon	–	Ryvarden (2020)
	G. citriporum	Venezuela: Yutaje	–	Ryvarden (2004a)
	G. cocoicola sp. nov.	Australia	√T	This study
	G. concinnum	Colombia: Choco State	√	Ryvarden (2000)
	G. corrugatum	Zaire: Kasai	–	Steyaert (1961)
	G. cupreum	Guinea	√	Moncalvo & Ryvarden (1997), this study
	G. curranii	Philippines: Luzon	–	Murrill (1908a)
	G. curtisii	USA: South Carolina	√	Murrill (1908b)
	G. dejongii	Indonesia: Java	–	Steyaert (1972)
	G. destructans	South Africa: Gauteng	√T	Coetzee *et al.* (2015)
	G. dianzhongense	China: Yunnan	√T	He *et al.* (2021)
	G. dimidiatum	Japan	–	Papp (2016)
	G. donkii	Indonesia: West Java	–	Steyaert (1972)
	G. dorsale	Brazil	–	Moncalvo & Ryvarden (1997)
	G. dubio-cochlear	Madagascar	–	Moncalvo & Ryvarden (1997)
	G. dunense	South Africa: Western Cape	√T	Tchotet Tchoumi *et al.* (2018)
	G. dussii	Guadeloupe	–	Moncalvo & Ryvarden (1997)
	G. ecuadorense	Ecuador: Orellana	√T	Crous *et al.* (2016)
	G. eickeri	South Africa	√T	Tchotet Tchoumi *et al.* (2019)
	G. elegantum	Ecuador: Yasuni National Park	–	Ryvarden (2004a)
	G. ellipsoideum	China: Hainan	√T	Hapuarachchi *et al.* (2018b)
	G. endochrum	Uganda: Entebbe	–	Moncalvo & Ryvarden (1997)
	G. enigmaticum	South Africa: Gauteng	√T	Coetzee *et al.* (2015)
	G. esculentum	China: Yunnan	√T	He *et al.* (2021)
	G. fallax sp. nov.	USA	√T	This study
	G. fassii	Congo: Ubangi	–	Steyaert (1961)
	G. fassioides	Congo: Yangambi	–	Steyaert (1961)
	G. fici	Tunisia: Gafsa	–	Moncalvo & Ryvarden (1997)
	G. flexipes	Vietnam: Tonkin	√	Steyaert (1972)
	G. fuscum	Zaire: Shaba	–	Moncalvo & Ryvarden (1997)
	G. gabonensis	Gabon	–	Decock & Ryvarden (2020)
	G. ghesquierei	Zaire: Lukoleka	–	Moncalvo & Ryvarden (1997)
	G. gibbosum	Indonesia: Java	√	Moncalvo & Ryvarden (1997), this study
	G. gilletii	Zaire: Moanda	–	Moncalvo & Ryvarden (1997)
	G. guangxiense sp. nov.	China: Guangxi	√T	This study
	G. guianensis	French Guiana	–	Ryvarden (2004a)
	G. hildebrandii	Comores Islands	–	Moncalvo & Ryvarden (1997)
	G. hinnuleum	Zaire: Yangambi	–	Moncalvo & Ryvarden (1997)

Table 2. (Continued).

Genus	Species	Type locality	Sequences	References
	G. hochiminhense	Vietnam	√T	Luangharn *et al.* (2021)
	G. hoehnelianum	Indonesia: Java	√	Luangharn *et al.* (2021)
	G. hoploides	Congo: Virunga National Park	–	Steyaert (1961)
	G. impolitum	Malaysia: Pahang	–	Moncalvo & Ryvarden (1997)
	G. insulare	Seychelles	–	Ryvarden (2020)
	G. knysnamense	South Africa	√T	Tchotet Tchoumi *et al.* (2019)
	G. kosteri	The Netherlands: Gouda	–	Steyaert (1972)
	G. lamaoense	Philippines: Lamao	–	Steyaert (1972)
	G. leucocontextum	China: Tibet	√T	Li *et al.* (2015)
	G. leucocreas	Zaire: Loango	–	Moncalvo & Ryvarden (1997)
	G. leytense	Philippines: Leyte	–	Steyaert (1972)
	G. lingua	Indonesia: Java	–	Moncalvo & Ryvarden (1997)
	G. lingzhi	China: Hubei	√T	Cao *et al.* (2012)
	G. lobatoideum	Guyana	–	Steyaert (1980)
	G. lobatum	USA: North Carolina	√	Steyaert (1980)
	G. lobenense	Cameroon	–	Kinge & Mih (2014)
	G. longistipitatum	Venezuela	–	Ryvarden (2000)
	G. lucidum	England: London	√	Steyaert (1972)
	G. luteicinctum	Singapore	–	Foroutan & Vaidya (2007)
	G. magniporum	China: Guangxi	√	This study
	G. mangiferae	Tahiti	–	Moncalvo & Ryvarden (1997)
	G. manoutchehrii	Iran: Ramsar	–	Steyaert (1972)
	G. martinicense	Martinique	√T	Welti & Courtecuisse (2010)
	G. mbrekobenum	Ghana	√T	Crous *et al.* (2016)
	G. megalosporum	Kenya: Nairobi	–	Moncalvo & Ryvarden (1997)
	G. melanophaeum	Zaire: Shaba	–	Moncalvo & Ryvarden (1997)
	G. mexicanum	Mexico	√	Torres-Torres & Guzmán-Dávalos (2012)
	G. miniatocinctum	Malaysia: Banting	–	Steyaert (1967)
	G. mirabile	Malaysia: Pahang	√	Steyaert (1972)
	G. mizoramense	India: Mizoram	√T	Crous *et al.* (2017a)
	G. multicornum	Venezuela	–	Ryvarden (2000)
	G. multipileum	China: Taiwan	√	Wang *et al.* (2009)
	G. multiplicatum	French Guiana	√	Steyaert (1980), Ryvarden (2000)
	G. mutabile	China: Yunnan	√T	Cao & Yuan (2012)
	G. myanmarense	Myanmar	√T	Luangharn *et al.* (2021)
	G. namutambalaense	Uganda	–	Moncalvo & Ryvarden (1997)
	G. nasalaense	Laos	√T	Hapuarachchi *et al.* (2019b)
	G. neogibbosum	Martinica insula	–	Welti & Courtecuisse (2010)
	G. neojaponicum	Japan: Tokyo	√T	This study
	G. nitidum	Honduras: Puerto Sierra	√	Moncalvo & Ryvarden (1997), this study
	G. ochrolaccatum	Philippines: Manila	–	Moncalvo & Ryvarden (1997)
	G. oerstedii	USA: Puerto Rico	√	Moncalvo & Ryvarden (1997)
	G. orbiforme	Guinea	√	Ryvarden (2000)
	G. oregonense	USA: Oregon	√	Murrill (1908b)
	G. ostracodes	Vietnam: Tonkin	–	Moncalvo & Ryvarden (1997)
	G. parvigibbosum	Martinique	–	Welti & Courtecuisse (2010)

Table 2. (Continued).

Genus	Species	Type locality	Sequences	References
	G. parvulum	Nicaragua	√	Ryvarden (2004a), this study
	G. petchii	Sri Lanka: Hakgala	–	Steyaert (1972)
	G. pfeifferi	Germany	√	Foroutan & Vaidya (2007)
	G. philippii	Myanmar: Mergui	√	Steyaert (1972)
	G. piceum	Malaysia	–	Ryvarden (2015)
	G. platense	Argentina	√	Moncalvo & Ryvarden (1997), this study
	G. podocarpense	Ecuador	√T	Crous *et al.* (2017b)
	G. polychromum	USA: California	√	Moncalvo & Ryvarden (1997), this study
	G. puerense sp. nov.	China: Yunnan	√T	This study
	G. puglisii	Italy: Potenza	–	Steyaert (1972)
	G. pulchella	–	–	Bresadola (1912)
	G. pygmoideum	Brazil	–	Moncalvo & Ryvarden (1997)
	G. ramosissimum	China: Yunnan	√	Zhao (1989a), this study
	G. ravenelii	USA: South Carolina	√	Steyaert (1980)
	G. resinaceum	France: Blois	√	Ryvarden (2000), Ryvarden (2004a)
	G. reticulatosporum	Zimbabwe: Harare	–	Moncalvo & Ryvarden (1997)
	G. rhacodes	–	–	Patouillard (1914)
	G. rothwellii	Zimbabwe	–	Steyaert (1980)
	G. rufoalbum	Venezuela	–	Moncalvo & Ryvarden (1997)
	G. ryvardenii	Cameroon	√T	Kinge & Mih (2011)
	G. sanduense	China: Guizhou	√T	Hapuarachchi *et al.* (2019b)
	G. sarasinii	New Caledonia: Yate	–	Steyaert (1961)
	G. sculpturatum	Madagascar	–	Moncalvo & Ryvarden (1997)
	G. septatum	Zaire: Kivu	–	Moncalvo & Ryvarden (1997)
	G. sessile	USA: New York	√	Steyaert (1972), this study
	G. sessiliforme	Mexico	√	Torres-Torres & Guzmán-Dávalos (2012)
	G. shanxiense	China: Shanxi	√T	Liu *et al.* (2019)
	G. sichuanense	China: Sichuan	√T	Zhao *et al.* (1983)
	G. silveirae	Brazil: Madeire	–	Moncalvo & Ryvarden (1997)
	G. sinense	China: Hainan	√	Zhao *et al.* (1979)
	G. soyeri	Zaire: Shaba	–	Steyaert (1961)
	G. sp.	Vietnam	√	Le *et al.* (2018)
	G. steyaertianum	Indonesia: Tirtaganga	√	Smith & Sivasithamparam (2003)
	G. stipitatum	Nicaragua	√	Murrill (1908b)
	G. subangustisporum sp. nov.	China: Yunnan	√T	This study
	G. subellipsoideum sp. nov.	Malaysia	√T	This study
	G. subflexipes sp. nov.	China: Guangdong	√T	This study
	G. sublobatum sp. nov.	Australia	√T	This study
	G. sublucidum	Zaire: Eala	–	Moncalvo & Ryvarden (1997)
	G. substipitata	–	–	Bresadola (1915)
	G. subumbraculum	Japan	–	Moncalvo & Ryvarden (1997)
	G. testaceum	Brazil	–	Moncalvo & Ryvarden (1997)
	G. thailandicum	Thailand	√T	Luangharn *et al.* (2019)
	G. tongshanense sp. nov.	China: Hubei	√T	This study
	G. tornatum	Mariana Island	√	Moncalvo & Ryvarden (1997), this study
	G. torosum	Thailand: Nakhawn Strithamarat	–	Moncalvo & Ryvarden (1997)

Table 2. (Continued).

Genus	Species	Type locality	Sequences	References
	G. trengganuense	Malaysia: Trengganu	–	Foroutan & Vaidya (2007)
	G. tropicum	Indonesia: Java	√	Steyaert (1972)
	G. trulla	Indonesia: Java	–	Moncalvo & Ryvarden (1997)
	G. trulliforme	Indonesia: Java	–	Moncalvo & Ryvarden (1997)
	G. tsugae	USA: New York	√	Murrill (1902)
	G. tuberculosum	Belize	√	Murrill (1908b)
	G. turbinatum	Uganda: Kabale	–	Ipulet & Ryvarden (2005)
	G. umbrinum	Indonesia: Java	–	Moncalvo & Ryvarden (1997)
	G. valesiacum	Switzerland: Valais	–	Moncalvo & Ryvarden (1997)
	G. vanheurnii	Indonesia: Java	–	Steyaert (1972)
	G. vanmeelii	Zaire: Shaba	–	Steyaert (1961)
	G. vivianimercedianum	Mexico	–	Torres-Torres (2008)
	G. weberianum	Samoa Islands	√	Steyaert (1972)
	G. weixiense	China: Yunnan	√T	Ye *et al.* (2019)
	G. wiiroense	Ghana	√T	Crous *et al.* (2015)
	G. williamsianum	Philippines: Luzon	√	Murrill (1907)
	G. xylonoides	Zaire: Bongabo	–	Steyaert (1961)
	G. yunlingense sp. nov.	China: Yunnan	√T	This study
	G. zonatum	USA: Florida	√	Murrill (1902)
Haddowia (2)	***Ha. longipes***	French Guyana	√	Steyaert (1972)
	Ha. macropora sp. nov.	French Guyana	√T	This study
Humphreya (3)	*Hu. eminii*	Tanzania	–	Moncalvo & Ryvarden (1997)
	Hu. endertii	Indonesia	–	Steyaert (1972)
	Hu. lloydii	–	–	Steyaert (1972)
Magoderna (2)	*M. infundibuliforme*	Uganda	–	Steyaert (1972)
	M. subresinosum	Philippines: Luzon	√	Steyaert (1972)
Neoganoderma gen. nov. (1)	***N. neurosporum comb. nov.***	Panama	√	Furtado (1967a), Ryvarden (2004a)
Sanguinoderma (16)	***Sa. bataanense***	Philippines: Luzon	√	Murrill (1908a), Sun *et al.* (2020)
	Sa. elmerianum	Philippines: Luzon	√	Murrill (1907), Sun *et al.* (2020)
	Sa. flavovirens	Zambia	√T	Sun *et al.* (2020)
	Sa. guangdongense sp. nov.	China: Guangdong	√T	This study
	Sa. infundibulare sp. nov.	China: Guangdong	√T	This study
	Sa. laceratum	China: Yunnan	√T	Sun *et al.* (2020)
	Sa. longistipitum sp. nov.	China: Yunnan	√T	This study
	Sa. melanocarpum sp. nov.	Malaysia	√T	This study
	Sa. microporum	China: Hainan	√T	Sun *et al.* (2020)
	Sa. microsporum sp. nov.	Thailand	√T	This study
	Sa. perplexum	Malaysia	√	Corner (1983), Sun *et al.* (2020)
	Sa. reniforme	Zambia	√T	Sun *et al.* (2020)
	Sa. rude	Australia: Tasmania	√	Sun *et al.* (2020)
	Sa. rugosum	Indonesia: Java	√	Sun *et al.* (2020)
	Sa. sinuosum	Australia: Queensland	√T	Sun *et al.* (2020)
	Sa. tricolor sp. nov.	Malaysia	√T	This study
Sinoganoderma gen. nov. (1)	***Si. shandongense comb. nov.***	China: Shandong	√	This study

Table 2. (Continued).

Genus	Species	Type locality	Sequences	References
Tomophagus (2)	*To. cattienensis*	Vietnam	√[T]	Le *et al.* (2012)
	To. colossus	Costa Rica	√	Le *et al.* (2012)
Trachydermella (1)	***Tr. tsunodae comb. nov.***	Japan	√	Imazeki (1952)

[T] Sequences from type specimens.

Furtadoella biseptata (Costa-Rezende *et al.*) B.K. Cui & Y.F. Sun, ***comb. nov.*** MycoBank MB 843287.
Basionym: *Furtadoa biseptata* Costa-Rezende *et al.*, Persoonia 39: 265. 2017.

Notes: *Furtadoa biseptata* was described as a new species by its simple septate generative hyphae in the context. However, due to the illegality of *Furtadoa*, this species was transferred to *Furtadoella* as a new combination in this study. The description of *Fu. biseptata* can be found in Costa-Rezende *et al.* (2017).

Furtadoella brasiliensis (Singer) B.K. Cui & Y.F. Sun, ***comb. nov.*** MycoBank MB 843289.
Basionym: *Scutiger brasiliensis* Singer, Beih. Nova Hedwigia 77: 22. 1983.

Notes: Costa-Rezende *et al.* (2017) transferred *Scutiger brasiliensis* to *Furtadoa* based on its similar morphological characters. But the name *Furatadoa* is illegitimate, and therefore *S. brasiliensis* is placed in *Furtadoella*. The description of *Fu. brasiliensis* can be found in Coelho *et al.* (2007).

Furtadoella corneri (Gulaid & Ryvarden) B.K. Cui & Y.F. Sun, ***comb. nov.*** MycoBank MB 843290.
Basionym: *Amauroderma corneri* Gulaid & Ryvarden, Mycol. Helv. 10: 28. 1998.

Notes: This species was firstly described from Brazil, and it was recombined to *Furtadoa* by its monomitic hyphal system in context (Costa-Rezende *et al.* 2017). In this study, *Amauroderma corneri* was treated as a new combination in *Furtadoella* due to the illegality of *Furtadoa*. The detailed description of *Fu. corneri* can be found in Gulaid & Ryvarden (1998).

Ganoderma P. Karst., Revue Mycol., Toulouse 3: 17. 1881. MycoBank MB 17639.

Type species: *Ganoderma lucidum* (Curtis) P. Karst.

Description: *Basidiomata* annual to perennial, sessile or subsessile to stipitate. *Pilei* solitary or imbricate, of variable shape. *Pileal surface* pale brown, reddish brown to almost black, dull to laccate, with variable ornamentation. *Context* homogeneous or heterogeneous. *Tubes* stratified or not. *Hyphal system* trimitic,

Fig. 9. Basidiomata of *Ganoderma acaciicola*.

generative hyphae usually with clamp connections. *Basidiospores* subglobose to ellipsoid or ovoid, truncated, double-walled with thick walls, exospore wall semi-reticulate, endospore wall smooth or with conspicuous spinules.

Notes: In this study, 95 species of *Ganoderma* were included to construct the phylogenetic tree, and they formed an independent clade with proper support (Fig. 1). Based on morphological characters and phylogenetic evidence, 16 new species are described and illustrated. In addition, 28 known species are also described, and a key to confirmed species of *Ganoderma* in China is provided.

Ganoderma acaciicola B.K. Cui, J.H. Xing & Y.F. Sun, ***sp. nov.*** MycoBank MB 839670. Figs 9, 10.

Diagnosis: Differs from other species in the genus by its sessile and concrescent basidiomata with reddish brown and laccate pileal surface, homogeneous context, non-stratified tubes, cream to buff pore surface unchanging when bruised, broadly ellipsoid to ovoid basidiospores with truncated apex.

Etymology: *acaciicola* (*Lat.*), refers to this species growing on *Acacia*.

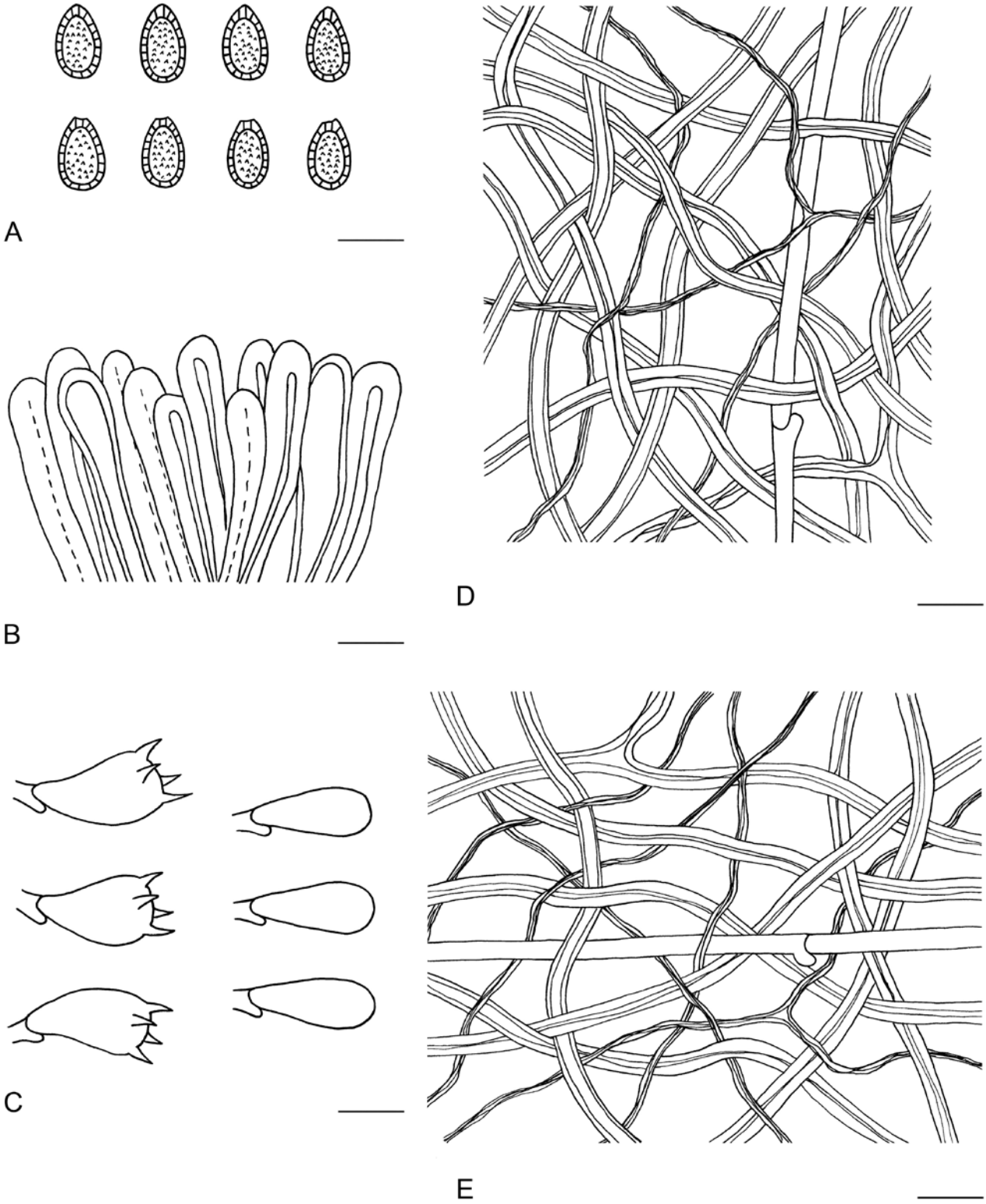

Fig. 10. Microscopic structures of *Ganoderma acaciicola* (drawn from Cui 16815). **A.** Basidiospores. **B.** Apical cells from cuticle. **C.** Basidia and basidioles. **D.** Hyphae from trama. **E.** Hyphae from context. Scale bars = 10 µm.

Typus: **Australia**, Queensland, Cairns, on stump of *Acacia*, 18 May 2018, Cui 16815 (**holotype** BJFC030114).

Additional materials examined: **Australia**, Queensland, Cairns, on stump of *Acacia*, 18 May 2018, Cui 16813 (BJFC030112), Cui 16814 (BJFC030113); on root of living *Acacia*, 18 May 2018, Cui 16817 (BJFC030116).

Description: *Basidiomata* annual, sessile or subsessile and broadly attached, usually concrescent, hard corky to woody hard. *Pilei* subcircular to flabelliform, up to 16.5 cm diam and 3 cm thick. *Pileal surface* rusty orange brown to reddish brown, laccate, glabrous, pileal margin distinct, cream buff; margin obtuse, entire, irregularly wavy. *Pore surface* cream to buff when fresh, unchanging when bruised, pale straw yellow when dry; pores circular to angular, 4–6 per mm; dissepiments moderately thick, entire. *Context* cinnamon brown to dark brown, homogeneous, with black melanoid lines, hard corky, up to 2 cm thick. *Tubes* yellowish brown to greyish brown, non-stratified, up to 1 cm long. *Hyphal system* trimitic; generative hyphae with clamp connections; all hyphae IKI –, CB +; tissues darkening in KOH. Generative hyphae in context colourless, thin-walled, 2–4 µm diam; skeletal hyphae in context dark brown, thick-walled with a wide to narrow lumen or sub-solid, arboriform and flexuous, 2–6 µm diam; binding hyphae in context colourless, thick-walled, branched and flexuous, up to 1 µm diam. Generative hyphae in tubes colourless, thin-walled, 2–3 µm diam; skeletal hyphae in tubes pale yellowish brown, thick-walled with a wide to narrow lumen or sub-solid, arboriform and flexuous, 2–4 µm diam; binding hyphae in tubes colourless, thick-walled, branched and flexuous, up to 1 µm diam. *Pileipellis* composed of clamped generative hyphae, thick-walled to sub-solid, apical cells clavate, inflated and flexuous, pale yellow to golden yellow, about 25–38 × 6–10 µm, forming a regular palisade. *Cystidia* and *cystidioles* absent. *Basidia* barrel-shaped, colourless, thin-walled, 15–20 × 9–12 µm; *basidioles* clavate, colourless, thin-walled, 15–20 × 6–10 µm. *Basidiospores* broadly ellipsoid to ovoid, truncated, yellowish brown, IKI –, CB +, double-walled with distinctly thick walls, exospore wall smooth, endospore wall with dense spinules, (9–)9.2–11.3(–11.6) × (5–)5.6–7 µm, L = 10.12 µm, W = 6.29 µm, Q = 1.61 (n = 60/2, with the turgid vesicular appendix excluded); (10.5–)10.7–11.8(–12.1) × (5.5–)5.8–7 µm, L = 11.12 µm, W = 6.31 µm, Q = 1.72–1.81 (n = 60/2, with the turgid vesicular appendix included).

Notes: *Ganoderma acaciicola* was collected from Australia on *Acacia*. It can be characterised by concrescent basidiomata without a stipe, rusty orange brown to reddish brown and laccate pileal surface, pore surface unchanging when bruised. In the phylogenetic analyses, *G. acaciicola* is closely related to *G. mizoramense* which was described from Mizoram, India; however, its stipitate basidiomata with irregular pileal surface, ellipsoid basidiospores in larger size (10–12.5 × 6–9 µm, Crous *et al.* 2017a) differentiate it from *G. acaciicola*.

Ganoderma acontextum B.K. Cui, J.H. Xing & Vlasák, ***sp. nov.*** MycoBank MB 805754. Figs 11, 12.

Diagnosis: Differs from other species in the genus by its ungulate pilei with non-laccate pileal surface, heterogeneous and thin context, non-stratified tubes, almond-shaped basidiospores without spinules on the endospore wall.

Etymology: *acontextum* (*Lat.*), refers to the basidiomata having extremely thin context.

Typus: **Guatemala**, San Mateo, on angiosperm tree, 22 Nov. 2006 (**holotype** JV 0611/21G).

Fig. 11. Basidiomata of *Ganoderma acontextum*.

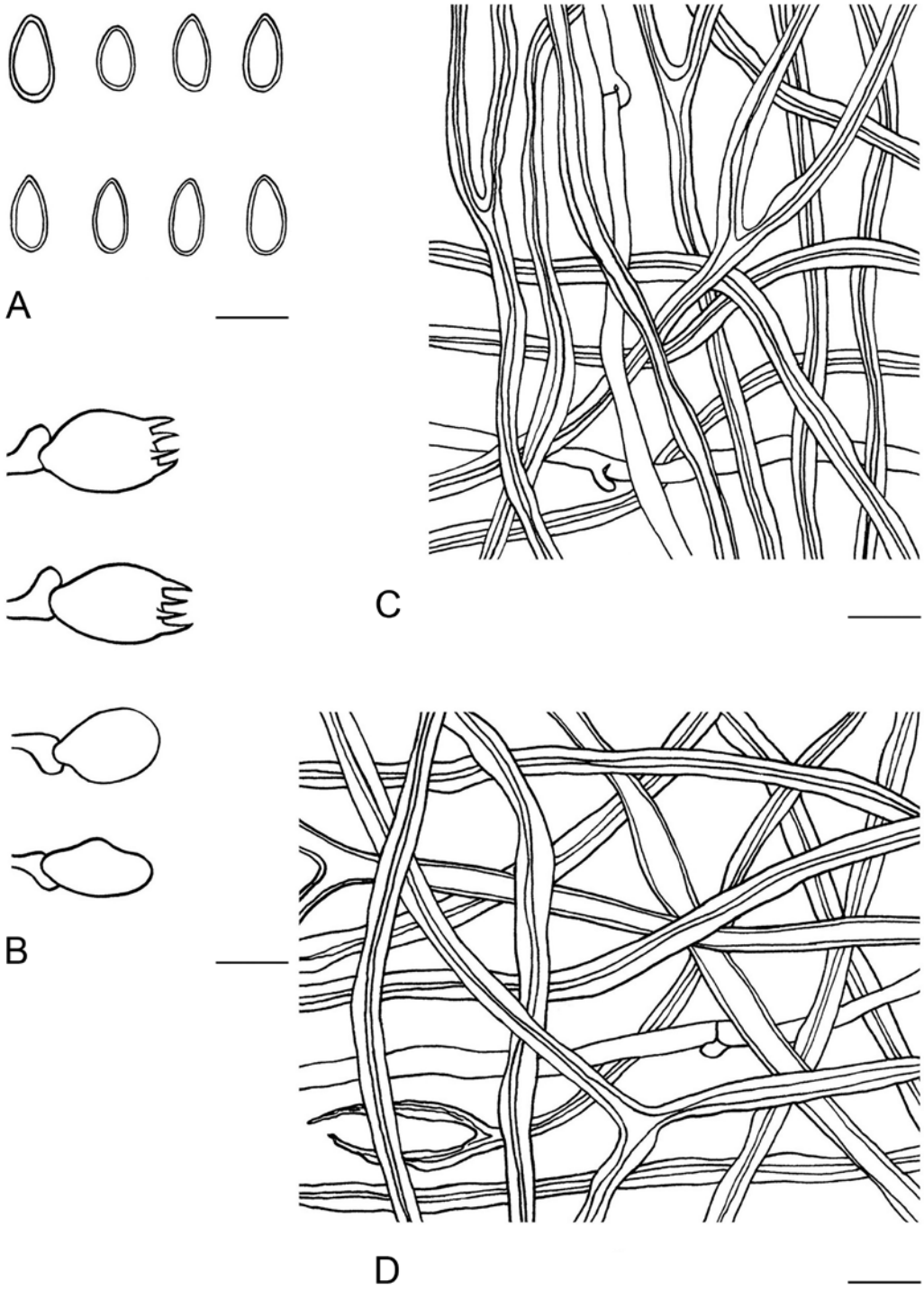

Fig. 12. Microscopic structures of *Ganoderma acontextum* (drawn from JV 0611/21G). **A.** Basidiospores. **B.** Basidia and basidioles. **C.** Hyphae from trama. **D.** Hyphae from context. Scale bars = 10 µm.

Additional materials examined: **USA**, Virginia, Woodbridge, Mason Neck State Park, on *Quercus*, 11 Aug. 2012, JV 1208/11J, JV 1407/64 (JV).

Diagnosis: *Basidiomata* perennial, sessile, woody hard. *Pilei* solitary, ungulate to columnar at maturity, up to 6 cm diam and 4 cm thick. *Pileal surface* reddish brown to dark brown, dull, glabrous, with dense concentric furrows; margin obtuse, entire, wavy. *Pore surface* white when fresh, turning darker when bruised, clay-buff to dark brown when dry; pores circular, 4–6 per mm; dissepiments thick, entire. *Context* dark brown, heterogeneous, composed of a strikingly light brown to ochre zone under pileal crust, followed by black melanoid lines, and dark brown context above the tubes, corky, thin, up to 3 mm thick altogether. *Tubes* dark brown, non-stratified, up to 4 cm long. *Hyphal system* trimitic; generative hyphae with clamp connections; skeletal hyphae occasionally with simple septa; all hyphae IKI –, CB +; tissues darkening in KOH. Generative hyphae in context colourless, thin-walled, 2–3 µm diam; skeletal hyphae in context yellow to brown, thick-walled with a wide to narrow lumen or sub-solid, arboriform and flexuous, 2–5 µm diam; binding hyphae in context colourless, thick-walled, branched and flexuous, 1.2–2.5 µm diam. Generative hyphae in tubes colourless, thin-walled, 2.2–2.8 µm diam; skeletal hyphae in tubes pale brown to brown, thick-walled with a wide to narrow lumen or sub-solid, arboriform and flexuous, 2.3–4 µm diam; binding hyphae in tubes colourless, thick-walled, branched and flexuous, 1–2.5 µm diam. *Cystidia* and *cystidioles* absent. *Basidia* broadly clavate, colourless, thin-walled, 20–30 × 7–11 µm; *basidioles* in shape like the basidia, colourless, thin-walled, 14–25 × 6–10 µm. *Basidiospores* almond-shaped, not obviously

truncated, golden-brown, IKI –, CB +, double-walled with slightly thick walls, exospore wall smooth, endospore wall without spinules, (9–)9.8–10.2(–11) × (4–)5.5–6.3(–6.5) µm, L = 9.89 µm, W = 5.73 µm, Q = 1.73 (n = 30/1, with the turgid vesicular appendix excluded).

Notes: *Ganoderma acontextum* was collected from Central America and the USA belonging to the non-laccate group. It has distinctive features such as ungulate pilei with densely concentrically furrowed pileal surface, heterogeneous and thin context, non-stratified tubes, almond-shaped basidiospores without an obviously truncated apex, and no spinules on the endospore wall.

Ganoderma alpinum B.K. Cui, J.H. Xing & Y.F. Sun, ***sp. nov.*** MycoBank MB 839671. Figs 13, 14.

Diagnosis: Differs from other species in the genus by its perennial and sessile basidiomata, pale brown to greyish brown pileal surface with concentric furrows and radial wrinkles, cracked margin, homogeneous context and non-stratified tubes.

Etymology: *alpinum* (*Lat.*), refers to this species being collected from an alpine area.

Typus: **China**, Yunnan, Shangri-La, Daxueshan, on stump of *Populus*, 12 Aug. 2019, Cui 17467 (**holotype** BJFC034326).

Additional materials examined: **China**, Sichuan, Yajiang County, on stump of *Pinus*, 8 Aug. 2019, Cui 17325 (BJFC034183); Xizang, Chayu County, on stump of *Cupressus*, 10 Sep. 2020, Cui 18402 (BJFC035263).

Description: *Basidiomata* perennial, sessile, woody hard. *Pilei* flabelliform to shell-shaped, applanate, up to 15 cm diam and 4 cm thick. *Pileal surface* pale brown to greyish brown, dull, glabrous, with concentric furrows and radial wrinkles; margin subacute to obtuse, entire, slightly wavy, cracked when dry. *Pore surface* white to cream when fresh, turning darker when bruised, clay buff to dark brown when dry; pores circular, 5–7 per mm; dissepiments slightly thick, entire. *Context* cinnamon brown to dark brown, homogeneous, with black melanoid lines, hard corky and fibrous, up to 2 cm thick. *Tubes* yellowish brown to dark brown, non-stratified, up to 2 cm long. *Hyphal system* trimitic; generative hyphae with clamp connections; all hyphae IKI –, CB +; tissues darkening in KOH. Generative hyphae in context colourless, thin-walled, 3–4 µm diam; skeletal hyphae in context pale yellowish brown, thick-walled with a wide to narrow lumen or sub-solid, arboriform and flexuous, 3–6 µm diam; binding hyphae in context colourless, thick-walled, branched and flexuous, up to 2 µm diam. Generative hyphae in tubes colourless, thin-walled, 2–4 µm diam; skeletal hyphae in tubes pale brown, thick-walled with a wide to narrow lumen or sub-solid, arboriform and flexuous, 3–5 µm diam; binding hyphae in tubes colourless, thick-walled, branched and flexuous, up to 2 µm diam. *Pileipellis* composed of clamped generative hyphae, thick-walled, apical cells clavate, slightly inflated and flexuous, yellowish brown, about 20–30 × 5–8 µm, forming a regular palisade. *Cystidia* and *cystidioles* absent. *Basidia* barrel-shaped, colourless, thin-walled, 20–30 × 11–16 µm; *basidioles* clavate, colourless, thin-walled, 12–18 × 6–10 µm. *Basidiospores* broadly ellipsoid to ovoid, truncated, yellowish brown, IKI –, CB +, double-walled with distinctly thick walls, exospore wall smooth, endospore wall with dense spinules, (6.2–)6.3–7.6(–7.8) × (4–)4.1–5.4(–5.5) µm, L = 6.97 µm, W = 4.83 µm, Q = 1.43–1.45 (n = 60/2,

Fig. 13. Basidiomata of *Ganoderma alpinum*.

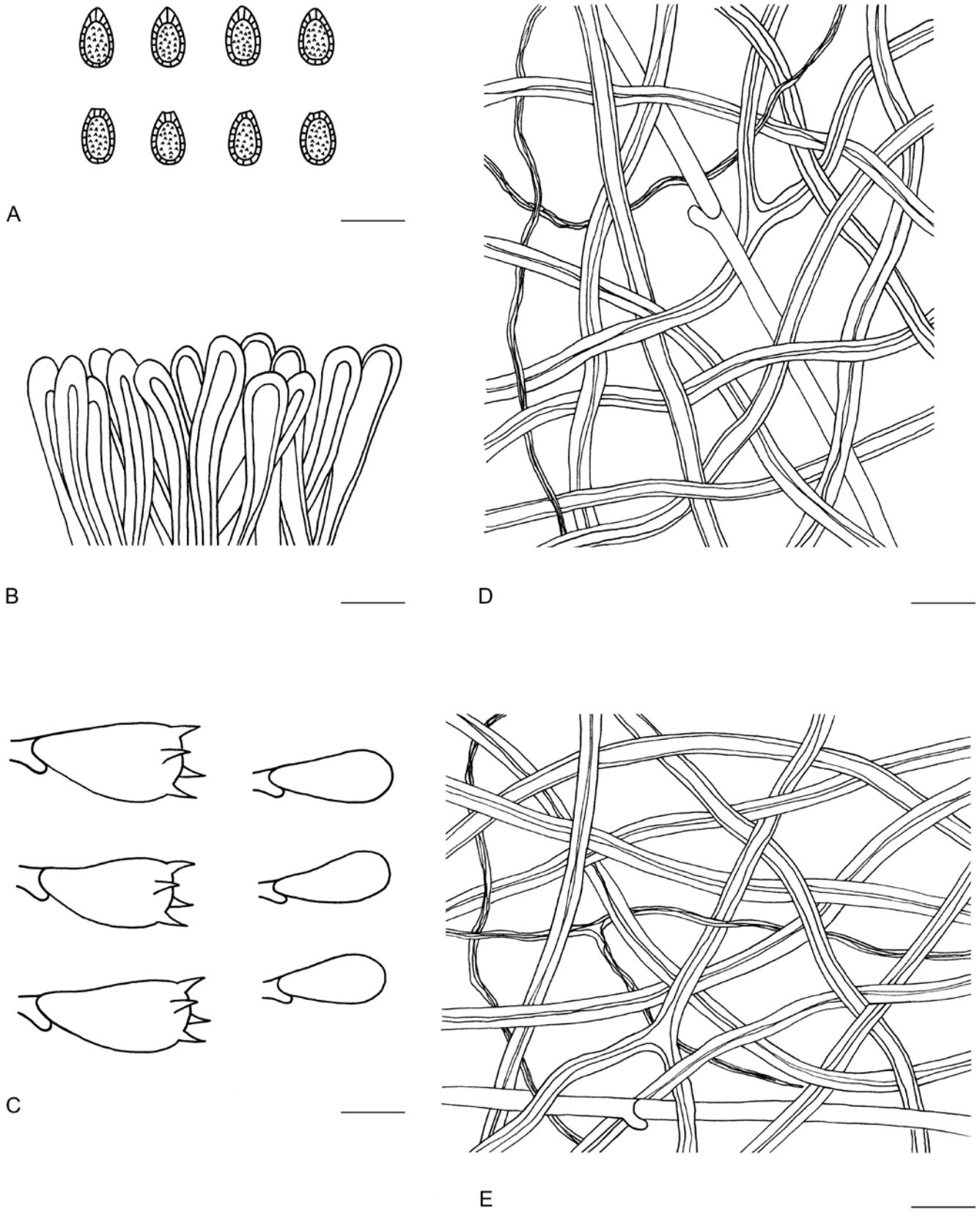

Fig. 14. Microscopic structures of *Ganoderma alpinum* (drawn from Cui 17467). **A.** Basidiospores. **B.** Apical cells from cuticle. **C.** Basidia and basidioles. **D.** Hyphae from trama. **E.** Hyphae from context. Scale bars = 10 µm.

with the turgid vesicular appendix excluded); (7.7–)7.8–9.2(–9.4) × (4–)4.1–5.4(–5.8) µm, L = 8.37 µm, W = 4.85 µm, Q = 1.71–1.74 (n = 60/2, with the turgid vesicular appendix included).

Notes: *Ganoderma alpinum* was collected from high altitude areas of southwestern China. It is hard to distinguish *G. alpinum* from *G. applanatum* on morphology, however, *G. alpinum* can be separated from *G. applanatum* by phylogenetic analyses and ecological distribution.

Ganoderma bubalinomarginatum B.K. Cui, J.H. Xing & Y.F. Sun, ***sp. nov.*** MycoBank MB 839672. Figs 15, 16.

Fig. 15. Basidiomata of *Ganoderma bubalinomarginatum*.

Diagnosis: Differs from other species in the genus by its pale-coloured basidiomata without stipe, laccate pileal surface with buff margin, homogeneous context and non-stratified tubes.

Etymology: *bubalinomarginatum* (*Lat.*), refers to the pilei with buff margin.

Typus: **China**, Guangxi, Nanning, Guangxi Academy of Forestry, on stump of *Castanopsis*, 4 Jul. 2019, Dai 20075 (**holotype** BJFC031749).

Additional material examined: **China**, Guangxi, Nanning, Guangxi Academy of Forestry, on living tree of *Phoebe*, 4 Jul. 2019, Dai 20074 (BJFC031748).

Description: *Basidiomata* annual, sessile and broadly attached, usually concrescent, hard corky. *Pilei* solitary, flabelliform to shell-shaped, up to 7.5 cm diam and 6 mm thick. *Pileal surface* reddish brown at the base, yellowish brown at the centre, buff at the margin, laccate, glabrous, with wide concentric furrows and slightly radial wrinkles; margin obtuse, entire, wavy when dry. *Pore surface* white to greyish white when fresh, turning darker when bruised, pale wood brown to greyish brown when dry; pores circular to angular, 5–6 per mm; dissepiments moderately thick, entire. *Context* straw yellow, homogeneous, without black melanoid lines, hard corky, up to 4 mm thick. *Tubes* pale brown, non-stratified, up to 3 mm long. *Hyphal system* trimitic; generative hyphae with clamp connections; all hyphae IKI –, CB +; tissues darkening in KOH. Generative hyphae in context colourless, thin-walled, 2–4 µm diam; skeletal hyphae in context pale yellow, thick-walled with a wide to narrow lumen or sub-solid, arboriform and flexuous, 2–5 µm diam; binding hyphae in context colourless, thick-walled, rarely branched and flexuous, up to 2 µm diam. Generative hyphae in tubes colourless, thin-walled, 2–3 µm diam; skeletal hyphae in tubes pale yellow, thick-walled with a wide to narrow lumen or sub-solid, arboriform and flexuous, 2–4 µm diam; binding hyphae in tubes colourless, thick-walled, rarely branched and flexuous, up to 1.5 µm diam. *Pileipellis* composed of clamped generative hyphae, thick-walled to sub-solid, apical cells clavate, inflated and flexuous, pale golden yellow, about 28–42 × 9–11 µm, forming a regular palisade. *Cystidia* and *cystidioles* absent. *Basidia* broadly clavate, colourless, thin-walled, 15–22 × 7–11 µm; *basidioles* in shape like the basidia, colourless, thin-walled, 12–20 × 5–9 µm. *Basidiospores* broadly ellipsoid to ovoid, truncated, pale yellowish brown, IKI –, CB +, with oily drop, double-walled with slightly thick walls, exospore wall smooth, endospore wall with dense spinules, (6.2–)6.5–7.4(–7.6) × (4.2–)4.5–5.3(–5.8) µm, L = 6.91 µm, W = 4.87 µm, Q = 1.41–1.43 (n = 60/2, with the turgid vesicular appendix excluded); (7–)7.2–8.3(–8.8) × (4.3–)4.5–5.6(–5.8) µm, L = 7.82 µm, W = 4.96 µm, Q = 1.57–1.59 (n = 60/2, with the turgid vesicular appendix included).

Notes: *Ganoderma bubalinomarginatum* has pale-coloured basidiomata without a stipe which differentiates it from the species described from Guangxi Autonomous Region: *G. daiqingshanense*, *G. guinanense* and *G. magniporum*. *Ganoderma*

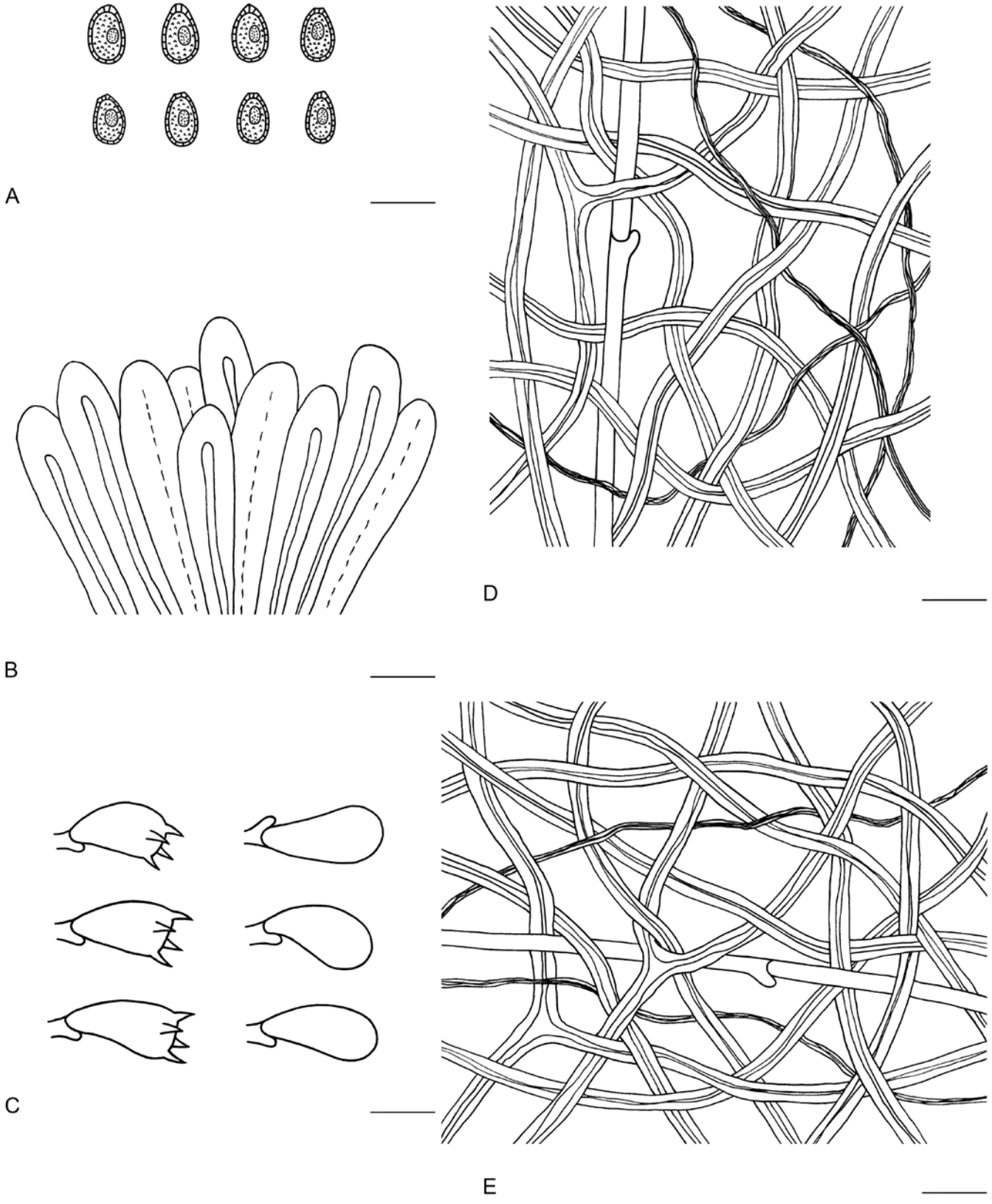

Fig. 16. Microscopic structures of *Ganoderma bubalinomarginatum* (drawn from Dai 20075). **A.** Basidiospores. **B.** Apical cells from cuticle. **C.** Basidia and basidioles. **D.** Hyphae from trama. **E.** Hyphae from context. Scale bars = 10 µm.

bubalinomarginatum is like *G. sessile*, described from America: it shares connate and sessile basidiomata, reddish brown to yellowish brown pileal surface, absence of black melanoid lines, white pore surface when fresh, homogeneous context and non-stratified tubes. However, *G. sessile* differs by the white, thin and acute pileal margin, larger pores (3–5 per mm), and larger basidiospores (9–11 × 6–8 µm, Murrill 1902).

Ganoderma castaneum B.K. Cui, J.H. Xing & Y.F. Sun, ***sp. nov.*** MycoBank MB 839673. Figs 17, 18.

Diagnosis: Differs from other species in the genus by its chestnut brown and laccate pileal surface with wide concentric ridges, heterogeneous context, and broadly ellipsoid basidiospores with smooth endospore wall.

Fig. 17. Basidiomata of *Ganoderma castaneum*.

Etymology: *castaneum* (*Lat.*), refers to the reddish brown pileal surface like a chestnut.

Typus: **China**, Hainan, Ledong County, Jianfengling Nature Reserve, on stump of angiosperm tree, 3 Jul. 2019, Cui 17283 (**holotype** BJFC034139).

Additional materials examined: **China**, Hainan, Ledong County, Jianfengling Nature Reserve, on stump of angiosperm tree, 17 Jun. 2014, Dai 13710 (BJFC017447); on fallen branch of angiosperm tree, 19 Jun. 2016, Cui 13893 (BJFC028759); Wuzhishan, Wuzhishan Forest Park, on stump of *Acacia*, 11 Jun. 2016, Dai 16500 (BJFC022616), Dai 16501 (BJFC022617).

Description: *Basidiomata* annual, sessile, broadly attached, hard corky to woody hard. *Pilei* solitary, flabelliform, applanate, up to 8.5 cm diam and 2 cm thick. *Pileal surface* reddish brown like chestnut, laccate, glabrous, with wide concentric ridges and slightly radial wrinkles; margin obtuse, entire, wavy. *Pore surface* white to cream when fresh, turning darker when bruised, buff to pale straw yellow when dry; pores circular, 4–6 per mm; dissepiments moderately thick, entire. *Context* heterogeneous, the upper layer pale straw yellow, the lower layer cinnamon brown to dark brown, with black melanoid lines, hard corky, up to 1.6 cm thick. *Tubes* pale greyish brown, non-stratified, up to 5 mm long. *Hyphal system* trimitic; generative hyphae with clamp connections; all hyphae IKI –, CB +; tissues darkening in KOH. Generative hyphae in context colourless, thin-walled, 2–4 µm diam; skeletal hyphae in context pale yellowish brown, thick-walled with a wide to narrow lumen or sub-solid, arboriform and flexuous, 3–6 µm diam; binding hyphae in context colourless, thick-walled, branched and flexuous, up to 2 µm diam. Generative hyphae in tubes colourless, thin-walled, 2–4 µm diam; skeletal hyphae in tubes pale yellowish brown, thick-walled with a wide to narrow lumen or sub-solid, arboriform and flexuous, 2–6 µm diam; binding hyphae in tubes colourless, thick-walled, branched and flexuous, up to 1 µm diam. *Pileipellis* composed of clamped generative hyphae, slightly thick-walled, apical cells clavate, flexuous, pale yellow, about 25–40 × 3–5 µm, forming a regular palisade. *Cystidia* and *cystidioles* absent. *Basidia* barrel-shaped, colourless, thin-walled, 14–21 × 7–12 µm; *basidioles* broadly clavate, colourless, thin-walled, 9–12 × 5–10 µm. *Basidiospores* broadly ellipsoid, not obviously truncated, golden yellow, IKI –, slightly CB +, double-walled with distinctly thick walls, exospore and endospore walls smooth, (6.2–)6.7–8.3(–8.5) × (4.2–)4.8–6(–6.3) µm, L = 7.42 µm, W = 5.43 µm, Q = 1.37 (n = 60/1, with the turgid vesicular appendix excluded).

Notes: *Ganoderma castaneum* was collected from a tropical rainforest of Hainan Province. When compared with the species in the checklist of *Ganoderma* reported from Hainan Island by Hapuarachchi *et al.* (2018b), *G. castaneum* has distinguished features such as chestnut-coloured and laccate pileal surface with wide concentric ridges, heterogeneous context, broadly ellipsoid and basidiospores not obviously truncated with smooth endospore walls.

Ganoderma chuxiongense B.K. Cui, J.H. Xing & Y.F. Sun, ***sp. nov.*** MycoBank MB 840397. Figs 19, 20.

Diagnosis: Differs from other species in the genus by its thin basidiomata, dimidiate and lobate pileus with reddish brown and laccate pileal surface, pale light-yellow pore surface.

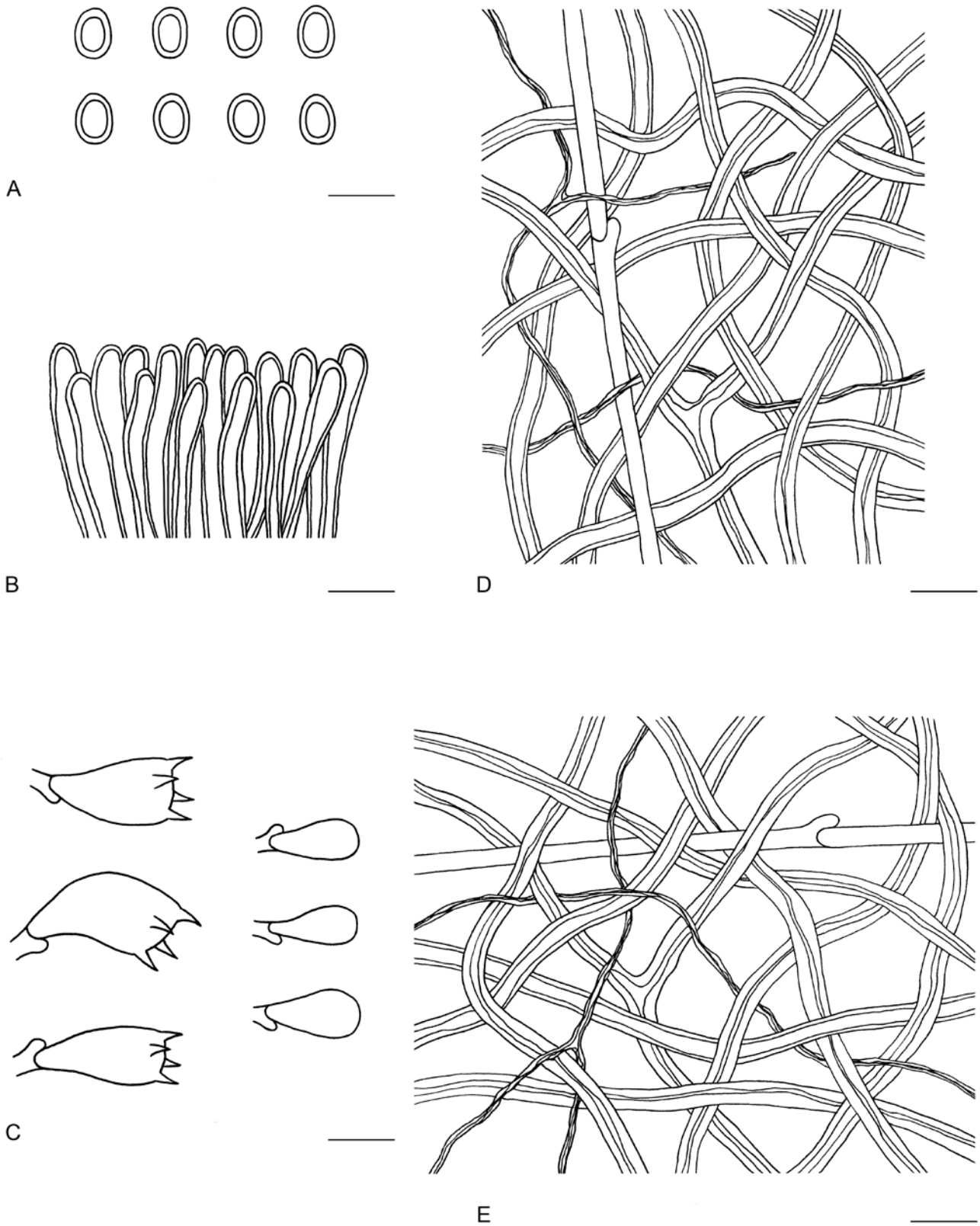

Fig. 18. Microscopic structures of *Ganoderma castaneum* (drawn from Cui 17283). **A.** Basidiospores. **B.** Apical cells from cuticle. **C.** Basidia and basidioles. **D.** Hyphae from trama. **E.** Hyphae from context. Scale bars = 10 µm.

Etymology: chuxiongense (*Lat.*), refers to the holotype of this species being found in Chuxiong City of Yunnan Province.

Typus: **China**, Yunnan, Chuxiong, Xishan Park, on stump of angiosperm tree, 25 Aug. 2018, Cui 17262 (**holotype** BJFC034120).

Description: *Basidiomata* annual, laterally stipitate, corky. *Pilei* solitary, flabelliform, dimidiate and lobate, up to 6 cm diam and 4 mm thick. *Pileal surface* reddish brown when fresh becoming dark-red when dry, laccate, glabrous, with concentric bands and slightly radial rugose; margin pale yellow, acute to obtuse, entire. *Pore surface* pale light-yellow when fresh, turning darker when bruised, buff to pale straw yellow when dry; pores circular, 4–6 per mm; dissepiments slightly thick, entire. *Context* dark wood brown, not obviously stratified, without black melanoid lines, soft corky, up to 2 mm thick. *Tubes* pale to dark wood brown, non-

Fig. 19. Basidiomata of *Ganoderma chuxiongense*.

stratified, up to 2 mm long. *Stipe* concolorous with pileal surface, cylindrical and solid, up to 7 cm long and 6 mm diam. *Hyphal system* trimitic; generative hyphae with clamp connections; all hyphae IKI –, CB +; tissues darkening in KOH. Generative hyphae in context colourless, thin-walled, 2–3 µm diam; skeletal hyphae in context pale yellow, thick-walled with a wide to narrow lumen or sub-solid, arboriform and flexuous, 2–4 µm diam; binding hyphae in context colourless, thick-walled, branched and flexuous, up to 2 µm diam. Generative hyphae in tubes colourless, thin-walled, 2–3 µm diam; skeletal hyphae in tubes pale yellow, thick-walled with a wide to narrow lumen or sub-solid, arboriform and flexuous, 2–4 µm diam; binding hyphae in tubes colourless, thick-walled, branched and flexuous, up to 1.5 µm diam. *Pileipellis* composed of clamped generative hyphae, slightly thick-walled, apical cells clavate, slightly inflated and flexuous, golden yellow, about 23–30 × 6–11 µm, forming a regular palisade. *Cystidia* and *cystidioles* absent. *Basidia* barrel-shaped, colourless, thin-walled, 15–20 × 10–12 µm; *basidioles* broadly clavate, colourless, thin-walled, 13–18 × 7–11 µm. *Basidiospores* broadly ellipsoid to ovoid, truncated, pale yellowish brown, IKI –, CB +, double-walled with distinctly thick walls, exospore wall smooth, endospore wall with dense spinules, (7.9–)8–9(–9.2) × (6–)6.2–7(–7.1) µm, L = 8.45 µm, W = 6.58 µm, Q = 1.28 (n = 60/1, with the turgid vesicular appendix excluded); (9.5–)10–11.3(–11.5) × (6.2–)6.5–7.3 µm, L = 10.35 µm, W = 6.88 µm, Q = 1.5 (n = 60/1, with the turgid vesicular appendix included).

Notes: *Ganoderma chuxiongense* is characterised by its stipitate basidiomata with lobate pilei, reddish brown pileal surface and pale-yellow pore surface when fresh. *Ganoderma kunmingense* described from Yunnan Province is like *G. chuxiongense* in the thin basidiomata with laccate and reddish brown pileal surface, margin entire or incised, but it has no concentric bands on the pileal surface, a cream pore surface, and broadly ellipsoid to subglobose basidiospores without obvious spinules on the endospore wall (Zhao 1989a).

Ganoderma cocoicola B.K. Cui, J.H. Xing & Y.F. Sun, ***sp. nov.*** MycoBank MB 839674. Figs 21, 22.

Diagnosis: Differs from other species in the genus by its small and hard basidiomata without stipe, dark and laccate pileal surface, homogeneous context, non-stratified tubes, oblong-ellipsoid and truncated basidiospores.

Etymology: *cocoicola* (*Lat.*), refers to this species growing on *Cocos*.

Typus: **Australia**, Queensland, Cairns, Cairns Botanical Garden, on stump of *Cocos*, 17 May 2018, Cui 16791 (**holotype** BJFC030090).

Additional material examined: **Australia**, Queensland, Cairns, Cairns Botanical Garden, on stump of *Cocos*, 17 May 2018, Cui 16792 (BJFC030091).

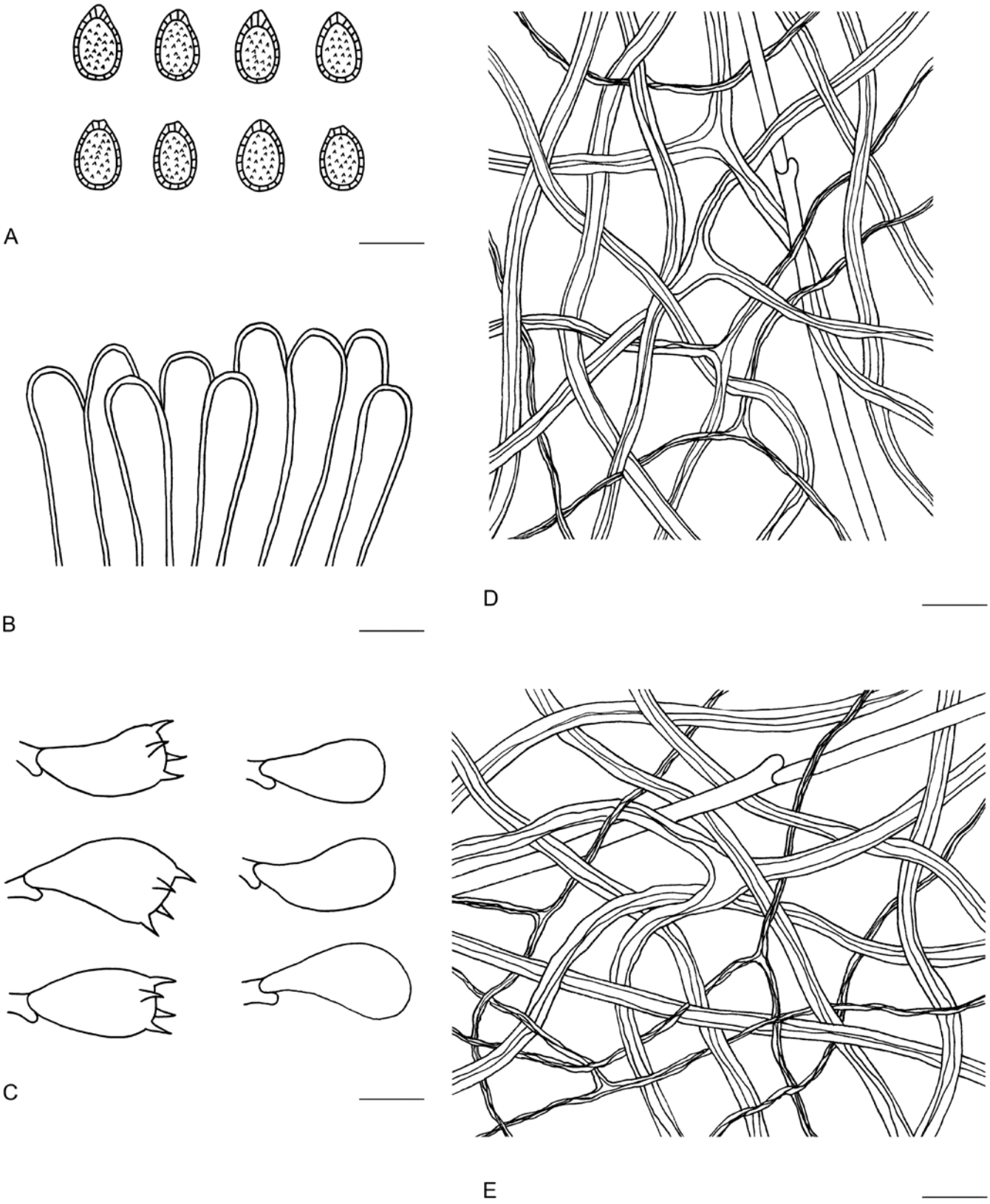

Fig. 20. Microscopic structures of *Ganoderma chuxiongense* (drawn from Cui 17262). **A.** Basidiospores. **B.** Apical cells from cuticle. **C.** Basidia and basidioles. **D.** Hyphae from trama. **E.** Hyphae from context. Scale bars = 10 µm.

Description: *Basidiomata* annual to perennial, sessile or sometimes sub-stipitate, hard corky to woody hard. *Pilei* solitary, flabelliform to ungulate, up to 3.5 cm diam and 1.5 cm thick. *Pileal surface* dark-red to near black, laccate, glabrous, with concentric furrows and slightly radial wrinkles; margin obtuse, entire. *Pore surface* white when fresh, turning darker when bruised, straw yellow to pale brown when dry; pores circular to angular, 4–6 per mm; dissepiments distinctly thick, entire. *Context* dark brown to cinnamon brown, homogeneous, without black melanoid lines, hard corky, up to 3 mm thick. *Tubes* dark grey to greyish brown, non-stratified, up to 1.2 cm long. *Hyphal system* trimitic; generative hyphae with clamp connections; all hyphae IKI –, CB +; tissues darkening in KOH. Generative hyphae in context colourless, thin-walled, 2–3 µm diam; skeletal hyphae in context pale yellowish brown, thick-walled

Fig. 21. Basidiomata of *Ganoderma cocoicola*.

with a wide to narrow lumen or sub-solid, frequently arboriform and flexuous, 2.5–5 µm diam; binding hyphae in context colourless, thick-walled, branched and flexuous, up to 2 µm diam. Generative hyphae in tubes colourless, thin-walled, 2–3 µm diam; skeletal hyphae in tubes pale yellowish brown, thick-walled with a wide to narrow lumen or sub-solid, frequently arboriform and flexuous, 3–5 µm diam; binding hyphae in tubes colourless, thick-walled, branched and flexuous, up to 1.5 µm diam. *Pileipellis* composed of clamped generative hyphae, thick-walled to sub-solid, apical cells clavate, flexuous, yellowish brown, about 27–35 × 5–7 µm, forming a regular palisade. *Cystidia* and *cystidioles* absent. *Basidia* broadly clavate, colourless, thin-walled, 16–22 × 7–10 µm; *basidioles* in shape like the basidia, colourless, thin-walled, 13–20 × 7–10 µm. *Basidiospores* oblong-ellipsoid, truncated, pale yellowish brown, IKI –, CB +, double-walled with moderately thick walls, exospore wall smooth, endospore wall with dense spinules, 9–9.8(–10) × 4.2–5.4(–5.6) µm, L = 9.42 µm, W = 4.77 µm, Q = 1.91–2.04 (n = 60/2, with the turgid vesicular appendix excluded); (9.6–)9.7–10.7(–10.8) × (4.2–)4.4–5.4(–5.5) µm, L = 10.15 µm, W = 4.83 µm, Q = 2.08–2.12 (n = 60/2, with the turgid vesicular appendix included).

Notes: *Ganoderma cocoicola* was collected from Australia on *Cocos*. It is characterised by small and hard basidiomata without a stipe, blackish brown and laccate pileal surface, homogeneous context, non-stratified tubes, oblong-ellipsoid and truncated basidiospores. In the phylogenetic analyses, *G. cocoicola* clustered with *G. zonatum*, *G. ryvardenii*, *G. boninense*, and *G. hochiminhense* with high support (Fig. 1); all these species grow on palm trees (Patouillard 1889, Murrill 1902, Kinge & Mih 2011, Zhou *et al.* 2015), except *G. hochiminhense* which grows on *Areca* (Luangharn *et al*. 2021).

Ganoderma fallax B.K. Cui, J.H. Xing & Vlasák, ***sp. nov.*** MycoBank MB 839677. Figs 23, 24.

Diagnosis: Differs from other species in the genus by its non-laccate pileal surface with faintly concentric furrows, stratified tubes, and basidiospores not obviously truncated with dense spinules on the endospore wall.

Etymology: *fallax* (*Lat.*), refers to this species being easily confused morphologically with other non-laccate species.

Typus: **USA**, Pennsylvania (**holotype** JV 1009/27).

Materials examined: **USA**, Arizona, JV 1209/60J (JV); New Jersey, JV 0109/B1-J (JV); Pennsylvania, JV 0709/39 (JV); Tennessee, JV 0509/93K, JV 1410/14J (JV).

Description: *Basidiomata* perennial, sessile, hard corky to woody hard. *Pilei* solitary, flabelliform to ungulate or shell-shaped, up to 11 cm diam and 3 cm thick. *Pileal surface* yellowish brown to dark brown, dull, glabrous, with faint concentric furrows; margin acute, entire, slightly wavy. *Pore surface* white to pale brown when fresh,

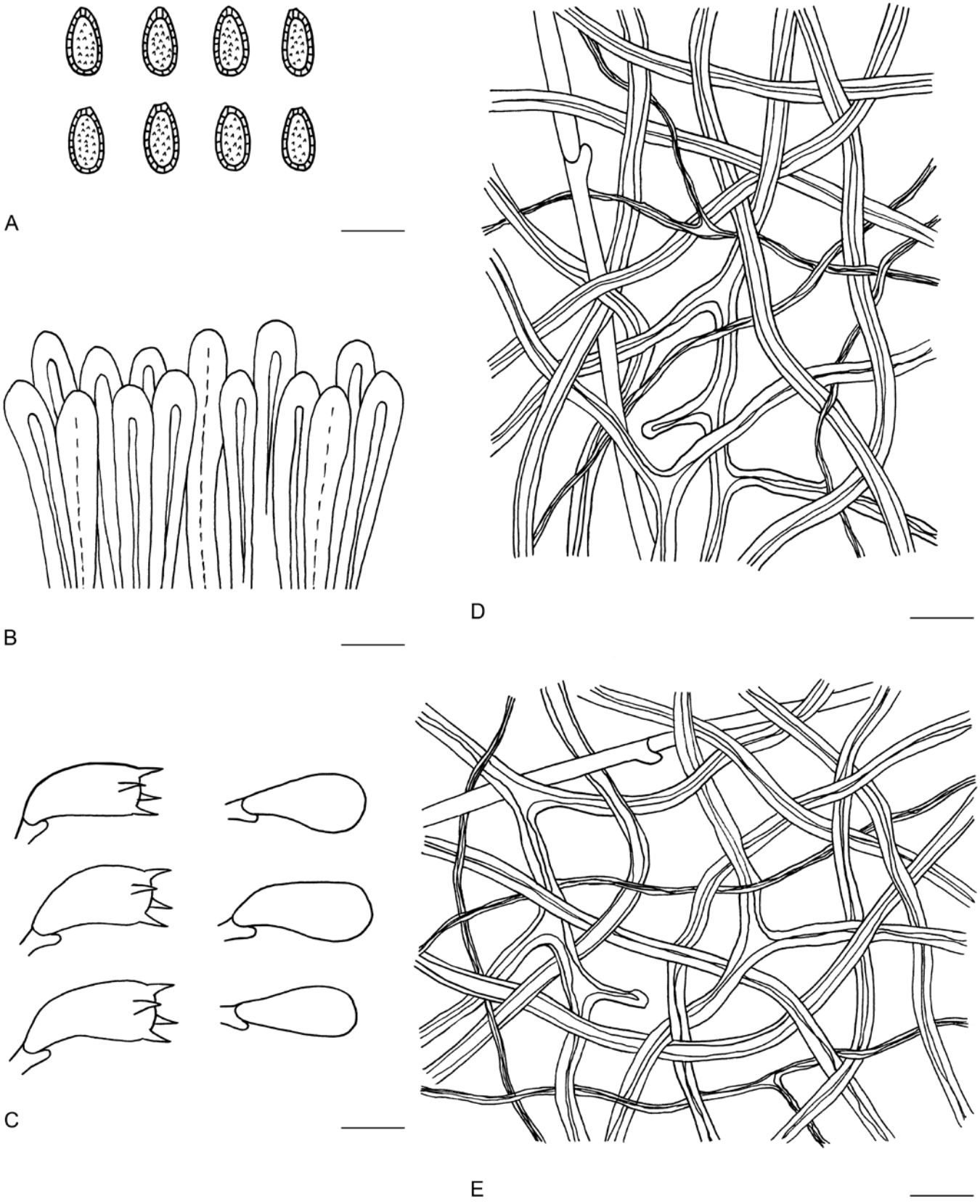

Fig. 22. Microscopic structures of *Ganoderma cocoicola* (drawn from Cui 16791). **A.** Basidiospores. **B.** Apical cells from cuticle. **C.** Basidia and basidioles. **D.** Hyphae from trama. **E.** Hyphae from context. Scale bars = 10 µm.

turning darker when bruised, straw yellow when dry; pores circular, 4–6 per mm; dissepiments slightly thick, entire. *Context* yellowish brown to dark brown, homogeneous, with black melanoid lines, corky, up to 7 mm thick. *Tubes* concolorous with context, stratified, up to 1.2 cm long. *Hyphal system* trimitic; generative hyphae with clamp connections; all hyphae IKI –, CB +; tissues darkening in KOH. Generative hyphae in context colourless, thin-walled, 2.5–5.5 µm diam; skeletal hyphae in context pale yellowish brown, thick-walled with narrow lumen or sub-solid, arboriform and flexuous, 3–6 µm diam; binding hyphae in context colourless, thick-walled, branched and flexuous, 2–3 µm diam. Generative hyphae in tubes colourless, thin-walled, 2–3.5 µm diam; skeletal hyphae in tubes

Fig. 23. Basidiomata of *Ganoderma fallax*.

pale brown, thick-walled with narrow lumen or sub-solid, arboriform and flexuous, 2–5 µm diam; binding hyphae in tubes colourless, thick-walled, branched and flexuous, 2–2.5 µm diam. *Cystidia* and *cystidioles* absent. *Basidia* barrel-shaped to clavate, colourless, thin-walled, 25–30 × 14–21 µm; *basidioles* in shape like the basidia, colourless, thin-walled, 16–17 × 9–18 µm. *Basidiospores* ovoid, not obviously truncated, pale yellowish brown, IKI –, CB +, double-walled with distinctly thick walls, exospore wall smooth, endospore wall with dense spinules, (8.5–)9–10(–10.5) × 6–7.5 µm, L = 9.25 µm, W = 6.56 µm, Q = 1.37 (n = 30/1, with the turgid vesicular appendix included).

Notes: *Ganoderma fallax* may be confused with the non-laccate species *G. adspersum*, which has large basidiomata with a yellowish brown pileal surface, homogeneous context and stratified tubes, but *G. adspersum* has larger and more obviously truncated basidiospores, and lacks concentric ornamentation on the pileal surface. In the phylogenetic analyses, *G. fallax* formed an independent lineage then clustered with *G. adspersum* (Fig. 1).

Ganoderma guangxiense B.K. Cui, J.H. Xing & Y.F. Sun, ***sp. nov.*** MycoBank MB 839678. Figs 25, 26.

Diagnosis: Differs from other species in the genus by its sessile basidiomata, greyish brown to near black pileal surface with obvious concentric furrows, cracked when dry, homogeneous context, non-stratified tubes, ellipsoid to ovoid and truncated basidiospores.

Etymology: *guangxiense* (*Lat.*), refers to the holotype of this species located at Guangxi.

Typus: **China**, Guangxi, Tianlin County, Cenwanglaoshan Nature Reserve, on stump of angiosperm tree, 8 Jul. 2017, Cui 14453 (**holotype** BJFC029321).

Additional materials examined: **China**, Guangxi, Tianlin County, Cenwanglaoshan Nature Reserve, on stump of angiosperm tree, 8 Jul. 2017, Cui 14454 (BJFC029322), Cui 14455 (BJFC029323); Jinxiu County, Dayaoshan Nature Reserve, on fallen trunk of angiosperm tree, 15 Jul. 2017, Cui 14500 (BJFC029369), Cui 14508 (BJFC029377).

Description: *Basidiomata* annual, sessile and broadly attached, hard corky to woody hard. *Pilei* solitary, flabelliform to shell-shaped, up to 11 cm diam and 4.3 cm thick. *Pileal surface* greyish brown to near black when fresh, dull, glabrous, with obvious concentric furrows, cracked when dry; margin obtuse, entire. *Pore surface* cream when

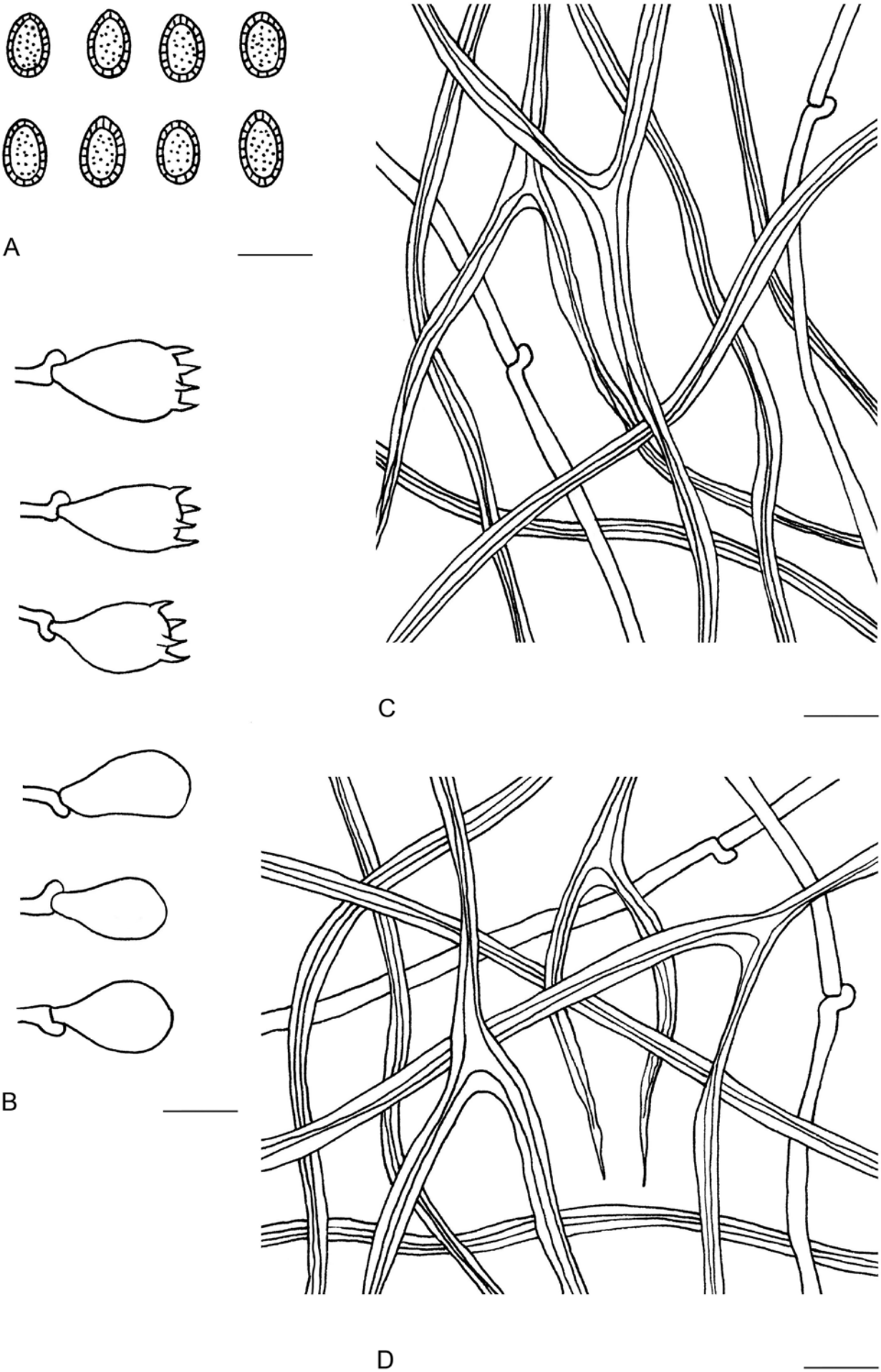

Fig. 24. Microscopic structures of *Ganoderma fallax* (drawn from JV 1009/27). **A.** Basidiospores. **B.** Basidia and basidioles. **C.** Hyphae from trama. **D.** Hyphae from context. Scale bars = 10 µm.

Fig. 25. Basidiomata of *Ganoderma guangxiense*.

fresh, turning darker when bruised, dark straw yellow to pale brown when dry; pores circular, 5–7 per mm; dissepiments moderately thick, entire. *Context* dark brown to cinnamon brown, homogeneous, with black melanoid lines, hard corky, up to 3 cm thick. *Tubes* slightly paler than context, non-stratified, up to 2 cm long. *Hyphal system* trimitic; generative hyphae with clamp connections; all hyphae IKI –, CB +; tissues darkening in KOH. Generative hyphae in context colourless, thin-walled, 2–3 µm diam; skeletal hyphae in context reddish brown, thick-walled with a wide to narrow lumen or sub-solid, arboriform and flexuous, 2–6 µm diam; binding hyphae in context colourless, thick-walled, branched and flexuous, up to 2 µm diam. Generative hyphae in tubes colourless, thin-walled, 2–3 µm diam; skeletal hyphae in tubes reddish brown, thick-walled with a wide to narrow lumen or sub-solid, arboriform and flexuous, 2–4 µm diam; binding hyphae in tubes colourless, thick-walled, branched and flexuous, up to 2 µm diam. *Pileipellis* composed of clamped generative hyphae, thick-walled to sub-solid, apical cells clavate, inflated and flexuous, golden yellow, about 28–37 × 5–8 µm, forming a regular palisade. *Cystidia* and *cystidioles* absent. *Basidia* barrel-shaped, colourless, thin-walled, 15–20 × 7–11 µm; *basidioles* broadly clavate, colourless, thin-walled, 12–15 × 7–9 µm. *Basidiospores* ellipsoid to ovoid, truncated, yellowish brown, IKI –, CB +, double-walled with moderately thick walls, exospore wall smooth, endospore wall with dense spinules, (7.5–)7.8–8.8(–8.9) × (4.9–)5–6(–6.5) µm, L = 8.23 µm, W = 5.49 µm, Q = 1.47–1.53 (n = 60/2, with the turgid vesicular appendix excluded); 8.7–9.8(–10) × (4.9–)5–6(–6.1) µm, L = 9.23 µm, W = 5.52 µm, Q = 1.67–1.68 (n = 60/2, with the turgid vesicular appendix included).

Notes: Morphologically, *Ganoderma guangxiense* is very similar to *G. australe* and they are not easy to separate. However, phylogenetically, *G. guangxiense* and *G. australe* are divided into two independent lineages with good support (Fig. 1). *Ganoderma daiqingshanense* also has sessile and hard basidiomata with blackish pilei, but it differs from *G. guangxiense* by having a heterogeneous context, larger pores (4–5 per mm) and irregular palisade of pileipellis structure (Zhao 1989a).

Ganoderma puerense B.K. Cui, J.H. Xing & Y.F. Sun, ***sp. nov.*** MycoBank MB 839679. Figs 27, 28.

Diagnosis: Differs from other species in the genus by its woody hard and thin basidiomata, yellowish brown pileal surface with dense concentric black bands or furrows, and a margin lacerated like petals.

Etymology: *puerense* (*Lat.*), refers to this species being collected from Puer City of Yunnan Province.

Typus: **China**, Yunnan, Puer, Puer Forest Park, on living tree of *Cinnamomum*, 17 Aug. 2019, Dai 20427 (**holotype** BJFC032095).

Description: *Basidiomata* annual, sessile or with short stipe, usually growing together, imbricate, woody hard. *Pilei* solitary, sub-orbicular to flabelliform, applanate, up to 7.5 cm diam and 8 mm thick. *Pileal surface* yellowish brown to dark brown, dull,

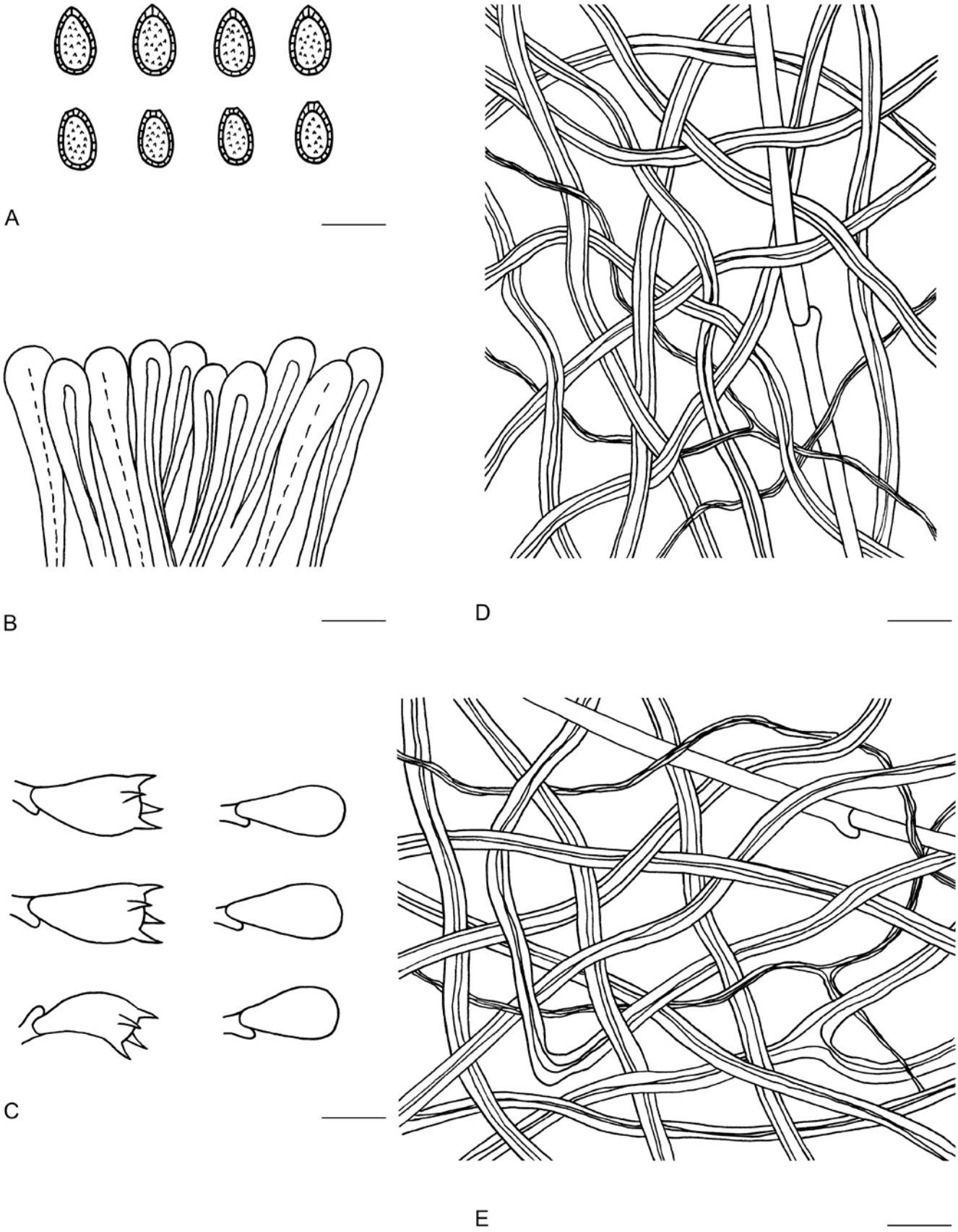

Fig. 26. Microscopic structures of *Ganoderma guangxiense* (drawn from Cui 14453). **A.** Basidiospores. **B.** Apical cells from cuticle. **C.** Basidia and basidioles. **D.** Hyphae from trama. **E.** Hyphae from context. Scale bars = 10 µm.

glabrous, with dense concentric black bands or furrows and slightly radial wrinkles; margin acute to obtuse, lacerated like petals. *Pore surface* white when fresh, turning darker when bruised, buff to pale brown when dry; pores circular to angular, 5–7 per mm; dissepiments moderately thick, entire. *Context* straw yellow to dark brown, homogeneous, with black melanoid lines, hard corky, up to 3 mm thick. *Tubes* dark brown, non-stratified, up to 5 mm long. *Stipe* concolorous with pileal surface, cylindrical

Fig. 27. Basidiomata of *Ganoderma puerense*.

and solid, up to 1.5 cm long and 3 mm diam. *Hyphal system* trimitic; generative hyphae with clamp connections; all hyphae IKI –, CB +; tissues darkening in KOH. Generative hyphae in context colourless, thin-walled, 2–3 µm diam; skeletal hyphae in context pale yellowish brown, thick-walled with a wide to narrow lumen or sub-solid, frequently arboriform and flexuous, 2–5 µm diam; binding hyphae in context colourless, thick-walled, rarely branched and flexuous, 1–2 µm diam. Generative hyphae in tubes colourless, thin-walled, 2–3 µm diam; skeletal hyphae in tubes pale yellowish brown, thick-walled with a wide to narrow lumen or sub-solid, arboriform and flexuous, 2–4 µm diam; binding hyphae in tubes colourless, thick-walled, rarely branched and flexuous, 1–2 µm diam. *Pileipellis* composed of clamped generative hyphae, thick-walled to sub-solid, apical cells clavate, faintly inflated and flexuous, yellowish brown, about 25–40 × 5–7 µm, forming a regular palisade. *Cystidia* and *cystidioles* absent. *Basidia* barrel-shaped, colourless, thin-walled, 12–20 × 7–10 µm; *basidioles* clavate to fusiform, colourless, thin-walled, 11–18 × 7–10 µm. *Basidiospores* ellipsoid to ovoid, truncated, yellowish brown, IKI –, CB +, double-walled with slightly thick walls, exospore wall smooth, endospore wall with dense spinules, (7–)7.2–8.5(–8.8) × (4.8–)5–6(–6.4) µm, L = 7.83 µm, W = 5.31 µm, Q = 1.47 (n = 60/1, with the turgid vesicular appendix excluded); (8.5–)8.8–9.5(–9.8) × (4.8–)5–6.2(–6.8) µm, L = 9.1 µm, W = 5.52 µm, Q = 1.65 (n = 60/1, with the turgid vesicular appendix included).

Notes: *Ganoderma bicharacteristicum* also has a dull pileal surface, homogeneous context and was described from Yunnan Province, but *G. bicharacteristicum* can be distinguished from *G. puerense* by its stipitate basidiomata with black pileal surface, wood brown pore surface and subglobose basidiospores (6.3–9 × 5.6–8.7 µm, Zhang 1994).

Ganoderma subangustisporum B.K. Cui, J.H. Xing & Y.F. Sun, ***sp. nov.*** MycoBank MB 839680. Figs 29, 30.

Diagnosis: Differs from other species in the genus by its dark-red to near black pileal surface with concentric bands and radial rugosities made by dark and continuous spots, margin acute and thin, and ellipsoid basidiospores with truncated apex.

Etymology: *subangustisporum* (*Lat.*), refers to this species being closely related to *Ganoderma angustisporum*.

Typus: **China**, Yunnan, Pingbian County, Daweishan National Nature Reserve, on stump of angiosperm tree, 3 Aug. 2019, Cui 18592 (**holotype** BJFC035453).

Materials examined: **China**, Yunnan, Pingbian County, Daweishan National Nature Reserve, on stump of angiosperm tree, 3 Aug. 2019, Cui 18593 (BJFC035454), Cui 18594 (BJFC035455), Cui 18595 (BJFC035456), Cui 18596 (BJFC035457), Cui 18597 (BJFC035458).

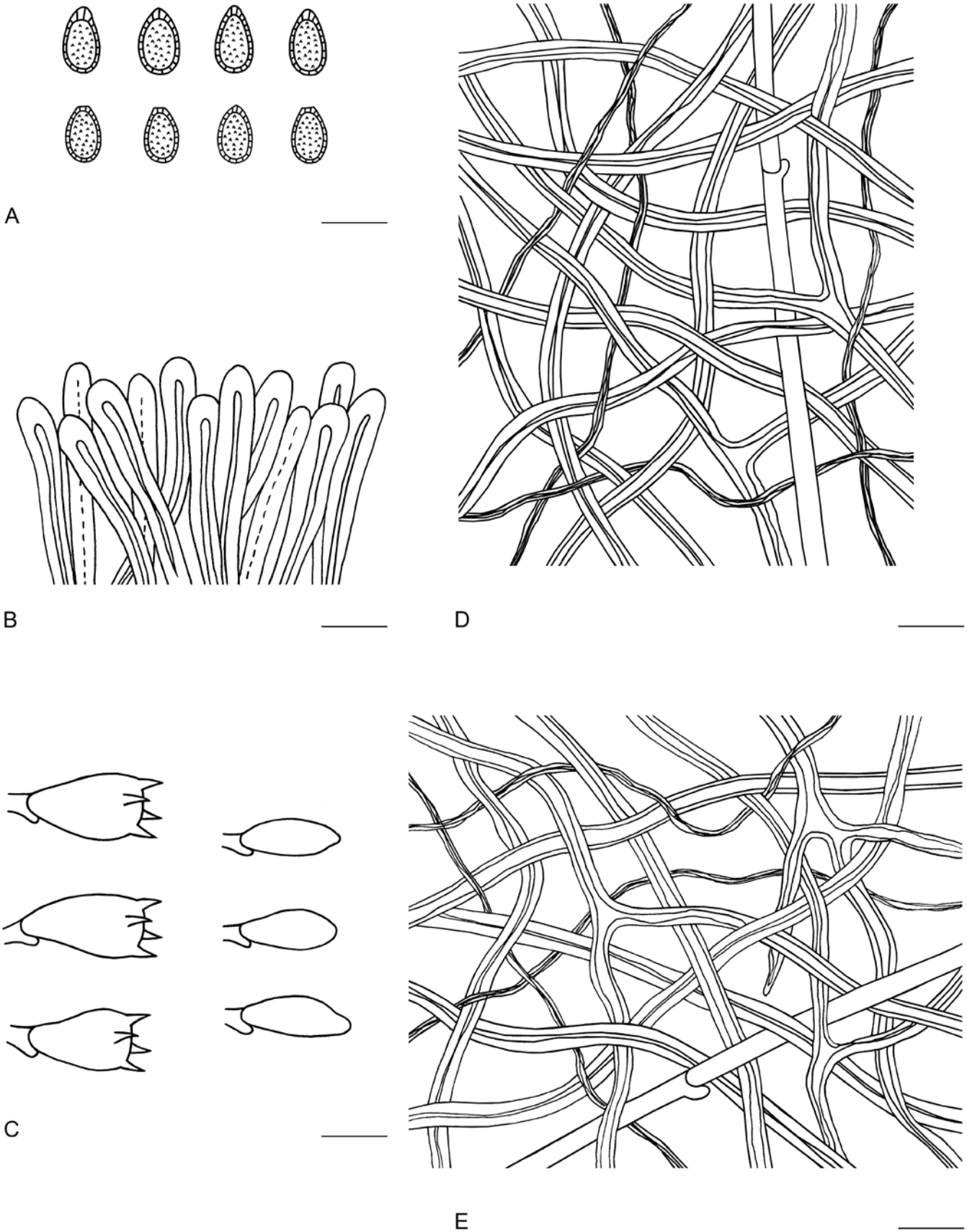

Fig. 28. Microscopic structures of *Ganoderma puerense* (drawn from Dai 20427). **A.** Basidiospores. **B.** Apical cells from cuticle. **C.** Basidia and basidioles. **D.** Hyphae from trama. **E.** Hyphae from context. Scale bars = 10 µm.

Description: *Basidiomata* annual, sessile or with short and lateral stipe, hard corky. *Pilei* solitary, sub-circular to flabelliform, up to 8 cm diam and 1.6 cm thick. *Pileal surface* dark reddish brown, laccate, glabrous, with concentric bands and radial rugose made by dark and continuous spots; margin acute, thin, entire. *Pore surface* white when fresh, turning darker when bruised, buff to pale straw yellow when dry; pores circular to angular, 4–6 per mm; dissepiments slightly thick, entire. *Context* cinnamon brown, homogeneous, with pale melanoid lines, hard corky, up to 9 mm thick. *Tubes* pale brown, non-stratified, up to 9 mm long. *Stipe*

Fig. 29. Basidiomata of *Ganoderma subangustisporum*.

concolourous with pileal surface, cylindrical and solid, up to 1 cm long and 1.5 cm diam. *Hyphal system* trimitic; generative hyphae with clamp connections; all hyphae IKI –, CB +; tissues darkening in KOH. Generative hyphae in context colourless, thin-walled, 3–4 µm diam; skeletal hyphae in context yellowish brown, thick-walled with a wide to narrow lumen or sub-solid, arboriform and flexuous, 3–5 µm diam; binding hyphae in context colourless, thick-walled, branched and flexuous, up to 2 µm diam. Generative hyphae in tubes colourless, thin-walled, 3–4 µm diam; skeletal hyphae in tubes yellowish brown, thick-walled with a wide to narrow lumen or sub-solid, arboriform and flexuous, 2–5 µm diam; binding hyphae in tubes colourless, thick-walled, branched and flexuous, up to 2 µm diam. *Pileipellis* composed of clamped generative hyphae, thick-walled to sub-solid, apical cells clavate, inflated and flexuous, dark yellowish brown to reddish brown, about 32–50 × 7–12 µm, forming a regular palisade. *Cystidia* and *cystidioles* absent. *Basidia* barrel-shaped, colourless, thin-walled, 13–19 × 10–13 µm; *basidioles* broadly clavate, colourless, thin-walled, 13–18 × 6–12 µm. *Basidiospores* broadly ellipsoid to ellipsoid, truncated, yellowish brown, IKI –, CB +, double-walled with distinctly thick walls, exospore wall smooth, endospore wall with dense spinules, 10–11.8(–12.1) × (5–)5.1–7(–7.3) µm, L = 10.88 µm, W = 6.13 µm, Q = 1.72–1.84 (n = 60/2, with the turgid vesicular appendix excluded); (10.3–)10.7–12.8(–13.1) × (5–)5.2–7(–7.3) µm, L = 11.72 µm, W = 6.02 µm, Q = 1.93–1.97 (n = 60/2, with the turgid vesicular appendix included).

Notes: *Ganoderma subangustisporum* clusters with *G. angustisporum* with high support in the phylogenetic analyses (Fig. 1). Morphologically, *G. angustisporum* differs from *G. subangustisporum* by having large basidiomata with lacerated margin, darker pileal surface with concentric furrows, and narrower basidiospores (9–11.3 × 4–5.2 µm, Xing *et al.* 2018).

Ganoderma subellipsoideum B.K. Cui, J.H. Xing & Y.F. Sun, ***sp. nov.*** MycoBank MB 839681. Figs 31, 32.

Diagnosis: Differs from other species in the genus by its subsessile and hard basidiomata, dark yellowish brown to blackish pileal surface with dense concentric furrows, small pores and stratified tubes, and ellipsoid basidiospores with truncated apex.

Etymology: *subellipsoideum* (*Lat.*), refers to this species being closely related to *Ganoderma ellipsoideum*.

Typus: **Malaysia**, Kuala Lumpur, Ecological Forest Park, on fallen trunk of angiosperm tree, 8 Dec. 2019, Cui 18325 (**holotype** BJFC035184).

Additional materials examined: **Malaysia**, Selangor, Kota Damansara, National Forest Reserve, on fallen trunk of angiosperm tree, 6 Dec. 2019, Cui 18241 (BJFC035100); Kuala Lumpur, Ecological Forest Park, on fallen trunk of angiosperm tree, 8 Dec. 2019, Cui 18327(BJFC035186).

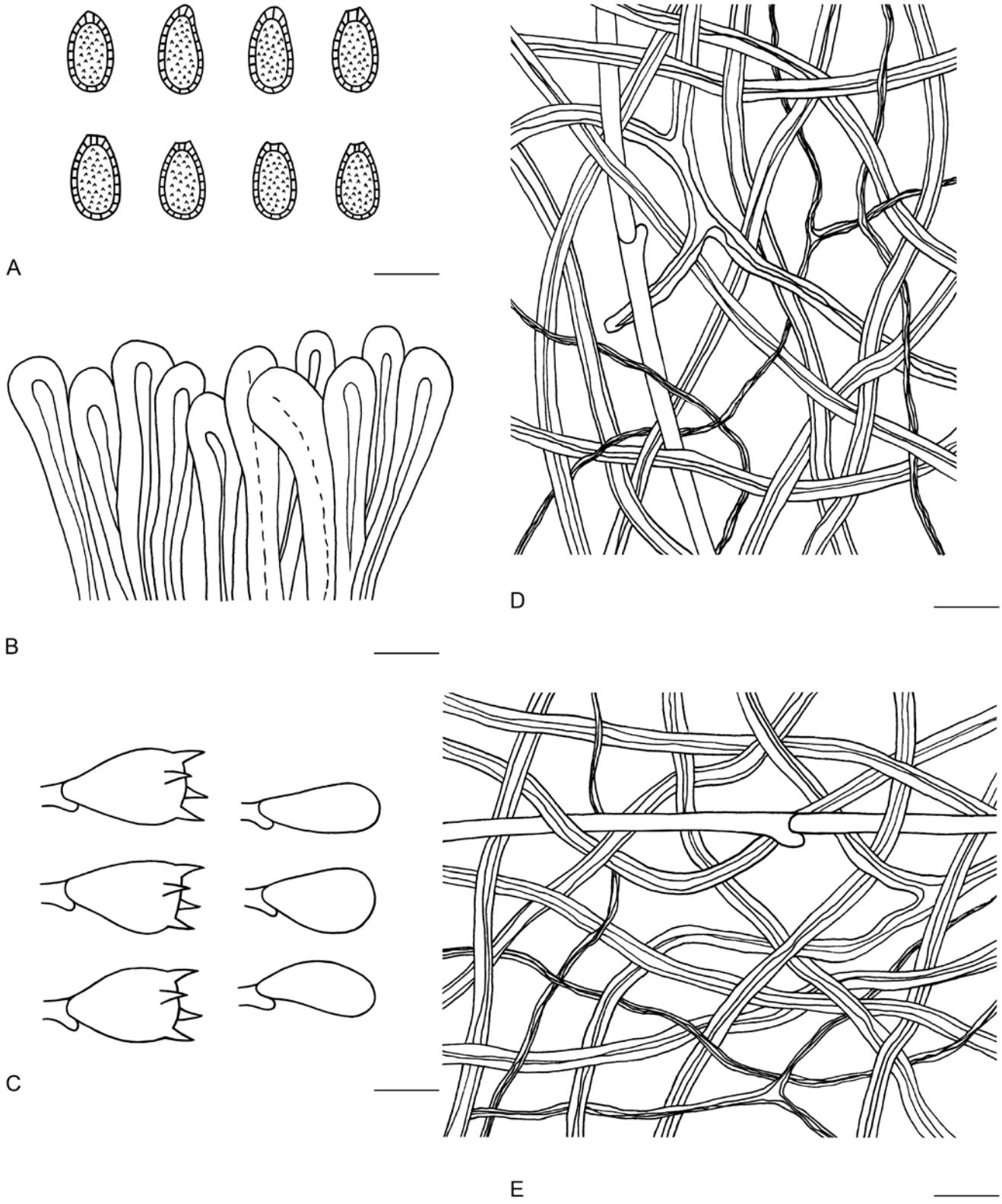

Fig. 30. Microscopic structures of *Ganoderma subangustisporum* (drawn from Cui 18592). **A.** Basidiospores. **B.** Apical cells from cuticle. **C.** Basidia and basidioles. **D.** Hyphae from trama. **E.** Hyphae from context. Scale bars = 10 µm.

Description: *Basidiomata* annual, sessile or with short and lateral stipe, woody hard. *Pilei* solitary, sub-circular to flabelliform, applanate, up to 9.5 cm diam and 2 cm thick. *Pileal surface* dark yellowish brown to near black when fresh becoming yellowish brown or greyish brown when dry, slightly laccate when fresh becoming dull when dry, glabrous, with dense concentric furrows; margin obtuse, entire. *Pore surface* white when fresh, turning darker when bruised, cream to buff when dry; pores circular, 6–8 per mm; dissepiments moderately thick, entire. *Context* cinnamon brown, homogeneous, with black melanoid lines, hard corky, up to 1 cm thick. *Tubes* dark brown, stratified by a layer of context, up to 9 mm long. *Stipe* concolourous with pileal surface, cylindrical and solid, up to 1.2 cm long and 1.3 cm diam. *Hyphal system* trimitic; generative hyphae with clamp connections; all hyphae IKI –, CB +; tissues darkening in KOH. Generative hyphae in context colourless, thin-walled, 2–4 µm diam; skeletal hyphae in context

Fig. 31. Basidiomata of *Ganoderma subellipsoideum*.

pale brown, thick-walled with a wide to narrow lumen or sub-solid, arboriform and flexuous, 2–5 µm diam; binding hyphae in context colourless, thick-walled, branched and flexuous, up to 1.5 µm diam. Generative hyphae in tubes colourless, thin-walled, 2–3 µm diam; skeletal hyphae in tubes yellowish brown, thick-walled with a wide to narrow lumen or sub-solid, arboriform and flexuous, 2–4 µm diam; binding hyphae in tubes colourless, thick-walled, branched and flexuous, up to 1 µm diam. *Pileipellis* composed of clamped generative hyphae, thick-walled, apical cells clavate, flexuous, pale yellowish brown, about 30–40 × 3–5 µm, forming a regular palisade. *Cystidia* and *cystidioles* absent. *Basidia* barrel-shaped, colourless, thin-walled, 12–17 × 9–11 µm; *basidioles* broadly clavate, colourless, thin-walled, 11–15 × 6–10 µm. *Basidiospores* ellipsoid, truncated, yellowish brown, IKI –, CB +, double-walled with moderately thick walls, exospore wall smooth, endospore wall with dense spinules, 6–6.9(–7) × 4–5.3(–5.5) µm, L = 6.46 µm, W = 4.62 µm, Q = 1.36–1.44 (n = 60/2, with the turgid vesicular appendix excluded); (8–)8.2–9.6(–10) × (4–)4.2–5.2(–6) µm, L = 8.89 µm, W = 4.69 µm, Q = 1.89–1.9 (n = 60/2, with the turgid vesicular appendix included).

Notes: In the phylogenetic analyses, *G. subellipsoideum* is closely related to *G. ellipsoideum*. *Ganoderma ellipsoideum* was described from Hainan Province and it has a yellowish brown pileal surface with alternating brownish orange to yellowish brown zones, heterogeneous context and non-stratified tubes, and ellipsoid basidiospores of smaller size (6.1–7.3 × 3.7–4.6 µm, Hapuarachchi *et al.* 2018b) which make it different from *G. subellipsoideum*.

Ganoderma subflexipes B.K. Cui, J.H. Xing & Y.F. Sun, ***sp. nov.*** MycoBank MB 839675. Figs 33, 34.

Diagnosis: Differs from other species in the genus by its small and dorso-laterally stipitate basidiomata, dark yellow to orange-brown and laccate pileal surface, wavy margin, and obviously truncated basidiospores.

Etymology: *subflexipes* (*Lat.*), refers to this species being closely related to *Ganoderma flexipes*.

Typus: **China**, Guangdong, Renhua County, Danxiashan Nature Reserve, on stump of angiosperm tree, 4 Jun. 2019, Cui 17257 (**holotype** BJFC034115).

Additional materials examined: **China**, Guangdong, Renhua County, Danxiashan Nature Reserve, on root of angiosperm tree, 4 Jun. 2019, Cui 17247 (BJFC034105); on stump of angiosperm tree, 4 Jun. 2019, Cui 17258 (BJFC034116); Jiangxi, Shangrao, Daomaoshan Park, on the ground of *Cyclobalanopsis jenseniana*, 30 Aug. 2021, Dai 23665 (BJFC038237).

Description: *Basidiomata* annual, dorso-laterally stipitate, hard corky. *Pilei* solitary, flabelliform to shell-shaped, up to 3 cm diam and 1 cm thick. *Pileal surface* dark yellow to orange-brown, laccate, glabrous, with concentric bands and slightly radial rugose; margin obtuse, entire, wavy when fresh, incurved when dry. *Pore surface* buff to straw yellow when dry; pores circular to angular, 5–7 per mm; dissepiments slightly thick to moderately thick, entire. *Context*

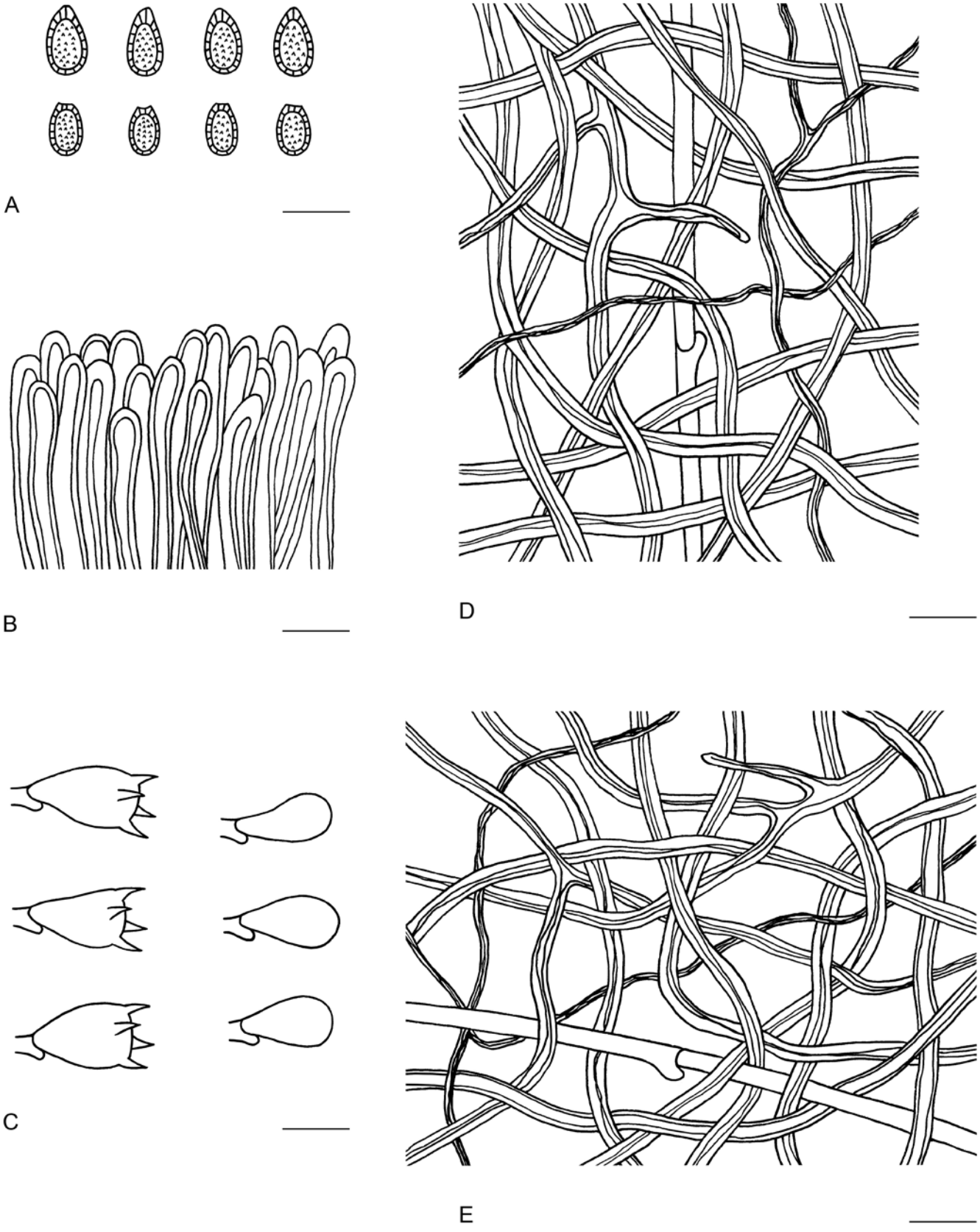

Fig. 32. Microscopic structures of *Ganoderma subellipsoideum* (drawn from Cui 18325). **A.** Basidiospores. **B.** Apical cells from cuticle. **C.** Basidia and basidioles. **D.** Hyphae from trama. **E.** Hyphae from context. Scale bars = 10 µm.

yellowish brown, homogeneous, without black melanoid lines, soft corky, up to 1.6 mm thick. *Tubes* buff, non-stratified, up to 7 mm long. *Stipe* dark-red, cylindrical and solid, sometimes budding without pilei, up to 14cm long and 6 mm diam. *Hyphal system* trimitic; generative hyphae with clamp connections; all hyphae IKI –, CB +; tissues darkening in KOH. Generative hyphae in context colourless, thin-walled, 2–3 µm diam; skeletal hyphae in context pale yellow, thick-walled with a wide to narrow lumen or sub-solid, arboriform and flexuous, 2–5 µm diam; binding hyphae in context colourless, thick-walled, branched and flexuous, up to 2 µm diam. Generative hyphae in tubes colourless, thin-walled, 2–3 µm diam; skeletal hyphae in tubes pale yellow, thick-walled with a wide to

Fig. 33. Basidiomata of *Ganoderma subflexipes*.

narrow lumen or sub-solid, arboriform and flexuous, 2–4 µm diam; binding hyphae in tubes colourless, thick-walled, branched and flexuous, up to 2 µm diam. *Pileipellis* composed of clamped generative hyphae, thick-walled to sub-solid, apical cells clavate, slightly inflated and flexuous, golden yellow, about 27–35 × 4–8 µm, forming a regular palisade. *Cystidia* and *cystidioles* absent. *Basidia* barrel-shaped, colourless, thin-walled, 15–22 × 9–11 µm; *basidioles* broadly clavate, colourless, thin-walled, 14–18 × 7–10 µm. *Basidiospores* ellipsoid to ovoid, truncated, yellowish brown, IKI –, CB +, double-walled with distinctly thick walls, exospore wall smooth, endospore wall with dense spinules, (6.3–)6.7–9.8(–10.1) × (4–)4.2–6.5(–7) µm, L = 8.2 µm, W = 5.37 µm, Q = 1.53–1.65 (n = 60/2, with the turgid vesicular appendix excluded); (7.6–)7.8–11(–11.5) × (4–)4.2–6.6(–6.8) µm, L = 9.25 µm, W = 5.46 µm, Q = 1.64–1.74 (n = 60/2, with the turgid vesicular appendix included).

Notes: *Ganoderma subflexipes* is distinguished by its small and dorso-laterally stipitate basidiomata, dark yellow to orange-brown pileal surface, wavy margin, and obviously truncated basidiospores. *Ganoderma flexipes* is sister to *G. subflexipes* in phylogenetic tree (Fig. 1), that species also has small and dorso-laterally stipitate basidiomata with a laccate pileal surface, but it differs from *G. subflexipes* by its reddish brown pileal surface, round and smooth margin, and basidiospores not obviously truncated (Steyaert 1972, Ryvarden 1983, Wang & Wu 2014).

Ganoderma sublobatum B.K. Cui, J.H. Xing & Y.F. Sun, ***sp. nov.*** MycoBank MB 839682. Figs 35, 36.

Diagnosis: Differs from other species in the genus by its annual basidiomata, non-laccate pileal surface with shallow concentric furrows and radial rugose, homogeneous context, non-stratified tubes and ellipsoid basidiospores with truncated apex.

Etymology: *sublobatum* (*Lat.*), refers to this species being closely related to *Ganoderma lobatum*.

Typus: **Australia**, Queensland, Cairns, Mount Whitfield Conservation Park, on stump of angiosperm tree, 18 May 2018, Cui 16804 (**holotype** BJFC030103).

Additional materials examined: **Australia**, Queensland, Cairns, Mount Whitfield Conservation Park, on stump of angiosperm tree, 18 May 2018, Cui 16805 (BJFC030104), Cui 16806 (BJFC030105).

Description: *Basidiomata* annual, sessile or subsessile, hard corky to woody hard. *Pilei* solitary, flabelliform to reniform or shell-shaped, applanate, up to 8 cm diam and 7 cm thick. *Pileal surface* pale brown to dark brown, dull, glabrous, with shallowly concentric furrows and radial rugose; margin obtuse, entire. *Pore surface* white to pale brown when fresh, turning darker when bruised, pale grey when

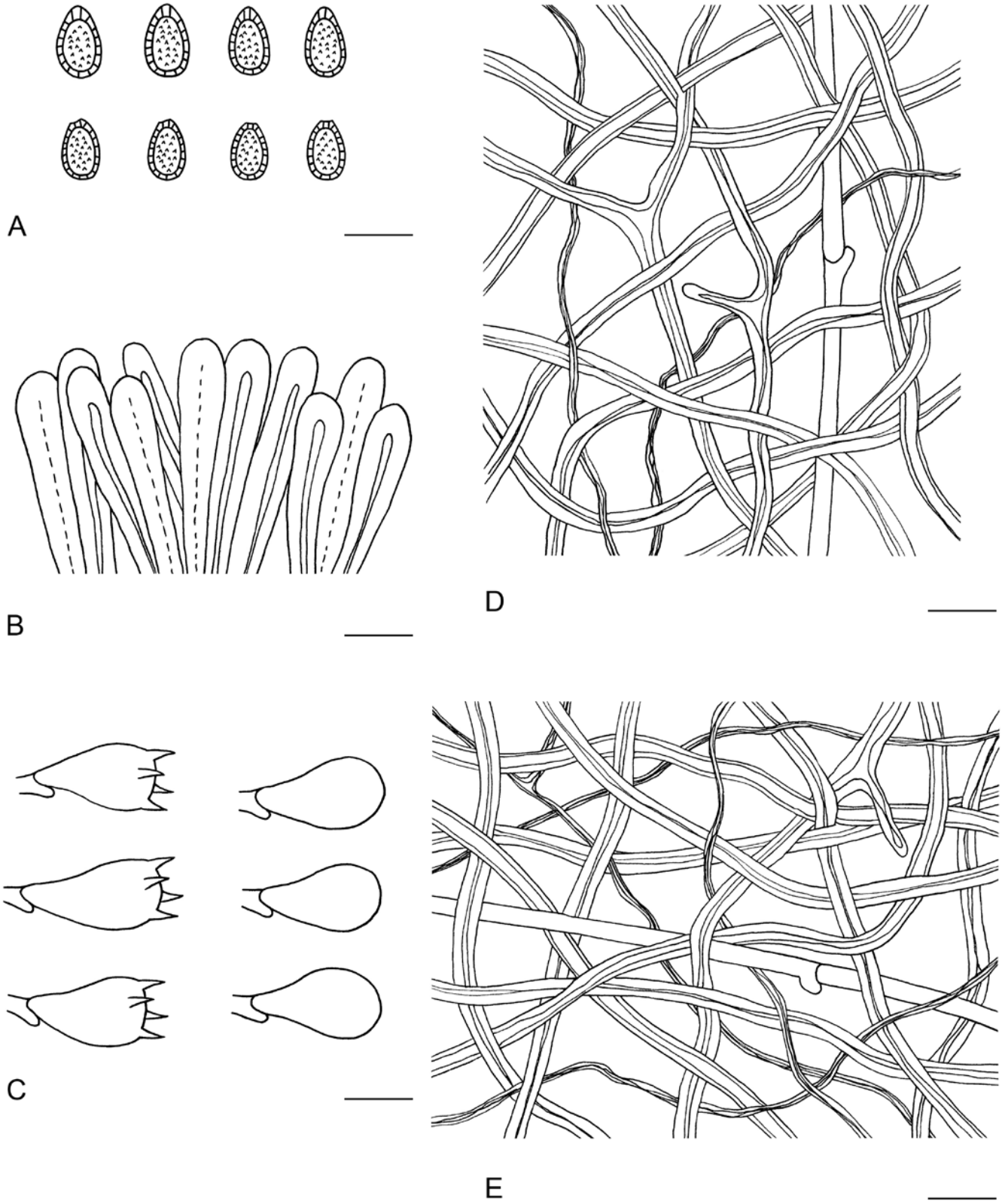

Fig. 34. Microscopic structures of *Ganoderma subflexipes* (drawn from Cui 17257). **A.** Basidiospores. **B.** Apical cells from cuticle. **C.** Basidia and basidioles. **D.** Hyphae from trama. **E.** Hyphae from context. Scale bars = 10 µm.

dry; pores circular, 5–6 per mm; dissepiments moderately thick, entire. *Context* dark brown, homogeneous, with black melanoid lines, corky, up to 3 mm thick. *Tubes* dark brown, non-stratified, up to 7 mm long. *Hyphal system* trimitic; generative hyphae with clamp connections; all hyphae IKI –, CB +; tissues darkening in KOH. Generative hyphae in context colourless, thin-walled, 2.5–5 µm diam; skeletal hyphae in context pale brown, thick-walled with narrow lumen or sub-solid, arboriform and flexuous, 3.5–6.5 µm diam; binding hyphae in context colourless, thick-walled, branched and flexuous, 2–3 µm diam. Generative hyphae in tubes colourless, thin-walled, 2–3.5 µm diam; skeletal hyphae in tubes pale brown, thick-walled with narrow lumen or sub-solid, arboriform and flexuous, 2–4.5 µm diam; binding hyphae in tubes colourless, thick-walled, branched and flexuous, 1.2–2.5 µm diam. *Pileipellis* composed of clamped generative hyphae, thin to slightly thick-walled, apical cells clavate, faintly constricted with obvious branch,

Fig. 35. Basidiomata of *Ganoderma sublobatum*.

dark brown, about 30–40 × 3–6 µm, forming an untidy palisade. *Cystidia* and *cystidioles* absent. *Basidia* barrel-shaped, colourless, thin-walled, 15–25 × 10–17 µm; *basidioles* clavate, colourless, thin-walled, 16–22 × 7–14 µm. *Basidiospores* ellipsoid, truncated, pale yellowish brown, IKI –, CB +, double-walled with distinctly thick walls, exospore wall smooth, endospore wall with dense spinules, (7.5–)9–11(–11.5) × (6–)6.5–8(–8.5) µm, L = 9.67 µm, W = 7.3 µm, Q = 1.32 (n = 30/1, with the turgid vesicular appendix excluded); (10.5–)11–12.5(–13) × 6.5–8.5(–9) µm, L = 11.41 µm, W = 7.25 µm, Q = 1.57 (n = 30/1, with the turgid vesicular appendix included).

Notes: *Ganoderma sublobatum* was collected from Queensland in Australia, it is closely related to *G. lobatum*. However, *G. lobatum* has perennial basidiomata with darker pilei, white pore surface, and smaller basidiospores (7–8.6 × 5–5.5 µm) which are different from *G. sublobatum*.

Ganoderma tongshanense B.K. Cui, J.H. Xing & Y.F. Sun, ***sp. nov.*** MycoBank MB 839683. Figs 37, 38.

Diagnosis: Differs from other species in the genus by its pale yellowish brown pileal surface, large pores, homogeneous context, non-stratified tubes, and ellipsoid and truncated basidiospores.

Etymology: *tongshanense* (*Lat.*), refers to the holotype of this species being found at Tongshan County of Hubei Province.

Typus: **China**, Hubei, Tongshan County, Jiugongshan National Park, on fallen trunk of angiosperm tree, 20 Oct. 2018, Cui 17168 (**holotype** BJFC030468).

Description: *Basidiomata* annual, sessile and broadly attached, hard corky. *Pilei* solitary, flabelliform, up to 7 cm diam and 2.5 cm thick. *Pileal* surface clay buff to pale yellowish brown, dull, glabrous, with concentric furrows and slightly radial wrinkles; margin obtuse, entire. *Pore surface* greyish white when fresh, turning darker when bruised, pale brown when dry; pores circular, shallow, 3–4 per mm; dissepiments moderately thick, entire. *Context* dark brown, homogeneous, without black melanoid lines, hard corky, up to 1.6 cm thick. *Tubes* slightly paler than context, non-stratified, stuffed with white mycelium, up to 9 mm long. *Hyphal system* trimitic; generative hyphae with clamp connections; all hyphae IKI –, CB +; tissues darkening in KOH. Generative hyphae in context colourless, thin-walled, 2–4 µm diam; skeletal hyphae in context dark brown, thick-walled with a wide to narrow lumen or sub-solid, arboriform and flexuous, 2–5 µm diam; binding hyphae in context colourless, thick-walled, branched and flexuous, up to 2 µm diam. Generative hyphae in tubes colourless, thin-walled, 2–4 µm diam; skeletal hyphae in tubes dark brown, thick-walled with a wide to narrow lumen or sub-solid, arboriform and flexuous, 2–5 µm diam; binding hyphae in tubes colourless, thick-walled, branched and flexuous, up to 2 µm diam. *Pileipellis* composed of clamped generative hyphae, thick-walled to sub-solid, apical cells clavate, inflated and

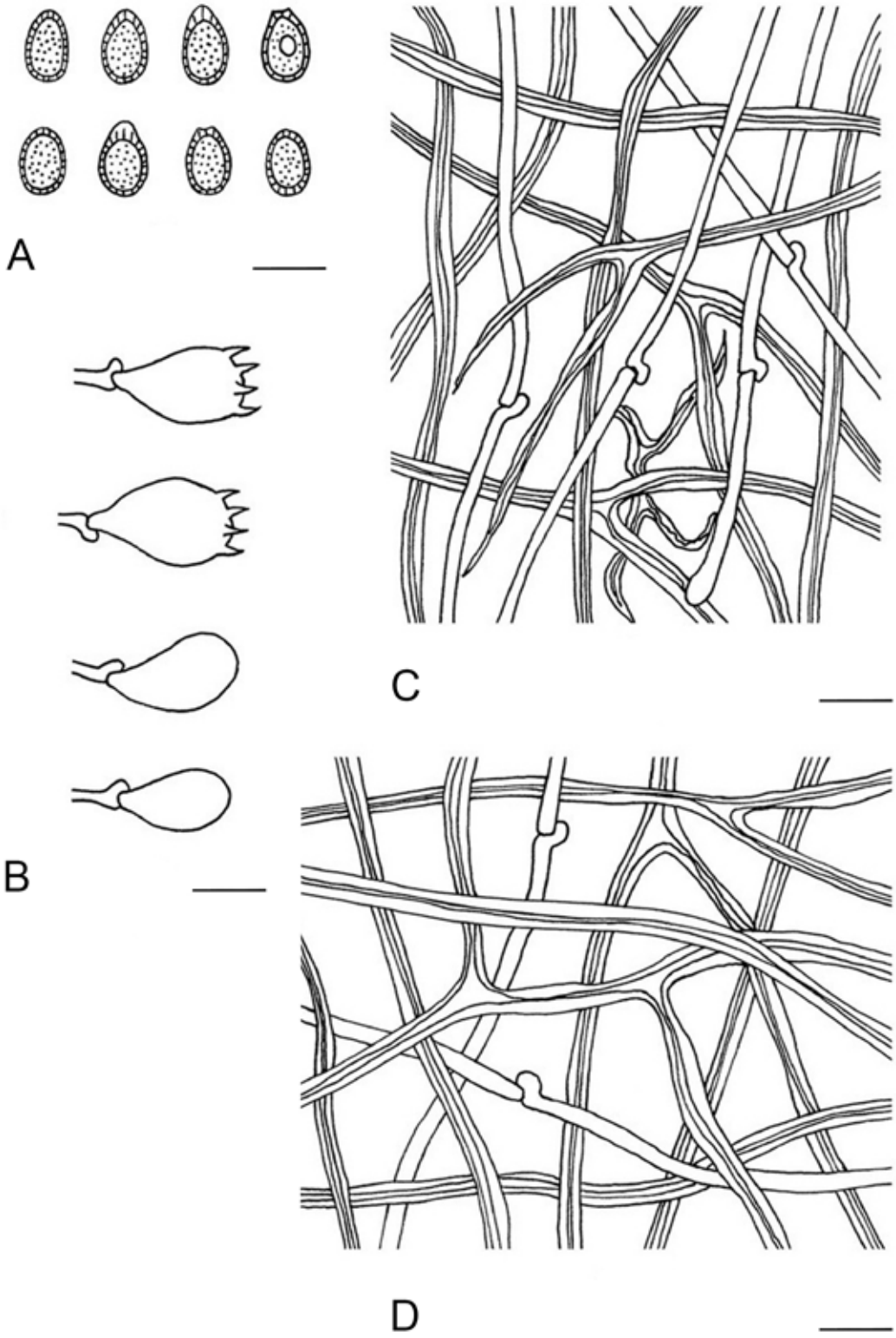

Fig. 36. Microscopic structures of *Ganoderma sublobatum* (drawn from Cui 16804). **A.** Basidiospores. **B.** Basidia and basidioles. **C.** Hyphae from trama. **D.** Hyphae from context. Scale bars = 10 µm.

flexuous, pale yellowish brown, about 30–45 × 6–8 µm, forming a regular palisade. *Cystidia* and *cystidioles* absent. *Basidia* clavate, colourless, thin-walled, 10–13 × 3–5 µm; *basidioles* in shape like the basidia, colourless, thin-walled, 8–11 × 4–6 µm. *Basidiospores* ellipsoid, truncated, pale yellowish brown, IKI –, CB +, double-walled with distinctly thick walls, exospore wall smooth, endospore wall with dense spinules, (8–)8.2–9.8(–10) × (5–)5.2–6.2(–6.5) µm, L = 8.91 µm, W = 5.62 µm, Q = 1.59 (n = 60/1, with the turgid vesicular appendix excluded); (9.2–)9.4–10.5(–11) × (5–)5.2–6.1(–6.3) µm, L = 9.81 µm, W = 5.65 µm, Q = 1.74 (n = 60/1, with the turgid vesicular appendix included).

Notes: Morphologically, *G. tongshanense* may be confused with *G. australe* which is widely distributed in South China. They share similar macro-morphological characters, but the latter has perennial and larger basidiomata and stratified tubes (Patouillard 1889, Ryvarden & Johansen 1980, Corner 1983). In the phylogenetic analyses, *G. tongshanense* and *G. australe* are distinct from each other (Fig. 1).

Fig. 37. Basidiomata of *Ganoderma tongshanense*.

Ganoderma yunlingense B.K. Cui, J.H. Xing & Y.F. Sun, ***sp. nov.*** MycoBank MB 839684. Figs 39, 40.

Diagnosis: Differs from other species in the genus by its non-laccate pileal surface with concentrically irregular ridges, extremely thin context, stratified tubes, and ovoid to almond-shaped basidiospores without spinules on the endospore wall.

Etymology: *yunlingense* (*Lat.*), refers to this species being collected from the Yunling Mountains of Yunnan Province.

Typus: **China**, Yunnan, Lanping County, Luoguqing, on fallen trunk of *Quercus*, 9 Sep. 2017, Cui 16288 (**holotype** BJFC029587).

Additional materials examined: **China**, Yunnan, Lijiang, Yulongxueshan, on stump of *Quercus*, 16 Sep. 2018, Cui 17043 (BJFC030342), Cui 17060 (BJFC030359); Lanping County, Luoguqing, on fallen trunk of *Quercus semecarpifolia*, 18 Sep. 2018, Cui 17161 (BJFC030461).

Description: *Basidiomata* perennial, sessile, hard corky to woody hard. *Pilei* solitary, flabelliform to shell-shaped, occasionally dimidiate, up to 11.5 cm diam and 10 cm thick. *Pileal surface* greyish brown to grey, dull, glabrous, with concentrically irregular ridges; margin acute, entire, wavy and sometimes lacerated as petals. *Pore surface* white when fresh, turning darker when bruised, straw yellow when dry; pores circular to angular, 4–6 per mm; dissepiments moderately thick, entire. *Context* extremely thin, without black melanoid lines. *Tubes* brown to dark brown, distinctly stratified, up to 5 cm long. *Hyphal system* trimitic; generative hyphae with clamp connections; all hyphae IKI –, CB +; tissues darkening in KOH. Generative hyphae in context colourless, thin-walled, 2–3.5 µm diam; skeletal hyphae in context yellowish brown, thick-walled with narrow lumen or sub-solid, arboriform and flexuous, 3–5.5 µm diam; binding hyphae in context colourless, thick-walled, branched and flexuous, 1.5–3 µm diam. Generative hyphae in tubes colourless, thin-walled, 2–3 µm diam; skeletal hyphae in tubes yellowish brown, thick-walled with narrow lumen or sub-solid, arboriform and flexuous, 2.5–5 µm diam; binding hyphae in tubes colourless, thick-walled, branched and flexuous, 1.5–3 µm diam. *Pileipellis* composed of clamped generative hyphae, thick-walled, apical cells clavate, flexuous, golden yellow to pale brown, about 25–40 × 4–7 µm, forming a regular palisade. *Cystidia* and *cystidioles* absent. *Basidia* barrel-shaped, colourless, thin-walled, 15–20 × 8–13 µm; *basidioles* clavate, colourless, thin-walled, 13–17 × 6–10 µm. *Basidiospores* ovoid to almond-shaped, not obviously truncated, pale yellowish brown, IKI –, CB +, double-walled with slightly thick walls, exospore wall smooth, endospore wall without spinules, (7.5–)8–10(–10.5) × (4.3–)4.8–5.5(–6) µm, L = 8.93 µm, W = 5.16 µm, Q = 1.70–1.73 (n = 60/2, with the turgid vesicular appendix excluded).

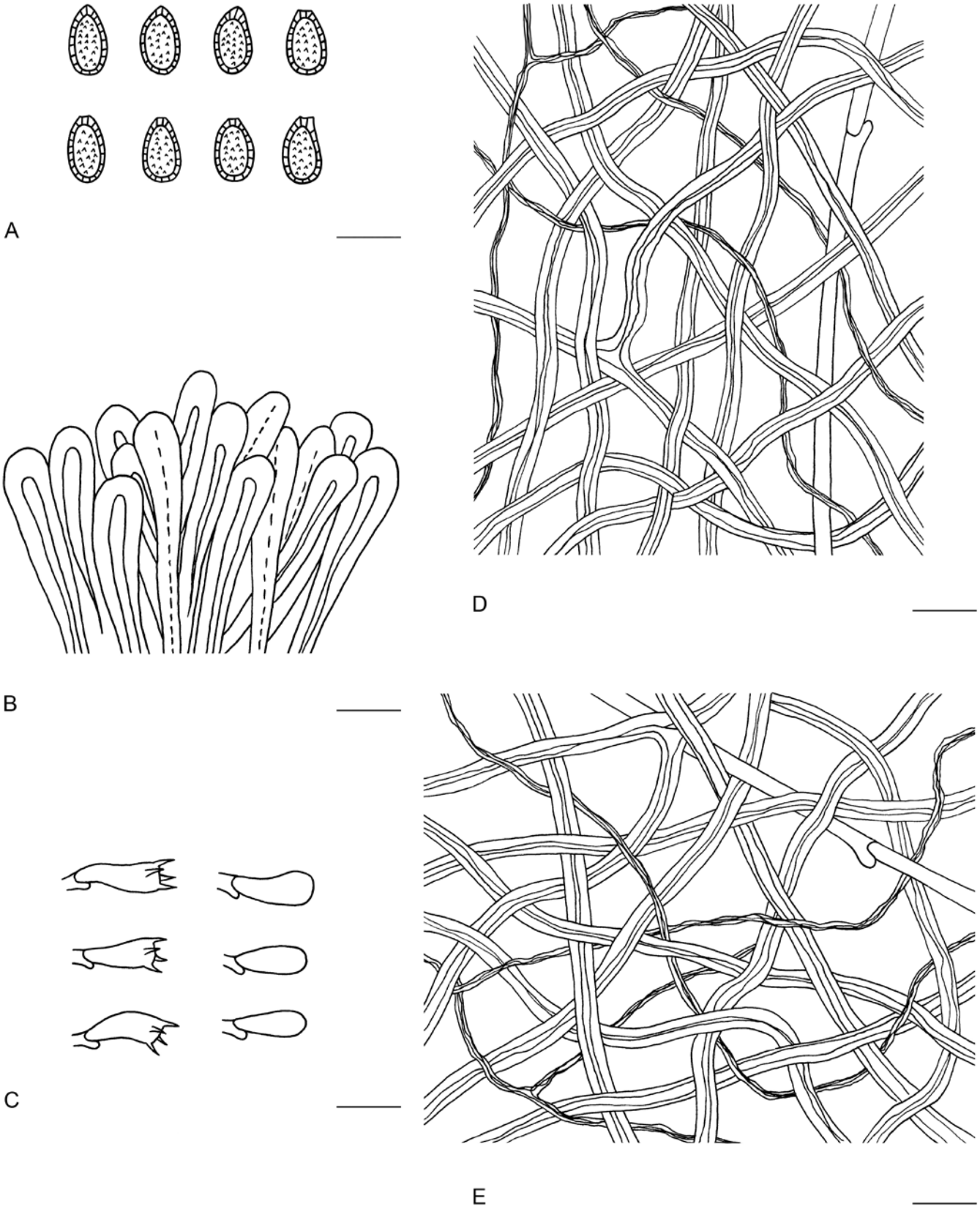

Fig. 38. Microscopic structures of *Ganoderma tongshanense* (drawn from Cui 17168). **A.** Basidiospores. **B.** Apical cells from cuticle. **C.** Basidia and basidioles. **D.** Hyphae from trama. **E.** Hyphae from context. Scale bars = 10 µm.

Notes: *Ganoderma yunlingense* is characterised by its non-laccate pileal surface with concentrically irregular ridges, extremely thin context, stratified and long tubes, basidiospores not obviously truncated, without spinules on the endospore wall. It may be confused with *G. acontextum* because of the dull pileal surface, thin context and basidiospores not obviously truncated without any ornamentation; however, *G. acontextum* was collected from the United States of America and has reddish brown pileal surface with dense concentric furrows, and non-stratified tubes.

Fig. 39. Basidiomata of *Ganoderma yunlingense*.

Notes on accepted species of *Ganoderma* recorded from China

Ganoderma ahmadii Steyaert, Persoonia 7: 91. 1972. MycoBank MB 314303.

For a detailed description of *Ganoderma ahmadii*, see Steyaert (1972) and Zhao (1989b).

Notes: *Ganoderma ahmadii* was described from Pakistan by Steyaert (1972). Zhao (1989b) examined an authentic specimen collected from Pakistan, but the description regarding the reddish brown pileal surface and homogeneous context is different to the original description. Wang (2005) studied one specimen of *G. ahmadii* collected from Sichuan Province in China and the ITS1-ITS2 sequences are similar to the records in GenBank. So, *G. ahmadii* was confirmed in Sichuan Province in China based on morphological and phylogenetic analyses.

Ganoderma angustisporum J.H. Xing *et al.*, MycoKeys 34: 98. 2018. MycoBank MB 823320.

For a detailed description of *Ganoderma angustisporum*, see Xing *et al.* (2018).

Notes: *Ganoderma angustisporum* was recently described from China and classified in *Ganoderma* according to its narrow and truncated basidiospores in *Ganoderma* (Xing *et al.* 2018). It is also found in Malaysia, Sri Lanka and Thailand.

Ganoderma applanatum (Pers.) Pat., Hyménomyc. Eur. (Paris): 143. 1887. MycoBank MB 119872. Figs 41, 42.
Basionym: *Boletus applanatus* Pers., Observ. Mycol. (Lipsiae) 2: 2. 1800.

Description: *Basidiomata* perennial, sessile and broadly attached, hard corky to woody hard. *Pilei* solitary or imbricate, variable, applanate, flabelliform to shell-like or ungulate, up to 23 cm diam and 7 cm thick. *Pileal surface* pale brown to dark brown, dull, glabrous, with shallow to deep concentric furrows; margin obtuse, entire and wavy. *Pore surface* white to pale brown when fresh, turning darker when bruised, greyish white to straw yellow when dry; pores circular to angular, 4–7 per mm; dissepiments moderately thick, mostly entire. *Context* yellowish brown to dark brown, homogeneous, with black melanoid lines when mature, corky, up to 3 cm thick. *Tubes* concolorous with context, stratified by a layer of context, up to 4 cm long. *Hyphal system* trimitic; generative hyphae with clamp connections; all hyphae IKI –, CB +; tissues darkening in KOH. Generative hyphae in context colourless, thin-walled, 2.5–7 µm diam; skeletal hyphae in context pale yellowish brown, thick-walled with a wide to narrow lumen or sub-solid, frequently arboriform and flexuous, 3.5–6.5 µm diam; binding hyphae in context colourless, thick-walled, branched and flexuous, 2–3 µm diam. Generative hyphae in tubes colourless, thin-walled, 2–3.5 µm diam; skeletal hyphae in tubes pale brown to dark brown, thick-walled with a wide to narrow lumen or sub-solid, frequently arboriform and flexuous, 2–4.5 µm diam; binding hyphae in tubes colourless, thick-walled, branched and flexuous, 1–2.5 µm diam. *Cystidia*, *cystidioles*, *basidia* and *basidioles*

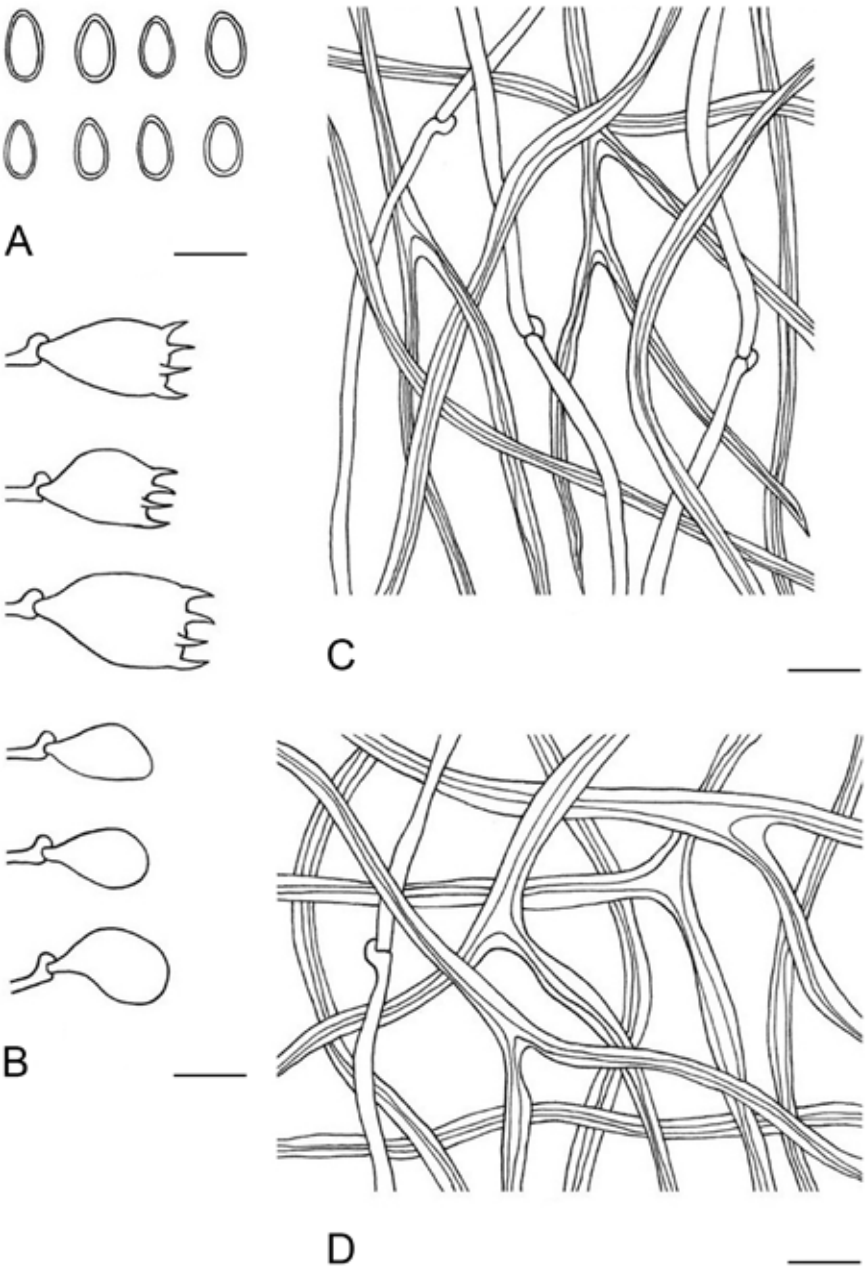

Fig. 40. Microscopic structures of *Ganoderma yunlingense* (drawn from Cui 16288). **A.** Basidiospores. **B.** Basidia and basidioles. **C.** Hyphae from trama. **D.** Hyphae from context. Scale bars = 10 µm.

absent. *Basidiospores* ellipsoid, truncated, yellowish to pale brown, IKI –, CB +, double-walled with moderately thick walls, exospore wall smooth, endospore wall with dense spinules, (5–)5.5–7(–8) × (4–)4.1–5.2(–6) µm, L = 6.25 µm, W = 4.56 µm, Q = 1.37 (n=30/1, with the turgid vesicular appendix included).

Additional materials examined: **China**, Jilin, Jiaohe, Hongyegu Park, on stump of angiosperm tree, 1 Aug. 2016, Cui 14062 (BJFC028930); on stump of *Betula*, 1 Aug. 2016, Cui 14070 (BJFC028938); Fusong County, Changbaishan Nature Reserve, on fallen trunk of angiosperm tree, 3 Aug. 2016, Cui 14121 (BJFC028989).

Notes: *Ganoderma applanatum* was firstly described from Europe and has a Holarctic distribution (Steyaert 1972, Moncalvo & Ryvarden 1997, Hapuarachchi *et al.* 2019b). *Ganoderma applanatum* is similar with *G. australe* based on perennial and sessile basidiomata, non-laccate and pale pileal surface, brown to dark brown context, but the latter has larger basidiospores (7–12 × 5–8 µm, Ryvarden 2004b). Besides, *G. applanatum* and *G. australe* can be separated in the phylogenetic analyses (Fig. 1).

Ganoderma australe (Fr.) Pat., Bull. Soc. Mycol. Fr. 5: 65. 1889. MycoBank MB 100745.
Basionym: *Polyporus australis* Fr., Elench. Fung. (Greifswald) 1: 108. 1828.
Synonyms: *Ganoderma triangulum* J.D. Zhao & L.W. Hsu, Acta Mycol. Sin. 3: 18. 1984.
Ganoderma ungulatum J.D. Zhao & X.Q. Zhang, Acta Mycol. Sin. 3: 19. 1984.
Ganoderma bawanglingense J.D. Zhao & X.Q. Zhang, Acta Mycol. Sin. 6: 205. 1987.
Ganoderma mirivelutinum J.D. Zhao, Acta Mycol. Sin. 7: 206. 1987.

For a detailed description of *G. australe*, see Ryvarden (2004b) and Hapuarachchi *et al.* (2018b).

Fig. 41. Basidiomata of *Ganoderma applanatum*.

Notes: *Ganoderma australe* was described from an island in the Pacific Ocean, but the type specimen has been lost and the only specimen deposited at the Royal Botanic Gardens Kew was from Europe which is inconsistent with its tropical distribution (Moncalvo & Ryvarden 1997). Cao (2013) suggested that *G. bawanglingense*, *G. mirivelutinum*, *G. triangulum* and *G. ungulatum* should be regarded as the synonyms of *G. applanatum*, but their tropical distribution and morphological similarity of *G. australe* support that they should be treated as the synonyms of *G. australe*. *Ganoderma australe* may be confused with *G. adspersum*, *G. applanatum* and *G. gibbosum* in morphology. Previously, many specimens collected from South China were identified as "*Ganoderma australe*". Two specimens from Australia are recognised as *G. australe* by Costa-Rezende *et al.* (2017), and most specimens collected from South China clustered with *G. gibbosum* (Fig. 1). Whether there is true *G. australe* in China is unknown and more detailed studies about the *G. australe* complex should be done.

Ganoderma boninense Pat., Bull. Soc. Mycol. Fr. 5: 72. 1889. MycoBank MB 100062.

For a detailed description of *G. boninense*, see Steyaert (1967) and Ryvarden (1983).

Notes: *Ganoderma boninense* was described from the Bonin Islands in Japan, and it has been recognised as the main pathogen of oil palm trees causing a basal stem rot (Pilotti 2005). *Ganoderma boninense* can be distinguished by its reddish and shiny pileal surface, irregular apical cells with swellings and protuberance of pileipellis, and oblong ellipsoid basidiospores (Ryvarden 1983). Cao (2013) compared the specimens collected from Hainan Province and Japan, and they showed very similar morphological characters and ITS sequences.

Ganoderma calidophilum J.D. Zhao *et al.*, Acta Microbiol. Sin. 19: 270. 1979. MycoBank MB 314307.

For a detailed description of *G. calidophilum*, see Zhao *et al.* (1979) and Luangharn *et al.* (2021).

Notes: Zhao *et al.* (1979) described *Ganoderma calidophilum* from Hainan Province based on its small basidiomata with heterogenous context, whitish pore surface and large basidiospores (10–12.1 × 6.2–8.7 µm). The sequences of *G. calidophilum* used in this study were downloaded from GenBank, and showed to be distinct from *G. flexipes* (Fig. 1), which has been considered as a doubtful synonym (Wang & Wu 2014).

Ganoderma casuarinicola J.H. Xing *et al.*, MycoKeys 34: 100. 2018. MycoBank MB 823321.

For a detailed description of *G. casuarinicola*, see Xing *et al.* (2018) and Luangharn *et al.* (2019).

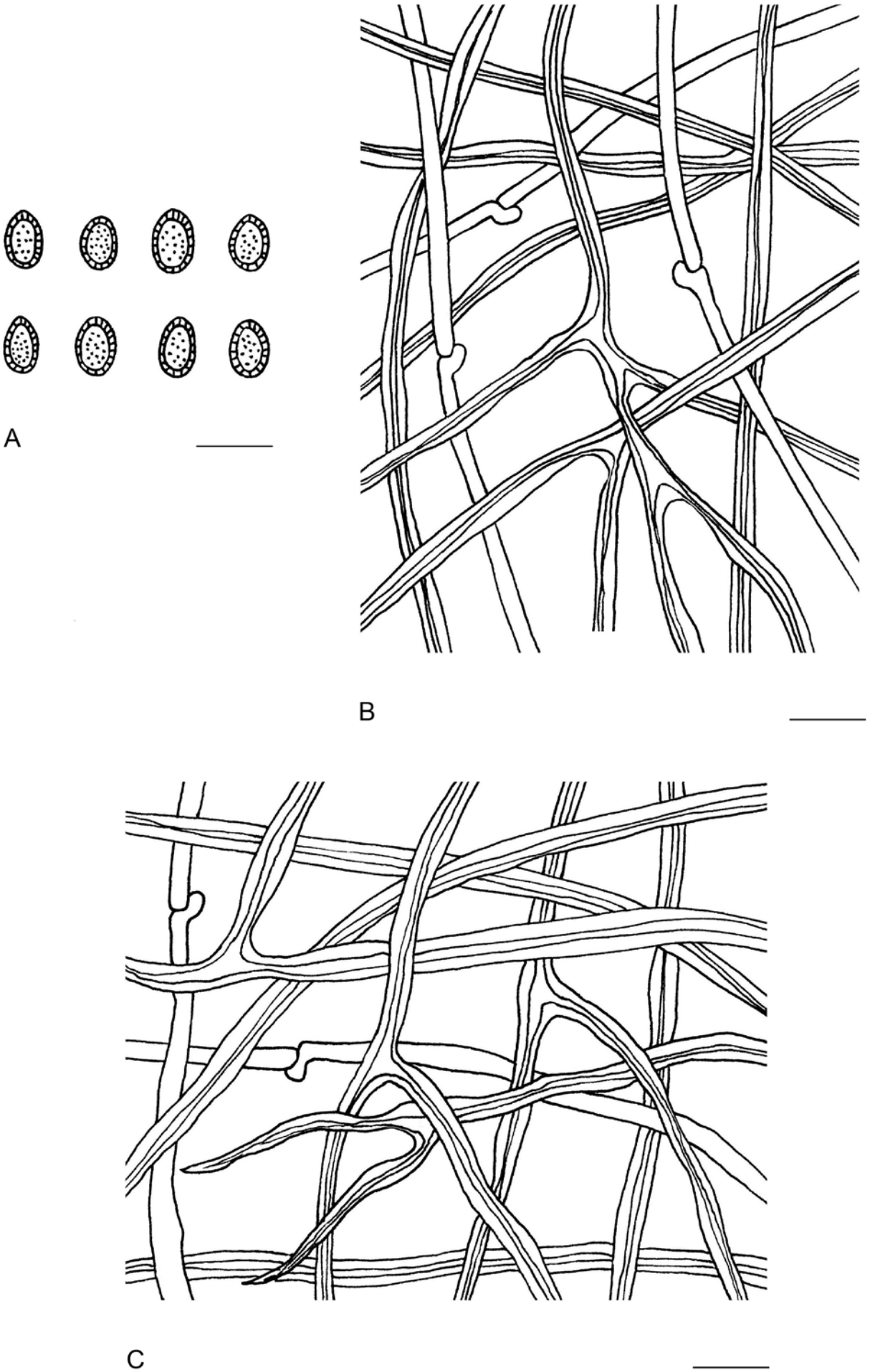

Fig. 42. Microscopic structures of *Ganoderma applanatum* (drawn from He 2139). **A.** Basidiospores. **B.** Hyphae from trama. **C.** Hyphae from context. Scale bars = 10 µm.

Notes: *Ganoderma casuarinicola* was collected on a living tree of *Casuarina equisetifolia* from Guangdong Province in China by Xing *et al.* (2018). Luangharn *et al.* (2019) reported *G. casuarinicola*, where it was found on *Pinus kesiya* stump, as a new record from Thailand. There are some differences such as applanate to dimidiate pilei, longer tubes and larger basidiospores when comparing these specimens with the type of *G. casuarinicola* (Dai 16336). Geographical and climatic divergences may be the reason for the intraspecific differences (Boddy *et al.* 2014).

Ganoderma ellipsoideum Hapuar. *et al.*, Mycosphere 9: 951. 2018. MycoBank MB 554384.

For a detailed description of *G. ellipsoideum*, see Hapuarachchi *et al.* (2018b).

Notes: *Ganoderma ellipsoideum* is distinguished by its ellipsoid spores (6.1–7.3 × 3.7–4.6 µm) with distinct spinules on the endospore wall. Hapuarachchi *et al.* (2018b) stated that *G. ellipsoideum* was known only from the type locality of Hainan Province in China. In this study, several specimens collected from Yunnan and Guangdong provinces showed similar morphological features and close phylogenetic relationships with *G. ellipsoideum*.

Ganoderma flexipes Pat., Bull. Soc. Mycol. Fr. 23: 75. 1907. MycoBank MB 249905. Figs 43, 44.
Synonyms: *Ganoderma atrum* J.D. Zhao *et al.*, Acta Microbiol. Sin. 19: 268. 1979.
Ganoderma hainanense J.D. Zhao *et al.*, Acta Microbiol. Sin. 19: 269. 1979.
Ganoderma parviungulatum J.D. Zhao & X.Q. Zhang, Acta Mycol. Sin. 5: 88. 1986.

Description: *Basidiomata* annual, dorso-laterally stipitate, hard corky to woody hard. *Pilei* solitary, variable, flabelliform to shell-like or circular, up to 5 cm diam and 1.5 cm thick. *Pileal surface* dark brown to reddish brown, strongly laccate, glabrous, with obvious concentric furrows and slightly radial rugose; margin obtuse, entire, slightly incurved. *Pore surface* white when fresh, turning darker when bruised, light buff when dry; pores circular to angular, 4–6 per mm; dissepiments slightly thick, entire. *Context* heterogeneous, the upper layer pale yellowish brown, the lower layer dark brown, with black melanoid lines, corky, up to 3 mm thick. *Tubes* dark brown, non-stratified, up to 1.2 cm long. *Stipe* reddish brown to purplish black, flattened to cylindrical, up to 25 cm long and 6 mm diam. *Hyphal system* trimitic; generative hyphae with clamp connections; all hyphae IKI –, CB +; tissues darkening in KOH. Generative hyphae in context colourless, thin-walled, 1.5–3.5 µm diam; skeletal hyphae in context pale yellowish brown, thick-walled with a narrow lumen or sub-solid, arboriform and flexuous, 2.5–6 µm diam; binding hyphae in context colourless, thick-walled, branched and flexuous, 1–2 µm diam. Generative hyphae in tubes colourless, thin-walled, occasionally branched, 2–3 µm diam; skeletal hyphae in tubes pale brown to dark brown, thick-walled with a narrow lumen to sub-solid, frequently arboriform and flexuous, 2–4 µm diam; binding hyphae in tubes colourless, thick-walled, branched and flexuous, 0.5–1 µm diam. *Pileipellis* composed of clamped generative hyphae, thick-walled to sub-solid, apical cells clavate, slightly inflated, pale brown to yellowish brown, 30–45 × 5–10 µm, forming a regular palisade. *Cystidia* and *cystidioles* absent. *Basidia* barrel-shaped, colourless, thin-walled, 23–30 × 12–17 µm; *basidioles* in shape like the basidia, colourless, thin-walled, 17–23 × 8–13 µm. *Basidiospores* ellipsoid, not obviously truncated, pale yellowish brown, IKI –, CB +, double-walled with moderately thick walls, exospore wall smooth, endospore walls with dense spinules, (6.5–)7–9(–9.5) × (4–)4.8–5.5(–6) µm, L = 8.17 µm, W = 5.23 µm, Q = 1.56 (n = 30/1, with the turgid vesicular appendix excluded).

Materials examined: **China**, Guangdong, Guangzhou, campus of Sun Yat-Sen University, on stump of angiosperm tree, 20 Jul. 2012, Cui 17209 (BJFC030563); Hainan, Qiongzhong County, Limushan Forest Park, on ground of angiosperm forest, 16 Jun. 2016, Cui 13841 (BJFC028707); Changjiang County, Bawangling Nature Reserve, on ground of angiosperm forest, 18 Jun. 2016, Cui 13863 (BJFC028729); Yunnan, Puer, Puer Forest Park, on rotten angiosperm wood, 17 Aug. 2019, Dai 20461 (BJFC032129).

Notes: *Ganoderma flexipes* was first described from Vietnam by Patouillard (1907), and many researchers have conducted detailed studies on it (Steyaert 1972, Ryvarden 1983, Hapuarachchi *et al.* 2019b). Cao (2013) considered *G. atrum*, *G. hainanense*

Fig. 43. Basidiomata of *Ganoderma flexipes*.

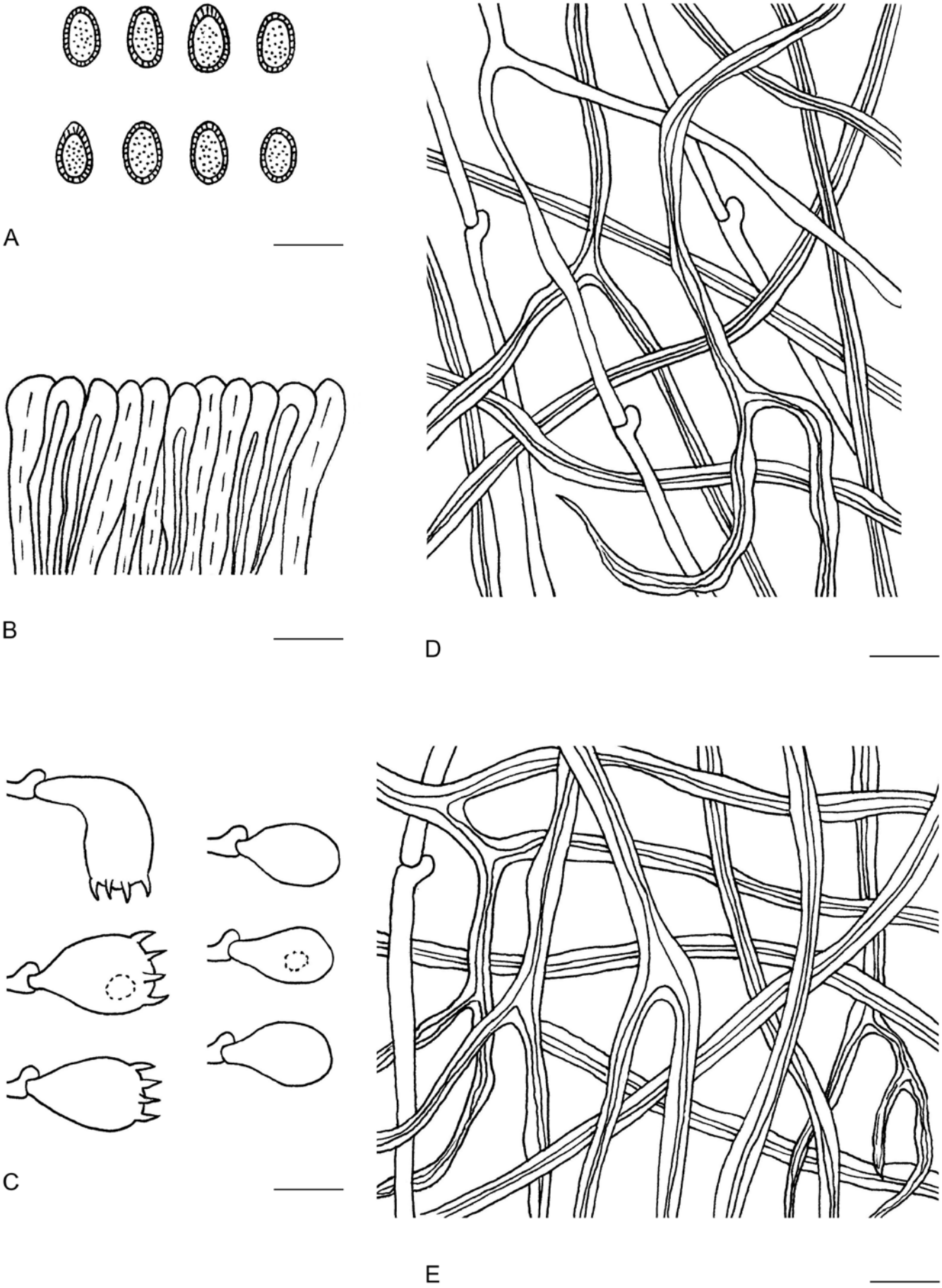

Fig. 44. Microscopic structures of *Ganoderma flexipes* (drawn from Cui 13882). **A.** Basidiospores. **B.** Apical cells from cuticle. **C.** Basidia and basidioles. **D.** Hyphae from trama. **E.** Hyphae from context. Scale bars = 10 µm.

and *G. parviungulatum* as synonyms of *G. flexipes* based on comprehensive observations of the holotype specimens.

Ganoderma gibbosum (Blume & T. Nees) Pat., Ann. Jard. Bot. Buitenzorg, suppl. 1: 114. 1897. MycoBank MB 250058.
Basionym: *Polyporus gibbosus* Blume & T. Nees, Nova Acta Phys.-Med. Acad. Caes. Leop.-Carol. Nat. Cur. 13: 19. 1826.

For a detailed description of *G. gibbosum*, see Luangharn *et al.* (2020).

Notes: *Ganoderma gibbosum* was first described from Java, however, the type specimen was lost (Moncalvo & Ryvarden, 1997). In previous studies, *G. gibbosum* was regarded as a synonym of *G. applanatum* or classified in the *G. applanatum–australe* complex based on the non-laccate basidiomata (Zhao 1989b, Moncalvo & Ryvarden 1997). Luangharn *et al.* (2020) conducted a study on the taxonomy of *G. gibbosum* collected from Kunming, China, and the results showed that samples of *G. gibbosum* from Asia and South America formed two different lineages. In this study, specimens of *G. gibbosum* collected from Guangdong, Guangxi and Sichuan provinces clustered together and formed a well-supported lineage (Fig. 1).

Ganoderma hoehnelianum Bres., Annls Mycol. 10: 502. 1912. MycoBank MB 243431. Figs 45, 46.
Synonym: *Ganoderma shangsiense* J.D. Zhao, Acta Mycol. Sin. 7: 17. 1988.

Description: *Basidiomata* perennial, sessile or broadly attached to laterally stipitate, hard corky to woody hard. *Pilei* solitary, variable, flabelliform or shell-like to reniform, applanate, up to 10 cm diam and 2.2 cm thick. *Pileal surface* yellowish brown to dark brown, dull, glabrous, with obvious concentric furrows; margin acute to obtuse, entire. *Pore surface* white when fresh, turning darker when bruised, straw yellow to pale yellowish brown when dry; pores circular to angular, 3–6 per mm; dissepiments moderately thick, entire. *Context* heterogeneous, the upper layer pale yellowish brown, the lower layer dark brown, with black melanoid lines, corky, up to 1 cm thick. *Tubes* light buff to greyish brown, stratified, up to 1.2 cm long. *Stipe* dark brown, flattened, up to 3 cm long and 6 mm diam. *Hyphal system* trimitic; generative hyphae with clamp connections; all hyphae IKI –, CB +; tissues darkening in KOH. Generative hyphae in context absent; skeletal hyphae in context pale yellowish brown, thick-walled with a wide to narrow lumen or sub-solid, frequently arboriform and flexuous, 2–4 µm diam; binding hyphae in context colourless, thick-walled, branched and flexuous, 1–2.5 µm diam. Generative hyphae in tubes colourless, thin-walled, 2.3–3.5 µm diam; skeletal hyphae in tubes pale brown to dark brown, thick-walled with a narrow lumen or sub-solid, frequently arboriform and flexuous, 2–5 µm diam; binding hyphae in tubes colourless, thick-walled, branched and flexuous, 1.5–3 µm diam. *Cystidia* and *cystidioles* absent. *Basidia* absent; *basidioles* barrel-shaped, colourless, thin-walled, 21–30 ×9–13 µm. *Basidiospores* subglobose, not obviously truncated, pale yellowish brown, IKI –, CB +, double-walled with distinctly thick walls, exospore walls smooth, endospore walls with dense spinules, (6.5–)7–8.2(–9) × (–5.5)5.8–7.8(–8) µm, L = 7.43 µm, W = 6.73 µm, Q = 1.1 (n = 30/1).

Fig. 45. Basidiomata of *Ganoderma hoehnelianum*.

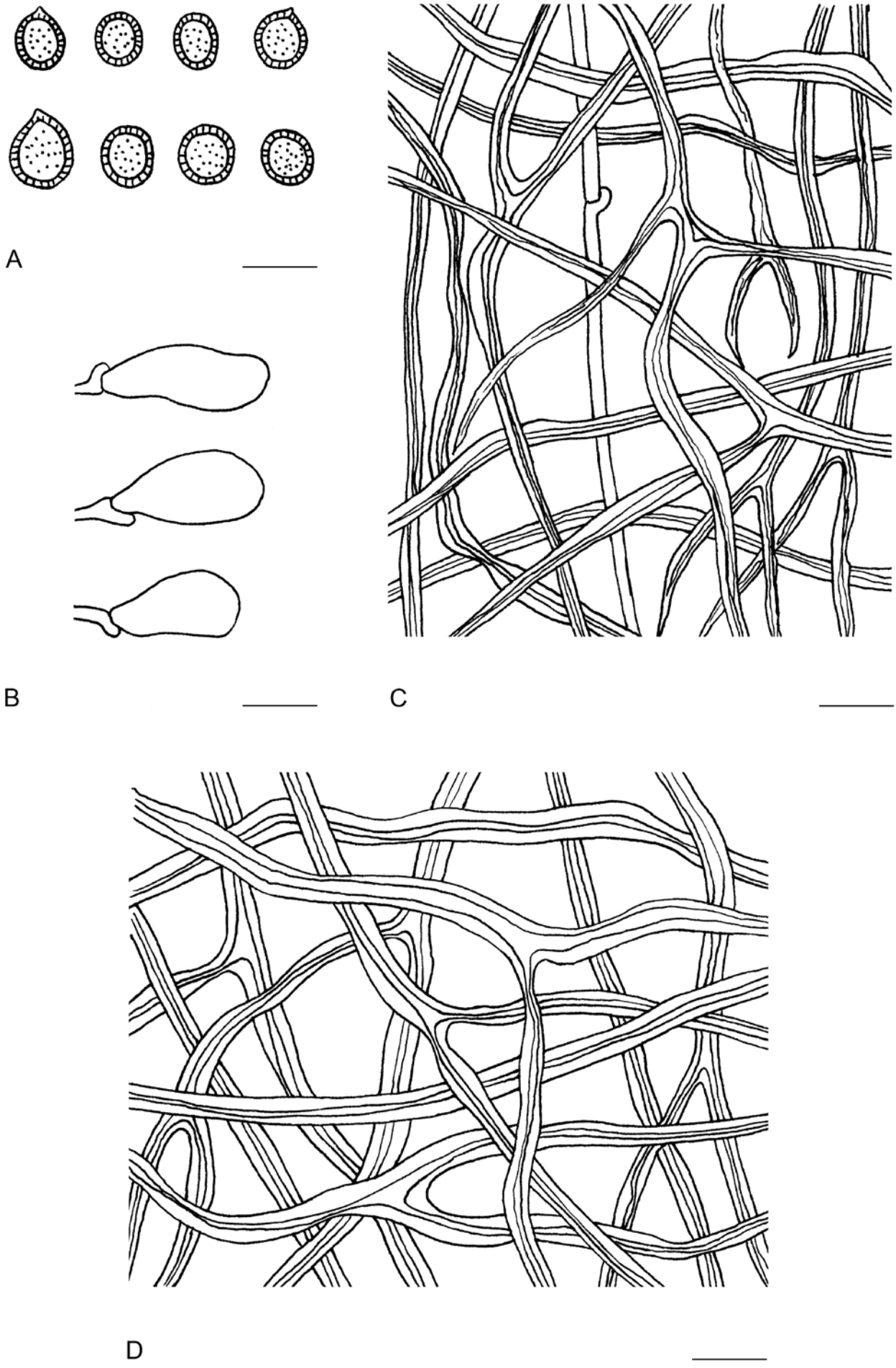

Fig. 46. Microscopic structures of *Ganoderma hoehnelianum* (drawn from Dai 16166). **A.** Basidiospores. **B.** Basidioles. **C.** Hyphae from trama. **D.** Hyphae from context. Scale bars = 10 µm.

Materials examined: **China**, Hainan, Ledong County, Jianfengling Nature Reserve, on stump of angiosperm tree, 19 Jun. 2016, Cui 13904 (BJFC028770); Guangxi, Shangsi County, Shiwandashan Forest Park, on dead tree of angiosperm, 6 Jul. 2016, Cui 13982 (BJFC028850); Nanning, Guangxi Academy of Forestry, on living tree of angiosperm, 21 Aug. 2019, Dai 20783 (BJFC032450); Yunnan, Mengla County, Wangtianshu Park, 20 Jul. 2014, Dai 13915 (BJFC017645).

Notes: *Ganoderma hoehnelianum* was described by Bresadola from Java. It has typically ganodermoid macro-morphological features, but the obviously amaurodermoid basidiospores make *G. hoehnelianum* different from other species. In the phylogenetic analyses, *G. hoehnelianum* grouped in the *Ganoderma* clade, and formed an independent lineage with high support (Fig. 1). Wang & Wu (2010) and Cao (2013) regarded *G. shangsiense* as a synonym of *G. hoehnelianum* after the studies on the holotype of *G. shangsiense*.

Ganoderma leucocontextum T.H. Li *et al.*, Mycoscience 56: 82. 2015. MycoBank MB 804187.

For a detailed description of *G. leucocontextum*, see Li *et al.* (2015).

Notes: *Ganoderma leucocontextum* as a member of the *G. lucidum* complex shares reddish brown and laccate pilei and truncated basidiospores, but it is distinguished by the white context Li *et al.* (2015). In the current study, *G. leucocontextum* grouped with *G. weixiense* (Fig. 1). According to the comparison between *G. leucocontextum* and *G. weixiense* in Ye *et al.* (2019), the size of pores (4–6 per mm *vs* 2–4 per mm) and basidiospores (9.5–12.5 × 7–9 µm *vs* 6–8 × 3–4 µm) are the main differences.

Ganoderma lingzhi Sheng H. Wu *et al.*, Fungal Divers. 56: 54. 2012. MycoBank MB 564240.

For a detailed description of *G. lingzhi*, see Cao *et al.* (2012).

Notes: Cao *et al.* (2012) revised the taxonomic status of the widely cultivated "*Ganoderma lucidum*" in China and described it as a new species called *G. lingzhi* based on geographical distribution, morphological features and phylogenetic analyses. *Ganoderma lingzhi* is widely distributed in temperate and subtropical areas of China, and it has also been reported from Korea and Laos (Kim *et al.* 2001, Hapuarachchi *et al.* 2019b).

Ganoderma lucidum (Curtis) P. Karst., Revue Mycol., Toulouse 3: 17. 1881. MycoBank MB 148413. Figs 47, 48.
Basionym: *Boletus lucidus* Curtis, Fl. Londin. 1: 72. 1781.
Synonym: *Ganoderma cantharelloideum* M.H. Liu, Acta Mycol. Sin. 8: 279. 1989.

Description: *Basidiomata* annual, laterally stipitate, hard corky to woody hard. *Pilei* solitary, variable, flabelliform or shell-like to circular, up to 11 cm diam and 3 cm thick. *Pileal surface* yellowish brown to reddish brown, laccate, glabrous, with concentric furrows; margin acute to obtuse, entire, slightly wavy. *Pore surface* white when fresh, turning darker when bruised, pale yellow to straw yellow when dry; pores circular, 4–6 per mm; dissepiments slightly thick, mostly entire. *Context* heterogeneous, the upper layer cream to buff, the lower layer clay-buff, without black melanoid lines, soft corky, up to 1.8 cm thick. *Tubes* pale brown, non-stratified, up to 1.2 cm long. *Stipe* reddish brown to purplish black, flattened to cylindrical, up to 12 cm long and 1.5 cm diam. *Hyphal system* trimitic; generative hyphae with clamp connections; all hyphae IKI –, CB +; tissues darkening in KOH. Generative hyphae in context colourless, thin-walled, 2.5–4 µm diam; skeletal hyphae in context pale yellowish brown, thick-walled with a narrow lumen or sub-solid, frequently arboriform and flexuous, 3–10 µm diam; binding hyphae in context colourless, thick-walled, branched and flexuous, 2–3 µm diam. Generative hyphae in tubes colourless, thin-walled, 2–3 µm diam; skeletal hyphae in tubes pale brown to dark brown, thick-walled with a narrow lumen or sub-solid, frequently arboriform and flexuous, 2–8 µm diam; binding hyphae in tubes colourless, thick-walled, branched and flexuous, 1–2.5 µm diam. *Pileipellis* composed of clamped generative hyphae, thick-walled to sub-solid, apical cells clavate, strongly inflated and flexuous, pale yellowish brown, about 30–50 × 8–16 µm, forming a regular palisade. *Cystidia* and *cystidioles* absent. *Basidia* absent; *basidioles* barrel-shaped, colourless, thin-walled, 20–25 ×9–12 µm. *Basidiospores* ellipsoid, truncated, pale yellowish brown, IKI –, CB +, double-walled with moderately to distinctly thick walls, exospore walls smooth, endospore walls with dense spinules, (7–)7.5–9.5(–10) × (5–)5.5–7(–7.5) µm, L = 8.52 µm, W = 6.2 µm, Q = 1.37 (n = 30/1, with the turgid vesicular appendix excluded); (8–)9–11(–11.5) × (5–)5.5–7(–8) µm, L = 10.05 µm, W = 6.45 µm, Q = 1.56 (n = 30/1, with the turgid vesicular appendix included).

Materials examined: **China**, Sichuan, Qingchuan County, Qingxi Town, on stump of *Quercus*, 31 Oct. 2016, Cui 14404 (BJFC029272), Cui 14405 (BJFC029273), Cui 14406 (BJFC029274); Yunnan, Kunming, Xiaoshao Forest Farm, on rotten angiosperm wood, 1 Jul. 2019, Dai 20017 (BJFC031691).

Notes: *Ganoderma lucidum* was firstly described from London in the UK. It is the type species of *Ganoderma* and has the typical ganodermoid characters, such as stipitate basidiomata with laccate pileal surface, and truncated basidiospores with spinules on the endospore walls (Steyaert 1972, Ryvarden 2004b). Cao (2013) suggested that *G. cantharelloideum* should be treated as a synonym of *G. lucidum* according to the original description and observations on the holotype of *G. cantharelloideum*. In the current phylogenetic study, the *G. lucidum* lineage consisted of specimens collected from the UK, Czech Republic and China with high divergence (Figs 1, 2). The divergence in *G. lucidum* groups also appeared in phylogenetic analyses inferred from single or multiple genes by Zhou *et al.* (2015), Hapuarachchi *et al.* (2018b), Liu *et al.* (2019) and Luangharn *et al.* (2021). This may be caused by geographic separation. An essential systemic study of the *G. lucidum* lineage should be conducted based on more specimens from different regions and more gene markers.

Ganoderma magniporum J.D. Zhao & X.Q. Zhang, Acta Mycol. Sin. 3: 15. 1984. MycoBank MB 124473.

For a detailed description of *G.a magniporum*, see Zhao *et al.* (1984).

Notes: *Ganoderma magniporum* was described from Guangxi of South China based on its small and nearly black pilei, large pores (2–2.5 per mm), and ellipsoid basidiospores (8.7–10.4 × 5.2–7 µm, Zhao *et al.* 1984). Cao (2013) observed the type specimen (HMAS 42696) of *G. magniporum*, and stated it was immature and had smaller basidiospores than another specimen (Zhou 439) collected from Guangxi. In the current study, one specimen collected from Yunnan grouped with *G. magniporum*.

Fig. 47. Basidiomata of *Ganoderma lucidum*.

Ganoderma multipileum Ding Hou, Quarterly Journal of the Taiwan Museum 3: 101. 1950. MycoBank MB 344109.
Synonym: *Ganoderma chenghaiense* J.D. Zhao, Acta Mycol. Sin. 8: 31. 1989.

For a detailed description of *Ganoderma multipileum*, see Wang *et al.* (2009).

Notes: *Ganoderma multipileum* was described from Taiwan (China) based on its imbricate basidiomata with yellowish brown to reddish brown pileal surface, small pores (6–8 per mm), corky context, and ellipsoid to ovoid basidiospores (Wang *et al.* 2009). Cao (2013) studied the holotype of *G. multipileum* and *G. chenghaiense*, and suggested that the latter should be a synonym of *G. multipileum* based on the morphological characters. As more specimens were collected, the distribution of *G. multipileum* became widespread, found in South China, Laos and India. In the phylogenetic analysis, one specimen collected from the type locality was included and *G. multipileum* formed a stable lineage with good support (Fig. 1).

Ganoderma mutabile Y. Cao & H.S. Yuan, Mycol. Prog. 12: 122. 2013. MycoBank MB 563047. Figs 49, 50.

Description: *Basidiomata* perennial, sessile, hard corky to woody hard. *Pilei* solitary, flabelliform to shell-like, up to 18 cm diam and 7 cm thick. *Pileal surface* reddish brown to purplish brown, laccate, glabrous, with concentric furrows; margin obtuse, entire, slightly wavy. *Pore surface* white when fresh, turning darker when bruised, dark brown when dry; pores circular to angular, 4–5 per mm; dissepiments moderately thick, entire. *Context* brown, homogeneous, with black melanoid lines, hard corky, up to 3 cm thick. *Tubes* brown, stratified, up to 4 cm long. *Hyphal system* trimitic; generative hyphae with clamp connections; all hyphae IKI –, CB +; tissues darkening in KOH. Generative hyphae in context colourless, thin-walled, 2–3.5 µm diam; skeletal hyphae in context pale brown, thick-walled with a narrow lumen or sub-solid, frequently arboriform and flexuous, 2–5.5 µm diam; binding hyphae in context colourless, thick-walled, branched and flexuous, 1–2.5 µm diam. Generative hyphae in tubes colourless, thin-walled, 2–3 µm diam; skeletal hyphae in tubes pale brown, thick-walled with a narrow lumen or sub-solid, frequently arboriform and flexuous, 2–4.5 µm diam; binding hyphae in tubes colourless, thick-walled, branched and flexuous, 1–2.5 µm diam. *Pileipellis* composed of clamped generative hyphae, thick-walled to sub-solid, apical cells mostly with lateral outgrowths and protuberances, branched and flexuous, yellowish brown, about 40–65 × 4–9 µm, forming an irregular palisade. *Cystidia*, *cystidioles*, *basidia* and *basidioles* absent. *Basidiospores* broadly ellipsoid, truncated, pale yellowish brown, IKI –, CB +, double-walled with distinctly thick walls, exospore walls smooth, endospore walls with dense spinules, (7.5–)8–11(–11.5) × 5.5–7(–7.5) µm, L = 9.1 µm, W = 6.25 µm, Q = 1.46 (n = 30/1, with the turgid vesicular appendix excluded); (8.5–)9–12.5(–13) × (5.5–)6–7.5(–8) µm, L = 10.57 µm, W = 6.83 µm, Q = 1.55 (n = 30/1, with the turgid vesicular appendix included).

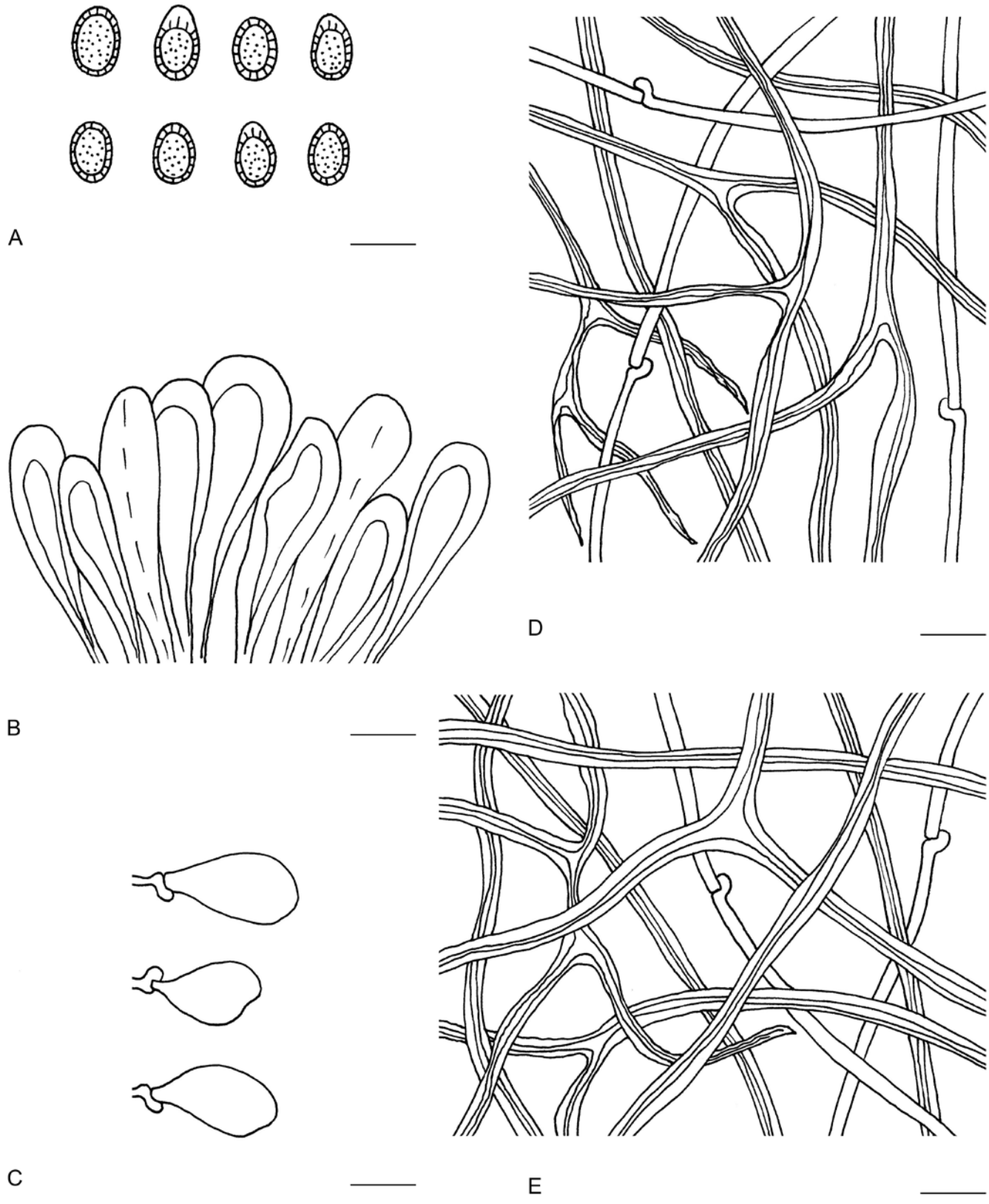

Fig. 48. Microscopic structures of *Ganoderma lucidum* (drawn from Dai 15805). **A.** Basidiospores. **B.** Apical cells from cuticle. **C.** Basidioles. **D.** Hyphae from trama. **E.** Hyphae from context. Scale bars = 10 μm.

Materials examined: **China**, Yunnan, Chuxiong, Zixishan Forest Park, on living tree of angiosperm, 8 Sep. 2006, **holotype** Yuan 2289 (IFP); Xinping County, Mopanshan Forest Park, on ground of mixed forest, 16 Aug. 2019, Dai 20414 (BJFC032082); Xizang, on angiosperm wood, Dec. 2018, Cui 17189 (BJFC030489).

Notes: *Ganoderma mutabile* was described from Yunnan in China based on the irregular apical cells of the pileipellis which are strongly flexuous and frequently branched Cao & Yuan (2012). Only one specimen was included in the original description, and in this study additional specimens were collected from Yunnan and Xizang.

Fig. 49. Basidiomata of *Ganoderma mutabile*.

Ganoderma orbiforme (Fr.) Ryvarden, Mycologia 92: 187. 2000. MycoBank MB 464692.
Basionym: *Polyporus orbiformis* Fr., Epicr. Syst. Mycol. (Upsaliae): 463. 1838.
Synonyms: *Ganoderma fornicatum* (Fr.) Pat., Bull. Soc. Mycol. Fr. 5: 71. 1889.
Ganoderma mastoporum (Lév.) Pat., Bull. Soc. Mycol. Fr. 5: 75. 1889.
Ganoderma subtornatum Murrill, Bull. Torrey Bot. Club 34: 477. 1907.
Ganoderma pygmoideum Steyaert, Bull. Jard. Bot. État Brux. 32: 103. 1962.
Ganoderma crebrostriatum J.D. Zhao & L.W. Hsu, Acta Mycol. Sin. 2: 161. 1983.
Ganoderma densizonatum J.D. Zhao & X.Q. Zhang, Acta. Mycol. Sin. 5: 86. 1986.
Ganoderma limushanense J.D. Zhao & X.Q. Zhang, Acta. Mycol. Sin. 5: 219. 1986.
Ganoderma diaoluoshanense J.D. Zhao & X.Q. Zhang, Acta Mycol. Sin. 6: 1. 1987.

For a detailed description of *G. orbiforme*, see Ryvarden (2000) and Wang *et al.* (2014).

Notes: *Polyporus orbiformis* was combined as *Ganoderma orbiforme* by Ryvarden (2000), while *G. boninense* and *G. pygmoideum* were considered as synonyms of *G. orbiforme* by Ryvarden (2000). The treatment of *G. boninense* as a synonym of *G. orbiforme* is not accepted by most other mycologists (Pilotti 2005). Wang *et al.* (2014) clarified the taxonomic status of *G. orbiforme* based on morphological and molecular data. *Ganoderma cupreum*, *G. densizonatum*, *G. fornicatum*, *G. limushanense*, *G. mastoporum* and *G. subtornatum* were treated as synonyms of *G. orbiforme* by Wang *et al.* (2014). Cao (2013) regarded *G. crebrostriatum* and *G. diaoluoshanense* as synonyms of *G. mastoporum* based on the observation of holotype specimens, while *G. crebrostriatum* and *G. diaoluoshanense* should be regarded as the synonyms of *G. orbiforme* according to the revision of *G. mastoporum* by Wang *et al.* (2014). In this study, two specimens of *G. cupreum* from Cameroon were included in the phylogenetic analyses, and they formed an independent lineage which is distinct from *G. orbiforme* (Fig. 1). Thus, *G. cupreum* should be treated as an independent species.

Ganoderma philippii (Bres. et Henn.) Bres., Iconogr. Mycol. 21: 1014. 1932. MycoBank MB 314321. Figs 51, 52.
Basionym: *Fomes philippii* Bres. & Henn. ex Sacc., Syll. Fung. (Abellini) 9: 180. 1891.

Description: *Basidiomata* annual or perennial, sessile and broadly attached, sometimes growing together, hard corky. *Pilei* solitary, variable, flabelliform to circular, applanate, up to 26 cm diam and 1.6 cm thick. *Pileal surface* pale brown to purplish black, dull, glabrous, with dense concentric zones; margin acute to obtuse, wavy like petal. *Pore surface* white when fresh, turning darker when bruised, pale brown when dry; pores circular to angular, 5–6 per mm;

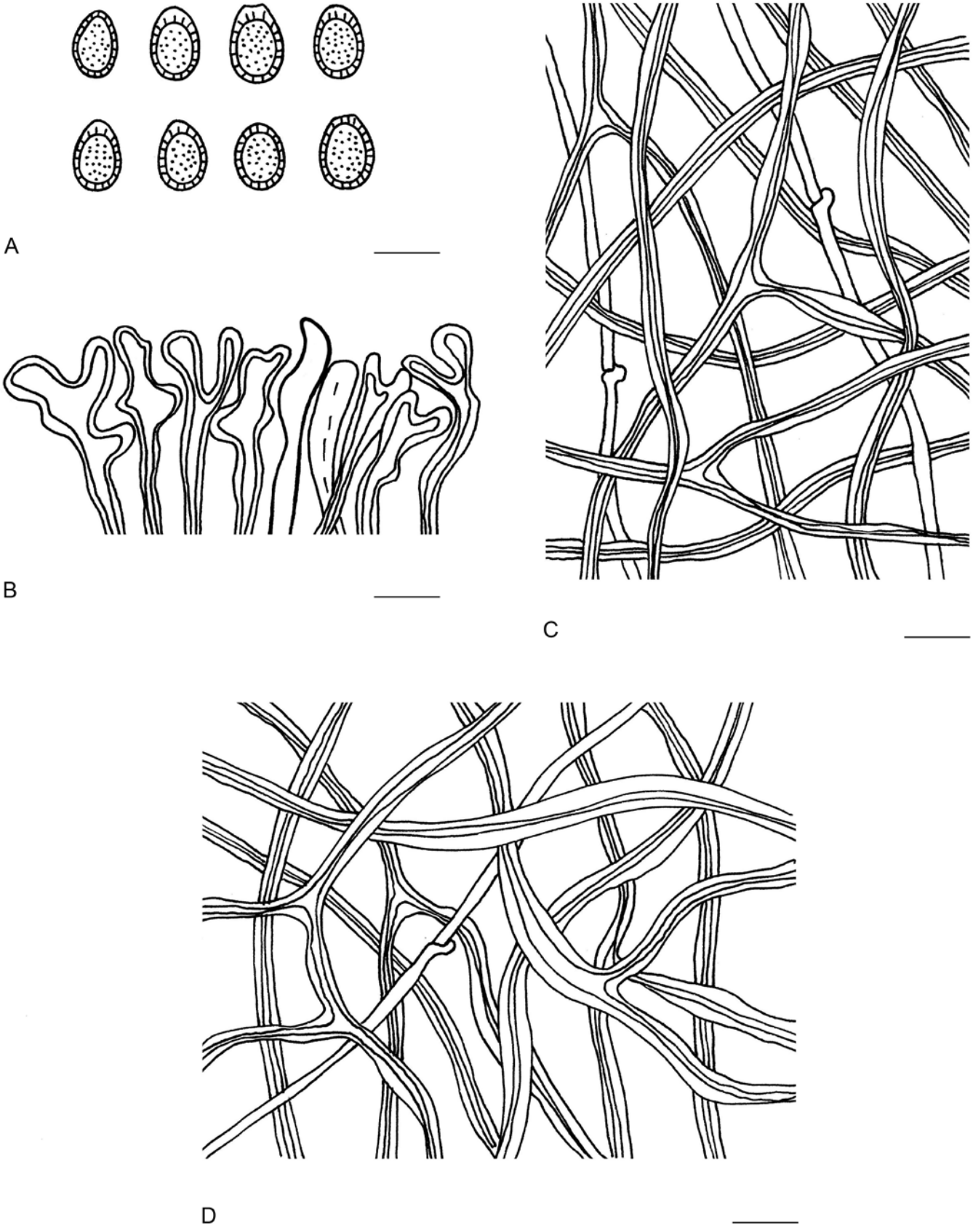

Fig. 50. Microscopic structures of *Ganoderma mutabile* (drawn from Cui 17189). **A.** Basidiospores. **B.** Apical cells from cuticle. **C.** Hyphae from trama. **D.** Hyphae from context. Scale bars = 10 µm.

dissepiments thin, mostly entire. *Context* brown, homogeneous, with black melanoid lines, hard corky, up to 1.4 cm thick. *Tubes* yellowish brown, non-stratified, up to 2 mm long. *Hyphal system* trimitic; generative hyphae with clamp connections; all hyphae IKI –, CB +; tissues darkening in KOH. Generative hyphae in context colourless, thin-walled, 2–3 µm diam; skeletal hyphae in context pale yellowish brown, thick-walled with a narrow lumen or sub-solid, arboriform and flexuous, 3–5 µm diam; binding hyphae in

Fig. 51. Basidiomata of *Ganoderma philippii*.

context colourless, thick-walled, branched and flexuous, 1–2 µm diam. Generative hyphae in tubes colourless, thin-walled, 1–3 µm diam; skeletal hyphae in tubes pale brown to dark brown, thick-walled with a narrow lumen or sub-solid, frequently arboriform and flexuous, 2–5 µm diam; binding in tubes colourless, thick-walled, branched and flexuous, 1–2 µm diam. *Cystidia*, *cystidioles*, *basidia* and *basidioles* absent. *Basidiospores* obovoid, not obviously truncated, with obvious vesicular appendix, pale yellowish brown, IKI –, CB +, double-walled with slightly thick walls, exospore walls smooth, endospore walls with dense spinules, 5–6 × 3–4 µm, L = 5.63 µm, W = 3.38 µm, Q = 1.67 (n = 30/1, with the turgid vesicular appendix excluded); 6–8 × 3–4 µm, L = 7.32 µm, W = 3.36 µm, Q = 2.18 (n = 30/1, with the turgid vesicular appendix included).

Materials examined: **China**, Hainan, Qiongzhong County, Limushan, on stump of *Hevea*, 9 Sep. 2016, Cui 14443 (BJFC029311), Cui 14444 (BJFC029311). **Singapore**, Bukit Timah Nature Reserve, on fallen trunk of angiosperm tree, 19 Jul. 2017, Dai 17828 (BJFC025360).

Notes: *Ganoderma philippii* was firstly described from Myanmar, and it has a wide distribution in South-East Asia including South China, Indonesia, Malaysia and Singapore (Steyaert 1972, Moncalvo & Ryvarden 1997). *Ganoderma philippii* can be distinguished by the sessile basidiomata with variable pilei, pale brown to purplish black pileal surface with dense concentric zones, small and obovoid basidiospores.

Ganoderma sanduense Hapuar. *et al.*, Mycosphere 8: 274. 2019. MycoBank MB 634622.

For a detailed description of *Ganoderma sanduense*, see Hapuarachchi *et al.* (2019b).

Notes: The type locality of *Ganoderma sanduense* is Sandu County of Guizhou Province in southwestern China. *Ganoderma stratoideum* was also described from Sandu County, and it shares layered, reddish black and laccate pilei, moderately sized pores (3–5 per mm), and heterogenous context with *G. sanduense* (He & Yu 1989). However, the small pilei (2–4 × 1–2.5 cm), greyish brown pore surface and larger basidiospores (12.1–13.8 × 9.2–10.5 µm) differentiate *G. sanduense* (Hapuarachchi *et al.* 2019b). The type specimen of *G. stratoideum* has been lost, and its taxonomic status is doubtful.

Ganoderma shanxiense L. Fan & H. Liu, Phytotaxa 406: 132. 2019. MycoBank MB 830632.

For a detailed description of *Ganoderma shanxiense*, see Liu *et al.* (2019).

Notes: *Ganoderma shanxiense* was described from Shanxi Province in China and is characterised by its basidiospores with a tapering and obtuse end at maturity (Liu *et al.* 2019). In the phylogenetic tree, *G. shanxiense* clustered with *G. chuxiongense* (Fig. 1) which

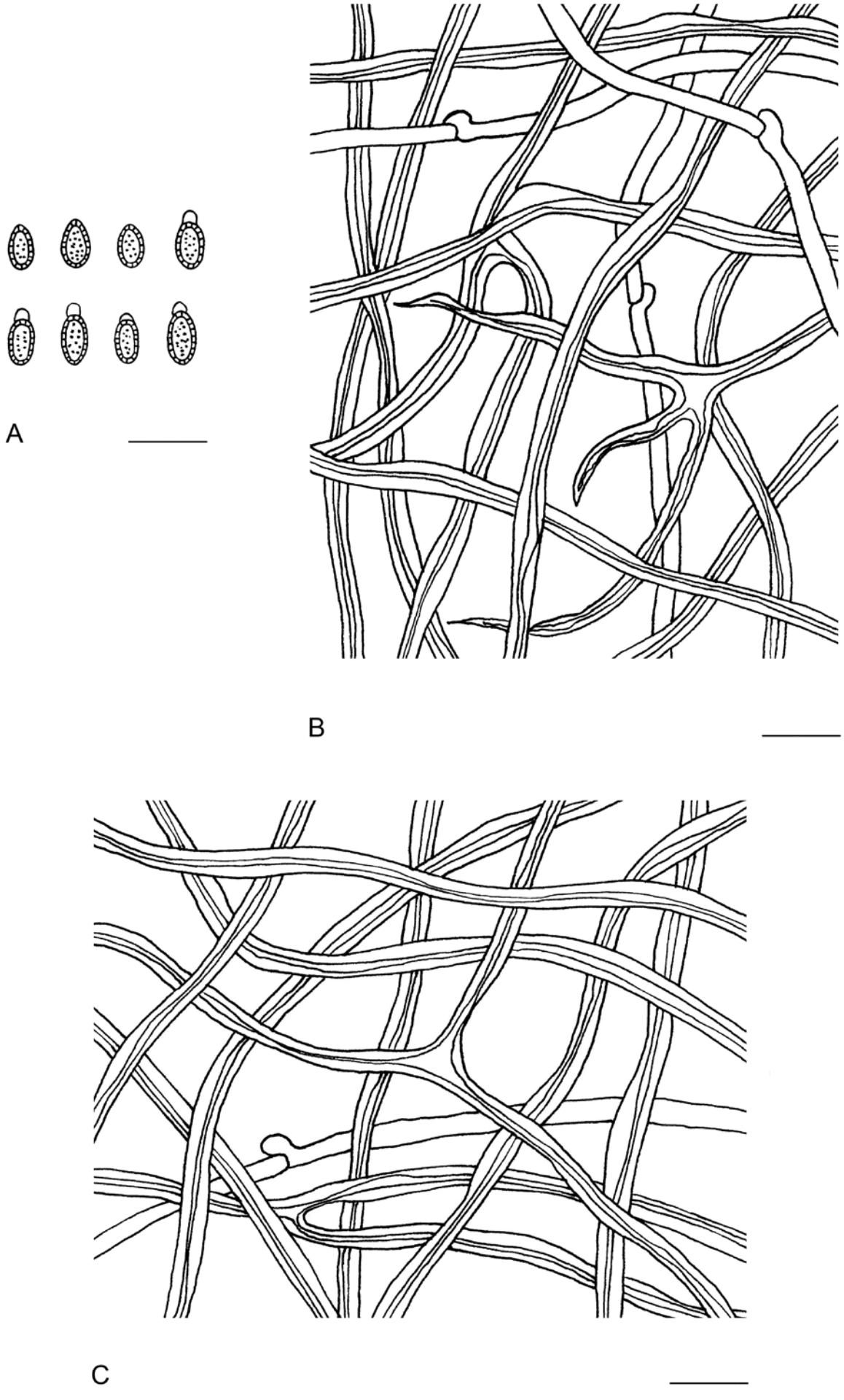

Fig. 52. Microscopic structures of *Ganoderma philippii* (drawn from Cui 14443). **A.** Basidiospores. **B.** Hyphae from trama. **C.** Hyphae from context. Scale bars = 10 µm.

was described from Yunnan Province, but the latter species differs by a purplish black and laccate pileal surface, greyish white pore surface with small pores (7–8 per mm), and broadly ellipsoid to ovoid basidiospores (10–12 × 7–8.5 µm).

Ganoderma sichuanense J.D. Zhao & X.Q. Zhang, Acta. Mycol. Sin. 2: 159. 1983. MycoBank MB 107984.

For a detailed description of *Ganoderma sichuanense*, see Zhao *et al.* (1983) and Wang *et al.* (2012).

Notes: *Ganoderma sichuanense* was first described from Sichuan Province by Zhao *et al.* (1983). Since then, more specimens have been collected from Guangdong, Guangxi of China and Sri Lanka. Phylogenetically, *G. weberianum* grouped with *G. sichuanense* which is consistent with Hapuarachchi *et al.* (2019b). Further studies are needed to clarify the relationship between *G. weberianum* and *G. sichuanense*.

Ganoderma sinense J.D. Zhao *et al.*, Acta Microbiol. Sin. 19: 272. 1979. MycoBank MB 314325. Figs 53, 54.
Synonyms: *Ganoderma austrofujianense* J.D. Zhao *et al.*, Acta Microbiol. Sin. 19: 274. 1979.
Ganoderma luteomarginatum J.D. Zhao *et al.*, Acta Microbiol. Sin. 19: 274. 1979.
Ganoderma formosanum T.T. Chang & T. Chen, Trans. Br. Mycol. Soc. 82: 731. 1984.
Ganoderma guinanense J.D. Zhao & X.Q. Zhang, Acta Mycol. Sin. 6: 4. 1987.
Ganoderma mediosinense J.D. Zhao, Acta Mycol. Sin. 7: 205. 1988.

Description: *Basidiomata* annual, laterally stipitate, hard corky to woody hard. *Pilei* solitary, variable, flabelliform to reniform or circular, up to 14 cm diam and 1.6 cm thick. *Pileal surface* reddish brown to purplish black, strongly laccate, glabrous, with concentric furrows and radial wrinkles; margin acute to obtuse, entire, slightly incurved. *Pore surface* white when fresh, turning darker when bruised, light buff when dry; pores circular to angular, 3–5 per mm; dissepiments thin, mostly entire. *Context* heterogeneous, the upper layer white to buff, the lower layer pale brown to yellowish brown, with black melanoid lines, hard corky, up to 3 cm thick. *Tubes* yellowish brown, non-stratified, up to 1.5 cm long. *Stipe* reddish brown to purplish black, flattened to cylindrical, up to 6 cm long and 2 cm diam. *Hyphal system* trimitic; generative hyphae with clamp connections; all hyphae IKI –, CB +; tissues darkening in KOH. Generative hyphae in context colourless, thin-walled, 2–4 µm diam; skeletal hyphae in context pale yellowish brown, thick-walled with a narrow lumen or sub-solid, arboriform and flexuous, 3–6 µm diam; binding hyphae in context colourless, thick-walled, branched and flexuous, 1.5–2.5 µm diam. Generative hyphae in tubes colourless, thin-walled, 1–3 µm diam; skeletal hyphae in tubes pale brown to dark brown, thick-walled with a narrow lumen or sub-solid, frequently arboriform and flexuous, 2–4 µm diam; binding hyphae in tubes colourless, thick-walled, branched and flexuous, 1–2 µm diam. *Pileipellis* composed of clamped generative hyphae, thick-walled to sub-solid, apical cells clavate, inflated, pale yellow to yellowish brown, about 40–55 × 6–12 µm, forming a

Fig. 53. Basidiomata of *Ganoderma sinense*.

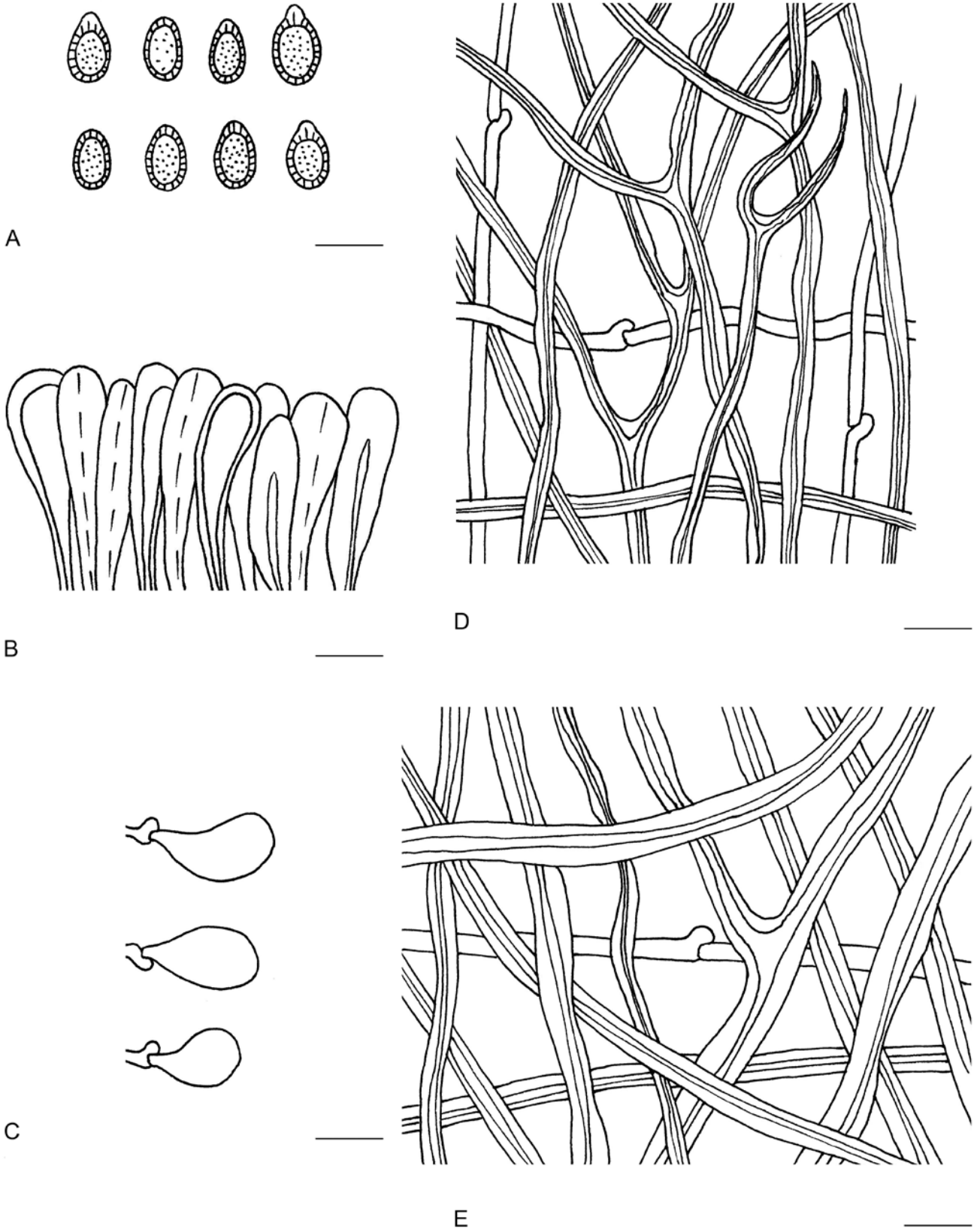

Fig. 54. Microscopic structures of *Ganoderma sinense* (drawn from Cui 14574). **A.** Basidiospores. **B.** Apical cells from cuticle. **C.** Basidioles. **D.** Hyphae from trama. **E.** Hyphae from context. Scale bars = 10 μm.

regular palisade. *Cystidia* and *cystidioles* absent. *Basidia* absent; *basidioles* barrel-shaped to clavate, colourless, thin-walled, 16–24 × 9–12 μm. *Basidiospores* ellipsoid, not obviously truncated, pale yellowish brown, IKI –, CB +, double-walled with moderately thick walls, exospore wall smooth, endospore wall with dense spinules, (11–)11.6–13.2(–13.7) × (7–)7.3–8.5(–8.8) μm, L = 12.39 μm, W = 7.99 μm, Q = 1.74 (n = 30/1, with the turgid vesicular appendix included).

Materials examined: **China**, Hainan, Lingshui County, Diaoluoshan Forest Park, on ground of angiosperm forest, 15 Jun. 2016, Cui 13825 (BJFC028691), Cui 13835 (BJFC028701); Guangxi, Jinxiu County,

Dayaoshan Nature Reserve, on stump of angiosperm tree, 15 Jul. 2017, Cui 14524 (BJFC029393), Cui 14526 (BJFC029395).

Notes: *Ganoderma sinense* was described from Hainan Province by Zhao *et al.* (1979), and it can be easily distinguished in the wild by its laterally stipitate basidiomata with dark reddish brown to purplish black and strongly laccate pileal surface. In this study, *G. sinense* clustered with *G. japonicum* with high support (Fig. 1) which is consistent with previous study by Hapuarachchi *et al.* (2019a). *Ganoderma japonicum* should be treated as a synonym of *G. sinense* temporarily based on the previous description and comments (Moncalvo & Ryvarden 1997, Liao *et al.* 2015, Hapuarachchi *et al.* 2019a). Wang (2005) and Cao (2013) also mentioned that *G. austrofujianense*, *G. formosanum*, *G. guinanense*, *G. luteomarginatum* and *G. mediosinense* are synonyms of *G. sinense* after studying the type specimens.

Ganoderma tropicum (Jungh.) Bres., Annls Mycol. 8: 586. 1910. MycoBank MB 149294. Figs 55, 56.
Basionym: *Polyporus tropicus* Jungh., Verh. Batav. Genootsch. Kunst. Wet. 17: 63. 1838.

Description: *Basidiomata* annual to perennial, usually sessile, sometimes laterally stipitate, hard corky to woody hard. *Pilei* solitary, variable, flabelliform to shell-shaped or circular, up to 17 cm diam and 3 cm thick. *Pileal surface* reddish brown to dark brown, strongly laccate, glabrous, with obvious concentric zones; margin acute to obtuse, entire or sometimes lacerated. *Pore surface* white when fresh, turning darker when bruised, straw yellow when dry; pores circular to angular, 4–6 per mm; dissepiments slightly thick to moderately thick, mostly entire. *Context* dark brown, homogeneous, with black melanoid lines, corky, up to 2.2 cm thick. *Tubes* brown, non-stratified, up to 8 mm long. *Stipe* reddish brown to purplish black, flattened to cylindrical, up to 6 cm long and 1.2 cm diam. *Hyphal system* trimitic; generative hyphae with clamp connections; all hyphae IKI –, CB +; tissues darkening in KOH. Generative hyphae in context colourless, thin-walled, 2.5–3.5 µm diam; skeletal hyphae in context pale yellowish brown, thick-walled with a wide to narrow lumen or sub-solid, frequently arboriform and flexuous, 2.5–6 µm diam; binding hyphae in context colourless, thick-walled, branched and flexuous, 1–2 µm diam. Generative hyphae in tubes colourless, thin-walled, 2–3 µm diam; skeletal hyphae in tubes pale brown to dark brown, thick-walled with a narrow lumen or sub-solid, frequently arboriform and flexuous, 2–4 µm diam; binding hyphae in tubes colourless, thick-walled, branched and flexuous, 0.5–1 µm diam. *Pileipellis* composed of clamped generative hyphae, thick-walled to sub-solid, apical cells clavate, sometimes branched or protuberant, inflated and flexuous, yellowish brown, about 19–32 × 4–9 µm, forming a regular palisade. *Cystidia*, *cystidioles*, *basidia* and *basidioles* absent. *Basidiospores* ellipsoid, truncated, pale yellowish brown, IKI –, CB +, double-walled with slightly thick walls, exospore walls smooth, endospore walls with dense spinules, (6.5–)7–8.5(–9) × (4.5–)5–6(–6.5) µm, L = 7.73 µm, W = 5.66 µm, Q = 1.37 (n = 30/1, with the turgid vesicular appendix excluded); (6.8–)7–9.6(–10) × (4–)4.5–6.2(–6.4) µm, L = 8.90 µm, W = 5.56 µm, Q = 1.60 (n = 30/1, with the turgid vesicular appendix included).

Materials examined: **China**, Hainan, Haikou, Jinniuling Park, on stump of *Acac*ia, 7 Jun. 2016, Dai 16434 (BJFC022551); Guangdong, Maoming, Dianbai, on dead tree of *Casuarina*, 3 Jun. 2019, Dai 19679 (BJFC031355); Guangxi, Baise, Baise Uprising Memorial Park, on living tree of *Acacia*, 1 Jul. 2019, Cui 20029 (BJFC031703). **Sri Lanka**, Colombo, Dombagaskarda Forest Reserve, on living tree of angiosperm, 27 Feb. 2019, Dai 19491 (BJFC031171). **Vietnam**, Ho Chi Minh City, Botanical Garden, on living tree of *Diospyros bejandii*, 11 Oct. 2017, Cui 16369 (BJFC029668).

Fig. 55. Basidiomata of *Ganoderma tropicum*.

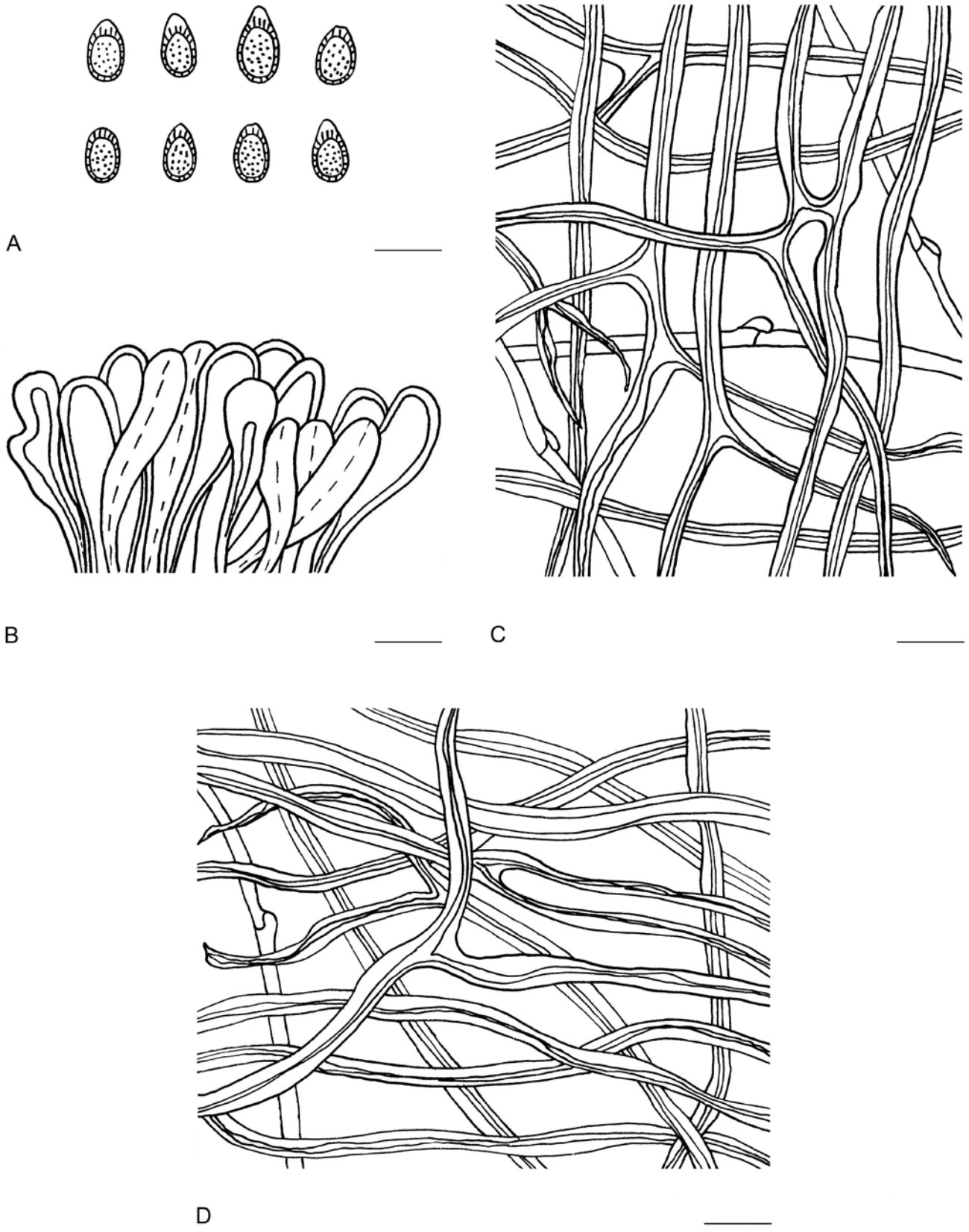

Fig. 56. Microscopic structures of *Ganoderma tropicum* (drawn from Cui 16341). **A.** Basidiospores. **B.** Apical cells from cuticle. **C.** Hyphae from trama. **D.** Hyphae from context. Scale bars = 10 µm.

Notes: *Ganoderma tropicum* was described from Indonesia, and it is characterised by the sessile to woody hard basidiomata, a strongly laccate pileal surface with obvious concentric zones, dark brown context, sometimes branched or protuberant apical cells of pileipellis, and ellipsoid basidiospores with dense spinules on the endospore walls (Steyaert 1972, Ryvarden 1981). These features are consistent with the observation in this study, and all specimens used in the phylogenetic analysis clustered together with high support (Fig. 1).

Ganoderma tsugae Murrill, Bull. Torrey Bot. Club 29: 601. 1902. MycoBank MB 239416. Figs 57, 58.

Description: *Basidiomata* annual, laterally stipitate, hard corky to woody hard. *Pilei* solitary, flabelliform, up to 20 cm diam and 4 cm thick. *Pileal surface* pale yellowish brown to reddish brown, strongly laccate, glabrous, with distinct concentric furrows and slightly radial wrinkles; margin acute to obtuse, lacerated like petals, slightly incurved when dry. *Pore surface* white when fresh, turning darker when bruised, pale yellowish brown when dry; pores circular to angular, 4–6 per mm; dissepiments moderately thick, mostly entire. *Context* heterogeneous, the upper layer white, the lower layer pale brown to yellowish brown, without black melanoid lines, hard corky, up to 2.2 cm thick. *Tubes* yellowish brown, non-stratified, up to 1.5 cm long. *Stipe* reddish brown to purplish black, flattened to cylindrical, up to 6 cm long and 2 cm diam. *Hyphal system* trimitic; generative hyphae with clamp connections; all hyphae IK I–, CB +; tissues darkening in KOH. Generative hyphae in context colourless, thin-walled, 2–3 µm diam; skeletal hyphae in context pale yellowish brown, thick-walled with a narrow lumen or sub-solid, arboriform and flexuous, 2.5–6.5 µm diam; binding hyphae in context colourless, thick-walled, branched and flexuous, 0.5–2 µm diam. Generative hyphae in tubes colourless, thin-walled, 1.5–3 µm diam; skeletal hyphae in tubes pale brown to dark brown, thick-walled with a narrow lumen or sub-solid, frequently arboriform and flexuous, 1.5–4 µm diam; binding hyphae in tubes colourless, thick-walled, branched and flexuous, 0.5–2 µm diam. *Pileipellis* composed of clamped generative hyphae, thick-walled, apical cells clavate, inflated, yellowish brown, about 30–45 × 5–10 µm, forming a regular palisade. *Cystidia* and *cystidioles* absent. *Basidia* barrel-shaped, colourless, thin-walled, 22–28 × 12–18 µm; *basidioles* broadly clavate, colourless, thin-walled, 18–23 × 11–14 µm. *Basidiospores* ellipsoid, truncated, pale yellowish brown, IKI –, CB +, double-walled with moderately thick walls, exospore walls smooth, endospore walls with dense spinules, 8–10(–11) × 5–6.2 µm, L = 9.12 µm, W = 5.49 µm, Q = 1.66 (n = 30/1, with the turgid vesicular appendix excluded); 9–11(–12) × 5–6(–7) µm, L = 10.21 µm, W = 5.88 µm, Q = 1.74 (n = 30/1, with the turgid vesicular appendix included).

Materials examined: **China**, Jilin, Fusong County, Songjianghe Forest Park, on stump of *Larix*, 2 Aug. 2016, Cui 14110 (BJFC028978), Cui 14112 (BJFC028980); Xinjiang, Habahe County, Baihabahe Forest Park, on stump of *Larix*, 10 Sep. 2015, Dai 15851 (BJFC019952), Dai 15856 (BJFC019957). **USA**, Connecticut, on living tree of *Tusga*, 19 Jul. 2012, Dai 12751b (BJFC013059).

Notes: *Ganoderma tsugae* was described from the USA growing on *Tsuga canadensis* by Murrill (1902); it has been reported occurring on several genera of coniferous trees such as *Abies*, *Larix*, *Picea* and *Tsuga* (Steyaert 1980, Adaskaveg & Gilbertson 1986). *Ganoderma tsugae* grouped in the *G. lucidum* complex in the phylogenetic analyses (Fig. 1).

Ganoderma weberianum (Bres. & Henn. ex Sacc.) Steyaert, Persoonia 7: 79. 1972. MycoBank MB 314330. Figs 59, 60.

Fig. 57. Basidiomata of *Ganoderma tsugae*.

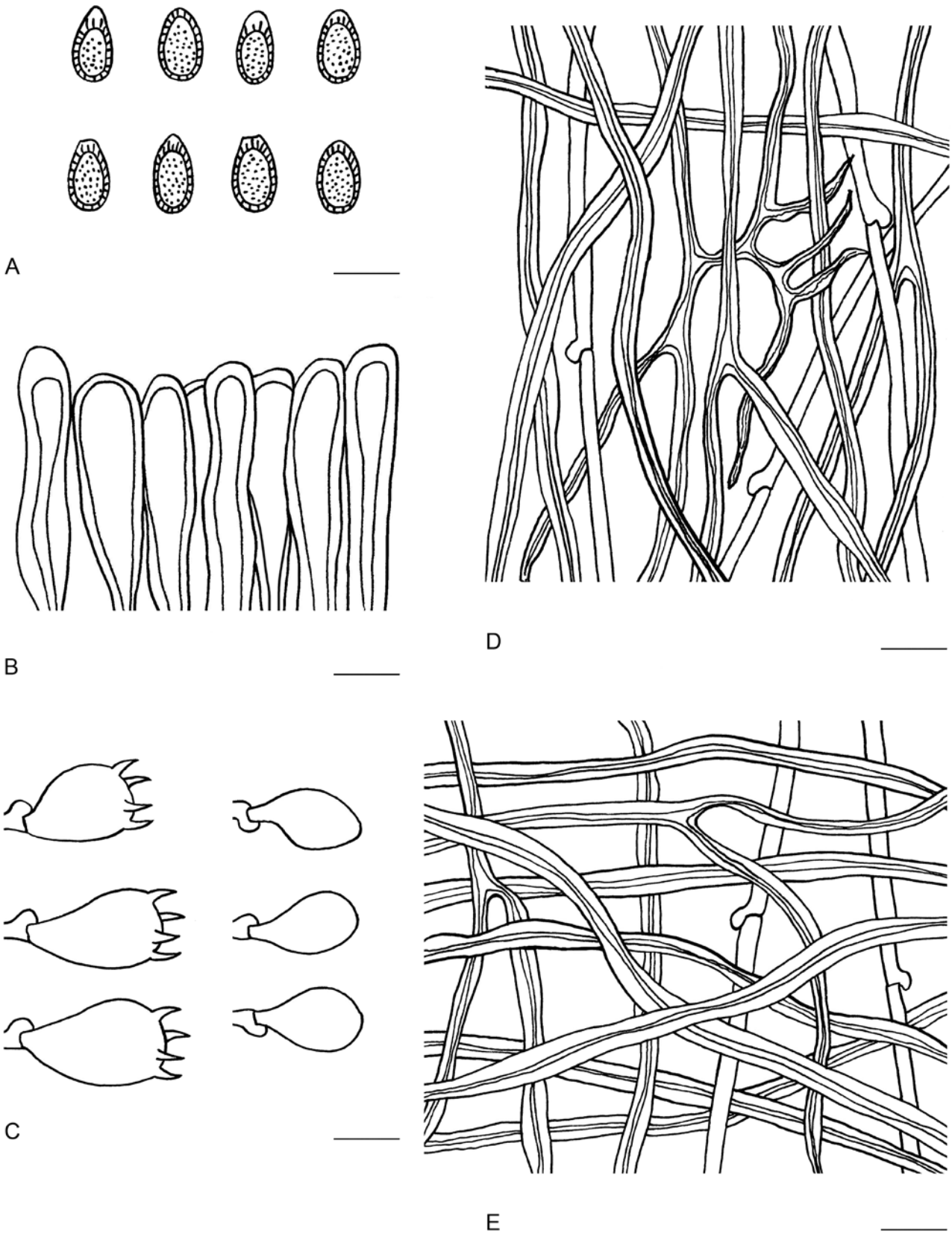

Fig. 58. Microscopic structures of *Ganoderma tsugae* (drawn from Cui 14554). **A.** Basidiospores. **B.** Apical cells from cuticle. **C.** Basidia and basidioles. **D.** Hyphae from trama. **E.** Hyphae from context. Scale bars = 10 µm.

Basionym: *Fomes weberianus* Bres. & Henn. ex Sacc., Syll. Fung. (Abellini) 9: 174. 1891.
Synonyms: *Ganoderma microsporum* R.S. Hseu, Mycotaxon 35: 36. 1989.
Ganoderma tenue J.D. Zhao *et al.*, Acta Microbiol. Sin. 19: 271. 1979.

Description: *Basidiomata* annual, sessile or with short stipe, usually growing together, imbricate, hard corky to woody hard. *Pilei* solitary, flabelliform, applanate, up to 14 cm diam and 8 mm thick. *Pileal surface* reddish brown to purplish black or near black, strongly laccate, glabrous, with concentrical bands and slightly radial wrinkles; margin acute, lacerated like petal, slightly incurved when

Fig. 59. Basidiomata of *Ganoderma weberianum*.

dry. *Pore surface* white when fresh, turning darker when bruised, pale yellow when dry; pores circular to angular, 4–6 per mm; dissepiments thin to slightly thick, mostly entire. *Context* greyish brown, homogeneous, without black melanoid lines, hard corky, up to 2 mm thick. *Tubes* pale brown to pale grey, non-stratified, up to 6 mm long. *Hyphal system* trimitic; generative hyphae with clamp connections; all hyphae IKI –, CB +; tissues darkening in KOH. Generative hyphae in context colourless, thin-walled, 2–4 µm diam; skeletal hyphae in context pale yellowish brown, thick-walled with a wide to narrow lumen or sub-solid, frequently arboriform and flexuous, 2.5–7 µm diam; binding hyphae in context colourless, thick-walled, branched and flexuous, 2–3 µm diam. Generative hyphae in tubes colourless, thin-walled, slightly swollen at the distal end, 2–3.5 µm diam; skeletal hyphae in tubes pale brown to dark brown, thick-walled with a narrow lumen or sub-solid, frequently arboriform and flexuous, 2–4.5 µm diam; binding hyphae in tubes colourless, thick-walled, branched and flexuous, 1.5–3 µm diam. *Pileipellis* composed of clamped generative hyphae, thick-walled to sub-solid, apical cells clavate, inflated, golden yellow, about 60–90 × 6–12 µm, forming a regular palisade. *Cystidia* and *cystidioles* absent. *Basidia* barrel-shaped, colourless, thin-walled, 15–35 × 13–18 µm; *basidioles* in shape like the basidia, colourless, thin-walled, 14–25 × 9–15 µm. *Basidiospores* subglobose to broadly ellipsoid, not obviously truncated, pale yellowish brown, IKI –, CB +, double-walled with slightly thick walls, exospore wall smooth, endospore wall with dense spinules, 6–7 × 4–6 µm, L = 6.53 µm, W = 5.13 µm, Q = 1.27 (n = 30/1, with the turgid vesicular appendix excluded).

Materials examined: **China**, Guangdong, Yangjiang, Jinshan Botanical Garden, on rotten stump of angiosperm tree, 3 Jun. 2019, Dai 19673 (BJFC031349); Maoming, Dianbai Region, on living tree of *Casuarina*, 3 Jun. 2019, Dai 19682 (BJFC031358); Zhanjiang, Guangdong Ocean University (Huguang Campus), on living tree of *Cinnamomum*, 4 Jun. 2019, Dai 19689 (BJFC031365). **Vietnam**, Ho Chi Minh City, United Palace Park, on living tree of *Cynometra dongnaiensis*, 10 Oct. 2017, Cui 16359 (BJFC029658), Cui 16360 (BJFC029659).

Notes: *Ganoderma weberianum* was first described from the Samoa Islands, and it probably has a worldwide tropical distribution (Steyaert 1972). Moncalvo *et al.* (1995) and Smith & Sivasithamparam (2003) mentioned that the ITS sequences of *G. weberianum* is almost the same to *G. microsporum* and suggested that *G. microsporum* should be treated as a synonym of *G. weberianum*. Cao (2013) regarded *Ganoderma tenue* as a synonym of *G. weberianum* based on the similar morphological characters such as reddish brown to purplish black pileal surface, apical cells of pileipellis regularly palisaded, and subglobose to broadly ellipsoid basidiospores.

Ganoderma weixiense Karun. & J.C. Xu, Phytotaxa 423: 78. 2019. MycoBank MB 646645.

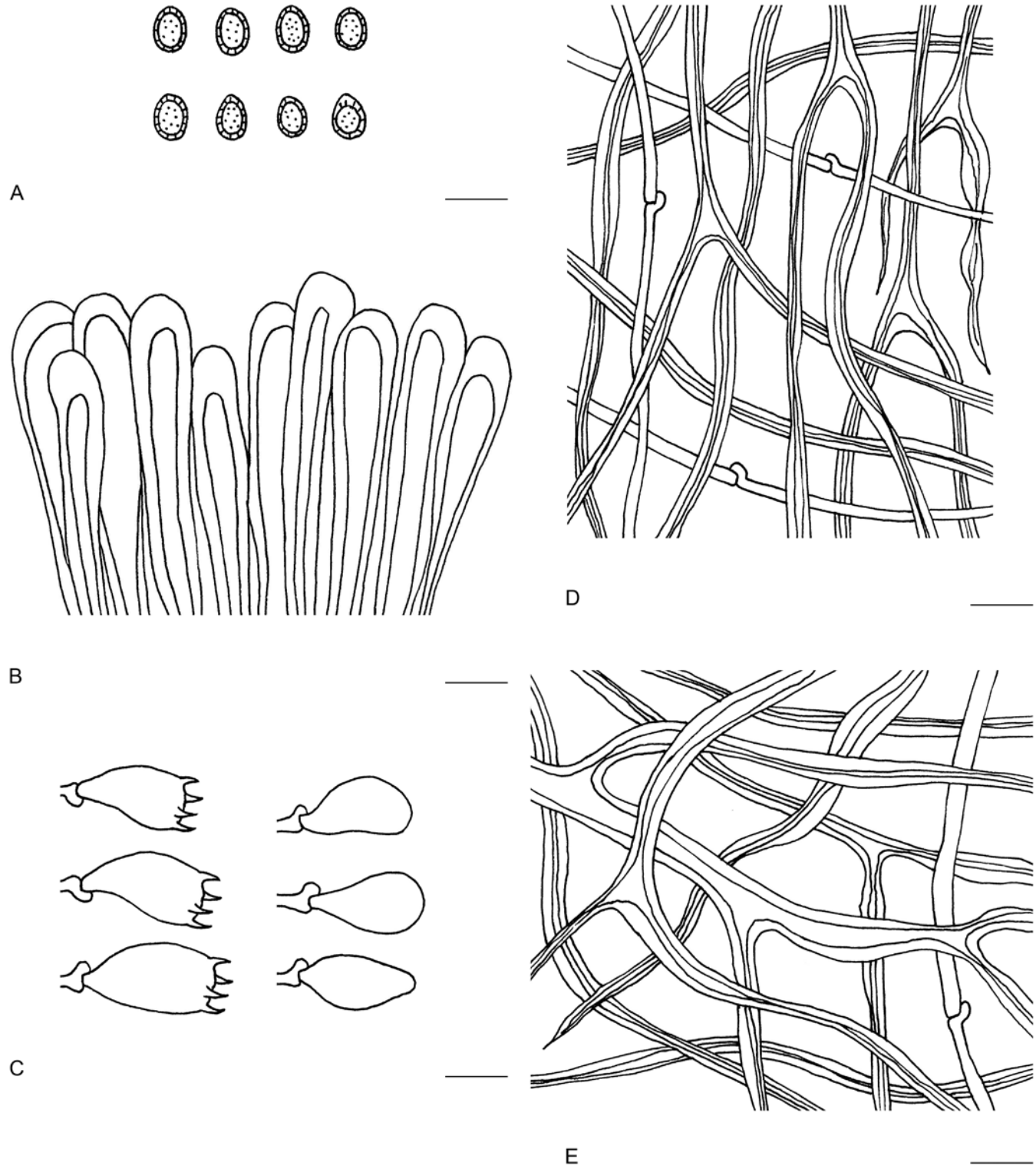

Fig. 60. Microscopic structures of *Ganoderma weberianum* (drawn from Cui 16360). **A.** Basidiospores. **B.** Apical cells from cuticle. **C.** Basidia and basidioles. **D.** Hyphae from trama. **E.** Hyphae from context. Scale bars = 10 µm.

For a detailed description of *Ganoderma weixiense*, see Ye *et al.* (2019).

Notes: *Ganoderma weixiense* was described from high altitude areas (altitude > 2 000 m) of Weixi County and Jinning in Yunnan Province. *Ganoderma leucocontextum* has similar morphological characters and close phylogenetic relationship with *G. weixiense* except the size of pores and basidiospores (details in notes of *G. leucocontextum*). In addition, *G. leucocontextum* shares similar climate and altitude habits with *G. weixiense*. In the current study, these two species grouped together, and it is quite difficult to separate them in morphology, ecology and phylogeny. The taxonomic status of *G. weixiense* needs to be clarified in further studies.

Ganoderma williamsianum Murrill, Bull. Torrey Bot. Club 34: 478. 1907. MycoBank MB 141987.
Synonym: *Ganoderma meijiangense* J.D. Zhao, Acta Mycol. Sin. 7: 16. 1988.

For a detailed description of *Ganoderma williamsianum*, see Wang &Wu (2010).

Notes: *Ganoderma williamsianum* was described from the Philippines and is easily confused with *G. acontextum*, *G. australe* and other non-laccate *Ganoderma* species in the wild as they all shared a hard and dull pileal surface. *Ganoderma williamsianum* is widely distributed in tropical areas of the Philippines, China, Malaysia, Singapore, Sri Lanka, Thailand and Vietnam. Wang & Wu (2010) studied specimens of *G. williamsianum* collected from Hainan and Yunnan provinces in China and the type specimen of *G. meijiangense*, and the latter was treated as a synonym of *G. williamsianum*.

Key to accepted species of *Ganoderma* in China

1a. Endospore wall smooth 2
1b. Endospore wall ornamented 3

2a. Basidiomata annual, pileal surface chestnut-colour, tubes non-stratified ..... *G. castaneum*
2b. Basidiomata perennial, pileal surface greyish brown, tubes stratified ..... *G. yunlingense*

3a. Pileal surface dull 4
3b. Pileal surface laccate 13

4a. Pilei imbricate, margin lacerated like petals ..... *G. puerense*
4b. Pilei solitary, margin entire 5

5a. Basidiospores subglobose ..... *G. hoehnelianum*
5b. Basidiospores broadly ellipsoid to ellipsoid or ovoid 6

6a. Tubes stratified 7
6b. Tubes non-stratified 8

7a. Context homogeneous; basidiospores 5.5–7 × 4.1–5.2 µm ..... *G. applanatum*
7b. Context heterogeneous; basidiospores 7–12 × 5–8 µm ..... *G. australe*

8a. Pores < 4 per mm ..... *G. tongshanense*
8b. Pores > 4 per mm 9

9a. Context without black melanoid lines; apical cells in cuticle branched ..... *G. ellipsoideum*
9b. Context with black melanoid lines; apical cells in cuticle unbranched 10

10a. Distributed in higher altitudes ..... *G. alpinum*
10b. Distributed in lower altitudes 11

11a. Apical cells in cuticle irregularly branched or with protuberances ..... *G. williamsianum*
11b. Apical cells in cuticle unbranched or without protuberances 12

12a. Pileal surface reddish brown to greyish brown, pores angular ..... *G. gibbosum*
12b. Pileal surface greyish brown to nearly black, pores circular ..... *G. guangxiense*

13a. Basidiomata sessile 14
13b. Basidiomata stipitate or with constricted short stipe 17

14a. Basidiospores almond-shaped ..... *G. angustisporum*
14b. Basidiospores ellipsoid to ovoid 15

15a. Apical cells in cuticle irregularly branched or with protuberances ..... *G. mutabile*
15b. Apical cells in cuticle unbranched or without protuberances 16

16a. Basidiomata small, pileal surface yellowish brown to reddish brown; basidiospores > 4 µm in width ..... *G. bubalinomarginatum*
16b. Basidiomata large, pileal surface dark brown to near black; basidiospores < 4 µm in width ..... *G. philippii*

17a. Pores < 3 per mm ..... *G. magniporum*
17b. Pores > 3 per mm 18

18a. Pileal surface nearly black 19
18b. Pileal surface pale brown to yellowish brown or reddish brown 23

19a. Stipe short or constricted at base, < 4 cm in length 20
19b. Stipe obviously long, > 4 cm in length 21

20a. Basidiospores subglobose to broadly ellipsoid, < 6 µm in width ..... *G. weberianum*
20b. Basidiospores broadly ellipsoid to ellipsoid or ovoid, > 6 µm in width ..... *G. orbiforme*

21a. Basidiospores truncated ..... *G. sanduense*
21b. Basidiospores not obviously truncated 22

22a. Pore surface grey to pale brown, pores 5–6 per mm; basidiospores 8–11 × 5.5–7 µm ..... *G. ahmadii*
22b. Pore surface white to buff, pores 3–5 per mm; basidiospores 11.6–13.2 × 7.3–8.5 µm ..... *G. sinense*

23a. Pore surface yellowish when fresh 24
23b. Pore surface white to cream or greyish white when fresh 25

24a. Pilei lobate, with dark red pileal surface ..... *G. chuxiongense*
24b. Pilei semicircle, shell-like, reniform to circular, with yellowish brown to reddish brown pileal surface ..... *G. lingzhi*

25a. Distributed in temperate or subtropical areas 26
25b. Distributed in subtropical or tropical areas 31

26a. Context white to cream ..... *G. leucocontextum*
26b. Context buff to brown 27

27a. Growing on coniferous trees ..... *G. tsugae*
27b. Growing on broad-leaf trees 28

28a. Basidiospores < 4 µm in width ..... *G. weixiense*
28b. Basidiospores > 4 µm in width 29

29a. Context with black melanoid lines ..... *G. sichuanense*
29b. Context without black melanoid lines 30

30a. Context heterogeneous; basidiospores 9–11 × 5.5–7 µm ..... *G. lucidum*
30b. Context homogeneous; basidiospores 11–13 × 8–9.5 µm ..... *G. shanxiense*

31a. Stipe short or constricted at base, < 6 cm in length 32
31b. Stipe obviously long, > 6 cm in length 34

32a. Growth on palm trees ..... *G. boninense*
32b. Growth on other trees 33

33a. Basidiomata small; apical cells in cuticle unbranched, basidiospores 10.7–12.8 × 5.7–9 µm ..... *G. subangustisporum*
33b. Basidiomata large; apical cells in cuticle branched or with protuberances, basidiospores 7–9.6 × 4.5–6.2 µm ..... *G. tropicum*

34a. Basidiomata laterally stipitate 35
34b. Basidiomata dorso-laterally stipitate 36

35a. Pilei solitary ..... *G. casuarinicola*
35b. Pilei imbricate ..... *G. multipileum*

36a. Context homogeneous, without black melanoid lines ..... *G. subflexipes*
36b. Context heterogeneous, with black melanoid lines 37

37a. Basidiospores larger, 8.5–12.6 × 7.2–9.1 µm ..... *G. calidophilum*
37b. Basidiospores smaller, 7–9 × 4.8–5.5 µm ..... *G. flexipes*

Haddowia Steyaert, Persoonia 7: 108. 1972. MycoBank MB 17717.

Type species: *Haddowia longipes* (Lév.) Steyaert

Description: *Basidiomata* annual, laterally stipitate, corky. *Pilei* solitary, sub-orbicular to flabelliform. *Pileal surface* yellowish brown to reddish brown or blackish brown, laccate, tomentose, concentrically zonate and furrowed, radial rugose. *Pore surface* white when fresh becoming straw yellow when dry; pores circular to angular; dissepiments thick, entire. *Context* white, corky. *Hyphal system* trimitic; generative hyphae colourless, thin-walled, with clamp connections; skeletal hyphae colourless to pale yellow, thick-walled, arboriform and flexuous; binding hyphae colourless, sub-solid, branched and flexuous. *Basidiospores* globose to ellipsoid, non-truncated, yellow to pale yellowish brown, double-walled with thick walls, exospore wall smooth and covering longitudinal crests, endospore wall with two longitudinal crests and transverse membranes.

Notes: *Haddowia* has similar basidiomata in shape and colour to *Ganoderma*, but differs by its non-truncated basidiospores which are double and thick-walled, a smooth exospore wall covering longitudinal crests, and an endospore wall with two longitudinal crests and transverse membranes. Although no outer wall on the basidiospores of *Haddowia* was observed by Steyaert (1972), and a smooth exospore wall exists according to the scanning electron micrographs of *Haddowia* species taken by Costa-Rezende *et al.* (2020b) and the current study (Fig. 8 E). In the phylogenetic analyses, *Ha. longipes* and *Ha. macropora* formed a distinct well-supported clade of *Ganodermataceae* (Fig. 1).

Haddowia macropora B.K. Cui, Vlasák & Y.F. Sun, ***sp. nov.*** MycoBank MB 839663. Figs 61, 62.

Diagnosis: Differs from other species in the genus by its yellowish brown to reddish brown pileal surface and large pores.

Etymology: *macropora* (*Lat.*), refers to the large pores.

Typus: **French Guiana** (**holotype** JV 1908/46).

Description: *Basidiomata* annual, laterally stipitate, corky. *Pilei* solitary, sub-orbicular to flabelliform, up to 4 cm diam and 1 mm thick. *Pileal surface* yellowish brown to reddish brown, strongly laccate, glabrous, with obvious concentric furrows and irregularly radial wrinkles; margin obtuse, entire, wavy when dry. *Pore surface* cream when fresh becoming dark when bruised; pores angular to irregular, 1–2 per mm; dissepiments slightly thick, entire. *Context* cream, without dark melanoid lines, soft corky, up to 1.5 mm thick. *Tubes* concolorous with context, up to 8.5 mm long. *Stipe* reddish-brown to purple-black, cylindrical and solid, up to 16.5 cm long and 6 mm diam. *Hyphal system* trimitic; generative hyphae with clamp connections, all the hyphae IKI + (dextrinoid), CB +; tissues darkening in KOH. Generative hyphae in context colourless, thin-walled, 2–3 µm diam; skeletal hyphae in context colourless to pale yellow, thick-walled with a wide to narrow lumen or sub-solid, frequently arboriform and flexuous, 2–5 µm diam; binding hyphae in context colourless, thick-walled, rarely branched and flexuous, 1–1.5 µm diam. Generative hyphae in tubes colourless, thin-walled, 2–3 µm diam; skeletal hyphae in tubes pale yellow, thick-walled with a wide to narrow lumen or sub-solid, frequently arboriform and flexuous, 2–4 µm diam; binding hyphae in tubes colourless, thick-

Fig. 61. Basidiomata of *Haddowia macropora*.

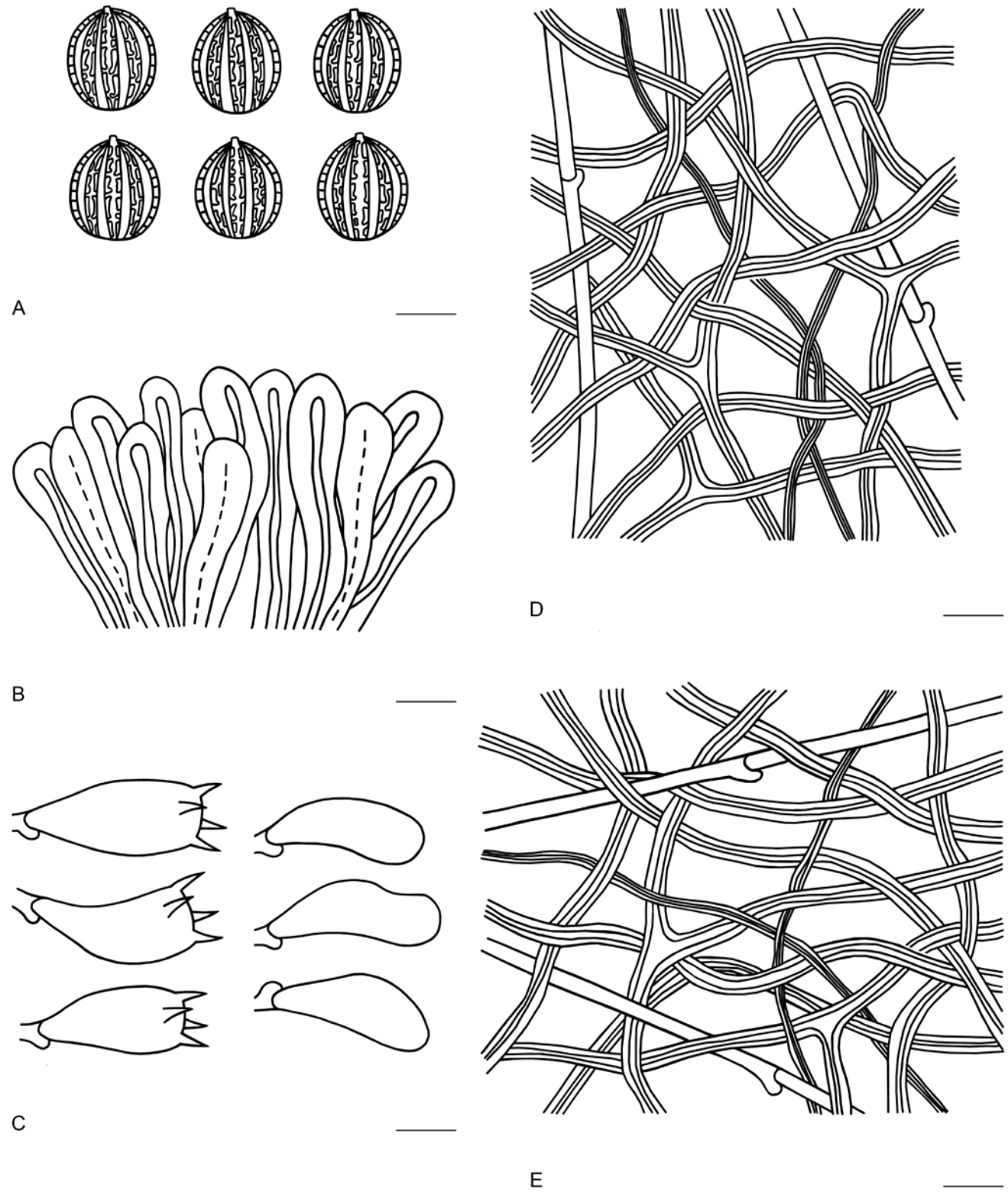

Fig. 62. Microscopic structures of *Haddowia macropora* (drawn from JV 1908/46). **A.** Basidiospores. **B.** Apical cells from cuticle. **C.** Basidia and basidioles. **D.** Hyphae from trama. **E.** Hyphae from context. Scale bars = 10 µm.

walled, rarely branched and flexuous, up to 1.5 µm diam. *Pileipellis* composed of clamped generative hyphae, thick-walled to subsolid, apical cells clavate, inflated and flexuous, yellowish brown, about 32–48 × 6–12 µm, forming a regular palisade. *Cystidia* and *cystidioles* absent. *Basidia* barrel-shaped, colourless, thin-walled, 23–32 × 14–17 µm; *basidioles* clavate, colourless, thin-walled, 21–30 × 7–15 µm. *Basidiospores* subglobose to broadly ellipsoid, pale yellowish brown, IKI + (dextrinoid), CB +, double-walled with distinctly thick walls, exospore wall smooth and covering longitudinal crests, endospore wall with intermittently longitudinal crests and transverse membranes, (13.6–)14–15.5(–16) × (12–)12.3–13.8(–14) µm, L = 14.64 µm, W = 13.08 µm, Q = 1.12 (n = 60/1).

Notes: *Haddowia macropora* has the typical basidiospores of *Haddowia* which differ from other genera in *Ganodermataceae* having intermittently longitudinal crests and transverse membranes on the endospore walls (Steyaert 1972). It can further be

distinguished by the yellowish brown to reddish brown pileal surface, and large pores. *Haddowia longipes* as the type species in this genus is quite different to *Ha. macropora* by the blackish brown pileal surface, thick context (4–5 mm), and ellipsoid basidiospores (12–19 × 10–14.5 µm, Steyaert 1972).

Key to accepted species of *Haddowia*

1a. Pileal surface yellowish brown to reddish brown, context thin (< 1.5 mm) ..... *Ha. macropora*
1b. Pileal surface blackish brown, context thick (4–5 mm) ..... *Ha. longipes*

Humphreya Steyaert, Persoonia 7: 98. 1972. MycoBank MB 17778.

Type species: *Humphreya lloydii* (Pat. & Har.) Steyaert.

For a detailed description of *Humphreya*, see Steyaert (1972).

Notes: *Humphreya* basidiospores have a typical ornamentation of reticulate or disjointed crests on the endospore walls which are different from other genera of *Ganodermataceae* (Steyaert 1972). Until now, *Humphreya* contained three species, *viz*., *Hu. eminii*, *Hu. endertii* and *Hu. lloydii*. No sequence data are available for *Humphreya*; thus, it is not included in the phylogenetic analyses of *Ganodermataceae*.

Key to accepted species of *Humphreya*

1a. Basidiospores more than 20 µm in length ..... *Hu. eminii*
1b. Basidiospores less than 20 µm in length 2

2a. Basidiomata up to 12 cm diam; basidiospores with reticulate ornamentation on the endospore wall ..... *Hu. lloydii*
2b. Basidiomata about 3 cm diam; basidiospores with disjointed crests on the endospore wall ..... *Hu. endertii*

Magoderna Steyaert, Persoonia 7: 111. 1972. MycoBank MB 18011.

Type species: *Magoderna subresinosum* (Murrill) Steyaert

Description: *Basidiomata* annual, sessile or stipitate, woody hard. *Pilei* solitary, sub-orbicular to infundibuliform. *Pileal surface* hair brown to coal black, dull to slightly shiny, glabrous, with concentric furrows and radial wrinkles. *Pore surface* buffy brown to pale grey brown when dry; pores circular to angular; dissepiments thick, entire. *Context* cream to buff, sometimes with dark melanoid lines, woody hard. *Hyphal system* trimitic; generative hyphae colourless, thin-walled, with clamp connections; skeletal hyphae near colourless, sub-solid, arboriform and flexuous; binding hyphae colourless, thick-walled, branched and flexuous. *Basidiospores* ellipsoid to ovoid, non- truncated, pale yellow, double and thick walled, exospore wall faintly verrucose, endospore wall with dense spinules.

Notes: *Magoderna* has a fibrous and pale white context, anticlinal hyphae in pileipellis, and ellipsoid to ovoid basidiospores without a truncated apex. Until now, *M. infundibuliforme* and *M. subresinosum* were accepted in *Magoderna*. In the phylogenetic analyses, the *Magoderna* clade was well supported and grouped with the *Neoganoderma* clade (Fig. 1).

Magoderna subresinosum (Murrill) Steyaert, Persoonia 7: 112. 1972. MycoBank MB 317117. Figs 63, 64.
Basionym: *Fomes subresinosus* Murrill, Bull. Torrey Bot. Club 35: 410. 1908.

Description: *Basidiomata* annual, sessile, woody hard. *Pilei* solitary, flabelliform, up to 12 cm diam and 3 cm thick. *Pileal surface* coal black, slightly shiny, glabrous, sticky, with obvious concentric furrows and strong radial wrinkles; margin subacute to obtuse, entire, incurved when dry. *Pore surface* pale greyish brown when dry; pores circular to angular, 4–5 per mm; dissepiments distinctly thick, entire. *Context* cream to pale wood brown, without dark melanoid lines, woody hard and fibrous, up to 1.3 cm thick. *Tubes* pale yellowish brown, up to 1.6 cm long. *Hyphal system* trimitic; generative hyphae with clamp connections, all hyphae IKI –, CB +; tissues slightly darkening in KOH. Generative hyphae in context colourless, thin-walled, 2–4 µm diam; skeletal hyphae in context colourless, sub-solid, arboriform and flexuous, 2–6 µm diam; binding hyphae in context colourless, thick-walled, branched and flexuous, up to 1 µm diam. Generative hyphae in tubes colourless, thin-walled, 2–3 µm diam; skeletal hyphae in tubes colourless, sub-solid, arboriform and flexuous, 2–4 µm diam; binding hyphae in tubes colourless, thick-walled, branched and flexuous, up to 1 µm diam. *Pileipellis* composed of clamped generative hyphae, thick-walled, apical cells clavate, inflated, dark brown, about 20–35 × 5–9 µm, anticlinal, forming a regular palisade. *Cystidia* and *cystidioles* absent. *Basidia* barrel-shaped, colourless, thin-walled, 20–25 × 18–20 µm; *basidioles* in shape like the basidia, colourless, thin-walled, 18–20 × 11–15 µm. *Basidiospores* ellipsoid to ovoid, non-truncated, pale yellow, IKI –, CB +, double-walled with slightly thick walls, exospore wall faintly verrucose, endospore wall with dense spinules, (14.7–)14.9–17.3(–18) × (9.6–)9.8–11.3(–11.8) µm, L = 15.88 µm, W = 10.52 µm, Q = 1.51 (n = 60/2).

Materials examined: **China**, Guangdong, Maoming, on living tree of *Casuarina*, Jun. 2017, Cui 14579 (BJFC029448), Cui 14580 (BJFC029449), Cui 14581 (BJFC029450). **Malaysia**, Selangor, Kota Damansara, National Forest Reserve, on dead angiosperm tree, 17 Apr. 2018, Dai 18626 (BJFC026914); on stump of angiosperm tree, 6 Dec. 2019, Cui 18262 (BJFC035121), Cui 18280 (BJFC035139).

Fig. 63. Basidiomata of *Magoderna subresinosum*.

Notes: *Magoderna subresinosum* is widely distributed in tropical and subtropical areas of Asia and Africa (Steyaert 1972). The taxonomic status of *M. subresinosum* was controversial for a long time. Humphrey (1938) regarded it as *Ganoderma subresinosum* due to the ganodermoid basidiomata. Corner (1983) suggested it should be placed in *Amauroderma* based on a similar hyphal system and similar basidiospores. However, it can be distinguished by a slightly shiny and sticky coal black pileal surface, pale and fibrous context, ellipsoid to ovoid and non-truncated basidiospores with faintly verrucose exospore wall and dense spinules on the endospore wall.

Key to accepted species of *Magoderna*

1a. Pileal surface snuff brown and dull; basidiospores smaller (9–10.5 × 8–9 µm ..... *M. infundibuliforme*
1b. Pileal surface coal black and slightly shiny; basidiospores larger (14.9–17.3 × 9.9–11.3 µm) ..... *M. subresinosum*

Neoganoderma B.K. Cui & Y.F. Sun, ***gen. nov.*** MycoBank MB 840978.

Diagnosis: Differs from other genera by its flat to convex pilei with brown pileal surface, cream context, slightly truncated basidiospores with longitudinal ridges on the endospore wall which are equal in length to the basidiospores.

Etymology: *neoganoderma* (*Lat.*), refers to the genus producing *Ganoderma*-like basidiomata and the distribution in the Neotropics.

Type species: *Neoganoderma neurosporum* (J.S. Furtado) B.K. Cui & Y.F. Sun

Description: *Basidiomata* annual, laterally stipitate or sessile, corky. *Pilei* solitary, flat to convex. *Pileal surface* reddish brown to dark brown, dull, glabrous, concentrically zonate and furrowed. *Pore surface* cream to pale cinnamon brown; pores circular. *Context* pallid white or cream, soft corky. *Hyphal system* dimitic; generative hyphae colourless, thin-walled, branched, with clamp connections; skeletal hyphae colourless to pale yellow, terminal arboriform or unbranched. *Basidiospores* ellipsoid, slightly truncated, pale yellow, double and thick-walled, endospore wall with longitudinal ridges which equal in length to the basidiospores.

Notes: So far, *Neoganoderma* includes *N. neurosporum* which has only been collected from Neotropics. The ganoderma-like basidiomata and haddowia-like ornamentation of endospore wall make *Neoganoderma* easily confused with *Ganoderma* and *Haddowia*, but *Neoganoderma* has unique basidiospores with longitudinal ridges on the endospore wall without obvious traverse ridges which are equal in length to the basidiospores. In the

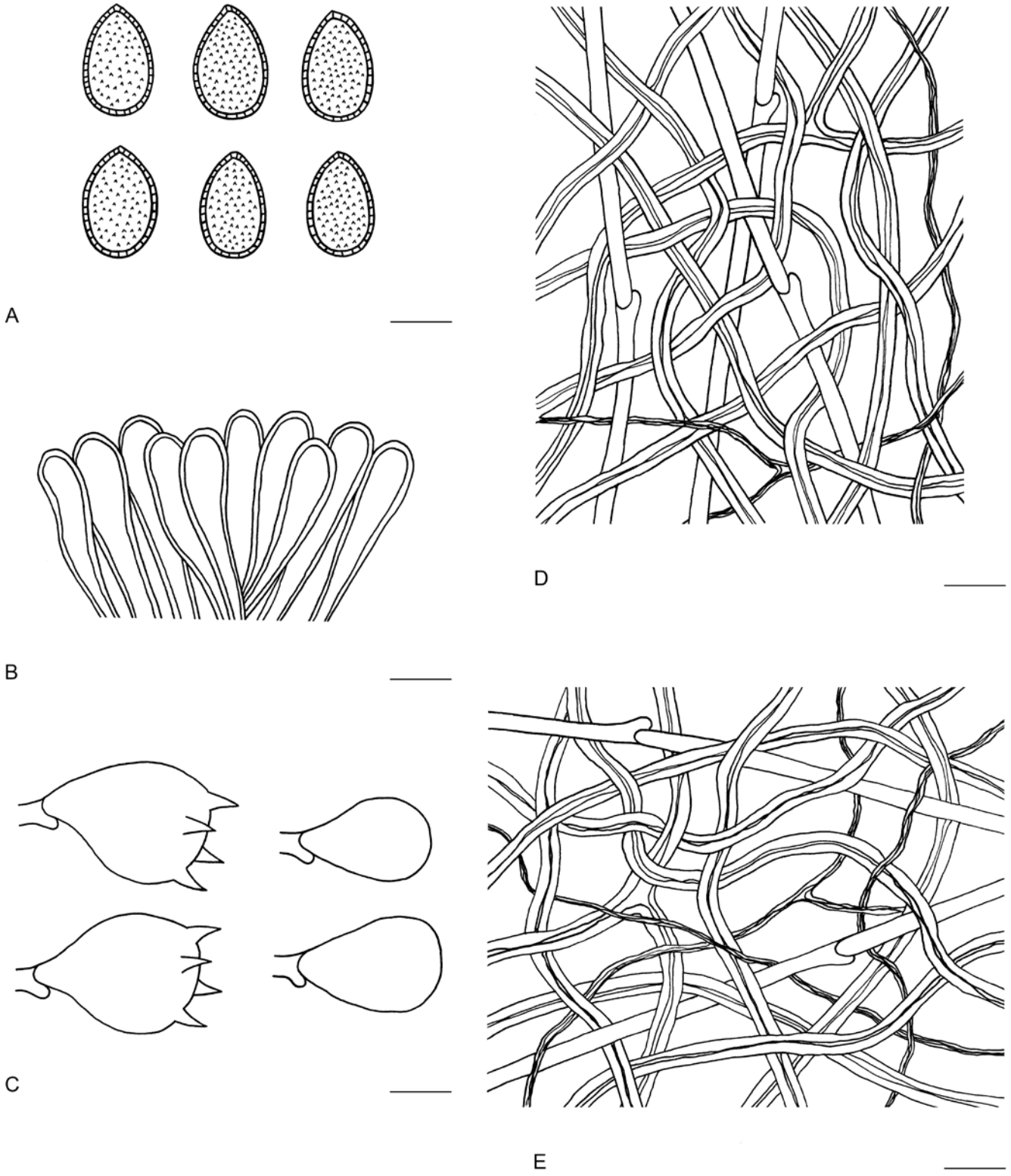

Fig. 64. Microscopic structures of *Magoderna subresinosum* (drawn from Cui 18280). **A.** Basidiospores. **B.** Apical cells from cuticle. **C.** Basidia and basidioles. **D.** Hyphae from trama. **E.** Hyphae from context. Scale bars = 10 µm.

phylogenetic analyses, *Neoganoderma* formed an independent clade distinct from other genera within *Ganodermataceae* and, so far, it is monotypic (Fig. 1).

Neoganoderma neurosporum (J.S. Furtado) B.K. Cui & Y.F. Sun, ***comb. nov.*** MycoBank MB 840979.
Basionym: *Ganoderma neurosporum* Furtado, Persoonia 4: 386. 1967.

Description: *Basidiomata* annual, laterally stipitate or sessile, corky. *Pilei* solitary, flat to convex, up to 15 cm diam and 3 cm thick. *Pileal surface* reddish brown to dark brown, dull, glabrous, with concentric furrows; margin obtuse, entire. *Pore surface* cream to pale cinnamon brown; pores circular, 4–5 per mm. *Context* pallid white or cream, soft corky, up to 2.5 cm thick. *Tubes* pale greyish brown, up to 1.5 cm long. *Stipe* dark brown, slightly swollen at base, up to 10 cm long and 1.5 cm diam. *Hyphal system* dimitic;

generative hyphae with clamp connections, colourless, thin-walled, branched, 2–5 µm diam; skeletal hyphae terminal arboriform or unbranched, colourless to pale yellow, 3–7 µm diam. *Pileipellis* composed of irregularly to slight anticlinal skeletal hyphae and thin generative hyphae. *Basidiospores* ellipsoid, slightly truncated, pale yellow, IKI–, double-walled with thick walls, endospore wall with longitudinal ridges which equal in length to basidiospores, 16–20 × 11–15 µm.

Notes: The brief description of *Neoganoderma neurosporum* was taken from Ryvarden (2004b) and Costa-Rezende *et al.* (2020b). According to the records, *N. neurosporum* is known from dead wood of deciduous trees in Neotropics. *Neoganoderma neurosporum* was placed in *Haddowia* by its similar endospore wall ornamentation, but no obvious traverse ridges were observed in *N. neurosporum* under SEM. Besides, *N. neurosporum* formed an independent lineage in the phylogenetic analyses (Fig. 1). More detailed description of *N. neurosporum* need to be made from future collections.

Sanguinoderma Y.F. Sun *et al.*, Persoonia 44: 224. 2020. MycoBank MB 828433.

Type species: *Sanguinoderma rude* (Berk.) Y.F. Sun *et al*.

For a detailed description of *Sanguinoderma*, see Sun *et al.* (2020).

Notes: *Sanguinoderma* was established by Sun *et al.* (2020) and 10 species were included in this genus. In this study, six new species are described based on the main distinguishing character of *Sanguinoderma i.e*., the fresh pore surface changes rapidly to blood red when bruised; there are other morphological features that differentiate it too.

Sanguinoderma guangdongense B.K. Cui & Y.F. Sun, ***sp. nov.*** MycoBank MB 839664. Figs 65, 66.

Diagnosis: Differs from other species in the genus by its dark pileal surface with shades of brown concentric zones and dense radial lines, fibrous context.

Etymology: *guangdongense* (*Lat.*), refers to the holotype of this species located at Guangdong.

Typus: **China**, Guangdong, Huizhou, on ground, 19 May 2019, Cui 17259 (**holotype** BJFC034117).

Additional materials examined: **China**, Guangdong, Shaoguan, Danxiashan Nature Reserve, on ground, 4 Jun. 2019, Cui 17240 (BJFC034098); Yunnan, Yuxi, Longquan Park, on ground of forest, 16 Aug. 2019, Dai 20419 (BJFC032087). **Thailand**, Chiang Mai, Doi Saket, on ground, 24 Jul. 2016, Dai 16724 (BJFC022831).

Description: *Basidiomata* annual, centrally to laterally stipitate, hard corky to woody hard. *Pilei* solitary, sub-orbicular to umbelliform, up to 8 cm diam and 7 mm thick. *Pileal surface* dark yellowish brown to near black, dull, tomentose, with shades of brown concentric zones and dense radial lines; margin obtuse, entire, wavy and obviously incurved when dry. *Pore surface* pale straw yellow when fresh

Fig. 65. Basidiomata of *Sanguinoderma guangdongense*.

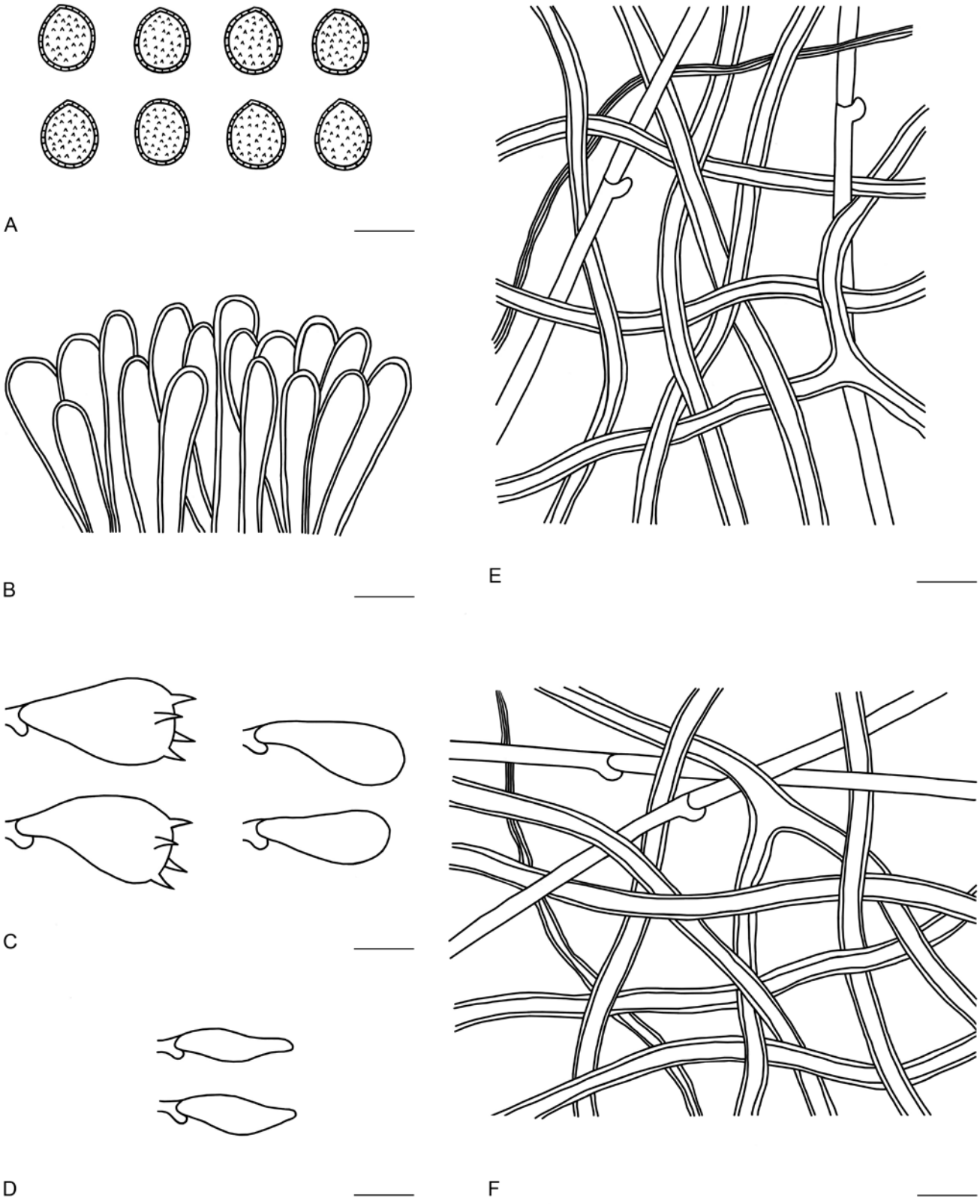

Fig. 66. Microscopic structures of *Sanguinoderma guangdongense* (drawn from Cui 17259). **A.** Basidiospores. **B.** Apical cells from cuticle. **C.** Basidia and basidioles. **D.** Cystidioles. **E.** Hyphae from trama. **F.** Hyphae from context. Scale bars = 10 µm.

becoming blood red when bruised and then quickly darkening; pores circular to angular or irregular, 5–7 per mm; dissepiments slightly thick, entire. *Context* wood brown to dark straw yellow, with dark melanoid lines, hard corky, fibrous, up to 4 mm thick. *Tubes* pale straw yellow to dark yellowish brown, up to 3 mm long. *Stipe* slightly darker than pileal surface, cylindrical and hollow, slightly swollen at base, up to 9.5 cm long and 6 mm diam. *Hyphal system* trimitic; generative hyphae with clamp connections, all hyphae IKI –, CB +; tissues darkening in KOH. Generative hyphae in context colourless, thin-walled, 4–5 µm diam; skeletal hyphae in context pale yellow, thick-walled with a wide lumen, arboriform and flexuous, 3–7 µm diam; binding hyphae in context colourless, thick-walled, rarely branched and flexuous, 1–2 µm diam. Generative hyphae in tubes colourless, thin-walled, 3–4 µm diam; skeletal hyphae in

tubes pale yellow, thick-walled with a wide lumen, arboriform and flexuous, 3–6 µm diam; binding hyphae in tubes colourless, thick-walled, rarely branched and flexuous, up to 2 µm diam. *Pileipellis* composed of clamped generative hyphae, slightly thick-walled, apical cells clavate, faintly inflated, dark yellowish brown, about 28–37 × 6–10 µm, forming a regular palisade. *Cystidia* absent; *cystidioles* fusiform, colourless, thin-walled, 14–20 × 4–7 µm. *Basidia* barrel-shaped to clavate, colourless, thin-walled, 18–25 × 10–15 µm; *basidioles* clavate, colourless, thin-walled, 14–20 × 8–13 µm. *Basidiospores* subglobose to broadly ellipsoid, pale yellow, IKI –, CB +, double-walled with slightly thick walls, exospore wall smooth, endospore wall with dense spinules, (9.4–)9.7–10.8(–11.2) × (8.8–)9–9.8(–10.2) µm, L = 10.26 µm, W = 9.28 µm, Q = 1.1 (n = 60/2).

Notes: *Sanguinoderma guangdongense* can be distinguished by a dark brown to almost black pileal surface with shades of brown concentric zones and dense radial lines. *Sanguinoderma microporum* shares the woody hard basidiomata and similar ornamentation of pilei with *Sa. guangdongense,* but *Sa. microporum* has a pale pileal surface, extremely thick dissepiments of micro pores and larger basidiospores (11–12 × 8.7–9.8 µm, Sun *et al.* 2020).

Sanguinoderma infundibulare B.K. Cui & Y.F. Sun, ***sp. nov.*** MycoBank MB 839665. Figs 67, 68.

Diagnosis: Differs from other species in the genus by its funnel-shaped pilei, yellowish brown to greyish brown pileal surface with dense and radial fine wrinkles.

Etymology: *infundibulare* (*Lat.*), refers to the funnel-shaped pilei.

Typus: **China**, Guangdong, Shaoguan, Danxiashan Nature Reserve, on ground, 4 Jun. 2019, Cui 17248 (**holotype** BJFC034106).

Additional materials examined: **China**, Guangdong, Shaoguan, Danxiashan Nature Reserve, on ground of angiosperm forest, 17 Dec. 2017, Dai 18148 (BJFC025677), Dai 18149 (BJFC025678), Dai 18151 (BJFC025680); 4 Jun. 2019, Cui 17238 (BJFC034096), Cui 17256 (BJFC034114).

Description: *Basidiomata* annual, centrally to laterally stipitate, hard corky. *Pilei* solitary, funnel-shape, up to 7.5 cm diam and 6 mm thick. *Pileal surface* yellowish brown to greyish brown, dull, tomentose, with obvious concentric zones, dense and radial fine wrinkles; margin slightly acute to obtuse, entire and slightly wavy when dry. *Pore surface* greyish white when fresh becoming to blood red when bruised and then quickly darkening; pores circular to angular, 4–6 per mm; dissepiments slightly thick, entire. *Context* pale wood brown to greyish brown, sometimes with dark melanoid lines, corky, up to 4 mm thick. *Tubes* pale grey to greyish brown, up to 2 mm long. *Stipe* concolorous with pileal surface, cylindrical and hollow, slightly swollen at base, up to 10 cm long and 7 mm diam. *Hyphal system* trimitic; generative hyphae with clamp connections, all hyphae IKI –, CB +; tissues darkening in

Fig. 67. Basidiomata of *Sanguinoderma infundibulare*.

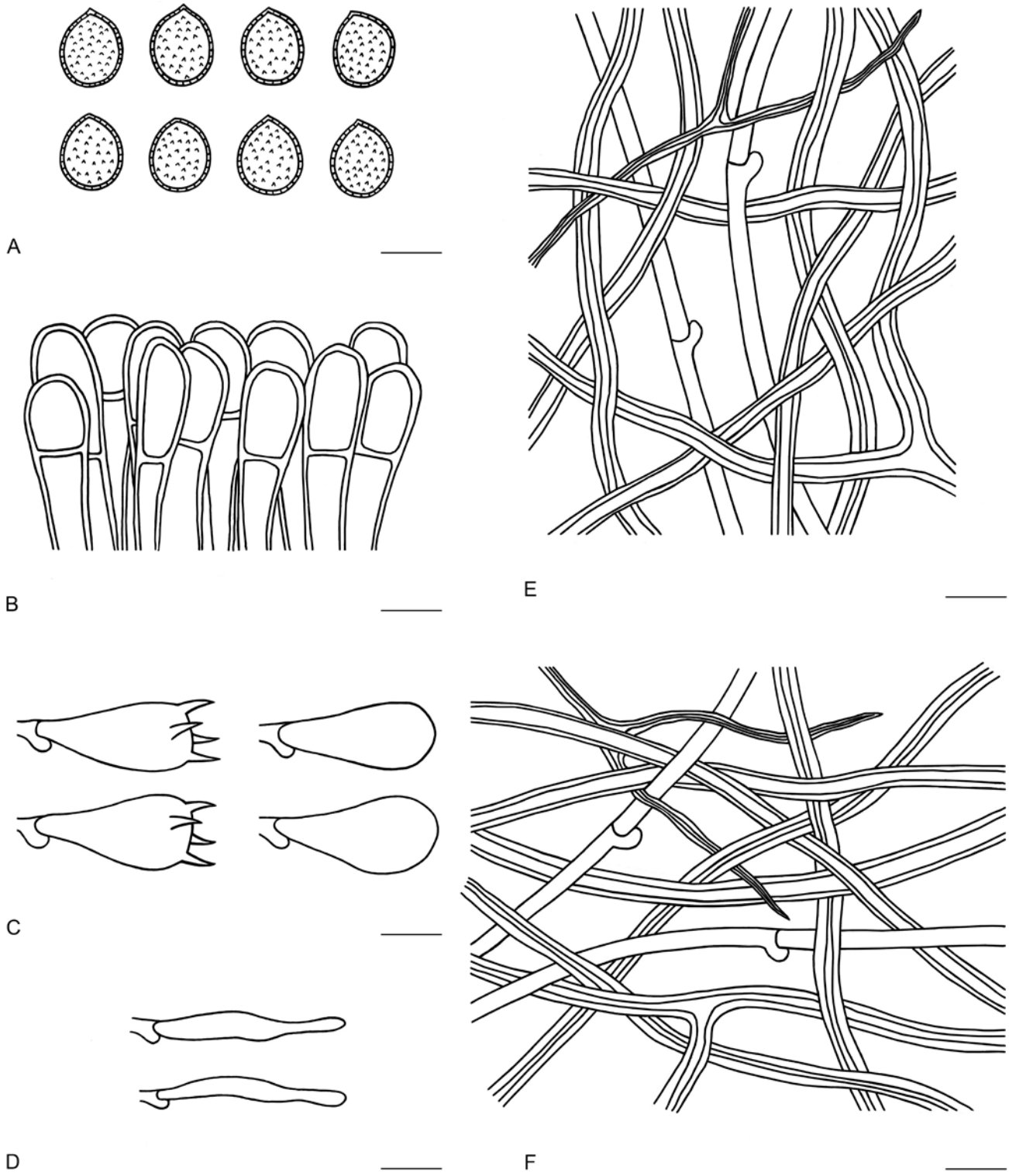

Fig. 68. Microscopic structures of *Sanguinoderma infundibulare* (drawn from Cui 17248). **A.** Basidiospores. **B.** Apical cells from cuticle. **C.** Basidia and basidioles. **D.** Cystidioles. **E.** Hyphae from trama. **F.** Hyphae from context. Scale bars = 10 µm.

KOH. Generative hyphae in context colourless, thin-walled, 3–4 µm diam; skeletal hyphae in context pale yellow, thick-walled with a wide to narrow lumen or sub-solid, arboriform and flexuous, 3–7 µm diam; binding hyphae in context colourless, sub-solid, branched and flexuous, 1–2 µm diam. Generative hyphae in tubes colourless, thin-walled, 3–4 µm diam; skeletal hyphae in tubes pale yellowish brown, thick-walled with a wide to narrow lumen or sub-solid, arboriform and flexuous, 3–6 µm diam; binding hyphae in tubes colourless, sub-solid, branched and flexuous, up to 2 µm diam. *Pileipellis* composed of clamped generative hyphae, thick-walled, apical cells clavate, faintly inflated and with obvious septa, pale yellowish brown, about 23–30 × 6–11 µm, forming a regular palisade. *Cystidia* absent; *cystidioles* clavate and apices constricted, colourless, thin-walled, 20–35 × 2–6 µm. *Basidia* barrel-shaped to clavate, colourless, thin-walled, 22–30 × 14–18 µm; *basidioles* in shape like the basidia, colourless, thin-walled, 15–25 × 9–19 µm. *Basidiospores* subglobose to broadly ellipsoid, pale yellow, IKI –, CB +, double-walled with slightly thick walls, exospore wall smooth, endospore wall with slightly dense spinules, (10–)10.2–12(–12.2) × (8.5–)9–10.2(–10.6) µm, L = 11.04 µm, W = 9.53 µm, Q = 1.16 (n = 60/1).

Notes: *Sanguinoderma infundibulare* was collected from the subtropical areas of China. It is like *Amauroderma preussii* in the thin and funnel-shaped pilei with obvious radial wrinkles, but *A. preussii* was described from Cameroon with darker and incurved pilei when dry, larger pores (2–4 per mm) and smaller basidiospores (7–9.1–11.5 × 6.5–8.5–10 µm, Steyaert 1972, Hapuarachchi *et al.* 2018a).

Sanguinoderma longistipitum B.K. Cui & Y.F. Sun, ***sp. nov.*** MycoBank MB 839666. Figs 69, 70.

Diagnosis: Differs from other species in the genus by basidiomata with small pilei and long stipe.

Etymology: *longistipitum* (*Lat.*), refers to the basidiomata with a long stipe.

Typus: **China**, Yunnan, Honghe, Huanglianshan Forest Park, on ground of forest, 11 Aug. 2019, Dai 20696 (**holotype** BJFC032363).

Additional materials examined: **China**, Yunnan, Jinghong, Xishuangbanna Botanical Garden, on ground, 23 Jul. 2014, Dai 13891 (BJFC017621); Hainan, Ledong County, Jianfengling Nature Reserve, on ground of angiosperm forest, 19 Jun. 2016, Cui 13903 (BJFC028769). **Thailand**, Chiang Rai, Doi Mae Salong, on ground of angiosperm forest, 22 Jul. 2016, Dai 16635 (BJFC022745).

Description: *Basidiomata* annual, laterally stipitate, hard corky. *Pilei* solitary, sub-orbicular to flabelliform, auricular or spathulate, up to 4 cm diam and 5 mm thick. *Pileal surface* greyish brown to almost black, dull, glabrous, with concentric zones and radial wrinkles; margin obtuse, entire, slightly wavy and incurved when dry. *Pore surface* greyish white when fresh becoming to blood red when bruised and then quickly darkening; pores circular to angular, 6–8 per mm; dissepiments moderately thick, entire. *Context* wood brown to greyish brown, sometimes with dark melanoid lines, corky, up to 2 mm thick. *Tubes* dark grey, up to 4 mm long. *Stipe* concolorous with pileal surface, cylindrical and solid, swollen at base, up to 14.5 cm long and 5 mm diam. *Hyphal system* trimitic; generative hyphae with clamp connections, all hyphae IKI –, CB +; tissues darkening in KOH. Generative hyphae in context colourless, thin-walled, 3–4 µm diam; skeletal hyphae in context pale yellow, thick-walled with a wide to narrow lumen or sub-solid, frequently arboriform and flexuous, 3–6 µm diam; binding hyphae in context colourless, sub-solid, branched and flexuous, 1–2 µm diam. Generative hyphae in tubes colourless, thin-walled, 3–4 µm diam; skeletal hyphae in tubes pale yellow, thick-walled with a wide to narrow lumen or sub-solid, arboriform and flexuous, 3–5 µm diam; binding hyphae in tubes colourless, sub-solid, frequently branched and flexuous, up to 2 µm diam. *Pileipellis* composed of clamped generative hyphae, thick-walled, apical cells finger-shape, with multiple obvious septa, pale greyish brown, about 22–40 × 5–10 µm, forming a regular palisade. *Cystidia* absent; *cystidioles* fusiform, colourless, thin-walled, 16–22 × 5–10 µm. *Basidia* barrel-shaped, colourless, thin-walled, 20–27 × 12–17 µm; *basidioles* in shape like the basidia, colourless, thin-walled, 19–25 × 5–16 µm. *Basidiospores* broadly ellipsoid, pale yellow, IKI –, CB +, double-walled with slightly thick walls, exospore wall smooth, endospore wall with dense spinules, 10–11(–11.3) × (8–)8.4–9.6(–9.8) µm, L = 10.58 µm, W = 8.94 µm, Q = 1.18–1.19 (n = 60/2).

Notes: *Sanguinoderma longistipitum* is a distinct species on account of its auricular or spathulate pilei with a long stipe. *Sanguinoderma guangdongense* has a similar distribution with *Sa. longistipitum* which can be collected from Yunnan Province, but the former can be distinguished by larger basidiomata with sub-orbicular to umbelliform pilei, shorter stipe and subglobose basidiospores. *Sanguinoderma longistipitum* is similar with the small specimens of *Sa. rugosum*, which also have broadly ellipsoid basidiospores in similar size (10.2–11.3 × 8.3–9.2 µm, Sun et al. 2020). However, the longer stipe and fusiform cystidioles of *Sa. longistipitum* distinguish it from *Sa. rugosum*. *Amauroderma auriscalpium* which was described from the Neotropics has similar-shaped pilei, but the basidiospores in *A. auriscalpium* are subglobose and smaller (6–8 µm, Torrend 1920).

Fig. 69. Basidiomata of *Sanguinoderma longistipitum*.

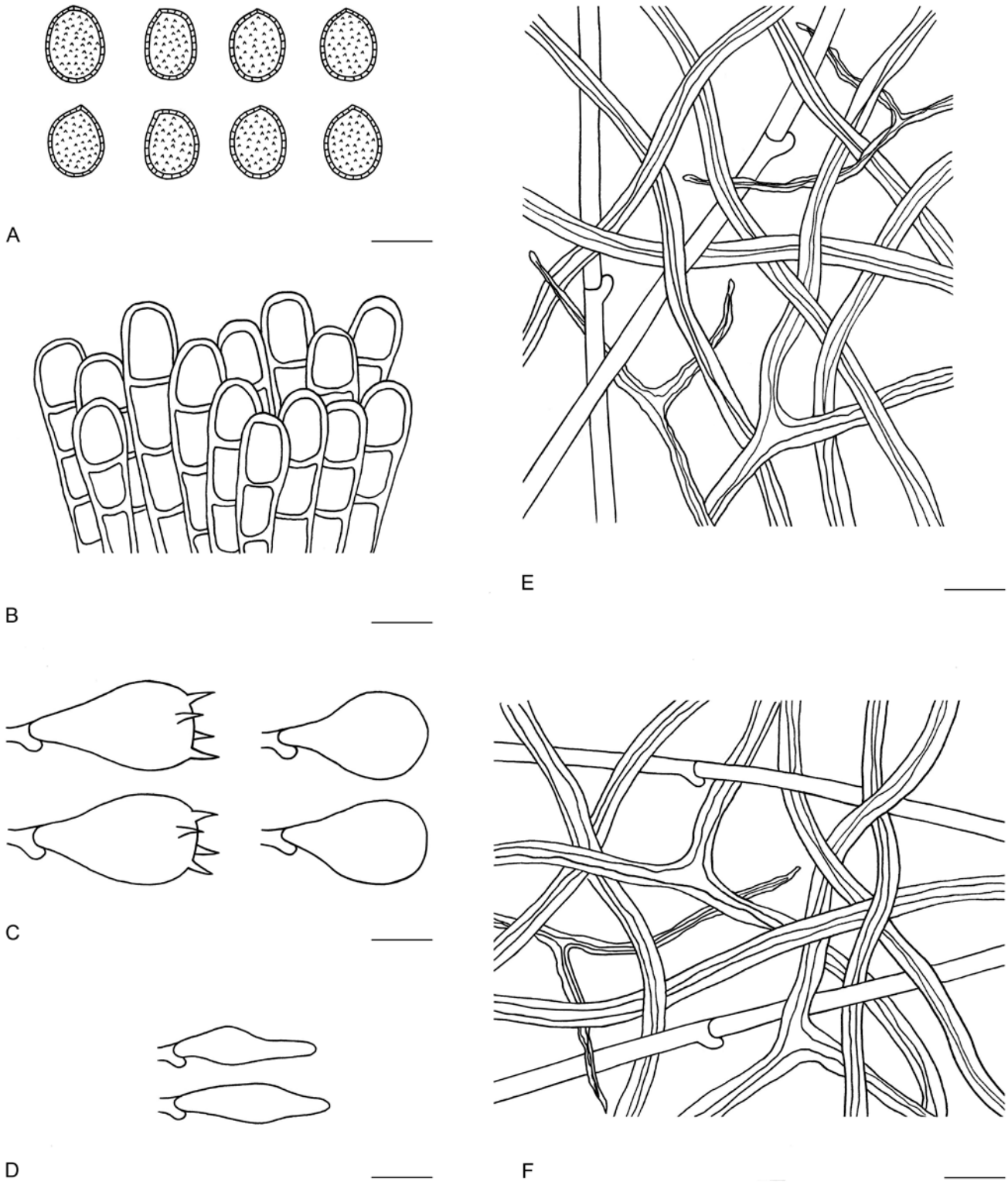

Fig. 70. Microscopic structures of *Sanguinoderma longistipitum* (drawn from Dai 20696). **A.** Basidiospores. **B.** Apical cells from cuticle. **C.** Basidia and basidioles. **D.** Cystidioles. **E.** Hyphae from trama. **F.** Hyphae from context. Scale bars = 10 µm.

Sanguinoderma melanocarpum B.K. Cui & Y.F. Sun, ***sp. nov.*** MycoBank MB 839667. Figs 71, 72.

Diagnosis: Differs from other species in the genus by its small and sub-orbicular pilei, coal black pileal surface with alternating dark to light concentric furrows and strong radial wrinkles.

Etymology: *melanocarpum* (*Lat.*), refers to the coal black pileal surface.

Typus: **Malaysia**, Selangor, Kota Damansara, Community Forest Reserve, on ground, 16 Apr. 2018, Dai 18603 (**holotype** BJFC026891).

Additional material examined: **Malaysia**, Selangor, Taman Botani Negara Shah Alam, on stump of angiosperm tree, 12 Apr. 2018, Dai 18512 (BJFC026801).

Description: *Basidiomata* annual, laterally stipitate, hard corky to woody hard. *Pilei* solitary, sub-orbicular to flabelliform, up to 4.5

cm diam and 5 mm thick. *Pileal surface* coal black when fresh, dull, glabrous, with alternating dark to light concentric furrows and strong radial wrinkles, centre navel-shaped; margin obtuse, entire, wavy and incurved when dry. *Pore surface* cream to greyish white when fresh becoming to blood red when bruised and then quickly darkening; pores circular to angular, 6–8 per mm; dissepiments distinctly thick, entire. *Context* straw yellow to yellowish brown, with dark melanoid lines, hard corky, up to 3 mm thick. *Tubes* greyish brown to dark grey, up to 3 mm long. *Stipe* concolorous with pileal surface, cylindrical and hollow, slightly swollen at base, up to 12 cm long and 5 mm diam. *Hyphal system* trimitic; generative hyphae with clamp connections, all the hyphae IKI + (slightly dextrinoid), CB +; tissues darkening in KOH. Generative hyphae in context colourless, thin-walled, 3–5 µm diam; skeletal hyphae in context pale yellow, thick-walled with a wide to narrow lumen or sub-solid, arboriform and flexuous, 3–7 µm diam; binding hyphae in context colourless, sub-solid, branched and flexuous, 1–1.5 µm diam. Generative hyphae in tubes colourless, thin-walled, 3–4 µm diam; skeletal hyphae in tubes pale yellow, thick-walled with a wide to narrow lumen or sub-solid, slightly arboriform and flexuous, 3–6 µm diam; binding hyphae in tubes colourless, sub-solid, branched and flexuous, up to 1.5 µm diam. *Pileipellis* composed of clamped generative hyphae, thick-walled to sub-solid, apical cells clavate, faintly constricted and flexuous, yellowish brown, about 28–32 × 5–7 µm, forming a regular palisade. *Cystidia* and *cystidioles* absent. *Basidia* barrel-shaped, colourless, thin-walled, 20–25 × 12–17 µm; *basidioles* clavate, colourless, thin-walled, 16–22 × 10–16 µm. *Basidiospores* subglobose to broadly ellipsoid, pale yellow, IKI + (slightly dextrinoid), CB +, double-walled with slightly thick walls, exospore wall smooth, endospore wall with dense spinules, (10–)10.4–11.8(–12) × (8.8–)9–10.5(–10.8) µm, L = 10.98 µm, W = 9.77 µm, Q = 1.10–1.15 (n = 60/2).

Notes: *Sanguinoderma melanocarpum* was collected from Malaysia and it has sub-orbicular pilei, a dark pileal surface with strongly concentric furrows and radial wrinkles which are similar to *Sa. rugosum*, but *Sa. rugosum* differs from *Sa. melanocarpum* by dark brown pilei, slightly thick dissepiments of pores, clavate cystidioles and elliptical basidiospores (10.2–11.3 × 8.3–9.2 µm) without amyloid or dextrinoid reaction (Sun *et al.* 2020).

Fig. 71. Basidiomata of *Sanguinoderma melanocarpum*.

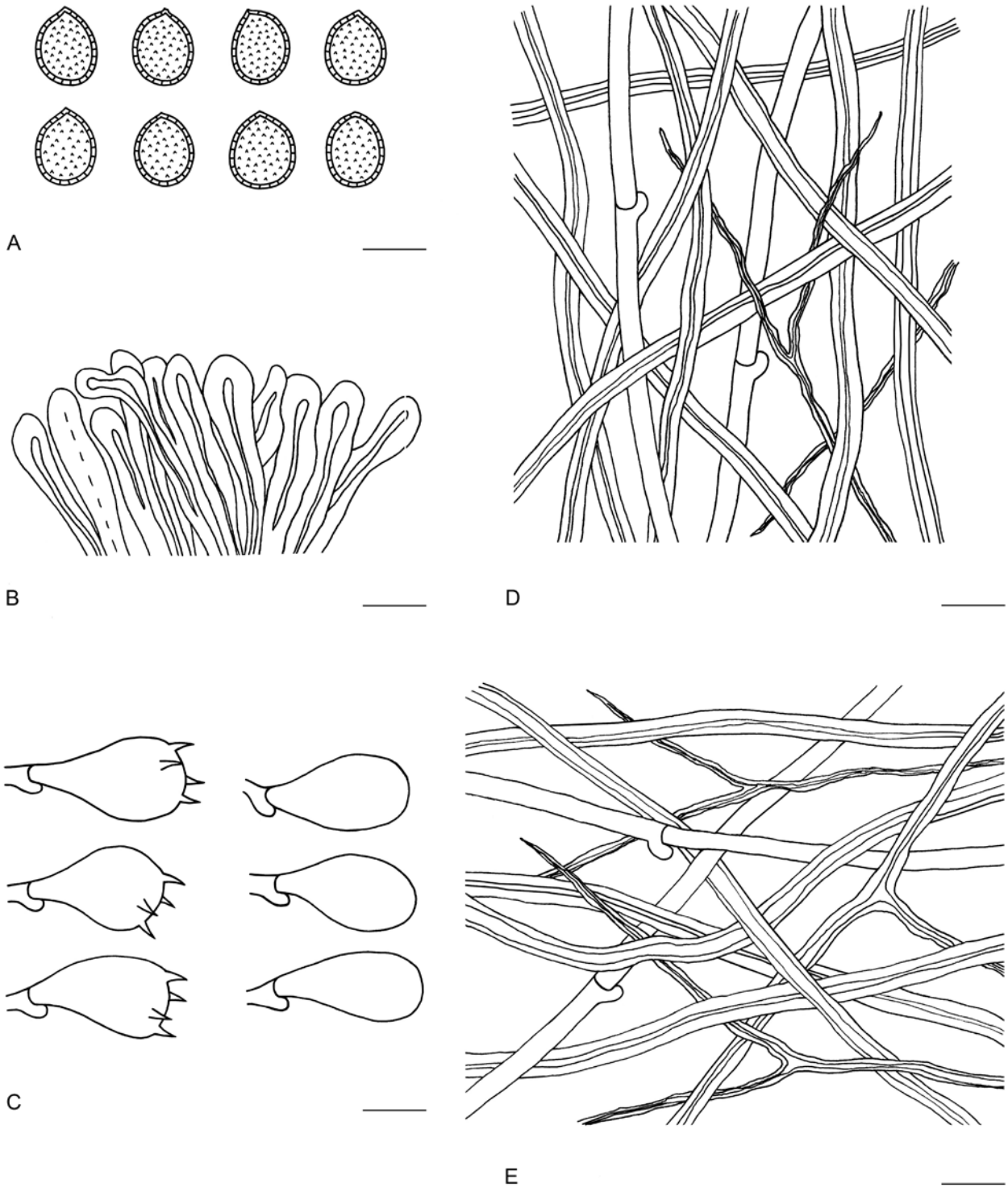

Fig. 72. Microscopic structures of *Sanguinoderma melanocarpum* (drawn from Dai 18603). **A.** Basidiospores. **B.** Apical cells from cuticle. **C.** Basidia and basidioles. **D.** Hyphae from trama. **E.** Hyphae from context. Scale bars = 10 µm.

Sanguinoderma microsporum B.K. Cui & Y.F. Sun, ***sp. nov.*** MycoBank MB 839668. Figs 73, 74.

Diagnosis: Differs from other species in the genus by having the smallest basidiospores.

Etymology: *microsporum* (*Lat.*), refers to the small basidiospores.

Typus: **Thailand**, Chiang Mai, Doi Saket, on ground, 24 Jul. 2016, Dai 16726 (**holotype** BJFC022833).

Additional materials examined: **China**, Hainan, Ledong County, Jianfengling Nature Reserve, on ground of angiosperm forest, 19 Jun. 2016, Cui 13897 (BJFC028763), Cui 13901 (BJFC028767).

Description: *Basidiomata* annual, centrally to laterally stipitate, hard corky. *Pilei* solitary, near orbicular, up to 4.5 cm diam and 3 mm thick. *Pileal surface* dark yellowish brown to almost black, dull, glabrous, with concentric zones and radial wrinkles; margin acute to obtuse, entire, incurved when dry. *Pore surface* pale yellowish brown to pale grey when dry, becoming to blood red when bruised

Fig. 73. Basidiomata of *Sanguinoderma microsporum*.

and then quickly darkening; pores circular to angular, 5–7 per mm; dissepiments slightly thick, entire. *Context* straw yellow, without dark melanoid lines, corky, up to 2 mm thick. *Tubes* pale straw yellow, up to 1 mm long. *Stipe* concolorous with pileal surface, cylindrical and hollow, up to 11 cm long and 7 mm diam. *Hyphal system* trimitic; generative hyphae with clamp connections, all hyphae IKI –, CB +; tissues darkening in KOH. Generative hyphae in context colourless, thin-walled, 3–5 µm diam; skeletal hyphae in context yellowish brown, thick-walled with a wide to narrow lumen or sub-solid, arboriform and flexuous, 4–7 µm diam; binding hyphae in context colourless, sub-solid, branched and flexuous, 1–2 µm diam. Generative hyphae in tubes colourless, thin-walled, 3–4 µm diam; skeletal hyphae in tubes pale yellow, thick-walled with a wide to narrow lumen or sub-solid, arboriform and flexuous, 3–6 µm diam; binding hyphae in tubes colourless, sub-solid, branched and flexuous, up to 1.5 µm diam. *Pileipellis* composed of clamped generative hyphae, slightly thick-walled, apical cells clavate, slightly inflated, reddish brown, about 30–40 × 5–8 µm, forming a regular palisade. *Cystidia* and *cystidioles* absent. *Basidia* clavate, colourless, thin-walled, 14–23 × 9–11 µm; *basidioles* in shape like the basidia, colourless, thin-walled, 12–17 × 5–10 µm. *Basidiospores* subglobose to broadly ellipsoid, pale brown, IKI –, CB +, double-walled with slightly thick walls, exospore wall smooth, endospore wall with dense spinules, (4.3–)4.7–5.6(–5.9) × (4–)4.3–5.2(–5.4) µm, L = 5.22 µm, W = 4.79 µm, Q = 1.06–1.12 (n = 60/2).

Notes: *Sanguinoderma microsporum* is unique in the genus due to its small basidiospores. It is like *Sa. melanocarpum* in the almost black orbicular pilei with long stipe, but the latter can be distinguished by smaller pores (6–8 per mm) with distinctly thick dissepiments, harder context with dark melanoid lines, and larger basidiospores (10.4–11.8 × 9.0–10.5 µm) with slightly dextrinoid reaction.

Sanguinoderma tricolor B.K. Cui & Y.F. Sun, ***sp. nov.*** MycoBank MB 839669. Figs 75, 76.

Diagnosis: Differs from other species in the genus by its hard basidiomata with concentric zonate pileal surface in three different colours when fresh.

Etymology: *tricolor* (*Lat.*), refers to the pileal surface with obvious concentric zones in three different colours.

Typus: **Malaysia**, Selangor, Kota Damansara, National Forest Reserve, on ground, 7 Dec. 2019, Cui 18292 (**holotype** BJFC035151).

Additional materials examined: **Malaysia**, Selangor, Kota Damansara, National Forest Reserve, on ground, 6 Dec. 2019, Cui 18242 (BJFC035101); Forest Research Institute of Malaysia, on stump of *Hopea*, 15 Apr. 2018, Dai 18574 (BJFC026862).

Description: *Basidiomata* annual, laterally stipitate, hard corky to woody hard. *Pilei* solitary, flabelliform to reniform, up to 12 cm diam and 1 cm thick. *Pileal surface* rust colour, dark brown to almost black when fresh, dull, glabrous, with obvious concentric zones in different colours and radial wrinkles; margin obtuse, entire, very

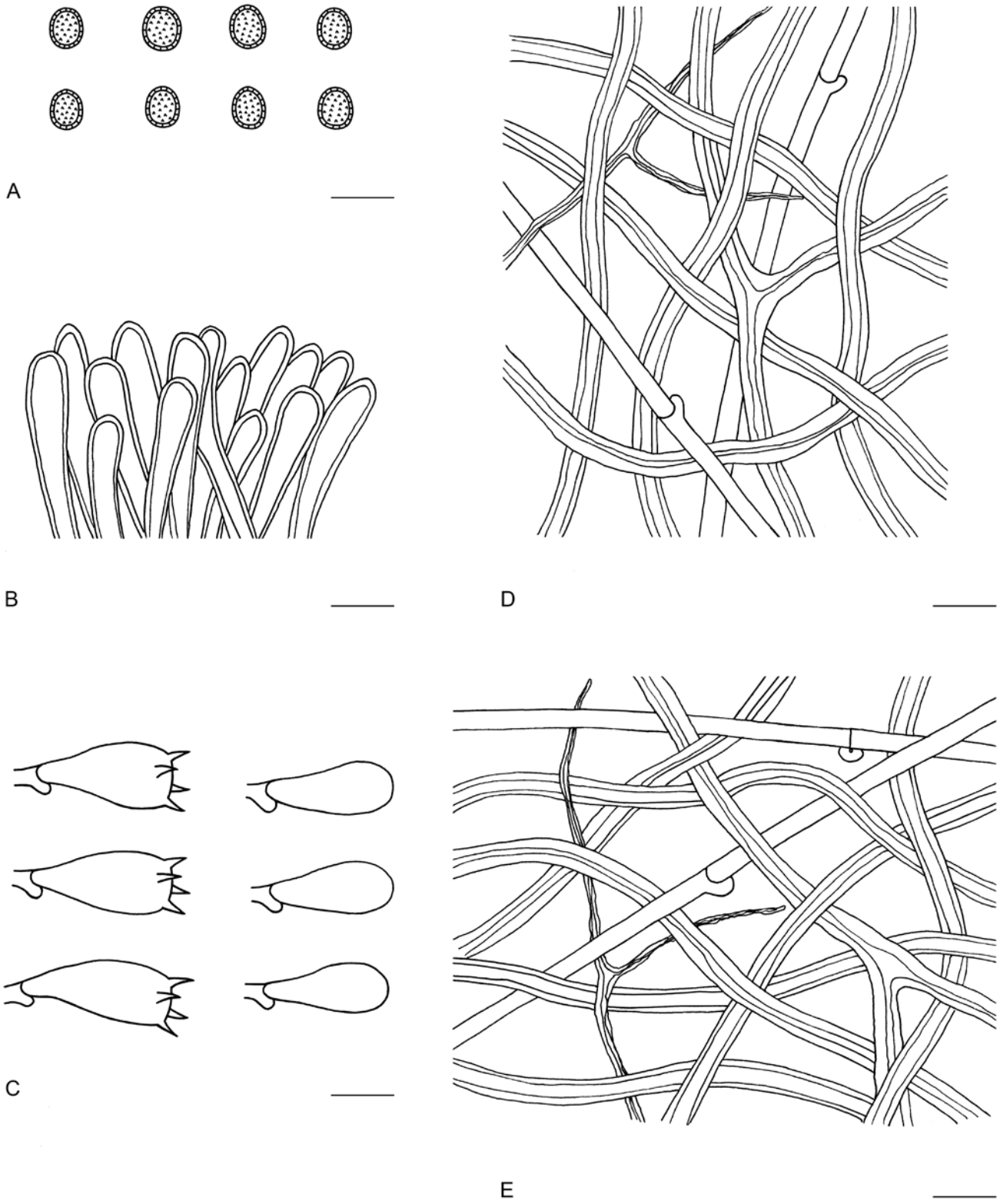

Fig. 74. Microscopic structures of *Sanguinoderma microsporum* (drawn from Dai 16726). **A.** Basidiospores. **B.** Apical cells from cuticle. **C.** Basidia and basidioles. **D.** Hyphae from trama. **E.** Hyphae from context. Scale bars = 10 µm.

wavy and incurved when dry. *Pore surface* cream to yellowish brown when fresh becoming to blood red when bruised and then quickly darkening, or unchanging in old specimens; pores circular, 5–7 per mm; dissepiments extremely thick (about 0.11–0.14 mm thick), entire. *Context* pale straw yellow to wood brown, without dark melanoid lines, hard corky, up to 3 mm thick. *Tubes* dark straw yellow to pale brown, up to 8 mm long. *Stipe* concolourous with pileal surface, cylindrical and solid, swollen at base, up to 5.5 cm long and 1.5 cm diam. *Hyphal system* trimitic; generative hyphae with clamp connections, all hyphae IKI –, CB +; tissues darkening in KOH. Generative hyphae in context colourless, thin-walled, 3–4 µm diam; skeletal hyphae in context pale golden yellow, thick-walled with a wide to narrow lumen or sub-solid, arboriform and flexuous, 3–7 µm diam; binding hyphae in context colourless, sub-solid, branched and flexuous, 1–2 µm diam. Generative hyphae in tubes colourless, thin-walled, 3–5 µm diam; skeletal hyphae

Fig. 75. Basidiomata of *Sanguinoderma tricolor*.

in tubes pale yellowish brown, thick-walled with a wide to narrow lumen or sub-solid, arboriform and flexuous, 3–6 µm diam; binding hyphae in tubes colourless, sub-solid, branched and flexuous, up to 2 µm diam. *Pileipellis* composed of clamped generative hyphae, thick-walled to sub-solid, apical cells clavate, inflated and flexuous, yellowish brown, about 18–27 × 5–7 µm, forming a regular palisade. *Cystidia* and *cystidioles* absent. *Basidia* barrel-shaped to clavate, colourless, thin-walled, 15–25 × 10–15 µm; *basidioles* in shape like the basidia, colourless, thin-walled, 14–17 × 9–13 µm. *Basidiospores* subglobose to broadly ellipsoid, pale yellow, IKI –, CB +, double-walled with slightly thick walls, exospore wall smooth, endospore wall with dense spinules, (10–)10.2–11.5(–12) × (8.3–8.8–10.2(–10.5) µm, L = 10.91 µm, W = 9.53 µm, Q = 1.13–1.16 (n = 60/2).

Notes: *Sanguinoderma tricolor* is a distinct species on account of its pileal surface with concentric zones in three different colours when fresh. It can be confused with *Sa. microporum* by having hard basidiomata, and small pores (5–7 per mm) with extremely thick dissepiments (about 0.12–0.16 mm thick), but *Sa. microporum* differs from *Sa. tricolor* by the monochromatic pileal surface, context with dark melanoid lines, larger and more elliptical basidiospores (11–12 × 8.7–9.8 µm, Q = 1.23–1.28, Sun *et al.* 2020).

Key to accepted species of *Sanguinoderma*

1a. Pore dissepiments extremely thick 2
1b. Pore dissepiments thin to distinctly thick 3

2a. Pileal surface pale yellowish brown, pore surface yellowish brown, context with dark melanoid lines ..... *Sa. microporum*
2b. Pileal surface rust brown to almost black, pore surface white to pale yellow, context without dark melanoid lines ..... *Sa. tricolor*

3a. Pore dissepiments lacerate, tubes fascicular when dry ..... *Sa. laceratum*
3b. Pore dissepiments entire, tubes unchanged when dry 4

4a. Pores ≤ 4 per mm 5
4b. Pores > 4 per mm 7

5a. Pores sinuate; basidiospores > 13.5 µm in length ..... *Sa. sinuosum*
5b. Pores circular to irregular; basidiospores < 13.5 µm in length 6

6a. Pore dissepiments thin; basidiospores globose to subglobose ..... *Sa. bataanense*
6b. Pore dissepiments slightly thick; basidiospores subglobose to broadly ellipsoid ..... *Sa. rude*

7a. Basidiospores < 6 µm in length ..... *Sa. microsporum*
7b. Basidiospores > 6 µm in length 8

8a. Pileal surface coal black; basidiospores slightly dextrinoid in Melzer's reagent ..... *Sa. melanocarpum*
8b. Pileal surface brown to almost black; basidiospores IKI– in Melzer's reagent 9

9a. Pileipellis composed of apical cells with obvious septa 10
9b. Pileipellis composed of apical cells without obvious septa 12

10a. Basidiomata with long stipe; apical cells of pileipellis digitate, with multiple septa ..... *Sa. longistipitum*
10b. Basidiomata with short stipe; apical cells of pileipellis clavate, with simple septa 11

11a. Pilei applanate, reniform, pileal surface dark brown to almost black ..... *Sa. elmerianum*
11b. Pilei funnel-shape, pileal surface yellowish brown to greyish brown ..... *Sa. infundibulare*

12a. Cystidioles absent 13
12b. Cystidioles present 14

13a. Pore surface yellowish green when fresh; basidiospores subglobose to broadly ellipsoid ..... *Sa. flavovirens*
13b. Pore surface pale grey when fresh; basidiospores reniform ..... *Sa. reniforme*

14a. Basidiomata sessile to subsessile; basidiospores ≥ 14 µm in length ..... *Sa. perplexum*
14b. Basidiomata stipitate; basidiospores < 14 µm in length 15

15a. Pileal surface with shades of brown concentric zones and slender radial lines, context fibrous ..... *Sa. guangdongense*
15b. Pileal surface with concentric furrows and radial wrinkles, context corky ..... *Sa. rugosum*

Sinoganoderma B.K. Cui, J.H. Xing & Y.F. Sun, ***gen. nov.*** MycoBank MB 839661.

Diagnosis: Differs from other genera by its ganodermoid basidiomata, applanate pilei with pale yellow pileal surface, cream context, thin dissepiments of pores, truncated basidiospores with an uneven or foveolate exospore wall and solid spinules on the endospore wall.

Etymology: *sinoganoderma* (*Lat.*), refers to the genus producing ganoderma-like basidiomata and distributed in China.

Type species: *Sinoganoderma shandongense* (J.D. Zhao & L.W. Xu) B.K. Cui *et al*.

Description: *Basidiomata* annual, stipitate, corky. *Pilei* solitary, flabelliform to shell-shaped, applanate. *Pileal surface* pale yellow to reddish brown, slightly laccate, glabrous, with concentric furrows and radial wrinkles. *Pore surface* near white when fresh; pores circular; dissepiments thin, entire. *Context* cream to pale wood brown, without dark melanoid lines, soft corky. *Hyphal system* trimitic; generative hyphae colourless, thin-walled, with clamp connections; skeletal hyphae near colourless to pale yellow, with narrow lumen or sub-solid, arboriform and flexuous; binding hyphae colourless, thick-walled, branched and flexuous. *Basidiospores* ellipsoid to ovoid, truncated, pale yellowish brown, double-walled and distinctly thick-walled, exospore wall uneven or foveolate, endospore wall with solid spinules.

Notes: *Sinoganoderma* is established due to its pale yellow pileal surface, cream context, thin dissepiments of pores, and truncated basidiospores with an uneven or foveolate exospore wall and solid spinules on the endospore wall. It is composed of one species which has been only collected from China. The ornamentation of the exospore wall of basidiospores observed under SEM is similar to *Foraminispora*, but the hollow and columnar spinules which persist until the exospore wall forming visible holes make *Foraminispora* different from other genera in *Ganodermataceae*. In the phylogenetic analyses, *Sinoganoderma* formed an independent clade distinct from other genera within *Ganodermataceae* and, so far, is monotypic (Fig. 1).

Sinoganoderma shandongense (J.D. Zhao & L.W. Xu) B.K. Cui, J.H. Xing & Y.F. Sun, ***comb. nov.*** MycoBank MB 839662. Figs 77, 78.
Basionym: *Ganoderma shandongense* J.D. Zhao & L.W. Xu, Acta Mycol. Sin. 5: 90. 1986.

Description: *Basidiomata* annual, laterally stipitate, corky. *Pilei* solitary, flabelliform to shell-shaped, applanate, up to 6.5 cm diam and 2.5 mm thick. *Pileal surface* pale yellow to reddish brown, slightly laccate, glabrous, with concentric furrows and radial wrinkles; margin obtuse, entire. *Pore surface* near white when fresh; pores circular, 3–5 per mm; dissepiments thin, entire. *Context* cream to pale wood brown, without dark melanoid lines, soft corky, up to 6 mm thick. *Tubes* cream, up to 4.3 mm long. *Stipe* purplish-red, slightly laccate, cylindrical and solid, slightly

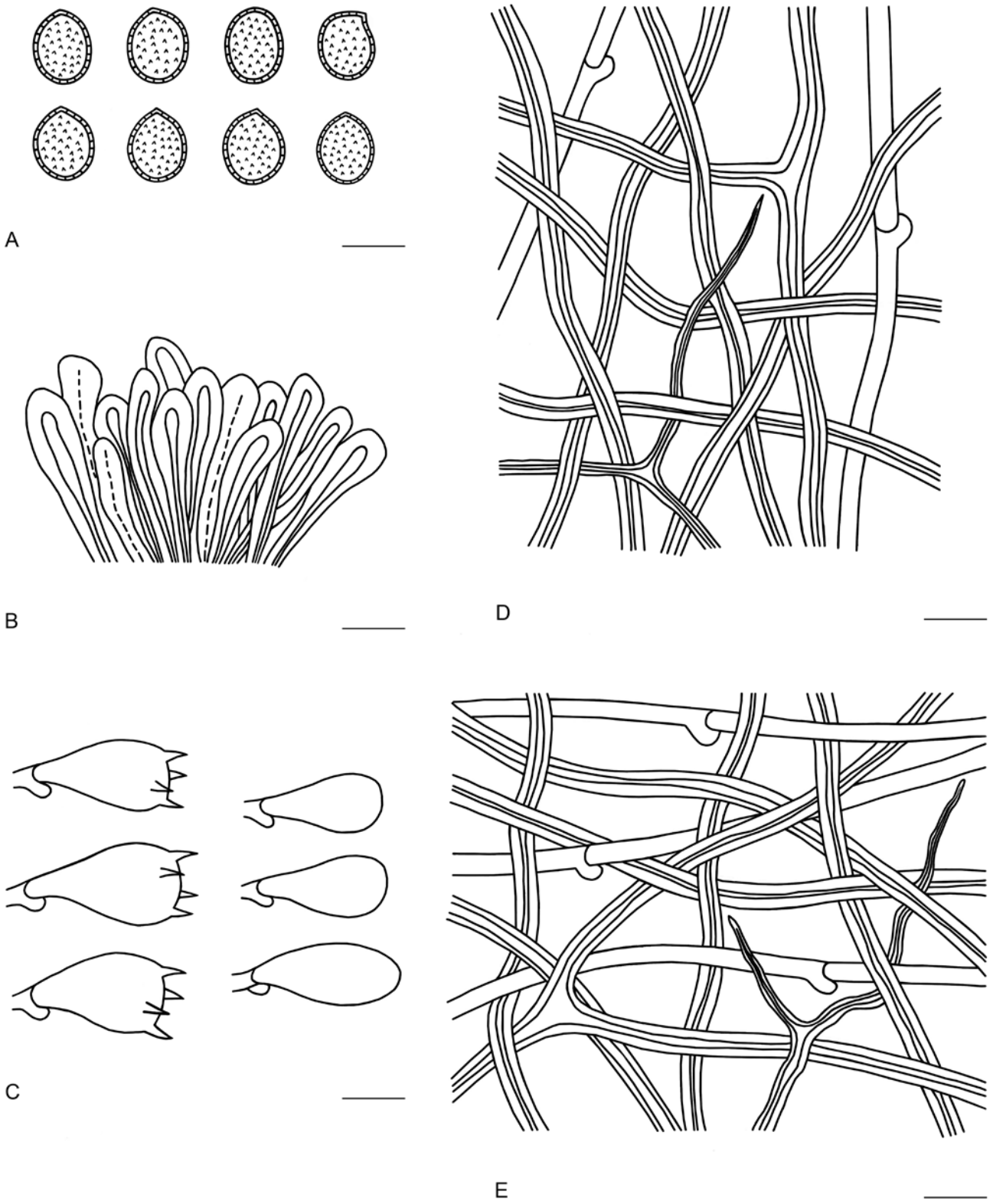

Fig. 76. Microscopic structures of *Sanguinoderma tricolor* (drawn from Cui 18292). **A.** Basidiospores. **B.** Apical cells from cuticle. **C.** Basidia and basidioles. **D.** Hyphae from trama. **E.** Hyphae from context. Scale bars = 10 μm.

swollen at base, up to 5.6 cm long and 1.2 cm diam. *Hyphal system* trimitic; generative hyphae with clamp connections, all hyphae IKI –, CB +; tissues slightly darkening in KOH. Generative hyphae in context colourless, thin-walled, 2–4 μm diam; skeletal hyphae in context near colourless to pale yellow, with narrow lumen or sub-solid, arboriform and flexuous, 2–5 μm diam; binding hyphae in context colourless, thick-walled, branched and flexuous, 1–2 diam. Generative hyphae in tubes colourless, thin-walled, 3–4 μm diam; skeletal hyphae in tubes near colourless, almost sub-solid, arboriform and flexuous, 2–4 μm diam; binding hyphae in tubes colourless, thick-walled, branched and flexuous, up to 1.5 μm diam. *Pileipellis* composed of clamped generative hyphae, thick-walled, apical cells clavate, inflated and flexuous, pale yellowish brown, about 37–45 × 5–9 μm, forming a regular palisade. *Cystidia* and *cystidioles* absent. *Basidia* barrel-shaped to clavate, colourless, thin-walled, 13–19 × 10–18 μm; *basidioles* in shape like the basidia,

Fig. 77. Basidiomata of *Sinoganoderma shandongense*.

colourless, thin-walled, 12–16 × 8–10 µm. *Basidiospores* ellipsoid to ovoid, truncated, pale yellowish brown, IKI –, CB +, double-walled with distinctly thick walls, exospore wall uneven or foveolate, endospore wall with solid spinules, (11.9–)12–13.2(–13.3) × (7.8–)8–9(–9.2) µm, L = 12.66 µm, W = 8.42 µm, Q = 1.49–1.52 (n = 60/2, with the turgid vesicular appendix included).

Materials examined: **China**, Shandong, Changqing County, Liantaishan Forest Park, on stump of *Albizia*, 24 Aug. 2015, Dai 15785 (BJFC019889), Dai 15786 (BJFC019890); on living tree of *Albizia*, 24 Aug. 2015, Dai 15787 (BJFC019891), Dai 15788 (BJFC019892), Dai 15790 (BJFC019894), Dai 15791 (BJFC019895); on living tree of *Albizia*, 6 Aug. 2019, Dai 20243 (BJFC031911), Dai 20244 (BJFC031912).

Notes: *Sinoganoderma shandongense* was firstly described by Zhao & Zhang (1986a) as *Ganoderma shandongense*. It has typical ganodermoid morphology, but *Si. shandongense* formed an independent lineage in the phylogenetic analyses (Fig. 1). It is worth mentioning that the sequences of two specimens (xsd08032 and xsd08085) uploaded into GenBank as *G. ramosissimum* are identical with *Si. shandongense* based on phylogenetic results in this study, and therefore the name of the two specimens (xsd08032 and xsd08085) needs to change to *Si. shandongense.*

Tomophagus Murrill, Torreya 5: 197. 1905. MycoBank MB 18657.

Type species: *Tomophagus colossus* (Fr.) Murrill

Description: *Basidiomata* annual, sessile, soft corky. *Pilei* solitary, flabelliform. *Pileal surface* pale straw yellow to reddish brown, slightly laccate, glabrous, without ornamentation or not obvious. *Pore surface* white to straw yellow; pores circular; dissepiments thick, entire. *Context* white to wood brown, soft corky. *Hyphal system* dimitic; generative hyphae colourless, thin-walled, branched, with clamp connections; skeletal hyphae colourless to pale yellow, thick-walled, thick-walled with narrow lumen or sub-solid, arboriform, strongly collapsed and flexuous. *Basidiospores* ellipsoid to ovoid, truncated, yellow to pale yellowish brown, double-walled with distinctly thick walls, exospore wall slightly foveolate to verrucose or reticulate, endospore wall with short and irregular ridges.

Notes: *Tomophagus* has typical ganodermoid basidiospores, but its pale white and soft context make it different from other genera (Murrill 1905, Le *et al.* 2012). Two species, *To. colossus* and *To. cattienensis* are accepted in *Tomophagus*. In the phylogenetic analyses, *Tomophagus* formed an independent clade within *Ganodermataceae* (Fig. 1).

Tomophagus cattienensis X.T. Le & Moncalvo, Mycol. Prog. 11: 777. 2012. MycoBank MB 561806. Figs 79, 80.

Description: *Basidiomata* annual, sessile, soft corky. *Pilei* solitary, flabelliform, up to 8 cm diam and 3 cm thick. *Pileal surface* pale straw yellow when fresh, slightly laccate, glabrous, without ornamentation;

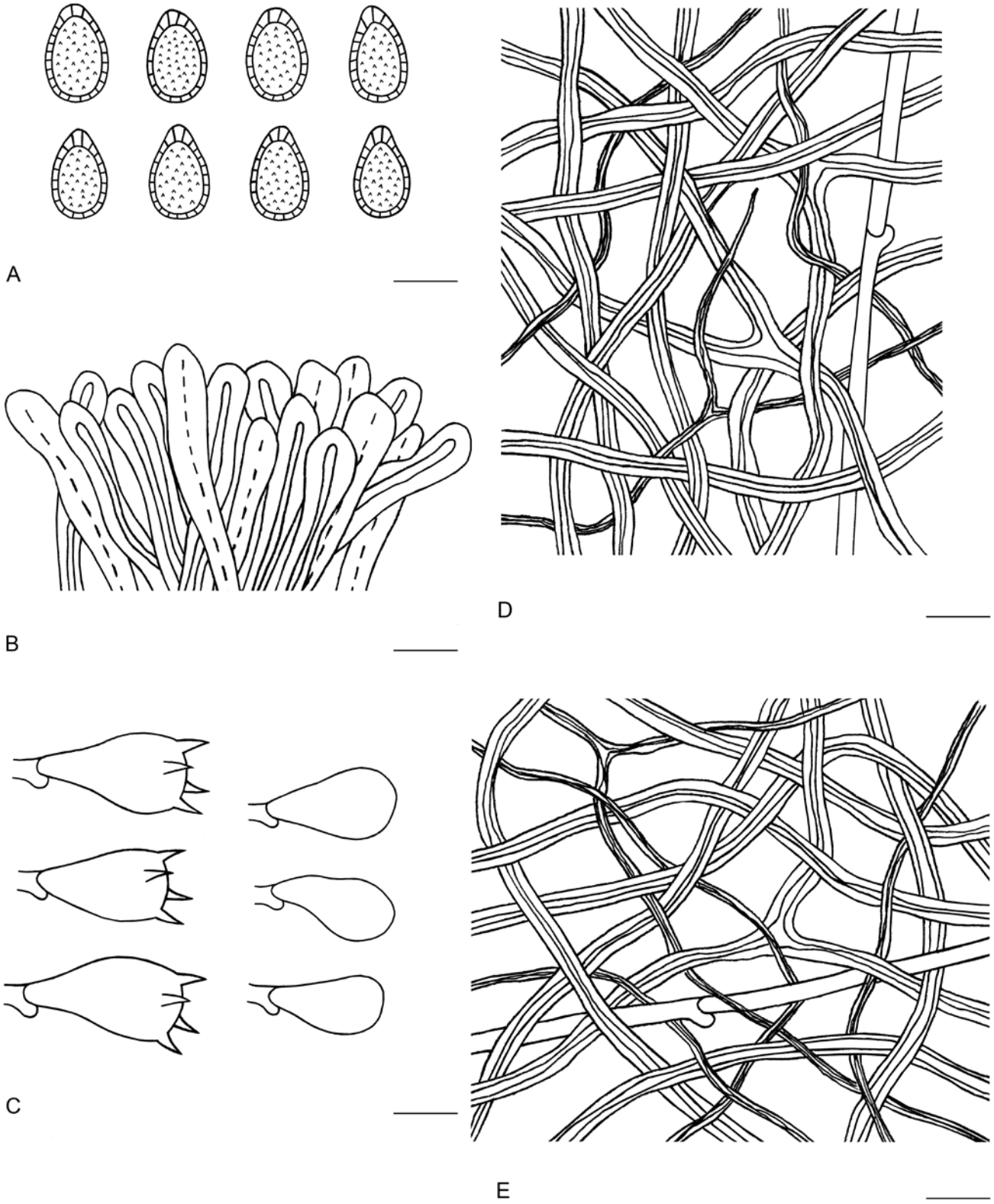

Fig. 78. Microscopic structures of *Sinoganoderma shandongense* (drawn from Dai 20244). **A.** Basidiospores. **B.** Apical cells from cuticle. **C.** Basidia and basidioles. **D.** Hyphae from trama. **E.** Hyphae from context. Scale bars = 10 μm.

margin obtuse, entire, and incurved when dry. *Pore surface* pale wood brown to straw yellow becoming dark when bruised; pores circular to oval, 3–5 per mm; dissepiments moderately thick, entire. *Context* wood brown, with dark resinous lines, soft corky, slightly fibrous and powdery, up to 3 cm thick. *Tubes* pale greyish brown, corky, up to 5 mm long. Hyphal system dimitic; generative hyphae with clamp connections, all hyphae IKI –, CB +; tissues darkening in KOH. Generative hyphae in context colourless, thin-walled, branched, 3–4 μm diam; skeletal hyphae in context pale yellow, thick-walled with narrow lumen or sub-solid, arboriform, strongly collapsed and flexuous, 3–5 μm diam. Generative hyphae in tubes colourless, thin-walled, branched, 3–4 μm diam; skeletal hyphae in tubes colourless to pale yellow, thick-walled with narrow lumen or sub-solid, arboriform, strongly collapsed and flexuous, 3–4 μm diam. *Pileipellis* composed of clamped generative hyphae, thin- to slightly thick-walled, apical cells clavate, faintly inflated,

Fig. 79. Basidiomata of *Tomophagus cattienensis*.

colourless to pale yellow, about 32–45 × 4–7 µm, forming a regular palisade. *Cystidia* and *cystidioles* absent. *Basidia* barrel-shaped to clavate, colourless, thin-walled, 18–27 × 10–13 µm; *basidioles* in shape like the basidia, colourless, thin-walled, 15–20 × 9–12 µm. *Basidiospores* ellipsoid to ovoid, truncated, pale yellowish brown, IKI –, CB +, double-walled with distinctly thick walls, exospore wall slightly foveolate, endospore wall with short and irregular ridges, (10–)10.2–11.8(–11.9) × (6.3–)6.5–7.8(–8) µm, L = 11.09 µm, W = 7.22 µm, Q = 1.54 (n = 60/1, with the turgid vesicular appendix excluded); (11.2–)11.3–12.7(–13) × (6.8–)7–8(–8.2) µm, L = 12.04 µm, W = 7.39 µm, Q = 1.63 (n = 60/1, with the turgid vesicular appendix included).

Material examined: **Malaysia**, Selangor, Jeram, on dead tree of *Elaeis*, 10 Apr. 2018, Dai 18487 (BJFC026776).

Notes: *Tomophagus cattienensis* was described from South Vietnam, and it can be distinguished from *To. colossus* by its pale red-brown and laccate pileal surface, pale brown context when dry, and slightly larger basidiospores (17.5–21.5 × 11.5–14.5 µm, Le *et al.* 2012). The specimen of *To. cattienensis* used in this study was collected from Malaysia, and it grouped with another *To. cattienensis* specimen in the phylogenetic analyses (Fig. 1). However, the specimens used in Le *et al.* (2012) showed different morphological characters to our specimen, such as a reddish brown pileal surface, larger pores (2–3 per mm), and larger basidiospores (17.5–21.5 × 11.5–14.5 µm).

Key to accepted species of *Tomophagus*

1a. Pileal surface reddish brown; basidiospores smaller (10.2–11.8 × 6.5–7.8 µm) ..... *To. cattienensis*
1b. Pileal surface yellow; basidiospores larger (14–20 × 9–14 µm) ..... *To. colossus*

Trachydermella B.K. Cui & Y.F. Sun, ***gen. nov.*** MycoBank MB 840976.

Diagnosis: Differs from other genera by its sessile basidiomata with flatly flabelliform pilei, trachytic and ochraceous to yellowish brown pileal surface, watery context.

Etymology: *trachydermella* (*Lat.*), refers to the genus having trachytic pileal surface.

Type species: *Trachydermella tsunodae* (Yasuda ex Lloyd) B.K. Cui & Y.F. Sun

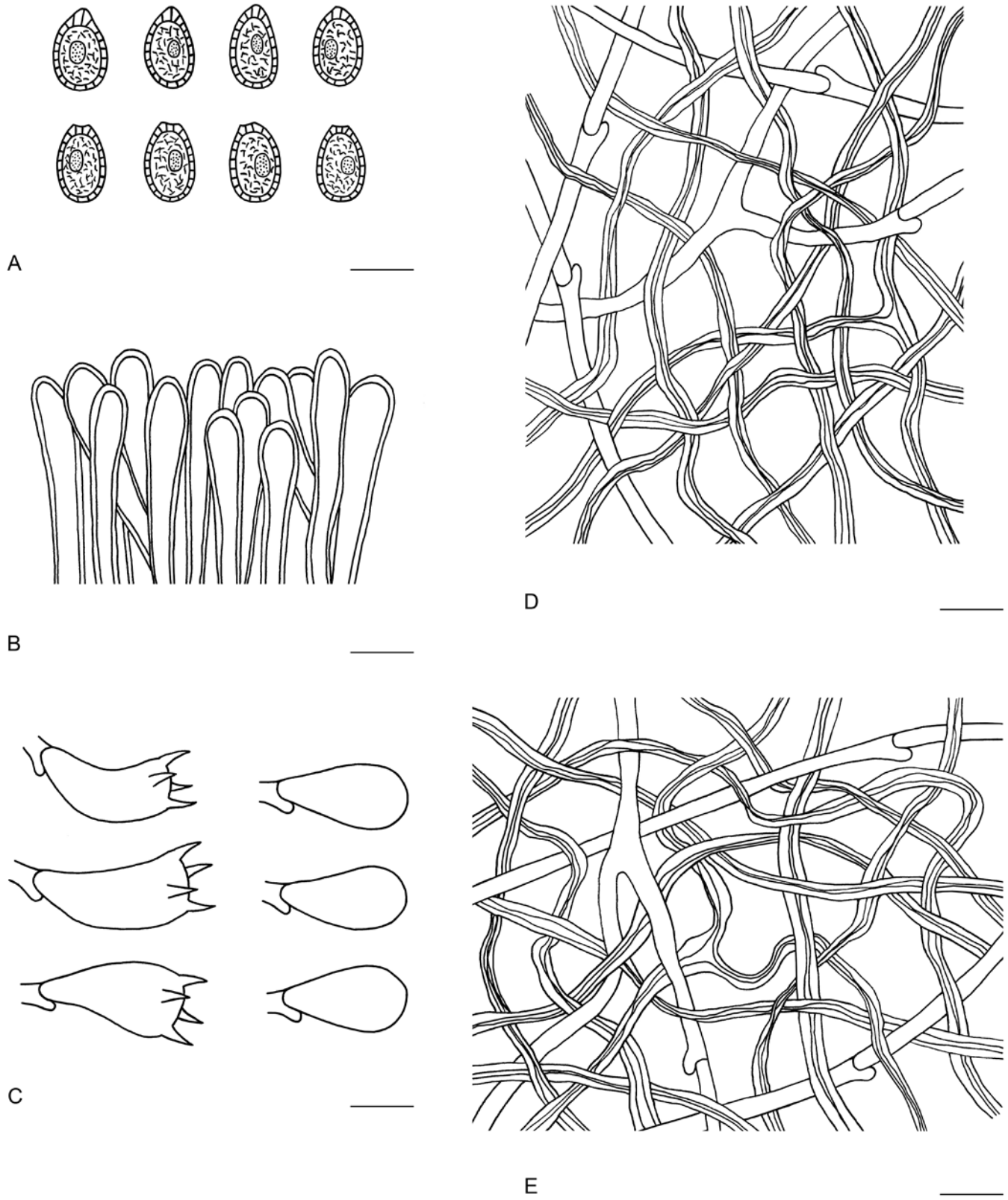

Fig. 80. Microscopic structures of *Tomophagus cattienensis* (drawn from Dai 18487). **A.** Basidiospores. **B.** Apical cells from cuticle. **C.** Basidia and basidioles. **D.** Hyphae from trama. **E.** Hyphae from context. Scale bars = 10 μm.

Description: *Basidiomata* annual, sessile, soft when fresh. *Pilei* solitary, flatly flabelliform. *Pileal surface* ochraceous to yellowish brown when fresh, dull, glabrous, trachytic, with concentric zones and radial wrinkles. *Pore surface* wood brown when dry; pores circular; dissepiments thick, entire. *Context* cream, watery when fresh and turning hard corky when dry. *Hyphal system* trimitic; generative hyphae colourless, thin-walled, with clamp connections; skeletal hyphae pale yellow, thick-walled with narrow lumen or sub-solid, arboriform and flexuous; binding hyphae colourless, thick-walled, rarely branched and flexuous. *Basidiospores* ellipsoid to ovoid, truncated, pale yellow, double-walled with distinctly thick walls, exospore wall verrucose to vermicular, endospore wall with conspicuous spinules.

Notes: *Trachyderma* is an illegitimate name as homonym of a lichen genus in *Pannariaceae* and was renamed as *Trachydermella*

in this study. *Trachydermella* is similar to *Tomophagus* in the pale white and soft context when fresh, but pale straw yellow pilei with non-obvious ornamentation, dimitic hyphal system with branched generative hyphae, and smaller basidiospores of *Tomophagus* can distinguish them easily (Murrill 1905, Le *et al.* 2012). In the phylogenetic analyses, *Trachydermella* formed an independent clade within *Ganodermataceae* (Fig. 1).

Trachydermella tsunodae (Yasuda ex Lloyd) B.K. Cui & Y.F. Sun, ***comb. nov.*** MycoBank MB 306952. Figs 81, 82.
Basionym: *Polyporus tsunodae* Yasuda ex Lloyd, Mycol. Writ. (Cincinnati) 5: 792. 1918.

Description: *Basidiomata* annual, sessile, soft corky when fresh. *Pilei* solitary, flatly flabelliform, up to 8 cm diam and 3 mm thick. *Pileal surface* ochraceous to yellowish brown when fresh, dull, glabrous, with obvious dark concentric zones and radial wrinkles; margin obtuse, entire, incurved when dry. *Pore surface* wood brown when dry; pores circular, 3–5 per mm; dissepiments moderately thick, entire. *Context* cream to pale wood brown, with dark melanoid lines, watery when fresh and turning hard corky when dry, up to 1.5 mm thick. *Tubes* straw yellow, up to 1.2 mm long. *Hyphal system* trimitic; generative hyphae with clamp connections, all the hyphae IKI + (dextrinoid), CB +; tissues darkening in KOH. Generative hyphae in context colourless, thin-walled, 2–3 µm diam; skeletal hyphae in context pale yellow, thick-walled with narrow lumen or sub-solid, arboriform and flexuous, 2–5 µm diam; binding hyphae in context colourless, thick-walled, rarely branched and flexuous, 1–1.5 µm diam. Generative hyphae in tubes colourless, thin-walled, 2–3 µm diam; skeletal hyphae in tubes pale yellow, thick-walled with narrow lumen or sub-solid, arboriform and flexuous, 2–4 µm diam; binding hyphae in tubes colourless, thick-walled, rarely branched and flexuous, up to 1.5 µm diam. *Pileipellis* composed of clamped generative hyphae, thin- to slightly thick-walled, apical cells clavate, flexuous, yellowish brown, about 25–43 × 3–7 µm, forming a patchy palisade. *Cystidia* and *cystidioles* absent. *Basidia* barrel-shaped, colourless, thin-walled, 25–35 × 22–24 µm; *basidioles* in shape like the basidia, colourless, thin-walled, 20–27 × 12–20 µm. *Basidiospores* ellipsoid to ovoid, truncated, pale yellow, IKI + (dextrinoid), CB +, double-walled with distinctly thick walls, exospore wall verrucose to vermicular, endospore wall with conspicuous spinules, (19.4–)19.8–21.5(–22) × (12.5–)12.7–15(–15.2) µm, L = 20.48 µm, W = 13.96 µm, Q = 1.47 (n = 60/1, with the turgid vesicular appendix included).

Material examined: **China**, Guizhou, on dead tree of *Litsea cubeba*, 17 Jun. 2000, Dai 3221c (BJFC018543).

Notes: The holotype of *Trachydermella tsunodae* was collected from Japan, and is distinguished by its pale white and watery context when fresh, large basidia (25–35 × 22–24 µm) and basidioles (20–27 × 12–20 µm), and truncated basidiospores with verrucose to vermicular exospore walls. The specimens of *Tr. tsunodae* used in this study were collected from Guizhou Province in southwest China. Our observations of *Tr. tsunodae* are generally consistent with the original description, but the obvious binding hyphae observed in this specimen are contrary to the dimitic hyphal system recorded by Imazeki (1952).

Fig. 81. Basidiomata of *Trachydermella tsunodae*.

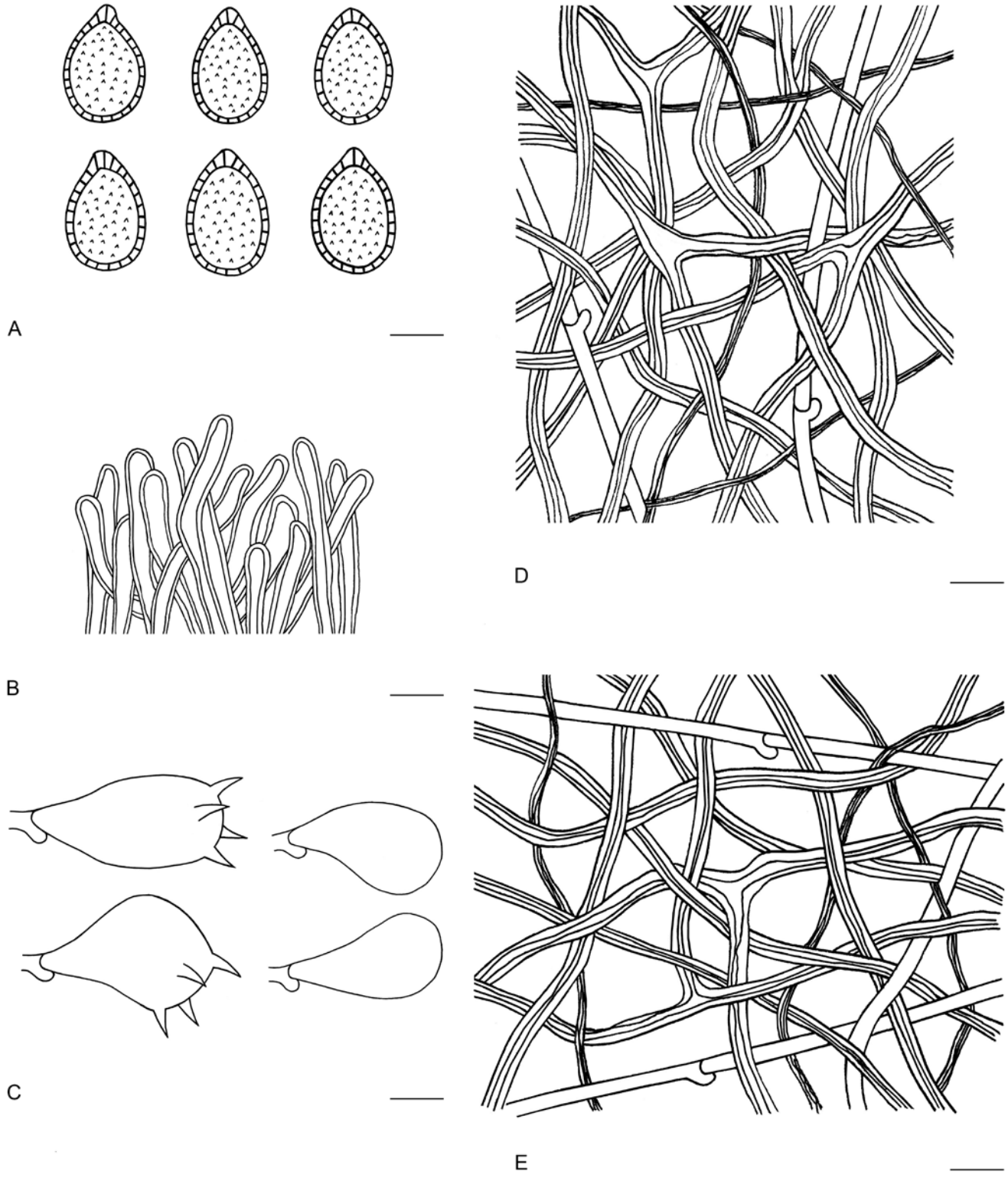

Fig. 82. Microscopic structures of *Trachyderma tsunodae* (drawn from Dai 3221c). **A.** Basidiospores. **B.** Apical cells from cuticle. **C.** Basidia and basidioles. **D.** Hyphae from trama. **E.** Hyphae from context. Scale bars = 10 μm.

DISCUSSION

Ganodermataceae is one of the most important families of macrofungi with many species having important ecological and economic values (Pilotti 2005, Dai *et al.* 2009, Glen *et al.* 2009, Cao *et al.* 2012, Chan *et al.* 2013, Zhou *et al.* 2015, Jong *et al.* 2017, Rodríguez-Couto 2017, Zhang *et al.* 2019, Wang *et al.* 2021). As species of the family have medicinal, agricultural and biotechnological application, accurate classification of *Ganodermataceae* has been pursued for a long time (Murrill 1905, Donk 1948, Imazeki 1952, Steyaert 1972, Moncalvo & Ryvarden 1997, Ryvarden 2004b, Costa-Rezende *et al.* 2017, 2020b, Sun *et al.* 2020). *Ganodermataceae* is a large and complex family and although many studies have focused on *Ganodermataceae*, the species diversity, geographic distribution, species classification, taxonomy and phylogeny of *Ganodermataceae* remained uncertain.

Donk (1948) proposed *Ganodermataceae* as a family, but it was not widely accepted until the sixth edition of the "Dictionary of Fungi" published by Ainsworth & Bisby (1971). Since then, *Ganodermataceae* has been treated as a family with unique

double-walled basidiospores with particular ornamentation on the endospore walls in the *Polyporales* (Ryvarden 2004b, Costa-Rezende *et al.* 2017, 2020b, Hapuarachchi *et al.* 2019b). Based on morphological observations and the six-gene combined phylogenetic analyses, 14 genera were confirmed in *Ganodermataceae*: *Amauroderma*, *Amaurodermellus*, *Cristataspora*, *Foraminispora*, *Furtadoella gen. nov.*, *Ganoderma*, *Haddowia*, *Humphreya*, *Magoderna*, *Neoganoderma gen. nov.*, *Sanguinoderma*, *Sinoganoderma gen. nov.*, *Tomophagus* and *Trachydermella gen. nov*. Besides the four new genera, detailed descriptions for *Ganoderma*, *Haddowia*, *Humphreya*, *Magoderna*, *Sanguinoderma* and *Tomophagus* are also provided in this study. The details of *Amauroderma*, *Amaurodermellus*, *Cristataspora*, *Foraminispora* and *Furtadoella gen. nov.* are well-presented in Costa-Rezende *et al.* (2017, 2020b) and Sun *et al.* (2020). In our work, SEM micrographs of basidiospores of 10 genera in *Ganodermataceae* were presented (Fig. 8). The keys for six genera of *Ganodermataceae* are provided, and 56 species including 23 new species are described and illustrated.

Neoganoderma was presented as a new genus with one species, *N. neurosporum*. The study of *N. neurosporum* is limited due to the scarcity of specimens from the Neotropics, and detailed description was provided by Ryvarden (2004b) and Costa-Rezende *et al.* (2020b). *Neoganoderma* can be distinguished by its unique basidiospores with longitudinal ridges which equal in length to basidiospores on the endospore wall.

Sinoganoderma has similar morphological characters with *Ganoderma*, such as flabelliform pilei with pale reddish brown and laccate pileal surface, truncated basidiospores with ornamentation on the endospore wall. However, *Sinoganoderma* differs by its applanate pilei with paler pileal surface, cream context, large pores with thin dissepiments, truncated basidiospores with an uneven or foveolate exospore wall and solid spinules on the endospore wall (Fig. 8 H). *Sinoganoderma shandongense* is the only species recognised in *Sinoganoderma*. It was originally described as *G. shandongense* from temperate areas of Shandong Province, East China (Zhao & Zhang 1986a).

Ganoderma is the largest genus in *Ganodermataceae* including 459 taxa recorded in Index Fungorum (http://www.indexfungorum.org/) as of 17 April 2021. Considering previous studies and the current morphological and phylogenetic analyses, 181 species of *Ganoderma* are confirmed, including 16 new species; 40 species was confirmed for China (Moncalvo & Ryvarden 1997, Ryvarden 2004b, Cao *et al.* 2012, Dai 2012, Hapuarachchi *et al.* 2018b, Xing *et al.* 2018, Hapuarachchi *et al.* 2019b, Decock & Ryvarden 2020, Ryvarden 2020). In this study, 95 taxa of *Ganoderma* with available molecular data were involved in the phylogenetic analyses and divided into 10 clades based on the laccate or dull pileal surface (Fig. 1). The species in subclade I (84 % ML, 1.00 BPP) have laccate pileal surface except *G. mirabile*. Subclade II (100 % ML, 1.00 BPP) and subclade III (100 % ML, 1.00 BPP) constituted monophyletic laccate species. Subclade IV (100 % ML, 1.00 BPP) and subclade VI (98 % ML, 1.00 BPP) were only composed of the species with a dull pileal surface. Subclade V (93 % ML, 1.00 BPP) included the species with dull pileal surface except *G. destructans*, *G. dunense*, *G. mutabile* and *G. pfeifferi* which have visibly obviously laccate pileal surface. Except for *G. hoehnelianum* and *G. puerense sp. nov.*, subclade VII (75 % ML, 0.99 BPP), subclade VIII, subclade IX (100 % ML, 1.00 BPP) and subclade X (99 % ML, 1.00 BPP) were formed by the laccate species. According to the evolutionary progress in the phylogenetic tree, it might be assumed that *Ganoderma* species have evolved from laccate to dull. Whether the feature of laccate or dull pileal surface can be the key evidence for reconstructing classification system of *Ganoderma* remains to be explored in the future.

Fryssouli *et al*. (2020) performed a single-gene phylogenetic analysis for 80 *Ganoderma* species based on ITS sequences, and the *Ganoderma* species were divided into five clades: Clade A (including clusters A1, A2, A3), Clade B, Clade C (including clusters C1, C2), Clade D (including clusters D1, D2, D3, D4), Clade E (including clusters E1, E2, E3, E4, E5). Clade A consisted of both laccate species and dull species, and these species form four different subclades (subclade VII, subclade VIII, subclade IX, subclade X) in our study. Clade B consisted of dull species, which is corresponding to subclade VI composed of the species with dull pileal surface in our study. Clade C includes six species from Paleotropics with laccate pileal surface in corresponding to subclade II in our study. Clade D included four clusters, cluster D1 only include *G. mbrekobenum*, which is corresponding to subclade III in our study, while clusters D2, D3 and D4 all including laccate species which formed subclade I in our study. Clade E (including clusters E1, E2, E3, E4, E5) is consisted of species with both laccate and dull pileal surface, cluster E1 only includes dull species which formed subclade IV in our study, while clusters E2, E3, E4 and E5 including both laccate and dull species which formed subclade V in our study. This indicated that the division of *Ganoderma* species by ITS based analysis by Fryssouli *et al*. (2020) is different from the division of *Ganoderma* species by our multiple gene-based analysis (Fig. 1). Moreover, the ITS based phylogenetic analysis (Fig. 2) for species of *Ganoderma* and related genera in our current study shown that species of *Ganoderma* were mixed together with other genera, which indicated that the single ITS based analysis is not sufficient to investigate the relationship of *Ganoderma* and related genera.

Amauroderma s. str., *Foraminispora*, *Furtadoella* and *Sanguinoderma* were separated from *Amauroderma s. lat.* based on morphological and phylogenetic studies (Costa-Rezende *et al.* 2017, Sun *et al.* 2020). As of 17 April 2021, 137 taxa of *Amauroderma* had been recorded in Index Fungorum (http://www.indexfungorum.org/), among them 58 species were confirmed as independent species (Table 2). According to Costa-Rezende *et al.* (2020a), 24 *Amauroderma* species were reported from the Neotropics, among those 16 species were phylogenetically supported. The previous studies have recorded 24 species of *Amauroderma* in China (Zhao & Zhang 2000, Li & Yuan 2015, Song et al. 2016), however, 16 of them have been demonstrated as synonyms or with confused nomenclatures (Steyaert 1972, Moncalvo & Ryvarden 1997, Li & Yuan 2015, Sun *et al.* 2020), and the others need to be abandoned because of incorrect descriptions or misidentifications; for the time being, there are no species of *Amauroderma s. str.* Known from China. *Foraminispora* was established by Costa-Rezende *et al.* (2017) and typified by *Fo. rugosa* from the Neotropics. Sun *et al.* (2020) proposed that, *Fo. austrosinensis*, *Fo. concentrica*, *Fo. yinggelingensis* and *Fo. yunnanensis* which were described from China should be included in *Foraminispora* based on similar spore ultrastructure characters and phylogenetic analysis. *Furtadoella* consisted of three species from the Neotropics based on soft basidiomata with dull pileal surface and pale context, dimitic hyphal system in trama but a monomitic hyphal system in context, with both clamped and simple-septate generative hyphae (Costa-Rezende *et al.* 2017). *Sanguinoderma* is composed of species from tropical Asia, Africa and Oceania, with the colour of fresh pore surface changing to blood red when bruised. In this study, six new species were described with effective morphological differences

and phylogenetic support, and a total of 16 species were confirmed in *Sanguinoderma*.

Costa-Rezende *et al.* (2020b) established two genera in *Ganodermataceae* with adequate analyses, which was further confirmed in this study. *Amaurodermellus* is proposed to contain the Neotropical species: *Amauroderma ovisporum* based on amaurodermoid basidiomata with ovoid and non-truncated basidiospores. *Cristataspora* is composed of *Ganoderma coffeatum* and *G. flaviporum*, which are distinguished by stipitate basidiomata with white context, and truncated basidiospores with vertical or transverse ridges on the endospore walls. *Ganoderma coffeatum* was recorded by Zhao & Zhang (2000) as *Humphreya coffeata* in China, but the specimens stored in HMAS has been determined as *G. lucidum* through morphological observation.

Haddowia was established by Steyaert (1972) including *Ha. aëtii* and *Ha. longipes* based on non-truncated basidiospores with longitudinal ridges partly connected with short transverse walls on exospore walls (Fig. 8 E). Zmitrovich (2018) combined *Ha. aëtii* to *Ganoderma* as *G. aetii*. In this study, *Ha. macropora* was described from French Guiana as a new species with yellowish brown pileal surface, large pores, intermittently longitudinal crests and transverse membranes on the exospore walls.

Humphreya has unique basidiospores with truncated apex and reticular or erratic irregularly ridged double walls. *Humphreya coffeata* has been combined to *Cristataspora* due to the longitudinally orientated crests as an independent phylogenetic branch (Costa-Rezende *et al.* 2020b). The taxonomic status of *Hu. eminii*, *Hu. endertii* and *Hu. lloydii* need to be further clarified based on more specimens.

In comparison to other genera, *Magoderna* has anticlinal hyphae in the pileipellis, ellipsoid to ovoid basidiospores with faintly verrucose exospore wall and tiny spinules on the endospore wall (Fig. 8 F). *Magoderna infundibuliforme*, *M. subresinosum* and *M. vansteenisii* were first included in *Magonderna* when it was established as a genus (Steyaert 1972). *Magoderna vansteenisii* has since been combined as *Sanguinoderma rugosum* by Corner (1983) without type specimen examination. And no available specimen of *M. infundibuliforme* was examined in this study, so, it should be kept as separate species in *Magoderna* before studying type specimens.

Tomophagus can be distinguished by the pale and soft context, and dimitic hyphal system with branched generative hyphae (Le *et al.* 2012). *Tomophagus colossus* and *To. cattienensis* were included into *Tomophagus* and formed an independent clade with good support in the phylogenetic tree (Fig. 1). One specimen of *To. cattienensis* collected from Malaysia was examined by macro-morphology, and microscopic examinations together with ultrastructural observations. The exospore wall of the basidiospores in *Tomophagus* was slightly foveolate to verrucose to reticulate which resembles *Ganoderma*, but the ornamentation of the latter is deeper (Fig. 8D, I). The detailed descriptions of *Tomophagus* given in this study make it more credible and recognisable as genus in *Ganodermataceae*.

Trachyderma was renamed as *Trachydermella* due to its illegitimacy, and has one species so far, *Tr. tsunodae*. In this study, *Tr. tsunodae* showed to be an independent clade with high support in the phylogenetic tree (Fig. 1). The specimen collected in southwestern China was confirmed by the watery context when fresh and large hyphae, spores and basidia, since no sequence could be generated. The ornamentation of basidiospores in *Trachydermella* has been observed under SEM, and shows a similar verrucose to reticulate exospore wall to that in *Amauroderma* and *Furtadoella*. However, the distinctly truncated apex of the basidiospores distinguishes *Trachydermella* from *Amauroderma* and *Furtadoella* (Fig. 8A, C, J).

After several studies, 642 taxa of *Ganodermataceae* were recorded in Index Fungorum (http://www.indexfungorum.org/) as of 10 March 2022, among which *Amauroderma* which has 141 records, *Amaurodermellus* has one species, *Cristataspora* has two species, *Foraminispora* has five species, *Furtadoella* has three species, *Ganoderma* has 467 records, *Haddowia* has three records, *Humphreya* has four records, *Magoderna* has three records, *Tomophagus* has two species, *Trachydermella* has one species and *Sanguinoderma* has 10 species. According to the nomenclatural study of *Ganodermataceae* by Moncalvo & Ryvarden (1997) and other studies, there are four major reasons to abandon some species: i) they are synonyms of already named species, ii) the type specimens are lost or immature, iii) they represent invalid names, and iv) there are errors in sequencing and nomenclature. Based on these reasons, we have now confirmed 278 species in the world (Table 2), and 145 of them have molecular data.

In the past few decades, many scholars have focused on exploring the diversity of *Ganodermataceae* with 130 taxa of *Ganodermataceae* in China (Zhao & Zhang 2000, Cao & Yuan 2012, Dai 2012, Wang & Wu 2014, Li *et al.* 2015, Zhou *et al.* 2015, Hapuarachchi *et al.* 2018b, Xing *et al.* 2018, Ye *et al.* 2019, Sun *et al.* 2020, He *et al.* 2021). Previously, the mostly recorded species were recognised only based on morphological characters. However in recent years, phylogenetic analyses have applied to the studies of *Ganodermataceae*. As a result of these studies, more than 30 species have been regarded as synonyms, and several taxa should be abandoned due to being immature specimens without basidiospores or confusing original descriptions (Wang 2005, Cao 2013, Li & Yuan 2015, Xing 2019). Sun *et al.* (2020) classified seven species originally reported as *Amauroderma* in China as other species, and Costa-Rezende *et al.* (2020b) combined *Humphreya coffeatum* to *Cristataspora*. In this study, the remnant of the species was checked based on morphological comparisons and geographic distribution together with phylogenetic analyses. For the time being, 59 species of *Ganodermataceae* are recognised in China, of which only one without available sequences. The recorded taxa of *Ganodermataceae* reported in China and its current taxonomic status are presented in Table 3.

Just recently, two additional new species of *Ganoderma*, *G. dianzhongense* and *G. esculentum* were described by He *et al.* (2021), the morphological characters and molecular evidence were sufficient to recognize their legitimacy even if they were not included in our current phylogenetic analyses. Both of them have been listed in Tables 2 and 3 along with other species of *Ganoderma* in China.

Since ITS and nLSU sequences were first used to identify *Ganoderma* species in Moncalvo *et al.* (1995), many DNA sequences have been uploaded to GenBank (https://www.ncbi.nlm.nih.gov/). These sequences are mostly generated from eight genes: ITS, nLSU, *rpb1*, *rpb2*, *tef1*, *tub*, mtSSU and nSSU; *rpb1* and *tub* are not widely for *Ganodermataceae* due to insufficient quantity. To evaluate the practicability and reliability of six genes, the phylogenetic analyses of *Ganodermataceae* based on ITS, nLSU, *rpb2*, *tef1*, mtSSU and nSSU sequences were carried out respectively (Figs 2–7). The internal transcribed spacer region (ITS) was considered as the universal barcode of fungi (Schoch *et al.* 2012), but its limitation in identifying complex groups or potential species cannot be ignored (Badotti *et al.* 2017) even if ITS is the most abundant gene region in *Ganodermataceae*. Loci such as *rpb2* and *tef1* are very useful for identifying the species

Table 3. Taxonomic status of *Ganodermataceae* reported from China.

Genus	Taxa	Current status	References
Amauroderma (24)	*A. amoiense*	= *Sanguinoderma rugosum*	Li & Yuan (2015)
	A. auriscalpium	Nomenclature unclear and holotype sterile	Moncalvo & Ryvarden (1997)
	A. austrosinense	= *Foraminispora austraosinensis*	Sun *et al.* (2020)
	A. bataanense	= *Sanguinoderma bataaense*	Sun *et al.* (2020)
	A. concentricum	= *Foraminispora concentrica*	Sun *et al.* (2020)
	A. conjunctum	Inconsistent with original description	This study
	A. dayaoshanense	= *Pyrrhoderma sendaiense*	Li & Yuan (2015)
	A. elmerianum	= *Sanguinoderma elmerianum*	Sun *et al.* (2020)
	A. exile	Specimens lost and only distributed in Neotropics	This study
	A. fujianense	= *Ganoderma fornicatum*	Li & Yuan (2015)
	A. guangxiense	Type specimen lost	This study
	A. hongkongense	Holotype polluted and sterile	This study
	A. jiangxiense	Ganodermoid basidiocarps and sterile	This study
	A. longgangense	Ganodermoid basidiocarps and sterile	This study
	A. nigrum	Nomenclature unclear	Moncalvo & Ryvarden (1997)
	A. perplexum	= *Sanguinoderma perplexum*	Sun *et al.* (2020)
	A. preussii	= *Sanguinoderma infundibulare sp. nov.*	This study
	A. rude	= *Sanguinoderma rude*	Sun *et al.* (2020)
	A. rugosum	= *Sanguinoderma rugosum*	Sun *et al.* (2020)
	A. schomburgkii	= *Sanguinoderma elmerianum*	This study
	A. sikorae	= *Amauroderma preussii*	Steyaert (1972)
	A. subresinosum	= *Magoderna subresinosum*	Sun *et al.* (2020)
	A. wuzhishanense	= *Amauroderma rugosum*	Li & Yuan (2015)
	A. yunnanense	= *Foraminispora yunnanensis*	Sun *et al.* (2020)
Ganoderma (104)	*G. ahmadii*	√	This study
	G. albomarginatum	Nomenclature repeated with same specimen	Xing (2019)
	G. amboinense	Nomenclature unclear	Moncalvo & Ryvarden (1997)
	G. angustisporum	√	Xing *et al.* (2018)
	G. annulare	= *Ganoderma australe*	Ryvarden (1989)
	G. applanatum	√	Dai (2012)
	G. atrum	= *Ganoderma flexipes*	Cao (2013)
	G. australe	√	Dai (2012)
	G. austrofujianense	= *Ganoderma sinense*	Cao (2013)
	G. bawanglingense	= *Ganoderma australe*	This study
	G. bicharacteristicum	Holotype sterile	Xing (2019)
	G. boninense	√	Wang (2005)
	G. brownii	Inconsistent with original description	Wang (2005)
	G. calidophilum	√	This study
	G. cantharelloideum	= *Ganoderma lucidum*	Cao (2013)
	G. capense	= *Ganoderma weberianum*	Wang (2005)
	G. casuarinicola	√	Xing *et al.* (2018)
	G. chalceum	Inconsistent with original description	This study
	G. chenghaiense	= *Ganoderma multipileum*	Cao (2013)
	G. chiungchungense	Description and type specimen unclear	Xing (2019)
	G. cochlear	Nomenclature unclear and type specimen lost	Moncalvo & Ryvarden (1997)
	G. colossus	= *Tomophagus colossus*	Cao (2013)
	G. crebrostriatum	= *Ganoderma mastoporum*	Cao (2013)
	G. cupulatiprocerum	= *Ganoderma duropora*	Zhao & Zhang 2000
	G. curtisii	Inconsistent with original description	Xing (2019)

Table 3. (Continued).

Genus	Taxa	Current status	References
	G. daiqingshanense	= *Ganoderma multiplicatum*	Cao (2013)
	G. densizonatum	= *Ganoderma orbiforme*	Wang *et al.* (2014)
	G. dianzhongense	√	He *et al.* (2021)
	G. diaoluoshanense	= *Ganoderma mastoporum*	Cao (2013)
	G. dimidiatum	Description and type specimen unclear	This study
	G. donkii	Inconsistent with original description	Moncalvo & Ryvarden (1997)
	G. duropora	Inconsistent with original description	This study
	G. ellipsoideum	√	Hapuarachchi *et al.* (2018b)
	G. esculentum	√	He *et al.* (2021)
	G. flexipes	√	Dai (2012)
	G. formosanum	= *Ganoderma sinense*	Cao (2013)
	G. fornicatum	= *Ganoderma orbiforme*	Wang *et al.* (2014)
	G. fulvellum	= *Fomes fulvellus*	This study
	G. gibbosum	√	Luangharn *et al.* (2020)
	G. guinanense	= *Ganoderma sinense*	Cao (2013)
	G. guizhouense	Description and type specimen unclear	Xing (2019)
	G. hainanense	= *Ganoderma flexipes*	Cao (2013)
	G. hoehnelianum	√	This study
	G. jianfenglingense	Description and type specimen unclear	Xing (2019)
	G. kunmingense	Holotype sterile	Cao (2013)
	G. leucocontextum	√	Li *et al.* (2015)
	G. limushanense	= *Ganoderma orbiforme*	Wang *et al.* (2014)
	G. lingzhi	√	Cao *et al.* (2012)
	G. lobatum	Inconsistent with original description	This study
	G. lucidum	√	This study
	G. luteomarginatum	= *Ganoderma sinense*	Cao (2013)
	G. magniporum	√	This study
	G. mastoporum	= *Ganoderma orbiforme*	Wang *et al.* (2014)
	G. mediosinense	= *Ganoderma sinense*	Cao (2013)
	G. meijiangense	= *Ganoderma williamsianum*	Wang & Wu (2010)
	G. microsporum	= *Ganoderma weberianum*	Cao (2013)
	G. mirabile	Climate different with type locality	This study
	G. mirivelutinum	= *Ganoderma australe*	This study
	G. mongolicum	Unlike *Ganoderma*	Wang (2005)
	G. multipileum	√	Dai (2012)
	G. multiplicatum	Inconsistent with original description	This study
	G. mutabile	√	Cao & Yuan (2012)
	G. neojaponicum	Inconsistent with original description	Wang (2005)
	G. nigrolucidum	Inconsistent with original description	Wang (2005)
	G. nitidum	Climate different with type locality	This study
	G. ochrolaccatum	Inconsistent with original description	This study
	G. orbiforme	√	Wang *et al.* (2014)
	G. ostracodes	Inconsistent with original description	Wang (2005)
	G. parviungulatum	= *Ganoderma flexipes*	Cao (2013)
	G. petchii	Inconsistent with original description	This study
	G. pfeifferi	Inconsistent with original description	Wang (2005)
	G. philippii	√	Dai (2012)
	G. ramosissimum	Holotype sterile	Cao (2013)
	G. renii	Description unclear and type specimen lost	Cao (2013)

Table 3. (Continued).

Genus	Taxa	Current status	References
	G. resinaceum	Inconsistent with original description	Xing (2019)
	G. rotundatum	= *Ganoderma multiplicatum*	Cao (2013)
	G. sanduense	√	Hapuarachchi *et al.* (2019b)
	G. sanmingense	Holotype sterile	Cao (2013)
	G. shandongense	= *Sinoganoderma shandongense comb. nov.*	This study
	G. shangsiense	= *Ganoderma hoehnelianum*	Wang & Wu (2010)
	G. shanxiense	√	Liu *et al.* (2019)
	G. sichuanense	√	Wang *et al.* (2012)
	G. simaoense	Holotype sterile	Cao (2013)
	G. sinense	√	Dai (2012)
	G. stipitatum	= *Ganoderma tropicum*	Wang (2005)
	G. stratoideum	Description unclear and type specimen lost	Xing (2019)
	G. subumbraculum	= *Ganoderma weberianum*	Wang (2005)
	G. tenue	= *Ganoderma weberianum*	Cao (2013)
	G. theaecola	= *Ganoderma multiplicatum*	Cao (2013)
	G. tibetanum	Description and type specimen unclear	Xing (2019)
	G. triangulum	= *Ganoderma australe*	This study
	G. tropicum	√	Dai (2012)
	G. trulla	Inconsistent with original description	This study
	G. tsugae	√	Dai (2012)
	G. tsunodae	= *Trachydermella tsunodae comb. nov.*	This study
	G. ungulatum	= *Ganoderma australe*	This study
	G. valesiacum	Inconsistent with original description	Wang (2005)
	G. weberianum	√	Dai (2012)
	G. weixiense	√	Ye *et al.* (2019)
	G. williamsianum	√	Dai (2012)
	G. wuhuense	Description unclear and type specimen lost	Xing (2019)
	G. wuzhishanense	Molecular sequence error	Xing (2019)
	G. xingyiense	Description unclear and type specimen lost	Xing (2019)
	G. zhenningense	Description and type specimen unclear	Xing (2019)
Haddowia (1)	*Ha. longipes*	√	Dai (2012)
Humphreya (1)	*Hu. coffeatum*	Inconsistent with original description	This study

in *Ganodermataceae*, but the instability of them usually produces uncontrollable mutations. Compared to other genes, nLSU, mtSSU and nSSU are so conservative that it is hard to delimit the species in *Ganodermataceae* using just these genes. Thus, phylogenetic analyses based on a gene locus alone is insufficient and a combined multi-gene dataset with ITS, nLSU, *rpb2*, *tef1*, *rpb1* and *tub*, is better recommended for phylogenetic analyses of *Ganodermataceae*. In this study, 1 382 sequences from 391 specimens were used in the phylogenetic analyses which included 63 type specimens. There were 817 sequences newly generated and uploaded to GenBank, including 132 sequences of ITS, 139 sequences of nLSU, 83 sequences of *rpb2*, 124 sequences of *tef1*, 150 sequences of mtSSU and 189 sequences of nSSU. The reliability of these sequences was referenced by literature citations, released information on NCBI and practical application, which suggests that the sequences used in this study should be the basis of future phylogenetic analyses of *Ganodermataceae*.

ACKNOWLEDGEMENTS

We express our gratitude to Prof Yu-Cheng Dai (China) for providing specimens and pictures for our study. The curators of herbaria of HMAS, HKAS, GDGM, IFP and Drs Tom May (Australia), Hai-Jiao Li (China), Jie Song (China), Lu-Lu Shen (China), Mei-Ling Han (China), Jun-Liang Zhou (China) and Ms. Xing Ji (China), Yan Wang (China), Yu-Li Han (China) are thanked for help during field collections and molecular studies. Drs Shuang-Hui He (China), Fang Wu (China), Hai-Sheng Yuan (China), Yu-Lian Wei (China), Li-Wei Zhou (China), Jun-Zhi Qiu (China), Hai-Xia Ma (China), Bo Zhang (China), Shi-Liang Liu (China), Ming Zhang (China), De-Wei Li (USA) are thanked for companionship during field collections. Dr Sheng-Hua Wu (China) is thanked for providing valuable suggestions on this study. The research was supported by the National Natural Science Foundation of China (Nos. U2003211, 31870008, 31670016), the Scientific and Technological Tackling Plan for the Key Fields of Xinjiang Production and Construction Corps (No. 2021AB004) and Beijing Forestry University Outstanding Young Talent Cultivation Project (No. 2019JQ03016).

DECLARATION ON CONFLICT OF INTEREST

The authors declare that there is no conflict of interest.

REFERENCES

Adaskaveg JE, Gilbertson RL (1986). Cultural studies and genetics of sexuality of *Ganoderma lucidum* and *G. tsugae* in relation to the taxonomy of the *G. lucidum* complex. *Mycologia* **78**: 694–705.

Aime MC, Henkel TW, Ryvarden L (2003). Studies in Neotropical polypores 15: New and interesting species from Guyana. *Mycologia* **95**: 614–619.

Aime L, Ryvarden L, Henkel TW (2007). Studies in Neotropical polypores 22. Additional new and rare species from Guyana. *Synopsis Fungorum* **23**: 15–31.

Ainsworth GC, Bisby GR (1971). *Dictionary of the fungi*. Commonwealth Mycological Institute, UK.

Badotti F, de Oliveira FS, Garcia CF, *et al.* (2017). Effectiveness of ITS and sub-regions as DNA barcode markers for the identification of *Basidiomycota* (Fungi). *BMC Microbiology* **17**: 1–42.

Binder M, Justo A, Riley R, *et al.* (2013). Phylogenetic and phylogenomic overview of the *Polyporales*. *Mycologia* **105**: 1350–1373.

Boddy L, Büntgen U, Egli S, *et al.* (2014). Climate variation effects on fungal fruiting. *Fungal Ecology* **10**: 20–33.

Bolaños AC, Bononi VLR, de Mello Gugliotta A, *et al.* (2016). New records of *Ganoderma multiplicatum* (Mont.) Pat. (*Polyporales*, *Basidiomycota*) from Colombia and its geographic distribution in South America. *Check List* **12**: 1–7.

Bresadola G (1912). *Polyporaceae* Javanicae. *Annales Mycologici* **10**: 492–508.

Bresadola G (1915). *Basidiomycetes* Philippinenses. Series III. *Hedwigia* **56**: 289–307.

Cabarroi-Hernández M, Villalobos-Arámbula AR, Torres-Torres MG, *et al.* (2019). The *Ganoderma weberianum-resinaceum* lineage: multilocus phylogenetic analysis and morphology confirm *G. mexicanum* and *G. parvulum* in the neotropics. *MycoKeys* **59**: 95–131.

Campacci TVS, Gugliotta AM (2009). A review of *Amauroderma* in Brazil, with the new record of *A. oblongisporum* in the Neotropics. *Mycotaxon* **110**: 423–436.

Cao Y (2013). *Taxonomy and phylogeny of Ganoderma in China*. Ph.D. dissertation. The University of Chinese Academy of Sciences in Shenyang, China.

Cao Y, Yuan HS (2012). *Ganoderma mutabile sp. nov.* from southwestern China based on morphological and molecular data. *Mycological Progress* **12**: 121–126.

Cao Y, Wu SH, Dai YC (2012). Species clarification of the prize medicinal *Ganoderma* mushroom 'Lingzhi'. *Fungal Diversity* **56**: 49–62.

Chan PM, Kanagasabapathy G, Tan YS, *et al.* (2013). *Amauroderma rugosum* (Blume & T. Nees) Torrend: nutritional composition and antioxidant and potential anti-inflammatory properties. *Evidence-Based Complementary and Alternative Medicine* **2013**: 1–10.

Coelho G, Cortez VG, Guerrero RT (2007). New morphological data on *Amauroderma brasiliense* (Polyporales, Basidiomycota). *Mycotaxon* **2007**: 177–183.

Coetzee MPA, Marincowitz S, Muthelo VG, *et al.* (2015). *Ganoderma* species, including new taxa associated with root rot of the iconic *Jacaranda mimosifolia* in Pretoria, South Africa. *IMA Fungus* **6**: 249–256.

Corner EJH (1983). Ad Polyporaceas I. *Amauroderma* and *Ganoderma*. *Beihefte zur Nova Hedwigia* **75**: 1–182.

Costa-Rezende DH, Gugliotta AM, Góes-Neto A, *et al.* (2016). *Amauroderma calcitum sp. nov.* and notes on taxonomy and distribution of *Amauroderma* species (*Ganodermataceae*). *Phytotaxa* **244**: 101–124.

Costa-Rezende DH, Robledo GL, Góes-Neto A, *et al.* (2017). Morphological reassessment and molecular phylogenetic analyses of *Amauroderma s. lat.* raised new perspectives in the generic classification of the *Ganodermataceae* family. *Persoonia* **39**: 254–269.

Costa-Rezende DH, Góes-Neto A, Drechsler-Santos ER (2020a). Studies on Brazilian *Amauroderma s. str.* reveal a new species from the Atlantic forest, *Amauroderma robledoi sp. nov.* (*Polyporales*, *Ganodermataceae*). *The Journal of the Torrey Botanical Society* **147**: 199–205.

Costa-Rezende DH, Robledo GL, Drechsler-Santos ER, *et al.* (2020b). Taxonomy and phylogeny of polypores with ganodermatoid basidiospores (*Ganodermataceae*). *Mycological Progress* **19**: 725–741.

Crous PW, Wingfield MJ, Schumacher RK, *et al.* (2014). Fungal Planet Description Sheets: 281–319. *Persoonia* **33**: 212–289.

Crous PW, Wingfield MJ, Le Roux, *et al.* (2015). Fungal Planet Description Sheets: 371–399. *Persoonia* **35**: 264–327.

Crous PW, Wingfield MJ, Richardson DM, *et al.* (2016). Fungal Planet description sheets: 400–468. *Persoonia* **36**: 316–458.

Crous PW, Wingfield MJ, Burgess TI, *et al.* (2017a). Fungal Planet description sheets: 558–624. *Persoonia* **38**: 240–384.

Crous PW, Wingfield MJ, Burgess TI, *et al.* (2017b). Fungal Planet description sheets: 625–715. *Persoonia* **39**: 270–467.

Crous PW, Luangsa-ard JJ, Wingfield MJ, *et al.* (2018). Fungal Planet Description Sheets: 785–867. *Persoonia* **41**: 238–417.

Cui BK, Li HJ, Ji X, *et al.* (2019). Species diversity, taxonomy and phylogeny of *Polyporaceae* (*Basidiomycota*) in China. *Fungal Diversity* **97**: 137–392.

Dai YC (2012). Polypore diversity in China with an annotated checklist of Chinese polypores. *Mycoscience* **53**: 49–80.

Dai YC, Yang ZL, Cui BK, *et al.* (2009). Species diversity and utilization of medicinal mushrooms and fungi in China. *International Journal of Medicinal Mushrooms* **11**: 287–302.

De Lima Júnior N, Gibertoni BT, Malosso E (2014). Delimitation of some Neotropical laccate *Ganoderma* (*Ganodermataceae*): molecular phylogeny and morphology. *Revista de Biologia Tropical* **62**: 1197–1208.

Decock C, Ryvarden L (2020). *Aphyllophorales* of Africa 41. Some polypores from Gabon. *Synopsis Fungorum* **42**: 5–15.

Donk MA (1948). Notes on Malesian fungi. I. *Bulletin du Jardin Botanique de Buitenzorg* **17**: 473–482.

Douanla-Meli C, Langer E (2009). *Ganoderma carocalcareus sp. nov.*, with crumbly-friable context parasite to saprobe on *Anthocleista nobilis* and its phylogenetic relationship in *G. resinaceum* group. *Mycological Progress* **8**: 145–155.

Farris JS, Kallersjo M, Kluge AG, *et al.* (1994). Testing significance of incongruence. *Cladistics* **10**: 315–319.

Foroutan A, Vaidya JG (2007). Record of new species of *Ganoderma* in Maharashtra, India. *Asian Journal of Plant Sciences* **6**: 913–919.

Fryssouli V, Zervakis GI, Polemis E, *et al.* (2020). A global meta-analysis of ITS rDNA sequences from material belonging to the genus *Ganoderma* (*Basidiomycota*, *Polyporales*) including new data from selected taxa. *MycoKeys* **75**: 71–143.

Furtado JS (1967a). Some tropical species of *Ganoderma* (*Polyporaceae*) with pale context. *Persoonia* **4**: 379–389.

Furtado JS (1967b). Species of *Amauroderma* Murr. with the laccate appearance of *Ganoderma* Karst. *Bulletin du Jardin Botanique National de Belgique* **37**: 309–317.

Gibertoni T, Bernicchia A, Ryvarden L, *et al.* (2008). Bresadola's polypore collection at the Natural History Museum of Trento, Italy 2. *Mycotaxon* **104**: 321–323.

Glen M, Bougher NL, Francis AA, *et al.* (2009). *Ganoderma* and *Amauroderma* species associated with root-rot disease of *Acacia mangium* plantation trees in Indonesia and Malaysia. *Australasian Plant Pathology* **38**: 345–356.

Gomes-Silva AC, Baltazar JM, Ryvarden L, *et al.* (2010). *Amauroderma calcigenum* (*Ganodermataceae*, *Basidiomycota*) and its presumed synonym *A. partitum*. *Nova Hedwigia* **90**: 449–455.

Gomes-Silva AC, Gibertoni TB (2012). Neotypification of *Amauroderma picipes* Torrend, 1920 (*Ganodermataceae*, *Agaricomycetes*). *Mycosphere* **3**: 23–27.

Gomes-Silva AC, De Lima-Júnior NC, Malosso E, *et al.* (2015). Delimitation of taxa in *Amauroderma* (*Ganodermataceae*, *Polyporales*) based

in morphology and molecular phylogeny of Brazilian specimens. *Phytotaxa* **227**: 201–228.
Gottlieb AM, Ferrer E, Wright JE (2000). rDNA analyses as an aid to the taxonomy of species of *Ganoderma*. *Mycological Research* **104**: 1033–1045.
Gulaid H, Ryvarden L (1998). Two new species of *Amauroderma* (*Ganodermataceae*, *Basidiomycetes*). *Mycologia Helvetica* **10**: 25–30.
Hall TA (1999). Bioedit: a user-friendly biological sequence alignment editor and analysis program for Windows 95/98/NT. *Nucleic Acids Symposium Series* **41**: 95–98.
Hapuarachchi KK, Karunarathna SC, Phengsintham P, *et al.* (2018a). *Amauroderma* (*Ganodermataceae*, *Polyporales*) – bioactive compounds, beneficial properties and two new records from Laos. *Asian Journal of Mycology* **1**: 121–136.
Hapuarachchi KK, Karunarathna SC, Raspé O, *et al.* (2018b). High diversity of *Ganoderma* and *Amauroderma* (*Ganodermataceae*, *Polyporales*) in Hainan Island, China. *Mycosphere* **9**: 931–982.
Hapuarachchi KK, Karunarathna SC, McKenzie EHC, *et al.* (2019a). High phenotypic plasticity of *Ganoderma sinense* (*Ganodermataceae*, *Polyporales*) in China. *Asian Journal of Mycology* **2**: 1–47.
Hapuarachchi KK, Karunarathna SC, Phengsintham P, *et al.* (2019b). *Ganodermataceae* (*Polyporales*): diversity in greater Mekong subregion countries (China, Laos, Myanmar, Thailand and Vietnam). *Mycosphere* **10**: 221–309.
He J, Luo ZL, Tang SM, *et al.* (2021). Phylogenetic analyses and morphological characters reveal two new species of *Ganoderma* from Yunnan Province, China. *MycoKeys* **84**: 141–162.
He SC, Yu HF (1989). The family *Ganodermataceae* from Guizhou Province of China II. *Acta Mycologica Sinica* **8**: 282–288.
Henao-M LG (1997). Afiloforales de Colombia III: *Amauroderma* (*Basidiomycetes*: *Ganodermataceae*) en el Herbario Nacional Colombiano. *Caldasia* **19**: 131–143.
Humphrey CJ (1938). Notes on some *Basidiomycetes* from the Orient. *Mycologia* **30**: 327–335.
Imazeki R (1952). A contribution to the fungus flora of Dutch New Guinea. *Bulletin of the Government Forest Experimental Station Meguro* **57**: 87–128.
Ipulet P, Ryvarden L (2005). New and interesting polypores from Uganda. *Synopsis Fungorum* **20**: 87–99.
Jong WYL, Show PL, Ling TC, *et al.* (2017). Recovery of lignin peroxidase from submerged liquid fermentation of *Amauroderma rugosum* (Blume & T. Nees) Torrend using polyethylene glycol/salt aqueous two-phase system. *Journal of Bioscience and Bioengineering* **124**: 91–98.
Justo A, Miettinen O, Floudas D, *et al.* (2017). A revised family-level classification of the *Polyporales* (*Basidiomycota*). *Fungal Biology* **121**: 798–824.
Katoh K, Standley DM (2013). MAFFT Multiple sequence alignment software version 7: improvements in performance and usability. *Molecular Biology Evolution* **30**: 772–780.
Kim HK, Seo GS, Kim HG (2001). Comparison of characteristics of *Ganoderma lucidum* according to geographical origins: consideration of morphological characteristics (II). *Mycobiology* **29**: 80–84.
Kinge TR, Mih AM (2011). *Ganoderma ryvardense sp. nov.* associated with basal stem rot (BSR) disease of oil palm in Cameroon. *Mycosphere* **2**: 179–188.
Kinge TR, Mih AM (2014). *Ganoderma lobenense* (*Basidiomycetes*), a new species from oil palm (*Elaeis guineensis*) in Cameroon. *Journal of Plant Sciences* **2**: 242–245.
Le XT, Le QHN, Pham ND, *et al.* (2012). *Tomophagus cattienensis sp. nov.*, a new *Ganodermataceae* species from Vietnam: evidence from morphology and ITS DNA barcodes. *Mycological Progress* **11**: 775–780.
Le XT, Le QHN, Bui HT, *et al.* (2018). Current status of *Humphreya endertii* and a new species (*Ganodermataceae*) recorded in South Vietnam. *Agrica* **7**: 102–109.
Li MJ, Yuan HS (2015). Type studies on *Amauroderma* species described by J.D. Zhao *et al.* and the phylogeny of species in China. *Mycotaxon* **130**: 79–89.
Li TH, Hu HP, Deng WQ, *et al.* (2015). *Ganoderma leucocontextum*, a new member of the *G. lucidum* complex from southwestern China. *Mycoscience* **56**: 81–85.
Liao B, Chen XC, Han JP, *et al.* (2015). Identification of commercial *Ganoderma* (Lingzhi) species by ITS2 sequences. *Chinese Medicine* **10**: 22.
Liu H, Guo LJ, Li SL, *et al.* (2019). *Ganoderma shanxiense*, a new species from northern China based on morphological and molecular evidence. *Phytotaxa* **406**: 129–136.
Liu YJ, Whelen S, Hall BD (1999). Phylogenetic relationships among ascomycetes: evidence from an RNA polymerase II subunit. *Molecular Biology Evolution* **16**: 1799–1808.
Loyd AL, Held BW, Barnes CW, *et al.* (2018). Elucidating '*lucidum*': distinguishing the diverse laccate *Ganoderma* species of the United States. *PLoS ONE* **13**: e0199738.
Luangharn T, Karunarathna SC, Mortimer PE, *et al.* (2019). Additions to the knowledge of *Ganoderma* in Thailand: *Ganoderma casuarinicola*, a new record; and *Ganoderma thailandicum sp. nov. MycoKeys* **59**: 47–65.
Luangharn T, Karunarathna SC, Mortimer PE, *et al.* (2020). Morphology, phylogeny and culture characteristics of *Ganoderma gibbosum* collected from Kunming, Yunnan Province, China. *Phyton-International Journal of Experimental Botany* **89**: 743–764.
Luangharn T, Karunarathna SC, Dutta AK, *et al.* (2021). *Ganoderma* (*Ganodermataceae*, *Basidiomycota*) species from the greater Mekong subregion. *Journal of Fungi* **7**: 819.
Maddison WP, Maddison DR (2017). *Mesquite: a modular system for evolutionary analysis.* Version 3.2. http://mesquiteproject.org.
Moncalvo JM, Wang HF, Hseu RS (1995). Phylogenetic relationships in *Ganoderma* inferred from the internal transcribed spacers and 25S ribosomal DNA sequences. *Mycologia* **87**: 223–1238.
Moncalvo JM, Ryvarden LA (1997). Nomenclatural study of the *Ganodermataceae* Donk. *Synopsis Fungorum* **11**: 1–114.
Murrill WA (1902). The *Polyporaceae* of North America: I. The genus *Ganoderma*. *Bulletin of the Torrey Botanical Club* **29**: 599–608.
Murrill WA (1905). *Tomophagus* for *Dendrophagus*. *Torreya* **5**: 197.
Murrill WA (1907). Some Philippine *Polyporaceae*. *Bulletin of the Torrey Botanical Club* **34**: 465–481.
Murrill WA (1908a). Additional Philippine *Polyporaceae*. *Bulletin of the Torrey Botanical Club* **35**: 391–416.
Murrill WA (1908b). *Polyporaceae*, Part 2. *North American Flora* **9**: 73–131.
Náplavová K, Beck T, Pristaš P, *et al.* (2020). Molecular data reveal unrecognized diversity in the European *Ganoderma resinaceum*. *Forests* **11**: 850–864.
Nylander JAA (2004). *MrModeltest v2.* Evolutionary Biology Centre, Uppsala University, Program distributed by the author.
Otieno NC (1968). *Polyporaceae* of eastern Africa: II. The genus *Amauroderma* Murrill. *Sydowia* **22**: 173–178.
Papp V (2016). The first validly published laccate *Ganoderma* species from East-Asia: *G. dimidiatum comb. nov.*, the correct name for *G. japonicum*. *Studia Botanica Hungarica* **47**: 263–268.
Patouillard NT (1887). *Les hyménomycètes d'Europe*. Paris.
Patouillard NT (1889). Le genre *Ganoderma*. *Bulletin de la Société Mycologique de France* **5**: 64–80.
Patouillard NT (1907). Champignons nouveaux du Tonkin. *Bulletin de la Société Mycologique de France* **23**: 69–79.
Patouillard NT (1914). Quelques Champignons du Congo. *Bulletin de la Société Mycologique de France* **30**: 336–346.
Petersen JH (1996). *Farvekort. The Danish Mycological Society's colour-chart*. Foreningen til Svampekundskabens Fremme. Greve.
Pilotti CA (2005). Stem rots of oil palm caused by *Ganoderma boninense*: pathogen biology and epidemiology. *Mycopathologia* **159**: 129–137.
Rehner SA, Buckley E (2005). A *Beauveria* phylogeny inferred from nuclear ITS and EF1-α sequences: evidence for cryptic diversification and links to *Cordyceps teleomorphs*. *Mycologia* **97**: 84–98.
Robledo GL, Newman DS, Popoff OF, *et al.* (2015). *Amauroderma trichodermatum* (*Ganodermataceae*, *Basidiomycota*): first record from Bolivia and geographic distribution map, with notes on nomenclature and morphology. *Check List* **11**: 1–5.

Ronquist F, Huelsenbeck JP (2003). MrBayes 3: bayesian phylogenetic inference under mixed models. *Bioinformatics* **19**: 1572–1574.

Ryvarden L (1974). Type studies in the *Polyporaceae* 2. Species described by M. Beeli. *Bulletin du Jardin Botanique National de Belgique* **44**: 65–76.

Ryvarden L (1981). Type studies in the *Polyporaceae* 12. Species described by F. W. Junghuhn. *Persoonia* **11**: 369–372.

Ryvarden L (1983). Type studies in the *Polyporaceae* 14. Species described by N. Patouillard, either alone or with other mycologists. *Occasional Papers of the Farlow Herbarium of Cryptogamic Botany* **18**: 1–39.

Ryvarden L (1989) Type studies in the *Polyporaceae* 21. Species described by C.G. Lloyd in *Cyclomyces*, *Daedalea*, *Favolus*, *Fomes*, and *Hexagonia*. *Mycotaxon* **35**: 229–236.

Ryvarden L (2000). Studies in neotropical polypores 2. A preliminary key to neotropical species of *Ganoderma* with a laccate pileus. *Mycologia* **92**: 180–191.

Ryvarden L (2004a). Studies in neotropical polypores 19. Two wood-inhabiting *Amauroderma* species. *Synopsis Fungorum* **18**: 57–61.

Ryvarden L (2004b). Neotropical polypores. Part 1. Introduction, *Hymenochaetaceae* and *Ganodermataceae*. *Synopsis Fungorum* **19**: 1–227.

Ryvarden L (2015). Type studies in *Polyporaceae* 31. Species described by V. Cesati. *Synopsis Fungorum* **33**: 5–8.

Ryvarden L (2018). Studies in African *Aphyllophorales* 25. New poroid species from East and Central Africa. *Synopsis Fungorum* **38**: 25–32.

Ryvarden L (2020). A new African *Ganoderma* species. *Synopsis Fungorum* **41**: 1–49.

Ryvarden L, Johansen I (1980). *A preliminary polypores flora of East Africa*. Fungiflora, Oslo: 1–636.

Schoch CL, Seifert KA, Huhndorf S, *et al.* (2012). Nuclear ribosomal internal transcribed spacer (ITS) region as a universal DNA barcode marker for fungi. *Proceedings of the National Academy of Sciences of the United States of America* **109**: 6241–6246.

Shen LL, Wang M, Zhou JL, *et al.* (2019). Taxonomy and phylogeny of *Postia*. Multi-gene phylogeny and taxonomy of the brown-rot fungi: *Postia* (*Polyporales*, *Basidiomycota*) and related genera. *Persoonia* **42**: 101–126.

Smith BJ, Sivasithamparam K (2003). Morphological studies of *Ganoderma* (*Ganodermataceae*) from the Australasian and Pacific regions. *Australian Systematic Botany* **16**: 487–503.

Song J, Cui BK (2017). Phylogeny, divergence time and historical biogeography of *Laetiporus* (*Basidiomycota*, *Polyporales*). *BMC Evolutionary Biology* **17**: 102.

Song J, Xing JH, Decock C, *et al.* (2016). Molecular phylogeny and morphology reveal a new species of *Amauroderma* (*Basidiomycota*) from China. *Phytotaxa* **260**: 47–56.

Sotome K, Hattori T, Ota Y (2011). Taxonomic study on a threatened polypore, *Polyporus pseudobetulinus*, and a morphologically similar species, *P. subvarius*. *Mycoscience* **52**: 319–326.

Stamatakis A (2014). RAxML Version 8: a tool for phylogenetic analyses and post analyses of large phylogenies. *Bioinformatics* **30**: 1312–1313.

Steyaert RL (1961). Genus *Ganoderma* (*Polyporaceae*). Taxa nova-I. *Bulletin du Jardin Botanique de l'État à Bruxelles* **31**: 69–83.

Steyaert RL (1967). Les *Ganoderma* palmicoles. *Bulletin Du Jardin Botanique National de Belgique* **37**: 465–492.

Steyaert RL (1972). Species of *Ganoderma* and related genera mainly of the Bogor and Leiden Herbaria. *Persoonia* **7**: 55–118.

Steyaert RL (1980). Study of Some *Ganoderma* Species. *Bulletin Du Jardin Botanique National de Belgique* **50**: 135–186.

Sun YF, Costa-Rezende DH, Xing JH, *et al.* (2020). Multi-gene phylogeny and taxonomy of *Amauroderma s. lat.* (*Ganodermataceae*). *Persoonia* **44**: 206–239.

Swofford DL (2002). *PAUP*: phylogenetic analysis using parsimony (*and other methods), version 4.0b10*. Sinauer Associates, Sunderland.

Tchotet Tchoumi JM, Coetzee MPA, Rajchenberg M, *et al.* (2019). Taxonomy and species diversity of *Ganoderma* species in the Garden Route National Park of South Africa inferred from morphology and multilocus phylogenies. *Mycologia* **111**: 730–747.

Tchotet Tchoumi JM, Coetzee MPA, Rajchenberg M, *et al.* (2018). Three *Ganoderma* species, including *Ganoderma dunense sp. nov.*, associated with dying *Acacia cyclops* trees in South Africa. *Australasian Plant Pathology* **47**: 431–447.

Teixeira AR (1992). New combinations and new names in the *Polyporaceae*. *Revista Brasileira de Botânica* **15**: 125–127.

Teng SC (1963). *Fungi of China*. Beijing Science Press, China.

Torrend C (1920). Les polyporacées du Brésil 1. Polyporacées stipités. *Brotéria Série Botânica* **18**: 121–143.

Torres-Torres MG, Guzmán-Dávalos L (2012). The morphology of *Ganoderma* species with a laccate surface. *Mycotaxon* **119**: 201–216.

Torres-Torres MG, Guzmán-Dávalos L, De Mello AG (2008). *Ganoderma vivianimercedianum sp. nov.* and the related species, *G. perzonatum*. *Mycotaxon* **105**: 447–454.

Vilgalys R, Hester M (1990). Rapid genetic identification and mapping of enzymatically amplified ribosomal DNA from several *Cryptococcus* species. *Journal of Bacteriology* **172**: 4238–4246.

Wang DM (2005). *Phylogenetic study of Ganoderma in China*. Ph.D. dissertation. The University of Chinese Academy of Sciences in Beijing, China.

Wang DM, Wu SH (2010). *Ganoderma hoehnelianum* has priority over *G. shangsiense*, and *G. williamsianum* over *G. meijiangense*. *Mycotaxon* **113**: 343–349.

Wang DM, Wu SH (2014). Two species of *Ganoderma* new to Taiwan. *Mycotaxon* **102**: 373–378.

Wang DM, Yao YJ (2005). Intrastrain internal transcribed spacer heterogeneity in *Ganoderma* species. *Canadian Journal of Microbiology* **51**: 113–121.

Wang DM, Wu SH, Su CH, *et al.* (2009). *Ganoderma multipileum*, the correct name for '*G. lucidum*' in tropical Asia. *Botanical Studies* **50**: 451–458.

Wang DM, Wu SH, Yao YJ (2014). Clarification of the concept of *Ganoderma orbiforme* with high morphological plasticity. *PLoS ONE* **9**: e98733.

Wang H, Deng W, Shen MH, *et al.* (2021). A laccase Gl-LAC-4 purified from white-rot fungus *Ganoderma lucidum* had a strong ability to degrade and detoxify the alkylphenol pollutants 4-n-octylphenol and 2-phenylphenol. *Journal of Hazardous Materials* **408**: 1–16.

Wang XC, Xi RJ, Li Y, *et al.* (2012). The species identity of the widely cultivated *Ganoderma*, "*G. lucidum*" (Ling-Zhi), in China. *PLoS ONE* **7**: e40857.

Welti S, Courtecuisse R (2010). The *Ganodermataceae* in the French West Indies (Guadeloupe and Martinique). *Fungal Diversity* **43**: 103–126.

White TJ, Bruns T, Lee S, *et al.* (1990). Amplification and direct sequencing of fungal ribosomal RNA genes for phylogenetics. In: Innis MA, Gelfand DH, Sninsky JJ, *et al.* (eds) *PCR protocols: a guide to methods and applications*. Academic Press, San Diego: 315–322.

Xing JH (2019). *Species diversity, taxonomy and phylogeny of Ganoderma*. Ph.D. dissertation. Beijing Forestry University, China.

Xing JH, Song J, Decock C, *et al.* (2016). Morphological characters and phylogenetic analysis reveal a new species within the *Ganoderma lucidum* complex from South Africa. *Phytotaxa* **266**: 115–124.

Xing JH, Sun YF, Han YL, *et al.* (2018). Morphological and molecular identification of two new *Ganoderma* species on *Casuarina equisetifolia* from China. *MycoKeys* **34**: 93–108.

Ye L, Karunarathna SC, Mortimer PE, *et al.* (2019). *Ganoderma weixiensis* (*Polyporaceae*, *Basidiomycota*), a new member of the *G. lucidum* complex from Yunnan Province, China. *Phytotaxa* **423**: 75–86.

Zhang XQ (1994). One new species and one new record of *Ganoderma* from China (*Aphyllophorales*, *Basidiomycota*). *Mycosystema* **7**: 105–110.

Zhang Y, Jiang Y, Zhang M, *et al.* (2019). *Ganoderma sinense* polysaccharide: An adjunctive drug used for cancer treatment. *Progress in Molecular Biology and Translational Science* **163**: 165–177.

Zhao CL, Cui BK (2013). Morphological and molecular identification of four new resupinate species of *Perenniporia* (*Polyporales*) from southern China. *Mycologia* **105**: 945–958.

Zhao JD (1989a) Studies on the taxonomy of *Ganodermataceae* in China. XI. Subgen. *Ganoderma* Sect. *Ganoderma*. *Acta Mycologica Sinica* **8**: 25–34.

Zhao JD (1989b). The *Ganodermataceae* in China. *Bibliotheca Mycologica* **132**: 1–176.

Zhao JD, Zhang XQ (1986a). Taxonomic studies on *Ganodermataceae* of China V. *Acta Mycologica Sinica* **5**: 219–225.

Zhao JD, Zhang XQ (1986b). Taxonomic studies on *Ganodermataceae* of China VII – the genus *Amauroderma*. *Acta Mycologica Sinica, Supplement* **1**: 258–272.

Zhao JD, Zhang XQ (2000). *Chinese Fungi No.1 vol. 18. Ganodermataceae*. Beijing Science Press, China.

Zhao JD, Xu LW, Zhang XQ (1979). Taxonomic studies on the subfamily *Ganodermoideae* of China. *Acta Microbiologica Sinica* **19**: 265–279.

Zhao JD, Xu LW, Zhang XQ (1983). Taxonomic studies on *Ganodermataceae* of China II. *Acta Mycologica Sinica* **2**: 159–167.

Zhao JD, Zhang XQ, Xu LW (1984). Studies on the taxonomy of *Ganodermataceae* in China III. *Acta Mycologica Sinica* **3**: 15–23.

Zhou LW, Cao Y, Wu SH, *et al.* (2015). Global diversity of the *Ganoderma lucidum* complex (*Ganodermataceae*, *Polyporales*) inferred from morphology and multilocus phylogeny. *Phytochemistry* **114**: 7–15

Zmitrovich IV (2018). Conspectus systematis Polyporacearum v. 1.0. *Folia Cryptogamica Petropolitana* **6**: 68.

Studies in Mycology 101: 417–564 (2022).

Genera of phytopathogenic fungi: GOPHY 4

Q. Chen[1], M. Bakhshi[2], Y. Balci[3], K.D. Broders[4], R. Cheewangkoon[5], S.F. Chen[6], X.L. Fan[7], D. Gramaje[8], F. Halleen[9, 10], M. Horta Jung[11], N. Jiang[7], T. Jung[11], T. Májek[11], S. Marincowitz[12], I. Milenković[11], L. Mostert[9], C. Nakashima[13], I. Nurul Faziha[14], M. Pan[7], M. Raza[1], B. Scanu[15], C.F.J. Spies[16], L. Suhaizan[14], H. Suzuki[12], C.M. Tian[7], M. Tomšovský[11], J.R. Úrbez-Torres[17], W. Wang[6], B.D. Wingfield[12], M.J. Wingfield[12], Q. Yang[7], X. Yang[18, 19], R. Zare[2], P. Zhao[1], J.Z. Groenewald[20], L. Cai[1*], P.W. Crous[20, 21, 22*]

[1]*State Key Laboratory of Mycology, Institute of Microbiology, Chinese Academy of Sciences, Beijing 100101, China;* [2]*Department of Botany, Iranian Research Institute of Plant Protection, P.O. Box 19395-1454, Agricultural Research, Education and Extension Organization (AREEO), Tehran, Iran;* [3]*USDA-APHIS Plant Protection and Quarantine, 4700 River Road, Riverdale, Maryland, 20737 USA;* [4]*Smithsonian Tropical Research Institute, Apartado Panamá, República de Panamá;* [5]*Entomology and Plant Pathology Department, Faculty of Agriculture, Chiang Mai University, Chiang Mai, Thailand, 50200;* [6]*China Eucalypt Research Centre (CERC), Chinese Academy of Forestry (CAF), Zhanjiang 524022, Guangdong Province, China;* [7]*The Key Laboratory for Silviculture and Conservation of the Ministry of Education, Beijing Forestry University, Beijing 100083, China;* [8]*Instituto de Ciencias de la Vid y del Vino (ICVV). Consejo Superior de Investigaciones Cientificas - Universidad de La Rioja - Gobierno de La Rioja. Ctra. LO-20 Salida 13, 26007 Logroño. Spain;* [9]*Department of Plant Pathology, University of Stellenbosch, Private Bag X1, Matieland, 7602, South Africa;* [10]*Plant Protection Division, ARC Infruitec-Nietvoorbij, Private Bag X5026, Stellenboscvh, 7599, South Africa;* [11]*Phytophthora Research Centre, Faculty of Forestry and Wood Technology, Mendel University in Brno, Zemědělská 3, 613 00 Brno, Czech Republic;* [12]*Department of Biochemistry, Genetics and Microbiology, Forestry and Agricultural Biotechnology Institute (FABI), University of Pretoria 0002, South Africa;* [13]*Graduate school of Bioresources, Mie University, Kurima-machiya 1577, Tsu, Mie, 514-8507, Japan;* [14]*Faculty of Fisheries and Food Science, Universiti Malaysia Terengganu, 21030 Kuala Nerus, Terengganu, Malaysia;* [15]*Department of Agricultural Sciences, University of Sassari, Viale Italia 39, 07100 Sassari, Italy;* [16]*ARC-Plant Health and Protection, Private Bag X5017, Stellenbosch, 7599, South Africa;* [17]*Agriculture and Agri-Food Canada, Summerland Research and Development Centre, Summerland, British Columbia V0H 1Z0, Canada;* [18]*USDA-ARS, Foreign Disease-Weed Science Research Unit, 1301 Ditto Avenue, Fort Detrick, Maryland, 21702 USA;* [19]*Oak Ridge Institute for Science and Education, ARS Research Participation Program, P.O. Box 117, Oak Ridge, Tennessee, 37831 USA;* [20]*Westerdijk Fungal Biodiversity Institute, P.O. Box 85167, 3508 AD Utrecht, The Netherlands;* [21]*Microbiology, Department of Biology, Faculty of Science, Utrecht University, Padualaan 8, 3584 CT Utrecht, The Netherlands;* [22]*Wageningen University and Research Centre (WUR), Laboratory of Phytopathology, Droevendaalsesteeg 1, 6708 PB Wageningen, The Netherlands*

**Correspondence*: L. Cai, cail@im.ac.cn; P.W. Crous, p.crous@wi.knaw.nl

Abstract: This paper is the fourth contribution in the Genera of Phytopathogenic Fungi (GOPHY) series. The series provides morphological descriptions and information about the pathology, distribution, hosts and disease symptoms, as well as DNA barcodes for the taxa covered. Moreover, 12 whole-genome sequences for the type or new species in the treated genera are provided. The fourth paper in the GOPHY series covers 19 genera of phytopathogenic fungi and their relatives, including *Ascochyta*, *Cadophora*, *Celoporthe*, *Cercospora*, *Coleophoma*, *Cytospora*, *Dendrostoma*, *Didymella*, *Endothia*, *Heterophaeomoniella*, *Leptosphaerulina*, *Melampsora*, *Nigrospora*, *Pezicula*, *Phaeomoniella*, *Pseudocercospora*, *Pteridopassalora, Zymoseptoria*, and one genus of oomycetes, *Phytophthora*. This study includes two new genera, 30 new species, five new combinations, and 43 typifications of older names.

Key words: DNA barcodes, Fungal systematics, New taxa, Typifications.

Taxonomic novelties: New genera: *Heterophaeomoniella* L. Mostert, C.F.J. Spies, Halleen & Gramaje, *Pteridopassalora* C. Nakash. & Crous; **New species:** *Ascochyta flava* Qian Chen & L. Cai, *Cadophora domestica* L. Mostert, R. van der Merwe, Halleen & Gramaje, *Cadophora rotunda* L. Mostert, R. van der Merwe, Halleen & Gramaje, *Cadophora vinacea* J.R. Úrbez-Torres, D.T. O'Gorman & Gramaje, *Cadophora vivarii* L. Mostert, Havenga, Halleen & Gramaje, *Celoporthe foliorum* H. Suzuki, Marinc. & M.J. Wingf., *Cercospora alyssopsidis* M. Bakhshi, Zare & Crous, *Dendrostoma elaeocarpi* C.M. Tian & Q. Yang, *Didymella chlamydospora* Qian Chen & L. Cai, *Didymella gei* Qian Chen & L. Cai, *Didymella ligulariae* Qian Chen & L. Cai, *Didymella qilianensis* Qian Chen & L. Cai, *Didymella uniseptata* Qian Chen & L. Cai, *Endothia cerciana* W. Wang. & S.F. Chen, *Leptosphaerulina miscanthi* Qian Chen & L. Cai, *Nigrospora covidalis* M. Raza, Qian Chen & L. Cai, *Nigrospora globospora* M. Raza, Qian Chen & L. Cai, *Nigrospora philosophiae-doctoris* M. Raza, Qian Chen & L. Cai, *Phytophthora transitoria* I. Milenković, T. Májek & T. Jung, *Phytophthora panamensis* T. Jung, Y. Balci, K. Broders & I. Milenković, *Phytophthora variabilis* T. Jung, M. Horta Jung & I. Milenković, *Pseudocercospora delonicicola* C. Nakash., L. Suhaizan & I. Nurul Faziha, *Pseudocercospora farfugii* C. Nakash., I. Araki, & Ai Ito, *Pseudocercospora hardenbergiae* Crous & C. Nakash., *Pseudocercospora kenyirana* C. Nakash., L. Suhaizan & I. Nurul Faziha, *Pseudocercospora perrottetiae* Crous, C. Nakash. & C.Y. Chen, *Pseudocercospora platyceriicola* C. Nakash., Y. Hatt, L. Suhaizan & I. Nurul Faziha, *Pseudocercospora stemonicola* C. Nakash., Y. Hatt., L. Suhaizan & I. Nurul Faziha, *Pseudocercospora terengganuensis* C. Nakash., Y. Hatt., L. Suhaizan & I. Nurul Faziha, *Pseudocercospora xenopunicae* Crous & C. Nakash.; **New combinations:** *Heterophaeomoniella pinifoliorum* (Hyang B. Lee *et al.*) L. Mostert, C.F.J. Spies, Halleen & Gramaje, *Pseudocercospora pruni-grayanae* (Sawada) C. Nakash. & Motohashi., *Pseudocercospora togashiana* (K. Ito & Tak. Kobay.) C. Nakash. & Tak. Kobay., *Pteridopassalora nephrolepidicola* (Crous & R.G. Shivas) C. Nakash. & Crous, *Pteridopassalora lygodii* (Goh & W.H. Hsieh) C. Nakash. & Crous; **Typification: Epitypification:** *Botrytis infestans* Mont., *Cercospora abeliae* Katsuki, *Cercospora ceratoniae* Pat. & Trab., *Cercospora cladrastidis* Jacz., *Cercospora cryptomeriicola* Sawada, *Cercospora dalbergiae* S.H. Sun, *Cercospora ebulicola* W. Yamam., *Cercospora formosana* W. Yamam., *Cercospora fukuii* W. Yamam., *Cercospora glochidionis* Sawada, *Cercospora ixorana* J.M. Yen & Lim, *Cercospora liquidambaricola* J.M. Yen, *Cercospora pancratii* Ellis & Everh., *Cercospora pini-densiflorae* Hori & Nambu, *Cercospora profusa* Syd. & P. Syd., *Cercospora pyracanthae* Katsuki, *Cercospora horiana* Togashi & Katsuki, *Cercospora tabernaemontanae* Syd. & P. Syd., *Cercospora trinidadensis* F. Stevens & Solheim, *Melampsora laricis-urbanianae* Tak. Matsumoto, *Melampsora salicis-cupularis* Wang, *Phaeoisariopsis pruni-grayanae* Sawada, *Pseudocercospora angiopteridis* Goh & W.H. Hsieh, *Pseudocercospora basitruncata* Crous, *Pseudocercospora boehmeriigena* U. Braun, *Pseudocercospora coprosmae* U. Braun & C.F. Hill, *Pseudocercospora cratevicola* C. Nakash. & U. Braun, *Pseudocercospora cymbidiicola* U. Braun & C.F. Hill, *Pseudocercospora dodonaeae* Boesew., *Pseudocercospora euphorbiacearum* U. Braun, *Pseudocercospora lygodii* Goh & W.H. Hsieh, *Pseudocercospora metrosideri* U. Braun, *Pseudocercospora paraexosporioides* C. Nakash. & U. Braun, *Pseudocercospora symploci* Katsuki & Tak. Kobay. ex U. Braun & Crous, *Septogloeum punctatum* Wakef.; **Neotypification:** *Cercospora aleuritis* I. Miyake; **Lectotypification**: *Cercospora dalbergiae* S.H. Sun, *Cercospora formosana* W. Yamam., *Cercospora fukuii* W. Yamam., *Cercospora glochidionis* Sawada, *Cercospora profusa* Syd. & P. Syd., *Melampsora laricis-urbanianae* Tak. Matsumoto, *Phaeoisariopsis pruni-grayanae* Sawada, *Pseudocercospora symploci* Katsuki & Tak. Kobay. ex U. Braun & Crous.

Studies in Mycology

Citation: Chen Q, Bakhshi M, Balci Y, Broders KD, Cheewangkoon R, Chen SF, Fan XL, Gramaje D, Halleen F, Horta Jung M, Jiang N, Jung T, Májek T, Marincowitz S, Milenković T, Mostert L, Nakashima C, Nurul Faziha I, Pan M, Raza M, Scanu B, Spies CFJ, Suhaizan L, Suzuki H, Tian CM, Tomšovský M, Úrbez-Torres JR, Wang W, Wingfield BD, Wingfield MJ, Yang Q, Yang X, Zare R, Zhao P, Groenewald JZ, Cai L, Crous PW (2022). Genera of phytopathogenic fungi: GOPHY 4. *Studies in Mycology* **101**: 417–564. doi: 10.3114/sim.2022.101.06.
Received: 7 January 2022; **Accepted:** 4 May 2022; **Effectively published online:** 2 June 2022
Corresponding editor: Robert A. Samson

INTRODUCTION

Genera of Phytopathogenic Fungi (GOPHY) is a series of publications introduced in 2017, which aims to provide a comprehensive framework for the taxonomy of major phytopathogenic fungal genera. The papers focus on the genera that are related to plant diseases, although it must be acknowledged that pathogenicity of some species has not been verified through Koch's postulates. The most important purpose of the series is to resolve generic and species boundaries of the fungi studied, because many taxa represent species complexes, or are accommodated in poly- and paraphyletic genera (Crous *et al.* 2015b, 2021). This series links to a larger initiative known as the "The Genera of Fungi Project" (www.MycoBank.org, Crous *et al.* 2014a, 2015a, Giraldo *et al.* 2017), which aims to revise the generic names of all currently accepted fungal genera (Kirk *et al.* 2013). Since many genera and species were described before the molecular era, type materials for many of these taxa have not been designated or are missing, and consequently lack DNA barcodes (Schoch *et al.* 2012). Another aim of this project is to validate the application of names by deriving DNA barcodes of type species of genera and type specimens of species (Crous *et al.* 2021). If type material has not been indicated or preserved, then either type species need to be recollected, or epitypes/neotypes designated and registered in MycoBank (Robert *et al.* 2013). The final objective is to have a single scientific name for each fungal taxon (Wingfield *et al.* 2012, Crous *et al.* 2015b, 2021).

Morphological descriptions and information about the pathology, distribution, hosts and disease symptoms, DNA barcodes, whole-genome sequences for the type species or a new species are provided for selected taxa. The whole-genome sequence provides the most fundamental and complete genetic background of each fungus (Chio & Kim 2017), which can resolve issues pertaining to taxonomy, biology, lifestyles, adaptability to stress and host specificity (Haridas *et al.* 2020).

Three issues of GOPHY have been published to date, in which 62 genera were treated, including the introduction of five new genera, 88 new species, 38 new combinations, four new names and 13 typifications of older names (Marin-Felix *et al.* 2017, 2019a, b). In this fourth contribution, a further 19 genera are treated, resulting in the clarification of their taxonomy and phylogenetic relationships, and the introduction of two new genera, 30 new species, five new combinations and 43 typifications of older names. In addition, 12 whole genomes are newly sequenced, assembled and annotated, and five genome sequences are cited from literature.

Mycologists who wish to contribute to future issues of the GOPHY series are encouraged to contact Pedro Crous (p.crous@wi.knaw.nl) before submission, to ensure there is no overlap with activities arising from other research groups. Preference will be given to genera that include novel species, combinations or typifications. Contributions of the treated genera published in each issue of the series, will be placed on www.plantpathogen.org.

MATERIAL AND METHODS

Isolates and morphological analysis

Descriptions of the new taxa and typifications are based on cultures obtained from the following biobanks: Bioresource Collection and Research Center, Food Industry Research and Development Institute, Hsinchu, Taiwan (BCRC); Westerdijk Fungal Biodiversity Institute, Utrecht, The Netherlands (CBS); working collection of P.W. Crous (CPC), housed at the Westerdijk Fungal Biodiversity Institute (WI); China Forestry Culture Collection Center, Beijing, China (CFCC); Chinese General Microbiological Culture Collection Center, Beijing, China (CGMCC); Culture Collection of the Forestry and Agricultural Biotechnology Institute (FABI), Pretoria, South Africa (CMW); Coleção Octávio de Almeida Drumond, Universidade Federal de Viçosa, Brazil (COAD); Collections at China Eucalypt Research Centre, Chinese Academy of Forestry, Zhanjiang, Guangdong, China (CSF); Lei Cai's personal collection, housed at the Chinese Academy of Sciences (CAS), China (LC); Culture collection of Mendel University in Brno, Czech Republic (CZ and PA); Mycological Herbarium of the Institute of Microbiology, Chinese Academy of Sciences, China (HMAS); Iranian Fungal Culture Collection, Iranian Research Institute of Plant Protection, Tehran, Iran (IRAN), the Genebank Project, NARO, Tsukuba, Ibaraki, Japan (MAFF); Culture Collection, Laboratory of Plant Pathology, Mie University, Tsu, Mie Prefecture, Japan (MUCC); NBRC Culture Collection, Biological Resource Center, National Institute of Technology and Evaluation, Chiba, Japan (NBRC); herbarium, Department of National Chung Hsing University, Taichung, Taiwan (NCHUPP); Pacific Agri-Food Research Centre Fungal Collection, Summerland, BC, Canada (PARC); Culture collection of the South African National Collection of Fungi (NCF), Roodeplaat, Pretoria, South Africa (PPRI), and the Mycological Herbarium of the Graduate School of Life and Environmental Sciences, University of Tsukuba, Tsukuba, Japan (TSH). For fresh collections, we followed the procedures previously described in Crous *et al.* (1991). Colonies were transferred to different media, *i.e.* carrot agar (CA), cornmeal agar (CMA), malt extract agar (MEA), potato dextrose agar (PDA), synthetic nutrient-poor agar (SNA), oatmeal agar (OA), V8-juice agar (V8A), water agar (WA) (Crous *et al.* 2019c), pine needle agar (PNA; Smith *et al.* 1996), and incubated under different conditions to induce sporulation. Requirements of media and conditions of incubation are specified for each genus. Reference strains and specimens are maintained at CBS, CPC, CGMCC, HMAS, LC and PARC.

Vegetative and reproductive structures were mounted in 100 % lactic acid or Shear's solution either directly from specimens or from colonies sporulating on CMA, MEA, OA, PCA, PDA, PNA, SNA or WA. For cultural characterisation, isolates were grown and incubated on different culture media and temperatures as indicated for each genus. Colour notations were rated according to the colour charts of Rayner (1970). For some taxa, the NaOH spot test was carried out on MEA cultures to detect the production of metabolite E (Boerema *et al.* 2004). Taxonomic novelties were deposited in MycoBank (www.MycoBank.org; Crous *et al.* 2004).

DNA isolation, amplification and analyses

Fungal DNA was extracted and purified directly from the colonies or host material as specified for each genus. Primers and protocols for the amplification and sequencing of gene loci, and software used for phylogenetic analyses can be found in the bibliography related to the phylogeny presented for each respective genus. Phylogenetic analyses consisted of Maximum-Likelihood (ML), Bayesian Inference (BI) and Maximum Parsimony (MP). The ML and the BI were carried out using methods described by Hernández-Restrepo *et al.* (2016), and the MP using those described by Crous *et al.* (2006c). Sequence data generated in this study were deposited in GenBank and the alignments and trees in TreeBASE (http://www.treebase.org).

Genome sequencing, assembly and annotation

Five to eight 5-mm-diam discs from the edges of 7-d-old PDA cultures were inoculated in 100 mL autoclaved potato dextrose broth (PDB) for each isolate. The flasks were shaken at 150 rpm for 3–7 d at 25 °C. Mycelia were collected and dried on sterilised filter paper, and then lyophilised. Twelve samples were sent to Annoroad Gene Technology Company Limited (Beijing, China) for genomic DNA extraction and Illumina sequencing on a Novaseq 6000.

Paired reads of 150 bp were assembled using SPAdes v. 3.12.0 (Bankevich *et al.* 2012). The quality of genome assembly was assessed using QUAST v. 5.0.2 (Gurevich *et al.* 2013). Protein-coding gene predictions were performed using Funannotate v. 1.7.0 (Love *et al.* 2019). The inferred proteins were functionally annotated using EggNOG-mapper v. 2.0.0 (Huerta-Cepas *et al.* 2017) with diamond as the mapping mode and the eukaryotic taxonomic scope.

RESULTS

Ascochyta Lib.***,*** *emend*. Qian Chen & L. Cai, Stud. Mycol. 82: 185. 2015. Fig. 1.

Classification: *Dothideomycetes*, *Pleosporomycetidae*, *Pleosporales*, *Didymellaceae*.

Type species: *Ascochyta pisi* Lib. Isotype: BR 5020059493320. Epitype and ex-epitype strain: HMAS 246705, CBS 122785 = PD 78/517.

DNA barcodes (genus): LSU, ITS.

DNA barcodes (species): *rpb2*, *tub2*. Table 1. Fig. 2.

Ascomata pseudothecial, immersed or erumpent, subglobose to flattened, or irregular, solitary or confluent, ostiolate, sometimes developing an elongated neck. *Asci* (sub-)cylindrical to (sub-) clavate, or saccate, sometimes slightly curved, 8-spored, bitunicate, sometimes short-stipitate. *Pseudoparaphyses* filamentous, hyaline, thin-walled, septate, conspicuous in immature fructifications, and disappear at maturity. *Ascospores* ovoid to ellipsoidal, slightly biconic, hyaline to yellowish into the ascus, may become brown when released, smooth, 1-septate, sometimes 3-septate, symmetrical or asymmetrical, constricted at the septum, uniseriate or biseriate; muriform, 4−6-transversely septate, with one vertical septum, slightly constricted at the septa, hyaline to pale yellow, becoming brown to dark brown at maturity, surrounded by a thick mucilaginous sheath. *Conidiomata* pycnidial, subglobose or ampulliform to mammiform, sometimes irregularly shaped, superficial on or immersed into the agar, solitary or confluent, ostiolate or poroid opening formed at the end of the growing process; *conidiomatal wall* pseudoparenchymatous, multi-layered. *Conidiogenous cells* annellidic or phialidic, hyaline, smooth, variable in shape, *i.e.* globose to subglobose, cylindrical, flask-shaped, obpyriform, lageniform, ampulliform to doliiform. *Conidia* hyaline or sometimes slightly coloured (yellow to pale brown), smooth- and thin-walled, aseptate or septate, mostly uniseptate, sometimes 2–3-septate, variable in shape, *i.e*. ovoid, oblong, (sub-)cylindrical, ellipsoidal, cymbiform, bacilliform, fusiform, allantoid, straight or slightly curved, eguttulate or guttulate (Boerema & Bollen 1975, Boerema *et al.* 2004, Chen *et al.* 2015b, 2017). *Chlamydospores* may occur in old cultures (Jellis & Punithalingam 1991, Trapero-Casas & Kaiser 1992, Kaiser *et al.* 1997, Chilvers *et al.* 2009).

Cultural characteristics: Colonies on OA white or slightly grey, pale olivaceous to olivaceous black, yellowish brown to dark brown, or dull green, becoming pale luteous-citrine, buff towards the periphery, aerial mycelium floccose, flat or with scant aerial mycelium, sometimes hazel with honey sterile zones, or with darker concentric zones due to pycnidia, margin regular or irregular.

Optimal media and cultivation conditions: OA or sterile pine needles placed on OA under nuv-light (12 h light, 12 h dark) to promote sporulation at 25 °C.

Distribution: Worldwide.

Hosts: Occurring as saprobes on dead stems of diverse herbaceous plants, polluted lake water and soil, and as weak or noxious pathogens on *Fabaceae*, especially on peas, also on *Apiaceae*, *Caryophyllaceae*, *Lamiaceae*, *Liliaceae*, *Oleaceae* and *Juglandaceae*.

Disease symptoms: Black stem, stem spots, fruit (bean pods) lesions, leaf spots, seed-borne diseases.

Notes: Libert (1830) established the asexually typified genus *Ascochyta*, based on its type species *A. pisi*, to accommodate some phytopathogenic species characterised by producing predominately uniseptate hyaline conidia and phialidic conidiogenous cells. Species in *Ascochyta* are highly similar to *Phoma* spp. in morphology, physiology, pathogenicity and molecular sequences, resulting in ambiguous generic boundaries (Aveskamp *et al.* 2010). Conidiogenesis and conidial septation were used to discriminate species of *Phoma* and *Ascochyta* in the Saccardoan system (Boerema & Bollen 1975, Aveskamp *et al.* 2010, Chen *et al.* 2015b), but Punithalingam (1979) considered that these characters were not appropriate as taxonomic criteria for distinguishing species. Chen *et al.* (2015b) clarified conidiogenesis to be phialidic in both genera. Recent molecular phylogenetic studies revealed both *Ascochyta* and *Phoma*, as traditionally defined, to be highly polyphyletic (Aveskamp *et al.* 2010). A later systematic revision of the *Didymellaceae*, however, redefined both genera as two monophyletic groups based on multi-locus sequence typing (Chen *et al.* 2015b, 2017, Hou *et al.* 2020a).

Currently, 20 species are recognised in the genus *Ascochyta* that are supported by ex-type or representative cultures and DNA

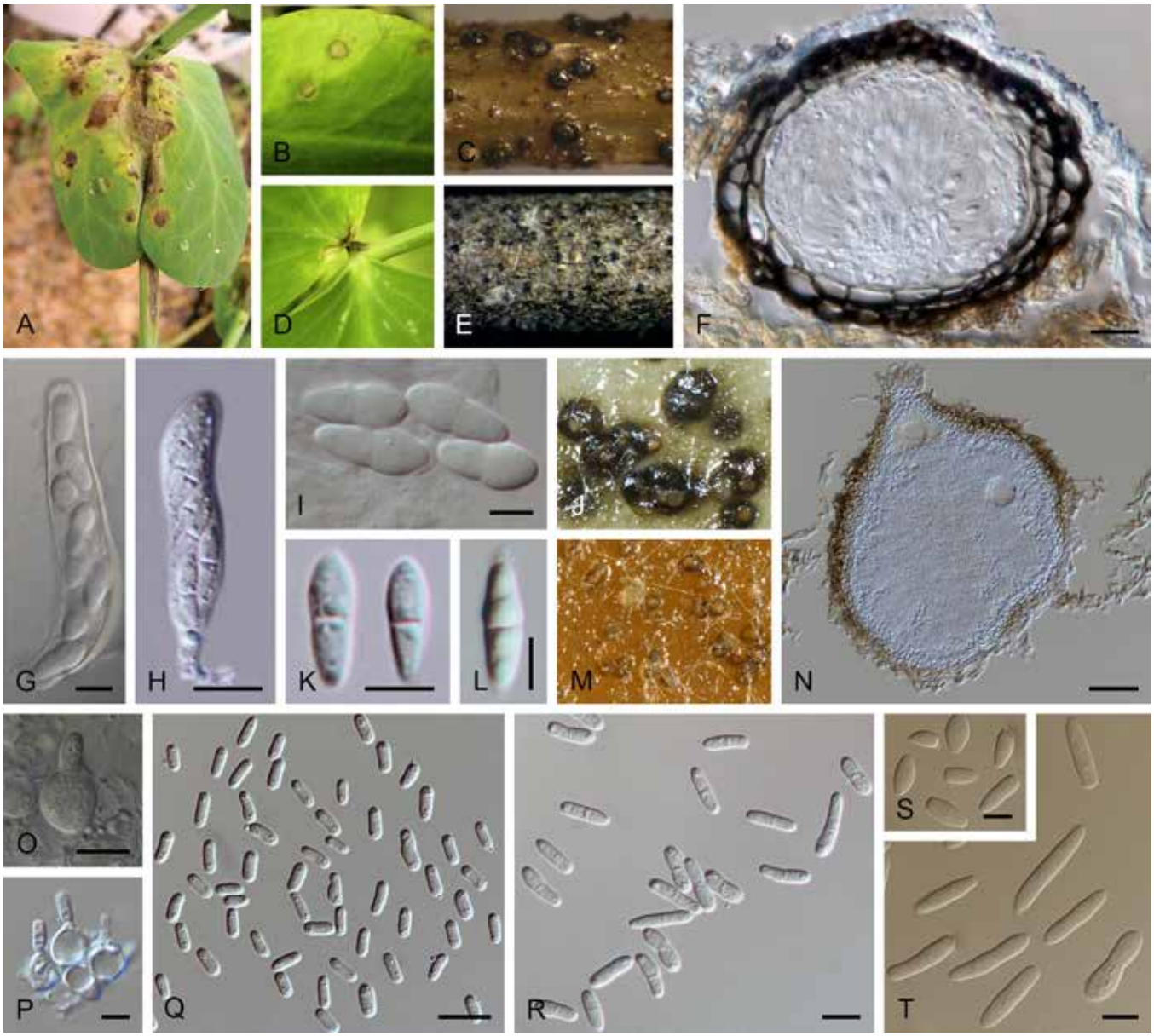

Fig. 1. *Ascochyta* spp. **A, B, D.** Disease symptoms. **A.** Symptoms caused by *Ascochyta koolunga* on field pea seedlings. **B, D.** Symptoms caused by *Ascochyta pisi* on *Pisum sativum* cv. 'Lifter'. **C, E–L.** Sexual morph. **C, E.** Ascomata on host surface. **C.** Ascomata of *Ascochyta pisi* on stem of *Pisum sativum* cv. 'Lifter'. **E.** Ascomata of *Ascochyta clinopodiicola* (holotype MFLU 17-1034) on dead aerial stem of *Clinopodium nepeta*. **F.** Section through ascoma of *Ascochyta clinopodiicola* (holotype MFLU 17-1034). **G, H.** Asci. **G.** *Ascochyta pisi* (WSP 71448). **H.** *Ascochyta clinopodiicola* (holotype MFLU 17-1034). **I, K, L.** Ascospores. **I.** *Ascochyta phacae* (holotype ZT Myc 54988). **K.** *Ascochyta clinopodiicola* (holotype MFLU 17-1034). **L.** *Ascochyta rosae* (ex-type MFLUCC 15-0063). **J, M–T.** Asexual morph. **J, M.** Conidiomata forming on OA. **J.** *Ascochyta benningiorum* (ex-type CBS 144957). **M.** *Ascochyta koolunga* (CBS 372.84). **N.** Section through the conidioma of *Ascochyta benningiorum* (ex-type CBS 144957). **O, P.** Conidiogenous cells. **O.** *Ascochyta koolunga* (CBS 372.84). **P.** *Ascochyta pilosella* (ex-type CBS 583.97). **Q–T.** Conidia. **Q.** *Ascochyta clinopodiicola* (CBS 123526). **R.** *Ascochyta pisi* (ex-epitype CBS 122785). **S, T.** *Ascochyta koolunga* (CBS 372.84). Scale bars: N = 50 µm; F = 15 µm; G, H, O, Q–T = 10 µm; I, K, L, P = 5 µm. Picture A taken from Davidson *et al.* (2009); B–D, G from Chilvers *et al.* (2009); E, F, H, K from Hyde *et al.* (2018); I, R from Chen *et al.* (2015b); L from Tibpromma *et al.* (2017); J, N from Hou *et al.* (2020b); M, O, S, T from Chen *et al.* (2017); P, Q from Hou *et al.* (2020a).

barcodes. Most species in this genus are plant pathogens, on *Fabaceae* and plants in other families (Kaiser *et al.* 1997, Peever *et al.* 2007, Chilvers *et al.* 2009, Hyde *et al.* 2018, Wanasinghe *et al.* 2018a, Hou *et al.* 2020a), while some are saprobes on dead plant tissue, or occur in different environments, such as lake water and soil.

Although names recorded in *Ascochyta* are mostly known only from asexual morphs, some species have both asexual and sexual morphs, such as *A. coronillae-emeri, A. fabae, A. lentis, A. phacae, A. pisi, A. rabiei* and *A. rosae* (Corbaz 1955, 1957, Corlett 1981, Jellis & Punithalingam 1991, Trapero-Casas & Kaiser 1992, Kaiser *et al.* 1997, Chilvers *et al.* 2009, Aveskamp *et al.* 2010, Chen *et al.* 2015b, Tibpromma *et al.* 2017, Wanasinghe *et al.* 2018a), while *A. astragalina* (Syn: *Didymella astragalina*) and *A. clinopodiicola* are only observed as sexual morphs (Corbaz 1957, Hyde *et al.* 2018, Hou *et al.* 2020a).

References: Boerema *et al.* 2004 (morphology, distribution and pathogenicity); Aveskamp *et al.* 2010, Chen *et al.* 2015b, 2017, Hou *et al.* 2020a (morphology, phylogeny and pathogenicity).

Table 1. DNA barcodes of accepted *Ascochyta* spp.

Species	Isolates[1]	GenBank accession numbers[2]				References
		LSU	ITS	*rpb2*	*tub2*	
Ascochyta astragalina	CBS 113797	KT389699	KT389482	MT018257	KT389776	Chen *et al.* (2015b), Hou *et al.* (2020a)
A. benningiorum	CBS 144957^{T}	MN823432	MN823581	MN824606	MN824755	Hou *et al.* (2020b)
A. clinopodiicola	CBS 123524	MN943793	MN973587	—	MT005693	Hou *et al.* (2020a)
	MFLUCC 18-0344^{T}	MH017429	MH017431	—	—	Hyde *et al.* (2018)
A. coronillae-emeri	MFLUCC 13-0820^{T}	MH069667	MH069661	MH069679	MH069686	Wanasinghe *et al.* (2018)
A. fabae	CBS 524.77	GU237963	GU237880	MT018241	GU237526	Aveskamp *et al.* (2010), Hou *et al.* (2020a)
A. flava	CGMCC 3.20067 = LC 13574^{T}	MT229670	MT229693	MT239090	MT249261	Present study
	LC 13575	MT229664	MT229687	MT239084	MT249255	Present study
	LC 13576	MT229665	MT229688	MT239085	MT249256	Present study
	LC 13577	MT229666	MT229689	MT239086	MT249257	Present study
	LC 13578	MT229667	MT229690	MT239087	MT249258	Present study
	LC 13579	MT229668	MT229691	MT239088	MT249259	Present study
	LC 13580	MT229669	MT229692	MT239089	MT249260	Present study
A. herbicola	CBS 629.97	GU238083	GU237898	KP330421	GU237614	Aveskamp *et al.* (2010), Chen *et al.* (2015c)
A. koolunga	CBS 372.84^{T} (*Ascochyta boeremae*)	KT389697	KT389480	—	KT389774	Chen *et al.* (2015b)
	DAR 78535^{T}	—	EU338416	EU874849	—	Davidson *et al.* (2009)
A. lentis	CBS 370.84	KT389691	KT389474	MT018246	KT389768	Chen *et al.* (2015b), Hou *et al.* (2020a)
A. medicaginicola	CBS 112.53^{T}	GU238101	GU237749	MT018251	GU237628	Aveskamp *et al.* (2010), Hou *et al.* (2020a)
A. nigripycnidia	CBS 116.96^{T}	GU238118	GU237756	MT018253	GU237637	Aveskamp *et al.* (2010), Hou *et al.* (2020a)
A. phacae	CBS 184.55^{T}	KT389692	KT389475	MT018255	KT389769	Chen *et al.* (2015b), Hou *et al.* (2020a)
A. pilosella	CBS 583.97^{T}	MN943796	MN973590	MT018258	MT005696	Hou *et al.* (2020a)
A. pisi	CBS 122785^{ET}	GU237969	GU237763	MT018244	GU237532	Aveskamp *et al.* (2010), Hou *et al.* (2020a)
A. rabiei	CBS 237.37^{T}	KT389696	KT389479	MT018256	KT389773	Chen *et al.* (2015b), Hou *et al.* (2020a)
A. rosae	MFLUCC 15-0063^{T}	KY496731	KY496751	KY514409	—	Tibpromma *et al.* (2017)
A. syringae	CBS 545.72	KT389700	KT389483	MT018245	KT389777	Chen *et al.* (2015b), Hou *et al.* (2020a)
A. viciae	CBS 451.68	KT389701	KT389484	KT389562	KT389778	Chen *et al.* (2015b)
A. viciae-pannonicae	CBS 254.92	KT389702	KT389485	MT018250	KT389779	Chen *et al.* (2015b), Hou *et al.* (2020a)
A. viciae-villosae	CBS 255.92	MN943790	MN973584	MT018249	MT005690	Hou *et al.* (2020a)

[1] CBS: Westerdijk Fungal Biodiversity Institute, Utrecht, the Netherlands; CGMCC: Chinese General Microbiological Culture Collection Center, Beijing, China; DAR: New South Wales Plant Pathology Herbarium, NSW, Australia; LC: Dr Lei Cai's personal collection deposited in laboratory, housed at Chinese Academy of Sciences (CAS), China; MFLUCC: Mae Fah Luang University Culture Collection, Chiang Rai, Thailand. ^{ET} and ^{T} indicate ex-epitype and ex-type strains, respectively.

[2] ITS: internal transcribed spacers and intervening 5.8S nrDNA; LSU: partial 28S large subunit nrRNA gene; *rpb2*: partial RNA polymerase II second largest subunit gene; *tub2*: partial β-tubulin gene.

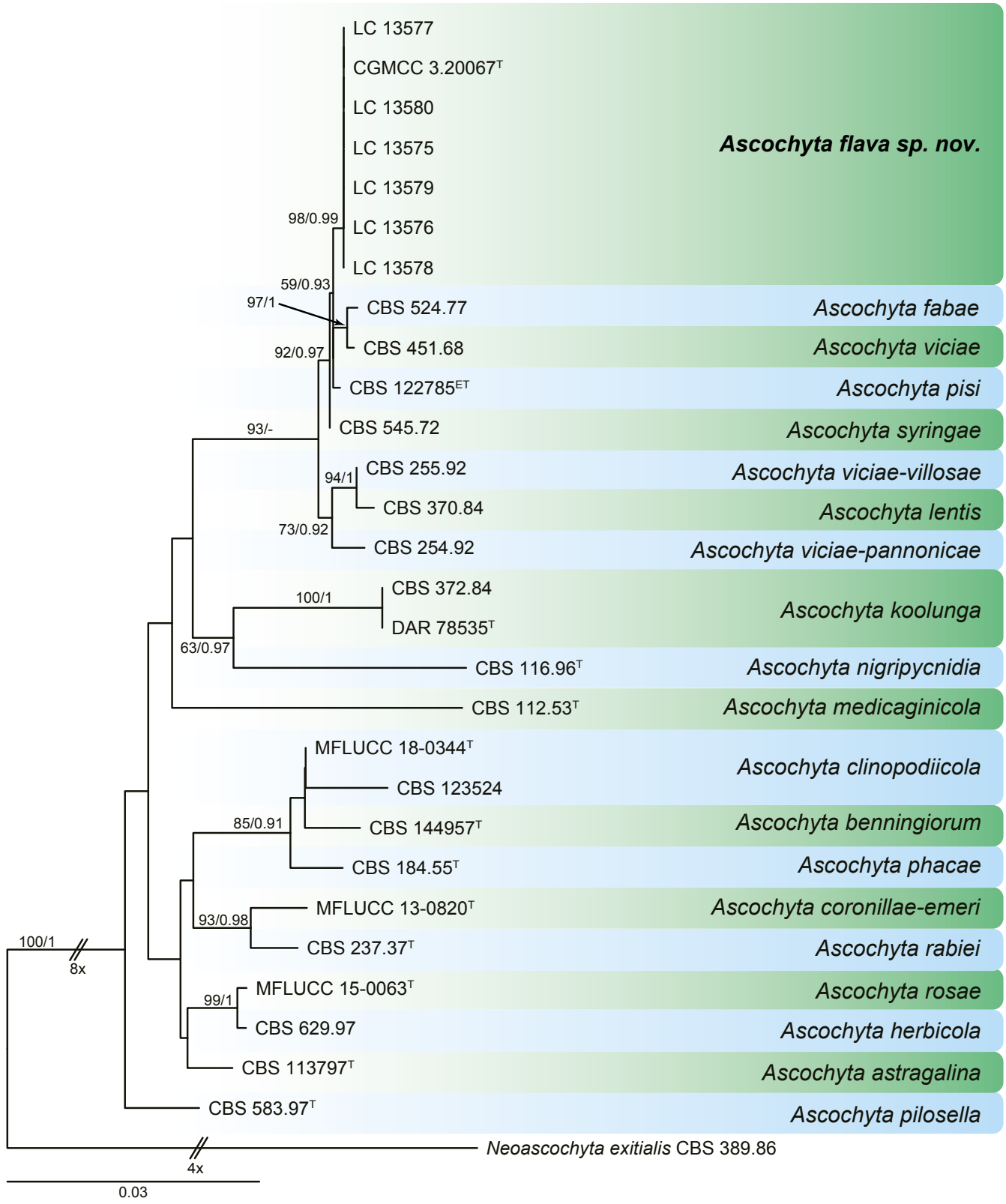

Fig. 2. Phylogenetic tree constructed from LSU (960 bp), ITS (454 bp), *tub2* (333 bp) and *rpb2* (596 bp) sequences of all accepted species of *Ascochyta*. RAxML bootstrap support values (> 70 %) and Bayesian posterior probability scores (> 0.90) are shown at the nodes. The novel taxon is printed in **bold**. The phylogenetic tree was rooted to *Neoascochyta exitialis* CBS 389.86. GenBank accession numbers are indicated in Table 1. T and ET indicate ex-type and ex-epitype strains, respectively. TreeBASE: S26038.

Ascochyta flava Qian Chen & L. Cai, ***sp. nov.*** MycoBank MB 834955. Fig. 3.

Etymology: Named after the colour of the colony reverse on OA, flava = yellowish.

Conidiomata pycnidial, mostly aggregated and confluent, globose to subglobose, pale brown, with some hyphal outgrows, superficial or semi-immersed, ostiolate, 60–380 × 55–330 µm; *ostioles* single, non-papillate; *conidiomatal wall* pseudoparenchymatous 3–5-layered, 12.5–30.5 µm thick, composed of isodiametric cells. *Conidiogenous cells* phialidic, hyaline, smooth, globose,

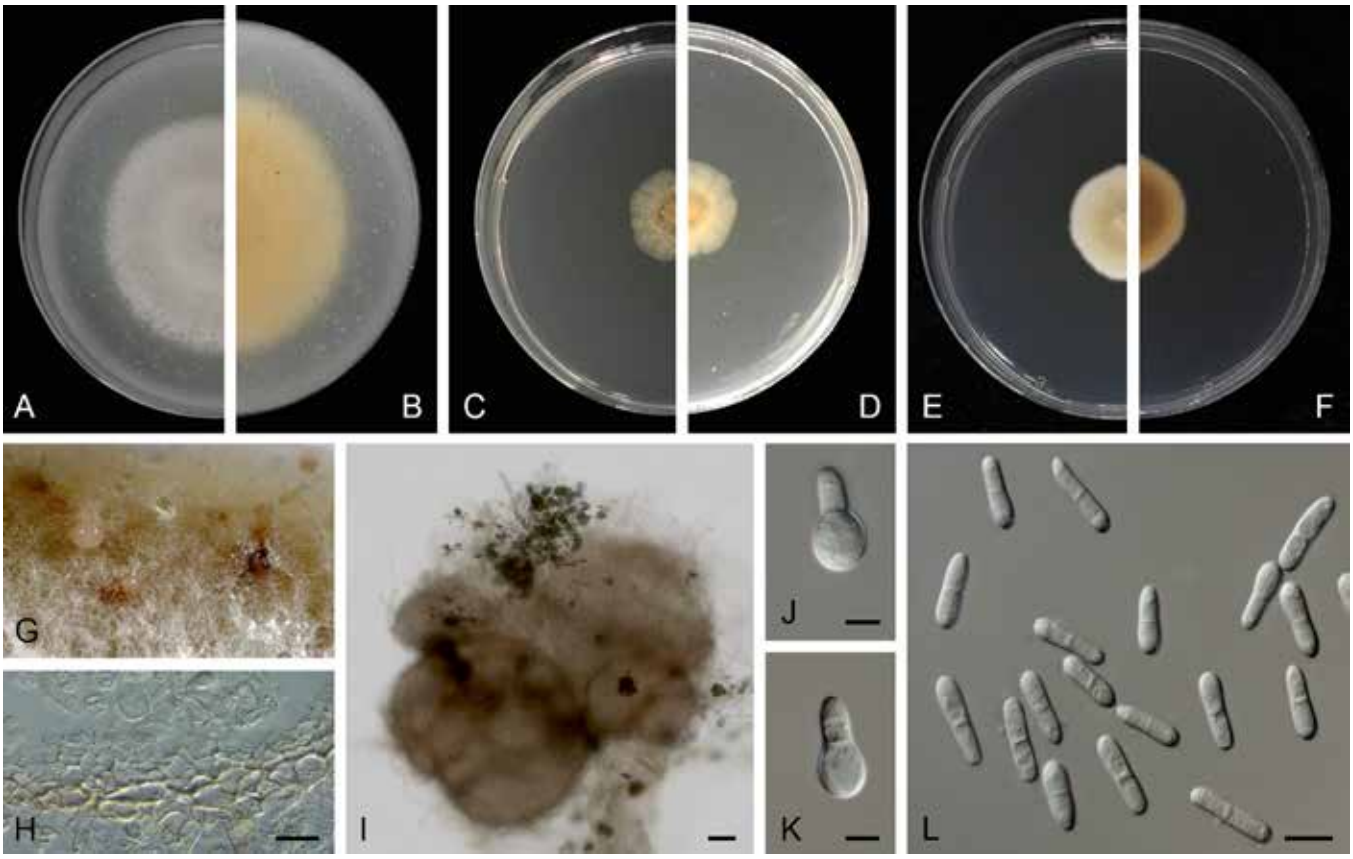

Fig. 3. *Ascochyta flava* (ex-type CGMCC 3.20067). **A, B.** Colony on OA (front and reverse). **C, D.** Colony on MEA (front and reverse). **E, F.** Colony on PDA (front and reverse). **G.** Conidiomata sporulating on OA. **H.** Section of conidiomatal wall. **I.** Conidiomata. **J, K.** Conidiogenous cells. **L.** Conidia. Scale bars: I = 50 µm; H, L = 10 µm; J, K = 5 µm.

ampulliform to obpyriform, 6–12 × 5–9.5 µm. *Conidia* oblong to bacilliform, or narrowly ovoid, always somewhat constricted at the septum, smooth- and thin-walled, hyaline, 0–1-septate, 9–17 × 3.5–5.5 µm, with numerous minute guttules. *Conidial matrix* pale pink.

Culture characteristics: Colonies on OA, 25–30 mm diam after 1 wk, margin regular, floccose to woolly, white; reverse buff. Colonies on MEA 10–15 mm diam after 1 wk, margin regular, floccose to woolly, compact, pale greenish yellow to buff; reverse concolourous. Colonies on PDA, 15–20 mm diam after 1 wk, margin regular, floccose, pale yellow, white near the margin; reverse pale saffron to hazel toward the centre, pale yellow near the margin. Application of NaOH results in a pale saffron discolouration of the agar.

Typus: **China**, Qinghai, Menyuan County, on leaves of *Angelica dahurica* (*Apiaceae*), 7 Aug. 2019, M.M. Wang (**holotype** HMAS 248350, dried culture, culture ex-type CGMCC 3.20067 = LC 13574).

Additional materials examined: **China**, Qinghai, Menyuan, on leaves of *Vicia sativa* (*Fabaceae*), 7 Aug. 2019, L.W. Hou, culture LC 13575; *ibid*. culture LC 13576; *ibid*. culture LC 13577; *ibid*. culture LC 13578; *ibid*. culture LC 13579; *ibid*. culture LC 13580.

Notes: *Ascochyta flava* is phylogenetically closely related to *A. pisi* and *A. fabae* (Fig. 2), but differs from *A. pisi* in producing larger conidiogenous cells (6–12 × 5–9.5 µm *vs* 5.5–8.5 × 4.5–8 µm, Chen *et al.* 2015b), and from *A. fabae* in the shorter conidia [9–17 × 3.5–5.5 µm *vs* (14–)16–25 × 3.5–6 µm, Punithalingam 1975, Jellis & Punithalingam 1991].

Genome sequenced strain: *Ascochyta pisi.* **The Netherlands,** on *Pisum sativum*, date unknown, M.M.J. Dorenbosch, culture ex-epitype CBS 122785. This Whole Genome Shutgun project has been deposited at GenBank under the accession JALRMB000000000 (BioProject : PRJNA827019, BioSample : SAMN27594410; present study).

Authors: Q. Chen & L. Cai

Cadophora Lagerb. & Melin, Svensk Skogsvårdsfören.Tidskr. 2 (2): 263. 1927. Fig. 4.

Classification: *Leotiomycetes*, *Leotiomycetidae*, *Helotiales*, *Ploettnerulaceae.*

Type species: *Cadophora fastigiata* Lageberg & Melin. Holotype and ex-type strain: A168, CBS 307.49.

DNA barcode (genus): ITS.

DNA barcodes (species): ITS, *tef1* and *tub2*. Table 2. Fig. 5.

Ascomata apothecial, arising singly or in small groups, sessile, slightly erumpent from the substrate, black when fresh. *Receptacle* cupulate, black. *Disc* concave, black. *Ectal excipulum* in lower flanks or in margins and upper flanks, composed of, thin-walled, palebrown to hyaline cells of *textura angularis*, or thick-walled, blackish cells of *textura globulosa*. *Medullary excipulum* in lower flanks, composed of thin-walled, hyaline cells of *textura porrecta*, or in upper flanks, composed of narrow, long, thin-walled, hyaline cells of *textura epidermoidea*. *Hymenium* hyaline. *Paraphyses*

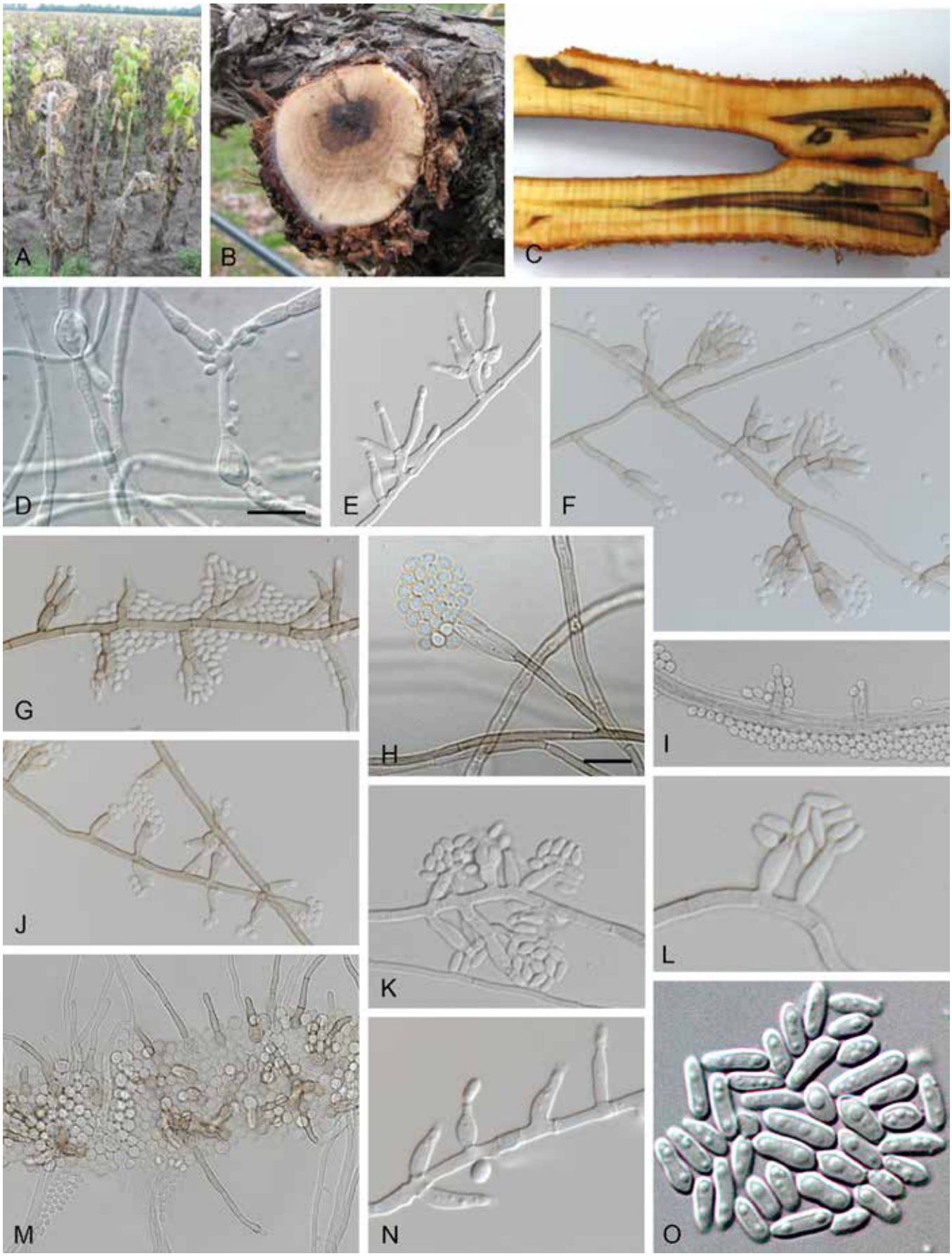

Fig. 4. *Cadophora* spp. **A–C.** Disease symptoms. **A.** Yellowing, leaf necrosis and sudden death caused by *Cadophora helianthi* in a sunflower field. **B.** Black spots and central necrosis on grapevine caused by *Cadophora vinacea*. **C.** Wood discolouration on plum trees caused by *Cadophora domestica*. **D–O**. Asexual morph. **D.** Hyphal swellings of *Cadophora luteo-olivacea* (ex-type CBS 128576). **E–H.** Conidiophores. **E.** *Cadophora helianthi* (ex-type CBS 144752). **F, G.** *Cadophora novi-eboraci* (ex-type OCR1). **H.** *Cadophora rotunda* (ex-type CBS 146264). **I–L, N.** Phialides. **I.** *Cadophora rotunda* (ex-type CBS 146264). **J.** *Cadophora novi-eboraci* (ex-type OCR1). **K, L.** *Cadophora viticola* (ex-type CBS 139.517). **M.** Over-mature conidia of *Cadophora rotunda* (ex-type CBS 146264). **N.** *Cadophora helianthi* (ex-type CBS 144752). **O.** Conidia of *Cadophora luteo-olivacea* (ex-type CBS 128576). Scale bars: D, H = 10 µm; O = 5 µm. D applies to E–G, I, J; H applies to K–N. Pictures D and O taken from Gramaje *et al*. (2011); E and N from Crous *et al*. (2019).

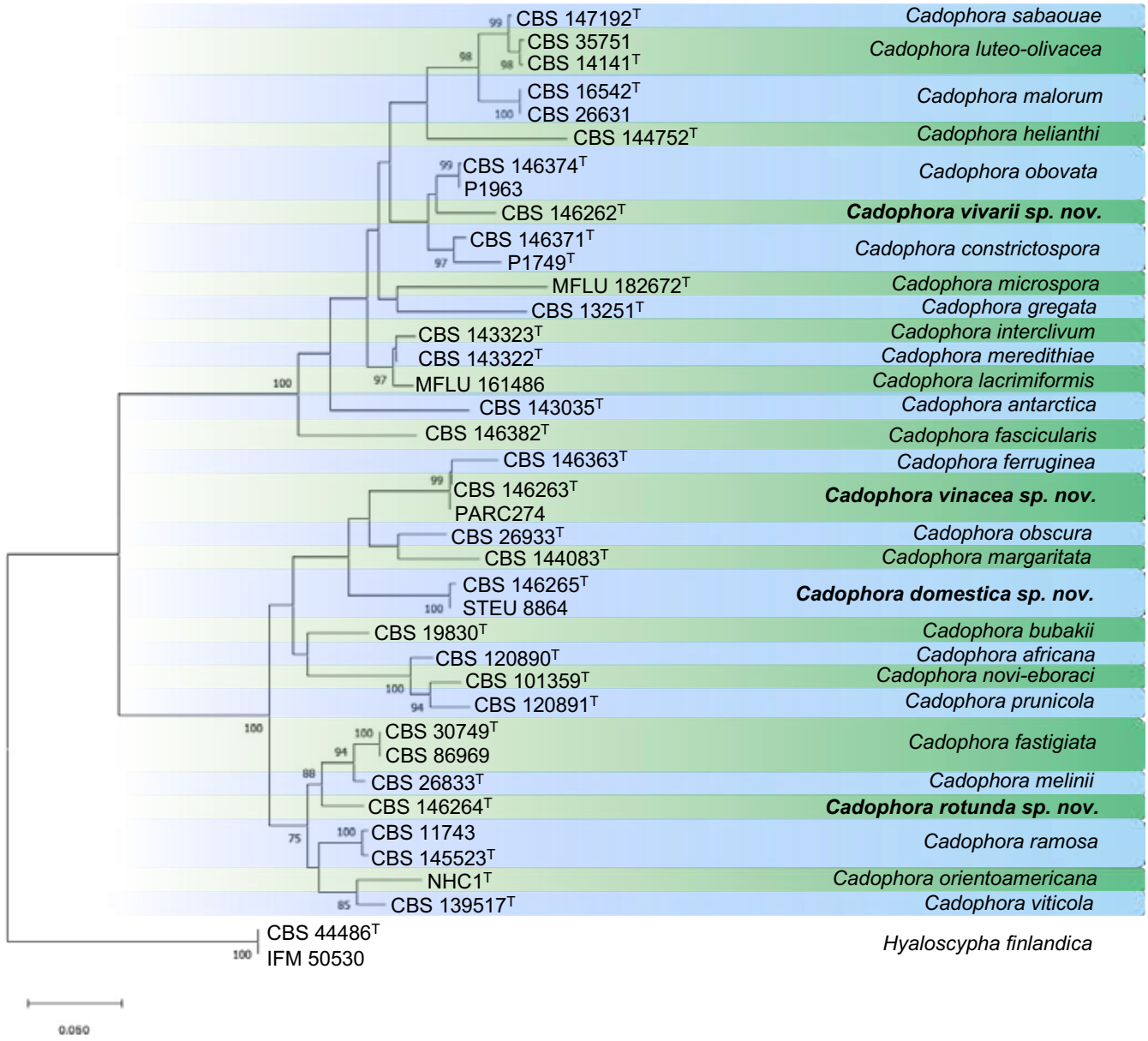

Fig. 5. Maximum likelihood (ML) phylogram obtained from the ITS (500 bp), *tef1* (352 bp) and *tub2* (544 bp) sequences of all accepted species of *Cadophora*. Bootstrap support values (> 70 %) are shown at the nodes. The novel taxa are printed in **bold**. The phylogenetic tree was rooted to *VHyaloscypha finlandica* CBS 44486 and IFM 50530. GenBank accession numbers are indicated in Table 2. T indicates ex-type strain. TreeBASE: S25577.

numerous, filiform, branched, septate, hyaline, acute at the apex or obtuse and slightly swollen at the apex, not exceed asci in length. *Asci* 8-spored, unitunicate, cylindrical-clavate, rounded or medium conical at the apex, amyloid, stipitate base, arising from croziers. *Ascospores* 1–2-seriate or multi-seriate, teardrop-shaped, fusoid to ellipsoid or fusoid-clavate, aseptate or sometimes 1-septate, hyaline, guttulate. *Hyphae* single or in bundles of up to 13, branched, septate, tuberculate with warts up to 3 µm diam, verruculose to smooth, hyaline or medium brown. *Conidiophores* mostly short, unbranched or branched, arising from aerial or submerged hyphae, erect to flexuous, up to 7-septate, pale brown. *Phialides* terminal or lateral, mostly single, smooth to verruculose or obclavate, mostly hyaline, but some vinaceous buff to fawn. *Collarettes* short, flaring, cup-shaped, cylindrical, subcylindrical, elongate-ampulliform, attenuated at the base or navicular, mostly hyaline. *Conidia* guttulate, sometimes aggregated in slimy heads, pyriform, ovoid, cylindrical or oblong ellipsoidal, aseptate, mostly hyaline, but some pale hazel.

Cultural characteristics: Colonies on MEA white or vinaceous buff to fawn, brown to pale brown, olivaceousblack or greyolivaceous, flat, felty, with an even edge. Some species produce aerial tufts of hyphae toward the centre and yellow pigmentation on PDA and/or MEA plates.

Optimal media and cultivation conditions: 2 % MEA at 25 ºC to induce sporulation of the asexual morph.

Distribution: Worldwide.

Hosts: The known *Cadophora* species occur in several habitats such as soil (Kerry 1990, Aislabie *et al.* 2001, Arenz *et al.* 2006, Hujslová *et al.* 2010, Crous *et al.* 2017b), decaying wood (Nilsson 1973, Morrell & Zabel 1985, Blanchette *et al.* 2004, Held *et al.* 2005, Arenz *et al.* 2006), or as plant pathogens (Halleen *et al.* 2003, Di Marco *et al.* 2004, Gramaje *et al.* 2011, Spadaro *et al.* 2011, Úrbez-Torres *et al.* 2014, Travadon *et al.* 2015, Crous *et al.* 2019a). The most prominent diseases in which *Cadophora* spp.

Table 2. DNA barcodes of accepted *Cadophora* spp.

Species	Isolates[1]	GenBank accession numbers[2]			References
		ITS	*tub2*	*tef1*	
Cadophora africana	CBS 120890^T	MN232936	MN232967	MN232988	Bien & Damm (2020)
Ca. antarctica	CBS 143035^T	MG385664	MK993426	MK993427	Crous *et al.* (2017)
Ca. bubakii	CBS 198.30^T	MH855111	—	MN232989	Bien & Damm (2020)
Ca. constrictospora	CBS 146371	KT269023	—	MN325874	Macià-Vicente *et al*. (2020)
Ca. domestica	CBS 146265^T	MN873024	MN873028	MN873031	Present study
Ca. fascicularis	CBS 146382^T	KT269992	—	MN325918	Macià-Vicente *et al*. (2020)
Ca. fastigiata	CBS 307.49^T	AY249073	KM497131	KM497087	Harrington & McNew (2003), Travadon *et al.* (2015)
Ca. ferruginea	CBS 146363^T	KT268618	—	MN325861	Macià-Vicente *et al*. (2020)
Ca. gregata	ATCC 11073^T	U66731	MF677920	MF979586	Harrington & McNew (2003)
Ca. helianthi	CBS 144.752^T	MK813837	MH733391	MH719029	Crous *et al.* (2019a)
Ca. interclivum	CBS 143323^T	MF979577	MF677917	MF979583	Walsh *et al.* (2018)
Ca. lacrimiformis	MFLU 16-1486	MK585003	—	—	Ekanayaka *et al*. (2019)
Ca. luteo-olivacea	CBS 141.41^T	AY249066	KM497133	KM497089	Harrington & McNew (2003)
Ca. malorum	CBS 165.42^T	AY249059	KM497134	KM497090	Gams (2000)
Ca. margaritata	CBS 144083^T	KJ702027	MH327786	—	Linnakoski *et al.* (2018)
Ca. melinii	CBS 268.33^T	AY249072	KM497132	KM497088	Harrington & McNew (2003), Travadon *et al.* (2015)
Ca. meredithiae	CBS 143322^T	MF979574	MF677914	MF979580	Walsh *et al.* (2018)
Ca. microspora	MFLU 18-2672	MK591966	—	—	Ekanayaka *et al*. (2019)
Ca. novi-eboraci	NYC14^T	KM497037	KM497118	KM497074	Travadon *et al.* (2015)
Ca. obovata	CBS 146374^T	KT269230	—	MN325888	Macià-Vicente *et al*. (2020)
Ca. obscura	CBS 269.33	MN232948	—	MN232996	Bien & Damm (2020)
Ca. orientoamericana	NHC1^T	KM497018	KM497099	KM497055	Travadon *et al.* (2015)
Ca. prunicola	CBS 120891^T	MN232949	MN232979	MN232997	Bien & Damm (2020)
Ca. ramosa	CBS 145523^T	MN232956	MN232984	MN233002	Bien & Damm (2020)
Ca. rotunda	CBS 146264^T	MN873023	MN873029	MN873030	Present study
Ca. sabaouae	CBS 147192^T	MT644187	MT646749	MT646746	Aigoun-Mouhous *et al*. (2021)
Ca. vinacea	CBS 146263^T	MN873025	MN873027	MN873032	Present study
Ca. viticola	CBS 139.517^T	HQ661096	HQ661066	HQ661081	Crous *et al.* (2015c)
Ca. vivarii	CBS 146262^T	KY312633	MN873026	MN873033	Present study

[1] ATCC: American Type Culture Collection, Virginia, USA; CBS: Westerdijk Fungal Biodiversity Institute, Utrecht, the Netherlands; MFLU: Mae Fah Luang University Herbarium, Chiang Rai, Thailand; NYC: New York Collection, New York, USA; NHC: New Hampshire Collection, New Hampshire, USA; UAMH: Centre for Global Microfungal Biodiversity, University of Toronto, Toronto, Canada. ^{T} indicates ex-type strain.

[2] ITS: internal transcribed spacers and intervening 5.8S nrDNA; *tef1*: partial translation elongation factor 1-α gene; *tub2*: partial β-tubulin gene.

are involved are Petri disease and esca, which occur on young and mature grapevines (*Vitaceae*), respectively.

Disease symptoms: Brown wood vascular streaking, plant decline, fruit skin pitting and brown spot, fruit rot.

Notes: The genus *Cadophora* was recently included within the family *Ploettnerulaceae* (Ekanayaka *et al.* 2019). It has morphological similarities with *Mollisia, Phialocephala* and *Collembolispora. Mollisia* can be differentiated from *Cadophora* by its phialocephala-like asexual morphs (Walsh *et al.* 2018). *Phialocephala* often produces densely packed head of phialides while *Cadophora* produces phialides singly or in groups of two or three (Day *et al.* 2012). *Collembolispora* differs from *Cadophora* in producing septate macroconidia (Crous *et al.* 2012a). Species delimitation based on morphology alone is limited since many species have overlapping characters. Moreover, the morphology of the sexual morph cannot be used because only two taxa are known to have a sexual morph. The three loci used most frequently for phylogenetic analyses are ITS, translation elongation factor 1-alpha (*tef1*) and partial beta-tubulin (*tub2*) genes (Crous *et al.* 2015c, 2019a, Travadon *et al.* 2015). Phylogenetic analyses combining these three regions allow for the resolution of almost all currently known *Cadophora* species (Fig. 5).

References: Gams 2000, Harrington & McNew 2003, Gramaje *et al.* 2011, Day *et al.* 2012 (morphology); Halleen *et al.* 2007, Gramaje *et al.* 2010, 2011, 2014, Úrbez-Torres *et al.* 2014, Travadon *et al.*

2015 (pathogenicity); Agustí-Brisach *et al.* 2011, 2013, Gramaje *et al.* 2011 (epidemiology); Gramaje *et al.* 2014 (population genetics); Day *et al.* 2012, Travadon *et al.* 2015, Crous *et al.* 2015c, 2019a, Linnakoski *et al.* 2018, Walsh *et al.* 2018, Ekanayaka *et al.* 2019, Bien & Damm 2020, Maciá-Vicente *et al*. 2020, Aigoun-Mouhous *et al*. 2021, Koukol & Maciá-Vicente 2022 (taxonomy and phylogeny); Navarrete *et al.* 2011, Spadaro *et al.* 2011, Úrbez-Torres *et al.* 2015, Maldonado-González *et al.* 2020 (detection and identification); Rédou *et al.* 2016, Knapp *et al.* 2018 (genome sequence).

Cadophora domestica L. Mostert, R. van der Merwe, Halleen & Gramaje, ***sp. nov.*** MycoBank MB 833823. Fig. 6.

Etymology: Named after its host, *Prunus domestica*.

Mycelium composed of branched, septate hyphae occurring singly or in bundles of up to 7; hyphae tuberculate with warts up to 2 µm diam, verruculose to smooth, olivaceous brown, 2.5–3.5 µm diam. *Conidiophores* mostly short, usually branched, arising from aerial or submerged hyphae, erect to flexuous, up to 4-septate, hyaline to pale brown, (7.5–)9.5–38(–48) (av. = 17) µm long and 2–3 (av. = 2.5) µm wide. *Phialides* terminal or lateral, mostly monophialidic, smooth to verruculose, hyaline, with 1.5–3.5 µm long, 2–2.5 µm wide, mostly cylindrical collarettes, (4.5–)6.5–13.5(–14.5) × 1.5–3(–4) (av. = 8 × 2.5) µm. *Conidia* hyaline, oblong ellipsoidal, (3–)3.5–5.5 × 1.5–2.5 (av. = 4.5 × 2) µm.

Culture characteristics: Colonies reaching19–25 mm after 8 d at 25 ºC. The minimum temperature for growth was 5 ºC, the optimum 20–25 ºC and the maximum 30 ºC. Colonies on MEA flat, felty, with even margins after 16 d, straw with a purple stripe close to the centre; reverse concolourous. Colonies on PDA flat, felty, with even margins after 16 d, white to umber toward the centre; reverse concolourous.

Typus: **South Africa**, Western Cape Province, Montagu, from necrotic tissues from crown of *Prunus domestica* (*Rosaceae*) nursery tree, 2017, R. van der Merwe (**holotype** CBS H-24306, culture ex-type STEU 8865 = CBS 146265).

Additional material examined: **South Africa**, Western Cape Province, Montagu, from necrotic tissues from crown of *Prunus domestica* nursery tree, 2017, R. van der Merwe, culture STEU 8864.

Notes: The two strains of *Ca. domestica* that were evaluated here exhibited very similar morphological characteristics. Conidiophores of strain STEU 8864 are on average longer (av. = 21 µm) than those of STEU 8865 (av. = 17 µm).

Cadophora rotunda L. Mostert, R. van der Merwe, Halleen & Gramaje, ***sp. nov.*** MycoBank MB 833822. Fig. 7.

Etymology: Latin, *rotundum*, meaning circular. In reference to the circular conidia.

Mycelium composed of branched, septate hyphae occurring singly or in bundles of up to 8; hyphae tuberculate with warts up to 2.5 µm diam, verruculose to smooth, olivaceous brown, 2.5–3.0 µm diam. *Conidiophores* usually branched, arising from aerial or submerged hyphae, erect to flexuous, up to 6-septate, pale brown

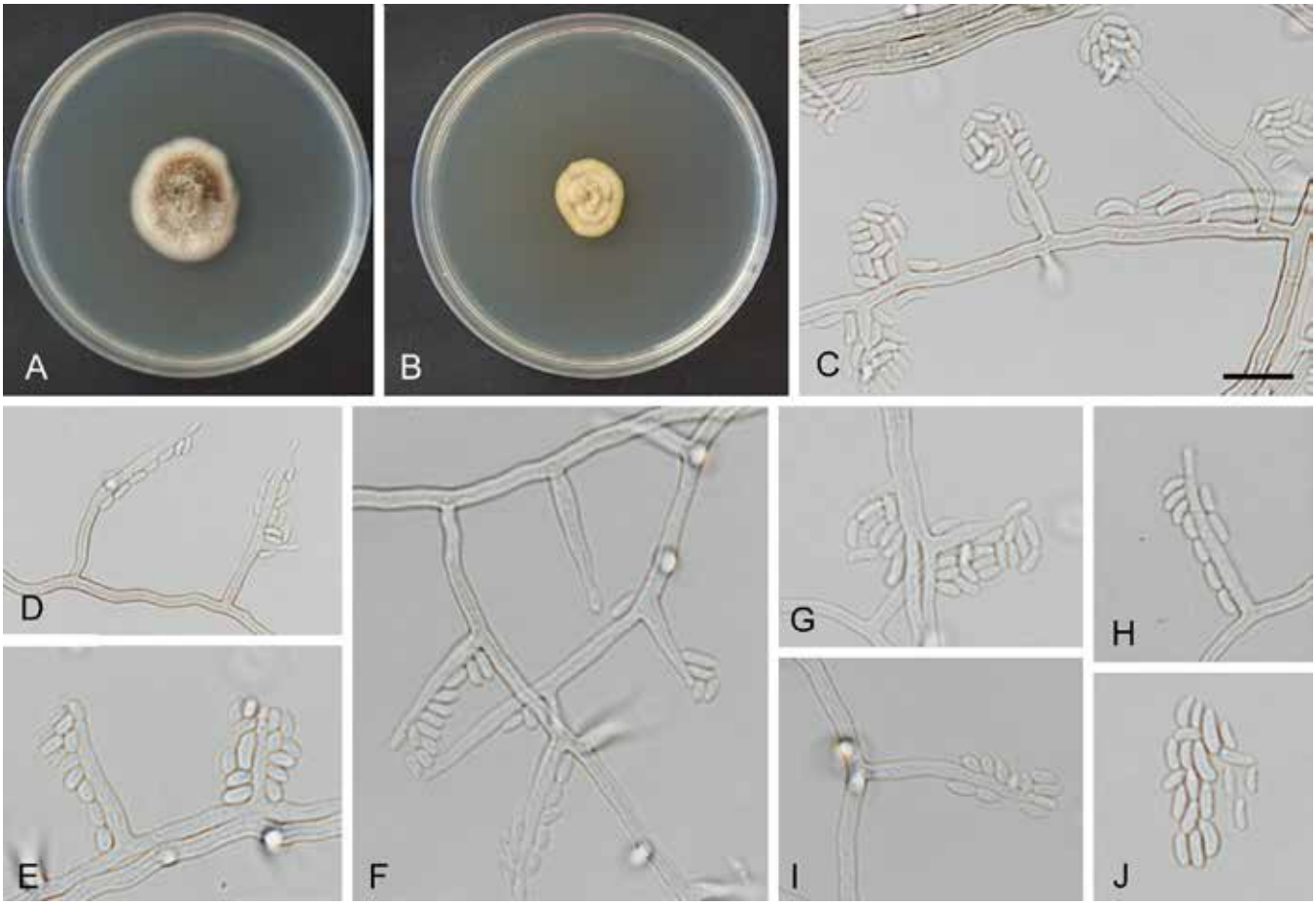

Fig. 6. *Cadophora domestica* (ex-type CBS 146265). **A.** Colony on PDA. **B.** Colony on MEA. **C, D.** Conidiophores and phialides. **E–I.** Phialides. **J.** Conidia. Scale bars: C = 10 µm. C applies to D–J.

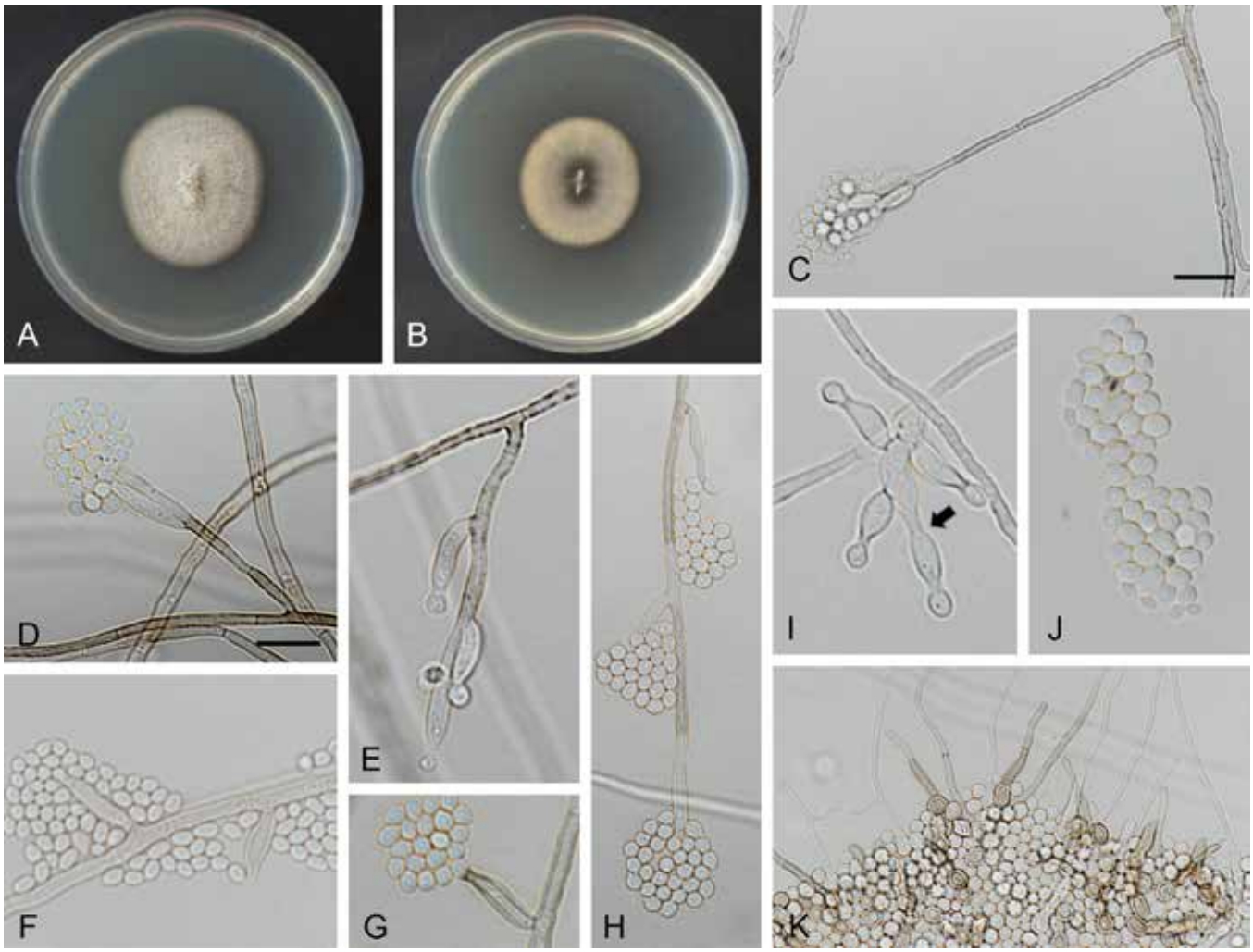

Fig. 7. *Cadophora rotunda* (ex-type CBS 146264). **A.** Colony on PDA. **B.** Colony on MEA. **C–E.** Conidiophores. **F–I.** Phialides. **I.** Percurrently proliferated phialide (indicated by arrow). **J.** Conidia. **K.** Over-mature conidia, some aggregating, some germinating. Scale bars: C, D = 10 µm. C applies to K; D applies to E–J.

to brown, (10–)12.5–59(–71) (av. = 35) µm long and 2–3.5 (av. = 2.5) µm wide. *Phialides* terminal or lateral, mostly monophialidic, smooth, hyaline, with 2–3 µm long, 2–3 µm wide, mostly cylindrical collarettes, some elongate-ampulliform, attenuated at the base or navicular, (3.5–)6–13.5(–15) × 1.5–3(–3.5) (av. = 8 × 2.5) µm. Phialides sometimes produce more than one collarette as a result of percurrent proliferation. *Conidia* hyaline, spherical, (3–)3.5–5.5 × 2.5–3.5 (av. = 4.5 × 3) µm.

Culture characteristics: Colonies reaching 27–28 mm diam after 8 d at 25 ºC. The minimum temperature for growth was 5 ºC, the optimum 20–25 ºC and the maximum 35 ºC. Colonies on MEA flat, felty, with even margins after 16 d, white to grey olivaceous close to the centre; reverse concolourous. Colonies on PDA flat, felty, with even margins after 16 d, white to pale grey; reverse concolourous.

Typus: **South Africa**, Western Cape Province, Montagu, from necrotic tissues from crown of *Prunus domestica* (*Rosaceae*) nursery tree, 2017, R. van der Merwe (**holotype** CBS H-24306, culture ex-type STEU 8862 = CBS 146264).

Notes: *Cadophora rotunda* is currently only known from a single isolate that is phylogenetically related to *Ca. melinii* and *Ca. fastigiata* (Fig. 5). *Cadophora rotunda* differs from *Ca. melinii* in the length of the conidiophores (*Ca. rotunda*: av. 35 µm long; *Ca. melinii*: av. 18.8 µm long) and the conidial morphology (*Ca. rotunda*: spherical; *Ca. melinii*: cylindrical to oblong ellipsoidal; Travadon *et al*. 2015). A total of 60 bp polymorphisms can distinguish *Ca. rotunda* from *Ca. melinii*: 23 bp in *tef1* locus, 28 bp in *tub2* locus, and 9 bp in ITS. *Cadophora rotunda* differs from *Ca. fastigiata* in the colony growth (*Ca. rotunda*: 27–28 mm after 8 d; *Ca. fastigiata*: 23–25 mm after 10 d) and the presence of light brown phialides in *Ca. fastigiata* (Cole & Kendrick 1973). A total of 78 bp polymorphisms can distinguish *Ca. rotunda* from *Ca. fastigiata*: 23 bp in *tef1* locus, 43 bp in the *tub2* locus, and 12 bp in ITS.

Cadophora vinacea J.R. Úrbez-Torres, D.T. O'Gorman & Gramaje, ***sp. nov.*** MycoBank MB 833825. Fig. 8.

Etymology: Latin, *vinum*, meaning wine. In reference to the red vinaceous colour of colonies on PDA.

Mycelium composed of branched, septate hyphae occurring singly or in bundles of up to 10; hyphae tuberculate with warts up to 2.5 µm diam, verruculose to smooth, olivaceous brown, 2.5–3 µm diam. *Conidiophores* mostly short, usually branched, arising from aerial or submerged hyphae, erect to flexuous, up to 5-septate, hyaline to pale brown, (8–)9.5–35.5(–44) (av. = 19) µm long and 2–3.5 (av. = 2.5) µm wide. *Phialides* terminal or lateral, mostly monophialidic, smooth to verruculose, hyaline, with 1.5–2.5 µm long, 2–2.5 µm wide, mostly cylindrical collarettes, (5–)7.5–15.5(–18) × 1.5–3(–3.5) (av. = 11 × 2.5) µm. *Conidia* hyaline, ovoid to oblong ellipsoidal, (3–)4–5.5 × 1.5–2.5 (av. = 4.5 × 2) µm.

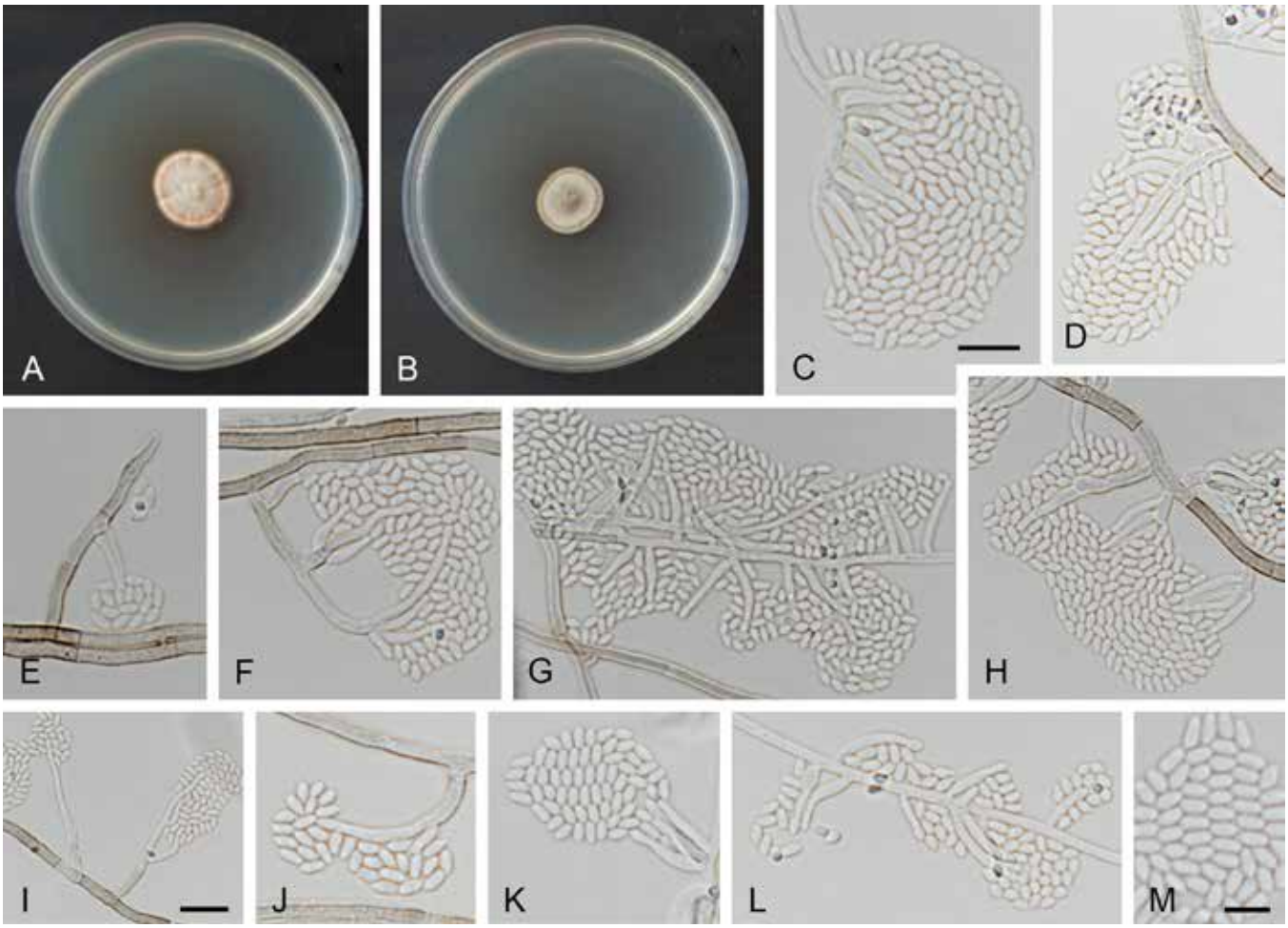

Fig. 8. *Cadophora vinacea* (ex-type CBS 146263). **A.** Colony on PDA. **B.** Colony on MEA. **C–L.** Conidiophores and phialides. **M.** Conidia. Scale bars: C, I = 10 µm; M = 5 µm. C applies to D–H, J–L.

Culture characteristics: Colonies reaching 21–24 mm after 8 d at 25 ºC. The minimum temperature for growth was 5 ºC, the optimum 20–25 ºC and the maximum 30 ºC. Colonies on MEA flat, felty, with even margins, after 16 d, buff with a vinaceous stripe near the centre; reverse concolourous. Colonies on PDA flat, felty, with even margins, after 16 d, buff to vinaceous toward the margin; reverse concolourous.

Typus: **Canada**, British Columbia, Okanagan Valley, from necrotic tissue in trunk of *Vitis vinifera* cv. Ehrenfelser (*Vitaceae*), 2011, J.R. Úrbez-Torres (**holotype** CBS H-24307, culture ex-type PARC199 = CBS 146263).

Additional material examined: **Canada**, British Columbia, Okanagan Valley, from necrotic tissue in cordon of *V. vinifera* cv. Gewurztraminer, 2011, J.R. Úrbez-Torres, culture PARC274.

Notes: *Cadophora vinacea* is phylogenetically related to *Ca. ferruginea* (Fig. 5). Cultures CBS 146263 (ex-type) and PARC274 differ from *Ca. ferruginea* in its fastest colony growth on PDA (*Ca. vinacea*: 21–24 mm after 8 d; *Ca. ferruginea*: 18–19 mm after 10 d), and the production of reddish globules and mycelium by *Ca. ferruginea* (Macià-Vicente *et al*. 2020). A total of 19 bp polymorphisms can distinguish *Ca. vinacea* from *Ca. ferruginea*: 17 bp in *tef1* locus, and two in ITS.

Cadophora vivarii L. Mostert, Havenga, Halleen & Gramaje, ***sp. nov.*** MycoBank MB 833824. Fig. 9.

Etymology: Latin, from *vivarium*, meaning "of the nursery". In reference to the environment where it was collected.

Mycelium composed of branched, septate hyphae occurring singly or in bundles of up to 10; hyphae tuberculate with warts up to 2 µm diam, verruculose to smooth, olivaceous brown, 2.5–4 µm diam. *Conidiophores* mostly short, usually branched, arising from aerial or submerged hyphae, erect to flexuous, up to 4-septate, pale brown to brown, (7.5–)8.5–41(–43) (av. = 18) µm long and 2–3.5 (av. = 2.5) µm wide. *Phialides* terminal or lateral, mostly monophialidic, smooth to verruculose, hyaline, with 1.5–3 µm long, 2–3 µm wide, mostly cylindrical collarettes, some elongate-ampulliform, attenuated at the base or navicular, (3.5–)5.5–10(–12) × 1.5–3(–4) (av. = 6.5 × 2.5) µm. *Conidia* hyaline, ovoid or oblong ellipsoidal, 3–5 × 1.5–2.5 (av. = 4 × 2) µm.

Culture characteristics: Colonies reaching 17–22 mm after 8 d at 25 ºC. The minimum temperature for growth was 5 ºC, the optimum 20–25 ºC and the maximum 35 ºC. Colonies on MEA flat, felty, with entire to undulate margin, producing yellow pigment, after 16 d, pale yellow toward the edge; reverse concolourous. Colonies on PDA flat, felty, with entire to undulate margin, after 16 d white to buff close to the centre; reverse concolourous.

Typus: **South Africa**, Western Cape Province, Kouebokkeveld, from necrotic tissue of bud union of *Malus domestica* (*Rosaceae*) nursery tree, 2015, M. Havenga (**holotype** CBS H-24304, culture ex-type STEU 8310 = CBS 146262).

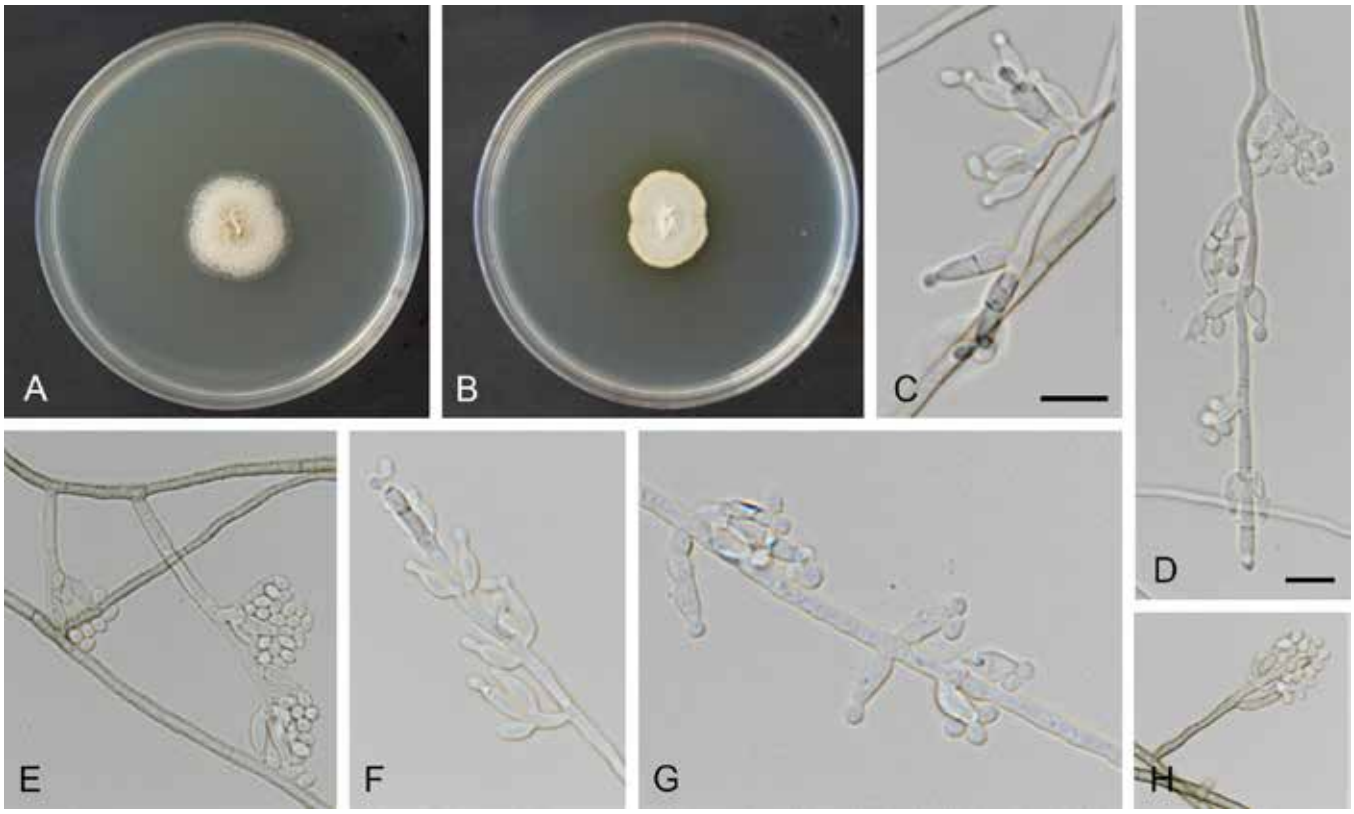

Fig. 9. *Cadophora vivarii* (ex-type CBS 146262). **A.** Colony on PDA. **B.** Colony on MEA. **C–H.** Conidiophores, phialides and conidia. Scale bars: C, D = 10 µm. C applies to F–G; D applies to E, H.

Notes: *Cadophora vivarii* is currently only known from a single isolate that is phylogenetically related to *Ca. obovata* (Fig. 5). *Cadophora vivarii* differs from *Ca. obovata* in conidial morphology (*Ca. vivarii*: ovoid or oblong ellipsoidal; *Ca. obovata*: obovate) and the absence of conidiophores in *Ca. obovata*.

Genome sequenced strain: *Cadophora luteo-olivacea*. **Spain,** Valencia, grapevine rootstock 110 Richter, 2007, D. Gramaje, culture ex-type CBS 128576 = Clo-18. This Whole Genome Shutgun project has been deposited at GenBank under the accession JALRMC000000000 (BioProject: PRJNA827019, BioSample: SAMN27594411; present study).

Authors: D. Gramaje, J.R. Úrbez-Torres, L. Mostert & F. Halleen

Celoporthe Nakab. *et al.*, Stud. Mycol. 55: 261. 2006. Fig. 10.

Classification: *Sordariomycetes*, *Sordariomycetidae*, *Diaporthales*, *Cryphonectriaceae*.

Type species: *Celoporthe dispersa* Nakab. *et al.* Holotype and ex-type strains: PREM 58896, CBS 118782 = CMW 9976.

DNA barcode (genus): ITS.

DNA barcodes (species): *tub1, tub2*, *tef1*. Table 3. Fig. 11.

Ascomata pseudothecial, semi-immersed to immersed in bark, erumpent, mostly gregarious or single, recognisable by papilla (short emerged perithecial necks). *Stromatic tissues* surrounding perithecia except for the base, orange to umber, pseudoparenchymatous to prosenchymatous depending on regions. *Perithecia* valsoid, bases immersed, globose to ellipsoidal. *Perithecial walls* dark olivaceous brown to black, pseudoparenchymatous. *Perithecial necks* black, embedded in stromatic tissue. *Asci* 8-spored, unitunicate, fusoid to ellipsoid, clavate to cylindrical, with a non-amyloid refractive ring in apex. *Ascospores* hyaline, oblong to ellipsoidal, straight or slightly curved, 1-median septate. *Conidiomata* superficial to immersed, single or gregarious, orange to umber when young, fuscous to black when mature, globose to conical, pulvinate, with or without short attenuated neck, uni- or multilocular, convoluted. *Stromatic tissues* pseudoparenchymatous to prosenchymatous. *Conidiophores* hyaline, branched irregularly at base, branching out along the length just below septum. *Conidiogenous cells* enteroblastic, cylindrical to lageniform with or without attenuated apices. *Paraphyses* or *cylindrical sterile cells* present or absent. *Conidia* hyaline, aseptate, oblong to cylindrical or ovoid, occasionally allantoid, exuded as bright luteous to orange tendrils or droplets.

Culture characteristics: Colonies grown on 2 % MEA in dark showing abundant floccose aerial mycelia, white, yellow white, pale luteous, and umber when immature, with age turning to sulfur yellow, luteous, umber, hazel, chestnut, or greenish black.

Optimal media and cultivation conditions: *Celoporthe* spp. display optimal growth on 2 % MEA between 25 °C and 30 °C: *Cel. borbonica*, *Cel. cerciana* *Cel. dispersa* and *Cel. woodiana* at 25 °C; *Cel. eucalypti*, *Cel. fontana* *Cel. guangdongenesis*, *Cel. hauoliensis*, *Cel. hawaiiensis*, *Cel. indonensiensis*, *Cel. paradisiaca*, *Cel. syzygii* and *Cel. tibouchinae* at 30 °C.

Distribution: China, Indonesia, La Réunion, South Africa, USA (Hawaii), Zambia.

Fig. 10. *Celoporthe* spp. **A–C.** Disease symptoms caused by *Celoporthe cerciana* on *Eucalyptus grandis* hybrid. **A.** Bark cracks of tree. **B.** Fruiting structures on canker. **C.** Close-up of canker. **D–G.** Asexual morph. **D, E.** *Celoporthe tibouchinae* (ex-type CMW 44126 = PPRI 25130). **D.** Conidiomata. **E.** Vertical section of conidioma. **F.** Paraphyses in conidioma of *Celoporthe borbonica* (CMW 44139). **G.** Conidia of *Celoporthe borbonica* (ex-type CMW 44128). **H–L.** Sexual morph of *Celoporthe borbonica* (ex-type CMW 44128). **H, I.** Ascostromata. **J.** Vertical section of ascostromata and perithecium. **K.** Ascus. **L.** Ascospores with some germinating. Scale bars: D = 500 µm; H, I = 250 µm; E, J = 100 µm; K, L = 10 µm; F, G = 5 µm. Picture B taken from Wang *et al*. (2018); F, J, K from Ali *et al*. (2018).

Hosts: *Eucalyptus*, *Heteropyxis*, *Psidium*, *Syzygium* (*Myrtaceae*), *Melastoma* and *Tibouchina* (*Melastomataceae*).

Disease symptoms: Cankers, branch dieback and leaf spots.

Notes: *Celoporthe* was introduced to accommodate a fungus that is closely related to *Chrysoporthe* and *Holocryphia* but distinctly different based on DNA sequence data and morphology (Nakabonge *et al.* 2006). The most notable difference between *Celoporthe* and *Chrysoporthe* is in the lengths of perithecial necks; *Celoporthe* with short necks appearing as papillae and *Chrysoporthe* with a long and easily distinguishable necks. *Celoporthe* accommodates 14 species, including the new species presented here (references in Table 3). Three species, *Cel. dispersa*, *Cel. borbonica* and *Cel. syzygii* are known from both sexual and asexual morphs (Nakabonge *et al.* 2006, Chen *et al.* 2011, Ali *et al.* 2018). Only asexual morphs are known for the remaining species.

The morphologies and characteristics of growth in culture overlap for various species of *Celoporthe*. Although species can be distinguished using a combination of morphological

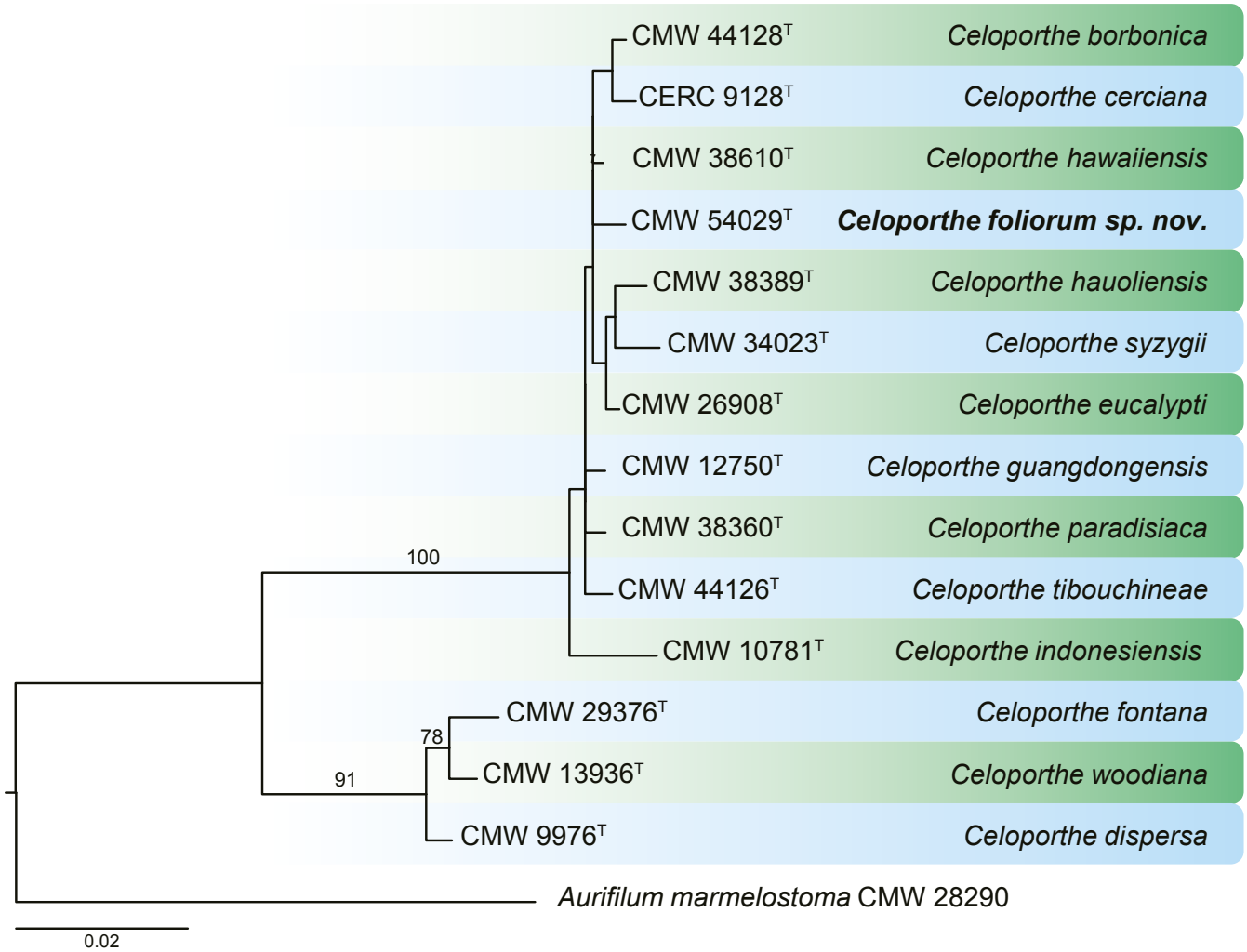

Fig. 11. Maximum likelihood (ML) phylogram constructed using the combined dataset of the ITS (506 bp), *tub1* (434 bp), and *tub2* (399 bp) gene regions of all accepted species of *Celoporthe*. Bootstrap support values (> 70 %) are indicated at the nodes. The novel taxon is printed in **bold**. The phylogenetic tree was rooted to *Aurifilum marmelostoma* CMW28290. GenBank accession numbers are indicated in Table 3. ^{T} indicates ex-type strain. TreeBASE: S28873.

Table 3. DNA barcodes of accepted *Celoporthe* spp.

Species	Isolates[1]	GenBank accession numbers[2]					References
		LSU	ITS	*tub1*	*tub2*	*tef1*	
Celoporthe borbonica	CMW 44128 = PPRI 25133^{T}	—	MG585741	MG585725	—	—	Ali *et al.* (2018)
Cel. cerciana	CERC 9128^{T}	—	MH084352	MH084382	MH084412	MH084442	Wang *et al.* (2018)
Cel. dispersa	CMW 9976 = CBS 118782^{T}	HQ730853	DQ267130	DQ267136	DQ267142	HQ730840	Nakabonge *et al.* (2006)
Cel. eucalypti	CMW 26908 = CBS 127190^{T}	HQ730863	HQ730837	HQ730817	HQ730827	HQ730850	Chen *et al.* (2011)
Cel. foliorum	CMW 54029 = PPRI 27961^{T}	—	LC537846	LC537847	LC537848	—	Present study
Cel. fontana	CMW 29376 = CBS 132008^{T}	—	GU726941	GU726953	GU726953	JQ824074	Vermeulen *et al.* (2013)
Cel. guangdongensis	CMW 12750 = CBS 128341^{T}	HQ730856	HQ730830	HQ730810	HQ730820	HQ730843	Chen *et al.* (2011)
Cel. hauoliensis	CMW 38389 = CBS 140640^{T}	—	KJ027502	KJ027478	—	—	Roux *et al.* (2020)
Cel. hawaiiensis	CMW 38610 = CBS 140642^{T}	—	KJ027499	KJ027475	—	—	Roux *et al.* (2020)

Table 3. (Continued).

Species	Isolates[1]	GenBank accession numbers[2]					References
		LSU	ITS	*tub1*	*tub2*	*tef1*	
Cel. indonesiensis	CMW 10781 = CBS 115844[T]	HQ730855	AY084009	AY084033	AY084021	HQ730842	Chen *et al.* (2011)
Cel. paradisiaca	CMW 38360 = CBS 147170[T]	—	KJ027498	KJ027474	—	—	Roux *et al.* (2020)
Cel. syzygii	CMW 34023 = CBS 127218[T]	HQ730857	HQ730831	HQ730811	HQ730821	HQ730844	Chen *et al.* (2011)
Cel. tibouchinae	CMW 44126 = PPRI 25130[T]	—	MG585747	MG585731	LC537849	—	Ali *et al.* (2018)
Cel. woodiana	CMW 13936 = CBS 118785[T]	—	DQ267131	DQ267137	DQ267143	JQ824071	Vermeulen *et al.* (2013)

[1] CBS: Westerdijk Fungal Biodiversity Institute, Utrecht, the Netherlands; CERC: Culture Collection of China Eucalypt Research Center, Guangdong Province, China; CMW: Tree Protection Co-operative Program, Forestry and Agricultural Biotechnology Institute, University of Pretoria, South Africa; PPRI: Culture collection of the South African National Collection of Fungi (NCF), Roodeplaat, Pretoria, South Africa. [T] indicates ex-type strain.

[2] ITS: internal transcribed spacers and intervening 5.8S nrDNA; LSU: partial 28S large subunit nrRNA gene; *tef1*: partial translation elongation factor 1-α gene; *tub1, tub2*: partial β-tubulin gene.

characteristics such as sizes of conidia or ascospores and optimal growth temperature, DNA sequence data are essential to confirm identifications. The ITS and *tef1* regions do not provide accurate species resolution when used alone (Vermeulen *et al.* 2013, Wang *et al.* 2018). The *tub1* and *tub2* regions are most useful for species resolution, but provide stronger support in combination with ITS and *tef1* data. *Celoporthe* spp. are all tree pathogens but they have been shown to vary in pathogenicity in controlled inoculation tests on *Eucalyptus* clones (Nakabonge *et al.* 2006, Chen *et al.* 2011, Vermeulen *et al.* 2013, Ali *et al.* 2018, Wang *et al.* 2018).

References: Gryzenhout *et al.* 2009 (classification); Nakabonge *et al.* 2006, Chen *et al.* 2011, Vermeulen *et al.* 2013, Ali *et al.* 2018, Wang *et al.* 2018 (morphology, nomenclature, phylogeny and pathogenicity).

Celoporthe foliorum H. Suzuki, Marinc. & M.J. Wingf., ***sp. nov.*** MycoBank MB 835419. Fig. 12.

Etymology: The name refers to its habitat, occurring on leaves.

Asexual morph observed on 2 % MEA grown in dark for 30 d. *Conidiomata* stromatic, gregarious, formed among aerial mycelium or on the medium, uni- or multi-locular, oozing a yellow and murky spore mass; *conidiomatal walls* pseudoparenchymatous, consisting of a few layers of thick-walled cells, pigmented, 5–21 µm thick (av. 11.2 µm), the outermost layer prosenchymatous. *Conidiophores* borne along locular walls, upright, simple, branched at basal cell or lateral, 12–30 µm long (av. 17.5 µm). *Paraphyses* not observed. *Conidiogenous cells* enteroblastic, hyaline, flask-shaped, abruptly attenuated toward apex, 4–12.5 × 1–2 µm (av. 6.9 × 1.8 µm). *Conidia* hyaline, aseptate, oblong to ellipsoidal with a pointed base, 3–4 × 1–2 µm (av. 3.6 × 1.5 µm). *Sexual morph* not observed.

Culture characteristics: On 2 % MEA showing optimum growth at 30 °C at 14.2 mm / d, followed by at 25 °C at 12.6 mm/d, showing slower growth at 15, 20, 35 °C. Cultures circular with uneven margin, aerial mycelium floccose, white when young, umber to hazel to chestnut when mature.

Typus: **Indonesia**, Riau, isolated from a leaf spot of a native *Syzygium* sp. (*Myrtaceae*), Oct. 2018, M.J. Wingfield (**holotype** PREM 62887, culture ex-type CMW 54029 = PPRI 27961).

Additional material examined: **Indonesia**, Riau, isolated from a leaf spot of a native *Syzygium* sp., Oct. 2018, M.J. Wingfield, PREM 62886, living culture CMW 54028 = PPRI 27960.

Note: Unlike the other *Celoporthe* spp. isolated from bark tissue, *Cel. foliorum* was isolated from leaf spots. Due to the scarcity of specimens, *in vivo* characteristics were not observed. A distinctive morphological feature of *Cel. foliorum* is a lack of paraphyses among conidiophores that is reported present in other species. Long paraphysis-like structures were occasionally observed but they were atypical conidiogenous cells. *Celoporthe hawaiiensis* is a phylogenetic closest relative to *Cel. foliorum* (Fig. 11). *Celoporthe hawaiiensis* was reported from Hawaii on *Pisidium* and *Syzygium* infected by *Austropuccinia psidii* (Roux *et al.* 2020). They are morphologically similar to each other based on the observation of *in vitro* cultures with *Eucalyptus* stem sections: their optimal growth temperature is 30 °C and conidial dimensions are 2.5–4 × 1–1.5 µm in *Cel. hawaiiensis* and 3–4 × 1–2 µm in *Cel. foliorum*. However, conical conidiomata with necks which were present in *Cel. hawaiiensis* were not observed in *Cel. foliorum*. *Celoporthe foliorum* is the second *Celoporthe* sp. to be reported from Indonesia. The other species from this region, *Cel. indonesiensis* was isolated from *Syzygium aromaticum* from North Sumatra in 1997 (Chen *et al.* 2011).

Genome sequenced strain: *Celoporthe dispersa.* **South Africa**, on *Syzigium cordatum,* 2001, M. Gryzenhout, culture ex-type CBS 118782. This Whole Genome Shutgun project has been deposited at GenBank under the accession WAID00000000 (BioProject: PRJNA574566, BioSample: SAMN12860070; Liu *et al.* 2019).

Authors: H. Suzuki, S. Marincowitz, S.F. Chen, B.D. Wingfield, M.J. Wingfield

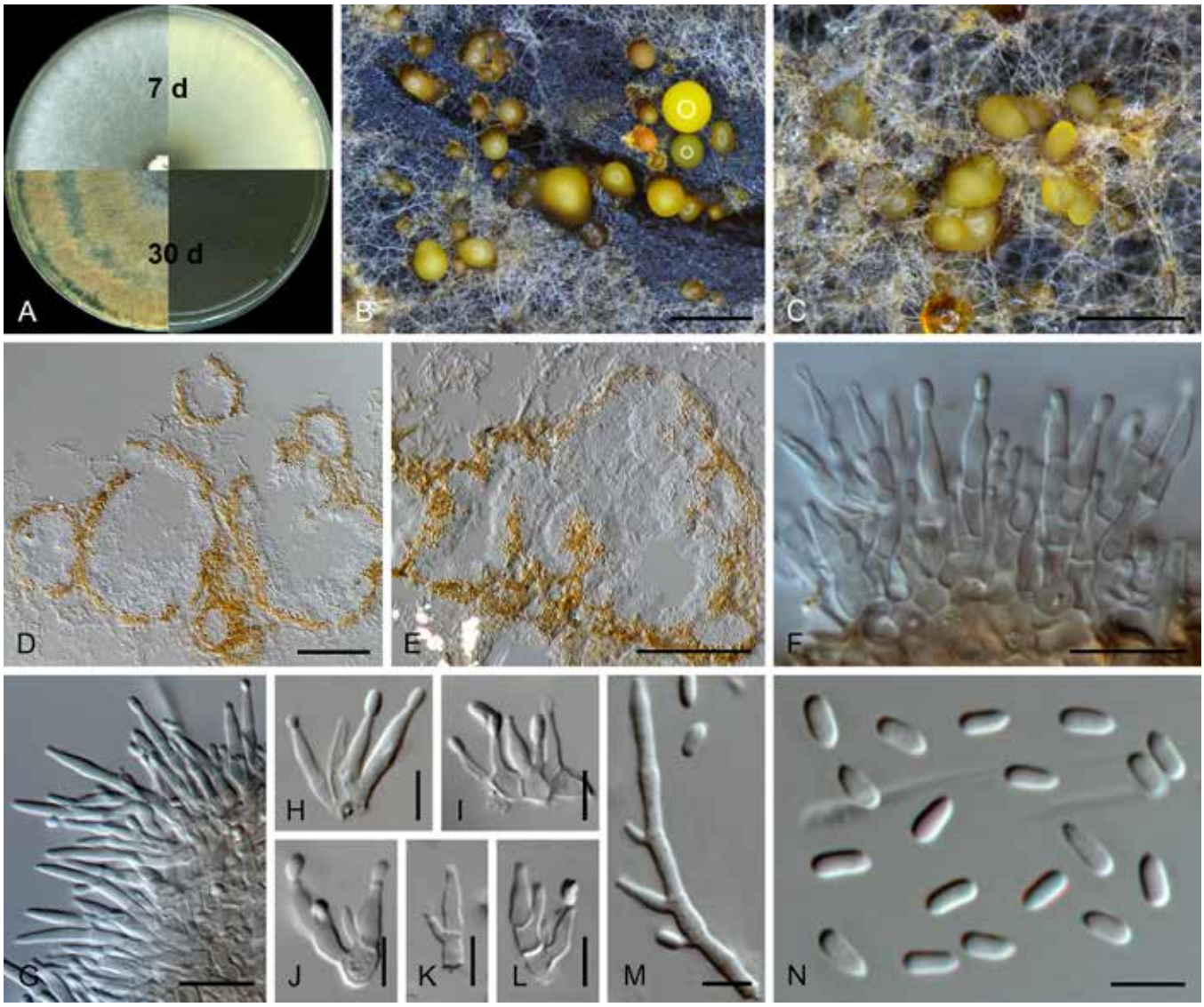

Fig. 12. *Celoporthe foliorum* (ex-type CMW 54029). **A.** Culture grown on 2 % MEA in 7 d and 30 d in dark (left: front, right: reverse). **B, C.** Conidiomata formed on agar surface (B) and on mycelial mass (C) with yellow oozing conidial mass. **D, E.** Vertical section through conidiomata showing multilocular, lobated chambers. **F, G.** Conidiophores. **H–M.** Conidiophores and conidiogenous cells. **N.** Conidia. Scale bars: B, C = 500 µm; D, E = 50 µm; F, G = 10 µm; H–N = 5 µm.

Cercospora Fresen. ex Fuckel, Fungi Rhen. Exs.: No. 117. 1863; Hedwigia 2: 133. Apr–Jun 1863, *nom. cons. prop*. Fig. 13.
Synonyms: *Virgasporium Cooke*, Grevillea 3: 182. 1875.
Cercosporina Speg., Anales Mus. Nac. Buenos Aires 3, 13: 424. 1911.

Classification: *Dothideomycetes*, *Dothideomycetidae*, *Mycosphaerellales*, *Mycosphaerellaceae*.

Type species: *Cercospora apii* Fresen., *typ. cons. prop*. Lectotype designated by Groenewald *et al.* (2005): Fuckel, Fungi rhen. 117, in HAL. Epitype designated by Groenewald *et al.* (2005), ex-epitype strain: CBS 116455 = CPC 11556.

DNA barcodes (genus): LSU, ITS, *rpb2*.

DNA barcodes (species): *actA*, *cmdA*, *gapdh*, *his3*, *tef1*, *tub2*. Table 4. Fig. 14.

Hyphomycetous. *Mycelium* internal, rarely external; hyphae branched, septate, hyaline or almost so to usually pigmented, thin-walled, smooth, rarely faintly rough-walled. *Stromata* lacking to well-developed, substomatal, intraepidermal to deeply immersed, mostly pigmented, composed of *textura angulata* or *textura globosa*. *Conidiophores* macronematous, mononematous, solitary or fasciculate, in small to large fascicles, rarely in sporodochial conidiomata, emerging through stomata or erumpent, very rarely arising from superficial hyphae, erect, continuous to pluriseptate, mostly pigmented, pale olivaceous to dark brown, rarely hyaline or almost so, straight or flexuous, sometimes geniculate, unbranched or rarely branched, wall smooth to somewhat rough, thin to moderately thick. *Conidiogenous cells* integrated, terminal or intercalary, sometimes conidiophores aseptate, *i.e.* reduced to conidiogenous cells, monoblastic, determinate to usually polyblastic, proliferation sympodial, rarely percurrent. *Conidiogenous loci* (scars) conspicuous, thickened and darkened-refractive, planate with minute central pore. *Conidia* solitary, rarely in short chains (mainly under high humidity), mostly scolecosporous, obclavate cylindrical, acicular, filiform and pluriseptate, rarely amero- to phragmosporous, broadly ellipsoid-ovoid to broadly obclavate-cylindrical, but always hyaline or subhyaline (with a pale green tinge), thin-walled, smooth or almost so, hila thickened and

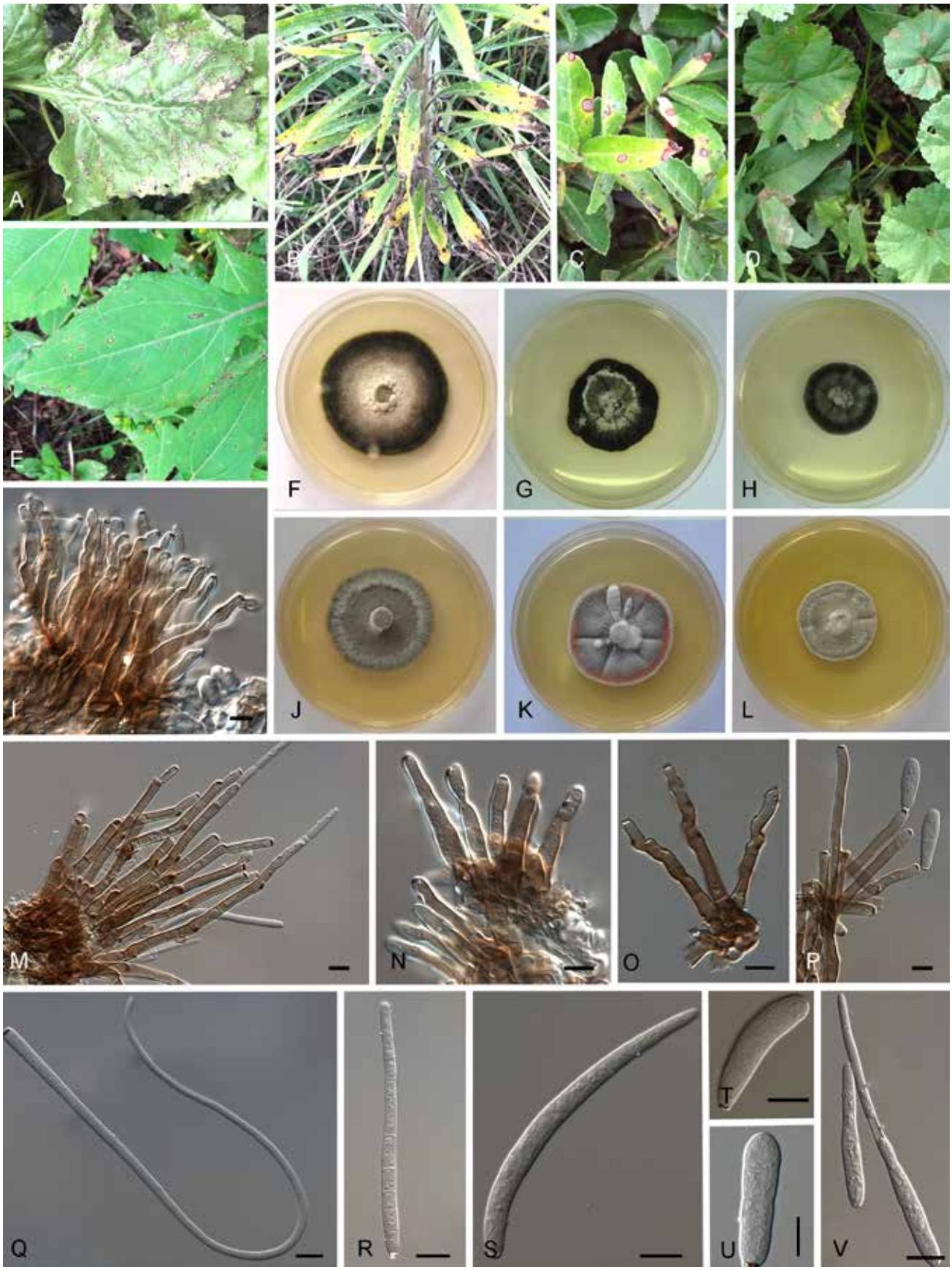

Fig. 13. *Cercospora* spp. **A–E.** Disease symptoms. **A.** *Cercospora beticola* on *Beta vulgaris*. **B.** *Cercospora conyzae-canadensis* on *Conyza canadensis*. **C.** *Cercospora cf. flagellaris* on *Buxus microphylla*. **D.** *Cercospora gamsiana* on *Malva neglecta*. **E.** *Cercospora cf. richardiicola* on *Bidens tripartita*. **F–H, J–L.** Colonies on MEA. **F.** *Cercospora althaeina* (IRAN 2674C). **G.** *Cercospora cylindracea* (ex-type IRAN 2654C). **H.** *Cercospora pseudochenopodii* (ex-type IRAN 2649C). **J.** *Cercospora uwebrauniana* (ex-type CBS 138581). **K.** *Cercospora cf. flagellaris* (IRAN 2668C). **L.** *Cercospora cf. flagellaris* (IRAN 2648C). **I, M–P.** Conidiophores. **I.** *Cercospora cf. gossypii* (CBS 136137). **M.** *Cercospora beticola* (CCTU 1135). **N.** *Cercospora rautensis* (CBS 136134). **O.** *Cercospora cylindracea* (ex-type CBS 138580). **P.** *Cercospora uwebrauniana* (ex-type CBS 138581). **Q–V.** Conidia. **Q.** *Cercospora beticola* (CCTU 1135). **R.** *Cercospora cylindracea* (ex-type CBS 138580). **S.** *Cercospora sorghicola* (ex-type CBS 136448). **T.** *Cercospora chenopodii* (CCTU 1033). **U.** *Cercospora uwebrauniana* (ex-type CBS 138581). **V.** *Cercospora gamsiana* (CBS 144962). Scale bars = 10 µm. Pictures D, I, M, P, Q, U, V taken from Bakhshi *et al.* (2018); O, R–T from Bakhshi *et al.* (2015a); N from Bakhshi (2019).

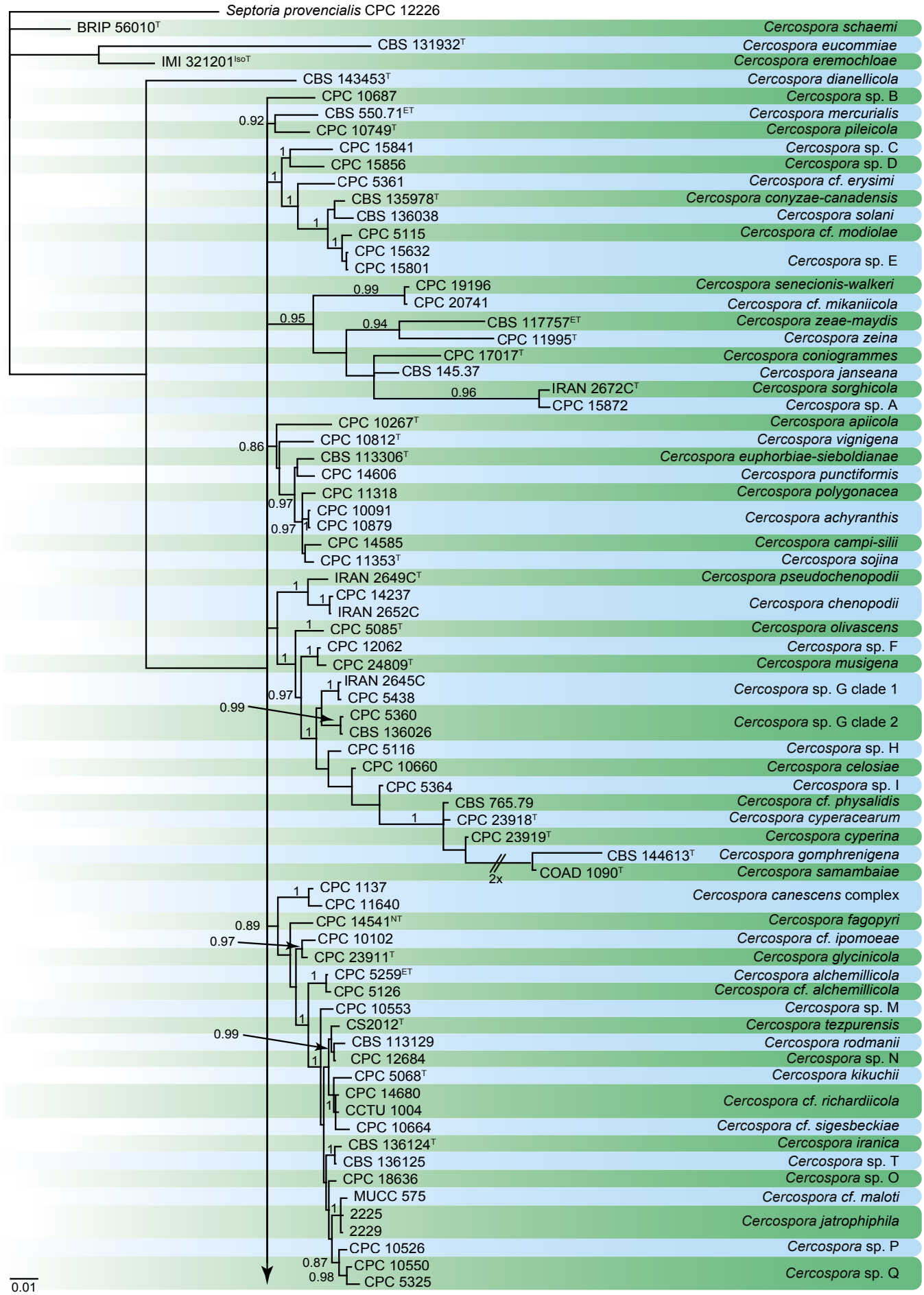

Fig. 14. Bayesian phylogram constructed from ITS (478 bp), *actA* (209 bp), *cmdA* (259 bp), *gapdh* (870 bp), *his3* (363 bp), *rpb2* (1 230 bp), *tef1* (352 bp) and *tub2* (415 bp) sequences of all accepted species of *Cercospora*. Bayesian posterior probability scores (≥ 0.85) are shown at the nodes. The novel taxon is printed in **bold**. The phylogenetic tree was rooted to *Septoria provencialis* CPC 12226. ^{T} and ^{ET} indicate ex-type and ex-epitype strains, respectively. TreeBASE: S26138.

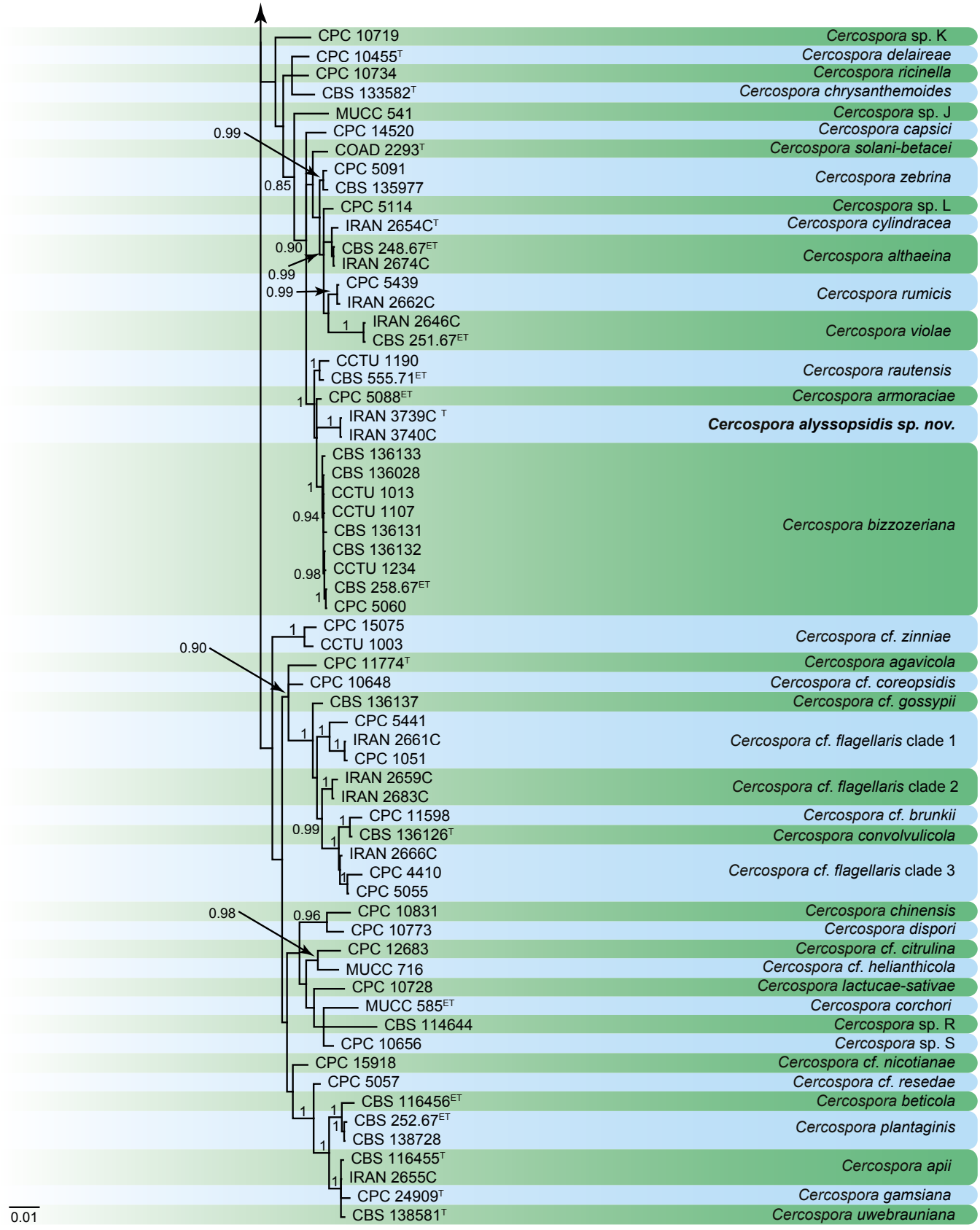

Fig. 14. (Continued).

darkened, conidial secession schizolytic. *Sexual morph* unknown (adapted from Ellis 1971, Crous & Braun 2003, Braun *et al.* 2013).

Cultural characteristics: Colonies on MEA, flat to folded, with smooth, even margins and sparse to moderate aerial mycelium, sometimes radially striated, surface white, olivaceous green, smoke grey, sometimes with different colour (*e.g.* vinaceous grey) in outer region, reverse olivaceous grey to iron grey. Colony colour sometimes changes with subculturing.

Optimal media and cultivation conditions: MEA incubated at 25 °C in dark for 2–4 wk, to determine growth rates, colour and shape of the colony.

Table 4. DNA barcodes of accepted *Cercospora* spp.

Species	Isolates[1]	GenBank accession numbers[2]								References
		ITS	*actA*	*cmdA*	*gapdh*	*his3*	*rpb2*	*tef1*	*tub2*	
Cercospora achyranthis	CBS 132613 = CPC 10879	JX143523	JX143031	JX142785	—	JX142539	—	JX143277	—	Groenewald *et al.* (2013)
	CPC 10091	JX143524	JX143032	JX142786	—	JX142540	—	JX143278	—	Groenewald *et al.* (2013)
Cer. agavicola	CBS 117292 = CPC 11774^{T}	AY647237	AY966898	AY966899	—	AY966900	—	AY966897	—	Groenewald *et al.* (2013)
Cer. alchemillicola	CPC 5259^{ET}	JX143525	JX143033	JX142787	—	JX142541	—	JX143279	—	Groenewald *et al.* (2013)
Cer. cf. alchemillicola	CPC 5126	JX143526	JX143034	JX142788	—	JX142542	—	JX143280	—	Groenewald *et al.* (2013)
Cer. althaeina	CBS 248.67 = CPC 5117^{ET}	JX143530	JX143038	JX142792	MH496170	JX142546	—	JX143284	MH496340	Groenewald *et al.* (2013), Bakhshi *et al.* (2018)
	CCTU 1194 = IRAN 2674C	KJ886397	KJ885914	KJ885753	MH496171	KJ886075	MH511837	KJ886236	MH496341	Bakhshi *et al.* (2015a, 2018)
Cer. alyssopsidis	IRAN 3739C^{T}	MT338042	MT334647	MT334651	MT334649	MT334645	—	MT334643	—	Present study
	IRAN 3740C	MT338043	MT334648	MT334652	MT334650	MT334646	—	MT334644	—	Present study
Cer. apii	CBS 116455 = CPC 11556^{T}	AY840519	AY840450	AY840417	MH496173	AY840384	—	AY840486	MH496343	Groenewald *et al.* (2013), Bakhshi *et al.* (2018)
	CCTU 1086 = CBS 136037 = IRAN 2655C	KJ886411	KJ885928	KJ885767	MH496176	KJ886089	MH511841	KJ886250	MH496346	Bakhshi *et al.* (2015a, 2018)
Cer. apiicola	CBS 116457 = CPC 10267^{T}	AY840536	AY840467	AY840434	—	AY840401	—	AY840503	—	Groenewald *et al.* (2013)
Cer. armoraciae	CBS 250.67 = CPC 5088^{ET}	JX143545	JX143053	JX142807	MH496181	JX142561	—	JX143299	MH496351	Groenewald *et al.* (2013), Bakhshi *et al.* (2018)
Cer. beticola	CBS 116456 = CPC 11557^{ET}	AY840527	AY840458	AY840425	MH496185	AY840392	KT216555	AY840494	MH496355	Groenewald *et al.* (2013), Bakhshi *et al.* (2018)
Cer. bizzozeriana	CBS 258.67 = CPC 5061^{ET}	JX143546	JX143054	JX142808	MH496198	JX142562	—	JX143300	MH496368	Groenewald *et al.* (2013), Bakhshi *et al.* (2018)
	CBS 540.71 = IMI 161110 = CPC 5060	JX143548	JX143056	JX142810	MH496199	JX142564	—	JX143302	MH496369	Groenewald *et al.* (2013), Bakhshi *et al.* (2018)
	CCTU 1013	KJ886414	KJ885931	KJ885770	MH496192	KJ886092	MH511855	KJ886253	MH496362	Bakhshi *et al.* (2015a, 2018)
	CCTU 1022 = CBS 136028	KJ886415	KJ885932	KJ885771	MH496193	KJ886093	MH511856	KJ886254	MH496363	Bakhshi *et al.* (2015a, 2018)
	CCTU 1040 = CBS 136131	KJ886416	KJ885933	KJ885772	MH496200	KJ886094	MH511861	KJ886255	MH496370	Bakhshi *et al.* (2015a, 2018)
	CCTU 1107	KJ886417	KJ885934	KJ885773	MH496197	KJ886095	MH511860	KJ886256	MH496367	Bakhshi *et al.* (2015a, 2018)
	CCTU 1117 = CBS 136132	KJ886418	KJ885935	KJ885774	MH496195	KJ886096	MH511858	KJ886257	MH496365	Bakhshi *et al.* (2015a, 2018)
	CCTU 1127 = CBS 136133	KJ886420	KJ885937	KJ885776	MH496194	KJ886098	MH511857	KJ886259	MH496364	Bakhshi *et al.* (2015a, 2018)
	CCTU 1234	KJ886419	KJ885936	KJ885775	MH496196	KJ886097	MH511859	KJ886258	MH496366	Bakhshi *et al.* (2015a, 2018)
Cer. cf. brunkii	CBS 132657 = CPC 11598	JX143559	JX143067	JX142821	—	JX142575	—	JX143313	—	Groenewald *et al.* (2013)
Cer. campi-silii	CBS 132625 = CPC 14585	JX143561	JX143069	JX142823	—	JX142577	KX288415	JX143315	—	Groenewald *et al.* (2013), Videira *et al.* (2017)
Cer. canescens complex	CBS 111133 = CPC 1137	AY260065	DQ835103	DQ835130	—	DQ835157	—	DQ835084	—	Groenewald *et al.* (2013)
	CPC 11640 = IMI 186563	JX143566	JX143074	JX142828	—	JX142582	—	JX143320	—	Groenewald *et al.* (2013)
Cer. capsici	CBS 132622 = CPC 14520	JX143568	JX143077	JX142831	—	JX142585	MF951456	JX143323	—	Groenewald *et al.* (2013)
Cer. celosiae	CBS 132600 = CPC 10660	JX143570	JX143080	JX142834	—	JX142588	—	JX143326	—	Groenewald *et al.* (2013)
Cer. chenopodii	CBS 132620 = CPC 14237	JX143571	JX143081	JX142835	—	JX142589	—	JX143327	—	Groenewald *et al.* (2013)
	CCTU 1060 = IRAN 2652C	KJ886438	KJ885955	KJ885794	MH496201	KJ886116	MH511862	KJ886277	MH496371	Bakhshi *et al.* (2015a, 2018)
Cer. chinensis	CBS 132612 = CPC 10831	JX143578	JX143088	JX142842	—	JX142596	—	JX143334	—	Groenewald *et al.* (2013)
Cer. chrysanthemoidis	CBS 133582 = CPC 20529^{T}	KC005779	KC005764	KC005767	—	—	—	KC005813	—	Crous *et al.* (2012a)
Cer. cf. citrulina	CBS 132669 = CPC 12683	EU514223	JX143090	JX142844	—	JX142598	—	JX143336	—	Groenewald *et al.* (2013)
Cer. coniogrammes	CBS 132634 = CPC 17017^{T}	JX143583	JX143095	JX142849	—	JX142603	—	JX143341	—	Groenewald *et al.* (2013)
Cer. convolvulicola	CCTU 1083 = CBS 136126^{T}	KJ886441	KJ885958	KJ885797	MH496204	KJ886119	MH511865	KJ886280	MH496374	Bakhshi *et al.* (2015a, 2018)
Cer. conyzae-canadensis	CCTU 1119 = CBS 135978^{T}	KJ886445	KJ885962	KJ885801	MH496207	KJ886123	MH511868	KJ886284	MH496377	Bakhshi *et al.* (2015a, 2018)

Table 4. (Continued).

Species	Isolates[1]	GenBank accession numbers[2]								References
		ITS	*actA*	*cmdA*	*gapdh*	*his3*	*rpb2*	*tef1*	*tub2*	
Cer. corchori	MUCC 585 = MUCNS 72 = MAFF 238191[ET]	JX143584	JX143096	JX142850	—	JX142604	—	JX143342	—	Groenewald *et al.* (2013)
Cer. cf. coreopsidis	CBS 132598 = CPC 10648	JX143585	JX143097	JX142851	—	JX142605	—	JX143343	—	Groenewald *et al.* (2013)
Cer. cylindracea	CCTU 1081 = CBS 138580 = IRAN 2654C[T]	KJ886449	KJ885966	KJ885805	MH496211	KJ886127	MH511872	KJ886288	MH496381	Bakhshi *et al.* (2015a, 2018)
Cer. cyperacearum	CPC 23918[T]	KT193667	—	KT193727	—	—	—	—	—	Nguanhom *et al.* (2016)
Cer. cyperina	CPC 23919[T]	KT193669	—	KT193729	—	—	—	—	—	Nguanhom *et al.* (2016)
Cer. delaireae	CBS 132595 = CPC 10455 = GV2 PPRI number: C558[T]	JX143587	JX143099	JX142853	—	JX142607	—	JX143345	—	Groenewald *et al.* (2013)
Cer. dianellicola	CBS 143453 = CPC 32597[T]	MG386075	MG674152	MG674153	—	—	—	—	—	Crous *et al.* (2017b)
Cer. dispori	CBS 132608 = CPC 10773	JX143591	JX143103	JX142857	—	JX142611	—	JX143349	—	Groenewald *et al.* (2013)
Cer. eremochloae	IMI 321201[IsoT]	HM235405	—	—	—	—	—	—	—	Crous *et al.* (2011a)
Cer. cf. erysimi	CBS 115059 = CPC 5361	JX143592	JX143104	JX142858	—	JX142612	—	JX143350	—	Groenewald *et al.* (2013)
Cer. eucommiae	CBS 131932 = CPC 10802[T]	GU269851	GU320555	—	—	—	—	GU384563	—	Crous *et al.* (2013)
Cer. euphorbiae-sieboldianae	CBS 113306[T]	JX143593	JX143105	JX142859	—	JX142613	MF951462	JX143351	—	Groenewald *et al.* (2013), Videira *et al.* (2017)
Cer. fagopyri	CBS 132623 = CPC 14541[NT]	JX143594	JX143106	JX142860	—	JX142614	MF951463	JX143352	—	Groenewald *et al.* (2013), Videira *et al.* (2017)
Cer. cf. flagellaris clade 1	CCTU 1128 = CBS 136141 = IRAN 2661C	KJ886476	KJ885993	KJ885832	MH496223	KJ886154	MH511884	KJ886315	MH496393	Bakhshi *et al.* (2015a, 2018)
	CPC 1051	AY260069	JX143121	JX142875	MH496225	JX142629	MH511886	JX143367	MH496395	Bakhshi *et al.* (2015a, 2018)
	CPC 5441	JX143611	JX143124	JX142878	MH496217	JX142632	MH511878	JX143370	MH496387	Bakhshi *et al.* (2015a, 2018)
Cer. cf. flagellaris clade 2	CCTU 1115 = CBS 136139 = IRAN 2659C	KJ886473	KJ885990	KJ885829	MH496232	KJ886151	MH511893	KJ886312	MH496402	Bakhshi *et al.* (2015a, 2018)
	CCTU 1223 = CBS 136154 = IRAN 2683C	KJ886512	KJ886029	KJ885868	MH496236	KJ886190	MH511897	KJ886351	MH496406	Bakhshi *et al.* (2015a, 2018)
Cer. cf. flagellaris clade 3	CBS 115482 = A207 Bs+ = CPC 4410	AY260070	DQ835114	DQ835141	MH496249	DQ835168	MH511910	DQ835095	MH496419	Bakhshi *et al.* (2015a, 2018)
	CBS 143.51 = CPC 5055	JX143607	JX143119	JX142873	MH496246	JX142627	MH511907	JX143365	MH496416	Bakhshi *et al.* (2015a, 2018)
	CCTU 1140 = CBS 136143 = IRAN 2666C	KJ886481	KJ885998	KJ885837	MH496248	KJ886159	MH511909	KJ886320	MH496418	Bakhshi *et al.* (2015a, 2018)
Cer. gamsiana	CCTU 1074 = CPC 24909[T]	KJ886426	KJ885943	KJ885782	MH496276	KJ886104	MH511937	KJ886265	MH496446	Bakhshi *et al.* (2015a, 2018)
Cer. glycinicola	CPC 23911[T]	KT193670	—	KT193730	—	—	—	—	—	Nguanhom *et al.* (2016)
Cer. gomphrenigena	CBS 144613 = CPC 32470[T]	MK442573	—	MK442650	—	MK442658	—	MK442690	MK442728	Crous *et al.* (2019b)
Cer. cf. gossypii	CCTU 1070 = CBS 136137	KJ886467	KJ885984	KJ885823	MH496282	KJ886145	MH511943	KJ886306	MH496452	Bakhshi *et al.* (2015a, 2018)
Cer. cf. helianthicola	MUCC 716	JX143615	JX143128	JX142882	—	JX142636	—	JX143374	—	Groenewald *et al.* (2013)
Cer. cf. ipomoae	CBS 132639 = CPC 10102	JX143616	JX143129	JX142883	—	JX142637	—	JX143375	—	Groenewald *et al.* (2013)
Cer. iranica	CCTU 1137 = CBS 136124[T]	KJ886513	KJ886030	KJ885869	MH496285	KJ886191	MH511946	KJ886352	MH496455	Bakhshi *et al.* (2015a, 2018)
Cer. ischaemi	BRIP 56010[T]	KM055428	—	—	—	—	—	—	—	Shivas *et al.* (2015)
Cer. janseana	CBS 145.37; IMI 303642	KF251314	—	—	—	—	MF951464	—	—	Videira *et al.* (2017)
Cer. jatrophiphila	CMHUB 21035 Strain 2225	KJ186790	—	KJ186792	—	KJ186794	—	—	—	Dianese *et al.* (2014)
	CMHUB 21035 Strain 2229	KJ186791	—	KJ186793	—	KJ186795	—	—	—	Dianese *et al.* (2014)

Table 4. (Continued).

Species	Isolates[1]	GenBank accession numbers[2]								References
		ITS	*actA*	*cmdA*	*gapdh*	*his3*	*rpb2*	*tef1*	*tub2*	
Cer. kikuchii	CBS 128.27 = CPC 5068^{T}	DQ835070	DQ835107	DQ835134	—	DQ835161	—	DQ835088	—	Groenewald *et al.* (2013)
Cer. lactucae-sativae	CBS 132604 = CPC 10728	JX143621	JX143134	JX142888	—	JX142642	—	JX143380	—	Groenewald *et al.* (2013)
Cer. cf. malloti	MUCC 575 = MUCNS 582 = MAFF 237872	JX143625	JX143138	JX142892	—	JX142646	—	JX143384	—	Groenewald *et al.* (2013)
Cer. mercurialis	CBS 550.71^{ET}	JX143628	JX143141	JX142895	—	JX142649	—	JX143387	—	Groenewald *et al.* (2013)
Cer. cf. mikaniicola	CPC 20741	KT193693	—	KT193753	—	—	—	—	—	Nguanhom *et al.* (2016)
Cer. cf. modiolae	CPC 5115	JX143630	JX143143	JX142897	—	JX142651	—	JX143389	—	Groenewald *et al.* (2013)
Cer. musigena	CPC 24809^{T}	KT193698	—	KT193758	—	—	—	—	—	Nguanhom *et al.* (2016)
Cer. cf. nicotianae	CBS 132632 = CPC 15918	JX143631	JX143144	JX142898	—	JX142652	—	JX143390	—	Groenewald *et al.* (2013)
Cer. olivascens	CBS 253.67 = IMI 124975 = CPC 5085^{T}	JX143632	JX143145	JX142899	—	JX142653	—	JX143391	—	Groenewald *et al.* (2013)
Cer. cf. physalidis	CBS 765.79	JX143633	JX143146	JX142900	—	JX142654	—	JX143392	—	Groenewald *et al.* (2013)
Cer. pileicola	CBS 132607 = CPC 10749^{T}	JX143634	JX143147	JX142901	—	JX142655	—	JX143393	—	Groenewald *et al.* (2013)
Cer. plantaginis	CBS 252.67 = CPC 5084^{ET}	DQ233318	DQ233368	DQ233394	MH496291	DQ233420	—	DQ233342	MH496461	Groenewald *et al.* (2013), Bakhshi *et al.* (2018)
	CCTU 1082 = CBS 138728	KJ886402	KJ885919	KJ885758	MH496286	KJ886080	MH511947	KJ886241	MH496456	Bakhshi *et al.* (2015a, 2018)
Cer. polygonacea	CBS 132614 = CPC 11318	JX143637	JX143150	JX142904	—	JX142658	—	JX143396	—	Groenewald *et al.* (2013)
Cer. pseudochenopodii	CCTU 1038 = CBS 136022 = IRAN 2649C^{T}	KJ886516	KJ886033	KJ885872	MH496294	KJ886194	MH511954	KJ886355	MH496464	Bakhshi *et al.* (2015a, 2018)
Cer. punctiformis	CBS 132626 = CPC 14606	JX143638	JX143151	JX142905	—	JX142659	—	JX143397	—	Groenewald *et al.* (2013)
Cer. rautensis	CBS 555.71 = IMI 161117 = CPC 5082^{ET}	JX143550	JX143058	JX142812	MK531772	JX142566	—	JX143304	MK531770	Groenewald *et al.* (2013), Bakhshi (2019)
	CCTU 1190 = CBS 136134	KJ886422	KJ885939	KJ885778	MK531771	KJ886100	MK564169	KJ886261	MK531769	Bakhshi *et al.* (2015a), Bakhshi (2019)
Cerc. cf. resedae	CBS 257.67 = CPC 5057	DQ233319	DQ233369	DQ233395	—	DQ233421	—	DQ233343	—	Groenewald *et al.* (2013)
Cer. cf. richardiicola	CBS 132627 = CPC 14680	JX143640	JX143153	JX142907	—	JX142661	—	JX143399	—	Groenewald *et al.* (2013)
	CCTU 1004	KJ886519	KJ886036	KJ885875	MH496295	KJ886197	MH511955	KJ886358	MH496465	Bakhshi *et al.* (2015a, 2018)
Cer. ricinella	CBS 132605 = CPC 10734	JX143646	JX143159	JX142913	—	JX142667	—	JX143405	—	Groenewald *et al.* (2013)
Cer. rodmanii	CBS 113129 = RC397 = WH9-BR	DQ835081	DQ835127	DQ835154	—	DQ835181	—	AF146143	—	Groenewald *et al.* (2013)
Cer. rumicis	CCTU 1129 = IRAN 2662C	KJ886522	KJ886039	KJ885878	MH496297	KJ886200	MH511957	KJ886361	MH496467	Bakhshi *et al.* (2015a, 2018)
	CPC 5439	JX143648	JX143161	JX142915	—	JX142669	—	JX143407	—	Groenewald *et al.* (2013)
Cer. samambaiae	CPC 24673 = COAD 1090^{T}	KT037508	KT037590	KT037457	—	—	—	KT037468	—	Guatimosim *et al.* (2016)
Cer. senecionis-walkeri	CBS 132636 = CPC 19196	JX143649	JX143162	JX142916	—	JX142670	MF951466	JX143408	—	Groenewald *et al.* (2013), Videira *et al.* (2017)
Cer. cf. sigesbeckiae	CBS 132601 = CPC 10664	JX143650	JX143163	JX142917	—	JX142671	—	JX143409	—	Groenewald *et al.* (2013)
Cer. sojina	CBS 132615 = CPC 11353^{T}	JX143659	JX143173	JX142927	—	JX142681	—	JX143419	KX288419	Groenewald *et al.* (2013), Videira *et al.* (2017)
	CCTU 1043 = CBS 136038	KJ886523	KJ886040	KJ885879	MH496299	KJ886201	MH511959	KJ886362	MH496469	Bakhshi *et al.* (2015a, 2018)
Cer. solani-betacei	COAD 2293^{T}	MH223464	MH445457	MH428037	—	—	—	—	—	Crous *et al.* (2018a)
Cer. sorghicola	CCTU 1173 = CBS 136448 = IRAN 2672C^{T}	KJ886525	KJ886042	KJ885881	MH496301	KJ886203	MH511961	KJ886364	MH496471	Bakhshi *et al.* (2015a, 2018)
Cercospora sp. A	CBS 132631 = CPC 15872	JX143675	JX143189	JX142943	—	JX142697	—	JX143435	—	Groenewald *et al.* (2013)
Cercospora sp. B	CBS 132602 = CPC 10687	JX143676	JX143190	JX142944	—	JX142698	—	JX143436	—	Groenewald *et al.* (2013)
Cercospora sp. C	CBS 132629 = CPC 15841	JX143677	JX143191	JX142945	—	JX142699	—	JX143437	—	Groenewald *et al.* (2013)

Table 4. (Continued).

Species	Isolates[1]	GenBank accession numbers[2]								References
		ITS	*actA*	*cmdA*	*gapdh*	*his3*	*rpb2*	*tef1*	*tub2*	
Cercospora sp. D	CBS 132630 = CPC 15856	JX143678	JX143192	JX142946	—	JX142700	—	JX143438	—	Groenewald *et al.* (2013)
Cercospora sp. E	CBS 132628 = CPC 15632	JX143679	JX143193	JX142947	—	JX142701	—	JX143439	—	Groenewald *et al.* (2013)
Cercospora sp. F	CBS 132618 = CPC 12062	DQ185071	DQ185095	DQ185107	—	DQ185119	—	DQ185083	—	Groenewald *et al.* (2013)
Cercospora sp. G clade 1	CCTU 1015 = CBS 136024 = IRAN 2645C	KJ886528	KJ886045	KJ885884	MH496303	KJ886206	MH511963	KJ886367	MH496473	Bakhshi *et al.* (2015a, 2018)
	CPC 5438	JX143682	JX143196	JX142950	MH496304	JX142704	—	JX143442	MH496474	Groenewald *et al.* (2013), Bakhshi *et al.* (2018)
Cercospora sp. G clade 2	CBS 115518 = CPC 5360	JX143681	JX143195	JX142949	MH496310	JX142703	—	JX143441	MH496480	Groenewald *et al.* (2013), Bakhshi *et al.* (2018)
	CCTU 1030 = CBS 136026	KJ886530	KJ886047	KJ885886	MH496311	KJ886208	MH511969	KJ886369	MH496481	Bakhshi *et al.* (2015a, 2018)
Cercospora sp. H	CBS 115205 = CPC 5116	JX143683	JX143197	JX142951	—	JX142705	—	JX143443	—	Groenewald *et al.* (2013)
Cercospora sp. I	CBS 114815 = CPC 5364	JX143685	JX143199	JX142953	—	JX142707	—	JX143445	—	Groenewald *et al.* (2013)
Cercospora sp. J	MUCC 541	JX143695	JX143209	JX142963	—	JX142717	—	JX143455	—	Groenewald *et al.* (2013)
Cercospora sp. K	CBS 132603 = CPC 10719	JX143696	JX143210	JX142964	—	JX142718	—	JX143456	—	Groenewald *et al.* (2013)
Cercospora sp. L	CBS 115477 = CPC 5114	JX143699	JX143213	JX142967	—	JX142721	—	JX143459	—	Groenewald *et al.* (2013)
Cercospora sp. M	CBS 132596 = CPC 10553	JX143700	AY752203	AY752234	—	AY752265	—	AY752175	—	Groenewald *et al.* (2013)
Cercospora sp. N	CBS 132619 = CPC 12684	EU514224	JX143214	JX142968	—	JX142722	—	JX143460	—	Groenewald *et al.* (2013)
Cercospora sp. O	CBS 132635 = CPC 18636	JX143701	JX143215	JX142969	—	JX142723	—	JX143461	—	Groenewald *et al.* (2013)
Cercospora sp. P	CBS 116365 = CPC 10526	AY752141	AY752204	AY752235	—	AY752266	—	AY752176	—	Groenewald *et al.* (2013)
Cercospora sp. Q	CBS 113997 = CPC 5325	JX143717	JX143230	JX142984	JX142521	JX142738	—	JX143476	JX142478	Groenewald *et al.* (2013)
	CPC 10550	AY752139	AY752200	AY752231	JX142533	AY752262	—	AY752172	JX142484	Groenewald *et al.* (2013)
Cercospora sp. R	CBS 114644	JX143732	JX143245	JX142999	—	JX142753	—	JX143491	—	Groenewald *et al.* (2013)
Cercospora sp. S	CBS 132599 = CPC 10656	JX143733	JX143246	JX143000	—	JX142754	—	JX143492	—	Groenewald *et al.* (2013)
Cercospora sp. T	CCTU 1148 = CBS 136125	KJ886541	KJ886058	KJ885897	MH496318	KJ886219	MH511976	KJ886380	MH496488	Bakhshi *et al.* (2015a, 2018)
Cer. tezpurensis	CS2012^{T}	KC351743	KC355808	KC513745	—	KC355807	—	KC513746	—	Meghvansi *et al.* (2013)
Cer. uwebrauniana	CCTU 1200 = CBS 138581^{T}	KJ886408	KJ885925	KJ885764	MH496319	KJ886086	MH511977	KJ886247	MH496489	Bakhshi *et al.* (2015a, 2018)
Cer. vignigena	CBS 132611 = CPC 10812^{T}	JX143734	JX143247	JX143001	—	JX142755	—	JX143493	—	Groenewald *et al.* (2013)
Cer. violae	CBS 251.67 = CPC 5079^{ET}	JX143737	JX143250	JX143004	MH496322	JX142758	—	JX143496	MH496492	Groenewald *et al.* (2013), Bakhshi *et al.* (2018)
	CCTU 1025 = IRAN 2646C	KJ886543	KJ886060	KJ885899	MH496321	KJ886221	MH511979	KJ886382	MH496491	Bakhshi *et al.* (2015a, 2018)
Cer. zeae-maydis	CBS 117757 = JV-WI-02 = A360^{ET}	DQ185074	DQ185098	DQ185110	—	DQ185122	—	DQ185086	—	Groenewald *et al.* (2013)
Cer. zebrina	CBS 108.22 = CPC 5091	JX143744	JX143257	JX143011	MH496324	JX142765	—	JX143503	MH496494	Groenewald *et al.* (2013), Bakhshi *et al.* (2018)
	CCTU 1239 = CBS 135977	KJ886551	KJ886068	KJ885907	MH496334	KJ886229	MH511987	KJ886390	MH496504	Bakhshi *et al.* (2015a, 2018)
Cer. zeina	CBS 118820 = CPC 11995^{T}	DQ185081	DQ185105	DQ185117	—	DQ185129	MF951469	DQ185093	—	Groenewald *et al.* (2013)
Cer. cf. zinniae	CBS 132676 = CPC 15075	JX143757	JX143273	JX143027	—	JX142781	—	JX143519	—	Groenewald *et al.* (2013)
	CCTU 1003	KJ886552	KJ886069	KJ885908	MH496335	KJ886230	MH511988	KJ886391	MH496505	Bakhshi *et al.* (2015a, 2018)

[1] BRIP: Queensland Plant Pathology Herbarium, Brisbane, Australia; CBS: Westerdijk Fungal Biodiversity Institute, Utrecht, the Netherlands; CCTU: Culture Collection of Tabriz University, Tabriz, Iran; COAD: Coleção Octávio Almeida Drummond, Universidade Ferderal de Viçosa, Viçosa, Brazil; CPC: Culture collection of Pedro Crous, housed at CBS; IMI: International Mycological Institute, Kew, UK; IRAN: Iranian Fungal Culture Collection, Iranian Research Institute of Plant Protection, Tehran, Iran; MAFF: Ministry of Agriculture, Forestry and Fisheries, Tsukuba, Ibaraki, Japan; MUCC: Murdoch University, Perth, Western Australia. $^{T, ET, IsoT}$ and ^{NT} indicate ex-type, ex-epitype, ex-isotype and ex-neotype strains, respectively.

[2] ITS: internal transcribed spacers and intervening 5.8S nrDNA; *actA*: partial actin gene; *cmdA*: partial calmodulin gene; *gapdh*: partial glyceraldehyde-3-phosphate dehydrogenase gene; *his3*: partial histone H3 gene; *rpb2*: partial RNA polymerase II second largest subunit gene; *tef1*: partial translation elongation factor 1-α gene; *tub2*: partial beta-tubulin gene.

Not sporulating well in culture. The descriptions are based on fungal structures *in planta*.

Distribution: Worldwide, but mostly in humid, tropical and subtropical climates.

Hosts: A wide range of woody and herbaceous plants including agricultural crops, cereals, vegetables, ornamentals, oil crops, forest trees and weeds of different plant families (Crous & Braun 2003, Groenewald *et al*. 2013, Bakhshi *et al.* 2018).

Disease symptoms: Often associated with leaf spots, but also causing necrotic lesions on flowers, fruits, bracts, seeds and pedicels.

Notes: Species of *Cercospora* are morphologically similar and hard to differentiate from one another. The most relevant differential morphological traits are the presence or absence of external mycelium, conidiophore morphology and conidial shape and size, but they are not always reliable as too much intraspecific variation exists (Crous & Braun 2003). Chupp (1954) provided the first monograph of the genus and stated that species of *Cercospora* are commonly host-specific and each plant host genus or family would have its own *Cercospora* species. At the moment, the connection between a *Cercospora* isolate and the host plant from which it was isolated, is still a major factor in the taxonomic description of most *Cercospora* species. Crous & Braun (2003) reassessed Chupp's work and recognised 659 species as true species of *Cercospora* using morphological criteria, with a further 281 species names reduced to synonyms under *Cer. apii s. lat.* since they were morphologically not or barely distinguishable from *Cer. apii s. str.* on celery. In recent years, Braun *et al.* (2013, 2014, 2015a, b, 2016) published a series of papers to produce a modern monograph of *Cercospora* and allied genera in a stepwise approach at plant family level based on morphological features and host data. However, as there are only few distinctive morphological characters useful for species discrimination and since specialised as well as plurivorous species are involved, molecular data are essential for accurate identification of species within this genus.

The ITS barcode has limited discriminatory power to distinguish *Cercospora* species (Stewart *et al.* 1999, Crous *et al.* 2000, 2009a, b, Goodwin *et al.* 2001), making multi-locus sequence analysis with several protein-coding loci essential for accurate species identification in this genus. Groenewald *et al.* (2013) provided a backbone phylogeny for *Cercospora* spp. based on a multi-locus DNA sequence dataset of five genomic loci (ITS, *actA*, *cmdA*, *his3* and *tef1*) of a large sampling of species. Since then, numerous molecular examinations of *Cercospora* species have been carried out based on multi-gene approaches (Dianese *et al.* 2014, Bakhshi *et al.* 2015a, Shivas *et al.* 2015, Soares *et al.* 2015, Albu *et al.* 2016, Guatimosim *et al.* 2016, Nguanhom *et al.* 2016, Guillin *et al.* 2017). Bakhshi *et al.* (2018) applied three more potential candidate gene regions including *gapdh*, *rpb2*, and *tub2* to perform an eight-gene phylogeny (ITS, *actA*, *cmdA*, *gapdh*, *his3*, *rpb2*, *tef1* and *tub2*) for *Cercospora* species. With the classifications presented by Groenewald *et al.* (2013) and Bakhshi *et al.* (2018), none of the genes analysed provided an effective barcode on its own across the entire genus. However, *gapdh* emerged as a strong candidate for improved species delimitation in *Cercospora* and provides better insight, especially into species complexes (Bakhshi *et al.* 2018, Bakhshi 2019). However, the *gapdh* marker has not yet been applied for the phylogeny of most of the reference taxa studied by Groenewald *et al.* (2013).

Based on molecular studies done in recent years, we have several issues in *Cercospora* taxonomy: 1. *Cercospora* collections on certain hosts with agreeing morphology found in different geographical regions do often not belong to a single species, thus most of the clades treated as "*cf*." based on their morphological similarities to existing species and pending comparison of those species with DNA sequence data of (epi-)type material from the original country and host; 2. Most of the *Cercospora* clades studied, have uncertain identity (*Cercospora* sp. A–T) (Groenewald *et al.* 2013, Bakhshi *et al.* 2015a), and it was not possible to unequivocally assign a species name since these clades contained isolates from multiple hosts and/or countries and the same hosts occurred in multiple clades, or the host information was not available. The speciation within *Cercospora s. str.*, above all is more complicated than previously presumed and beside specialised species, the genus includes many complex species with a wide host range, often with overlapping host ranges between different taxa. Therefore, typification and epitypification of the species within this genus is essential to stabilise the names of different taxa, and to provide connections between specimens assessed through morphological and molecular methods.

At the generic level, the genus *Cercospora* is well distinguished from other cercosporoid genera by the smooth hyphae (*vs Stenella s. lat.*), conspicuous, thickened and darkened conidiogenous loci and conidial hila (*vs Pseudocercospora s. lat.*) and hyaline or subhyaline conidia (*vs Passalora s. lat.*) (Crous & Braun 2003). However, the monophyly of *Cercospora s. str.* was rejected by Bakhshi *et al.* (2015b) who introduced the genus *Neocercospora* with cercospora-like morphology, clustering in a clade in *Mycosphaerellaceae* apart from *Cercospora s. str.*, suggesting that also at generic level, molecular identification is practically mandatory for the classification of cercospora-like taxa.

Cercospora is a very successful pathogenic genus that causes disease on a great number of agricultural crops, including cereals, vegetables, ornamentals, oil crops and forest trees, but is rarely saprobic or a secondary invader (Crous & Braun 2003, Groenewald *et al.* 2013). Species of the genus are commonly described causing leaf spots, but are also associated with necrotic lesions on flowers, fruits, seeds, bracts and pedicels of many cultivated and native plants in a range of climates worldwide (Crous & Braun 2003, Groenewald *et al.* 2013). Some species are considered potential biocontrol agents of weeds, including *Cer. caricis* on *Cyperus rotundus* and *Cer. rodmanii* on *Eichhornia crassipes* (Inglis *et al.* 2001, Tessmann *et al.* 2001, Praveena & Naseema 2004). Examples of the most relevant plant pathogens are *Cer. apii* on celery (Groenewald *et al.* 2006a), *Cer. beticola* on sugar beet (Groenewald *et al.* 2008), *Cer. canescens* on beans (Chand *et al.* 2015, Duangsong *et al.* 2016), *Cer. carotae* on carrots (Kushalappa *et al.* 1989), *Cer. kikuchii* on soybean (Sautua *et al.* 2019), *Cer. zeae-maydis* and *Cer. zeina* on maize (Crous *et al.* 2006a) and *Cer. zonata* on faba beans (Kimber 2011). Some of these pathogens produce a photo-activated perylinquinone toxin called cercosporin, which helps the fungus to obtain its nourishment by killing host cells (Daub 1982, Chen 2007, Santos Rezende *et al.* 2020). Elucidation of the draft genome sequence of *Cercospora* species, especially the plant pathogenic taxa, will provide insights to better understand the genes involved in various biosynthesis pathways including cercosporin (secondary metabolites) production, pathogenicity, virulence and other important molecular functions. In addition, it will enable the proper classification of *Cercospora* spp.

References: Ellis 1971, Chupp 1954, Crous & Braun 2003, Braun *et al.* 2013, 2014, 2015a, b, 2016 (morphology and host range); Groenewald *et al.* 2006b, 2008, Soares *et al.* 2015, Albu *et al.* 2016, Vaghefi *et al.* 2018, Santos Rezende *et al.* 2020 (pathogenicity);

Groenewald *et al.* 2013, Bakhshi *et al.* 2015a, 2018, Guatimosim *et al.* 2016, Nguanhom *et al.* 2016 (morphology and phylogeny).

Cercospora alyssopsidis M. Bakhshi, Zare & Crous, ***sp. nov.*** MycoBank MB 835420. Fig. 15.

Etymology: Name derived from the host genus, *Alyssopsis*.

Leaf spots amphigenous, circular, 3–6 mm, grey with definite border and yellow halo. *Mycelium* internal. *Caespituli* amphigenous, brown. *Conidiophores* aggregated in moderately dense fascicles, arising from a moderately developed, brown stroma, to 55 µm diam; conidiophores brown, 1–5-septate, straight to geniculate-sinuous due to sympodial proliferation, simple, sometimes branched, uniform in width, sometimes constricted at the proliferating point, (40–)130–210(–240) × 3–5 µm. *Conidiogenous cells* integrated, terminal or lateral, pale brown to brown, proliferating sympodially, 15–30 × 3–5 µm, multi-local; loci distinctly thickened, darkened and somewhat refractive, apical, lateral or formed on shoulders caused by geniculation, 1.5–3 µm diam. *Conidia* solitary, obclavate-cylindrical, straight to slightly curved, hyaline, (25–)35–70(–105) × 3–6 µm, 3–10-septate, with obtuse to subobtuse apices and subtruncate or obconically truncate bases; hila thickened, darkened, refractive, 1.5–3 µm diam.

Culture characteristics: Colonies on MEA slow-growing, reaching 18 mm diam after 20 d at 25 °C in the dark; raised, folded, with smooth, even margins and sparse aerial mycelium, radially striated, surface grey olivaceous, reverse iron grey. Colonies on PDA reaching 27 mm diam after 20 d at 25 °C, flat, with smooth, even margins and moderate aerial mycelium, surface grey olivaceous, reverse iron grey.

Typus: **Iran**, Golestan Province, Gorgan, 36°50'26.22"N, 54°27'24.98"E, 150 m a.s.l., on leaves of *Alyssopsis mollis* (*Brassicaceae*), 1 Nov. 2017, M. Bakhshi (**holotype** IRAN 17628F, culture ex-type IRAN 3739C).

Additional material examined: **Iran**, Golestan Province, Gorgan, on *Alyssopsis mollis*, Oct. 2018, M. Bakhshi (IRAN 17629F, culture IRAN 3740C).

Notes: Based on the results of the combined phylogenetic tree, two isolates obtained from *Alyssopsis mollis* cluster in a distinct well-supported clade (Fig. 14). No *Cercospora* species is presently known from *Alyssopsis* (Crous & Braun 2003, Farr & Rossman 2022). As *Arabis secunda*, *Nasturtium sagittatum* and *Sisymbrium molle* are synonyms of *Alyssopsis mollis*, we also checked the *Cercospora* species reported on these genera. *Cercospora armoraciae*, *Cer. cruciferarum, Cer. kuznetzoviana* and *Cer. nasturtii* are species of *Cercospora* that have been described from these plant genera (Crous & Braun 2003, Farr & Rossman 2022). *Cercospora alyssopsidis* is phylogenetically distinct from *Cer. armoraciae*. Among the other candidate species, no type material could be located for *Cer. kuznetzoviana*, but possibly this species is allied to *Pseudocercosporella capsellae* (Crous & Braun 2003). *Cercospora cruciferarum* is in the *Cer. apii s. lat.* complex (Crous & Braun 2003) and causes different leaf spots (0.5–2 mm diam, white centre, pale to dark brown border). *Cercospora nasturtii* also differs morphologically from this species by the shorter and somewhat wider conidiophores (20–100 × 4–6.5 µm) and indistinctly septate conidia (Hsieh & Goh 1990). *Cercospora alyssopsidis* is the first *Cercospora* species reported until now on the host genus *Alyssopsis* and appears to be specific to *Alyssopsis mollis*.

Genome sequenced strain: *Cercospora apii*. **Germany**, Heilbron, Landwirtschaftsamt, on *Apium graveolens* (*Apiaceae*), 10 Aug. 2004, K. Schrameyer, culture ex-epitype CBS 116455 = CPC 11556. This Whole Genome Shutgun project has been deposited at GenBank under the accession JALRMD000000000 (BioProject: PRJNA827019, BioSample: SAMN27594412; present study).

Authors: M. Bakhshi & R. Zare

Fig. 15. *Cercospora alyssopsidis* (ex-type IRAN 3739C). **A.** Leaf spots. **B–D.** Fasciculate conidiophores. **E–I.** Conidia. Scale bars = 10 µm.

Coleophoma Höhn., Sber. Akad. Wiss. Wien, Math,-naturw. Kl., Abt. I, 116: 637. 1907. Fig 16.
Synonyms: *Rhabdostromellina* Höhn., Ann. Mycol. 15: 303. 1917.
Bactropycnis Höhn., Hedwigia 62: 65. 1920.
Xenodomus Petr., in Sydow & Petrak, Ann. Mycol. 20: 206. 1922.
Parafabraea Chen Chen *et al*., Fungal Biol. 120: 1317. 2016.

Classification: *Leotiomycetes*, *Leotiomycetidae*, *Helotiales*, *Dermateaceae*.

Type species: *Coleophoma crateriformis* (Durieu & Mont.) Höhn., basionym: *Ascospora crateriformis* Durieu & Mont. Holotype: FH 00304449, ex-type or reference living culture not available.

DNA barcode (genus): ITS.

DNA barcodes (species): *tef1* and *tub2*. Table 5. Fig. 17.

Mycelium immersed, septate, branched, hyaline to pale brown hyphae. *Ascomata* apothecial, short-stalked, pale to dark brown, sessile to sub-sessile, gregarious or confluent, semi-immersed, cluster on basal stroma. *Disc* pale brown, turbinate. Seta-like structures surrounding apothecia, pale brown, rigid, septate, straight or curved, cylindrical, slightly enlarged at truncate apex. *Stroma* sub-immersed, composed of irregular, pale to brown cells. *Hamathecium* composed of hyaline to pale brown, slender, cylindrical, septate, filamentous paraphyses. *Asci* hyaline to pale brown, clavate to cylindrical-clavate, inoperculate, short-pedicellate, apex rounded, base truncate, 8-spored. *Ascospores* hyaline, fusoid to ellipsoid, thin-walled, rounded ends, guttulate, aseptate, straight or slightly curved. *Conidiomata* pycnidial, black, immersed, globose or flattened at base, with single, non-papillate ostiole; *conidiomata wall* multi-layer, brown, comprised of *textura angularis*, with inner layer thin, pale brown and outer layer thick, brown to dark brown. *Paraphyses* hyaline, cylindrical to long clavate, septate at base, intermingled among conidiophores. *Conidiophores* smooth, thin-walled, septate, branched, hyaline at apex, pale brown at base, formed from inner pycnidial wall, confined to the base or in short chains. *Conidiogenous cells* determinate, phialidic, integrated and subcylindrical, or discrete and ampulliform to lageniform, hyaline, determinate, smooth, with prominent periclinal thickening, and collarette minute. *Conidia* hyaline, straight, cylindrical, smooth, aseptate, guttulate, apex obtuse, acute at base.

Cultural characteristics: Colonies erumpent, flat, spreading with sparse aerial mycelium, feathery margin and fast growing on OA and PDA as compared to MEA. Colonies on OA, PDA and MEA are olivaceous grey, smoke grey with patches of honey and iron grey with patches of olivaceous grey respectively.

Optimal media and cultivation conditions: OA, PDA or MEA at 25 °C under continuous nuv-light to induce sporulation.

Distribution: Worldwide.

Hosts: Pathogens, saprophytes or endophytes on a variety of hosts such as *Amelanchier lamarckii* (*Rosaceae*), *Camellia japonica* (*Theaceae*), *Coptosperma littorale* (*Rubiaceae*), *Eucalyptus caliginosa*, *E. globulus*, *E. piperita*, *E. gummifera* (*Myrtaceae*), *Empetrum nigrum*, *Erica cinerea*, *Rhododendron* sp. (*Ericaceae*), *Helleborus* sp. (*Ranunculaceae*), *Hedera helix* (*Araliaceae*), *Hypericum* sp. (*Hypericaceae*), *Liriodendron tulipifera* (*Magnoliaceae*), *Protea caffra* (*Proteaceae*) and *Thuja plicata* (*Cupressaceae*).

Disease symptoms: Leaf spots or leaf blotch.

Notes: The genus *Coleophoma* typified by *Co. crateriformis* was established by von Höhnel (1907). This genus was previously listed as *incertae sedis* in *Pezizomycotina* in MycoBank and Index Fungorum, with confusing taxonomy. Crous & Groenewald (2016) confirmed it as a polyphyletic genus based on LSU/ITS sequence data and provided a backbone tree for *Coleophoma* employing ITS, *tef1* and *tub2* sequence data. Moreover, they established the sexual-asexual connection between *Coleophoma* and *Parafabraea*, thus reduced *Parafabraea* as synonymy under *Coleophoma*. Presently,

Table 5. DNA barcodes of accepted *Coleophoma* spp.

Species	Isolates[1]	GenBank accession numbers[2]			References
		ITS	*tef1*	*tub2*	
Coleophoma caliginosa	CBS 124806^T	GU973505	—	—	Cheewangkoon *et al.* (2010)
Co. camelliae	CBS 101376^T	KU728481	KU728558	KU728597	Crous & Groenewald (2016)
Co. coptospermatis	CPC 19864^T	KU728483	KU728560	KU728599	Crous & Groenewald (2016)
Co. cylindrospora	CBS 449.70	KJ663834	KU728561	KU728600	Crous *et al*. (2014b), Crous & Groenewald (2016)
	CBS 505.71	KU728485	KU728563	KU728602	Crous & Groenewald (2016)
Co. ericicola	CBS 301.72^T	KU728488	KU728566	KU728605	Crous & Groenewald (2016)
Co. eucalypticola	CBS 124810^T	GQ303279	—	—	Cheewangkoon *et al.* (2009)
Co. eucalyptorum	CBS 131314^T	JQ044430	KU728567	KU728606	Crous *et al*. (2011b), Crous & Groenewald (2016)
Co. paracylindrospora	CBS 109074^T	KU728491	KU728570	KU728609	Crous & Groenewald (2016)
Co. parafusiformis	CBS 132692^T	KU728494	KU728573	KU728612	Crous & Groenewald (2016)
Co. proteae	CBS 132532^T	JX069866	KU728574	KU728613	Crous *et al*. (2012b), Crous & Groenewald (2016)
Co. xanthosiae	CBS 142070^T	KY173396	—	KY173598	Crous *et al*. (2016)

[1] CBS: Westerdijk Fungal Biodiversity Institute, Utrecht, the Netherlands; CPC: Culture collection of Pedro Crous housed at CBS. ^{T} indicates ex-type strain.

[2] ITS: internal transcribed spacers and intervening 5.8S nrDNA; *tef1*: partial translation elongation factor 1-α gene; *tub2*: partial β-tubulin gene.

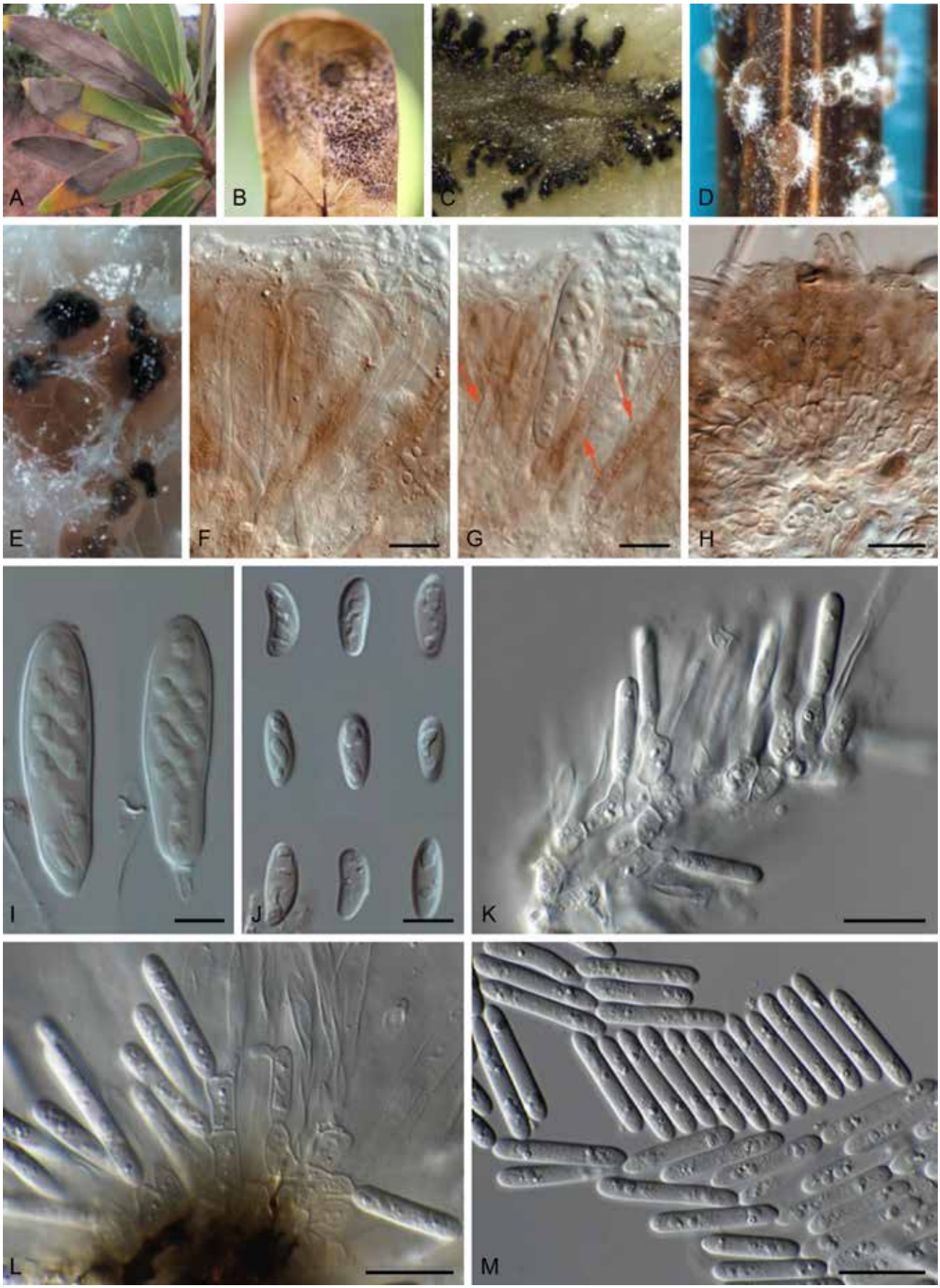

Fig. 16. *Coleophoma* spp. **A, B.** Disease symptoms. **A.** *Coleophoma proteae* (ex-type CBS 132532) on *Protea caffra*. **B.** *Coleophoma coptospermatis* (ex-type CPC 19864) on *Coptosperma littorale*. **C.** Sporulation on OA of *Coleophoma parafusiformis* (CBS 129169). **D, F–J.** Sexual morph (*Coleophoma eucalypticola* = *Neofabraea eucalypti*, ex-type CBS 124810). **D.** Ascomata on pine needle agar. **F.** Paraphyses. **G, H.** Paraphyses, asci and setae-like structures (arrows indicate setae-like structure). **I.** Asci. **J.** Ascospores. **E, K–M.** Asexual morph. **E.** Pycnidia of *Coleophoma eucalypticola* (ex-type CBS 124810) on OA. **K.** Conidiogenous cells and paraphyses of *Coleophoma eucalyptorum* (CPC 19865). **L.** Conidiogenous cells of *Coleophoma coptospermatis* (ex-type CPC 19864). **M.** Conidia of *Coleophoma paracylindrospora* (ex-type CBS 109074). Scale bars = 10 µm. Picture A taken from Crous *et al.* (2012b); B, C, K–M from Crous & Groenewald (2016); D–J from Cheewangkoon *et al.* (2009).

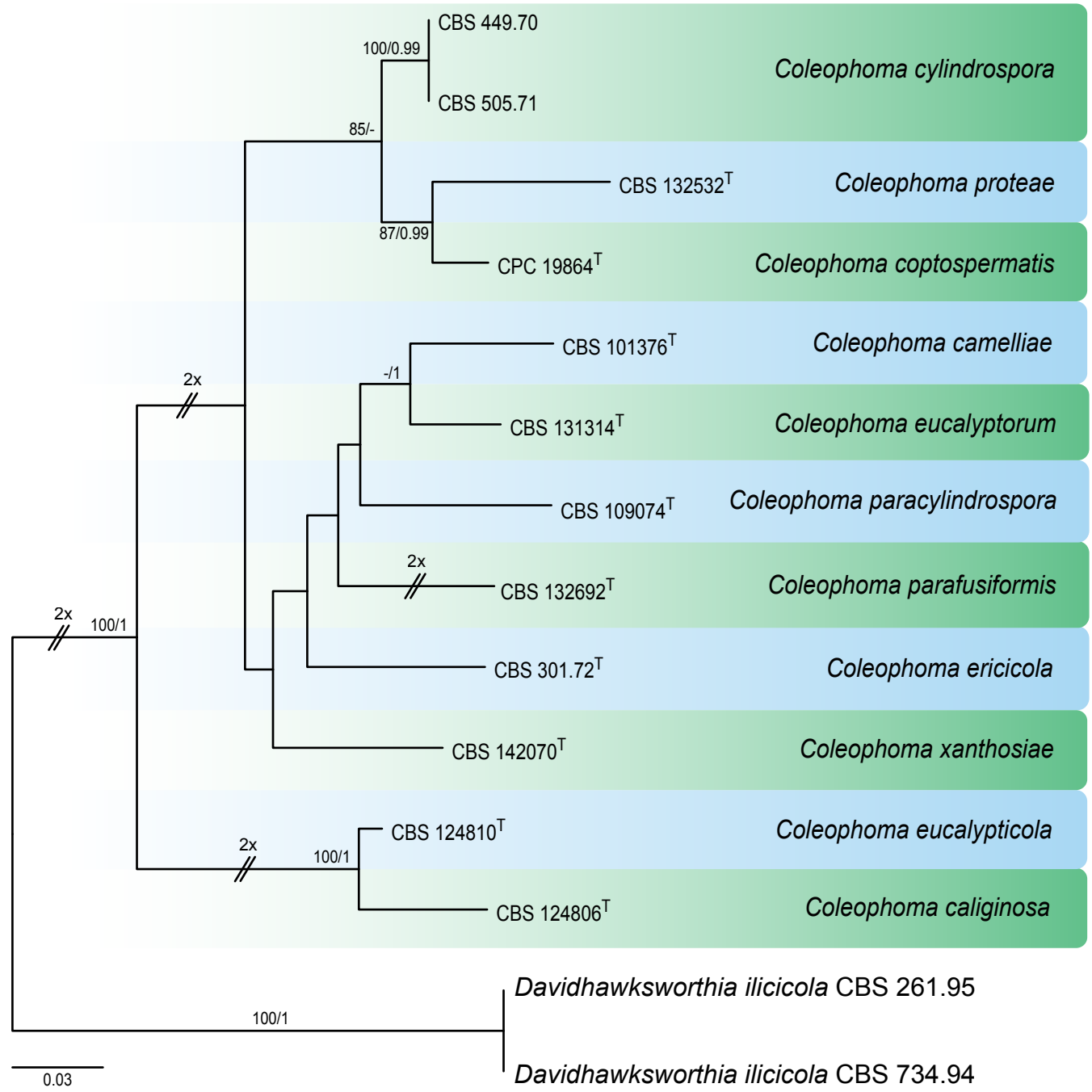

Fig. 17. RAxML phylogram constructed from ITS (528 bp), *tef1* (423 bp) and *tub2* (280 bp) sequences of all accepted species of *Coleophoma*. Maximum likelihood bootstrap support values (> 70 %) and Bayesian posterior probability scores (> 0.95) are indicated on the branches. The phylogenetic tree was rooted to *Davidhawksworthia ilicicola* CBS 261.95 and CBS 734.94. GenBank accession numbers are indicated in Table 5. ^{T} indicates ex-type strain. TreeBASE; S26189.

Coleophoma is placed in *Dermateaceae* (Johnston *et al.* 2019) but there is no available culture of its type species *Co. crateriformis*. Species of *Coleophoma* are characterised by pycnidial conidiomata, hyaline conidiophores intermingled with paraphyses and integrated phialidic conidiogenous cells with periclinal thickening and hyaline, smooth, straight cylindrical, guttulate conidia with obtuse ends (Sutton 1980, Crous & Groenewald 2016). This genus has been reported as saprobic or endophytic and plant pathogenic (Sutton 1980, Yuan 1996, Duan *et al.* 2007).

References: Sutton 1980, Yuan 1996, Duan *et al.* 2007 (pathogenicity); Cheewangkoon *et al.* 2009 (sexual/asexual connection); Cheewangkoon *et al.* 2009, Crous & Groenewald 2016 (morphology and phylogeny).

Genome sequenced strain: *Coleophoma eucalyptorum*. **Australia**, New South Wales, Blue Mountains, Kurrajong Heights, from leaves of *Eucalyptus piperita*, 16 Nov. 2010, B.A. Summerell, culture ex-type CBS 131314. This Whole Genome Shutgun project has been deposited at GenBank under the accession JALRME000000000 (BioProject: PRJNA827019, BioSample: SAMN27594413; present study).

Authors: M. Raza & L. Cai

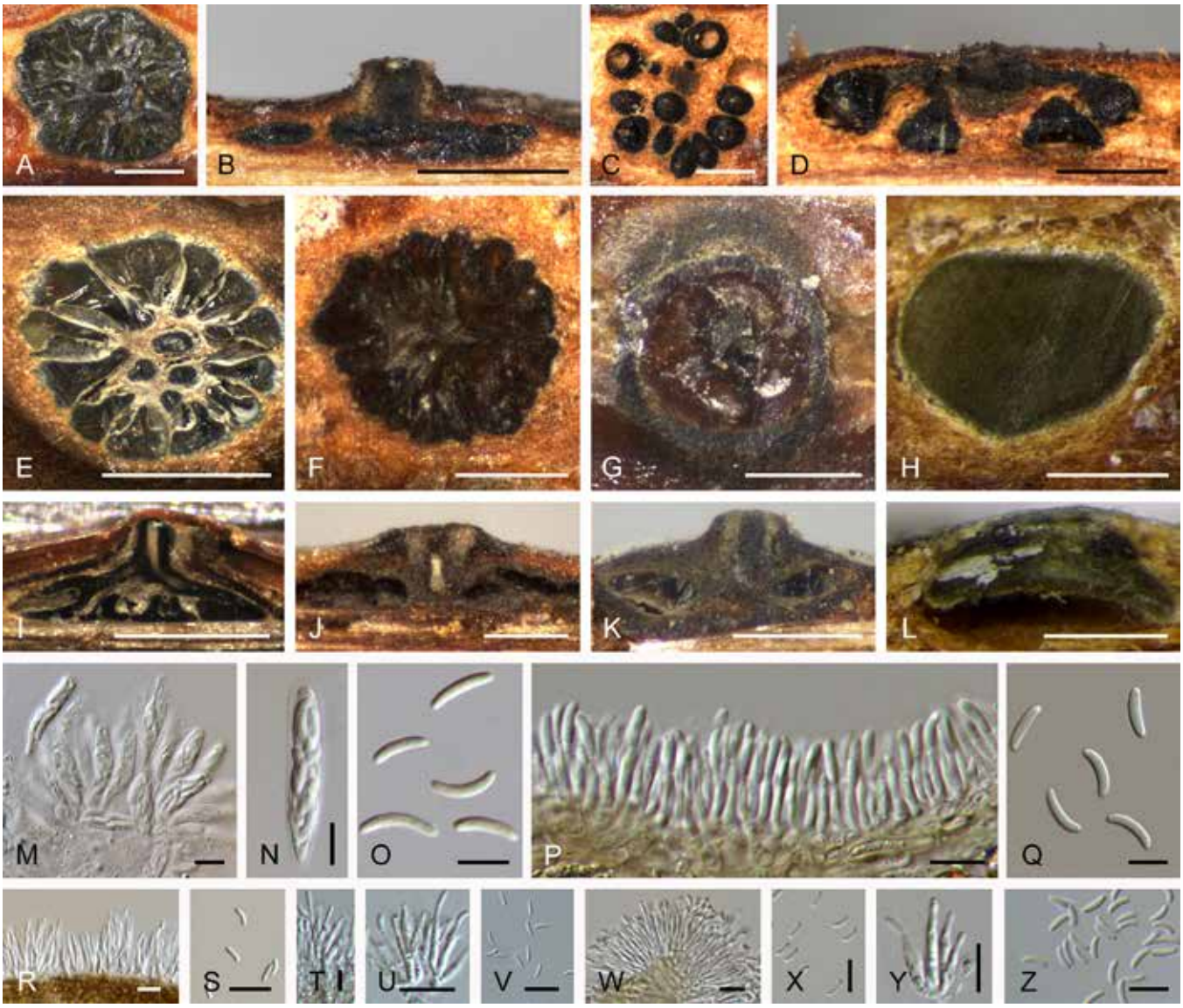

Fig. 18. *Cytospora* spp. **A, B.** Conidiomata of *Cytospora mali* (BJFC-S503) on *Malus pumila*. **C, D.** Ascomata of *Cytospora mali* (BJFC-S503) on *Malus pumila*. **E, I.** Lamyelloid conidioma of *Cytospora ceratosperma* (BJFC-S774) on *Juglans regia*. **F, J.** Cytosporoid conidioma of *Cytospora chrysosperma* (BJFC-S750) on *Populus alba* subsp. *pyramidalis*. **G, K.** Leucostosporoid conidioma of *Cytospora leucostoma* (BJFC-S918) on *Prunus persica*. **H, L.** Cytophomoid conidioma of *Cytospora pruinosa* (BJFC-S636) on *Syringa oblata*. **M–O.** Asci and ascospores of *Cytospora sibiraeae* (BJFC-S783) on *Sibiraea angustata*. **P–Z.** Conidiophores and conidia. **P, Q.** *Cytospora gigaspora* (BJFC-S975) on *Salix psammophila*. **R, S.** *Cytospora ceratosperma* (BJFC-S774) on *Juglans regia*. **T–V.** *Cytospora chrysosperma* (BJFC-S750) on *Populus alba* subsp. *pyramidalis*. **W, X.** *Cytospora leucostoma* (BJFC-S918) on *Prunus persica*. **Y, Z.** *Cytospora pruinosa* (BJFC-S636) on *Syringa oblata*. Scale bars: A–L = 500 µm; M–Z = 10 µm.

Cytospora Ehrenb., Sylvae Mycologicae Berolinenses: 28. 1818. Fig. 18.

Synonyms: *Valsa* Fr., Summa Veg. Scand., Sectio Post. (Stockholm): 410. 1849.

Valsella Fuckel, Jahrb. Nassauischen Vereins Naturk. 23–24: 203. 1870.

Leucocytospora (Pers.) Höhn., Ber. Deutch. Bot. Ges. 35: 352. 1917.

Leucostoma (Nitschke) Höhn., Ber. Deutch. Bot. Ges. 35: 637. 1917.

Valseutypella Höhn., Ann. Mycol. 16: 224. 1919.

Classification: *Sordariomycetes*, *Diaporthales*, *Diaporthomycetidae*, *Cytosporaceae*.

Type species: *Cytospora chrysosperma* (Pers.) Fr., basionym: *Sphaeria chrysosperma* Pers. (epitypification pending).

DNA barcodes (genus): ITS, LSU.

DNA barcodes (species): ITS, LSU, *act1*, *rpb2*, *tef1* and *tub2*. Table 6. Fig. 19.

Ascostromata solitary, immersed in vascular plant tissues, slightly to strongly erumpent through the bark surface. *Stromatic tissues* prosenchymatous or pseudoparenchymatous, sometimes delimited by a black marginal line (conceptacle). *Ascomata* perithecial inclined to upright, in valsoid or diatrypelloid configurations, immersed, usually embedded in ectostromatic disc, with beaks converging at surface. *Ostioles* numerous per disc, periphysate; walls of perithecia bilayered, narrow, outer layer of *textura epdermoidea* to *textura angularis*. *Paraphyses* may be lacking at maturity but usually present, often collapsed and broad. *Asci* free, narrow, ellipsoid to clavate, apical ring refractive. *Ascospores* hyaline, allantoid, aseptate, thin-walled, smooth, biseriate, 4–8 or polysporous per ascus. *Conidiomata* pycnidial,

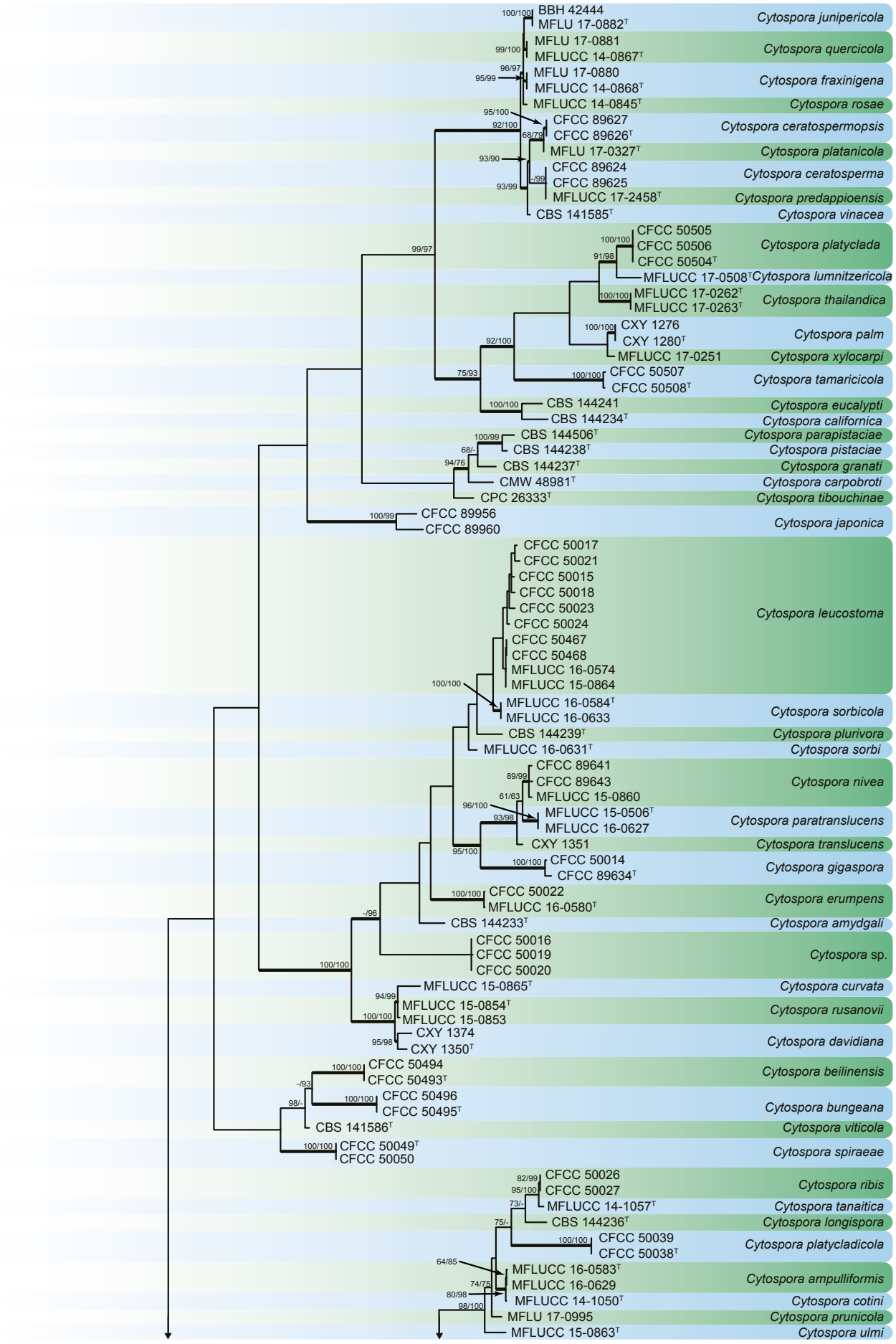

Fig. 19. Maximum parsimony phylogram constructed from ITS (662 bp), LSU (525 bp), *act1* (357 bp), *rpb2* (730 bp), *tef1*-α (796 bp) and *tub2* (635 bp) sequences of all accepted species of *Cytospora*. Maximum parsimony (MP) and Maximum likelihood (ML) bootstrap support values (> 50 %) are shown at the nodes (MP/ML). Thickened branches represent Bayesian posterior probability scores (> 0.95). The phylogenetic tree was rooted to *Diaporthe vaccinii* CBS 160.32. GenBank accession numbers are indicated in Table 6. ^{T} indicates ex-type strains. TreeBASE: S26220.

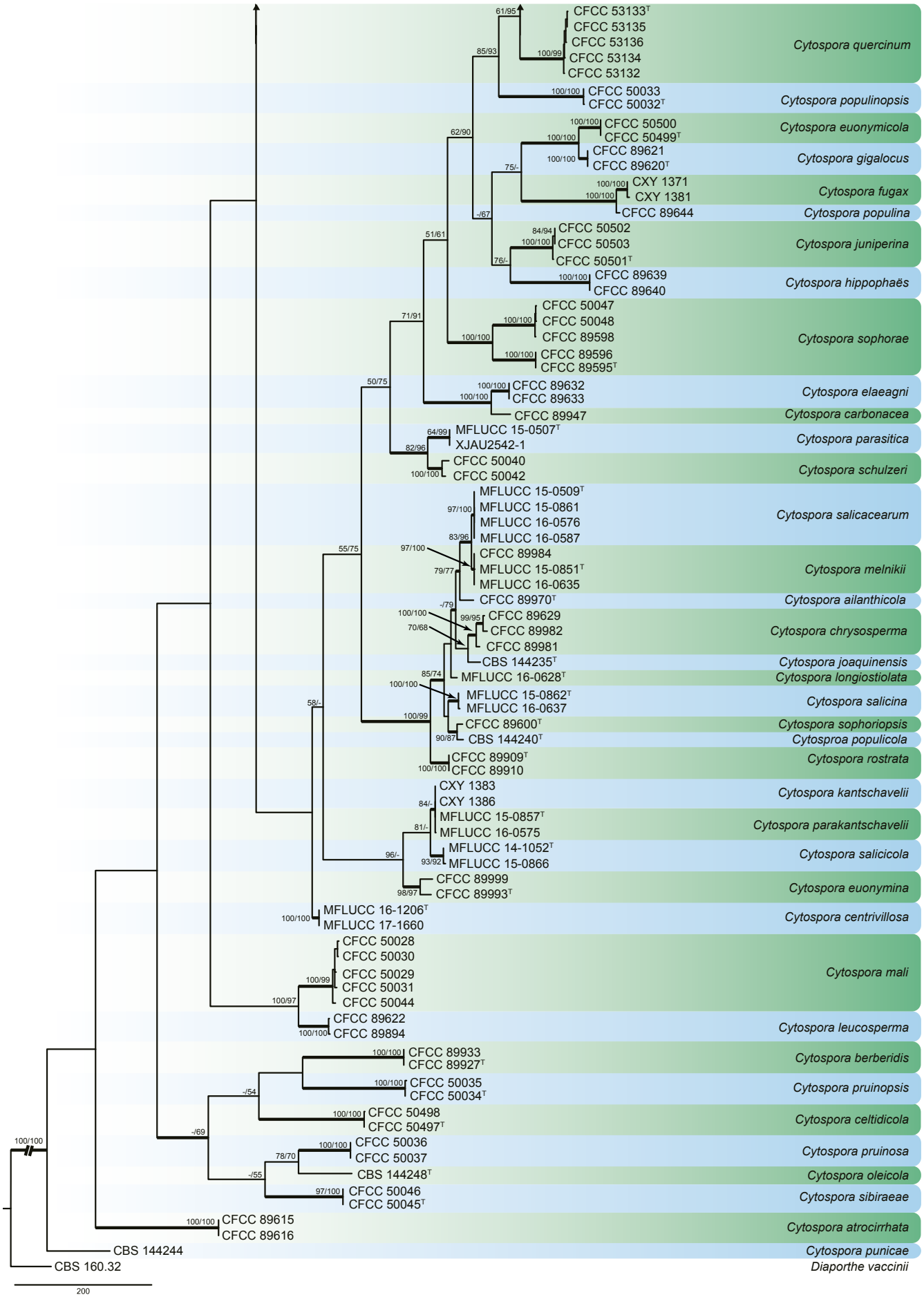

Fig. 19. (Continued).

Table 6. DNA barcodes of accepted *Cytospora* spp.

Species	Isolates[1]	GenBank accession numbers[2]						References
		ITS	LSU	*act1*	*rpb2*	*tef1*	*tub2*	
Cytospora ailanthicola	CFCC 89970^T	MH933618	MH933653	MH933526	MH933592	MH933494	MH933565	Fan *et al*. (2020)
Cy. ampulliformis	MFLUCC 16-0583^T	KY417726	KY417760	KY417692	KY417794	—	—	Norphanphoun *et al*. (2017)
	MFLUCC 16-0629	KY417727	KY417761	KY417693	KY417795	—	—	Norphanphoun *et al*. (2017)
Cy. amygdali	CBS 144233^T	MG971853	—	MG972002	—	MG971659	MG971718	Lawrence *et al*. (2018)
Cy. atrocirrhata	CFCC 89615	KR045618	KR045700	KF498673	KU710946	KP310858	KR045659	Fan *et al*. (2020)
	CFCC 89616	KR045619	KR045701	KF498674	KU710947	KP310859	KR045660	Fan *et al*. (2020)
Cy. beilinensis	CFCC 50493^T	MH933619	MH933654	MH933527	—	MH933495	MH933561	Fan *et al*. (2020)
	CFCC 50494	MH933620	MH933655	MH933528	—	MH933496	MH933562	Fan *et al*. (2020)
Cy. berberidis	CFCC 89927^T	KR045620	KR045702	KU710990	KU710948	KU710913	KR045661	Fan *et al*. (2020)
	CFCC 89933	KR045621	KR045703	KU710991	KU710949	KU710914	KR045662	Fan *et al*. (2020)
Cy. bungeana	CFCC 50495^T	MH933621	MH933656	MH933529	MH933593	MH933497	MH933563	Fan *et al*. (2020)
	CFCC 50496	MH933622	MH933657	MH933530	MH933594	MH933498	MH933564	Fan *et al*. (2020)
Cy. californica	CBS 144234^T	MG971935	—	MG972083	—	MG971645	—	Lawrence *et al*. (2018)
Cy. carbonacea	CFCC 89947	KR045622	KP310812	KP310842	KU710950	KP310855	KP310825	Fan *et al*. (2020)
Cy. carpobroti	CMW 48981^T	MH382812	MH411216	—	—	MH411212	MH411207	Jami *et al*. (2018)
Cy. celtidicola	CFCC 50497^T	MH933623	MH933658	MH933531	MH933595	MH933499	MH933566	Fan *et al*. (2020)
	CFCC 50498	MH933624	MH933659	MH933532	MH933596	MH933500	MH933567	Fan *et al*. (2020)
Cy. centrivillosa	MFLUCC 16-1206^T	MF190122	MF190068	—	MF377601	—	—	Senanayake *et al*. (2017)
	MFLUCC 17-1660	MF190124	MF190070	—	MF377600	—	—	Senanayake *et al*. (2017)
Cy. ceratosperma	CFCC 89624	KR045645	KR045724	—	KU710976	KP310860	KR045686	Fan *et al*. (2020)
	CFCC 89625	KR045646	KR045725	—	KU710977	KP31086	KR045687	Fan *et al*. (2020)
Cy. ceratospermopsis	CFCC 89626^T	KR045647	KR045726	KU711011	KU710978	KU710934	KR045688	Fan *et al*. (2020)
	CFCC 89627	KR045648	KR045727	KU711012	KU710979	KU710935	KR045689	Fan *et al*. (2020)
Cy. chrysosperma	CFCC 89629	KF765673	KF765689	—	KF765705	—	—	Fan *et al*. (2020)
	CFCC 89981	MH933625	MH933660	MH933533	MH933597	MH933501	MH933568	Fan *et al*. (2020)
	CFCC 89982	KP281261	KP310805	KP310835	—	KP310848	KP310818	Fan *et al*. (2020)
Cy. cotini	MFLUCC 14-1050^T	KX430142	KX430143	—	KX430144	—	—	Norphanphoun *et al*. (2017)
Cy. curvata	MFLUCC 15-0865^T	KY417728	KY417762	KY417694	KY417796	—	—	Norphanphoun *et al*. (2017)
Cy. davidiana	CXY 1350^T	KM034870	—	—	—	—	—	Wang *et al*. (2015)
	CXY 1374	KM034869	—	—	—	—	—	Wang *et al*. (2015)
Cy. elaeagni	CFCC 89632	KR045626	KR045706	KU710995	KU710955	KU710918	KR045667	Fan *et al*. (2020)
	CFCC 89633	KF765677	KF765693	KU710996	KU710956	KU710919	KR045668	Fan *et al*. (2020)
Cy. erumpens	CFCC 50022	MH933627	MH933661	MH933534	—	MH933502	MH933569	Fan *et al*. (2020)
	MFLUCC 16-0580^T	KY417733	KY417767	KY417699	KY417801	—	—	Norphanphoun *et al*. (2017)
Cy. eucalypti	CBS 144241	MG971907	—	MG972056	—	MG971617	MG971772	Lawrence *et al*. (2018)
Cy. euonymicola	CFCC 50499^T	MH933628	MH933662	MH933535	MH933598	MH933503	MH933570	Fan *et al*. (2020)
	CFCC 50500	MH933629	MH933663	MH933536	MH933599	MH933504	MH933571	Fan *et al*. (2020)
Cy. euonymina	CFCC 89993^T	MH933630	MH933664	MH933537	MH933600	MH933505	MH933590	Fan *et al*. (2020)
	CFCC 89999	MH933631	MH933665	MH933538	MH933601	MH933506	MH933591	Fan *et al*. (2020)
Cy. fraxinigena	MFLUCC 14-0868^T	MF190133	MF190078	—	—	—	—	Senanayake *et al*. (2017)
	MFLU 17-0880	MF190134	MF190079	—	—	—	—	Senanayake *et al*. (2017)

Table 6. (Continued).

Species	Isolates[1]	GenBank accession numbers[2]						References
		ITS	LSU	*act1*	*rpb2*	*tef1*	*tub2*	
Cy. fugax	CXY 1371	KM034852	—	—	—	—	KM034891	Wang *et al.* (2015)
	CXY 1381	KM034853	—	—	—	—	KM034890	Wang *et al.* (2015)
Cy. gigalocus	CFCC 89620[T]	KR045628	KR045708	KU710997	KU710957	KU710920	KR045669	Fan *et al.* (2020)
	CFCC 89621	KR045629	KR045709	KU710998	KU710958	KU710921	KR045670	Fan *et al.* (2020)
Cy. gigaspora	CFCC 50014	KR045630	KR045710	KU710999.	KU710959	KU710922	KR045671	Fan *et al.* (2020)
	CFCC 89634[T]	KF765671	KF765687	KU711000	KU710960	KU710923	KR045672	Fan *et al.* (2020)
Cy. granati	CBS 144237[T]	MG971799	—	MG971949	—	MG971514	MG971664	Lawrence *et al.* (2018)
Cy. hippophaës	CFCC 89639	KR045632	KR045712	KU711001	KU710961	KU710924	KR045673	Fan *et al.* (2020)
	CFCC 89640	KF765682	KF765698	KF765730	KU710962	KP310865	KR045674	Fan *et al.* (2020)
Cy. japonica	CFCC 89956	KR045624	KR045704	KU710993	KU710953	KU710916	KR045665	Fan *et al.* (2020)
	CFCC 89960	KR045625	KR045705	KU710994	KU710954	KU710917	KR045666	Fan *et al.* (2020)
Cy. joaquinensis	CBS 144235[T]	MG971895	—	MG972044	—	MG971605	MG971761	Lawrence *et al.* (2018)
Cy. junipericola	BBH 42444	—	—	—	—	MF377579	—	Senanayake *et al.* (2017)
	MFLU 17-0882[T]	MF190125	MF190072	—	—	MF377580	—	Senanayake *et al.* (2017)
Cy. juniperina	CFCC 50501[T]	MH933632	MH933666	MH933539	MH933602	MH933507	—	Fan *et al.* (2020)
	CFCC 50502	MH933633	MH933667	MH933540	MH933603	MH933508	MH933572	Fan *et al.* (2020)
	CFCC 50503	MH933634	MH933668	MH933541	MH933604	MH933509	—	Fan *et al.* (2020)
Cy. kantschavelii	CXY 1383	KM034867	—	—	—	—	—	Wang *et al.* (2015)
	CXY 1386	KM034866	—	—	—	—	—	Wang *et al.* (2015)
Cy. leucosperma	CFCC 89622	KR045616	KR045698	KU710988	KU710944	KU710911	KR045657	Fan *et al.* (2020)
	CFCC 89894	KR045617	KR045699	KU710989	KU710945	KU710912	KR045658	Fan *et al.* (2020)
Cy. leucostoma	MFLUCC 15-0864	KY417729	KY417763	KY417695	KY417797	—	—	Norphanphoun *et al.* (2017)
	MFLUCC 16-0574	KY417731	KY417764	KY417696	KY417798	—	—	Norphanphoun *et al.* (2017)
	CFCC 50015	KR045634	KR045714	KU711002	KU710963	KU710925	KR045675	Fan *et al.* (2020)
	CFCC 50017	MH933635	MH933669	MH933542	—	MH933510	MH933573	Fan *et al.* (2020)
	CFCC 50018	MH933636	MH933670	MH933543	—	MH933511	MH933574	Fan *et al.* (2020)
	CFCC 50021	MH933639	MH933673	MH933546	—	MH933512	MH933575	Fan *et al.* (2020)
	CFCC 50023	KR045635	KR045715	KU711003	KU710964	KU710926	KR045676	Fan *et al.* (2020)
	CFCC 50024	MH933640	MH933674	MH933547	MH933605	—	MH933576	Fan *et al.* (2020)
	CFCC 50467	KT732948	KT732967	—	—	—	—	Fan *et al.* (2020)
	CFCC 50468	KT732949	KT732968	—	—	—	—	Fan *et al.* (2020)
Cy. longiostiolata	MFLUCC 16-0628[T]	KY417734	KY417768	KY417700	KY417802	—	—	Norphanphoun *et al.* (2017)
Cy. longispora	CBS 144236[T]	MG971905	—	MG972054	—	MG971615	MG971764	Lawrence *et al.* (2018)
Cy. lumnitzericola	MFLUCC 17-0508[T]	MG975778	MH253461	MH253457	MH253453	—	—	Norphanphoun *et al.* (2018)
Cy. mali	CFCC 50028	MH933641	MH933675	MH933548	MH933606	MH933513	MH933577	Fan *et al.* (2020)
	CFCC 50029	MH933642	MH933676	MH933549	MH933607	MH933514	MH933578	Fan *et al.* (2020)
	CFCC 50030	MH933643	MH933677	MH933550	MH933608	MH933524	MH933579	Fan *et al.* (2020)
	CFCC 50031	KR045636	KR045716	KU711004	KU710965	KU710927	KR045677	Fan *et al.* (2020)
	CFCC 50044	KR045637	KR045717	KU711005	KU710966	KU710928	KR045678	Fan *et al.* (2020)
Cy. melnikii	CFCC 89984	MH933644	MH933678	MH933551	MH933609	MH933515	MH933580	Fan *et al.* (2020)
	MFLUCC 15-0851[T]	KY417735	KY417769	KY417701	KY417803	—	—	Norphanphoun *et al.* (2017)
	MFLUCC 16-0635	KY417736	KY417770	KY417702	KY417804	—	—	Norphanphoun *et al.* (2017)

Table 6. (Continued).

Species	Isolates[1]	GenBank accession numbers[2]						References
		ITS	LSU	*act1*	*rpb2*	*tef1*	*tub2*	
Cy. nivea	CFCC 89641	KF765683	KF765699	KU711006	KU710967	KU710929	KR045679	Fan *et al*. (2020)
	CFCC 89643	KF765685	KF765701	—	KU710968	KP310863	KP310829	Fan *et al*. (2020)
	MFLUCC 15-0860	KY417737	KY417771	KY417703	KY417805	—	—	Norphanphoun *et al*. (2017)
Cy. oleicola	CBS 144248^T	MG971944	—	MG972098	—	MG971660	MG971752	Lawrence *et al*. (2018)
Cy. palm	CXY 1276	JN402990	—	—	—	KJ781296	—	Zhang *et al*. (2014)
	CXY 1280^T	JN411939	—	—	—	KJ781297	—	Zhang *et al*. (2014)
Cy. parakantschavelii	MFLUCC 15-0857^T	KY417738	KY417772	KY417704	KY417806	—	—	Norphanphoun *et al*. (2017)
	MFLUCC 16-0575	KY417739	KY417773	KY417705	KY417807	—	—	Norphanphoun *et al*. (2017)
Cy. parapistaciae	CBS 144506^T	MG971804	—	MG971954	—	MG971519	MG971669	Lawrence *et al*. (2018)
Cy. parasitica	MFLUCC 15-0507^T	KY417740	KY417774	KY417706	KY417808	—	—	Norphanphoun *et al*. (2017)
	XJAU 2542-1	MH798884	MH798897	—	—	MH813452	—	Ma *et al*. (2018)
Cy. paratranslucens	MFLUCC 15-0506^T	KY417741	KY417775	KY417707	KY417809	—	—	Norphanphoun *et al*. (2017)
	MFLUCC 16-0627	KY417742	KY417776	KY417708	KY417810	—	—	Norphanphoun *et al*. (2017)
Cy. pistaciae	CBS 144238^T	MG971802	—	MG971952	—	MG971517	MG971667	Lawrence *et al*. (2018)
Cy. platanicola	MFLU 17-0327^T	MH253451	MH253452	MH253449	MH253450	—	—	Hyde *et al*. (2018)
Cy. platycladi	CFCC 50504^T	MH933645	MH933679	MH933552	MH933610	MH933516	MH933581	Fan *et al*. (2020)
	CFCC 50505	MH933646	MH933680	MH933553	MH933611	MH933517	MH933582	Fan *et al*. (2020)
	CFCC 50506	MH933647	MH933681	MH933554	MH933612	MH933518	MH933583	Fan *et al*. (2020)
Cy. platycladicola	CFCC 50038^T	KT222840	MH933682	MH933555	MH933613	MH933519	MH933584	Fan *et al*. (2020)
	CFCC 50039	KR045642	KR045721	KU711008	KU710973	KU710931	KR045683	Fan *et al*. (2020)
Cy. plurivora	CBS 144239^T	MG971861	—	MG972010	—	MG971572	MG971726	Lawrence *et al*. (2018)
Cy. populicola	CBS 144240^T	MG971891	—	MG972040	—	MG971601	MG971757	Lawrence *et al*. (2018)
Cy. populina	CFCC 89644	KF765686	KF765702	KU711007	KU710969	KU710930	KR045681	Fan *et al*. (2020)
Cy. populinopsis	CFCC 50032^T	MH933648	MH933683	MH933556	MH933614	MH933520	MH933585	Fan *et al*. (2020)
	CFCC 50033	MH933649	MH933684	MH933557	MH933615	MH933521	MH933586	Fan *et al*. (2020)
Cy. predappioensis	MFLUCC 17-2458^T	MG873484	MG873480	—	—	—	—	Jayawardena *et al*. (2019)
Cy. pruinopsis	CFCC 50034^T	KP281259	KP310806	KP310836	KU710970	KP310849	KP310819	Fan *et al*. (2020)
	CFCC 50035	KP281260	KP310807	KP310837	KU710971	KP310850	KP310820	Fan *et al*. (2020)
Cy. pruinosa	CFCC 50036	KP310800	KP310802	KP310832	—	KP310845	KP310815	Fan *et al*. (2020)
	CFCC 50037	MH933650	MH933685	MH933558	—	MH933522	MH933589	Fan *et al*. (2020)
Cy. prunicola	MFLU 17-0995	MG742350	MG742351	MG742353	MG742352	—	—	Hyde *et al*. (2018)
Cy. punicae	CBS 144244	MG971943	—	MG972091	—	MG971654	MG971798	Lawrence *et al*. (2018)
Cy. quercicola	MFLU 17-0881	MF190129	MF190074	—	—	—	—	Senanayake *et al*. (2017)
	MFLUCC 14-0867^T	MF190128	MF190073	—	—	—	—	Senanayake *et al*. (2017)
Cy. quercinum	CFCC 53132	MT360044	MT360032	MT363981	MT363990	MT364000	MT364010	Pan *et al*. (2021)
	CFCC 53133^T	MT360045	MT360033	MT363982	MT363991	MT364001	MT364011	Pan *et al*. (2021)
	CFCC 53134	MT360046	MT360034	MT363983	MT363992	MT364002	MT364012	Pan *et al*. (2021)
	CFCC 53135	MT360047	MT360035	MT363984	MT363993	MT364003	MT364013	Pan *et al*. (2021)
	CFCC 53136	MT360048	MT360036	MT363985	MT363994	MT364004	MT364014	Pan *et al*. (2021)

Table 6. (Continued).

Species	Isolates[1]	GenBank accession numbers[2]						References
		ITS	LSU	*act1*	*rpb2*	*tef1*	*tub2*	
Cy. ribis	CFCC 50026	KP281267	KP310813	KP310843	KU710972	KP310856	KP310826	Fan *et al.* (2020)
	CFCC 50027	KP281268	KP310814	KP310844	—	KP310857	KP310827	Fan *et al.* (2020)
Cy. rosae	MFLUCC 14-0845[T]	MF190131	MF190076	—	—	—	—	Senanayake *et al.* (2017)
Cy. rostrata	CFCC 89909[T]	KR045643	KR045722	KU711009	KU710974	KU710932	KR045684	Fan *et al.* (2020)
	CFCC 89910	KR045644	KR045723	KU711010	KU710975	KU710933	—	Fan *et al.* (2020)
Cy. rusanovii	MFLUCC 15-0853	KY417743	KY417777	KY417709	KY417811	—	—	Norphanphoun *et al.* (2017)
	MFLUCC 15-0854[T]	KY417744	KY417778	KY417710	KY417812	—	—	Norphanphoun *et al.* (2017)
Cy. salicacearum	MFLUCC 16-0576	KY417747	KY417781	KY417713	KY417815	—	—	Norphanphoun *et al.* (2017)
	MFLUCC 15-0509[T]	KY417746	KY417780	KY417712	KY417814	—	—	Norphanphoun *et al.* (2017)
	MFLUCC 15-0861	KY417745	KY417779	KY417711	KY417813	—	—	Norphanphoun *et al.* (2017)
	MFLUCC 16-0587	KY417748	KY417782	KY417714	KY417816	—	—	Norphanphoun *et al.* (2017)
Cy. salicicola	MFLUCC 14-1052[T]	KU982636	KU982635	KU982637	—	—	—	Li *et al.* (2018)
	MFLUCC 15-0866	KY417749	KY417783	KY417715	KY417817	—	—	Norphanphoun *et al.* (2017)
Cy. salicina	MFLUCC 15-0862[T]	KY417750	KY417784	KY417716	KY417818	—	—	Norphanphoun *et al.* (2017)
	MFLUCC 16-0637	KY417751	KY417785	KY417717	KY417819	—	—	Norphanphoun *et al.* (2017)
Cy. schulzeri	CFCC 50040	KR045649	KR045728	KU711013	KU710980	KU710936	KR045690	Fan *et al.* (2020)
	CFCC 50042	KR045650	KR045729	KU711014	KU710981	KU710937	KR045691	Fan *et al.* (2020)
Cy. sibiraeae	CFCC 50045[T]	KR045651	KR045730	KU711015	KU710982	KU710938	KR045692	Fan *et al.* (2020)
	CFCC 50046	KR045652	KR045731	KU711015	KU710983	KU710939	KR045693	Fan *et al.* (2020)
Cy. sophorae	CFCC 50047	KR045653	KR045732	KU711017	KU710984	KU710940	KR045694	Fan *et al.* (2020)
	CFCC 50048	MH820401	MH820394	MH820409	MH820397	MH820405	MH820390	Fan *et al.* (2020)
	CFCC 89598	KR045654	KR045733	KU711018	KU710985	KU710941	KR045695	Fan *et al.* (2020)
Cy. sophoricola	CFCC 89595[T]	KR045655	KR045734	KU711019	KU710986	KU710942	KR045696	Fan *et al.* (2020)
	CFCC 89596	KR045656	KR045735	KU711020	KU710987	KU710943	KR045697	Fan *et al.* (2020)
Cy. sophoriopsis	CFCC 89600[T]	KR045623	KP310804	KU710992	KU710951	KU710915	KP310817	Fan *et al.* (2020)
Cy. sorbi	MFLUCC 16-0631[T]	KY417752	KY417786	KY417718	KY417820	—	—	Norphanphoun *et al.* (2017)
Cy. sorbicola	MFLUCC 16-0584[T]	KY417755	KY417789	KY417721	KY417823	—	—	Norphanphoun *et al.* (2017)
	MFLUCC 16-0633	KY417758	KY417792	KY417724	KY417826	—	—	Norphanphoun *et al.* (2017)
Cytospora sp.	CFCC 50016	MH820400	MH820393	MH820408	—	MH820404	MH820389	Fan *et al.* (2020)
	CFCC 50019	MH933637	MH933671	MH933544	—	—	—	Fan *et al.* (2020)
	CFCC 50020	MH933638	MH933672	MH933545	—	—	—	Fan *et al.* (2020)
Cy. spiraeae	CFCC 50049[T]	MG707859	MG707643	MG708196	MG708199	—	—	Fan *et al.* (2020)
	CFCC 50050	MG707860	MG707644	MG708197	MG708200	—	—	Fan *et al.* (2020)
Cy. tamaricicola	CFCC 50507	MH933651	MH933686	MH933559	MH933616	MH933525	MH933587	Fan *et al.* (2020)
	CFCC 50508[T]	MH933652	MH933687	MH933560	MH933617	MH933523	MH933588	Fan *et al.* (2020)

Table 6. (Continued).

Species	Isolates[1]	GenBank accession numbers[2]						References
		ITS	LSU	*act1*	*rpb2*	*tef1*	*tub2*	
Cy. tanaitica	MFLUCC 14-1057[T]	KT459411	KT459412	KT459413	—	—	—	Ariyawansa *et al*. (2015)
Cy. thailandica	MFLUCC 17-0262[T]	MG975776	MH253463	MH253459	MH253455	—	—	Norphanphoun *et al*. (2018)
	MFLUCC 17-0263[T]	MG975777	MH253464	MH253460	MH253456	—	—	Norphanphoun *et al*. (2018)
Cy. tibouchinae	CPC 26333[T]	KX228284	KX228335	—	—	—	—	Norphanphoun *et al*. (2018)
Cy. translucens	CXY 1351	KM034874	—	—	—	—	KM034895	Wang *et al*. (2015)
Cy. ulmi	MFLUCC 15-0863[T]	KY417759	—	—	—	—	—	Norphanphoun *et al*. (2017)
Cy. vinacea	CBS 141585[T]	KX256256	—	—	—	KX256277	KX256235	Lawrence *et al*. (2018)
Cy. viticola	CBS 141586[T]	KX256239	—	—	—	KX256260	KX256218	Lawrence *et al*. (2018)
Cy. xylocarpi	MFLUCC 17-0251	MG975775	MH253462	MH253458	MH253454	—	—	Norphanphoun *et al*. (2018)

[1] BBH: BIOTEC Bangkok Herbarium, National Science and Technology Development Agency, Thailand; CBS: Westerdijk Fungal Biodiversity Institute, Utrecht, the Netherlands; CFCC: China Forestry Culture Collection Centre, Beijing, China; CMW: Tree Protection Co-operative Program, Forestry and Agricultural Biotechnology Institute, University of Pretoria, South Africa; CPC: Culture collection of Pedro Crous, housed at CBS; MFLU: Mae Fah Luang University herbarium, Thailand; MFLUCC: Mae Fah Luang University Culture Collection, Chiang Rai, Thailand; XJAU: Xinjiang Agricultural University, Xinjiang, China. [T] indicates ex-type strain.

[2] ITS: internal transcribed spacers and intervening 5.8S nrDNA; LSU: partial 28S large subunit nrRNA gene; *act1*: partial actin gene; *rpb2*: partial RNA polymerase II second largest subunit gene; *tef1*: partial translation elongation factor1-α gene; *tub2*: partial β-tubulin gene.

ostiolate, immersed in vascular plant tissues, slightly to strongly erumpent through the bark surface, sometimes delimited by a black marginal line (conceptacle). *Ectostromatic disc* prominent or lacking, one to few ostioles per disc. *Locules* single, undivided to multiple chambered with invaginations, globoid to flattened toroid, in ectostroma or embedded in entostroma, sometimes with a column; wall bilayered, outer layer prosenchymatous, ultimately sclerenchymatous. *Conidiophores* borne along the locules, hyaline, branched or not, thin-walled, normally embedded in a gelatinous layer. *Conidiogenous cells* enteroblastic, phialidic, sub-cylindrical to cylindrical, tapering towards apices. *Conidia* hyaline, allantoid, eguttulate, smooth, aseptate, thin-walled, relatively small and narrow (adapted from Adams *et al.* 2005, Fan *et al.* 2020).

Culture characteristics: Colonies growing fast on MEA and PDA, covering the medium within 5 d at 25 °C, with surface mycelium flattened, dense and felty. Colonies initially white, becoming cream to yellowish, producing brownish dots with age, with visible solitary conidiomata at maturity on all media.

Optimal media and cultivation conditions: On MEA and PDA under nuv-light (12 h light, 12 h dark) at 25 °C for 3 wk; drought stress and scratches on media induce sporulation of the asexual morph.

Distribution: Worldwide.

Hosts: Pathogens on a wide range of woody plants.

Disease symptoms: Canker and dieback.

Notes: *Cytospora* was established by Ehrenberg (1818) and subsequently resulted in a confusing taxonomy due to identifications that were largely based on host affiliation and similar morphological characters. More than 660 species epithets named *Cytospora* have been recorded in Index Fungorum (http://www.indexfungorum.org/; 2020) but most of them have no available materials with DNA sequences. Adams *et al.* (2005) described 28 species of *Cytospora* from *Eucalyptus* based on combined morphology and ITS sequence data, of which 11 species were new to science. Adams *et al.* (2006) described 14 additional species from South Africa using the same methodology. Recent studies have subsequently focussed on *Cytospora* species from specific hosts using a polyphasic approach (Fan *et al.* 2014a, b, 2015a, b, Yang *et al.* 2015, Lawrence *et al.* 2017, Norphanphoun *et al.* 2017, 2018, Zhu *et al.* 2018, 2020, Pan *et al.* 2019, 2020). Fan *et al.* (2020) summarised 52 species of *Cytospora* associated with canker and dieback disease in China using a six-gene matrix (ITS, LSU, *act1*, *rpb2*, *tef1* and *tub2*), of which 13 species were new to science. Morphologically, six locule types were widely accepted (Spielman 1983, 1985). Lamyelloid refers to multiple independent locules with multiple ostioles, *e.g. Cy. ceratosperma* (Fig. 18E, I). Cytosporoid refers to a divided locule and shared walls, including most species of *Cytospora*, *e.g. Cy. chrysosperma* (Fig. 18F, J). Torsellioid refers to multiple independent locules with one ostiole. Cyclocytosporoid refers to a toruloid locule with a central column. Leucostosporoid refers to divided locule and shared walls surrounded by a black circle (conceptacle), *e.g. Cy. leucostoma* (Fig. 18G, K). Cytophomoid refers to an undivided locule and wing-like ectostroma around the ostiole (sometimes it is inconspicuous), *e.g. Cy. pruinosa* (Fig. 18H, L).

References: Adams *et al.* 2005, Fan *et al.* 2020 (morphology and phylogeny).

Genome sequenced strain: *Cytospora chrysosperma*. **China**, Shaanxi Province, poplar tree in temperate region, collection date and collector unknown, strain YSFL. This Whole Genome Shutgun project has been deposited at GenBank under the accession LJZO00000000 (BioProject: PRJNA296468, BioSample: SAMN04099705); CFL2056 v1.0 in MycoCosm (Yin & Huang, unpublished).

Authors: M. Pan & X.L. Fan

Dendrostoma X.L. Fan & C.M. Tian, Persoonia 40: 126. 2018. Fig. 20.

Classification: *Sordariomycetes*, *Diaporthomycetidae*, *Diaporthales*, *Erythrogloeaceae.*

Type species: *Dendrostoma mali* X.L. Fan & C.M. Tian. Holotype and ex-type strain: CF 2017445, CFCC 52102.

DNA barcode (genus): LSU.

DNA barcodes (species): ITS, *rpb2*, *tef1.* Table 7. Fig. 21.

Pseudostromata small to large, distinct, circular, erumpent, consisting of an inconspicuous ectostromatic disc, semi-immersed to superficial, causing a pustulate bark surface. *Ectostromatic disc* flat or concave, orange, surrounded by bark flaps. *Central column* beneath the disc more or less conical. *Stromatic zones* lacking. *Ascomata* perithecial, conspicuous, umber to fuscous black, embedded in orange to umber pseudostromatic tissue, regularly scattered, surrounding the ectostromatic disc, with small to long ostioles that emerge within the ectostromatic disc. *Ostioles* flat in the disc or sometimes slightly projecting, cylindrical, sometimes obscuring the disc, covered by an orange, umber to fuscous black crust. *Paraphyses* deliquescent. *Asci* fusoid, 8-spored, 2–3-seriate, with an apical ring, becoming detached from the perithecial wall. *Ascospores* hyaline, fusoid to cylindrical, symmetrical to asymmetrical, straight to curved, bicellular, with a median septum, constricted at the septum, smooth, multiguttulate. *Conidiomata* acervular, spherical to conical to pulvinate, occurring separately, immersed to semi-immersed in bark; wall of several layers of yellow *textura angularis*. *Central column* beneath the disc conical or not. *Conidiophores* reduced to conidiogenous cells. *Conidiogenous cells* lining the inner walls of cavity, hyaline, smooth, subcylindrical to ampulliform. *Conidia* hyaline, aseptate, smooth, multiguttulate or not, thin-walled, ellipsoid to fusoid, straight to curved (adapted from Fan *et al.* 2018, Jaklitsch & Voglmayr 2019, Jiang *et al.* 2019a).

Culture characteristics: Colonies on PDA circular to irregular, reaching 70 mm diam with 5–20 d at 25 °C in darkness, originally flat with white felted aerial mycelium, becoming yellow, grey to black mycelium due to different pigment formation, producing sexual ascomata or not after 1 mo.

Optimal media and cultivation conditions: MEA and PDA at 25 °C under continuous nuv-light to promote sporulation.

Distribution: Australia, China and Europe (Austria, Croatia, France, Greece, Italy, Poland, Spain).

Hosts: Tree genera including *Castanea*, *Quercus* (*Fagaceae*), *Elaeocarpus* (*Elaeocarpaceae*), *Malus* (*Rosaceae*) and *Osmanthus* (*Oleaceae*).

Disease symptoms: Stem canker.

Notes: *Dendrostoma* is characterised by having multiguttulate and bicellular ascospores that are constricted at the septum and acervular conidiomata, with subcylindrical to ampulliform conidiogenous cells and hyaline to olivaceous, aseptate conidia (Fan *et al. 2018,* Jiang *et al.* 2019a). This genus was initially described by Fan *et al.* (2018) based on the type species, *De. mali* from *Malus spectabilis*, together with two other species, *De. osmanthi* and *De. quercinum*. Subsequently, *De. leiphaemia* on *Quercus* trees in Europe was transferred from *Amphiporthe* (Senanayake *et al.* 2018). Another 15 species from *Castanea* and *Quercus* trees were added, which revealed a high diversity of *Dendrostoma* on *Fagaceae* hosts (Jaklitsch & Voglmayr 2019, Jiang *et al.* 2019a, Zhu *et al.* 2019).

The family *Erythrogloeaceae* comprises four genera, namely *Chrysocrypta*, *Dendrostoma*, *Disculoides* and *Erythrogloeum*. Species of *Dendrostoma* are all known from bark, while those of the other three genera are all foliar pathogens (Jiang *et al.* 2019a). Additionally, the only genus of this family for which sexual morphs are known is *Dendrostoma*. Although all *Dendrostoma* species have been described from symptomatic tissues, no pathogenicity tests have thus far been conducted.

References: Fan *et al.* 2018 (morphology and phylogeny); Jiang *et al.* 2019a (morphology and phylogeny).

Dendrostoma elaeocarpi C.M. Tian & Q. Yang, ***sp. nov.*** MycoBank MB 829528. Fig. 22.

Etymology: Named after the host genus from which it was collected, *Elaeocarpus*.

Pseudostromata erumpent, consisting of an inconspicuous yellowish to orange ectostromatic disc, semi-immersed to superficial, causing a pustulate bark surface, 540–750 µm diam. *Ectostromatic* disc flat or concave, orange, or brown to black, sometimes concealed by ostioles, surrounded by bark flaps, 395–490 µm diam. *Central column* yellowish to brownish. *Stromatic zones* lacking. *Perithecia* conspicuous, umber to fuscous black, regularly scattered, surrounding the ectostromatic disc, (170–) 205–245(–300) µm diam. *Ostioles* 2–5 per disc, flat in the disc or sometimes slightly projecting, cylindrical, covered by an orange, umber to fuscous black crust, 75–100 µm diam. *Paraphyses* deliquescent. *Asci* fusoid, 8-spored, biseriate or triserial, with an apical ring, (40.5–)43–44.5(–47) × (8.5–)10.5–12 µm. *Ascospores* hyaline, ellipsoidal to fusoid, smooth, biguttulate, symmetrical to asymmetrical, straight to slightly curved, bicellular, with a median septum distinctly constricted, (10.5–)11–13 × 3–3.5 µm.

Culture characteristics: Colonies on PDA circular to irregular, reaching 70 mm diam after 10 d at 25 °C in darkness, originally flat with white felted aerial mycelium, becoming saffron yellow mycelium due to pigment formation, producing ascomata after 1 mo.

Typus: **China**, Jiangxi Province, Ganzhou, Jinpenshan Forest Farm, 25°14'08.51"N, 115°12'41.21"E, on branches of *Elaeocarpus decipiens* (*Elaeocarpaceae*), 19 Jul. 2018, Q. Yang, Y. Liu, Y.M. Liang & C.M. Tian (**holotype** BJFC-S1682, culture ex-type CFCC 53113).

Additional material examined: **China**, Jiangxi Province, Ganzhou, Jinpenshan Forest Farm, 25°14'08.51"N, 115°12'41.21"E, on branches of *Elaeocarpus decipiens*, 19 Jul. 2018, Q. Yang, Y. Liu, Y.M. Liang & C.M. Tian, culture CFCC 53114.

Fig. 20. *Dendrostoma* spp. **A–D.** Disease symptoms on host barks. **A.** *Osmanthus fragrans*. **B–D.** *Quercus* spp. **E.** Pseudostroma. **F.** Transverse section through pseudostroma. **G.** Longitudinal section through pseudostroma. **E–G.** *Dendrostoma osmanthi* (CF 2017474) on *Osmanthus fragrans*. **H.** Conidioma of *Dendrostoma dispersum* (BJFC-S1537) on *Quercus* sp. **I.** Transverse section through conidioma of *Dendrostoma aurorae* (BJFC-S1561) on *Castanea mollissima*. **J.** Longitudinal section through conidioma of *Dendrostoma qinlingense* (BJFC-S1539) on *Quercus wutaishanica*. **K, L.** Ascus and ascospores of *Dendrostoma osmanthi* (CF 2017474) on *Osmanthus fragrans*. **M, N.** Conidiogenous cells and conidia of *Dendrostoma dispersum* (BJFC-S1538) on *Quercus* sp. Scale bars: E–H, J = 500 µm; I = 200 µm; K–N = 10 µm.

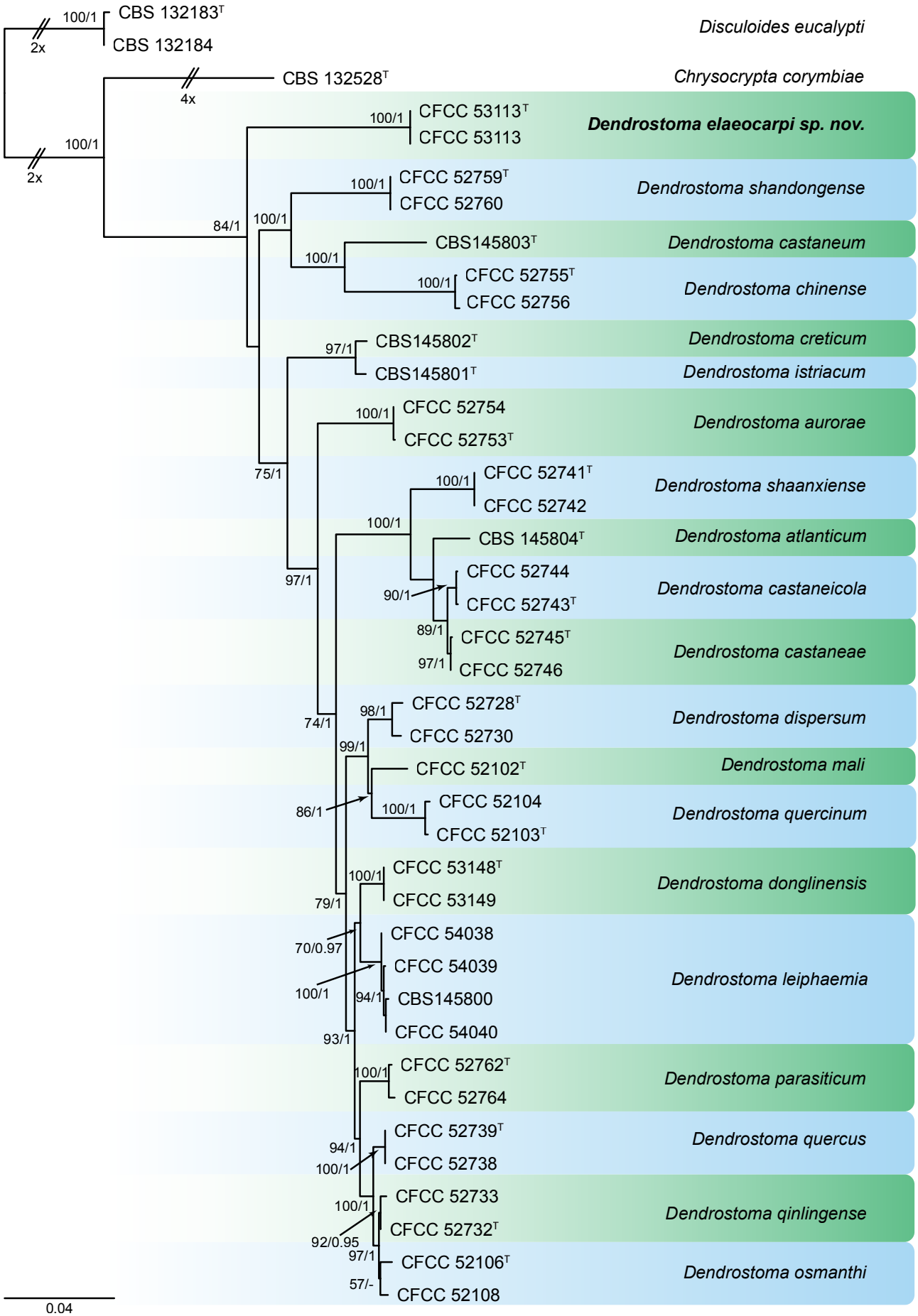

Fig. 21. Maximum Likelihood (ML) phylogram constructed from ITS (495 bp), *rpb2* (1 075 bp) and *tef1* (402 bp) sequences of all accepted species of *Dendrostoma*. Bootstrap support values (> 50 %) for ML and Bayesian posterior probabilities (> 0.95) are shown at the nodes. The novel taxon is printed in **bold**. The phylogenetic tree was rooted to *Disculoides eucalypti* CBS 132183 and CBS132184. GenBank accession numbers are indicated in Table 7. [T] indicates ex-type strain. TreeBASE: S26124.

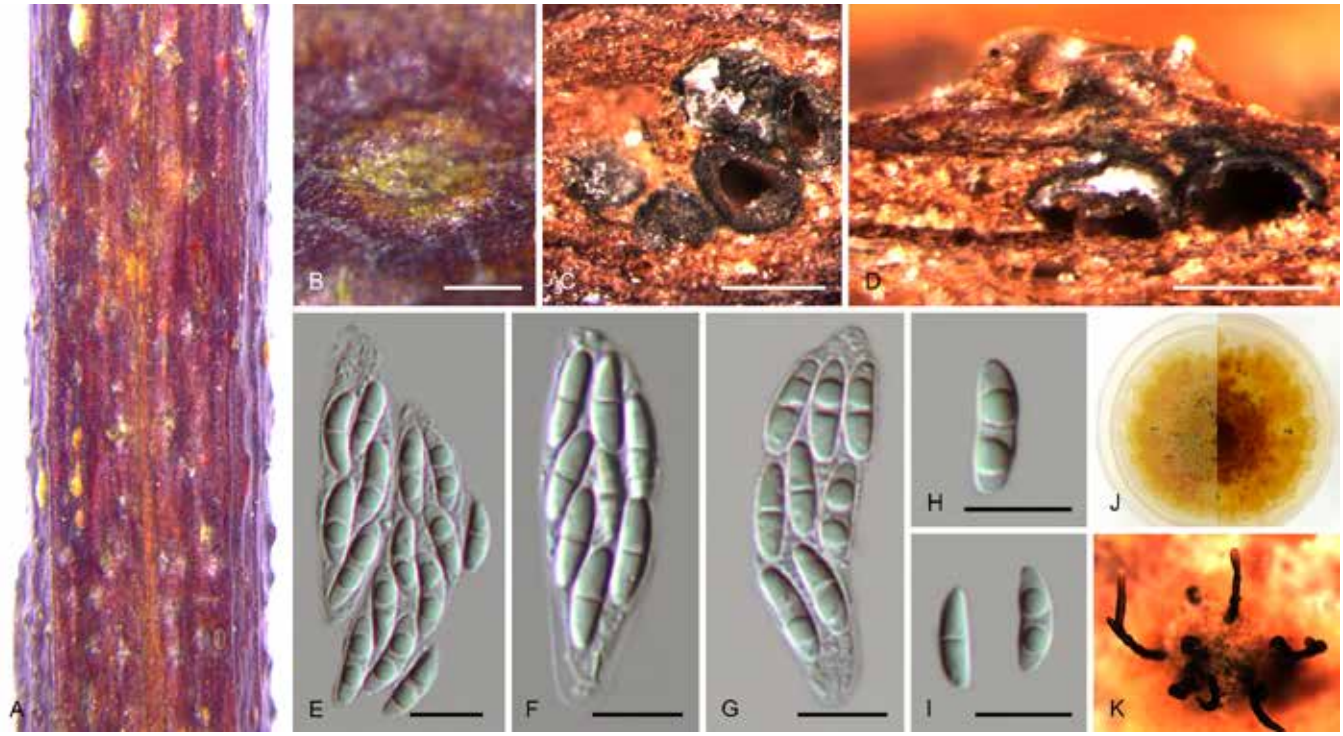

Fig. 22. *Dendrostoma elaeocarpi* (holotype BJFC-S1682). **A, B.** Habit of pseudostromata on twigs. **C.** Transverse section of pseudostromata. **D.** Longitudinal section through pseudostromata. **E–G.** Asci. **H, I.** Ascospores. **J.** The colony on PDA (front and reverse). **K.** Sexual ascomata on PDA. Scale bars: B–D = 200 µm; E–I = 10 µm.

Table 7. DNA barcodes of accepted *Dendrostoma* spp.

Species	Isolates[1]	GenBank accession numbers[2]			References
		ITS	*tef1*	*rpb2*	
Dendrostoma atlanticum	CBS 145804^T	MN447223	MN432167	MN432160	Jaklitsch *et al.* (2019)
De. aurorae	CFCC 52753^T	MH542498	MH545447	MH545405	Jiang *et al.* (2019a)
	CFCC 52754	MH542499	MH545448	MH545406	Jiang *et al.* (2019a)
De. castaneae	CFCC 52745^T	MH542488	MH545437	MH545395	Jiang *et al.* (2019a)
	CFCC 52746	MH542489	MH545438	MH545396	Jiang *et al.* (2019a)
De. castaneicola	CFCC 52743^T	MH542496	MH545445	MH545403	Jiang *et al.* (2019a)
	CFCC 52744	MH542497	MH545446	MH545404	Jiang *et al.* (2019a)
De. castaneum	CBS 145803^T	MN447225	MN432169	MN432162	Jaklitsch *et al.* (2019)
De. chinense	CFCC 52755^T	MH542500	MH545449	MH545407	Jiang *et al.* (2019a)
	CFCC 52756	MH542501	MH545450	MH545408	Jiang *et al.* (2019a)
De. creticum	CBS 145802^T	MN447228	MN432171	MN432163	Jaklitsch *et al.* (2019)
De. dispersum	CFCC 52730	MH542467	MH545416	MH545374	Jiang *et al.* (2019a)
	CFCC 52728^T	MH542469	MH545418	MH545376	Jiang *et al.* (2019a)
De. donglinensis	CFCC 53148^T	MN266206	MN315480	MN315491	Zhu *et al.* (2019)
	CFCC 53149	MN266207	MN315481	MN315492	Zhu *et al.* (2019)
De. elaeocarpi	CFCC 53113^T	MK432638	MK578096	MK578114	Present study
	CFCC 53114	MK432639	MK578097	MK578115	Present study
De. istriacum	CBS 145801^T	MN447229	MN432172	MN432164	Jaklitsch *et al.* (2019)
De. leiphaemia	CFCC 54038	MN545571	MN551288	MN551291	Present study
	CFCC 54039	MN545572	MN551289	MN551292	Present study
	CFCC 54040	MN545573	MN551290	MN551293	Present study
	CBS 145800	MN447230	MN432173	MN432165	Jaklitsch *et al.* (2019)
De. mali	CFCC 52102^T	MG682072	MG682052	MG682032	Fan *et al.* (2018)
De. osmanthi	CFCC 52106^T	MG682073	MG682053	MG682033	Fan *et al.* (2018)
	CFCC 52108	MG682074	MG682054	MG682034	Fan *et al.* (2018)

Table 7. (Continued).

Species	Isolates[1]	GenBank accession numbers[2]			References
		ITS	*tef1*	*rpb2*	
De. parasiticum	CFCC 52762[T]	MH542482	MH545431	MH545389	Jiang *et al.* (2019a)
	CFCC 52764	MH542483	MH545432	MH545390	Jiang *et al.* (2019a)
De. qinlingense	CFCC 52732[T]	MH542471	MH545420	MH545378	Jiang *et al.* (2019a)
	CFCC 52733	MH542472	MH545421	MH545379	Jiang *et al.* (2019a)
De. quercinum	CFCC 52103[T]	MG682077	MG682057	MG682037	Fan *et al.* (2018)
	CFCC 52104	MG682078	MG682058	MG682038	Fan *et al.* (2018)
De. quercus	CFCC 52739[T]	MH542476	MH545425	MH545383	Jiang *et al.* (2019a)
	CFCC 52738	MH542477	MH545426	MH545384	Jiang *et al.* (2019a)
De. shaanxiense	CFCC 52741[T]	MH542486	MH545435	MH545393	Jiang *et al.* (2019a)
	CFCC 52742	MH542487	MH545436	MH545394	Jiang *et al.* (2019a)
De. shandongense	CFCC 52759[T]	MH542504	MH545453	MH545411	Jiang *et al.* (2019a)
	CFCC 52760	MH542505	MH545454	MH545412	Jiang *et al.* (2019a)

[1] CBS: Westerdijk Fungal Biodiversity Institute, Utrecht, the Netherlands; CFCC: China Forestry Culture Collection Center, Beijing, China. [T] indicates ex-type.

[2] ITS: internal transcribed spacers and intervening 5.8S nrDNA; *rpb2*: partial RNA polymerase II second largest subunit gene; *tef1*: partial elongation factor 1-α gene.

Notes: *Dendrostoma elaeocarpi* is associated with canker disease of *Elaeocarpus decipiens*, representing a first report from this host. *Dendrostoma elaeocarpi* can be distinguished from other *Dendrostoma* species by host associations and ellipsoidal to fusoid, biguttulate ascospores.

Genome sequenced strain: *Dendrostoma leiphaemia*. **The Netherlands**, on *Quercus* sp., 25 Apr. 2019, N. Jiang, culture ex-epitype CFCC 54038. This Whole Genome Shutgun project has been deposited at GenBank under the accession JALRMF000000000 (BioProject: PRJNA827019, BioSample: SAMN27594414; present study).

Authors: N. Jiang, Q. Yang & C.M. Tian

Didymella Sacc. *ex* Sacc. *emend*. Qian Chen & L. Cai, Stud. Mycol. 82: 173. 2015. Fig. 23.
Synonym: *Peyronellaea* Goid. *ex* Togliani, Ann. Sperim. Agrar. II 6: 93. 1952.

Classification: *Dothideomycetes*, *Pleosporomycetidae*, *Pleosporales*, *Didymellaceae*.

Type species: *Didymella exigua* (Niessl) Sacc., basionym: *Didymosphaeria exigua* Niessl, Oesterr. bot. Z. 25: 165. 1875. Neotype and ex-neotype strain: CBS H-20123, CBS 183.55.

DNA barcodes (genus): LSU, ITS.

DNA barcodes (species): *rpb2*, *tub2*. Table 8. Fig. 24.

Ascomata pseudothecial, immersed or erumpent, (sub-)globose to flattened, solitary or confluent, ostiolate; *ascomatal wall* multi-layered, composed of pseudoparenchymatous cells. *Asci* cylindrical to clavate or saccate, 8-spored, bitunicate, arising from a broad hymenium among pseudoparaphyses. *Ascospores* mostly hyaline or brownish, ellipsoidal to cymbiform, uniseptate, symmetrical or asymmetrical, constricted at the septum, or multiseptate. *Conidiomata* pycnidial, (sub-)globose to ellipsoidal, flask-shaped, or obpyriform, becoming irregular, superficial on or immersed into the agar, solitary or confluent, ostiolate or poroid, sometimes with elongated necks; micropycnidia occur in some species; *conidiomatal wall* pseudoparenchymatous, multi-layered. *Conidiogenous cells* phialidic, hyaline, smooth, flask-shaped, subglobose, lageniform, ampulliform or doliiform. *Conidia* generally aseptate, variable in shape, smooth and thin-walled, *i.e.* ellipsoidal to (sub-)globose, cylindrical, oblong, ovoid, sometimes allantoid, hyaline, but in older cultures conidia may become pigmented, larger or septate conidia may occur in at least one species, mostly guttulate. *Unicellular chlamydospores* often abundantly formed in and on the agar and in the aerial mycelium, globose, intercalary, brown or (pale) olivaceous pigmented; *multicellular chlamydospores* mainly alternarioid, muriformly septate, terminal or intercalary, often in chains, brown or (pale) olivaceous (de Gruyter *et al.* 2009, Aveskamp *et al.* 2010, Zhang *et al.* 2012, Crous *et al.* 2014, Chen *et al.* 2015b, 2017, Hou *et al.* 2020a).

Cultural characteristics: Colonies on OA covered by flat, felted, or floccose, white to pale olivaceous grey, pale luteous to buff, or yellow olivaceous to dull green aerial mycelium, margin mostly regular, white to smoke/mouse/iron/yellowish grey, buff, amber to brown, pale olivaceous to dark olivaceous, yellowish green to dull green, fuscous-black, sometimes with saffron, salmon, red to dark vinaceous colour.

Optimal media and cultivation conditions: OA or sterile pine needles placed on OA under nuv-light (12 h light, 12 h dark) to promote sporulation at 25 °C.

Distribution: Worldwide.

Hosts: Mainly found as saprobes on dead stems or bark, and (opportunistic) parasites of herbaceous and woody plants on a wide range of plant families, *i.e.* *Aceraceae*, *Actinidiaceae*, *Amaryllidaceae*, *Anacardiaceae*, *Aquifoliaceae*, *Araceae*, *Araliaceae*, *Asphodelaceae*, *Asteraceae*, *Berberidaceae*, *Bromeliaceae*, *Cactaceae*, *Caprifoliaceae*, *Chenopodiaceae*, *Combretaceae*, *Cucurbitaceae*, *Elaeagnaceae*, *Ericaceae*, *Fabaceae*, *Gentianaceae*,

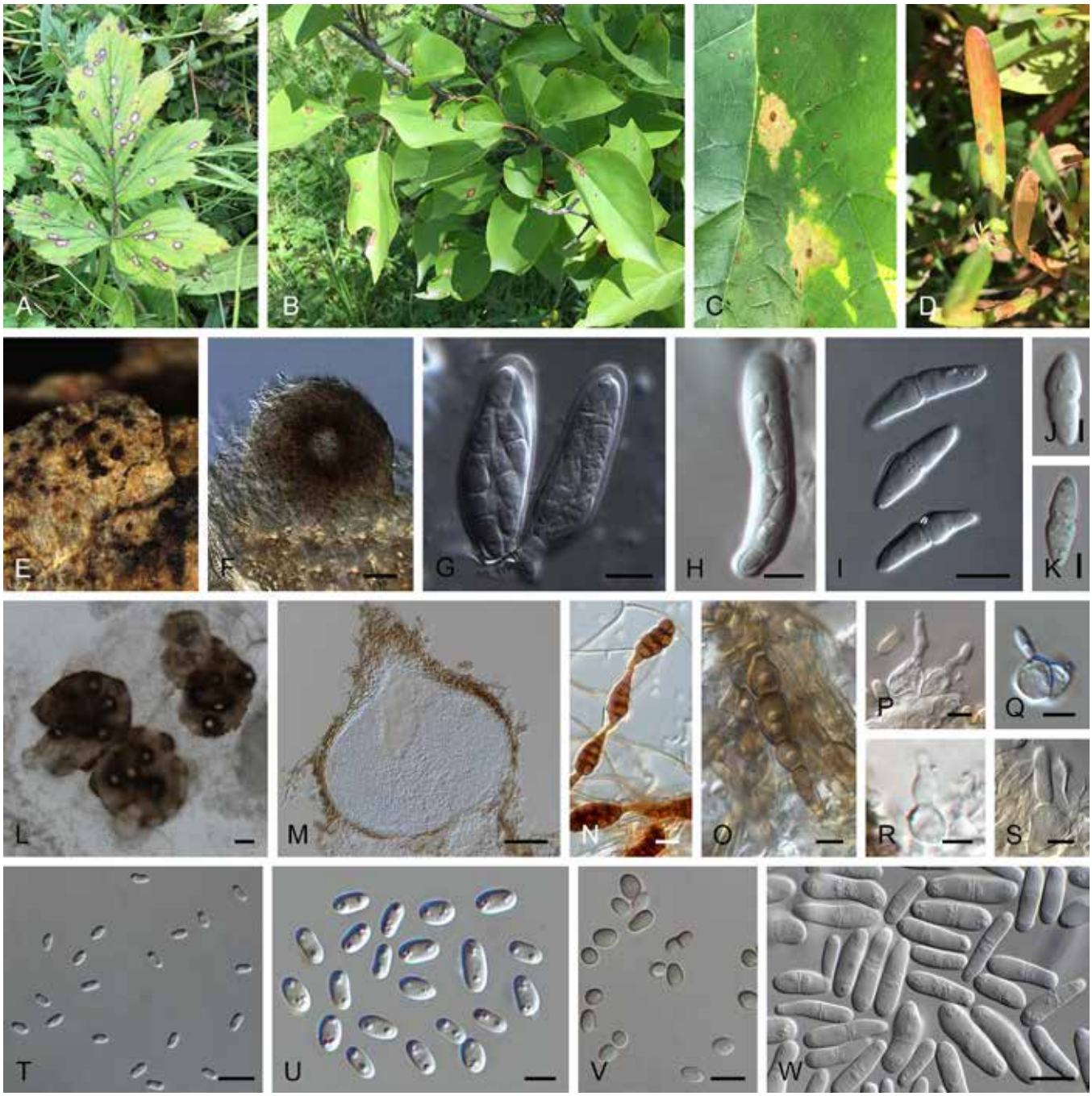

Fig. 23. *Didymella* spp. **A–D.** Disease symptoms. **A.** Symptoms caused by *Didymella gei* (ex-type CGMCC 3.20068) on *Geum* sp. **B.** Symptoms caused by *Didymella uniseptata* (ex-type CGMCC 3.20069) on *Syringa vulgaris*. **C.** Symptoms caused by *Didymella qilianensis* (ex-type CGMCC 3.20071) on *Rheum officinale*. **D.** Symptoms caused by *Didymella chlamydospora* (LC13589) on *Polygonum sibiricum*. **E–K.** Sexual morph. **E.** Ascomata on host of *Didymella exigua* (ex-neotype CBS 183.55). **F.** Ascoma of *Didymella exigua* (ex-neotype CBS 183.55). **G, H.** Asci. **G.** *Didymella exigua* (ex-neotype CBS 183.55). **H.** *Didymella pinodes* (holotype K 56275). **I–K.** Ascospores. **I.** *Didymella exigua* (ex-neotype CBS 183.55). **J.** *Didymella pinodes* (holotype K 56275). **K.** *Didymella sinensis* (ex-type CGMCC 3.18348). **L–W.** Asexual morph. **L.** Conidiomata of *Didymella aquatica* (ex-type CGMCC 3.18349). **M.** Section through the conidioma of *Didymella degraaffiae* (ex-type CBS 144956). **N, O.** Chlamydospores. **N.** Alternaroid chlamydospores of *Didymella glomerata* (UTHSCD I16-205). **O.** *Didymella degraaffiae* (ex-type CBS 144956). **P–S.** Conidiogenous cells. **P.** *Didymella brunneospora* (ex-type CBS 115.58). **Q.** *Didymella degraaffiae* (ex-type CBS 144956). **R.** *Didymella ilicicola* (ex-type CGMCC 3.18355). **S.** *Didymella cari* (ex-type CBS 144497). **T–W.** Conidia. **T.** *Didymella aquatica* (ex-type CGMCC 3.18349). **U.** *Didymella degraaffiae* (ex-type CBS 144956). **V.** *Didymella infuscatispora* (CGMCC 3.18356). **W.** *Didymella cari* (ex-type CBS 144497). Scale bars: L = 50 µm; F–I, M, N, S, T, V, W = 10 µm; J, K, O–R, U = 5 µm. Pictures E–J taken from Chen *et al.* (2015b); K, L, R, T, V from Chen *et al.* (2017); M, O, Q, U from Hou *et al.* (2020b); N, P from Valenzuela-Lopez *et al.* (2018); S, W from Crous *et al.* (2018c).

Geraniaceae, *Hamamelidaceae*, *Lamiaceae*, *Liliaceae*, *Lythraceae*, *Myrtaceae*, *Oleaceae*, *Orchidaceae*, *Pinaceae*, *Poaceae*, *Polygonaceae*, *Pteridaceae*, *Rosaceae*, *Rubiaceae*, *Saxifragaceae*, *Scrophulariaceae*, *Simaroubaceae*, *Solanaceae*, *Theaceae*, *Umbelliferae*, *Urticaceae* and *Vitaceae*, and also from different human and environment samples.

Disease symptoms: Blossom blight, flower-stalk diseases, leaf spots, leaf scorch, neck rot, stem lesions, seed-borne diseases, wood discolouration, damping-off of seedlings, red spot disease, and black root rot.

Table 8. DNA barcodes of accepted *Didymella* spp.

Species	Isolates[1]	GenBank accession numbers[2]				References
		LSU	ITS	*rpb2*	*tub2*	
Didymella acetosellae	CBS 631.76[ET]	MN943749	MN973542	MT018176	MT005645	Hou *et al.* (2020a)
Di. aeria	CGMCC 3.18353[T]	KY742205	KY742051	KY742137	KY742293	Chen *et al.* (2017)
Di. aliena	CBS 379.93	GU238037	GU237851	KP330416	GU237578	Aveskamp *et al.* (2010), Chen *et al.* (2015c)
Di. aloeicola	CBS 562.88[T]	MN943742	MN973535	MT018164	MT005638	Hou *et al.* (2020a)
Di. americana	CBS 185.85	GU237990	FJ426972	KT38 9594	FJ427088	Aveskamp *et al.* (2009, 2010), Chen *et al.* (2015b)
Di. anserina	CBS 360.84	GU237993	GU237839	KT389596	GU237551	Aveskamp *et al.* (2010), Chen *et al.* (2015b)
Di. aquatica	CGMCC 3.18349[T]	KY742209	KY742055	KY742140	KY742297	Chen *et al.* (2017)
Di. arachidicola	CBS 333.75[IsoT]	GU237996	GU237833	KT389598	GU237554	Aveskamp *et al.* (2010), Chen *et al.* (2015b)
Di. aurea	CBS 269.93[T]	GU237996	GU237833	KT389598	GU237554	Aveskamp *et al.* (2010), Chen *et al.* (2015b)
Di. bellidis	CBS 714.85	GU238046	GU237904	KP330417	GU237586	Aveskamp *et al.* (2010), Chen *et al.* (2015c)
Di. boeremae	CBS 109942[NT]	GU238048	FJ426982	KT389600	FJ427097	Aveskamp *et al.* (2009, 2010), Chen *et al.* (2015b)
Di. brunneospora	CBS 115.58[T]	KT389723	KT389505	KT389625	KT389802	Chen *et al.* (2015b), Valenzuela-Lopez *et al.* (2018)
Di. calidophila	CBS 448.83[NT]	GU238052	FJ427059	MT018170	FJ427168	Aveskamp *et al.* (2009, 2010), Hou *et al.* (2020a)
Di. cari	CBS 144497[T]	MH327861	MH327825	—	MH327899	Crous *et al.* (2018c)
Di. chenopodii	CBS 128.93	GU238055	GU237775	KT389602	GU237591	Aveskamp *et al.* (2010), Chen *et al.* (2015b)
Di. chlamydospora	LC 13586	MT229671	MT229694	MT239091	MT249262	Present study
	CGMCC 3.20072 = LC 13587[T]	MT229672	MT229695	MT239092	MT249263	Present study
	LC 13588	MT229673	MT229696	MT239093	MT249264	Present study
	LC 13589	MT229674	MT229697	MT239094	MT249265	Present study
Di. chloroguttulata	CGMCC 3.18351[T]	KY742211	KY742057	KY742142	KY742299	Chen *et al.* (2017)
Di. coffeae-arabicae	CBS 123380[T]	GU238005	FJ426993	KT389603	FJ427104	Aveskamp *et al.* (2009, 2010), Chen *et al.* (2015b)
Di. combreti	CBS 137982[T]	KJ869191	KJ869134	MT018139	MT005626	Crous *et al.* (2014), Hou *et al.* (2020a)
Di. curtisii	CBS 251.92	GU238013	FJ427038	MT018131	FJ427148	Aveskamp *et al.* (2009, 2010), Hou *et al.* (2020a)
Di. dactylidis	CBS 124513[T]	GU238061	GU237766	MT018173	GU237599	Aveskamp *et al.* (2010), Hou *et al.* (2020a)
Di. degraaffiae	CBS 144956[T]	MN823295	MN823444	MN824470	MN824618	Hou *et al.* (2020b)
Di. dimorpha	CBS 346.82[T]	GU238068	GU237835	MT018158	GU237606	Aveskamp *et al.* (2010), Hou *et al.* (2020a)
Di. ellipsoidea	CGMCC 3.18350[T]	KY742214	KY742060	KY742145	KY742302	Chen *et al.* (2017)
Di. eucalyptica	CBS 377.91	GU238007	GU237846	KT389605	GU237562	Aveskamp *et al.* (2010), Chen *et al.* (2015b)
Di. exigua	CBS 183.55[T]	EU754155	GU237794	EU874850	GU237525	Chilvers *et al.* (2009), de Gruyter *et al.* (2009), Aveskamp *et al.* (2010)
Di. finnmarkica	CBS 145572[T]	MK876429	MK876388	MK876484	—	Crous *et al.* (2019a)
Di. gardeniae	CBS 626.68[IT]	GQ387595	FJ427003	KT389606	FJ427114	Aveskamp *et al.* (2009), de Gruyter *et al.* (2010), Chen *et al.* (2015b)
Di. gei	CGMCC 3.20068 = LC 13581[T]	MT229675	MT229698	MT239095	MT249266	Present study
Di. glomerata	CBS 528.66	EU754184	FJ427013	GU371781	FJ427124	Aveskamp *et al.* (2009), de Gruyter *et al.* (2009), Schoch *et al.* (2009)
Di. guttulata	CBS 127976[T]	MN943730	MN973524	MT018138	MT005625	Hou *et al.* (2020a)
Di. heteroderae	CBS 109.92[T]	GU238002	FJ426983	KT389601	FJ427098	Aveskamp *et al.* (2009, 2010), Chen *et al.* (2015b)
Di. ilicicola	CGMCC 3.18355[T]	KY742219	KY742065	KY742150	KY742307	Chen *et al.* (2017)
Di. indica	CBS 653.77[T]	MN943741	MN973534	MT018159	MT005637	Hou *et al.* (2020a)
Di. infuscatispora	CGMCC 3.18356[T]	KY742221	KY742067	KY742152	KY742309	Chen *et al.* (2017)
Di. keratinophila	CBS 143032[T]	LN907343	LT592901	LT593039	LT592970	Valenzuela-Lopez *et al.* (2018)
Di. kooimaniorum	CBS 144951[T]	MN823299	MN823448	MN824474	MN824622	Hou *et al.* (2020b)
Di. lethalis	CBS 103.25	GU238010	GU237729	KT389607	GU237564	Aveskamp *et al.* (2010), Chen *et al.* (2015b)
Di. ligulariae	CGMCC 3.20070 = LC 13583[T]	MT229676	MT229699	MT239096	MT249267	Present study
Di. longicolla	CBS 124514[T]	GU238095	GU237767	MT018161	GU237622	Aveskamp *et al.* (2010), Hou *et al.* (2020a)
Di. macrophylla	CGMCC 3.18357[T]	KY742224	KY742070	KY742154	KY742312	Chen *et al.* (2017)

Table 8. DNA barcodes of accepted *Didymella* spp.

Species	Isolates[1]	GenBank accession numbers[2]				References
		LSU	ITS	*rpb2*	*tub2*	
Di. macrostoma	CBS 223.69	GU238096	GU237801	KT389608	GU237623	Aveskamp *et al.* (2010), Chen *et al.* (2015b)
Di. maydis	CBS 588.69^{T}	EU754192	FJ427086	GU371782	FJ427190	Aveskamp *et al.* (2009), de Gruyter *et al.* (2009), Schoch *et al.* (2009)
Di. microchlamydospora	CBS 105.95^{T}	GU238104	FJ427028	KP330424	FJ427138	Aveskamp *et al.* (2009, 2010), Chen *et al.* (2015c)
Di. mitis	CBS 443.72^{T}	MN943729	MN973523	MT018137	MT005624	Hou *et al.* (2020a)
Di. molleriana	CBS 229.79	GU238067	GU237802	KP330418	GU237605	Aveskamp *et al.* (2010), Chen *et al.* (2015c)
Di. musae	CBS 463.69	GU238011	FJ427026	MT018148	FJ427136	Aveskamp *et al.* (2009, 2010), Hou *et al.* (2020a)
Di. negriana	CBS 358.71	GU238116	GU237838	KT389610	GU237635	Aveskamp *et al.* (2010), Chen *et al.* (2015b)
Di. nigricans	CBS 444.81^{IsoT}	GU238000	GU237867	MT018146	GU237558	Aveskamp *et al.* (2010), Hou *et al.* (2020a)
Di. ocimicola	CGMCC 3.18358^{T}	KY742232	KY742078	MT018181	KY742320	Chen *et al.* (2017), Hou *et al.* (2020a)
Di. pedeiae	CBS 124517^{T}	GU238127	GU237770	KT389612	GU237642	Aveskamp *et al.* (2010), Chen *et al.* (2015b)
Di. pinodella	CBS 531.66	GU238017	FJ427052	KT389613	FJ427162	Aveskamp *et al.* (2009, 2010), Chen *et al.* (2015b)
Di. pinodes	CBS 525.77^{ET}	GU238023	GU237883	KT389614	GU237572	Aveskamp *et al.* (2010), Chen *et al.* (2015b)
Di. pomorum	CBS 539.66	GU238028	FJ427056	KT389618	FJ427166	Aveskamp *et al.* (2009, 2010), Chen *et al.* (2015b)
Di. prolaticolla	CBS 126182^{T}	MN943740	MN973533	MT018157	MT005636	Hou *et al.* (2020a)
Di. prosopidis	CBS 136414^{T}	KF777232	KF777180	MT018149	MT005631	Crous *et al.* (2013b)
Di. protuberans	CBS 381.96^{NT}	GU238029	GU237853	KT389620	GU237574	Aveskamp *et al.* (2010), Chen *et al.* (2015b)
Di. pteridis	CBS 379.96^{T}	KT389722	KT389504	KT389624	KT389801	Chen *et al.* (2015b), Chen *et al.* (2017)
Di. qilianensis	LC 13584	MT229677	MT229700	MT239097	MT249268	Present study
	CGMCC 3.20071 = LC 13585^{T}	MT229678	MT229701	MT239098	MT249269	Present study
Di. rhei	CBS 109177	GU238139	GU237743	KP330428	GU237653	Aveskamp *et al.* (2010), Chen *et al.* (2015c)
Di. rumicicola	CBS 683.79^{IsoT}	KT389721	KT389503	KT389622	KT389800	Chen *et al.* (2015b)
Di. sancta	CBS 281.83^{T}	GU238030	FJ427063	KT389623	FJ427170	Aveskamp *et al.* (2009, 2010), Chen *et al.* (2015b)
Di. segeticola	CGMCC 3.17489^{T}	KP330455	KP330443	KP330414	KP330399	Chen *et al.* (2015c), Chen *et al.* (2017)
Di. senecionicola	CBS 160.78	GU238143	GU237787	MT018177	GU237657	Aveskamp *et al.* (2010), Hou *et al.* (2020a)
Di. sinensis	CGMCC 3.18348^{T}	KY742239	KY742085	MT018127	KY742327	Chen *et al.* (2017), Hou *et al.* (2020a)
Di. subglobispora	CBS 364.91^{T}	MN943737	MN973531	MT018153	MT005634	Hou *et al.* (2020a)
Di. subglomerata	CBS 110.92	GU238032	FJ427080	KT389626	FJ427186	Aveskamp *et al.* (2009, 2010), Chen *et al.* (2015b)
Di. subherbarum	CBS 250.92^{T}	GU238145	GU237809	MT018162	GU237659	Aveskamp *et al.* (2010), Hou *et al.* (2020a)
Di. subrosea	CBS 733.79^{T}	MN943747	MN973540	MT018174	MT005643	Hou *et al.* (2020a)
Di. suiyangensis	CGMCC 3.18352^{T}	KY742243	KY742089	KY742168	KY742330	Chen *et al.* (2017)
Di. uniseptata	CGMCC 3.20069 = LC 13582^{T}	MT229679	MT229702	MT239099	MT249270	Present study
Di. variabilis	CBS 254.79^{T}	MN943751	MN973544	MT018182	MT005647	Hou *et al.* (2020a)
Di. viburnicola	CBS 523.73	GU238155	GU237879	KP330430	GU237667	Aveskamp *et al.* (2010), Chen *et al.* (2015c)

[1] CBS: Westerdijk Fungal Biodiversity Institute, Utrecht, the Netherlands; CGMCC: Chinese General Microbiological Culture Collection Center, Beijing, China; LC: Dr Lei Cai's personal collection deposited in laboratory, housed at Chinese Academy of Sciences, China. $^{T,\ ET,\ IsoT}$ and ^{NT} indicate ex-type, ex-epitype, ex-isotype and ex-neotype strains, respectively.

[2] ITS: internal transcribed spacers and intervening 5.8S nrDNA; LSU: partial 28S large subunit nrRNA gene; *rpb2*: partial RNA polymerase II second largest subunit gene; *tub2*: partial β-tubulin gene.

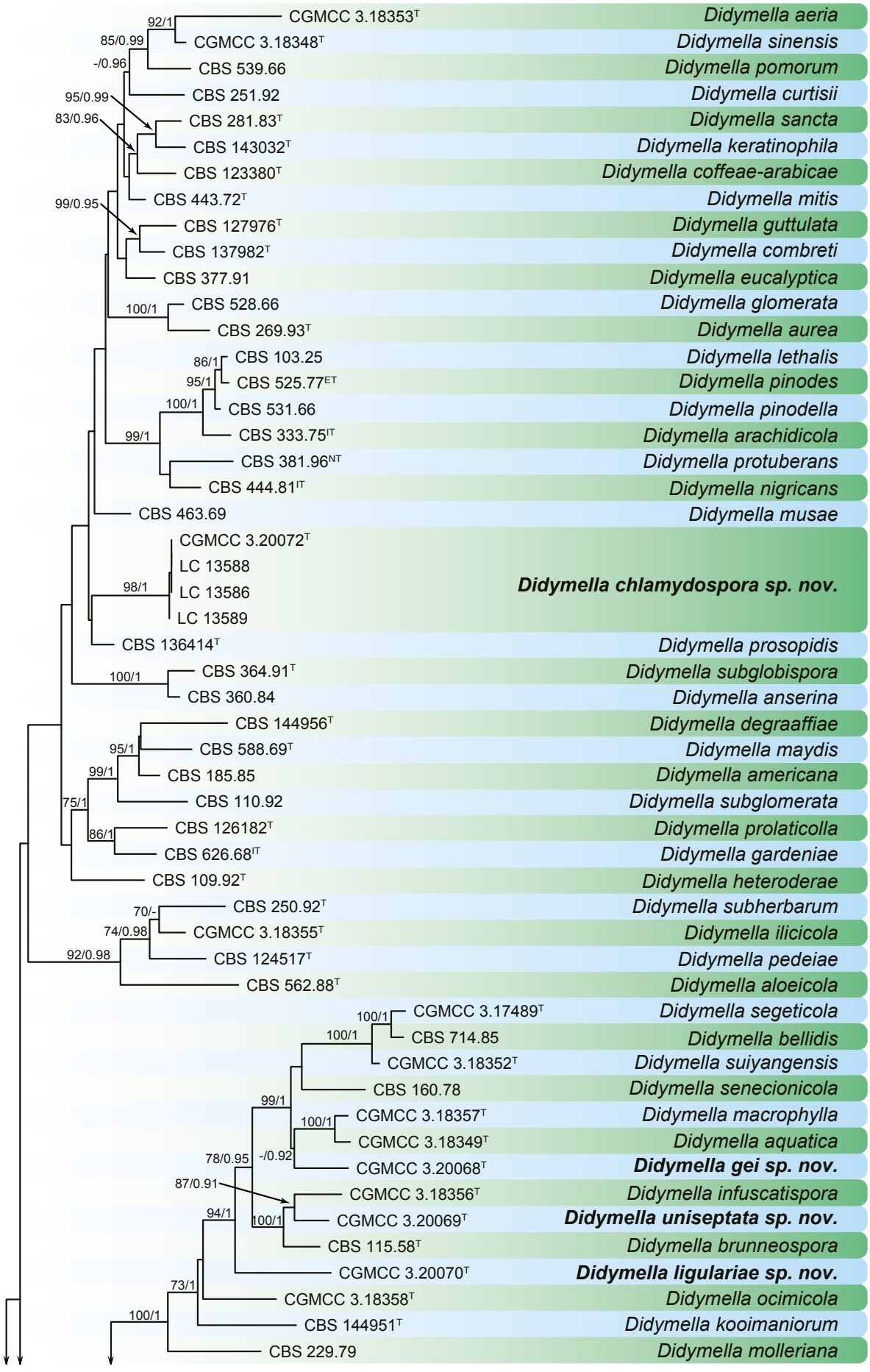

Fig. 24. Maximum Likelihood (ML) phylogram constructed from LSU (962 bp), ITS (462 bp), *tub2* (346 bp) and *rpb2* (596 bp) sequences of all accepted species of *Didymella*. RAxML bootstrap support values (> 70 %) and Bayesian posterior probability scores (> 0.90) are shown at the nodes. Novel taxa are printed in **bold**. The phylogenetic tree was rooted to *Neoascochyta exitialis* CBS 389.86. GenBank accession numbers are indicated in Table 8. $^{T, ET, IsoT}$ and ^{NT} indicate ex-type, ex-epitype, ex-isotype and ex-neotype strains, respectively. TreeBASE: S26040.

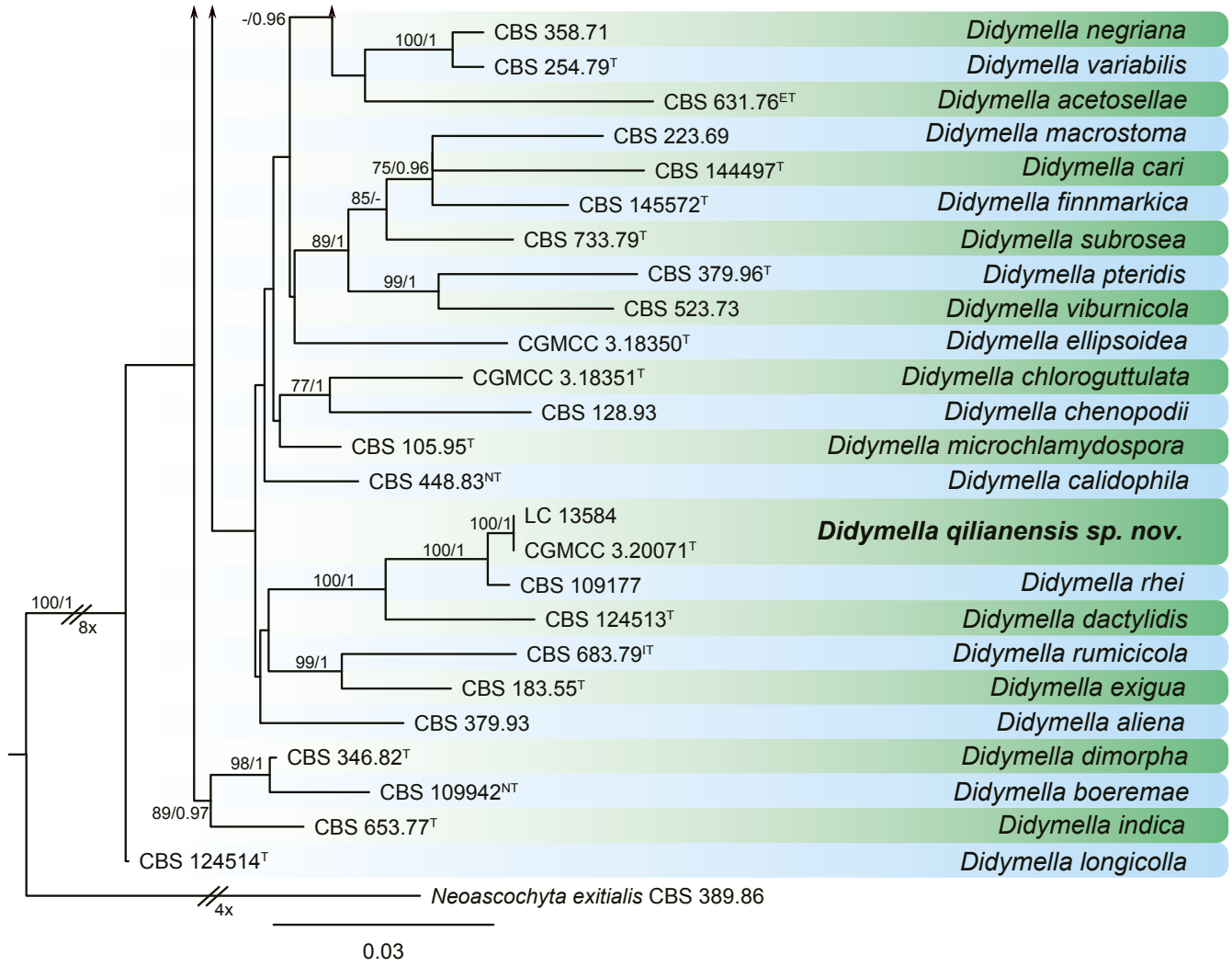

Fig. 24. (Continued).

Notes: *Didymella* was introduced as genus name in 1880, with the description of the type species *Di. exigua*, and later validated when a Latin diagnosis was provided (Saccardo 1880, 1882, de Gruyter *et al*. 2009). It was introduced in the *Mycosphaerellaceae* at first, and subsequently accommodated in several different families, such as *Pleosporaceae*, *Phaeosphaeriaceae*, *Venturiaceae*, and in the *Pleosporales* as *incertae sedis* (de Gruyter *et al*. 2009). The family *Didymellaceae* was established with *Didymella* as type genus, comprising species mostly from two related asexually typified genera *Ascochyta* and *Phoma*. The taxonomy of *Didymellaceae* has been recently revised by Aveskamp *et al*. (2010) and Chen *et al*. (2015b), in which *Ascochyta*, *Didymella* and *Phoma* were resolved based on their phylogenetic relationships, each restricted to a monophyletic group. *Didymella* species are variable in morphology and DNA sequences are necessary for accurate species identification. Among the four DNA barcodes studied, *rpb2* performed best at both generic and species level (Chen *et al*. 2015b, 2017, Valenzuela-Lopez *et al*. 2018, Hou *et al*. 2020a). Currently circumscribed *Didymella* includes phytopathogenic and saprobic fungi associated with more than 40 plants families, and those from clinical samples, such as human lesion, skin, toenails and sputum, and also environmental origin, such as air, soil and lake water (Corlett 1981, Aveskamp *et al*. 2010, Chen *et al*. 2015b, 2017, Valenzuela-Lopez *et al*. 2018, Hou *et al*. 2020a).

References: Boerema *et al*. *2004* (morphology and pathogenicity); Aveskamp *et al*. 2009, 2010, Chen *et al*. 2015b, c, 2017, Valenzuela-Lopez *et al*. 2018, Hou *et al*. 2020a, b (morphology, phylogeny and pathogenicity).

Didymella chlamydospora Qian Chen & L. Cai, ***sp. nov.*** MycoBank MB 834961. Fig. 25.

Etymology: Name reflects its production of chlamydospores.

Conidiomata pycnidial, aggregated, globose to subglobose, later merging into a large irregular one, glabrous, mostly produced on the surface, 130–230 × 90–290 µm; *ostiole* single, elongated to a short wide neck with age; *conidiomatal wall* pseudoparenchymatous 2–4-layered, 11–30 µm thick, composed of isodiametric cells, the outer layer slightly pigmented. *Conidiogenous cells* phialidic, hyaline, smooth, lageniform to ampulliform, doliiform, 4–8.5 × 4–6 µm. *Conidia* variable in shape, ellipsoidal, ovoid or oblong, incidentally slightly curved, smooth- and thin-walled, hyaline, aseptate, 3.5–6.5(–8) × 2.5–3.5 µm, with several polar guttules. *Conidial exudates* pale pink. *Chlamydospores* unicellular, occasionally 1-septate, hyaline or pale brown to brown, thin-walled, intercalary, globose to subglobose, solitary or in short chains, eguttulate, 8–18 µm diam.

Culture characteristics: Colonies on OA, 60–65 mm diam after 1 wk, margin regular, floccose, white, pale olivaceous brown near the centre; reverse cream-white, pale olivaceous to dark olivaceous

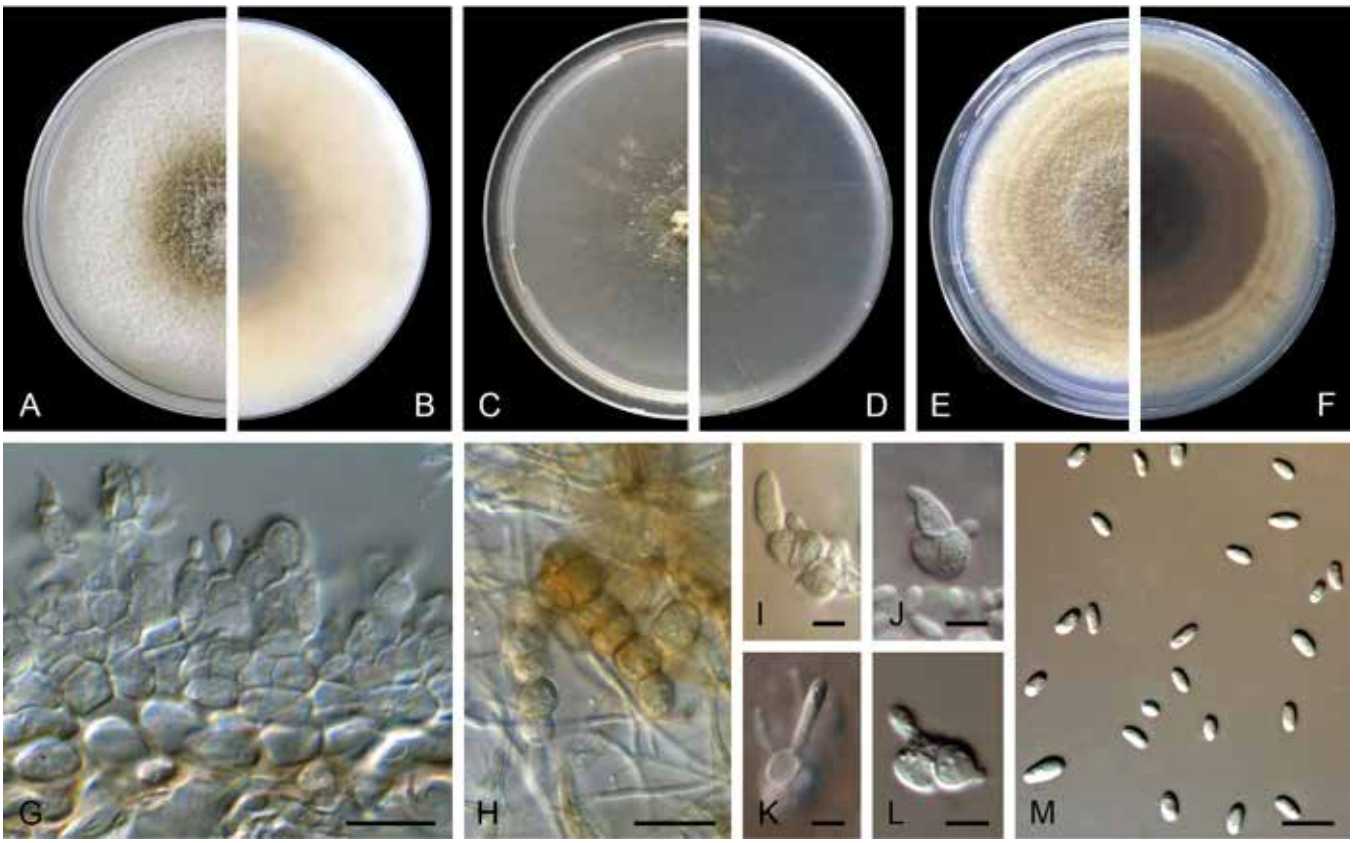

Fig. 25. *Didymella chlamydospora* (ex-type CGMCC 3.20072). **A, B.** Colony on OA (front and reverse). **C, D.** Colony on MEA (front and reverse). **E, F.** Colony on PDA (front and reverse). **G.** Section of conidiomatal wall. **H.** Chlamydospores. **I–L.** Conidiogenous cells. **M.** Conidia. Scale bars: H = 20 µm; G, M = 10 µm; I–L = 5 µm.

towards the centre. Colonies on MEA 55–65 mm diam after 1 wk, margin regular, aerial mycelium sparsely floccosse, pale yellowish olivaceous; reverse concolourous. Colonies on PDA, 55–65 mm diam after 1 wk, margin regular, floccose to woolly, hazel to pale brown, grey near the centre, cream-white near the margin, with pale brown concentric rings; reverse brown, leaden grey to dark brown near the centre, hazel near the margin, with pale brown concentric rings. Application of NaOH results in a pale yellowish green discolouration of the agar.

Typus: **China**, Qinghai Province, Menyuan County, Gangshika snow-capped Mountain, from diseased leaves of *Elymus glaucus* (*Poaceae*), 9 Aug. 2019, L.W. Hou (**holotype** HMAS 248355, dried culture, culture ex-type CGMCC 3.20072 = LC 13587).

Additional materials examined: **China**, Qinghai Province, Menyuan County, Gangshika snow-capped Mountain, from diseased leaves of *Elymus glaucus* (*Poaceae*), 9 Aug. 2019, L.W. Hou, culture LC 13586; Qinghai, Qilian County, Ladong, from diseased leaves of *Polygonum viviparum* (*Polygonaceae*), 9 Aug. 2019, L.W. Hou, culture LC 13588; from diseased leaves of *Polygonum sibiricum* (*Polygonaceae*), 9 Aug. 2019, L.W. Hou, culture LC 13589.

Notes: *Didymella chlamydospora* is phylogenetically closely related to *Didymella prosopidis* (Fig. 24; 5 bp difference in ITS, 2 in LSU, 19 in *rpb2* and 17 in *tub2*), but differs in the size of chlamydospores (8–18 µm diam) from the latter (5–9 µm diam; Crous *et al.* 2013b).

Didymella gei Qian Chen & L. Cai, ***sp. nov.*** MycoBank MB 834956. Fig. 26.

Etymology: Named after the host genus from which the holotype was collected, Geum.

Conidiomata pycnidial, aggregated and confluent, globose to subglobose, brown, glabrous or with few hyphal outgrows, superficial on the agar, 105–260 × 85–225 µm; *ostiole* inconspicuous; *conidiomatal wall* pseudoparenchymatous 2–3-layered, 10–27 µm thick, composed of oblong or isodiametric cells. *Conidiogenous cells* phialidic, hyaline, smooth, ampulliform to doliiform, 5–8.5 × 4–7 µm. *Conidia* oval to oblong, smooth- and thin-walled, hyaline, aseptate, 4–6.5 × 2–2.5 µm, with 1–2 guttules. Conidial exudates not recorded.

Culture characteristics: Colonies on OA, 60–65 mm diam after 1 wk, margin regular, woolly, white near the centre, hazel, abundant brown pycnidia visible; reverse hazel, white to pale saffron near the centre. Colonies on MEA 50–60 mm diam after 1 wk, margin regular, aerial mycelium pale olivaceous grey, floccose to woolly, olivaceous; reverse brownish olivaceous, greyish hazel. Colonies on PDA, 50–60 mm diam after 1 wk, margin regular, floccose to woolly, pale grey to hazel; reverse hazel to pale salmon, dark brown dots forming by pycnidia. Application of NaOH results in a pale brownish green discolouration of the agar.

Typus: **China**, Qinghai Province, Menyuan County, Xianmi National Forest Park, from leaf spots on *Geum* sp. (*Rosaceae*), 8 Aug. 2019, L.W. Hou (**holotype** HMAS 248351, dried culture, culture ex-type CGMCC 3.20068 = LC13581).

Notes: *Didymella gei* formed a distinct lineage sister to *Di. aquatica* and *Di. macrophylla* (Fig. 24). Morphologically, the conidiogenous

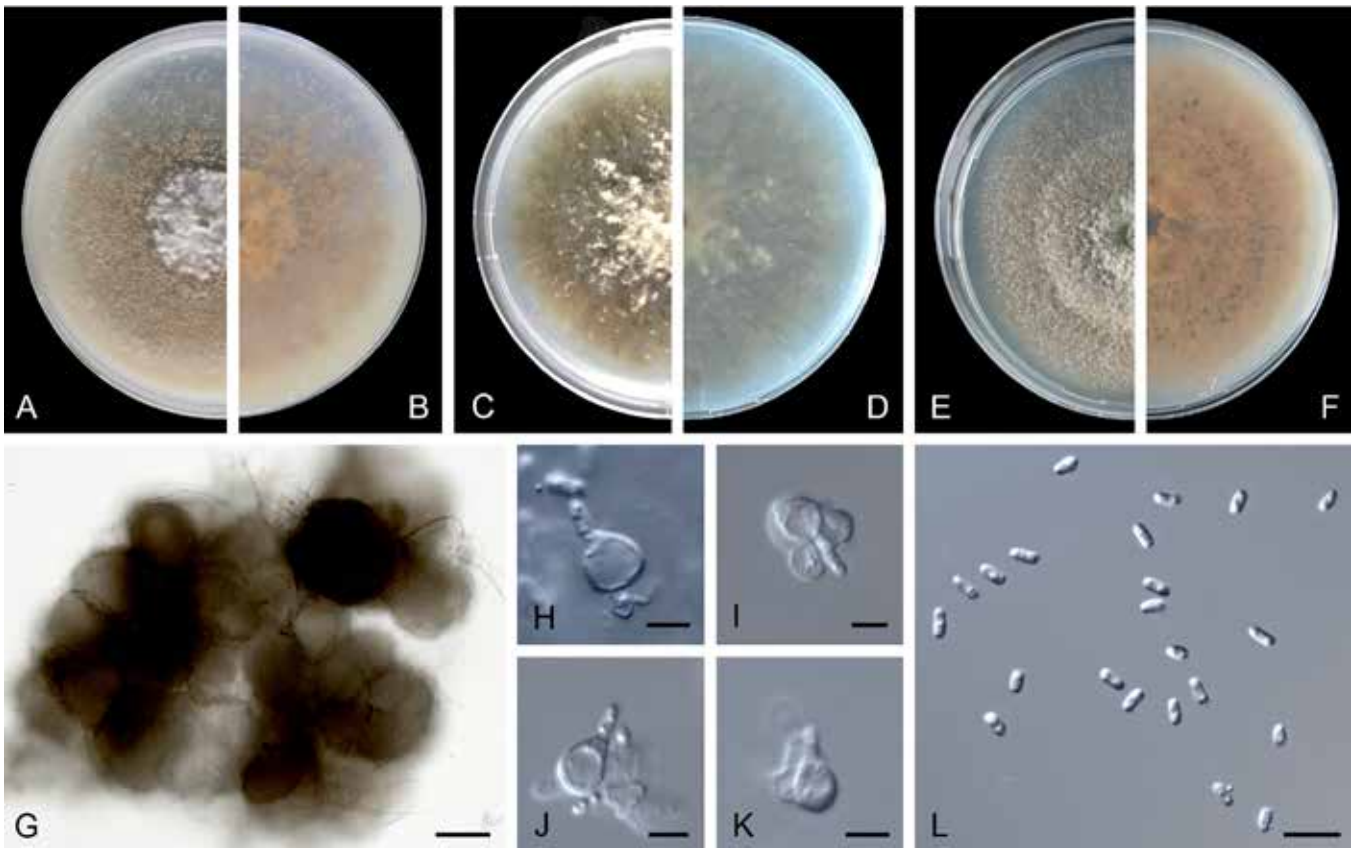

Fig. 26. *Didymella gei* (ex-type CGMCC 3.20068). **A, B.** Colony on OA (front and reverse). **C, D.** Colony on MEA (front and reverse). **E, F.** Colony on PDA (front and reverse). **G.** Conidiomata. **H–K.** Conidiogenous cells. **L.** Conidia. Scale bars: G = 100 µm; L = 10 µm; H–K = 5 µm.

cells of *Di. gei* (5–8.5 × 4–7 µm) are larger than those of *Di. aquatica* (4–5 × 3.5–5 µm). In addition, the ostiole of *Di. gei* is inconspicuous, while the latter have 2–13 ostioles on pycnidia (Chen *et al.* 2017). *Didymella gei* also differs from *Di. macrophylla* in the NaOH test (a pale brownish green discolouration *vs*. negative).

Didymella ligulariae Qian Chen & L. Cai, ***sp. nov.*** MycoBank MB 834957. Fig. 27.

Etymology: Named after the host genus *Ligularia*, from which the holotype of the species was isolated.

Conidiomata pycnidial, mostly solitary, sometimes 2–3 aggregated, globose to subglobose, dark brown, glabrous or with few hyphal outgrows, superficial or (semi-)immersed, 95–260 × 75–190 µm; *ostiole* single, papillate, sometimes elongated to a wide short neck, pale brown; *conidiomatal wall* pseudoparenchymatous, 3–5-layered, 15.5–30 µm thick, composed of oblong or isodiametric cells, outer two layers slightly pigmented. *Conidiogenous cells* phialidic, hyaline, smooth, ampulliform to doliiform, 5.5–8.5 × 4–7.5 µm. *Conidia* oblong to cylindrical, ovoid, incidentally slightly curved, smooth- and thin-walled, hyaline, aseptate, 6–10 × 2.5–4 µm, with large guttules. Conidial exudates not recorded. *Chlamydospores* unicellular, pale brown, intercalary, in chains, globose to subglobose, 8.5–23 µm diam, thick-walled.

Culture characteristics: Colonies on OA, 40–50 mm diam after 1 wk, margin regular, floccose, white aerial mycelium, smoky grey near the centre, buff to pale brown near the margin; reverse buff to pale salmon, olivaceous brown near the centre. Colonies on MEA 45–50 mm diam after 1 wk, margin regular, with scant floccose aerial mycelium, buff; reverse white to buff, with olivaceous shade. Colonies on PDA, 15–40 mm diam after 1 wk, margin regular, covered by woolly, flat, pale grey aerial mycelium, grey near the centre, with several concentric rings forming by aerial mycelium; reverse hazel to brown, with some concentric rings, buff towards the margin. Application of NaOH results in a pale yellowish green discolouration on OA.

Typus: **China**, Qinghai Province, Menyuan County, Xianmi National Forest Park, on diseased leaves of *Ligularia sibirica* (*Asteraceae*), 8 Aug. 2019, M. Li (**holotype** HMAS 248353, dried culture, culture ex-type CGMCC 3.20070 = LC 13583).

Notes: *Didymella ligulariae* clustered in a well-supported clade (MLBS = 94 %; BPP = 1) containing *Di. aquatica*, *Di. bellidis*, *Di. brunneospora*, *Di. gei*, *Di. infuscatispora*, *Di. macrophylla*, *Di. segeticola*, *Di. senecionicola*, *Di. suiyangensis* and *Di. uniseptata* (Fig. 24). *Didymella ligulariae* can be differentiated from all these species by the production of chlamydospores, and differs from *Di. aquatica*, *Di. segeticola* and *Di. suiyangensis* in producing larger conidiogenous cells (5.5–8.5 × 4–7.5 µm *vs* 4–5 × 3.5–5 µm, 5–6.5 × 4–5.5 µm and 4–4.5 × 3–4 µm), from *Di. bellidis*, *Di. brunneospora*, *Di. gei*, *Di. macrophylla* and *Di. senecionicola* in producing larger conidia (6–10 × 2.5–4 µm *vs* 3.8–6.4 × 1.8–2.6 µm, 4.5–7 × 3–3.5 µm, 4–6.5 × 2–2.5 µm, 3.5–5.5 × 1.5–2.5 µm and 4–6.4 × 1.6–2.4 µm), and from *Di. infuscatispora* and *Di. uniseptata* in the colour of conidia (hyaline *vs* hyaline to brown) (de Gruyter *et al.* 1993, Chen *et al.* 2015c, 2017, Valenzuela-Lopez *et al.* 2018). *Didymella ligulariae* is the first species of *Didymella* described from the plant genus *Ligularia.*

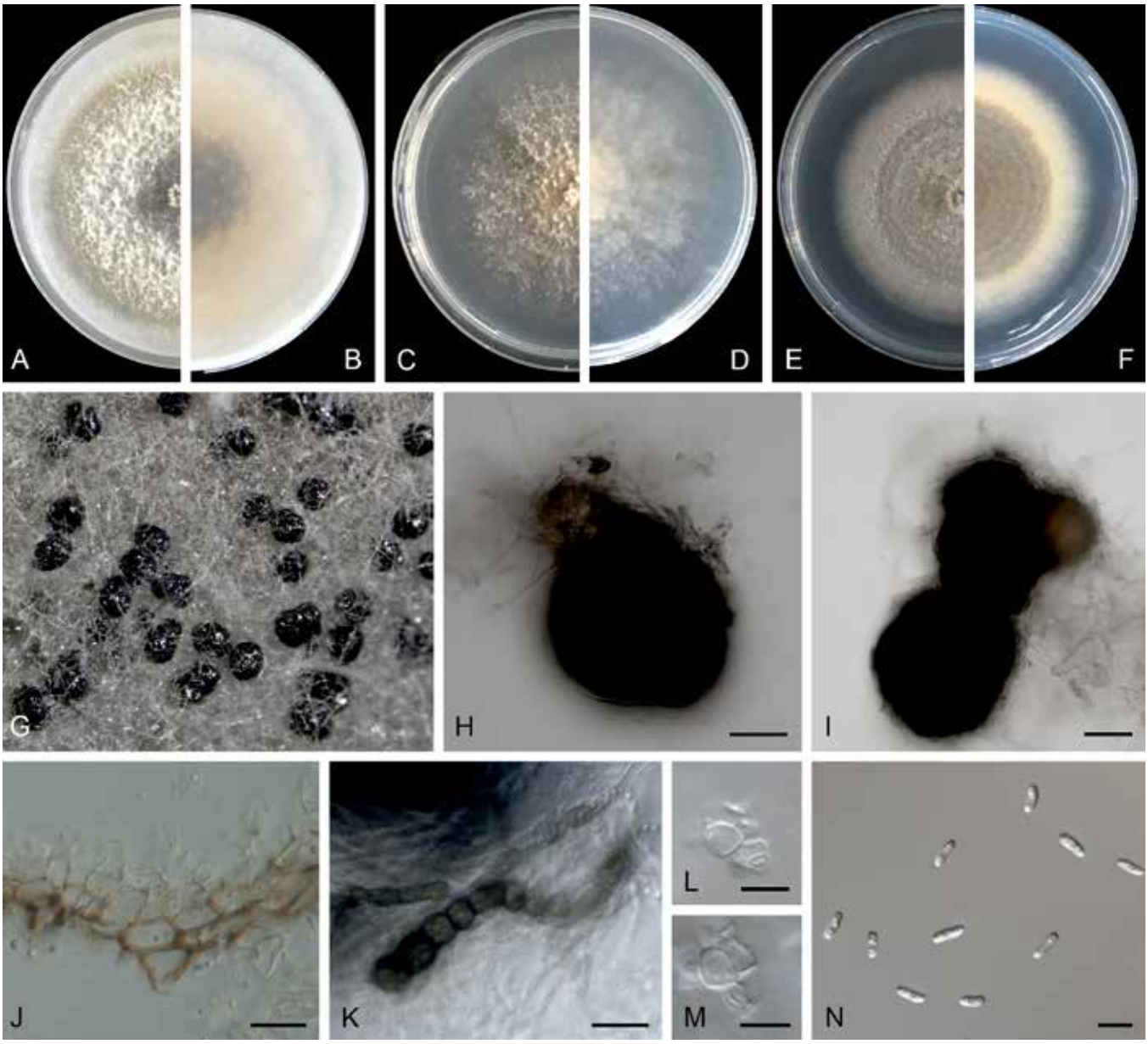

Fig. 27. *Didymella ligulariae* (ex-type CGMCC 3.20070). **A, B.** Colony on OA (front and reverse). **C, D.** Colony on MEA (front and reverse). **E, F.** Colony on PDA (front and reverse). **G.** Conidiomata sporulating on OA. **H, I.** Conidiomata. **J.** Section of conidiomatal wall. **K.** Chlamydospores. **L, M.** Conidiogenous cells. **N.** Conidia. Scale bars: H, I = 50 µm; K = 20 µm; J, L–N = 10 µm.

Didymella qilianensis Qian Chen & L. Cai, ***sp. nov.*** MycoBank MB 834958. Fig. 28.

Etymology: Epithet derived from the location of origin, Qilian County, Qinghai Province in China.

Conidiomata pycnidial, solitary or aggregated, globose to subglobose, pale brown, glabrous, superficial on the agar or semi-immersed, 75–310 × 65–225 µm; *ostiole* single, slightly papillate; *conidiomatal wall* pseudoparenchymatous 2–4-layered, 15.5–28 µm thick, composed of isodiametric cells. *Conidiogenous cells* phialidic, hyaline, smooth, flask-shaped, ampulliform to doliiform, 4.5–8 × 3–6.5 µm. *Conidia* oval, oblong, ovoid, smooth- and thin-walled, hyaline, aseptate, 3.5–7.5(–13.5) × 2–3.5 µm, with several polar guttules. *Conidial matrix* whitish cream.

Culture characteristics: Colonies on OA, 50–55 mm diam after 1 wk, margin regular, floccose to woolly, white aerial mycelium, smoky grey, with buff to pale salmon concentric rings forming by the conidial exudate; reverse smoky grey to leaden dark, buff near the centre, white to pale purple near the margin. Colonies on MEA 40–45 mm diam after 1 wk, margin regular, floccose aerial mycelium, olivaceous; reverse concolourous. Colonies on PDA, 45–50 mm diam after 1 wk, margin regular, floccose to woolly, pale greyish olivaceous to olivaceous, pale salmon near the centre forming by the conidial exudate, pale brown near the margin; reverse dull green. Application of NaOH results in a pale yellowish green discolouration of the agar.

Typus: **China**, Qinghai Province, Qilian County, Ladong, from leaf spots on *Rheum officinale* (*Polygonaceae*), 9 Aug. 2019, L.W. Hou (**holotype** HMAS 248354, dried culture, culture ex-type CGMCC 3.20071 = LC 13585).

Additional material examined: **China**, Qinghai Province, Qilian County, Ladong, from leaf spots on *Rheum officinale* (*Polygonaceae*), 9 Aug. 2019, L.W. Hou, culture LC 13584.

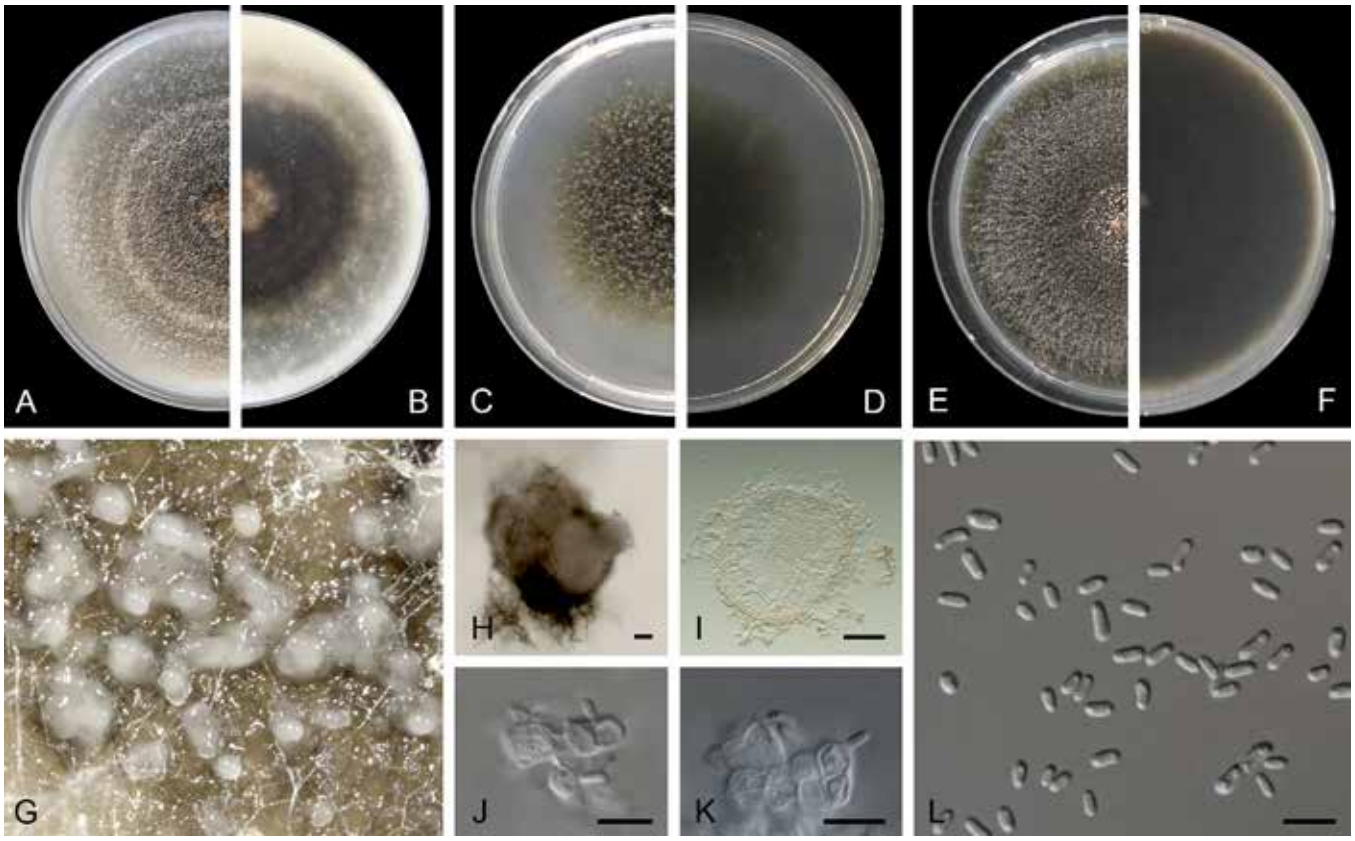

Fig. 28. *Didymella qilianensis* (ex-type CGMCC 3.20071). **A, B.** Colony on OA (front and reverse). **C, D.** Colony on MEA (front and reverse). **E, F.** Colony on PDA (front and reverse). **G.** Conidiomata sporulating on OA. **H.** Conidiomata. **I.** Section through conidiomata. **J, K.** Conidiogenous cells. **L.** Conidia. Scale bars: H, I = 50 µm; J–L = 10 µm.

Notes: *Didymella qilianensis* is closely related to *Di. rhei* (Fig. 24) but differs from the latter species mainly in DNA sequences of *rpb2* and *tub2*. Moreover, *Di. qilianensis* produces narrower conidiogenous cells (4.5–8 × 3–6.5 µm) than those of *Di. rhei* (3–8 × 5–8.5 µm). The NaOH spot test on OA showed a pale yellowish green discolouration of *Di. qilianensis*, while it proved negative for *Di. rhei* (de Gruyter *et al*. 2002).

Didymella uniseptata Qian Chen & L. Cai, ***sp. nov.*** MycoBank MB 834959. Fig. 29.

Etymology: *Name reflects the fact that conidia are 1-septate.*

Conidiomata pycnidial, mostly solitary, sometimes several aggregated, globose to subglobose, dark brown, glabrous or with few hyphal outgrowths, abundant, scattered, mostly produced on the surface, but sometimes partly in the agar, 215–525 × 210–445 µm; *ostiole* inconspicuous; *conidiomatal wall* pseudoparenchymatous 2–6-layered, 16.5–36 µm thick, composed of isodiametric cells, outer 2–3 cell layers slightly pigmented. *Conidiogenous cells* phialidic, hyaline, smooth, ampulliform to doliiform, 8.5–16.5 × 6–11.5 µm. *Conidia* ellipsoidal, ovoid, smooth- and thin-walled, hyaline, later becoming pale brown to brown, 0–1-septate, 8–13 × 4.5–6.5 µm, with numerous minute guttules. Conidial exudates not recorded.

Culture characteristics: Colonies on OA, 40–50 mm diam after 1 wk, margin irregular, aerial mycelium sparse, hazel to pale olivaceous, with an irregular black zone near the centre forming by abundant black pycnidia; reverse concolourous. Colonies on MEA 25–30 mm diam after 1 wk, margin regular, aerial mycelium sparse, woolly, white to pale olivaceous; reverse concolourous. Colonies on PDA, 25–35 mm diam after 1 wk, margin regular, woolly, compact, buff, abundant black pycnidia visible, forming a concentric ring near the centre, white near the margin; reverse buff, black dots and a concentric ring forming by pycnidia. NaOH spot test negative on OA.

Typus: **China**, Qinghai Province, Datong County, Yaozigou National Forest Park, from leaf spots on *Syringa vulgaris* (*Oleaceae*), 6 Aug. 2019, L.W. Hou (**holotype** HMAS 248352, dried culture, culture ex-type CGMCC 3.20069 = LC 13582).

Notes: *Didymella uniseptata* and *Di. infuscatispora* clustered in a well-supported clade (Fig. 24). Morphologically, *Di. uniseptata* can be easily differentiated from the latter by producing larger conidiogenous cells (8.5–16.5 × 6–11.5 µm *vs* 6–8.5 × 5.5–8 µm) and conidia (8–13 × 4.5–6.5 µm *vs* 5–8.5 × 3.5–5.5 µm; Chen *et al.* 2017).

Genome sequenced strain: *Didymella exigua.* **France,** Menise sur Tholon, from *Rumex alpestris* (=*Rumex arifolius*), deposited in CBS May 1955, E. Müller, culture ex-neotype CBS 183.55. This Whole Genome Shutgun project has been deposited at GenBank under the accession JALRMG000000000 (BioProject: PRJNA827019, BioSample: SAMN27594415; present study).

Authors: Q. Chen & L. Cai

Endothia Fr., Sum. Veg. Scand: 385. 1849. Fig. 30.

Classification: *Sordariomycetes*, *Sordariomycetidae*, *Diaporthales*, *Cryphonectriaceae.*

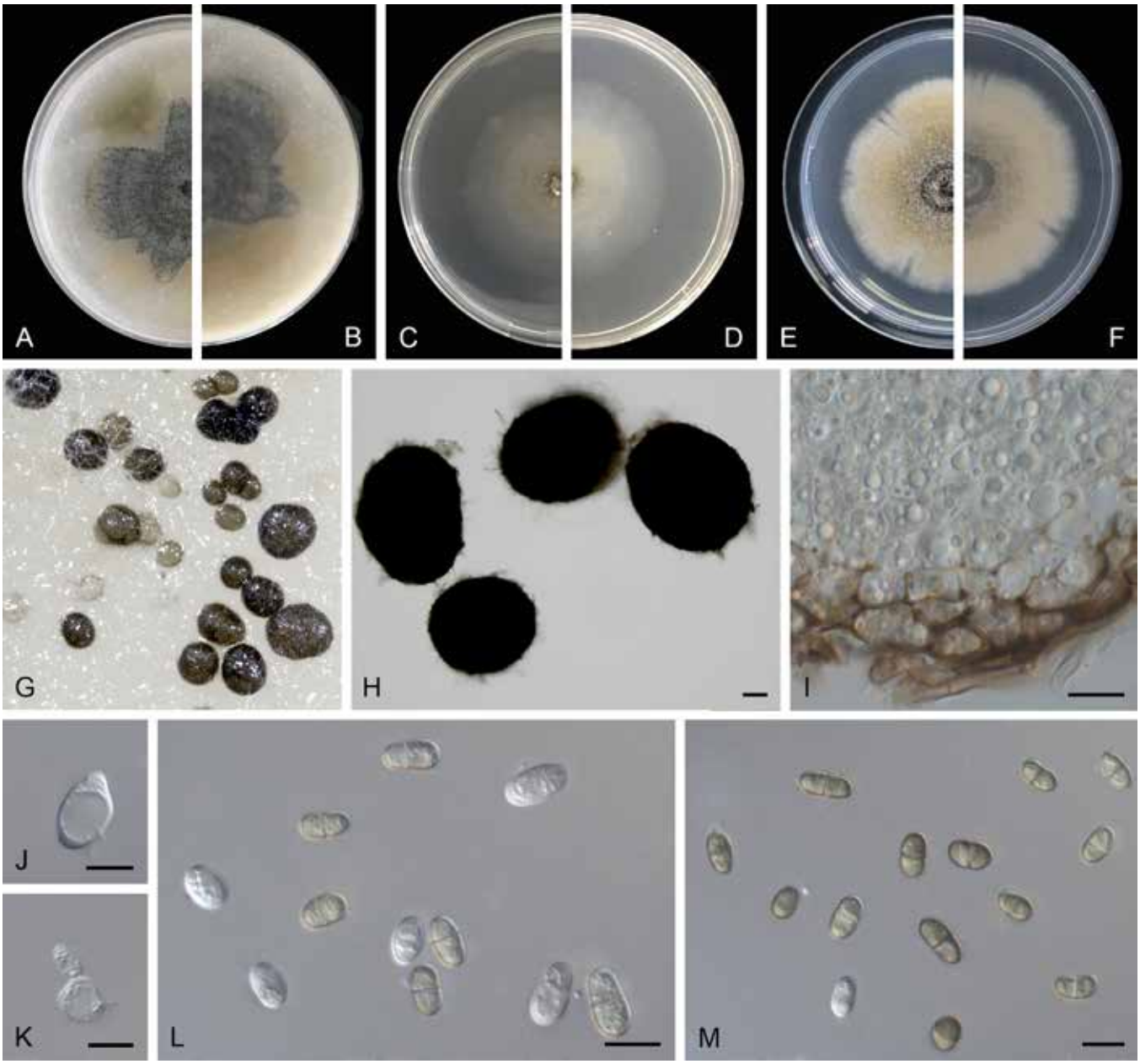

Fig. 29. *Didymella uniseptata* (ex-type CGMCC 3.20069). **A, B.** Colony on OA (front and reverse). **C, D.** Colony on MEA (front and reverse). **E, F.** Colony on PDA (front and reverse). **G.** Conidiomata sporulating on OA. **H.** Conidiomata. **I.** Section of conidiomatal wall. **J, K.** Conidiogenous cells. **L, M.** Conidia. Scale bars: H = 50 µm; I–M = 10 µm.

Type species: *Endothia gyrosa* (Schwein.: Fr.) Fr., basionym: *Sphaeria gyrosa* Schwein.; *Melogramma gyrosum* (Schwein.: Fr.) Tul. & C. Tul.; *Endothia gyrosum* (Schwein.: Fr.) Fuckel. Holotype could not be located, and a neotype from USA is required. Representative strains: CBS 112915 = CMW 2091, CBS 118850 = CMW 10442.

DNA barcodes (genus): LSU, ITS.

DNA barcodes (species): ITS, *tef1*, *tub1*, *tub2*. Table 9. Fig. 31.

Ascostromata large, erumpent, pulvinate to clavate, superficial to semi-immersed to immersed in bark, orange, upper region eustromatic, lower region pseudostromatic. *Stromatic tissues* pseudoparenchymatous on edge of stroma, prosenchymatous in centre. *Perithecia* usually diatrypoid, embedded in stromata at irregular levels, fuscous black. *Perithecial necks* emerge at stromatal surface as black ostioles covered with orange stromatal tissue to form papillae. *Asci* 8-spored, fusiform. *Ascospores* hyaline, cylindrical to fusoid, aseptate. *Conidiomata* part of ascostromata as conidial locules or as separate structures, large, pulvinate, superficial to semi- immersed, orange, multiloculate, non-ostiolate. *Conidiophores* cylindrical or flask-shaped, occasionally with separating septa and branching. *Conidiogenous cells* phialidic. *Paraphyses* or *cylindrical sterile cells* absent. *Conidia* minute, hyaline, cylindrical, aseptate, exuded as orange to sienna droplets.

Culture characteristics: Colonies grown on MEA and PDA showing abundant floccose aerial mycelia, white, yellow white, buff to cinnamon when immature, margins smooth or crenate.

Optimal media and cultivation conditions: *Endothia cerciana*, *E. chinensis*, *E. gyrosa*, *E. singularis*, all display optimal growth on 2 % MEA or 1.8 % PDA at 25 °C.

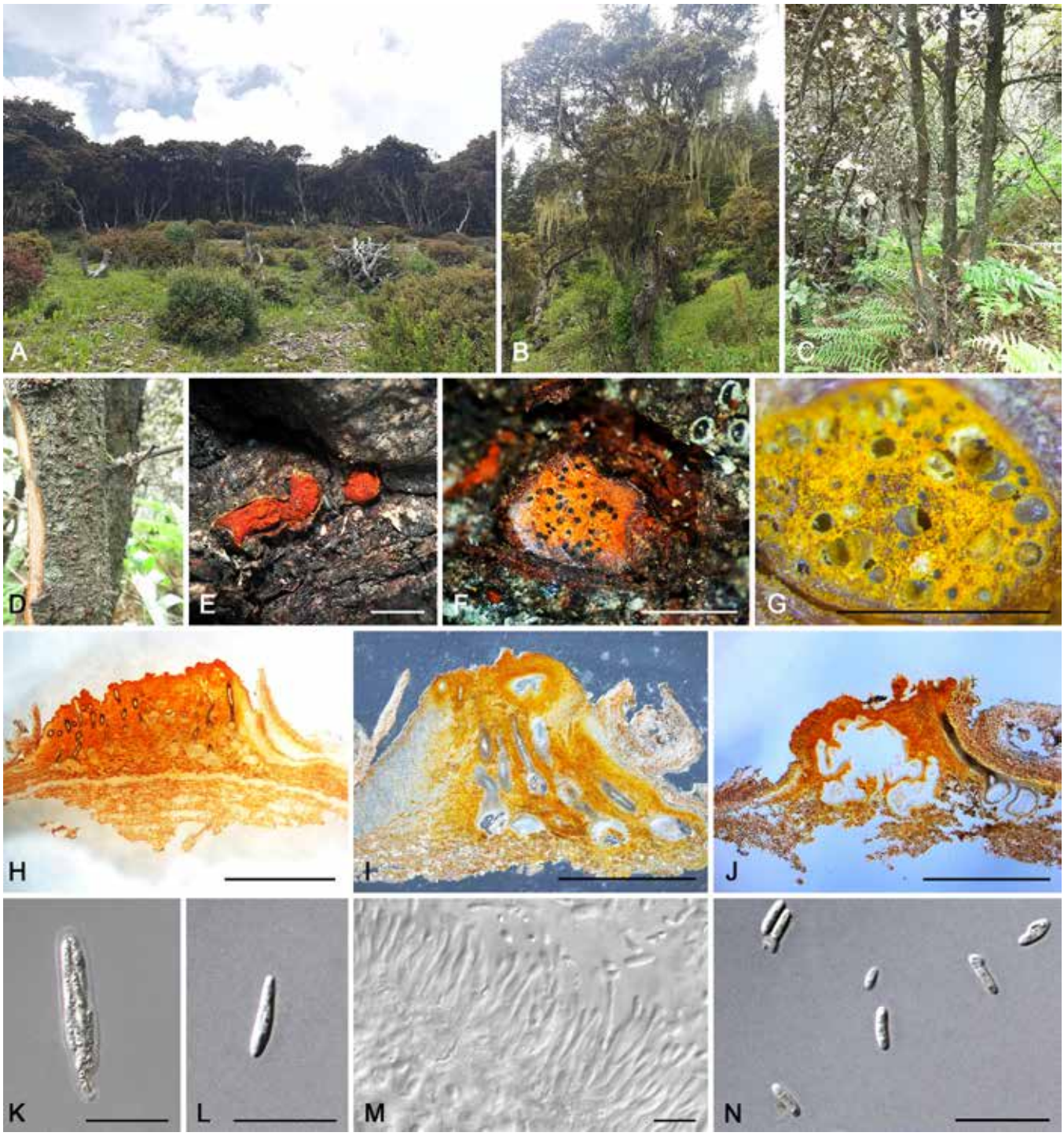

Fig. 30. *Endothia* spp. **A–C.** Host of *Endothia cerciana*. **A, B.** *Quercus aquifolioides*. **C.** *Quercus semecarpifolia*. **D.** Disease symptoms of *Endothia cerciana* on *Quercus semecarpifolia*, showing fruiting structures on bark. **E.** Orange fruiting structures of *Endothia cerciana* on *Quercus semecarpifolia*. **F, G.** Transverse section through ascostromata. **F.** *Endothia cerciana* (HMAS 255732). **G.** *Endothia chinensis* (BJFC-S1432). **H, I.** Longitudinal section through ascostromata of *Endothia cerciana* (HMAS 255732). **J.** Longitudinal section through conidiomata and ascostromata of *Endothia cerciana* (HMAS 255732). **K.** Ascus of *Endothia cerciana* (HMAS 255732). **L.** Ascospore of *Endothia cerciana* (HMAS 255732). **M.** Conidiophores of *Endothia gyrosa* (not available). **N.** Conidia of *Endothia cerciana* (HMAS 255732). Scale bars: E–J = 1 mm; K–N = 10 µm. Picture G taken from Jiang *et al*. (2019b); M from Gryzenhout *et al*. (2009).

Distribution: China, USA.

Hosts: *Acer* (*Aceraceae*), *Castanea*, *Fagus*, *Quercus* (*Fagaceae*), *Corylus* (*Corylaceae*), *Ilex* (*Aquifoliaceae*), *Liquidambar* (*Hamamelidaceae*), *Prunus* (*Rosaceae*), *Ulmus* (*Ulmaceae*) and *Vitis* (*Vitaceae*).

Disease symptoms: Cankers on branches, stems or roots, die-back and defoliation.

Notes: *Endothia* presents the oldest generic name in the *Cryphonectriaceae* (Fries 1849). Previously, *Cryphonectria* was treated as a synonym of *Endothia* (Shear *et al.* 1917, Kobayashi 1970, Roane 1986), and the genus *Endothia* has accommodated most of the known species of *Cryphonectria* and *Endothia* (Micales & Stipes 1987). Currently, *Endothia* and *Holocryphia* are the only genera in *Cryphonectriaceae* with aseptate ascospores. These two genera can be distinguished by their stromatal structures: the stromata of *Endothia* are large, erumpent, and no paraphyses

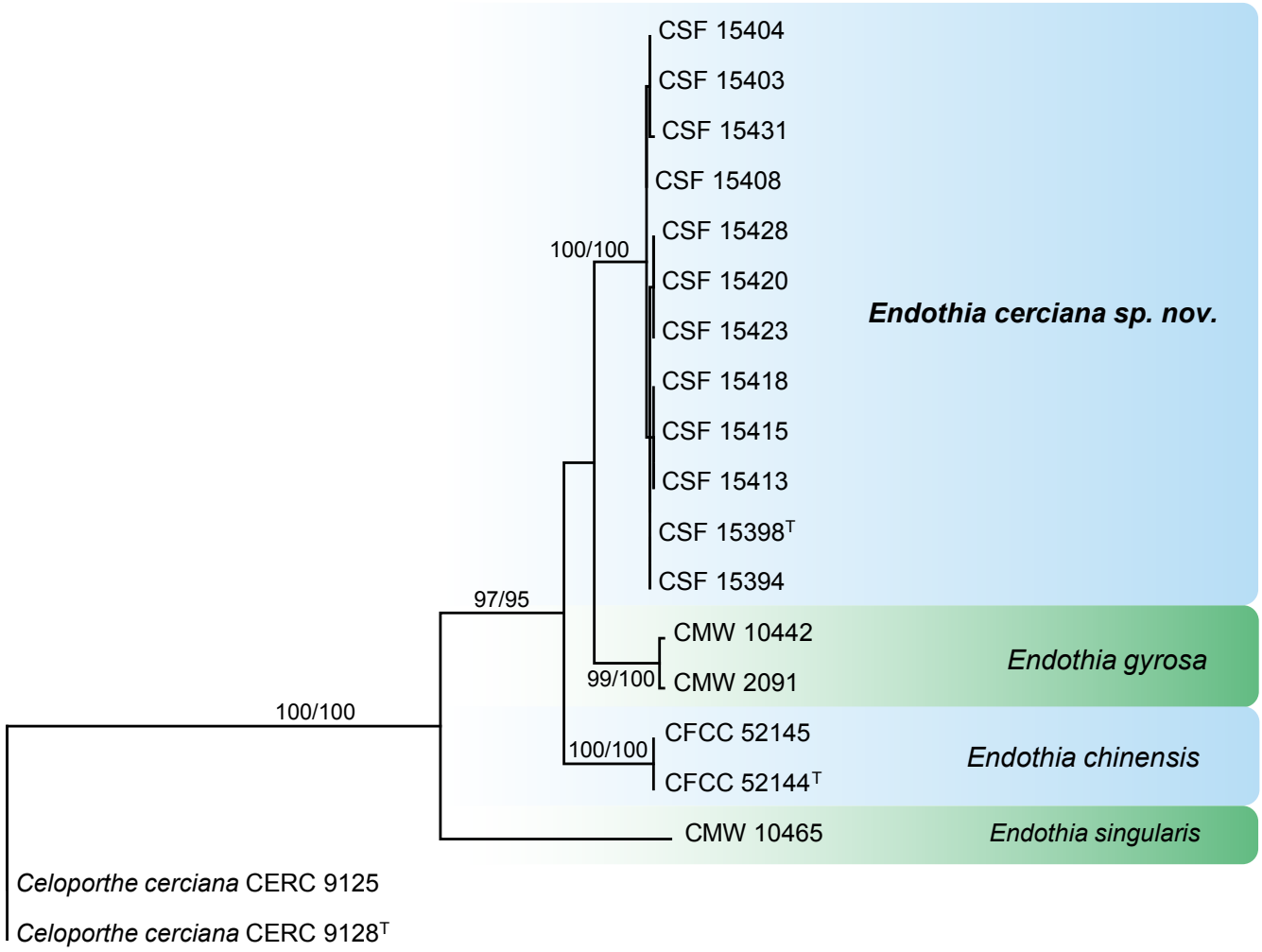

Fig. 31. Maximum Likelihood (ML) phylogram constructed from ITS (480 bp), *tub2* (360 bp), *tub1* (410 bp) and *tef1* (185 bp) sequences of all accepted species of *Endothia*. Bootstrap support values (> 70 %) for ML and maximum parsimony (MP) analyses are presented at the nodes (ML/MP). The novel taxon is printed in **bold**. The phylogenetic tree was rooted to *Celoporthe cerciana* CERC 9125 and CERC 9128. GenBank accession numbers are indicated in Table 9. [T] indicates ex-type strains. TreeBASE: S26038.

are produced among conidiophores (Barr 1978, Myburg *et al.* 2004, Gryzenhout *et al.* 2009, Jiang *et al.* 2019b), while stromata of *Holocryphia* are smaller, and prominent paraphyses are present among conidiophores (Venter *et al.* 2002, Gryzenhout *et al.* 2009). Four species reside in *Endothia*, *i.e. E. cerciana*, *E. chinensis*, *E. gyrosa* and *E. singularis* (Fries 1849, Shear *et al.* 1917, Gryzenhout *et al.* 2009, Jiang *et al.* 2019b). Although some morphological differences exist among these species, such as sizes of ascospores and conidia, DNA sequence data are essential to species identifications (Venter *et al.* 2002, Myburg *et al.* 2004, Gryzenhout *et al.* 2009, Jiang *et al.* 2019b). The ITS and *tub* (*tub1* and *tub2*) regions provide accurate species resolution when used alone, and the combination of these regions provide stronger support (Venter *et al.* 2002, Myburg *et al.* 2004, Gryzenhout *et al.* 2009, Jiang *et al.* 2019b). *Endothia gyrosa* was the first species described from what now represents the *Cryphonectriaceae* (Fries 1849). This species has been reported from many different woody plant hosts, including species of *Acer*, *Castanea*, *Corylus*, *Fagus*, *Ilex*, *Liquidambar*, *Prunus*, *Quercus*, *Ulmus* and *Vitis* (Shear *et al.* 1917, Snow *et al.* 1974, Roane 1986) and it has an extensive distribution in North America (Shear *et al.* 1917). *Endothia singularis* was reported from several species of *Quercus* in the USA (Gryzenhout *et al.* 2009). *Endothia cerciana* and *E. chinensis* were both only reported in China, *E. cerciana* from *Quercus aquifolioides* and *Q. semecarpifolia*, and *E. chinensis* from *Castanea mollissima* (Jiang *et al.* 2019b). *Endothia gyrosa* caused cankers on branches, stems or roots that results in die-back, defoliation and decline of trees (Stipes & Phipps 1971, Roane *et al.* 1974), and *E. chinensis* is pathogenic to detached *C. mollissima* branches (Jiang *et al.* 2019b), but whether *E. cerciana* is pathogenic to its original hosts is unknown.

References: Venter *et al.* 2002, Myburg *et al.* 2004, Gryzenhout *et al.* 2009, Jiang *et al.* 2019b (morphology, nomenclature, phylogeny and pathogenicity); Gryzenhout *et al.* 2006, 2009, Wang *et al.* 2020b, Jiang *et al.* 2020 (higher classification).

Endothia cerciana W. Wang & S.F. Chen, ***sp. nov.*** MycoBank MB 842889. Fig. 32.

Etymology: The name refers to CERC, a research institute that is pioneering the study of tree diseases caused by *Cryphonectriaceae* in China.

Table 9. DNA barcodes of accepted *Endothia* spp.

Species	Isolates[1]	GenBank accession numbers[2]				References
		ITS	*tub2*	*tub1*	*tef1*	
Endothia cerciana	CSF 15394	OM801200	OM685025	OM685037	OM685049	Present study
	CSF 15398 = CGMCC 3.20105^T	OM801201	OM685026	OM685038	OM685050	Present study
	CSF 15403	OM801202	OM685027	OM685039	OM685051	Present study
	CSF 15404	OM801203	OM685028	OM685040	OM685052	Present study
	CSF 15408	OM801204	OM685029	OM685041	OM685053	Present study
	CSF 15413	OM801205	OM685030	OM685042	OM685054	Present study
	CSF 15415	OM801206	OM685031	OM685043	OM685055	Present study
	CSF 15418	OM801207	OM685032	OM685044	OM685056	Present study
	CSF 15420 = CGMCC 3.20106	OM801208	OM685033	OM685045	OM685057	Present study
	CSF 15423	OM801209	OM685034	OM685046	OM685058	Present study
	CSF 15428	OM801210	OM685035	OM685047	OM685059	Present study
	CSF 15431	OM801211	OM685036	OM685048	OM685060	Present study
E. chinensis	CFCC 52144^T	MH514027	MH539690	MH539680	MN271860	Jiang *et al*. (2019b, 2020)
	CFCC 52145	MH514028	MH539691	MH539681	—	Jiang *et al*. (2019b, 2020)
E. gyrosa	CMW 2091 = CBS 112915	AF368325	AH011601	AH011601	—	Venter *et al*. (2002), Gryzenhout *et al*. (2006)
	CMW 10442 = CBS 118850	AF368326	AH011602	AH011602	—	Venter *et al*. (2002), Gryzenhout *et al*. (2006)
E. singularis	CMW 10465 = CBS 112921	AF368323	AH011599	AH011599	—	Venter *et al*. (2002), Myburg *et al*. (2004)

[1] CBS: Westerdijk Fungal Biodiversity Institute, Utrecht, Netherlands; CSF: Collections at China Eucalypt Research Centre, Chinese Academy of Forestry, Zhanjiang, Guangdong, China; CFCC: China Forestry Culture Collection Center, Beijing, China; CGMCC: Chinese General Microbiological Culture Collection Center, Beijing, China; CMW: Tree Protection Co-operative Program, Forestry and Agricultural Biotechnology Institute, University of Pretoria, South Africa. ^{T} indicates ex-type strain.

[2] ITS: internal transcribed spacers and intervening 5.8S nrDNA; *tef1*: partial translation elongation factor 1-α gene; *tub1*, *tub2*: partial β-tubulin gene.

Ascostromata on host single, pulvinate, large, semi-immersed to immersed in bark, orange, 850–1500 µm high, 800–4250 µm diam, upper region eustromatic, lower region pseudostromatic. *Stromatic tissues* pseudoparenchymatous on edge of stroma, prosenchymatous in centre. *Perithecia* usually diatrypoid, embedded in stromata at irregular levels, fuscous black. *Perithecial necks* emerge at stromatal surface as black ostioles covered with orange stromatal tissue to form papillae extending up to 200 µm above stromatal surface. *Asci* (21–)24.5–35(–39) × (4.5–)5–7(–8.5) µm (av. 30 × 6 µm), oblong ellipsoidal to sub-clavate, 8-spored. *Ascospores* (7–)8.5–10.5(–12) × (1–)1.5–2 µm (av. 9.5 × 1.6 µm), hyaline, ellipsoidal to fusoid, ends round, aseptate. *Conidiomata* part of ascostromata as conidial locules or separate structures, large, pulvinate, semi-immersed to immersed in bark, orange, multiloculate structures with the same tissue morphology, stromatic structure and size to the ascostromata, locules numerous in labyrinthine pattern, non-ostiolate. *Conidiophores* (6–)8–10(–14) µm long, occasionally with separating septa and branching, hyaline. *Conidiogenous cells* 1–1.5 µm wide, cylindrical or flask-shaped with attenuated apices. *Paraphyses* or *cylindrical sterile cells* absent. *Conidia* (3.5–)4.5–5.5(–6) × 1–1.5 µm (av. 5 × 1.3 µm), hyaline, cylindrical, aseptate.

Culture characteristics: Colonies grown on 2 % MEA showing abundant floccose aerial mycelia, white when young, turning buff to cinnamon after 2 wk, margins smooth or crenate; reverse white to buff, often makes growth medium perilla purple. Optimal growth temperature 25 °C, grow slowly at 5 °C and 35 °C. After 1 wk, the colonies at 5 °C, 10 °C, 15 °C, 20 °C, 25 °C, 30 °C, and 35 °C reached 8.5, 18, 31, 65, 82, 17, and 8 mm, respectively.

Typus: **China**, Sichuan Province, Ganzi Region, Batang County, Moduo Town, Moduo Village, 30°14'0.1032"N, 99°15'19.8252"E, from the stem bark of *Quercus semecarpifolia* (*Fabaceae*), 28 Jun. 2018, S.F. Chen, W. Wang & Q.C. Wang (**holotype** HMAS 255732, culture ex-type CSF 15398 = CGMCC 3.20105).

Additional materials examined: **China**, Sichuan Province, Ganzi Region, Yajiang County, Bajiao Town, Rimu Village, 30°4'22.44"N, 101°9'58.6164"E, from the stem bark of *Quercus aquifolioides* (*Fagaceae*), 30 Jun. 2018, S.F. Chen, W. Wang & Q.C. Wang, HMAS 255733, culture CSF 15420 = CGMCC 3.20106; *ibid.* cultures CSF 15394, CSF 15403, CSF 15404, CSF 15408, CSF 15413, CSF 15415, CSF 15418, CSF 15423, CSF 15428, CSF 15431.

Notes: *Endothia cerciana* isolated from *Quercus* species in China represents a fourth species in this genus (Table 9). It is closely related to *E. gyrosa* in the phylogenetic analysis (Fig. 31). *Endothia cerciana*, *E. chinensis*, *E.* gyrosa and *E. singularis* all produce perithecia embedded in stromata at irregular levels, with paraphyses or cylindrical sterile cells absent (asexual morph is unknown for *E. chinensis*) (Gryzenhout *et al.* 2009, Jiang *et al.* 2019b). Some differences have been observed among the four species in ascospore and conidial dimensions. The ascospores of

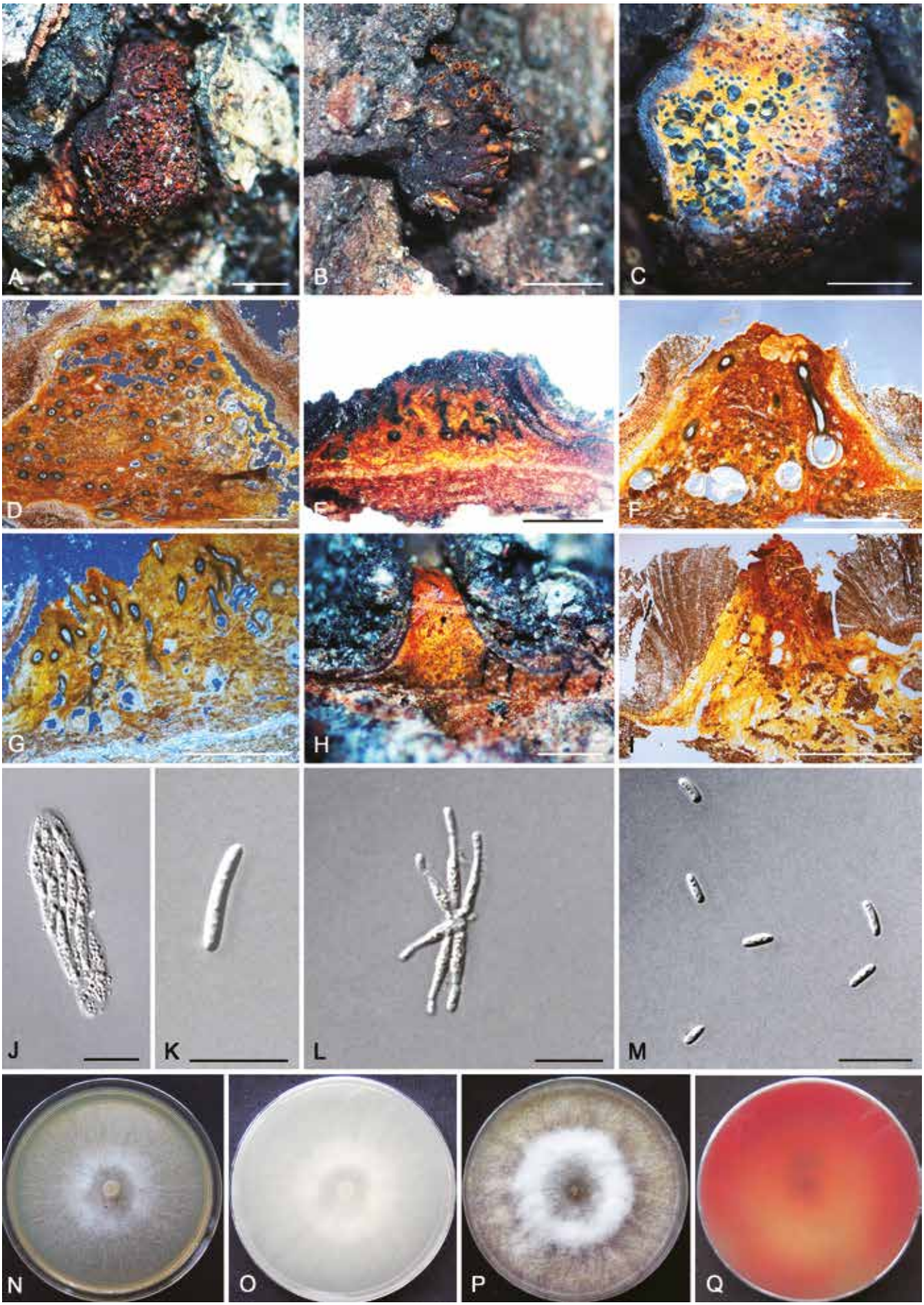

Fig. 32. *Endothia cerciana* (ex-type CGMCC 3.20105). **A, B.** Fruiting structures on canker. **C, D.** Transverse section through ascostromata. **E–G.** Longitudinal section through ascostromata. **H, I.** Longitudinal section through conidiomata. **J.** Ascus. **K.** Ascospore. **L.** Conidiophores. **M.** Conidia. **N–Q.** Colonies on 2 % MEA in 1 wk (N: front, O: reverse) and 30 d (P: front, Q: reverse) in dark. Scale bars: A–I = 1 mm; J–M = 10 µm.

E. gyrosa (av. 10 × 2 µm) are longer than *E. cerciana* (av. 9.5 × 1.6 µm), *E. chinensis* (av. 8.5 × 1.5 µm) and *E. singularis* (av. 9 × 2.5 µm), and the ascospores of *E. chinensis* are the smallest, while *E. singularis* are the widest. The conidia of *E. cerciana* (av. 5 × 1.3 µm) are narrower than those of *E. gyrosa* (av. 3.75 × 1.5 µm) and *E. singularis* (av. 3.5 × 1.5 µm) (Gryzenhout *et al.* 2009, Jiang *et al.* 2019b).

Genome sequenced strain: *Endothia cerciana.* **China**, from the stem bark of *Quercus semecarpifolia*, 28 Jun. 2018, S.F. Chen, W. Wang & Q.C. Wang, culture ex-type CSF 15398 = CGMCC 3.20105. This Whole Genome Shutgun project has been deposited at GenBank under the accession JALRMH000000000 (BioProject: PRJNA827019, BioSample: SAMN27594416; present study).

Authors: W. Wang & S.F. Chen

Leptosphaerulina McAlpine, Fungus Diseases of stone-fruit trees in Australia: 103. 1902. Fig. 33.

Fig. 33. *Leptosphaerulina* spp. **A–C.** Disease symptoms. **A.** Symptoms caused by *Leptosphaerulina miscanthi* (ex-type CGMCC 3.20073) on *Miscanthus floridulus*. **B.** Symptoms caused by *Leptosphaerulina miscanthi* (LC 13590) on *Swertia tetraptera*. **C.** Symptoms caused by *Leptosphaerulina miscanthi* (LC 13591) on *Sonchus asper*. **D–R.** Sexual morph. **D.** Ascoma with asci of *Leptosphaerulina conyzicola* (ex-type VIC 31627). **E.** Ascoma of *Leptosphaerulina sisyrinchiicola* (ex-type CBS 121688). **F, G.** Sections through ascoma. **F.** *Leptosphaerulina longiflori* (holotype MFLU18–2527). **G.** *Leptosphaerulina obtusispora* (ex-type CBS 569.94). **H–L.** Asci. **H.** *Leptosphaerulina conyzicola* (ex-type VIC 31627). **I.** *Leptosphaerulina saccharicola* (holotype MFLU11-0205). **J.** *Leptosphaerulina longiflori* (holotype MFLU18–2527). **K.** *Leptosphaerulina obtusispora* (ex-type CBS 569.94). **L.** *Leptosphaerulina sisyrinchiicola* (ex-type CBS 121688). **M–R.** Ascospores. **M.** *Leptosphaerulina conyzicola* (ex-type VIC 31627). **N.** *Leptosphaerulina saccharicola* (holotype MFLU11-0205). **O.** *Leptosphaerulina longiflori* (holotype MFLU18–2527). **P.** *Leptosphaerulina obtusispora* (ex-type CBS 569.94). **Q.** *Leptosphaerulina sisyrinchiicola* (ex-type CBS 121688). **R.** *Leptosphaerulina australis* (CBS 116307). Scale bars: E = 50 µm; D, G, K, L = 20 µm; F, H, I, P–R = 10 µm; J, M–O = 5 µm. Pictures D, H, M taken from Duarte *et al.* (2016); E, G, K, L, P, Q from Hou *et al.* (2020a); F, J, O from Tennakoon *et al.* (2019); I, N from Phookamsak *et al.* (2013); R from Crous *et al.* (2011c).

Classification: *Dothideomycetes*, *Pleosporomycetidae*, *Pleosporales*, *Didymellaceae*.

Type species: *Leptosphaerulina australis* McAlpine. Reference strain: CBS 317.83.

DNA barcodes (genus): LSU, ITS.

DNA barcodes (species): *rpb2*, *tub2*. Table 10. Fig. 34.

Ascomata pseudothecial, immersed or erumpent, solitary or clustered, obpyriform to subglobose, globose, membranous, ostiolate; *ascomatal* wall multi-layers, composed of cells in *textura angularis*. *Asci* clavate to ovoid, or obovoid, subglobose, obpyriform, saccate, oblong, bitunicate, 8-spored. *Ascospores* muriform or phragmosporous, oblong to cylindrical, ellipsoidal to obovoid, subfusoid, hyaline to brown, smooth, 1(–9)-septate (including transverse and longitudinal), sometimes slightly constricted at the septum, biseriate or triseriate, sometimes surrounded by a thin mucilaginous sheath (Saccardo 1905, Graham & Luttrell 1961, Roux 1986, Inderbitzin *et al.* 2000, Abler 2003, Crous *et al.* 2011c, Hou *et al.* 2020a). *Conidiophores* mononematous, solitary, with one apical pore, mostly unbranched, septate, hyaline to pale brown, smooth-walled. *Conidiogenous cells* holoblastic, integrated, terminal, cylindrical, hyaline to brown. *Conidia* solitary thalloconidia, oblong to cylindrical or ellipsoidal, muriform or phragmosporous,

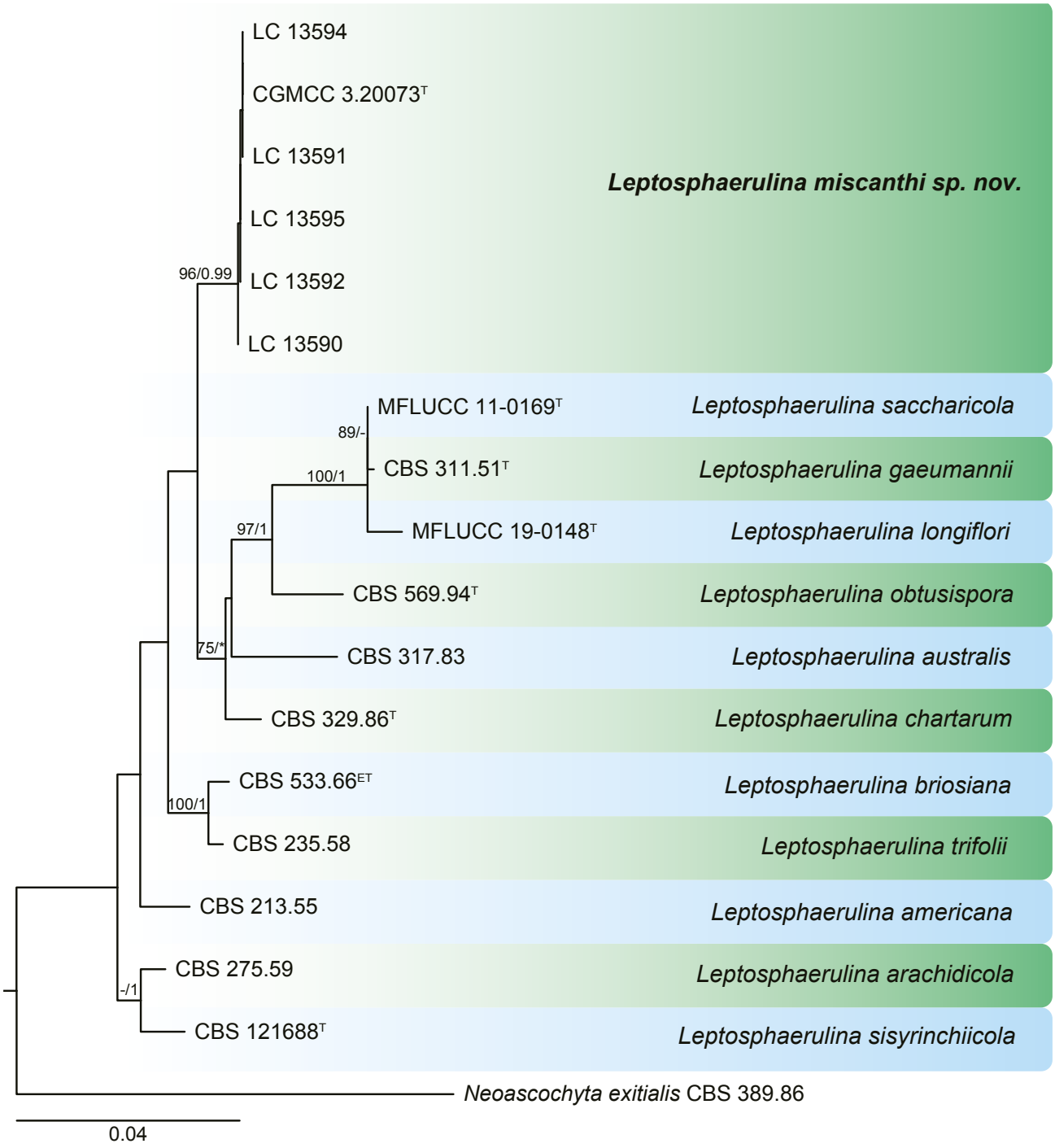

Fig. 34. Maximum Likelihood (ML) phylogram constructed from LSU (960 bp), ITS (453 bp), *tub2* (333 bp) and *rpb2* (596 bp) sequences of all accepted species of *Leptosphaerulina*. RAxML bootstrap support values (> 70 %) and Bayesian posterior probability scores (> 0.90) are shown at the nodes. The novel taxon is printed in **bold**. The phylogenetic tree was rooted to *Neoascochyta exitialis* CBS 389.86. GenBank accession numbers are indicated in Table 10. T and ET indicate ex-type and ex-epitype strains, respectively. TreeBASE: S26039.

Table 10. DNA barcodes of accepted *Leptosphaerulina* spp.

Species	Isolates[1]	GenBank accession numbers[2]				References
		LSU	ITS	*rpb2*	*tub2*	
Leptosphaerulina americana	CBS 213.55	GU237981	GU237799	KT389641	GU237539	Aveskamp *et al.* (2010), Chen *et al.* (2015b)
L. arachidicola	CBS 275.59	GU237983	GU237820	MT018278	GU237543	Aveskamp *et al.* (2010), Hou *et al.* (2020a)
L. australis	CBS 317.83	EU754166	GU237829	GU371790	GU237540	de Gruyter *et al.* (2009), Aveskamp *et al.* (2010)
L. briosiana	CBS 533.66^{ET}	MN943804	EU167575	MT018266	MT005704	Simon *et al.* (2009), Hou *et al.* (2020a)
L. chartarum	CBS 329.86^{T}	MN943813	MN973604	MT018277	MT005714	Hou *et al.* (2020a)
L. gaeumannii	CBS 311.51^{T}	MN943810	MN973601	MT018274	MT005711	Hou *et al.* (2020a)
L. longiflori	MFLUCC 19-0148^{T}	MK503811	MK503800	MK503805	—	Tennakoon *et al.* (2019)
L. miscanthi	LC 13590	MT229680	MT229703	MT239100	MT249271	Present study
	LC 13591	MT229681	MT229704	MT239101	MT249272	Present study
	LC 13592	MT229682	MT229705	MT239102	MT249273	Present study
	CGMCC 3.20073 = LC 13593^{T}	MT229683	MT229706	MT239103	MT249274	Present study
	LC 13594	MT229684	MT229707	MT239104	MT249275	Present study
	LC 13595	MT229685	MT229708	MT23910	MT249276	Present study
L. obtusispora	CBS 569.94^{T}	MN943811	MN973602	MT018275	MT005712	Hou *et al.* (2020a)
L. saccharicola	MFLUCC 11-0169^{T}	KF670716	KF670717	KF670714	—	Phookamsak *et al.* (2013)
L. sisyrinchiicola	CBS 121688^{T}	MN943814	MN973605	MT018279	MT005715	Hou *et al.* (2020a)
L. trifolii	CBS 235.58	GU237982	GU237806	MT018271	GU237542	Aveskamp *et al.* (2010), Hou *et al.* (2020a)

[1] CBS: Westerdijk Fungal Biodiversity Institute, Utrecht, the Netherlands; CGMCC: Chinese General Microbiological Culture Collection Center, Beijing, China; LC: Dr Lei Cai's personal collection deposited in laboratory, housed at Chinese Academy of Sciences, China; MFLUCC: Mae Fah Luang University Culture Collection, Chiang Rai, Thailand. ^{T} and ^{ET} indicate ex-type and ex-epitype strains, respectively.

[2] ITS: internal transcribed spacers and intervening 5.8S nrDNA; LSU: partial 28S large subunit nrRNA gene; *rpb2*: partial RNA polymerase II second largest subunit gene; *tub2*: partial β-tubulin gene.

initially hyaline, becoming brown to dark brown, mostly with 3–4 transverse septa and 0–1 longitudinal septa (Phookamsak *et al.* 2013).

Cultural characteristics: Colonies on OA covered by flat aerial mycelium, pale olivaceous to olivaceous black, sometimes dirty white near the centre, olivaceous grey to iron-grey near the margin, margin regular.

Optimal media and cultivation conditions: OA or sterile pine needles placed on OA under nuv-light (12 h light, 12 h dark) to promote sporulation at 20 to 25 °C.

Distribution: Worldwide.

Hosts: Occurring on forage plants as saprobes and pathogens, mainly found in members of *Fabaceae*, and also on other plants of *Aizoaceae*, *Asteraceae*, *Caprifoliaceae*, *Gentianaceae*, *Iridaceae*, *Liliaceae*, *Myrtaceae*, *Poaceae*, *Rhizophoraceae*, *Rosaceae* and *Vitaceae*.

Disease symptoms: Leaf blight, leaf scorch, leaf spot, pepper spot, stem spots.

Notes: *Leptosphaerulina comprises plant pathogenic species that cause leaf spot and pepper spot mainly on* legumes and turfgrasses, and saprophytes on decaying or dead branches, stems or leaves (Graham & Luttrell 1961, Inderbitzin *et al.* 2000, Abler 2003, Phookamsak *et al.* 2013, Chen *et al.* 2015b, Tennakoon *et al.* 2019). This genus is well characterised by small, immersed-erumpent ascomata, bitunicate, saccate, obpyriform or oblong asci, and muriform, hyaline or pigmented ascospores (Graham & Luttrell 1961, Barr 1972, Chen *et al.* 2015b, Tennakoon *et al.* 2019). *Leptosphaerulina chartarum* was reported to be the sexual morph of *Pithomyces chartarum* (Roux 1986), but this has been refuted by molecular evidence. Recent phylogenetic studies showed that the genus *Pithomyces* resided in the family *Astrosphaeriellaceae*, clearly distant from *Didymellaceae* (Pratibha & Prabhugaonkar 2015, Wanasinghe *et al.* 2019). To date, the asexual morph of *Leptosphaerulina w*as only recorded for *L. saccharicola* by Phookamsak *et al.* (2013), which produced hyaline to brown, muriform or phragmosporous conidia from mononematous conidiophores on hyphae. Among the names under *Leptosphaerulina*, 13 have been recognised based on both morphology and molecular data. Nevertheless, *L. conyzicola* from the weed *Conyza canadensis* was not included in the phylogenetic tree, because only LSU sequence data are available (Duarte *et al.* 2016).

References: Graham & Luttrell 1961, Roux 1986, Inderbitzin *et al.* 2000, Abler 2003, Crous *et al.* 2011c, Phookamsak *et al.* 2013, Tennakoon *et al.* 2019, Hou *et al.* 2020a (morphology and pathogenicity); de Gruyter *et al.* 2009, Aveskamp *et al.* 2010, Chen *et al.* 2015b (phylogeny).

Leptosphaerulina miscanthi Qian Chen & L. Cai, ***sp. nov.*** MycoBank MB 834960. Fig. 35.

Etymology: Name after *Miscanthus*, the grass genus from which it was collected.

Ascomata pseudothecial, superficial or semi-immersed, solitary or aggregated, uniloculate, globose to subglobose, membranous, brown, 165–330 × 125–210 µm; *ostioles* circular, central, papillate; *pseudothecial wall pseudoparenchymatous*, of *textura angularis*, 2–4 layers, outer wall 2–3-layered, brown, 17–48 µm thick. *Pseudoparaphyses* not observed. *Asci* hyaline, subclavate, saccate, obpyriform or ovoid, 8-spored, bitunicate, fissitunicate, 72–173 × 23.5–58.5 µm. *Ascospores* 32–42.5 × 13.5–18 µm, irregularly biseriate or overlapping, crowned in the ascus, fusoid, muriform, hyaline to pale brown, with 4–5 transverse septa, and 2–4 longitudinal septa, apex obtuse, base broadly obtuse to subobtuse, usually widest in the second cell, slightly constricted at the septum, smooth-walled.

Culture characteristics: Colonies on OA, 30–35 mm diam after1 wk, margin entire, regular, covered by flat aerial mycelium, buff to pale olivaceous, buff near the margin; reverse buff to olivaceous, black pseudothecia visible. Colonies on MEA, 30–35 mm diam after 1 wk, margin regular, aerial mycelium sparse, dark green; reverse concolourous, with a greenish brown concentric ring near the centre. Colonies on PDA, 30 mm diam after 1 wk, margin regular, covered by flat aerial mycelium, buff to hazel, greyish olivaceous toward the periphery, some irregular radially furrowed zones near the margin; reverse buff to pale salmon, brownish olivaceous near the centre, some irregular radially furrowed zones near the margin. Application of NaOH results in a pale yellowish green discolouration of the agar.

Typus: **China**, Qinghai Province, Qilian County, Arou, on leaves of *Miscanthus floridulus* (*Poaceae*), 10 Aug. 2019, M. Li (**holotype** HMAS 248356, culture ex-type CGMCC 3.20073 = LC 13593).

Additional materials examined: **China**, Qinghai Province, Qilian County, Ladong, on leaves of *Elymus dahuricus* (*Poaceae*), 9 Aug. 2019, M. Li, culture LC 13592; Menyuan County, Haomen, on leaves of *Swertia tetraptera* (*Gentianaceae*), 7 Aug. 2019, M. Li, culture LC 13590; Menyuan County, Xianmi National Forest Park, on leaves of *Sonchus asper* (*Asteraceae*), 8 Aug. 2019, M. Li, culture LC 13591; on leaves of *Iris lacteal* (*Iridaceae*), 8 Aug. 2019, L.W. Hou, culture LC 13594; on leaves of *Spiraea* sp. (*Rosaceae*), 8 Aug. 2019, L.W. Hou, culture LC 13595.

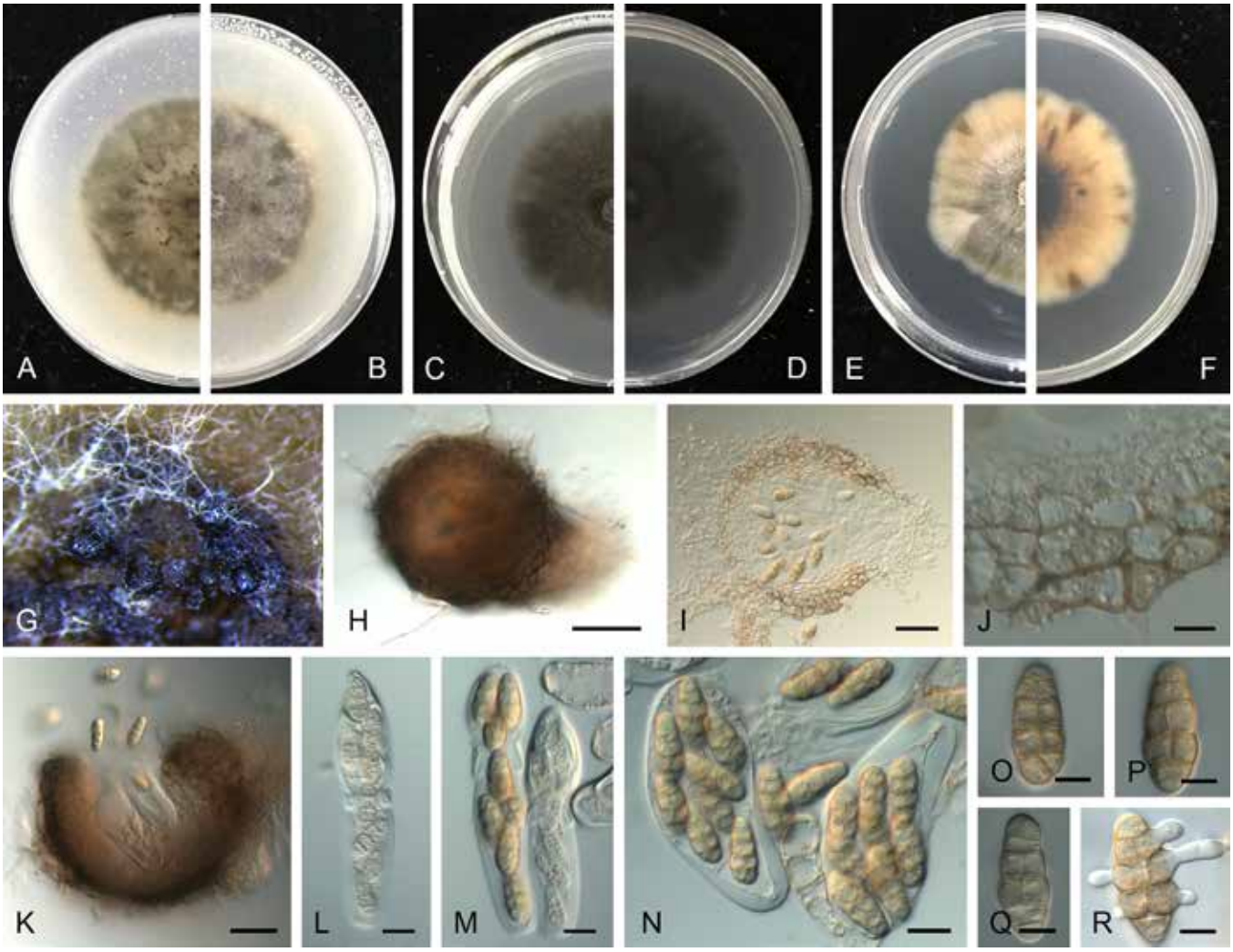

Fig. 35. *Leptosphaerulina miscanthi* (ex-type CGMCC 3.20073). **A, B.** Colony on OA (front and reverse). **C, D.** Colony on MEA (front and reverse). **E, F.** Colony on PDA (front and reverse). **G.** Pseudothecia sporulating on OA. **H.** Pseudothecium. **I.** Section of pseudothecium. **J.** Section of pseudothecial wall. **K.** Pseudothecium with asci. **L–N.** Asci. **O–Q.** Ascospores. **R.** Germinating ascospore. Scale bars: H, I, K = 50 µm; L–N = 20 µm; J, O–R = 10 µm.

Notes: *Leptosphaerulina miscanthi* formed a sister clade to *L. briosiana* and *L. trifolii* in the phylogenetic analysis based on four loci (Fig. 34; LSU, ITS, *rpb2* and *tub2*), but differs from *L. briosiana* in producing slightly longer asci (72–173 × 23.5–58.5 µm *vs* 109–122 × 55–59 µm), and from *L. trifolii* in its narrower asci (72–173 × 23.5–58.5 µm *vs* 91–137 × 65–71 µm) and smaller ascospores (32–42.5 × 13.5–18 µm *vs* 38–62 × 17–26 µm) (Graham & Luttrell 1961).

Genome sequenced strain: *Leptosphaerulina australis.* **Indonesia**, Lampung, from *Syzygium aromaticum* (= *Eugenia aromatica*), Dec. 1982, H. Vermeulen, reference culture CBS 317.83. This Whole Genome Shutgun project has been deposited at GenBank under the accession JALRMI000000000 (BioProject: PRJNA827019, BioSample: SAMN27594417; present study).

Authors: Q. Chen & L. Cai

Melampsora Castagne, Observ. Uréd. 2: 18. 1843. Fig 36.

Classification: *Basidiomycota*, *Pucciniomycotina*, *Pucciniomycetes*, *Pucciniales*, *Melampsoraceae*, *Melampsora*.

Type species: *Melampsora euphorbiae* (Ficinus & C. Schub.) Castagne on *Euphorbia exigua*, basionym: *Xyloma euphorbiae* Ficinus & C. Schub., Fl. Geg. Dresd. 2: 310. 1823. Reference specimen: BPI 871135.

DNA barcodes (genus): ITS, LSU.

DNA barcodes (species): *CO1*, ITS, LSU, *MS208*, *MS277* and *Nad6*. Table 11. Fig. 37.

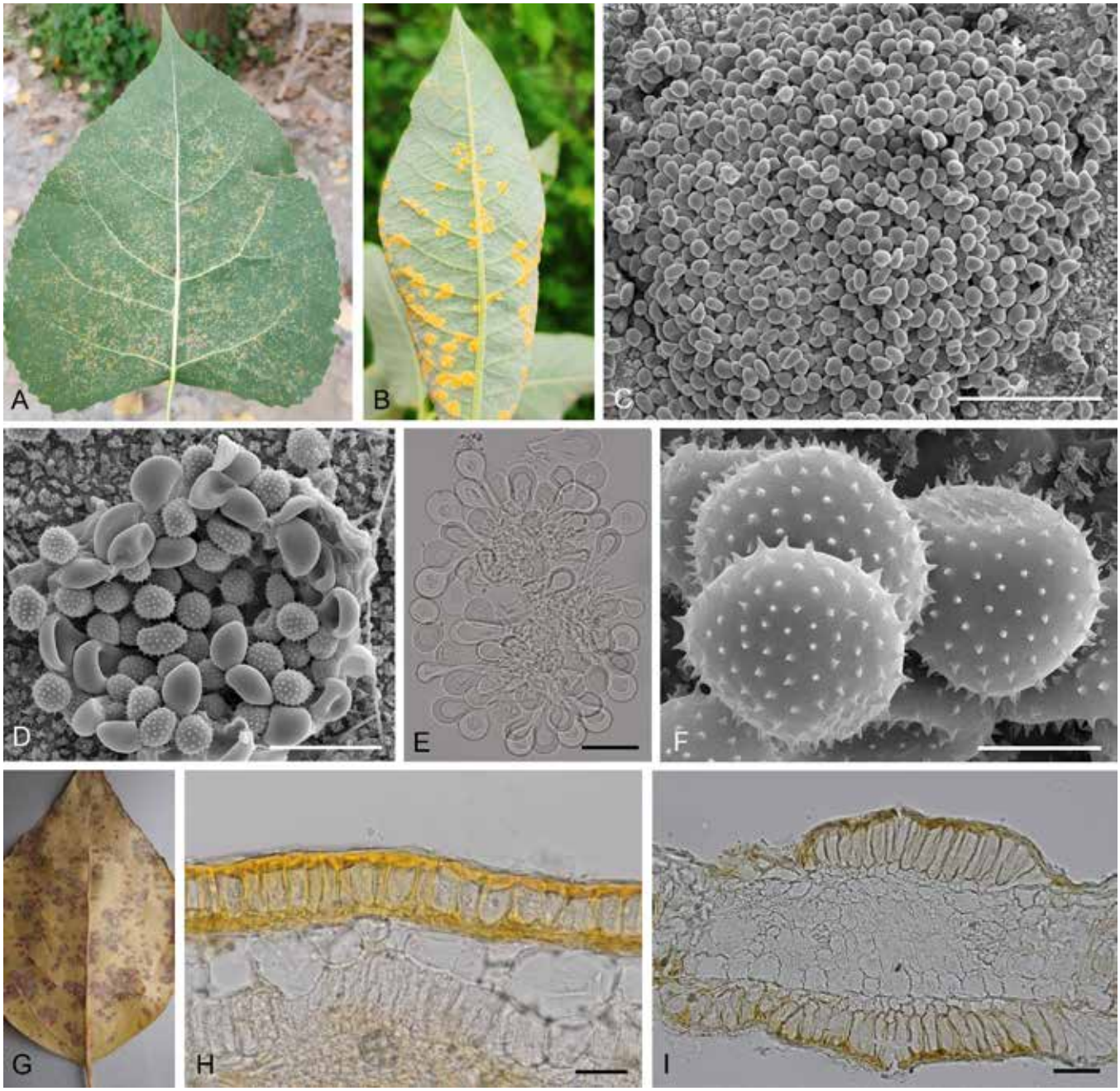

Fig. 36. *Melampsora* spp. **A–F.** Uredinial stage. **A, B.** Disease symptoms. **A.** *Melampsora medusae* on poplar leaf. **B.** *Melampsora salicis-albae* on willow leaf. **C, D.** Scanning electron micrographs of uredinia. **C.** *Melampsora epitea* (epitype TNS-F-121034). **D.** *Melampsora salicis-futurae* (holotype TSH-R9620). **E.** Capitate paraphyses of *Melampsora epitea* (epitype TNS-F-121034). **F.** Scanning electron micrographs of urediniospores of *Melampsora epitea* (epitype TNS-F-121034). **G–I.** Telial stage. **G.** Disease symptoms of *Melampsora medusae* on the poplar leaf. **H, I.** Teliospores. **H.** *Melampsora salicis-bakko* (epitype TSH-R3879). **I.** *Melampsora ribesii-purpureae* (TSH-R7549). Scale bars: C = 100 µm; D, E = 50 µm; H, I = 20 µm; F = 10 µm.

Table 11. DNA barcodes of accepted *Melampsora* spp.

Species	Specimen[1]	GenBank accession numbers[2]						References
		CO1	ITS	LSU	*MS208*	*MS277*	*Nad6*	
Melampsora abietis-canadensis	1399MEA-POG-USA	JQ011188	JN881733	JN934918	JQ011098	JQ011008	JN985832	Vialle *et al.* (2013)
M. abietis-caprearum	KR-M-0048700	–	MK697300	–	–	–	–	Scholler *et al.* (2020)
M. abietis-populi	HMAS 55410	–	AB116870	AB116799	–	–	–	Tian *et al.* (2004)
M. aecidioides	380ME-PO-BC7	EU702405	EU808041	JN934930	JQ011114	JQ011021	JN985844	Vialle *et al.* (2013)
M. albertensis	BPI 0021209	–	JX416848	JX416843		–	–	Vialle *et al.* (unpublished)
M. allii-populina	1260MEAP-POC-HU	JQ011172	JN881728	JN934902	JQ011082	JQ010992	JN985816	Vialle *et al.* (2013)
M. amygdalinae	HMAAC4082	–	MK372149	MK372182	–	–	–	Wang *et al.* (2020a)
M. apocyni	LYR3	–	KR296802	KR296803	–	–	–	Gao *et al.* (unpublished)
M. arctica	HMAS 8629	–	KX386084	KX386113	–	–	–	Zhao *et al.* (2017)
M. bigelowii	1268MEB-SAN-SKA	–	GQ479205	–	–	–	–	Vialle *et al.* (unpublished)
M. capraearum	NYS-F-003819[T]	–	KU550034	KU550033	–	–	–	Zhao *et al.* (2016)
M. chelidonii-pierotii	TSH-R7713	–	AB646769	–	–	–	–	Shinyama & Yamaoka (2012)
M. coleosporioides	HNMAP3114	–	KF780755	KF780638	–	–	–	Zhao *et al.* (2015)
M. epiphylla	TSH-R12280[ET]	–	KF780789	KF780672	–	–	–	Zhao *et al.* (2017)
M. epitea	TNS-F-121034[ET]	–	KX386070	KX386097	–	–	–	Zhao *et al.* (2017)
M. euonymi-caprearum	Iran 13124 F	–	FJ455132	–	–	–	–	Eslami *et al.* (unpublished)
M. euphorbiae	BPI 871135	–	DQ351722	–	–	–	–	Deadman *et al.* (2006)
M. euphorbiae-gerardianae	BRIP 39560	–	EF192199	–	–	–	–	Aime *et al.* (unpublished)
M. ferrinii	SAG 21943	–	KY053852	KY053853	–	–	–	Zapata (2016)
M. gelmii	PUR N6744	–	KJ136571	KJ136569	–	–	–	Tomme & Aime (2015)
M. helioscopiae	WM 1029	–	–	AF426197	–	–	–	Maier *et al.* (2003)
M. humilis	TSH-R7650[ET]	–	KF780812	KF780695	–	–	–	Zhao *et al.* (2017)
M. hypericorum	PDD 97325	–	KJ716353	–	–	–	–	Padamsee & McKenzie (2014)
M. idesiae	KUS-F29304	–	KX944285	–	–	–	–	Lee *et al.* (2017)
M. iranica	HMAAC4055	–	MK372158	MK372191	–	–	–	Wang *et al.* (2020a)
M. kamikotica	HNMAP3186	–	KF780760	KF780643	–	–	–	Zhao *et al.* (2015c)
M. kupreviczii	TSH-R6016	–	KX386080	KX386109	–	–	–	Zhao *et al.* (2015c)
M. kiusiana	HH-77887[T]	–	KF780808	KF780691	–	–	–	Zhao *et al.* (2015c)
M. laricis	HMAS 46905	–	AB116867	AB116809	–	–	–	Tian *et al.* (2004)
M. laricis-miyabeana	TSH-R950826	–	KX386072	KX386099	–	–	–	Zhao *et al.* (2015c)
M. laricis-pentandrae	HNMAP3201	–	KF780801	KF780684	–	–	–	Zhao *et al.* (2015c)
M. laricis-populina	880MLP-LAD-QC	JQ011213	GQ479844	JN934946	JQ011130	JQ011040	JN985860	Vialle *et al.* (2013)
M. laricis-tremulae	PFH-99-1	JQ011224	JN881745	JN934957	JQ011142	JQ011052	JN985871	Vialle *et al.* (2013)
M. laricis-urbanianae	TSH-R7420[ET]	–	KF780778	KF780661	–	–	–	Zhao *et al.* (2015c)
M. lini	5261	–	–	L20283	–	–	–	Berres *et al.* (1995)
M. magnusiana	1426MEG-CJ-DSD	JQ011196	GQ479845	JN934927	JQ011108	JQ011018	JN985841	Vialle *et al.* (2013)
M. medusae	97CN5	JQ011228	GQ479302	JN934961	JQ011146	JQ011056	JN985875	Vialle *et al.* (2013)
M. medusae-populina	97G13	–	AY375276	–	–	–	–	Vialle *et al.* (2013)
M. microsora	HH-53150[T]	–	KF780834	KF780717	–	–	–	Zhao *et al.* (2015c)

Table 11. (Continued).

Species	Specimen[1]	GenBank accession numbers[2]						References
		CO1	ITS	LSU	*MS208*	*MS277*	*Nad6*	
M. microspora	1407MEMI-PON-IRQ	JQ011199	JN881737	JN934931	JQ011115	JQ011025	JN985845	Vialle *et al.* (2013)
M. nujiangensis	1423MEN-POY-CHI^{T}	JQ011201	JN881739	JN934933	JQ011117	JQ011027	JN985847	Vialle *et al.* (2013)
M. occidentalis	411MEO-PO-BC13	JQ011205	GQ479885	JN934937	JQ011121	JQ011031	JN985851	Vialle *et al.* (2013)
M. pakistanica	BAQAU13^{T}	—	KU097001	KU847978	—	—	—	Ali *et al.* (2016)
M. paradoxa	649ME-LAL-ZM45.1	—	GQ479269	—	—	—	—	Vialle *et al.* (unpublished)
M. pinitorqua	1367MPI-PNI-FI	JQ011238	GQ479897	JN934973	JQ011158	JQ011068	JN985887	Vialle *et al.* (2013)
M. populnea	AAH00-1	—	AY444772	AY444786	—	—	—	Pei *et al.* (2005)
M. pruinosae	1366MEPR-POPRURT	JQ011207	GQ479898	JN934939	JQ011122	JQ011034	JN985853	Vialle *et al.* (2013)
M. pulcherrima	O8ZK4	JQ011209	GQ479320	JN934941	JQ011125	JQ011035	JN985855	Vialle *et al.* (2013)
M. reticulatae	TNS-F-107037	—	KF780844	KF780727	—	—	—	Zhao *et al.* 2015c)
M. ribesii-purpureae	NWC-06843	—	KF780830	KF780713	—	—	—	Zhao *et al.* (2015b)
M. ribesii-viminalis	HNMAP3218	—	KF780796	KF780679	—	—	—	Zhao *et al.* (2015c)
M. ricini	PDD 98363	—	KJ716352	—	—	—	—	Padamsee & McKenzie (2014)
M. rostrupii	PFH-08-3	JQ011246	JN881752	JN934981	JQ011169	JQ011079	JN985895	Vialle *et al.* (2013)
M. salicis-albae	NWC-09234	—	KF780774	KF780657	—	—	—	Zhao *et al.* (2015c)
M. salicis-argyraceae	HMAS52984^{T}	—	KF780733	KF780616	—	—	—	Zhao *et al.* (2015a)
M. salicis-bakko	TSH-R3879^{ET}	—	KC631854	KC685611	—	—	—	Zhao *et al.* (2015c)
M. salicis-cavaleriei	HMAAC4043	—	MK277296	MK277301	—	—	—	Zhao *et al.* (2015c)
M. salics-cupularis	HMAS 76122^{ET}	—	KF780752	KF780635	—	—	—	Zhao *et al.* (2015c)
M. salicis-futurae	TSH-R9620^{T}	—	KC631860	KC685617	—	—	—	Zhao *et al.* (2017)
M. salicis-purpureae	HMAS 62584^{T}	—	KF780766	KF780649	—	—	—	Zhao *et al.* (2015a)
M. salicis-reinii	TSH-R10306^{T}	—	KF780777	KF780660	—	—	—	Zhao *et al.* (2015c)
M. salicis-sinicae	HNMAP1710^{T}	—	KC631839	KC685596	—	—	—	Zhao *et al.* (2014)
M. salicis-triandrae	HNMAP3181^{T}	—	KF780829	KF780712	—	—	—	Zhao *et al.* (2015b)
M. salicis-viminalis	HMAS 38658^{T}	—	KF780732	KF780615	—	—	—	Zhao *et al.* (2015c)
M. salicis-warburgii	HH-53135^{T}	—	KF780837	KF780720	—	—	—	Zhao *et al.* (2015c)
M. tsinlingensis	HNMAP3185	—	KF780748	KF780631	—	—	—	Zhao *et al.* (2015c)
M. yezoensis	HH-99463^{T}	—	KF780833	KF780730	—	—	—	Zhao *et al.* (2015c)
Melampsora cf. yezoensis	PUR N6744	—	KJ13657	KJ136569	—	—	—	Tomme & Aime (2015)
Melampsora x *columbiana*	SN-35	—	JQ042235	—	—	—	—	Busby *et al.* (2012)

[1] BPI: Systematic Mycology and Microbiology Laboratory, Agricultural Research Service, USDA, USA; BRIP: Queensland Plant Pathology Herbarium, Queensland, Australia; HH: Hiratsuka Herbarium, Tokyo, Japan; HMAAC: Mycological Herbarium of Xinjiang Agricultural University, Xinjiang, China; HMAS: Mycological Herbarium of Institute of Microbiology, Chinese Academy of Sciences, China; HMNWFC: Mycological Herbarium of College of Forestry, Northwest A & F University, China; HNMAP: Mycological Herbarium of Inner Mongolia Agricultural University, Inner Mongolia, China; PDD: New Zealand Fungarium, Lincoln, New Zealand; PUR: Arthur Fungarium, Purdue University, West Lafayette, IN, USA; TNS: National Museum of Nature and Science, Tsukuba, Japan; TSH: Mycological Herbarium of the Graduate School of Life and Environmental Sciences, University of Tsukuba, Tsukuba, Japan. ^{T} and ^{ET} indicate type and epitype, respectively.

[2] *CO1*: partial cytochrome oxidase subunit 1 gene; ITS: internal transcribed spacers and intervening 5.8S nrDNA; LSU: partial 28S large subunit nrRNA gene; *MS208*: gene for DNA replication-licensing factor required for DNA replication initiation and cell proliferation; *MS277*: gene required for rRNA accumulation during biogenesis of the ribosome; *Nad6*: partial dehydrogenase subunit 6 gene.

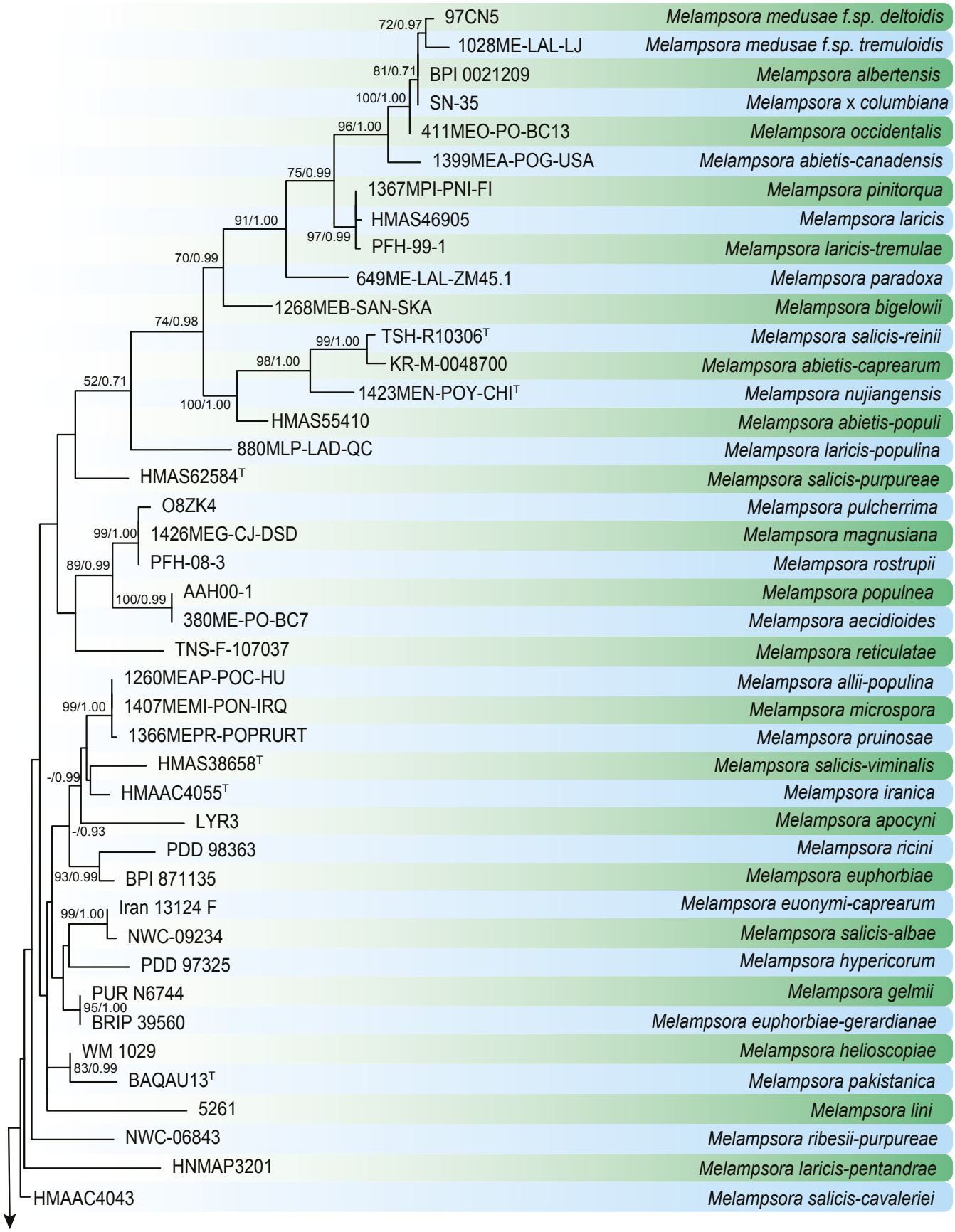

Fig. 37. Phylogenetic tree constructed based on ITS (550 bp) and LSU (700 bp) sequences of all accepted species of *Melampsora*. RAxML bootstrap support values (> 50 %) and Bayesian posterior probability scores (> 0.70) are shown at the nodes. The phylogenetic tree was rooted to *Chrysomyxa monesis* 1361CHM-PCS-BC and *C. empetri* 287CHE-EMN-SA1. GenBank accession numbers are indicated in Table 11. ^{T} and ^{ET} indicate type and epitype, respectively. TreeBASE: S26038.

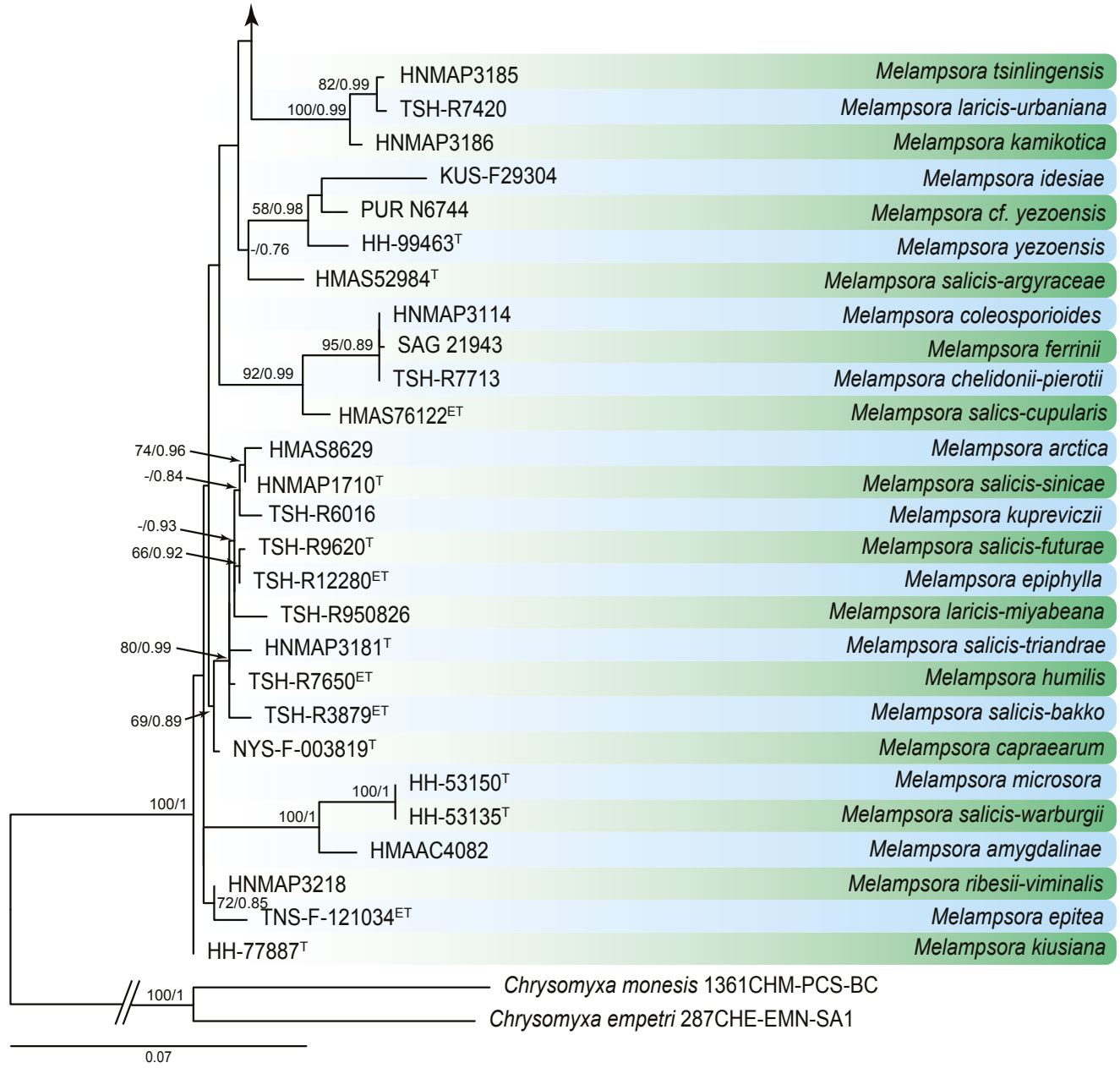

Fig. 37. (Continued).

Spermogonia Group I (type 2 or type 3), subepidermal or subcuticular, determinate, with flat hymenia, bounding structures lacking. *Aecia Caeoma*-type, subepidermal, with rudimentary or no peridia, occasionally some species have peridial cells adherent to host epidermis. *Aeciospore* catenulate, with intercalary cells, verrucose with rodlike columns or blocks. *Uredinia Uredo*-type, subepidermal, erumpent, brightly yellow or orange when fresh, fading to nearly hyaline, with abundant capitate paraphyses, occasionally with a partial peridium. *Urediniospores* borne singly, echinulate, germ pores scattered or bizonate. *Telia* subepidermal or subcuticular, not erumpent, consisting of laterally adherent teliospores in crusts one spore deep or some species also with subjacent spore-like cells. *Teliospores* aseptate, sessile, pigmented. *Basidia* external.

Distribution: Worldwide.

Life cycle: This genus includes either heteroecious or autoecious life cycles, and most species are recorded as macrocyclic, with five different spore stages, *i.e.* spermogonium, aecium, uredinium, telium and basidium. Heteroecious species have their uredinia and telia on willows (*Salix*) and poplars (*Populus*) belonging to *Salicaceae*, and spermogonia and aecia of these species occur on coniferous trees of *Pinaceae* such as *Abies*, *Larix*, *Picea*, *Pinus*, *Pseudotsuga* and *Tsuga*, or on various herbaceous plants such as *Allium* (*Alliaceae*), *Chelidonium*, *Corydalis* (*Papaveraceae*), *Ribes* (*Grossulariaceae*), *Saxifraga* (*Saxifragaceae*), and several orchidaceous genera. Most autoecious species of *Melampsora* occur on dicotyledonous plants, including *Euphorbiaceae* and *Linaceae*.

Disease symptoms: Yellow aecia are sometimes visible on cones or needles of coniferous trees and other aecial hosts, infected needles shrivel and die soon after sporulation; yellow to brownish uredinia in small orange-yellow pustules on one or both leaf surfaces on telial hosts, commonly with yellow spots on leaves, eventually become necrotic; the whole trees have a golden appearance in severe infection; heavily infected leaves turn brown, wither, and curl at the margin before falling.

Notes: The family *Melampsoraceae* contains only one genus, *Melampsora*, which possesses Group I spermogonia and unicellular teliospores embedded under the host epidermis or cuticular layers (Sydow & Sydow 1915, Kuprevich & Tranzschel 1957, Cummins & Hiratsuka 2003). Since *Melampsora* was established in 1843 with *M. euphorbiae* on *Euphorbia exigua* as type species, there have been approximately 212 species described (Farr & Rossman 2022). *Melampsora lini* was listed as one of the *Top 10* most important fungal plant pathogens based on its scientific/economic importance as the cause of rust on cultivated flax (Dean *et al.* 2012). Species recognition in *Melampsora* has been based on the ecological species concept that focused on aecial or telial host ranges, together with a few morphological characters in uredinial and telial stages. More recently, molecular data has revealed interspecific relationships in *Melampsora*, and taxonomic identities have been resolved via rDNA phylogenies (Zhao *et al.* 2020). There have been several systematic studies at the species level in *Melampsora* (Tian *et al.* 2004, Pei *et al.* 2005, Feau *et al.* 2009, Zhao *et al.* 2015c, 2017). Molecular barcodes for identification at both generic and species level are available. At generic level, LSU is used, while for species, *CO1*, ITS, LSU, *MS208*, *MS277* and *Nad6*, are useful barcodes. Among the 212 reported species, nucleotide sequences from 71 species of *Melampsora* are presently available.

References: Hiratsuka & Kaneko 1982 (morphology and host range); Bagyanarayana 2005 (morphology, host range and key of *Melampsora* species on willows); Pei 2005 (morphology and host range); Vialle *et al.* 2011 (morphology, host range and key of *Melampsora* species on poplar); Tian *et al.* 2004, Feau *et al.* 2009, Zhao *et al.* 2015c, Zhao *et al.* 2017, Zhao *et al.* 2020 (phylogeny).

Melampsora laricis-urbanianae Tak. Matsumoto, Ann. Missouri Bot. Gard. 6: 311. 1920. Fig. 38.

Spermogonia amphigenous, subcuticular. *Aecia* caeomata type, hypophyllous; aeciospores globose or broadly ellipsoid, 15–25 × 13–21 µm, finely and densely verrucose, walls 1.5–2 µm thick, germ pores scattered. *Uredinia* hypophyllous, 0.2–0.6 mm; *urediniospores* obovoid or ellipsoid, 16–30 × 9–21 µm, walls 2–2.5 µm thick at sides, 4–6.9 µm thick at apex, echinulate, germ pores 2–4, tending to bizonate. *Paraphyses* intermixed 30–79 × 11–24 µm, walls slightly thickened at apex up to 12 µm. *Telia* hypophyllous,

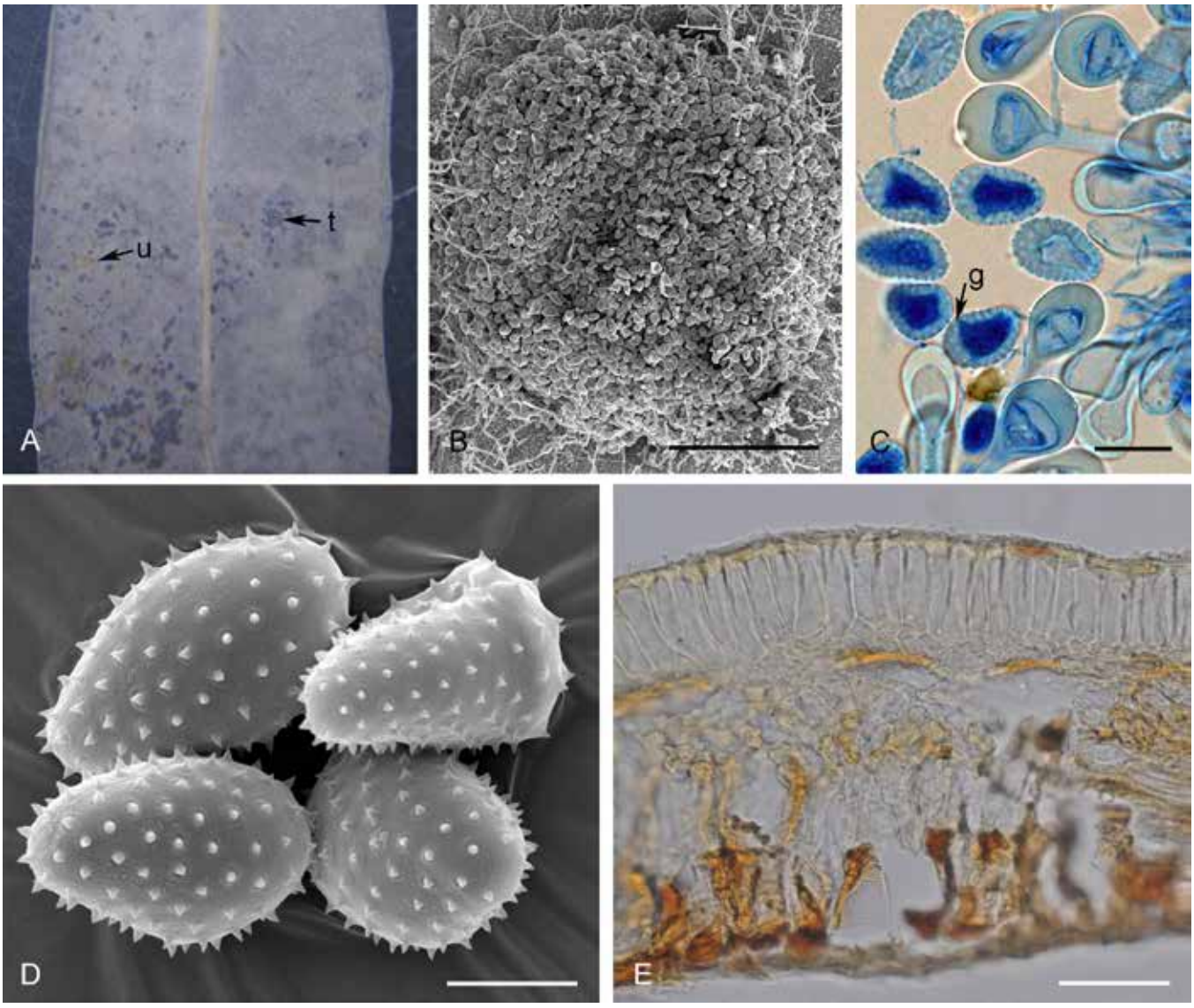

Fig. 38. *Melampsora laricis-urbaniana* (epitype TSH-R7420). **A.** Uredinia (u) and telia (t) on leaves of epitype specimen. **B.** Scanning electron micrographs of uredinia with intermixed paraphyse. **C.** Urediniospores with biozonate germ pores (g), urediniospores and paraphyses with apparently thickened apical wall. **D.** Scanning electron micrographs of urediniospores with echinulate spines. **E.** Section of telia and teliospores. Scale bars: B = 150 µm; E = 30 µm; C = 20 µm; D = 10 µm.

subepidermal, 0.2–0.6 mm; *teliospores* 20–49 × 6–16 µm, walls 1–2.5 µm thick at sides, up to 4.7 µm thick at apex, an apical germ pore sometimes visible.

Host range: Spermogonia and aecia on *Larix leptolepis*, and uredinia and telia on *Toisusu urbaniana*.

Typus: **Japan**, Hokkaido, Sapporo-shi, on *Toisusu urbaniana* (*Salicaceae*), Tak. Matsumoto (Ann. Missouri Bot. Gard. 6: 311. 1920, figs 1–3, **lectotype** designated here, MBT 10005755); Hokkaido, Sapporo-shi, on *T. urbaniana*, data unknown, Y. Yamaoka (**epitype** designated here TSH-R7420, MBT 10005047).

Additional materials examined: **Japan,** Hokkaido, Sapporo-shi, Toyohira, on *T. urbaniana*, 18 Nov. 1925, N. Hiratsuka, HH-53303; Hokkaido, Sapporo-shi, on *Toisusu urbaniana*, 4 Oct. 1901, J. Hanzawa, HH-78307; *ibid.* HH-53302; Hokkaido, Sapporo-shi, on *T. urbaniana*, 21 Aug. 1905, K. Miyabe, HH-53305; Hokkaido, Sapporo-shi, on *T. urbaniana*, date unknown, Y. Yamaoka, TSH-R7419; Nagano, on *T. urbaniana*, date unknown, Y. Yamaoka, TSH-R9834.

Notes: *Melampsora laricis-urbanianae* was first reported on *T. urbaniana* in Sapporo-shi of Hokkaido in Japan and Matsumoto (1920) validly described this species with description and line drawings. Matsumoto (1920) did not cite the materials examined by him, thus, Hiratsuka & Kaneko (1982) designated a neotype and isoneotype during their systematic studies of *Melampsora* species on willows in Japan. However, the neotypification of Hiratsuka & Kaneko (1982) is not Code compliant as original material is available for lectotypification. For this reason, we have designated illustrations of Matsumoto (1920) as lectotype. We also designated an epitype specimen, which was collected by Y. Yamaoka in the Sapporo-shi of Hokkaido in Japan, from which we derived ITS and LSU sequences: TSH-R7420 (ITS: KF780778; LSU: KF780661), TSH-R9834 (ITS: KF164453; LSU: KF164446) and TSH-R9835 (ITS: KF164454; LSU: KF164447). This species was only found in Japan with its aecial stage on *Larix* species and telial stage on *Toisusu*.

Melampsora salicis-cupularis Wang, Contr. Inst. Bot. Natl. Acad. Peiping 6: 225. 1949. Fig. 39.

Spermogonia and *aecia* not found. *Uredinia* hypophyllous, 0.2–0.6 mm; *Urediniospores* globoid or ellipsoid, echinulate, 14–30 × 12–27 µm, wall 1.5–3 µm thick, mean distance between spines 1.01–1.12 µm, germ pores 3–5, scattered. *Paraphyses* mainly capitate, 41–93 × 16–37 µm, with evenly thickened or slightly thickened apex, up to 8 µm. *Telia* amphigenous, mainly hypophyllous, 0.2–0.8 mm; *Teliospores* subepidermal, 20–40 × 5–14 µm, wall 1 µm thick, not thickened at apex.

Host range: Uredinia and telia on *Salix cupularis.*

Typus: **China**, Shaanxi Province, Taibai Mountains, on *Salix cupularis* (*Salicaceae*), 14 Aug. 1942, Y.C. Wang (**holotype** HMAS 957); *ibid*., 26 Aug. 1996, Z.M. Cao (**epitype** designated here HMAS 76122, MBT 10005048).

Additional materials examined: **China**, Shaanxi Province, Taibai Mountains, on *S. cupularis*, 26 Aug. 1996, Z.M. Cao, HMNWFC-T8540; Inner Mongolia, Alxa, He Lan Mountains on *S. cupularis*, 16 Aug. 1963, Y.Z. Shang, HNMAP3152.

Notes: *Melampsora salicis-cupularis* was first detected on *Salix cupularis* from the Taibai Mountains in China, and it was characterised by relatively large urediniospores, capitate paraphyses in uredinia, amphigenous telia and subepidermal teliospores with evenly thickened apical wall (Wang 1949). This species resembles *M. epiphylla* in amphigenous telia and subepidermal teliospores, but the two species differ in urediniospores dimensions and teliospore shape (Hiratsuka & Kaneko 1982, Zhao *et al.* 2017). We failed to generate molecular data from the holotype material, and therefore a specimen collected from the host and location in the Taibai Mountains of China was designated as epitype. We successfully characterised its morphological features, as well as phylogenetic placement based on the epitype material. This species is hitherto only known from China (Shaanxi and Inner Mongolia).

Genome sequenced strain: *Melampsora lini*. **Unknown**, collection information unknown, culture CH5 (a hybrid strain obtained from crossing self-fertilised New Zealand "race" 5 and a North American "race" 228 strain . This Whole Genome Shutgun project has been deposited at GenBank under the BioProject: PRJNA239538; Melli1 in MycoCosm (Nemri *et al.* 2014).

Authors: P. Zhao & L. Cai

Nigrospora Zimm., Zentralbl. Bakteriol. Parasitenk., Abt. I, 8: 220. 1902. Fig. 40.

Classification: *Sodariomycetes*, *Xylariomycetidae*, *Xylariales*, *Apiosporaceae*.

Type species: *Nigrospora panici* Zimm. Type or reference material not available.

DNA barcode (genus): LSU.

DNA barcodes (species): ITS, *tef1, tub2*. Table 12. Fig 41.

Ascomata perithecial, black, aggregated, subepidermal, erumpent, spherical or ovoid, with papillate ostioles. *Asci* short pedicellate, rounded at the apex, unitunicate-operculate, clavate, 8–spored. *Paraphyses* septate, longer than asci, thin-walled. *Ascospores* granular, hyaline, curved, inequilateral, biseriate, initially unicellular, usually unequally two-celled with a transverse septum. *Conidiophores* smooth, branched, micronematous or semi-macronematous, flexuous, hyaline to brown, usually reduced to conidiogenous cells. *Conidiogenous cells* hyaline, discrete, solitary, monoblastic, subspherical, determinate, ampulliform, doliiform, sub-cylindrical to clavate. *Conidia* solitary, sparse, acrogenous, aseptate, globose or sub-globose or ellipsoidal or pyriform, shiny, smooth, simple, pale brown to black, rarely with violent discharge mechanism. *Setae* straight to irregular, curved, subcylindrical, smooth, black, tapering at apex, obtuse or subobtuse, base truncate (adapted from Hudson 1963, Wang *et al.* 2017, Raza *et al.* 2019).

Cultural characteristics: Colonies on PDA filamentous with shiny, small, black conidia, white or pale yellow when are young, floccose, cottony, brown or black when mature with abundant sporulation. Colonies on SNA flat, mycelia immersed, white to greyish surface, greyish reverse with or without patches.

Optimal media and cultivation conditions: Fast growth on PDA and slow growth on SNA media. On SNA at 25 °C to induce sporulation of the asexual morph.

Distribution: Worldwide.

Fig. 39. *Melampsora salicis-cupularis* (epitype HMAS 76122). **A.** Label of epitype specimen. **B.** Uredinia (u) and telia (t) on leaves of *Salix cupularis*. **C.** Scanning electron micrographs of uredinia with intermixed paraphyses. **D.** Urediniospores with scattered germ pores (g). **E.** Capitate paraphyses. **F.** Scanning electron micrographs of urediniospores with echinulate spines and paraphyses with smooth wall. **G.** Section of telia and teliospores. Scale bars: C = 100 µm; D, E = 50 µm; G = 20 µm; E, F = 10 µm.

Hosts: *Nigrospora* species are cosmopolitan with wide host ranges and occur as saprobes, endophytes, plant and human pathogens. *Nigrospora sphaerica* (reported from 40 different host genera), *N. oryzae* (reported from 20 different host genera) and *N. chinensis* (reported from 10 different host genera) are the three most ubiquitous species. Overall, *Nigrospora* species lacks host specificity.

Disease symptoms: Leaf spots, twig and shoot or leaf blights, rots.

Notes: *Nigrospora* as recently redefined is a monophyletic genus, and phylogenetic studies employing ITS, *tef1* and *tub2* sequence data were performed for species identification and delimitation (Wang *et al.* 2017, Raza *et al.* 2019). The type of the genus was reported from *Panicum amphibium* from Java and its holotype has been lost. Unfortunately, to date attempts to locate a suitable specimen to neotypify this species have been unsuccessful. The sexual morph of *Nigrospora* species is rarely observed. *Arthrinium* and *Apiospora* are similar in producing deeply pigmented conidia with or without germ slit and the presence of setae. The distinction among these genera is obscure, but the most characteristic difference is the production of a single conidium produced on each conidiogenous cell in *Nigrospora*, while conidia are produced in clusters in

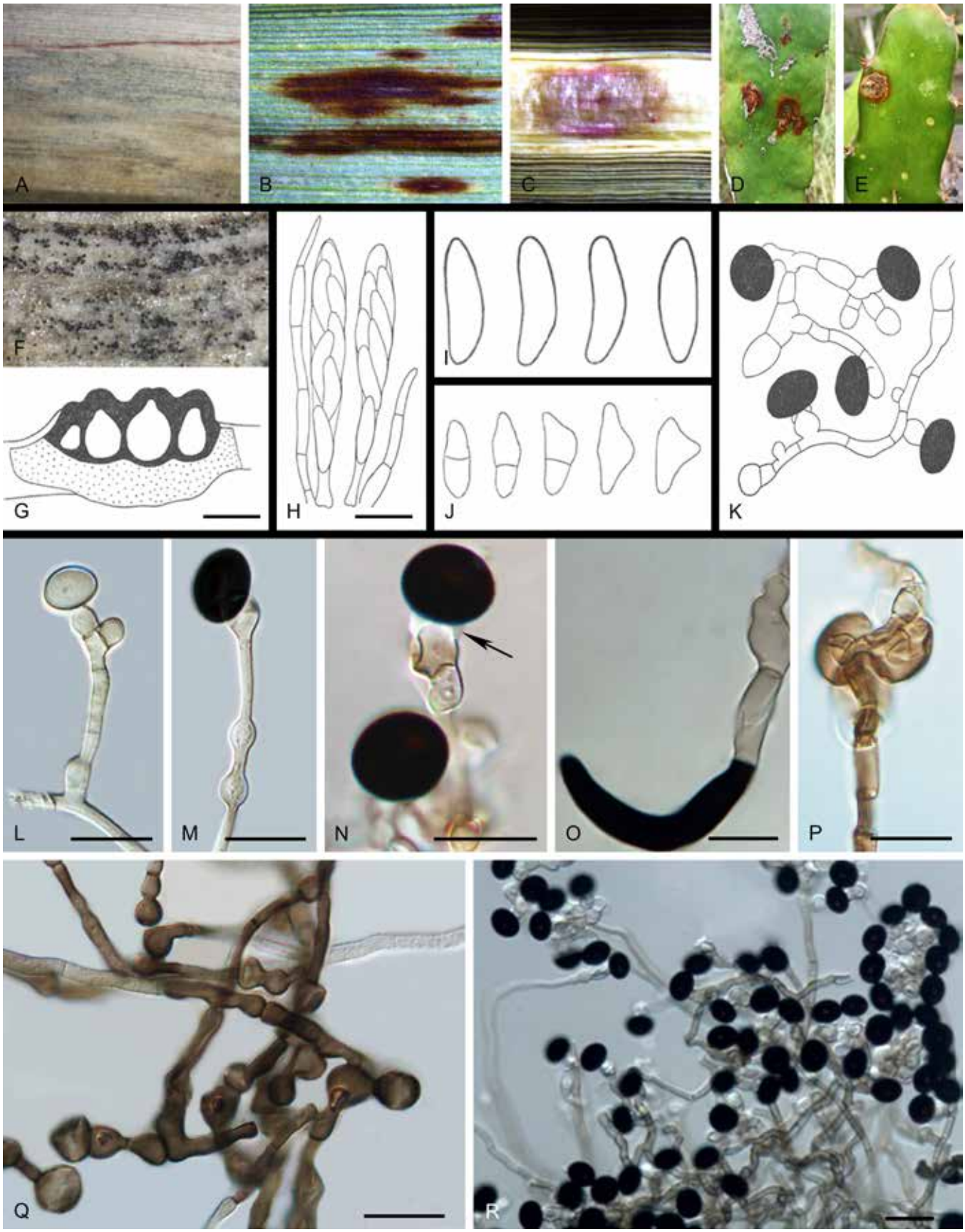

Fig. 40. *Nigrospora* spp. **A–F.** Disease symptoms. **A, F.** *Nigrospora hainanensis* on *Saccharum officinarum*. **B.** *Nigrospora aurantiaca* on *Saccharum officinarum*. **C.** *Nigrospora camelliae-sinensis* on *Saccharum officinarum.* **D.** *Nigrospora lacticolonia* on *Selenicereus undatus*. **E.** *Nigrospora sphaerica* on *Selenicereus undatus*. **G–K.** Sexual morph of *Nigrospora oryzae* (Herb. IMI 79239). **G.** Perithecia. **H.** Asci and paraphyses. **I.** Ascospores, all from *Saccharum officinarum*. **J.** Discharged ascospores. **K.** Germinating ascospores producing conidia. **L–R.** Asexual morph. **L, M.** Conidiophores with conidia of *Nigrospora falsivesicularis* (ex-type CGMCC 3.19678). **N.** Conidiogenous cells giving rise to conidia (arrow indicates the vesicles surrounding the septum) of *Nigrospora sacchari-officinarum* (ex-type CGMCC 3.19335). **O.** Seta of *Nigrospora hainanensis* (ex-type CGMCC 3.18129). **P, Q.** Sterile conidia of *Nigrospora saccharicola* (ex-type CGMCC 3.19362). **R.** Conidia of *Nigrospora guilinensis* (ex-type CGMCC 3.18124). Scale bars: G = 200 µm; H, J–M, P–R = 20 µm; I, N, O = 10 µm. Pictures A–C, F, L–N, P, Q taken from Raza *et al.* (2019); D, E from Kee *et al.* (2019); G–K from Hudson (1963); O, R from Wang *et al.* (2017).

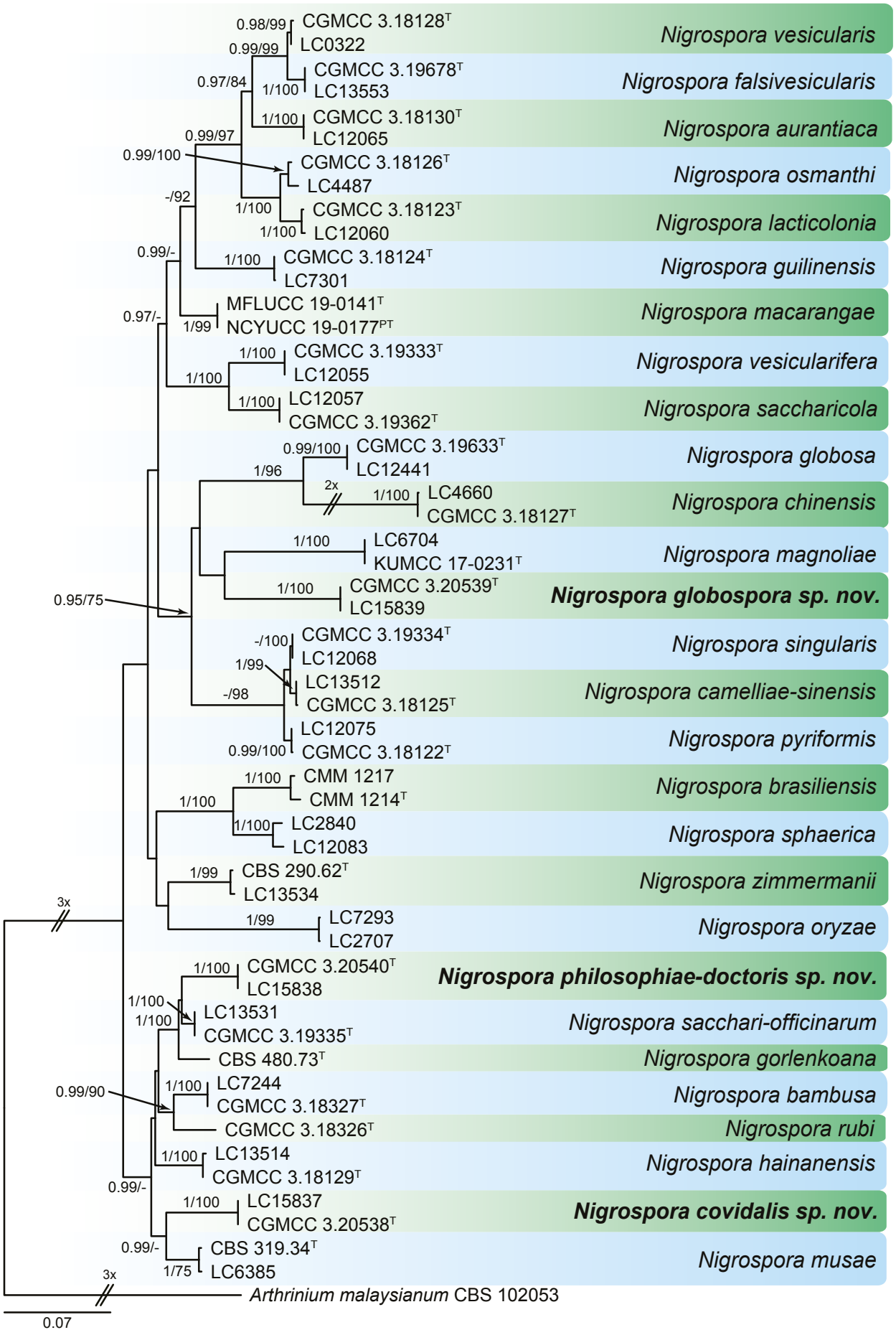

Fig. 41. RAxML phylogram constructed from ITS (521 bp), *tub2* (433 bp) and *tef1* (543 bp) sequences of all accepted species of *Nigrospora*. Maximum likelihood bootstrap support values (> 70 %) and Bayesian posterior probability scores (> 0.95) are indicated on the branches. The novel taxa are printed in **bold**. The phylogenetic tree was rooted to *Arthrinium malaysianum* CBS 102053. GenBank accession numbers are indicated in Table 12. ^{T} and ^{PT} indicate ex-type and ex-paratype strains, respectively. TreeBASE: S26190.

Table 12. DNA barcodes of accepted *Nigrospora* spp.

Species	Isolates[1]	GenBank accession numbers[2]			References
		ITS	*tub2*	*tef1*	
Nigrospora aurantiaca	CGMCC 3.18130^{T}	KX986064	KY019465	KY019295	Wang *et al.* (2017)
	LC 12065	MN215771	MN329935	MN264010	Raza *et al.* (2019)
N. bambusae	CGMCC 3.18327^{T}	KY385307	KY385319	KY385313	Wang *et al.* (2017)
	LC 7244	KY385306	KY385320	KY385314	Wang *et al.* (2017)
N. brasiliensis	CMM 1214^{T}	KY569629	MK720816	MK753271	Crous *et al.* (2019)
	CMM 1217	KY569630	MK720817	MK753272	Crous *et al.* (2019)
N. camelliae-sinensis	CGMCC 3.18125^{T}	KX985986	KY019460	KY019293	Wang *et al.* (2017)
	LC 13512	MN215775	MN329939	MN264014	Raza *et al.* (2019)
N. chinensis	CGMCC 3.18127^{T}	KX986023	KY019462	KY019422	Wang *et al.* (2017)
	LC 4660	KX986026	KY019548	KY019445	Wang *et al.* (2017)
N. covidalis	CGMCC 3.20538 = LC 4566^{T}	OK335209	OK431479	OK431485	Present study
	LC 158337	OK335210	OK431480	OK431486	Present study
N. falsivesicularis	CGMCC 3.19678^{T}	MN215778	MN329942	MN264017	Raza *et al.* (2019)
	LC 13553	MN215779	MN329943	MN264018	Raza *et al.* (2019)
N. globosa	CGMCC 3.19633^{T}	MK329121	MK336134	—	Zhang *et al.* (2021)
	LC 12441	MK329122	MK336135	—	Zhang *et al.* (2021)
N. globospora	CGMCC 3.20539 = LC 8397^{T}	OK335211	OK431481	OK431487	Present study
	LC 15839	OK335212	OK431482	OK431488	Present study
N. gorlenkoana	CBS 480.73^{T}	KX986048	KY019456	KY019420	Wang *et al.* (2017)
N. guilinensis	CGMCC 3.18124^{T}	KX985983	KY019459	KY019292	Wang *et al.* (2017)
	LC 7301	KX986063	KY019608	KY019404	Wang *et al.* (2017)
N. hainanensis	CGMCC 3.18129^{T}	KX986091	KY019464	KY019415	Wang *et al.* (2017)
	LC 13514	MN215780	MN329944	MN264019	Raza *et al.* (2019)
N. lacticolonia	CGMCC 3.18123^{T}	KX985978	KY019458	KY019291	Wang *et al.* (2017)
	LC 12060	MN215784	MN329948	MN264023	Raza *et al.* (2019)
N. macarangae	MFLUCC 19–0141^{T}	MW114318	—	—	Tennakoon *et al.* (2021)
	NCYUCC 19–0177^{PT}	MW114319	—	—	Tennakoon *et al.* (2021)
N. magnoliae	MFLUCC 19–0112 = KUMCC 17–0246^{T}	MW285092	MW438334	—	de Silva *et al.* (2021)
	LC 6704	KX986047	KY019571	KY019373	Wang *et al.* (2017)
N. musae	CBS 319.34^{T}	KX986076	KY019455	KY019419	Wang *et al.* (2017)
	LC 6385	KX986042	KY019567	KY019371	Wang *et al.* (2017)
N. oryzae	LC 7293	KX985931	KY019601	KY019396	Wang *et al.* (2017)
	LC 2707	KX985954	KY019481	KY019307	Wang *et al.* (2017)
N. osmanthi	CGMCC 3.18126^{T}	KX986010	KY019461	KY019421	Wang *et al.* (2017)
	LC 4487	KX986017	KY019540	KY019438	Wang *et al.* (2017)
N. philosophiae-doctoris	CGMCC 3.20540 = LC 13398^{T}	OK335213	OK431483	OK431489	Present study
	LC 15838	OK335214	OK431484	OK431490	Present study
N. pyriformis	CGMCC 3.18122^{T}	KX985940	KY019457	KY019290	Wang *et al.* (2017)
	LC 12075	MN215787	MN329988	MN264026	Raza *et al.* (2019)
N. rubi	CGMCC 3.18326^{T}	KX985948	KY019475	KY019302	Wang *et al.* (2017)
N. sacchari-officinarum	CGMCC 3.19335^{T}	MN215791	MN329954	MN264030	Raza *et al.* (2019)
	LC 13531	MN215792	MN329955	MN264031	Raza *et al.* (2019)
N. saccharicola	CGMCC 3.19362^{T}	MN215788	MN329951	MN264027	Raza *et al.* (2019)
	LC 12057	MN215789	MN329952	MN264028	Raza *et al.* (2019)
N. singularis	CGMCC 3.19334^{T}	MN215793	MN329956	MN264032	Raza *et al.* (2019)
	LC 12068	MN215794	MN329957	MN264033	Raza *et al.* (2019)
N. sphaerica	LC 2840	KX985965	KY019492	KY019318	Wang *et al.* (2017)

Table 12. (Continued).

Species	Isolates[1]	GenBank accession numbers[2]			References
		ITS	*tub2*	*tef1*	
	LC 12083	MN215811	MN329974	MN264050	Raza *et al.* (2019)
N. vesicularifera	CGMCC 3.19333[T]	MN215812	MN329975	MN264051	Raza *et al.* (2019)
	LC 12055	MN215814	MN329977	MN264053	Raza *et al.* (2019)
N. vesicularis	CGMCC 3.18128[T]	KX986088	KY019463	KY019294	Wang *et al.* (2017)
	LC 0322	KX985939	KY019467	KY019296	Wang *et al.* (2017)
N. zimmermanii	CBS 290.62[T]	KY385309	KY385317	KY385311	Wang *et al.* (2017)
	LC 13534	MN215824	MN329987	MN264063	Raza *et al.* (2019)

[1] CBS: Westerdijk Fungal Biodiversity Institute, Utrecht, the Netherlands; CMM: Culture Collection of Phytopathogenic Fungi Prof. Maria Menezes; CGMCC: China General Microbiological Culture Collection Center, Institute of Microbiology, Beijing, China; LC: Dr Lei Cai's personal collection deposited in laboratory, housed at Chinese Academy of Sciences (CAS), China. [T] and [PT] indicate ex-type and ex-paratype strains, respectively.

[2] ITS: internal transcribed spacers and intervening 5.8S nrDNA; *tub2*: partial β-tubulin gene; *tef1*: partial translation elongation factor 1-α gene.

Arthrinum and *Apiospora* (Minter 1985, Crous & Groenewald 2013, Wang *et al.* 2017, Raza *et al.* 2019, Pintos & Alvarado 2021).

References: Hudson 1963 (sexual connection), Wang *et al.* 2017, Crous *et al.* 2019a, Raza *et al.* 2019, Pintos & Alvarado 2021 (morphology and phylogeny), Kee *et al.* 2019 (morphology and pathogenicity).

Nigrospora covidalis M. Raza, Qian Chen & L. Cai, ***sp. nov.*** MycoBank MB 840804. Fig. 42.

Etymology: Refers to the COVID-19 pandemic.

Asexual morph on SNA: *Hyphae* branched, septate, guttulate, hyaline to pale brown, 2–4 µm diam. *Conidiophores* micronematous or semi-macronematous, flexuous or straight, hyaline to pale brown. *Conidiogenous cells* monoblastic, solitary, discrete, pale brown, doliiform to ampulliform, 5–8.5 × 4.5–7 µm (av. = 6.70 ± 1.4 × 5.91 ± 1.2). *Conidia* sparse, discrete on aerial hyphae, pale brown to black, globose or subglobose, 9–14 µm diam (av. = 12.03 ± 1.3).

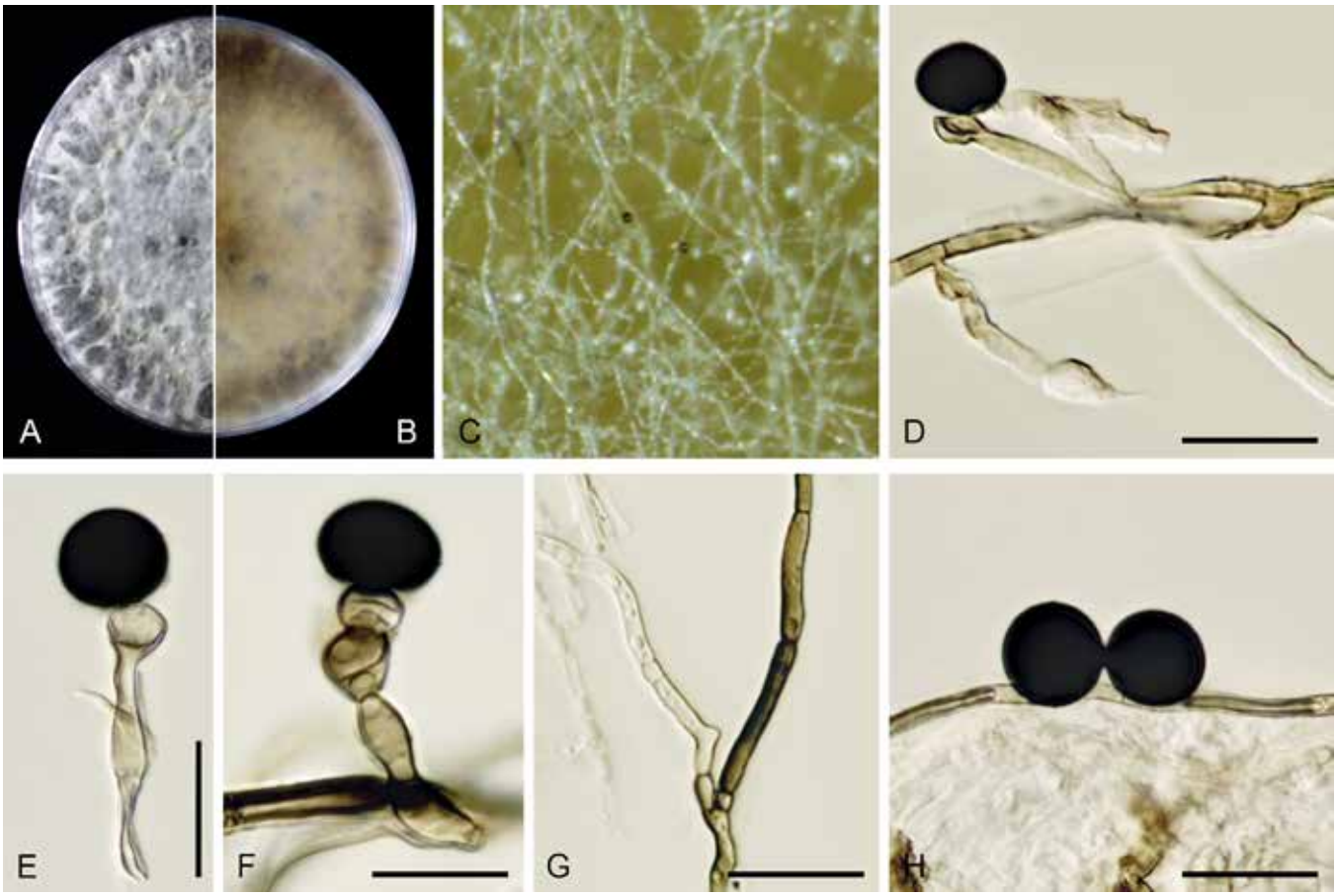

Fig. 42. *Nigrospora covidalis* (ex-type CGMCC 3.20538). **A, B.** Colony on PDA (front and reverse). **C.** Sporulation on SNA medium. **D–F.** Conidiophores with conidia. **G.** Hyphal growth. **H.** Conidia. Scale bars = 5 µm.

Culture characteristics: Colony on PDA fast growing, reaching 86 mm diam in 1 wk after incubation at 25 ± 1 °C; colony sparse, rough surface with fimbriate edge, elevation raised, floccose and irregular at margin; colony from above rough, sparse, white; from below white to black, not producing pigment in PDA media.

Cardinal temperature for growth: Optimum 25 °C, maximum 37 °C, minimum 5 °C.

Typus: **China**, Jiangxi Province, on *Lithocarpus* sp. (*Fagaceae*), Oct. 2013, Y.H. Gao, N. Zhou & Y. Zhang (**holotype** HMAS 350622, culture ex-type CGMCC 3.20538 = LC 4566).

Additional material examined: **China**, Jiangxi Province, on *Lithocarpus*, Oct. 2013, Y.H. Gao, N. Zhou & Y. Zhang, culture LC 158337.

Notes: *Nigrospora covidalis* clustered in a well-supported clade closely related to *N. musae* (Fig. 41). Morphologically, *N. covidalis* can be differentiated from *N. musae* in the smaller size of its conidiogenous cells (5–8.5 × 4.5–7 µm *vs* 6.5–14 × 6–9 µm) and conidia (9–14 µm *vs* 15–19.5 µm). Additionally, vesicles were present in *N. musae* but absent in *N. covidalis*.

Nigrospora globospora M. Raza, Qian Chen & L. Cai, ***sp. nov.*** MycoBank MB 840805. Fig. 43.

Etymology: Refers to the globose shape of its conidia.

Asexual morph on SNA: *Hyphae* smooth, septate, branched, hyaline to pale brown, 1.5–4.5 µm diam. *Conidiophores* reduced to conidiogenous cells. *Conidiogenous cells* monoblastic, solitary,

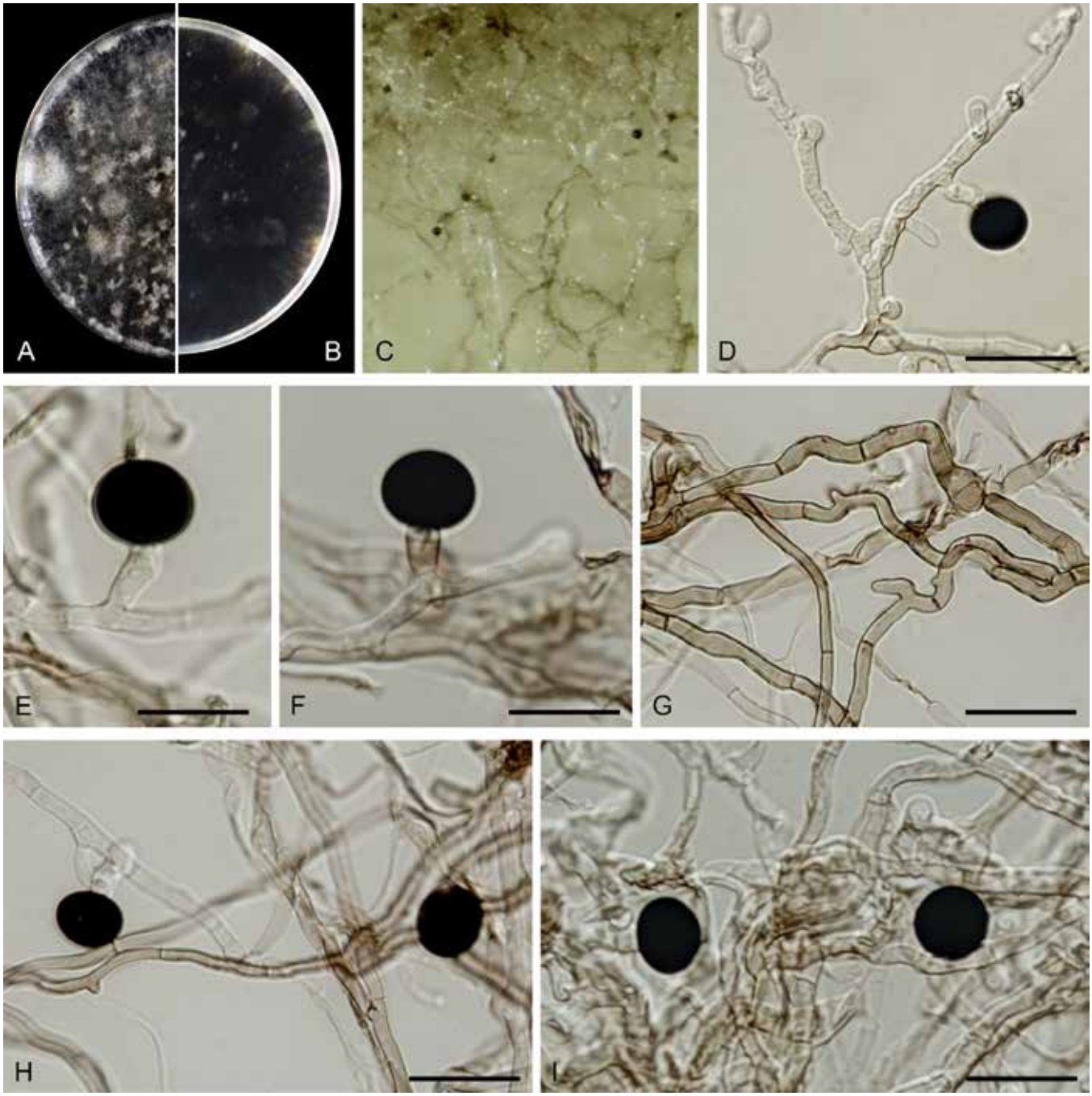

Fig. 43. *Nigrospora globospora* (ex-type CGMCC 3.20539). **A, B.** Colony on PDA (front and reverse). **C.** Sporulation on SNA medium. **D–F.** Conidiophores with conidia. **G.** Hyphal growth. **H, I.** Conidia. Scale bars = 5 µm.

discrete, determinate, sub-spherical or ampulliform, 8.5–9 × 3–4.5 µm (av. = 7.39 ± 1.1 × 3.8 ± 0.4). *Conidia* sparse, discrete on aerial hyphae, black, shiny, mostly ellipsoidal, 8.5–12 × 10.5–13.5 µm (av. = 10.51 ± 0.9 × 12.11 ± 0.6).

Culture characteristics: Colony on PDA fast growing, reaching 89 mm diam in 1 wk after incubation at 25 ± 1 °C, colony with rough surface and erose edge, elevation raised, effuse and strongly irregular at margin; colony from above rough, whitish black; from below white to black, not producing pigment in PDA media.

Cardinal temperature for growth: Optimum 25 °C, maximum 37 °C, minimum 5 °C.

Typus: **China**, Fujian Province, Fuzhou, Wuyishan country, on *Petasites hybridus* (*Asteraceae*), Aug. 2016, L. Cai (**holotype** HMAS 350624, culture ex-type CGMCC 3.19633 = LC 8397).

Additional material examined: **China**, Fujian Province, Fuzhou, Wuyishan country, on *Petasites hybridus*, Aug. 2016, L. Cai, culture LC 12441.

Notes: *Nigrospora globospora* clustered with *N. magnoliae* and formed a distinct clade (Fig. 41). Morphologically, *N. globosporium* can be differentiated from *N. magnoliae* by its larger conidiogenous cells (8.5–9 × 3–4.5 µm *vs* 5–7× 5–6 µm) and smaller conidia (8.5–12 × 10.5–13.5 µm *vs* 10–14 × 10–13 µm).

Nigrospora philosophiae-doctoris M. Raza, Qian Chen & L. Cai, ***sp. nov.*** MycoBank MB 840803. Fig. 44.

Etymology: Refers to a PhD career in academia, PhD represents the *Latin* phrase "*philosophiae doctor*".

Asexual morph on SNA: *Hyphae* septate, branched, flexuous or straight, hyaline to pale brown, 1.5–3.5 µm diam. *Conidiophores* reduced to conidiogenous cells. *Conidiogenous cells* monoblastic, discrete, solitary, pale brown, subglobose to ampulliform, 4–9.5 × 3–7.5 µm (av. = 6.66 ± 1.6 × 5.83 ± 1.4). *Conidia* discrete on aerial hyphae, sparse, pale brown to brown, globose or subglobose, 11–16 × 8–14 µm (av. = 14.02 ± 1.4 × 11.38 ± 1.6).

Culture characteristics: Colony on PDA fast growing, reaching 88 mm diam in 1 wk after incubation at 25 ± 1 °C, colony medium sparse, rough surface with fimbriate edge, elevation raised, downy, funiculate, floccose and irregular at margin; colony from above; rough, sparse, white; from below; black, not producing pigment in PDA media.

Cardinal temperature for growth: Optimum 25 °C, maximum 37 °C, minimum 5 °C.

Typus: **China**, Guangxi Region, Baise, Leye country, on *Disporum sessile* (*Colchicaceae*), Aug. 2017, Z.Y. Ma & L.W. Hou (**holotype** HMAS 350623, culture ex-type CGMCC 3.20540 = LC 13398).

Additional materials examined: **China**, Guangxi Region, Baise, Leye country, on *Disporum sessile*, Aug. 2017, Z.Y. Ma and L.W. Hou, culture LC 15838.

Notes: *Nigrospora philosophiae-doctoris* clustered in a well-supported clade closely related to *N. sacchari-officinarum* and *N.*

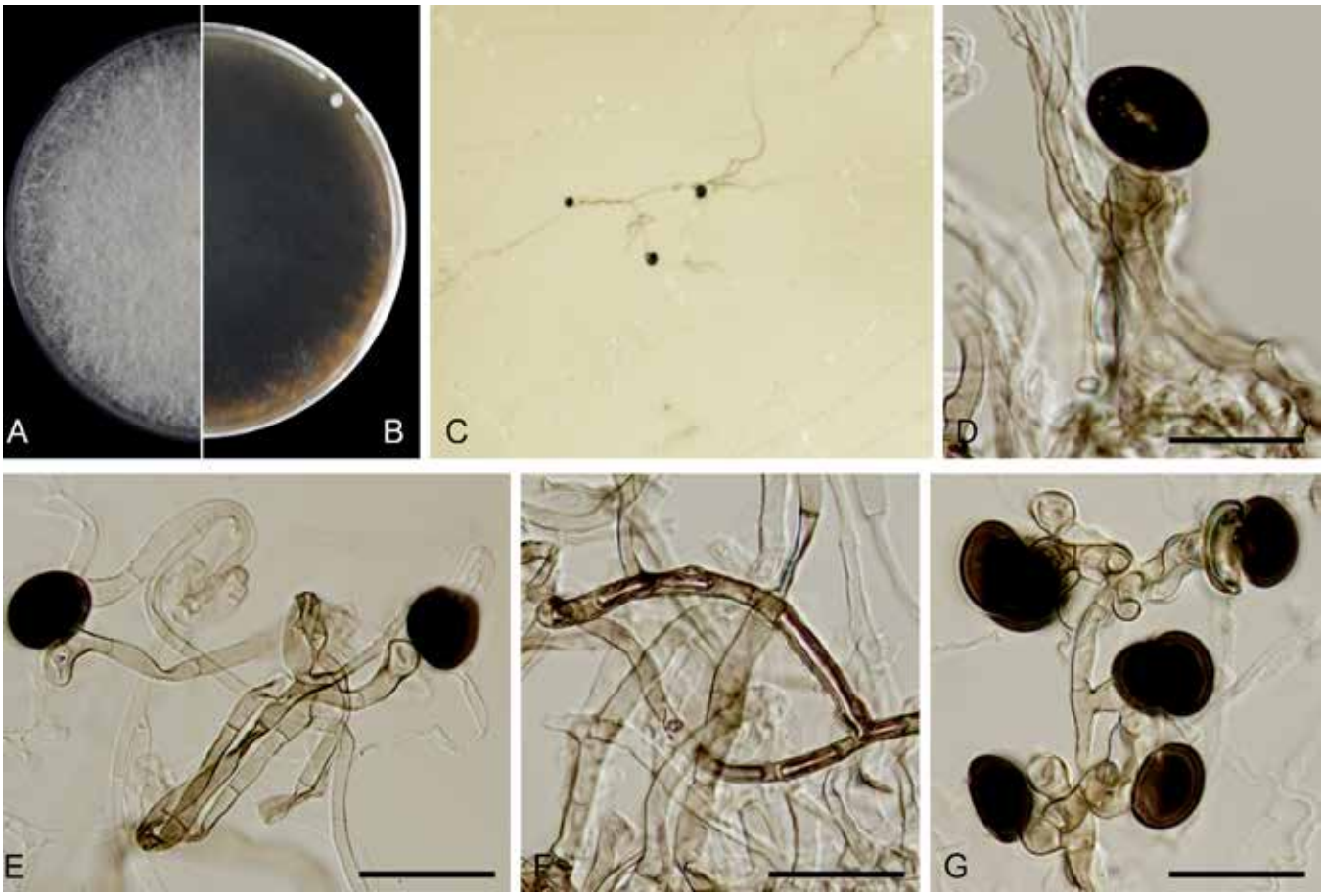

Fig. 44. *Nigrospora philosophiae-doctoris* (ex-type CGMCC 3.20540). **A, B.** Colony on PDA (front and reverse). **C.** Sporulation on SNA medium. **D, E.** Conidiophores with conidia. **F.** Hyphal growth. **G.** Conidia. Scale bars = 5 µm.

gorlenkoana (Fig. 41). *Nigrospora philosophiae-doctoris* produces smaller conidiogenous cells when compared to those in *N. sacchari-officinarum* and *N. gorlenkoana* (4–9.5 × 3–7.5 µm in *N. philosophiae-doctoris*; 7–15.5 × 9 5–9.5 µm in *N. sacchari-officinarum*; 7–13.5 × 4–9 µm in *N. gorlenkoana*), and smaller conidia than those of *N. sacchari-officinarum*. Additionally, vesicles were present in *N. sacchari-officinarum* but absent in *N. philosophiae-doctoris*.

Genome sequenced strain: *Nigrospora sphaerica.* **Unknown**, from fruit of *Musa* × *paradisiaca* (= *Musa sapientum*), collection date and collector unknown, culture CBS 166.26. This Whole Genome Shutgun project has been deposited at GenBank under the accession JALRMJ000000000 (BioProject: PRJNA827019, BioSample: SAMN27594418; present study).

Authors: M. Raza, Q. Chen & L. Cai

Pezicula Tul & C. Tul., Select. fung. carpol. (Paris) 3: 182. 1865. Fig. 45.

Classification: *Leotiomycetes*, *Leotiomycetidae*, *Helotiales*, *Dermateaceae*.

Type species: *Pezicula carpinea* (Pers.) Tul. & C. Tul. ex Fuckel., basionym: *Peziza carpinea* Pers., Syn. meth. fung.: 673. 1801. Holotype: L 910.261-293. Epitype and ex-epitype strain designated by Chen *et al.* (2016): CBS H-17476, CBS 923.96.

DNA barcodes (genus): ITS, LSU.

DNA barcode (species): *rpb2*. Table 13. Fig. 46.

Ascomata apothecial, erumpent, solitary or in clusters, sessile to short pedicellate. *Disc* pruinose, circular to irregular, pale whitish, orange, yellow, olivaceous, or orange brown to dark brown. *Receptacle* dark brown to olivaceous black, with entire margin, persistent or irregular, often with slightly raised rim. *Peridium* thickened, unequally, two-layered, outer layer comprising of hyaline to dark brown, thick-walled cells, inner layer comprising of thin-walled, hyaline to brown cells. *Hamathecium* comprising smooth, septate, filiform, septate or branched, filamentous paraphyses, tapering towards apex. *Asci* 8- or 4-spored, cylindrical-clavate to clavate, inoperculate, short pedicillate with knob-like pedicle, sometimes crozier present, apically well-developed, thickened, amyloid, with a J+. *Ascospores* smooth, thin-walled, straight or curved, ovoid, fusoid or ellipsoidal, hyaline, guttulate, aseptate to septate, or muriform. *Conidiomata* erumpent, single or clustered, immersed, subglobose, irregular pulvinate to conical or claviform, sometimes stromatic acervular, plane to pustulate. *Conidiophores* smooth, hyaline, simple, branched, acrogenous or acropleurogenous. *Conidiogenous cells* determinate, discrete or integrated, phialidic or indeterminate, proliferating percurrently, cylindrical to ampulliform, giving rise to macro- or micro-conidia. *Macroconidia* usually present, smooth, thin-walled, aseptate to septate, hyaline, ellipsoidal, pyriform, fusoid or claviform, rounded or pointed at apex, attenuated or rounded with protruding scar at base, guttulate, sometimes form micro-conidia from minute opening. *Microconidia* usually present, hyaline, smooth, aseptate, thin-walled, cylindrical, rounded at apex, truncate at base, content granular (adapted from Verkley 1999, Chen *et al.* 2016).

Cultural characteristics: Colonies on OA growing fast compared to MEA. Colonies on OA, flat, entire or discrete margins, aerial mycelium absent or weakly developed with patches, hyaline to buff, reverse concolourous. Colonies on MEA, flat, slightly raised, entire or discrete margins, moderately to well-developed white aerial mycelium, pigmented or non-pigmented.

Optimal media and cultivation conditions: OA and MEA at 18 °C with nuv-light (12 h light, 12 h dark).

Distribution: Worldwide.

Hosts: Pathogens, saprophytes or endophytes on a variety of hosts such as *Abies alba*, *A. balsamea*, *Larix decidua*, *Tsuga canadensis* (*Pinaceae*), *Acer spicatum* (*Sapindaceae*), *Alnus crispa*, *A. glutinosa*, *Carpinus betulus* (*Betulaceae*), *Chamaecyparis* sp. (*Cupressaceae*), *Cornus rugosa* (*Cornaceae*), *Eucalyptus* sp. (*Myrtaceae*), *Fagus sylvatica*, *Quercus robur*, *Castanea sativa* (*Fagaceae*), *Gaultheria shallon* (*Ericaceae*), *Taxus baccata* (*Taxaceae*), *Tilia cordata* (*Malvaceae*), *Rhamnus frangula* (*Rhamnaceae*), *Rubus* sp. (*Rosaceae*).

Disease symptoms: Cankers, but also saprobic.

Notes: *Pezicula*, a discomycetous gejnus typified by *Pe. carpinea* was established by Tulasne & Tulasne (1865). The type species of *Cryptosporiopsis* (*Cryp. nigra*) was considered the asexual morph of *Pezicula ocellata* (Chen *et al.* 2016), *Cryptosporiopsis* has therefore been synonymised under *Pezizula* (Johnston *et al.* 2014). Previous studies considered *Pezicula*, *Phlyctema* and *Rhizodermea* as congeneric to *Neofabraea*, but these groups present great variation in morphology (Réblová *et al.* 2011, Johnston *et al.* 2014). Recently, Chen *et al.* (2016) emphasised the usefulness of *rpb2* in resolving the phylogenetic relationships among *Cryptosporiopsis*, *Neofabraea*, and *Pezicula*, and concluded that *Pezicula* represents a separate genus. The genera *Neofabraea* and *Pezicula* have similar apothecia but the excipular tissues are less differentiated in *Neofabraea*. Phialidic conidiogenous cells and strongly curved macroconidia are present in *Neofabraea* species while species of *Pezicula* have two types of conidiogenesis (determinate and phialidic or indeterminate and proliferating percurrently). Species of *Pezicula* and related genera vary in host specificity, but most studies to date have focussed on northern America or Europe. Epitypification of species from *Pezicula* and related genera therefore remains of great importance to stabilise the application of names in this generic complex.

References: Verkley 1999, Abeln *et al.* 2000, Chen *et al.* 2016, Ekanayaka *et al.* 2016 (morphology and phylogeny).

Genome sequenced strain: *Pezicula carpinea.* **Germany**, Bad Bentheim, Bentheimer relictwald, near Kuhrort, on recently fallen *Carpinus betulus*, 9 Jul. 1996, G. Verkley, culture ex-epitype CBS 923.96. This Whole Genome Shutgun project has been deposited at GenBank under the accession JALRMK000000000 (BioProject: PRJNA827019, BioSample: SAMN27594419; present study).

Authors: M. Raza & L. Cai

Phaeomoniella Crous & W. Gams, Phytopathol. Medit. 39: 113. 2000. Fig 47.

Classification: *Eurotiomycetes*, *Chaetothyriomycetidae*, *Phaeomoniellales*, *Celotheliaceae.*

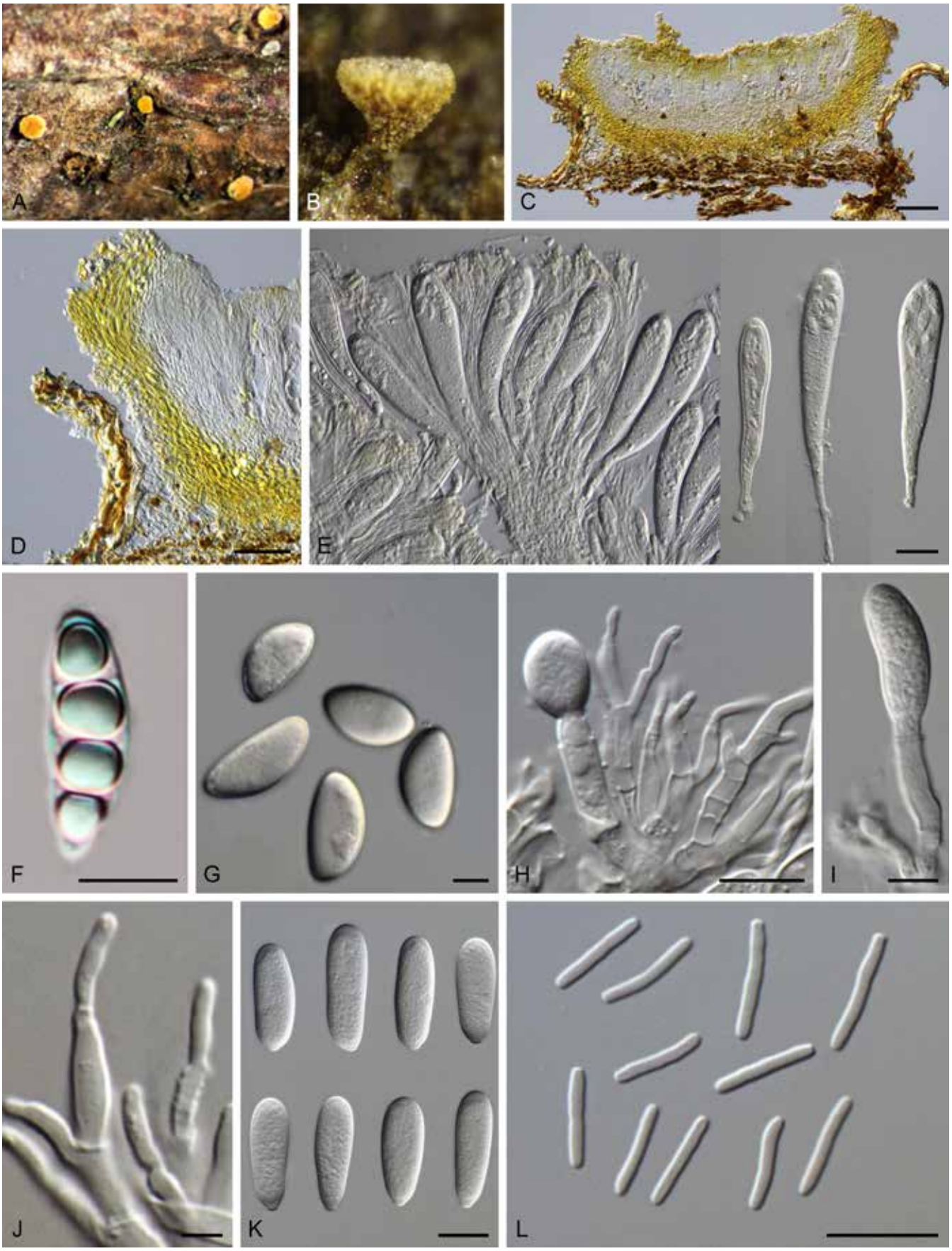

Fig. 45. *Pezicula* spp. **A–G.** Sexual morph. **A, B.** Living on substrate. **A.** Ascomata of *Pezicula chiangraiensis* (holotype MFLU 15-3566). **B.** Dry apothecium of *Pezicula neocinnamomea* (ex-type CBS 100248). **C.** Section through apothecium of *Pezicula ocellata* (CBS 949.97). **D.** Section through peridium of *Pezicula ocellata* (CBS 949.97). **E.** Asci and paraphyses of *Pezicula carpinea* (ex-epitype CBS 923.96). **F.** Fusoid ascospore of *Pezicula chiangraiensis* (holotype MFLU 15-3566). **G.** Ascospores of *Pezicula ocellata* (CBS 949.97). **H–L.** Asexual morph. **H.** Conidiophores, macro- and microconidiogenous cells of *Pezicula fagacearum* (ex-type CBS 112400). **I.** Macroconidiogenous cells giving rise to macrocondia with phialides of *Pezicula fagacearum* (ex-type CBS 112400). **J.** Microconidiogenous cells giving rise to microcondia with phialides of *Pezicula fagacearum* (ex-type CBS 112400). **K.** Macroconidia of *Pezicula neocinnamomea* (ex-type CBS 100248). **L.** Microconidia of *Pezicula pseudocinnamomea* (ex-type CBS 101000). Scale bars: C = 100 µm, E = 20 µm, F–I, K, L = 10 µm, J = 5 µm. Pictures A, F taken from Ekanayaka *et al.* (2016); B–E, G–L from Chen *et al.* (2016).

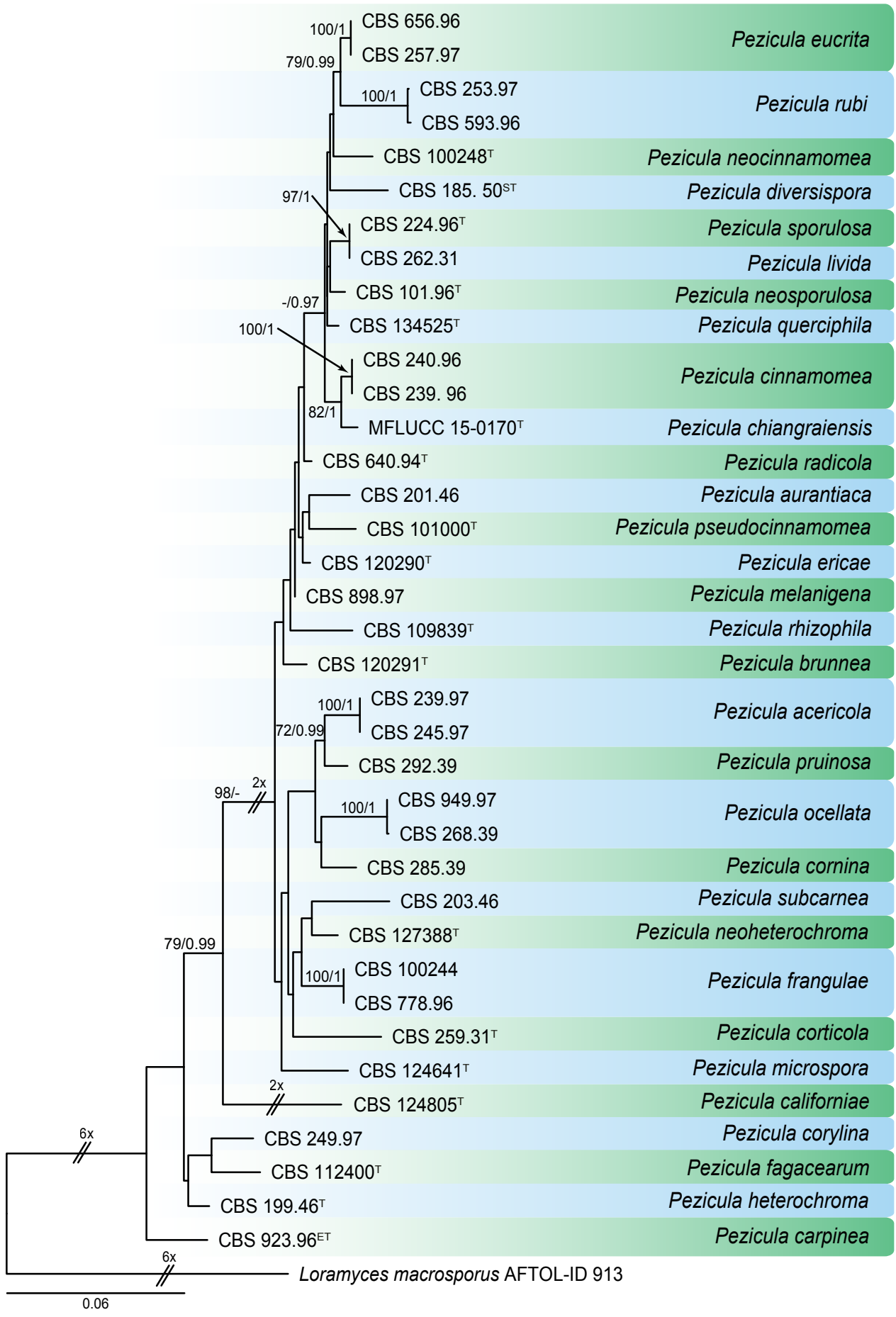

Fig. 46. RAxML phylogram constructed from ITS (490 bp), LSU (799 bp) and *rpb2* (1 045 bp) sequences of all accepted species of *Pezicula*. Maximum likelihood bootstrap support values (> 70 %) and Bayesian posterior probability scores (> 0.95) are indicated on the branches. The tree was rooted to *Loramyces macrosporus* AFTOL-ID 913. GenBank accession numbers are indicated in Table 13. [T, ET] and [ST], indicate ex-type, ex-epitype and ex-syntype strains, respectively. TreeBASE: S26191.

Table 13. DNA barcodes of accepted *Pezicula* spp.

Species	Isolates[1]	GenBank accession numbers[2]			References
		ITS	LSU	*rpb2*	
Pezicula acericola	CBS 239.97	KF376154	KR858884	KF376214	Chen *et al.* (2016), Ekanayaka *et al.* (2016)
	CBS 245.97	KF376153	KR858889	KF376213	Chen *et al.* (2016), Ekanayaka *et al.* (2016)
Pe. aurantiaca	CBS 201.46	KF376150	KR858893	KF376210	Chen *et al.* (2016), Ekanayaka *et al.* (2016)
Pe. brunnea	CBS120291^{T}	KR859103	KR858894	—	Chen *et al.* (2016)
Pe. californiae	CBS 124805^{T}	KR859104	KR858895	KR859332	Chen *et al.* (2016), Ekanayaka *et al.* (2016)
Pe. carpinea	CBS 923.96^{ET}	KR859108	KR858899	KF376158	Chen *et al.* (2016), Ekanayaka *et al.* (2016)
Pe. chiangraiensis	MFLUCC 15-0170^{T}	KU310621	KU310622	KU310623	Ekanayaka *et al.* (2016)
Pe. cinnamomea	CBS 239.96	KF376102	KR858915	KF376165	Chen *et al.* (2016), Ekanayaka *et al.* (2016)
	CBS 240.96	KF376105	KR858916	KF376163	Chen *et al.* (2016), Ekanayaka *et al.* (2016)
Pe. cornina	CBS 285.39	AF141182	—	—	Abeln *et al.* (2000)
Pe. corticola	CBS 259.31^{T}	KR859164	KR858956	—	Chen *et al.* (2016), Ekanayaka *et al.* (2016)
Pe. corylina	CBS 249.97	KF376106	KR858960	KF376161	Chen *et al.* (2016), Ekanayaka *et al.* (2016)
Pe. diversispora	CBS 185.50ST	KR859170	KR858962	—	Chen *et al.* (2016)
Pe. ericae	CBS120290^{T}	KR859173	KR858965	—	Chen *et al.* (2016)
Pe. eucrita	CBS 656.96	KF376144	KR858977	KF376208	Chen *et al.* (2016), Ekanayaka *et al.* (2016)
	CBS 257.97	KR859177	KR858969	—	Chen *et al.* (2016)
Pe. fagacearum	CBS 112400^{T}	KR859201	KR858993	—	Chen *et al.* (2016)
Pe. frangulae	CBS 778.96	KF376151	KR859001	KF376212	Chen *et al.* (2016), Ekanayaka *et al.* (2016)
	CBS 100244	KF376152	KR858996	KF376211	Chen *et al.* (2016), Ekanayaka *et al.* (2016)
Pe. heterochroma	CBS 199.46^{T}	KR859210	KR859002	—	Chen *et al.* (2016)
Pe. livida	CBS 262.31	AF141180	—	—	Abeln *et al.* (2000)
Pe. melanigena	CBS 898.97	KR859211	KR859003	—	Chen *et al.* (2016)
Pe. microspora	CBS 124641^{T}	KR859212	KR859004	KR859337	Chen *et al.* (2016)
Pe. neocinnamomea	CBS 100248^{T}	KR859213	KR859005	KF376209	Chen *et al.* (2016)
Pe. neoheterochroma	CBS 127388^{T}	KR859221	KR859013	KR859338	Chen *et al.* (2016)
Pe. neosporulosa	CBS 101.96^{T}	KR859223	KR859015	KF376193	Chen *et al.* (2016), Ekanayaka *et al.* (2016)
Pe. ocellata	CBS 949.97	KF376149	KR859025	KF376215	Chen *et al.* (2016) Ekanayaka *et al.* (2016)
	CBS 268.39	KR859232	KR859024	KR859339	Chen *et al.* (2016)
Pe. pruinosa	CBS 292.39	AF141188	KR859026	—	Abeln *et al.* (2000), Chen *et al.* (2016)
Pe. pseudocinnamomea	CBS 101000^{T}	KR859235	KR859027	KR859340	Chen *et al.* (2016)
Pe. querciphila	CBS 134525^{T}	JX144750	—	—	Chen *et al.* (2016)
Pe. radicicola	CBS 640.94^{T}	KR859236	KR859028	—	Chen *et al.* (2016)
Pe. rhizophila	CBS 109839^{T}	KR859238	KR859030	—	Chen *et al.* (2016)
Pe. rubi	CBS 253.97	KF376100	KR859042	KF376204	Chen *et al.* (2016), Ekanayaka *et al.* (2016)
	CBS 593.96	KF376101	KR859045	KF376203	Chen *et al.* (2016), Ekanayaka *et al.* (2016)
Pe. sporulosa	CBS 224.96^{T}	AF141172	KR859053	KF376201	Chen *et al.* (2016), Ekanayaka *et al.* (2016)
Pe. subcarnea	CBS 203.46	AF141171	KR859059	—	Abeln *et al.* (2000), Chen *et al.* (2016)

[1] CBS: Westerdijk Fungal Biodiversity Institute, Utrecht, the Netherlands; MFLUCC: Mae Fah Luang University Culture Collection, Chiang Rai, Thailand. $^{T, ET}$ and ST indicate ex-type, ex-epitype and ex-syntype strains, respectively.

[2] ITS: internal transcribed spacers and intervening 5.8S nrDNA; LSU: partial 28S large subunit nrRNA gene; *rpb2*: partial RNA polymerase II second largest subunit gene.

Type species: *Phaeomoniella chlamydospora* (W. Gams *et al.*) Crous & W. Gams, basionym: *Phaeoacremonium chlamydosporum* W. Gams *et al.*, Mycologia 88: 792. 1996. Holotype and ex-type strain: CBS H-5709, CBS 229.95.

DNA barcode (genus): LSU.

DNA barcodes (species): ITS and *tef1*. Table 14. Fig. 48.

Mycelium consisting of branched, septate hyphae. *Hyphae* simple, or occurring in strands, verruculose to tuberculate, green-brown, becoming paler to hyaline towards the conidiogenous region. Chlamydospore-like structures present, forming microsclerotia on water agar. *Conidiophores* micronematous, arising from aerial or

Fig. 47. *Phaeomoniella chlamydospora* (culture STE-U 6384). **A–C.** Symptoms of Petri disease on grapevines. **A, B.** Brown-black discolouration of vascular tissue of grapevine rootstock. **C.** Brown-black streaking in vertical section of an infected rootstock. **D, E.** Conidiomata on grapevine wood. **F.** Section through a conidioma. **G, H.** Conidiogenous cells from conidiomata. **I.** Conidia from conidiomata. **J–R.** Structures from the hyphomycetous stage. **J.** Mycelium and conidial droplets. **K–M, O.** Conidiophores. **N, P.** Condiogenous cells. **Q.** Adelophialide. **R.** Conidia. Scale bars: D = 500 µm; E, J = 100 µm; F, G, I, K, O, P, R = 10 µm. G applies to H; K applies to L–N; P applies to Q.

submerged hyphae, erect, simple, subcylindrical, green-brown, becoming paler toward the tip, verruculose to smooth, septate. *Conidiogenous cells* terminal, monophialidic, elongate-ampulliform to lageniform or subcylindrical, with a terminal, narrowly funnel-shaped collarette. *Conidia* becoming aggregated into round, slimy heads at the apices of conidiogenous cells, pigmented, aseptate, smooth-walled, oblong-ellipsoidal to obovate, straight. *Synasexual morph* phoma-like, induced in culture and on infected canes. *Conidiomata* brown, pycnidial, globose, up to 70 µm diam. *Conidiophores* pale brown, subcylindrical, smooth, 1- to

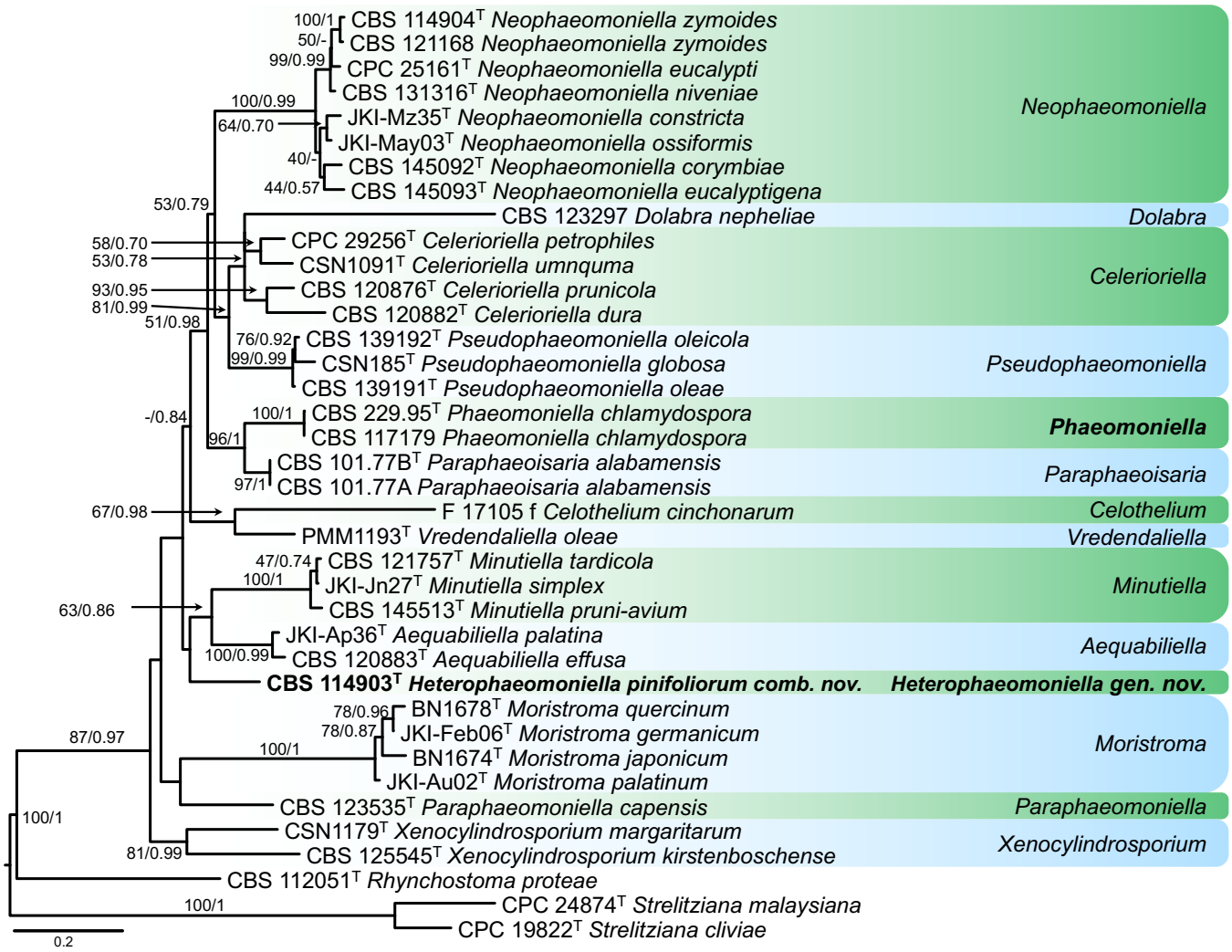

Fig. 48. Maximum likelihood phylogram of the *Phaeomoniellales* constructed from ITS (636 bp), 28S (869 bp), *tef1* (274 bp) and *tub2* (423 bp) sequences. Maximum likelihood bootstrap support values (> 40 %) and Bayesian posterior probability scores (> 0.70) are shown at the nodes. The novel taxon is printed in **bold**. The phylogenetic tree was rooted to *Rhynchostoma proteae* CBS 112051, *Strelitziana cliviae* CPC 19822 and *S. malaysiana* CPC 24874. GenBank accession numbers of *Phaeomoniella* and *Heterophaeomoniella* are listed in Table 14. [T] indicates ex-type strain. TreeBASE: S27583.

Table 14. DNA barcodes of accepted species in *Phaeomoniella* and *Heterophaeomoniella*.

Species	Isolates[1]	GenBank accession numbers[2]				References
		ITS	LSU	*tef1*	*tub2*	
Phaeomoniella chlamydospora	CBS 229.95[T]	NR_155612	NG_066265	—	AF253968	Groenewald *et al.* (2001), Vu *et al.* (2019)
	CBS 117179	KF764544	—	KF764636	KF764683	Úrbez-Torres *et al.* (2014)
Heterophaeomoniella pinifoliorum	CBS 114903[T]	DQ270240	MN861685	MN861678	KR260452	Lee *et al.* (2006), Úrbez-Torres *et al.* (2015), present study

[1] CBS: Westerdijk Fungal Biodiversity Institute, Utrecht, the Netherlands; [T] indicates ex-type strain.

[2] ITS: internal transcribed spacer regions, including the 5.8S nrDNA; LSU: partial 28S large subunit nrRNA gene; *tef1*: partial translation elongation factor 1-α gene.

multiseptate. *Conidiogenous cells* monophialidic, terminal and intercalary, variable in shape, but frequently subcylindrical to oblong-ellipsoidal. *Conidia* exuding from pycnidia in a droplet or cirrus, hyaline, oblong-ellipsoidal to obovate, permanently straight. *Sexual morph* unknown.

Cultural characteristics: Colonies on MEA (reverse) grey olivaceous to olivaceous black, with sparse aerial mycelium.

Optimal media and cultivation conditions: PDA or MEA to induce sporulation of the asexual morph, while for the synasexual morph WA with sterilised pine needles is recommended, incubated at 25 °C.

Distribution: Worldwide.

Hosts: Mainly pathogen of grapevine (*Vitis vinifera* and *Vitis* spp.; *Vitaceae*). One of the causal agents of Petri disease and esca on

grapevines. Once reported on kiwi fruit in Italy (di Marco *et al.* 2000) and olive trees in California (Úrbez-Torres *et al.* 2013).

Disease symptoms: Brown to black discolouration of vascular tissue; streaking symptoms when vertically sectioned and brown to black spots (goo-like) when cross-sectioned. Young vines with Petri disease show stunted growth, shoot dieback and in severe conditions, the young vines can die.

Notes: Currently only one species resides in the genus *Phaeomoniella*. *Phaeomoniella pinifoliorum* groups together with *Paraphaeomoniella capensis*, being distinctly different from *Pa. chlamydospora*. Several species described in *Phaeomoniella* were placed into new genera including *Aequabiliella*, *Celerioriella*, *Minutiella*, *Neophaeomoniella* and *Paraphaeomoniella*. Morphological variation motivated the introduction of new genera with some genera that only formed the coelomycetous morph and no hyphomycete morph (Crous *et al.* 2015c). Available sequence data mostly include ITS and LSU, only limited *tef1* sequences are available.

Genome sequenced strain: *Phaeomoniella chlamydospora*. **USA**, California, Riverside County, Coachella Valley, 33.617467 N, 116.065139 W, Nov. 2011, collector unknown, isolate UCR-PC4. This Whole Genome Shutgun project has been deposited at GenBank under the accession LCWF00000000 (BioProject: PRJNA261774, BioSample: SAMN03077702; Morales-Cruz *et al*., 2015).

Heterophaeomoniella L. Mostert, C.F.J. Spies, Halleen & Gramaje, ***gen. nov.*** MycoBank MB 835744. Table 14. Fig. 48.

Etymology: "*Heter*" meaning other; morphologically similar, but phylogenetically different from *Phaeomoniella*.

Mycelium densely interwoven, forming globular to ovoid vesicles. *Phialides* commonly simple, inflated, sometimes integrated as swollen cells into toruloid hyphal segments, usually without an obvious collarette. *Conidia* hyaline, cylindrical to ovoid, often slightly curved to allantoid, potentially reproducing in a yeast-like fashion after dehiscence, secondary conidiation common with the yeast-like conidia arising mostly from phialidic apertures at the ends of primary conidia. Vesicular *chlamydospores* abundant, hyaline or subhyaline, globose to subglobose, formed singly or in chains (from Lee *et al.* 2006).

Type species: *Heterophaeomoniella pinifoliorum* (Hyang B. Lee *et al*.) L. Mostert, C.F.J. Spies, Halleen & Gramaje. Holotype and ex-type culture: SFC P00327, CBS 114903 = SFCCW202.

Notes: A new genus name is proposed for *Phaeomoniella pinifoliorum.* Only one isolate of *Phaeomoniella pinifoliorum* has been found to date. This isolate is phylogenetically distant from *Phaeomoniella* (Fig. 48). *Phaeomoniella zymoides* and *Pa. pinifoliorum* were described by Lee *et al.* (2006) from pine needles in Korea. *Phaeomoniella zymoides* was renamed as *Neophaeomoniella zymoides* (H.B. Lee *et al*.) Crous (Crous *et al.* 2015c), being distinct from *Pa. chlamydospora*, although it was initially a sister clade to *P.a chlamydospora* when less taxa were included the phylogeny of Lee *et al.* (2006). *Phaeomoniella pinifoliorum* was found to differ from *Pa. chlamydospora* in optimal growth in culture (Lee *et al. 2006*). Furthermore, *Pa. pinifoliorum* produced little to no aerial mycelium in comparison with *Pa. chlamydospora* (Lee *et al.* 2006).

Heterophaeomoniella pinifoliorum (Hyang B. Lee *et al.*) L. Mostert, C.F.J. Spies, Halleen & Gramaje, ***comb. nov.*** MycoBank MB 835759.
Basionym: *Phaeomoniella pinifoliorum* Hyang B. Lee *et al.,* Mycologia 98: 605. 2006.

Description and illustration: Lee *et al.* (2006).

Typus: **Korea**, Mount Juwang, Gyungsangbug-do, on needles of *Pinus densiflora* (*Pinaceae*), 20 Jan 2004, H.B. Lee (**holotype** SFC P00327, culture ex-type CBS 114903 = SFCCW202).

References: Crous *et al.* 1996, Crous & Gams 2000, Damm *et al*. 2010, Chen *et al*. 2015a, Crous *et al*. 2015c (morphology and systematics); Larignon & Dubos 1997, Mugnai *et al*. 1999, Pascoe & Cottral 2000, Gatica *et al*. 2001, Halleen *et al*. 2003, Luque *et al*. 2009, Gramaje *et al*. 2010, White *et al*. 2011, Diaz & Latorre 2014 (symptoms and pathogenicity); Groenewald *et al.* 2000, Ridgway *et al*. 2002, Whiteman *et al*. 2002, Overton *et al*. 2004, Retief *et al*. 2005, Martos *et al*. 2011, Martín *et al*. 2012, Pouzoulet *et al*. 2013, Úrbez-Torres *et al*. 2015 (detection); Mostert *et al*. 2000, Tegli *et al*. 2000, Borie *et al*. 2002, Pottinger *et al*. 2002, Tello *et al*. 2010 (genetic diversity); Antonielli *et al*. 2014, Morales-Cruz *et al*. 2015 (genomes).

Authors: L. Mostert, C.F.J. Spies, F. Halleen & D. Gramaje

Phytophthora de Bary, J. Roy. Agric. Soc. England 12: 240. 1876. Figs 49–51.

Classification: *Stramenipila*, *Oomycota*, *Peronosporomycetes*, *Peronosporales*, *Peronosporaceae*.

Fig. 49. Morphological structures of *Phytophthora*. **A.** Coenocytic, irregular coralloid hyphae of *Phytophthora* ×*heterohybrida*. **B.** Catenulate, globose to subglobose and irregular hyphal swellings of *Phytophthora pseudosyringae*. **C, D.** Papillate, slightly asymmetric caducous sporangia of *Phytophthora tropicalis* with basal plug. **C.** Elongated-ovoid with medium-length pedicel. **D.** Pyriform with long pedicel. **E.** Compound sympodium of *Phytophthora tropicalis* sporangia. **F.** Bipapillate, laterally attached distorted sporangium of *Phytophthora citrophthora*. **G.** Semipapillate, ovoid to obpyriform sporangium of *Phytophthora plurivora*. **H.** Ovoid nonpapillate sporangium of *Phytophthora* ×*cambivora*. **I.** Internal extended sporangial proliferation of *Phytophthora* ×*cambivora*. **J.** Internal nested sporangial proliferation of *Phytophthora* ×*cambivora* and release of zoospores with flagella (arrows). **K.** Zoospore cysts of *Phytophthora cinnamomi* germinating directly with a hypha and after release of a secondary zoospore (arrow; diplanetism). **L.** Zoospore cysts of *Phytophthora cinnamomi* germinating directly with hyphae or by forming a microsporangium (arrow). **M.** Terminal thin-walled chlamydospore of *Phytophthora cinnamomi*. **N.** Lateral, sessile thick-walled chlamydospore of *Phytophthora meadii*. **O.** Elongated oogonium of *Phytophthora attenuata* with long-tapering curved base, a conspicuous basal plug, a subglobose plerotic oospore containing a lipid globule, and a paragynous antheridium. **P.** Globose oogonium of *Phytophthora plurivora* with tapering curved base, a plerotic oospore containing a lipid globule and a paragynous antheridium with finger-like projection (arrow). **Q.** Oogonium of the heterothallic *Phytophthora cinnamomi* resulting from an A1×A2 cross, with golden-brown wall, thick-walled plerotic oospore containing multiple lipid globules, and an amphigynous bicellular antheridium. **R.** Oogonia of the heterothallic *Phytophthora* ×*cambivora* resulting from an A1×A2 cross, with an ornamented-wavy wall, a plerotic oospore and a bicellular amphigynous antheridium (arrow) or smooth-walled with an aplerotic oospore and a unicellular amphigynous antheridium. **S.** Oogonium of *Phytophthora uniformis* with a thin stalk and wavy wall, an aplerotic oospore containing a large lipid globule, a bicellular amphigynous and a secondary paragynous (arrow) antheridium. **T.** Comma-shaped oogonium of *Phytophthora* ×*multiformis*, with ornamented, golden-brown wall and unicellular amphigynous antheridium. Scale bars = 25 µm; T applies to A–D and F–T.

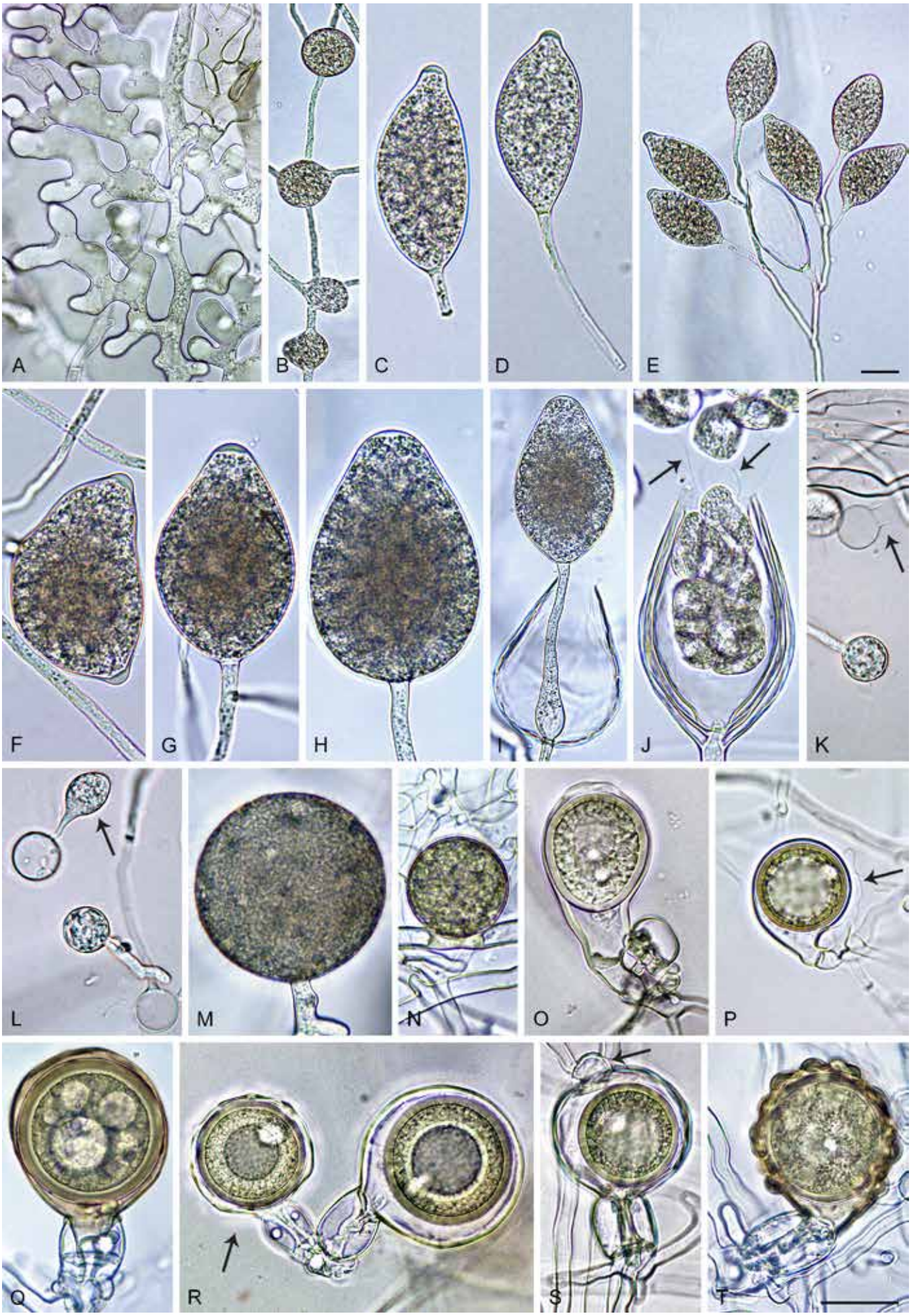
A
B
C
D
E
F
G
H
I
J
K
L
M
N
O
P
Q
R
S
T

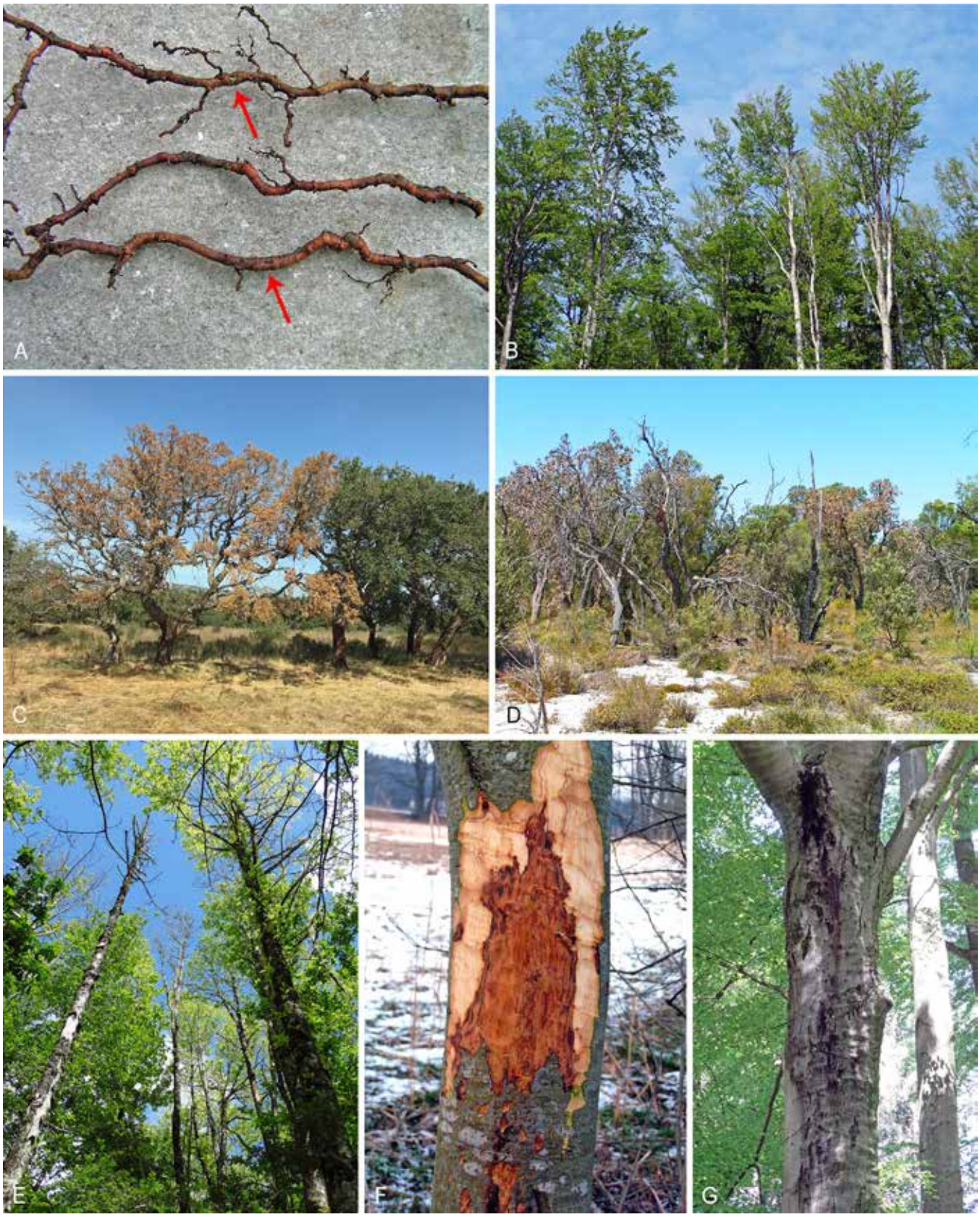

Fig. 50. Phytophthora diseases of forest trees. **A.** Small woody roots of a mature *Quercus robur* with severe losses of fine roots and lateral roots and bark lesions (arrows) caused by *Phytophthora plurivora* and *Phytophthora quercina*. **B.** Chlorosis, microphylly, thinning and dieback of *Fagus sylvatica* due to root and collar rot caused by *Phytophthora ×cambivora*. **C.** Acute wilting and death of *Quercus suber* due to a girdling collar rot lesion caused by *Phytophthora cinnamomi*. **D.** Extensive dieback and collapse of a *Banksia* woodland caused by *Phytophthora cinnamomi*. **E.** Chlorosis, thinning, dieback and mortality of *Castanea sativa* caused by *Phytophthora cinnamomi*. **F.** Orange-brown, tongue-shaped, active inner bark lesion caused by *Phytophthora ×alni* on *Alnus incana*. **G.** Aerial bleeding canker caused by *Phytophthora ×cambivora* on *Fagus sylvatica*.

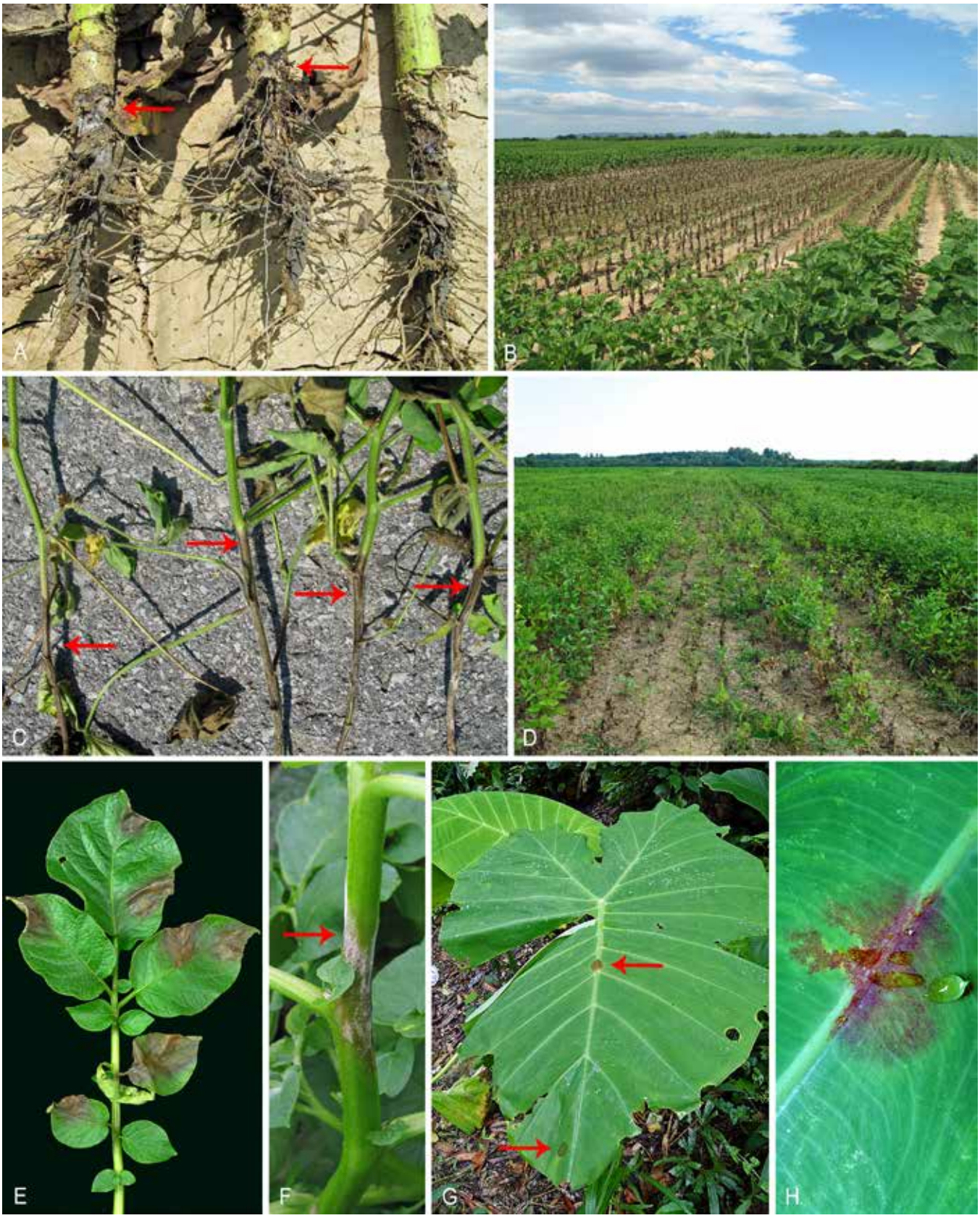

Fig. 51. Phytophthora diseases of agricultural plants. **A.** Root and collar rot (arrows) of *Helianthus annuus* caused by *Phytophthora rosacearum*. **B.** Patch dieback and mortality of *Helianthus annuus* caused by *Phytophthora rosacearum* following heavy rain and temporary waterlogging. **C.** Stem rot (arrows) of *Glycine max* caused by *Phytophthora sojae*. **D.** Patch dieback and mortality of *Glycine max* caused by *Phytophthora sojae* following heavy rain and temporary waterlogging. **E.** Late blight on *Solanum tuberosum* leaves caused by *Phytophthora infestans*. **F.** Late blight on *Solanum tuberosum* stem with white masses of sporangia (arrow). **G, H.** Necrotic lesions (arrows) caused by *Phytophthora colocasiae* on leaves of *Colocasia esculenta*. Pictures A–D courtesy to Dr Željko Tomić, Center for Plant Protection, Zagreb, Croatia; E, F courtesy to Dr David Cooke, The James Hutton Institute, Dundee, UK.

Type species: *Phytophthora infestans* (Mont.) de Bary, basionym: *Botrytis infestans* Mont., Bull. Sci. Soc. Philom. Paris 13: 313. 1845; **holotype** of *B. infestans*: **France**, from leaves of *Solanum tuberosum* (*Solanaceae*) "Sur les fanes de pomme de terre" M. Vernois, coll. H. Montagne, dep. on 18 Aug. 1845, Hi.C. Montagne FUSION94490 in PC; additional synonym: *Peronospora infestans* (Mont.) Casp., in Rabenhorst, Klotzschii Herb. Viv. Mycol. Ed. II, Cent. 19: no. 1879 (1854). **Netherlands**, from infected *Solanum tuberosum*, 1993, A. Drenth (**epitype** designated here CBS H-24657, MBT 10005612, culture ex-epitype CBS 147289).

DNA barcodes (genus): LSU, ITS, *cox1.*

DNA barcodes (species): ITS, *Btub*, *TigA*, *cox1*. Table 15. Figs 52–56.

Mycelium hyaline, consisting of individual hyphae 3–8 µm diam, generally coenocytic (Fig. 49A) with septa occurring only in ageing cultures. *Hyphae* branched with a conspicuous constriction at the base of lateral hyphae, coralloid, nodose, smooth, swollen, tuberculate or undulate (Fig. 49A); *hyphal swellings* spherical, ellipsoid, appressoria-like or irregular-elongated shape, occurring terminally, laterally or intercalary, often in chains (catenulate; Fig. 49B) or groups; *hyphal aggregations* occasionally present, originated by clusters of lateral hyphae or hyphae twisting around each other. *Sporangia*, or *zoosporangia*, borne on thin-walled sporangiophores, variable in shape and size (Fig. 49C–J), mostly spherical, subspherical, ovoid, obovoid, ellipsoid, elongated, limoniform, pyriform, obpyriform to turbinate, obturbinate, ampulliform and distorted, sometimes containing a large vacuole at maturity; *sporangial tip* either with a conspicuous protruding papilla at the apex (papillate; Fig. 49C–E), sometimes laterally displaced, bipapillate (Fig. 49F) or tripapillate, or with an inconspicuous papilla (semipapillate; Fig. 49G), or nonpapillate (Fig. 49H–I); *sporangial base* round or tapered, often with a prominent plug, a globose swelling or a conspicuous narrowing, and occasionally with laterally attached sporangiophore (Fig. 49F); persistent or caducous breaking off below a basal plug separating a short (< 5 µm), intermediate (5–20 µm; Fig. 49C) or long pedicel (> 20 µm; Fig. 49D) from the bearing sporangiophore; pedicel length mostly species specific; *sporangial proliferation* externally with hyphae arising close to sporangial base and forming monochasial or dichasial, lax or dense-compound sympodia (Fig. 49E), and internally, both in an extended or nested way (Fig. 49I–J), only occurring in species with nonpapillate sporangia; *Phytophthora* species with a primarily aerial lifestyle usually form papillate or semipapillate, caducuous sporangia in more or less compound sympodia (Fig. 49E). In contrast, *Phytophthora* species with a primarily aquatic or soilborne lifestyle form nonpapillate or semipapillate, persistent sporangia on unbranched sporangiophores or in lax sympodia; sporangia usually germinate indirectly via release of zoospores or — on solid agar or in oxygen-depleted aqueous solutions — directly with one or more germ tubes which usually emerge at the sporangial apex. *Zoospores* are fully differentiated inside the sporangium and discharged through a narrow to wide exit pore at the sporangial apex into an ephemeral membranous vesicle, reniform (kidney-like), motile with two heterokont flagella developing from the concave side; chemotactically attracted to and encysting on the surface of host tissues; *zoospore cysts* germinate directly by forming hyphae or a secondary microsporangium (Fig. 49K–L) or indirectly by releasing a secondary zoospore (= diplanetism; Fig. 49K). *Chlamydospores* are produced by some *Phytophthora* species, thin-walled in soilborne and aquatic species (Fig. 49M) or thick-walled in aerial species (Fig. 49N), formed either individually or in clusters, differentiated at the tip of hyphae (terminal; Fig. 49M), laterally on short hyphae or sessile (Fig. 49N) or intercalary, with globose, ellipsoid or irregular shape, sometimes with one or multiple radiating hyphal extensions. *Gametangia* produced by homothallic species in single culture and by heterothallic species only when individuals of the opposite compatibility types (= mating types) A1 and A2 are paired; *oogonia* globose to subglobose (Fig. 49P–S), sometimes elongated (Fig. 49O), pyriform, ellipsoid, comma-shaped (Fig. 49T), tubular or excentric, with a tapering (Fig. 49O, Q, T) or rounded base (Fig. 49P, R, S), occasionally with a curved, twisted or long thick oogonial stalk; oogonial wall smooth (Fig. 49P, R), wavy (Fig. 49Q, S), flexuose (Fig. 49O) or ornamented with bullate protuberances (verrucose; Fig. 49R, T), mostly hyaline but they may become pigmented golden- to dark-brown with age (Fig. 49Q, T); *oospores* mostly globose to subglobose (Fig. 49P–T) or less frequently elongated (Fig. 49O), thick-walled, near-plerotic to plerotic (Fig. 49O–Q, T) or aplerotic (Fig. 49R–S), usually containing one large or less frequently multiple smaller lipid globules (ooplasts); *antheridia* attached to the oogonium laterally (paragynous; Fig. 49O–P) or surrounding the oogonial stalk (amphigynous; Fig. 49Q–T)), single- (Fig. 49O–R, T) or two-celled (Fig. 49Q–S), sometimes with finger-like hyphal projections (Fig. 49P); homothallic *Phytophthora* species amphigynous, paragynous or with both types of antheridial insertion; heterothallic *Phytophthora* species always form amphigynous antheridia but sometimes one or multiple additional paragynous antheridia can be observed, in particular when A2 mating type isolates are selfing (main references for morphology: Blackwell 1949, Brasier & Griffin 1979, Erwin & Ribeiro 1996, Jung *et al.* 1999, 2003, 2011, 2017a, b, Jung & Burgess 2009).

Culture characteristics: Colonies always white with chrysanthemum, petallate, petaloid, radiate, stellate, striate, rosaceous, dendroid or uniform patterns; on V8-juice agar (V8A) and carrot agar (CA) appressed, felty, or with limited to fluffy aerial mycelium, in some species umbonate in the centre of the colony, with round or irregular margins; largely submerged on CMA; on PDA and MEA often with slow growth, felty to cottony aerial mycelium, and round to irregular, sometimes submerged margins (Brasier & Griffin 1979, Erwin & Ribeiro 1996, Jung *et al.* 1999, 2002, 2003, 2011, 2017a, b, 2021, Brasier *et al.* 2004, Jung & Burgess 2009, Rea *et al.* 2010, 2011, Bertier *et al.* 2013a, Yang & Hong 2013, Henricot *et al.* 2014, Scanu *et al.* 2014a, 2015, Burgess *et al.* 2018).

Optimal media and cultivation conditions: A range of selective agar media available for *Phytophthora* isolations with PARPNH agar and Synthetic Mucor Agar (SMA) being most commonly used (Elliott *et al.* 1966, Masago *et al.* 1977, Jeffers & Martin 1986, Erwin & Ribeiro 1996, Jung *et al.* 2000, 2002, 2021). V8A, CA prepared from grated carrots or carrot juice and — for *Phy. infestans* — rye agar at 20 °C in the dark to stimulate the production of gametangia (Brasier 1967, Erwin & Ribeiro 1996, Jung *et al.* 1999, Scanu *et al.* 2014a) which, depending on the *Phytophthora* species, predominantly occurs in the centre of the colony, confined to fertile patches of dense mycelium or at the margins of the colony close to the Petri dish walls. Chlamydospores and hyphal swellings frequently differentiated at the margins of the colony. V8A or CA discs from growing colonies submerged in nonsterile soil extract water under natural daylight at 18–24 °C to induce the production of sporangia (Erwin & Ribeiro 1996, Jung *et al.* 1996). Release of zoospores from mature sporangia occurs readily in most *Phytophthora* species but

can be stimulated by incubation for 30 min at 5–8 °C and returning to room temperature (chilling; Erwin & Ribeiro 1996). Long-term storage either cryogenic under liquid nitrogen (Mchau & Coffey 1995) or conventional on V8A, CA or PDA, sealed and double-bagged, in Petri dishes, on agar slants or as agar discs in tubes, either submerged in sterile distilled water or non-submerged, or on sterile hemp seeds submerged in sterile distilled water; incubation temperature 15–25 °C for tropical species and 5–14 °C for species from other climatic regions (*cf*. Boesewinkel 1976, Brasier & Griffin 1979, Erwin & Ribeiro 1996, Aragaki & Uchida 2001, Jung *et al.* 2002, 2017a, 2020, Pérez-Sierra *et al.* 2013, Ann *et al.* 2016).

Distribution: Worldwide.

Hosts: Apart from primarily aquatic species from phylogenetic Clades 6 and 9 with a predominant lifestyle as saprotrophic litter decomposers and opportunistic pathogens (Brasier *et al.* 2003a, Jung *et al.* 2011, 2020, Yang & Hong 2013), most *Phytophthora* species are primary plant pathogens causing serious damage to horticultural, ornamental, forestry and natural terrestrial, riparian and marine ecosystems. The genus *Phytophthora* has a particularly wide range of host plants within the *Dicotyledoneae*, *Monocotyledoneae*, *Acrogymnospermae* and *Polypodiopsida*. Many *Phytophthora* species are host-specific or have very limited host ranges, often within a plant genus or family, *i.e*. *Phy. abietivora* on *Abies fraseri*, *Phy. agathidicida* on *Agathis australis*, *Phy. aleatoria* and *Phy. pinifolia* on *Pinus radiata*, *Phy. amaranthi* on *Amaranthus tricolor*, *Phy. andina*, *Phy. betacei* and *Phy. infestans* on *Solanaceae* species, *Phy. austrocedrae* on *Austrocedrus chilensis* and *Juniperus communis*, *Phy. botryosa* on *Hevea brasiliensis*, *Phy. cajani* on *Cajanus cajan*, *Phy. captiosa* and *Phy. fallax* on *Eucalyptus* spp., *Phy. castanetorum* on *Castanea sativa*, *Phy. clandestina* on *Trifolium subterraneum*, *Phy. chesapeakensis* and *Phy. gemini* on *Zostera* spp., *Phy. cocois* on *Cocos nucifera*, *Phy. cyperi* on *Cyperus* spp., *Phy. flexuosa* on *Fagus hayatae*, *Phy. fragariae* on *Fragaria* × *ananassa*, *Phy. glovera* on *Nicotiana tabacum*, *Phy. idaei* and *Phy. rubi* on *Rubus idaeus*, *Phy. ilicis* on *Ilex aquifolium, Phy. intricata* on *Quercus tarokoensis*, *Phy. ipomoeae* on *Ipomoea* spp., *Phy. lateralis* on *Chamaecyparis* spp. and *Taxus brevifolia*, *Phy. medicaginis* on *Medicago sativa*, *Phy. megakarya* on *Theobroma cacao*, *Phy. mirabilis* on *Mirabilis jalapa*, *Phy. oleae* on *Olea europea*, *Phy. phaseoli* on *Phaseolus lunata*, *Phy. pisi* on *Pisum sativum* and *Vicia faba*, *Phy. pistaciae* on *Pistacia vera*, *Phy. pluvialis* on *Pseudotsuga menziesii* and *Pinus radiata*, *Phy. primulae* on *Primula* spp., *Phy. pseudotsugae* on *Pseudotsuga menziesii*, *Phy. quercina*, *Phy. quercetorum* and *Phy. tyrrhenica* on *Quercus* spp., *Phy. quininea* on *Cinchona* spp., *Phy. sojae* on *Glycine max*, *Phy. terminalis* on *Pachysandra terminalis*, *Phy. trifolii* on *Trifolium* spp., *Phy. tubulina* and *Phy. vulcanica* on *Fagus sylvatica*, *Phy. vignae* on *Vigna unguiculata* and *V. angularis*, *Phy.* ×*alni*, *Phy.* ×*multiformis* and *Phy. uniformis* on *Alnus* spp. (Crandall 1947, Buddenhagen & Young 1957, Amin *et al.* 1978, Brasier & Griffin 1979, Hamm & Hansen 1983, Galindo & Hohl 1985, Taylor *et al.* 1985, Hansen & Maxwell 1991, Wilcox *et al.* 1993, Kennedy & Duncan 1995, Erwin & Ribeiro 1996, Jung *et al.* 1999, 2000, 2017a, b, 2018a, Mirabolfathy *et al.* 2001, Hansen *et al.* 2000, 2012, Flier *et al.* 2002, Brasier *et al.* 2004, Dick *et al.* 2006, Greslebin *et al.* 2007, Tyler 2007, Balci *et al.* 2008, Durán *et al.* 2008, Abad *et al.* 2011, Man in't Veld *et al.* 2011, 2015, 2019, Forbes *et al.* 2013, Green *et al.* 2013, 2015, Heyman *et al.* 2013, Reeser *et al.* 2013, Scanu *et al.* 2014b, Scott & Williams 2014, Weir *et al.* 2015, Ann *et al.* 2016, Mideros *et al.* 2018, Ruano-Rosa *et al.* 2018, Li *et al.* 2019, Scott *et al.* 2019). Species from Clade 8b, *Phy. brassica*, *Phy. cichorii*, *Phy. dauci*, *Phy. lactucae*, *Phy. porri*, *Phy. pseudolactucae* and interspecific hybrids between them are host specific pathogens of various vegetable species (Erwin & Ribeiro 1996, Man in 't Veld *et al.* 2002, Bertier *et al.* 2013a, b, Rahman *et al.* 2015). In contrast, the notorious *Phy. cinnamomi* arguably has the widest host range of all plant pathogens infecting more than 5 000 woody and herbaceous, dicotyledonous, monocotyledonous and coniferous plant species (Erwin & Ribeiro 1996, Shearer *et al.* 2004, Cahill *et al.* 2008, Jung *et al.* 2013a, Hardham & Blackman 2018). Numerous *Phytophthora* species infect multiple plant species, *i.e. Phy. arenaria*, *Phy. attenuata*, *Phy. bisheria*, *Phy. capsici*, *Phy. castaneae*, *Phy. chlamydospora*, *Phy. citricola*, *Phy. condilina*, *Phy. constricta*, *Phy. crassamura*, *Phy. elongata*, *Phy. erythroseptica*, *Phy. europaea*, *Phy. gonapodyides*, *Phy. gregata*, *Phy. gibbosa*, *Phy. hedraiandra*, *Phy. hibernalis*, *Phy. inundata*, *Phy. kernoviae*, *Phy. lacustris*, *Phy. litoralis*, *Phy. heveae*, *Phy. kwongonina*, *Phy. meadii*, *Phy. pachypleura*, *Phy. parvispora*, *Phy. pseudorosacearum*, *Phy. pseudosyringae*, *Phy. psychrophila*, *Phy. rosacearum*, *Phy. sansomeana*, *Phy. syringae*, *Phy. tentaculata*, *Phy. thermophila* and *Phy. versiformis* (Mchau & Coffey 1995, Erwin & Ribeiro 1996, Abad *et al.* 2008, Jung *et al.* 2002, 2003, 2011, 2013b, 2016, 2017a, c, 2018a, b, 2020, Brasier *et al.* 2003b, 2005, de Cock & Lévesque 2004, Rea *et al.* 2010, 2011, Nechwatal *et al.* 2013, Pérez-Sierra *et al.* 2013, Henricot *et al.* 2014, Scanu *et al.* 2014a, 2015, Hansen *et al.* 2012, 2015, Paap *et al.* 2017, Burgess *et al.* 2018) and some have diverse host ranges of up to 100 and more woody and herbal plant species, *i.e*. *Phy. cactorum*, *Phy. citrophthora*, *Phy. cryptogea*, *Phy. drechsleri*, *Phy. megasperma*, *Phy. nicotianae*, *Phy. palmivora*, *Phy. plurivora*, *Phy. ramorum*, *Phy. tropicalis* and *Phy.* ×*cambivora* (Brasier & Griffin 1979, Erwin & Ribeiro 1996, Aragaki & Uchida 2001, Grünwald *et al.* 2008, Jung & Burgess 2009, Panabières *et al.* 2016, Jung *et al.* 2018a). The emerging pathogens *Phy. multivora* and *Phy. niederhauserii* have rapidly expanding host ranges (Scott *et al.* 2009, Abad *et al.* 2014). Generally, the *Cupressaceae*, *Ericaceae*, *Fabaceae*, *Fagaceae*, *Lauraceae*, *Myrtaceae*, *Nothofagaceae*, *Proteaceae* and *Rosaceae* families contain many susceptible woody hosts of *Phytophthora* spp.

Disease symptoms: Soilborne *Phytophthora* species cause damping-off, losses of fine roots and small lateral roots (Fig. 50A), necrotic bark lesions on woody roots (Fig. 50A), root rots (Fig. 51A), collar and stem rots (Fig. 50F, 51A, C) and bark lesions along the stem up to the canopy (aerial bark cankers or stem cankers; Fig. 50G) (Day 1938, Crandall *et al.* 1945, Tsao 1990, Shearer & Tippet 1989, Erwin & Ribeiro 1996, Harris 1991, Jung *et al.* 1996, 1999, 2000, 2013a, b, 2017c, 2018a, b, 2020, Hansen *et al.* 2000, 2012, Jung & Blaschke 2004, Tyler 2007, Jung 2009, Green *et al.* 2013, 2015, Pérez-Sierra *et al.* 2013, Ginetti *et al.* 2014, Bellgard *et al.* 2016). On woody plants collar rot and aerial bark lesions are characterised by orange-brown to black exudations at the surface of the bark and orange to dark-brown, tongue-shaped lesions of the inner bark (Fig. 50F, G; Crandall *et al.* 1945, Erwin & Ribeiro 1996, Hansen *et al.* 2000, Jung 2009, Jung *et al.* 2013a, b, 2018a, 2020, Green *et al.* 2013, Bellgard *et al.* 2016). In *Acacia*, *Citrus* and *Prunus* species bark cankers on stems and branches are characterised by gum-like exudations (gummosis; Erwin & Ribeiro 1996, Graham & Menge 2000, Pérez-Sierra *et al.* 2010, Jung *et al.* 2016, Puglisi *et al.* 2017, Albuquerque Alves *et al.* 2019). Since *Phytophthora* pathogens are advancing first in the cambium layer, the front of active lesions in the cambium and inner bark is usually considerably ahead of the exudate spots on the bark surface. Depending on the proportion of circumference, affected bark lesions on stems cause starvation of parts of the root system and reduced water transport.

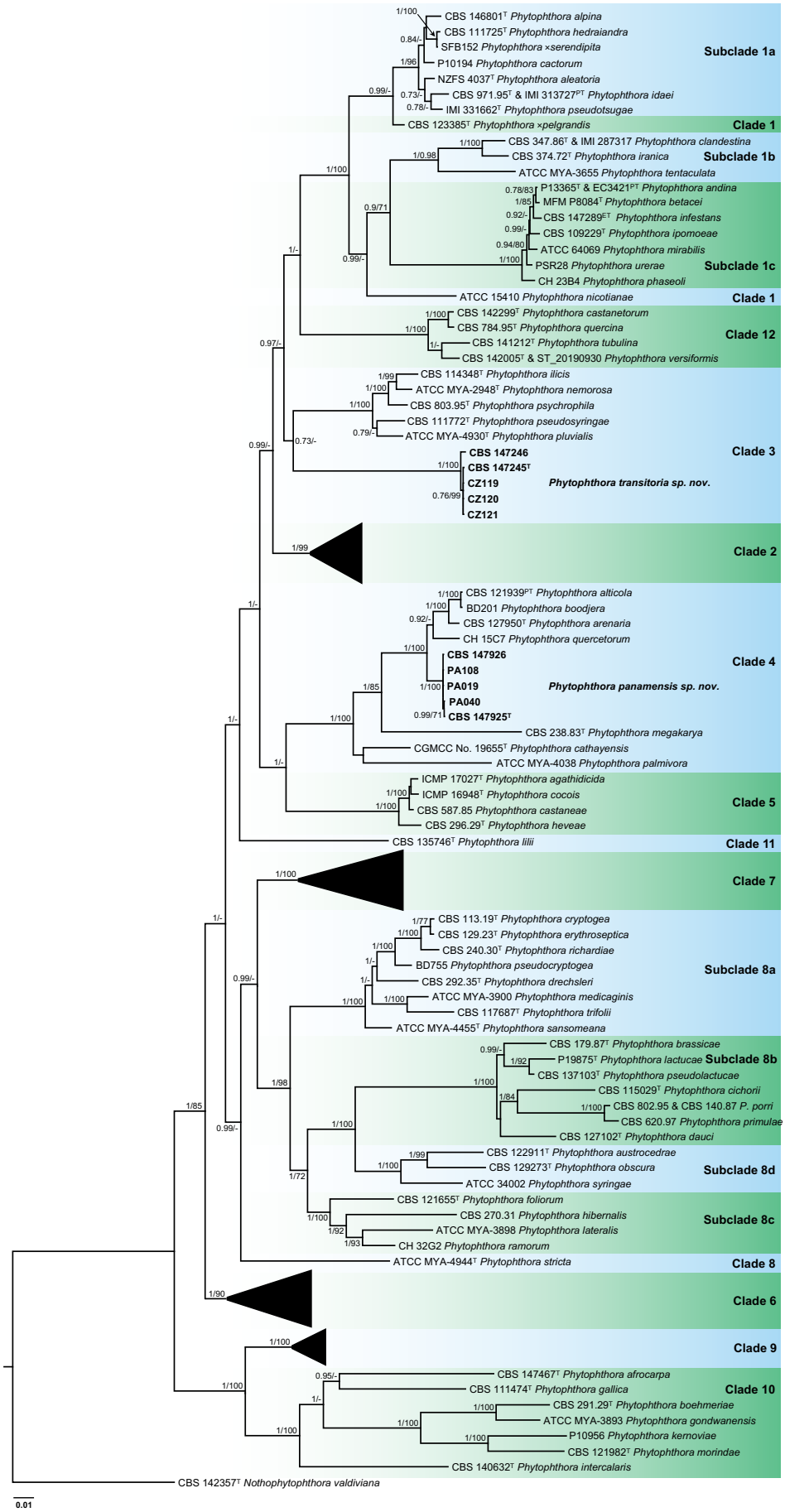

Fig. 52. Bayesian Inference phylogram constructed from ITS (1 185 bp), *Btub* (1 136 bp), *tigA* (1 669 bp) and *cox1* (867 bp) sequences of all accepted species of *Phytophthora*. Bayesian posterior probability scores (> 0.90) and RAxML bootstrap support values (> 70 %) are shown at the nodes. Detailed structures of Clades 2, 6, 7 and 9 are shown in Figs 53–56, respectively. The novel taxa are printed in **bold**. The phylogenetic tree was rooted to *Nothophytophthora valdiviana* CBS 142357. GenBank accession numbers are listed in Table 15. ^{T}, ^{ET} and ^{PT} indicate ex-type, ex-epitype and ex-paratype strains, respectively. TreeBASE: S28641.

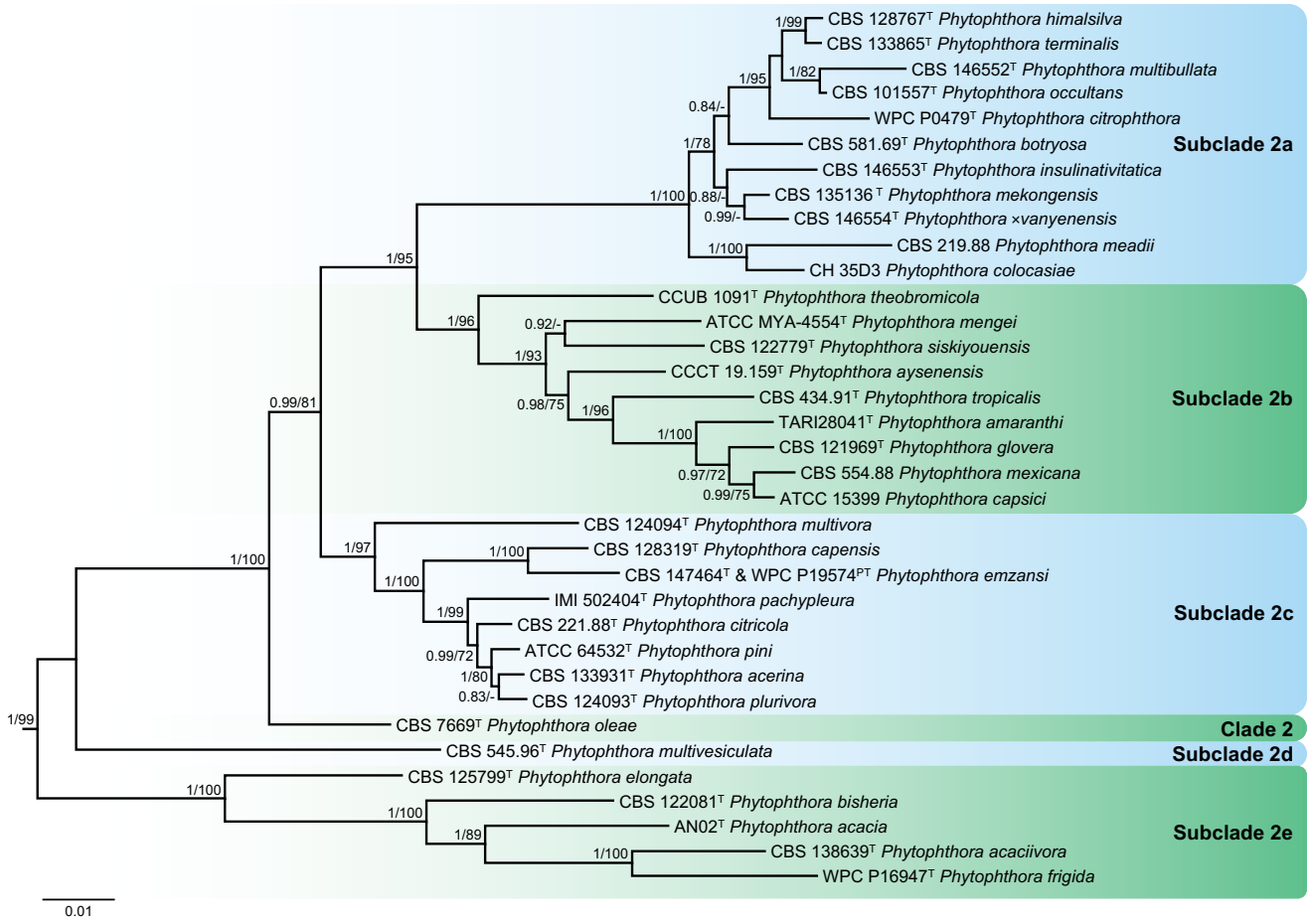

Fig. 53. Structure of *Phytophthora* Clade 2 in the Bayesian Inference phylogram constructed from ITS (1 185 bp), *Btub* (1 136 bp), *tigA* (1 669 bp) and *cox1* (867 bp) sequences of all accepted species of *Phytophthora* (Fig. 52). Bayesian posterior probability scores (> 0.90) and RAxML bootstrap support values (> 70 %) are shown at the nodes. GenBank accession numbers are listed in Table 15. ^{T} and ^{PT} indicate ex-type and ex-paratype strains, respectively. TreeBASE: S28641.

Reduced water uptake due to fine root losses and reduced water transport cause non-specific symptoms of drought and malnutrition in the crown such as increased transparency of the crown, sparse ramification resulting in whip-like branches, chlorotic, wilting, small-sized leaves which often cluster at the ends of branches (Fig. 50B–E; Erwin & Ribeiro 1996, Jung *et al.* 2000, 2013b, 2016, 2017c, 2018a, b, 2020, Jönsson *et al.* 2005, Jung 2009, Pérez-Sierra *et al.* 2010, 2013, Orlikowski *et al.* 2011, Pérez-Sierra & Jung 2013, Scanu *et al.* 2015, Bellgard *et al.* 2016, Milenković *et al.* 2018, Corcobado *et al.* 2020). In mature trees it can take decades of multicyclic inoculum build-up and infections until the destruction of the fine root system results in visible above-ground symptoms. Eventually trees and whole ecosystems can show dieback and die (Fig. 50B–E; Erwin & Ribeiro 1996, Shearer & Tippett 1989, Jung *et al.* 1996, 2000, 2013a, b, 2018a, b, Jung 2009). Girdling of large roots or the stem by bark lesions results in acute wilting and mortality (Fig. 50C, D). Temporary waterlogging after heavy or prolonged rain or flooding provides ideal conditions for continuous zoospore production and infections often leading to acute patch dieback and mortality, in particular in agricultural ecosystems with highly susceptible, often clonal crops (Fig. 51A–D) and in riparian ecosystems (Davison 1988, Harris 1991, Shearer & Tippett 1989, Erwin & Ribeiro 1996, Streito *et al.* 2002, Jung & Blaschke 2004, Dorrance 2013, Jung *et al.* 2018a). Splash-dispersal of soilborne sporangia and zoospores by heavy rain or sprinkler irrigation can cause leaf necroses, shoot dieback and fruit rot up to 2 m above the ground (Erwin & Ribeiro 1996, Nechwatal *et al.* 2011, Pérez-Sierra & Jung 2013).

Airborne *Phytophthora* species cause necrotic lesions on leaves, shoots and fruits (Fig. 51E–H), shoot dieback, defoliations, bleeding bark lesions and also root and foot rot (Erwin & Ribeiro 1996, Aragaki & Uchida 2001, Werres *et al.* 2001, Rizzo *et al.* 2002, Brasier *et al.* 2005, Brown & Brasier 2007, Brasier & Webber 2010, Reeser *et al.* 2013, Scanu & Webber 2016, Jung *et al.* 2016, 2018a, 2021, Hansen *et al.* 2017). Analogous to fine root diseases *Phytophthora*-induced leaf and fruit diseases are multicyclic and prolonged foggy and rainy periods or excessive sprinkler irrigation can result in epidemic disease outbreaks in temperate crops like *Solanum tuberosum* (late blight of leaves, shoots and tubers), *Solanum lycopersicum* (buckeye fruit rot, leaf blight) and *Piper nigrum* (damping-off, root, foot and fruit rot); tropical crops like *Artocarpus altilis* (leaf blight, fruit rot), *Theobroma cacao* (Black pod), *Cocos nucifera* (bud rot), *Durio zibethinus* (leaf blight, fruit rot, stem canker), *Artocarpus heterophyllus* (root rot, trunk cankers and gummosis, chlorosis, wilt, leaf blight, defoliation, fruit rot), *Carica papaya* (damping-off, leaf and shoot blight, pod rot), *Hevea brasiliensis* (early leaf fall, pod rot, black stripe and stem canker) and *Colocasia esculenta* (leaf blight) by *Phy. botryosa*, *Phy. colocasiae*, *Phy. meadii*, *Phy. palmivora* and *Phy. tropicalis*; forest trees and shrubs like *Larix kaempferi* and *Larix* × *eurolepis* (defoliation, bark cankers on twigs and stems), *Rhododendron ponticum* and *Umbellularia californica* laurel (leaf and shoot blight) by *Phy. ramorum*, *Pinus radiata* by *Phy. pinifolia* and *Phy. pluvialis*

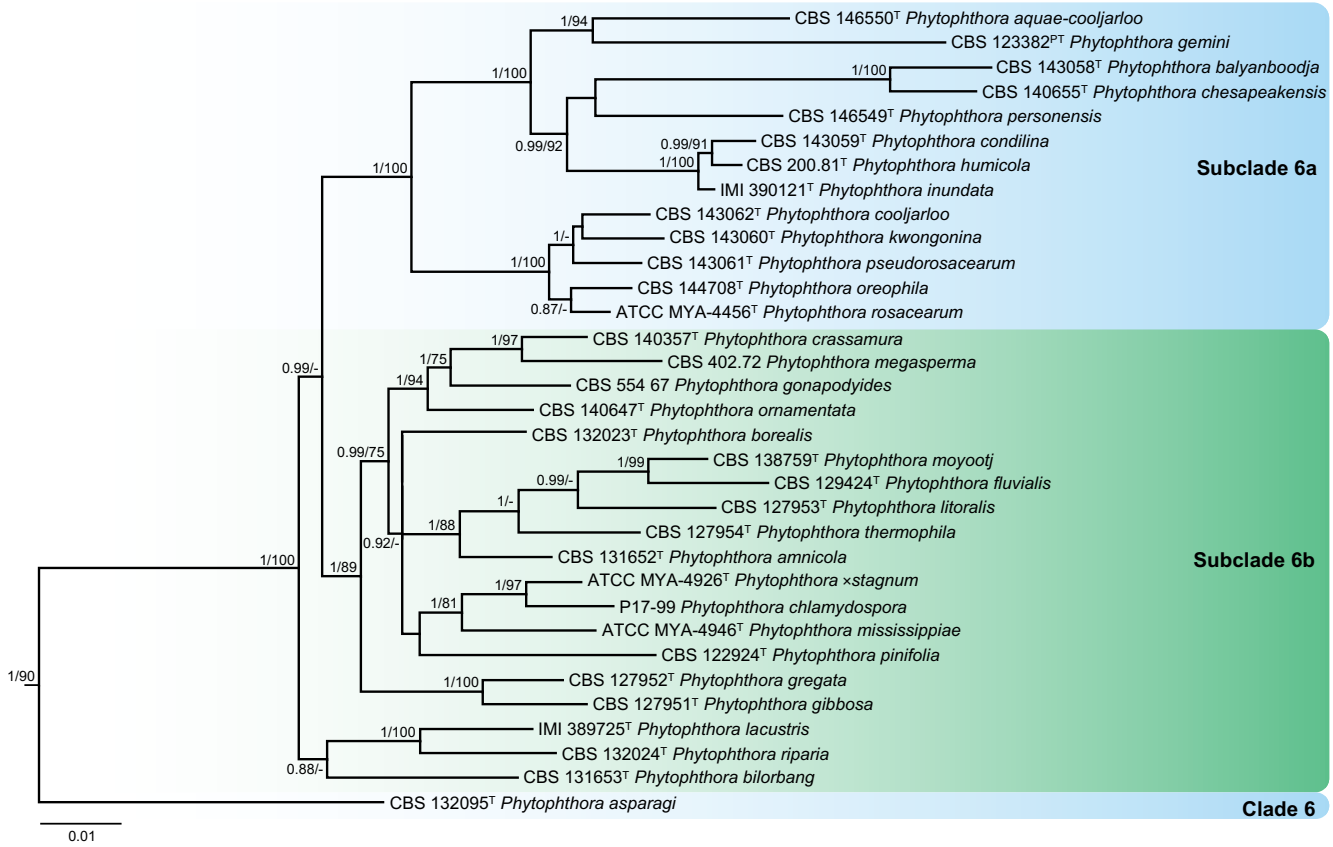

Fig. 54. Structure of *Phytophthora* Clade 6 in the Bayesian Inference phylogram constructed from ITS (1 185 bp), *Btub* (1 136 bp), *tigA* (1 669 bp) and *cox1* (867 bp) sequences of all accepted species of *Phytophthora* (Fig. 52). Bayesian posterior probability scores (> 0.90) and RAxML bootstrap support values (> 70 %) are shown at the nodes. GenBank accession numbers are listed in Table 15. ^{T} and ^{PT} indicate ex-type and ex-paratype strains, respectively. TreeBASE: S28641.

(needle cast), *Chamaecyparis* spp. by *Phy. lateralis* (needle and shoot necroses) or *Ilex aquifolium* by *Phy. ilicis* (leaf and shoot blight, fruit rot); and many ornamental plants like *Rhododendron* spp. (Brasier & Griffin 1979, Erwin & Ribeiro 1996, Aragaki & Uchida 2001, Werres *et al.* 2001, Rizzo *et al.* 2002, Drenth & Guest 2004, Durán *et al.* 2008, Grünwald *et al.* 2008, Brasier & Webber 2010, Robin *et al.* 2011, Webber *et al.* 2012, Forbes *et al.* 2013, Granke *et al.* 2013, Miyasaka *et al.* 2013, Sanogo & Bosland 2013, Jung *et al.* 2016, 2018a, Akrofi 2015, Tri *et al.* 2015, Puglisi *et al.* 2017).

Notes: The potato late blight epidemic caused by *Phy. infestans* was responsible for the Irish potato famine, which resulted in death and emigration of millions of people from Ireland (Haas *et al.* 2009). Worldwide control measure expenses and crop losses are estimated to be $6.7 billion per year (Haverkort *et al.* 2008). When the genus *Phytophthora* (Greek for 'plant destroyer') was established in 1876 by Anton de Bary with *Phy. infestans*, the causal agent of potato late blight, as type species, no culture was retained linked to this specimen. Therefore, we designate here an epitype for *Phy. infestans*. Isolate CBS 147289 (= T30–4) was chosen as ex-epitype strain because it has an A1 mating type, like the original strains causing the potato late blight epidemic of the 19th century studied by de Bary, with known parents resulting from a sexual cross between two Dutch *Phy. infestans* isolates from late-blighted potatoes, 80029 (A1 mating type, race 2.4.7, isolated in 1980) and 88133 (A2 mating type, race 1.3.7.10.11, isolated in 1988) performed in potato leaves under natural conditions (Drenth *et al.* 1995); it was used in numerous studies including the sequencing of the *Phy. infestans* reference genome ASM14294v1 (genome size 240 Mbp; GenBank assembly accession GCA_000142945.1, RefSeq assembly accession GCF_000142945.1) (Haas *et al.* 2009); and proved to contain all six avirulence genes studied in the experiments of van der Lee *et al.* (2001).

Until the end of the 20th century the number of described *Phytophthora* species was gradually increasing to 50 (Erwin & Ribeiro 1996, Jung *et al.* 1999). However, during the past two decades the number of new species descriptions was skyrocketing and the genus currently comprises 192 described and accepted culturable species (Table 15; Figs 52–56) and six unculturable species (*Phy. cyperi*, *Phy. cyperi-bulbosi*, *Phy. lepironiae*, *Phy. leersiae*, *Phy. polygoni* and *Phy. verrucosa*). The latter were not included in the phylogenetic analyses of the present study. Several factors contributed to this exponential increase of *Phytophthora* species numbers. The advent and advance of molecular sequencing techniques and phylogenetic inference analyses allowed the sorting out of several morphospecies complexes (*cf.* Brasier *et al.* 2003b, Jung *et al.* 2003, 2011, 2017b, Man In' t Veld 2002, 2007, Hansen *et al.* 2009, 2015, Hong *et al.* 2009, 2011, Jung & Burgess 2009, Scott *et al.* 2009, Rea *et al.* 2010, Bertier *et al.* 2013a, Nechwatal *et al.* 2013, Scanu *et al.* 2014b, Burgess *et al.* 2018) and correct identifications of isolates in culture collections (Burgess *et al.* 2009, Rahman *et al.* 2015). Further, surveys in previously unexplored natural and semi-natural ecosystems in Africa, Asia, Australia, Europe, the USA and South America uncovered an unprecedented diversity of both known and unknown *Phytophthora* species (*cf.* Jung *et al.* 1999, 2000, 2002, 2003, 2011, 2017a–d, 2018b, 2020, Hansen *et al.* 2003, 2012, Dick *et al.* 2006, Balci *et al.* 2008, Reeser *et al.* 2011, 2013, Vettraino *et al.* 2011, Oh *et al.* 2013, Ginetti *et al.* 2014, Scanu *et al.* 2015, Paap *et al.* 2017, Burgess *et al.* 2017, 2018) supporting the prediction of 200–600 unknown *Phytophthora* species in natural ecosystems (Brasier 2009).

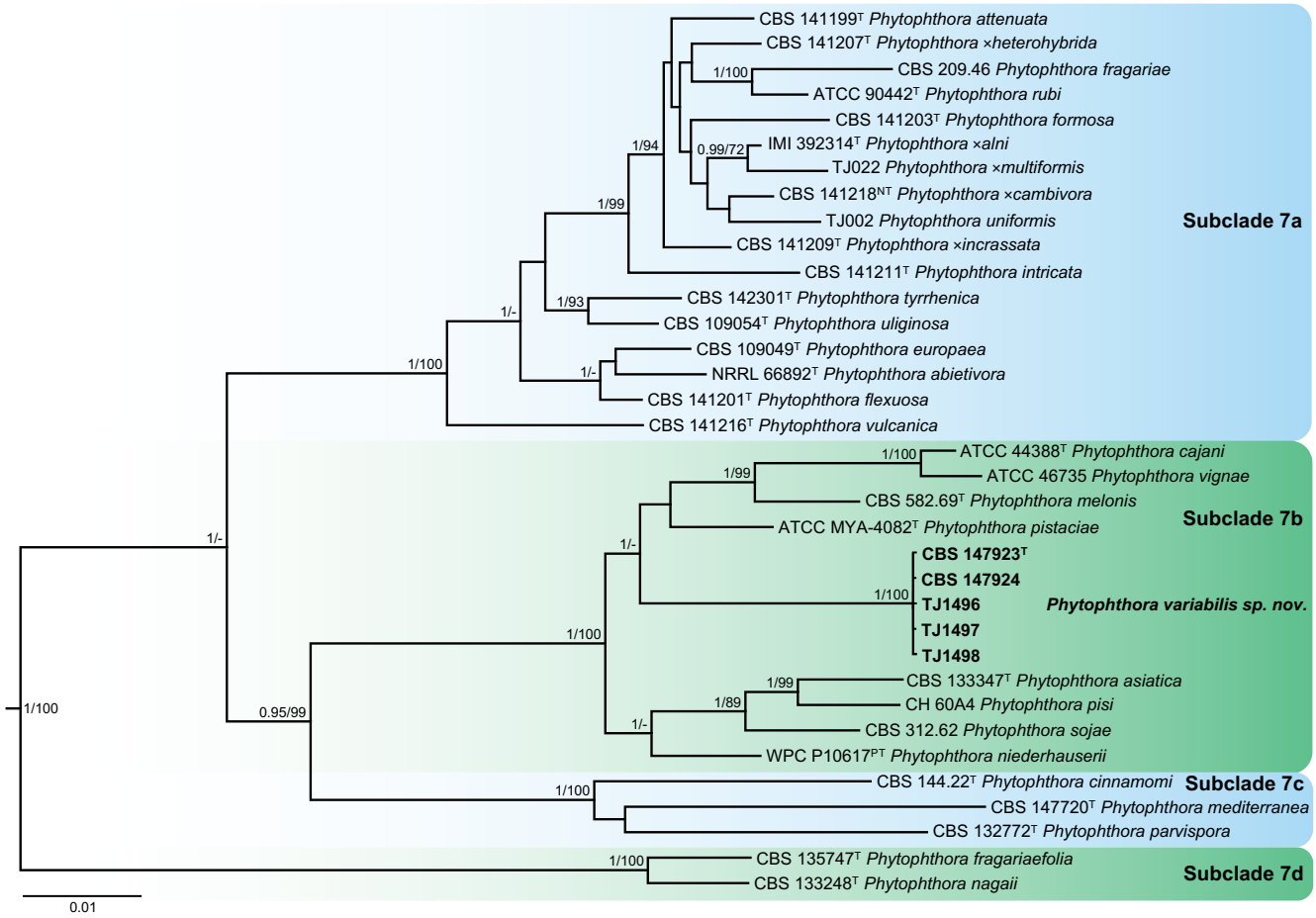

Fig. 55. Structure of *Phytophthora* Clade 7 in the Bayesian Inference phylogram constructed from ITS (1 185 bp), *Btub* (1 136 bp), *tigA* (1 669 bp) and *cox1* (867 bp) sequences of all accepted species of *Phytophthora* (Fig. 52). Bayesian posterior probability scores (> 0.90) and RAxML bootstrap support values (> 70 %) are shown at the nodes. The novel taxon is printed in **bold**. GenBank accession numbers are listed in Table 15. T, PT and NT indicate ex-type, ex-paratype and ex-neotype strains, respectively. TreeBASE: S28641.

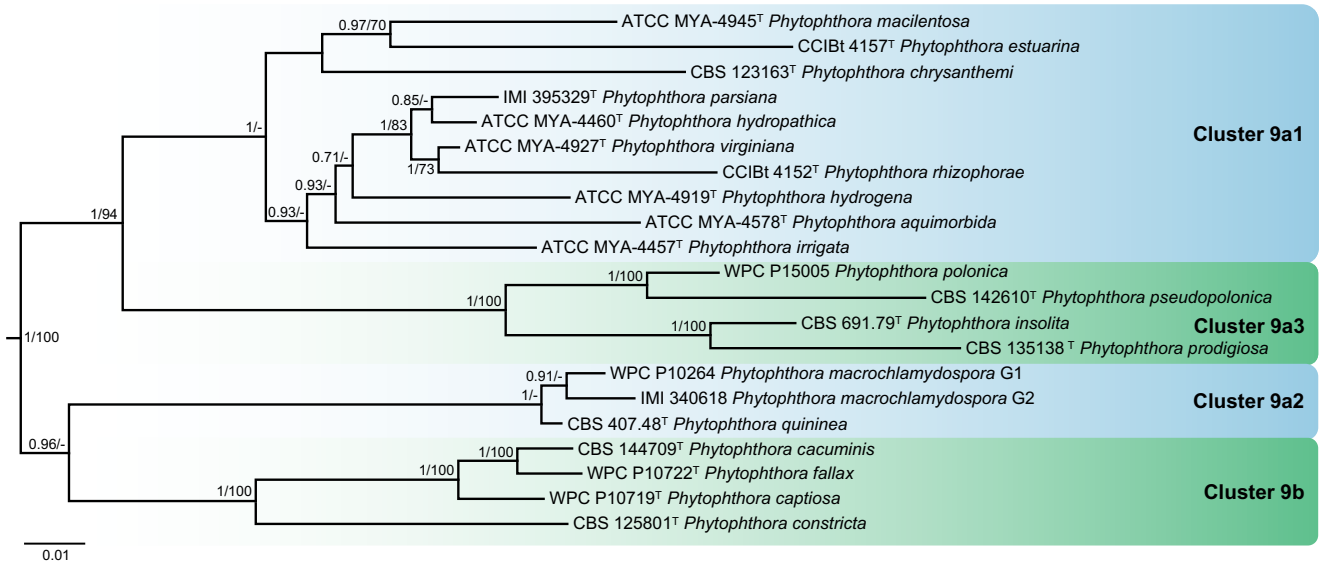

Fig. 56. Structure of *Phytophthora* Clade 9 in the Bayesian Inference phylogram constructed from ITS (1 185 bp), *Btub* (1 136 bp), *tigA* (1 669 bp) and *cox1* (867 bp) sequences of all accepted species of *Phytophthora* (Fig. 52). Bayesian posterior probability scores (> 0.90) and RAxML bootstrap support values (> 70 %) are shown at the nodes. GenBank accession numbers are listed in Table 15. T indicates ex-type strain. TreeBASE: S28641.

Table 15. DNA barcodes of accepted *Phytophthora* spp.

Species	(Sub) clade	Isolates[1]	GenBank accession numbers[2]				References
			cox1	ITS	*Btub*	*tigA*	
Phy. abietivora	7a	NRRL 66892^{T}	MK164270	MK163944	MK164274	–	Li *et al.* (2019)
Phy. acaciae	2d	AN02^{T}	KX396267	KX396303	KX396338	–	Albuquerque Alves *et al.* (2019)
Phy. acaciivora	2d	CBS 138639^{T}	MN991991	KX011264	MN991984	–	Paap *et al.* (2017), Burgess *et al.* (2020)
Phy. acerina	2c	CBS 133931^{T}	MH620026	JX951285	KX250713	KX250718	Ginetti *et al.* (2014), Yang *et al.* (2017), Yang & Hong (2018)
Phy. afrocarpa	10	CBS 147467^{T}	MT762315	MT762306	MT762324	–	Bose *et al.* (2021)
Phy. agathidicida	5	ICMP 17027^{T}	MH620036	KP295308	KX251077	KX251082	Weir *et al.* (2015), Yang *et al.* (2017), Yang & Hong (2018)
Phy. alpina	1a	CBS 146801^{T}	MT729668	MT707332	MT729673	–	Bregant *et al.* (2020)
Phy. alticola	4	CBS 121939^{PT}	KF317106	KF317084	KX251007	KX251012	Yang *et al.* (2017), Yang & Hong (2018)
Phy. amaranthi	2b	TARI28041^{T}	MH477739	GU111585	KJ179949	–	Ann *et al.* (2016)
Phy. amnicola	6b	CBS 131652^{T}	MH620041	MH620126	KX251168	KX251173	Yang *et al.*(2017), Yang & Hong (2018)
Phy. andina	1c	WPC P13365^{T}	–	FJ801734	EU080183	EU080188	Blair *et al.* (2008)
		EC3421^{PT}	AY564160				Kroon *et al.* (2004)
Phy. aquae-cooljarloo	6a	CBS 146550^{T}	MT210466	MT210484	MT210475	–	Crous *et al.* (2020a)
Phy. aquimorbida	9a (cluster 9a1)	ATCC MYA-4578^{T}	GQ294536	FJ666127	KX252239	KX252244	Hong *et al.* (2012)
Phy. arenaria	4	CBS 127950^{T}	MH620034	MH620120	KX251014	KX251019	Yang *et al.* (2017), Yang & Hong (2018)
Phy. asiatica	7b	CBS 133347^{T}	MH620062	MH620142	KX251666	KX251671	Yang *et al.* (2017), Yang & Hong (2018)
Phy. asparagi	6	CBS 132095^{T}	MH620053	MH620137	KX251474	KX251479	Yang *et al.* (2017), Yang & Hong (2018)
Phy. attenuata	7a	CBS 141199^{T}	MH620054	KU517154	KX251610	KX251615	Jung *et al.* (2017a), Yang *et al.* (2017), Yang & Hong (2018)
Phy. austrocedrae	8d	CBS 122911^{T}	KF358233	KF358220	KX252169	KX252174	Yang *et al.* (2017), Yang & Hong (2018)
Phy. aysenensis	2b	CCCT 19.159^{T}	–	MN557838	MN557840	–	Crous *et al.* (2020b)
Phy. balyanboodja	6a	CBS 143058^{T}	MF326863	KJ372258	MF326806	–	Burgess *et al.* (2018)
Phy. betaceae	1c	MFM-P8084T	–	JAANHX010000146[3]	JAANHX010000299[3]	JAANHX010000345[3]	Mideros *et al.* (2018)
Phy. bilorbang	6b	CBS 131653^{T}	MH620042	MH620127	KX251182	KX251186	Yang *et al.* (2017), Yang & Hong (2018)
Phy. bisheria	2d	CBS 122081^{T}	MH620030	MH620116	EU080742	EU080747	Blair *et al.* (2008), Yang & Hong (2018)
Phy. boehmeriae	10	CBS 291.29^{T}	KT183047	KT183036	EU080162	EU080167	Blair *et al.* (2008), Yang *et al.* (2016)
Phy. boodjera	4	BD201	MZ736426	MZ753913	MZ736452	MZ736479	Present study
Phy. borealis	6b	CBS 132023^{T}	MH620043	MH620128	KX251188	KX251193	Yang *et al.* (2017), Yang & Hong (2018)
Phy. botryosa	2a	CBS 581.69^{T}	MH620019	MH620107	KX250538	KX250543	Yang *et al.* (2017), Yang & Hong 2018
Phy. brassicae	8b	CBS 179.87^{T}	MH620082	MH620158	KX252001	KX252006	Yang *et al.* (2017), Yang & Hong (2018)
Phy. cactorum	1a	WPC P10194	MH620014	MH620100	KX250370	KX250375	Yang *et al.* (2017), Yang & Hong 2018
Phy. cacuminis	9b	CBS 144709^{T}	MG543010	MG542997	MG543045	–	Khaliq *et al.* (2019)
Phy. cajani	7b	ATCC 44388^{T}	MH620063	MH620143	KX251687	KX251692	Yang *et al.* (2017), Yang & Hong (2018)

Table 15. (Continued).

Species	(Sub) clade	Isolates[1]	GenBank accession numbers[2]				References
			cox1	ITS	*Btub*	*tigA*	
Phy. capensis	2c	CBS 128319^{T}	MH620027	MH620113	KX250727	KX250732	Yang *et al.* (2017), Yang & Hong (2018)
Phy. capsici	2b	ATCC 15399	KF317094	KF317073	KX250636	KX250641	Yang *et al.* (2017), Yang & Hong (2018)
Phy. captiosa	9b	WPC P10719^{T}	KC733449	MH620174	EU079659	EU079664	Blair *et al.* (2008), Yang *et al.* (2014a), Yang & Hong (2018)
Phy. castaneae	5	CBS 587.85	AY564190	MH620122	KX251098	KX251103	Kroon *et al.* (2004), Yang *et al.* (2017), Yang & Hong (2018)
Phy. castanetorum	12	CBS 142299^{T}	MZ736427	MF036182	MZ736453	MZ736480	Jung *et al.* (2017b), present study
Phy. cathayensis	4	CGMCC No. 19655^{T}	MN692211	MN385741	MT063102	–	Morales-Rodríguez *et al.* (2020)
Phy. chesapeakensis	6a	CBS 140655^{T}	KX172096	KX172092	–	–	Man In't Veld *et al.* (2019)
Phy. chlamydospora	6b	P17-99	CM022726	JAABLK0 10000522[3]	JAABLK0 10000021[3]	JAABLK0 10000299[3]	Mc Gowan *et al.* (2020)
Phy. chrysanthemi	9a (cluster 9a1)	CBS 123163^{T}	MH620093	KT183038	KX252267	KX252272	Yang *et al.* (2016, 2017), Yang & Hong (2018)
Phy. cichorii	8b	CBS 115029^{T}	MH620083	MH620159	KX252008	KX252013	Yang *et al.* (2017), Yang & Hong (2018)
Phy. cinnamomi	7c	CBS 144.22^{T}	MH620070	MH620147	KX251812	KX251817	Yang *et al.* (2017), Yang & Hong (2018)
Phy. citricola	2c	CBS 221.88^{T}	KF317095	KF317074	KX250748	KX250753	Yang *et al.* (2017), Yang & Hong (2018)
Phy. citrophthora	2a	WPC P0479^{T}	MH136872	MG865476	MH493923	–	https://idtools.org/id/phytophthora/
Phy. clandestina	1b	CBS 347.86^{T}	–	MH620101	EU079867	EU079872	Blair *et al.* (2008), Yang & Hong (2018)
		IMI 287317	AY564172				Kroon *et al.* (2004)
Phy. cocois	5	ICMP 16948^{T}	MH620037	KP295304	KX251105	KX251110	Weir *et al.* (2015), Yang *et al.* (2017), Yang & Hong (2018)
Phy. colocasiae	2a	CH 35D3	KF317097	KF317076	KX250566	KX250571	Yang *et al.* (2014a, 2017)
Phy. condilina	6a	CBS 143059^{T}	MF326843	KJ372262	MF326814	–	Burgess *et al.* (2018)
Phy. constricta	9b	CBS 125801^{T}	KC733450	MH620175	KX252562	KX252567	Yang *et al.* (2014a, 2017), Yang & Hong (2018)
Phy. cooljarloo	6a	CBS 143062^{T}	HQ012881	HQ012957	MF326816	–	Jung *et al.* (2011), Burgess *et al.* (2018)
Phy. crassamura	6b	CBS 140357^{T}	MH620044	KP863493	KX251202	KX251207	Scanu *et al.* (2015), Yang *et al.* (2017), Yang & Hong (2018)
Phy. cryptogea	8a	CBS 113.19^{T}	MH620075	MH620151	KX251868	KX251873	Yang *et al.* (2017), Yang & Hong (2018)
Phy. dauci	8b	CBS 127102^{T}	MH620084	MH620160	KX252015	KX252020	Yang *et al.* (2017), Yang & Hong (2018)
Phy. drechsleri	8a	CBS 292.35^{T}	MH620076	MH620152	KX251889	KX251894	Yang *et al.* (2017), Yang & Hong (2018)
Phy. elongata	2d	CBS 125799^{T}	MH620031	MH620117	KX250895	KX250900	Yang *et al.* (2017), Yang & Hong (2018)
Phy. emzansi	2c	CBS 147464^{T}	MT762309	MT762301	–	–	Bose *et al.* (2021)
		WPC P19574^{PT}	–	–	KX250860	KX250865	Yang *et al.* (2017)
Phy. erythroseptica	8a	CBS 129.23^{T}	MH620077	MH620153	KX251896	KX251901	Yang *et al.* (2017), Yang & Hong (2018)
Phy. estuarina	9a (cluster 9a1)	CCIBt 4157^{T}	KT886051	KT886034	–	–	Li *et al.* (2016)
Phy. europaea	7a	CBS 109049^{T}	MH620055	MH620138	KX251523	KX251528	Yang *et al.* (2017), Yang & Hong (2018)

Table 15. (Continued).

Species	(Sub) clade	Isolates[1]	GenBank accession numbers[2]				References
			cox1	ITS	*Btub*	*tigA*	
Phy. fallax	9b	WPC P10722^{T}	KC733451	MH620176	KX252569	KX252574	Blair *et al.* (2008), Yang *et al.* (2014a), Yang & Hong (2018)
Phy. flexuosa	7a	CBS 141201^{T}	MH620056	KU517152	KX251617	KX251622	Jung *et al.* (2017a), Yang *et al.* (2017), Yang & Hong (2018)
Phy. fluvialis	6b	CBS 129424^{T}	MH620045	MH620129	KX251209	KX251214	Yang *et al.* (2017), Yang & Hong (2018)
Phy. foliorum	8c	CBS 121655^{T}	EU124918	MH620164	KX252113	KX252118	Yang *et al.* (2017), Yang & Hong (2018)
Phy. formosa	7a	CBS 141203^{T}	MH620057	KU517153	KX251624	KX251629	Jung *et al.* (2017a), Yang *et al.* (2017), Yang & Hong (2018)
Phy. fragariae	7a	CBS 209.46^{T}	MH620058	MH620139	KX251544	KX251549	Yang *et al.* (2017), Yang & Hong (2018)
Phy. fragariaefolia	7d	CBS 135747^{T}	MH620073	MH620149	KX251854	KX251859	Yang *et al.* (2017), Yang & Hong (2018)
Phy. frigida	2d	WPC P16947^{T}	KF317098	KF317077	KX250916	KX250921	Yang *et al.* (2017) , Yang & Hong (2018)
Phy. gallica	10	CBS 111474^{T}	KF317112	KF317090	KX252590	KX252595	Yang *et al.* (2017) , Yang & Hong (2018)
Phy. gemini	6a	CBS 123382^{PT}	MH620038	FJ217680	KX251126	KX251131	Man In't Veld *et al.* (2011), Yang *et al.* (2017), Yang & Hong (2018)
Phy. gibbosa	6b	CBS 127951^{T}	MH620046	MH620130	KX251223	KX251228	Yang *et al.* (2017), Yang & Hong (2018)
Phy. glovera	2b	CBS 121969^{T}	MH620022	MH620110	KX250650	KX250655	Yang *et al.* (2017), Yang & Hong (2018)
Phy. gonapodyides	6b	CBS 554.67	KC733448	KF112854	KX251237	KX251242	Yang *et al.* (2013, 2014a, 2017)
Phy. gondwanensis	10	ATCC MYA-3893	KT183046	KT183035	KX252604	KX252609	Yang *et al.* (2016, 2017)
Phy. gregata	6b	CBS 127952^{T}	MH620047	MH620131	KX251251	KX251256	Yang *et al.* (2017), Yang & Hong (2018)
Phy. hedraiandra	1a	CBS 111725^{T}	AY769115	AY707987	KX250398	KX250403	de Cock & Lévesque (2004), Yang *et al.* (2017)
Phy. heveae	5	CBS 296.29^{T}	AY564182	MH620123	KX251112	KX251117	Kroon *et al.* (2004), Yang *et al.* (2017), Yang & Hong (2018)
Phy. hibernalis	8c	CBS 270.31	MH620088	KT183039	KX252120	KX252125	Yang *et al.* (2016, 2017), Yang & Hong (2018)
Phy. himalsilva	2a	CBS 128767^{T}	MH620020	MH620108	KX250573	KX250578	Yang *et al.* (2017), Yang & Hong (2018)
Phy. humicola	6a	CBS 200.81^{T}	KF112862	KF112855	KX251140	KX251145	Yang *et al.* (2017), Yang & Hong (2018)
Phy. hydrogena	9a (cluster 9a1)	ATCC MYA-4919^{T}	KC249962	KC249959	KX252281	KX252286	Yang *et al.* (2014b, 2017)
Phy. hydropathica	9a (cluster 9a1)	ATCC MYA-4460^{T}	KC733452	EU583793	KX252295	KX252300	Hong *et al.* (2010), Yang *et al.* (2014b, 2017)
Phy. idaei	1a	CBS 971.95^{T}	–	FJ801946	EU080130	EU080135	Blair *et al.* (2008)
		IMI 313727^{PT}	AY564185				Kroon *et al.* (2004)
Phy. ilicis	3	CBS 114348^{T}	JX524159	JX524158	KX250951	KX250956	Yang *et al.* (2017)
Phy. infestans	1c	CBS 147289^{ET}	MZ736428	MZ753914	MZ736454	MZ736481	Present study
Phy. insolita	9a (cluster 9a3)	CBS 691.79^{T}	AY564188	GU111612	EU080176	EU080181	Kroon *et al.* (2004), Blair *et al.* (2008)
Phy. insulinativitatica	2a	CBS 146553^{T}	MT583646	KY212028	MT583631	–	Dang *et al.* (2021)
Phy. intercalaris	10	CBS 140632^{T}	KT163315	KT163268	KX252611	KX252616	Yang *et al.* (2016, 2017)
Phy. intricata	7a	CBS 141211^{T}	MH620059	KU517155	KX251631	KX251636	Jung *et al.* (2017a), Yang *et al.* (2017), Yang & Hong (2018)

Table 15. (Continued).

Species	(Sub) clade	Isolates[1]	GenBank accession numbers[2]				References
			cox1	ITS	*Btub*	*tigA*	
Phy. inundata	6a	IMI 390121^T	KF112863	KF112856	KX251154	KX251159	Yang *et al.* (2017), Yang & Hong (2018)
Phy. ipomoeae	1c	CBS 109229^T	MH620016	MH620104	EU080831	EU080836	Blair *et al.* (2008), Yang & Hong (2018)
Phy. iranica	1b	CBS 374.72^T	AY564189	MH620102	KX250440	KX250445	Kroon *et al.* (2004), Yang *et al.* (2017), Yang & Hong (2018)
Phy. irrigata	9a (cluster 9a1)	ATCC MYA-4457^T	KC733453	EU334634	KX252316	KX252321	Hong *et al.* (2008), Yang *et al.* (2014b, 2017)
Phy. kernoviae	10	WPC P10956	KT183048	MH620177	EU080042	KX252631	Blair *et al.* (2008), Yang *et al.* (2016), Yang & Hong (2018)
Phy. kwongonina	6a	CBS 143060^T	MF326847	JN547636	MF326824	–	Aghighi *et al.* (2012), Burgess *et al.* (2018)
Phy. lactucae	8b	WPC P19875^T	MH620085	MH620161	KX252043	KX252048	Yang *et al.* (2017), Yang & Hong (2018)
Phy. lacustris	6b	IMI 389725^T	JF896561	AF266793	EU080531	EU080536	Cooke *et al.* (2000), Blair *et al.* (2008), Nechwatal *et al.* (2013)
Phy. lateralis	8c	ATCC MYA-3898	MH620089	MH620165	KX252134	KX252139	Yang (2017), Yang & Hong (2018)
Phy. lilii	11	CBS 135746^T	AB856786	MG865523	AB856782	AB856800	Rahman *et al.* (2015)
Phy. litchii	4	CPHST BL 145^T	MH136919	MG865524	–	–	https://idtools.org/id/phytophthora/
Phy. litoralis	6b	CBS 127953^T	MH620048	MH620132	KX251279	KX251284	Yang *et al.* (2017), Yang & Hong (2018)
Phy. macilentosa	9a (cluster 9a1)	ATCC MYA-4945^T	KF192708	KF192700	KX252344	KX252349	Yang *et al.* (2014a, 2017)
Phy. macrochlamydospora-G1	9a (cluster 9a2)	WPC P10264	KC733454	KC733445	KX252511	KX252515	Yang *et al.* (2014a, 2017)
Phy. macrochlamydospora-G2	9a (cluster 9a2)	IMI 340618	MH620098	MH620172	KX252517	KX252521	Yang *et al.* (2017), Yang & Hong (2018)
Phy. meadii	2a	CBS 219.88	AY564192	MH620109	KX250594	KX250599	Kroon *et al.* (2004), Yang *et al.* (2017), Yang & Hong 2018
Phy. medicaginis	8a	ATCC MYA-3900	KF358236	KF358223	KX251903	KX251908	Yang *et al.* (2017) , Yang & Hong (2018)
Phy. mediterranea	7c	CBS 147720^T	MW900447	MW892398	MW900443	–	Bregant *et al.* (2021)
Phy. megakarya	4	CBS 238.83^T	MH620035	MH620121	KX251035	KX251040	Yang *et al.* (2017), Yang & Hong (2018)
Phy. megasperma	6b	CBS 402.72	MH620049	MH620133	KX251286	–	Yang *et al.* (2017), Yang & Hong (2018)
Phy. mekongensis	2a	CBS 135136^T	MZ813273	LC595792	MZ813274	MZ813275	present study
Phy. melonis	7b	CBS 582.69^T	MH620064	KT183041	KX251708	KX251713	Yang *et al.* (2016, 2017), Yang & Hong (2018)
Phy. mengei	2b	ATCC MYA-4554^T	MH620023	EU748545	KX250657	KX250662	Hong *et al.* (2009), Yang *et al.* (2017), Yang & Hong (2018)
Phy. mexicana	2b	CBS 554.88	MH620024	MH620111	KX250671	KX250676	Yang *et al.* (2017), Yang & Hong (2018)
Phy. mirabilis	1c	ATCC 64069	MH620017	MH620105	KX250482	KX250487	Yang *et al.* (2017), Yang & Hong 2018
Phy. mississippiae	6b	ATCC MYA-4946^T	KF112860	KF112852	KX251306	KX251311	Yang *et al.* (2013, 2017)
Phy. morindae	10	CBS 121982^T	KT183050	MH620178	KX252634	KX252639	Yang *et al.* (2016, 2017), Yang & Hong (2018)
Phy. moyootj	6b	CBS 138759^T	KJ396702	KJ372256	KJ372303	–	Crous *et al.* (2014)
Phy. multibullata	2a	CBS 146552^T	MT583658	MT568655	MT583643	–	Dang *et al.* (2021)

Table 15. (Continued).

Species	(Sub) clade	Isolates[1]	GenBank accession numbers[2]				References
			cox1	ITS	*Btub*	*tigA*	
Phy. multivesiculata	2e	CBS 545.96^{T}	MH620032	MH620118	EU080066	EU080071	Blair *et al.* (2008), Yang & Hong (2018)
Phy. multivora	2c	CBS 124094^{T}	FJ237508	FJ237521	KX250776	KX250781	Scott *et al.* (2009), Yang *et al.* (2017)
Phy. nagaii	7d	CBS 133248^{T}	MH620074	MH620150	KX251861	KX251866	Yang *et al.* (2017), Yang & Hong (2018)
Phy. nemorosa	3	ATCC MYA-2948^{T}	KF317104	KF317082	KX250965	KX250970	Yang *et al.* (2017), Yang & Hong (2018)
Phy. nicotianae	1	ATCC 15410	KF317091	KF317070	KX250510	KX250515	Yang *et al.* (2017), Yang & Hong (2018)
Phy. niederhauserii	7b	WPC P10617^{PT}	MH620065	MH620144	KX251729	KX251734	Yang *et al.* (2017), Yang & Hong (2018)
Phy. obscura	8d	CBS 129273^{T}	MH620091	MH620167	KX252176	KX252181	Yang *et al.* (2017), Yang & Hong (2018)
Phy. occultans	2a	CBS 101557^{T}	MH620021	JX978155	KX250601	KX250606	Man In 't Veld *et al.* (2015), Yang *et al.* (2017), Yang & Hong (2018)
Phy. oleae	2	CBS 7669^{T}	MF083569	KY982930	—	—	Ruano-Rosa *et al.* (2018)
Phy. oreophila	6a	CBS 144708^{T}	MG543002	MG542976	MG543037	—	Khaliq *et al.* (2019)
Phy. ornamentata	6b	CBS 140647^{T}	MH620050	KP863496	KX251320	KX251325	Scanu *et al.* (2015), Yang *et al.* (2017), Yang & Hong (2018)
Phy. pachypleura	2c	IMI 502404^{T}	MH620028	MH620114	KX250790	KX250795	Yang *et al.* (2017), Yang & Hong (2018)
Phy. palmivora	4	ATCC MYA-4038	KF317108	KF317086	KX251056	KX251061	Yang *et al.* (2017), Yang & Hong (2018)
Phy. panamensis	4	CBS 147925^{T}	MZ736433	MZ753919	MZ736459	MZ736486	Present study
		CBS 147926	MZ736432	MZ753918	MZ736458	MZ736485	Present study
		PA19	MZ736429	MZ753915	MZ736455	MZ736482	Present study
		PA40	MZ736430	MZ753916	MZ736456	MZ736483	Present study
		PA108	MZ736431	MZ753917	MZ736457	MZ736484	Present study
Phy. parsiana	9a (cluster 9a1)	IMI 395329^{T}	KC733455	KC733446	KX252358	KX252363	Yang *et al.* (2014a, 2017)
Phy. parvispora	7c	CBS 132772^{T}	MH620071	KC478667	KX251840	KX251845	Scanu *et al.* (2014), Yang *et al.* (2017), Yang & Hong (2018)
Phy. personensis	6a	CBS 146549^{T}	HQ012877	EU301169	MF326805	—	Jung *et al.* (2011), Crous *et al.* (2020b)
Phy. phaseoli	1c	CH 23B4	MH620018	MH620106	KX250496	KX250501	Yang *et al.* (2017), Yang & Hong (2018)
Phy. pini	2c	ATCC 64532^{T}	KF317100	KF317079	KX250811	KX250816	Yang *et al.* (2014a, 2017)
Phy. pinifolia	6b	CBS 122924^{T}	JN935960	MH620134	KX251334	KX251339	Aghighi *et al.* (2012), Yang *et al.* (2017), Yang & Hong (2018)
Phy. pisi	7b	CBS 130350^{T}	MH620066	KT183042	KX251736	KX251741	Yang *et al.* (2016, 2017), Yang & Hong (2018)
Phy. pistaciae	7b	ATCC MYA-4082^{T}	MH620067	KT183043	KX251749	KX251754	Yang *et al.* (2016), Yang & Hong (2018)
Phy. plurivora	2c	CBS 124093^{T}	Contig MH136959 _KC855435	FJ665225	MZ736460	MZ736487	Jung & Burgess (2009), present study
Phy. pluvialis	3	ATCC MYA-4930^{T}	MH620033	MH620119	KX250972	KX250977	Yang *et al.* (2017), Yang & Hong (2018)
Phy. polonica	9a (cluster 9a3)	WPC P15005	KC733456	KF358225	KX252546	EU080262	Blair *et al.* (2008), Yang *et al.* (2014a)
Phy. porri	8b	CBS 802.95	KC478717	KC478747	—	—	Bertier *et al.* (2013a)

Table 15. (Continued).

Species	(Sub) clade	Isolates[1]	GenBank accession numbers[2]				References
			cox1	ITS	*Btub*	*tigA*	
		CBS 140.87	–	–	LC595879	–	–
Phy. primulae	8b	CBS 620.97	KF358238	KF358226	KX252064	KX252069	Yang *et al.* (2014a, 2017)
Phy. prodigiosa	9a (cluster 9a3)	CBS 135138^T	LC595937	LC595799	LC595880	–	-
Phy. pseudocryptogea	8a	BD755	MZ736434	MZ753920	MZ736461	MZ736488	Present study
Phy. pseudolactucae	8b	CBS 137103^T	AB894396	AB894388	–	–	Rahman *et al.* (2015)
Phy. pseudopolonica	9a (cluster 9a3)	CBS 142610^T	–	KY707115	KY707104	–	Li *et al.* (2017)
Phy. pseudorosacearum	6a	CBS 143061^T	MF326858	KJ372267	MF326827	–	Burgess *et al.* (2018)
Phy. pseudosyringae	3	CBS 111772^T	KF317105	KF317083	KX250979	KX250984	Yang *et al.* (2014a, 2017)
Phy. pseudotsugae	1a	IMI 331662^T	AY564199	FJ802112	EU080427	EU080432	Kroon *et al.* (2004), Blair *et al.* (2008)
Phy. psychrophila	3	CBS 803.95^T	KF358239	KF358227	KX250993	KX250998	Yang *et al.* (2014a, 2017)
Phy. quercetorum	4	CH 15C7	KF358240	KF358228	KX251063	KX251068	Yang *et al.* (2014a, 2017)
Phy. quercina	12	CBS 784.95^T	KF358241	KF358229	KX252655	KX252660	Yang *et al.* (2014a, 2017)
Phy. quininea	9a (cluster 9a2)	CBS 407.48^T	MH620099	MH620173	EU079803	EU079807	Blair *et al.* (2008), Yang & Hong (2018)
Phy. ramorum	8c	CH 32G2	MH620090	MH620166	KX252148	KX252153	Yang *et al.* (2017), Yang & Hong (2018)
Phy. rhizophorae	9a (cluster 9a1)	CCIBt 4152^T	KT886048	KT886031	–	–	Li *et al.* (2016)
Phy. richardiae	8a	CBS 240.30^T	MH620078	MH620154	KX251924	KX251929	Yang *et al.* (2017), Yang & Hong (2018)
Phy. riparia	6b	CBS 132024^T	MH620051	MH620135	KX251348	KX251353	Yang *et al.* (2017), Yang & Hong (2018)
Phy. rosacearum	6a	ATCC MYA-4456^T	MH620039	MH620124	KX251446	KX251451	Yang *et al.* (2017), Yang & Hong (2018)
Phy. rubi	7a	ATCC 90442^T	DQ674736	HQ643340	KX251565	KX251570	Man In't Veld (2007), Robideau *et al.* (2011), Yang *et al.* (2017)
Phy. sansomeana	8a	ATCC MYA-4455^T	MH620079	MH620155	KX251931	KX251936	Yang *et al.* (2017), Yang & Hong (2018)
Phy. siskiyouensis	2b	CBS 122779^T	KF317102	KF317081	KX250678	KX250683	Yang *et al.* (2014a, 2017)
Phy. sojae	7b	CBS 312.62	MH620068	MH620145	KX251763	KX251768	Yang *et al.* (2017), Yang & Hong (2018)
Phy. stricta	8	ATCC MYA-4944^T	KF192702	KF192694	KX252211	KX252216	Yang *et al.* (2014a, 2017)
Phy. syringae	8d	ATCC 34002	MH620092	MH620168	KX252197	KX252202	Yang *et al.* (2017), Yang & Hong (2018)
Phy. tentaculata	1b	ATCC MYA-3655	MH620015	MH620103	KX250454	KX250459	Yang *et al.* (2017), Yang & Hong 2018
Phy. terminalis	2a	CBS 133865^T	JX978168	JX978167	KX250608	KX250613	Man In 't Veld *et al.* (2015), Yang (2017)
Phy. theobromicola	2b	CCUB 1091^T	MW597344	MT074263	MT074223	–	Decloquement *et al.* (2021)
Phy. thermophila	6b	CBS 127954^T	MH620052	MH620136	KX251355	KX251360	Yang *et al.* (2017), Yang & Hong (2018)
Phy. transitoria	3	CBS 147245^T	MZ736439	MZ753925	MZ736466	MZ736493	Present study
		CBS 147246	MZ736435	MZ753921	MZ736462	MZ736489	Present study
		CZ119	MZ736436	MZ753922	MZ736463	MZ736490	Present study
		CZ120	MZ736437	MZ753923	MZ736464	MZ736491	Present study
		CZ121	MZ736438	MZ753924	MZ736465	MZ736492	Present study
Phy. trifolii	8a	CBS 117687^T	MH620080	MH620156	KX251959	KX251964	Yang *et al.* (2017), Yang & Hong (2018)

Table 15. (Continued).

Species	(Sub) clade	Isolates[1]	GenBank accession numbers[2]				References
			cox1	ITS	*Btub*	*tigA*	
Phy. tropicalis	2b	CBS 434.91^{T}	MH620025	MH620112	KX250699	KX250704	Yang *et al.* (2017), Yang & Hong (2018)
Phy. tubulina	12	CBS 141212^{T}	MZ736440	MF036196	MZ736467	MZ736494	Jung *et al.* (2017b), present study
Phy. tyrrhenica	7a	CBS 142301^{T}	MZ736441	KU899188	KU899265	MZ736495	Jung *et al.* (2017b), present study
Phy. uliginosa	7a	CBS 109054^{T}	MH620060	MH620140	EU080012	KX251573	Blair *et al.* (2008), Yang *et al.* (2017), Yang & Hong (2018)
Phy. uniformis	7a	TJ002	MZ736442	KU899173	KU899249	MZ736496	Jung *et al.* (2017a), present study
Phy. urerae	1c	PSR27^{T}	KR632858	KR632862	KR632888	—	Grünwald *et al.* (2019)
Phy. variabilis	7b	CBS 147923^{T}	MZ736447	MZ753930	MZ736472	MZ736501	Present study
		CBS 147924	MZ736443	MZ753926	MZ736468	MZ736497	Present study
		TJ1496	MZ736444	MZ753927	MZ736469	MZ736498	Present study
		TJ1497	MZ736445	MZ753928	MZ736470	MZ736499	Present study
		TJ1498	MZ736446	MZ753929	MZ736471	MZ736500	Present study
Phy. versiformis	12	CBS 142005^{T}	KX011222	KX011279	KX011321	—	Paap *et al.* (2017)
Phy. vignae	7b	ATCC 46735	MH620069	MH620146	KX251777	KX251782	Yang *et al.* (2017), Yang & Hong (2018)
Phy. virginiana	9a (cluster 9a1)	ATCC MYA-4927^{T}	KC295546	KC295544	KX252379	KX252384	Yang & Hong (2013), Yang *et al.* (2017)
Phy. vulcanica	7a	CBS 141216^{T}	MZ736448	MF036209	MZ736473	MZ736502	Jung *et al.* (2017b), present study
Phytophthora aleatoria	1a	NZFS 4037^{T}	MK294177	MK282209	MK294172	—	Scott *et al.* (2019)
Phy. ×*alni*	7a	IMI 392314^{T}	KU681017	MH620141	KX251589	KX251594	Jung *et al.* (2017a), Yang *et al.* (2017), Yang & Hong (2018)
Phy. ×*cambivora*	7a	CBS 141218^{NT}	MZ736422	KU899179	KU899255	MZ736475	Jung *et al.* (2017a), present study
Phy. ×*heterohybrida*	7a	CBS 141207^{T}	KU517145	KU517151	KX251638	KX251643	Jung *et al.* (2017a), Yang *et al.* (2017)
Phy. ×*incrassata*	7a	CBS 141209^{T}	KU517150	KU517156	KX251645	KX251650	Jung *et al.* (2017a), Yang *et al.* (2017)
Phy. ×*multiformis*	7a	TJ022	MZ736423	KU899184	KU899261	MZ736476	Jung *et al.* (2017a), present study
Phy. ×*pelgrandis*	1	CBS 123385^{T}	MZ736424	MZ753911	MZ736450	MZ736477	Present study
Phy. ×*serendipita*	1a	SFB152	MZ736425	MZ753912	MZ736451	MZ736478	Present study
Phy. ×*stagnum*	6b	ATCC MYA-4926^{T}	KC631619	—	KX251376	KX251381	Yang *et al.* (2014c, 2017)
Phy. ×*vanyenensis*	2a	CBS 146554^{T}	MT583648	MT568651	MT583634	—	Dang *et al.* (2021)

[1] ATCC: American Type Culture Collection, Virginia, USA; CBS: Westerdijk Fungal Biodiversity Institute, Utrecht, the Netherlands; BD and TJ: Dr Thomas Jung's personal culture collection, housed at Mendel University in Brno, Czech Republic and the University of Algarve, Faro, Portugal; CCIBt: Culture collection of the Instituto de Botânica, São Paulo State, Brazil; CCUB: Culture Collection at the University of Brasilia, Brazil; CGMCC: China General Microbial Culture Collection Center, Beijing, China; CH: Chuanxue Hong laboratory at Virginia Polytechnic Institute and State University, Virginia Beach, VA, USA; CPHST BL: USDA-APHIS-PPQ-Center for Plant Health, Science & Technology-Beltsville Laboratory, Beltsville, MD, USA; CZ, PA and SFB: Culture collection of Mendel University in Brno, Czech Republic; ICMP: International Collection of Microorganisms from Plants, Auckland, New Zealand; IMI: International Mycological Institute, Kew, UK; NRRL: ARS Culture Collection, Peoria, IL, USA; NZFS: New Zealand Forest Research Culture Collection, Rotorua, New Zealand; TARI: Taiwan Agricultural Research Institute, Taichung, Taiwan; WPC: The World Phytophthora Genetic Resource Collection at University of California, Riverside, USA; all other codes refer to local collections. $^{T, ET, NT}$ and ^{PT} indicate ex-type, ex-epitype, ex-neotype and ex-paratype strains, respectively.

[2] *cox1*: partial cytochrome-c oxidase 1 gene; ITS: internal transcribed spacers and intervening 5.8S nrDNA; *Btub*: partial β-tubulin gene; *tigA*, *tigA*: gene fusion protein. PDL Phytophthora Database (www.phytophthoradb.org).

[3] Genome sequences.

The continuously growing imports of rooted plants from overseas to Europe and North America and the increasing intensity and complexity of the international nursery trade have caused the accidental introduction of many exotic *Phytophthora* species and their subsequent widespread dissemination through the nursery industry and into the wider environment (Brasier 2008, Davison *et al.* 2006, Schwingle *et al.* 2007, Moralejo *et al.* 2009, Bienapfl & Balci 2014, Jung *et al.* 2016). Consequently, since the 1960s the number of devastating forest epidemics caused by exotic and often previously unknown, invasive *Phytophthora* species has been exponentially increasing (Jung *et al.* 2018a). Recently, Jung *et al.* (2021) demonstrated that *Phy. ramorum*, the causal agent of the devastating "Sudden Oak Death" and "Sudden Larch Death" epidemics in the USA and the UK, respectively, originates from natural forests in East Asia. The centre of origin of the wide-host range pathogen *Phy. cinnamomi* was recently shown to be in Taiwan and Southeast Asia (Shakya *et al.* 2021).

Before 2000 the genus *Phytophthora* was organised in six non-natural morphological groups, named Waterhouse groups 1–6 (Waterhouse 1963, Erwin & Ribeiro 1996). Based on multigene analyses it is currently structured in 12 phylogenetic clades (Table 15; Fig. 52; Yang *et al.* 2017, Jung *et al.* 2017b). The first ITS-based phylogeny of the genus already suggested that *Peronospora* resides within *Phytophthora* (Cooke *et al.* 2000). Subsequent multigene phylogenetic studies confirmed the paraphyly of *Phytophthora* by demonstrating that the brassicolous downy mildews, the graminicolous downy mildews, the downy mildews with coloured conidia and the downy mildews with pyriform haustoria, altogether comprising *ca*. 600 species in 19 genera, reside as two distinct clades within *Phytophthora* (Thines & Choi 2016, Bourret *et al.* 2018). The availability of whole genome sequences for a wide range of *Phytophthora* and downy mildew species enabled phylogenomic analyses and also confirmed its paraphyletic structure with downy mildews having evolved from hemibiotrophic phytophthora-like ancestors (McCarthy & Fitzpatrick 2017, Fletcher *et al.* 2018, 2019).

Phytophthora and its recently described sister genus *Nothophytophthora* share many morphological characters like the production of chlamydospores, hyphal swellings, both persistent and caducous sporangia with internal zoospore differentiation and both external and internal extended and nested proliferation, and both amphigynous and paragynous antheridial insertion to the oogonia. The most significant morphological difference between the two genera is the presence of a conspicuous, opaque plug inside the sporangiophore close to the base of most mature sporangia in all known *Nothophytophthora* species enabling sporangial caducity in several *Nothophytophthora* species (Jung *et al.* 2017d, O' Hanlon *et al.* 2021).

Interspecific hybridisations play an important evolutionary role in *Phytophthora* by facilitating adaptation to new host plants and environments. Nine of 16 new *Phytophthora* taxa detected in natural forests and streams in Taiwan and many *Phytophthora* isolates retrieved from aquatic ecosystems in Australia, South Africa, Chile and Vietnam were shown to be interspecific hybrids (Hüberli *et al.* 2013, Nagel *et al.* 2013, Oh *et al.* 2013, Burgess 2015, Jung *et al.* 2017a, c, 2018b, 2020). Particularly prone to interspecific hybridisations are *Phytophthora* Clades 1 (*i.e. Phy. andina*, *Phy.* ×*pelgrandis*, *Phy.* ×*serendipita*; Goss *et al.* 2011, Man In' t Veld *et al.* 2012), 2a (*Phytophthora* sp. ×botryosa-like, *Phytophthora* sp. ×meadii-like; Jung *et al.* 2017c), 6 (*Phy.* ×*stagnum* and multiple hybrids between *Phy. amnicola*, *Phy. chlamydospora*, *Phy. fluvialis*, *Phy. gonapodyides*, *Phy. litoralis*, *Phy. moyootj* and *Phy. thermophila*; Nagel *et al.* 2013, Yang *et al.* 2014c, Burgess 2015, Jung *et al.* 2018b) , 7a (*Phy.* ×*alni*, *Phy.* ×*cambivora*, *Phy.* ×*incrassata*, *Phy.* ×*heterohybrida*, *Phy.* ×*multiformis*; Brasier *et al.* 2004, Husson *et al.* 2015, Jung *et al.* 2017a, 2020), 7b (hybrids of *Phy. sojae* and *Phy. vignae*; May *et al.* 2003), 8b (multiple hybrids of *Phy. primulae*, *Phytophthora* taxon Parsley and several unknown species; Bertier *et al.* 2013b) and 9 (multiple hybrids of *Phy. insolita*, *Phy. virginiana*, *Phytophthora* sp. Grenada 3, *Phytophthora* sp. kunnunara and *Phytophthora* sp. Peru 4; Jung *et al.* 2017, 2020). All known *Phytophthora* hybrids are allopolyploid with known genome sizes ranging from 236 Mbp in *Phy.* ×*alni*, 230–510 Mbp in *Phy.* ×*cambivora* to 654.3 Mbp in *Phy.* ×*incrassata* (Feau *et al.* 2016; Jung *et al.* 2017a), and resulted from sexual crossings rather than from somatic fusions (*cf.* May *et al.* 2003, Burgess 2015, Jung *et al.* 2017a, c, 2018b, 2020). *Phytophthora* ×*alni*, *Phy.* ×*cambivora* and *Phy.* ×*multiformis* are the causal agents of widespread root and collar rot epidemics of *Alnus* and *Fagaceae* forests while *Phy.* ×*pelgrandis*, *Phy.* ×*serendipita* and the Clade 8d hybrids cause serious diseases of ornamentals, vegetables and poplar trees (Brasier *et al.* 2004, Jung & Blaschke 2004, Jung *et al.* 2000, 2013a, 2018a, b, Man in' t Veld *et al.* 2012, Bertier *et al.* 2013b, Milenković *et al.* 2018). *Phytophthora* ×*incrassata*, *Phy.* ×*heterohybrida* and hybrids of *Phy. sojae* and *Phy. vignae* demonstrated in pathogenicity trials high aggressiveness to forest trees and soybean and cowpea cultivars, respectively (May *et al.* 2003, Jung *et al.* 2017a). Using phylogenomics and genome size estimation, van Poucke *et al.* (2021) confirmed and characterised 27 previously described hybrid species and discovered 16 new hybrid species.

References: Blackwell 1949 (morphology and terminology); Erwin & Ribeiro 1996 (morphology, physiology and pathogenicity); Cooke *et al.* 2000, Yang *et al.* 2017, Bourret *et al.* 2018, van Poucke *et al.* 2021 (phylogeny); Lamour 2013, Jung *et al.* 2018a (pathogenicity); Burgess 2015, Husson *et al.* 2015, van Poucke *et al.* 2021 (hybridization); Jung *et al.* 2017a (hybridization, morphology, phylogeny); Jung *et al.* 2021, Shakya *et al.* 2021 (centre of origin).

Phytophthora transitoria I. Milenković, T. Májek & T. Jung, ***sp. nov.*** MycoBank MB 839452. Fig. 57.

Etymology: Referring to the transitional role of most primary sporangia releasing their cytoplasm into a secondary emerging sporangium which forms and releases zoospores.

Morphological structures on V8A: *Sporangia* infrequently observed in solid agar of 1–3-mo-old cultures and produced commonly in non-sterile soil extract; 32.5 ± 4.9 × 25.7 ± 3.8 µm (overall range 20.0–42.5 × 14.9–33.3 µm) with a length/breadth ratio of 1.33 ± 0.3 (overall range 1.05–3.0); primary sporangia nonpapillate, borne terminally on unbranched sporangiophores, almost exclusively transitional, releasing their undifferentiated cytoplasm gradually into secondary nonpapillate sporangia instead of releasing zoospores (Fig. 57A–R); secondary sporangia emerging from mature primary sporangia at or near the apex (Fig. 57B–N, P–R, T–V) or laterally (Fig. 57O, S), sessile (Fig. 57J, K, M, N, Q–S) or on short stalks (Fig. 57L, O, P, T–V); nonpapillate (Fig. 57K–M, O–R); primary and secondary sporangia usually with a conspicuous basal plug (Fig. 57C–W) and often 1 or 2 additional plugs inside the sporangiophore close to the sporangial base (Fig. 57D–H, J, M–P, T–V) forming short or medium-length pedicels; despite pedicels non-caducous; sporangial shapes varying from subglobose (8 %; Fig. 57B, C, J, K, O, P, T, U), ovoid or broad-ovoid (60 %; Fig. 57A, D, E, G–I, K–N, Q, R), obpyriform (8 %; Fig. 57F) and pyriform (6 %; Fig. 57S) to limoniform (1 %; Fig. 57O, P); lateral attachment of the sporangiophore to the primary sporangia commonly observed

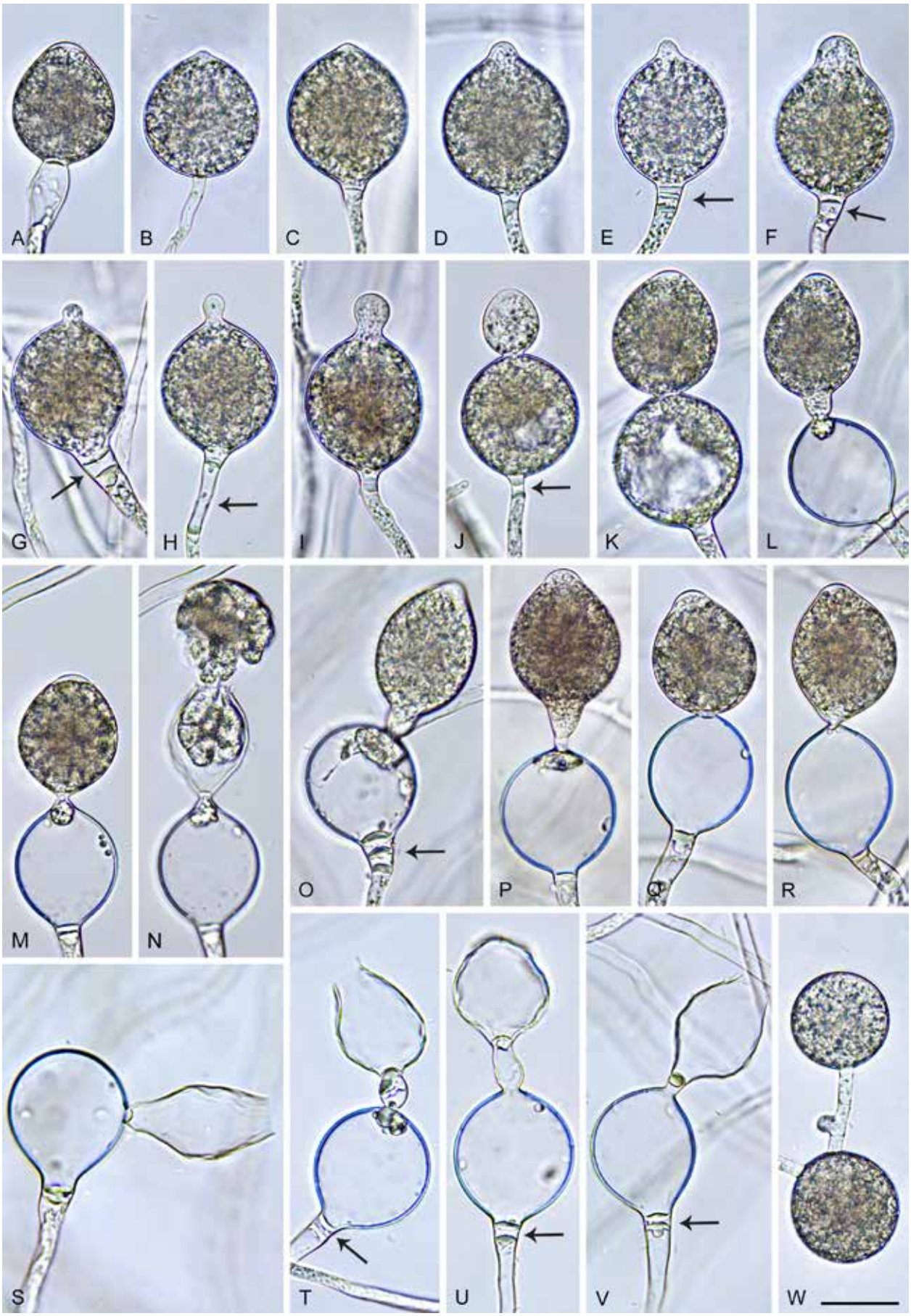

Fig. 57. *Phytophthora transitoria* (ex-type CBS 147245). **A–V.** Sporangia formed on V8 agar (V8A) flooded with soil extract. **A.** Nonpapillate, ovoid primary sporangium with widened sporangiophore. **B–D.** Primary transitional sporangia in different stages of development of secondary sporangia, with conspicuous basal plugs. **E.** With three basal plugs (arrow). **F–H, J.** With pedicels (arrows). **L–R.** Empty, primary transitional sporangia with conspicuous basal plugs and secondary mature sporangia after completion of cytoplasm transfer from the primary sporangia. **N.** Release of zoospores by the secondary sporangium. **O.** With three basal plugs. **S–V.** Empty, primary transitional sporangia and attached, empty secondary sporangia after zoospore release; all sporangia with one or multiple (arrows) basal plugs. **W.** Globose intercalary and terminal chlamydospores formed in solid V8A. Scale bar = 25 µm; W applies to A–V.

(26 %; Fig. 57G, R). *Zoospores* differentiate almost exclusively inside secondary sporangia (Fig. 57N-O), discharged through an exit pore 5.2–11.3 µm wide (av. 7.4 ± 1.5 µm; Fig. 57N, S–V), limoniform to reniform whilst motile, becoming spherical (av. diam = 9.9 ± 1.2 µm) on encystment. *Chlamydospores* globose to subglobose, 28.9 ± 4.9 µm diam (overall range 17.4–38.1 µm), terminal or intercalary, sometimes catenulate (Fig. 57W). *Gametangia* not observed in single culture or in mating tests with A1 and A2 tester strains of *Phytophthora cinnamomi*, suggesting a sterile breeding system.

Culture characteristics: Colonies on V8A and CA uniform and submerged; on PDA uniform, dense-felty and appressed with irregular submerged margins and slow growth (Fig. 60).

Cardinal temperatures and growth rates: Optimum 22.5 °C with 4.0 mm/d radial growth on V8A, maximum 30 °C, minimum < 10 °C.

Typus: **Czech Republic**, Central Bohemian region, Obříství, isolated from rhizosphere soil of a *Quercus robur* (*Fagaceae*) seedling, Mar. 2018, I. Milenković (**holotype** CBS H-24578, dried culture on V8A, culture ex-type CBS 147245 = CZ001).

Additional materials examined: **Czech Republic,** Central Bohemian region, Obříství, isolated from rhizosphere soil of nursery-grown *Quercus robur* seedlings, Mar. 2018, I. Milenković (cultures CBS 147246 = CZ118, CZ119, CZ120, CZ121, CZ123).

Notes: *Phytophthora transitoria* differs from all other known *Phytophthora* species by releasing zoospores almost exclusively from secondary sporangia which emerge from primary transient sporangia. In addition, *Phy. transitoria* has a sterile breeding system and produces nonpapillate persistent sporangia differentiating it from all other known species from phylogenetic Clade 3 (Fig. 52) which are homothallic with semipapillate, predominantly caducous sporangia.

Phytophthora panamensis T. Jung, Y. Balci, K. Broders & I. Milenković, ***sp. nov.*** MycoBank MB 840175. Fig. 58.

Etymology: Name refers to Panama, the country where this species was first isolated.

Morphological structures on V8A: *Sporangia* commonly observed in solid agar and abundantly produced in non-sterile soil extract; borne terminally on long unbranched sporangiophores (8.8 %), in lax sympodia (14.8 %) or on short lateral sporangiophores (70.4 %; Fig. 58E, I) or less frequently intercalary (6.0 %; Fig. 58D); non-caducous, predominantly ovoid or elongated ovoid (94.4 %; Fig. 58A–D, F, G, K), less frequently limoniform (3.6 %; Fig. 58J), obpyriform (1.2 %; Fig. 58I), mouse-shaped (0.4 %; Fig. 58E, H) or distorted (0.4 %); lateral attachment of the sporangiophore (50.4 %; Fig. 58B, C, E) and a conspicuous basal plug (60 %; Fig. 58K) commonly observed; sometimes forming short hyphal appendices (Fig. 58B); apices papillate or rarely bipapillate (<1 %; Fig. 58J), frequently asymmetric to curved (31.2 %; Fig. 58E–I); occasionally external proliferation (Fig. 58I, K); sporangial dimensions averaging 44.1 ± 5.3 x 29.8 ± 3.5 µm (overall range 28.5–62.9 × 20.3–41.3 µm) with a length/breadth ratio of 1.49 ± 0.16 (overall range 0.95–1.97); sporangial germination usually indirectly with zoospores discharged through an exit pore 3.9–8.3 µm wide (av. 6.2 ± 0.9 µm) (Fig. 58G, K). *Zoospores* limoniform to reniform whilst motile, becoming spherical (av. diam = 9.5 ± 1.1 µm) on encystment. *Hyphal swellings* subglobose to mostly globose, intercalary, averaging 11.4 ± 3.2 µm (Fig. 58W). *Chlamydospores* not observed. *Oogonia* abundantly produced in single culture (homothallic breeding system), terminal on short to medium-length, often twisted lateral hyphae (Fig. 58L–V), smooth-walled, globose to slightly subglobose (74.4 %; Fig. 58L–Q), less frequently slightly excentric or elongated (25.6 %; Fig. 58R–V), relatively small (mean diam 24.6 ± 2.1 µm, overall range 16.0–31.0 µm); plerotic or almost plerotic (62.8 %; Fig. 58M–P, S) or aplerotic (37.2 %; Fig. 58L, Q, R, T–V). *Oospores* globose with a large lipid globule (Fig. 58L–V), wall thickness 1.9 ± 0.3 µm (overall range 1.1–2.7 µm), oospore wall index 0.43 ± 0.04; abortion 16–33 % after 4 wk. *Antheridia* exclusively paragynous and club-shaped to subglobose (Fig. 58L–V), frequently formed on hyphal branches arising close to the oogonia-bearing hyphal branch (Fig. 58V), sometimes with a finger-like projection (1.2 %).

Culture characteristics: Colonies on V8A and CA mostly submerged to appressed, radiate on V8A and uniform on CA; on PDA dense-felty to cottony, petaloid with submerged margins (Fig. 60).

Cardinal temperatures and growth rates: Optimum 27.5 or 30 °C with 9.5–9.7 mm/d radial growth on V8A, maximum 30–32.5 °C, minimum >10–15 °C.

Notes: *Phytophthora panamensis* differs from its closest relative *Phy. quercetorum* in phylogenetic Clade 4 (Fig. 52) by producing on average smaller oogonia and oospores and larger sporangia, having higher minimum and optimum temperatures and lower maximum temperature for growth, showing considerably faster growth between 15 °C and 30 °C and different colony morphology on V8A and CA.

Typus: **Panama**, Parque Nacional Sobernia, isolated from necrotic lesion on a naturally fallen leaf of a non-identified tree species in a tropical lowland forest, Nov. 2019, K.D. Broders & Y. Balci (**holotype** CBS H-24773, dried culture on V8A, culture ex-type CBS 147925 = PA328).

Additional materials examined: **Panama**, Parque Nacional Sobernia, isolated from necrotic lesions on naturally fallen leaves of non-identified tree species in tropical lowland forests, Nov. 2019, K.D. Broders & Y. Balci (cultures CBS 147926 = PA329, PA019, PA040, PA108).

Phytophthora variabilis T. Jung, M. Horta Jung & I. Milenković, ***sp. nov.*** MycoBank MB 840174. Fig. 59.

Etymology: Name refers to the variable shapes of the oogonia with both amphigynous and paragynous antheridia.

Morphological structures on V8A: *Sporangia* not observed in solid agar but abundantly produced in non-sterile soil extract; borne terminally on mostly long unbranched or less frequently short lateral sporangiophores (72.4 %; Fig. 59A–J) or via internal nested and extended proliferation (18.8 %; Fig. 59I, J) or external proliferation (8.8 %); nonpapillate, non-caducous, predominantly ovoid, broad ovoid or elongated ovoid (83.2 %; Fig. 59A–D, I), less frequently ellipsoid or elongated ellipsoid (4.8 %; Fig. 59F, G) or elongated obpyriform (0.4 %; Fig. 59E); basal plug common (39.2 %; Fig. 59A, F, H); lateral attachment of the sporangiophore (8.8 %) and a slightly displaced apex (2.8 %) infrequently observed; sporangial dimensions averaging 61.0 ± 7.0 × 37.7 ± 3.9 µm (overall range 47.2–82.5 × 25.3–47.9 µm) with a length/breadth ratio of 1.62 ± 0.16 (overall range 1.28–2.25); sporangial germination indirectly with zoospores discharged through a wide exit pore of 8.2–18.6 µm (av. 13.1 ± 2.1 µm) into a short-lived vesicle (Fig. 59H, J). *Zoospores* limoniform to reniform whilst motile (Fig. 59H, J), becoming spherical (av. diam = 10.3 ± 1.0 µm) on encystment. *Hyphal swellings* and

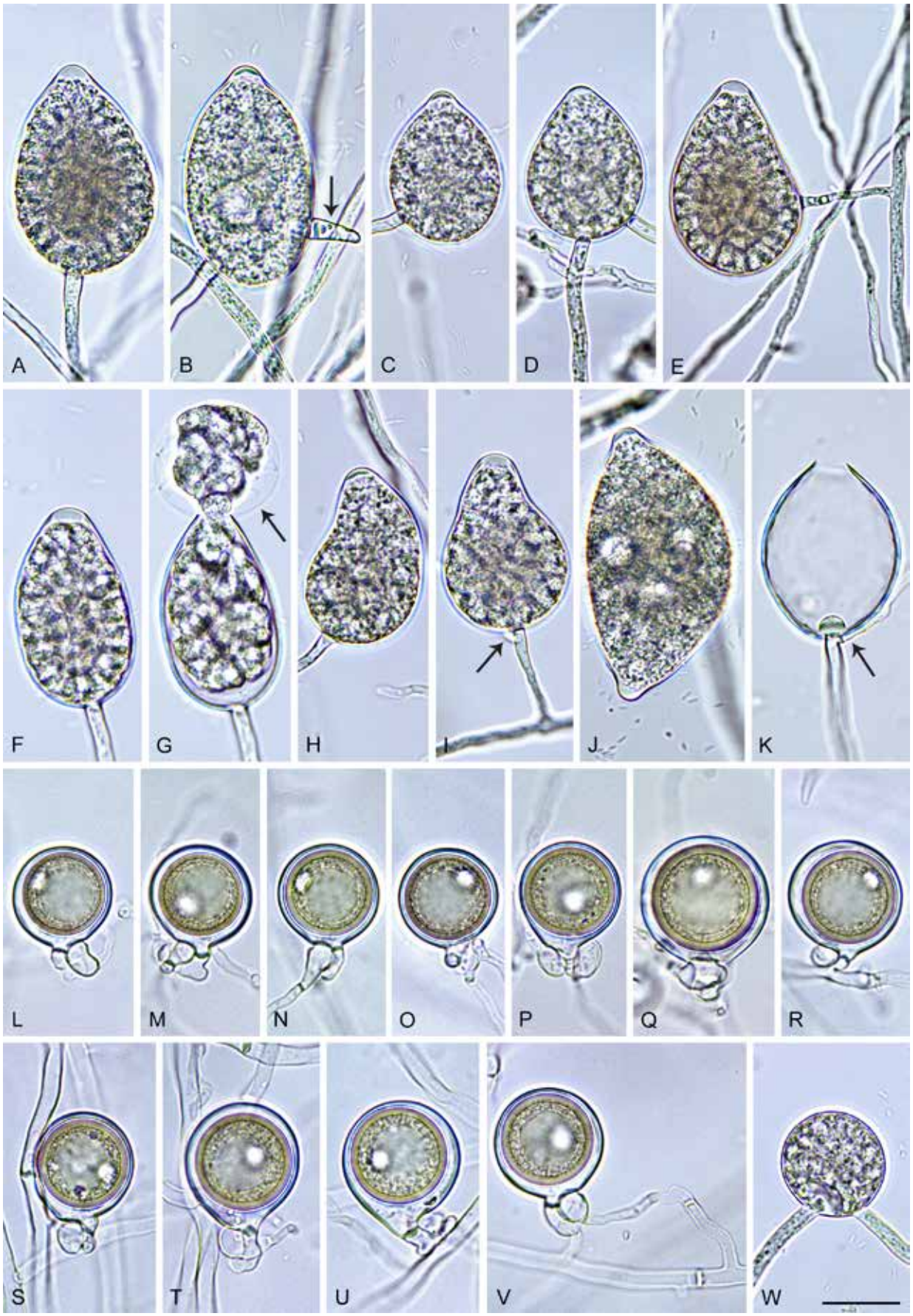

Fig. 58. *Phytophthora panamensis* (ex-type CBS 147925). **A–K.** Papillate sporangia formed on V8 agar (V8A) flooded with soil extract. **A.** Ovoid, with differentiated zoospores inside the sporangium. **B.** Ovoid with hyphal projection (arrow), laterally attached. **C.** Ovoid, laterally attached. **D.** Ovoid, intercalary. **E.** Asymmetric-obpyriform with differentiated zoospores, laterally attached, on short lateral hypha. **F, G.** Elongated-ovoid, releasing zoospores into short-lived vesicle (arrow). **H.** Mouse-shaped. **I.** Obpyriform, with external proliferation (arrow), on short lateral hypha. **J.** Limoniform, bipapillate. **K.** Ovoid, after zoospore release, with conspicuous basal plug and external proliferation (arrow). **L–V.** Oogonia with thick-walled oospores, containing large lipid globules, and paragynous antheridia, formed in solid V8A. **L–Q.** Globose to subglobose. **R–V.** Slightly excentric or elongated. **M–P, S.** Plerotic or almost plerotic oospores. **Q, R, T–V.** Aplerotic oospores. **W.** Intercalary globose hyphal swelling in solid V8A. Scale bar = 25 µm; W applies to A–V.

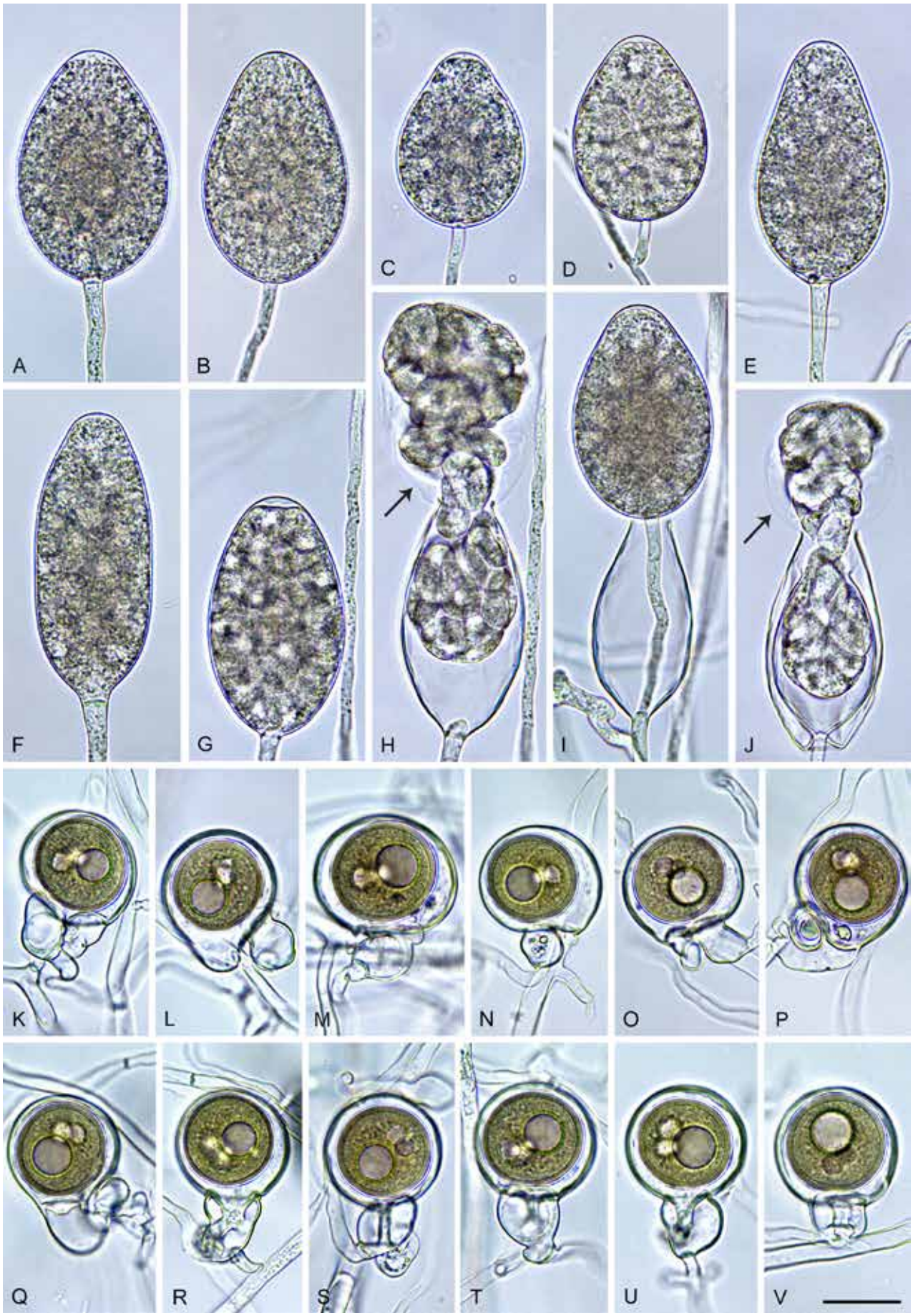

Fig. 59. *Phytophthora variabilis* (ex-type CBS 147923). **A–J.** Non-caducous sporangia formed on V8 agar (V8A) flooded with soil extract. **A–F, I.** Nonpapillate. **A–D.** Ovoid. **D.** On short lateral hypha. **E.** Elongated-obpyriform. **F.** Elongated-ellipsoid. **G, H.** Ellipsoid, releasing zoospores into short-lived vesicle (arrow). **I.** Ovoid, internal extended proliferation. **J.** Internal nested proliferation, zoospore release into short-lived vesicle (arrow). **K–V.** Oogonia containing thick-walled, brown, aplerotic oospores with large lipid globules formed in solid V8A, variable shapes. **K, M, O.** Excentric. **L, P.** Elongated with tapering base. **N.** Comma-shaped. **Q–V.** Globose to slightly subglobose. **K–Q.** Paragynous antheridia. **R–V.** Amphigynous antheridia. Scale bar = 25 µm; V applies to A–U.

chlamydospores not observed. *Oogonia* abundantly produced in single culture (homothallic breeding system), sessile (12.5 %; Fig. 59M, N) or on short stalks which are often unusually thin (Fig. 59S, T) or thick (Fig. 59K, P, Q) and sometimes curved (Fig. 59P, Q); smooth-walled with variable shapes ranging from globose to slightly subglobose (55.5 %; Fig. 59Q–V), elongated (10.5 %; Fig. 59L, P) or excentric (25.5 %; Fig. 59K, M, O) to comma-shaped (19.5 %; Fig. 59N); av. diam. 33.0 ± 3.9 µm with an overall range of 24.0–49.9 µm; largely aplerotic (Fig. 59K–V). *Oospores* globose to subglobose with a medium-large lipid globule (Fig. 59K–V); wall diam 1.4 ± 0.2 µm (overall range 0.8–2.0 µm) and oospore wall index 0.30 ± 0.04; turning brown during maturation (Fig. 59K–V); abortion 2–7 % after 4 wk. *Antheridia* paragynous (68.5 %; Fig. 59K–Q) or amphigynous (31.5 %; Fig. 59R–V), 1-celled, and club-shaped, ovoid, subglobose or elongated to irregular (Fig. 59K–V).

Culture characteristics: Colonies on V8A and CA with limited aerial mycelium, radiate on V8A and uniform on CA; on PDA uniform and cottony (Fig. 60).

Cardinal temperatures and growth rates: Optimum 27.5 °C with 6.1–6.3 mm/d radial growth on V8A, maximum 32.5–35 °C, minimum <10 °C.

Notes: *Phytophthora variabilis* differs from all other species from Clade 7b (Fig. 55) by its distinct phylogenetic position and by having highly variable oogonial shapes. In addition, it is distinguished from the heterothallic *Phy. niederhauserii* and *Phy. melonis* (Erwin & Ribeiro 1996, Mirabolfathy *et al.* 2001, Abad *et al.* 2014) by its homothallic breeding system. The production of both amphigynous and paragynous antheridia separate *Phy. variabilis* from *Phy. cajani*, *Phy. melonis*, *Phy. sinensis* and *Phy. vignae* which

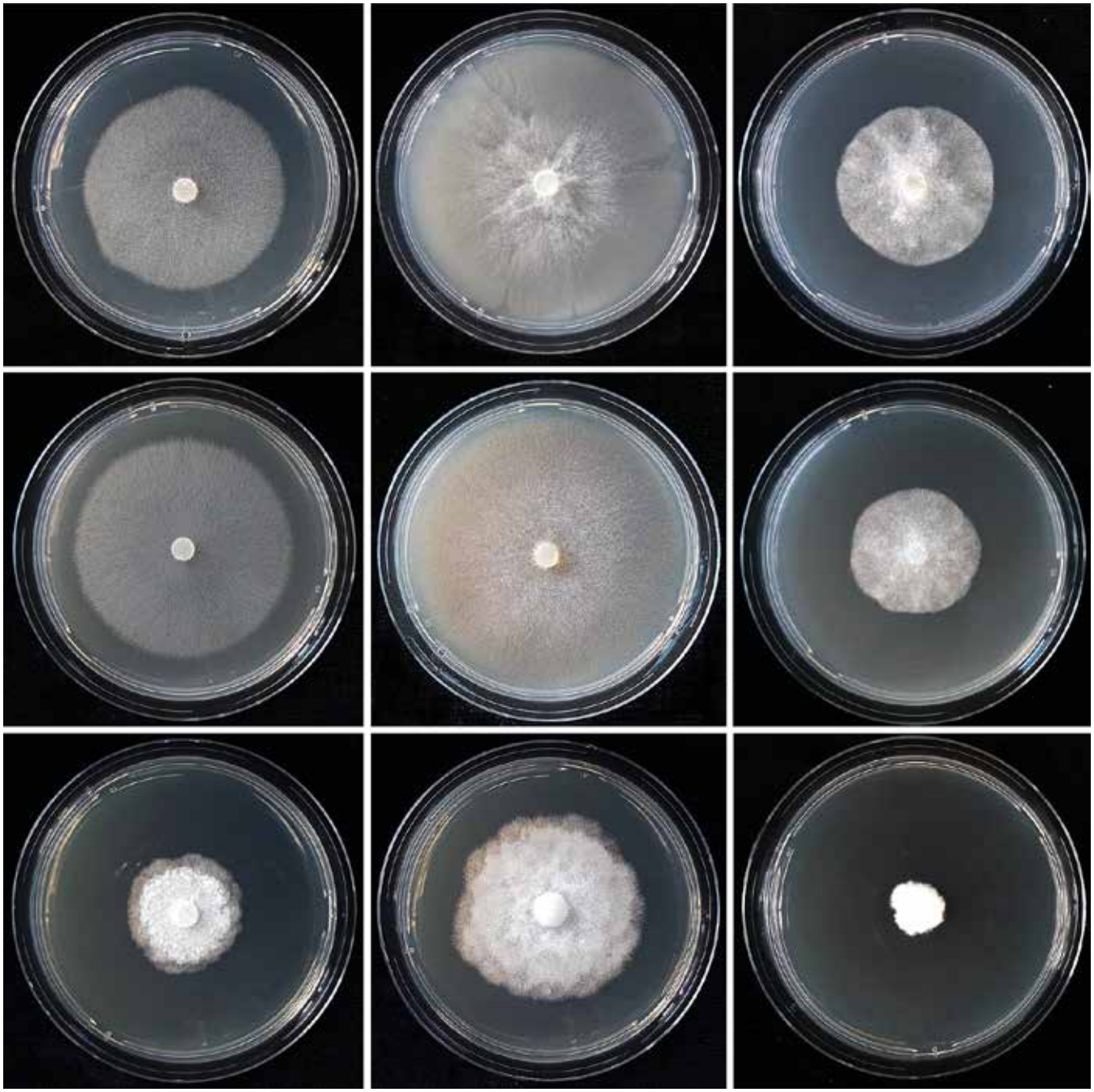

Fig. 60. Colony morphology of *Phytophthora transitoria*, *Phytophthora panamensis* and *Phytophthora variabilis* (from left to right) after 7 d growth at 20 ºC in the dark on V8-agar, carrot agar and potato-dextrose agar (from top to bottom).

all have exclusively amphigynous antheridia (Erwin & Ribeiro 1996, Mirabolfathy *et al.* 2001) and from *Phy. asiatica* which produces paragynous antheridia only rarely (Rahman *et al.* 2015).

Typus: **Slovakia**, Bratislava, Marianka, isolated from a commercial tree planting substrate, Jun. 2013, T. Jung (**holotype** CBS H-24772, dried culture on V8A, culture ex-type CBS 147923 = TJ915).

Additional materials examined: **Slovakia**, Bratislava, Marianka, isolated from a commercial tree planting substrate, Jun. 2013, T. Jung (cultures CBS 147924 = TJ1495, TJ1496, TJ1497, TJ1498).

Genome sequenced strain: *Phytophthora infestans*. **Netherlands**, collection information unknown, isolate T30-4 (F_1 individual from a genetic cross used to construct a linkage of *Phy. infestans*). This Whole Genome Shutgun project has been deposited at GenBank under the accession AATU01000000 (BioProject: PRJNA17665, BioSample: SAMN02953670; Haas *et al*. 2009).

Authors: T. Jung, Y. Balci, X. Yang, M. Horta Jung, I. Milenković, K.D. Broders, M. Tomšovský, T. Májek, B. Scanu

Pseudocercospora Spegazzini, Anales Mus. Nac. Buenos Aires, Ser. 3 13: 437. 1911. Fig. 61.
Synonyms: For synonyms see Braun *et al.* (2013).

Classification: *Dothideomycetes*, *Dothideomycetidae*, *Mycosphaerellales*, *Mycosphaerellaceae.*

Type species: *Pseudocercospora vitis* (Lév.) Spegazzini, basionym: *Septonema vitis* Lév., Annls Sci. Nat., Bot., sér. 3 9: 261. 1848. The state of type material is unclear.

DNA barcode (genus): ITS.

DNA barcodes (species): *act*, *rpb2* and *tef1*. Table 16. Fig. 62.

Sexual morph (*fide* Crous 1998, Aptroot 2006) "mycosphaerella-like". *Ascomata* invariably carbonised, uniformly rather large-cellular with parenchymatous cells, dispersed or aggregated. *Ascomatal wall* extended also below the hamathecium. *Clypeus* not observed. *Ostiole* apical, cells of ostiole arranged regularly. *Hamathecium* filaments (paraphyses, pseudoparaphyses, paraphysoids) always absent. *Asci* bitunicate, pyriform cylindrical, or cylindrical-clavate, variable in size, plerotic, containing 8 ascospores. *Ascospores* arranged irregularly uniseriate to irregularly biseriate or multiseriate, hyaline, median to conspicuously supramedian uniseptate (rarely 3-septate), variable in shape, rounded or slightly pointed at both ends, with thin wall. *Stromata* lacking to well developed, pigmented, subhyaline to dark brown, stomatal, epidermal, erumpent, often with superficial hyphae. *Pycnidial conidioma* rarely formed. *Conidiophores* solitary arising from superficial hyphae or loosely to densely fasciculate from upper part of stromata, rarely synnematous, straight to flexuous or geniculate, subhyaline to dark brown, simple or branched, thin- or thick-walled, smooth to verruculose, aseptate or septate. *Conidiogenous cells* integrated, terminal or intercalary, proliferating sympodially or percurrently, with unthickened conidial loci, rarely cicatrized or ring-shaped. *Conidia* solitary, rarely bearing micro-cyclic conidia in moist condition, holoblastic, cylindrical, acicular to obclavate, straight to mildly curved, subhyaline, pale or dark brown, reddish brown or pale to deep olivaceous, thin- or thick-walled, smooth- to verruculose-walled, aseptate to septate, often more than 10-disto- or euseptate, with unthickened and not darkened hilum, rarely slightly thickened along the rim.

Cultural characteristics: Colonies on PDA and MEA pale grey, smoke grey, grey olivaceous, pale olivaceous grey, pale greenish grey, olivaceous grey to greenish grey (Rayner 1970) on the upper surface, greenish grey, olivaceous black to greenish black on the under surface, floccose, cottony, flat, raised or convex, margin lobate, undulate, entire or sometimes rhizoid. Seldom with citrine green to greyish yellow green diffusible pigmentation in agar medium (Fig. 63).

Optimal media and artificial sporulation: Sterilised banana leaves placed on 1.5 % water agar (WA) or slide cultures of V-8 juice agar under nuv-light to induce sporulation of the asexual morph, while for the sexual morph Sach's agar (Crous *et al*. 2019d) with sterilised pine needles is recommended, incubated at 20–25 °C, pH 4–9. Inoculation tests using conidia formed on artificial media are required to confirm pathogenicity. Oatmeal agar prepared with host-leaf decoction water (tomato leaf: Hartman *et al.* 1991), sclerotia bodies formed by shake culture (Zinno 1970), and cultivation under nuv-light (Suto 1985). The following method has successfully been used for *Ps. fuligena*: 1) incubate isolate on MEA Petri dish for 1 wk. The medium should be kept somewhat dry; 2) the colony is scratched and spread with a spreader; 3) leaves of the host plant are dipped and lightly waved in boiling water (in the case of tomato leaves, approx. 40 s); 4) leaf pieces are cut out in 5 mm squares, and completely dried under a laminar flow fume hood; 5) several leaf pieces are placed on the spreading colony and incubated for 2 wk under diffused light, without sealing the dishes. Conidia are collected with sterile water and a brush.

Distribution: Worldwide.

Hosts: Wide host range, including ferns, monocots, and dicots.

Disease symptoms: Leaf spots, leaf blight, shot-hole, sooty spots and early defoliation, twig cankers, fruit and husk spots (Fig. 63).

Notes: The taxonomic criteria for distinguishing genera and species of cercosporoid fungi, including *Pseudocercospora*, are sequentially published in a series by Braun *et al.* (2013, 2014, 2015a, b, 2016). The distinguishable morphological characteristics from other cercosporoid fungi are: pale to dark olivaceous caespituli, pigmented conidia with unthickened and not refractive scars on the conidiogenous cells and hila at the basal ends of conidium *in vivo* (Braun *et al.* 2013, Crous *et al*. 2013a, Videira *et al*. 2017). Species criteria of *Pseudocercospora* are based on morphological differences on the host plants as in other cercosporoid fungal genera. This criterion postulates that *Pseudocercospora* species are chiefly host specific. However, inoculation tests on various hosts are largely lacking. Host specificity is supported by the overall DNA phylogeny of *Pseudocercospora* as presented in Crous *et al*. (2013a). Recently, Nakashima *et al*. (2016) indicated that the *rpb2* locus should be added to the concatenated ITS-*actA*-*tef1* alignment as a robust secondary DNA barcode for recognition of species within the genus *Pseudocercospora*.

References: Deighton 1976 (re-evaluation of the genus *Pseudocercospora*); Crous 1998 (sexual morph); Crous & Braun 2003 (morphology, host range and list of species); Crous *et al*. 2013a (phylogeny); Braun *et al*. 2013, 2014, 2015a, b, 2016 (morphology, host range and list of species by the host family); Nakashima *et al*. 2016 (morphology and DNA barcodes for species); Videira *et al*. 2017 (morphology in culture and phylogeny).

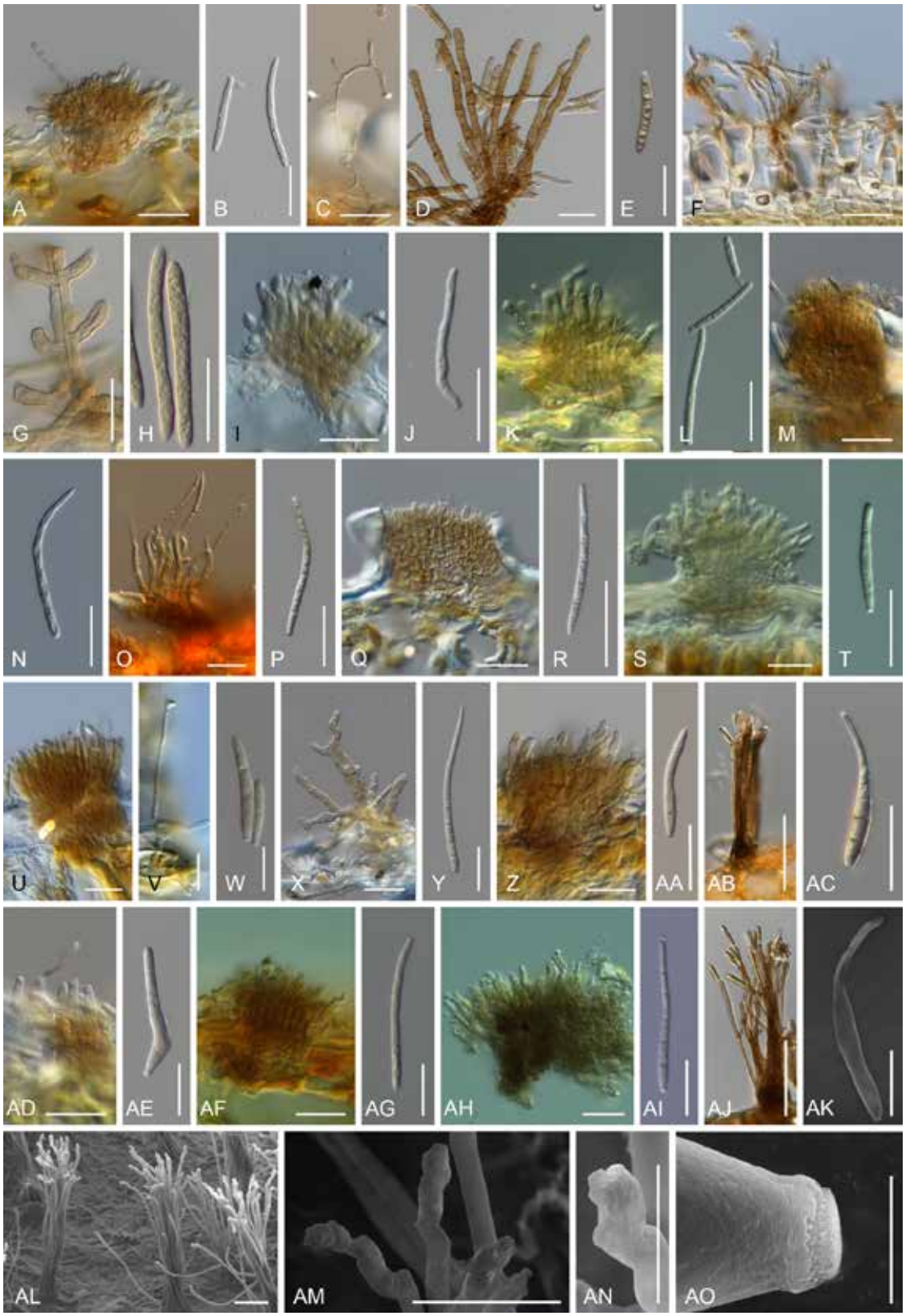

Fig. 61. *Pseudocercospora* spp. on host plants. **A, I, K, M, O, Q, S, U, Z, AF, AH, AJ.** Substomatal or erumpent stromata. **D, F, G, X, AB, AD.** Small stromata composed of few brown cells. **A, D, F, I, K, M, O, Q, S, U, X, Z, AB, AD, AF, AH, AJ.** Conidiophores emerging from stromata. **C, F, G, V.** Short conidiophores branched from superficial hypha. **AB, AJ, AL.** Synnematous conidiophores. **B, E, H, J, L, N, P, R, T, W, Y, AA, AC, AE, AG, AI, AK.** Conidia. **AM.** Sympodially proliferating conidiogenous cell. **AN.** Unthickened and truncated conidiogenous loci at the shoulder of conidiogenous cells. **AO.** Unthickened basal end of conidia. **A–C.** *Pseudocercospora amelanchieris* (holotype TSU-MUMH11539). **D, E.** *Pseudocercospora araliae* (epitype TFM: FPH-8094). **F.** *Pseudocercospora avicenniae* (isotype CPC17304). **G, H.** *Pseudocercospora bruceae* (TSU-MUMH11880). **I, J.** *Pseudocercospora chibaensis* (holotype TFM: FPH-6914). **K, L.** *Pseudocercospora chionanthi-retusi* (epitype NCHUP 3205). **M, N.** *Pseudocercospora daphniphylli* (holotype TFM: FPH-4431). **O, P.** *Pseudocercospora elaeocarpicola* (holotype TFM: FPH-7447). **Q, R.** *Pseudocercospora eriobotryae* (epitype TSU-MUMH11284). **S, T.** *Pseudocercospora eriobotryicola* (epitype NCHUP 3201). **U–W.** *Pseudocercospora hiratsukana* (epitype TNS-F-61275). **X, Y.** *Pseudocercospora houttuyniae* (holotype TNS-F-243809). **Z, AA.** *Pseudocercospora humuli* (holotype NIAES C487). **AB, AC.** *Pseudocercospora pruni-grayanae* (epitype TSU-MUMH11475). **AD, AE.** *Pseudocercospora stephanandrae* (holotype TFM: FPH-4411). **AF, AG.** *Pseudocercospora tinea* (epitype NCHUPP 3203). **AH, AI.** *Pseudocercospora violamaculans* (neotype TSU-MUMH11409). **AJ–AO.** *Pseudocercospora vitis* (TSU-MUMH 11593). Pictures A–E, G–J, M–AC, AF–AK were taken from Nakashima *et al*. (2016). Scale bars: A–AL = 20 µm; AM, AN = 5 µm, AO = 2.5 µm.

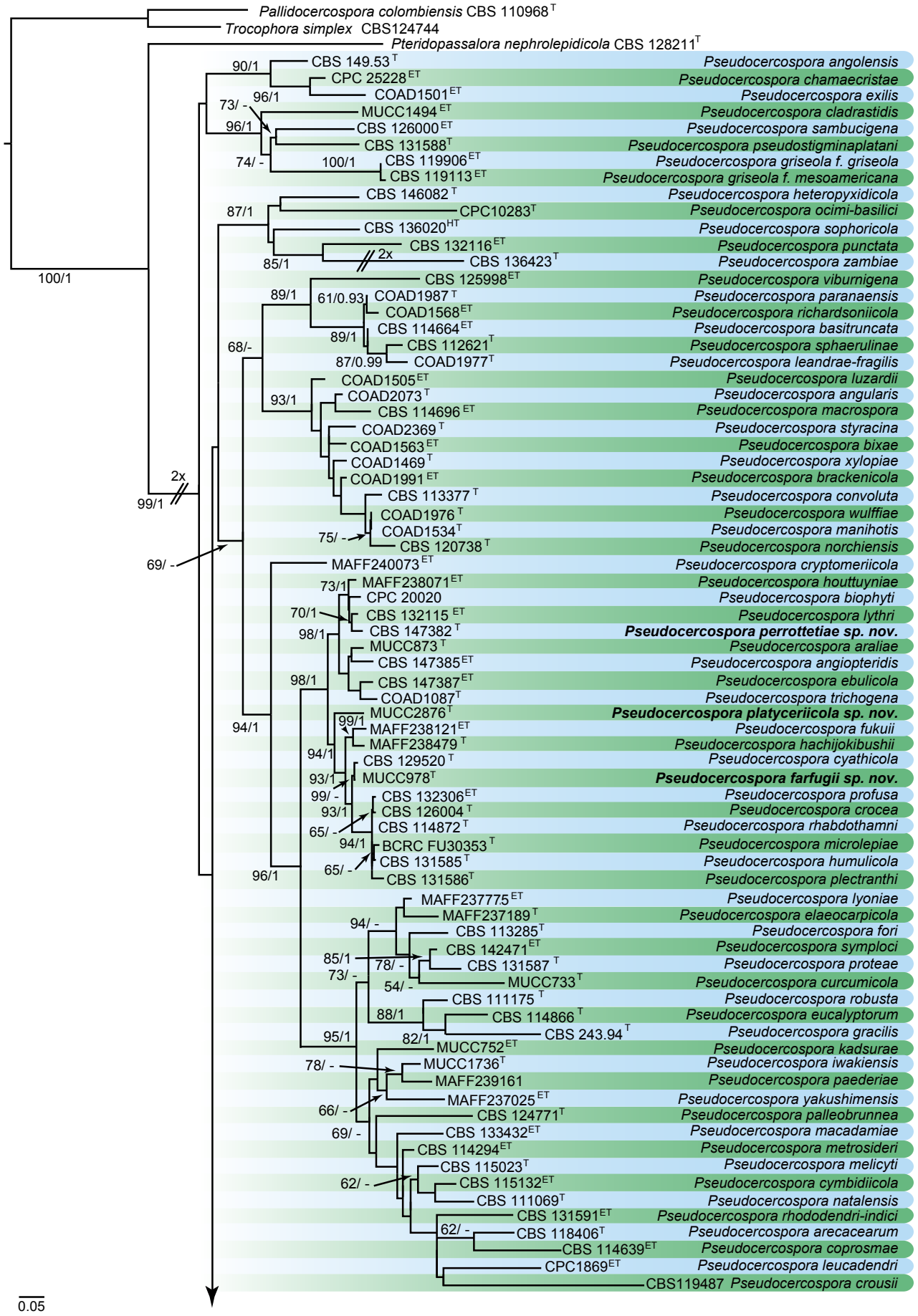

Fig. 62. Maximum Likelihood (ML) phylogram constructed from *actA* (254 bp), ITS (520 bp), *tef1* (615 bp), and *rpb2* (676 bp) sequences of all accepted species of *Pseudocercospora*. Maximum Likelihood bootstrap support values (> 50 %) and Bayesian posterior probability scores (> 0.90) are shown at the nodes. The novel taxa are printed in **bold**. The phylogenetic tree was rooted to *Pallidocercospora colombiensis* CBS 110968 and *Trocophora simplex* CBS 124744. GenBank accession numbers are indicated in Table 16. $^{T, ET, IsoT}$ and ^{NT} indicate ex-type, ex-epitype, ex-isotype and ex-neotype strains, respectively. TreeBASE: S27432.

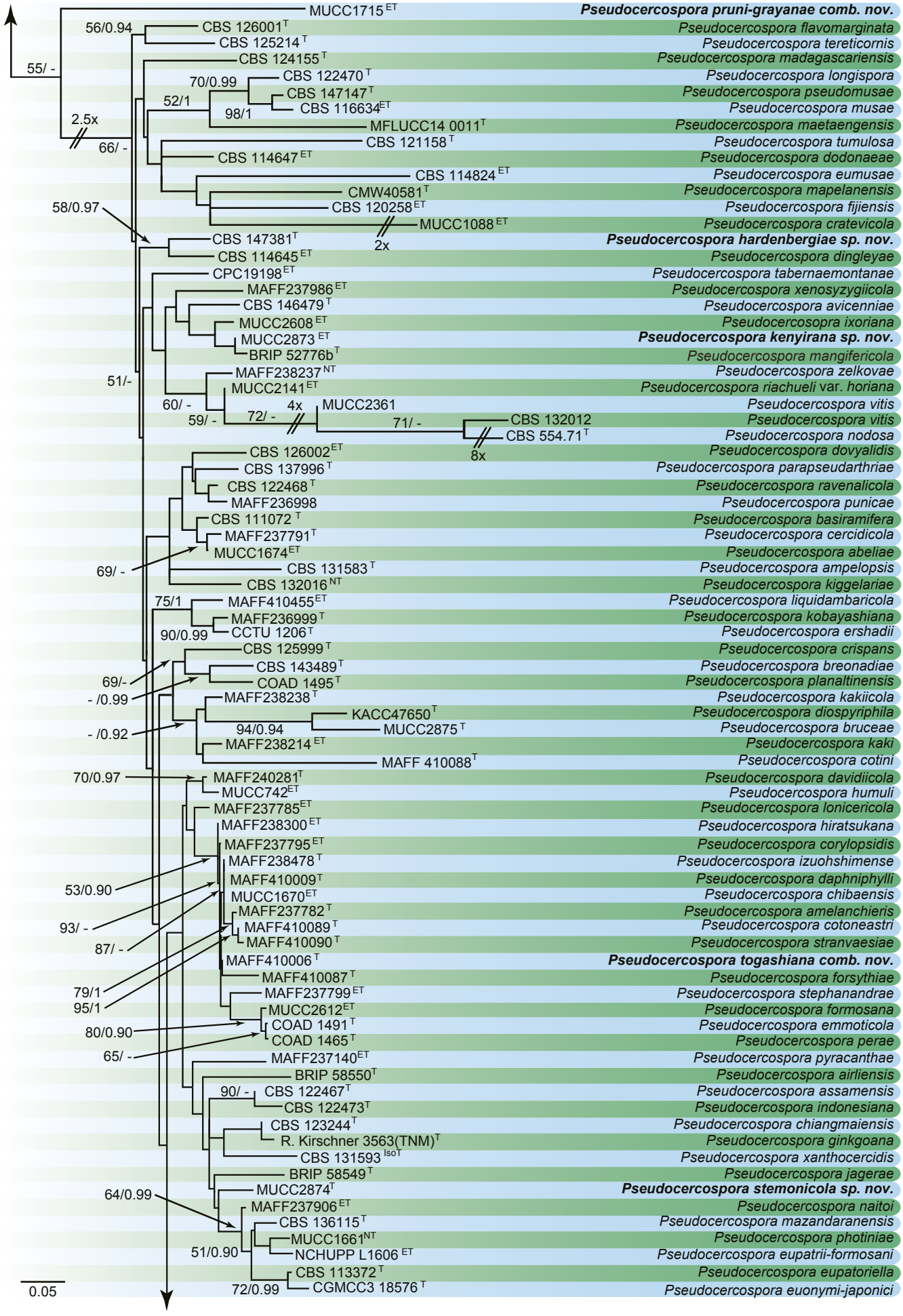

Fig. 62. (Continued).

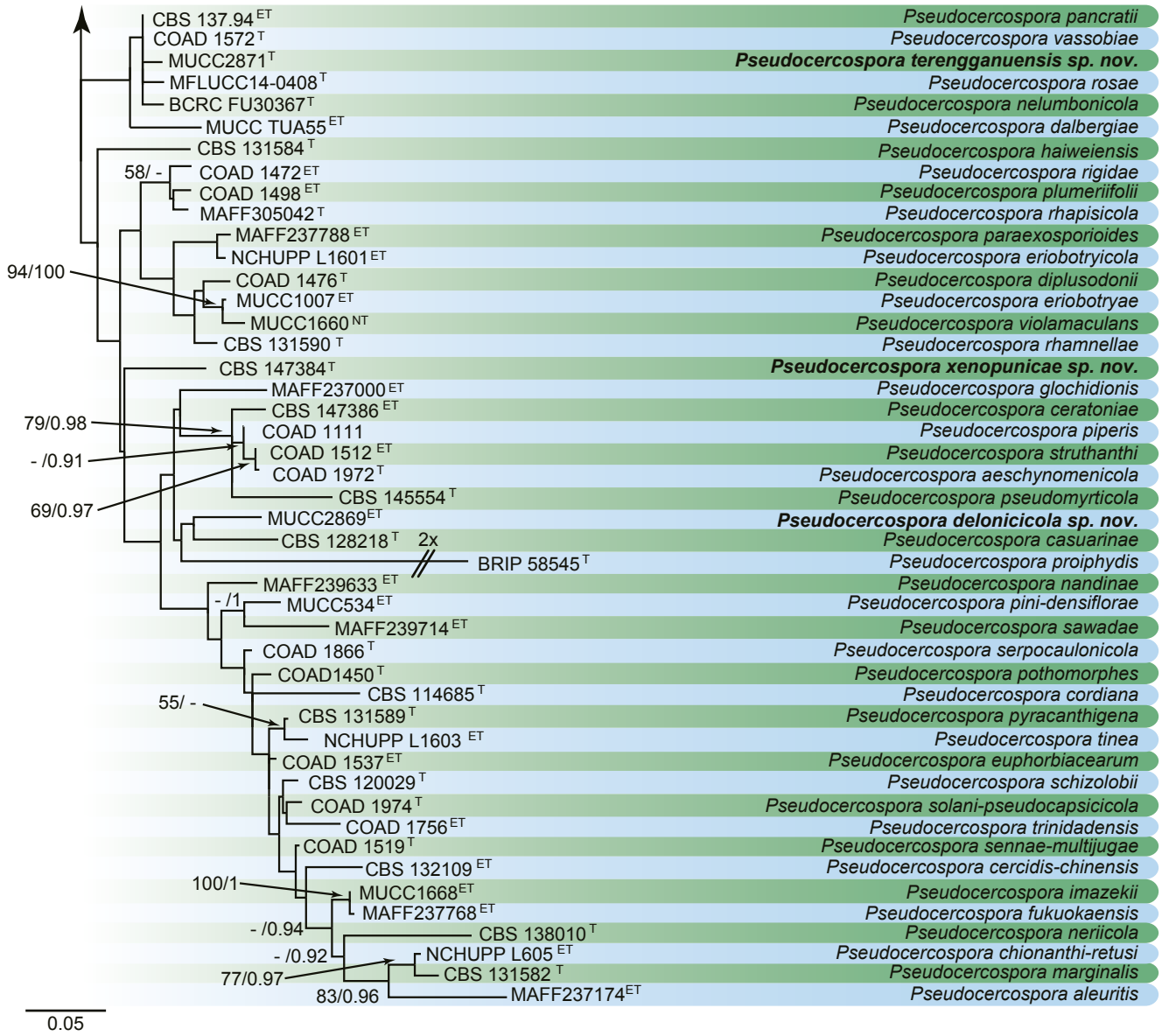

Fig. 62. (Continued).

Table 16. DNA barcodes of accepted *Pseudocercospora* spp.

Species	Isolates[1]	GenBank accession numbers[2]					References
		LSU	ITS	*actA*	*tef1*	*rpb2*	
Ps. abeliae	MUCC1674[ET]	—	LC599330	LC599407	LC599448	LC599587	Present study
Ps. aeschynomenicola	CPC 25227 = COAD 1972[T]	KT290173	KT290146	KT313501	KT290200	—	Silva *et al.* (2016)
Ps. airliensis	BRIP 58550[T]	KM055433	KM055429	—	KM055436	—	Shivas *et al.* (2015)
Ps. aleuritis	MAFF237174 = MUCC1230[ET]	—	LC599331	LC599408	LC599449	LC599588	Present study
Ps. amelanchieris	MAFF 237782 = MUCC885[T]	—	KX462583	KX462550	KX462669	KX462616	Nakashima *et al.* (2016)
Ps. ampelopsis	CBS 131583 = CPC 11680[T]	GU253846	GU269830	GU320534	GU384542	—	Crous *et al.* (2013a)
Ps. angiopteridis	CBS 147385[ET]	—	LC599332	LC599409	LC599450	LC599589	Present study
Ps. angolensis	CBS 149.53[T]	JQ324941	JQ324975	JQ325011	JQ324988	—	Silva *et al.* (2016)
Ps. angularis	COAD 2073[T]	—	KX793125	KX793124	—	—	Crous *et al.* (2017a)
Ps. araliae	MUCC 873[ET]	GU253702	GU269653	GU320361	GU384371	KX462617	Crous *et al.* (2013a), Nakashima *et al.* (2016)

Table 16. (Continued).

Species	Isolates[1]	GenBank accession numbers[2]					References
		LSU	ITS	*actA*	*tef1*	*rpb2*	
Ps. arecacearum	CBS 118406^{T}	GU253704	GU269655	GU320363	GU384373	—	Crous *et al.* (2013a)
Ps. assamensis	CBS 122467^{T}	GU253705	GU269656	GU320364	GU384374	—	Crous *et al.* (2013a)
Ps. avicenniae	CBS 146479^{T}	—	GU188047	LC599410	LC599451	LC599590	Shivas *et al*. (2009a)
Ps. basiramifera	CBS 111072 = CPC 1266 ^{T}	GU253709	GU269661	GU320368	DQ211677	—	Crous *et al.* (2013a)
Ps. basitruncata	CBS 114664 = CPC 1202^{ET}	GU253710/ DQ204759	DQ267600/ GU269662	DQ147622	DQ211675	—	Crous *et al.* (2013a)
Ps. biophyti	CPC 20020	—	LC599333	LC599411	LC599452	LC599591	Present study
Ps. bixae	CPC 25244 = COAD 1563^{ET}	KT290180	KT290153	KT313508	KT290207	—	Silva *et al.* (2016)
Ps. brackenicola	CPC 24695 = COAD 1991^{T}	KT037565	KT037524	KT037606	KT037484	—	Guatimosim *et al.* (2016)
Ps. breonadiae	CBS 143489 = CPC 30153^{T}	MH107959	MH107913	MH107985	MH108026	MH108006	Crous *et al.* (2018b)
Ps. bruceae	MUCC 2875^{T}	—	LC599334	LC599412	LC599453	—	Present study
Ps. casuarinae	CBS 128218^{T}	HQ599604	HQ599603	LC599413	LC599454	—	Crous *et al.* (2010b)
Ps. ceratoniae	CBS 147386^{ET}	—	LC599335	LC599414	LC599455	LC599592	Present study
Ps. cercidicola	MAFF 237791 = MUCC 896^{T}	GU253719	GU269671	GU320377	GU384388	KX462618	Crous *et al.* (2013a), Nakashima *et al*. (2016)
Ps. cercidis-chinensis	CBS 132109 = CPC 14481^{ET}	GU253718	GU269670	GU320376	GU384387/ LC599456	LC599593	Crous *et al.* (2013a)
Ps. chamaecristae	CPC 25228 = COAD 1973^{ET}	KT290174	KT290147	KT313502	KT290201	—	Silva *et al.* (2016)
Ps. chiangmaiensis	CBS 123244^{T}	MH863288	EU882113	EU882147	KF903544	—	Cheewangkoon *et al.* (2008), Vu *et al*. (2019)
Ps. chibaensis	MUCC1670^{ET}	—	KX462584	KX462551	KX462670	KX462619	Nakashima *et al.* (2016)
Ps. chionanthi-retusi	TUA50 = NCHUPP L1605^{ET}	—	KX462585	KX462552	KX462671	KX462620	Nakashima *et al.* (2016)
Ps. cladrastidis	MUCC1494^{ET}	—	LC599336	LC599415	LC599457	LC599594	Present study
Ps. convoluta	CBS 113377 = MJM 1533 = C488^{T}	MF951226	DQ676519	—	—	MF951617/ LC599595	Videira *et al.* (2017)
Ps. coprosmae	CBS 114639^{ET}	JQ324946	GU269680	GU384397	GU320386	—	Present study
Ps. cordiana	CBS 114685 = CPC 2552^{T}	GU214472	AF362054/ GU269681	GU320387	GU384398	—	Crous *et al.* (2013a)
Ps. corylopsidis	MAFF 237795 = MUCC 908^{ET}	—	GU269684	GU320390	GU384401	KX462621	Nakashima *et al.* (2016)
Ps. cotini	MAFF410088 = MUCC1415^{T}	—	LC599337	LC599416	LC599458	LC599596	Present study
Ps. cotoneastri	MAFF 410089 = MUCC1416^{T}	—	KX462586	KX462553	KX462672	KX462622	Nakashima *et al.* (2016)
Ps. cratevicola	MUCC1088^{ET}	MF951233	MF951372	LC599417	LC599459	LC599597	Present study
Ps. crispans	CBS 125999 = CPC 14883^{T}	GU253825	GU269807	GU320510	GU384518	KX462623	Crous *et al.* (2013a), Nakashima *et al.* (2016)
Ps. crocea	CBS 126004 = CPC 11668^{T}	JQ324947	GU269792	GU320493	GU384502	—	Crous *et al.* (2013a)
Ps. crousii	CBS 119487	GU253729	GU269686	GU384403	GU320392	—	Crous *et al.* (2013a)

Table 16. (Continued).

Species	Isolates[1]	GenBank accession numbers[2]					References
		LSU	ITS	*actA*	*tef1*	*rpb2*	
Ps. cryptomeriicola	MAFF240073 = NBRC 102150[ET]	—	LC599338	LC599418	LC599460	LC599598	Present study
Ps. curcumicola	MUCC733[T]	—	LC599339	LC599419	LC599461	LC599599	Present study
Ps. cyathicola	CBS 129520 = CPC 17047[T]	JF951159	JF951139	KX462554	KX462673	KX462624	Guatimosim *et al.* (2016), Nakashima *et al.* (2016)
Ps. cymbidiicola	CBS 115132[ET]	GU253733	GU269692	GU320397	GU384408	—	Crous *et al.* (2013a)
Ps. dalbergiae	TUA55[ET]	—	LC599340	LC599420	LC599462	LC599600	Present study
Ps. daphniphylli	MAFF 410009 = MUCC1399[T]	—	KX462587	KX462555	KX462674	KX462625	Nakashima *et al.* (2016)
Ps. davidiicola	MAFF 240281 = MUCC296[T]	GU253734	GU269693	GU320398	GU384409	KX462626	Nakashima *et al.* (2016)
Ps. delonicicola	MUCC2869[T]	—	LC599341	LC599421	LC599463	LC599601	Present study
Ps. dingleyae	CBS 114645[ET]	KX286997	KX287299	—	—	KX288454	Videira *et al.* (2017)
Ps. diospyriphila	KACC47650[T]		GU512009	LC515790	LC512003	—	Braun *et al.* (2020)
Ps. diplusodonii	CPC 25179 = COAD 1476[T]	KT290162	KT290135	KT313490	KT290189	—	Silva *et al.* (2016)
Ps. dodonaeae	CBS 114647[ET]	JQ324948	GU269697	JQ325013	GU384413	—	Crous *et al.* (2013a)
Ps. dovyalidis	CBS 126002 = CPC 13771[ET]	GU253818	GU269800	GU320503	GU384513	—	Crous *et al.* (2013a)
Ps. ebulicola	CBS 147387[ET]	—	LC599342	LC599422	—	LC599602	Present study
Ps. elaeocarpicola	MAFF 237189 = MUCC1236[T]	—	KX462588	KX462556	KX462675	KX462627	Nakashima *et al.* (2016)
Ps. emmoticola	CPC 25187 = COAD 1491[T]	KT290163	KT290136	KT313491	KT290190	—	Silva *et al.* (2016)
Ps. eriobotryae	MUCC 1007[ET]	—	KX462589	KX462557	KX462676	KX462628	Nakashima *et al.* (2016)
Ps. eriobotryicola	TUA12 = NCHUPPL1601[ET]	—	KX462590	KX462558	KX462677	KX462629	Nakashima *et al.* (2016)
Ps. ershadii	CBS 136114 = CCTU 1206[T]	KP717032	KM452867	KM452844	KM452889	MN786459	Bakhshi *et al.* (2014), Braun *et al.* (2020)
Ps. eucalyptorum	CBS 114866 = CPC 11[T]	JQ739817	KF901720	KF903474	KF903195	MF951618	Videira *et al.* (2017)
Ps. eumusae	CBS 114824[ET]	—	EU514238	LFZN0100 0053	LFZN0100 0037	—	Crous *et al.* (2020)
Ps. euonymi-japonici	CGMCC 3.18576[T]	—	MH255812	MH392525	—	MH392531	Wang *et al.* (2019)
Ps. eupatoriella	CBS 113372[T]	GU253743	GU269704	GU320408	GU384420	MH392531	Crous *et al.* (2013a)
Ps. eupatorii-formosani	TUA59 = NCHUPP L1606[ET]	—	KX462591	KX462559	KX462678	KX462630	Nakashima *et al.* (2016)
Ps. euphorbiacearum	COAD 1537[ET]	KT290172	KT290145	KT313500	KT290199	—	Silva *et al.* (2016)
Ps. exilis	CPC 25193 = COAD 1501[ET]	KT290166	KT290139	KT313494	KT290193	—	Silva *et al.* (2016)
Ps. farfugii	MUCC978[T]	—	LC599343	LC599423	LC599464	LC599603	Present study
Ps. fijiensis	CBS 120258 = CIRAD 86[ET]	JQ324952	EU514248	NW006921533	NW006921532	NW006921535	Crous *et al.* (2013a)
Ps. flavomarginata	CBS 126001[T]	GU253822	GU269804	GU320507	GU384515 / LC599465	LC599604	Crous *et al.* (2013a)
Ps. fori	CBS 113285[T]	DQ204748	AF468869	DQ147618	DQ211664	KT356874	Crous *et al.* (2013a), Ismail *et al.* (2016)
Ps. formosana	MUCC2612[ET]	—	LC599344	LC599424	LC599466	LC599605	Present study
Ps. forsythiae	MAFF 410087 = MUCC1414[T]	—	LC599345	LC599425	LC599467	—	Present study

Table 16. (Continued).

Species	Isolates[1]	GenBank accession numbers[2]					References
		LSU	ITS	*actA*	*tef1*	*rpb2*	
Ps. fukuii	MAFF238121 = MUCC1297^{ET}	—	LC599347	LC599427	LC599469	LC599607	Present study
Ps. fukuokaensis	MAFF 237768 = MUCC 887^{ET}	GU253751	GU269714	GU320418	GU384430	KX462632	Nakashima *et al.* (2016)
Ps. ginkgoana	R. Kirschner 3563 (TNM)^{T}	—	JX134048	—	—	—	Kirschner & Okuda (2013)
Ps. glochidionis	MAFF 237000; MUCC1211^{ET}	—	LC599348	LC599428	LC599470	LC599608	Present study
Ps. gracilis	CBS 242.94^{T}	DQ204750	DQ267582	DQ147616	DQ211666	—	Crous *et al.* (2013a)
Ps. griseola f. griseola	CBS 119906^{ET}	—	DQ289812.	DQ289879	—	—	Crous *et al. (*2006b)
Ps. griseola f. mesoamericana	CBS 119113^{ET}	—	DQ289824	DQ289891	—	—	Crous *et al.* (2006b)
Ps. hachijokibushii	MAFF 238479^{T}	—	KX462593	KX462561	KX462680	KX462633	Nakashima *et al.* (2016)
Ps. haiweiensis	CBS 131584 = CPC 14084^{T}	GU253821	GU269803	GU320506	GU384514	KX462634	Crous *et al.* (2013a), Nakashima *et al.* (2016)
Ps. hardenbergiae	CBS 147381^{T}	—	LC599349	LC599429	LC599471	LC599609	Present study
Ps. heteropyxidicola	CBS 146082 = CPC 38030^{T}	MN567658	MN562151	MN556791	—	—	Crous *et al.* (2019e)
Ps. hiratsukana	MAFF 238300 = MUCC1105^{ET}	—	KX462594	KX462562	KX462681	KX462635	Nakashima *et al.* (2016)
Ps. houttuyniae	MAFF 238071 = MUCC1289^{ET}	—	KX462595	KX462563	KX462682	KX462636	Nakashima *et al.* (2016)
Ps. humuli	MUCC 742^{ET}	GU253758	GU269725	GU320428	GU384439	KX462637	Crous *et al.* (2013a), Nakashima *et al.* (2016)
Ps. humulicola	CBS 131585^{T}	JQ324956	GU269723	GU320427	GU384438	—	Crous *et al.* (2013a)
Ps. imazekii	MUCC 1668^{ET}	—	KX462596	KX462564	KX462683	KX462638	Nakashima *et al.* (2016)
Ps. indonesiana	CBS 122473^{T}	GU253765	GU269735	GU320437 EU514340	GU384448	—	Crous *et al.* (2013a)
Ps. iwakiensis	MUCC 1736^{T}	—	KX462607	KX462574	KX462693	KX462657	Nakashima *et al.* (2016)
Ps. ixoriana	MUCC2608^{ET}	—	LC599350	LC599430	LC599472	LC599610	Present study
Ps. izuohshimense	MAFF 238478 = MUCC1336^{T}	—	KX462597	KX462565	KX462684	KX462639	Nakashima *et al.* (2016)
Ps. jagerae	BRIP 58549^{T}	KM055435	KM055431	—	KM055438	—	Shivas *et al.* (2015)
Ps. kadsurae	MUCC 752^{ET}	—	KX462598	KX462566	KX462685	KX462640	Nakashima *et al.* (2016)
Ps. kaki	MAFF 238214^{ET}	—	LC512001	LC512007	LC515783	LC515794	Braun *et al.* (2020)
Ps. kakiicola	MAFF 238238 = MUCC 900^{T}	GU253761	GU269729	GU320431	GU384442	LC515786	Crous *et al.* (2013a), Braun et al. (2020)
Ps. kenyirana	MUCC 2873^{T}	—	LC599351	LC599431	LC599473	—	Present study
Ps. kiggelariae	CBS 132016 = CPC 11853^{NT}	GU253762	GU269730	GU320432	GU384443	—	Crous *et al.* (2013a)
Ps. kobayashiana	MAFF 236999^{T}	—	LC511998	LC512004	LC515780	LC515791	Braun *et al.* (2020)
Ps. leandrae-fragilis	COAD 1977^{T}	KY574287	KY574288	—	—	—	Crous *et al.* (2017a)
Ps. leucadendri	CPC 1869^{ET}	GU214480	GU269842	GU320545	GU384555	—	Crous *et al.* (2013a)
Ps. liquidambaricola	MAFF410455^{ET}		LC599352	LC599432	LC599474	LC599611	Present study
Ps. longispora	CBS 122470^{T}	GU253764	GU269734	GU320436 EU514342	GU384447	—	Crous *et al.* (2013a)

Table 16. (Continued).

Species	Isolates[1]	GenBank accession numbers[2]					References
		LSU	ITS	*actA*	*tef1*	*rpb2*	
Ps. lonicericola	MUCC 889 = MAFF 237785[ET]	GU253766	GU269736	GU320438	JQ324999	KX462641	Crous *et al.* (2013a), Nakashima *et al.* (2016)
Ps. luzardii	CPC 25196 = COAD 1505[ET]	KT290167	KT290140	KT313495	KT290194	—	Silva *et al.* (2016)
Ps. lyoniae	MAFF 237775 = MUCC 910[ET]	GU253768	GU269739	GU320441	GU384451	KX462642	Crous *et al.* (2013a), Nakashima *et al.* (2016)
Ps. lythri	CBS 132115 = CPC 14588[ET]	GU253771	GU269742	GU320444	GU384454/ LC599475	LC599612	Crous *et al.* (2013a)
Ps. macadamiae	CBS 133432[ET]	KX286998	KX287300	KU878551	KU878504	KX288455	Ong *et al.* (2017), Videira *et al.* (2017)
Ps. macrospora	CBS 114696 = CPC 2553[ET]	GU214478	AF362055/ GU269745	GU320447	GU384457	—	Crous *et al.* (2013a)
Ps. madagascariensis	CBS 124155[T]	—	GQ852767	KF253625	KF253265	KX462643	Nakashima *et al.* (2016)
Ps. maetaengensis	MFLUCC 14-0411[T]	MN648328	MN648323	—	—	—	Hyde *et al.* (2020)
Ps. mangifericola	BRIP 52776b[T]	—	GU188048	—	—	—	Shivas *et al*. (2009b)
Ps. manihotis	CPC 25219 = COAD 1534[T]	KT290171	KT290144	KT313499	KT290198	—	Silva *et al.* (2016)
Ps. mapelanensis	CMW40581[T]	KM203121	KM203118	KM203127	KM203124	—	Osorio *et al.* (2015)
Ps. marginalis	CBS 131582 = CPC 12497[T]	GU253812	GU269794	GU320495	GU384504	—	Crous *et al.* (2013a)
Ps. mazandaranensis	CCTU 1102 = CBS 136115[T]	KP717020	KM452854	KM452831	KM452876	LC599613	Bakhshi *et al.* (2014)
Ps. melicyti	CBS 115023[T]	JQ324968	GU269769	GU320472	GU384481	—	Crous *et al.* (2013a)
Ps. metrosideri	CBS 114294[ET]	KX286999	KX287301	—	—	KX288456	Videira *et al.* (2017)
Ps. microlepiae	BCRC FU30353[T]	—	KR348740	—	—	—	Kirschner & Wang (2015)
Ps. musae	CBS 116634[ET]	GU253775	GU269747	GU320449	GU384459	LFZO01000453	Crous *et al.* (2013, 2020)
Ps. naitoi	MAFF 237906 = MUCC1072[ET]	—	KX462599	KX462567	KX462686	KX462644	Nakashima *et al.* (2016)
Ps. nandinae	MAFF 237633 = MUCC1260[ET]	—	KX462600	KX462568	KX462687	KX462645	Nakashima *et al.* (2016)
Ps. natalensis	CBS 111069 = CPC 1263[T]	DQ267576	DQ303077	DQ147620	JQ325000	—	Crous *et al.* (2013a)
Ps. nelumbonicola	BCRC FU30367[T]	—	KY304492	—	—	LC199940	Chen & Kirschner (2017)
Ps. neriicola	CBS 138010 = CPC 23765[T]	KJ869222	KJ869165	KJ869231	KJ869240	KX462647	Crous *et al.* (2014c), Nakashima *et al.* (2016)
Ps. nodosa	CBS 554.71[T]	MF951227	MF951367	—	—	MF951620	Videira *et al.* (2017)
Ps. norchiensis	CBS 120738 = CPC 13049[T]	GU253780	EF394859	GU320455	GU384464	KX462648	Crous *et al.* (2013a), Nakashima *et al.* (2016)
Ps. ocimi-basilici	CPC 10283[T]	GU214678	GU269754	GU320456	GU384465	—	Crous *et al.* (2013a)
Ps. paederiae	MAFF 239161	—	KX462603	KX462570	KX462689	KX462651	Nakashima *et al.* (2016)
Ps. palleobrunnea	CBS 124771 = CPC 13387[T]	GQ303319	GQ303288	GU320500	GU384509	KX462652	Crous *et al.* (2013a), Nakashima *et al.* (2016)

Table 16. (Continued).

Species	Isolates[1]	GenBank accession numbers[2]					References
		LSU	ITS	*actA*	*tef1*	*rpb2*	
Ps. pancratii	CBS 137.94[ET]	GU253784	GU269759	GU320460	GU384470	—	Crous *et al.* (2013a)
Ps. paraexosporioides	MAFF237788[ET]	GU253746	GU269707	GU320411	GU384423	—	Crous *et al.* (2013a)
Ps. paranaensis	CPC 24680 = COAD 1987[T]	KT037563	KT037522	KT037604	KT037482	—	Guatimosim *et al.* (2016)
Ps. parapseudarthriae	CBS 137996 = CPC 23449[T]	KJ869208	KJ869151	KJ869229	KJ869238	—	Crous *et al.* (2014c), Guatimosim *et al.* (2016)
Ps. perae	CPC 25171 = COAD 1465[T]	KT290159	KT290132	KT313487	KT290186	—	Silva *et al.* (2016)
Ps. perrottetiae	CBS 147382[T]	—	LC599353	LC599433	LC599477	LC599614	Present study
Ps. photiniae	MUCC 1661[NT]	—	KX462604	KX462571	KX462690	KX462653	Nakashima *et al.* (2016)
Ps. pini-densiflorae	MUCC 1714[ET]	—	LC599354	LC599434	LC599478	LC599615	Crous *et al.* (2013a)
Ps. piperis	COAD 1111	JX875063	JX875062	—	JX896123	—	Rocha *et al*. (2013)
Ps. planaltinensis	CPC 25189 = COAD 1495[T]	KT290164	KT290137	KT313492	KT290191	—	Silva *et al.* (2016)
Ps. platyceriicola	MUCC2876[T]	—	LC599355	LC599435	LC599479	LC599616	Present study
Ps. plectranthi	CBS 131586 = CPC 11462[T]	JQ324962	GU269791	GU320492	GU384501	—	Crous *et al.* (2013a)
Ps. plumeriifolii	CPC 25191 = COAD 1498[ET]	KT290165	KT290138	KT313493	KT290192	—	Silva *et al.* (2016)
Ps. pothomorphes	CPC 25166 = COAD 1450[T]	KT290158	KT290131	KT313486	KT290185	—	Silva *et al.* (2016)
Ps. profusa	CBS 132306 = CPC 10055[ET]	GU253787	GU269762	GU320463	GU384473	—	Crous *et al.* (2013a)
Ps. proiphydis	BRIP 58545[T]	KM055434	KM055430	—	KM055437	—	Shivas *et al.* (2015)
Ps. proteae	CBS 131587 = CPC 15217[T]	GU253826	GU269808	GU320511	GU384519/ LC599480	LC599617	Crous *et al.* (2013a)
Ps. pruni-grayanae comb.nov.	MUCC 1715[ET]	—	LC599356	—	LC599481	LC599618	Present study
Ps. pseudomusae	CBS 147147[T]	—	MW063423	MW070772	MW071091	MW070919	Crous *et al.* (2020)
Ps. pseudomyrticola	CBS 145554 = CPC 35448[T]	MK876446	MK876405	MK876461	MK876499	MK876490	Crous *et al.* (2019a)
Ps. pseudostigminaplatani	CBS 131588 = CPC 11726[T]	JQ324963	GU269857	GU320560	GU384568	—	Crous *et al.* (2013a)
Ps. punctata	CBS 132116 = CPC 14734[ET]	GU253791	GU269765	GU320468	GU384477	MF951622	Crous *et al.* (2013a), Videira *et al*. (2017)
Ps. punicae	MAFF236998 = MUCC 1209	—	KX462606	KX462573	KX462692	KX462655	Nakashima *et al.* (2016)
Ps. pyracanthae	MAFF237140 = MUCC 1226[ET]	GU253792	GU269767	GU320470	GU384479/ LC599482	LC599619	Crous *et al.* (2013a)
Ps. pyracanthigena	CBS 131589 = CPC 10808[T]	—	GU269766	GU320469	GU384478	—	Crous *et al.* (2013a)
Ps. ravenalicola	CBS 122468[T]	GU253828	GU269810	GU320513	GU384521	—	Crous *et al.* (2013a)
Ps. rhabdothamni	CBS 114872[T]	JQ324964	GU269768	GU320471	GU384480	—	Crous *et al.* (2013a)
Ps. rhamnellae	CBS 131590 = CPC 12500[T]	GU253813	GU269795	GU320496	GU384505	—	Crous *et al.* (2013a)
Ps. rhapisicola	MAFF305042 = MUCC1484[T]	—	LC599357	LC599436	LC599483	LC599620	Present study
Ps. rhododendri-indici	CBS 131591 = CPC 10822[T]	JQ324965	GU269722	GU320426	—	—	Crous *et al.* (2013a)

Table 16. (Continued).

Species	Isolates[1]	GenBank accession numbers[2]					References
		LSU	ITS	*actA*	*tef1*	*rpb2*	
Ps. riachueli var. *horiana*	MUCC2141[ET]	—	LC599358	LC599437	LC599484	LC599621	Present study
Ps. richardsoniicola	CPC 25248 = COAD 1568[ET]	KT290181	KT290154	KT313509	KT290208	—	Silva *et al.* (2016)
Ps. rigidae	CPC 25175 = COAD 1472[ET]	KT290161	KT290134	KT313489	KT290188	—	Silva *et al.* (2016)
Ps. robusta	CBS 111175 = CPC 1269 = CMW 5151[T]	DQ204767	AY309597	DQ147617	DQ211683	KX462656	Crous *et al.* (2013a), Nakashima *et al.* 2016
Ps. rosae	MFLUCC 14-0408[T]	MG829063	MG828952	—	—	—	Wanasinghe *et al.* (2018b)
Ps. sambucigena	CBS 126000[ET]	GU253809	GU269788	GU320508	GU384498	—	Crous *et al.* (2013a)
Ps. sawadae	MAFF 239714		LC599359	LC599438	LC599485	LC599622	Present study
Ps. schizolobii	CBS 120029 = CPC 12962[T]	KF251826	KF251322	KF253628	KF253269	—	Guatimosim *et al.* (2016)
Ps. sennae-multijugae	CPC 25206 = COAD 1519[T]	KT290169	KT290142	KT313497	KT290196	—	Silva *et al.* (2016)
Ps. serpocaulonicola	CPC 25077 = COAD 1866[T]	KT037566	KT037525	KT037607	KT037485	—	Guatimosim *et al.* (2016)
Ps. solani-pseudocapsicicola	CPC 25229 = COAD 1974[T]	KT290175	KT290148	KT313503	KT290202	—	Silva *et al.* (2016)
Ps. sophoricola	CCTU 1037 = CBS 136020[T]	KP717027	KM452861	KM452838	KM452883	LC599486	Bakhshi *et al.* (2014)
Ps. sphaerulinae	CBS 112621[T]	GQ852652	KF901625	—	KF903215	—	Crous *et al.* (2009b), Quaedvlieg *et al.* (2014)
Ps. stemonicola	MUCC2874[T]	—	LC599360	LC599439	LC599487	—	Present study
Ps. stephanandrae	MAFF237799 = MUCC914[ET]	GU253831	GU269814	GU320516	GU384526	KX462658	Silva *et al.* (2016), Nakashima *et al.* (2016)
Ps. stranvaesiae	MAFF410090 = MUCC1417[T]	—	LC599361	LC599440	LC599488	LC599623	Present study
Ps. struthanthi	CPC 25199 = COAD 1512[ET]	KT290168	KT290141	KT313496	KT290195	—	Silva *et al.* (2016)
Ps. styracina	COAD 2369[T]	MH480643	MH397664	MH480641	MH480642	—	Crous *et al.* (2018a)
Ps. symploci	NCHUPP L1685 = CBS142471[ET]	—	LC599362	LC599441	LC599489	LC599624	Present study
Ps. tabernaemontanae	CPC 19198[ET]	—	LC599363	LC599442	—	LC599625	Present study
Ps. tereticornis	CBS 125214 = CPC 13299[T]	—	GQ852770	GU320499	GU384508	KX462659	Nakashima *et al.* (2016)
Ps. terengganuensis	MUCC2871[T]	—	LC599364	LC599443	LC599490	—	Present study
Ps. tinea	TUA40 = NCHUPP L1603[ET]	—	KX462608	KX462577	KX462696	KX462660	Nakashima *et al.* (2016)
Ps. togashiana	MAFF410006[T] (*Mycosphaerella togashiana*)	—	LC599365	LC599444	LC599491	LC599626	Present study
Ps. trichogena	CPC 24664 = COAD 1087[T]	KT037560	KT037519	KT037601	KT037479	—	Guatimosim *et al.* (2016)
Ps. trinidadensis	COAD 1756[ET]	KT290184	KT290157	—	KT290210	—	Present study
Ps. tumulosa	CBS 121158[T]	—	DQ530217	—	—	—	Crous *et al.* (2019d)
Ps. vassobiae	CPC 25251 = COAD 1572[T]	KT290182	KT290155	KT313510	—	—	Silva *et al.* (2016)
Ps. viburnigena	CBS 125998 = CPC 15249[ET]	GU253827	GU269809	GU384520	GU320512	—	Crous *et al.* (2013a)

Table 16. (Continued).

Species	Isolates[1]	GenBank accession numbers[2]					References
		LSU	ITS	*actA*	*tef1*	*rpb2*	
Ps. violamaculans	MUCC 1660^{NT}	—	KX462610	KX462579	KX462698	KX462662	Nakashima *et al.* (2016)
Ps. vitis	CBS 132012 = CPC 11595	GU214483	GU269829	GU320533	GU384541	KX462663	Crous *et al.* (2013a), Nakashima *et al.* (2016)
	MUCC2361	—	LC599366	LC599445	LC599492	LC599627	Present study
Ps. wulffiae	CPC 25232 = COAD 1976^{T}	KT290177	KT290150	KT313505	KT290204	—	Silva *et al.* (2016)
Ps. xanthocercidis	CBS 131593 = CPC 11665^{IsoT}	JQ324971	JQ324983	JQ325026	JQ325005	—	Crous *et al.* (2013a)
Ps. xenopunicae	CBS 147384^{T}	—	LC599367	LC599446	LC599493	LC599628	Present study
Ps. xenosyzygiicola	MAFF237986 = MUCC1481^{ET}	—	KX462611	KX462580	KX462699	KX462664	Nakashima *et al.* (2016)
Ps. xylopiae	CPC 25173 = COAD 1469^{T}	KT290160	KT290133	KT313488	KT290187	—	Silva *et al.* (2016)
Ps. yakushimensis	MAFF237025 = MUCC1214^{ET}		LC599368	LC599447	LC599494	LC599629	Present study
Ps. zambiae	CBS 136423 = CPC 22686^{T}	KF777228	KF777175	—	—	MF951630	Videira *et al.* (2017)
Ps. zelkovae	MAFF 238237 = MUCC872^{NT}	—	GU269835	GU320537	GU384547	KX462665	Nakashima *et al.* (2016)

[1] BCRC: Bioresource Collection and Research Center, Food Industry Research and Development Institute, Hsinchu, Taiwan; CBS: Westerdijk Fungal Biodiversity Institute, Utrecht, the Netherlands; CCTU: Culture Collection of Tabriz University, Tabriz, Iran; COAD: Coleção Octávio de Almeida Drumond,Universidade Federal de Viçosa, Brazil; CPC: Culture collection of Pedro Crous, housed at the Westerdijk Fungal Biodiversity Institute; MAFF: Genebank Project, NARO, Tsukuba, Ibaraki, Japan; MFLUCC: Mae Fah Luang University Culture Collection, Chiang Rai, Thailand; MUCC: Culture Collection, Laboratory of Plant Pathology, Mie University, Tsu, Mie Prefecture, Japan; NBRC: Biological Resource Center, National Institute of Technology and Evaluation, Chiba, Japan; NCHUPP: the herbarium, Department of National Chung Hsing University, Taichung, Taiwan.$^{T, ET, IsoT}$ and ^{NT} indicate ex-type, ex-epitype, ex-isotype and ex-neotype strains, respectively.

[2] ITS: internal transcribed spacers and intervening 5.8S nrDNA; LSU: partial 28S large subunit nrRNA gene; *actA*: partial actin gene; *tef1*: partial translation elongation factor 1-α gene; *rpb2*: partial RNA polymerase II second largest subunit gene.

Pseudocercospora abeliae (Katsuki) Nishij. *et al.*, Mycoscience 40: 269. 1999. Fig. 64A–C.
Basionym: *Cercospora abeliae* Katsuki, Ann. Phytopathol. Soc. Japan 20: 71. 1955.

Leaf spots amphigenous, angular to irregular, subcircular, blackish brown to dark brown, often greyish white at the centre, 2–5 mm. *Caespituli* amphigenous, visible as dark olivaceous grey masses composed of superficial hyphae and conidia. *Mycelium* internal. *Stromata* amphigenous, substomatal, epidermal, erumpent, 20–50 µm diam, pale olivaceous brown to pale brown. *Conidiophores* densely to loosely fasciculate, arising from the upper part of stromata, rarely branched from superficial hyphae, straight to sinuous-geniculate, subcylindrical, unbranched, 25–65 × 2–3.8 µm, 0–2-septate, pale olivaceous brown to pale brown, paler toward the apex, smooth. *Conidiogenous cells* integrated, terminal, proliferating sympodially, rounded at the apex, with unthickened loci, 2 µm diam. *Conidia* solitary, holoblastic, cylindrical to obclavate, 25–55 × 2.5–5 µm, 3–6-septate, hyaline, or pale olivaceous, smooth to rough, subacute to rounded at the apex, obconically truncated and unthickened at the base, not darkened, 2 µm diam (adapted from Nakashima *et al.* 1999).

Typus: **Japan,** Fukuoka, Fukuoka, on *Abelia chinensis* (*Caprifoliaceae*), 15 Sep. 1954, S. Katsuki (**holotype**, in the Katsuki collection, TNS-F); Toyama, Kureha, Family Park, 25 Sep. 1998, T. Kobayashi & E. Imaizumi (**epitype** designated here TSU-MUMH11438, MBT 10005049, dried culture, culture ex-epitype TSU-MUCC1674).

Additional materials examined: **Japan,** on *Abelia glandiflora*, Tochigi, Sano, 4 Sep. 1998, T. Kobayashi; Ibaraki, Oarai, on *Abelia glandiflora*, 24 Sep. 1979, T. Kobayashi, TFM: FPH-5007; Ibaraki, Inashiki, Kukisaki, FFPRI, on *Abelia glandiflora*, 15 Oct. 1981, T. Kobayashi, TFM: FPH-5472; Ibaraki, Tsukuba, Tsukuba Medical Plant Research Station, on *Abelia glandiflora*, 9 Oct. 1997, T. Kobayashi & C. Nakashima; Ibaraki, Iwai, on *Abelia glandiflora*, 10 Sep. 1998, T. & Y. Kobayashi; Chiba, Kisaradzu, Fukuda, on *Abelia glandiflora*, 20 Sep. 1974, T. Kobayashi, TFM: FPH-4243; Tokyo, Chofu, Jindaiji, on *Abelia glandiflora*, 25 Sep. 1974, T. Kobayashi, TFM: FPH-4346; Tokyo, Setagaya, Tokyo University of Agriculture, on *Abelia glandiflora*, 6 Oct. 1998, C. Nakashima; Shizuoka, Hamamtsu, Fruit Park, on *Abelia glandiflora*, 1 Nov. 1996, T. Kobayashi, C. Nakashima & T. Nishijima; Fukuoka, Yame, Kuroki, Fukuoka For. Exp. Stn., on *Abelia glandiflora*, 20 Sep. 1974, S. Ogawa, TFM: FPH-4191; on *Abelia tetrasepala*, Tokyo, Jindaiji, Jindai Bot. Park, 7 Nov. 1998, C. Nakashima & E. Imaizumi, TSU-MUMH CNS504.

Illustrations: Nakashima *et al.* (1999).

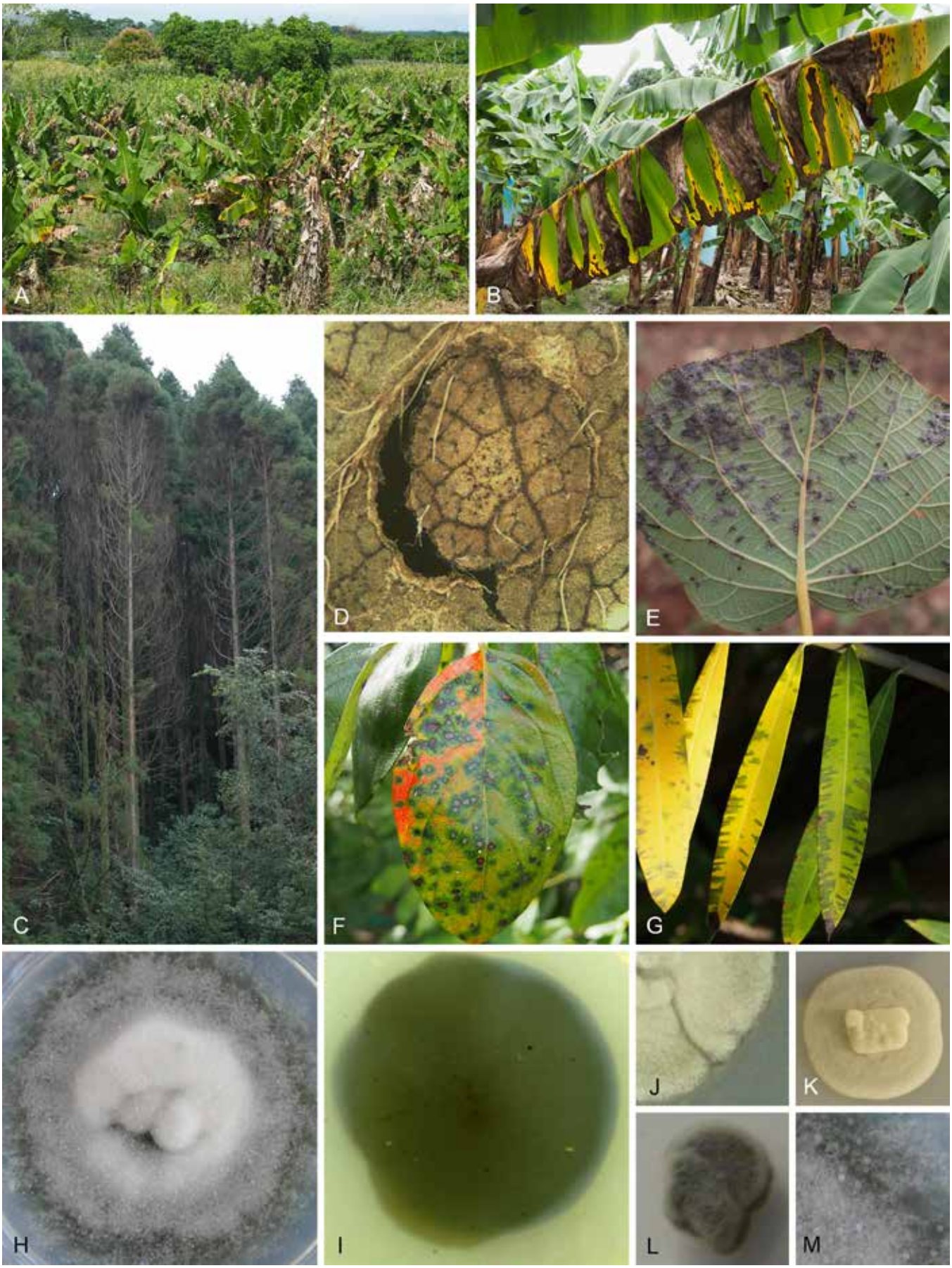

Fig. 63. Symptoms caused by *Pseudocercospora* spp. and cultural characteristics. **A, B.** Black Sigatoka disease of *Musa* spp. caused by *Pseudocercospora fijiensis*. **C.** Early defoliation of *Cryptomeria japonica* caused by *Pseudocercospora cryptomeriicola*. **D.** Shot hole of *Prunus* sp. caused by *Pseudocercospora prunicola*. **E.** Sooty spot of *Actinidia deliciosa* caused by *Pseudocercospora actinidiae*. **F.** Angular leaf spot of *Diospyros kaki* caused by *Pseudocercospora kaki*. **G.** Obscure leaf spot of *Nerium oleander* var. *indicum* caused by *Pseudocercospora kurimensis*. **H.** Upper surface of colony on MEA (*Pseudocercospora fuligena* TSU-MUCC460). **I.** Under surface of colony on MEA (*Pseudocercospora actinidiae* TSU-MUCC1454). **J–M.** Various colony morphologies on MEA. **J, K.** *Pseudocercospora actinidiae* (culture TSU-MUCC1454). **L.** *Pseudocercospora farfugii* (ex-type culture TSU-MUCC978). **M.** *Pseudocercospora fuligena* (culture TSU-MUCC460).

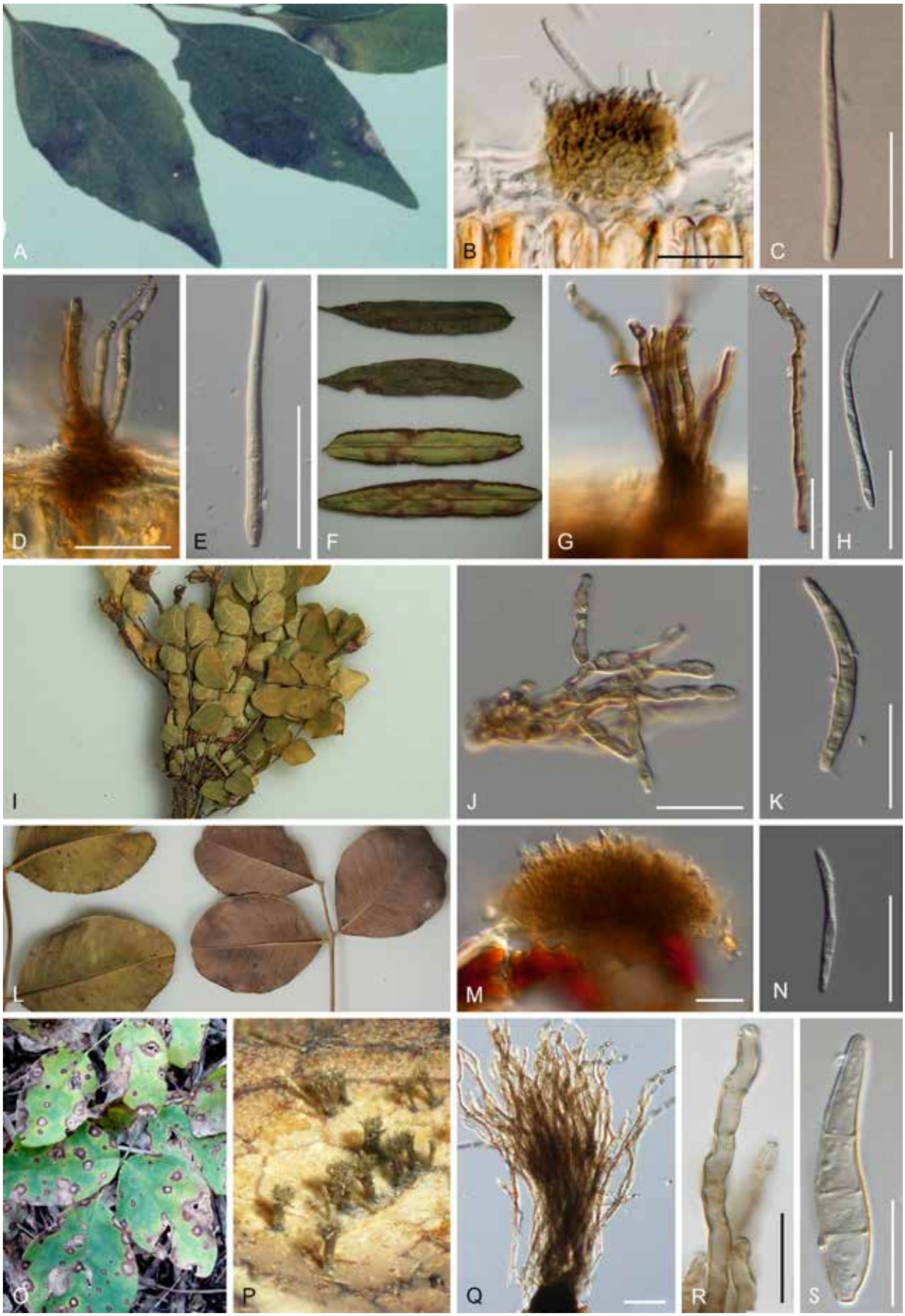

Fig. 64. *Pseudocercospora* spp. plate 1. **A–C.** *Pseudocercospora abeliae* (epitype TSU-MUMH11438). **A.** Disease symptoms on *Abelia grandiflora*. **B.** Stroma and conidiophores. **C.** Conidium. **D, E.** *Pseudocercospora aleuritis* (neotype TSU-MUMH1934). **D.** Stroma and conidiophores. **E.** Conidium. **F–H.** *Pseudocercospora angiopteridis* (epitype CBS H-24676). **F.** Disease symptoms on *Angiopteris evecta*. **G.** Stroma and conidiophores. **H.** Conidium. **I–K**. *Pseudocercospora biophyti* (epitype KRAM F-49038). **I.** Disease symptoms on *Biophytum petersianum*. **J.** Conidiophores. **K**. Conidium. **L–N.** *Pseudocercospora ceratoniae* (epitype CBS H-24677). **L.** Disease symptoms on *Ceratonia siliqua*. **M.** Stroma and conidiophores. **N.** Conidium. **O–S.** *Pseudocercospora cladrastidis* (epitype HHUF30085). **O.** Disease symptoms on *Cladrastis amurensis*. **P.** Synnematous conidiophores on the leaf spot. **Q.** Conidiophores. **R.** Conidiogenous cell on conidiophore. **S.** Conidium. Scale bars = 20 µm. Pictures O–S were taken from Sasaki *et al*. (2012).

Note: Holotype material was examined, and an epitype selected for further molecular phylogenetic studies.

Pseudocercospora aleuritis (I. Miyake) Deighton, Mycol. Pap. 140: 138. 1976. Fig. 64D, E.
Basionym: *Cercospora aleuritis* I. Miyake [as *'aleuritidis'*], Bot. Mag. (Tokyo) 26: 66. 1912.

Leaf spots amphigenous, circular to subcircular, blackish on upper leaf surface, yellowish brown at the centre with dark brown margin on hypophyllous leaf surface, 6–10 mm (*fide* Miyake 1912). *Caespituli* amphigenous. *Mycelium* internal, pale brown. *Stromata* amphigenous, mainly epiphyllous, substomatal, epidermal, erumpent, 38–65 µm diam, brown to dark brown, without superficial hyphae. *Conidiophores* densely to loosely fasciculate, emerging from the upper part of stromata, simple, rarely branched, straight to sinuous-geniculate, cylindrical, 20–65 × 2.5–3.8 µm, 0–4-septate, pale brown to brown, smooth. *Conidiogenous cells* integrated, terminal, proliferating sympodially or percurrently, with unthickened loci, 2.5 µm diam. *Conidia* solitary, holoblastic, cylindrical to obclavate, 25–76 × 3.8–5 µm, 0–3-septate, hyaline or pale brown, smooth to rough, thick-walled, subacute to rounded at the apex, obconically truncated and unthickened at the base, not darkened, 2.5 µm diam.

Typus: **Japan,** Okinawa, Okinawa Is., Kunigami, Yona Field centre, Univ. of Ryukyu, on *Aleurites montanus* (= *Vernicia montana*) (*Euphorbiaceae*), Nov. 1994, T. Kobayashi (**neotype** designated here TSU-MUMH1934, MBT 10005050, culture ex-neotype MAFF237174 = MUCC1230).

Additional materials examined: **Japan,** Nagasaki, Omura, on *Aleurites fordii* (= *Vernicia fordii*), 15 Oct. 1951, E. Kurosawa, MUMH-CNS362; Okayama, on *Aleurites cordatus,* 20 Nov. 1960, H. Tanaka, TFM: FPH-3243; Kobe, Hyogo, 21 Nov. 1960, S. Akai, TFM: FPH-3244.

Notes: The herbarium where the holotype specimen (on *Aleurites cordatus* = *V. montana*, China, Hynan, Pron. Sangteh, 12 Oct. 1908, I. Miyake.) has been deposited is unknown, and the specimen could not be located. A neotype was selected from Japanese specimens based on the similarity of the morphological description.

Pseudocercospora angiopteridis Goh & W.H. Hsieh, Trans. Mycol. Soc. Republ. China 4: 27. 1989. Fig. 64F–H.

Leaf spots amphigenous, water-soaked, with indefinite margin, pale brown with dark brown and indefinite border, 10–30 mm. *Caespituli* epiphyllous, visible as black and loose fascicles. *Mycelium* internal, brown to pale brown. *Stromata* small to well developed, epiphyllous, submerged, erumpent, 20–50 µm diam, dark brown. *Conidiophores* arising from upper part of stromata, straight at the basal part, sinuous-geniculate to geniculate at the upper part, subcylindrical, loosely fasciculate in 2–10, simple, 20–140 × 3.8–5 µm, 3–7-septate, brown, pale brown at the apex, smooth. *Conidiogenous cells* integrated, terminal and intercalary, proliferating sympodially or percurrently, conically truncated at the apex, with unthickened, sometimes rim-like, and slightly convexed conidial loci at shoulder or at the apex caused by sympodial proliferation, 2.5–3.5 µm. *Conidia* solitary, holoblastic, variable in shape, cylindrical to obclavate, acicular, 52–82 × 2–5 µm, 6–9-septate, hyaline, or very pale coloured, smooth to rough, straight to curved, rounded to subacute at the apex, long obconically truncated and unthickened at the base, not darkened, 2–3.5 µm diam.

Typus: **Taiwan Island**, Hwalien Hsieh, Taluke, on *Angiopteris lygodiifolia* (*Marattiaceae*), 1 Feb. 1985, T.K. Goh (**holotype** NCHUPP-148a; **isotype** K(M) IMI 312070). **Thailand,** on *Angiopteris evecta*, Chiang Mai, Chiang Mai Botanical Garden, 2 Nov. 2012, P.W. Crous (**epitype** designated here CBS H-24676, MBT 10005051, culture ex-epitype CBS 147385 = CPC 21666).

Notes: The epitype chosen from the specimens on the same host genus in Asia closely corresponds with the morphology of the holotype. The tabular key to *Pseudocercospora* species on ferns based on the morphology is provided in Braun *et al*. (2013). No DNA data are available from the holotype.

Pseudocercospora basitruncata Crous, Mycol. Mem. 21: 123. 1998.

Description and illustrations: Crous (1998).

Typus: **Colombia**, Astorga, Nemocon, Cundinamarca, on *Eucalyptus* sp. (*Myrtaceae*), 5 Jan. 1942, J. Orjuela-Navarrete (**holotype** BPI 436146; **isotypes** Herbario de Fitopatologia Dept. de Agric. Bogota 00990; BPI 436141, 436142, Herbario de Fitopatologia Dept. de Agric. Bogota 00993, 00999); on *Eucalyptus* sp., 11 Jan. 1972, E. Feliu, BPI 436195, 436196; on *Eucalyptus grandis*, Sinai, May 1995, M.J. Wingfield (**epitype** designated here PREM 54408, MBT 10005052, cultures ex-epitype CPC 1202–1204 = CBS 114664).

Notes: The epitype was chosen from specimens collected in Colombia, the type locality. It closely corresponds with the morphology of the holotype. No DNA data are available from the holotype.

Pseudocercospora biophyti (Syd. & P. Syd.) Deighton, Mycol. Pap. 140: 140. 1976. Fig. 64I–K.
Basionym: *Cercospora biophyti* Syd. & P. Syd., Philipp. J. Sci., C, Bot. 8: 284. 1913.

Leaf spots indistinct. *Caespituli* mainly hypophyllous, visible as dark olivaceous grey to brown mycelial mat composed of superficial hyphae and conidia, or as a sooty mold. *Mycelium* internal and external, developed at the leaf surface. *Stromata* lacking to small, hypophyllous, substomatal, epidermal, erumpent, up to 25 µm diam, pale brown to brown, with superficial hyphae. *Conidiophores* densely to loosely fasciculate, arising from the upper part of stromata or branched from superficial hyphae, straight to sinuous-geniculate, creeping on the surface of leaf, subcylindrical, branched, tangled, 10–80 × 2.5–5 µm, multi-septate, pale brown to brown, smooth to rough. *Conidiogenous cells* integrated, terminal, proliferating sympodially or percurrently, rounded at the apex, with unthickened or small rim-like loci, 1.5–2 µm. *Conidia* solitary, holoblastic, cylindrical to obclavate, 25–55 × 2.5–5 µm, 3–6-septate, hyaline or pale brown, smooth to rough, subacute to rounded at the apex, long obconically truncated and unthickened at the base, not darkened, 1.5–2 µm diam.

Typus: **Philippines**, Los Banos, on *Biophytum sensitivum* (*Oxalidaceae*), 7 Jan. 1913, H. Sydow (**isotype** CUP-039199).

Material examined: **Benin**, Collines, on *Biophytum petersianum*, 22 Oct. 2011, M. Piatek & N. Yourou (**reference strain** designated here KRAM F-49038, culture CPC 20020).

Notes: The type material of *Ps. biophyti* was collected from the Philippines and has not been examined in this study. The symptoms and morphology of the specimen from Benin were identical to that described for *Ps. biophyti*. In this study, we propose a reference strain to facilitate further studies.

Pseudocercospora boehmeriigena U. Braun, Trudy Bot. Inst. Komarova 20: 42. 1997.

Descriptions and ilustrations: Braun & Melnik (1997), Silva *et al.* (2016).

Typus: **USA,** New York, Saratoga, South Ballston, on *Boehmeria cylindrica*, Sep., C.H. Peck (**holotype** NYS f494). **Brazil**, Minas Gerais, Viçosa, Universidade Federal de Viçosa, on *Boehmeria nivea* (*Urticaceae*), 21 May 2013, R.W. Barreto (**epitype** designated here CBS H-22170, MBT 10005053, culture ex-epitype COAD 41562 = CPC 25243).

Notes: *Pseudocercospora boehmeriigena* was recently described by Braun & Melnik (1997). Although the species was treated by Silva *et al*. (2016), they did not designate an epitype. The host plant of this species, *Boehmeria cylindrica*, is widely distributed in North and South America. Based on the distribution of this fungus, and its morphology, we designate an epitype for the species.

Pseudocercospora ceratoniae (Pat. & Trab.) Deighton, Mycol. Pap. 140: 141. 1976. Fig. 64L–N.
Basionym: *Cercospora ceratoniae* Pat. & Trab., Bull. Soc. Mycol. France 19(3): 260. 1903.

Leaf spots amphigenous, scattered, angular to irregular, vein limited, 2–5 mm, greyish at the centre, blackish brown. *Caespituli* amphigenous. *Mycelium* internal and external, hyaline to pale brown. *Stromata* amphigenous, substomatal, epidermal, erumpent, well-developed, 22.5–97.5 µm diam, pale to dark brown, with superficial hyphae. *Conidiophores* well-developed, dense, arising from the upper part of stromata, short, straight to curved, subcylindrical, unbranched, rarely branched at the basal part, 12–20 × 2–3.8 µm, septate, pale brown to brown, paler towards the tip, smooth. *Conidiogenous cells* integrated, terminal, proliferating percurrently, conically truncated at the apex, with unthickened and truncated conidial loci, 1–1.5 µm. *Conidia* solitary, holoblastic, cylindrical to filamentous, obclavate, 12–60 × 2–2.5 µm, 1–6-septate, hyaline, straight to sinuous, smooth, acute at the apex, obconically truncated and unthickened at the base, not darkened, 1–1.5 µm wide.

Typus: **Algeria**, Algier, on *Ceratonia siliqua* (*Fabaceae*), 1901, Par N. Patouillard (**holotype** FH 7806). **Italy**, on *Ceratonia siliqua,* Nov. 2011, G. Polizzi (**epitype** designated here CBS H-24677, MBT 10005054, culture ex-epitype CPC 19998 = CBS 147386).

Notes: The epitype was selected from the same host based on the similarity of morphological characters to that of the holotype. The disease symptoms and morphological characters are similar to that observed on a specimen from Taiwan island (See Hsieh & Goh 1990).

Pseudocercospora cladrastidis (Jacz.) J.K. Bai & M.Y. Cheng, Acta Mycol. Sin. 11: 121, 1992. Fig. 64O–S.
Basionym: *Cercospora cladrastidis* Jacz., in Jaczewski *et al*., Fungi Ross. Exs. no. 350. 1899.

Leaf spots amphigenous, circular, scattered, pale brown to brown with reddish brown margin, 1–5 mm diam. *Caespituli* hypophyllous, synnematous with blackish brown conidiophores. *Mycelium* internal, hyaline to brown. *Stromata* hypophyllous, substomatal, epidermal, erumpent, well-developed, subglobose to globose, dark brown to blackish, 31–60 µm diam. *Conidiophores* well-developed, densely fasciculate, synnematous, or loosely fasciculate, arising from the upper part of stromata, straight at the base, sometimes curved, cylindrical, unbranched, geniculated at the upper part, 78–170(–450) × 1.6–5 µm, multi-septate, pale to dark brown, paler towards the tip, smooth to rough. *Conidiogenous cells* integrated, terminal, proliferating sympodially or percurrently, conically truncated at the apex, with unthickened and truncated conidial loci, 1–2 µm diam. *Conidia* solitary, holoblastic, obclavate, 24–49 × 2–7 µm, 4–5-septate, hyaline, or slightly pigmented, straight to curved, smooth, rounded at the apex, obconically truncated and unthickened at the base, not darkened, 1–2 µm diam.

Typus: **Japan**, Aomori, Nishimeya, Shirakami, on *Maackia amurensis* (*Fabaceae*), 28 Aug. 2010, K. Tanaka, K. Hirayama, & K. Honda (**epitype** designated here HHUF30085, MBT 10005056, culture ex-epitype TSU-MUCC1494). **Russia**, Amurskaja Oblast, Khabarovsk Kraj, Primoskij Kraj, 1895, on *Maackia amurensis* (**lectotype** LE40382).

Additional materials examined: **Japan**, Aomori, Nishimeya, Shirakami, on *Maackia amurensis*, 29 Aug. 2010, K. Tanaka & K. Honda, HHUF30086, culture TSU-MUCC1495; *ibid*., on *Maackia amurensis*, 17 Sep. 2010, K. Tanaka, A. Hashimoto & K. Honda, HHUF30087, culture TSU-MUCC1496; *ibid*., on *Maackia amurensis*, 8 Jul. 2014, C. Nakashima, K. Shibayama & K. Motohashi, TSU-MUMH11492, culture TSU-MUCC1722.

Notes: Braun & Melnik (1997) examined the lectotype (LE 40382) of the present species. In addition, some *exsiccatae* specimens have been deposited (BPI 976394, BPI 976395, and WIS-F-0012808). The epitype for further molecular studies was selected from Japanese materials based on the similarity of morphological characters to the lectotype description by Braun & Melnik (1997).

Pseudocercospora coprosmae U. Braun & C.F. Hill, Australas. Pl. Pathol. 32: 88. 2003.

Description and illustrations: Braun *et al.* (2003).

Typus: **New Zealand**, Auckland, Grey Lynn, Western Springs Park, on *Coprosma robusta* (*Rubiaceae*), 29 Apr. 2001, C.F. Hill 404 (**holotype** HAL 1731); Auckland, Grey Lynn, Western Springs Park, on *Coprosma robusta*, 21 Dec. 2003, C.F. Hill (**epitype** designated here PDD 89282, MBT 10005058, **iso-epitypes** U. Braun: Fungi selecti exsiccati 57 & Hill 957 in CBS H, culture ex-epitype ICMP 15279 = CBS 114639).

Notes: To fix the phylogenetic application of the name, an epitype was selected from topotypic material.

Pseudocercospora cratevicola C. Nakash. & U. Braun, IMA Fungus 4: 271. 2013. Fig. 65A, B.

Description: Braun *et al.* (2013).

Typus: **India**, Madras, Coimbatore, Government Farm, on *Crateva religiosa* (*Capparaceae*), 5 Feb. 1912, W. McRae (**holotype** S, F42112). **Japan**, Chiba, Tateyama, Fujiwara, on *Crateva religiosa*, 18 Sep. 1998, C. Nakashima & S. Uematsu (**epitype** designated here TSU-MUMH CNS462, MBT 10005059, culture ex-epitype TSU-MUCC1088).

Additional materials examined: **Japan**, Shizuoka, Ito, on *Crateva formosensis*, 29 Sep. 1999, T. Kobayashi & C. Nakashima (TSU-MUMH CNS797 and HAL 2597 F).

Notes: An epitype was selected for further molecular studies from the Japanese specimens on *C. religiosa*. Based on a morphological study of the type material, Japanese specimens on *Prathigada crataevae* were described as a new species (Braun *et al.* 2013).

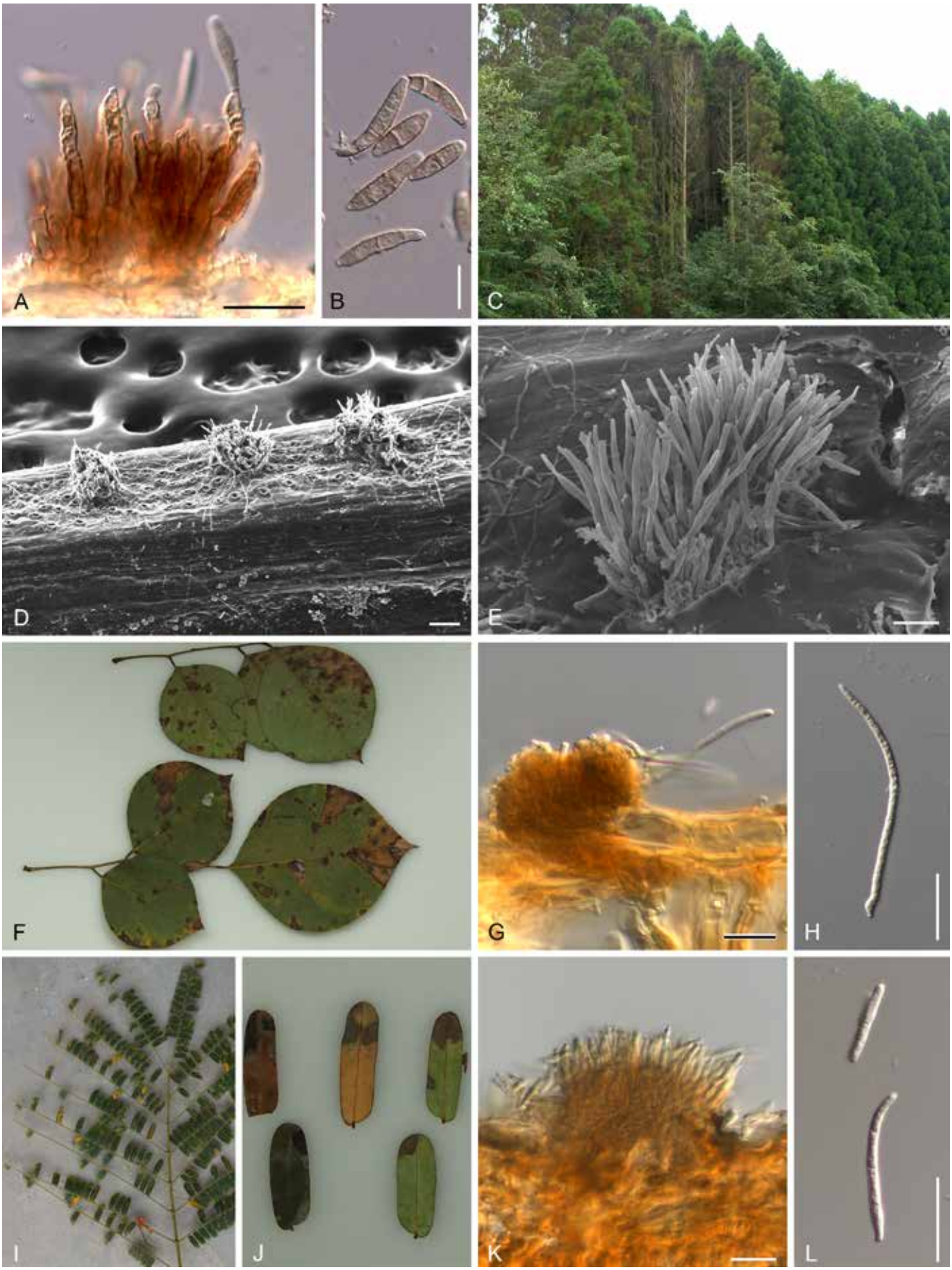

Fig. 65. *Pseudocercospora* spp. plate 2. **A, B.** *Pseudocercospora cratevicola* (epitype TSU-MUMH CNS462). **A.** Stroma and conidiophores on *Crateva formosensis*. **B.** Conidia. **C–E.** *Pseudocercospora cryptomeriicola* (epitype TFM: FPH-7851). **C.** Early defoliation of diseased leaves of *Cryptomeria japonica*. **D.** Caespituli on a leaf. **E.** Conidophores and conidia bearing from stroma. **F–H.** *Pseudocercospora dalbergiae* (epitype TSU-MUMH TUA55). **F.** Disease symptoms on *Dalbergia sissoo*. **G.** Stroma and conidiophores. **H.** Conidium. **I–L.** *Pseudocercospora delonicicola* (holotype UMT201901). **I.** Disease symptoms on *Delonix* sp. **J.** Magnified symptoms. **K.** Stroma and conidiophores. **L.** Conidia. Scale bars = 20 µm.

Pseudocercospora cryptomeriicola (Sawada) C. Nakash. *et al.*, Mycoscience 48: 254, 2007. Fig. 65C–E.
Basionym: *Cercospora cryptomeriicola* Sawada, Bull. Gov. Forest Exp. Sta. Meguro 45: 53. 1950.

Descriptions and illustrations: Nakashima *et al.* (2007), Braun *et al.* (2013).

Typus: **Japan**, Yamagata, Kamabuchi, on *Cryptomeria japonica* (*Cupressaceae*), 8 Aug. 1949, K. Sato (**holotype** IUM-FS 62); Kumamoto, Kikuchi, on *Cryptomeria japonica*, 7 Nov. 2005, C. Nakashima, K. Motohashi & T. Akashi (**epitype** designated here TFM: FPH-7851, MBT 10005060, culture ex-epitype MAFF 240073 = NBRC102150 = MUCC145).

Additional materials examined: **Japan**, Aichi, Shitara, Furiwake, on *Cr. japonica*, 16 Jun. 1954, I. Ando, TFM: FPH-1085; Kumamoto, Kikuchi, on *Cr. japonica*, 1 Jun. 2004, C. Nakashima, K. Motohashi & T. Akashi, TFM: FPH-7850, culture MAFF240072; Miyazaki, Shiiba, on *Cr. japonica*, 8 Jun. 2001, T. Sanui, culture TSU-MUCC170 = MAFF 238328 = MUCC1088.

Notes: *Pseudocercospora cryptomeriicola* is a pathogen of an endemic plant in Japan, *Cr. japonica*, and is only known from Japan. The epitype was selected based on the similarity of morphological characters to that of the holotype specimen on *Cr. japonica*.

Pseudocercospora cymbidiicola U. Braun & C.F. Hill, Mycol. Prog. 1: 23, 2002.

Description and illustrations: Braun & Hill (2002).

Typus: **New Zealand**, Auckland, Mt. Albert, on *Cymbidium* sp. (*Orchidaceae*), 24 Sep. 2000, C.F. Hill (**holotype** HAL 1585); Auckland, Mt. Albert, on *Cymbidium* sp., 25 Mar. 2004, C.F. Hill 1007 (**epitype** designated here PDD 81460, MBT 10005061, culture ex-epitype CBS 115132).

Note: The epitype was selected from topotypic material based on the similarity of morphological characters.

Pseudocercospora dalbergiae (S.H. Sun) J.M. Yen, Bull. Trimestriel Soc. Mycol. France 94: 386. 1979. Fig. 65F–H.
Basionym: *Cercospora dalbergiae* S.H. Sun, J. Agric. Forest., Taiwan 9: 43. 1955.

Leaf spots amphigenous, circular to irregular, scattered, dark brown with greyish brown centre, 1–10 mm diam, often enlarged and confluent. *Caespituli* amphigenous. *Mycelium* internal and external, hyaline, or pale brown. *Stromata* amphigenous, small to developed, substomatal, epidermal, erumpent, brown to pale brown, 24–55 µm diam. *Conidiophores* dense, arising from the upper part of stromata, or solitary, branched from superficial hyphae, straight or strongly geniculate, cylindrical, 5–25 × 2.5 µm, 0–2-septate, pale brown, smooth. *Conidiogenous cells* integrated, terminal, or intercalary, proliferating sympodially, conically truncated at the apex, with unthickened and truncated conidial loci, 1.5–2 µm. *Conidia* solitary, holoblastic, obclavate to filamentous, 28–80 × 1.5–2.5 µm, 3–6-septate, hyaline, straight to curved, smooth, rounded to subacute at the apex, truncated and unthickened at the base, not darkened, 1.5–2 µm diam.

Typus: **Taiwan Island**, Taichun, Taichun, on *Dalbergia sissoo* (*Fabaceae*), 17 Aug. 1955, S.H. Sun (**holotype** deposited in unknown fungarium); (line drawing, in Sun SH (1955) Studies on the genus *Cercospora* found in Taiwan (I). Journal of Agriculture and Forestry Taiwan 4: 141, fig. 3, **lectotype** designated here MBT 10005062); Taichun, Dakengdizhen Park, on *Dalbergia sissoo*, 9 Oct. 2014, C. Nakashima, K. Motohashi, Y. Hattori & C.Y. Chen (**epitype** designated here TSU-MUMH TUA55, MBT 10005063, culture ex-epitype TSU-MUCC TUA55).

Notes: The location of the type material is unknown. A lectotype was therefore selected from the protologue. An epitype was selected from a newly collected topotypic specimen to facilitate further molecular studies.

Pseudocercospora delonicicola C. Nakash., L. Suhaizan & I. Nurul Faziha, ***sp. nov.*** MycoBank MB 838198. Fig. 65I–L.

Etymology: Derived from the name of host plant, *Delonix*.

Diseased leaves are easily defoliating. *Leaf spots* amphigenous, angular to irregular, 1–10 mm diam, dark brown to blackish brown, with black border at upper surface, often surrounded yellowish halo, brown to dark brown at lower surface. *Caespituli* amphigenous, punctiform, scattered, visible as olivaceous brown masses. *Mycelium* internal. *Stromata* amphigenous, substomatal to epidermal, erumpent, well developed, 25–75 µm diam, pale brown to olivaceous brown, without superficial hyphae. *Conidiophores* dense, short, arising from the upper part of stromata, straight to geniculate-sinuous, subcylindrical, unbranched, 7.5–25 × 2–2.5 µm, 0–1-septate, pale brown to brown, paler towards the tip, smooth. *Conidiogenous cells* integrated, terminal, proliferating sympodially or percurrently, with unthickened conidial loci. *Conidia* solitary, irregular in shape, cylindrical to obclavate, 10–50 × 2–2.5 µm, 1–5-septate, hyaline, smooth, rounded at the apex, truncate and unthickened at the base, not darkened, 2–2.5 µm diam.

Typus: **Malaysia**, Terengganu, Universiti Malaysia Terengganu, on *Delonix* sp. (*Fabaceae*), 22 Jun. 2019, C. Nakashima & Y. Hattori (**holotype** UMT201901, isotype TSU-MUMH11874, culture ex-type TSU-MUCC2869).

Note: Present species differs from *Ps. delonicis* (on *Delonix regia*, Singapore) in having small stromata and well-developed superficial hyphae.

Pseudocercospora dodonaeae Boesew., Trans. Brit. Mycol. Soc. 77: 453, 1981.

Description and illustration: Crous & Braun (1996).

Typus: **New Zealand**, on *Dodonaea viscosa*, Auckland, H.J. Boesewinkel, Jul. 1978 (**holotype** PDD 41332); *ibid*., Grey Lynn, Western Springs Park, on *Dodonaea viscosa*, 2 Dec. 2003, C.F. Hill 826-B (**epitype** designated here PDD 93500, MBT 10005064, culture ex-epitype CBS 114647 = ICMP 15283).

Notes: Three cercosporoid species on *Dodonaea* plants, *Passalora dodonaeae, Pseudocercospora dodonaeae*, and *Ps. mitteriana*, were examined by Crous & Braun (1996). The epitype of *Ps. dodonaeae* was selected from topotypic material for further phylogenetic studies.

Pseudocercospora ebulicola (W. Yamam.) Deighton, Mycol. Pap. 140: 143. 1976. Fig. 66A–C.
Basionym: *Cercospora ebulicola* W. Yamam., Trans. Sapporo Nat. Hist. Soc. 13: 139. 1934.

Leaf spots amphigenous, indistinct, vein limited, 1–10 mm, dark brown to pale brown. *Caespituli* mainly hypophyllous, visible as sooty or pale olivaceous brown mycelial mat. *Mycelium* internal and external, superficial hyphae creeping at lower leaf surface, brown to

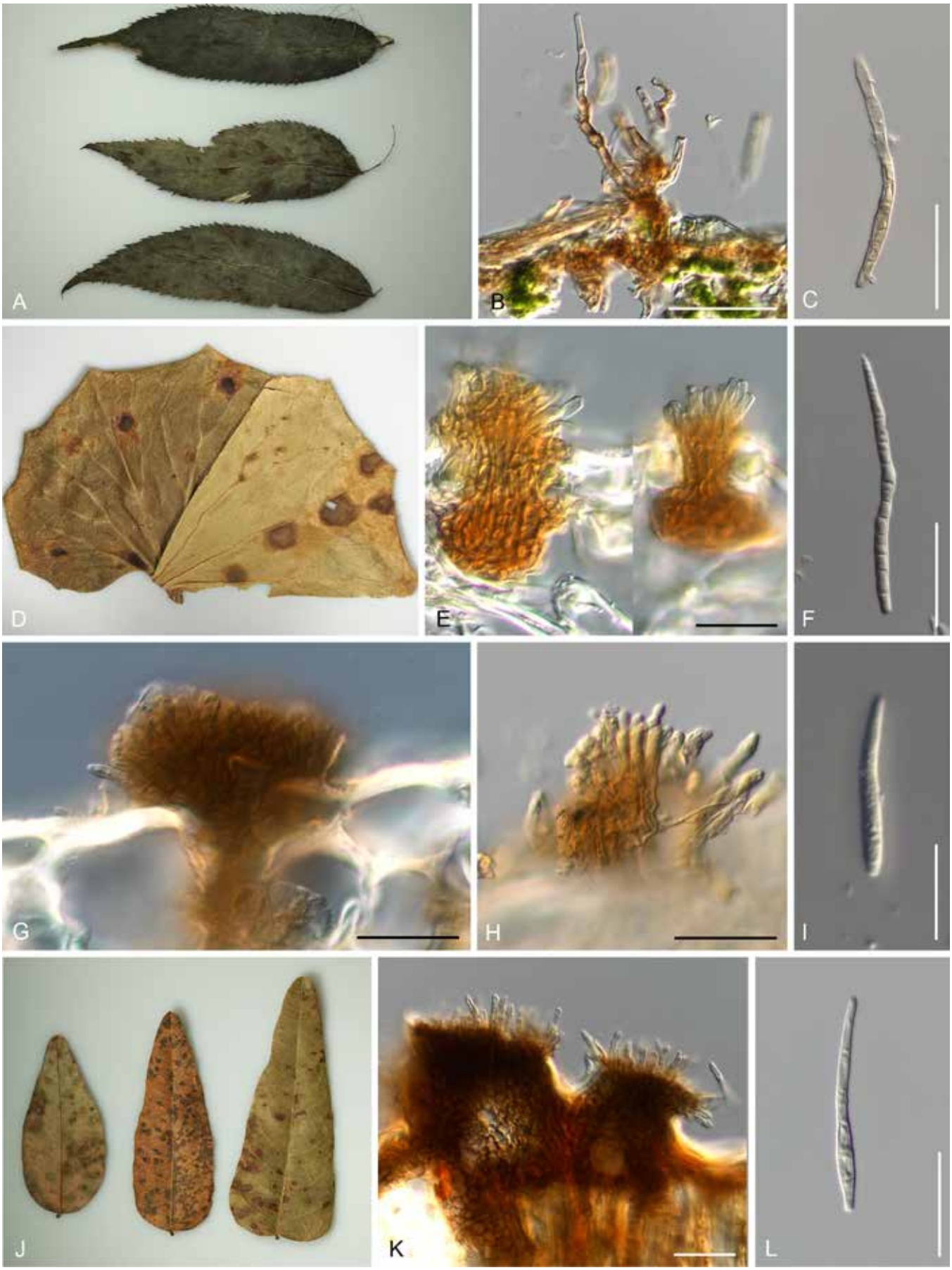

Fig. 66. *Pseudocercospora* spp. plate 3. **A–C.** *Pseudocercospora ebulicola* (epitype CBS H-24678). **A.** Disease symptoms on *Sambucus* sp. **B.** Stroma and conidiophores. **C.** Conidium. **D–F.** *Pseudocercospora farfugii* (holotype TSU-MUMH11202). **D.** Disease symptoms on *Farfugium japonicum*. **E.** Stromata and conidiophores. **F.** Conidium. **G–I.** *Pseudocercospora glochidionis* (epitype TSU-MUMH11940). **G, H.** Stroma and conidiophores. **I.** Conidium. **J–L.** *Pseudocercospora hardenbergiae* (holotype CBS H-24673). **J.** Disease symptoms on *Hardenbergia violacea*. **K.** Stroma and conidiophores. **L.** Conidium. Scale bars = 20 µm.

pale brown. *Stromata* lacking to developed, amphigenous, mainly hypophyllous, substomatal to epidermal, erumpent, globose, up to 47 µm diam, brown to dark brown, with superficial hyphae on lower leaf surface. *Conidiophores* loose to dense, emerging from the upper part of stromata, straight to sinuous, subcylindrical, simple or branched, irregular in width, 10–120 × 2–5 µm, multi-septate, hyaline to dark brown, irregular in width, smooth. *Conidiogenous cells* integrated, terminal or intercalary, proliferating sympodially, with unthickened and reflective conidial loci at shoulder caused by sympodial proliferation, 2–2.5 µm diam. *Conidia* solitary, variable in shape, acicular, cylindrical to obclavate, 38–100 × 2–5 µm, 3–8-septate, hyaline, or pale coloured, smooth, acute to rounded at the apex, obconically truncated and unthickened at the base, not darkened, 2–2.5 µm wide.

Typus: **Taiwan Island**, Sozan, on *Sambucus javanica* (*Adoxaceae*), 3 Dec. 1933, W. Yamamoto (**lectotype** CUP-039732, MBT 202795); on *Sambucus* sp., 18 Dec. 2011, P.W. Crous (**epitype** designated here CBS H-24678, MBT 10005065, culture ex-epitype CBS 147387 = CPC 20159).

Notes: *Pseudocercospora ebulicola* is a well-known species, and numerous collections are also maintained in Japanese fungaria. The epitype was selected from specimens collected on Taiwan Island based on the morphological similarity to that of the original description of lectotype, designated by Braun *et al*. (2015b).

Pseudocercospora euphorbiacearum U. Braun, Biblioth. Lichenol. 86: 89. 2003.

Description and illustration: Braun (2003).

Typus: **Dominican Republic**, Haina, on *Dalechampia scandens* (*Euphorbiaceae*), 26 Jan. 1926, R. Ciferri (**holotype** MA Ciferri 886[7669] B). **Brazil**, on *Dalechampia* sp., Minas Gerais, Viçosa, Reserva Floresta I Mata do Paraíso, 5 Aug. 2013, M. Silva (**epitype** designated here CBS H-22163, MBT 10005066, **iso-epitype** VIC 42797, culture ex-epitype COAD 1537 = CPC 25222).

Notes: The holotype material has not been examined. Silva *et al*. (2016) examined four *Pseudocercospora* species on *Euphorbiaceae* plants and indicated that species on different host genera clustered phylogenetically apart. The epitype was selected based on the similarity of morphological characters on the same host genus to that of the original description.

Pseudocercospora farfugii C. Nakash., I. Araki, & Ai Ito, ***sp. nov.*** MycoBank MB 838200. Fig. 66D–F.

Etymology: Derived from the name of host genus, *Farfugium*.

Leaf spots amphigenous, pale brown to dark brown on the upper leaf surface, pale brown to brown with dark brown border on the lower leaf surface, scattered, circular to orbicular, 10–20 mm diam, later enlarged, irregular. *Caespituli* amphigenous, scattered. *Mycelium* internal. *Stromata* amphigenous, small to developed, substomatal, epidermal, erumpent, subglobose, 20–70 µm diam, pale brown to brown. *Conidiophores* loose to densely fasciculate, arising from the upper part of stromata, straight to mildly geniculate, cylindrical, 10–30 × 2.5–3.8 µm, 0–1-septate, hyaline or pale brown, paler towards the apex, smooth. *Conidiogenous cell*s integrated, terminal, proliferating sympodially or percurrently, rounded or truncated at the apex, with unthickened conidial loci, 2.5–3 µm diam. *Conidia* solitary, holoblastic, cylindrical to acicular, 60–180 × 2.5–5 µm, 6–14-septate, hyaline, smooth, acute at the apex, truncate and unthickened at the base, 2.5–3 µm diam.

Typus: **Japan**, Mie, Tsu, Mie University, on *Farfugium japonicum* (*Asteraceae*), 28 Nov. 2008, I. Araki & A. Ito (**holotype** TSU-MUMH11202, culture ex-type TSU-MUCC978).

Additional material examined: **Japan**, Shizuoka, Kanzanji, on *Farfugium japonicum*, J. Nishikawa, TSU-MUMH11203, culture TSU-MUCC137.

Pseudocercospora formosana (W. Yamam.) Deighton, Mycol. Pap. 140: 144. 1976.
Basionym: *Cercospora formosana* W. Yamam., J. Soc. Trop. Agric., Formosa 6: 600. 1934.

Diseased leaves are easily defoliating. *Leaf spots* amphigenous, scattered, angular to irregular, vein limited, later enlarged, confluent, 1–3 mm diam, pale to dark brown. *Mycelium* internal and external. *Caespituli* amphigenous, mainly hypophyllous, visible as olivaceous brown masses composed of conidiophores and conidia. *Stromata* lacking or small, composed of a few brown cells, substomatal, erumpent, submerged. *Conidiophores* emerging from stromata, branched from creeping superficial hyphae, short, loose, straight to geniculate-sinuous, subcylindrical, 2–12.5 × 2–2.5 µm, 0–1-septate, pale brown to brown, paler towards the tip, smooth. *Conidiogenous cells* integrated, terminal or intercalary, proliferating sympodially, with unthickened conidial loci, 1.5–2 µm diam. *Conidia* solitary, holoblastic, cylindrical to obclavate, straight to curved, 30–40 × 2–2.5 µm, 2–4-septate, hyaline, smooth, acute at the apex, obconical truncate and unthickened at the base, not darkened, 1.5–2 µm diam.

Typus: **Japan**, Chiba, Tateyama, on *Lantana camara* (*Verbenaceae*), 4 Jun. 1997, C. Nakashima & S. Uematsu (**epitype** designated here TSU-MUMH11939, MBT 10005067, culture ex-epitype MAFF 238239). **Taiwan Island,** Taihoku, on *Lantana camara*, 20 Jan. 1934, W. Yamamoto (**lectotype** designated here NTU-PPE, hb. Sawada, MBT 10005893, **isotype** IMI 8570).

Additional materials examined: **Japan**, Okinawa, Kunigami, Onna, on *Lantana camara*, 17 Nov. 2007, C. Nakashima & T. Akashi, TSU-MUMH10957, culture TSU-MUCC855. **Malaysia**, Terengganu, Universiti Malaysia Terengganu, on *Lantana* sp., 22 Aug. 2018, C. Nakashima & Y. Hattori, culture TSU-MUCC2612.

Notes: Isotypes have been deposited in fungaria (IMI 8570 *fide* Crous & Braun 2003, and NTU-PPE). An isotype specimen preserved at NTU-PPT was selected as lectotype. Nishikawa *et al.* (2001) concluded that *Ps. formosana* was a synonym of *Ps. guianensis* on *Lantana* spp. based on the overlapping size of stromata and density of conidiophores on stromata. However, these morphological characters should be treated as distinguishing features for the two species. Furthermore, Crous *et al.* (2013a) showed that the Jamaican isolate of *Ps. guianensis* on *Lantana camara* (see *Ps. guianensis*) was located in a distinct clade from *Ps. formosana*. For Asian *Pseudocercospora* species on *Lantana* spp., *Ps. formosana* represents the most appropriate name.

Pseudocercospora fukuii (W. Yamam.) W.H. Hsieh & Goh, Trans. Mycol. Soc. Rep. China 2: 115. 1987.
Basionym: *Cercospora fukuii* W. Yamam. [as *'fukui'*], J. Soc. Trop. Agric., Formosa 6: 601. 1934.

Description and illustrations: Goh & Hsieh (1987).

Typus: **Japan**, Tokyo, Akiruno, Itsukaichi, on *Boehmeria nivea* var. *concolor*

f. nipononivea (*Urticaceae*), May 1999, E. Imaizumi (**epitype** designated here TSU-MUMH11938, MBT 10005068, culture ex-epitype MAFF 238121). **Taiwan Island**, Taipei, on *Boehameria cylindrica*, 20 Feb. 1934, W. Yamamoto (**lectotype** designated here CUP-039844, MBT 10005896, **isotype** IMI 8555).

Additional materials examined: **Japan**, Tokyo, Jindaiji, on *Boehmeria nivea* var. *concolor f. nipononivea,* 19 Jul. 1997, C. Nakashima, TSU-MUMH CNS200, culture MAFF238074; Okinawa, Okinawa Is, Nakijin, on *Boehmeria nivea* var. *concolor f. nipononivea,* 28 Mar. 2000, C. Nakashima, TSU-MUMH CNS902, culture MAFF238235.

Notes: The lectotype was selected from isotype materials preserved at fungaria. In addition, the epitype was selected from Japanese specimens. Morphological characters of the epitype were identical to the description and illustrations based on IMI 8555 in Goh & Hsieh (1987). Many fungarium specimens from Japan are maintained in TSU-MUMH and other fungaria.

Pseudocercospora glochidionis (Sawada) Goh & W.H. Hsieh, Trans. Mycol. Soc. Rep. China 2: 136. 1987. Fig. 66G–I.
Basionym: *Cercospora glochidionis* Sawada, Rept. Dept. Agric, Res. Inst. Taiwan 1: 670, 1919 [1920].
= *Gloeosporium glochidionis* Sawada, Trans. Nat. Hist, Soc. Formosa 24: 78, 1916.

Caespituli amphigenous. *Mycelium* internal or external, pale brown. *Stromata* small to well developed, amphigenous, mainly epiphyllous, substomatal, epidermal, erumpent, 20–110 µm diam, pale brown to brown. *Conidiophores* short, dense, emerging from the upper part of stromata, simple, straight to mildly sinuous, cylindrical, 17–25 × 2–2.5 µm, 0–4-septate, pale brown, smooth. *Conidiogenous cells* integrated, terminal, proliferating percurrently, conically truncated at the apex, with unthickened loci, 1–2 µm diam. *Conidia* solitary, holoblastic, obclavate, 32–55 × 2–2.5 µm, 0–4-septate, hyaline, smooth, subacute at the apex, obconically truncated and unthickened at the base, not darkened, 1.5–2 µm diam.

Typus: **Japan**, Kagoshima, Amami-Ohshima Is, Tatsugo, on *Glochidion zeylanicum* (*Phyllanthaceae*), 10 Nov. 1993, T. Kobayashi & M. Muramoto (**epitype** designated here TSU-MUMH11940, MBT 10005069, culture ex-epitype MAFF237000). **Taiwan Island**, Taipei, on *Glochidion hongkongense*, 19 Feb. 1916, K. Sawada (**lectotype** designated here NTU-PPE, hb. Sawada, MBT 10005838); *ibid*., 10 Mar. 1918 (**syntype**, NTU-PPE, hb. Sawada).

Notes: The lectotype material was selected from syntypes maintained at NTU-PPE, hb. Sawada. The specimen collected from Amami island, located in the same island arc, was selected as epitype based on the similarity of morphological characters to that of the original description.

Pseudocercospora hardenbergiae Crous & C. Nakash., ***sp. nov.*** MycoBank MB 838650. Fig. 66J–L.

Etymology: Derived from the name of host plant, *Hardenbergia*.

Leaf spots amphigenous, scattered, angular, vein limited, often enlarged and confluent, 1–3 mm diam, pale brown to brown. *Caespituli* amphigenous, visible as black conidial masses. *Mycelium* internal. *Stromata* amphigenous, small to well-developed, substomatal, epidermal, submerged, erumpent, dark blackish brown to pale brown, 22–150 µm diam. *Conidiophores* dense, arising from the upper part of stromata, straight to sinuous-geniculated, cylindrical, unbranched, pale brown to brown, paler towards the apex, 2.5–15 × 2–2.5 µm, 0–2-septate, smooth. *Conidiogenous cells* integrated, terminal, proliferating percurrently or sympodially, with unthickened and truncated conidial loci, 2 µm diam. *Conidia* solitary, holoblastic, cylindrical to obclavate, 25–68 × 2.5–3 µm, 1–7-septate, hyaline to pale coloured, smooth, acute at the apex, obconically truncated, unthickened and not darkened at the base, 2 µm diam.

Typus: **Australia**, Queensland, on *Hardenbergia violacea* (*Fabaceae*), 16 Jul. 2009, P.W. Crous (**holotype** CBS H-24673, culture ex-type CBS 147381 = CPC 17177).

Notes: *Pseudocercospora hardenbergiae* is proposed as a new taxon, occurring on *Hardenbergia violacea,* which is endemic to Australia, ranging from Queensland to Tasmania.

Pseudocercospora ixorana (J.M. Yen & Lim) U. Braun & Crous [as '*ixoriana*'], *Mycosphaerella* and its anamorphs: 1. Names published in *Cercospora* and *Passalora*: 230. 2003. Fig. 67A–C.
Basionym: *Cercospora ixorana* J.M. Yen & Lim [as *'ixoriana'*], Bull. Trimestiel Soc. Mycol. France 85(4): 471. 1969 (1970).

Leaf spots large, amphigenous, circular to subcircular, 8–10 mm diam, dark brown, greyish white at the centre, irregular at marginal area, dark brown upper, often enlarged, up to 30 mm diam. *Caespituli* hypophyllous, punctiform, scattered, visible as olivaceous brown masses composed of conidiophores and conidia. *Mycelium* internal and external. *Stromata* hypophyllous, small, composed of few brown cells or up to 30 µm diam, substomatal to epidermal, erumpent. *Conidiophores* densely fasciculate, arising from the upper part of stromata or solitary from superficial hyphae, straight to geniculate-sinuous, subcylindrical, 5–30 × 2–3 µm, 0–1-septate, dark brown to pale blackish, paler towards the tip, smooth. *Conidiogenous cells* integrated, terminal, proliferating sympodially, with unthickened conidial loci, 2–3 µm diam. *Conidia* solitary, holoblastic, obclavate, 40–50 × 2–3 µm, 3–4-septate, hyaline to pale brown, smooth, rounded at the apex, obconically truncate and unthickened at the base, 2 µm diam.

Typus: **Malaysia**, Terengganu, Universiti Malaysia Terengganu, on *Ixora chinensis* (*Rubiaceae*), 22 Aug. 2018, C. Nakashima & Y. Hattori (**epitype** designated here UMT201801KL, MBT 10005070, **iso-epitype** TSU-MUMH11942, cultures ex-epitype TSU-MUCC2608–2609). **Singapore**, on *Ixora chinensis*, 2 Aug. 1969, G. Lim (**holotype** PC).

Notes: The holotype material has not been examined. Symptoms and morphological characters of the epitype selected in this study are similar to that of the protologue. Although conidial length was slightly shorter than in the description (36–109 µm; Yen & Lim 1970), the line drawings (fig. 6; Yen & Lim 1970), depicted two classes of conidia, namely longer and shorter conidia. The shorter conidia are comparable to those observed in this study.

Pseudocercospora kenyirana C. Nakash., L. Suhaizan & I. Nurul Faziha, ***sp. nov.*** MycoBank MB 838201. Fig. 67D–F.

Etymology: Derived from the collection site in Malaysia.

Leaf spots amphigenous, scattered, angular to irregular, vein limited, enlarged and confluent, 2–10 mm diam, pale brown, surrounded by dark brown coloured vein. *Caespituli* amphigenous. *Mycelium* internal and external. *Stromata* amphigenous, well-developed on the upper leaf surface,

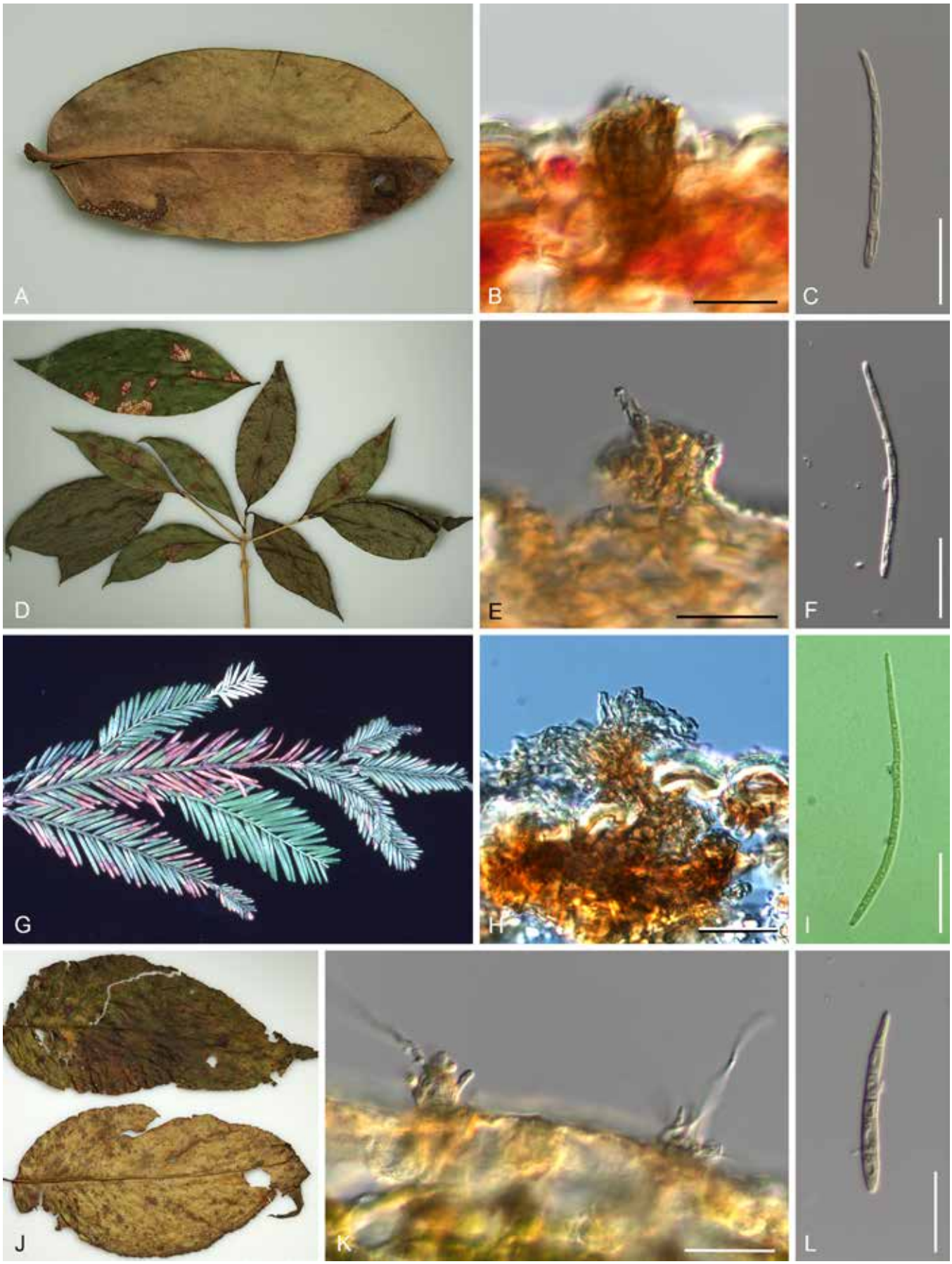

Fig. 67. *Pseudocercospora* spp. plate 4. **A–C.** *Pseudocercospora ixoriana* (epitype UMT201801KL). **A.** Disease symptoms on *Ixora chinensis*. **B.** Stroma and conidiophores. **C.** Conidium. **D–F.** *Pseudocercospora kenyirana* (holotype UMT201916KL). **D.** Disease symptoms on *Trigoniastrum* sp. **E.** Stroma and conidiophores. **F.** Conidium. **G–I.** *Pseudocercospora paraexosporioides* (epitype TSU-MUMH CNS448). **G.** Disease symptoms on *Sequoia sempervirens*. **H.** Stroma and conidiophores. **I.** Conidium. **J–L.** *Pseudocercospora perrottetiae* (holotype CBS H-24674). **J.** Disease symptoms on *Perrottetia arisanensis*. **K.** Stromata and conidiophores. **L.** Conidium. Scale bars = 20 µm.

epidermal, erumpent, subglobose, brown to dark brown, 25–30 µm diam, lacking or small on the lower leaf surface, brown, substomatal, up to 30 µm diam. *Conidiophores* short, arising from the upper part of stromata or branched from superficial hyphae, straight to slightly curved, cylindrical, unbranched, pale brown to brown, paler towards the apex, 2.5–15 × 2–2.5 µm, 0–1-septate, smooth. *Conidiogenous cells* integrated, terminal, proliferating percurrently, with unthickened and truncated conidial loci, 2–2.5 µm diam. *Conidia* solitary, holoblastic, cylindrical to obclavate, 35–55 × 2–2.5 µm, 1–8-septate, hyaline, smooth, acute at the apex, obconical truncate and unthickened, not darkened, at the base, 2–2.5 µm diam.

Typus: **Malaysia**, Terengganu, Hulu Terengganu, Kenyir Lake, on *Trigoniastrum* sp. (*Polygalaceae*), 23 Jun. 2019, C. Nakashima, Y. Hattori, L. Suhaizan & I. Nurul Faziha Faziha (**holotype** UMT201916KL, isotype TSU-MUMH11878, culture ex-type TSU-MUCC2873).

Note: No cercosporoid species are known from *Trigoniastrum*, which is an endemic plant to Malaysia and Indonesia.

Pseudocercospora liquidambaricola (J.M. Yen) U. Braun, Schlechtendalia 5: 44. 2000.
Basionym: *Cercospora liquidambaricola* J.M. Yen, Bull. Trimestiel Soc. Mycol. France 94(1): 54. 1978.

Descriptions and illustrations: Kobayashi *et al.* (2002), Braun *et al.* (2015b).

Typus: **Japan,** Okinawa, Ishigaki Island, Ishigaki, Maesato, on *Liquidambar formosana* (*Altingiaceae*), 18 Nov. 1988, T. Kobayashi & M. Tsurumachi (**epitype** designated here TFM: FPH-7026, MBT 10005071, culture ex-epitype MAFF 410455). **Taiwan Island**, Taichung, on *Liquidambar formosana*, 29 Oct. 1971, J.M. Yen (**holotype** PC Yen 71255); Taipei, on *Liquidambar formosana*, 14 Oct. 1928, K. Sawada (**neotype** NTU-PPE, hb. Sawada, *fide* Braun *et al.* 2015b).

Additional material examined: **Japan,** Okinawa, Ishigaki Island, Ishigaki, Maesato, on *Liquidambar formosana*, Nov. 1988, T. Kobayashi & M. Tsurumachi, TFM: FPH-7027.

Notes: Braun *et al.* (2015b) designated a neotype for this species because holotype material could not be traced in PC or UC. In this study, an epitype was selected to facilitate further molecular studies from the specimens collected in the same archipelago as the type locality.

Pseudocercospora metrosideri U. Braun, Fungal Diversity 8: 44. 2001.

Description and illustrations: Braun (2001a).

Typus: **New Zealand**, North Island, New Plymouth, on *Metrosideros parkinsonii* (*Myrtaceae*), 16 Dec. 1965, G.F. Laundon (**holotype** IMI 116995); Auckland, Blockhouse Bay, Boundary Road, on *Metrosideros excelsa*, 17 Oct. 2003 (**epitype** designated here HAL C.F. Hill 929, MBT 10005077, culture ex-epitype CBS 114294 = ICMP 15227).

Notes: The holotype material has not been examined. An epitype was selected based on the similarity of morphological characters to the original description and illustrations.

Pseudocercospora pancratii (Ellis & Everh.) U. Braun & R.F. Castañeda, Cryptog. Bot. 2: 294. 1991.

Basionym: *Cercospora pancratii* Ellis & Everh., J. Mycol. 3(2): 15. 1887.

Description and illustrations: Braun & Castaneda (1991), Braun *et al.* (2014).

Typus: **Cuba**, Guisa, Hranma, on *Hippeastrum equestre* (*Amarydillaceae*), 8 Nov. 1988, R.F. Castañeda (**epitype** designated here as metabolically inactive culture, CBS 137.94, MBT 10005078, culture ex-epitype CBS 137.94). **USA**, Louisiana, Plaquemines Parish, on *Pancratium coronarium*, 4 Jun. 1886, A.B. Langlois (**holotype** NY 00838178, **isotype** BPI 457098).

Notes: The holotype material has not been examined, and the epitype is based on similarity to published descriptions and illustrations. See also *Ps. terengganuensis.*

Pseudocercospora paraexosporioides C. Nakash. & U. Braun, IMA Fungus 4: 336. 2013. Fig. 67G–I.

Description: Braun *et al.* (2013).

Typus: **Japan**, Tokushima, on *Sequoia sempervirens* (*Cupressaceae*), 4 Sep. 1959, K. Ito (**holotype** TFM: FPH-551); *ibid*., Ibaraki, Tsukuba, 11 Sep. 1998, T. Kobayashi & C. Nakashima (**epitype** designated here TSU-MUMH CNS448, MBT 10005079, culture ex-epitype MAFF237788).

Additional material examined: **Japan**, Fukuoka, Tanushimaru, on *Sequoia sempervirens*, 20 Jun. 2000, T. Kobayashi & Y. Ono, TSU-MUCNS 970.

Notes: *Pseudocercospora paraexosporioides* was separated from *Ps. exosporioides* occurring in European countries. It differs from *Ps. paraexosporioides* in having much larger stromata, up to 300 µm diam, large sporodochial conidiomata, and much shorter, usually subcylindrical conidia with few septa (Braun *et al*. 2013). To facilitate further phylogenetic studies, an epitype was selected based on the similarity of morphological characters to that of the holotype specimen.

Pseudocercospora perrottetiae Crous, C. Nakash. & C.Y. Chen, ***sp. nov.*** MycoBank MB838651. Fig. 67J–L.

Etymology: Derived from the host plant, *Perrottetia.*

Leaf spots amphigenous, angular to irregular with distinct border, 5–10 mm, dark brown on the upper leaf surface, somewhat paler and indistinct on the lower surface, often confluent. *Caespituli* amphigenous, mainly hypogenous. *Mycelium* internal, pale brown, rarely external. *Stromata* hypogenous, small to developed, substomatal to intraepidermal, erumpent, subglobose, up to 32 µm diam. *Conidiophores* emerging from upper part of stromata, mildly sinuous, cylindrical, unbranched, smooth, 10–15 × 2.5–3 µm, 0–1-septate, hyaline to pale brown, paler towards the apex. *Conidiogenous cells* integrated, terminal, proliferating sympodially, rounded at the apex, with unthickened conidial loci, 2 µm diam. *Conidia* solitary, holoblastic, obclavate, straight to slightly curved, 32–50 × 2.5–3 µm, 3–4-septate, hyaline to pale olivaceous brown, smooth to rough, obconically truncated and unthickened at the base, 2 µm diam, subacute at the apex.

Typus: **Taiwan Island**, on *Perrottetia arisanensis* (*Streptaxidae*), 18 Dec. 2011, P.W. Crous (**holotype** CBS H-24674, cultures ex-type CBS 147382 = CPC 20074, CBS 147383 = CPC 20066).

Notes: No cercosporoid taxa are known from *Perrottetia*, and therefore the present collection is described as new.

Pseudocercospora pini-densiflorae (Hori & Nambu) Deighton, Trans. Brit. Mycol. Soc. 88: 390. 1987.
Basionym: *Cercospora pini-densiflorae* Hori & Nambu, J. Pl. Prot., Tokyo 4: 353. 1917.

Description and illustrations: Braun *et al.* (2013).

Typus: **Japan**, Kagoshima, Magome, on *Pinus densiflora* (*Pinaceae*), 20 Sep. 1915 (**holotype** not preserved); Kagoshima, Magome, on *Pinus densiflora*, 1 Oct. 1915, K. Hara (**neotype** NIAES C-511, MBT 176152, topotypic material of type); Aichi, Nagoya, Chikusa, Higashiyama Botanical Garden, on *Pinus strobus*, 1 Sep. 2012, K. Motohashi & S. Ukita (**epitype** designated here TSU-MUMH11935, MBT 10005080, culture ex-epitype TSU-MUCC1714).

Notes: The holotype specimen could not be traced and a neotype was selected from topotypic specimens (Braun *et al.* 2013). Although *Ps. pini-densiflora* is a plant quarantine targeted species in European countries and Japan, the ex-type isolate for reference has not been preserved. An epitype was designated based on the similarity of morphological characters to that of the protologue to facilitate molecular examination and further studies.

Pseudocercospora platyceriicola C. Nakash., Y. Hatt, L. Suhaizan & I. Nurul Faziha, ***sp. nov.*** MycoBank MB 838202. Fig. 68A–D.

Etymology: Derived from the host genus, *Platycerium* sp.

Leaf spots amphigenous, subcircular to fusiform, water soaked, indefinite border, 3–18 mm diam, brown to reddish brown, scattered, later enlarged and confluent. *Caespituli* hypophyllous, punctiform, scattered, visible as blackish conidial masses. *Mycelium* internal and external. *Stromata* lacking or small, substomatal to intraepidermal, composed of a few dark brown cells, 10–20 µm diam, with dark brown external hyphae. *Conidiophores* emerging loosely from small stromata or solitary from external hyphae, straight to distinctly geniculate, subcylindrical, irregular in width, unbranched, smooth to rough, 2.5–45 × 2.5–3 µm, 0–3-septate, hyaline to dark brown, paler towards the apex. *Conidiogenous cells* integrated, terminal, proliferating sympodially or percurrently, with unthickened conidial loci, 2–2.5 µm diam. *Conidia* solitary, cylindrical to obclavate, straight to slightly curved, 25–50 × 2–2.5 µm, 2–6-septate, hyaline to pale blackish brown, smooth to rough, obconically truncated and unthickened at the base, 2–2.5 µm diam, rounded or acute at the apex.

Typus: **Malaysia**, Terengganu, Hulu Terengganu, Kenyir Lake, on *Platycerium* sp. (*Polypodiaceae*), 23 Jun. 2019, C. Nakashima, Y. Hattori, L. Suhaizan & I. Nurul Faziha (**holotype** UMT201939KL, **isotype** TSU-MUMH11881, culture ex-type TSU-MUCC2876).

Notes: *Pseudocercospora platyceriicola* differs from *Cercospora platycerii* (also on *Platycerium*), as the latter has hyaline, acicular conidia.

Pseudocercospora profusa (Syd. & P. Syd.) Deighton, Trans. Brit. Mycol. Soc. 88: 388. 1987.
Basionym: *Cercospora profusa* Syd. & P. Syd., Ann. Mycol. 7(2): 175. 1909.

Description and illustrations: Shin & Kim (2001), Crous *et al.* (2013a).

Typus: **Japan,** Tosa, Hoki-ga-mine, on *Acalypha australis* (*Euphorbiaceae*), 17 Oct. 1908, T. Yoshinaga (**lectotype** designated here S, hb. Sydow F37710, MBT 100005719). **South Korea**, Seoul, on *Acalypha australis*, 17 Sep. 2003, H.D. Shin (**epitype** designated here CBS H-20882, MBT 10005081, cultures ex-epitype CPC 10713–10715).

Additional materials examined: **Japan,** Tosa, Hoki-ga-mine, on *Acalypha australis* (*Euphorbiaceae*), 17 Oct. 1908, T. Yoshinaga (syntype NIAES C-267). **South Korea**, Wonju, on *Acalypha australis*, 18 Oct. 2002, H.D. Shin, CBS H-20881, culture CPC 10055.

Notes: Many specimens of this taxon are preserved in Japanese fungaria, although they are not linked to cultures. To facilitate molecular phylogenetic studies, an epitype was selected from South Korean specimens based on the similarity of morphological characters to the original description.

Pseudocercospora pruni-grayanae (Sawada) C. Nakash. & Motohashi., ***comb. nov.*** MycoBank MB 838210. Fig. 61AB, AC, 68E–H.
Basionym: *Phaeoisariopsis pruni-grayanae* Sawada, Bull. Gov. Forest Exp. Sta. Meguro 105: 113. 1958.

Leaf spots amphigenous, scattered, angular to irregular, enlarged and confluent, 3–8 mm, dark brown to brown. *Caespituli* amphigenous, mainly hypophyllous, scattered, visible as synnematous fascicles. *Mycelium* internal, pale brown. *Stromata* amphigenous, mainly hypophyllous, small, epidermal, erumpent, substomatal, brown to dark brown, 20–25 µm diam. *Conidiophores* densely fasciculate, synnematous to divergent, arising from the upper part of stromata, straight, divergent or geniculate at the upper part, cylindrical, unbranched, blackish brown to olivaceous brown, paler towards the apex, 50–120 × 3.5–5 µm, 1–4-septate, smooth to rough. *Conidiogenous cells* integrated, terminal, proliferating sympodially, with unthickened or rim-like and refractive loci, 2.5–3.8 µm diam. *Conidia* solitary, holoblastic, obclavate, 30–65 × 5–7.5 µm, 3–5-septate, hyaline, or pale brown at central part, smooth to rough, rounded to subacute at the apex, obconical truncate and unthickened or rim-like, not darkened, at the base, 2.5–3.5 µm diam.

Typus: **Japan**, Iwate, Morioka, Sakurayama, on *Padus grayana* (*Rosaceae*), 7 Sep. 1947, K. Sawada (**lectotype** designated here IUM-FS424, MBT 10005840); *ibid*., Koma, on *Padus grayana*, 27 Aug. 1948, K. Sawada (**syntype** IUM-FS425); *ibid*., 10 Sep. 2013, C. Nakashima & K. Motohashi (**epitype** designated here TSU-MUMH 11475, MBT 10005082, culture ex-epitype TSU-MUCC1715).

Notes: The lectotype specimen designated here is maintained in the IUM fungarium. The topotypic material with similar morphological characters, characterised by synnematous conidiophores and beak-like basal ends of conidia was selected as epitype for further molecular phylogenetic studies.

Pseudocercospora punctata (Wakef.) B. Sutton, Mycol. Res. 97: 125. 1993.
Basionym: *Septogloeum punctatum* Wakef., Bull. Misc. Inf., Kew: 204. 1931.

Description and illustrations: Crous (1999).

Typus: **South Africa**, Kwazulu-Natal Province, Durban, P.A. van der Bijl 323, on *Eugenia cordata* (= *Syzygium cordatum*) (*Myrtaceae*), 1922 (**holotype** in K, IMI 352712); Limpopo Province, Gundani, on living leaves of *Syzygium cordatum* 18 Dec. 2015, J. Roux (**epitype** designated here, CBS H-24919, MBT 10005841, culture ex-epitype CPC 39344).

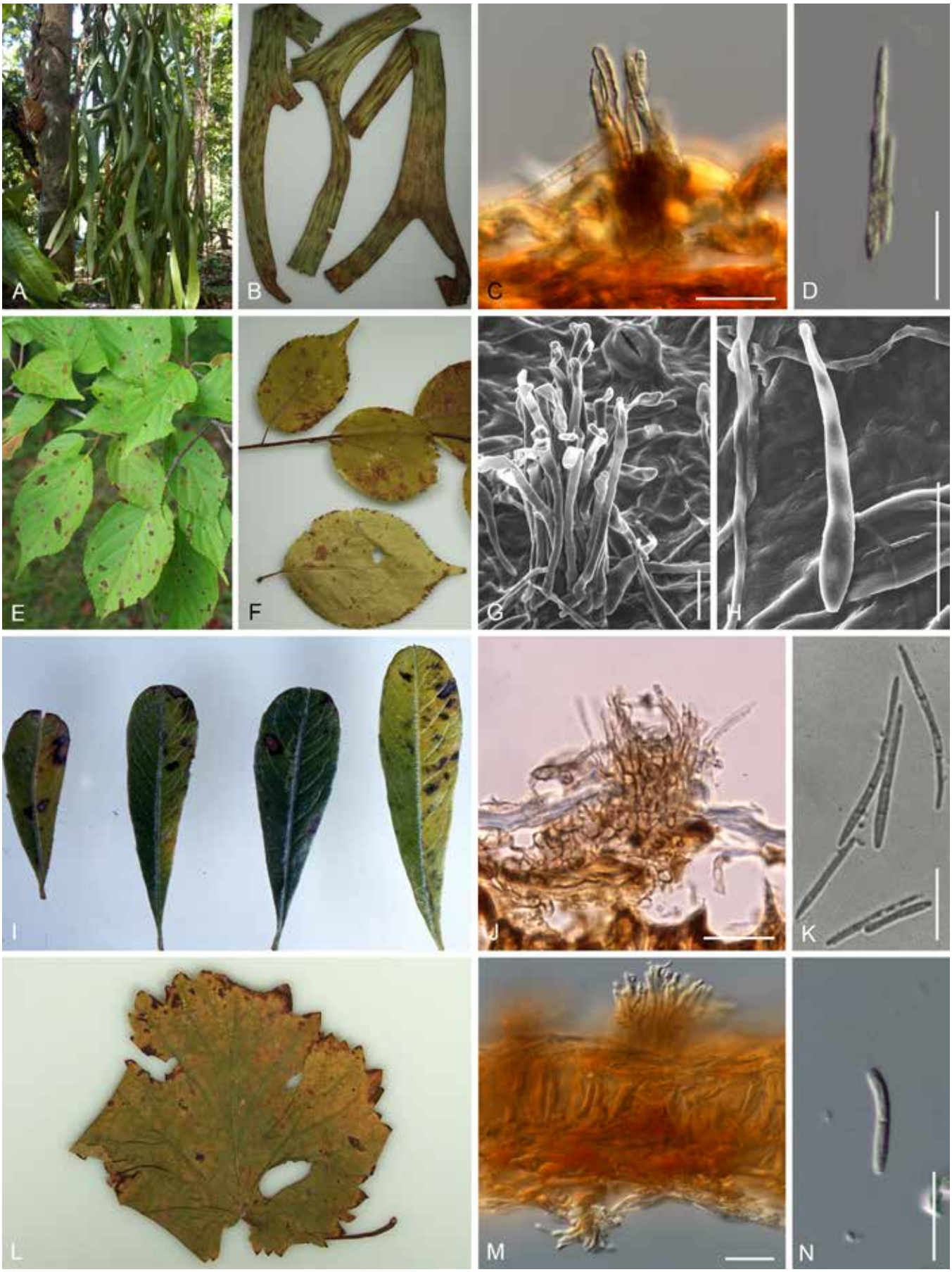

Fig. 68. *Pseudocercospora* spp. plate 5. **A–D.** *Pseudocercospora platyceriicola* (holotype UMT201939KL). **A.** Disease symptoms on *Platycerium* sp. **B.** Magnified symptoms. **C.** Stroma and conidiophores. **D.** Conidium. **E–H.** *Pseudocercospora pruni-grayanae* (epitype TSU-MUMH 11475). **E.** Disease symptoms on *Padus grayana*. **F.** Magnified symptoms. **G.** Conidiophores. **H.** Conidium. **I–K.** *Pseudocercospora pyracanthae* (epitype TSU-MUMH11941). **I.** Disease symptoms on *Pyracantha angustifolia*. **J.** Stroma and conidiophores. **K.** Conidia. **L–N.** *Pseudocercospora riachueli* var. *horiana* (epitype TSU-MUMH11544). **L.** Disease symptoms on *Vitis* sp. **M.** Stromata and conidiophores. **N.** Conidium. Scale bars = 20 µm.

Additional materials examined: **Madagascar**, on *Syzygium* sp., 25 Oct. 2007, P.W. Crous, cultures CPC 14734 = CBS 132116, CPC 14737, CPC 14740. **South Africa** near Mozambique border, *Syzygium cordatum*, 19 Oct. 2020, M.J. Wingfield, HPC 3498, culture CPC 40081; Kwazulu-Natal Province, on *Syzygium cordatum*, M.J. Wingfield, culture CBS 113315.

Note: The epitype was selected based on the similarity of morphological characters to those of the holotype specimen (Crous 1999). *Pseudocercospora punctata* is a common foliar pathogen on leaves of *Syzygium cordatum* in South Africa.

Pseudocercospora pyracanthae (Katsuki) C. Nakash. & Tak. Kobay., Ann. Phytopathol. Soc. Japan 63: 313, 1997. Fig. 68I–K.
Basionym: *Cercospora pyracanthae* Katsuki [as *'pyrecanthae'*], Bull. Agric. Impr. Sect. Econ. Dept. Fukuoka Prefecture Japan 1: 19. 1949.

Description: Nakashima & Kobayashi (1997).

Typus: **Japan**, Fukuoka, Kurume, on *Pyracantha angustifolia* (*Rosaceae*), 6 Nov. 1947, S. Katsuki (**holotype** TNS-F-243829); Ibaraki, Tsukuba, Nov. 1994, T. Nishijima (**epitype** designated here TSU-MUMH11941, MBT 10005083, culture ex-epitype MAFF 237140).

Additional materials examined: **Japan**, Chiba, Sanmu, Oct., on *Pyracantha angustifolia*, 1976, E. Ishizawa, TFM: FPH-4432; Okayama, Okayama, on *Pyracantha angustifolia*, 20 Nov. 1960, H. Tanaka, TFM: FPH-3247; Ibaraki, Tsukuba, on *Pyracantha angustifolia*, 15 Apr. 1995, T. Koboyashi & C. Nakashima, TSU-MUMH CNS446, culture TSU-MUCC892; Kumamoto, on *Pyracantha crenulata*, 1973, T. Kobayashi, culture MAFF 410022.

Notes: Many specimens of *P*s. *pyracanthae* are maintained in fungaria in Japan. The epitype was selected based on the similarity of morphological characters to that of the examined holotype specimen.

Pseudocercospora riachueli* var. *horiana (Togashi & Katsuki) U. Braun & Crous, *Mycosphaerella* and its anamorphs: 1. Names published in *Cercospora* and *Passalora*: 354. 2003. Fig. 68L–N.
Basionym: *Cercospora horiana* Togashi & Katsuki, Sci. Rep. Yokohama Natl. Univ., Sect. 2 1: 4. 1952.

Caespituli amphigenous. *Mycelium* internal, pale brown. *Stromata* small to developed, amphigenous, substomatal, epidermal, erumpent, 15–43 µm diam, brown, without superficial hyphae. *Conidiophores* dense, emerging from the upper part of stromata, simple, straight, cylindrical, short, 10–28 × 2–2.5 µm, 0–1-septate, pale brown, paler towards apex, smooth. *Conidiogenous cells* integrated, terminal, proliferating percurrently, rounded at the apex, with unthickened loci, 2 µm diam. *Conidia* solitary, holoblastic, cylindrical to obclavate, 22–30 × 2.5 µm, 0–2-septate, hyaline or pale brown, smooth, subacute to rounded at the apex, truncated and unthickened at the base, not darkened, 2 µm diam.

Typus: **Japan**, Tokyo, Minamitama, Nanao, on *Parthenocissus tricuspidata* (*Vitaceae*), 7 Oct. 1951, E. Kurosawa (**holotype** TNS-F 243957); Mie, Tsu, on *Vitis* sp., 27 Aug. 2016, C. Nakashima (**epitype** designated here TSU-MUMH11544, MBT 10005084, culture ex-epitype MUCC2141).

Notes: Although the host plant of the holotype is *Parthenocissus tricuspidata* (*Vitaceae*), the morphological characters of the specimen on *Vitis*, the host plant of the epitype designated in this study, are identical.

Pseudocercospora stemonicola C. Nakash., Y. Hatt., L. Suhaizan & I. Nurul Faziha, ***sp. nov.*** MycoBank MB 838203. Fig. 69A–C.

Etymology: Derived from the host genus, *Stemona.*

Leaf spots amphigenous, angular, vein limited, distinct, greyish brown to brown, surrounded by blackish brown border, later enlarged and confluent, 3–15 mm diam, often holed. *Caespituli* amphigenous. *Mycelium* internal. *Stromata* epidermal, substomatal, erumpent, subglobose, 25–73 µm diam. *Conidiophores* emerging from upper part of stromata, unbranched, straight to sinuous-geniculate, cylindrical, irregular in width, unbranched, smooth to rough, conically truncated at the apex, 12–40 × 2.5–5 µm, 0–2-septate, blackish brown, paler towards the apex. *Conidiogenous cells* integrated, terminal, terminal, proliferating sympodially or percurrently, with unthickened conidial loci, 2 µm diam. *Conidia* solitary, holoblastic, acicular, cylindrical, or obclavate, straight to curved, subhyaline, smooth to rough, 20–75 × 2–2.5 µm, 1–6-septate, obconically truncated and unthickened at the base, 2–2.5 µm diam, acute at the apex.

Typus: **Malaysia**, Terengganu, Hulu Terengganu, Kenyir Lake, on *Stemona tuberosa* (*Stemonaceae*), 23 Jun. 2019, C. Nakashima, Y. Hattori, L. Suhaizan & I. Nurul Faziha (**holotype** UMT201923KL, **isotype** TSU-MUMH11879, culture ex-type MUCC2874).

Notes: *Pseudocercospora stemonae*, which also occurs on this host (Braun 2001b), is distinct in having larger and olivaceous brown conidia (60–150 × 3–3.5 µm, 5–14-septate).

Pseudocercospora symploci Katsuki & Tak. Kobay. ex U. Braun & Crous, *Mycosphaerella* and its anamorphs: 1. Names published in *Cercospora* and *Passalora*: 394. 2003. Fig. 69D, E.

Leaf spots subcircular to irregular, 5–20 mm diam, on the upper leaf surface, at first a purplish brown speck, later frequently extending to the edge of the leaf, becoming tan to dark brown with a purplish margin, on the hypophyllous surface greyish brown (*fide* Katsuki & Kobayashi 1975). *Caespituli* amphigenous. *Mycelium* internal. *Stromata* amphigenous, small to well-developed, epidermal, erumpent, brown to pale brown, 20–75 µm diam. *Conidiophores* short, dense, arising from the upper part of stromata, straight to mildly geniculate, cylindrical, unbranched, hyaline or pale brown, paler towards the apex, 5–15 × 2–2.5 µm, 0–1-septate, smooth. *Conidiogenous cells* integrated, terminal, proliferating sympodially or percurrently, with unthickened and truncated conidial loci at the apex, 2–2.5 µm diam. *Conidia* solitary, holoblastic, long obclavate to acicular, 38–70 × 2.5–3 µm, 4–8-septate, hyaline, or pale olivaceous brown, smooth to rough, subacute at the apex, truncate and unthickened at the base, 2–2.5 µm diam.

Typus: **Taiwan Island**, Hsinchu, on *Symplocos crataegoides* var. *chinensis* (*Symplocaceae*), 27 Apr. 1930, K. Sawada (**lectotype** designated here NTU-PPE, hb. Sawada, MBT 10005897, **isotype** TNS-F220525); Taichung, Chisuim, on *Symplocos crategoides* var. *chinensis*, 25 Jul. 1931, K. Sawada (**syntype**); Taichung City, Heping Dist., Mt. Dashueshan, on *Symplocos paniculata,* 9 Oct. 2014, C. Nakashima, K. Motohashi, Y. Hattori & C.Y. Chen (**epitype** designated here NCHUPP 3352, MBT 10005085, culture ex-epitype NCHUPP L1685 = CBS 142471).

Notes: In this study, a lectotype was selected from syntype specimens. The morphological characteristics of the isotype (TNS-F220525) were examined. The chosen epitype specimen (NCHUPP 3352) is morphologically similar to the isotype.

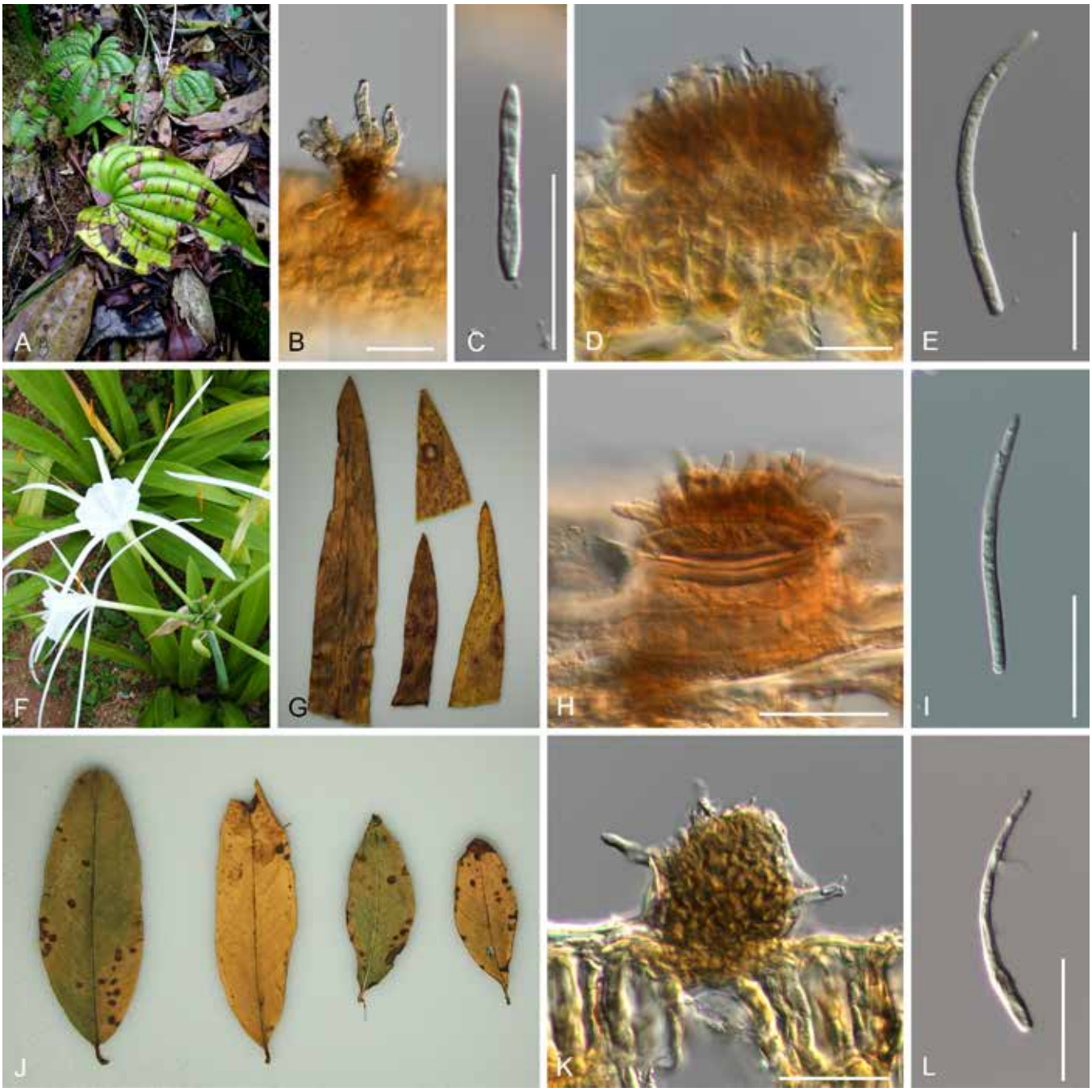

Fig. 69. *Pseudocercospora* spp. plate 6. **A–C.** *Pseudocercospora stemonicola* (holotype UMT201923KL). **A.** Disease symptoms on *Stemona tuberosa*. **B.** Stroma and conidiophores. **C.** Conidium. **D, E.** *Pseudocercospora symploci* (epitype NCHUPP3352). **D.** Stroma and conidiophores on *Symplocos paniculata*. **E.** Conidium. **F–I.** *Pseudocercospora terengganuensis* (holoype UMT201909). **F, G.** Disease symptoms on *Hymenocallis speciosa*. **H.** Stroma and conidiophores. **I.** Conidium. **J–L.** *Pseudocercospora xenopunicae* (holotype CBS H-24675). **J.** Disease symptoms on *Punica granatum*. **K.** Stroma and conidiophores. **L.** Conidium. Scale bars = 20 µm.

Pseudocercospora tabernaemontanae (Syd. & P. Syd.) Deighton, Mycol. Pap. 140: 154. 1976.
Basionym: *Cercospora tabernaemontanae* Syd. & P. Syd., Philipp. J. Sci., C, 8(5): 507. 1913.

Description and illustrations: Hsieh & Goh (1990).

Typus: **Laos**, Vientiane Capital, Xaythany District, Xay Village, on *Tabernaemontana coronaria* (*Apocynaceae*), 25 Jul. 2006, P. Phengsintham (**epitype** designated here HAL P107, MBT 10005086, culture ex-epitype CPC 19198). **Philippines**, Los Banos, P.I., on *Tabernaemontana pandacaqui*, 20 Apr. 1913, M.B. Raimundo (**holotype** S F37811).

Notes: The holotype material has not been examined, but the present collection from Laos is a good fit for the species (Phengsintham *et al.* 2010).

Pseudocercospora terengganuensis C. Nakash., Y. Hatt., L. Suhaizan & I. Nurul Faziha, ***sp. nov.*** MycoBank MB 838267. Fig. 69F–I.

Etymology: Derived from the collection site in Malaysia.

Leaf spots amphigenous, cirucular to subcircular, 3–10 mm diam, brown, reddish brown at centre, blackish brown, with definite border. *Caespituli* amphigenous, punctiform, scattered. *Mycelium* internal

and external; internal hyphae hyaline to pale brown, external hyphae brown to reddish brown. *Stromata* amphigenous, substomatal to epidermal, erumpent, 35–50 µm diam, brown to reddish brown, with superficial hyphae. *Conidiophores* dense, emerging from upper part of stromata, or solitary from superficial hyphae, short, straight to geniculate-sinuous, cylindrical, unbranched, 2.5–30 × 2.5–3 µm, 0–1-septate, pale brown, paler towards the apex, smooth. *Conidiogenous cells* integrated, terminal, proliferating percurrently, rarely sympodially, with conically truncate and unthickened conidial loci. *Conidia* solitary, acicular to narrowly obclavate, 26–75 × 2–2.5 µm, 3–7-septate, hyaline or pale coloured, smooth, acute to rounded at the apex, truncate and unthickened at the base, not darkened, 2–2.5 µm wide.

Typus: **Malaysia**, Terengganu, University of Malaysia Terengganu, on *Hymenocalis speciosa* (*Amaryllidaceae*), 22 Jun. 2019, C. Nakashima, Y. Hattori, L. Suhaizan, & I. Nurul Faziha (**holotype** UMT201909, **isotype** TSU-MUMH11876, culture ex-type TSU-MUCC 2871).

Notes: *Pseudocercospora pancratii* is also known on *Hymenocalis*, and has been reported from Middle and North America, India, Japan, Kenya and Myanmar (see *Ps. pancratii*). Morphologically, *Ps. terengganunensis* is distinct in having hyaline to very pale coloured conidia that form on stromata and superficial hyphae, and somewhat smaller stromata with superficial hyphae. Moreover, their phylogenetic relationships indicate that these are two different species on the same host plant.

Pseudocercospora togashiana (K. Ito & Tak. Kobay.) C. Nakash. & Tak. Kobay., ***comb. nov.*** MycoBank MB 838225.
Basionym: *Mycosphaerella togashiana* K. Ito & Tak. Kobay. Bull. Gov. Forest Exp. Sta.: 23. 1953.

Typus: **Japan**, Tokyo, Meguro, Forest Experimental Station, on *Populus simonii* (*Salicaceae*), 24 Jul. 1951, T. Kobayashi (**holotype** of *Mycosphaerella togashiana* TFM: FPH 3703, culture ex-type MAFF410006, **isotype** TFM: FPH-3563).

Additional materials examined: **Japan**, Tokyo, Meguro, Forest Experimental Station, on *Populus alba*, 20 Oct. 1948, K. Ito, TFM: FPH-38; Tokyo, Meguro, Forest Experimental Station, on *Populus maximowiczii* (= *Populus suaveolens*), 19 Oct. 1948, K. Ito, TFM: FPH-36; Tokyo, Meguro, Forest Experimental Station, on *Populus monilifera* (= *Populus deltoides* subsp. *monilifera*), 19 Oct. 1948, K. Ito, TFM: FPH-37; *ibid*., 15 Sep. 1950, T. Kobayashi, TFM: FPH-166.

Illustrations: Ito & Kobayashi (1953).

Notes: Eleven "mycosphaerella-like" species have been described from *Populus* and *Salix*. However, the relationships of asexual and sexual morphs remain unclear, except for *M. togashiana,* and its *Pseudocercospora* asexual morph. In this study, we propose the new combination in *Pseudocercospora* based on *M. togashiana* (Deighton 1976).

Pseudocercospora trinidadensis (F. Stevens & Solheim) Crous *et al.*, Mycotaxon 72: 179. 1999.
Basionym: *Cercospora trinidadensis* F. Stevens & Solheim, Mycologia 23(5): 376. 1931.

Description and illustrations: Crous *et al.* (1999), Silva *et al.* (2016).

Typus: **Brazil**, Rio de Janeiro, Nova Friburgo, Fazenda Barreto II, on *Croton urucurana*, 1 Jun. 2014, R.W. Barreto (**epitype** designated here VIC 42851, MBT 10005842, culture ex-epitype COAD 1756 = CPC 26082). **Trinidad and Tobago**, St. Augustine, Trinidad, on *Croton gossypiifolius* (*Euphorbiaceae*), 13 Aug. 1922, F.L. Stevens (No.839) (**holotype** BPI 442019).

Notes: Crous *et al*. (1999) recognised the present species as separate from *Cercospora tiglii*, and proposed a new combination under the genus *Pseudocercospora*. The specimen examined by Silva *et al.* (2016) is selected as the epitype based on the similarity of morphological characters to the holotype specimen.

Pseudocercospora xenopunicae Crous & C. Nakash., ***sp. nov.*** MycoBank MB838652. Fig. 69J–L.

Etymology: Derived from the host genus, *Punica,* with prefix "*xeno*-".

Leaf spots amphigenous, circular to subcircular, 2–3 mm diam, dark brown, pale brown at the centre. *Caespituli* amphigenous. *Mycelium* internal and external, hyaline to pale olivaceous brown. *Stromata* amphigenous, substomatal to epidermal, erumpent, submerged, globose, olivaceous brown to brown, 12.5–42 µm diam, with superficial hyphae. *Conidiophores* dense, emerging from upper part of stromata, or solitary from superficial hyphae, straight to sinuous-geniculate, cylindrical, unbranched, 2.5–30 × 2–2.5 µm, 0–2-septate, pale brown, paler towards the apex, smooth, conically truncated at the apex. *Conidiogenous cells* integrated, terminal, proliferating sympodially, with truncated and unthickened conidial loci, 2–2.5 µm. *Conidia* solitary, cylindrical to obclavate, straight to curved, 25–55 × 2–2.5 µm, 1–4-septate, hyaline to olivaceous brown, smooth, acute at the apex, obconical truncated and unthickened at the base, not darkened, 2–2.5 µm diam.

Typus: **South Africa**, Limpopo Province, Westfalia, Tzaneen, on *Punica granatum* (*Lythraceae*), 8 Jul. 2011, P.W. Crous (**holotype** CBS H-24675, culture ex-type CBS 147384 = CPC 19712).

Notes: *Pseudocercospora punicae* is a well-known species on *Punica*. *Pseudocercospora xenopunicae* is distinct in that it has amphigenous caespituli, superficial hyphae with branching conidiophores, and narrower conidia than that of *Ps. punicae*. Moreover, the phylogenetic position of *Ps. xenopunicae* is quite removed from that of *Ps. punicae*. According to the USDA Fungal Databases (Farr & Rossman 2022), *Ps. punicae* has been reported worldwide from 45 countries. More detailed studies using phylogeny and morphology will be required to elucidate the species diversity of *Pseudocercospora* on *Punica*.

Genome sequenced strain: *Pseudocercospora vitis*. **Japan**, Mie, Iga, on *Vitis vinifera*, 31 Jul. 2017, H. Kondo, culture HUCC 2361. This Whole Genome Shutgun project has been deposited at GenBank under the accession JALRML000000000 (BioProject: PRJNA827019, BioSample: SAMN27594420; present study)

Authors: C. Nakashima, M. Bakhshi, R. Cheewangkoon, L. Suhaizan, I. Nurul Faziha, J.Z. Groenewald & P.W. Crous

Pteridopassalora C. Nakash. & Crous, ***gen. nov.*** MycoBank MB 841508.

Etymology: Derived from *Passalora* and *pteridophyte.*

Classification: *Dothideomycetes*, *Dothideomycetidae*, *Mycosphaerellales*, *Mycosphaerellaceae*.

Stromata small to well-developed. *Conidiophores* emerging from stromata or superficial hyphae, cylindrical, smooth to rough. *Conidiogenous cells* integrated to terminal on conidiophore, with unthickened or slightly thickened loci. *Conidia* solitary, variable in shape, cylindrical, filamentous to narrowly-obclavate, multi-septate, truncate and unthickened hilum at the base. *Sexual morph* not observed.

Cultural characteristics: Colonies growing slowly; on PDA surface smoke grey with patches of grey olivaceous, iron grey in reverse; on MEA pale olivaceous grey (surface), iron grey in reverse; on OA olivaceous grey with patches of pale olivaceous grey.

Type species: *Pteridopassalora nephrolepidicola* (Crous & R.G. Shivas) C. Nakash. & Crous. Holotype and ex-type culture: CBS H-20492, CBS 128211 = CPC 17049, CPC 17050.

DNA barcodes (genus): LSU and *rpb2*.

DNA barcodes (species): LSU, ITS and *rpb2*. Table 17. Fig. 70.

Optimal media and cultivation conditions: on CMA, sporulation of the asexual morph as *in situ* are observed (Kirschner & Wang 2015).

Distribution: Australia, mainland China and Taiwan Island.

Hosts: Known only from the pteridophytes, *Nephrolepis falcata* and *Lygodium japonicum*.

Disease symptoms: Leaf spots and leaf blight.

Notes: The unthickened or slightly thickened conidiogenous loci of *Pteridopassalora* are also seen in *Passalora s. lat.* and *Pseudocercospora.* The unresolved taxonomic position of the basionym *Pseudocercospora nephrolepidicola* has been discussed before (Kirschner & Wang 2015, Nakashima *et al*. 2016). Phylogenetic analysis using the combined matrix composed of LSU+ITS+*RPB2* regions, which are barcodes for *Passalora s. lat.* (Videira *et al*. 2017), showed *Pseudocercospora nephrolepidicola* warranted transfer to a new genus, *Pteridopassalora*. Many species of *Passalora* and *Pseudocercospora* that have been reported on ferns in recent years (Crous *et al*. 2010, Braun *et al*. 2013, Kirschner & Liu 2014, Kirschner & Wang 2015, Guatimosim *et al*. 2016, Nakashima *et al*. 2016), have morphological characteristics that resembling those of *Pteridopassalora.* Further studies are required to clarify their molecular phylogeny.

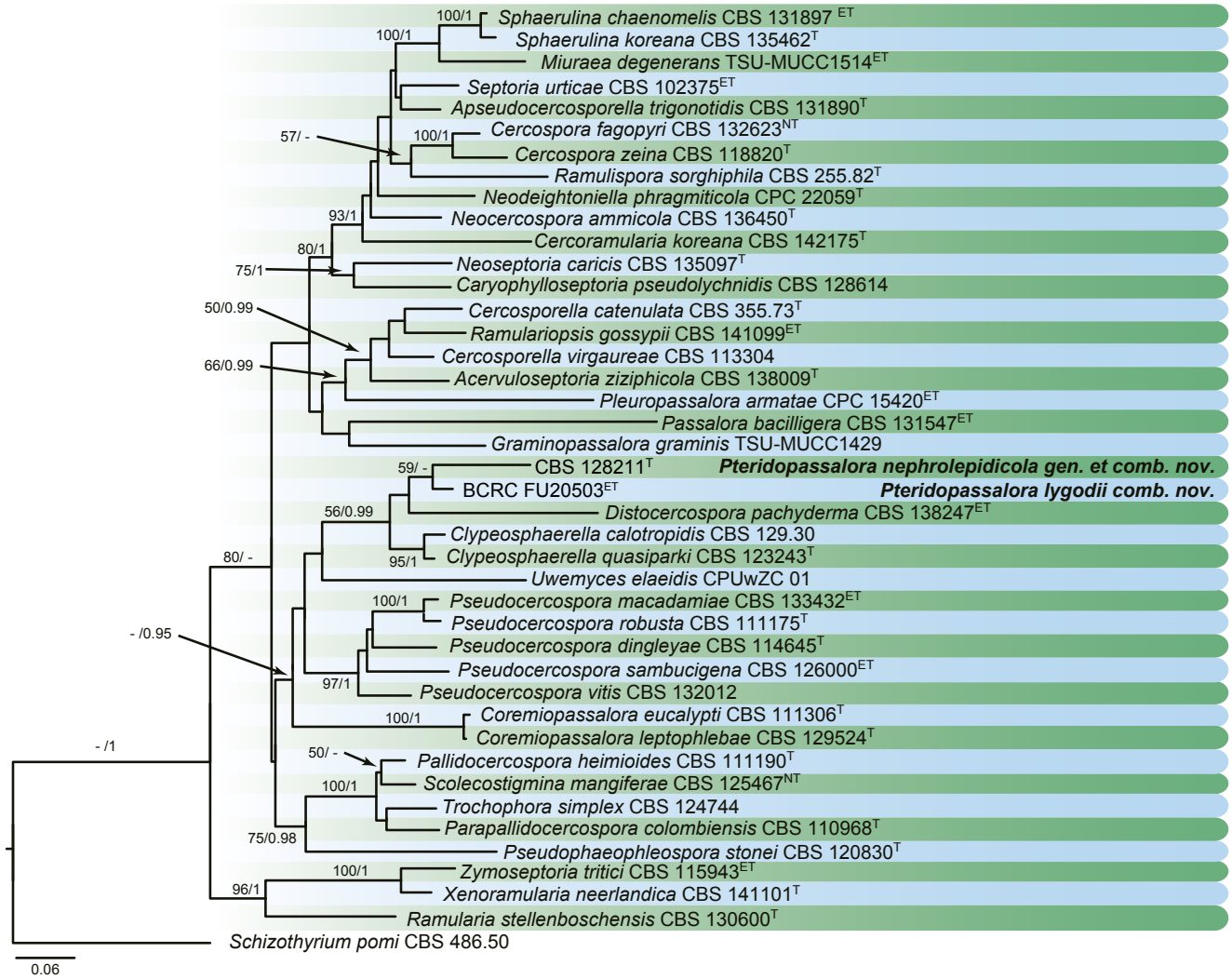

Fig. 70. Maximum Likelihood (ML) phylogram constructed from LSU (750 bp), ITS (583 bp), and *rpb2* (766 bp) sequences of *Pteridopassalora* spp. within *Passalora s. lat.* Maximum Likelihood bootstrap support values (> 50 %) and Bayesian posterior probability scores (> 0.95) are shown at the nodes. The novel taxa are printed in **bold**. The phylogenetic tree was rooted to *Schizothyrium pomi* CBS 486.50. GenBank accession numbers are indicated in Table 17. [T, ET] and [NT] indicate ex-type, ex-epitype, and ex-neotype strains, respectively. TreeBASE: S28912.

Table 17. DNA barcodes of accepted *Pteridopassalora* spp.

Species	Isolates[1]	GenBank accession numbers[2]			References
		LSU	ITS	*rpb2*	
Pteridopassalora lygodii	BCRC FU30503[ET]	—	KR527201	—	Kirschner & Wang (2015)
Pt. nephrolepidicola	CBS 128211 = CPC 17049[T]	HQ599591	HQ599590	KX462646	Crous *et al.* (2010), Nakashima *et al.* (2016)

[1] BCRC: Bioresource Collection and Research Center, Food Industry Research and Development Institute, Hsinchu, Taiwan; CBS: Westerdijk Fungal Biodiversity Institute, Utrecht, the Netherlands; CPC: Culture collection of Pedro Crous, housed at CBS. [T] and [ET] indicate ex-type and ex-epitype strains, respectively.

[2] LSU: partial 28S large subunit nrRNA gene; ITS: internal transcribed spacers and intervening 5.8S nrDNA; *rpb2*: partial RNA polymerase II second largest subunit gene.

References: Crous *et al.* 1998 (morphology); Kirschner & Wang 2015 (morphology); Nakashima *et al.* 2016 (phylogeny); Videira *et al.* 2017 (phylogeny and DNA barcodes).

Pteridopassalora nephrolepidicola (Crous & R.G. Shivas) C. Nakash. & Crous, ***comb. nov.*** MycoBank MB 841683.
Basionym: *Pseudocercospora nephrolepidicola* Crous & R.G. Shivas, Persoonia 25: 139. 2010.

Description and illustrations: Crous *et al.* (2010a).

Typus: **Australia**, Queensland, Brisbane Botanical Garden, on fronds of *Nephrolepis falcata* (*Nephrolepidaceae*), 14 Jul. 2009, P.W. Crous & R.G. Shivas (**holotype** CBS H-20492, cultures ex-type CBS 128211 = CPC 17049, CPC 17050).

Pteridopassalora lygodii (Goh & W.H. Hsieh) C. Nakash. & Crous, ***comb. nov.*** MycoBank MB 841767.
Basionym: *Pseudocercospora lygodii* Goh & W.H. Hsieh, Trans. Mycol. Soc. Rep. China 2 (2): 131. 1987.

Description and illustrations: Kirschner & Wang (2015).

Typus: **Taiwan Island**, Hsinchu County, Hsinpu, on pinnules of *Lygoium japonicum* (*Lygodiaceae*), 2 May 1920, E. Kurosawa (**holotype** PPMH); Taipei City, Tianmu Trail, on pinnules of *Lygoium japonicum*, 4 Apr. 2015 (**epitype** designated here TNM R. Kirschner 4182, MBT 10003650, culture ex-epitype BCRC FU30503).

Notes: An epitype collected on the same host from Taiwan island is proposed based on morphological similarity to that of the holotype.

Authors: C. Nakashima & P.W. Crous

Zymoseptoria Quaedvlieg & Crous, Persoonia 26: 64. 2011. Fig 71.

Classification: *Dothideomycetes*, *Dothideomycetidae*, *Mycosphaerellales*, *Mycosphaerellaceae*.

Type species: *Zymoseptoria tritici* (Desm.) Quaedvlieg & Crous, basionym: *Septoria tritici* Desm., Ann. Sci. Nat., Bot., sér. 2, 17: 107. 1842. Holotype: France, on *Triticum* sp., PC. Epitype and ex-type strain designated by Quaedvlieg *et al.* (2011): CBS H-20545, CBS 115943 = IPO 323.

DNA barcodes (genus): ITS, LSU.

DNA barcodes (species): *rpb2*, *tef1*. Table 18. Fig. 72.

Ascomata pseudothecial, globose, subepidermal, substomatal, brown, produced in older pale grey lesions; pseudothecia with central periphysate ostiole; wall of 2–3 layers of brown *textura angularis*. *Hamathecium* tissues absent. *Asci* stipitate, bitunicate, hyaline, smooth, obovoid to fusoid-ellipsoid, 8-spored, with apical chamber. *Ascospores* multiseriate, hyaline, smooth, fusoid-ellipsoid, medianly 1-septate, with bipolar, heterothallic mating

Table 18. DNA barcodes of accepted *Zymoseptoria* spp.

Species	Isolates[1]	GenBank accession numbers[2]				References
		ITS	LSU	*tef1*	*rpb2*	
Zymoseptoria ardabiliae	CBS 130977[T]	JQ739806	JQ739846	JQ739790	JN982483	Quaedvlieg *et al.* (2011), Stukenbrock *et al.* (2012)
Z. brevis	CBS 128853[T]	JF700867	JQ739833	JQ739777	JF700799	Quaedvlieg *et al.* (2011), Stukenbrock *et al.* (2012)
Z. crescenta	CBS 144410[T]	MH259304	MH267287	MH271694	MH271695	Crous *et al.* (2018c)
Z. halophila	CBS 128854[T]	JF700876	JQ739842	JQ739786	JF700808	Quaedvlieg *et al.* (2011), Stukenbrock *et al.* (2012)
Z. passerinii	CBS 120382[ET]	JF700877	JQ739843	JQ739787	JF700809	Quaedvlieg *et al.* (2011), Stukenbrock *et al.* (2012)
Z. pseudotritici	CBS 130976[T]	JN982480	JQ739828	JQ739772	JN982482	Quaedvlieg *et al.* (2011), Stukenbrock *et al.* (2012)
Z. tritici	CBS 115943[ET]	AF181692	GU214436	—	KX348112	Stukenbrock *et al.* (2012), Videira *et al.* (2016)
Z. verkleyi	CBS 133618[T]	KC005781	KC005802	—	—	Crous *et al.* (2012a)

[1] CBS: Westerdijk Fungal Biodiversity Institute, Utrecht, the Netherlands. [T] and [ET] indicate ex-type and ex-epitype strains, respectively.

[2] ITS: internal transcribed spacers and intervening 5.8S nrDNA; LSU: partial 28S large subunit nrRNA gene; *tef1*: partial translation elongation factor 1-α gene; *rpb2*: partial RNA polymerase II second largest subunit gene.

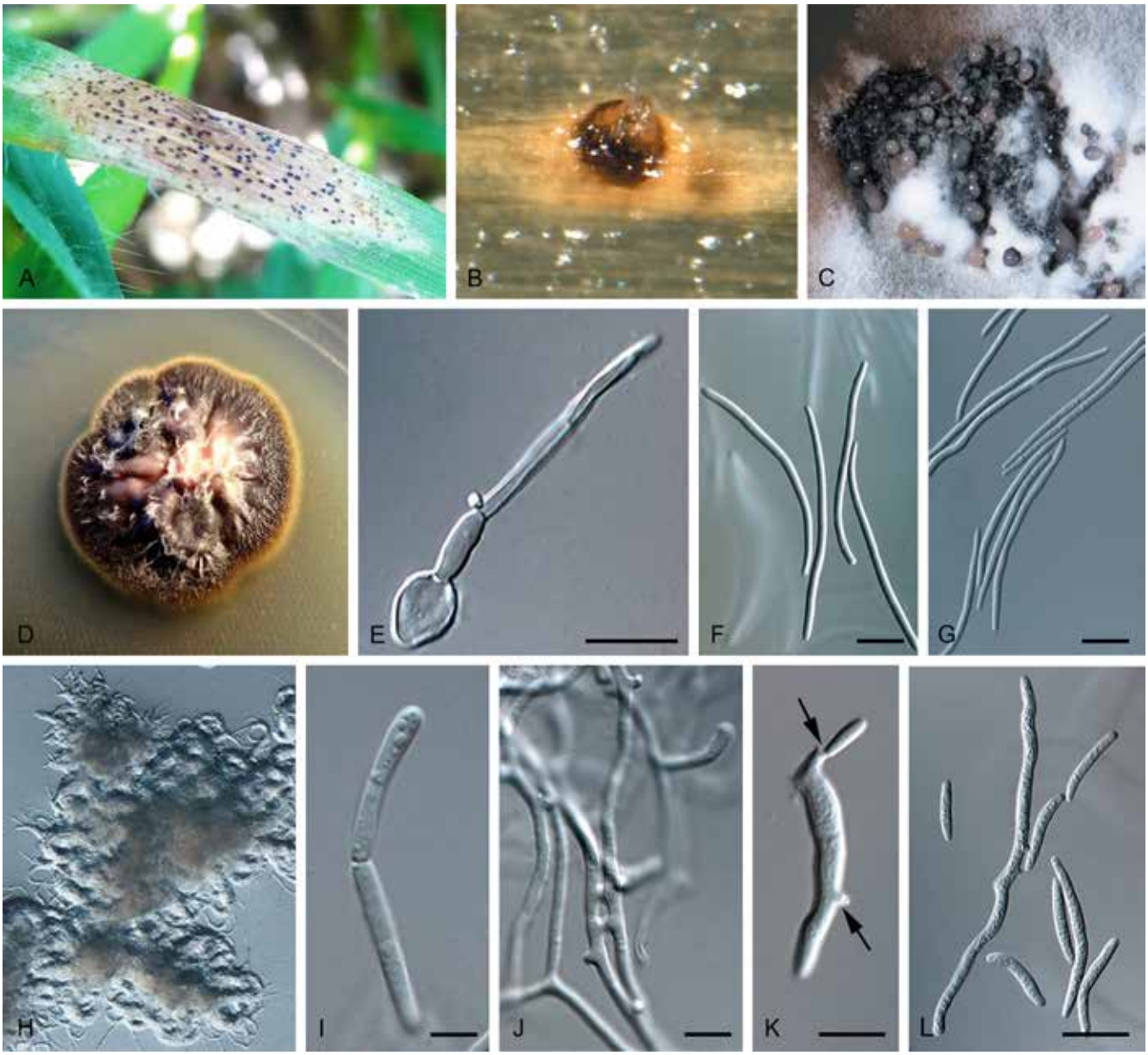

Fig. 71. *Zymoseptoria* spp. **A, B.** Disease symptoms. **A.** *Zymoseptoria crescent* (ex-type CBS 144410) on living leaves of *Aegilops triuncialis*. **B.** *Zymoseptoria brevis* (ex-type CBS 128853) forming a pycnidium on leaves of *Hordeum vulgare*. **C, D.** Colony sporulation on PDA. **C.** *Zymoseptoria brevis* (ex-type CBS 128853). **D.** *Zymoseptoria crescenta (*ex-type CBS 144410*)*. **E.** Conidiogenous cell of *Zymoseptoria passerinii* (ex-epitype CBS 120382) formed inside pycnidium. **F, G.** Conidia (Type I). **F.** *Zymoseptoria tritici* (ex-epitype CBS 115943). **G.** *Zymoseptoria halophila* (ex-type CBS 128854). **H.** *Zymoseptoria halophila* (ex-type CBS 1288545) colony with yeast-like growth on synthetic nutrient-poor agar. **I, J.** Conidia (Type II) of *Zymoseptoria halophila* (ex-type CBS 128854) formed as phragmospores in aerial hyphae. **K, L.** Conidia (Type III). **K.** *Zymoseptoria brevis* (ex-type CBS 128853) formed via microcyclic conidiation (arrows indicate Type III). **L.** *Zymoseptoria tritici* (ex-epitype CBS 115943). Scale bars = 10 µm. Pictures A, D taken from Crous *et al.* (2018c); B, C, E–L from Quaedvlieg *et al.* (2011).

system. *Conidiomata* pycnidial, dark brown to black, semi-immersed to erumpent, subglobose, with an ostiole. *Conidiomata wall* multi-layer, comprised of *textura angularis*. *Conidiophores* smooth, hyaline, septate, or reduced to conidiogenous cells. *Conidiogenous cells* aggregated, subcylindrical, ampulliform to doliiform, phialidic with periclinal thickening, or inconspicuous, percurrent proliferation at apex. *Hilum* not thickened nor darkened. *Type I conidia* hyaline, solitary, guttulate, smooth, cylindrical to subulate, tapering towards rounded apex with rounded to truncate base. *Type II conidia* disarticulate from aerial hyphae into phragmospores via microcyclic conidiation. *Type III conidia* microcyclic conidiation with yeast-like growth. *Sexual morph* unknown (adapted from Quaedvlieg *et al.* 2011, Stukenbrock *et al.* 2012).

Cultural characteristics: Colonies on PDA flat, with moderate aerial mycelium, surface pale olivaceous grey to olivaceous grey, iron grey from reverse. Colonies on MEA erumpent, with less mycelium, surface iron grey with patches or without patches, greenish black to black from reverse. Colonies on OA filamentous, with sparse aerial mycelium, somewhat erumpent, with patches.

Optimal media and cultivation conditions: OA, PDA or SNA at 25 °C under nuv-light to induce sporulation.

Distribution: Worldwide.

Hosts: Pathogens or saprobes on a variety of grass hosts including *Aegilops triuncialis, Dactylis* sp., *Elymus* sp., *Hordeum vulgare*,

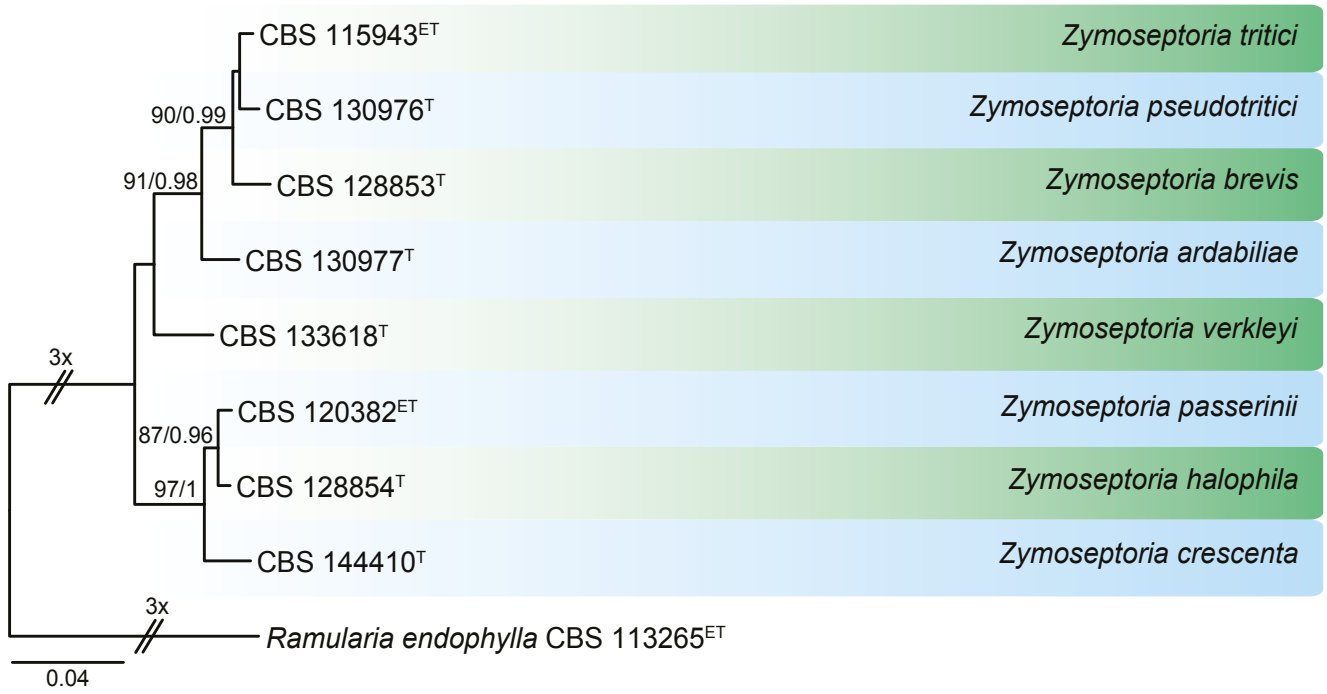

Fig. 72. RAxML phylogram constructed from ITS (471 bp), LSU (728 bp), *tef1* (270 bp) and *rpb2* (293) sequences of all accepted species of *Zymoseptoria*. Maximum likelihood bootstrap support values (> 70 %) and Bayesian posterior probability scores (> 0.95) are indicated on the branches. The phylogenetic tree was rooted to *Ramularia endophylla* CBS 113265. GenBank accession numbers are indicated in Table 18. ^{T} and ^{ET} indicate ex-type and ex-epitype strains, respectively. TreeBASE: S26192.

Lolium sp., *Poa annua* and *Triticum eastivum* (*Poaceae*).

Disease symptoms: Leaf spots or leaf blotch.

Notes: *Zymoseptoria* was introduced by Quaedvlieg *et al.* (2011) to accommodate septoria-like species pathogenic to grass hosts. Species of *Zymoseptoria* mostly have phialides with periclinal thickening, or percurrent proliferation at the apex of conidiogenous cells. Presently, this genus contains eight accepted species, which exhibit a yeast-like growth on artificial media and produces up to three types of conidia (Type I, pycnidial conidia; Type II, phragmospores on aerial hyphae; Type III, yeast-like growth proliferating via microcyclic conidiation) typical for the genus (Quaedvlieg *et al.* 2011, Stukenbrock *et al.* 2012).

References: Quaedvlieg *et al.* 2011, Stukenbrock *et al.* 2012, Crous *et al.* 2012a, 2018c (morphology and phylogeny).

Genome sequenced strain: *Zymoseptoria crescenta.* **Iran**, East Azarbaijan Province, Kaleybar, on living leaves of *Aegilops triuncialis*, May 2012, M. Abrinbana, culture ex-type CBS 144410. This Whole Genome Shutgun project has been deposited at GenBank under the accession JALRMM000000000 (BioProject: PRJNA827019, BioSample: SAMN27594421; present study).

Authors: M. Raza & L. Cai

ACKNOWLEDGEMENTS

Meng Li, Lingwei Hou, Yahui Gao, Nan Zhou, Yu Zhang, Mengmeng Wang and Ziying Ma are thanked for help with sample collection, as well as providing cultures. The study of *Ascochyta*, *Didymella* and *Leptosphaerulina* were supported by the National Natural Science Foundation of China (31750001) and the National Science and Technology Fundamental Resources Investigation Program of China (MOST: 2021FY100900). The study of the genus *Phytophthora* was supported by the Project Phytophthora Research Centre Reg. No. CZ.02.1.01/0.0/0.0/15_003/0000453 cofinanced by the European Regional Development Fund. ShuaiFei Chen acknowledges the National Key R&D Program of China (China-South Africa Forestry Joint Research Centre Project; 2018YFE0120900) for financial support. Mounes Bakhshi and Rasoul Zare gratefully acknowledge the Iran National Science Foundation (INSF), and Research Deputy of the Iranian Research Institute of Plant Protection, Agricultural Research, Education and Extension Organization (AREEO), for financial support. The study of the genera *Pseudocercospora* and *Pteridopassalora* were partially supported by JSPS KAKENHI Grant Numbers JP20K06146 to Chiharu Nakashima.

DECLARATION ON CONFLICT OF INTEREST

The authors declare that there is no conflict of interest.

REFERENCES

Abad ZG, Abad JA, Cacciola SO, *et al.* (2014). *Phytophthora niederhauserii sp. nov.*, a polyphagous species associated with ornamentals, fruit trees and native plants in 13 countries. *Mycologia* **106**: 431–447.

Abad ZG, Abad JA, Coffey MD, *et al.* (2008). *Phytophthora bisheria sp. nov.*, a new species identified in isolates from the Rosaceous raspberry, rose and strawberry in three continents. *Mycologia* **100**: 99–110.

Abad ZG, Ivors K, Gallup CA, *et al.* (2011). Morphological and molecular characterization of *Phytophthora glovera sp. nov.* from tobacco in Brazil. *Mycologia* **103**: 341–350.

Abeln EC, Pagter MA, Verkley GJ. (2000). Phylogeny of *Pezicula*, *Dermea* and *Neofabraea* inferred from partial sequences of the nuclear ribosomal RNA gene cluster. *Mycologia* **92**: 685–93.

Abler SW (2003). *Ecology and Taxonomy of Leptosphaerulina* spp. *associated with Turfgrasses in the United States*. Virginia Polytechnic Institute and State University. Blacksburg, Virginia, USA.

Adams GC, Roux J, Wingfield MJ, *et al.* (2005). Phylogenetic relationships and morphology of *Cytospora* species and related teleomorphs (*Ascomycota, Diaporthales, Valsaceae*) from *Eucalyptus*. *Studies in Mycology* **52**: 1–144.

Adams GC, Roux J, Wingfield MJ (2006). *Cytospora* species (*Ascomycota, Diaporthales, Valsaceae*), introduced and native pathogens of trees in South Africa. *Australasian Plant Pathology* **35**: 521–548.

Agustí-Brisach C, Gramaje D, García-Jiménez J, *et al.* (2013). Detection of black-foot and Petri disease pathogens in natural soils of grapevine nurseries and vineyards. *Plant and Soil* **364**: 5–13.

Agustí-Brisach C, Gramaje D, León M, *et al.* (2011). Evaluation of vineyard weeds as potential hosts of black-foot and Petri disease pathogens. *Plant Disease* **95**: 803–810.

Aigoun-Mouhous W, Eddine-Mahamedi A, León M, *et al.* (2021). *Cadophora sabaouae sp. nov. and Phaeoacremonium* species associated with Petri Disease on grapevine propagation material and young grapevines in Algeria. *Plant Disease* **105**: 3657–3668.

Aislabie J, Fraser R, Duncan S, *et al.* (2001). Effect of oil spills in microbial heterotrophs in Antarctic soils. *Polar Biology* **24**: 308–313.

Akrofi A (2015). *Phytophthora megakarya*: A review on its status as a pathogen on cacao in West Africa. *African Crop Science Journal* **23**: 67–87.

Albu S, Schneider R, Price P, *et al.* (2016). *Cercospora cf. flagellaris* and *Cercospora cf. sigesbeckiae* are associated with Cercospora leaf blight and purple seed stain on soybean in North America. *Phytopathology* **106**: 1376–1385.

Albuquerque Alves TC, Tessmann DJ, Ivors KL, *et al.* (2019). *Phytophthora acaciae sp. nov*., a new species causing gummosis of black wattle in Brazil. *Mycologia* **111**: 445–455.

Ali B, Sohail Y, Toome-Heller M, *et al.* (2016). *Melampsora pakistanica sp. nov.*, a new rust fungus on *Euphorbia helioscopia* (Sun spurge) from Pakistan. *Mycological Progress* **15**: 1285–1292.

Ali DB, Marincowitz S, Wingfield MJ, *et al.* (2018). Novel *Cryphonectriaceae* from La Réunion and South Africa, and their pathogenicity on *Eucalyptus*. *Mycological Progress* **17**: 953–966.

Amin KS, Baldev B, Williams FJ (1978). *Phytophthora cajani*, a new species causing stem blight on *Cajanus cajan*. *Mycologia* **70**: 171–176.

Ann PJ, Huang JH, Tsai JN, *et al.* (2016). Morphological, molecular and pathological characterization of *Phytophthora amaranthi sp. nov.* from amaranth in Taiwan. *Journal of Phytopathology* **164**: 94–101.

Antonielli L, Compant S, Strauss J, *et al.* (2014). Draft genome sequence of *Phaeomoniella chlamydospora* strain RR-HG1, a grapevine trunk disease (Esca)-related member of the *Ascomycota*. *Genome Announcements* **2**: e00098–00014.

Aptroot A (2006). *Mycosphaerella and its anamorphs: 2. Conspectus of Mycosphaerella.* CBS Biodiversity Series 5. CBS-KNAW Fungal Biodiversity Centre, Utrecht, The Netherlands.

Aragaki M, Uchida JY (2001). Morphological distinctions between *Phytophthora capsici* and *P. tropicalis sp. nov*. *Mycologia* **93**: 137–145.

Arenz BE, Held BW, Jurgens JA, *et al*. (2006). Fungal diversity in soils and historic wood from the Ross Sea Region of Antarctica. *Soil Biology and Biochemistry* **38**: 3057–3064.

Ariyawansa HA, Hyde KD, Jayasiri SC, *et al.* (2015). Fungal diversity notes 111–252 taxonomic and phylogenetic contributions to fungal taxa. *Fungal Diversity* **75**: 27–274.

Aveskamp MM, de Gruyter J, Woudenberg JHC, *et al.* (2010). Highlights of the *Didymellaceae*: A polyphasic approach to characterise *Phoma* and related pleosporalean genera. *Studies in Mycology* **65**: 1–60.

Aveskamp MM, Verkley GJ, De Gruyter J, *et al.* (2009). DNA phylogeny reveals polyphyly of *Phoma* section *Peyronellaea* and multiple taxonomic novelties. *Mycologia* **101**: 363–382.

Bagyanarayana G (2005). The species of *Melampsora* on *Salix* (*Salicaceae*). In: *Rust diseases of willow and poplar* (Pei MH, McCracken AR, eds). CABI Publishing, Wallingford, UK: 29–50.

Bakhshi M (2019). Epitypification of *Cercospora rautensis*, the causal agent of leaf spot disease on *Securigera varia*, and its first report from Iran. *Fungal Systematics and Evolution* **3**: 157–163.

Bakhshi M, Arzanlou M, Babai-Ahari A, *et al.* (2014). Multi-gene analysis of *Pseudocercospora* spp. from Iran. *Phytotaxa* **184**: 245–264.

Bakhshi M, Arzanlou M, Babai-ahari A, *et al.* (2015a). Application of the consolidated species concept to *Cercospora* spp. from Iran. *Persoonia* **34**: 65–86.

Bakhshi M, Arzanlou M, Babai-ahari A, *et al.* (2015b). Is morphology in *Cercospora* a reliable reflection of generic affinity? *Phytotaxa* **213**: 22–34.

Bakhshi M, Arzanlou M, Babai-ahari A, *et al.* (2018). Novel primers improve species delimitation in *Cercospora*. *IMA Fungus* **9**: 299–332.

Balci Y, Balci S, Blair JE, *et al.* (2008). *Phytophthora quercetorum sp. nov*. a novel species isolated from eastern and north-central USA oak forest soils. *Mycological Research* **112**: 906–916.

Bankevich A, Nurk S, Antipov D, *et al.* (2012). SPAdes: a new genome assembly algorithm and its applications to single-cell sequencing. *Journal of Computational Biology* **19**: 455–477.

Barr ME (1972). Preliminary studies on the *Dothideales* in temperate North America. *Contributions from the University of Michigan Herbarium* **9**: 523–638.

Barr ME (1978). The *Diaporthales* in North America with emphasis on *Gnomonia* and its segregates. *Mycologia Memoir* **7**: 1–232.

Bellgard SE, Pennycook SR, Weir BS, *et al.* (2016). *Phytophthora agathidicida*. *Forest Phytophthoras* **6**. doi: 10.5399/osu/fp.5.1.3748.

Berres ME, Szabo LJ, McLaughlin DJ (1995). Phylogenetic relationships in auriculariaceous basidiomycetes based on 25S ribosomal DNA sequences. *Mycologia* **87**: 821–840.

Bertier L, Brouwer H, de Cock AWAM, *et al.* (2013a). The expansion of *Phytophthora* clade 8b: three new species associated with winter grown vegetable crops. *Persoonia* **31**: 63–76.

Bertier L, Leus L, D'hondt L, *et al.* (2013b). Host adaptation and speciation through hybridization and polyploidy in *Phytophthora*. *PLoS ONE* **8**: e85385.

Bien F, Damm U (2020). *Arboricolonus simplex gen. et sp. nov.* and novelties in *Cadophora, Minutiella* and *Proliferodiscus* from *Prunus* wood in Germany. *MycoKeys* **63**: 119–161.

Bienapfl JC, Balci Y (2014). Movement of *Phytophthora* spp. in Maryland's nursery trade. *Plant Disease* **98**: 134–144.

Blackwell E (1949). *Terminology in Phytophthora*. *Mycological Papers 30*. Commonwealth Mycological. Institute, Kew, Surrey, England.

Blanchette RA, Held BW, Jurgens JA, *et al*. (2004). Wood-destroying soft rot fungi in the historic expedition huts of Antarctica. *Applied and Environmental Microbiology* **70**: 1328–1335.

Boerema GH, Bollen GJ (1975). Conidiogenesis and conidial septation as differentiating criteria between *Phoma* and *Ascochyta*. *Persoonia* **8**: 111–444.

Boerema GH, de Gruyter J, Noordeloos ME, *et al.* (2004). *Phoma identification manual. Differentiation of specific and infra-specific taxa in culture*. CABI Publishing, Wallingford, UK.

Boesewinkel HJ (1976). Storage of fungal cultures in water. *Transactions of the British Mycological Society* **66**: 183–185.

Borie B, Jacquiot L, Jamaux-Despreaux I, *et al.* (2002). Genetic diversity in populations of the fungi *Phaeomoniella chlamydospora* and *Phaeoacremonium aleophilum* on grapevine in France. *Plant Pathology* **51**: 85–96.

Bose T, Hulbert JM, Burgess TI, *et al.* (2021). Two novel *Phytophthora* species from the southern tip of Africa. *Mycological Progress* **20**: 755–767.

Bourret TB, Choudhury RA, Mehl HK, *et al.* (2018). Multiple origins of downy mildews and mito-nuclear discordance within the paraphyletic genus *Phytophthora*. *PLoS ONE* **13**: e0192502.

Brasier CM (1967). *Physiology of reproduction in Phytophthora*. PhD. Thesis, University of Hull, UK.

Brasier CM (2008). The biosecurity threat to the UK and global environment from international trade in plants. *Plant Pathology* **57**: 792–808.

Brasier CM (2009). *Phytophthora* biodiversity: How many *Phytophthora* species are there? In: *Phytophthoras in Forests and Natural Ecosystems: Fourth Meeting of the International Union of Forest Research Organizations (IUFRO) Working Party S07.02.09* (Goheen

EM, Frankel SJ, eds.). USDA Forest Service, Pacific Southwest Research Station, Albany, California. General Technical Report PSW-GTR-221: 101–115.

Brasier CM, Griffin MJ (1979). Taxonomy of *Phytophthora palmivora* on cocoa. *Transactions of the British Mycological Society* **72**: 111–143.

Brasier CM, Webber J (2010). Sudden larch death. *Nature* **466**: 824–825.

Brasier CM, Beales PA, Kirk SA, *et al.* (2005). *Phytophthora kernoviae sp. nov.* an invasive pathogen causing bleeding stem lesions on forest trees and foliar necrosis of ornamentals in Britain. *Mycological Research* **109**: 853–859.

Brasier CM, Cooke DEL, Duncan JM, *et al.* (2003a). Multiple new phenotypic taxa from trees and riparian ecosystems in *Phytophthora gonapodyides – P. megasperma* ITS Clade 6, which tend to be high-temperature tolerant and either inbreeding or sterile. *Mycological Research* **107**: 277–290.

Brasier CM, Kirk SA, Delcan J, *et al.* (2004). *Phytophthora alni sp. nov.* and its variants: designation of emerging heteroploid hybrid pathogens spreading on *Alnus* trees. *Mycological Research* **108**: 1172–1184.

Brasier CM, Sanchez-Hernandez E, Kirk SA (2003b). *Phytophthora inundata sp. nov*., a part heterothallic pathogen of trees and shrubs in wet or flooded soils. *Mycological Research* **107**: 477– 484.

Braun U (2001a). Taxonomic notes on some species of the *Cercospora* complex (VII). *Fungal Diversity* **8**: 41–71.

Braun U (2001b). Revision of *Cercospora* species described by K.B. Boedijn. *Nova Hedwigia* **73**: 419–436.

Braun U (2003). Miscellaneous notes on some cercosporoid *Hyphomycetes*. *Bibliotheca Lichenologica* **86**: 79–98.

Braun U, Castaneda RR (1991). *Cercospora* and allied genera of Cuba (II). *Cryptogamie Botany* **2/3**: 289–297.

Braun U, Crous PW (2016). (2415) Proposal to conserve the name *Cercospora* (*Ascomycota*: *Mycosphaerellaceae*) with a conserved type. *Taxon* **65**: 185.

Braun U, Crous PW, Nakashima C (2014). Cercosporoid fungi (*Mycosphaerellaceae*) 2. Species on monocots (*Acoraceae* to *Xyridaceae*, excluding *Poaceae*). *IMA Fungus* **5**: 203–390.

Braun U, Crous PW, Nakashima C (2015a). Cercosporoid fungi (*Mycosphaerellaceae*) 3. Species on monocots (*Poaceae*, true grasses). *IMA Fungus* **6**: 25–97.

Braun U, Crous PW, Nakashima C (2015b). Cercosporoid fungi (*Mycosphaerellaceae*) 4. Species on dicots (*Acanthaceae* to *Amaranthaceae*). *IMA Fungus* **6**: 373–469.

Braun U, Crous PW, Nakashima C (2016). Cercosporoid fungi (*Mycosphaerellaceae*) 5. Species on dicots (*Anacardiaceae* to *Annonaceae*). *IMA Fungus* **7**: 161–216.

Braun U, Hill CF (2002). Some new micromycetes from New Zealand. *Mycological Progress* **1**: 19–30.

Braun U, Hill CF, Dick M (2003). New cercosporoid leaf spot diseases from New Zealand. *Australasian Plant Pathology* **32**: 87–97.

Braun U, Melnik VA (1997). Cercosporoid fungi from Russia and adjacent countries. *Trudy Botanicheskogo Instituta Imeni V.L. Komarova, Rossijskaya Akademiya Nauk St. Petersburg* **20**: 1–130.

Braun U, Nakashima C, Bakhshi M, *et al.* (2020). Taxonomy and phylogeny of cercosporoid ascomycetes on *Diospyros* spp. with special emphasis on *Pseudocercospora* spp. *Fungal Systematics and Evolution* **6**: 95–127.

Braun U, Nakashima C, Crous PW (2013). Cercosporoid fungi (*Mycosphaerellaceae*) 1. Species on other fungi, *Pteridophyta* and *Gymnospermae*. *IMA Fungus* **4**: 265–345.

Brown AV, Brasier CM (2007). Colonization of tree xylem by *Phytophthora ramorum*, *P. kernoviae* and other *Phytophthora* species. *Plant Pathology* **56**: 227–241.

Buddenhagen IW, Young RA (1957). Leaf and twig disease of English holly caused by *Phytophthora ilicis n. sp. Phytopathology* **47**: 95–100.

Burgess TI (2015). Molecular characterization of natural hybrids formed between five related indigenous Clade 6 *Phytophthora* species. *PLoS ONE* **10**: e0134225.

Burgess TI, Dang QN, Le BV, *et al*. (2020). *Phytophthora acaciivora sp. nov.* associated with dying *Acacia mangium* in Vietnam. *Fungal Systematics and Evolution* **6**: 243–252.

Burgess TI, Simamora AV, White D, *et al.* (2018). New species from *Phytophthora* Clade 6a: evidence for recent radiation. *Persoonia* **41**: 1–17.

Burgess TI, Webster JL, Ciampini JA, *et al.* (2009). Re-evaluation of *Phytophthora* species isolated during 30 years of vegetation health surveys in Western Australia using molecular techniques. *Plant Disease* **93**: 215–223.

Burgess TI, White D, McDougall KM, *et al.* (2017). Distribution and diversity of *Phytophthora* across Australia. *Pacific Conservation Biology* **23**: 1–13.

Busby PE, Aime MC, Newcombe G (2012). Foliar pathogens of *Populus angustifolia* are consistent with a hypothesis of Beringian migration into North America. *Fungal Biology* **116**: 792–801.

Cahill DM, Rookes JE, Wilson BA, *et al.* (2008). Turner Review No. 17. *Phytophthora cinnamomi* and Australia's biodiversity: impacts, predictions and progress towards control. *Australian Journal of Botany* **56**: 279–310.

Chand R, Pal C, Singh V, *et al.* (2015). Draft genome sequence of *Cercospora canescens*: a leaf spot causing pathogen. *Current Science* **109**: 2103–2110.

Cheewangkoon R, Crous PW, Hyde KD, *et al.* (2008). Species of *Mycosphaerella* and related anamorphs on *Eucalyptus* leaves from Thailand. *Persoonia* **21**: 77–91.

Cheewangkoon R, Groenewald JZ, Summerell BA, *et al.* (2009). *Myrtaceae*, a cache of fungal biodiversity. *Persoonia* **23**: 55–85.

Cheewangkoon R, Groenewald JZ, Verkley GJ, *et al.* (2010). Re-evaluation of *Cryptosporiopsis eucalypti* and Cryptosporiopsis-like species occurring on *Eucalyptus* leaves. *Fungal Diversity* **44**: 89–105.

Chen C, Verkley GJ, Sun G, *et al.* (2016). Redefining common endophytes and plant pathogens in *Neofabraea*, *Pezicula*, and related genera. *Fungal Biology* **120**: 1291–322.

Chen H, Lee MH, Daub ME, *et al.* (2007). Molecular analysis of the cercosporin biosynthetic gene cluster in *Cercospora nicotianae*. *Molecular Microbiology* **64**: 755–770.

Chen KH, Miadlikowska J, Molnár K, *et al.* (2015a). Phylogenetic analyses of eurotiomycetous endophytes reveal their close affinities to *Chaetothyriales*, *Eurotiales*, and a new order – *Phaeomoniellales*. *Molecular Phylogenetics and Evolution* **85**: 117–130.

Chen KL, Kirschner R (2017). Fungi from leaves of lotus (*Nelumbo nucifera*). *Mycological Progress* **17**: 275–293.

Chen Q, Hou LW, Duan WJ, *et al.* (2017). *Didymellaceae* revisited. *Studies in Mycology* **87**: 105–159.

Chen Q, Jiang JR, Zhang GZ, *et al.* (2015b). Resolving the *Phoma* enigma. *Studies in Mycology* **82**: 137–217.

Chen Q, Zhang K, Zhang GZ, *et al.* (2015c). A polyphasic approach to characterise two novel species of *Phoma* (*Didymellaceae*) from China. *Phytotaxa* **197**: 267–281.

Chen SF, Gryzenhout M, Roux J, *et al.* (2011). Novel species of *Celoporthe* from *Eucalyptus* and *Syzygium* trees in China and Indonesia. *Mycologia* **103**: 1384–1410.

Chilvers MI, Rogers JD, Dugan FM, *et al.* (2009). *Didymella pisi sp. nov*., the teleomorph of *Ascochyta pisi*. *Mycological Research* **113**: 391–400.

Chupp C (1954). *A monograph of the fungus genus Cercospora*. Ithaca, New York.

Cole GT, Kendrick B (1973). Taxonomic studies of *Phialophora*. *Mycologia* **65**: 661–668.

Cooke DEL, Drenth A, Duncan JM, *et al.* (2000). A molecular phylogeny of *Phytophthora* and related oomycetes. *Fungal Genetics and Biology* **30**: 17–30.

Corbaz R (1955). Sur *Didymella phacae* Corbaz. *Sydowia* **9**: 229–230.

Corbaz R (1957). Recherches sur le genre *Didymella* Sacc. *Phytopathologische Zeitschrift* **28**: 375–414.

Corcobado T, Cech TL, Brandstetter M, *et al.* (2020). Decline of European beech in Austria: involvement of *Phytophthora* spp. and contributing biotic and abiotic factors. *Forests* **11**: 895.

Corlett M (1981). A taxonomic survey of some species of *Didymella* and Didymella-like species. *Canadian Journal of Botany* **59**: 2016–2042.

Crandall BS (1947). A new *Phytophthora* causing root and collar rot of

Cinchona in Peru. *Mycologia* **39**: 218–223.
Crandall BS, Gravatt GF, Ryan MM (1945). Root disease of *Castanea* species and some coniferous and broadleaf nursery stocks, caused by *Phytophthora cinnamomi*. *Phytopathology* **35**: 162–180.
Crous PW (1998). *Mycosphaerella* spp. and their anamorphs associated with leaf spot diseases of *Eucalyptus*. *Mycologia Memoir* **21**: 1–170.
Crous PW (1999). Species of *Mycosphaerella* and related anamorphs occurring on *Myrtaceae* (excluding *Eucalyptus*). *Mycological Research* **103**: 607–621.
Crous PW, Aptroot A, Kang JC, *et al.* (2000). The genus *Mycosphaerella* and its anamorphs. *Studies in Mycology* **45**: 107–121.
Crous PW, Braun U (1996). Notes on cercosporoid fungi occurring on *Dodonaea*. *South African Journal of Botany* **62**: 247–249.
Crous PW, Braun U (2003). *Mycosphaerella and its Anamorphs. 1. Names published in Cercospora and Passalora.* CBS Biodiversity Series 1. CBS-KNAW Fungal Biodiversity Centre, Utrecht, The Netherlands.
Crous PW, Braun U, Alfenas AC (1999). Cercosporoid Fungi from Brazil. 3. *Mycotaxon* **72**: 171–193.
Crous PW, Braun U, Hunter GC, *et al.* (2013a). Phylogenetic lineages in *Pseudocercospora*. *Studies in Mycology* **75**: 37–114.
Crous PW, Carlier J, Roussel V, *et al.* (2020). *Pseudocercospora* and allied genera associated with leaf spots of banana (*Musa* spp.). *Fungal Systematics and Evolution* **7**: 1–19.
Crous PW, Carnegie AJ, Wingfield MJ, *et al.* (2019a). Fungal Planet description sheets: 868–950. *Persoonia* **42**: 291–473.
Crous PW, Carris LM, Giraldo A, *et al.* (2015a). The Genera of Fungi – fixing the application of the type species of generic names – G2: *Allantophomopsis*, *Latorua*, *Macrodiplodiopsis*, *Macrohilum*, *Milospium*, *Protostegia*, *Pyricularia*, *Robillarda*, *Rotula*, *Septoriella*, *Torula*, and *Wojnowicia*. *IMA Fungus* **6**: 163–198.
Crous PW, Gams W (2000). *Phaeomoniella chlamydospora gen. et comb. nov*., a causal organism of Petri grapevine decline and esca. *Phytopathologia Mediterranea* **39**: 112–118.
Crous PW, Gams W, Stalpers JA, *et al.* (2004). MycoBank: an online inititive to launch mycology into the 21st century. *Studies in Mycology* **50**: 19–22.
Crous PW, Gams W, Wingfield MJ, *et al.* (1996). *Phaeoacremonium gen. nov.* associated with wilt and decline diseases of woody hosts and human infections. *Mycologia* **88**: 786–796.
Crous PW, Giraldo A, Hawksworth DL, *et al.* (2014a). The Genera of Fungi: fixing the application of the type species of generic names. *IMA Fungus* **5**: 141–160.
Crous PW, Groenewald JZ (2013). A phylogenetic re-evaluation of *Arthrinium*. *IMA Fungus* **4**: 133–54.
Crous PW, Groenewald JZ (2016). They seldom occur alone. *Fungal Biology* **120**: 1392–415.
Crous PW, Groenewald JZ, Groenewald M, *et al.* (2006a). Species of *Cercospora* associated with grey leaf spot of maize. *Studies in Mycology* **55**: 189–197.
Crous PW, Groenewald JZ, Shivas RG (2010a). *Pseudocercospora nephrolepidicola* Crous & R.G. Shivas, *sp. nov*. Fungal Planet 59. *Persoonia* **25**: 138–139.
Crous PW, Groenewald JZ, Shivas RG (2010b). *Pseudocercospora casuarinae* Crous & R.G. Shivas, *sp. nov.* Fungal Planet 66. *Persoonia* **25**: 152–153.
Crous PW, Groenewald JZ, Shivas RG, *et al.* (2011a). Fungal Planet description sheets: 69–91. *Persoonia* **26**: 108–156.
Crous PW, Hawksworth DL, Wingfield MJ (2015b). Identifying and naming plantpathogenic fungi: past, present, and future. *Annual Review of Phytopathology* **53**: 247–267.
Crous PW, Liebenberg MM, Braun U, Groenewald JZ (2006b). Re-evaluating the taxonomic status of *Phaeoisariopsis griseola*, the causal agent of angular leaf spot of bean. *Studies in Mycology* **55**: 163–173.
Crous PW, Luangsa-ard JJ, Wingfield MJ, *et al.* (2018a). Fungal Planet description sheets: 785–867. *Persoonia* **41**: 238–417.
Crous, PW, Quaedvlieg W, Hansen K, *et al.* (2014b). *Phacidium* and *Ceuthospora* (*Phacidiaceae*) are congeneric: taxonomic and nomenclatural implications. *IMA Fungus* **5**: 173–193.
Crous PW, Rossman AY, Aime MC, *et al*. (2021). Names of phytopathogenic fungi: a practical guide. *Phytopathology* **111**: 1500–1508.
Crous PW, Schoch CL, Hyde KD, *et al.* (2009a). Phylogenetic lineages in the *Capnodiales*. *Studies in Mycology* **64**: 17–47.
Crous PW, Schumacher RK, Wingfield MJ, *et al.* (2018b). New and Interesting Fungi. 1. *Fungal Systematics and Evolution* **1**: 169–215.
Crous PW, Schumacher RK, Akulov A, *et al.* (2019b). New and interesting fungi. 2. *Fungal Systematics and Evolution* **3**: 57–134.
Crous PW, Shivas RG, Quaedvlieg W, *et al.* (2014c). Fungal Planet description sheets: 214–280. *Persoonia* **32**: 184–306.
Crous PW, Shivas RG, Wingfield MJ, *et al.* (2012a). Fungal Planet description sheets: 128–153. *Persoonia* **29**: 146–201.
Crous PW, Slippers B, Wingfield MJ, *et al.* (2006c). Phylogenetic lineages in the *Botryosphaeriaceae*. *Studies in Mycology* **55**: 235–253.
Crous PW, Summerell BA, Carnegie AJ, *et al.* (2009b). Unravelling *Mycosphaerella*: do you believe in genera? *Persoonia* **23**: 99–118.
Crous PW, Summerell BA, Shivas RG, *et al.* (2011b). Fungal Planet description sheets: 92–106. *Persoonia* **27**: 130–162.
Crous PW, Summerell BA, Shivas RG, *et al.* (2012b). Fungal Planet description sheets: 107–127. *Persoonia* **28**: 138–182.
Crous PW, Summerell BA, Swart L, *et al.* (2011c). Fungal pathogens of *Proteaceae*. *Persoonia* **27**: 20–45.
Crous PW, Verkley GJM, Groenewald JZ, *et al*. (2019c). *Westerdijk Laboratory Manual Series 1: Fungal Biodiversity*. Westerdijk Fungal Biodiversity Institute, Utrecht, The Netherlands.
Crous PW, Wingfield MJ, Burgess TI, *et al.* (2016). Fungal Planet description sheets: 469–557. *Persoonia* **37**: 218–403.
Crous PW, Wingfield MJ, Burgess TI, *et al.* (2017a). Fungal Planet description sheets: 558–642. *Persoonia* **38**: 240–384.
Crous PW, Wingfield MJ, Burgess TI, *et al.* (2017b). Fungal Planet description sheets: 625–715. *Persoonia* **39**: 270–467.
Crous PW, Wingfield MJ, Burgess TI, *et al.* (2018c). Fungal Planet description sheets: 716–784. *Persoonia* **40**: 240–393.
Crous PW, Wingfield MJ, Cheewangkoon R, *et al.* (2019d). Foliar pathogens of eucalypts. *Studies in Mycology* **94**: 125–298.
Crous PW, Wingfield MJ, Guarro J, *et al.* (2013b). Fungal Planet description sheets: 154–213. *Persoonia* **31**: 188–296.
Crous PW, Wingfield MJ, Guarro J, *et al.* (2015c). Fungal Planet description sheets: 320–370. *Persoonia* **34**: 167–266.
Crous PW, Wingfield MJ, Lombard L, *et al.* (2019e). Fungal Planet description sheets: 951–1041. *Persoonia* **43**: 223–425.
Crous PW, Wingfield MJ, Park RF (1991). *Mycosphaerella nubilosa* a synonym of *M. molleriana*. *Mycological Research* **95**: 628–632.
Cummins GB, Hiratsuka Y (2003). *Illustrated genera of rust fungi.* 3rd ed. American Phytopathological Society Press, St Paul, Minnesota, USA.
Damm U, Fourie PH, Crous PW (2010). *Coniochaeta* (*Lecythophora*), *Collophora gen. nov.* and *Phaeomoniella* species associated with wood necroses of *Prunus* trees. *Persoonia* **24**: 60–80.
Daub ME (1982). Cercosporin, a photosensitizing toxin from *Cercospora* species. *Phytopathology* **72:** 370–374.
Davidson JA, Hartley D, Priest M, *et al.* (2009). A new species of *Phoma* causes ascochyta blight symptoms on field peas (*Pisum sativum*) in South Australia. *Mycologia* **101**: 120–128.
Davison EM (1988). The role of waterlogging and *Phytophthora cinnamomi* in the decline and death of *Eucalyptus marginata* in Western Australia. *GeoJournal* **17**: 239–244.
Davison EM, Drenth A, Kumar S, *et al.* (2006). Pathogens associated with nursery plants imported into Western Australia. *Australasian Plant Pathology* **35**: 473–475.
Day MJ, Hall JC, Currah RS (2012). Phialide arrangement and character evolution in the helotialean anamorph genera *Cadophora* and *Phialocephala*. *Mycologia* **104**: 371–381.
Day WR (1938). Root-rot of sweet chestnut and beech caused by species of *Phytophthora*. I. Cause and symptoms of disease: Its relation to soil conditions. *Forestry* **12**: 101–116.
De Bary A (1876). Researches into the nature of the potato fungus. *Journal of the Royal Agricultural Society of England* **12**: 239–269.
De Cock AWAM, Lévesque CA (2004). New species of *Pythium* and *Phytophthora*. *Studies in Mycology* **50**: 481–487.

De Gruyter J, Aveskamp MM, Woudenberg JHC, *et al.* (2009). Molecular phylogeny of *Phoma* and allied anamorph genera: towards a reclassification of the *Phoma* complex. *Mycological Research* **113**: 508–519.

De Gruyter J, Boerema GH, van der Aa HA (2002). Contributions towards a monograph of *Phoma* (Coelomycetes) VI – 2. Section *Phyllostictoides*: outline of its taxa. *Persoonia* **18**: 1–53.

De Gruyter J, Noordeloos ME, Boerema GH (1993). Contributions towards a monograph of *Phoma* (Coelomycetes) – I. 2. Section *Phoma*: additional taxa with very small conidia and taxa with conidia up to 7 µm long. *Persoonia* **15**: 369–400.

De Gruyter J, Woudenberg JHC, Aveskamp MM, *et al.* (2010). Systematic reappraisal of species in *Phoma* section *Paraphoma*, *Pyrenochaeta* and *Pleurophoma*. *Mycologia* **102**: 1066–1081.

De Silva NI, Maharachchikumbura SSN, Thambugala KM, *et al.* (2021). Morpho-molecular taxonomic studies reveal a high number of endophytic fungi from *Magnolia candolli* and *M. garrettii* in China and Thailand. *Mycosphere* **11**: 163–237.

Deadman ML, Al Sa'di AM, Maqbali YM, *et al.* (2006). First report of the rust *Melampsora euphorbiae* on *Euphorbia heterophylla* in Oman. *Journal of Plant Pathology* **88**: 121.

Dean R, Van Kan JA, Pretorius ZA, *et al.* (2012). The Top 10 fungal pathogens in molecular plant pathology. *Molecular Plant Pathology* **13**: 414–430.

Deighton FC (1976). Studies on *Cercospora* and allied genera. VI. *Pseudocercospora* Speg., *Pantospora* Cif., and *Cercoseptoria* Petr. *Mycological Papers* **140**: 1–168.

Di Marco S, Calzarano F, Gams W, *et al.* (2000). A new wood decay of kiwifruit in Italy. *New Zealand Journal of Crop and Horticultural Science* **28**: 69–73.

Di Marco S, Calzarano F, Osti F, *et al*. (2004). Pathogenicity of fungi associated with a decay of kiwifruit. *Australasian Plant Pathology* **33**: 337–342.

Dianese AC, Vale HM, Souza ÉS, *et al.* (2014). New *Cercospora* species on *Jatropha curcas* in central Brazil. *Mycological Progress* **13**: 1069–1073.

Diaz GA, Latorre BA (2014). Infection caused by *Phaeomoniella chlamydospora* associated with esca-like symptoms in grapevine in Chile. *Plant Disease* **98**: 351–360.

Dick MA, Dobbie K, Cooke DEL, *et al.* (2006). *Phytophthora captiosa sp. nov.* and *P. fallax sp. nov.* causing crown dieback of *Eucalyptus* in New Zealand. *Mycological Research* **110**: 393–404.

Dorrance AE (2013). *Phytophthora sojae* on soybean. In: *Phytophthora a global perspective* (Lamour K, ed). CABI, Wallingford, UK: 79–86.

Drenth A Guest DI (eds.) (2004). Diversity and management of *Phytophthora* in Southeast Asia. Australian Centre for International Agricultural Research, Canberra, Australia.

Drenth A, Janssen EM, Govers F (1995). Formation and survival of oospores of *Phytophthora infestans* under natural conditions. *Plant Pathology* **44**: 86–94.

Duan JX, Liu XZ, Wu WP (2007). Reinstatement of *Coleonaema* for *Coleophoma oleae* and further notes on the genus *Coleophoma*. *Fungal Diversity* **26**: 187–204.

Duangsong U, Laosatit K, Somta P, *et al.* (2018). Genetics of resistance to Cercospora leaf spot disease caused by *Cercospora canescens* and *Psuedocercospora cruenta* in yardlong bean (*Vigna unguiculata* ssp. *sesquipedalis*) × grain cowpea (*V. unguiculata* ssp. *unguiculata*) populations. *Journal of Genetics* **97**: 1451–1456.

Duarte LL, Santos FMC, Barreto RW (2016). Mycobiota of the weed *Conyza canadensis* (*Asteraceae*) in Brazil. *Fungal Biology* **120**: 1118–1134.

Durán A, Gryzenhout M, Slippers B, *et al.* (2008). *Phytophthora pinifolia sp. nov*. associated with a serious needle disease of *Pinus radiata* in Chile. *Plant Pathology* **57**: 715–727.

Ehrenberg CG (1818). *Sylvae Mycologicae Berolinenses*. Berlin, Germany.

Ekanayaka AH, Daranagama DA, Ariyawansa HA, *et al.* (2016). *Pezicula chiangraiensis sp. nov*. from Thailand. *Mycotaxon* **131**: 739–748.

Ekanayaka AH, Hyde KD, Gentekaki E, *et al.* (2019). Preliminary classification of *Leotiomycetes. Mycosphere* **10**: 310–489.

Elliott CG, Hendrie MR, Knights BA (1966). The sterol requirement of *Phytophthora cactorum*. *Journal of General Microbiology* **42**: 425–435.

Ellis MB (1971). *Dematiaceous Hyphomycetes*. Commonwealth Mycological Institute, Kew, UK.

Erwin DC, Ribeiro OK (1996). *Phytophthora diseases worldwide*. APS Press, St. Paul, Minnesota, USA.

Fan XL, Bezerra JDP, Tian CM, *et al.* (2018). Families and genera of diaporthalean fungi associated with canker and dieback of tree hosts. *Persoonia* **40**: 119–134.

Fan XL, Bezerra JDP, Tian CM, *et al.* (2020). *Cytospora* (*Diaporthales*) in China. *Persoonia* **45**: 1–45.

Fan XL, Hyde KD, Liu M, *et al.* (2015a). *Cytospora* species associated with walnut canker disease in China, with description of a new species *C. gigalocus*. *Fungal Biology* **119**: 310–319.

Fan XL, Hyde KD, Yang Q, *et al.* (2015b). *Cytospora* species associated with canker disease of three anti-desertification plants in northwestern China. *Phytotaxa* **197**: 227–244.

Fan XL, Liang YM, Ma R, *et al.* (2014a). Morphological and phylogenetic studies of *Cytospora* (*Valsaceae*, *Diaporthales*) isolates from Chinese scholar tree, with description of a new species. *Mycoscience* **55**: 252–259.

Fan XL, Tian CM, Yang Q, *et al.* (2014b). *Cytospora* from *Salix* in northern China. *Mycotaxon* **129**: 303–315.

Farr DF, Rossman AY (2022). *Fungal Databases, Systematic Mycology and Microbiology Laboratory, ARS, USDA*. Available online at https://nt.ars-grin.gov/fungaldatabases.

Feau N, Taylor G, Dale AL, *et al.* (2016). Genome sequences of six *Phytophthora* species threatening forest ecosystems. *Genomics Data* **10**: 85–88.

Feau N, Vialle A, Allaire M, *et al*. (2009). Fungal pathogen (mis-) identifications: A case study with DNA barcodes on *Melampsora* rusts of aspen and white poplar. *Mycological Research* **113**: 713–724.

Fletcher K, Klosterman SJ, Derevnina L, *et al*. (2018). Comparative genomics of downy mildews reveals potential adaptations to biotrophy. *BMC Genomics* **19**: 8–10.

Fletcher K, Gil J, Bertier LD, *et al.* (2019). Genomic signatures of heterokaryosis in the oomycete pathogen *Bremia lactucae*. *Nature Communications* **10**: 1–13.

Flier WG, Grünwald NJ, Kroon LPNM, *et al.* (2002). *Phytophthora ipomoeae sp. nov*., a new homothallic species causing leaf blight on *Ipomoea longipedunculata* in the Toluca Valley of central Mexico. *Mycological Research* **106**: 848–856.

Forbes GA, Morales JG, Restrepo S, *et al.* (2013). *Phytophthora infestans* and *Phytophthora andina* on solanaceous hosts in South America. In: *Phytophthora a global perspective* (Lamour K, ed). CABI, Wallingford, UK: 46–58.

Fries EM (1849). *Summa Vegetabilium Scandinaviae*. Holmiae & Lipsiae, Uppsala.

Galindo AJ, Hohl HR (1985). *Phytophthora mirabilis*, a new species of *Phytophthora*. *Sydowia Annales Mycologici Series II* **38**: 87–96.

Gams W (2000). *Phialophora* and some similar morphologically little-differentiated anamorphs of divergent ascomycetes. *Studies in Mycology* **45**: 187–199.

Gatica M, Cesari C, Magnin S, *et al.* (2001). *Phaeoacremonium* species and *Phaeomoniella chlamydospora* in vines showing "hoja de malvon" and young vine decline symptoms in Argentina. *Phytopathologia Mediterranea* **40**: S317–S324.

Ginetti B, Moricca S, Squires JN, *et al.* (2014). *Phytophthora acerina sp. nov*., a new species causing bleeding cankers and dieback of *Acer pseudoplatanus* trees in planted forests in Northern Italy. *Plant Pathology* **63**: 858–876.

Giraldo A, Crous PW, Schumacher RK, *et al.* (2017). The Genera of Fungi – G3: *Aleurocystis*, *Blastacervulus*, *Clypeophysalospora*, *Licrostroma*, *Neohendersonia* and *Spumatoria*. *Mycological Progress* **16**: 325–348.

Goh TK, Hsieh WH (1987). Studies on *Cercospora* and Allied genera of Taiwan (IV): New combinations of *Cercospora* species. *Transaction of Mycological Society of Republic of China* **2**: 113-123.

Gomes RR, Glienke C, Videira SIR, *et al.* (2013). *Diaporthe*: a genus of endophytic, saprobic and plant pathogenic fungi. *Persoonia* **31**: 1–41.

Goodwin SB, Dunkle LD, Zismann VL (2001). Phylogenetic analysis of *Cercospora* and *Mycosphaerella* based on the internal transcribed spacer region of ribosomal DNA. *Phytopathology* **91**: 648–658.

Goss EM, Cardenas ME, Myers K, *et al.* (2011). The plant pathogen *Phytophthora andina* emerged via hybridization of an unknown *Phytophthora* species and the Irish potato famine pathogen, *P. infestans*. *PLoS ONE* **6**: e24543.

Graham JH, Luttrell ES (1961). Species of *Leptosphaerulina* on forage plants. *Phytopathology* **51**: 680–693.

Graham JH, Menge JA (2000). *Phytophthora*-induced diseases. In: *Compendium of Citrus Diseases*. 2nd edition. APS Press, St Paul, MN, USA: 12–15.

Gramaje D, García-Jiménez J, Armengol J (2010). Grapevine rootstock susceptibility to fungi associated with Petri disease and esca under field conditions. *American Journal of Enology and Viticulture* **61**: 512–520.

Gramaje D, León M, Santana M, *et al.* (2014). Multilocus ISSR markers reveal two major genetic groups in Spanish and South African populations of the grapevine fungal pathogen *Cadophora luteo-olivacea*. *PLoS ONE* **9**: e110417.

Gramaje D, Mostert L, Armengol J (2011). Chracterization of *Cadophora luteo-olivacea* and *C. melinii* isolates obtained from grapevines and environmental samples from grapevine nurseries in Spain. *Phytopathologia Mediterranea* **50**: S112–S126.

Granke L, Quesada-Ocampo L, Hausbeck M. (2013). *Phytophthora capsici* in the Eastern USA. In: *Phytophthora a global perspective* (Lamour K, ed). CABI, Wallingford, UK: 96–103.

Green S, Brasier CM, Schlenzig A, *et al.* (2013). The destructive invasive pathogen *Phytophthora lateralis* found on *Chamaecyparis lawsoniana* across the UK. *Forest Pathology* **43**: 19–28.

Green S, Elliot M, Armstrong A, *et al.* (2015). *Phytophthora austrocedrae* emerges as a serious threat to juniper (*Juniperus communis*) in Britain. *Plant Pathology* **64**: 456–466.

Greslebin AG, Hansen EM, Sutton W. (2007). *Phytophthora austrocedrae sp. nov*., a new species associated with *Austrocedrus chilensis* mortality in Patagonia Argentina. *Mycological Research* **111**: 308–316.

Groenewald M, Bellstedt DU, Crous PW (2000). A PCR-based method for the detection of *Phaeomoniella chlamydospora* in grapevines. *South African Journal of Science* **96**: 43–46.

Groenewald M, Kang JC, Crous PW, *et al.* (2001). ITS and β-tubulin phylogeny of *Phaeoacremonium* and *Phaeomoniella* species. *Mycological Research* **105**: 651–657.

Groenewald JZ, Nakashima C, Nishikawa J, *et al.* (2013). Species concepts in *Cercospora*: spotting the weeds among the roses. *Studies in Mycology* **75**: 115–170.

Groenewald M, Groenewald JZ, Crous PW (2005). Distinct species exist within the *Cercospora apii* morphotype. *Phytopathology* **95**: 951–959.

Groenewald M, Groenewald JZ, Braun U, *et al.* (2006a). Host range of *Cercospora apii* and *C. beticola* and description of *C. apiicola*, a novel species from celery. *Mycologia* **98**: 275–285.

Groenewald M, Groenewald JZ, Harrington TC, *et al.* (2006b). Mating type gene analysis in apparently asexual *Cercospora* species is suggestive of cryptic sex. *Fungal Genetics and Biology* **43**: 813–825.

Groenewald M, Linde CC, Groenewald JZ, *et al.* (2008). Indirect evidence for sexual reproduction in *Cercospora beticola* populations from sugar beet. *Plant Pathology* **57**: 25–32.

Grünwald NJ, Goss EM, Press CM (2008). *Phytophthora ramorum*: a pathogen with a remarkably wide host range causing Sudden Oak Death on oaks and ramorum blight on woody ornamentals. *Molecular Plant Pathology* **9**: 729–740.

Gryzenhout M, Myburg H, Wingfield BD, *et al.* (2006). *Cryphonectriaceae* (*Diaporthales*), a new family including *Cryphonectria*, *Chrysoporthe*, *Endothia* and allied genera. *Mycologia* **98**: 239–249.

Gryzenhout M, Wingfield BD, Wingfield MJ (2009). *Taxonomy, phylogeny, and ecology of barkinhabiting and tree pathogenic fungi in the Cryphonectriaceae*. St Paul, MN, USA: APS Press.

Guatimosim E, Schwartsburd PB, Barreto RW, *et al.* (2016). Novel fungi from an ancient niche: cercosporoid and related sexual morphs on ferns. *Persoonia* **37**: 106–141.

Guillin EA, de Oliveira LO, Grijalba PE, *et al.* (2017). Genetic entanglement between *Cercospora* species associating soybean purple seed stain. *Mycological Progress* **16**: 593–603.

Gurevich A, Saveliev V, Vyahhi N, *et al.* (2013). QUAST: quality assessment tool for genome assemblies. *Bioinformatics* **29**: 1072–1075.

Haas BJ, Kamoun S, Zody MC, *et al.* (2009). Genome sequence and analysis of the Irish potato famine pathogen *Phytophthora infestans*. *Nature* **461**: 393–398.

Halleen F, Crous PW, Petrini O (2003). Fungi associated with healthy grapevine cuttings in nurseries, with special reference to pathogens involved in the decline of young vines. *Australasian Plant Pathology* **32**: 47–52.

Halleen F, Mostert L, Crous PW (2007). Pathogenicity testing of lesser-known vascular fungi of grapevines. *Australasian Plant Pathology* **36**: 277–285.

Hamm PB, Hansen EM (1983). *Phytophthora pseudotsugae* a new species causing root rot of Douglas fir. *Canadian Journal of Botany* **61**: 2626–2631.

Hansen EM, Maxwell DP (1991). Species of the *Phytophthora megasperma* complex. *Mycologia* **83**: 376–381.

Hansen EM, Goheen DJ, Jules ES, *et al.* (2000). Managing Port-Orford-cedar and the introduced pathogen *Phytophthora lateralis*. *Plant Disease* **84**: 4–14.

Hansen EM, Reeser PW, Davidson JM, *et al.* (2003). *Phytophthora nemorosa*, a new species causing cankers and leaf blight of forest trees in California and Oregon, U.S.A. *Mycotaxon* **88**: 129–138.

Hansen EM, Reeser PW, Sutton W. (2012). *Phytophthora borealis* and *Phytophthora riparia*, new species in *Phytophthora* ITS Clade 6. *Mycologia* **104**: 1133–1142.

Hansen EM, Reeser P, Sutton W, *et al.* (2015). Redesignation of *Phytophthora* taxon Pgchlamydo as *Phytophthora chlamydospora sp. nov. North American Fungi* **10**: 1–14.

Hansen EM, Reeser PW, Sutton W (2017). Ecology and pathology of *Phytophthora* ITS clade 3 species in forests in western Oregon, USA. *Mycologia* **109**: 100–114.

Hansen EM, Wilcox WF, Reeser PW, *et al.* (2009). *Phytophthora rosacearum* and *P. sansomeana*, new species segregated from the *Phytophthora megasperma* "complex". *Mycologia* **101**: 129–135.

Hansen EM, Reeser PW, Sutton W (2012). *Phytophthora* beyond agriculture. *Annual Review of Phytopathology* **50**: 359–378.

Hardham AR, Blackman LM (2018). *Phytophthora cinnamomi*. *Molecular Plant Pathology* **19**: 260–285.

Haridas S, Albert R, Binder M, *et al.* (2020). 101 *Dothideomycetes* genomes: A test case for predicting lifestyles and emergence of pathogens. *Studies in Mycology* **96**: 141–153.

Harrington TC, McNew DL (2003). Phylogenetic analysis places the Phialophora-like anamorph genus *Cadophora* in the *Helotiales*. *Mycotaxon* **87**: 41–151.

Harris DC (1991). The Phytophthora disease of apple. *Journal of Horticultural Sciences* **66**: 513–544.

Hartman GL, Chen SC, Wang TC (1991). Cultural studies and pathogenicity of *Pseudocercospora fuligena,* the causal agent of Black leaf mold of Tomato. *Plant Disease* **75**: 1060–1063.

Haverkort AJ, Boonekamp PM, Hutten R, *et al.* (2008). Societal costs of late blight in potato and prospects of durable resistance through cisgenic modification. *Potato Research* **51**: 47–57.

Held BW, Jurgens JA, Arenz BE, *et al.* (2005). Environmental factors influencing microbial growth inside the historic expedition huts of Ross Island, Antarctica. *International Biodeterioration & Biodegradation* **55**: 45–53.

Henricot B, Pérez-Sierra A, Jung T (2014). *Phytophthora pachypleura sp. nov*., a new species causing root rot of *Aucuba japonica* and other ornamentals in the United Kingdom. *Plant Pathology* **63**: 1095–1109.

Hernández-Restrepo M, Groenewald JZ, Elliott ML, *et al.* (2016). Take-all or nothing. *Studies in Mycology* **83**: 19–48.

Heyman F, Blair JE, Persson L, *et al.* (2013). Root rot of pea and faba bean in southern Sweden caused by *Phytophthora pisi*, *sp. nov*. *Plant Disease* **97**: 461–471.

Hiratsuka N, Kaneko S (1982). A taxonomic revision of *Melampsora* on

willows in Japan. *Reports of the Tottori Mycological Institute* **20**: 1–32.
Hong CX, Gallegly ME, Browne GT, *et al.* (2009). The avocado subgroup of *Phytophthora citricola* constitutes a distinct species, *Phytophthora mengei sp. nov. Mycologia* **101**: 833–840.
Hong CX, Gallegly ME, Richardson PA, *et al.* (2011). *Phytophthora pini* Leonian resurrected to distinct species status. *Mycologia* **103**: 351–360.
Hou LW, Groenewald JZ, Pfenning LH, *et al.* (2020a). The phoma-like dilemma. *Studies in Mycology* **96**: 309–396.
Hou LW, Hernández-Restrepo M, Groenewald JZ, *et al.* (2020b). Citizen science project reveals high diversity in *Didymellaceae* (*Pleosporales, Dothideomycetes*). *MycoKeys* **65**: 49–99.
Hsieh WH, Goh TK (1990). *Cercospora and Similar Fungi from Taiwan*. Taiwan, Taipei: Maw Chang Book Company.
Hüberli D, Hardy GEStJ, White D, *et al.* (2013). Fishing for *Phytophthora* from Western Australia's waterways: a distribution and diversity survey. *Australasian Plant Pathology* **42**: 251–260.
Huerta-Cepas J, Forslund K, Coelho LP, *et al.* (2017). Fast genome-wide functional annotation through orthology assignment by eggNOG-mapper. *Molecular Biology and Evolution* **34**: 2115–2122.
Hudson HJ (1963). The perfect state of *Nigrospora oryzae*. *Transactions of the British Mycological Society* **46**: 355–360.
Hujslova M, Kubatova A, Chudıckova M, *et al.* (2010). Diversity of fungal communities in saline and acidic soils in the Soos National Natural Reserve, Czech Republic. *Mycological Progress* **9**: 1–15.
Husson C, Aguayo J, Revellin C, *et al.* (2015). Evidence for homoploid speciation in *Phytophthora alni* supports taxonomic reclassification in this species complex. *Fungal Genetics and Biology* **77**: 12–21.
Hyde KD, Chaiwan N, Norphanphoun C, *et al.* (2018). Mycosphere notes 169–224. *Mycosphere* **9**: 271–430.
Hyde KD, Dong Y, Phookamsak R, *et al.* (2020). Fungal diversity notes 1151–1276: taxonomic and phylogenetic contributions on genera and species of fungal taxa. *Fungal Diversity* **100**: 5–277.
Inderbitzin P, Jones EBG, Vrijmoed LLP (2000). A new species of *Leptosphaerulina* from decaying mangrove wood from Hong Kong. *Mycoscience* **41**: 233–237.
Inglis PW, Teixeira EA, Ribeiro DM, *et al.* (2001). Molecular markers for the characterization of Brazilian *Cercospora caricis* isolates. *Current Microbiology* **42**: 194–198.
Ismail SI, Batzer JC, Harrington TC, *et al.* (2016). Ancestral state reconstruction infers phytopathogenic origins of sooty blotch and flyspeck fungi on apple. *Mycologia* **108**: 292–302.
Ito K, Kobayashi T (1953). Contributions to the diseases of poplars in Japan-II. The Cercospora leaf spot of poplars with special reference to the life history of the causal fungus. *Bulletin of the Government Forest Experiment Station* **59**: 1–28.
Jaklitsch WM, Voglmayr H (2019). European species of *Dendrostoma* (*Diaporthales*). *MycoKeys* **59**: 1–26.
Jami F, Marincowitz S, Crous PW, *et al.* (2018). A new *Cytospora* species pathogenic on *Carpobrotus edulis* in its native habitat. *Fungal Systematics and Evolution* **2**: 37–43.
Jayawardena RS, Hyde KD, Jeewon R, *et al.* (2019). One stop shop II: taxonomic update with molecular phylogeny for important phytopathogenic genera: 26–50 (2019). *Fungal Diversity* **94**: 41–129.
Jeffers SN, Martin SB (1986). Comparison of two media selective for *Phytophthora* and *Pythium* species. *Plant Disease* **70**: 1038–1043.
Jellis GJ, Punithalingam E (1991). Discovery of *Didymella fabae sp. nov*., the teleomorph of *Ascochyta fabae*, on faba bean straw. *Plant Pathology* **40**: 150–157.
Jiang N, Fan XL, Crous PW, *et al.* (2019a). Species of *Dendrostoma* (*Erythrogloeaceae, Diaporthales*) associated with chestnut and oak canker diseases in China. *MycoKeys* **48**: 67–96.
Jiang N, Fan XL, Tian CM (2019b). Identification and pathogenicity of *Cryphonectriaceae* species associated with chestnut canker in China. *Plant Pathology* **68**: 1132–1145.
Jiang N, Fan XL, Tian CM, *et al.* (2020). Re-evaluating *Cryphonectriaceae* and allied families in *Diaporthales*. *Mycologia* **112**: 267–292.
Johnston PR, Quijada L, Smith CA, *et al.* (2019). A multigene phylogeny toward a new phylogenetic classification of *Leotiomycetes*. *IMA Fungus* **10**:1–22.
Johnston PR, Seifert KA, Stone JK, *et al.* (2014). Recommendations on generic names competing for use in *Leotiomycetes* (*Ascomycota*). *IMA Fungus* **5**: 91–120.
Jönsson U, Jung T, Sonesson K, *et al.* (2005). Relationships between *Quercus robur* health, occurrence of *Phytophthora* species and site conditions in southern Sweden. *Plant Pathology* **54**: 502–511.
Jung T (2009). Beech decline in Central Europe driven by the interaction between *Phytophthora* infections and climatic extremes. *Forest Pathology* **39**: 73–94.
Jung T, Blaschke M (2004). Phytophthora root and collar rot of alders in Bavaria: distribution, modes of spread and possible management strategies. *Plant Pathology* **53**: 197–208.
Jung T, Burgess TI (2009). Re-evaluation of *Phytophthora citricola* isolates from multiple woody hosts in Europe and North America reveals a new species, *Phytophthora plurivora sp. nov*. *Persoonia* **22**: 95–110.
Jung T, Blaschke H, Neumann P (1996). Isolation, identification and pathogenicity of *Phytophthora* species from declining oak stands. *European Journal of Forest Pathology* **26**: 253–272.
Jung T, Blaschke H, Osswald W (2000). Involvement of soilborne *Phytophthora* species in Central European oak decline and the effect of site factors on the disease. *Plant Pathology* **49**: 706–718.
Jung T, Chang TT, Bakonyi J, *et al.* (2017c). Diversity of *Phytophthora* species in natural ecosystems of Taiwan and association with disease symptoms. *Plant Pathology* **66**: 194–211.
Jung T, Colquhoun IJ, Hardy GEStJ (2013a). New insights into the survival strategy of the invasive soilborne pathogen *Phytophthora cinnamomi* in different natural ecosystems in Western Australia. *Forest Pathology* **43**: 266–288.
Jung T, Cooke DEL, Blaschke H, *et al.* (1999). *Phytophthora quercina sp. nov*., causing root rot of European oaks. *Mycological Research* **103**: 785–798.
Jung T, Durán A, Sanfuentes von Stowasser E, *et al.* (2018b). Diversity of *Phytophthora* species in Valdivian rainforests and association with severe dieback symptoms. *Forest Pathology* **48**: e12443.
Jung T, Hansen EM, Winton L, *et al.* (2002). Three new species of *Phytophthora* from European oak forests. *Mycological Research* **106**: 397–411.
Jung T, Horta Jung M, Cacciola SO, *et al.* (2017b). Multiple new cryptic pathogenic *Phytophthora* species from *Fagaceae* forests in Austria, Italy and Portugal. *IMA Fungus* **8**: 219–244.
Jung T, Horta Jung M, Scanu B, *et al.* (2017a). Six new *Phytophthora* species from ITS Clade 7a including two sexually functional heterothallic hybrid species detected in natural ecosystems in Taiwan. *Persoonia* **38**: 100–135.
Jung T, Horta Jung M, Webber JF, *et al.* (2021). The destructive tree pathogen *Phytophthora ramorum* originates from the Laurosilva forests of East Asia. *Journal of Fungi* **7**: 226.
Jung T, Nechwatal J, Cooke DEL, *et al.* (2003). *Phytophthora pseudosyringae sp. nov*., a new species causing root and collar rot of deciduous tree species in Europe. *Mycological Research* **107**: 772–789.
Jung T, Orlikowski L, Henricot B, *et al.* (2016). Widespread *Phytophthora* infestations in European nurseries put forest, semi-natural and horticultural ecosystems at high risk of Phytophthora diseases. *Forest Pathology* **46**: 134–163.
Jung T, Pérez–Sierra A, Durán A, *et al.* (2018a). Canker and decline diseases caused by soil- and airborne *Phytophthora* species in forests and woodlands. *Persoonia* **40**: 182–220.
Jung T, Scanu B, Bakonyi, J, *et al.* (2017d). *Nothophytophthora gen. nov*., a new sister genus of *Phytophthora* from natural and semi-natural ecosystems. *Persoonia* **39**: 143–174.
Jung T, Scanu B, Brasier CM, *et al.* (2020). A survey in natural forest ecosystems of Vietnam reveals high diversity of both new and described *Phytophthora* taxa including *P. ramorum*. *Forests* **11**: 93.
Jung T, Stukely MJC, Hardy GEStJ, *et al.* (2011). Multiple new *Phytophthora* species from ITS Clade 6 associated with natural ecosystems in Australia: evolutionary and ecological implications. *Persoonia* **26**: 13–39.

Jung T, Vettraino AM, Cech TL, *et al.* (2013b). The impact of invasive *Phytophthora* species on European forests. In: *Phytophthora a global perspective* (Lamour K, ed). CABI, Wallingford, UK: 146–158.

Kaiser WJ, Wang BC, Rogers JD (1997). *Ascochyta fabae* and *A. lentis*: Host specificity, teleomorphs (*Didymella*), hybrid analysis, and taxonomic status. *Plant Disease* **81**: 809–816.

Katsuki S, Kobayashi T (1975). Cercosporae of Japan (Supplement 3). *Transaction of Mycological Society of Japan* **16**: 1–15.

Kee YJ, Hafifi ABM, Huda-Shakirah AR, *et al.* (2019). First report of reddish brown spot disease of red-fleshed dragon fruit (*Hylocereus polyrhizus*) caused by *Nigrospora lacticolonia* and *Nigrospora sphaerica* in Malaysia. *Crop Protection* **122**: 165–170.

Kennedy DM, Duncan JM (1995). A papillate *Phytophthora* species with specificity to *Rubus*. *Mycological Research* **99**: 57–68.

Kerry E (1990). Microorganisms colonizing plants and soil subjected to different degrees of human activity, including petroleum contamination, in the Vestfold Hills and MacRobertson Land, Antarctica. *Polar Biology* **10**: 423–430.

Kimber RBE (2011). *Epidemiology and management of Cercospora leaf spot (Cercospora zonata) of faba beans (Vicia faba).* PhD thesis, Faculty of Sciences, University of Adelaide, Australia.

Kirk PM, Cannon PF, Minter DW, *et al.* (2008). *Dictionary of the fungi*, 10th edn. CABI, Wallingford, UK.

Kirk PM, Stalpers JA, Braun U, *et al.* (2013). A without-prejudice list of generic names of fungi for protection under the International Code of Nomenclature for algae, fungi and plants. *IMA Fungus* **4**: 381–443.

Kirschner R, Liu LC (2014). Mycosphaerellaceous fungi and new species of *Venustosynnema* and *Zasmidium* on ferns and fern allies in Taiwan. *Phytotaxa* **176**: 309–323.

Kirschner R, Okuda T (2013). A new species of *Pseudocercospora* and new record of *Bartheletia paradoxa* on leaves of *Ginkgo biloba*. *Mycological Progress* **12**: 421–426.

Kirschner R, Wang H (2015). New species and records of mycosphaerellaceous fungi from living fern leaves in East Asia. *Mycological Progress* **14**: 65.

Knapp DG, Németh JB, Barry K, *et al.* (2018). Comparative genomics provides insights into the lifestyle and reveals functional heterogeneity of dark septate endophytic fungi. *Scientific Reports* **8**: 6321.

Kobayashi T (1970). Taxonomic studies of Japanese *Diaporthaceae* with special reference to their life histories. *Bulletin of the Government Forest Experiment Station* **226**: 132–147.

Kobayashi T, Nakashima C, Nishijima T (2002). Addition and re-examination of Japanese species belonging to the genus *Cercospora* and allied genera. V. Collections from the Nansei Islands (2). *Mycoscience* **43**: 219–227.

Koukol O, Maciá-Vicnete JG (2022). *Leptodophora gen. nov*. (*Helotiales*, *Leotiomycetes*) proposed to accommodate selected root-associated members of the genus *Cadophora*. *Czech Mycology* **74**: 57–66.

Kuprevich VF, Tranzschel VG (1957). Rust fungi. 1. Family *Melampsoraceae*. In: *Cryptogamic plants of the USSR* (Savich VP, ed). Botanicheskogo Instituta, Komarova, Russia: 1–518.

Kushalappa AC, Boivin G, Brodeur L (1989). Forecasting incidence thresholds of Cercospora blight in carrots to initiate fungicide application. *Plant Disease* **73**: 979–983.

Lamour K. (ed) (2013). *Phytophthora* a global perspective. CABI, Wallingford, UK. 96.

Larignon P, Dubos B (1997). Fungi associated with esca disease in grapevine. *European Journal of Plant Pathology* **103**: 147–157.

Lawrence DP, Travadon R, Pouzoulet J, *et al.* (2017). Characterization of *Cytospora* isolates from wood cankers of declining grapevine in North America, with the descriptions of two new *Cytospora* species. *Plant Pathology* **5**: 713–725.

Lawrence DP, Holland LA, Nouri MT, *et al.* (2018). Molecular phylogeny of *Cytospora* species associated with canker diseases of fruit and nut crops in California, with the descriptions of ten new species and one new combination. *IMA Fungus* **9**: 333–370.

Lee HB, Park JY, Jung HS, *et al.* (2006). *Phaeomoniella zymoides* and *Phaeomoniella pinifoliorum spp. nov.*, new acid-tolerant epiphytic fungi isolated from pine needles in Korea. *Mycologia* **98**: 598–611.

Lee SH, Kim CS, Kang KS, *et al.* (2017). Morphological and molecular identification of *Melampsora idesiae* on *Idesia polycarpa* in Korea. *Australasian Plant Disease Notes* **12**: 46.

Li DW, Schultes NP, LaMondia JA, *et al.* (2019). *Phytophthora abietivora*, a new species isolated from diseased Christmas trees in Connecticut, USA. *Plant Disease* **103**: 3057–3064.

Li J, Jeewon R, Phookamsak R, *et al.* (2018). *Marinophialophora garethjonesii gen. et sp. nov.*: a new hyphomycete associated with *Halocyphina* from marine habitats in Thailand. *Phytotaxa* **345**: 1–12.

Libert MA (1830). *Plantae cryptogamicae, quas in Arduenna collegit*. Fascicle I (*exsiccata*).

Linnakoski R, Kasanen R, Lasarov I, *et al.* (2018). *Cadophora margaritata sp. nov.* and other fungi associated with the longhorn beetles *Anoplophora glabripennis* and *Saperda carcharias* in Finland. *Antonie van Leeuwenhoek* **111**: 2195–2211.

Liu F, Chen S, Ferreira MA, *et al.* (2019). Draft genome sequences of five *Calonectria* species from *Eucalyptus* plantations in China, *Celoporthe dispersa*, *Sporothrix phasma* and *Alectoria sarmentosa*. *IMA Fungus* **10**: 22.

Love J, Palmer J, Stajich J, *et al.* (2019). nextgenusfs/funannotate: funannotate v1.7.0 (1.7.0). *Zenodo*. https://doi.org/10.5281/zenodo.3534297.

Luque J, Martos S, Aroca A, *et al.* (2009). Symptoms and fungi associated with declining mature grapevine plants in Northeast Spain. *Journal of Plant Pathology* **91**: 381–390.

Ma R, Liu YM, Yin YX, *et al.* (2018). A canker disease of apple caused by *Cytospora parasitica* recorded in China. *Forest Pathology* **48**: 12–17.

Maciá-Vicente JG, Piepenbring M, Koukol O (2020). Brassicaceous roots as an unexpected diversity hot-spot of helotialean endophytes. *IMA Fungus* **11**: 16.

Maier W, Begerow D, Weiß M, *et al.* (2003). Phylogeny of the rust fungi: an approach using nuclear large subunit ribosomal DNA sequences. *Canadian Journal of Botany* **81**: 12–23.

Maldonado-González MM, Martínez-Diz MP, Andrés-Sodupe M, *et al.* (2020). Quantification of *Cadophora luteo-olivacea* from grapevine nursery stock and vineyard soil using droplet digital PCR. *Plant Disease* **104**: 2269–2274.

Man in' t Veld WA (2007). Gene flow analysis demonstrates that *Phytophthora fragariae* var. *rubi* constitutes a distinct species, *Phytophthora rubi comb. nov*. *Mycologia* **99**: 222–226.

Man in' t Veld WA, de Cock AWAM, Ilieva E, *et al.* (2002). Gene flow analysis of *Phytophthora porri* reveals a new species: *Phytophthora brassicae sp. nov*. *European Journal of Plant Pathology* **108**: 51–62.

Man in' t Veld WA, Rosendahl KCHM, Brouwer H, *et al.* (2015). *Phytophthora gemini sp. nov.*, a new species isolated from the halophilic plant *Zostera marina* in the Netherlands. *Fungal Biology* **115**: 724–732.

Man in' t Veld WA, Rosendahl KCHM, Hong C (2012). *Phytophthora xserendipita sp. nov*. and *P. xpelgrandis*, two destructive pathogens generated by natural hybridization. *Mycologia* **104**: 1390–1396.

Man in' t Veld WA, Rosendahl KCHM, van Rijswick PCJ, *et al.* (2011). *Phytophthora terminalis sp. nov.* and *Phytophthora occultans sp. nov.*, two invasive pathogens of ornamental plants in Europe. *Mycologia* **107**: 54–65.

Man in' t Veld WA, Rosendahl KCHM, van Rijswick PCJ, *et al.* (2019). Multiple *Halophytophthora* spp. and *Phytophthora* spp. including *P. gemini*, *P. inundata* and *P. chesapeakensis sp. nov*. isolated from the seagrass *Zostera marina* in the Northern hemisphere. *European Journal of Plant Pathology* **153**: 341–357.

Marin-Felix Y, Groenewald JZ, Cai L, *et al.* (2017). Genera of phytopathogenic fungi: GOPHY 1. *Studies in Mycology* **86**: 99–216.

Marin-Felix Y, Hernández-Restrepo M, Iturrieta-González I, *et al.* (2019a). Genera of phytopathogenic fungi: GOPHY 3. *Studies in Mycology* **94**: 1–124.

Marin-Felix Y, Hernández-Restrepo M, Wingfield MJ, *et al.* (2019b). Genera of phytopathogenic fungi: GOPHY 2. *Studies in Mycology* **92**: 47–133.

Martín MT, Cobos R, Martín L, *et al.* (2012). Real-Time PCR detection of *Phaeomoniella chlamydospora* and *Phaeoacremonium aleophilum*. *Applied Environmental Microbiology* **78**: 3985–3991.

Martos S, Torres E, El Bakali MA, *et al.* (2011). Co-operational PCR

coupled with dot blot hybridization for the detection of *Phaeomoniella chlamydospora* on infected grapevine wood. *Journal of Phytopathology* **159**: 247–254.

Masago H, Yoshikawa M, Fukada M, *et al.* (1977). Selective inhibition of *Pythium* spp. on a medium for direct isolation of *Phytophthora* spp. from soils and plants. *Phytopathology* **67**: 425–428.

Matsumoto T (1920). Culture experiments with *Melampsora* in Japan. *Annals of the Missouri Botanical Garden* **6**: 309–316.

May KJ, Drenth A, Irwin JAG (2003). Interspecific hybrids between the homothallic *Phytophthora sojae* and *Phytophthora vignae*. *Australasian Plant Pathology* **32**: 353–359.

McCarthy CGP, Fitzpatrick DA (2017). Phylogenomic reconstruction of the oomycete phylogeny derived from 37 genomes. *mSphere* **2**: e00095–17.

McGowan J, O'Hanlon R, Owens RA, *et al.* (2020). Comparative genomic and proteomic analyses of three widespread *Phytophthora* species: *Phytophthora chlamydospora*, *Phytophthora gonapodyides* and *Phytophthora pseudosyringae*. *Microorganisms* **8**: 653.

Mchau GRA, Coffey MD (1995). Evidence for the existence of two subpopulations in *Phytophthora capsici* and a redescription of the species. *Mycological Research* **99**: 89–102.

Meghvansi MK, Khan MH, Gupta R, *et al.* (2013). Identification of a new species of *Cercospora* causing leaf spot disease in *Capsicum assamicum* in northeastern India. *Research in Microbiology* **164**: 894–902.

Micales JA, Stipes RJ (1987). A re-examination of the fungal genera *Cryphonectria* and *Endothia*. *Phytopathology* **77**: 650–654.

Mideros MF, Turissini DA, Guayazán N, *et al.* (2018). *Phytophthora betacei*, a new species within *Phytophthora* clade 1c causing late blight on *Solanum betaceum* in Colombia. *Persoonia* **41**: 39–55.

Milenković I, Keča N, Karadžić D, *et al.* (2018). Isolation and pathogenicity of *Phytophthora* species from poplar plantations in Serbia. *Forests* **9**: 330.

Minter DW (1985). A re-appraisal of the relationships between *Arthrinium* and other hyphomycetes. *Proceedings / Indian Academy of Sciences* **94**: 281–308.

Mirabolfathy M, Cooke DEL, Duncan JM, *et al.* (2001). *Phytophthora pistaciae sp. nov*. and *P. melonis*: the principal causes of pistachio gummosis in Iran. *Mycological Research* **105**: 1166–1175.

Miyake I (1912). Studies in Chinese Fungi. *Botanical Magazine Tokyo* **26**: 51–66.

Miyasaka SC, Lamour K, Shintaku M, *et al.* (2013). Taro leaf blight caused by *Phytophthora colocasiae*. In: *Phytophthora a global perspective* (Lamour K, ed). CABI, Wallingford, UK: 104–112.

Montagne JFC (1845). Note sur la maladie qui ravage les pommes de terre et characteres du *Botrytis infestans* (Note on the disease that ravages potatoes and characters of *Botrytis infestans*). *Bulletin de la Société Philomatique de Paris* **13**: 312–313.

Moralejo E, Pérez-Sierra A, Alvarez LA, *et al.* (2009). Multiple alien *Phytophthora* taxa discovered on diseased ornamental plants in Spain. *Plant Pathology* **58**: 100–110.

Morales-Cruz A, Amrine KC, Blanco-Ulate B, *et al.* (2015). Distinctive expansion of gene families associated with plant cell wall degradation, secondary metabolism, and nutrient uptake in the genomes of grapevine trunk pathogens. *BMC Genomics* **16**: 469.

Morrell JJ, Zabel RA (1985). Wood strength and weight loss caused by soft-rot fungi isolated from treated southern pine utility poles. *Wood and Fiber Science* **17**: 132–143.

Mostert L, Abeln ECA, Halleen F, *et al.* (2006). Genetic diversity among isolates of *Phaeomoniella chlamydospora* on grapevines. *Australasian Journal of Plant Pathology* **35**: 453–460.

Mugnai L, Graniti A, Surico G (1999). Esca (black measles) and brown wood-streaking: two old and elusive diseases of grapevines. *Plant Disease* **83**: 404–418.

Myburg H, Gryzenhout M, Wingfield BD, *et al.* (2004). Phylogenetic relationships of *Cryphonectria* and *Endothia* species, based on DNA sequence data and morphology. *Mycologia* **96**: 990–1001.

Nagel JH, Gryzenhout M, Slippers B, *et al.* (2013). Characterization of *Phytophthora* hybrids from ITS clade 6 associated with riparian ecosystems in South Africa and Australia. *Fungal Biology* **117**: 329–347.

Nakabonge G, Gryzenhour M, Roux J, *et al.* (2006). *Celoporthe dispersa gen. et sp. nov.* from native *Myrtales* in South Africa. *Studies in Mycology* **55**: 255–267.

Nakashima C, Akashi T, Takahashi Y, *et al.* (2007). New species of the genus *Scolecostigmina* and revision of *Cercospora cryptomeriicola* on conifers. *Mycoscience* **48**: 250–254.

Nakashima C, Kobayashi T (1997). Etiological studies on brown spot disease of *Pyracantha*. *Annals of the Phytopathological Society of Japan* **63**: 309–315.

Nakashima C, Motohashi K, Chen CY, *et al.* (2016). Species diversity of *Pseudocercospora* from Far East Asia. *Mycological Progress* **15**: 1093–1117.

Nakashima C, Nishijima T, Kobayashi T (1999). Addition and reexamination of Japanese species belonging to the genus *Cercospora* and allied genera II. Species described by Japanese mycologists (1). *Mycoscience* **40**: 269–276.

Navarrete F, Abreo E, Martínez S, *et al.* (2011). Pathogenicity and molecular detection of Uruguayan isolates of *Greeneria uvicola* and *Cadophora luteo-olivacea* associated with grapevine trunk diseases. *Phytopathologia Mediterranea* **50**: S166–S175.

Nechwatal J, Bakonyi J, Cacciola SO, *et al.* (2013). The morphology, behaviour and molecular phylogeny of *Phytophthora* taxon Salixsoil and its redesignation as *Phytophthora lacustris sp. nov*. *Plant Pathology* **62**: 355–369.

Nechwatal J, Hahn J, Schönborn A, *et al.* (2011). A twig blight of understorey European beech (*Fagus sylvatica*) caused by soilborne *Phytophthora* spp. *Forest Pathology* **41**: 493–500.

Nemri A, Saunders DG, Anderson C, *et al.* (2014). The genome sequence and effector complement of the flax rust pathogen *Melampsora lini*. *Frontiers in Plant Science* **5**: 98.

Nguanhom J, Cheewangkoon R, Groenewald JZ, *et al.* (2016). Taxonomy and phylogeny of *Cercospora* spp. from Northern Thailand. *Phytotaxa* **233**: 27–48.

Nilsson T (1973). Studies on degradation and cellulolytic activity of microfungi. *Studia Forestalia Suecica* **104**: 1–40.

Nishikawa J, Nakashima C, Kobayashi T (2001). Brown leaf spot on *Lantana* spp. caused by *Pseudocercospora guianensis*. *Journal of General Plant Pathology* **67**: 281–284.

Norphanphoun C, Doilom M, Daranagama DA, *et al.* (2017). Revisiting the genus *Cytospora* and allied species. *Mycosphere* **8**: 51–97.

Norphanphoun C, Raspé O, Jeewon R, *et al.* (2018). Morphological and phylogenetic characterisation of novel *Cytospora* species associated with mangroves. *MycoKeys* **38**: 93–120.

O' Hanlon R, Destefanis M, Milenković I, *et al.* (2021). Two new *Nothophytophthora* species from streams in Ireland and Northern Ireland: *Nothophytophthora irlandica* and *N. lirii sp. nov*. *PLoS ONE* **16**: e0250527.

Oh E, Gryzenhout M, Wingfield BD, *et al.* (2013). Surveys of soil and water reveal a goldmine of *Phytophthora* diversity in South African natural ecosystems. *IMA Fungus* **4**: 123–131.

Ong CE, Henderson J, Akinsanmi OA (2017). Characterization and development of qPCR for early detection and quantification of *Pseudocercospora macadamiae* at different stages of infection process. *European Journal of Plant Pathology* **147**: 85–102.

Orlikowski LB, Ptaszek M, Rodziewicz A, *et al.* (2011). *Phytophthora* root and collar rot of mature *Fraxinus excelsior* in forest stands in Poland and Denmark. *Forest Pathology* **41**: 510–519.

Osorio JA, Wingfield MJ, de Beer ZW, *et al.* (2015). *Pseudocercospora mapelanensis sp. nov*., associated with a fruit and leaf disease of *Barringtonia racemosa* in South Africa. *Australasian Plant Pathology* **44**: 349–359.

Overton BE, Stewart EL, Qu X, *et al.* (2004). Qualitative real-time PCR SYBR® Green detection of Petri disease fungi. *Phytopathologia Mediterranea* **43**: 403–410.

Paap T, Croeser L, White D, *et al.* (2017). *Phytophthora versiformis sp. nov.*, a new species from Australia related to *P. quercina*. *Australasian Plant Pathology* **46**: 369–378.

Padamsee M, McKenzie EHC (2014). A new species of rust fungus on the New Zealand endemic plant, *Myosotidium*, from the isolated Chatham Islands. *Phytotaxa* **174**: 223–230.
Pan M, Zhu HY, Bonthond G, *et al.* (2019). *Cytospora piceae sp. nov*. associated with canker disease of *Picea crassifolia* in China. *Phytotaxa* **383**: 181–196.
Pan M, Zhu HY, Tian CM, *et al.* (2020). High diversity of *Cytospora* associated with canker and dieback of *Rosaceae* in China, with 10 new species described. *Frontiers in Plant Science* **11**: 690.
Panabières F, Ali GS, Allagui MB, *et al.* (2016). *Phytophthora nicotianae* diseases worldwide: new knowledge of a long-recognised pathogen. *Phytopathologia Mediterranea* **55**: 20−40.
Pascoe I, Cottral E (2000). Developments in grapevine trunk diseases research in Australia. *Phytopathologia Mediterranea* **39**: 68–75.
Peever TL, Barve MP, Stone LJ, *et al.* (2007). Evolutionary relationships among *Ascochyta* species infecting wild and cultivated hosts in the legume tribes *Cicereae* and *Vicieae*. *Mycologia* **99**: 59–77.
Pei MH, Bayon C, Ruiz C (2005). Phylogenetic relationships in some *Melampsora* rusts on *Salicaceae* assessed using rDNA sequence information. *Mycological Research* **109**: 401–409.
Pei MH (2005). A brief review of *Melampsora* rusts on *Salix*. In: *Rust diseases of willow and poplar* (Pei MH, McCracken AR, eds). CABI Publishing, Wallingford, UK: 11–28.
Pérez-Sierra A, Jung T (2013). *Phytophthora* in woody ornamental nurseries. In: *Phytophthora a global perspective* (Lamour K, ed). CABI, Wallingford, UK: 166–177.
Pérez-Sierra A, León M, Alvarez LA, *et al.* (2010). Outbreak of a new *Phytophthora* sp. associated with severe decline of almond trees in eastern Spain. *Plant Disease* **94**: 534–541.
Pérez-Sierra A, López-García C, León M, *et al.* (2013). Previously unrecorded low temperature *Phytophthora* species associated with *Quercus* decline in a Mediterranean forest in Eastern Spain. *Forest Pathology* **43**: 331–339.
Phengsintham P, Chukeatiorte E, Bahkali A, *et al.* (2010). *Cercospora* and allied genera from Laos 3. *Cryptogamie, Mycologie* **31**: 305–322.
Phookamsak R, Liu JK, Chukeatirote E, *et al.* (2013). Phylogeny and morphology of *Leptosphaerulina saccharicola sp. nov*. and *Pleosphaerulina oryzae* and relationships with *Pithomyces*. *Cryptogamie, Mycologie* **34**: 303–319.
Pintos Á, Alvarado P (2021). Phylogenetic delimitation of *Apiospora* and *Arthrinium*. *Fungal Systematics and Evolution* **7**: 197–221.
Pottinger B, Stewart A, Carpenter M, *et al.* (2002). Low genetic variation detected in New Zealand populations of *Phaeomoniella chlamydospora*. *Phytopathologia Mediterranea* **41**: 199–211.
Pouzoulet J, Mailhac N, Couderc C, *et al.* (2013). A method to detect and quantify *Phaeomoniella chlamydospora* and *Phaeoacremonium aleophilum* DNA in grapevine-wood samples. *Applied Microbiology and Biotechnology* **97**: 10163–10175.
Pratibha J, Prabhugaonkar A (2015). Multi-gene phylogeny of *Pithomyces* with the sexual morph of *P. flavus* Berk. & Broome. *Phytotaxa* **218**: 84–90.
Praveena R, Naseema A (2004). Fungi occurring on water hyacinth (*Eichhornia crassipes* (Mart.) Solms) in Kerala. *Journal of Tropical Agriculture* **42**: 21–23.
Puglisi I, De Patrizio A, Schena L, *et al.* (2017). Two previously unknown *Phytophthora* species associated with brown rot of Pomelo (*Citrus grandis*) fruits in Vietnam. *PLoS ONE* **12**: e0172085.
Punithalingam E (1975). *Ascochyta fabae*. *CMI Descriptions of Pathogenic Fungi and Bacteria*. No. **461**.
Punithalingam E (1979). Graminicolous *Ascochyta* species. *Mycological Papers* **142**: 1–214.
Quaedvlieg W, Binder M, Groenewald JZ, *et al.* (2014). Introducing the Consolidated Species Concept to resolve species in the *Teratosphaeriaceae*. *Persoonia* **33**: 1–40.
Quaedvlieg W, Kema GH, Groenewald JZ, *et al.* (2011). *Zymoseptoria gen. nov*.: a new genus to accommodate septoria-like species occurring on graminicolous hosts. *Persoonia* **26**: 57–69.
Rahman MZ, Uematsu S, Kimishima E, *et al.* (2015). Two plant pathogenic species of *Phytophthora* associated with stem blight of Easter lily and crown rot of lettuce in Japan. *Mycoscience* **56**: 419–433.
Rayner RW (1970). *A mycological colour chart*. Commonwealth Mycological Institute, Kew, UK.
Raza M, Zhang ZF, Hyde KD, *et al.* (2019). Culturable plant pathogenic fungi associated with sugarcane in southern China. *Fungal Diversity* **99**: 1–104.
Rea AJ, Burgess TI, Hardy GEStJ, *et al.* (2011). Two novel and potentially endemic species of *Phytophthora* associated with episodic dieback of kwongan vegetation in the south-west of Western Australia. *Plant Pathology* **60**: 1055–1068.
Rea AJ, Jung T, Burgess TI, *et al.* (2010). *Phytophthora elongata sp. nov*. a novel pathogen from the *Eucalyptus marginata* forest of Western Australia. *Australasian Plant Pathology* **39**: 477–491.
Réblová M, Gams W, Štěpánek V. (2011). The new hyphomycete genera *Brachyalara* and *Infundichalara*, the similar *Exochalara* and species of '*Phialophora* sect. *Catenulatae*' (*Leotiomycetes*). *Fungal Diversity* **46**: 67–86.
Rédou V, Kumar A, Hainaut M, *et al.* (2016). Draft genome sequence of the Deep-sea ascomycetous filamentous fungus *Cadophora malorum* Mo12 from the Mid-Atlantic ridge reveals its biotechnological potential. *Genome Announcements* **4**: e00467–16.
Reeser PW, Sutton W, Hansen EM, *et al.* (2011). *Phytophthora* species in forest streams in Oregon and Alaska. *Mycologia* **103**: 22–35.
Reeser P, Sutton W, Hansen EM (2013). *Phytophthora pluvialis*, a new species from mixed tanoak-Douglas-fir forests of western Oregon, U.S.A. *North American Fungi* **8**: 1–8.
Retief E, Damm U, van Niekerk M, *et al.* (2005). A protocol for molecular detection of *Phaeomoniella chlamydospora* in grapevine wood sample. *South African Journal of Science* **101**: 139–142.
Ridgway HJ, Sleight BE, Stewart A (2002). Molecular evidence for the presence of *Phaeomoniella chlamydospora* in New Zealand nurseries, and its detection in rootstock mothervines using species-specific PCR. *Australasian Plant Pathology* **31**: 267–271.
Rizzo DM, Garbelotto M, Davidson JM, *et al.* (2002). *Phytophthora ramorum* as the cause of extensive mortality of *Quercus* spp. and *Lithocarpus densiflorus* in California. *Plant Disease* **86**: 205–214.
Roane MK (1986). Taxonomy of the genus *Endothia*. In: *Chestnut blight, other Endothia diseases, and the genus Endothia* (MK Roane, GJ Griffin, JR Elkins, eds.). APS Press, St. Paul, Minnesota, USA: 28–39.
Roane MK, Stipes RJ, Phipps PM, *et al.* (1974). *Endothia gyrosa*, causal pathogen of pin oak blight. *Mycologia* **66**: 1042–1047.
Robert V, Vu D, Amor ABH, *et al.* (2013). MycoBank gearing up for new horizons. *IMA Fungus* **4**: 371–379.
Robin C, Piou D, Feau NF, *et al.* (2011). Root and aerial infections of *Chamaecyparis lawsoniana* by *Phytophthora lateralis*: a new threat for European countries. *Forest Pathology* **41**: 417–424.
Rocha FB, Hanada RE, de Albuquerque ST, *et al.* (2013). *Pseudocercospora piperis* associated with leaf spots on *Piper aduncum* in Brazil. *Australasian Plant Disease Notes* **8**: 101–103.
Roux C (1986). *Leptosphaerulina chartarum sp. nov*., the teleomorph of *Pithomyces chartarum*. *Transactions of the British Mycological Society* **86**: 319–323.
Roux J, Kamgan Nkuekam G, Marincowitz S, *et al.* (2020). *Cryphonectriaceae* associated with rust-infected *Syzygium jambos* in Hawaii. *MycoKeys* **76**: 49–79.
Ruano-Rosa D, Schena L, Agosteo GE, *et al.* (2018). *Phytophthora oleae sp. nov.* causing fruit rot of olive in southern Italy. *Plant Pathology* **67**: 1362–1373.
Saccardo PA (1880). Fungi Gallici ser. II. *Michelia* **2**: 39–135.
Saccardo PA (1882). *Sylloge Fungorum* **1**: i-xviii, 1–768. Italy, Padua.
Saccardo PA (1905). *Sylloge Fungorum omnium hucusque cognitorum: Supplementum Universale, Pars VI* **17**: 1–991. Padova, Italy.
Sanogo S, Bosland PW. (2013). Biology and management of *Phytophthora capsici* in the South-western USA. In: *Phytophthora a global perspective* (Lamour K, ed). CABI, Wallingford, UK: 87–95.
Santos Rezende J, Zivanovic M, Costa de Novaes MI, *et al.* (2020). The AVR4 effector is involved in cercosporin biosynthesis and likely affects the virulence of *Cercospora cf. flagellaris* on soybean. *Molecular Plant Pathology* **21**: 53–65.

Sasaki Y, Tanaka K, Nakamura A, *et al*. (2012). Identification and phylogenetic analyses of *Pseudocercospora cladrastidis* on *Maackia amurensis*. *Natural History Society of Aomori* **17**: 55–61.

Sautua FJ, Gonzalez SA, Doyle VP, *et al.* (2019). Draft genome sequence data of *Cercospora kikuchii*, a causal agent of Cercospora leaf blight and purple seed stain of soybeans. *Data in Brief* **27**: 104693.

Senanayake IC, Crous PW, Groenewald JZ, *et al.* (2017). Families of *Diaporthales* based on morphological and phylogenetic evidence. *Studies in Mycology* **86***:* 217–296.

Senanayake IC, Jeewon R, Chomnunti P, *et al.* (2018). Taxonomic circumscription of *Diaporthales* based on multigene phylogeny and morphology. *Fungal Diversity* **93**: 241–443.

Scanu B, Hunter GC, Linaldeddu BT, *et al.* (2014a). A taxonomic re-evaluation reveals that *Phytophthora cinnamomi* and *P. cinnamomi* var. *parvispora* are separate species. *Forest Pathology* **44**: 1–20.

Scanu B, Linaldeddu BT, Deidda A, *et al.* (2015). Diversity of *Phytophthora* species from declining Mediterranean maquis vegetation, including two new species, *Phytophthora crassamura* and *P. ornamentata sp. nov*. *PLoS ONE* **10**: e0143234.

Scanu B, Linaldeddu BT, Pérez-Sierra A, *et al.* (2014b). *Phytophthora ilicis* as a leaf and stem pathogen of *Ilex aquifolium* in Mediterranean islands. *Phytopathologia Mediterranea* **53**: 480–490.

Scanu B, Webber JF (2016). Dieback and mortality of *Nothofagus* in Britain: ecology, pathogenicity and sporulation potential of the causal agent *Phytophthora pseudosyringae*. *Plant Pathology* **65**: 26–36.

Schoch CL, Crous PW, Groenewald JZ, *et al.* (2009). A class-wide phylogenetic assessment of *Dothideomycetes*. *Studies in Mycology* **64**: 1–15.

Schoch CL, Seifert KA, Huhndorf S, *et al.* (2012). Nuclear ribosomal internal transcribed spacer (ITS) region as a universal DNA barcode marker for Fungi. *Proceedings of the National Academy of Sciences, USA* **109**: 6241–6246.

Schwingle BW, Smith JA, Blanchette RA (2007). *Phytophthora* species associated with diseased woody ornamentals in Minnesota nurseries. *Plant Disease* **91**: 97–102.

Scott P, Taylor P, Gardner J, *et al.* (2019). *Phytophthora aleatoria sp. nov*., associated with root and collar damage on *Pinus radiata* from nurseries and plantations. *Australasian Plant Pathology* **48**: 313–321.

Scott P, Williams N (2014). Phytophthora diseases in New Zealand forests. *New Zealand Journal of Forestry* **59**: 14–21.

Scott PM, Burgess TI, Barber PA, *et al.* (2009). *Phytophthora multivora sp. nov*., a new species recovered from declining *Eucalyptus*, *Banksia*, *Agonis* and other plant species in Western Australia. *Persoonia* **22**: 1–13.

Shakya SK, Grünwald NJ, Fieland VJ, *et al.* (2021). Phylogeography of the wide-host range panglobal plant pathogen *Phytophthora cinnamomi*. *Molecular Ecology* **30**: 5164–5178.

Shear CL, Stevens NE, Tiller RJ (1917). *Endothia parasitica* and related species. *United States Department of Agriculture Bulletin* **380**: 1–82.

Shearer BL, Tippett JT (1989). *Jarrah dieback: The dynamics and management of Phytophthora cinnamomi in the jarrah (Eucalyptus marginata) forests of south-western Australia.* Department of Conservation and Land Management, Perth, Australia.

Shearer BL, Crane CE, Cochrane A (2004). Quantification of the susceptibility of the native flora of the South-West Botanical Province, Western Australia, to *Phytophthora cinnamomi*. *Australian Journal of Botany* **52**: 435–443.

Shin HD, Kim JD (2001). *Cercospora* and allied genera from Korea. *Plant Pathogens of Korea* **7**: 1–303.

Shinyama Y, Yamaoka Y (2012). Ecology of two heteroecious *Melampsora* species that parasitize willows and *Papaveraceae* plants. *Japanese Journal of Mycology* **53**: 15–32.

Shivas RG, Marney TS, Tan YP, *et al.* (2015). Novel species of *Cercospora* and *Pseudocercospora* (*Capnodiales*, *Mycosphaerellaceae*) from Australia. *Fungal Biology* **119**: 362–369.

Shivas RG, Young AJ, Crous PW (2009a). *Pseudocercospora avicenniae*. Fungal Planet 40, *Persoonia* **23**: 192–193.

Shivas RG, Young AJ, Grice KRE (2009b). *Pseudocercospora mangifericola*. Fungal Planet 42, *Persoonia* **23**: 196–197.

Silva M, Barreto RW, Pereira OL, *et al.* (2016). Exploring fungal mega-diversity: *Pseudocercospora* from Brazil. *Persoonia* **37**: 142–172.

Simon UK, Groenewald JZ, Crous PW. (2009). *Cymadothea trifolii*, an obligate biotrophic leaf parasite of *Trifolium*, belongs to *Mycosphaerellaceae* as shown by nuclear ribosomal DNA analyses. *Persoonia* **22**: 49–55.

Snow GA, Beland JW, Czabator FJ (1974). Formosan sweetgum susceptible to North American *Endothia gyrosa*. *Phytopathology* **64**: 602–605.

Soares APG, Guillin EA, Borges LL, *et al.* (2015). More *Cercospora* species infect soybeans across the Americas than meets the eye. *PLoS ONE* **10**: e0133495.

Spadaro D, Pellegrino C, Garibaldi A, *et al.* (2011). Development of SCAR primers for the detection of *Cadophora luteo-olivacea* on kiwifruit and pome fruit and of *Cadophora malorum* on pome fruit. *Phytopathologia Mediterranea* **50**: 430–441.

Spegazzini C (1910). Mycetes Argentinenses (Series V). *Anales del Museo Nacional de Historia Natural de Buenos Aires* **20**: 329–467.

Spielman LJ (1983). *Taxonomy and biology of Valsa species on hardwoods in North America, with special reference to species on maples.* Cornell University, New York, USA.

Spielman LJ (1985). A monograph of *Valsa* on hardwoods in North America. *Canadian Journal of Botany* **63**: 1355–1378.

Stewart EL, Liu Z, Crous PW, *et al.* (1999). Phylogenetic relationships among some cercosporoid anamorphs of *Mycosphaerella* based on rDNA sequence analysis. *Mycological Research* **103**: 1491–1499.

Stipes RJ, Phipps PM (1971). A species of *Endothia* associated with a canker disease of pin oak (*Quercus palustris*) in Virginia. *Plant Disease Report* **55**: 467–469.

Streito JC, Legrand P, Tabary F, *et al.* (2002). Phytophthora disease of alder (*Alnus glutinosa*) in France: investigations between 1995 and 1999. *Forest Pathology* **32**: 179–191.

Stukenbrock EH, Quaedvlieg W, Javan-Nikhah M, *et al.* (2012). *Zymoseptoria ardabiliae* and *Z. pseudotritici*, two progenitor species of the septoria tritici leaf blotch fungus *Z. tritici* (synonym: *Mycosphaerella graminicola*). *Mycologia* **104**: 1397–407.

Suto Y (1985). Sporulation of several Cercosporae on culture media under the irradiation of a black-light fluorescent lamp. *Journal of the Japanese Forest Society* **67**: 51–56.

Sutton BC (1980). *The Coelomycetes. Fungi imperfecti with pycnidia*, *acervuli* and *stromata*. Commonwealth Mycological Institute, Kew, Surrey, England.

Sydow P, Sydow H (1915). *Monographia Uredinearum. III: Melampsoraceae, Zaghouaniaceae, Coleosporiaceae*. Leipzig, Berlin, Borntraeger, Germany.

Taylor PA, Pascoe IG, Greenhalgh FC (1985). *Phytophthora clandestina sp. nov*. in roots of subterranean clover. *Mycotaxon* **22**: 77–85.

Tegli S, Santilli E, Bertelli E, *et al.* (2000). Genetic variation within *Phaeoacremonium aleophilum* and *P. chlamydosporum* in Italy. *Phytopathologia Mediterranea* **39**: 125–133.

Tello ML, Gramaje D, Gómez A, *et al.* (2010). Analysis of phenotypic and molecular diversity of *Phaeomoniella chlamydospora* isolates in Spain. *Journal of Plant Pathology* **92**: 195–203.

Tennakoon DS, Kou CH, Maharachchikumbura SSN, *et al.* (2021). Taxonomic and phylogenetic contributions to *Celtis formosana*, *Ficus ampelas*, *F. septica*, *Macaranga tanarius* and *Morus australis* leaf litter inhabiting microfungi. *Fungal Diversity* **108**:1–215.

Tennakoon DS, Thambugala KM, De Silva NI, *et al.* (2019). Leaf litter saprobic Didymellaceae (Dothideomycetes): *Leptosphaerulina longiflori sp. nov.* and *Didymella sinensis*, a new record from *Roystonea regia*. *Asian Journal of Mycology* **2**: 87–100.

Tessmann DJ, Charudattan R, Kistler HC, *et al.* (2001). A molecular characterization of *Cercospora* species pathogenic to water hyacinth and emendation of *C. piaropi*. *Mycologia* **93**: 323–334.

Thines M, Choi Y–J (2016). Evolution, diversity and taxonomy of the *Peronosporaceae*, with focus on the genus *Peronospora*. *Phytopathology* **106**: 6–18.

Tian CM, Shang YZ, Zhuang JY, *et al.* (2004). Morphological and molecular phylogenetic analysis of *Melampsora* species on poplars in China.

Mycoscience **45**: 56–66.
Tibpromma S, Hyde KD, Jeewon R, *et al.* (2017). Fungal diversity notes 491–602: taxonomic and phylogenetic contributions to fungal taxa. *Fungal Diversity* **83**: 1–261.
Toome M, Aime MC (2015). Reassessment of rust fungi on weeping willows in the Americas and description of *Melampsora ferrinii sp. nov. Plant Pathology* **64**: 216–224.
Trapero-Casas A, Kaiser WJ (1992). Development of *Didymella rabiei*, the teleomorph of *Ascochyta rabiei*, on chickpea straw. *Phytopathology* **82**: 1261–1266.
Travadon R, Lawrence DP, Rooney-Latham S, *et al.* (2015). *Cadophora* species associated with wood-decay of grapevine in North America. *Fungal Biology* **119**: 53–66.
Tri MV, Van Hoa N, Minh Chau N, *et al.* (2015). Decline of jackfruit (*Artocarpus heterophyllus*) incited by *Phytophthora palmivora* in Vietnam. *Phytopathologia Mediterranea* **54**: 275–280.
Tsao PH. (1990). Why many phytophthora root rots and crown rots of tree and horticultural crops remain undetected. *Bulletin OEPP/EPPO Bulletin* **20**: 11–17.
Tulasne LR, Tulasne C (1865). *Selecta Fungorum Carpologia*. Vol. 3. Paris.
Tyler BM (2007). *Phytophthora sojae*: root rot pathogen of soybean and model oomycete. *Molecular Plant Pathology* **8**: 1–8.
Úrbez-Torres JR, Haag P, Bowen P, *et al.* (2014). Grapevine trunk diseases in British Columbia: incidence and characterization of the fungal pathogens associated with esca and Petri diseases of grapevine. *Plant Disease* **98**: 456–468.
Úrbez-Torres JR, Haag P, Bowen P, *et al.* (2015). Development of a DNA microarray for the detection and identification of fungal pathogens causing decline of young grapevines. *Phytopathology* **105:** 1373–1388.
Úrbez-Torres JR, Peduto F, Vossen PM, *et al.* (2013). Olive twig and branch dieback: Etiology, incidence, and distribution in California. *Plant Disease* **97**: 231–244.
Vaghefi N, Kikkert JR, Hay FS, *et al.* (2018). Cryptic diversity, pathogenicity, and evolutionary species boundaries in *Cercospora* populations associated with Cercospora leaf spot of *Beta vulgaris*. *Fungal Biology* **122**: 264–282.
Valenzuela-Lopez N, Cano-Lira JF, Guarro J, *et al.* (2018). Coelomycetous *Dothideomycetes* with emphasis on the families *Cucurbitariaceae* and *Didymellaceae. Studies in Mycology* **90**: 1–69.
Van der Lee T, Robold A, Testa A, *et al.* (2001). Mapping of avirulence genes in *Phytophthora infestans* with amplified fragment length polymorphism markers selected by bulked segregant analysis. *Genetics* **157**: 949–956.
Van Poucke K, Haegeman A, Goedefroit T, *et al.* (2021). Unravelling hybridization in *Phytophthora* using phylogenomics and genome size estimation. *IMA Fungus* **12**: 16.
Venter M, Myburg H, Wingfield BD, *et al.* (2002). A new species of *Cryphonectria* from South Africa and Australia, pathogenic on *Eucalyptus*. *Sydowia* **54**: 98–117.
Verkley GJM (1999). A monograph of *Pezicula* and its anamorphs. *Studies in Mycology* **44**: 1–176.
Vermeulen M, Gryzenhout M, Wingfield MJ, *et al.* (2013). Species delineation in the tree pathogen genus *Celoporthe* (*Cryphonectriaceae*) in southern Africa. *Mycologia* **105**: 297–311.
Vettraino AM, Brasier CM, Brown AV, *et al.* (2011). *Phytophthora himalsilva sp. nov.* an unusually phenotypically variable species from a remote forest in Nepal. *Fungal Biology* **115**: 275–287.
Vialle A, Feau N, Frey P, *et al.* (2013). Phylogenetic species recognition reveals host-specific lineages among poplar rust fungi. *Molecular Phylogenetics and Evolution* **66**: 628–644.
Vialle A, Frey P, Hambleton S, *et al.* (2011). Poplar rust systematics and refinement of *Melampsora* species delineation. *Fungal Diversity* **50**: 227–248.
Videira SIR, Groenewald JZ, Braun U, *et al.* (2016). All that glitters is not *Ramularia*. *Studies in Mycology* **83**: 49–163.
Videira SIR, Groenewald JZ, Nakashima C, *et al.* (2017). *Mycosphaerellaceae* – chaos or clarity? *Studies in Mycology* **87**: 257–421.
Von Höhnel F (1907). Fragmente zur Mykologie: IV. Mitteilung (Nr. 156 bis 168). *Sitzungsberichte der Kaiserlichen Akademie der Wissenschaften Mathematisch-Naturwissenschaftliche Klasse, Abteilung I* **116**: 615–647.
Vu D, Groenewald M, de Vries M, *et al.* (2019). Large-scale generation and analysis of filamentous fungal DNA barcodes boosts coverage for kingdom fungi and reveals thresholds for fungal species and higher taxon delimitation. *Studies in Mycology* **92**: 135–154.
Walsh E, Duan W, Mehdi M, *et al.* (2018). *Cadophora meredithiae* and *C. interclivum*, new species from roots of sedge and spruce in a western Canada subalpine forest. *Mycologia* **110**: 201–214.
Wanasinghe DN, Jeewon R, Jones EBG, *et al.* (2019). Novel palmicolous taxa within *Pleosporales*: multigene phylogeny and taxonomic circumscription. *Mycological Progress* **17**: 571–590.
Wanasinghe DN, Jeewon R, Peršoh D, *et al.* (2018a). Taxonomic circumscription and phylogenetics of novel didymellaceous taxa with brown muriform spores. *Studies in Fungi* **3**: 152–175.
Wanasinghe DN, Phukhamsakda C, Hyde KD, *et al.* (2018b). Fungal diversity notes 709–839: taxonomic and phylogenetic contributions to fungal taxa with an emphasis on fungi on *Rosaceae*. *Fungal Diversity* **89**: 1–236.
Wang LL, Li KM, Liu Y, *et al.* (2020a). *Melampsora salicis-michelsonii sp. nov.* on *Salix michelsonii* and *Melampsora salicis-cavaleriei* on *Salix serrulatifolia* from China. *Phytotaxa* **435**: 280–292.
Wang M, Liu F, Crous PW, *et al.* (2017). Phylogenetic reassessment of *Nigrospora*: ubiquitous endophytes, plant and human pathogens. *Persoonia* **39**:118–142.
Wang Q, Liu ZC, He W, *et al.* (2019). *Pseudocercospora* spp. from leaf spots of *Euonymus japonicus* in China. *Mycosystema* **38**:159–170.
Wang W, Li GQ, Liu QL, *et al.* (2020b). *Cryphonectriaceae* on *Myrtales* in China: phylogeny, host range, and pathogenicity. *Persoonia* **45**: 101–131.
Wang W, Liu QL, Li GQ, *et al.* (2018). Phylogeny and pathogenicity of *Celoporthe* species from plantation *Eucalyptus* in Southern China. *Plant Disease* **102**: 1915–1927.
Wang YL, Lu Q, Decock C, *et al.* (2015). *Cytospora* species from *Populus* and *Salix* in China with *C. davidiana sp. nov*. *Fungal Biology* **119**: 420–432.
Wang YZ (1949). *Uredinales* of Shensi. *Contributions from the Institute of Botany National Academy of Peiping* **6**: 221–232.
Waterhouse GM (1963). Key to the species of *Phytophthora* de Bary. Commonwealth Mycological Institute, Kew, Surrey, UK. *Mycological Papers* **92**: 22.
Webber JF, Vettraino AM, Chang TT, *et al.* (2012). Isolation of *Phytophthora lateralis* from *Chamaecyparis* foliage in Taiwan. *Forest Pathology* **42**: 136–143.
Weir BS, Paderes EP, Anand N, *et al.* (2015). A taxonomic revision of *Phytophthora* Clade 5, including two new species, *Phytophthora agathidicida* and *P. cocois*. *Phytotaxa* **205**: 21–38.
Werres S, Marwitz R, Man in 't Veld WA, *et al.* (2001). *Phytophthora ramorum sp. nov*., a new pathogen on *Rhododendron* and *Viburnum*. *Mycological Research* **105**: 1155–1165.
White C-L, Halleen F, Mostert L (2011). Symptoms and fungi associated with esca in South African vineyards. *Phytopathologia Mediterranea* **50**: S236–S246.
Whiteman SA, Jaspers MV, Stewart A, *et al.* (2002). Detection of *Phaeomoniella chlamydospora* in soil using species-specific PCR. *New Zealand Plant Protection* **55**: 139–145.
Wilcox WF, Scott PH, Hamm PB, *et al.* (1993). Identity of a *Phytophthora* species attacking raspberry in Europe and North America. *Mycological Research* **97**: 817–831.
Wingfield MJ, De Beer ZW, Slippers B, *et al.* (2012). One fungus, one name promotes progressive plant pathology. *Molecular Plant Pathology* **13**: 604–613.
Yang Q, Fan XL, Crous PW, *et al.* (2015). *Cytospora* from *Ulmus pumila* in northern China. *Mycological Progress* **14**: 1–12.
Yang X, Copes WE, Hong C (2013). *Phytophthora mississippiae sp. nov.*, a new species recovered from irrigation reservoirs at a plant nursery in Mississippi. *Journal of Plant Pathology and Microbiology* **4**: 180.

Yang X, Copes WE, Hong C (2014a). Two novel species representing a new clade and cluster of *Phytophthora*. *Fungal Biology* **118**: 72–82.

Yang X, Gallegly ME, Hong C (2014b). A high-temperature tolerant species in clade 9 of the genus *Phytophthora*: *P. hydrogena sp. nov. Mycologia* **106**: 57–65.

Yang X, Hong C (2013). *Phytophthora virginiana sp. nov*., a high-temperature tolerant species from irrigation water in Virginia. *Mycotaxon* **126**: 167–176.

Yang X, Hong C (2018). Differential usefulness of nine commonly used genetic markers for identifying *Phytophthora* species. *Frontiers in Microbiology* **9**: 2334.

Yang X, Richardson PA, Hong C (2014c). *Phytophthora* ×*stagnum nothosp. nov*., a new hybrid from irrigation reservoirs at ornamental plant nurseries in Virginia. *PLoS One* **9**: e103450.

Yang X, Tyler BM, Hong C (2017). An expanded phylogeny for the genus *Phytophthora*. *IMA Fungus* **8**: 355–384.

Yen JM, Lim G (1970). Étude sur les champignons parasites du sud-est Asiatique. XIV Huitième note sur les *Cercospora* de Malaisie. *Bulletin de la Société Mycologique de France* **85**: 459–474.

Yuan ZQ (1996). Fungi and associated tree diseases in Melville Island, Northern Territory, Australia. Australian *Systematic Botany* **9**: 337–360.

Zapata M (2016). First report of *Melampsora ferrinii* causing willow leaf rust in Chile. *New Disease Reports* **34**: 25.

Zhang QT, Lu Q, He M, *et al.* (2014). *Cytospora palm sp. nov.* (*Diaporthales, Ascomycota*), a canker agent on *Cotinus coggygria* (*Anacardiaceae*) in Northern China. *Cryptogamie*, *Mycologie* **35**: 211–220.

Zhang ZF, Zhou SY, Eurwilaichitr L, *et al.* (2021). Culturable mycobiota from Karst caves in China II, with descriptions of 33 new species. *Fungal Diversity* **106**:29–136.

Zhao P, Tian CM, Yao YJ, *et al.* (2014). *Melampsora salicis-sinicae* (*Melampsoraceae*, *Pucciniales*), a new rust fungus found on willows in China. *Mycoscience* **55**: 390–399.

Zhao P, Tian CM, Yao YJ, *et al.* (2015a). Two new species and one new record of *Melampsora* on willows from China. *Mycological Progress* **14**: 66.

Zhao P, Wang QH, Tian CM, *et al.* (2015b). A morphological and molecular survey of Japanese *Melampsora* species on willows reveals a new species and two new records. *Mycological Progress* **14**: 101.

Zhao P, Wang QH, Tian CM, *et al.* (2015c). Integrating a numerical taxonomic method and molecular phylogeny for species delimitation of *Melampsora* species (*Melampsoraceae*, *Pucciniales*) on willows in China. *PLoS ONE* **17**: e0144883.

Zhao P, Kakishima M, Wang Q, *et al.* (2017). Resolving the *Melampsora epitea* complex. *Mycologia* **109**: 391–407.

Zhao P, Qi XH, Crous PW, *et al.* (2020). *Gymnosporangium* species on *Malus*: species delineation, diversity and host alternation. *Persoonia* **45**: 68–100.

Zinno Y (1970). A new method for artificial sporulation of *Cercospora sequoiae* Ellis *et* Everhart, the needle blight fungus of *Cryptomeria* (I). *Journal of the Japanese Forest Society* **52**: 306–309.

Zhu HY, Pan M, Bezerra JDP, *et al.* (2020). Discovery of *Cytospora* species associated with canker disease of tree hosts from Mount Dongling of China. *MycoKeys* **62**: 97–121.

Zhu HY, Pan M, Bonthond G, *et al.* (2019). Diaporthalean fungi associated with canker and dieback of trees from Mount Dongling in Beijing, China. *MycoKeys* **59**: 67–94.

Zhu HY, Tian CM, Fan XL (2018). Multigene phylogeny and morphology reveal *Cytospora spiraeae sp. nov*. (*Diaporthales, Ascomycota*) in China. *Phytotaxa* **338**: 49–62.

Studies in Mycology (ISSN 0166-0616)

The Westerdijk Fungal Biodiversity Institute taxonomy series “Studies in Mycology” is issued as individual booklets. Regular subscribers receive each issue automatically. Prices of back-volumes are specified below.

For more information and ordering of other Westerdijk Institute books and publications see www.wi.knaw.nl and www.studiesinmycology.org.

101 Samson RA (ed) March 2022. Regular issue. 564 pp., online only. No hardcopy available.
100 Samson RA (ed) September 2021. Human fungal pathogens. 117 pp., online only. No hardcopy available.
99 Samson RA (ed) June 2021. Regular issue. 218 pp., online only. No hardcopy available.
98 Samson RA (ed) March 2021. Genera of fusarioid fungi in *Nectriaceae*. 184 pp., online only. No hardcopy available.
97 Samson RA (ed) September 2020. Regular issue. 92 pp., online only. No hardcopy available.
96 Samson RA (ed) June 2020. Regular issue. 396 pp., online only. No hardcopy available.
95 Samson RA, Crous PW (eds) March 2020. Genera of Hyphomycetes: a Tribute to Keith A. Seifert. 462 pp., online only. No hardcopy available.
94 Samson RA (ed) September 2019. Regular issue. 298 pp., online only. No hardcopy available.
93 Samson RA (ed) June 2019. Taxonomy of industrially important fungi. 252 pp., online only. No hardcopy available.
92 Samson RA (ed) March 2019. Regular issue. 415 pp., online only. No hardcopy available.
91 Samson RA (ed) December 2018. A (post-) genomic view on the diversity in *Aspergillus*. 100 pp., online only. No hardcopy available.
90 Crous PW (ed) June 2018. Regular issue. 190 pp., online only. No hardcopy available.
89 Samson RA (ed) March 2018. Leading women in fungal biology. 302 pp., online only. No hardcopy available.
88 Samson RA (ed) December 2017. Diversity and taxonomy of Food and Indoor Fungi. 268 pp., online only. No hardcopy available.
87 Crous PW (ed) June 2017. Dothideomycetes. 422 pp., online only. No hardcopy available.
86 Samson RA (ed) March 2017. Regular issue. 296 pp., online only. No hardcopy available.
85 Crous PW (ed) September 2016. Regular issue. 214 pp., online only. No hardcopy available.
84 Samson RA (ed) June 2016. Diversity and taxonomy of Indoor Fungi 1. 224 pp., online only. No hardcopy available.
83 Samson RA (ed) March 2016. Regular issue. 234 pp., online only. No hardcopy available.
82 Crous PW, Groenewald JZ (eds) 2015. Saprobic and phytopathogenic *Dothideomycetes*. 222 pp., online only. No hardcopy available.
81 Boekhout T, Bai F-Y (eds) 2015. Multigene phylogeny and reclassification of yeasts and related filamentous taxa in Basidiomycota. 190 pp., online only. No hardcopy available.
80 Lombard L, Groenewald JZ, Crous PW (eds) (2015). Hypocrealean lineages of industrial and phytopathological importance. 245 pp., € 70.00
79 Crous PW, Groenewald JZ (eds) (2014). Fungal pathogens of food and fibre crops. 288 pp., € 65.00
78 Samson RA, Visagie CM, Houbraken J (eds) (2014). Species diversity in *Aspergillus*, *Penicillium* and *Talaromyces*. 451 pp., € 75.00
77 Stadler M, Læssøe T, Fournier F, Decock C, Schmieschek B, Tichy H-V, Peršoh D (2014). A polyphasic taxonomy of *Daldinia* (*Xylariaceae*). 143 pp., € 60.00
76 Phillips AJL, Slippers B, Groenewald JZ, Crous PW (eds) (2013). Plant pathogenic and endophytic *Botryosphaeriales* known from culture. 167 pp., € 65.00
75 Crous PW, Verkley GJM, Groenewald JZ (eds) (2013). Phytopathogenic *Dothideomycetes*. 406 pp., € 70.00
74 Dijksterhuis J, Wösten H (eds) (2013). Development of *Aspergillus niger*. 85 pp., €40.00
73 Damm U, Cannon PF, Crous PW (eds) (2012). *Colletotrichum*: complex species or species complexes? 217 pp., € 65.00
72 Bensch K, Braun U, Groenewald JZ, Crous PW (2012). The genus *Cladosporium*. 401 pp., € 70.00
71 Hirooka Y, Rossmann AY, Samuels GJ, Lechat C, Chaverri P (2012). A monograph of *Allantonectria*, *Nectria*, and *Pleonectria* (*Nectriaceae*, *Hypocreales*, *Ascomycota*) and their pycnidial, sporodochial, and synnematous anamorphs. 210 pp., € 65.00
70 Samson RA, Houbraken J (eds) (2011). Phylogenetic and taxonomic studies on the genera *Penicillium* and *Talaromyces*. 183 pp., € 60.00
69 Samson RA, Varga J, Frisvad JC (2011). Taxonomic studies on the genus *Aspergillus*. 97 pp., € 40.00
68 Rossman AY, Seifert KA (eds) (2011). Phylogenetic revision of taxonomic concepts in the *Hypocreales* and other *Ascomycota* - A tribute to Gary J. Samuels. 256 pp., € 65.00
67 Bensch K, Groenewald JZ, Dijksterhuis J, Starink-Willemse M, Andersen B, Summerell BA, Shin H-D, Dugan FM, Schroers H-J, Braun U, Crous PW (2010). Species and ecological diversity within the *Cladosporium cladosporioides* complex (*Davidiellaceae*, *Capnodiales*). 96 pp., € 40.00
66 Lombard L, Crous PW, Wingfield BD, Wingfield MJ (2010). Systematics of *Calonectria*: a genus of root, shoot and foliar pathogens. 71 pp., € 40.00
65 Aveskamp M, Gruyter H de, Woudenberg J, Verkley G, Crous PW (2010). Highlights of the *Didymellaceae*: A polyphasic approach to characterise *Phoma* and related pleosporalean genera. 64 pp., € 40.00
64 Schoch CL, Spatafora JW, Lumbsch HT, Huhndorf SM, Hyde KD, Groenewald JZ, Crous PW (2009). A phylogenetic re-evaluation of *Dothideomycetes*. 220 pp., € 65.00
63 Jaklitsch WA (2009). European species of *Hypocrea*. Part I. The green-spored species. 93 pp., € 40.00
62 Sogonov MV, Castlebury LA, Rossman AY, Mejía LC, White JF (2008). Leaf-inhabiting genera of the *Gnomoniaceae*, *Diaporthales*. 79 pp., € 40.00
61 Hoog GS de, Grube M (eds) (2008). Black fungal extremes. 198 pp., € 60.00
60 Chaverri P, Liu M, Hodge KT (2008). Neotropical *Hypocrella* (anamorph *Aschersonia*), *Moelleriella*, and *Samuelsia*. 68 pp., € 40.00
59 Samson RA, Varga J (eds) (2007). *Aspergillus* systematics in the genomic era. 206 pp., € 65.00
58 Crous PW, Braun U, Schubert K, Groenewald JZ (eds) (2007). The genus *Cladosporium* and similar dematiaceous hyphomycetes. 253 pp., € 65.00
57 Sung G-H, Hywel-Jones NL, Sung J-M, Luangsa-ard JJ, Shrestha B, Spatafora JW (2007). Phylogenetic classification of *Cordyceps* and the clavicipitaceous fungi. 63 pp., € 40.00
56 Gams W (ed.) (2006). *Hypocrea* and *Trichoderma* studies marking the 90th birthday of Joan M. Dingley. 179 pp., € 60.00

For a complete list of the Studies in Mycology see www.wi.knaw.nl.